



EuCAP 2024

**18TH EUROPEAN CONFERENCE ON
ANTENNAS & PROPAGATION**

GLASGOW

17 - 22 March 2024

EuCAP

TECHNICAL PROGRAMME

16.03.2024

**Authors and
Programme**

eBook

EurAAP

Organized by



Supported by



**IEEE Antennas and
Propagation Society**



**The Institution of
Engineering and Technology**



EuCAP2024 Sponsors

Platinum Sponsors



The [Microwave Vision Group](#) offers cutting-edge technologies for the visualization of electromagnetic waves. With advanced test solutions for antenna characterization, radar signature evaluation and electromagnetic measurements, we support company R&D teams in their drive to innovate and boost product development.



Founded in 1987 with headquarters in Shenzhen, China, [Huawei](#) is a leading global provider of information and communications technology (ICT) infrastructure and smart devices. Huawei's products and solutions are used by 45 of the world's top 50 carriers in over 170 countries, serving around a third of the world's population. Huawei is a private company, 100% owned by its employees, and is constantly engaged in management development complying with the international best practices.

The company currently has 197,000 employees, over 45% of whom are employed in the Research & Development sector. Huawei has built 14 Research & Development centers, 36 Joint Innovation Centers and 45 Training Centers worldwide. In 2021, the company invested over \$22 billion in Research & Development, 22.4% of its global revenue.


Huawei has filed 112,849 patents and, according to the UN World Intellectual Property Organization (WIPO), in 2021 it is the first company in the world for international patent applications with 6,952 requests. In 2021, Huawei also ranks first for patent applications filed at the European Patent Office (EPO) with 3,544 applications.

Huawei ranked 44th in the 2021 Fortune Global 500 ranking and was the first Chinese company ever to enter the 'Top 100 Best Global Brands' by Interbrand, where in 2021 it ranked 85th.


With solutions integrated in four key domains (telecommunication networks, IT, smart devices and cloud services), Huawei is committed to bringing digital to every person, home and organization, for a fully connected and intelligent world. In 2021, Huawei recorded a revenue of \$99.9 billion with a net profit of \$17.8 billion.

Huawei operates in Italy since 2004 where it counts on +700 professionals (85% local), two main offices in Milan and Rome, offices in major cities, three centers of Global Research, six Innovation Centers and five Joint R&D Labs. Moreover, Huawei is currently carrying out

	<p>research collaborations with 36 universities in Italy providing for investments in joint projects on optical technologies, semiconductor technologies, 5G, Industry 4.0.</p>
--	---

	<p>Ansys Powering innovation that drives human advancement</p> <p>When visionary companies need to know how their world-changing ideas will perform, they close the gap between design and reality using Ansys simulation. For more than 50 years, Ansys software has enabled innovators across industries to push the boundaries of product design by using the predictive power of simulation. From sustainable transportation and advanced satellite systems to life-saving medical devices, Ansys powers innovation that drives human advancement.</p> <p>CADFEM</p> <p>Our mission is to develop, support and complement your simulation capacity and expertise. We have proven experience of driving innovation across a broad spectrum of engineering disciplines where simulation has the potential to accelerate, enhance and optimise product designs as well as reducing the time and cost of their design cycles. As a long standing partner of the leading software provider Ansys, we provide a single source contact for a broad range of engineering simulation solutions including RF, microwave and photonics, systems, structural, thermal and fluid dynamics. We also provide technical support, training, technology transfer, and consulting relating to Ansys software, plus we can help you with any associated IT requirements (including Cloud based solutions). Simulation is more than software!</p>
---	--

Gold Sponsors

	<p>Dassault Systèmes:</p> <p>Dassault Systèmes is a catalyst for human progress. We provide business and people with collaborative virtual environments to imagine sustainable innovations. By creating virtual twin experiences of the real world with our 3DEXPERIENCE platform and applications, our customers can redefine the creation, production and life-cycle-management processes of their offer and thus have a meaningful impact to make the world more sustainable. The beauty of the Experience Economy is that it is a human-centered economy for the benefit of all -consumers, patients and citizens.</p> <p>Dassault Systèmes brings value to more than 300,000 customers of all sizes, in all industries, in more than 150 countries. For more information, visit www.3ds.com</p>
---	--



SIMUSERV:

SIMUSERV, an established Dassault Systèmes Business partner, operates from offices in the UK, Germany, Australia, and New Zealand. We specialise in simulation and the SIMULIA Brand of Dassault Systèmes. Our team boasts extensive experience in Engineering Simulation, covering the full range of physics addressed by SIMULIA. Our primary areas of expertise lie in CST Studio Suite for Electromagnetic simulation and ABAQUS for structural analysis. At SIMUSERV, we recognize that precise simulation workflows are vital for success. Our core focus revolves around implementing Technology as a Business Solution to harness the "Art of Simulation" to attain the required specific business benefits.



For more than 75 years, [ETS-Lindgren](#) has been manufacturing a wide range of products renowned for setting the research, development, production, and service standards of the RF/ Microwave Test and Measurement Industry. Having the proven technical depth expected of an industry leader, with more than 50,000 RF Shielded installations worldwide, ETS-Lindgren can guide our customers to an optimal test and measurement solution for their specific product application. Solutions include turnkey systems for Government/Aerospace, Automotive, EMC, and Wireless applications. We offer RF/Microwave Far-Field, Near-Field, and Compact Range Chambers for Radar Cross Section as well as Antenna Measurement Systems for 5G NR, OTA, and MIMO OTA performance testing. ETS-Lindgren's popular antennas are available in standard and custom designs. Our diverse absorber product line is well known for its durability, high performance, non-hygroscopic design, and high-power handling capabilities. As an end-to-end integrated supplier, we also manufacture multi-axis positioners, field probes, and monitors, to name a few. Turnkey system solutions feature EMQuest™ software for fully automated 2- and 3-D antenna pattern measurement for passive antennas and active wireless devices. ETS-Lindgren's customers can count on continuous support through our six manufacturing sites and more than 750 employees worldwide.



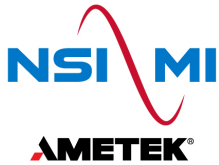
For over 100 years, [Leonardo](#) has designed world-leading airborne sensors that protect aircrews on operations around the globe.

The Centre of Excellence in Edinburgh is built upon an 80-year heritage of technological expertise in Airborne Radars, establishing Leonardo as a world-leader in radar design and manufacturing. Its products provide essential capability to military and civilian operations worldwide including the Eurofighter Typhoon primary sensor, the Captor radar, as well as its family of Osprey and Seaspray radars

Leonardo is a founding partner of Team Tempest (alongside UK MOD, BAE Systems, Rolls-Royce and MBDA) and is developing the Integrated Sensing and Non-Kinetic Effects (ISANKE) and Integrated Communications Systems (ICS) technology for the UK's Future Combat Air Systems (FCAS) including the Global Combat Air Programme (GCAP).

Leonardo is one of the UK's leading aerospace companies and one of biggest suppliers of defence and security equipment to the UK MOD. It makes a significant contribution to the UK economy with revenues of £1.9bn, around 45% of which are in export. The company operates from 8 main sites across the UK employing over 8,000 highly skilled people.

Our team is constantly looking for talented software, systems and electronics engineers to join our team and help drive our innovation in sensor technology.



[NSI-MI Technologies](#) is the premier source for advanced antenna measurement solutions for any aerospace, defence, satellite, or wireless application and beyond. Our elite team of experts oversee every step of the design, manufacturing, construction, and system integration process, and our broad customer service network will lend support long after delivery. Whether investing in a turnkey system, a precision component, or optimised instrumentation suite, we take your specific RF measurement requirements and execute a solution unparalleled in performance, accuracy, and quality.

You can always Test with Confidence™ at NSI-MI.



As technology pushes society forward at a staggering pace, we need to safeguard our future.

A fully connected world presents us with challenges. The potential impact of technology is the very reason why it needs to be as safe as possible. To make sure this and future generations can rest assured, we need to continuously put technology to the test. For the sake of everyone. Aiming to propel innovation to new heights.

At world-leading [Emerson & Cuming AC](#), we have been developing and manufacturing rf-absorbing materials and anechoic chambers since 1948. These are paramount to the constant optimisation and testing of new technologies. Working closely with universities and other research institutes, we offer sustainable solutions tailored to any specific needs to our customers in aerospace, automotive, defence, consumer electronics, telecommunications and academic and research institutions.

Step by step, we create a safer world through innovation and enable the great minds on their mission to make humankind flourish.

Step by step, we shape the future.



ROHDE & SCHWARZ
Make ideas real

The [Rohde & Schwarz](#) technology group is among the trailblazers when it comes to paving the way for a safer and connected world with its leading solutions in test & measurement, technology systems, and networks & cybersecurity. Founded nearly 90 years ago, the group is a reliable partner for industry and government customers around the globe. On June 30, 2022, Rohde & Schwarz had around 13,000 employees worldwide. The independent group achieved a net revenue of EUR 2.53 billion in the 2021/2022 fiscal year (July to June). The company is headquartered in Munich, Germany.



[TICRA](#) is the world's leading supplier of antenna modeling software for antenna industries, including spacecraft manufacturers and space agencies, earth-station antenna suppliers, defence industries and research institutions.

With more than 50 years of experience in developing trusted solutions for the space industry, TICRA provides highly accurate EM simulation software for reflector antennas and related feed systems, quasi-periodic surfaces, platform scattering as well as for antenna measurements. Our expert engineers are available to customers through software support and consultancy services.

Silver Sponsors



IMST GmbH is a development centre for customer-specific radio technology and microelectronic systems. More than 130 highly qualified engineers develop integrated circuits, hybrid modules and systems, radio modules, antennas, micro-controller circuits, embedded systems and 3D-EM simulation software. We support our customers from the first ideas all the way up to the prototype and we offer support also in the production phase. In order to always keep our extensive know-how in the various radio technologies up to date, IMST GmbH successfully participates in many funded research projects -including German funded projects, EU activities and ESA contracts.



We are **the IET** and we inspire, inform and influence the global engineering community to engineer a better world. As a diverse home across engineering and technology, we share knowledge that helps make better sense of the world in order to solve the challenges that matter. It's why we are uniquely placed to champion engineering.

Keep advancing with our wide range of engineering, science and technology content. Essential discovery tools for researchers, universities and organisations around the world.

Visit the IET stand to receive a discount on our latest antennas and propagation book titles and take a look at the opportunities to submit your research to our journal IET Microwaves, Antennas & Propagation.



At **Keysight** (NYSE: KEYS), we inspire and empower innovators to bring world-changing technologies to life. As an S&P 500 company, we're delivering market-leading design, emulation, and test solutions to help engineers develop and deploy faster, with less risk, throughout the entire product lifecycle. We're a global innovation partner enabling customers in communications, industrial automation, aerospace and defense, automotive, semiconductor, and general electronics markets to accelerate innovation to connect and secure the world. Learn more at www.keysight.com.



Optenni Ltd. is an innovator in antenna and RF design automation, developing professional design tools for antenna and RF engineers. Optenni employs customer-driven innovation, and partners with leading players in the wireless ecosystem.

Optenni's main product, Optenni Lab™, is the leading circuit synthesis software for antenna and RF optimization that features automatic matching circuit synthesis and optimization, antenna array beamforming with active impedance control, and many assessment tools to evaluate design candidate's performance. Optenni Lab links with major EM tools, and is applied, for example, in the design of tunable and multiband antenna systems and phased arrays.



[Rogers Corporation](#) (NYSE:ROG) is a global leader in engineered materials to power, protect and connect our world. Rogers delivers innovative solutions to help our customers solve their toughest material challenges. Rogers' advanced electronic and elastomeric materials are used in applications for EV/HEV, automotive safety and radar systems, mobile devices, renewable energy, wireless infrastructure, energy-efficient motor drives, industrial equipment and more. Headquartered in Chandler, Arizona, Rogers operates manufacturing facilities in the United States, Asia and Europe, with sales offices worldwide. For more information, visit www.rogerscorp.com.



[Antenna Systems Solutions \(ASYSOL\)](#) is a European company committed to delivering innovation and outstanding service worldwide in the field of antenna measurements.

Through our dedication, we strive to offer on putting customers first by presenting them with industry expertise as a supplier and producer of antenna metrology measuring systems for the Aerospace, Automotive, Academia, Commercial, and Defense industries. In the last years, Antenna Systems Solutions has installed over 60 Antenna Measurement Systems globally (23 countries in Europe, North America, Africa and Asia).

We design solutions for any RF communications test equipment requirements. We will work with your team to provide you with the optimal test setup for your application.

ASYSOL is a place where innovation is standard.

Bronze Sponsors



[Teleco Renta](#) is an outreach plan to attract talent for the development of future 5G networks in Spain. Please write to aamor@ing.uc3m.es to learn more about the different research centers and universities participating in the program.

		energy efficient space phased arrays; Dr. Hervé Laguey, Thales Alenia Space, France	Propagation Channel Characterization; Dr. Pekka Kyösti, University of Oulu, Finland																	
15:20-16:00		IN2: Self-Phasing Antenna Array Technology for Real World Wireless; Prof. Vincent Fusco, Queens University of Belfast, N Ireland, UK	IN4: Radiowave Propagation Development in the ITU-R; Carol Wilson, CSIRO Space & Astronomy, Australia																	

16:00-16:30 coffee-break

16:30-18:10		CS32: AMTA Session: Novel Antenna Measurement and Post Processing Techniques	EXR: Exhibitors' reception	A04: Shared apertures and multiband antennas	A21: Mm-wave antenna technologies II	A19: Antennas for space systems	P03: Detection and estimation	CS13: Applications of RFID Antennas and Systems	CS27: Implantable antennas and intra-body wave propagation	CS7: Antenna for emerging applications at sub-THz frequencies	CS11: AI-Driven Antenna Design Contemporary Methodologies and Practical Applications	IW11: Applying AI/ML to 6G PHY Research, Keysight Technologies	IW3: 5G & 6G Communication Testbeds, TMYTEK	E07: Optimization Methods in Metasurface Design	DA -: DA - EurAAP DA
-------------	--	--	----------------------------	--	--------------------------------------	---------------------------------	-------------------------------	---	--	---	--	--	---	---	----------------------

Wednesday, March 20

08:30-10:10		SW11a: Wi-Fi Antenna Innovation for FTR (Fiber-To-The-Room) Multi-Access Points FSG-A Scenarios	CS31: AMTA Session: New Applications for Compressive Sensing in Antenna Measurements	CS35a: Propagation for Smart Mobility Scenarios	A12a: Advances in modelling and design of phased arrays	A16: User terminal antennas for satellite systems	CS40a: New challenges on small antennas for emerging wireless technologies	CS23a: Recent Advances on Propagation Research and Its Impact on Localizations	CS45: Direct and inverse EM modelling for biomedical microwave imaging systems	A05: Optical, THz and sub-THz antennas	E10a: Electromagnetic Modelling and Analytical Methods	E08: Efficient Methods for Metasurfaces Design	IW6: Advances in TICRA Tools and Future Developments for AI and Array Antennas, TICRA	A08a: Leaky-wave antennas	SW12a: Open Source Electromagnetic Modelling Tools
-------------	--	---	--	---	---	---	--	--	--	--	--	--	---	---------------------------	--

10:10-10:40 coffee-break

10:40-12:20		SW11b: Wi-Fi Antenna Innovation for FTR (Fiber-To-The-Room) Multi-Access Points FSG-A Scenarios (continued)	SW13: 20 Years Anniversary ESoA	CS35b: Propagation for Smart Mobility Scenarios (continued)	A12b: Advances in modelling and design of phased arrays (continued)	A13: Emerging antennas for space systems	CS40b: New challenges on small antennas for emerging wireless technologies (continued)	CS23b: Recent Advances on Propagation Research and Its Impact on Localizations (continued)	E01: Inverse Scattering and Imaging for Biomedical Applications	E05: Periodic Structures for mmWave and THz Applications	E10b: Electromagnetic Modelling and Analytical Methods (continued)	IW12: Teleco Renta: An opportunity to conduct research in Spain	IWS: From Planar Antennas to Multi-Beam Phased Array Systems, Celestia	A08b: Leaky-wave antennas (continued)	SW12b: Open Source Electromagnetic Modelling Tools (continued)
-------------	--	---	---------------------------------	---	---	--	--	--	---	--	--	---	--	---------------------------------------	--

12:20-13:10 Lunch

PA4: Poster session on mm-wave and sub mm-wave Antennas I,
 PA6: Poster session on Metamaterials and metasurface antennas and systems,
 PA8: Poster session on Antenna systems,
 PE3: Poster Session on Electromagnetics II,
 PM2: Poster Session on Measurements II,
 PP02: Poster session on Propagation II

14:40-15:20		IN5: Terahertz Antennas and Systems for Space Applications; Dr. Goutam Chattopadhyay, NASA-JPL, USA	IN7: Spaceborne antenna testing: Status, Perspectives and Challenges; Dr. Luis Rolo, ESTEC, ESA, The Netherlands																	
-------------	--	---	--	--	--	--	--	--	--	--	--	--	--	--	--	--	--	--	--	--

15:20-16:00		IN6: Quasi-Optical Antenna Systems for THz Communications and Sensing; Prof. Nuria Llombart, Tu Delft, Netherlands	IN8: How Compressive Sensing Approaches Can Enhance RF Hardware Capability; Dr. Brian E. Fischer, Resonant Sciences, USA																	
-------------	--	--	--	--	--	--	--	--	--	--	--	--	--	--	--	--	--	--	--	--

16:00-16:30 coffee-break

16:30-18:10		SWM: In Memory of Ross Stone	M3: Innovative Approaches for Antenna Measurements	CS34: Propagation measurements and modelling for RIS-aided wireless communications	P09: Rain attenuation	A07: Lens antennas	E04: Electromagnetic Imaging	CS21: mm-Wave Antennas for Radar Applications	P06: Body propagation, sensing and communication	A23: Antenna modelling techniques	A22: Modelling and design techniques for lens antennas	SW9: Rydberg Atom-Based Sensors: Transforming Measurements and Detection of Radio-Frequency Fields and Communication Signals	E11: Fundamental Research and Emerging Technology	E12: Novel Materials, Metamaterials, and Metasurfaces II	WG Measurements: WG meeting
-------------	--	------------------------------	--	--	-----------------------	--------------------	------------------------------	---	--	-----------------------------------	--	--	---	--	-----------------------------

Thursday, March 21

08:30-10:10		SW2a: Activities of	CS22a: Quantum	A03a: Antenna analysis and	CS8: Advanced mm-	A18: Algorithms,	SW7a: Stand on the IEEE	A01a: Sensing,	M4: Measurements,	P10a: mmWave and	E02a: Computational	A06a: Advances in	CS33a: Multiscale,	A10: Metasurfaces	A25: Additive manufactured
-------------	--	---------------------	----------------	----------------------------	-------------------	------------------	-------------------------	----------------	-------------------	------------------	---------------------	-------------------	--------------------	-------------------	----------------------------

	ITU-R Study Group 3 on radio wave propagation	Electromagnetics - From Photonics to Quantum Computing	design for sub-6GHz	Wave Substrate Integrated Antennas and Systems for Future Wireless Communication	modelling and system analysis for aerospace systems	Antennas & Propagation Standards	communication and identification antennas and systems	characterization and apparatus	THz propagation modeling and measurements	Electromagnetics	reflectarray antennas for wave control, space and 5G applications	Multiphysics and Unconventional Techniques for Electromagnetic Imaging	and resonant cavity antennas	antennas	
10:10-10:40	coffee-break														
10:40-12:20	SW2b: Activities of ITU-R Study Group 3 on radio wave propagation (continued)	CS22b: Quantum Electromagnetics - From Photonics to Quantum Computing (continued)	A03b: Antenna analysis and design for sub-6GHz (continued)	A11: Developments in mm-wave antennas	CS4: Antennas for Radio Astronomy	SW7b: Stand on the IEEE Antennas & Propagation Standards (continued)	A01b: Sensing, communication and identification antennas and systems (continued)	CS41: Electrically Small Antenna Measurement Technique	P10b: mmWave and THz propagation modeling and measurements (continued)	E02b: Computational Electromagnetics (continued)	A06b: Advances in reflectarray antennas for wave control, space and 5G applications (continued)	CS33b: Multiscale, Multiphysics and Unconventional Techniques for Electromagnetic Imaging (continued)	IW8: Regulatory and Performance Testing Considerations for Future Wireless Communication Technologies, ETS-Lindgren	WG Active Array Antennas: wg meeting	IW14: IMST workshop: Efficient Dual Polarised Omnidirectional 5G/6G mmWave Tx/Rx Frontend Module Design using EMPIRE-XPU
12:20-13:10	Lunch														
13:10-14:40	PA1: Poster session on Antennas for biomedical and health applications, PA3: Poster session on mm-wave and sub mm-wave Antennas II, PA5: Poster session on Sub-6GHz antennas for terrestrial networks, PP03: Poster session on Propagation III, PS1: Best Paper Awards														

14:40-15:20	IN9: Versatile metamaterials for diverse field manipulation; Prof. Ariel Epstein, Technion - Israel Institute of Technology, Israel	IN12: Filtering Antenna Techniques for 5G/BSG Wireless Communication Applications; Prof. Wenquan Che, South China University of Technology, China													
15:20-16:00	IN10: Perfectly-Matched Metamaterials; Prof. Anthony Grbic, University of Michigan, USA	IN11: Crafting the Future of Smart EM Environments Through the System-by-Design - The SEME@Trentino Initiative; Prof. Paolo Rocca, University of Trento, Italy													
16:00-16:30	coffee-break														
16:30-18:10	SW4: EurAAP Early Careers and Women in Antennas and Propagation	CS18: Characteristic Modes Analysis for Next-Generation Wireless Technologies	A02: Emerging antenna technologies for sub-6GHz	A28: Antennas for 5G and beyond	A17: Deployable antenna solutions for space applications	P02: Imaging, detection and estimation	CS29: Propagation for Integrated Sensing and Communication	A20: Biomedical and health	P01: Channel modeling and measurements	A24: Superdirectivity and synthesis techniques	M2: MIMO, OTA and 6G Antenna Testing	ESoA: ESoA Board	E09: Frequency Selective Surfaces		

Friday, March 22

08:30-10:10	SW10a: Sub-Terahertz Antenna and Packaging Solutions for Future Radar and Wireless Communication	CS30a: Approaching optimal performance through automated design techniques	CS43a: COST-INTERACT, Propagation Measurement and Modelling for 6G and Beyond	CS48: MIMO Beamforming Design and Optimization in future 6G Wireless Systems	CS15: GigaScale Antenna Arrays for Space based Solar Power	CS1a: Advances in Microwave and mmWave Wireless Power Transfer	CS12a: AMTA Session: Robotic Antenna Measurements	CS19a: Fundamental challenges and novel methodologies in the next-generation computational electromagnetics	SW6a: Recent advances in antenna measurement traceability and uncertainty at reduced distances	CS26a: COST CA18223 (SyMat) Modeling and Applications of Higher Symmetries	A15a: Developments in antenna arrays	SW8a: Waveguide Antenna Array Technologies for Space and Beyond	CS14a: Shape-morphing metamaterials, antennas and electromagnetic components	RoE: RoE meeting
10:10-10:40	coffee-break													
10:40-12:20	SW10b: Sub-Terahertz Antenna and Packaging Solutions for Future Radar and Wireless Communication (continued)	CS30b: Approaching optimal performance through automated design techniques (continued)	CS43b: COST-INTERACT, Propagation Measurement and Modelling for 6G and Beyond (continued)	A26: Reconfigurable Intelligent Surface (RIS) technologies	CS46: GNSS Reflectometry Antenna Topics	CS1b: Advances in Microwave and mmWave Wireless Power Transfer (continued)	CS12b: AMTA Session: Robotic Antenna Measurements (continued)	CS19b: Fundamental challenges and novel methodologies in the next-generation computational electromagnetics (continued)	SW6b: Recent advances in antenna measurement traceability and uncertainty at reduced distances (continued)	CS26b: COST CA18223 (SyMat) Modeling and Applications of Higher Symmetries (continued)	A15b: Developments in antenna arrays (continued)	SW8b: Waveguide Antenna Array Technologies for Space and Beyond (continued)	CS14b: Shape-morphing metamaterials, antennas and electromagnetic components (continued)	
12:40-13:10	CC: Closing ceremony													
14:00-17:00		SC07: Fundamental equations of electromagnetics from classical to quantum	SC08: Microwave Imaging and Sensing and their Innovative Applications	SC02: Optimal Antennas: Operators, Limits, and Design	SC01: Modelling and Design of Space-Time Modulated Electromagnetic Structures	SC05: AI Techniques for Microwave Antenna Design	SC06: Machine Learning-Enabled Optimization and Synthesis of Metasurface Antennas	SC04: Multibeam Antennas and Beamforming Networks	SC03: Advanced impedance matching and impedance analysis for antenna applications	SC09: Planar near-field measurements of phased array antennas in millimetre-wave bands	SC10: Spherical Near-Field Antenna Measurements - Theory and Practical Implementation			

Monday, March 18 8:30 - 9:30

OC: Opening Ceremony

Room: Clyde Auditorium

Monday, March 18 9:30 - 10:15

KY1: Keynote 1: Innovation and developments in reflector antenna modelling and applications; Dr. Cecilia Cappellin, TICRA, Denmark

Room: Clyde Auditorium

Chair: Christophe Craeye (Université Catholique de Louvain, Belgium)

Monday, March 18 10:15 - 10:45

coffee-break

Room: Expo/Poster

Monday, March 18 10:45 - 11:30

KY2: Keynote 2: Absolute security for broadband terahertz wireless links; Prof. Daniel M. Mittleman, Brown University, USA

Room: Clyde Auditorium

Chair: Thomas Kürner (Technische Universität Braunschweig, Germany)

Monday, March 18 11:30 - 12:15

KY3 -: Keynote 3: Silicon-Based Phased-Arrays for SATCOM, 5G and 6G: We Solved the Puzzle! Now what else to do?; Prof. Rebeiz, The University of California, San Diego, USA

Room: Clyde Auditorium

Chair: George V. Eleftheriades (University of Toronto, Canada)

Monday, March 18 12:15 - 13:30

Lunch

Room: Expo/Poster

Monday, March 18 13:30 - 15:30

SW3a: Defence radar, antennas and electromagnetics: past present and future

Room: Clyde Auditorium

Chairs: Anthony Keith Brown (University of Manchester, United Kingdom (Great Britain)), David Conway (MIT Lincoln Labs, USA)

13:30 Introductory Remarks

Presenters: Tony Brown, David Conway (Queen Mary, University of London, UK; MIT Lincoln Labs, USA)

13:35 Historical Perspective of World War II Radar Development

Presenter: David Conway (MIT Lincoln Labs)

14:05 History and Future Directions of Airborne Radars

Presenter: Claudio Biancotto (Leonardo)

14:35 Development of Phased Array and Multi-Phase Centre Systems

Presenter: Stephen Harman (THALES, UK)

Monday, March 18 13:30 - 15:30

SW5a: Metrology for 5G and beyond in support of standard developments (IET workshop)

Room: Lomond Auditorium

Chairs: Fabien Heliot (University of Surrey, United Kingdom (Great Britain)), Anil K Shukla (QinetiQ, United Kingdom (Great Britain))

13:30 Opening Presentation by Organizers

Presenter: Anil Shukla (QinetiQ)

13:35 Needs and Measurements Challenges over Integrating Adaptive Antenna with Emerging Wireless Systems

Presenter: Anil Shukla (QinetiQ)

13:55 Array Calibration for Massive MIMO Antenna System: Challenges and Solutions

Presenter: Wei Fan (Aalborg University)

14:15 Plane Wave Generator for OTA Testing

Presenter: Lars Foged (Microwave Vision Group)

14:35 Traceability of 5G Measurements

Presenter: Emrah Tas (Federal institute of Metrology METAS)

14:55 A Metrological Full-Connected Hybrid Beamformer Testbed with a Large Antenna Array for Millimetre-Wave RF-EMF Testing

Presenter: Tian Hong Loh (National Physical Laboratory)

Monday, March 18 13:30 - 15:30

CS17a: Reconfigurable Intelligent Surfaces Recent Developments and Applications

T09 Fundamental research and emerging technologies / Convened Session / Antennas

Room: M1

Chairs: Mohsen Khalily (University of Surrey & 5G Innovation Centre, Institute for Communication Systems (ICS), United Kingdom (Great Britain)), Okan Yurduseven (Queen's University Belfast, United Kingdom (Great Britain))

13:30 Dual-Polarized Reconfigurable Metacavity Transceiver for Computational Polarimetric Imaging

Mengran Zhao (Queen's University Belfast, United Kingdom (Great Britain) & Xi'an Jiaotong University, China); Mohsen Khalily (University of Surrey & 5G Innovation Centre, Institute for Communication Systems (ICS), United Kingdom (Great Britain)); Okan Yurduseven (Queen's University Belfast, United Kingdom (Great Britain))

In this paper, a dual-polarized reconfigurable metacavity transceiver (DRMT) that can be applied in computational polarimetric imaging (CPI) is proposed. The transmitter and the receiver of a CPI system are replaced by two ports of the DRMT, which significantly simplifies the hardware architecture. The DRMT is an electrically over-sized metacavity with its back wall replaced by a reconfigurable metasurface and its top surface etched with leaky cross-shaped irises. By altering the PIN state of each metamaterial element, spatially orthogonal measurement modes can be obtained. Besides, measurement modes under different polarization states are also orthogonal to each other. The correlation coefficients are smaller than 0.2 and the singular values are close to each other, which proves the spatial-orthogonality of the measurement modes. The DRMT-based full-wave CPI simulations are also implemented and polarimetric images were reconstructed using different polarization components to showcase the benefits of the CPI method.

13:50 3D Method-Of-Moment Design of Huygens' Metasurfaces

Tianke Qiu, Vasileios G. Ataloglou and George V. Eleftheriades (University of Toronto, Canada)

Electromagnetic metasurfaces (MTSs) are often assumed to be passive and lossless, and can be modeled as purely reactive homogenized impedance sheets on dielectric substrates. In this paper, a 3-D design procedure for reflective metasurfaces based on the integral equation method and impedance boundary conditions is presented. The metasurface consists of impedance sheets placed on top of a grounded dielectric slab, and the impedance values are optimized to match certain far-field (FF) power patterns or to beamform using the gradient-descent method.

14:10 Exploring RIS Coverage Enhancement in Factories: From Ray-Based Modeling to Use-Case Analysis

Gurjot Singh Bhatia (Université Paris-Saclay, Laboratoire Des Signaux et Systèmes, France & SIRADEL, France); Yoann Corre and Thierry Tenoux (SIRADEL, France); Marco Di Renzo (CNRS & Paris-Saclay University, France)

Reconfigurable Intelligent Surfaces (RISs) have risen to the forefront of wireless communications research due to their proactive ability to alter the wireless environment intelligently, promising improved wireless network capacity and coverage. Thus, RISs are a pivotal technology in evolving next-generation communication networks. This paper demonstrates a system-level modeling approach for RIS. The RIS model, integrated with the Volcano ray-tracing (RT) tool, is used to analyze the far-field (FF) RIS channel properties in a typical factory environment and explore coverage enhancement at sub-6 GHz and mmWave frequencies. The results obtained in non-line-of-sight (NLOS) scenarios confirm that RIS application is relevant for 5G industrial networks.

14:30 Reflective Surfaces Based on Semi-Passive Reconfigurable Polymer Network Liquid Crystal

Pablo de la Rosa del Val, Robert Guirado, Gerardo Perez-Palomino, Eduardo Carrasco and Manuel Caño-García (Universidad Politécnica de Madrid, Spain)

Future telecommunication networks demand for innovative solutions that can improve the poor coverage conditions expected at millimeter-wave frequencies (>30 GHz). The devices composing those networks, apart from improving the coverage, must be of moderate cost, easy to manufacture and operate under strict low power consumption requirements. In this paper, a reflecting planar semi-passive device based on Polymer Network Liquid Crystal (PNLC) is proposed as an example of a single-time programmable RIS. Due to the PNLC properties, the device is easy to mass-produce, can be easily programmed for each working scenario, and behaves like a passive device after it is programmed. The envisioned implementation workflow is also discussed, together with its advantages and disadvantages. Finally, a single-time programmable reflectarray antenna based on PNLCs is designed at 100 GHz from experimentally validated data, and different radiation conditions or scenarios are presented.

14:50 Nonlinear Distortion Issues Created by Active Reconfigurable Intelligent Surfaces

Nikolaos Kolomvakis and Emil Björnson (KTH Royal Institute of Technology, Sweden)

Reconfigurable intelligent surfaces (RISs) can improve the propagation conditions over wireless channels but a passively reflecting RIS must be large to be effective. Active RIS with amplifiers can deal with this issue. In this paper, we study the distortion created by nonlinear amplifiers in active RIS. We analytically obtain the directions of the reflected distortion when the desired signals arrive from specific azimuth and elevation angles. The results are demonstrated numerically and we conclude that nonlinearities can both create in-band and out-of-band distortion that is beamformed in entirely new directions.

15:10 RIS-Enhanced MIMO Channels in Urban Environments: Experimental Insights

James Rains (University of Glasgow, United Kingdom (Great Britain)); Anvar Tukmanov (BT, United Kingdom (Great Britain)); Qammer H Abbasi and Muhammad Ali Imran (University of Glasgow, United Kingdom (Great Britain))

Can the smart radio environment paradigm measurably enhance the performance of contemporary urban macrocells? In this study, we explore the impact of reconfigurable intelligent surfaces (RISs) on a real-world sub-6 GHz MIMO channel. A rooftop-mounted macrocell antenna has been adapted to enable frequency domain channel measurements to be ascertained. A nature-inspired beam search algorithm has been employed to maximize channel gain at user positions, revealing a potential 50% increase in channel capacity in certain circumstances. Analysis reveals, however, that the spatial characteristics of the channel can be adversely affected through the introduction of a RIS in these settings. The RIS prototype schematics, Gerber files, and source code have been made available to aid in future experimental efforts of the wireless research community.

Monday, March 18 13:30 - 15:30

CS37a: Integration of Antennas and Electronic Circuits

T09 Fundamental research and emerging technologies / Convened Session / Antennas

Room: Alsh 1

Chairs: Nader Behdad (University of Wisconsin-Madison, USA), Nima Ghalichechian (Georgia Institute of Technology, USA)

13:30 3D-Printed Wearable Antenna Integrated with Rectifier for Wireless Power Transfer

Xiaoyang Yin (The University of Adelaide, Australia); Tucker Stuart (The University of Arizona, USA); Shengjian Jammy Chen (Flinders University, Australia & The University of Adelaide, Australia); Philipp Gutruf (The University of Arizona, USA); Christophe Fumeaux (University of Queensland, Australia)

Wireless power transfer (WPT) technology can facilitate battery-less and non-monitored operation for wearable devices. One core component in a WPT system is the rectenna, which integrates an antenna with a rectifier circuit. This paper discusses core factors including load impedance and received power level which will determine the rectenna topology. On this basis, a specific demonstration will be given based on a low-power bio-information monitoring platform. Co-simulations between CST Microwave Studio (CST) and Advanced Design System (ADS) are conducted for the purpose of realizing an optimal rectenna structure. Following the simulated predictions, 3D-printed rectenna prototypes have been fabricated and experimentally validated. A good agreement between simulation and measurements over several practical parameter sweeps successfully verifies the rectenna working performance.

13:50 Optimum Structured Phased Array with Novel Beam Forming Circuits for Beam Wireless Power Transfer

Naoki Shinohara, Bo Yang and Wenyi Shao (Kyoto University, Japan)

Wireless power transfer (WPT) is a transformative technology, with several startups actively pursuing its development worldwide. In 2022, Japan introduced new radio regulations for far beam WPT at 920 MHz, 2.4 GHz, and 5.7 GHz. To expand the applicability of far beam WPT, the need arises for a cost-effective phased array antenna system that boosts beam efficiency, received power, and mitigates interference with conventional wireless systems. This paper presents the research and development results of an optimal structured phased array with novel beamforming circuits for beam WPT.

14:10 A Class-E, Switched-Mode, Non-LTI Electrically-Small Transmit Antenna Design for Overcoming the Fundamental Bandwidth-Efficiency Product Limits

Nader Behdad (University of Wisconsin-Madison, USA); Dan C. Ludois (University of Wisconsin - Madison, USA); Mirhamed Mirmozafari and Marisa Liben (University of Wisconsin-Madison, USA)

We present a switched-mode, non-linear-time-invariant (non-LTI) electrically-small antenna (ESA) designed to overcome the theoretical bandwidth-efficiency product limitations governing the performances of passive, LTI ESAs. The proposed non-LTI ESA operates by integrating a class-E, switched-mode inverter, designed to act as an ideal voltage source, with an electrically-small, self-resonant radiator. There is no impedance matching between the output of the class-E inverter and the input of the self-resonant, ESA. This way, the class-E inverter is directly driving a resonant load with a small input resistance without using any intermediate impedance matching stage to 50Ω . To generate a digitally-modulated waveform, the current passing through the antenna is directly modulated by controlling the bias voltage and/or the gate driver signal of the class-E inverter. Through combined numerical electromagnetic simulation and transient circuit simulation, we demonstrate that a wide range of digitally-modulated waveforms may be generated.

14:30 Integrated Low-Loss mmWave On-Chip Arrays

Seung Yoon Lee (Georgia Institute of Technology, USA); Thomas G. Williamson (Georgia Tech Research Institute, USA); David L. West, Sree Adinarayana Dasari, Walter Royal Disharoon and Nima Ghalichechian (Georgia Institute of Technology, USA)

A 60 GHz coplanar folded slot antenna with an off-chip ground and a deep air cavity is proposed, featuring both a single element and a 1×8 linear array with corporate feed. The single-element on-chip antenna (OCA) operating at 60 GHz achieves a -10 dB measured fractional bandwidth of 6.9%. The measured peak gain is 5.6 dBi with a directivity of 6.4 dBi, and the antenna's efficiency is simulated to be 83%. The 1×8 array exhibits a 9.8 dBi realized gain with a radiation efficiency of 71%. We introduced a phase shifter using microfabricated vanadium dioxide (VO₂)-based switches. The resulting phase shifter demonstrated input impedance matching, indicating a fractional bandwidth of 182%. Integration of OCA with VO₂-based phase shifters will be instrumental in exhibiting beam steering capabilities up to 45°.

14:50 Display-Integrated MIMO Antennas for Gesture-Sensing Radars

Jin Myeong Heo, Hae Soo Eun, Phuong Linh Hoang and Kyuho Lee (Ulsan National Institute of Science and Technology (UNIST), Korea (South)); Kiseo Kim and Jaeuk Choi (Samsung Display Company Ltd., Korea (South)); Gangil Byun (Ulsan National Institute of Science and Technology (UNIST), Korea (South))

This paper proposes display-integrated MIMO antenna designs for gesture-sensing radars in mobile devices. The MIMO antennas consisting of 1 transmitting element and 3 receiving elements are implemented on a non-optical region of the display panel. Since this region is covered by a polarizer, optically clear adhesive, and a window, the proposed antennas are completely invisible to users. By placing the receiving antennas on horizontal and vertical edges, angular resolution in both azimuth and elevation directions can be achieved. For impedance matching, proximity-coupled slot dipole and monopole are employed for the antennas on the horizontal edge and vertical edge, respectively. To verify the proposed approach, the MIMO antennas are fabricated and measured, and the measured results are in good agreement with the simulated results. Moreover, the complete radar module with the proposed MIMO antennas is manufactured and tested for the feasibility of gesture-sensing.

15:10 A Completely Overlapped Ku- and Ka-Band Dual-Polarized Phased Array for Simultaneous Terrestrial and Satellite Communications

Bumhyun Kim and Wonbin Hong (Pohang University of Science and Technology (POSTECH), Korea (South))

This paper proposes an antenna designed with the shared aperture principle to operate in both the Ku and Ka bands and support dual polarization while the two antennas are completely overlapped on the same layer. Ku-band and Ka-band phased arrays are realized within the same volume without any increase in size. The inter-element spacing is optimized by using a shared aperture concept. The reflection coefficient features below -10 dB for each operating band. Additionally, both bands exhibit inter-port isolation exceeding 20 dB. Both simulated and measured results for the Ku band yield a beam steering angle greater than ± 40 degrees for both polarizations and a maximum gain of 10.3 dBi in a 1×3 array structure. For the Ka band, it is confirmed that a maximum beam steering angle is over ± 43 degrees for all polarizations, resulting in a peak gain of 13.1 dBi in a 1×5 phased array structure.

Monday, March 18 13:30 - 15:30

CS5a: Advances in mmWave and (sub-)THz channel sounding and measurements for 5G and Beyond

T02 Mm-wave for terrestrial networks 5G/6G / Convened Session / Propagation

Room: Alsh 2

Chairs: Diego Andrés Dupleich (Technische Universität Ilmenau, Germany & Fraunhofer Institute for Integrated Circuits IIS, Germany), Wei Fan (Southeast University, China)

13:30 Context-Aware Channel Sounder for AI-Assisted Radio-Frequency Channel Modeling

Camillo Gentile, Jelena Senic, Anuraag Bodi and Samuel Berweger (NIST, USA); Raied Caromi (National Institute of Standard and Technology, USA); Nada Golmie (NIST, USA)

We describe a context-aware channel sounder that consists of three separate systems: a radio-frequency system to extract multipaths scattered from the surrounding environment in the 3D geometrical domain, a Lidar system to generate a point cloud of the environment in the same domain as the multipaths - providing a geometrical means to associate the multipaths to the environment scatterers - and a camera system to identify and classify the scatterers. With the assistance of artificial intelligence (AI), the data acquired by the three systems can be automatically reduced into a scatter-specific channel model. Two such applications are presented.

13:50 Validation of Pseudo-Scale Model for the Air-Sea Two-Layer Near-Field Problem by Using FDTD Simulations and Measurements in a Tank

Nozomu Ishii and Makoto Goto (Niigata University, Japan); Masaharu Takahashi (Chiba University, Japan); Qiang Chen (Tohoku University, Japan)

A pseudo-scale model for the air-seawater two-layer problem, adjustable in two parameters, a scale factor with respect to length and a conductivity multiplier, is examined by using the results of FDTD simulations and scaled measurements in a tank. For the conversion of the sea region of the model, it can be derived assuming that the entire region is the sea, and for the conversion of the air region, it is assumed to be the extreme near-field of the source. The behavior of the electromagnetic field in the air region just above the sea surface can be validated by examining the field distribution in the region where lateral waves are dominant. The distributions of the dominant electric field component before and after the scale conversion almost coincide in the direct wave and lateral wave regions. This fact confirms the validity and effectiveness of the proposed pseudo-scale model.

14:10 Horn Antenna Phase Center Position Influence on Sub-THz Measurements Uncertainties

Mohamad Dawood Al-Dabbagh (Physikalisch-Technische Bundesanstalt (PTB), Germany); David Ulm (Physikalisch-Technische Bundesanstalt, Germany); Thomas Kleine-Ostmann (Physikalisch-Technische Bundesanstalt (PTB), Germany); David A. Humphreys (University of Bristol, United Kingdom (Great Britain) & Physikalisch-Technische Bundesanstalt, Germany)

Horn antenna phase center position is an essential parameter to perform antenna calibration at the sub-THz band. We present two measurement setups to measure the phase center, using the power delay profile (PDP) magnitude and using the PDP delay for two horn antennas at WR05 and WR03 bands compared to the antenna's dimensions.

14:30 Indoor Channel Characterization Based on Directional Measurements at 140 GHz

Jiahao Hu, Amar Al-Jzari and Sana Salous (Durham University, United Kingdom (Great Britain))

In this paper we present the results of 140 GHz propagation channel measurements in a corridor and indoor industrial environments at Durham University. Both Line-of-Sight (LoS) and Non-Line-of-Sight (NLoS) measurements were carried out with a rotated directional antenna at the transmitter to estimate the angle of departure of the multipath components (MPCs). Estimated channel parameters include Power Delay Profiles (PDP), Angular Spread (AS), and Root-Mean-Square (RMS) Delay Spread. In addition, the path loss coefficients are presented for both the Close-In (CI) and the Floating-Intercept (FI) Models.

14:50 A Modular COTS-Based High-Efficient Sub-THz Channel Sounder and Experimental Validations

Peize Zhang (University of Oulu, Finland); Cihan Barış Findik (CWC Radio Technologies - University of Oulu, Finland); Pekka Kyösti (Keysight Technologies & University of Oulu, Finland); Veikko Hovinen, Klaus Nevala, Nuutti Tervo, Marko E. Leinonen and Aarno Pärssinen (University of Oulu, Finland)

The prospect of offering huge amounts of available bandwidth to achieve extremely high data rates makes terahertz (THz) communication seen as a key enabler for 6G use cases requiring extreme throughputs on the order of 10s or 100s of Gbps. The design and planning of wireless communication systems are affected by the radio channels in which they will operate. Physical modeling of THz channels requires sufficient channel-sounding data collected across multiple frequency bands and environments for statistical analysis. In this paper, we present a modular correlation-based sub-THz channel sounder using commercial off-the-shelf instruments. It can be easily scaled for multi-band channel measurements by using different frequency extenders while sharing the same baseband units. The D-band validation measurements are conducted in an indoor corridor using the proposed sounder, together with the ray-tracing simulation results for performance validations in identical settings.

15:10 Excitation Signal Design for THz Channel Sounding and Propagation Parameter Estimation

Jonas Gedschold (Technische Universität Ilmenau, Germany); Sebastian Semper (Ilmenau University of Technology, Germany); Michael Döbereiner (Fraunhofer Institute for Integrated Circuits IIS & Technische Universität Ilmenau, Germany); Reiner S. Thomä (Ilmenau University of Technology, Germany)

In this publication, we analyze how the performance of propagation parameter estimation for THz channel sounding can be improved by the power spectrum design of a multicarrier waveform. To this end, we discuss the Fisher information of the propagation parameters and the corresponding deterministic Cramér-Rao lower bound (CRB) as well as their relation to the carrier powers of the excitation signal. We use these quantities to design waveforms that improve range estimation. In practice, evaluating the Fisher information requires prior knowledge of the propagation scenario which is usually unavailable. Hence, we propose two solutions which we compare numerically to the classical approach of equal power distribution. The evaluation shows that an optimized power distribution can improve the CRB comparable up to a 4 dB gain in signal-to-noise ratio (SNR) if knowledge about the propagation scenario is available and slightly less if the scenario is unknown.

Monday, March 18 13:30 - 15:30

CS20a: Physics-compliant models of reconfigurable intelligent surfaces

T08 EM modelling and simulation tools / Convened Session / Antennas

Room: Boisdale 1

Chairs: Raffaele D'Errico (CEA, LETI & Université Grenoble-Alpes, France), Philipp del Hougne (CNRS, Univ Rennes, France), Gabriele Gradoni (University of Surrey, United Kingdom (Great Britain))

13:30 Comparison of Simplistic System-Level RIS Models and Diffraction-Theory Solutions

Le Hao (Technische Universität Wien, Austria); Francisco S. Cuesta and Sergei Tretyakov (Aalto University, Finland)

We discuss and compare two recently published path-loss models for reconfigurable intelligent surfaces (RIS) derived from the electromagnetic and communication theory points of view. The electromagnetic model considers the RIS as a whole, taking into account field interactions of all metasurface elements, whereas the communication model is based on an assumption that each array element is an independent relay. The estimations given by the two models are rather different but, surprisingly, we find that the simplistic model gives the same result as the electromagnetic calculation for perfectly functioning anomalous reflectors if one replaces the effective areas of the unit cells by their geometrical areas, scaled by the corresponding angular factors. Simulation results validate our analysis and show the numerical differences between the two models when we vary the frequency and the number of elements in RISs.

13:50 Analysis and Optimization of Reconfigurable Intelligent Surfaces Based on S-Parameters Multiport Network Theory

Andrea Abrardo (University of Siena, Hong Kong); Alberto Toccafondi (University of Siena, Italy); Marco Di Renzo (CNRS & Paris-Saclay University, France)

In this paper, we consider a reconfigurable intelligent surface (RIS) and model it by using multiport network theory. We first compare the representation of RIS by using S -parameters and SS -parameters, by proving their equivalence and discussing their distinct features. Then, we develop an algorithm for optimizing the RIS configuration in the presence of electromagnetic mutual coupling. We show that the proposed algorithm based on optimizing the SS -parameters results in better performance than existing algorithms based on optimizing the S -parameters. This is attributed to the fact that small perturbations of the step size of the proposed algorithm result in larger variations of the SS -parameters, hence increasing the convergence speed of the algorithm.

14:10 Load Impedances Vs Polarizabilities: On the Compactness of Physics-Compliant Models of RIS-Parametrized Wireless Channels

Philipp del Hougne (CNRS, Univ Rennes, France)

Physics-compliant models of RIS-parametrized wireless channels currently describe the reconfigurability of the RIS elements either in terms of tunable load impedances or tunable polarizabilities. No efforts to compare or harmonize these two approaches exist to date, and similar results are independently derived with both approaches. Here, we compare the two approaches, notably in terms of their mathematical complexity. We argue that the polarizability approach is more "transparent" because polarizability is a local concept and the RIS configuration determines the radio environment's local scattering properties at the location of the RIS elements. In contrast, impedance is a non-local concept, and the impedance matrix only serves as a transit quantity in deriving the end-to-end channel matrix. We conclude that the polarizability formulation facilitates physical intuition and may offer lower computational complexity. The latter matters for physics-compliant channel estimation, as well as the latency and convergence of physics-compliant RIS optimization algorithms.

14:30 Accurate Design of Surface-Wave Enabled Reflective Intelligent Surfaces Through the Generalized Oliner Method

Talha Arshed, Enrica Martini and Stefano Maci (University of Siena, Italy)

This work, starting from the analysis of the sources of inefficiency and the limitations of the space wave (SPW)-to-surface wave (SW) conversion through sinusoidally modulated metasurfaces (MTSs), devises a synthesis process to achieve the impedance modulation profile providing optimum conversion performance. We apply a generalization of the Oliner's method, based on Floquet-wave expansion of the fields and Fourier-series of modulated impedance, to analytically derive a system of equations for the modulation parameters. The synthesized modulation provides control not only over the desired LW mode, but also over unwanted higher-order modes, leading to improved conversion efficiency for arbitrary beam angles. The synthesis process allows for a flexible selection of the operating wavenumber of the SW, thus, facilitating MTS implementation. The proposed approach is applied to the design of a reflective intelligent surface (RIS) operating upon a dual-conversion: first from incident SPW to SW and subsequently from SW to radiating SPW.

14:50 Recent Advances on Multi-Scale Wave Manipulation Through Reconfigurable Intelligent Surfaces

Giacomo Oliveri (University of Trento & ELEDIA Research Center, Italy); Marco Salucci (ELEDIA Research Center, Italy); Andrea Massa (University of Trento, Italy)

The Smart ElectroMagnetic Environment (SEME) concept is revolutionizing the design of wireless systems, exceeding current-generation capabilities. SEME manipulates electromagnetic waves to align with performance objectives, challenging traditional fixed propagation environments. Electromagnetic Skins (EMSs), including reconfigurable passive two-dimensional artificial structures, represent a crucial technology within this framework. These devices enable to perform advanced wave manipulation functionalities (e.g., anomalous reflection, beam shaping) through meta-atomic adjustments of their electrical properties (e.g., through electronically-controllable components). Despite complexity, EMSs offer cost-effective alternatives to traditional wireless equipment, prompting substantial research in the field. This work is aimed at discussing some of the latest RIS synthesis and wave manipulation developments, offering insights into advanced design and implementation strategies.

15:10 Electromagnetics-Based RIS Channel Model with Near-Field Accuracy Improvement

Ondřej Franek (Aalborg University & APMS Section, Denmark)

An enhanced electromagnetics-based channel model of communication between two devices via reconfigurable intelligent surface (RIS) that enables closer placement of the devices to the RIS is described. This improvement is achieved by decomposing the communication paths between the RIS and the devices into individual paths for each RIS element. Key features include the use of commercial simulation software for device characterization, physical-level modeling of RIS inter-element coupling, fast device linking using the scattering matrix formalism, and easy emulation of fading or blockage. The model is implemented as a MATLAB function and additionally offers higher-order interpolation for improved accuracy.

Monday, March 18 13:30 - 15:30

CS38: Advancements in IoT Antenna Systems Synthesis, Optimization, and Design Strategies

T04 RF sensing for automotive, security, IoT, and other applications / Convened Session / Antennas

Room: Boisdale 2

Chairs: Miloslav Capek (Czech Technical University in Prague, Czech Republic), Martijn van Beurden (Eindhoven University of Technology, The Netherlands)

13:30 Improving Scan Gain of Sparse Vivaldi Array with Parasitic Scatterers

Albert Salmi, Jan H. S. Bergman, Anu Lehtovuori and Juha Ala-Laurinaho (Aalto University, Finland); Ville Viikari (Aalto University & School of Electrical Engineering, Finland)

This paper presents a fully populated, but sparsely fed antipodal Vivaldi array. Every second element of the array is fed, and the others, parasitic scatterers, are terminated to passive loads. The appropriate terminations of the parasitic elements for improving scan gain of the array are computed using principal component analysis-based algorithm. Compared to a reference array without parasitic elements, the main beam realized gain is increased by up to 1.8 dB inside a desired beam-steering sector. The results are verified by measurements of manufactured prototypes.

13:50 Model Order Reduction for Parametric Dependence of Q-Factor Bounds in IoT Applications

Lars Jonsson (KTH Royal Institute of Technology, Sweden)

In Internet of Things (IoT) applications the antennas are often electrically small at their radiation frequency. This makes it hard to design antennas that meet desired bandwidth requirements. It is therefore interesting to consider the trade-off between antenna size and antenna position within the terminal with respect to its available bandwidth, as characterized by the Q-factor bound. To determine these quantities are associated with solving a non-trivial optimization problem.

Recent development of model order reduction techniques can include parametric dependencies. Here we apply the data-driven Loewner framework to the Q-factors as a function of size and position parameters, to investigate how well these methods work for the Q-factor bounds in IoT applications. We show that the Loewner framework can deliver a reduced-order model of the bound. Properties of the reduced model can be used to indicate how well the reduced order interpolates the parametric dependence.

14:10 Reconfigurable Architecture in a 130 x 80 mm² PCB with Antenna Booster Element for Multiband Operation in IoT Devices

Elena García and Aurora Andújar (Ignion, Spain); Joan Pijoan (Universitat Ramon Llull, Spain); Jaume Anguera (Ignion & Universitat Ramon Llull, Spain)

The rapid increase of IoT (Internet of Things) devices, including sensors and trackers, presents a significant challenge in terms of size and performance requirements. This challenge also extends to the design of the antenna system, which needs to be efficient and capable of operating across various frequency bands while maintaining a compact form factor. To address these demands, a 130mm x 80mm printed circuit board (PCB) is proposed and designed for analysis. The objective is to determine whether a passive matching network is sufficient for the desired frequency bands or if a reconfigurable architecture is necessary. This reconfigurable architecture incorporates a single SP4T (Single-Pole 4-Throw) switch, enabling operation in the frequency range of 698 MHz - 960 MHz and 1710 MHz - 2170 MHz. Additionally, the reconfigurable matching network provides flexibility in configuring and optimizing frequency bands as needed.

14:30 Ground Plane Width Analysis for IoT Devices Embedding Antenna Boosters

Alejandro Fernández and Aurora Andújar (Ignion, Spain); Jaume Anguera (Ignion & Universitat Ramon Llull, Spain)

This paper presents a $\lambda/30$ at 824 MHz antenna booster element on two PCB designs with ground planes of 120 mm x 60 mm and 120 mm x 20 mm, matched to operate in 824-960 MHz and 1710-2170 MHz. A study in terms of matching and total efficiency is performed for both designs. The use of characteristic modes analysis (CMA) is performed to seek the physical limitations of the antenna booster element. The horizontal modes help the 60 mm PCB width design achieve the best match in the high-frequency region, while the 20 mm design achieves a competitive performance thanks to the monomodal resonance at the low-frequency region.

14:50 Substructure Modes and Bounds

Mats Gustafsson (Lund University, Sweden); Lukas Jelinek and Miloslav Capek (Czech Technical University in Prague, Czech Republic); Kurt Schab (Santa Clara

University, USA); Johan Lundgren (Lund University, Sweden)

Antennas are often required to operate in environments containing objects that interact with radiating or receiving electromagnetic waves. For fixed objects in close proximity of antennas, such as a ground plane, it is frequently advantageous to include the surrounding objects in using substructure or numerical Green's function formulation. In this paper, we review how substructures are incorporated in fundamental bounds and modal expansions jointly formulated using controllable and uncontrollable regions. Moreover, a scattering theory is developed showing how substructures are treated using scattering matrices.

15:10 Estimating the Achievable Efficiency and Bandwidth of Small Terminal-Integrated Inverted-F Antennas Using Machine Learning

Julian Roqui (Université Côte d'Azur CNRS LEAT, France); Alain Pegatoquet (LEAT, France); Leonardo Lizzi (University Côte d'Azur, CNRS, LEAT, France)

This article explores the impact of dielectric substrate, terminal size and Printed Circuit Board (PCB) thickness on the achievable performance, namely efficiency and bandwidth, of small terminal-integrated inverted-F antennas (IFA). The study is based on the use of a machine learning estimation approach.

Monday, March 18 13:30 - 15:30

CS42a: AMTA Session: Post Processing Techniques in Antenna Measurements

T09 Fundamental research and emerging technologies / Convened Session / Measurements

Room: Carron 1

Chairs: Jeffrey Guerrieri (National Institute of Standards and Technology, USA), Francesco Saccardi (Microwave Vision Italy, Italy)

13:30 Inverse Source Solutions with Spectral Filtering

Thomas F. Eibert (Technical University of Munich (TUM) & Chair of High-Frequency Engineering (HFT), Germany); Matthias M. Saurer, Alexander H. Paulus and Josef Knapp (Technical University of Munich, Germany)

The radiation model of inverse source solvers representing an antenna under test (AUT) relies on a discretized spatial equivalent source distribution and the source expansion coefficients are found such that their radiation reproduces known field observations. The required number of field observations depends on the number of degrees of freedom of the radiation fields and, thus, on the spatial extent of the sources. For source distributions producing a narrow far-field radiation pattern, the number of degrees of freedom is reduced as compared to the general case and the spatial observation density can be reduced considerably. Since a general purpose inverse source solver requires the full set of observation samples as possibly supported by its spatial source distribution, we consider a solver with a spectrally filtered radiation operator, where the filtering is performed in the translation step of the underlying propagating plane-wave representation as known from the multilevel fast multipole method.

13:50 Quantification and Correction of Signal Averaging with On-The-Fly Sampling in Near-Field Antenna Measurements

Olav Breinbjerg (ElMaReCo, Denmark)

In order to achieve an acceptable signal-to-noise ratio in practical near-field antenna measurements, probe signal averaging is usually employed. Hence, the nominal sample of the probe signal at the nominal sampling point is actually an average of multiple - between two and several millions - actual samples. For on-the-fly sampling, these actual samples are not taken at the same nominal sampling point but at different actual sampling points over a sampling interval - where the probe signal is not constant. If the nominal sample of the probe signal is treated as a point quantity in the subsequent post-processing an error is thus introduced. The present work shows that this erroneous effect of signal averaging with on-the-fly sampling can be exactly quantified and exactly corrected for

14:10 Reconstruction of the Far-Field Pattern Radiated by an Elongated Antenna Measured over a Perfectly Electric Conducting Ground Plane in a Spherical Spiral Near-Field Facility

Claudio Gennarelli, Flaminio Ferrara, Rocco Guerriero and [Francesco D'Agostino](#) (University of Salerno, Italy)

Aim is to devise an effective spherical spiral near-to-far-field (NTFF) transformation for long antennas, which uses a reduced set of spiral near-field (NF) data measured in a hemispherical NF facility. The proposed technique properly exploits the theoretical foundations of spiral scanings for non-volumetric antennas to develop the non-redundant representation along the spiral wrapping the upper and lower hemispheres and the image theorem to synthesise the voltage NF data which would be collected along the spiral wrapping the lower hemisphere. Once these voltage NF data have been synthesised, then an efficient 2-D optimal sampling interpolation algorithm is conveniently used to recover the NF data required by the classical spherical NTFF transformation. It is here assumed that the considered antenna and its image exhibit a predominant dimension as compared to the other two and, hence, are effectively modeled by a rounded cylinder. Numerical tests show the accuracy of the devised NTFF transformation.

14:30 Planar Near-Field Phaseless Measurements Using Multi-Probe Arrays

Fernando Rodríguez Varela (Universidad Rey Juan Carlos de Madrid, Spain); [Manuel Sierra-Castañer](#) (Universidad Politécnica de Madrid, Spain); Francesco Saccardi (Microwave Vision Italy, Italy); Andrea Giacomini (SATIMO, Italy); Lars Foged (Microwave Vision Italy, Italy)

Near-field measurements of antennas with integrated sources is a challenge. The lack of a reference channel forces to apply phaseless techniques with high levels of oversampling and poor recovery guarantees. On this line, multi-probe systems bring numerous advantage. Not only they provide measurement time savings, but also enable the measurement of the relative phases between probes. This paper proposes a planar phaseless technique based on an optimized grid designed to minimize measurement time. The optimized grid is scanned by a probe array which extracts the magnitude and relative phase between the neighboring samples. This partial phase information is fed to a state-of-the-art phase retrieval technique which reconstructs the complete phase signal and the antenna far-field. To demonstrate the capabilities of the proposed technique, a simulation example with the VAST12 antenna is presented, where the total number of samples is reduced by a factor of 100 using a 4x4 probe array.

14:50 Antenna Coupling Evaluation in Arrays and Complex Structures Using Measured Sources and Simulations

[Lars Foged](#) (Microwave Vision Italy, Italy); Lucia Scialacqua (Italian Ministry of Health, Italy); Giorgia Giorgia Venturini (MVG, USA); Marlice Schoeman (Altair Engineering SA (Pty) Ltd, South Africa); Daniel LeRoux (Altair Engineering, SA (Pty) Ltd, South Africa); CJ Reddy (Altair, USA)

The success of antenna developments heavily relies on realistic numerical simulations of antennas and their intended operating environments. Central to this success is the accuracy of the antenna representation, which significantly enhances result reliability. Recent advancements have made it possible to derive precise mathematical models directly from measured antennas, seamlessly integrating them into Computational Electromagnetic tools. This approach proves invaluable in tackling complex structural challenges, large-scale scenarios, antenna placement intricacies, scattering phenomena, among others. An equally intriguing application arises when merging measurement data with simulations to assess antenna coupling. This becomes particularly important in designing large arrays, allowing an insight into element coupling from single-element measurements. Prior publications have predominantly concentrated on arrays featuring three identical cavity-backed cross-dipole antennas where we validated the coupling between multiple simulated near-field sources through numerical simulation, this paper extends the scope by including an experimental validation of the coupling evaluation employing measured sources

15:10 Hybrid Antenna Measurement and Post-Processing for 5G Small Cell Exposure Assessment with Site-Specific Mounting Conditions

Tobias Struck, Lisa-Marie Schilling, Willi Hofmann and Christian Bornkessel (Technische Universität Ilmenau, Germany); Matthias Hein (Ilmenau University of Technology, Germany)

Ongoing mobile radio small cell deployment requires detailed analysis of the electromagnetic exposure which is dependent on the installation environment. To facilitate site-specific small cell exposure analysis, a hybrid exposure assessment approach is utilized which combines antenna nearfield measurement and post-processing. An equivalent current antenna model is investigated under virtually varying installation conditions, considering three real applications of small cell installation. The equivalent current antenna model's results are in good agreement with reference measurements and geometry-based simulations. Antenna pattern deviations vary between 0.9 dB and 2.9 dB, depending on the installation environment selected. This highlights the advantages of using the hybrid exposure assessment approach which adequately captures and reflects changes in the installation surroundings. Additionally, it yields comparable results to established methods and provides extensive flexibility for virtual exposure estimations by taking into account varying installation environments.

Monday, March 18 13:30 - 15:30

CS2: Challenges in Human RF Exposure Assessment to Present and Future Mobile Radio Technologies including 5G and 6G

T06 Biomedical and health / Convened Session / Antennas

Room: Carron 2

Chairs: Wout Joseph (Ghent University/IMEC, Belgium), Lisa-Marie Schilling (Technische Universität Ilmenau, Germany)

13:30 *Instantaneous Vs Theoretical Maximum Exposure Under Real Traffic Conditions: Example in the City of Valencia*

Alvaro Villaescusa-Tebar (Universitat Politècnica de València, Spain); Alberto Najera and Jesus Gonzalez-Rubio (Universidad de Castilla La Mancha, Spain); Concepcion Garcia-Pardo (Universitat Politècnica de València & Institute of Telecommunications and Multimedia Applications (iTEAM), Spain)

With the ongoing deployment of the fifth generation (5G) mobile telecommunications, there is an increasing need for standardized methodologies to assess human exposure to radiofrequency electromagnetic fields from 5G base stations. Thus, the development of proper assessment methodologies will impact the adequate deployment of 5G systems as well as ensure the safe operation of devices for people. This work focuses on comparing total exposure and theoretical maximum exposure levels in commercial 5G operational networks in the City of Valencia for the frequency band below 6 GHz. This study is based on the use of a code-selective method using the R&S@TSME6 and EME Spy Evolution exposimeter in addition to an omnidirectional antenna and one user equipment (UE) to measure the downlink exposure.

13:50 *Characterization of Typical Instantaneous Exposure and Usage Scenarios in the Vicinity of 5G Massive-MIMO Base Stations*

Anna-Malin Schiffarth and Thanh Tam Julian Ta (RWTH Aachen University, Germany); Lisa-Marie Schilling and Christian Bornkessel (Technische Universität Ilmenau, Germany); Matthias Hein (Ilmenau University of Technology, Germany); Dirk Heberling (RWTH Aachen University, Germany)

A recurring discussion is whether it is useful to specify a typical exposure in addition to the theoretical maximum exposure for massive-MIMO systems, but currently no reliable method exists. Therefore, typical 5G use cases are investigated, grouped according to their throughput, and three typical data rates are derived. To evaluate the reproducibility of data rates and corresponding exposures, three measurement runs have been performed at four measurement points (MP) with different cell utilization by other users, while a 5G UE generated the typical data rates in the vicinity of the MP. Furthermore, temporal variations have been considered by evaluating three different averaging times. The results demonstrate that the exposure values are reproducible within typical measurement uncertainty across different averaging times and even across different measurement runs. Therefore, this method is considered to be capable of providing reproducible measurements of the typical exposure in addition to the maximum possible exposure.

14:10 *Long-Term Network-Based Assessment of the Actual Output Power of Base Stations in a 5G Network*

Paramananda Joshi, Davide Colombi, Bo Xu, Carla Di Paola, Jens Eilers Bischoff, Stanislav Stefanov Zhekov and Christer Törnevik (Ericsson AB, Sweden)

In this study, data were collected for 22 massive multi-input multi-output (MIMO) base stations in busy 5G sites over 15 months using a network monitoring tool. Logged precoding matrix index (PMI) data and time-averaged output power from the 5G base stations were used to obtain actual time-averaged output power statistics considering spatial distribution of power transmission corresponding to spreading of antenna beams in different directions over time. More than one billion output power samples were collected over the whole study period. The results show that the actual time-averaged output power per beam direction was significantly below the theoretical maximum power, with the mean and 95th percentile values being 2.9% and 7.4%, respectively, of the theoretical maximum. At the busiest site the 95th percentile and the maximum value were found to be 18.7% and 35.5%, respectively, of the theoretical maximum.

14:30 *Advanced Post-Processing Technique to Evaluate Specific Absorption Rate (SAR) for a Standard Dipole Antenna*

Shoaib Anwar (Microwave Vision Group, Satimo Industries, France); Lucia Scialacqua (Italian Ministry of Health, Italy); Aurelien Lelievre (MVG Industries Technopole Best Iroise - Plouzane, France); Mohamad Mantash (MVG Industries, France); Jerome Luc (MVG Industries Technopole Best Iroise - Plouzane, France); Nicolas Gross (MVG Industries, France); Francesco Saccardi and Lars Foged (Microwave Vision Italy, Italy)

In this paper, advanced post-processing techniques are combined with near-field measurements to evaluate the SAR of a standard SAR dipole antenna. The results are then compared to measurements on a legacy SAR measurement system and with full wave simulations. The results show very good comparison with just 0.94 dB difference w.r.t reference measurements evaluated for the standard SAR dipole antenna operating at 2.45 GHz frequency. This study demonstrates that the proposed method to use near-field data along with advanced post-processing techniques is reliable and promising. The goal is to use this technique for evaluation of modern communication devices for pre-compliance SAR testing in a more efficient way as compared to using legacy SAR evaluation techniques, which are more time consuming, and require more human and material resources.

14:50 *New Hybrid Ray-Tracing/FDTD for EMF Exposure in 6G Networks Using Semantically Classified Google Earth Photogrammetry with Measurement Validation*

Robin Wydaeghe (Ghent University & IMEC, Belgium); Arno Moerman, Olivier Caytan, Sergei Shikhantsov, Emmeric Tanghe, Gunter Vermeeren and Hendrik Rogier (Ghent University, Belgium); Sam Lemey (Ghent University-imec, Belgium); Piet Demeester (Ghent University - iMinds, Belgium); Wout Joseph (Ghent University/IMEC, Belgium)

State-of-the-art (SOTA) technologies are combined to make channel and exposure assessment in realistic environments anywhere on Earth a reality. The new API for 3D photorealistic tiles from the Google Earth dataset provides high Level of Detail (LoD) and high coverage photogrammetry. These meshes are semantically classified with a SOTA deep-learning model to distinguish classes such as buildings, terrain and vegetation. The environment is ray-traced at 26 GHz millimeter waves (mmWaves) with a 6G distributed massive MIMO (DMA-MIMO) antenna system as Tx. A scan measurement from an in-house beamforming 16-element DMA-MIMO antenna system in an anechoic room is performed. The EMFs of the created hotspot are compared with results from the hybridization component in the simulation pipeline, with a 1D Normalized Mean Absolute Error (NMAE) of 17%. The measurement validates the use of the simulations in realistic environments. A case-study near Central Park in New York City, USA, is examined.

15:10 *Reproducibility Studies of Instantaneous and 6-Minute Average Exposure Measurements Around 5G Massive-MIMO Base Stations*

Christian Bornkessel (Technische Universität Ilmenau, Germany); Alena Pikushina (TU Ilmenau, Germany); Lisa-Marie Schilling and Tobias Struck (Technische Universität Ilmenau, Germany); Matthias Hein (Ilmenau University of Technology, Germany)

Measurements of RF exposure to mobile radio base stations are important for risk communication. We measured instantaneous exposure with a focus on 5G with an exposimeter on an identical route on three afternoons to study the reproducibility. Due to different walking speeds, the relationship between time and place was not identical for the measurements, so time is not suitable as a reference for comparison. When the distance walked was used as reference, accuracy problems of the exposimeter's internal GPS system occurred, resulting in a mismatch between the actual location and the GPS location. This problem was successfully corrected by using the gradient descent with momentum method. The three measurements show a variation in maximum measured exposure of up to 5.4 dB for a selected section of the route, which is reduced to 2.8 dB when averaged over 6-minute intervals, which is acceptable given typical measurement uncertainties of ± 3 dB.

Monday, March 18 13:30 - 15:30

CS6a: Emerging Multiple Beam and Beamforming Technologies for 5G and Beyond

T02 Mm-wave for terrestrial networks 5G/6G / Convened Session / Antennas

Room: Dochart 1

Chairs: Simone Genovesi (University of Pisa, Italy), Lizhao Song (University of Technology Sydney, Australia)

13:30 *Irregular Subarray with Gathered Elements for Sidelobe Suppression*

Yihan Ma (University of Hertfordshire, United Kingdom (Great Britain)); Qi Luo (University of Hertfordshire, United Kingdom (Great Britain)); Wei Liu (Queen Mary University

of London, United Kingdom (Great Britain)); Steven Shichang Gao (Chinese University of Hong Kong, China)

Subarray technique is an effective approach for reducing the cost of a phased array system. Although integrating multiple elements into a subarray can reduce the number of radio frequency (RF) chains and system complexity, how to avoid grating lobes when performing beam-scanning remains a challenging research topic. This paper evaluates the scanning performance of three different types of polyomino-shaped irregular subarray configurations: domino-shaped, skew-tetromino-shaped & L-tetromino-shaped, and L-octomino-shaped subarray configurations, on both 8x8 and 16x16 arrays. By combining the Algorithm X technique to precisely tile polyomino-shaped subarrays and the Genetic Algorithm (GA) to find the optimal configuration, we are able to evaluate the maximum sidelobe levels (SLLs) at different scanning angles from numerical simulations.

13:50 Designing Transmissive Metasurface for Multibeam Transmitarray at 5G Millimeter-Wave Band

Weixu Yang, Ke Chen and Yijun Feng (Nanjing University, China)

In this paper, a frequency-multiplexed spin-decoupled transmissive metasurface is proposed by employing shared-aperture meta-atoms made of interleaved dual-band receiver-transmitter structures. As an application, a low-profile dual-band dual-CP shared-aperture transmitarray (TA) with four degrees of freedom for beamforming is designed in the 5G new radio millimeter-wave band. Simulated results show overall peak aperture efficiencies of 38.3% and 22.1%, simultaneously with joint gain variation < 3 dB and axial ratio < 3 dB relative bandwidths of two orthogonal CP beams better than 18.8% and 7.4%, for the low- and high-frequency bands, respectively. These features of the proposed TA make it a suitable candidate for 5G wireless and space communications.

14:10 Wideband Transmissive Metasurfaces for Sub-THz Frequency-Dependent Beam Scanning

Lizhao Song (University of Technology Sydney, Australia); Ting Zhang (CSIRO, Australia); Peiyuan Qin (University of Technology Sydney, Australia); Jia Du (CSIRO, Australia); Y Jay Guo (University of Technology Sydney, Australia)

A wideband transmissive metasurface is presented for frequency-dependent beam scanning at sub-terahertz (THz) band. Firstly, an anisotropic element model is developed to support low transmission losses and stable linear transmission phases in an ultrawide band. Secondly, theoretical analyses of transmissive frequency-scanning metasurfaces are provided. Design concepts and methods in terms of increasing beam angular coverages and transmission efficiencies are investigated. Finally, a prototype covering a beam range of $\pm 41^\circ$ is developed, exhibiting continuous scanning capability from 94 GHz to 220 GHz with enhanced transmission efficiencies up to 75%. The theoretical analyses and full-wave simulation results have been well validated by experiments.

14:30 A Beam-Scanning Metal-Only Folded Reflectarray Antenna

Haoran Jiang and Lu Guo (Nanjing University of Science and Technology, China)

A beam-scanning metal-only folded reflectarray is presented. It comprises two parts, namely a folded reflectarray and upper metasurfaces, which are all metallic. By rotating the metasurfaces on the top of folded reflectarray, the beams can be scanned in both elevation and azimuth planes. From the results of the simulation, the scanning range is $\pm 41^\circ$ in elevation plane with a 360° steering in azimuth plane. The proposed design exhibits various advantages such as low-cost, low-profile, and simple configuration, demonstrating its good potential for satellite communications.

14:50 Multibeam Phased Array with Reduced Transmit and Receive Modules

Francesco Alessio Dicandia (National Research Council (CNR), Italy); Simone Genovesi (University of Pisa, Italy)

Due to the high system demands of fifth generation (5G) wireless communication networks and the scarcity of available spectrum in traditional cellular frequencies, there has been significant research interest and active investigation into multibeam antenna systems. The need of a multibeam antenna is also shared with the increasing involvement of low-earth orbit (LEO) satellites systems as a mean to cope with the loss of the fixed link provided by geostationary orbit ones. A preliminary study is carried out to investigate the advantages offered by applying a subarray partitioning technique based on Penrose tessellation. A phased array able to generate a couple of main beams independently scanning five predefined areas is designed by pursuing the minimization of the transmit/receive modules (TRMs) as well as of the peak side lobe level together with the maximization of the minimum gain exhibited along the selected directions.

15:10 Development of a Circuit-Type Multiple-Agile Beamforming and Interference Mitigation Network

Yanki Aslan and Antoine Roederer (Delft University of Technology, The Netherlands); Nelson Fonseca (Anywaves, France); Piero Angeletti (European Space Agency, The Netherlands); Alexander Yarovoy (TU Delft, The Netherlands)

An innovative reconfigurable beamforming network concept for multiple high-gain agile and mutually zero-forced beam generation is proposed. Four-port couplers and variable phase shifters are used to synthesize the network. A 2 beam by 7 element beam former is designed and fabricated as proof of concept. A static scenario with the two beams separated by the approximated array beamwidth is considered in the prototype. At the operating frequency of 9 GHz, based on the array factor using the measured scattering parameters, it is demonstrated that the null levels stay below -37 dB, while the beam weights remain close to uniform for the best efficiency.

Monday, March 18 13:30 - 15:30

CS9a: Advances in 2-D Leaky-Wave Antennas Modelling and Design

T08 EM modelling and simulation tools / Convened Session / Antennas

Room: Dochart 2

Chairs: Paolo Baccarelli (Roma Tre University, Italy), Davide Comite (Sapienza University of Rome, Italy)

13:30 Dual-Frequency Metasurface Antenna for Earth Science Remote Sensing

Kristy Hecht (University of North Carolina at Charlotte, USA); Nacer Chahat (NASA-JPL, Caltech, USA); Goutam Chattopadhyay (NASA-JPL/Caltech, USA); Enrica Martini (University of Siena, Italy); Mario Junior Mencagli (University of North Carolina at Charlotte, USA)

This paper presents an innovative approach to designing dual-frequency Metasurface (MTS) antennas. These antennas cater to the growing demand for multifrequency capabilities in applications like Earth science, satellite communications, and remote sensing. Traditional multifrequency antenna designs have limitations, often requiring external feeds. The paper outlines the foundational principles of single-layer, single frequency MTS antenna design and expands upon them to introduce a dual-band, dual-layered antenna configuration. The proposed design leverages Foster's reactance theorem to enable independent operation of two patterned metallic sheet at two widely separated frequencies with coplanar excitation. Simulation results demonstrate the antenna's performance, not only in broadside operation but also at various pointing angles. This approach offers a promising solution for compact multifrequency antennas in space-constrained applications, addressing the needs of modern communication systems.

13:50 2D-Scanning of Circularly Polarized Beams via Array-Fed Fabry-Perot Cavity Antennas

Mikhail Madji and Davide Comite (Sapienza University of Rome, Italy); Walter Fuscaldo (Consiglio Nazionale delle Ricerche (CNR), Italy); Edoardo Negri, Alessandro Galli and Paolo Burghignoli (Sapienza University of Rome, Italy)

Fabry-Perot cavity antennas based on partially reflecting surfaces capable of converting linear into circular polarization have recently been proposed for the realization of broadside pencil beams. Here we consider the excitation of such structures by linear or rectangular phased arrays, with the aim of synthesizing fan beams or pencil beams, respectively. Such beams can be scanned in elevation by varying frequency and in azimuth by varying the array phasing. Angular scanning ranges where the axial ratio remains within specified bounds are studied through computationally efficient full-wave simulations that take advantage of reciprocity theorem.

14:10 Beam Focusing with a Conformal Leaky-Wave Antenna Described by a Spline Curve

Michael A Dittman and John Papapolymerou (Michigan State University, USA); Mauro Ettore (University of Rennes 1 & UMR CNRS 6164, France)

In this paper, a conformal leaky-wave antenna (CLWA) based on an aperiodic array of slots on a spline curve is analyzed and validated with full-wave simulations. A spline curve is a mathematical object that

is interpolated from a set of node points. The leaky-wave antenna consists of an array of slots on a double-grounded dielectric slab described by the spline profile. The contribution to the far field of each slot is engineered by varying the periodicity along the arc length of the structure to tailor the phase profile over the radiating aperture. The proposed design permits the control of the beam direction along complex shapes. The design procedure is validated using full-wave simulations and demonstrates the CLWA radiating a main beam around broadside.

14:30 **Characterization and Comparison of Formulas for Optimizing Broadside Radiation in a 2-D Leaky-Wave Antenna**

Walter Fuscaldo (Consiglio Nazionale delle Ricerche (CNR), Italy); David R. Jackson (University of Houston, USA); Alessandro Galli (Sapienza University of Rome, Italy)
Two-dimensional (2-D) leaky-wave antennas (LWAs) are commonly designed to radiate pencil beams at broadside and/or scanned conical beams. Recently, the possibility to radiate narrow null patterns at broadside has also been preliminarily explored. In this work, we first review the design rules to obtain a pencil beam from an infinite 2-D LWA and then show how they change for having a beam with a null at broadside. The effects of antenna truncation are also accounted for in both cases, and numerical results show how the optimum conditions are in turn affected.

14:50 **Beam Steering 2D Leaky Wave Resonant Cavity Antenna for Ka-Band Satellite Communication**

Maira I Nabeel (University of Technology Sydney & NUST, Australia); Muhammad Usman Afzal (School of Electrical and Data Engineering University of Technology Sydney, Australia); Dush Thalakituna and Karu Esselle (University of Technology Sydney, Australia)
This paper presents a Ka-band beam-steering antenna system based on near-field metasurfaces. The antenna system comprises a 2D leaky wave resonant cavity antenna (RCA) and a pair of phase-gradient metasurfaces (PGMs) stacked above RCA in its near-field region. To improve the performance of the overall antenna system, we have investigated higher resolution PGMs that have smaller fundamental cells having a lateral periodicity of a quarter wavelength to reduce the phase quantization error. Instead of square patches, these cells have metal loops printed on thin substrates, reducing the overall weight of the PGMs. The predicted results indicate that the proposed antenna system can steer its beam within a conical region having an apex angle of 100 degrees without reducing gain by more than 3dB from the maximum gain of 16.6 dBi. The maximum height of the antenna, including the feed, is 1.65 times the free space wavelength.

15:10 **Strategies for Enhancing the Gain Bandwidth of Fabry-Pérot Cavity Antennas: A Review of Recent Advances**

Ahmad T. Almutawa (Abdullah Al Salem University, Kuwait); Filippo Capolino (University of California, Irvine, USA)
We analyze strategies to realize high-gain wideband antennas using leaky waves excited in a Fabry-Pérot Cavity (FPC). Three main strategies are conceivable now: (1) implementing an electrically thick partially reflective surface (PRS) with its internal resonance, (2) exciting the FPC with a sparse array, and (3) combining these two methods. We also discuss other less practical methods that are still valid as principles. The broadside 3 dB gain bandwidth (GBW) is significantly enhanced compared to the conventional FPC antenna structure, which has a single feed and an electrically thin PRS.

Monday, March 18 13:30 - 15:30

P05: Radar, location and sensing

T05 Positioning, localization, identification & tracking //

Room: M2

Chairs: Joao M. Felicio (Escola Naval, Portugal & CINAV - Instituto de Telecomunicacoes, Portugal), Yannis Iliopoulos (TNO, The Netherlands)

13:30 **Small-Scale Passive Millimetre-Wave Imaging Measurements for Marine Litter Detection at W-Band**

Mario Vala (Instituto de Telecomunicações de Portugal, Portugal); Joao M. Felicio (Escola Naval, Portugal & CINAV - Instituto de Telecomunicacoes, Portugal); Tomás Soares da Costa (ULisboa - Instituto Superior Técnico & Instituto Telecomunicações, Portugal); Nuno R. Leonor (Polytechnic Institute of Leiria (IPL) & Instituto de Telecomunicações (IT), Leiria, Portugal); Jorge R. Costa (Instituto de Telecomunicações / ISCTE-IUL, Portugal); Paulo Marques (ISEL-IT Lisboa, Portugal); Antonio A Moreira (IST - University of Lisbon & Instituto de Telecomunicações/ Lisbon, Portugal); Sergio Matos (ISCTE-IUL / Instituto de Telecomunicações, Portugal); Rafael F. S. Caldeirinha (Polytechnic Institute of Leiria & Instituto de Telecomunicações, Portugal); Carlos A. Fernandes (Instituto de Telecomunicacoes, Instituto Superior Tecnico, Portugal); Nelson Fonseca (Anywaves, France); Peter de Maagt (European Space Agency, The Netherlands)
In this study, we explore the possibility of employing passive millimetre-wave imaging (PMMWI) as a means for remotely detecting plastic marine litter. We conducted measurements in both controlled pool and natural lake environments under static and agitated water conditions using a W-band radiometer. We assessed the radiometric response to different sized plastic objects and concentrations. By comparing the measurements with and without plastics allowed us to discern differences and visually detect the presence of objects in the water. Preliminary results indicate the promising potential of radiometric imaging for remote detection of floating plastics.

13:50 **Multifunction Over-The-Horizon Radar for Space Domain Awareness**

Simon Henault and Kyra Czarnowska (Defence Research and Development Canada, Canada); Yahia M. M. Antar (Royal Military College, Canada)
The possibility of using existing planar monopole arrays of an over-the-horizon radar (OTHR) for space domain awareness (SDA) is evaluated experimentally. The International Space Station was successfully tracked by the radar over the majority of an 11-minute pass, by exploiting the full azimuth and elevation steerability of the antenna arrays. As predicted using numerical models of the arrays, signal-to-noise ratios that can exceed 40 dB were measured. Range and Doppler measurements are compared with NASA provided truth data to identify ionospheric effects. SDA is determined to be a potential multifunction addition to existing OTHR systems for coarse orbital element measurements, but requires better ionospheric correction techniques to achieve the fine accuracies typically obtained with SDA radars operating at higher frequencies.

14:10 **Characterisation of Thin Glass-Fibre Substrates for Deployable SAR Antennas**

Simone Mencarelli (The University of Auckland, New Zealand); Annalisa Tresoldi (University of Auckland, New Zealand); Andrew C M Austin (University of Bristol, United Kingdom (Great Britain)); Michael J Neve (The University of Auckland, New Zealand); Guglielmo Aglietti (University of Auckland, New Zealand)
This paper investigates the electrical characteristics of a thin glass-fibre membrane to be employed as a support and dielectric substrate for a new kind of deployable antenna mechanical structure designed for space-borne Synthetic Aperture Radar sensors on nano-satellite platforms. The approach outlined in this paper relies on cost-effective test fixtures built from material samples originally designed for mechanical testing. A simple Time Domain Reflectometry / Transmissometry (TDR/T) procedure enables the extraction of the material's complex permittivity.

14:30 **A Small-Sized Antenna System for Direction Finding Applications on a Single Plane (1D) Using BT 5.1**

Ioannis Gouzouasis (U-blox, Greece); Mohamad Abou Nasa and Peter Karlsson (U-BLOX, Greece)
In this paper, an antenna system is presented for direction finding applications on a single plane (1D). The proposed system makes use of the Angle of Arrival (AoA) capabilities of BT 5.1 and is designed to be as small as possible. Novel antenna design ideas have been implemented to reduce size and counteract antenna interferences. The antenna design process is presented in detail along with antenna results. AoA measurements are taken outdoors and indoors with the proposed 1D system and a 2D system of previous work. The AoA results reveal the recommended azimuth range of the proposed 1D system to be -60 degrees to +60 degrees, where it can achieve a CDF of 50% at 5 degrees, 90% at 14 degrees, and 95% at 18 degrees of error indoors. The performance comparison with previous work is also presented in detail.

14:50 **Sequential Phase Optimization for Coherent Long-Range Distributed Wireless Power Transfer to a Non-Communicative Receiver**

Barnabas J Petit (Queen's University Belfast & QinetiQ Ltd, United Kingdom (Great Britain)); Richard Hoad and Sam J Hole (QinetiQ, United Kingdom (Great Britain)); Vincent Fusco (Queen's University Belfast, United Kingdom (Great Britain)); Neil Buchanan (Queens University Belfast, United Kingdom (Great Britain)); Muhammad Ali Babar Abbasi (Queen's University Belfast & The Institute of Electronics, Communications and Information Technology (ECIT), United Kingdom (Great Britain))
There are scenarios where Distributed Wireless Power Transfer (WPT) might be required to work without any steering (pilot signal) or information feedback from the power receiver. A new Sequential Phase

Optimization (SPO) technique has been developed to create coherence from independent, distributed transmitters at the spatial location of a non-communicative power receiver. This would increase the efficiency of the power transfer compared to incoherent systems. The proposed technique was tested under laboratory conditions.

15:10 Contactless Respiration Variability Detection and Accuracy Test Using UWB Radar

Muhammad Farooq, Hira Hameed, Ahmad Taha, Muhammad Ali Imran, Qammer H Abbasi and Hasan Abbas (University of Glasgow, United Kingdom (Great Britain))

This paper investigates the potential radar technology for the precise and non-intrusive detection of respiration rate variability. UWB radar, with its ultra-short pulses and extensive bandwidth, offers significant advantages in capturing subtle chest wall movements associated with respiration. It possesses the unique ability to penetrate clothing and physical barriers, making it an excellent candidate for remote physiological monitoring. This ultra-wideband radar system ensures the extraction of accurate respiration waveforms, and deep learning models, including VGG16, InceptionV3, and ResNet50, are employed to evaluate respiration rate variability. Remarkably, VGG16 attains outstanding accuracy in results. This study advances the field of radar-based respiration monitoring, emphasizing the importance of robust signal processing and deep learning techniques. It showcases the potential of UWB radar for non-contact respiration monitoring, with applications spanning healthcare and in-home environments, promising to revolutionize the assessment of well-being and health.

Monday, March 18 13:30 - 15:30

E13: Novel Materials, Metamaterials, and Metasurfaces I

T10 Novel materials, metamaterials, metasurfaces and manufacturing processes // Electromagnetics

Room: M3

Chairs: Mustafa Bakr (University of Oxford, United Kingdom (Great Britain)), Miguel Poveda-García (Technical University of Cartagena, Spain)

13:30 Ultrahigh Sensitive Terahertz Metasurface with 2D MoS₂ for Refractive Index Biosensing

Tomas Pires, Ruobin Han and Vaithinathan Karthikeyan (University of Glasgow, United Kingdom (Great Britain)); Abdoalbasat Abohmra (Glasgow University, United Kingdom (Great Britain)); Farooq A Tahir, Hasan Abbas, Muhammad Ali Imran and Qammer Abbasi (University of Glasgow, United Kingdom (Great Britain))

Terahertz (THz) metasurfaces possess extensive advantages for biosensing with their unique terahertz spectral signatures. Developing terahertz metasurfaces with ultrahigh sensitivity requires enhanced Q-factor for improved performance and functionality. High Q-factor resonance enhances the light-matter interaction for biosensing by exciting high order plasmonic modes. In this work, we demonstrate a methodology for increasing the Q-factor resonance of a polarization insensitive Electromagnetically Induced Transparency-like (EIT) terahertz metasurface by an addition of a 2D Molybdenum disulfide (MoS₂) layer. Our simulation results show a doubling of Q factor from 4.8 to 8.45 and an improved theoretical sensitivity of 661 GHz/RIU with respect to the metasurface at a resonant frequency of 2.02 THz. Our results prove the enhancement of Q-factor and the sensitivity of terahertz metasurface with the incorporation of 2D MoS₂ layer which will serve as an excellent platform for protein biosensing applications.

13:50 Magnetic Composites with M-Type Hexaferrites for Q/V-Band Electromagnetic Wave Absorption

Byeonjin Park (Korea Institute of Materials Science, Korea (South)); Horim Lee (Korea Institute of Materials Science, Korea (South)); Suk Jin Kwon, Jae Ryung Choi and Sang Bok Lee (Korea Institute of Materials Science, Korea (South))

While there are several composite absorbers proposed with magnetic materials, their working frequencies are usually limited under 30 GHz due to their low ferromagnetic resonance (FMR) frequency. In this study, a novel multi-band electromagnetic interference (EMI) absorbing composite film with M-type strontium ferrites is proposed. This film shows broadband EMI absorption performance including most of Q/V-band with sub-millimeter thickness. In addition, this film can absorb more than 97% of EMI in two mmWave frequency bands, and these ultrahigh absorption frequency bands are controllable by tuning FMR frequency of M-type strontium ferrites and composite layer geometries.

14:10 Superconducting Space-Time Modulation: Theoretical Implications and Mixing-Beamsplitting Functionality

Sajjad Taravati (University of Southampton & University of Oxford, United Kingdom (Great Britain)); Mustafa Bakr (University of Oxford, United Kingdom (Great Britain))

This paper explores a pioneering frontier in the domain of superconducting nonlinear space-time modulation, going beyond the established research on linear spatiotemporal modulation. It investigates wave propagation and incidence in superconducting space-time-modulated media, unveiling their unique properties and theoretical implications. The study introduces the distinctive functionalities of nonlinear space-time-modulated structures, with a focus on the pure frequency-conversion-beamsplitting capability. It further provides insights into scattered electromagnetic fields, and boundary conditions. The research employs full-wave finite-difference time domain (FDTD) simulations to provide a comprehensive understanding of the behavior of nonlinear superconducting space-time surfaces. Illustrative examples are presented, highlighting the exceptional functionalities of these surfaces, with the potential to advance the fields of quantum information processing and electromagnetic metamaterials, shaping the future of cutting-edge technologies.

14:30 Thin-Film Terahertz Metamaterials Manufactured by Laser Direct Writing

Yin-Han Cheng, Kai-Chun Hu, Chih-Han Lin and Yu-Hsiang Cheng (National Taiwan University, Taiwan)

In this paper, we present the split-ring resonators and the cross-shaped resonators in terahertz frequency range, which are made on flexible PET substrates using the low-cost laser direct writing technique. The transmission spectra obtained by terahertz time-domain spectroscopy match the simulation results.

14:50 Transmissive-Type Metagratings with Few Meta-Atoms for Beam Splitting

Zhen Tan (Xi'an Jiaotong University, France); Jianjia Yi (Xi'an Jiaotong University, China); Badreddine Ratni (Univ Paris Nanterre, France); André de Lustrac (C2N, Université Paris-Saclay, France); Shah Nawaz Burokur (LEME, France)

In this paper, we present a methodology to design symmetric and asymmetric beam splitting with arbitrary angle from transmissive-type metagratings. The metagratings consist of five meta-atoms and one layer dielectric substrate. Three of the meta-atoms are distributed on the upper layer of the substrate and the other two meta-atoms are on the lower layer. The meta-atom is composed of a microstrip line loaded with a capacitor. To validate the methodology, several designs with different angle and power ratio are performed in HFSS simulation at 10 GHz. Both the supercell (one period with periodic boundary) simulation results and array (multiple periods with finite size) simulation results show good agreement with the theoretical prediction.

15:10 Highly Efficient Polarization-Insensitive EM Energy Harvester

Majid Amiri (UTS, Australia); Mehran Abolhasan and Negin Shariati (University of Technology Sydney, Australia); Justin Lipman (University of Technology, Sydney (UTS), Australia)

The main challenge to converting electromagnetic waves into DC output is providing enough energy for non-linear rectification devices. This paper presents a highly efficient metamaterial perfect absorber (MPA) with stable absorption characteristics facing waves with different polarization and incident angles. Instead of connecting one rectifier to each unit cell, six cells have been channelled to increase the available energy at rectification sections. The final structure comprises six vertical and six horizontal channels with 12 rectifiers. The 6 × 6 structure shows almost 99% electromagnetic signal absorption efficiency. The absorbed signal is transferred to the rectifier with 88% efficiency. Finally, the proposed structure has been fabricated. A strong correlation between simulation and measurement results validates the design procedure.

Monday, March 18 13:30 - 15:30

CS3: CS3 Antennas on eco-friendly materials, environmental impact of devices and sustainable development

T10 Novel materials, metamaterials, metasurfaces and manufacturing processes / Convened Session / Antennas

Room: M4

13:30 *Chipless RFID Sensor on Paper Substrate*

[Cong Danh Bui](#) (Trinity College Dublin, Ireland & CONNECT Centre, Ireland); Adam Narbudowicz (Trinity College Dublin, Ireland & Wroclaw University of Science and Technology, Poland)

This paper proposes a chipless RFID sensor to detect permittivity changes in the Material Under Test (MUT) that is placed in a small container. The proposed design comprises an interrogator antenna and a miniaturized aluminium tag that is shaped as a meander line to reduce size and ensure high Q-factor. The detection of material is through the observation of the frequency peaks in the reflected signal S11, which corresponds to the resonating frequency of the tag modulated by the material inside the container. Experimental verification uses air and ice as MUT, due to the intended application in frozen food monitoring. Measurement of the proposed design shows that the resonating peaks of air and ice are 5.3 and 4.2 GHz, respectively, and are similar to the simulation results.

13:50 *From Reconfigurable Intelligent Surfaces to Holographic MIMO Surfaces and Back*

Ashwin Thelappilly Joy, [Anton Tishchenko](#) and Hamidreza Taghvaei (University of Surrey, United Kingdom (Great Britain)); Christopher P. Botham (BTexact, United Kingdom (Great Britain)); Fraser Burton (BT, United Kingdom (Great Britain)); Mohsen Khalily (University of Surrey & 5G Innovation Centre, Institute for Communication Systems (ICS), United Kingdom (Great Britain)); Rahim Tafazolli (University of Surrey, United Kingdom (Great Britain))

Holographic Beamforming is a promising concept to reduce the power consumption of MIMO antenna arrays. In a holographic approach, the impedance of antenna patches is varied through the inclusion of tuning elements, such as varactor diodes, which allows to electronically control the phase and amplitude of each antenna element. In this paper, we provide the electromagnetic framework for the design of a Holographic MIMO Surface (HMIMOS). We analyse its performance in terms of energy efficiency and compare it to passive Reconfigurable Intelligent Surfaces (RIS) and Active Phased Arrays (APA) at 5G mmWave. This work shows that the power consumption of HMIMOS is considerably lower than of APAs, and on par with RISs, due to many structural similarities, while HMIMOS can offer many benefits in terms of environmental awareness and intelligence for Integrated Sensing and Communication (ISAC).

14:10 *Reconfigurable Polarisation Conversion Metasurface for mm-Wave Applications Using Vanadium Dioxide (VO2)*

Grant Jack Gourley (Heriot-Watt University, United Kingdom (Great Britain)); Nelson Sepúlveda Alancastro (Michigan State University, United Kingdom (Great Britain)); Dimitris E. Anagnostou (Heriot Watt University, United Kingdom (Great Britain))

A reconfigurable wideband linear-to-linear polarisation converting metasurface (PCM) with 90% efficiency is presented. The design consists of metallic microstrips that are connected by a coplanar vanadium dioxide (VO2) film on a grounded sapphire wafer. The simulation results reveal that when the VO2 film is inactive, the PCM converts the polarisation of the electric field from the co-pol to the cross-pol from 24 to 28 GHz. When the VO2 is active the PCM acts as an ordinary reflector from 24 GHz to 28 GHz.

14:30 *Eco-Friendly Meta-Randomized Antenna for Millimeter Wave Radar*

[María Elena de Cos Gómez](#), Alicia Flórez Berdasco and Fernando Las-Heras (Universidad de Oviedo, Spain)

A compact and low-cost meta-randomized wearable grid array antenna (MTR-GAA) for Electronic-travel Assistance (ETA) radar application at 24 GHz is presented. It is based on eco-friendly aluminum-cladded Polypropylene (PP) substrate. The MTR-GAA size is 40 x 40 x 1.74 mm³. Prototypes are fabricated and tested, meeting typical requirements for the envisioned ETA applications in aid of visually impaired people. Comparison with state of the art 24 GHz wearable radar antennas is also provided.

14:50 *Exploring PLA/Flax Substrates for Antenna Applications: Assessing Moisture, Temperature and Dielectric Constant Homogeneity*

Vincent Grennerat (IMEP LAHC - University Grenoble Alpes, France); Georges Zakka El Nashef (& CISTEME, France); Ahmad Sabra (University of Limoges, France); [Pascal Xavier](#) (IMEP-LaHC, France); Thierry Lacrevez (Imep Lahc, France); Nicolas Corrao (IMEP-LAHC - University Grenoble Alpes - Grenoble INP, France); Haokai Liang (Grenoble INP-Phelma, France); Géczy Attila (Budapest Univ of Technology and Economics, France); Nicolas Chevalier (CISTEME, France)

This paper investigates the potential of PLA/Flax substrates as eco-friendly alternatives for RF (Radio Frequency) antenna applications in the context of sustainability within the electronics industry. As electronic waste continues to mount globally and the use of RF-connected devices proliferates, there is a growing need for sustainable materials. This study explores the dielectric properties of PLA/Flax substrates and their implications for antenna design and performance. Our findings reveal promising RF performance, highlighting the viability of bio-sourced and biodegradable materials in RF engineering to address environmental concerns. Subsequent sections delve into the impact of moisture, and substrate homogeneity, offering valuable insights for sustainable RF systems.

15:10 *Use of Ecofriendly Geopolymer Ceramics in Antenna Design and Microwave Applications*

[Guto G Silva](#), Ameni Gharzouni and Olivier Tantot (University of Limoges, France); Noel Feix (Université de Limoges, France); Edson Martinod and Sylvie Rossignol (University of Limoges, France)

Nowadays environmental sustainability and cost efficiency are important factors in new electronics systems design. Materials that are not usually used find new applications in this area. This is the case of geopolymers that represent an eco-friendly and cost-efficient solution for such applications. The objective of this paper is to show some of them in the field of absorbent materials, antennas and some future applications such as radomes.

Monday, March 18 16:00 - 18:00

SW3b: Defence radar, antennas and electromagnetics: past present and future (continued)

Room: Clyde Auditorium

Chairs: Anthony Keith Brown (University of Manchester, United Kingdom (Great Britain)), David Conway (MIT Lincoln Labs, USA)

16:00 *Recent Past, Current, and Future AESA Radar Development at Lincoln Lab*

Presenter: David Conway (MIT Lincoln Labs)

16:30 *Phased Array Antennas for Radar: Research Directions at TNO*

Presenter: Stefania Monni (TNO)

17:00 *Phased Array Technology at FHR - from Early Beginnings to High-End Solutions*

Presenter: Dirk Heberling (FHR Fraunhofer)

17:30 *Panel Discussion*

Monday, March 18 16:00 - 18:00

SW5b: Metrology for 5G and beyond in support of standard developments (IET workshop) (continued)

Room: Lomond Auditorium

Chairs: Fabien Hélot (University of Surrey, United Kingdom (Great Britain)), Anil K Shukla (QinetiQ, United Kingdom (Great Britain))

16:00 5G OTA Testbed of Full-Sized Vehicles in Reverberation Chamber

Presenter: Kristian Karlsson (Research Institute of Sweden)

16:20 Scattering Model on Rough Surfaces in the THz Band

Presenter: Ke Guan (Beijing Jiaotong University)

16:40 Characterisation of Frequency Selective Reflections off Indoor Surfaces for Sub-THz Band

Presenter: Mohsen Khalily (University of Surrey)

17:00 SW5 Panel Discussion

Monday, March 18 16:00 - 18:00

CS17b: Reconfigurable Intelligent Surfaces Recent Developments and Applications (continued)

T09 Fundamental research and emerging technologies / Convened Session / Antennas

Room: M1

Chairs: Mohsen Khalily (University of Surrey & 5G Innovation Centre, Institute for Communication Systems (ICS), United Kingdom (Great Britain)), Okan Yurduseven (Queen's University Belfast, United Kingdom (Great Britain))

16:00 On the Design of Static Passive Skins for Next Generation Fixed Wireless Access Applications

Giacomo Oliveri (University of Trento & ELEDIA Research Center, Italy); Marco Salucci (ELEDIA Research Center, Italy); Andrea Massa (University of Trento, Italy)

The possibility of passive flat patterned electromagnetic skins (EMSs) to support point-to-point fixed wireless access links that surpass the asymptotic free-space limit of total path attenuation (TPA) is discussed in this work. The design methodologies, technological challenges, and potential applicative scenarios of the proposed solutions are reviewed. Some proof-of-concept results are discussed to point out the feasibility of the proposed solution strategy in realistic scenarios.

16:20 Challenges and Opportunities of Amplified Information Metasurfaces for Simultaneous Wireless Communications and Power Transfers

Jiaqi Han (China); Xin Wang (Xidian University, China); Kai Zhou (Shanghai Radio Equipment Research Institute, China); Long Li (Xidian University, China); Tie Jun Cui (Southeast University, China)

In this paper, we summarized and pointed out the main challenges and opportunities in the design of amplified information metasurfaces for simultaneous wireless information and power transfer (SWIPT), such as instability, maximum output power, and operating bandwidth. Maximum output power and operating bandwidth directly determine the wireless charging distance and communication rates. And instability problems will break down the system. A scattering model is proposed to analyze these challenges. The instability is mainly due to the positive feedback of the power amplifier integrated with the element. Moreover, based on the scattering model and loadpull theory, the impedance of the amplifier is modeled for achieving its optimum performance including maximum output power and operating bandwidth.

16:40 Information Metasurface for Simultaneous Wave Manipulations and Signal Modulations

Qun Yan Zhou and Shengguo Meng (Southeast University, China); Qiao Chen (KTH Royal Institute of Technology, Sweden); Jun Yan Dai, Qiang Cheng and Tie Jun Cui (Southeast University, China)

Recently, digital and programmable metasurface has evolved into a new branch as information metasurface owing to its real-time manipulation of electromagnetic (EM) waves and simultaneous modulation of digital signals. Here, we present the theoretical model of information metasurface and analyze its capability of wave manipulation and signal modulation. Further, we extend the single-metasurface model into a multi-metasurface one, and discuss the feasibility and application of their joint operation. Our simulation results show its performance in high-precision harmonic scattering patterns, higher-order signal modulation, and spatial localization, demonstrating the potential of information metasurface in wireless communications and radar signal processing.

17:00 Indoor Coverage Enhancement Employing Liquid Crystal-Based Massive Reconfigurable Intelligent Surface Linked to 5G FR2 Base Station

Hyunjun Yang (SeoulNationalUniversity, Korea (South)); Sunghyun Kim (Korea Telecom, Korea (South)); Hogyeon Kim, Seungwoo Bang, Yongwan Kim and Jungsuek Oh (Seoul National University, Korea (South))

In this paper, we present indoor coverage enhancement enabled by the first experimental realization of an electrically large-size liquid crystal (LC)-based RIS, and its appropriate beam management with a commercial base station (BS) deployed in a 5G n257 frequency range 2 (FR2) band network. The RIS, featuring 2250 unit cells, ensures efficient beam receipt from the BS without spillover and provides -60 to 60-degree beam scanning, easing 5G deployment. We report the first confirmation of RIS's network coverage and capacity enhancement capabilities in an indoor scenario using a commercial FR2 band network. Verified improvements include a 225.4 percent throughput increase. This work, distinct from most existing studies, considers realistic RIS deployment in scenarios where the UE and BS are not fully obscured by obstacles, addressing the challenge of identifying coverage holes and suggesting an appropriate field trial construction employing our developed RIS-assisted ray-tracing to improve RIS coverage enhancement gain.

17:20 RIS-Based Over-The-Air Channel Equalization in Resource-Constrained Wireless Networks

Hugo Prodhomme (CNRS, France); Mohammadreza F. Imani (Arizona State University, USA); Sergi Abadal (Universitat Politècnica de Catalunya (UPC) & NaNoNetworking Center in Catalunya (N3Cat), Spain); Philipp del Hougne (CNRS, Univ Rennes, France)

Rich scattering yields long channel impulse responses (CIRs) with many taps that thwart communications in resource-constrained wireless networks limited to simple on-off-keying: the modulation rate must be throttled to avoid inter-symbol interference. Relevant examples include Internet-of-Things (IoT) networks and wireless networks-on-chips (WNoCs). If the radio environment is parametrized by a reconfigurable intelligent surface (RIS), the RIS configuration can be optimized to tailor the CIR between selected antenna pairs and make it (almost) pulse-like despite rich scattering by judiciously engineering the interferences of the multi-bounce paths. Thereby, the channel is equalized "over the air" in the physical domain, unlike conventional pre- and/or post-coding strategies. Here, using a physics-compliant model of a RIS-parametrized rich-scattering environment, we explore how the optimal choice of the time delay at which the CIR is shaped to have its most significant tap depends on the amount of reverberation in the environment and the latter's specific geometry.

17:40 Wave-Controlled Biasing of RIS for Multi-Beam Scattering Pattern Generation

Miguel Saavedra-Melo (University of California, Irvine, USA); Kasra Rouhi and Benjamin C Bradshaw (University of California Irvine, USA); Filippo Capolino (University of California, Irvine, USA)

We discuss the recent advances on an approach introduced recently to bias controllable varactors within the unit cells of a reconfigurable intelligent surface (RIS) to generate reflected beams in two different directions. This method leverages multiple resonant standing waves on a single biasing transmission line (TL) under the RIS elements, excited by an arbitrary time-domain periodic waveform. In this way, we eliminate the need for external biasing of each RIS element. To assess its effectiveness, an analytical model of the RIS is used to compare the farfield scattering patterns of the reflected waves in two main scenarios: one that incorporates varactor effects, and another that further includes the wave-control of the biasing voltage distribution, achieved through standing waves. Both of these scenarios are compared with the ideal case, where a constant phase shift is assumed and losses are neglected.

Monday, March 18 16:00 - 18:00

CS37b: Integration of Antennas and Electronic Circuits (continued)

T09 Fundamental research and emerging technologies / Convened Session / Antennas

Room: Alsh 1

Chairs: Nader Behdad (University of Wisconsin-Madison, USA), Nima Ghalichechian (Georgia Institute of Technology, USA)

16:00 3D Spatially Reconfigurable Circularly Polarized Antenna in Package with Embedded Electronics

Maria M Bermudez Arboleda and Atif Shamim (King Abdullah University of Science and Technology, Saudi Arabia)

Low-power applications require innovative antenna systems that can radiate in the full 3D sphere while reducing power wastage. However, the complexity of feeding structures for smart radiation reconfiguration has hindered the widespread use of spatially diverse antennas in Internet of Things (IoT) solutions. Therefore, this paper introduces a 2.4 GHz Antenna-in-Package (AiP) design comprising twelve microstrip patch antennas with circular polarization (CP) arranged on the faces of a dodecahedron package. This design enables dynamic beam focusing for both gain and polarization. The electromagnetic (EM) shielded core, formed by the twelve antenna grounds, accommodates the controlling electronics without affecting antenna performance. Moreover, an embedded control printed circuit board (PCB) enables automated reconfigurability of the radiation pattern. The AiP is compatible with cost-effective additive manufacturing techniques. With this efficient 3D sphere coverage, the presented AiP and integrated digital control offer a promising solution for future wireless networks, especially in energy-constrained devices.

16:20 Crack Stop as a Coupling Element Between an IC Chip and Antenna

Jan H. S. Bergman, Kaisa Ryyänen, Juha Ala-Laurinaho and Kari Stadius (Aalto University, Finland); Jussi Ryyänen (Finland); Ville Viikari (Aalto University & School of Electrical Engineering, Finland)

Millimeter-wave antenna arrays place integrated transceiver chips and antennas in close proximity to each other. As a result, the presence of the chip will affect the performance of the system significantly, with the metallic structures within the chip being a source for structural resonances. A transition which utilizes one of these metallic structures, the crack stop, as a coupling element is presented. The proposed design allows a non-galvanic connection between the IC chip and the antenna. The performance of the transition is analyzed through simulations, and is shown to reach above-70-percent power transmission between 42.3 GHz and 62 GHz, covering the majority of V-band.

16:40 Chessboard Focal Plane Array in Silicon Technologies for Terahertz Imaging

Martijn Hoogelander (Delft University of Technology, The Netherlands); Sven L van Berkel (NASA Jet Propulsion Laboratory, Caltech, USA); Satoshi Malotau (Tusk-IC, The Netherlands); Maria Alonso-delPino, Marco Spirito, Daniele Cavallo and Nuria LLombart (Delft University of Technology, The Netherlands)

Recently, we presented a focal plane array (FPA) integrated in 22 nm CMOS technology for terahertz imaging from 200 GHz to 600 GHz. The FPA has a chessboard topology and is integrated with direct-detectors. Measurements of a demonstrator showed that this array design yields excellent resolution, while also maintaining a good aperture efficiency, which was measured to be -4.1 dB at 400 GHz. Although the CMOS technology was a good platform to showcase the versatility of the chessboard configuration, the limited responsivity of the direct-detectors, prohibited passive performance. In this contribution, we show using preliminary simulation results that an improvement of almost two orders of magnitude in the noise-equivalent power can be realized by using diode-connected heterojunction bipolar transistors in a 130 μ m SiGe technology. As such, the proposed design can offer a fully-integrated solution for THz imaging applications in which both a high resolution and passive performance are required.

17:00 Increasing the Efficiency-Bandwidth Product and Impedance Bandwidth of Electrically-Small Antennas Through Parametric Space-Time Variation

Zachary Fritts, Amirhossein Babae and Steve M Young (University of Michigan, USA); Anthony Grbic (University of Michigan, Ann Arbor, USA)

A method for improving the efficiency-bandwidth product of electrically-small antennas (ESAs) through space-time variation is reported. By coupling radiative and non-radiative modes of the ESA using spatially-discrete traveling wave modulation (SDTWM), the time-varying antenna is made to radiate efficiently over an operating band that is 4.5 times larger than its LTI counterpart. Judicious choice of the modulation parameters allows this bandwidth enhancement to be obtained while keeping the reflected power more than 10 dB below the incident power.

17:20 Front-End Mismatching, Mutual Coupling, Bandwidth, Transmission Line Noise, and SNR

Majid Manteghi (Virginia Tech, USA); Sina Moradi (High-Frequency Engineering, Technical University of Munich (TUM))

This paper examines the novel technique of front-end mismatching, which offers benefits for a wide variety of antennas. This technique is especially effective for electrically small antennas (ESAs), which are typically constrained by bandwidth limitations. Notably, matching circuitry influences the scattering matrix and, consequently, the coupling between elements. Significantly, mismatching can reduce mutual coupling, thereby addressing issues in dense arrays and MIMO systems. First, the noise figure for a receiver chain with a significant mismatch is determined. Then, we discuss the advantages of incorporating an intentional impedance mismatch at the receiver end. To demonstrate the effectiveness of our proposed method, we apply it to a standard receiving chain.

17:40 Differentially-Fed Antenna-On-Display Module for SATCOM and Mobile Applications at Ka-Band

Junho Park, Inseok Jang and Baekjun Seong (KREEMO, Korea (South)); Wonbin Hong (Pohang University of Science and Technology (POSTECH), Korea (South)); Sehun Kim (KREEMO, Korea (South))

This work presents a one-dimensional (1-D) differentially-fed antenna-on-display (AoD) module, proficient in offering a polarization switchable radiation pattern across wideband spectrum from 24 GHz to 40 GHz. The antenna element employs a truncated radiator paired with a differential feedline, while also integrating two parasitic elements to enhance impedance bandwidth. A comprehensive exploration of the proposed antenna is conducted, encompassing input impedance, surface current distribution, and vector electric-field distribution. The AoD achieves polarization adaptability by altering the excitation current phase on the differential feedline. Two phased-array antenna models are designed, fabricated and verified. The first model employs a passive 1:4 power divider with a fixed-phase delay line, achieving a peak gain of 9.45/9.55 dBi at 28 GHz and 8.99/9.51 dBi at 39 GHz.

Monday, March 18 16:00 - 18:00

CS5b: Advances in mmWave and (sub-)THz channel sounding and measurements for 5G and Beyond (continued)

T02 Mm-wave for terrestrial networks 5G/6G / Convened Session / Propagation

Room: Alsh 2

Chairs: Diego Andrés Dupleich (Technische Universität Ilmenau, Germany & Fraunhofer Institute for Integrated Circuits IIS, Germany), Wei Fan (Southeast University, China)

16:00 **Enabling VNA Based Channel Sounder for 6G Research: Challenges and Solutions**

Wei Fan (Southeast University, China); Zhiqiang Yuan (Beijing University of Posts and Telecommunications, Denmark & Aalborg University, Denmark); Yejian Lyu and Gert Pedersen (Aalborg University, Denmark)

To support research and development for sixth-generation (6G) communication, it is imperative to understand the application needs and develop accurate and realistic channel models to meet the application needs. Several key radio technologies are identified for 6G research, including utilization of frequency bands ranging from sub-6 GHz to THz, antenna configuration covering simple single antenna to complicated gigantic multiple-input and multiple-output (MIMO) systems, and diverse deployment scenarios requiring various measurement ranges. This paper summarizes latest strategies to significantly extend the capabilities of current vector network analyzer (VNA)-based channel sounder, mainly radio-over-fiber (RoF) to enable longrange channel measurements, phase compensation to achieve accurate and coherent phase measurement, frequency extension to extend the carrier frequency and frequency bandwidth, and virtual antenna array (VAA) schemes to enable multiantenna/link channel measurements.

16:20 **Double-Directional Angle-Resolved Wideband Channel Measurements and Path Loss Characterization in Corridor at 300 GHz**

Riku Takahashi (Niigata University, Japan); Anirban Ghosh (SRM University Amaravati, India); Minseok Kim (Niigata University, Japan)

In this paper, a comprehensive double-directional channel measurement across 40 receiver (Rx) positions in a corridor using an in-house developed 300 GHz channel sounder is reported. During measurement, two types of antennae - horn and probe with different gain and half power beamwidth (HPBW) are used to investigate the impact of mentioned antenna parameters on signal propagation in the THz band. Finally, path loss model parameters are evaluated for both omnidirectional path loss (PL) and line of sight (LoS) PL by fitting the data with two popular existing channel models. It is observed that in the case of the corridor, irrespective of the model the path loss exponent (PLE) is always less when the more directional horn antenna is used while the shadowing effect is lower when a wider HPBW probe antenna is used at the Rx.

16:40 **Industrial Design Validation for a Plane Wave Generator at 28GHz**

Shoaib Anwar (Microwave Vision Group, Satimo Industries, France); Andrea Giacomini (Microwave Vision Italy SRL, Italy); Francesco Saccardi (Microwave Vision Italy, Italy); Francesco Scattone (Microwave Vision Group (MVG), Italy); Evgueni Kaverine and Nicolas Gross (MVG Industries, France); Per Iversen (Orbit/FR, USA); Lars Foged (Microwave Vision Italy, Italy)

In recent research, we introduced a pioneering concept: a Plane Wave Generator (PWG) optimized for millimeter-wave Over the Air (OTA) testing applications. The industrialized PWG incorporates substantial enhancements over the previously presented breadboard models. This industrial unit has been meticulously manufactured and subjected to rigorous testing within a state-of-the-art Planar Near-Field (PNF) measurement facility. The industrial design of the PWG, operates from 24.25 GHz to 29.5 GHz frequency range, with a Quiet Zone of 38cm diameter. The measured amplitude variations are ranging from ± 0.9 dB to ± 1.7 dB and phase variations between $\pm 9^\circ$ and $\pm 20^\circ$ inside the quiet zone. By harnessing a surrogate model for quiet zone synthesis, our proposed QZ evaluation technique now delivers results in just one day, marking a substantial advancement over the previous method, which necessitated nearly a week for measurements and subsequent post-processing

17:00 **Channel Measurements in Workspace with Robotic Manipulators at 300 GHz and Recent Results**

Varvara V. Elesina, Carla E. Reinhardt and Thomas Kürner (Technische Universität Braunschweig, Germany)

This paper presents an initial characterization of radio channel with robotic manipulators at low terahertz frequencies. The measurement scenarios include both time-invariant and time-variant settings, reconstructing channels between two robotic arms and between an access point and a sensor node on the manipulator. The evaluation results include path gain, power delay profile and delay spread for time-invariant setups. For the time-variant setups, the evaluation results include 3D power delay profile and path gain versus time for a fixed delay value. The findings presented here demonstrate the feasibility of wireless communication in workspaces containing robotic arms and lay the foundation for further channel measurements and models development for industrial environments.

17:20 **Design and Preliminary Indoor Assessment of a Long-Range Sub-THz VNA-Based Channel Sounder Between 500 GHz and 750 GHz**

Lawrence WG Carslake (National Physical Laboratory UK, United Kingdom (Great Britain)); James Skinner (National Physical Laboratory, United Kingdom (Great Britain)); Tian Hong Loh (UK, National Physical Laboratory, United Kingdom (Great Britain))

Practical, traceable sub-Terahertz (sub-THz) propagation channel characterization in real-world environments presents new measurement challenges as current systems utilizing coaxial cable setups suffer from high cable losses that restrict the range of the measurements when assessing meaningful real-world use cases and application scenarios. This paper presents, for the first time, a novel dynamic range adjustable design of a long-range sub-THz vector network analyzer (VNA)-based channel sounder system operating between 500 GHz and 750 GHz using both power adjustable radio-over-fiber (RoF) technologies and a phase compensation mechanism. The link budget with up to 600 m of optical fiber and preliminary indoor radio channel sounding assessments have been carried out to evaluate the functionality of the proposed system at distances of up to 4.49 m.

17:40 **Sub-Terahertz MassiveMIMO Channel Sounder for 6G Mobile Communication Systems**

Minoru Inomata, Wataru Yamada and Ryotaro Taniguchi (NTT, Japan); Nobuaki Kuno, Koshiro Kitao, Takahiro Tomie and Satoshi Suyama (NTT DOCOMO, INC., Japan); Michael Millhaem (Keysight Technologies, USA); Takao Miyake (Keysight Technologies, Japan); Roger Nichols (Keysight Technologies, USA)

6G mobile communications will require extremely high-speed data rates exceeding 100 Gbps using sub-terahertz (THz) bands. Sub-THz bands have extremely short wavelengths, and channel characteristics are affected by objects and people surrounding mobile stations. Therefore, we have developed a sub-THz Massive MIMO channel sounder using 896 antenna elements. This channel sounder offers a high time-spatial channel resolution. It can analyze the number of arriving paths with lower received power in real-time, which can contribute to constructing an accurate 6G channel model and feasible 6G system using sub-THz bands. In this paper, we introduce a newly developed sub-THz MassiveMIMO channel sounder and demonstrate the system performance in an outdoor environment.

Monday, March 18 16:00 - 18:00

CS20b: Physics-compliant models of reconfigurable intelligent surfaces (continued)

T08 EM modelling and simulation tools / Convened Session / Antennas

Room: Boisdale 1

Chairs: Raffaele D'Errico (CEA, LETI & Université Grenoble-Alpes, France), Gabriele Gradoni (University of Surrey, United Kingdom (Great Britain))

16:00 **1-Bit SubTHz RIS with Planar Tightly Coupled Dipoles: Beam Shaping and Prototypes**

Xianjun Ma and Yonggang Zhou (Nanjing University of Aeronautics and Astronautics, China); Qi Luo (University of Hertfordshire, United Kingdom (Great Britain)); Yihan Ma (University of Hertfordshire, United Kingdom (Great Britain)); Kyriakos Stylianopoulos and George C. Alexandropoulos (University of Athens, Greece)

In this paper, a proof-of-concept study of a 1-bit wideband reconfigurable intelligent surface (RIS) comprising planar tightly coupled dipoles (PTCD) is presented. The developed RIS operates at subTHz frequencies and obtained a 3-dB gain bandwidth of 27.4% with the center frequency at 110 GHz. The binary phase shift of each RIS unit element is enabled by changing the polarization of the reflected wave by 180°. The PTCD RIS has a planar configuration with one dielectric layer bonded to a ground plane, thus it can be fabricated by using cost-effective PCB technology. We analytically calculated the response of the RIS and good agreement is obtained between the simulated and calculated result. We also applied beamforming algorithms to calculate the response of the RIS with beam pointing at different directions by modifying the 1-bit phase distribution of the RIS. To prove the concept, several passive prototypes with frozen beams were fabricated.

16:20 **A Macroscopic Bilateral Modeling Approach for Reflective and Transmissive Metasurfaces**

Silvi Kodra, Enrico M. Vitucci and Marina Barbiroli (University of Bologna, Italy); Matteo Albani (University of Siena, Italy); Vittorio Degli-Esposti (University of Bologna, Italy)

This paper presents a macroscopic bilateral modeling approach for Reconfigurable Intelligent Surfaces (RIS) capable of simulating various cases, including transmissive and bilaterally reradiating RIS. Building on recent work, the approach is based on a general power balance at the RIS surface according to a few parameters, that accounts for both desired and parasitic radiation modes on both sides of the surface as

well as diffuse scattering and dissipation. The surface effect is described using a spatial modulation coefficient that embodies the wavefront transformation of each reradiation mode, including phase and amplitude modulation. Here the model is proposed and combined with a Huygens-based field calculation method to test its effectiveness in a few applications cases found on the literature.

16:40 Measurements of Reconfigurable Intelligent Surface in 5G System Within a Reverberation Chamber at mmWave

Luca Bastianelli (Università Politecnica delle Marche, Italy); Riccardo Diamanti (Telecom Italia, Italy); [Emanuel Colella](#) (CNIT, Parma & Università Politecnica Delle Marche, Italy); Valter Mariani Primiani (Polytechnic University of Marche, Italy); Franco Moglie (Università Politecnica delle Marche, Italy); Ayoub Toubal, Mikhail Odit, Jean-Baptiste Gros, Youssef Nasser, Geoffroy Lerosey and Luca Santamaria (Greenerwave, France); Andrea Allasia (Telecom Italia S.p.A., Italy); Maurizio Crozzoli, Mauro Boldi and Elisa Zimaglia (Telecom Italia, Italy); Valerio Lieti (Nokia, Italy); Michele Colombo (Nokia Networks Italia, Italy); Davide Micheli (Telecom Italia - TILAB, Italy)

In this paper we evaluated the performance of a reconfigurable intelligent surface tested with a fifth generation signal provided by a commercial fifth generation base station. We adopted a reverberation chamber as a real life propagating environment. Tests were conducted at the millimeter wave frequency range. This measurement campaign was carried out under the H2020 European project RISE-6G and a collaboration program between TIM S.p.A., Nokia and Università Politecnica delle Marche.

17:00 Impedance-Based RIS Channel Model and Optimization in Fast-Fading Environments

[Placido Mursia](#) and Vincenzo Sciancalopore (NEC Laboratories Europe GmbH, Germany); Gabriele Gradoni (University of Surrey, United Kingdom (Great Britain)); Marco Di Renzo (Paris-Saclay University / CNRS, France); Xavier Costa-Perez (ICREA and i2cat & NEC Laboratories Europe, Spain)

We extend a recently proposed electromagnetically-consistent RIS channel model based on mutually coupled loaded wire dipoles at the transmitter, RIS, receiver, and scattering objects. The original model is applicable in a static environment, where the position and load impedance of all the dipoles is fixed. The extended model includes fast multi-path fading, originated by rapidly varying channel conditions, through the random coupling model (RCM). Indeed, RCM allows for incorporating random fluctuations in the channel coefficients by modelling the propagation between any two dipoles as chaotic trajectories within a closed cavity, which is parameterized by an average loss factor. Numerical results demonstrate the validity of such model under different degrees of losses within the cavity, and its convergence to conventional deterministic channel models in the regime of large cavity losses. Moreover, we demonstrate how accurate modelling of such channel fluctuations leads to superior performance in terms of achievable rate.

17:20 Scattering Singularities of Complex Systems Probed with Continuously Variable Metasurfaces

Jared Erb and Thomas Antonsen (University of Maryland, USA); Steven Anlage (Quantum Materials Center)

We study the wave properties of complex enclosed scattering systems in the limit where the wavelength is much smaller than the size of the enclosure. In this limit the scattering properties (S-matrix, impedance matrix, etc.) are extremely sensitive to variations in frequency or perimeter structure of the cavity. We perform two-port S-matrix measurements of a variety of two-dimensional and three-dimensional scattering systems, all of which host two or more electronically tunable metasurfaces. We focus on two scattering singularities present in non-Hermitian systems, namely coherent perfect absorption (CPA), and exceptional points (EP), as a function of experimental parameters. We find that both CPAs and EPs are a generic and common feature of all of the experimental systems studied. Both types of singularity can be created and destroyed through variations in metasurface configuration. This establishes continuous metasurface tuning as a means to exploit CPA and EP scattering singularities for applications.

17:40 A Vector Differential Coding for Hybrid RIS Aided Zero-Padded OTFS Systems

Lingling Zhang and Jianan Zhang (Northwestern Polytechnical University, China); Chengkai Tang (northwestern polytechnical university)

This paper presents a vector differential encoding for the recently proposed orthogonal time frequency space (OTFS) modulation scheme applied in hybrid Reconfigurable Intelligent Surface (RIS) aided wireless communication. The basic idea is to eliminate the need to estimate the channel and simplified the symbol detection at the user equipment. The design of initial symbol vector and differential scheme result in constant modulus transmission. The maximum likelihood (ML) detector with interference cancellation is derived with low complexity. Simulation results show the the uncoded bit error ratio is below (10^{-2}) for SNR over 18 dB with data rate 1.26Mbps, despite the strong Doppler effect caused by the high speed at 120 km/hr.

Monday, March 18 16:00 - 18:00

CS47: Over-The-Air (OTA) testing of active array antennas

T02 Mm-wave for terrestrial networks 5G/6G / Convened Session / Measurements

Room: [Boisdale 2](#)

Chairs: Daniele Cavallo (Delft University of Technology, The Netherlands), A. B. (Bart) Smolders (Eindhoven University of Technology, The Netherlands)

16:00 Over-The-Air Measurements for mm-Wave Body-Centric Wireless Communication

Jonas Ørnkov Nielsen (Technical University of Denmark, Denmark); Ad Reniers and A. B. (Bart) Smolders (Eindhoven University of Technology, The Netherlands)

A preliminary study of the applicability of mm-waves for future body-centric wireless communication systems is presented. The loss levels associated with body-centric wireless propagation at lower mm-wave frequencies are quantified by over-the-air measurements of a propagation scenario, in which a custom-made human-head phantom is placed between two antennas to obstruct the line of sight. Both passive and active measurements within the frequency ranges 1–18 GHz and 22–30 GHz, respectively, are presented. The approximate loss levels for the passive measurements were found to be about 10 dB for the vertical polarization and more than 30 dB for the horizontal. The loss variation for the active measurements was high—between 10 and 50 dB, depending on the polarization, antenna aperture separation distance, and degree of obstruction by the phantom.

16:20 Advanced Thermal-Imaging for OTA Industrial-Testing of Active-In-Package, Antenna-On-Chip and Antenna on PCB

Mo Shakouri (Microsanj LLC, USA); Sidina Wane (eV-Technologies, France); Douglas A Gray (Microsanj LLC & Telewave.io, USA); Ali Shakouri (MicroSanj, USA)

Traditional design approaches individually optimize chip, package, printed circuit board, and antenna. Even with high success at each step the overall end-to-end result will fall far short of an optimal solution for the completed module. This contribution describes emSCOPE™, a new holistic Near-Field (NF) Over-the-Air (OTA) testing solution for Chip-Package-PCB-Antenna modules based on advanced Thermal-Imaging technologies. The proposed solution is demonstrated using advanced front-end-modules co-designed with AIP on WLCSF fan-in/fan-out integration technologies. The ability of the proposed testing solution to capture EM-Thermal distributions of antennas opens new possibilities for multi-physics testing of radiating devices and systems based on a unified Sub-10 GHz, mmWaves and THz platforms.

16:40 Millimeter-Wave Scattering from Building Facade: A Simulation and Verification Study

Javad Ebrahimzadeh (Kuleuven University, Belgium); Vahid Khorashadizadeh (Ku Leuven, Belgium); Xuesong Cai and Fredrik Tuvfesson (Lund University, Sweden); Guy Vandenbosch (Katholieke Universiteit Leuven (KU Leuven), Belgium)

This paper presents millimeter-wave scattering from a building facade predominantly composed of windows. These windows are integrated into the walls, forming dihedral structures that reflect waves toward the incident angle. The scattered field resulting from the building facade is simulated using the two-bounce Geometrical-Physics (GO) method. We analyze the channel in power loss and arrival angle along the receiver's trajectory path. It is observed that in the delay domain, the trajectory path due to a window appears as a line, and in the angular domain, it follows a hyperbolic curve. A comprehensive measurement campaign is conducted to verify the results in both the delay and angular domains. This measurement campaign takes place in a courtyard scenario, utilizing a multi-input-multi-output (MIMO) channel sounder operating within the frequency band of 27.5 GHz to 29.5 GHz. Notably, the results obtained through simulation exhibit a commendable level of agreement with the measurement data.

17:00 Over-The-Air Noise-Figure Measurements of Active Integrated Antennas at W-Band

[Remco Heijs](#) (Eindhoven University of Technology, The Netherlands); Tim Stek, Antonius Johannes van den Biggelaar, Roel X.F. Budé and Anouk Hubrechtsen (ANTENNEX, The Netherlands)

This paper applies an existing method for estimating the system gain and noise figure of active integrated antennas to W-band frequencies. The method uses a reverberation chamber as a wireless noise source, where the ENR can be tuned. Measurements, including different calibration steps, are performed to obtain the noise figure and system gain of a horn antenna connected to a low-noise amplifier as a proof of concept for measuring an integrated antenna. The preliminary measured results are within 1.0 dB of the datasheet value for part of the measured frequency span. Limits of this method are demonstrated through the measurement campaign and recommendations for improvement are provided.

17:20 In-Field Measurement of Total Radiated Power from Active Antenna Arrays

Jonas Fridén (Ericsson AB, Sweden); Aidin Razavi (Ericsson Research, Sweden); Bengt-Erik Olsson (Ericsson AB, Sweden)

Total radiated power is a key metric in 5G Base Station conformance testing. Therefore, assessment in live networks is required. Here, a power trace is measured at street level, while a User Equipment attracts a traffic beam. Three different methods are investigated: Beam directed to point of measurement, a fixed beam and measuring in different points, and fixed measurement location and directing the beam towards different points. GNSS coordinates are used to retrieve needed distances and directions to project the measured power trace to an EIRP trace. The radiated power is calculated in two ways. Firstly, a binned integration technique is used to sum the radiated power contributions from different solid angle bins. This overcomes the inherent problem of measuring the radiation pattern in a regular angular grid. Secondly, the ratio of peak EIRP and directivity is used. Here, peak directivity is assumed known or estimated via the beamwidths.

17:40 The Antenna Dome High-Speed Characterization System for OTA Characterization of FR2 5G Active Antenna Panels

Richard Coesoij and Ferry Musters (TU Delft, The Netherlands); Marco Spirito (Delft University of Technology, The Netherlands)

In this work we present the recent developments in the system architecture and the calibration techniques employed in the TU Delft high speed Antenna Dome system developed for the Characterization of FR2 5G Active Antenna Panels. In the current implementation the Antenna Dome employs 36 dual linearly-polarized scalar sensing nodes, to enable real-time 2D (theta and phi) radiation pattern acquisition. The system employs over-the-air characterization procedures to equalize the power conversion asymmetry within the nodes as well as across all the sensing nodes. Moreover, the system makes use of a controller area network (CAN) bus allowing to acquire power from all the nodes at synchronized timing interval and obtain a full 2D pattern acquisition with data transfer in less than 5 msec. The experimental data of a calibration horn (16dBi) are presented and compared to the nominal (EM response) at 26.5GHz.

Monday, March 18 16:00 - 18:00

CS42b: AMTA Session: Post Processing Techniques in Antenna Measurements (continued)

T09 Fundamental research and emerging technologies / Convened Session / Measurements

Room: Carron 1

Chairs: Jeffrey Guerrieri (National Institute of Standards and Technology, USA), Francesco Saccardi (Microwave Vision Italy, Italy)

16:00 An Antenna Measuring System Based on a Cable Suspended Dolly and Inverse Source

Marco Righero and [Giorgio Giordanengo](#) (LINKS Foundation, Italy); Giuseppe Musacchio Adorisio (Fondazione LINKS, Italy); Michael Maurer, Frederick Mayer and Georg Peters (Spidercam GmbH, Austria); Ines Barbary, Eric van der Houwen and Luis Rolo (European Space Agency, The Netherlands); Giuseppe Vecchi (Politecnico di Torino, Italy)

We present an innovative antenna measurement system where a cable-suspended dolly moves the probe antenna around the antenna under test. This flexible means allows covering large scanning areas while ensuring safety. Equivalent sources are used to process the acquired signals to characterize the antenna under test.

16:20 Multiple Reduced Order Models for Antenna Measurements

Samuel Corre (IETR, France); Nicolas Mezieres (Centre National d'Etudes Spatiales, France); Benjamin Fuchs (Federal Office of Communications, Switzerland); Michael Mattes (Technical University of Denmark, Denmark); Laurent Le Coq (University of Rennes 1 & IETR, France)

For the characterization of the radiated field of antennas, the Reduced Order Model method is a simple yet powerful numerical tool that allows to reduce significantly the number of field samples relatively to other techniques based on analytical signal expansions. To further improve the flexibility and versatility of this tool, this article focuses on building a set of multiple reduced models via subdivision of the source domain and on applying reference point method for ROM. Validations based on simulation and measurement data in the far field are shown.

16:40 Phaseless Characterization of Flat Sources with a Planar Wide-Mesh Scanning Strategy

Florindo Bevilacqua (Università di Salerno, Italy); Amedeo Capozzoli and Claudio Curcio (Università di Napoli Federico II, Italy); Francesco D'Agostino, Flaminio Ferrara, Claudio Gennarelli and Rocco Guerriero (University of Salerno, Italy); Angelo Liseno (Università di Napoli Federico II, Italy); Massimo Migliozi (University of Salerno, Italy); Yiannis Vardaxoglou (University of Loughborough, United Kingdom (Great Britain))

This work evaluates the performance of a phaseless near-field to far-field transformation when applied to a demanding antenna as test case. It is based on a smart scanning strategy, an effective representation of the unknowns of the problem, and a proper optimization method. The characterized source is a non-canonical planar source, formed by two disconnected subapertures, radiating a difference far-field pattern. The characterization has been accomplished by collecting the squared amplitude of the near-field samples on a planar wide-mesh scanning, based on a disk modeling of the source, which is convenient for planar flat sources, thus reducing the number of sampling points and simplifying the mathematical formulation. A numerical validation has been carried out to assess the effectiveness of the proposed approach.

17:00 Discretizing 2D Equivalent Radiating Panels by Legendre Quadrature

Amedeo Capozzoli and Claudio Curcio (Università di Napoli Federico II, Italy); Francesco D'Agostino (University of Salerno, Italy); Angelo Liseno (Università di Napoli Federico II, Italy); Luigi Pascarella (Università di Salerno, Italy)

We deal with the discretization of a 2D radiating panel. After dimensioning the panel by a properly developed approach, a non-uniform array can be a feasible solution for its practical implementation. In the proposed scheme, the determination of the number, the positions and the excitations of the array elements is accomplished by exploiting a Gaussian quadrature rule. Considering that the most significant singular functions supported on the region of interest are related to those supported on the equivalent panel by a radiation integral, the quadrature allows to replace the radiation integrals by weighted summations. The quadrature also provides a unique set of nodes, namely the elements positions, and a unique set of weights, which are involved in the definition of the excitation coefficients. Numerical results assess the effectiveness of the technique.

17:20 A Greedy Approach for Reducing Data in Near-Field Measurements

Maria Antonia Maisto (Università degli studi della Campania Luigi Vanvitelli, Italy); Antonio Ciociola (Università della Campania, Italy); Raffaele Solimene (Università degli studi della Campania Luigi Vanvitelli, Italy)

In this paper, a sampling strategy which allows to take advantage of all a priori information available on the Antenna under test in reducing the measurement number is proposed. Experimental results show that the required sampling points returned by the proposed method are lower than the ones needed by the standard warping and half-wavelength sampling.

17:40 Uncertainty Quantification of the Gain Budget for INCUS

Alessio Mancini (NASA Jet Propulsion Laboratory, USA); Gaurangi Gupta (NASA Jet Propulsion Laboratory, Caltech, USA); [Paolo Focardi](#) (Jet Propulsion Laboratory & California Institute of Technology, USA)

INCUS is an Earth Science project approved by NASA in 2022. The goal of the mission is to study in detail how water vapor and droplets move inside tropical storms and thunderstorms and understand their effects

on weather and climate models. To carry out this study, the mission will use three almost identical SmallSats, each one equipped with a Ka-band radar heritage of Raincube. The deployable mesh reflector antenna is a new 1.6m design provided by Tendeg. The bus for each of the three observatories is provided by Blue Canyon Technology (BCT), while Colorado State University leads the science team of the project. This paper presents the general architecture of the three observatories with particular emphasis on the radar antenna subsystem design. In particular, a statistical analysis to evaluate the impact of fabrication tolerances of the deployable mesh reflector surface and their effect on the antenna gain will be presented.

Monday, March 18 16:00 - 18:00

CS28: Biological tissue characterization as a basis for medical devices development

T06 Biomedical and health / Convened Session / Antennas

Room: Carron 2

Chairs: Raquel C. Conceição (Instituto de Biofísica e Engenharia Biomédica, Faculdade de Ciências, Universidade de Lisboa, Portugal), Daniela M. Godinho (Instituto de Biofísica e Engenharia Biomédica - Faculdade de Ciências - Universidade de Lisboa, Portugal)

16:00 Dielectric Characterisation of Human Parathyroid Glands at Microwave Frequencies

[Bilal Amin](#) (University of Galway, Ireland); [Atif Shahzad](#) (Centre for Systems Modelling and Quantitative Biomedicine, Ireland); [Ana González-Suárez](#), [Eoghan Dunne](#) and [Aoife Lowery](#) (University of Galway, Ireland); [Martin O'Halloran](#) (National University of Ireland, Galway, Ireland); [Adnan Elahi](#) (University of Galway, Ireland)

This paper reports the first comprehensive investigation of the ex vivo dielectric properties of human parathyroid glands in the microwave frequency range for the application of microwave imaging and microwave thermal ablation. The dielectric properties of the human parathyroid glands (N = 9) were measured using an open-ended coaxial probe measurement technique at frequencies ranging from 0.5 - 8.5 GHz. The measurements were conducted on freshly excised human parathyroid gland samples. A two-pole Debye model was fitted on the mean dielectric properties of the human parathyroid glands. The relative permittivity values ranged from 42 - 57 over the frequency range of 0.5 GHz to 8.5 GHz, and the conductivity ranged from 0.9 - 9 S/m for that frequency band. These insights into the dielectric properties of human parathyroid glands have the potential to advance the development of microwave-based techniques for non-invasive detection, localisation and functional assessment of parathyroid glands.

16:20 The Effect of Pressure of the Open-Ended Coaxial Probe on the Measurement of Ex Vivo Biological Tissues Dielectric Properties

[Ana Catarina Pelicano](#) (Instituto de Biofísica e Engenharia Biomédica, Fac. Ciências Un. Lisboa & FCIencias ID, Portugal); [Nuno Araújo](#) (Centro de Física Teórica e Computacional, Fac. Ciências Un. Lisboa, Portugal); [Daniela M. Godinho](#) (Instituto de Biofísica e Engenharia Biomédica - Faculdade de Ciências - Universidade de Lisboa, Portugal); [Raquel C. Conceição](#) (Instituto de Biofísica e Engenharia Biomédica, Faculdade de Ciências, Universidade de Lisboa, Portugal)

The impact of increasing evenly spaced pressures, between 2.58 and 25.8 kPa, on dielectric data ranging from 0.5 to 8.5 GHz was studied using 1×1×1 cm³ and 2×2×2 cm³ of bovine liver and chicken muscle samples. Results show a reduction exceeding 15% in tissue dielectric properties as pressure increased, until a breaking point is reached, and the trend reversed. The initial decline of dielectric properties aligns with existing literature, which suggests intracellular and interstitial fluid displacement due to probe pressure. We propose that the subsequent increase of dielectric properties may result from cellular membrane rupture, driving water towards the sample surface. Hence, maintaining consistent probe-tissue pressure during measurements is imperative to minimise data inaccuracies. We recommend conducting preliminary pressure tests prior to measuring biological tissue dielectric data. Moreover, we endorse the inclusion of applied pressure details in measurements metadata.

16:40 Dielectric Characterization of Biological Tissues at Microwave Frequencies Based on Water Content

[Flavia Liporace](#), [Gianluca Ciarleglio](#), [Maria Gabriella Santonicola](#) and [Marta Cavagnaro](#) (Sapienza University of Rome, Italy)

Nowadays, many medical techniques apply electromagnetic fields (EMF) on patients with therapeutic and/or diagnostic purposes. For this reason, to provide safe and effective treatments, it is necessary to comprehend the mechanisms of interaction between the biological system under exposure and the applied EMF. This interaction is described by the dielectric properties of the considered system. Biological tissues are complex and heterogeneous, and their dielectric properties change with frequency and under the influence of many factors. In particular, at frequencies higher than 1 GHz the main influence on the dielectric behaviour of a certain tissue is given by its water content. In this work, an approach is proposed for the reconstruction of the dielectric properties of biological tissues from their water content. An experimental validation is given on muscle and liver ex-vivo animal samples whose water content is measured through the desiccation technique.

17:00 Phantom Material with Biological Composition for Muscle Equivalent Radiofrequency, Thermal and Magnetic Resonance Properties

[Laura J.C. Barendsz](#), [Kemal Sumser](#) and [Steven Beumer](#) (Eindhoven University of Technology, The Netherlands); [Sergio Curto](#) (Erasmus University Medical Center, The Netherlands); [Rob Mestrom](#) and [Margarethus M. Paulides](#) (Eindhoven University of Technology, The Netherlands)

As research and development in the field of electromagnetic medical devices increases, so does the need for proper validation and calibration. This is typically done using tissue mimicking models known as phantoms. Magnetic resonance imaging (MRI) is becoming increasingly popular for electromagnetic device modelling and validation. Currently, there is no muscle phantom material that matches the properties of muscle tissue in MRI, electromagnetic and thermal properties. This study presents a novel muscle phantom made from inexpensive, household materials, that can approximate all three. Phantoms consist of water, agar-agar, peanut oil, and protein powder. These ingredients are used to model healthy, obese and dehydrated muscle tissue. While the phantoms exhibit behavior similar to those in existing literature, their values are consistently lower. We expect that future improvement is possible by reducing the protein and oil content, to bring the values even closer to the muscle tissue properties reported in literature.

17:20 Temperature-Dependent Electrical Characterization of a Thermally Sensitive Hepatic Tumor Phantom

[Ahmet Bilir](#) and [Sema Dumanli](#) (Bogazici University, Turkey)

Phantom design is a critical task in biomedical device development which gives strong indication for validity before going for animal/human testing. Microwave ablation therapy is no exception. The temperature change in the target tissue is measured in thermal phantoms after estimated with electromagnetic and thermal simulations. Establishing a visual feedback mechanism during thermal therapy would bring the testing process closer to a more realistic scenario. Here we propose a semi-transparent polyacrylamide gel based hepatic tumor phantom at 2.45 GHz of which absorbance changes as the temperature increases. It is shown that, the phantom can be optimized such that the absorbance converges to its maximum value at a specific target temperature value. The temperature-dependent permittivity and conductivity values, and temperature-dependent absorbance values of the proposed phantom is given.

Monday, March 18 16:00 - 18:00

CS6b: Emerging Multiple Beam and Beamforming Technologies for 5G and Beyond (continued)

T02 Mm-wave for terrestrial networks 5G/6G / Convened Session / Antennas

Room: Dochart 1

Chairs: [Simone Genovesi](#) (University of Pisa, Italy), [Lizhao Song](#) (University of Technology Sydney, Australia)

16:00 Multibeam Antenna for Wide-Angle 95-Beam Coverage at Ka-Band Using a Multifocal Transmit-Array

[Sergio Matos](#) (ISCTE-IUL / Instituto de Telecomunicações, Portugal); [João M. Felício](#) (Escola Naval, Portugal & CINAV - Instituto de Telecomunicações, Portugal); [Jorge R. Costa](#) (Instituto de Telecomunicações / ISCTE-IUL, Portugal); [Carlos A. Fernandes](#) (Instituto de Telecomunicações, Instituto Superior Técnico, Portugal); [Nelson Fonseca](#) (Anywaves, France)

Cost-effective multibeam millimeter wave antenna solutions are required to enable the deployment of 5G and beyond systems operating in the frequency range 2 (FR2). The trade-off between system complexity and

RF requirements (such as high gain, number of beams, beam forming/scanning capability, etc.) is a challenging problem fomenting the development of new antennas. Spatially fed transmit-arrays (TAs) where the aperture is illuminated by a planar array placed in a focal plane, is a canonical solution. However, the design is constrained by the focal distance to aperture diameter ratio (F/D). On the one hand, reducing the F/D allows designing more compact feeding array elements, on the other hand, it limits the maximum angle coverage due to scanning aberrations. In this work, we show that a TA optimized for operating simultaneously with low F/D and wide-angle coverage can improve the performance of this classical configuration. We design a Ka-band multibeam antenna with a TA fed by a 19x5 array of standard WR38 waveguide operating with F/D=0.34. It provides 25 dBi of gain with scan losses below 3 dB when scanning in a zenith plane up to -55 degrees, covering 80 degrees (-55 to 25 degrees) with cross-over levels around 3 dB.

16:20 Hybrid Analog-Digital Beamforming System with Quad-Steerable Beams Based on Programmable Transmitarray

Antonio Clemente (CEA-Leti, France); Samara Gharbieh (CEA-Leti Minatoc, Grenoble, France); David Demmer (CEA-LETI, France); Raffaele D'Errico (CEA, LETI & Université Grenoble-Alpes, France); Jean-Baptiste Doré (CEA-LETI, France)

A hybrid analog/digital beamforming system generating four independent steerable beams is presented. A quad-focal-source programmable transmitarray operating on the frequency band 24 - 31 GHz is optimized and demonstrated. The proposed antenna system is based on an array of 400 programmable unit-cells with a 1-bit phase resolution. Four 10-dBi pyramidal horn antennas are used to illuminate the transmitarray aperture. Inter-beam interference is mitigated numerically by applying an amplitude and phase precoder. This hybrid precoding techniques can be used to implement spatial division multiplexing in a multi-user system.

16:40 Anisotropic Metagrating for Beamforming with Polarization Conversion

Anh Mai Nguyen (Ulsan National Institute of Science and Technology, Korea (South)); Gangil Byun (Ulsan National Institute of Science and Technology (UNIST), Korea (South)); Ikmo Park (Ajou University, Korea (South))

This work presents a realistic simple printed circuit board typed metagrating structure to achieve near-unity efficiency for dual-polarization anomalous reflection. The proposed scatterers are meticulously designed using a set of electric dipoles, which effectively breaks the symmetry under normal incidence, allowing for high power coupling into the desired propagating mode. Furthermore, the inclusion of an artificial ground layer enhances the metagrating's capability for different polarization performance in wide-angle anomalous reflection. This advancement extends the practical applications and versatility of metagrating concepts.

17:00 Millimeter-Wave Beam-Steerable Lens with Reduced Profile and Enhanced Gain

Yang Cai and Peng Mei (Aalborg University, Denmark); XianQI Lin (University of Electronic Science and Technology of China, China); Shuai Zhang (Aalborg University, Denmark)

A 20x20 2-bit lens antenna is proposed utilizing the method of extracting actual phase shift (APS) by simulating element array (EA) for reduced profile and enhanced gain, which eliminates the effects of oblique incidences and simplifies the design process. Dielectric lenses elements are used to demonstrate the design. The proposed lens antenna exhibits enhanced gain and beam-steerable performance from 22 GHz - 30GHz. The gain enhances 3.4 dB at 26 GHz compared to the conventional design using the periodic boundary conditions. Moreover, the scan angle can maintain $\pm 30^\circ$ within the whole bandwidth by mechanically displacing the feed antenna.

17:20 Multi-Beam Arrays for Future LEO SatCom Payloads

Carlos Vazquez-Sogorb (Consiglio Nazionale delle Ricerche & Istituto di Elettronica e di Ingegneria dell'Informazione e Delle Telecomunicazioni, Italy); Roger Montoya-Roca (Consiglio Nazionale delle Ricerche, Italy); Giuseppe Addamo (Istituto di Elettr. e di Ingegneria dell'Inform. e delle Telecom. (IEIT-CNR), Italy); Oscar Peverini (IEIT-CNR, Italy); Giuseppe Virone (Consiglio Nazionale delle Ricerche, Italy)

LEO satellite antennas must provide several beams at the same time up to Ka-band over a large scanning angle (up to $\pm 60^\circ$). For this reason, high performance radiating elements and beamforming circuitry becomes crucial for the development of new constellations. This paper outlines the challenges and limitations of both waveguide-based and Vivaldi-based solutions and their impact on the beam-formed patterns.

17:40 3D-Printed Multi-Beam Flat Lens Antenna System

Maral Ansari (CSIRO, Australia); Lizhao Song and Peiyuan Qin (University of Technology Sydney, Australia); Stephanie Smith (CSIRO & Astronomy and Space Science, Australia); Y. Jay Guo (University of Technology Sydney, Australia)

This paper focus on the design of a multi-beam flat GRadiant INdex (GRIN) lens antenna. The lens profile is found analytically in combination with an arc feed trajectory to produce an approximate linear phase on the lens aperture for maximum radiation angle. This approach improves the scanning performance of the flat lens in 2D orthogonal plane when compared to equivalent lens designs previously reported. The variation in the refractive index profile of the lens is implemented using a partially filled dielectric periodic cubic unit cell. An array of microstrip patches is used as the feed source. The arrays are arranged in two orthogonal plane to demonstrate the 2D multiple beam performance of the lens antenna system. A prototype lens antenna is fabricated using 3D printing technology operating from 12 to 15 GHz. This design is suitable for high-gain multi-beam emerging fifth generation (5G) communication systems.

Monday, March 18 16:00 - 18:00

CS9b: Advances in 2-D Leaky-Wave Antennas Modelling and Design (continued)

T08 EM modelling and simulation tools / Convened Session / Antennas

Room: Dochart 2

Chairs: Paolo Baccarelli (Roma Tre University, Italy), Davide Comite (Sapienza University of Rome, Italy)

16:00 Emulating Spatial Dispersion Using Non-Spatially Dispersive Periodic Metasurfaces

Jordan R. Dugan, Tom Smy and Shulabh Gupta (Carleton University, Canada)

Spatially dispersive (or non-local) metasurfaces are an important class of surface where the induced currents on the surface are dependent on the fields over an extended region of the surface. These surfaces can be characterized using surface susceptibilities that take the form of rational polynomial functions in the spatial frequency domain. This representation allows us to model the field scattering from the surface as a higher-order boundary condition. Recently, a method was proposed to synthesize a set of susceptibilities to achieve any given field response in the spatial frequency domain. However, realizing these susceptibilities remains an open problem. In this paper, we demonstrate that spatially dispersive metasurfaces can be implemented as non-uniform metasurfaces composed of non-spatially dispersive unit cells.

16:20 Mechanically Re-Configurable Leaky-Wave Antenna for Fix-Frequency Beam Scanning

Miguel Poveda-García (Technical University of Cartagena, Spain); Samuel Arthur Rotenberg (Heriot-Watt University, United Kingdom (Great Britain)); Jose-Luis Gómez-Tornero (Polytechnic University of Cartagena, Spain); Symon K. Podilchak (University of Edinburgh, United Kingdom (Great Britain)); George Goussetis (Heriot-Watt University, United Kingdom (Great Britain))

In this paper we present a mechanically re-configurable leaky-wave antenna (LWA) for fix-frequency beam scanning. The structure consists of a meandered waveguide with coupling slots for radiation, constituting a periodic LWA. The beam direction is controlled with the phase shift between slots that is depending on the meandered length. Thus, a mechanism to change the length of the meander is presented, allowing for a beam scanning range from -65° to $+65^\circ$ with a 12.75 mm displacement of a moving metallic component. The structure has been validated with full-wave simulations, showing the proper synthesis of the scanned beams at the fixed frequency of 13 GHz.

16:40 Dual-Polarized Reconfigurable Metasurface for Leaky-Wave Antenna Design Using Air-Bridged Schottky Diode Technology

Ioannis Gerafentis, Alexandros Feresidis and Evangelos Vassos (University of Birmingham, United Kingdom (Great Britain))

A novel dynamically reconfigurable leaky wave antenna capable of performing beamsteering based on a tunable metasurface that supports dual polarization and uses air-bridged Schottky diodes is presented. The

electromagnetic waves produced by ideal dipoles in this case, propagate within a cavity which is formed by a Partially Reflective Surface (PRS) and a tuneable High-Impedance Surface (HIS). The beamsteering capability of the produced highly-directive beam is enabled by the air-bridged Schottky diodes embedded in the centre of each HIS unit cell by altering the capacitance of the diodes. This design operates at 37.5 GHz with a continuous beam scanning of 22° while the proposed HIS unit cell enables the support of dual-polarized excitation. The proposed leaky wave antenna design was simulated using CST Microwave Studio and is characterized by acceptable losses of 1-5.4dB for this frequency band, a bandwidth of 2GHz while the directivity varies within 20.72- 22.8 dBi.

17:00 Design of Modulated Dielectric Leaky-Wave Antennas for Efficient Bessel-Beam Synthesis

Tomas Lira (Pontificia Universidad Católica de Valparaíso, Chile); Francisco Pizarro (Pontificia Universidad Católica de Valparaíso, Chile); Eva Rajo-Iglesias (University Carlos III of Madrid, Spain); Jose-Luis Gómez-Tornero (Polytechnic University of Cartagena, Spain)

The synthesis of Bessel beams with a leaky wave antenna made of dielectric rings on a substrate is the focus of this study. Employing 3D-printing techniques, this particular two-dimensional Bull's-eye antenna design offers flexibility in modifying various parameters of the rings. These parameters include the material, thickness, width, and periodicity. The study illustrates how this flexibility facilitates the efficient design of a Bessel-beam launcher antenna, optimizing focusing properties such as the non-diffractive range and the spillover efficiency.

17:20 Modal Analysis in Woodpile Dielectric Structures

Vakhtang Jandieri (General and Theoretical Electrical Engineering (ATE), Faculty of Engineering, Germany); Guido Valerio (Sorbonne Université, France); Paolo Baccarelli (Roma Tre University, Italy)

We propose an efficient semi-analytical approach to analyze the real and complex modes in three-dimensional woodpile bandgap structures that consist of multilayered periodic arrays of circular dielectric cylinders. The reflection and transmission matrices through the woodpile structure are rigorously calculated using the transition-matrix approach combined with the lattice sums technique. The dispersion behavior of bound and complex modes in closed stop-band regions as well as of proper and improper leaky modes can be numerically calculated. The results for the bound modes are compared with a fully independent commercial EM software showing a very good agreement.

Monday, March 18 16:00 - 18:00

M5: Uncertainty analysis and measurements techniques

T09 Fundamental research and emerging technologies / /

Room: M2

Chairs: Giada Maria Battaglia (Università Mediterranea di Reggio Calabria, Italy), Vince Rodriguez (NSI-MI Technologies & University of Mississippi, USA)

16:00 On the RF Absorber Coverage of Antenna Under Test Positioners

Vince Rodriguez (NSI-MI Technologies & University of Mississippi, USA); Mark Ingerson (NSI-MI AMETEK, USA); Gwenael Dun (NSI-MI, c/o AMETEK, France)

In any antenna measurement, the antenna under test (AUT) must be positioned in front of the range antenna. Positioners are typically made from metal or dielectrics. Regardless of the material, they will reflect and diffract the electromagnetic waves and influence the measurement. It is common to cover them in RF absorber. However, RF absorber is not perfect, and it will also influence the measurement. In this paper, several treatments of absorber on a roll over azimuth AUT positioner are analyzed. The range is a spherical near field range, with an open-ended waveguide (OEWG) illuminating the AUT. The analysis shows that sometimes a minimal absorber coverage is sufficient to get accurate measurements within a given uncertainty level.

16:20 Uncertainty Analysis of Linear Multi-Probe Array Systems for Fast Antenna Measurements

Francesco Saccardi (Microwave Vision Italy, Italy); Andrea Giacomini (SATIMO, Italy); Nicolas Gross and Thierry Blin (MVG Industries, France); Per Iversen, Roni Braun and Lior Shmidov (Orbit/FR, USA); Meng He (MVG, Hong Kong); Chen Chen (MVG Hong-Kong, Italy); Xavier Bland (MVG, Hong Kong); Lars Foged (Microwave Vision Italy, Italy)

In this paper we present the measurement uncertainty analysis of a linear Multi Probe Array (MPA) system suited for fast testing of medium and high directive antennas. As proved in previous publications, a MPA allows to significantly reduce the measurement time of a conventional Planar Near Field (PNF) system based on the mechanical scanning with a single probe. Due to its unavoidable increased complexity, a MPA system requires dedicated calibration steps and corrections to compensate for the non-ideal uniformity of the sensors and their radiation pattern. The residual errors of such compensation techniques are taken into account in this analysis together with other error sources, such as multiple reflections, scan truncation, probe position errors and room scattering.

16:40 Simulation Based Uncertainty Analysis for Active Two-Way-Radiation Pattern Measurements of Circularly Polarized Antennas

Anna Granich (RWTH - Aachen University, Germany); Dirk Heberling (RWTH Aachen University, Germany)

Traditional antenna measurement systems are often ineffective in the case of integrated systems due to the lack of accessibility to the antenna's feed point. To address this issue, a frequency-modulated continuous wave (FMCW) radar system's two-way radiation pattern can be assessed by utilizing the radar's own transmit and receive modules while measuring against a reflector. However, it's important to note that this method introduces measurement uncertainties distinct from those encountered in conventional antenna measurements. In this study, we delve into the mechanical uncertainties through simulations to shed light on their impact and characteristics for circular polarized antennas, taking into account the polarization-dependent reflections of plate, dihedral and trihedral reflectors. Although discrepancies between the theoretically calculated two-way radiation pattern and the simulations can be found, the method can be validated in general and proves robustness against smaller misalignment errors.

17:00 Thermoelectric Cooling Solution for Active Antennas

Rania Khalifeh (IRSEEM ESIGELEC, France); Habib Boulzazen and Moncef Kadi (IRSEEM/ESIGELEC, France); Nabil Benjelloun (IRSEEM ESIGELEC, France)

An active antenna array cooling method is presented in this paper. As part of an industrial partnership, a 5G telecommunications array is provided. The proposed thermoelectric solution, with low power consumption, must maintain acceptable RF performances and small dimensions while cooling the transceivers supplying the antenna array.

17:20 Near Field Phase Recovery Exploiting Only One Measurement Surface and A Smart Warping Sampling Strategy

Giada Maria Battaglia (Università Mediterranea di Reggio Calabria, Italy); Tommaso Isernia (University of Reggio Calabria, Italy); Maria Antonia Maisto (Università degli studi della Campania Luigi Vanvitelli, Italy); Andrea Francesco Morabito (Università Mediterranea di Reggio Calabria, Italy); Roberta Palmeri (IREA-CNR, Napoli, Italy); Raffaele Solimene (Università degli studi della Campania Luigi Vanvitelli, Italy)

A recently introduced and successful strategy for addressing the phase retrieval problem from far-field measurements is now applied to the near-field case. This extension maintains its core methodology of treating 2-D phase retrieval as a series of 1-D recovery problems. These latter are effectively solved by integrating the Spectral Factorization method with a selection process reminiscent of solving a crossword puzzle. The expansion into the near-field domain involves leveraging key findings related to efficient planar near-field measurements through warping strategies. This approach restores the bandlimited nature of scattered fields, allowing the method to retain its advantages over state-of-the-art techniques. These advantages include the requirement for only a single measurement surface and the ability to achieve the optimal solution without resorting to computationally expensive global optimization algorithms.

17:40 Spherical Near-Field Measurement and Far-Field Characterization of a 300 GHz Band Antenna Based on an Electrooptic Probe with Compact Tabletop Robotic Arm

Yusuke Tanaka, Kento Ishihara and Shintaro Hisatake (Gifu University, Japan)

We demonstrate the photonics-based near-field measurements and far-field characterization of a horn antenna operating at 300 GHz based on a spherical scanning system. An electrooptic probe, which consists of an optical fiber and a small organic crystal, is mounted on a 6-axis tabletop compact robotic arm for the scanning. The far-field distribution calculated from the measured spherical near-field distribution without probe

compensation is agreed well with the simulation results.

Monday, March 18 16:00 - 18:00

EuCAP: EuCAP2025

//

Room: M3

Monday, March 18 16:00 - 18:00

CS16: Beam focusing for microwave and (sub-)millimeter-wave applications

T09 Fundamental research and emerging technologies / Convened Session / Antennas

Room: M4

Chairs: Walter Fuscaldo (Consiglio Nazionale delle Ricerche (CNR), Italy), Santi Concetto Pavone (Università degli Studi di Catania, Italy)

16:00 Analytical and Numerical Evaluation of Efficient Power Transfer of Bessel-Shaped Beams in Near-Field Through a Planar Layered Medium

Santi Concetto Pavone (Università degli Studi di Catania, Italy); Gino Sorbello (University of Catania, Italy)

We propose here the analytical and numerical evaluation of efficient power transfer through a planar layered medium of a Bessel-shaped beam (i.e., the 2-D equivalent of a Bessel beam), operating in the Fresnel region of the radiator. An analytical model is introduced together with a suitable figure of merit to estimate the amount of beam power that is efficiently transferred beyond the layered medium, by taking into account also the preservation of beam focusing in the main beam. The applications of such an approach are quite large, spanning from soil heating to near-field wireless power transfer and through-the-wall radars.

16:20 On the Data Rate Capability of Near-Field Communications Links Based on Bessel Beams

Adam Narbudowicz (Trinity College Dublin, Ireland & Wrocław University of Science and Technology, Poland); Mauro Ettore (University of Rennes 1 & UMR CNRS 6164, France)

This work proposes the numerical analysis of near-field communications using non-diffractive Bessel beams, in terms of Bit Error Rates when communicating with QAM-256 modulation. The study calculates BER for different locations within the near-field volume and non-diffractive range of the generated non-diffractive beam within the near field of the radiating aperture. It is demonstrated that, unlike the far-field analysis, the BER in the near-field can significantly vary, even when calculated at the same distance from the radiating aperture. The study also predicts that a communication link with BER $< 10e-4$ can be achieved - under certain conditions - over a distance up to 4 wavelengths.

16:40 All-Metal Perfectly-Matched Metamaterials

Jorge Ruiz-Garcia (University of Michigan, USA); Anthony Grbic (University of Michigan, Ann Arbor, USA)

This work introduces a method for designing all-metallic metamaterials that perform a prescribed field transformation in a reflectionless manner. First, Perfectly-Matched Metamaterials (PMMs) are reviewed. PMMs consist of subwavelength unit cells that remain impedance-matched to each other and the surrounding medium under any excitation. It is shown that for a given field transformation, the constitutive parameters of a PMM's unit cells can be analytically calculated. Using homogenization, the PMM's constitutive parameters are then realized as elliptical metallic pins in a parallel-plate waveguide environment. An all-metal perfectly-matched collimator is designed to validate the proposed design technique.

17:00 Leaky-Wave Design of Hybrid-, TE-, and TM-Polarized Resonant Bessel-Beam Launchers for Millimeter- and Submillimeter-Wave Applications

Edoardo Negri (Sapienza University of Rome, Italy); Walter Fuscaldo (Consiglio Nazionale delle Ricerche (CNR), Italy); Paolo Burghignoli and Alessandro Galli (Sapienza University of Rome, Italy)

Bessel beams (BBs) recently gained much interest thanks to their limited-diffractive and self-healing properties. Resonant BB launchers are compact, low-profile, cost-effective devices able to generate such field distribution in the microwave and low millimeter-wave frequency ranges. However, modern applications call for radiating devices able to focus the electromagnetic energy at higher frequencies. For this reason, the possibility to implement TM-, TE-, or hybrid-polarized BB launchers at millimeter and submillimeter waves is investigated in this work. In particular, three resonant BB launchers working at central frequency of 300 GHz are designed with different polarizations. Full-wave simulations of the proposed devices are in excellent agreement with those theoretically predicted by a rigorous, effective, and well-documented leaky-wave approach. Therefore, this work can be considered as a starting point for the implementation of innovative devices able to focus the electromagnetic energy in the submillimeter-wave range.

17:20 Radiation Control by Space-Time-Modulated Anisotropic Impedance Surfaces

Oscar Senlis (Univ Rennes, CNRS, IETR, France); David González-Ovejero (Centre National de La Recherche Scientifique - CNRS, France); Mauro Ettore (University of Rennes 1 & UMR CNRS 6164, France); Vincent Laquerbe (CNES, France); Pouliguen Philippe (DGA, France)

This paper builds on the holographic technique, previously used for the design of modulated metasurface antennas, to explore the radiation characteristics of space-time-modulated (STM) impedance surfaces. Space-time holography is employed here to derive the anisotropic impedance tensor for a metasurface antenna that, despite being excited by a monochromatic surface wave (SW), is capable of radiating at two different discrete frequencies with orthogonal polarizations. An example of space-time-modulated holographic antenna is provided and simulated with a commercial software to validate the proposed theoretical framework.

17:40 A Multiband Leaky-Wave Phased Array Antenna for 5G Fixed Link Communications

Darwin Blanco (Ericsson, Sweden)

A multi-band-single-layer leaky-wave antenna LW operating at k-band is reported. The designed array has a periodicity of two wavelengths at 28GHz while the excited grating lobes are mitigated by directive top flat LW patterns. The design is based on a single meta-surface layer MTS, allowing low profile and low cost while providing a versatile solution for 5G with multi-band operation mode. The single layer offers two operational high gain bands (low frequency band and high frequency band, LB/HB respectively) and a mid-band where the MTS is transparent that can be used in some scenarios as a control channel. Moreover, the MTS acts as a frequency selective surface (stop band) for the frequencies below and above the pass-band. Full-wave simulations, validate the current design showing two high-gain and one low-gain bands. A maximum gain of 26.2 dBi and 28.2 dBi with side lobe levels lower than -13 dBi is reported.

Monday, March 18 18:15 - 19:00

AW: Awards ceremony

Room: Lomond Auditorium

Monday, March 18 19:00 - 20:30

WC: Welcome Reception & Exhibition Opening

Room: Expo/Poster

Tuesday, March 19

Tuesday, March 19 8:30 - 10:10

SW1a: Active Array Antennas: Design concepts, technologies and over-the-air testing

Room: Lomond Auditorium

Chairs: Daniele Cavallo (Delft University of Technology, The Netherlands), A. B. (Bart) Smolders (Eindhoven University of Technology, The Netherlands)

8:30 Welcome and Introduction

Presenter: Bart Smolders (Eindhoven University of Technology)

8:40 Integration of Doherty Power Amplifiers with Antennas: Direct Impedance Matching, Active Load Modulation

Presenters: Oleg Lupikov/Marianna Ivashina (Chalmers University)

9:10 Packaging of mm-Wave Active Array Antennas for Car Radar: Concepts and Technologies

Presenter: Ralph van Schelven (NXP Semiconductors)

9:40 RF-Heterointegration for mm-Wave Radar and Communication Antenna-Arrays

Presenter: Fransesco Filice (IMEC)

Tuesday, March 19 8:30 - 10:10

E06a: Metasurface Design and Applications

T10 Novel materials, metamaterials, metasurfaces and manufacturing processes // Electromagnetics

Room: M1

Chairs: Sarah E Clendinning (KTH Royal Institute of Technology, Sweden), Marco Faenzi (University of Siena, Italy)

8:30 Contiguous Broadband Circularly Periodic High Impedance Surface Integrated with a Spiral Antenna

Kshitij Lele and Chris Bartone (Ohio University, USA)

A broadband circularly periodic High Impedance Surface is designed and integrated with a broadband spiral antenna to enable unidirectional broadband performance in a low-profile format. Performance is demonstrated between 2-6 GHz covering three contiguous sub-bands centered at 2.4 GHz, 3.5 GHz, and 5.0 GHz. The design methodology aligns the $\pm 90^\circ$ reflection-phase of consecutive sub-bands to enable good performance at the center of each sub-band, as well as the overlapping frequencies in between. The phase response is verified using simulations to ensure zero-degree reflection-phase at each sub-band design frequency and the $\pm 90^\circ$ reflection-phase at overlapping sub-band frequencies. A broadband spiral antenna is integrated with the HIS by placing the antenna above the HIS at a height of 0.09 λ . This HIS-backed spiral antenna is enclosed in an aluminum cavity to further suppress back-lobe radiation. The antenna S11, gain and radiation patterns are presented to demonstrate broadband performance of the integrated antenna structure.

8:50 On Solving Inverse Source Problems with Metasurfaces Performing Analog Computations

Mario Phaneuf and Puyan Mojabi (University of Manitoba, Canada)

We investigate the feasibility of solving inverse source problems with metasurfaces that perform analog computations. In particular, we consider the antenna diagnostics application wherein the fields radiating from an antenna under test (AUT) interact with a metasurface system. The output fields of this metasurface system will then represent the tangential fields near the aperture of the AUT, making them suitable for diagnostics. To this end, we present a general design framework while highlighting the potential difficulties of these metasurfaces. We show via simulation data that the approach can work in principle, and also present how a cascaded system of metasurfaces could potentially provide a form of hardware-based regularization to treat the ill-posedness of the underlying problem.

9:10 Fully Autonomous Reconfigurable Metasurfaces with Integrated Sensing and Communication

Hamidreza Taghvaei, Maryam Khodadadi and Gabriele Gradoni (University of Surrey, United Kingdom (Great Britain)); Mohsen Khalily (University of Surrey & 5G Innovation Centre, Institute for Communication Systems (ICS), United Kingdom (Great Britain))

One of the most controversial issues in Reconfigurable Intelligent Surfaces (RIS) is how to localize users. A potential solution is to integrate sensing and communication into the RIS platform to simultaneously detect a target and establish a communication link. By utilizing a shared spectrum, it is possible to optimize the channel with little to no mutual interference. To this end, a hybrid metasurface layout is proposed that supports beamforming while also enabling the sensing of incident signals from the user. This hybrid technology couples a small portion of the incident signal into a sensing layer. In the next step, a sensing scheme is introduced that leverages the inherent multiplexing of information within the metasurface's substrate to retrieve relevant information using a few sensing elements. The proposed metasurface can generate desired radiation patterns, and the addition of sensing capabilities has minimal impact on its primary functionality.

9:30 Design of a Low-Frequency Magnetic Metasurface for Extremely Focused and Long Range Wireless Power Transfer Applications

Martina Falchi, Pierpaolo Usai and Danilo Brizi (University of Pisa, Italy); Agostino Monorchio (University of Pisa & CNIT, Italy)

A methodology to design low-frequency metasurfaces for resonant inductive WPT applications able to extremely focus the magnetic field distribution at large distances from the source is presented. First, the optimal distribution of currents on the metasurface realizing the desired magnetic field hotspot is analytically defined. In this phase, the metasurface is considered to be composed of a planar distribution of ideal loops. Subsequently the corresponding real-scenario copper spiral unit-cells are designed. To verify the methodology, we conceived a numerical test-case by designing a 5x5 metasurface, opportunely excited by an actively fed driving coil. The obtained results at 4 MHz proved that a 40 mm diameter magnetic field beam was created between the plane of the metasurface and a point set 10 cm above the driver. The extreme focusing properties are achieved with any means of guiding structure and the volume around the system consists exclusively of air.

9:50 An Efficient Wheel-Integrated Wireless Power Transfer System Based on High-Permittivity Metasurface

Yu Yao and Maziar Nekovee (University of Sussex, United Kingdom (Great Britain))

Efficient wireless power transfer (WPT) systems seamlessly integrated with electric vehicles (EVs) are crucial to their successful massive rollout. This paper proposes a WPT system with a high-permittivity metasurface integrated with a wheel for efficiency enhancement. The single-turn coils with coupling-enhanced rings are explored as transmitter (Tx) and receiver (Rx). The metasurface is composed of high-permittivity elements placed on both surfaces. The symmetric system model ensures bidirectional transmission between EVs and power grids. With the aid of the metasurface, the efficiency of the WPT system is substantially enhanced and maintained within 400 mm.

Tuesday, March 19 8:30 - 10:10

CS39a: AMTA Session: Trends, Advancements and Challenges on Measurement Techniques for 5G and Beyond

T01 Sub-6 GHz for terrestrial networks (5G/6G) / Convened Session / Measurements

Room: Alsh 1

Chairs: Tian Hong Loh (UK, National Physical Laboratory, United Kingdom (Great Britain)), Janet O'Neil (ETS-Lindgren, USA)

8:30 A Comprehensive Mobile Phone Antenna Performance Evaluation Model Based on Deep Learning

Hui Zhao (China Academy of Information and Communications Technology, China)

Machine learning methods such as deep learning are beneficial to solving complex multidimensional modeling problems, so have great potential in electromagnetic(EM) structure research. In this work, we introduce a general method for predicting antenna performance using deep neural networks. Specifically, we use near-field data from artificial neural network (ANN) to estimate the far-field radiation and S 11 of antennas such as rectangular patch antennas in real time. This method is versatile because it can learn from a range of design parameters for various substrate materials and operating frequencies and can accurately predict all electromagnetic characteristics of the desired antenna (e.g., near and far field, S-parameters). Compared to numerical methods, we achieve acceptable antenna performance estimates.

8:50 Measurement of Total Radiated Power Using a TEM Cell

Kai Jiang and Yi Huang (University of Liverpool, United Kingdom (Great Britain)); Xiaoming Chen and Yanzhao Xie (Xi'an Jiaotong University, China)

This paper presents a study on measuring the total radiated power (TRP) of the equipment under test (EUT) using a transverse electromagnetic (TEM) cell, which has been a valuable tool for electromagnetic compatibility (EMC) measurements. It demonstrates that the utilization of the source-stirred method can generate an averaged uniform field inside the TEM cell at higher frequencies for measurement of total radiated power. Compared with other methods, such as the reverberation chamber method, this new approach exhibits a comparable accuracy but is faster and more cost-effective. The results are validated by both numerical simulations and experimental measurements.

9:10 Full Wave Modelling and Design of a Baffle for the HERTZ 2.0 Compact Antenna Test Range

Cecilia Cappellin, William Hamilton Yatman, Pasquale Giuseppe Nicolaci, Stig Sørensen and Mustafa Murat Bilgic (TICRA, Denmark); Damiano Trenta (European Space Agency, ESTEC, Italy); Luis Rolo (European Space Agency, The Netherlands)

A baffle has the purpose of preventing the feed of a compact antenna test range to radiate in the quiet zone and it is typically constituted by a cylindrical structure covered by pyramidal absorbers. In this paper we describe the electrical design of a baffle for the new compensated compact antenna test range for the HERTZ 2.0 facility at ESTEC. Two modelling approaches are shown and compared and the updated performance of the quiet zone field at L band is given.

9:30 Addressing PIM Challenges in Radio Base Stations: Field Issues and Testing Methods for Large-Scale Deployments

Queenie Zhang (Ericsson AB, Sweden); Chuanting Liu (Ericsson (China) Communications Co. Ltd, China); Ingolf Meier, Noor Choudhury, Lei Deng, Xiang Yue, Bo Xu and Yu Yang (Ericsson AB, Sweden); Frieso Damm (Ericsson Antenna Technology Germany GmbH, Germany); Hao An (Ericsson (China) Communications Co. Ltd, China); Nezahat Gunenc Tuncel and Martin Haun (Ericsson Antenna Technology Germany GmbH, Germany); Xiaoying Jiang (Ericsson (China) Communications Co. Ltd, China)

Mobile wireless broadband systems using 4G and 5G are being widely deployed and traffic demand is still growing with operators challenged for capacity from their spectrum. High transmitted power levels of multiple 3GPP broadband carriers tend to generate passive intermodulation (PIM) sources in such high electric-field situations. With the surge of compact integrated RBS, came an urgent demand for PIM requirements for site deployments as well as suitable testing methods. This paper addresses the complexity of real-world scenarios by conducting a comprehensive investigation into radio base station (RBS) equipment with PIM issues observed over the past few years. Using realistic measurements and empirical data, providing valuable insights into PIM test methodologies. Furthermore, this work contributes to the development of large-scale deployment testing methodologies, fostering a deeper understanding of PIM-related challenges in 5G wireless systems. This work can help manage PIM issues in the evolving landscape of 5G wireless communication systems.

9:50 Standardization Progress and Challenges for 5G OTA Testing

Siting Zhu and Xuan Yi (China Academy of Information and Communications Technology, China); Peng Wang, Long Pei and Guanghui Liu (China Academy of Information and Communication Technology, China)

Precise evaluation of MIMO performance and communication capacity measurement are essential to guarantee 5G product development and advance the 5G industry. The main developments in 3GPP Multiple-input Multiple-output (MIMO) Over-the-Air (OTA) standards for FR1 (450MHz-7.125GHz) and FR2 (24.25GHz-52.6GHz) are described in this paper along with the test methodologies and performance metrics. Furthermore, it is demonstrated the handheld test scenarios are important to the current MIMO OTA performance testing. Results of the channel model validation for FR2 MIMO OTA measurements are presented in our 3D-MPAC, confirming the successful application of the channel model in the test zone.

Tuesday, March 19 8:30 - 10:10

A27a: Mm-wave antenna technologies I

T02 Mm-wave for terrestrial networks 5G/6G // Antennas

Room: Alsh 2

Chairs: Oscar Quevedo-Teruel (KTH Royal Institute of Technology, Sweden), Lei Wang (Heriot-Watt University, United Kingdom (Great Britain))

8:30 Full-Metal Single-Block Antenna Arrays with Waveguide Corporate Feeding Networks at Ka and V Bands

Jorge Sánchez Castillo (Universidad Autónoma de Madrid, Spain); Jose Luis Masa-Campos (Universidad Politécnica de Madrid, Spain); Eduardo Garcia-Marin (Universidad Autonoma de Madrid, Spain); Pablo Sanchez-Olivares (Universidad Politecnica de Madrid, Spain); Jorge A Ruiz-Cruz (Universidad Politécnica de Madrid, Spain)

In this paper, we introduce a planar circularly polarized array with a corporate feeding network utilizing waveguide technology. The antenna is composed of three main layers: the radiating array and a two-stage feeding network. The intricate multi-layer design of the antenna poses manufacturing challenges, particularly at higher frequencies where potential power leakage between the layers is a concern. This study investigates the feasibility of producing the design as a single unified unit and assesses its reliability within such complex antenna structures. The array in question is tailored for applications in the lower millimeter-wave spectrum, specifically the Ka band (38 GHz) and the V band (60 GHz). These frequency bands are of significance due to the anticipated 5G satellite expansion and the deployment of WiGig technology respectively.

8:50 *Impact of Dielectric Substrate, Feed Connector, and Fabrication Tolerances on the Performance of Planar Millimeter-Wave Antenna Arrays*

Abdul Jabbar, Qammer H Abbasi, Muhammad Ali Imran and Masood Ur-Rehman (University of Glasgow, United Kingdom (Great Britain))

In this paper, the impact of dielectric substrate, feed connectors, and fabrication tolerances on the performance of planar microstrip mmWave antenna arrays is elucidated. Three similar prototypes of an 8-element wideband series-fed microstrip array, covering the entire 57-71 GHz ISM band, are designed by using three dielectric substrates (RO3003, RO5880, and RO4003C). The influence of the dielectric substrate on -10 dB impedance bandwidth, radiation efficiency, total efficiency, realized gain, sidelobe level, and radiation patterns is thoroughly analyzed through extensive numerical simulations. Moreover, a realistic 3D model of a microstrip edge-fed solderless 1.85mm V-connector is co-simulated with the array design, and its impact on mmWave antenna radiation characteristics is investigated. Furthermore, antenna fabrication tolerances and measurement effects at high frequencies are highlighted. These findings offer valuable insights when choosing dielectric substrates and taking into account connector effects while designing mmWave array antennas for a diverse range of futuristic applications.

9:10 *K-Band Microstrip ESPAR Antenna Integrated into Large Array*

Raffaele De Marco and Arman Bordbar (University of Calabria, Italy); Francesco Greco (Universita' delle Calabria, Italy); Carmine Mustacchio (CEA-LETI & Universita della Calabria, Italy); Sherif R. Zahran (University of Calabria, Italy & CNIT, Italy); Emilio Arneri (University of Calabria, Italy); Giandomenico Amendola (Universita della Calabria, Italy); Luigi Boccia (University of Calabria, Italy)

This study introduces a novel design for an microstrip electronically steerable parasitic array radiator (ESPAR), specifically employing a 5-element cluster configuration. Each cluster is composed of a single active element and four varactor-loaded parasitic elements, enabling beam steering in the E-plane and H-plane. The reported results show a continuous steering range of 50° along the E-plane and 80° along the H-plane. The operational bandwidth is approximately 13%, including the bandwidth reduction due to the beam scanning operation. The proposed subarray is integrated into a large array design comprising nine subarrays arranged in an interleaved triangular lattice. Notably, for each 5-element subarray, only one element necessitates phase control, leading to an 80% reduction in the number of required phase shifters compared to a standard phased array. The outcomes demonstrate a maximum scanning range of approximately 70 degrees on both E and H planes, with a maximum efficiency of 43%.

9:30 *Mechanical/Electrical Hybrid 2-Dimensional Beam Scanning Cylindrical Dielectric Lens Antenna*

Yoshiki Sugimoto, Takanori Narita and Kunio Sakakibara (Nagoya Institute of Technology, Japan); Tuan Hung Nguyen (Le Quy Don Technical University, Vietnam); Nobuyoshi Kikuma (Nagoya Institute of Technology, Japan)

A hybrid 2-dimensional beam scanning cylindrical lens antenna by combining a mechanical lens slide and a linear phased array is presented. The proposed antenna scans the main beam mechanically within the lens displacement plane by sliding the lens in one dimension. The proposed antenna also scans the beam electrically by a phased array of primary radiators arranged orthogonal to the mechanical beam scanning plane. The 2-dimensional beam scanning performance of the proposed antenna has been demonstrated through EM simulation; the proposed antenna capable of 2-dimensional beam scanning over a spherical angular range of $\pm 10^\circ$.

9:50 *A Novel Substrate Integrated Broadband Dielectric Resonator Antenna (DRA) in SICL for Millimeter Wave Application*

Naman Baghel and Soumava Mukherjee (Indian Institute of Technology Jodhpur, India)

In this study, a novel and compact substrate integrated broadband Dielectric Resonator Antenna (DRA) excited by Substrate Integrated Coaxial Line (SICL) is presented. In comparison to the traditional non-planar DRA configuration, that requires mounting of a dielectric over the feed, the presented work provides a simple alternative by utilizing the same substrate of the SICL feed network making it planar. This eliminates the major challenge of a complex fabrication process in designing DRA. Two semi-circular rings fed by the top and middle layer of SICL feed line forms the resonating structure of the DRA. The design procedure is shown to enhance the bandwidth of the proposed antenna. The field distribution attained in the suggested Dielectric Resonator Antenna (DRA) has similarities to the HEM₁₂ mode of the standard cylindrical DRA. The proposed DRA achieves a broadside unidirectional beam with a gain of 5.5 dBi at 26 GHz.

Tuesday, March 19 8:30 - 10:10

CS25: Antenna Systems for 6G SatCom

T03 Aerospace, new space and non-terrestrial networks / Convened Session / Antennas

Room: Boisdale 1

Chairs: Thomas Delamotte (Bundeswehr University Munich, Germany), Ulf Johannsen (Eindhoven University of Technology, The Netherlands)

8:30 *Beamforming Schemes for 6G Direct-To-Cell Connectivity Using Satellite Swarms*

Diego Tuzi (University of the Bundeswehr Munich, Germany); Thomas Delamotte and Andreas Knopp (Bundeswehr University Munich, Germany)

Direct-to-cell (D2C) connectivity, i.e., direct connectivity between satellite base stations and user terminals (UTs) with low power and low antenna gain, requires large satellite apertures to mitigate the performance gap with terrestrial network (TN). This paper focuses on innovative distributed space segment implementations using swarms of multiple small platforms, each embedding one or a subset of radiating elements, creating large virtual antenna apertures. The use of small satellites promises reduced production and launch costs and increased fault tolerance. This paper compares the multi-beam performance of a distributed implementation with that of a single platform implementation, using different beamforming schemes. The results show that distributed implementations overcome single-platform ones in terms of sum throughput. Furthermore, different beamforming schemes might be suitable for different system load conditions of the system. Recommendations for the use of beamforming schemes for swarms are outlined.

8:50 *A Modular, Low-Cost Ka-Band Antenna Subarray as Building Block for Phased Arrays of Arbitrary Size and Shape*

Federico Boulos, Ernest Ofosu Addo and Stefano Caizzone (German Aerospace Center (DLR), Germany); Ulf Johannsen (Eindhoven University of Technology, The Netherlands)

Recent and upcoming megaconstellations in LEO orbit will contribute to suppress the digital divide through satellite communication (satcom). The big obstacle, for an even more widespread use, is currently represented by the user terminal. The everyday consumer has still to deal with high power consumption and cost, exhibited by existing phased array-based antenna solutions. In this paper, a cost-effective phased array modular antenna concept, based on domino subarrays, is presented. The domino subarrays can be deployed in an arbitrary size and shape, opening to fully customizable phased arrays which can accommodate different designs for the upcoming 6G applications.

9:10 *Multibeam Phased Arrays Exploiting Frequency Dispersion for Massive MIMO Satellite Communications*

Margaux Pellet (Heriot-Watt University & Thales Alenia Space, France); George Goussetis and Joao Mota (Heriot-Watt University, United Kingdom (Great Britain)); Hervé Legay (Thalès Alenia Space, France); Giovanni Toso (European Space Agency, ESA ESTEC, The Netherlands); Piero Angeletti (European Space Agency, The Netherlands)

This article presents a frequency reuse methodology as applied to multibeam geostationary antennas that is suitable for different traffic scenarios. The maximization of the throughput is achieved adopting a strategy based on fixed grids of beams, each allocated to a frequency band that minimizes the dispersion effects. Each individual grid is associated with a lattice of orthogonal beams. The beam grids are independently positioned to best fit different traffic scenarios. Simulation results show that this positioning methodology has a significant impact on the overall throughput of the communication system and offers a substantial improvement as compared to a conventional scheme based on 4-colour frequency reuse.

9:30 *Aperture Distribution Method for Array-Fed Reflectors: A System Level Performance Case Study*

Francesco Lisi (Heriot-Watt University, United Kingdom (Great Britain)); Julien Maurin (Thales Alenia Space, France); Hervé Legay (Thalès Alenia Space, France); Piero Angeletti (European Space Agency, The Netherlands); George Goussetis (Heriot-Watt University, United Kingdom (Great Britain))

Array-Fed Reflectors provide the most favourable trade-off between performance, reconfigurability and cost for geostationary communication satellites. By combining the advantages of digital on-board processing,

active antenna technology and reflector magnification, these systems can generate hundreds of beams simultaneously and achieve sum rates up to hundreds of Gbps. However, their design can be a time-consuming operation due to the full system simulation required at each iteration of the optimization loop. While the Physical Optics-based Current Distribution method provides the most accurate results, the Geometrical Optics-based Aperture Distribution one can significantly reduce the simulation time at the expense of accuracy. In this manuscript, we analyse the impact of this trade-off for a specific architecture. By computing the Aperture Distribution method on the GPU, the simulation time can be reduced by two orders of magnitude within a tolerable C/I error. This result encourages the use of such method in the early design phase.

9:50 TX/RX Terminal Based on Metascreen Technology for Ka-Band Satcom with Dual Switchable Polarization

Francesco Caminita (Wave-Up SRL, Italy); Cristian Della Giovampaola (Wave Up srl, Italy); Massimo Nannetti (Wave Up Srl, Italy); Gabriele Minatti (Wave Up S. r. l., Italy); Nicola Bartolomei (Wave Up srl, Italy); Enrica Martini (University of Siena, Italy); Benedikt Byrne (European Space Agency, The Netherlands); Giovanni Toso (European Space Agency, ESA ESTEC, The Netherlands); Stefano Maci (University of Siena, Italy)

We present the design of a full TX/RX terminal with dual switchable polarization based on the Metascreen technology, for Ka-band operations. The two screens, which exploit the Pancharatnam-Berry phase technique, have been optimized in order to scan a highly-directive beam with reduced level of the grating lobes. Preliminary experimental results show that this technology can produce beam-steering antennas with high radiation efficiency greater than 80%.

Tuesday, March 19 8:30 - 10:10

A09a: Advances in reconfigurable antenna technologies

T10 Novel materials, metamaterials, metasurfaces and manufacturing processes // Antennas

Room: **Boisdale 2**

Chairs: Francesco Foglia Manzillo (CEA-LETI, France), James Kelly (Queen Mary University of London, United Kingdom (Great Britain))

8:30 Optical Microwave Metasurface Phased Arrays

Si Yu Miao and Feng Han Lin (ShanghaiTech University, China)

The concept, design and validation of the optical-microwave metasurface phased arrays (OMMPA) are introduced. The proposed OMMPA is composed of a microwave source, an optically-reconfigurable microwave metasurface, and an optical-control system. Different from microwave-photonics antennas that use light as the carrier for low-loss wideband microwave transmission (or light carries microwave), the proposed OMMPA uses light as the control signal for low-cost large-scale microwave tuning (or light controls microwave). Three important design considerations are highlighted with examples, concerning firstly the experimental modeling of tunable components, secondly the design of the optical-controlling system and thirdly the design of metasurfaces. Possible future directions and applications of the proposed OMMPA are also outlined.

8:50 Sub-Wavelength Anisotropic Unit-Cells for Low-Profile Transmitarray Antennas

Andrea Tummolo (Université de Rennes, France); Orestis Koutsos (CEA Leti, France); Francesco Foglia Manzillo (CEA-LETI, France); Antonio Clemente (CEA-Leti, France); Agnese Mazzinghi (University of Florence, Italy); Angelo Freni (Università degli studi Firenze, Italy); Ronan Sauleau (University of Rennes 1, France)

This paper presents the design of a sub-wavelength (sub-WL) element with anisotropic properties and demonstrates the performance enhancement it offers for realizing low-profile transmitarrays. The transmission characteristics are analyzed and compared to those of similar half-wavelength (half-WL) elements. The results reveal that, as opposed to the half-wavelength cell, the sub-wavelength element exhibits minimal sensitivity to oblique incidence effects, a key issue for low-profile transmitarrays. To evaluate the impact of the angular robustness of the element on the transmitarray performance, four distinct prototypes with 3-bit phase resolution and $10 \times 10 \lambda^2$ size, featuring the two unit-cell types and two different focal-to-diameter ratios ($F/D = 0.85, 0.3$) are designed at 30 GHz. The low-profile antenna with sub-wavelength elements attains a peak gain of 28.1 dBi with 46% aperture efficiency and a -3 dB gain bandwidth of 35%, outperforming the transmitarray based on half-wavelength elements.

9:10 1-Bit Reconfigurable Transmitted/Reflected Array (TRA) for 5G/6G Wireless Communication

Yujie Liu (Queen Mary University of London & Antenna Group, United Kingdom (Great Britain)); James Kelly (Queen Mary University of London, United Kingdom (Great Britain)); Mark Holm (Huawei Technologies (Sweden) AB, Sweden); Yuanwei Liu (Queen Mary University of London, United Kingdom (Great Britain))

This paper introduces a design for a 1-bit reconfigurable Transmitted/Reflected Array (TRA), capable of electronic beamforming in both transmission and reflection. The TRA is constructed using the Unit Cells (UCs) that respond differently to TE and TM incidences. By employing the PIN diodes, the UC achieves two phase states, 0° and 180° , for the transmission and reflection, respectively. Simulation results show that the proposed TRA has demonstrated independent control of the transmitted and reflected beams at the working frequency of 5.9 GHz. A peak gain of 18.1 dBi and a scanning range of 0° to 60° have been achieved in both transmission and reflection, making it suitable for applications in 5G/6G wireless communication systems.

9:30 Beam Training of LoS-MIMO Systems Using Subarray-Based Beamforming in the Presence of Ground Reflection

Masahiro Takigawa, Ryochi Kataoka and Issei Kanno (KDDI Research, Inc., Japan); Yoji Kishi (KDDI Corporation, Japan)

This paper proposes a beam training algorithm for line-of-sight (LoS) multi-input and multi-output (MIMO) system with subarray-based beamforming functionality. In general, a conventional beam training algorithm is conducted to maximize the signal power of each stream. As a result, each pair of subarrays directs its beam towards each other. In LoS-MIMO regime, however, the subarray positions at transmitter and receiver are optimized at a certain communication distance. The channel capacity degrades due to its higher spatial correlation depending on a distance. In this paper, a beam training algorithm utilizing the ground reflection is proposed to alleviate such degradation. The simulation results show that the proposed algorithm reduces the condition number of channel matrix and improves the channel capacities across communication distances.

9:50 Non-Volatile RF Frequency Reconfigurable Antenna for Wireless Communication

Xiaoyu Xiao (University of Manchester, United Kingdom (Great Britain)); Yize Li (The University of Manchester, United Kingdom (Great Britain)); Zirui Zhang and Zhirun Hu (University of Manchester, United Kingdom (Great Britain))

This paper presents the design, fabrication, and measurement of a frequency reconfigurable antenna by using non-volatile RF switches. The non-volatile switches were made by Nafion and glued to the antenna using silver epoxy to make it frequency reconfigurable. Due to the nature of their non-volatility, these switches do not need any DC power to sustain their states hence dissipate zero static power, significantly reducing the power consumption for antenna operation. The antenna can switch at three different operation modes between 1.8 GHz to 3.5 GHz without any static power supply.

Tuesday, March 19 8:30 - 10:10

CS36a: New antenna systems for Direction-of-Arrival estimation

T05 Positioning, localization, identification & tracking / Convened Session / Antennas

Room: **Carron 1**

Chairs: Jose-Luis Gómez-Tornero (Polytechnic University of Cartagena, Spain), Julien Sarrazin (Sorbonne Université, France)

8:30 Angle of Arrival Estimation Methods Using Spherical-Modes-Driven Multiport Antennas

Lintu Antony, Abel Abdul Zandamela and Nicola Marchetti (Trinity College Dublin, Ireland); Adam Narbudowicz (Trinity College Dublin, Ireland & Wroclaw University of Science and Technology, Poland)

Phased antenna arrays are traditionally used for Angle-of-Arrival (AoA) detection of radio signals. Yet, when size and weight are crucial, spherical mode-driven MIMO antennas present a compact alternative, significantly reducing dimensions. When applying traditional AoA estimation to multipoint antennas with non-linear configurations, the algorithm's intricacies need scrutiny. This paper investigates the optimal AoA estimation technique for spherical mode-driven MIMO antennas. In this work, various techniques for AoA estimation are evaluated, including the conventional Delay-and-Sum (DAS), the Minimum Variance Distortionless Response (MVDR), the subspace-based Multiple Signal Classifier (MUSIC), and the Estimation of Signal Parameters via Rotational Invariance Technique (ESPRIT). This study delves into the intricacies of each estimation technique for multipoint antennas, weighing estimation accuracy against computational demands. The performance of four methods on spherical mode-driven MIMO antennas is analyzed, pinpointing the best fits for compact IoT systems.

8:50 GHz Prism: Frequency-Scanned Antennas to Improve Localization with Separate-Channel Fingerprinting

Jose-Luis Gómez-Tornero (Polytechnic University of Cartagena, Spain); Jose A López Pastor (Universidad Politécnica de Cartagena, Spain); Alejandro Gil Martínez (Technical University of Cartagena Cartagena, Spain); Miguel Poveda-García (Technical University of Cartagena, Spain); Astrid Algaba-Brazález (Ericsson AB, Sweden)
We propose the application of frequency-scanning leaky-wave antennas to improve the performance of separate-channel fingerprinting techniques used for indoor localization. This paper reports initial evaluations conducted with microstrip leaky-wave antennas (LWA) and BLE (Bluetooth Low Energy) beacons. The LWA is designed to direct the three BLE advertising channels towards different angular sectors. As a result, it is demonstrated an increase of the spatial diversity of the separate-channel radiomaps. This significantly improves the location estimation accuracy by 30%, if compared to separate-channel BLE beacons using conventional antennas.

9:10 Compact Amplitude-Monopulse Microstrip Antenna Design for Wide Field-Of-View Direction Finding

Alejandro Gil Martínez (Technical University of Cartagena Cartagena, Spain); Miguel Poveda-García (Technical University of Cartagena, Spain); David Cafete Rebenague (Polytechnic University of Cartagena, Spain); Astrid Algaba-Brazález (Ericsson AB, Sweden); Jose-Luis Gómez-Tornero (Polytechnic University of Cartagena, Spain)
We investigate the challenges and possibilities to design short microstrip leaky-wave antennas (MLWA), which synthesize amplitude-monopulse patterns covering a wide angular field of view (FoV). It is shown that the standard design methodology requests the MLWA to operate in a radiation regime associated to a high scanning angle associated to poor radiation efficiency. Subsequently, we propose a new design technique to operate in a more relaxed dispersion regime, where the antenna is radiating close to broadside. Design examples working in the 2.45 GHz band are reported to validate the novel methodology, demonstrating the successful synthesis of monopulse patterns covering a wide FoV of 120° using a MLWA of length 9.8 cm (0.8 wavelengths). To the authors' knowledge, this is the most compact design and the widest FoV reported for this class of monopulse antennas, which might find useful application for integrated antenna sensors in the context of the IoT.

9:30 Compact Metamaterial Antenna for Three-Dimensional Angular Localization of Multiple Radio-Frequency Sources

Abdelwaheb Ourir (Institut Langevin ESPCI Paris CNRS, France); Julien de Rosny (CNRS, ESPCI Paris, PSL Research University, France)
We present an original technique of three-dimensional angular localization for multiple radio-frequency sources based on a single port metamaterial antenna. The designed antenna is a compact 4 by 4 finite periodic array of sub-wavelength $\lambda/6$ resonators. We show that a normalized dictionary of several complex radiation patterns can be constructed over a specific narrow frequency band. We implement numerical methods to estimate the direction of target antennas emitting uncorrelated signals by taking benefits of the complex frequency signatures over this band. We demonstrate that this single port antenna made of a finite array of metamaterial resonators is able to achieve the three-dimensional angular localization of an emitting target. Besides, we show that the proposed antenna can be used to retrieve the direction angles of multiple radiating radio-frequency sources.

9:50 A Parasitic Element Technique for Deep Null Synthesis and the Application to Received Signal Strength (RSS)-Based Localization

Jo Tamura and Hiroyuki Arai (Yokohama National University, Japan)
This paper presents an antenna system that uses received signal strength (RSS) for localization. The proposed system has the benefits of small size, low cost, precise estimation, and low power consumption, which is suitable for the Internet of Things (IoT) applications. It estimates angle-of-arrival (AoA) using an antenna radiation null. A parasitic element technique is applied to steer a deep null without attenuators. The technical challenge to build the system is that amplitude errors in the feeding circuit degrade the null-steering performance. The impact of the errors on the AoA estimation is investigated, and the specific criteria are clarified. The simulation results reveal that a properly designed antenna and phase shifter can reduce the error by up to 15 degrees. Consequently, the system can localize a target with an error of less than four degrees in a range of 120 degrees.

Tuesday, March 19 8:30 - 10:10

CS24a: Biomedical Microwave Techniques and Devices from Diagnosis to Treatment

T06 Biomedical and health / Convened Session / Antennas

Room: Carron 2

Chairs: Raquel C. Conceição (Instituto de Biofísica e Engenharia Biomédica, Faculdade de Ciências, Universidade de Lisboa, Portugal), Jorge A. Tobon Vasquez (Politecnico di Torino, Italy)

8:30 Advancements in the Experimental Validation of a Wearable Microwave Imaging System for Brain Stroke Monitoring

David O. Rodríguez-Duarte, Martina Gugliermio, Cristina Origlia and Jorge A. Tobon Vasquez (Politecnico di Torino, Italy); Rosa Scapaticci (CNR-National Research Council of Italy, Italy); Lorenzo Crocco (CNR - National Research Council of Italy, Italy); Francesca Vipiana (Politecnico di Torino, Italy)
Stroke is a disease that negatively affect brain oxygenation, so impacting short- and long-term people living conditions or, in the worst case, provoking the death. Brain stroke causes physiological variations in the affected tissues, which in turn produce relevant changes in the permittivity and conductivity of the involved tissues. Such changes can be detected and imaged by processing the scattering response at microwaves of the brain. This work advances the experimental validation of a microwave-based scanner to generate 3-D contrast dielectric maps, using low-complexity microwave hardware and a real-time standalone linear inversion algorithm based on the distorted Born approximation. The validation herein presented faces non-trivial conditions using anthropomorphic multi-tissue head and stroke phantoms, so replicating a laboratory set-up very close to the clinical scenario.

8:50 Microwave Imaging for Monitoring Bone Healing Using Magnetic Scaffolds: An Initial Analysis

Sonia Zappia (IREA-CNR, Italy); Matteo Bruno Lodi (University of Cagliari, Italy); Roberta Palmeri (IREA-CNR, Napoli, Italy); Nicola Curreli (Italian Institute of Technology, Italy); Ilaria Catapano (IREA-CNR, Italy); Lorenzo Crocco (CNR - National Research Council of Italy, Italy); Alessandro Fanti (University of Cagliari, Italy); Rosa Scapaticci (CNR-National Research Council of Italy, Italy)
Magnetic scaffolds are a particular class of multifunctional and electromagnetic-responsive biomaterials, in which traditional biomaterials are loaded with magnetic nanoparticles. These biomedical devices are able to accelerate bone healing repair under the action of electromagnetic fields. To date, limited efforts have been spent to provide monitoring tools for the follow up of bone tissue regeneration for these theranostic devices. In this work, the possibility of using microwave imaging to monitor tissue regeneration is investigated. In particular, a preliminary analysis on the signal level variations that can be observed during bone regeneration is performed, as this provides the necessary initial guideline to design a monitoring device.

9:10 Evaluating System Design in Breast Microwave Sensing: Data and Image Quality in Multiple Systems

Tyson Reimer, Fatimah Eashour, Gabrielle Fontaine, Jordan Krenkevich and Stephen Pistorius (University of Manitoba, Canada)
Numerous microwave-based breast imaging (MBI) systems have been developed to investigate the potential of microwave-based breast cancer detection. Despite the diversity in system design, relatively little research has compared systems and evaluated the impact of design parameters. This work evaluates the spatial resolution, noise, and shift-dependence of three imaging systems. These systems vary with respect to key design parameters and have been designed for different purposes – a bed-based system was designed for deployment to a permanent clinic, a bench-top system was designed for laboratory use, and a portable prototype system was designed for deployment to remote communities. The bed-based system was found to have the best spatial resolution with respect to both image and data quality, achieving a best-case resolution of (12.4 +/- 0.5)-mm, and the best signal-to-noise ratio of (26 +/- 2)-dB.

9:30 Analytical and Numerical Solution of the One Dimensional Steady State Bioheat Transfer Equation

[Marco Di Cristofano](#) and Marta Cavagnaro (Sapienza University of Rome, Italy)

This work describes the comparison between the analytical and numerical solution of the one dimensional steady state bioheat equation along the axis of a muscle slab. Aim of the work is the definition of an analytical framework for hyperthermia devices design and optimization. Oncological hyperthermia is a medical technique aimed at generating a temperature increase in the tumour region of the patient through the application of an electromagnetic field. The absorbed electromagnetic power per unit mass is the specific absorption rate (SAR). In this study a plane wave at 434 MHz is considered as electromagnetic source, and the analytical solution is calculated solving the bioheat equation in case of an exponential approximation of the SAR distribution, in order to predict the temperature distribution along the axis of the tissue. Results show an optimum agreement between the analytical and numerical temperature distributions.

9:50 Polynomial Basis Functions for Qualitative Head Tissue Segmentation via Linearized Microwave Imaging

[Darko Ninković](#) (University of Belgrade, Serbia); Álvaro Yago Ruiz (CNR, National Research Council, Italy); Symeon Nikolaou (Frederick Research Center & Frederick University, Cyprus); Lorenzo Crocco (CNR - National Research Council of Italy, Italy); Branko Kolundzija and [Marija Stevanović](#) (University of Belgrade, Serbia)

Microwave imaging of head tissue is a complex task due to the nonlinearity of the underlying inverse scattering problem. Such a difficulty can be alleviated by providing a convenient starting guess to inversion algorithms. To this end, we present an approach to provide a qualitative segmentation of the head tissue, i.e., an image able to identify the different tissue boundaries but not their electromagnetic properties. The proposed approach uses three-dimensional polynomial basis functions for the permittivity distribution under the first-order Born approximation and generalized Tikhonov regularization. To illustrate the possibilities of the proposed method, we apply it to the problem of permittivity reconstruction of the realistic head phantom comprising five tissues. Preliminary results show that the boundaries of all five tissues are identifiable.

Tuesday, March 19 8:30 - 10:10

CS44a: Near Field mmWave and THz Communication and Sensing Systems

T07 THz and high frequency technologies / Convened Session / Antennas

Room: Dochart 1

Chairs: Josep M Jornet (Northeastern University & Institute for the Wireless Internet of Things, USA), Mauricio Rodríguez (Pontificia Universidad Católica de Valparaíso, Chile)

8:30 Development of a Shaped Quartz Lens Antenna for Wide Scanning Sub-Millimeter Imagers

[Huasheng Zhang](#), Shahab Oddin Dabironezare and Nuria LLombart (Delft University of Technology, The Netherlands)

Focal plane arrays (FPAs) with dielectric lenses are promising candidates for achieving wide field-of-view sub-millimeter imaging. A field-correlation method was proposed to analyze the scanning performance of such an FPA coupled to a reflector. In this work, we implement this methodology to develop a shaped quartz lens combined with a leaky-wave feed to achieve a scanning angle up to 20.3 degrees. The simulations show a scanning gain loss of 2.6 dB which is much lower than that associated with the direct fields coming from the reflector (about 6 dB). The shaped lens was fabricated and measured at 180 GHz to validate the proposed concept of lens shaping. The measured reflection coefficient is below -10 dB from 150 GHz to 210 GHz. Moreover, the measured far-field patterns and gain are in excellent agreement with the simulations over the considered frequency band.

8:50 Dual Functional mmWave RIS for Radar and Communication Coexistence in near Field

[Anton Tishchenko](#) and Ahmed Elzanaty (University of Surrey, United Kingdom (Great Britain)); Anna Guerra (University of Bologna, Italy); Francesco Guidi (National Research Council of Italy (CNR) - IEIT, Italy); Alberto Zanella (National Research Council of Italy (CNR), Italy); Mohsen Khalily (University of Surrey & 5G Innovation Centre, Institute for Communication Systems (ICS), United Kingdom (Great Britain))

The paper deals with an integrated sensing and communications system aided by a Reconfigurable Intelligent Surface in the mmWave Near-Field

9:10 A Wideband Reflector-Based Mm-Wave/THz Nearfield Line Scanner for Rapidly Sensing Materials in Envelopes

Carey Rappaport (Northeastern University, USA); Michael Geraghty (Kirtland AFB, USA)

For non-invasive detection of illicit materials arriving at postal facilities, it is important to rapidly scan envelopes. Illegal drugs, shipped in thin packages, can be identified based on form factor (pills) or wideband sub-terahertz frequency signature. To image efficiently, a millimeter-wave or sub-terahertz signal can be focused to a spot on the surface of the package, providing sufficient intensity and resolution to penetrate and distinguish the contents. A flying beam scanner is developed, using a wideband focusing reflector with a small physically rotating feed. The novel shaped reflector scans focal spots along a line on the surface of the envelope, sensing in one dimension. It is assumed that the envelope moves on a conveyor belt. The line scanning time is limited by the mechanical rotation speed of the small feed, which can be accomplished in ~0.01 sec., and the entire envelope could be scanned in less than 1/5th second.

9:30 High Data-Rate Sub-THz Coherent Near-Field Wireless Links Enabled by Spine-Profile Bessel Launchers

Jérôme Taillieu (Université de Rennes 1, France); David González-Ovejero (Centre National de La Recherche Scientifique - CNRS, France); Walter Fuscaldo (Consiglio Nazionale delle Ricerche (CNR), Italy); Laurent Bramerie (Foton CNRS UMR & ENSSAT / Université de Rennes 1, France); Paul Desombre (IETR/CentraleSupélec, France); Mathilde Gay (ENSSAT / Université de Rennes 1, France); Mehdi Alouini (Institut de Physique de Rennes - Université Rennes 1 - CNRS, France); Haifa Farès (Centrale Supélec, France); Yves Louet (CentraleSupélec, France); Mauro Ettorre (University of Rennes 1 & UMR CNRS 6164, France)

This paper presents a robust high data-rate link using two broadband Bessel beam launchers at sub-THz frequencies enabled by photonic down-conversion. An error-free link at 15.5 Gb/s with QPSK modulation format has been achieved in an offline configuration. Bit Error Rate curves at 2.75 Gb/s are measured to demonstrate the resilience of Bessel beams in the presence of an opaque metallic obstacle in the line of sight.

9:50 Interference-Free Transmission for Near-Field Communication with Unlimited Antennas

Zhexuan Yu and Yu Han (Southeast University, China); Jun Zhang (Nanjing University of Posts and Telecommunications, China); Shi Jin (Southeast University, China); Michail Matthaiou (Queen's University Belfast, United Kingdom (Great Britain))

Extra large-scale (XL) multiple-input multiple-output (MIMO) is a potential key technology for the sixth-generation (6G) mobile communication systems. An important conclusion in the early literature is that intra-cell interference vanishes when the number of BS antennas tends to infinity under the far-field channel assumption. However, as the number of antennas increases, users may fall in the near, Fresnel, and far fields. In this paper, we check whether intra-cell interference still vanishes by investigating the correlation among near-field, Fresnel-field and far-field user channels, and find that the channel of a near-field user does not have asymptotic orthogonality with another user in any field. To achieve interference-free transmission, we further propose a novel antenna allocation and power control scheme. Our numerical results show that when the number of antennas is large enough, this transmission scheme can achieve the same performance as the ideal case without any interfering user.

Tuesday, March 19 8:30 - 10:10

P04a: Propagation theory and modeling

T08 EM modelling and simulation tools // Propagation

Room: Dochart 2

Chairs: Thomas Kürner (Technische Universität Braunschweig, Germany), Claude Oestges (Université Catholique de Louvain, Belgium)

8:30 On the Use of Adaptive-Density Point Cloud for Site-Specific Ray-Optics Simulations

Pasi Koivumäki and Katsuyuki Haneda (Aalto University, Finland); Andreas F. Molisch (University of Southern California, USA)

Multipath channel simulations at millimeter-wave frequencies require more accurate knowledge of the geometry of physical environments than at below-6 GHz frequencies because of the shorter wavelength. The accurate geometry can be obtained as a point cloud through LIDAR (light detection and ranging) scanning of the environment. While the use of point clouds for ray-optics simulations of multipath channels has become a popular approach recently, optimized point cloud parameters -- for example its density -- that allow accurate reproduction of multipath channels are not yet known. We propose to use a point cloud that is denser for environments near antennas and is sparser when further from antennas. Compared to using a uniform-density point cloud with 10 cm resolution on average, the use of such an adaptive-density point cloud in ray tracing simulations shows better reproduction of measured multipath channel properties, e.g., delay and angular spreads.

8:50 Improvements of Scintillation Modelling from Radiosonde Observations in the Arctic Region

Florian Quatresooz (UCLouvain, Belgium); Martin Rytir (Norwegian Defence Research Establishment (FFI), Norway); Danielle Vanhoenacker-Janvier (Université catholique de Louvain, Belgium); Claude Oestges (Université Catholique de Louvain, Belgium)

Satellite-to-ground communications at radio-frequencies above 10 GHz and low elevation angles suffer from increased scintillation. Hence, accurate modelling of this effect is required for the design and operation of those communication links. This work presents two new models for predicting the long-term scintillation standard deviation. They are based on radiosonde observations and vertical profiles of the refractive index structure parameter. Comparisons between the models and one year of scintillation measurements in Norway show good correlations and excellent agreement in terms of statistical distributions. They also enable physical insights about the seasonally observed in the measurements.

9:10 Analysis of Propagation Models for Frequency Coordination Between 5G Base Stations and Satellite Earth Stations at FR1

Ahmad Hamada and Thomas Kürner (Technische Universität Braunschweig, Germany)

The deployment of 5G Time Division Duplex (TDD) technology in the 3.6GHz band has revealed novel challenges in the field of interference management w.r.t sharing the spectrum with other radio services in the same or adjacent bands. In order to protect the potential interference victims, propagation models are applied to predict the expected harmful interference in the regulatory process. In such a regulatory process the use widely agreed models usually based on ITU-R recommendations is common practice. In this paper measurements of the received interference at a high-sensitive satellite earth station originating from a 5G base station mimicked by a drone has been used to analyse four propagation models at the 5G Frequency Range 1 (FR1).

9:30 Fully Differentiable Ray Tracing via Discontinuity Smoothing for Radio Network Optimization

Jérôme Eertmans (UCLouvain, Belgium); Claude Oestges (Université Catholique de Louvain, Belgium); Laurent Jacques (University of Louvain, Belgium)

Recently, Differentiable Ray Tracing has been successfully applied in the field of wireless communications for learning radio materials or optimizing the transmitter orientation. However, in the frame of gradient-based optimization, obstruction of the rays by objects can cause sudden variations in the related objective functions or create entire regions where the gradient is zero. As these issues can dramatically impact convergence, this paper presents a novel Ray Tracing framework that is fully differentiable with respect to any scene parameter, but also provides a loss function continuous everywhere, thanks to specific local smoothing techniques. Previously non-continuous functions are replaced by a smoothing function, that can be exchanged with any function having similar properties. This function is also configurable via a parameter that determines how smooth the approximation should be. The present method is applied on a basic one-transmitter-multi-receiver scenario, and shows that it can successfully find the optimal solution.

9:50 Proposal on Application of Quantum Annealers for Analysis of Multiple Scattered Waves

Tetsuro Imai and Keita Fujita (Tokyo Denki University, Japan); Minoru Inomata and Wataru Yamada (NTT, Japan)

Radio wave propagation analysis with raytracing is based on searching for radio propagation paths. Here, to improve the analysis accuracy, it is necessary to search for multiple paths that contribute to the propagation characteristics, but the amount of calculation increases exponentially as the number of structures to be considered and the number of interactions with structures increase. On the other hand, at present, attention is focused on quantum annealing (QA) computer that enable ultra-high-speed operations for combinatorial optimization problems. Here, it can be said that the searching for propagation paths is one of the combinatorial optimization problems. Therefore, we have proposed models applicable to QA for finding propagation paths with multiple scattering. However, these models did not consider the dependence of the scattering pattern on the direction of incidence. In this paper, the model in which scattering pattern depends on incident direction, and its performance is shown.

Tuesday, March 19 8:30 - 10:10

IW7: Advanced materials and manufacturing methods enable new antenna solutions - application use-cases with 3D printable RF lenses, Rogers

Room: M2

8:30 Advanced Materials and Manufacturing Methods Enable New Antenna Solutions - Application Use-Cases with 3D Printable RF Lenses

Presenters: Henrik Ramberg; Romeo Premerlani; Stefano Dada (Rogers GmbH)

Tuesday, March 19 8:30 - 10:10

IW1: Design of tunable antennas, Optenni Ltd

Jussi Rahola, Optenni Ltd

Room: M3

Overview of Frequency Tunable Antenna Concepts, Especially Aperture Tuning

Overview of Closed-Loop Tuning to Adapt to Varying Impedance Environments

Overview of Tunable Components: Capacitor Banks, Switches and Tuner Chips

Efficiency Use of Electromagnetic and Circuit Simulation Tools for Tunable Antennas

Discussion on the Optimization Goals and Methods for Tunable Antenna Design

How to Take Layout Effects into Account in Circuit Optimization

Tuesday, March 19 8:30 - 10:10

IW10: Advanced Simulation Toolchain for Electromagnetic and Radiofrequency Compatibility Applications in Realistic Automotive and Aerospace Application Scenarios, BETA CAE Systems SA

Room: M4

8:30 *Electromagnetic Compatibility for Automotive Applications*

Presenter: Christos Liontas (BETA CAE Systems SA)

9:20 *Radiofrequency Compatibility for Aerospace Applications*

Presenter: Benoît Chaigne (IMACS)

Tuesday, March 19 10:40 - 12:20

SW1b: Active Array Antennas: Design concepts, technologies and over-the-air testing (continued)

Room: Lomond Auditorium

Chairs: Daniele Cavallo (Delft University of Technology, The Netherlands), A. B. (Bart) Smolders (Eindhoven University of Technology, The Netherlands)

10:40 *Active Array Antennas for Non-Terrestrial Communications*

Presenter: Maria Carolina Vigano (Viasat)

11:10 *Over-The-Air Measurements of Integrated Antennas Using a Reverberation Chamber*

Presenter: Anouk Hubrechtsen (ANTENNEX)

11:40 *Front-End Topologies and Calibration Strategies of Active Phased Arrays*

Presenter: Yanki Aslan (Delft University of Technology)

12:10 *SW1 Panel Discussion: Discuss on Future Research Challenges*

Tuesday, March 19 10:40 - 12:20

E06b: Metasurface Design and Applications (continued)

T10 Novel materials, metamaterials, metasurfaces and manufacturing processes // Electromagnetics

Room: M1

Chairs: Dimitris E. Anagnostou (Heriot Watt University, United Kingdom (Great Britain)), Christos Bilitos (University of Rennes, France)

10:40 *Variable Multi-Band Metasurface Reflector with Controllable Direction Using Varactor Diodes Mounted Large-Via Mushroom-Type Structure*

Taisei Urakami (Nara Institute of Science and Technology, Japan); Tamami Maruyama (National Institute of Technology, Hakodate College, Japan); Akira Ono (National Institute of Technology (KOSEN), Kagawa College, Japan); Na Chen and Minoru Okada (Nara Institute of Science and Technology, Japan)

Reconfigurable metasurface reflectors, which are key components of the intelligent reflecting surface (IRS) have recently been considered as the countermeasures for the coverage hole problem in the fifth- and sixth-generation (5G/6G) mobile communication systems. In this paper, a novel varactor diodes mounted large-via mushroom-type (VDLM) structure with a wide reflection phase range is proposed to realize the variable multi-band metasurface reflector with controllable direction. Specifically, two varactor diodes for controlling the reflection direction and frequency band are mounted on the unit cell of the metasurface. In addition, the proposed VDLM structure consists of a large grounding conductor cylinder (large-via) to expand the reflection phase range, and mitigate the influence of the design gap that is caused between each frequency. According to our electromagnetic simulation results, the reflector with the proposed VDLM structure could control the reflection direction at selected frequency with a low sidelobe suppression ratio.

11:00 *Direction-Of-Arrival Estimation by a Programmable Metasurface*

Nawel Meftah and Badreddine Ratni (Univ Paris Nanterre, France); Mohammed Nabil El Korso (Université Paris-Saclay, France); Shah Nawaz Burokur (LEME, France)

We propose a methodology for estimating the direction of arrival (DOA) by a programmable metasurface exploited as an electronically scanned virtual parabolic reflector. Each parabolic reflector configuration fixes its own reception angle, making the incident beams converge to the common focal point where the receiving antenna is located. The DOA is estimated by finding the maximum power recovered by the receiving antenna. Experimental measurements are conducted in an anechoic chamber to validate the proposed method.

11:20 *Multi-Beam Dual Polarised Metasurface Antenna in Ka-Band*

Ravikanth Thanikonda and Marco Faenzi (University of Siena, Italy); David González-Ovejero (Centre National de La Recherche Scientifique - CNRS, France); Enrica Martini and Stefano Maci (University of Siena, Italy)

This paper presents a novel design strategy for a Multi-Beam dual-polarized Metasurface (MTS)-based aperture by leveraging inward and outward surface wave (SW) duplexing. Two approaches are introduced to achieve dual-polarized beams in desired directions. The first method divides the aperture into sectors, each responsible for generating one beam, while the second method employs multiple modulations across the aperture. In both cases, a vertical dipole at the aperture center launches an outward radial SW, interacting with the modulated MTS to create simultaneous beams with either right-hand or left-hand circular polarization. Additionally, edge excitation generates an inward traveling SW, resulting in multiple beams at the same angles but with opposite polarization. An innovative triaxial feeding system is integrated to excite both inward and outward traveling SW, ensuring a low-profile design while maintaining power handling and structural simplicity.

11:40 *A Reconfigurable Phase Gradient Metasurface Rasorber Offering Enhanced Beam Steering Capability and a Tuneable Transmission Band*

Callum J Hodgkinson (University of Edinburgh & Heriot Watt University, United Kingdom (Great Britain)); Dimitris E. Anagnostou (Heriot Watt University, United Kingdom (Great Britain)); Symon K. Podilchak (University of Edinburgh, United Kingdom (Great Britain))

A reconfigurable phase gradient metasurface (PGMS) rasorber design is presented that can provide antenna beam steering and wideband absorption. By creating a varactor loaded, three-layer frequency selective surface (FSS), and individually biasing the adjacent columns, a reconfigurable PGMS can be formed. Then, by further adding a resistive layer with embedded varactors above this PGMS, the structure also becomes

a tuneable rasorber with adjustable absorption bands. As further shown in the paper, the PGMS rasorber can steer a beam from broadside by 30 degrees in either direction, with the ability to tune to intermediate angles by modifying the gradient of the PGMS. Furthermore, by applying a common bias to the columns, the structure can also operate as a rasorber with a tuneable transmission band between 4.1 and 6.4 GHz. To the best knowledge of the authors, no similar multi-functional design achieves combined reconfigurable beam steering and absorption.

12:00 Metasurface Solution for Generating 3D-Curved Beams in Road Environments: A Numerical Study

Narimane awada Mismiani (University of Gustave Eiffel & IFSTTAR-LEOST, France); Divitha Seetharamdoo (Univ Gustave Eiffel COSYS LEOST Univ Lille Nord de France & Univ Lille Nord de France, France)

Cooperative Intelligent Transport Systems (C-ITS) are currently being deployed in Europe and the number of connected vehicles and infrastructure is expected to increase. In this paper, an anomalous metasurface reflector at toll gates is proposed for connected vehicles in IEEE 802.11p. Three-dimensional curved beam relying on holographic technique is introduced to solve the propagation issues due to the highly scattering environment of metallic road infrastructure. It is based on the design of unconventional two-dimensional planar and passive metasurface. Full-wave simulations results at 5.9 GHz are shown to be in good agreement with the curved trajectory specified.

Tuesday, March 19 10:40 - 12:20

CS39b: AMTA Session: Trends, Advancements and Challenges on Measurement Techniques for 5G and Beyond (continued)

T01 Sub-6 GHz for terrestrial networks (5G/6G) / Convened Session / Measurements

Room: Alsh 1

Chairs: Tian Hong Loh (UK, National Physical Laboratory, United Kingdom (Great Britain)), Janet O'Neil (ETS-Lindgren, USA)

10:40 Exploring the Properties of Reverberation Chambers in the THz Range: A Pilot Study

John Kvarnstrand (Bluetest AB, Sweden); Samar Hosseinzadegan (Bluetest, Sweden); [Rutger van Boeijen](#) (University of Twente & Bluetest a. b., The Netherlands); Lawrence Moore and Anders Fransson (Ericsson AB, Sweden)

The rapid evolution of wireless communication technology and the emergence of 6G have led to the exploration of new segments of the electromagnetic spectrum, specifically the THz region. These high frequencies promise exceptionally high data rates, yet they also introduce substantial technical challenges. One primary challenge involves measurement techniques, encompassing component design, instrument manufacturing, and the creation of practical testing environments suitable for these frequencies. In this paper, we focus on employing reverberation chambers as testing environments within the THz region. Firstly, we examine the chamber's characteristics, particularly addressing losses up to 220 GHz. Subsequently, we present the hardware components and introduce a dedicated new mode stirrer designed for operation at these frequencies. The paper also offers insights and establishes a theoretical foundation for loss calculations within the reverberation chamber at high frequencies.

11:00 Estimation of Obtainable Data-Rates in an Over-The-Air mm-Wave MIMO Testbed

Koen Buisman (University of Surrey, United Kingdom (Great Britain) & Chalmers University of Technology, Sweden); Thomas Eriksson (Chalmers University of Technology, Sweden)

In the era of 5G and the forthcoming 6G technology, the demand for advanced communication systems has surged, driving the need for innovative testbeds. These testbeds are vital for the rapid development of hardware and algorithms. Estimation of the capacity potential of mm-wave transceiver arrays is essential to maximise performance. Moreover, an efficient and effective estimation method is indispensable to ensure swift iterations during the development process. Such rapid experimentation is essential for identifying and addressing potential bottlenecks. Here we demonstrate a method based on cross correlation to estimate data-rates in a mm-wave testbed using Over-The-Air measurements only. The method is tested using the Chalmers mm-wave testbed MATE at 29 GHz.

11:20 Broadband Performance Assessment of Compensated Compact Antenna Test Range CCR 75/60 of Airbus at L-Band for Navigation Applications

Björn Niclas Möhring and Engin Gülten (Airbus Defence and Space GmbH, Germany); Josef Migl (Airbus DS GmbH, Germany)

For navigation application, a facility assessment and qualification is performed to measure the antenna group delay of a low gain navigational antenna in a compact antenna test range (CATR) facility at L-band. Motivated is this work by verifying and assuring that the measurement accuracy and limitations of a CATR at low frequencies are sufficient for high precision phase and hence group delay demands for novel GNSS applications. Through facility optimization techniques, echo suppression as well and applying APC technique, very precise group delay results are recorded.

11:40 Millimeter Wave Vector Measurement System Using Low Frequency Band Oscilloscope

Satoru Kurokawa (National Institute of Advanced Industrial Science and Technology, Japan); Masanobu Hirose (7G aa Co., Ltd., Japan); Michitaka Arneya (NMIJ/AIST, Japan)

We have newly developed a millimeter-wave band vector measurement system using a time-domain measurement setup. The system consists of an optical fiber link millimeter-wave transmission system, an IF substitution method configuration as a receiving system, and a low-frequency band-type oscilloscope. In this paper, we show the developed millimeter-wave measurement system configuration. Then, we demonstrate a time-domain antenna pattern measurement for two standard gain horn antennas. Then, we show the radiation pattern for the estimated magnitude and phase.

12:00 Antennas and Power Measurement Techniques for Wireless Applications

Walid El Hajj (Intel Corporation, France); Juan Antonio Del Real (Wireless Telecom Group Inc., France); Tsitoha Andriamiharivolamena (Intel Corporation, France); Bob Buxton (Boonton- Wireless Telecom Group- Parsippany- NJ, USA); Nawfal Asrih (Intel Corporation, France)

This paper explores the time variation power measurement complexities of multi-output systems in dynamic scenarios, focusing on advanced power measurement techniques for regulatory compliance. Time Average Specific Absorption Rate (TAS); a critical feature commonly used in wireless devices as human exposure mitigation method, is a typical illustration for dynamic scenarios. While TAS measurement is straightforward in single-band, single-output scenario, it becomes more challenging, when involving multiple outputs and multiple bands requiring simultaneous measurements. In this paper multiple architecture of power time varying measurement solutions will be presented in multi-output context. These are illustrated in two cases: one with multi-band simultaneous transmission from the same antenna, and the other with multi-antenna simultaneous transmission on the same band.

Tuesday, March 19 10:40 - 12:20

A27b: Mm-wave antenna technologies I (continued)

T02 Mm-wave for terrestrial networks 5G/6G // Antennas

Room: Alsh 2

Chairs: Oscar Quevedo-Teruel (KTH Royal Institute of Technology, Sweden), Lei Wang (Heriot-Watt University, United Kingdom (Great Britain))

10:40 A Wideband High-Gain Circularly-Polarized Metasurface Antenna with a Large Element Spacing SIW Array at Ka Band

Yuehe Ge and Jiahong Chen (Fuzhou University, China); Jingru Wang (Motorola Mobile Internet Technology Co Ltd, China); Zhizhang (David) Chen (Dalhousie University,

Canada)

In this paper, a novel Ka-band circularly-polarized planar metasurface antenna is proposed, which is based on an innovation technique for suppressing grating lobes in antenna arrays featuring large element spacing. It consists of a substrate-integrated-waveguide (SIW) array with a large element spacing and a metasurface lens. The SIW array and the compact meta-lens are first developed separately. They are then integrated to construct the metasurface antenna, where the grating lobes are effectively suppressed and the gain is significantly improved. Simulations are carried out to validate the antenna design, yielding impressive results, including a peak gain of 26.92 dBi and an expansive 3-dB axial ratio (AR) bandwidth of over 23%. This innovative antenna design provides an alternative way to realize high-gain antenna arrays, offering distinct advantages of design simplicity and the ability to overcome difficulties associated with processing, tuning, and reliability, especially in the millimeter-wave band.

11:00 A Radial Waveguide Power Divider Inspired Antenna for mmWave IoT Sensing Applications

Md. Abu Sufian (Chungbuk National University, Korea (South)); Niamat Hussain (Sejong University, Korea (South)); Domin Choi (Korea Radio Promotion Association, Korea (South)); Yangbae Chun (KAIST, Korea (South)); Qasid Hussain (Chungbuk National University, South Korea, Korea (South)); Nam Kim (Chungbuk National University, Korea (South))

This paper presents the design and investigation of a radial waveguide power divider (RWPD) based antenna with omnidirectional radiation characteristics for the 5G millimeter-wave IoT sensing applications. The presented antenna consists of a circular radiating loop, shorting vias, and eight non-uniform array dipole structures. The radiating circular loop is fed by an SMA connector, while the shorting vias are utilized to create a one-to-eight radial waveguide power divider to supply power to the eight different dipole structures. The antenna is modeled and manufactured on an 8 mils thick Rogers-RO003C substrate. The simulated and tested findings confirm that the antenna offers a -10 impedance bandwidth ranging from 28.39 - 28.97 GHz and a peak gain of 5.46 dBi with an omnidirectional radiation pattern. Due to its comprehensive set of performance attributes, particularly for the omnidirectional radiation characteristics, the suggested antenna is a viable candidate for 5G millimeter wave IoT sensing applications.

11:20 Single Material Multilayer Radome for D Band Applications

Arto Hujanen and Vladimir Ermolov (VTT Technical Research Centre of Finland, Finland)

The paper presents results of design and testing of a single material multilayer (SMML) radome for applications in D-band. The two-layer radome is designed and tested. Both layers are fabricated of a single material plate of PREPERM RS260 material. The first layer is a homogeneous layer, and the second layer has a pattern of cavities configured to decrease an effective dielectric constant of the material. The radome demonstrates transmission losses 0.15 dB at the frequency 150 GHz. It has a wider bandwidth than a wavelength radome fabricated from the same material. Possibility of realization of a single material multi-layer wideband radome is studied.

11:40 Design of a Hollow-Waveguide Slot Array Antenna for a Channel Sounder in the 150 GHz Band

Jiro Hirokawa, Rikako Yamaguchi and Takashi Tomura (Tokyo Institute of Technology, Japan); Minoru Inomata and Wataru Yamada (NTT, Japan)

A hollow-waveguide slot array antenna is designed for a channel sounder operating in the 150 GHz band. The antenna design features a narrow-wall slot array on four rectangular waveguides fed by an E-plane horn. Laminated thin metal plates will be diffusion bonded to enable precise fabrication of the antenna. During this process, a triangular corner and a reflection canceling wall with gaps will be formed. A 16x4 slot array accomplishes uniform excitation and 24.8 dBi realized gain at 158 GHz through the utilization of a hollow waveguide structure, resulting in high antenna efficiency.

12:00 Flexible Phase-Reconfigurable Branch Line Coupler for Millimeter-Wave Phased Array Antenna

Fayyadh Ahmed (University of Sheffield, United Kingdom (Great Britain) & University of Duhok, Iraq); Rola Saad (The University of Sheffield, United Kingdom (Great Britain)); Salam Khamas (University of Sheffield, United Kingdom (Great Britain))

This paper presents a reconfigurable phase-shift branch line coupler (BLC) design. The proposed design is developed based on a defective microstrip line (DML), where all of the conventional microstrip lines of an ordinary BLC are replaced by the DML structure. To realize the phase delay line, four PIN diode switches are used in the DML structure, which redirect the current paths between the input and output ports of the BLC, consequently providing a variety of phase differences at the output ports. Changing PIN diode switch states enables phase shifts between 100 and 150 degrees. The proposed design operates millimeter-wave (mmWave) with a resonant frequency of 25.5 GHz. The design parameters are studied and analyzed using the CST Studio Suite software package. The proposed reconfigurable BLC can be employed as phase shifters, offering a flexible, low-cost solution for mmWave phase array antennas.

Tuesday, March 19 10:40 - 12:20

CS10: Dome antennas for the next generation of terrestrial and satellite communication systems

T03 Aerospace, new space and non-terrestrial networks / Convened Session / Antennas

Room: Boisdale 1

Chairs: Astrid Algaba-Brazález (Ericsson AB, Sweden), Maria Carolina Vigano (Viasat Antenna Systems SA, Switzerland)

10:40 Efficient Ray-Tracing Model for Generalized 2D Dielectric Lenses Combined with Arrays

Maria Pubill-Font (University of Technology Sydney (UTS), Australia); Francisco Mesa (University of Seville, Spain); Astrid Algaba-Brazález (Ericsson AB, Sweden); Martin Johansson and Lars Manholm (Ericsson Research, Sweden); Pilar Castillo-Tapia and Sarah E Clendinning (KTH Royal Institute of Technology, Sweden); Can Ding (University of Technology Sydney (UTS), Australia); Y. Jay Guo (University of Technology Sydney, Australia); Oscar Quevedo-Teruel (KTH Royal Institute of Technology, Sweden)

In this paper a simple and efficient ray-tracing model is presented to evaluate two-dimensional (2D) multilayer dielectric lenses combined with arrays. The proposed algorithm is capable of accurately evaluating the reflection and absorption losses of the lens. Two examples have been simulated with the proposed algorithm and compared with a commercial full-wave simulator. We demonstrate that the proposed method provides a very good agreement with the simulations, reducing considerably the computation time, and thus offering an effective tool for design optimization.

11:00 Design of a Dielectric Lens Using a Ray-Tracing Model for Satellite Communications

Núria Flores-Espinosa and Pilar Castillo-Tapia (KTH Royal Institute of Technology, Sweden); Francisco Mesa (University of Seville, Spain); Maria Carolina Vigano (Viasat Antenna Systems SA, Switzerland); Oscar Quevedo-Teruel (KTH Royal Institute of Technology, Sweden)

In millimeter-wave applications, it is essential to use highly directional and steerable antennas. Phased array antennas are the most common choice, but they have restricted scanning coverage because of their effective aperture. To enhance the scanning coverage, a dielectric lens can be placed on top of the array. However, full-wave simulations require a lot of computing time to simulate this type of structure. In this work, a two-dimensional ray-tracing model has been adapted and improved to efficiently compute the radiation pattern of arrays combined with multilayered dielectric radomes for satellite communications applications. Moreover, this model can also calculate the absorption and reflection losses and the transmitted power required to comply with the regulatory mask. This model has been used to design a lens that increases the scanning range of an array while maintaining a maximum height and ensuring that it complies with the regulatory masks for satellite communications.

11:20 D-Band Active Antenna Array with Lens Enabling Quasi-Optical and Analogue Beam Reconfiguration for 6G Applications

Marta Arias Campo, Simona Bruni, Wolfgang Wischmann, Andreas Lauer and Aline Friedrich (IMST GmbH, Germany); Michael Wleklinski (IMST, Germany); Christos Oikonomopoulos-Zachos and Oliver Litschke (IMST GmbH, Germany); Karthik Krishnegowda (IHP GmbH, Innovations for High Performance Microelectronics, Germany); Christoph Herold (IHP, Germany); Nicolò Moroni (IHP GmbH, Germany); Wilhelm Keusgen (Technische Universität Berlin, Germany)

In this paper, a proof-of-concept at D-band (110-170 GHz) is presented for a hybrid quasi-optic and analogue beamforming approach, involving an elliptical lens and an active focal plane array. The quasi-optic technique reduces the beam squint over frequency. Analogue phase shift in the focal plane array is used to increase the lens steering range. A prototype including two 4-channel D-band transceivers with on-chip antennas has been built as a first demonstrator. The resulting active focal plane array consists of 2x4 antenna elements, which are tuned in amplitude and phase to reconfigure the beam. The concept will be scaled to larger focal plane arrays in future development steps.

11:40 *Metasurface Dome Enhancing Beam Scanning of AESA Panels*

Joaquín García Fernández (WAVE UP SRL & University of Siena, Italy); Enrica Martini and Stefano Maci (University of Siena, Italy)

Active Electronically Scanned Arrays (AESA) provide a limited beam scanning range without experiencing impedance mismatch or producing secondary lobes. This field of view (FoV) limitation becomes critical for the implementation of localization systems, such as a monopulse radars. This study evaluates the improvement in the scanning performance of an AESA panel when it is combined with a dome-shaped metasurface. We present a general technique to achieve wide-angle matching for the AESA panel system by jointly designing the dome's phase profile and the array's complex excitation. The approach for the design of the metasurface implementing the desired phase profile is also discussed. Numerical results are reported, demonstrating the riddance of the field of view (FoV) restriction in monopulse active phased arrays.

12:00 *On the Scanning Properties of Bidimensional Discrete Lens Antennas with 1, 3, Infinite Focal Points*

Giovanni Toso (European Space Agency, ESA ESTEC, The Netherlands); Piero Angeletti (European Space Agency, The Netherlands)

Discrete lens beamforming networks and antennas are also known as bootlace lenses, constrained lenses, or discretized array lenses. The main benefits associated to this type of discrete lens BFN are associated to the simple implementation in Printed Circuit Board Technology (PCB), the excellent scanning capabilities, the free-space beamforming, and the true-time delay behavior. While two-dimensional bootlace lenses have been investigated intensively in the literature starting from some seminal contributions, three-dimensional lenses have been investigated mainly in the last years. The main objective of this communication is to compare 2D and 3D discrete lens antennas identifying pros and cons of both type of architectures.

Tuesday, March 19 10:40 - 12:20

A09b: Advances in reconfigurable antenna technologies (continued)

T10 Novel materials, metamaterials, metasurfaces and manufacturing processes // Antennas

Room: Boisdale 2

Chairs: Francesco Foglia Manzillo (CEA-LETI, France), James Kelly (Queen Mary University of London, United Kingdom (Great Britain))

10:40 *X-Band Reconfigurable Phase Shifters Based on SIW and Liquid Metal Technologies*

Shaker Alkarak (University of Nottingham, United Kingdom (Great Britain)); Quan Wei Lin (City University of Hong Kong, Hong Kong); Syeda Fizzah Jilani (Aberystwyth University, United Kingdom (Great Britain)); Hang Wong (City University of Hong Kong, Hong Kong); Alejandro L. Borja (Universidad de Castilla-La Mancha, Spain); Shiyang Tang (University of Southampton, United Kingdom (Great Britain)); Yi Wang (University of Birmingham, United Kingdom (Great Britain)); James Kelly (Queen Mary University of London, United Kingdom (Great Britain))

This paper presents three reconfigurable phase shifters operate at X-band and designed utilizing liquid metal (LM). The phase shifters operate at 10 GHz and they have very low insertion loss performance and able to handle high levels of radio frequency (RF) power. Besides, the proposed phase shifters able to achieve a total of 360° phase shift and they are compact in size as they are designed using substrate integrated waveguides (SIW). This enable the proposed phase shifters to be integrated within SIW based feeding structures to realize complete phased array antenna systems. The phase shift is realized by inserting a series of liquid metal vias in the SIW. When a single or multiple via connection is needed, the via hole is filled with liquid metal and conversely, the liquid metal is withdrawn from the via when the connection is no longer required.

11:00 *Recent Advances in Plasma Surfaces*

Mirko Magarotto (University of Padova, Italy); Luca Schenato (National Research Council, Italy); Marco Santagiustina, Andrea Galtarossa and Antonio-D. Capobianco (University of Padova, Italy)

Plasma-based surfaces represent an innovative alternative approach for reconfiguring electromagnetic (EM) signals. These structures comprise an array of plasma discharges, which can integrate a metallic ground plane if the surface is operated in reflection mode. Recent developments in theoretical and numerical models demonstrate that plasma-based surfaces offer beam steering and polarization control capability. This is achievable by tuning the EM response of plasma through its properties, such as density, which can be electronically controlled. Furthermore, the range for the plasma properties enabling plasma-based reflective or transmit surfaces is consistent with the discharge technologies at the state-of-the-art. This paper presents a comprehensive overview of the recent progress made in plasma-based surfaces, emphasizing their relevance and outlining the roadmap toward realizing the first proof-of-concepts.

11:20 *Ultra-Low-Loss Millimeter Wave Beam Scanning Antenna Using Piezoelectric Actuation*

James Churm (University of Birmingham, United Kingdom (Great Britain)); Muhammad S Rabbani (Plextek, United Kingdom (Great Britain)); Ioannis Gerafentis and Alexandros Feresidis (University of Birmingham, United Kingdom (Great Britain))

An enhanced beam scanning angle, leaky-wave, antenna is presented with high efficiencies at millimeter wave frequencies and above, enabled by the tuning mechanism residing wholly outside the millimeter wave circuit. This is achieved by forming a cavity between a Partially Reflective Surface (PRS) and a phase tuneable High Impedance Surface (HIS). A phase change is achieved by the micro-motion of the HIS ground plane, provided by a piezoelectric actuator. This phase change translates to a beam steer of the leaky wave radiating from the PRS. In order to compensate for limited beam scan, a dual cavity has been incorporated into a single antenna, in which resides a switchable feed that can selectively energize parts of the cavity to create a $\pm 40^\circ$ beam steer with radiation losses of 0.65-0.92 dB, total losses ranging between 1.6-2.58 dB, realized gain between 17.8 and 20.63 dBi, and bandwidth of 2 GHz.

11:40 *Loss Analysis for Compact Liquid Crystal Delay Lines Based on Defective Ground Structures*

Robin Neuder (Technical University Darmstadt, Germany); Marc Späth (Technische Universität Darmstadt, Germany); Martin Schüßler (TU Darmstadt, Germany); Alejandro Jiménez-Sáez (Technische Universität Darmstadt, Germany)

This paper analyzes loss contributions in novel, high-performance Liquid Crystal (LC) microstrip delay lines with defected ground structures. While providing a significant miniaturization of the tunable delay line, the aforementioned topology enables low losses despite thin LC layer thickness, which is a requirement for millisecond LC response times. These features result in a wide range of potential applications, including but not limited to phased arrays, reflectarrays and reconfigurable intelligent surfaces. Within this contribution, we conduct a comprehensive comparative analysis with a focus on dielectric and conductor loss contributions between a conventional inverted microstrip line (IMSL) and the defected ground structure IMSL (DGS-IMSL). The DGS-IMSL achieves a high FoM above 70 °dB in a bandwidth of 8.8 GHz (30%) at 28.8 GHz in measurements, despite a thin LC layer of only 4.6 µm.

12:00 *Liquid Metal Reconfigurable Phased Array Antenna*

Shaker Alkarak (University of Nottingham, United Kingdom (Great Britain)); Quan Wei Lin (City University of Hong Kong, Hong Kong); Fuad Erman (Nablus University for Vocational and Technical Education, Palestine); Syeda Fizzah Jilani (Aberystwyth University, United Kingdom (Great Britain)); Zhengpeng Wang (Beihang University, China); Hang Wong (City University of Hong Kong, Hong Kong); James Kelly (Queen Mary University of London, United Kingdom (Great Britain))

A design for a phased array antenna using liquid metal (LM) technology is presented. The phased array antenna uses substrate integrated waveguides (SIW) to excite a 1x4 printed dipole antenna array. The phase distribution on SIW power dividers is managed using LM shorting pins/vias inside the SIW. The integrated LM vias offers an extensive phase tuning range of 360°, delivering stable, low-loss, and broad-frequency performance. In more detail, the reconfigurability of phase control within the array can be realized by manipulating the presence or absence of liquid metals in designated vias in the SIW. A prototype of the LM phased array antenna, operating at 10 GHz, has been measured, demonstrating an impedance bandwidth exceeds 10% with maximum gain of higher than 8 dBi and a scanning range spanning approximately $\pm 40^\circ$ along the end-fire direction. This technology holds promise as a reliable and cost-effective solution for wideband phased array applications.

Tuesday, March 19 10:40 - 12:20

CS36b: New antenna systems for Direction-of-Arrival estimation (continued)

T05 Positioning, localization, identification & tracking / Convened Session / Antennas

Room: Carron 1

Chairs: Jose-Luis Gómez-Tornero (Polytechnic University of Cartagena, Spain), Julien Sarrazin (Sorbonne Université, France)

10:40 Safe Beamforming Based on Human Area Estimation for Microwave Wireless Power Transfer

[Kentaro Murata](#), Haruki Yamamoto, Kyoshiro Muramatsu and Naoki Honma (Iwate University, Japan)

This paper proposes a safe beamforming (BF) method based on human area estimation for microwave wireless power transfer (MWPT). The proposed method assumes that multiple MPWT transmitting/receiving (Tx/Rx) arrays operate cooperatively and configure a multistatic multiple-input multiple-output radar. This enables human width estimation by combining the human channel and location information acquired using only the radio-frequency front-end. Finally, a safe BF maximises the Rx power density while maintaining the power density in the estimated human width range below the maximum permissible exposure (MPE). Electromagnetic simulation results show that the proposed method achieves a high Rx power density, with only a 1.4 dB difference from the achievable maximum, and satisfies the MPE in the entire human area, even without prior human geometry information. The above results prove the superiority of the proposed BF method over conventional methods in terms of the safe and secure operation of MWPT.

11:00 Direction-Of-Arrival Ambiguities Mitigation in Multibeam Leaky-Wave Antennas

Julien Sarrazin and Guido Valerio (Sorbonne Université, France)

The inherent frequency beam scanning behavior of leaky-wave antennas (LWA) enables estimating directions of arrival (DoA) with a reduced complexity with respect to antenna-array-based DoA estimation. It has been shown recently that making use of multiple fast Floquet harmonics in periodic LWA can drastically reduce the frequency bandwidth required to scan a large angular field of view. However, with this multibeam operation, the columns of the LWA response matrix are not linearly independent which gives rise to ambiguities, i.e., spurious peaks in the MUSIC pseudo spectrum, in the DoA estimation. Indeed, if the number of snapshots and/or SNR is not sufficiently high, DoA ambiguities arise which leads to false detection. To tackle this issue, this paper investigates an approach to make use of signals received by both ports of a 1-D LWA in order to effectively mitigate those ambiguities.

11:20 Towards a Reconfigurable Metacavity Antenna for Computational Imaging and DoA Estimation

[Mengran Zhao](#) (Queen's University Belfast, United Kingdom (Great Britain) & Xi'an Jiaotong University, China); Luyi Wang and Shitao Zhu (Xi'an Jiaotong University, China); Muhammad Ali Babar Abbasi (Queen's University Belfast & The Institute of Electronics, Communications and Information Technology (ECIT), United Kingdom (Great Britain)); Thomas Fromenteze (University of Limoges & Xlim Research Institute CNRS, France); Okan Yurduseven (Queen's University Belfast, United Kingdom (Great Britain))

In this paper, a reconfigurable metacavity antenna (RMA) that can be used for microwave computational imaging (CI) and direction of arrival (DoA) estimation applications is proposed. The RMA is an electrically over-sized metacavity with its back wall replaced by a 1-bit reconfigurable metasurface and its top surface etched with leaky circular irises. By leveraging the frequency-diversity and the dynamic aperture techniques, spatio-temporally low-correlated radiation patterns can be generated by the RMA at different operating frequencies and under different PIN states. The correlation coefficients are smaller than 0.3 and the singular values are close to each other, which demonstrates the spatial-orthogonality of the measurement modes. Simulated experiments are implemented to validate the feasibility of the proposed RMA for CI and DoA estimation. Using the developed RMA, the target image has been reconstructed and the far-field source has been estimated. The proposed design is validated through simulations in CST Microwave Studio.

11:40 Simplified Frequency-Diverse Array Architecture for Surveillance Purposes

Enrico Fazzini (Università di Bologna, Italy); Tommaso Tiberi (University of Bologna, Italy); Lorenzo Bastia (Università di Bologna, Italy); Alessandra Costanzo (DEI, University of Bologna, Italy); Diego Masotti (University of Bologna, Italy)

This work presents a novel analysis of frequency diverse arrays (FDAs) for radar applications when real radiating structures are involved. A straight comparison with the ideal FDA behavior has demonstrated the limits of real radiating architectures and the characteristics that they should have in terms of half-power beamwidth (HPBW) and directivity for optimal FDA performance. The best topology has been identified in series-fed arrays as single radiating element, offering a wide visible range in the plane where the frequency diversity scheme is applied and improved directivity in the orthogonal one. The analytical results are supported by a measurement campaign where the characterization of a wideband planar series-fed frequency diverse array working at 1.95 GHz is provided. The results have highlighted this topology as one of the most promising solutions for localization purposes if frequency diversity is exploited.

12:00 Multi-Directional Leaky-Wave Antenna with Independent Beam-Scanning Laws

Francis Baccin-Smith and Shulabh Gupta (Carleton University, Canada)

A multi-directional periodic leaky-wave antenna (LWA) is presented for the X-band frequencies with suppressed stop-band and independent beam-scanning laws for left, right, and top sides of the antenna, respectively, using tri-directional LWA as an example. The tri-directional antenna is designed to radiate out-of-plane beams along three directions on the top face and each antenna edge. The antenna is a combination of a top-radiating slot-pair array and side-fire Vivaldi array to achieve flexible placements of the beams at a given design frequency along three unique directions. The antenna can be engineered to emit high gain beams along specified angles, and can be adapted to provide precision control of the independent output beams in various frequency bands.

Tuesday, March 19 10:40 - 12:20

CS24b: Biomedical Microwave Techniques and Devices from Diagnosis to Treatment (continued)

T06 Biomedical and health / Convened Session / Antennas

Room: Carron 2

Chairs: Raquel C. Conceição (Instituto de Biofísica e Engenharia Biomédica, Faculdade de Ciências, Universidade de Lisboa, Portugal), Jorge A. Tobon Vasquez (Politecnico di Torino, Italy)

10:40 Microwave Tomography Bone Imaging: Analysing the Impact of Skin Thickness on the Reconstruction of Numerical Bone Phantoms

Alessia Cannatà (University of Pavia, Italy); Adnan Elahi and Martin O Halloran (University of Galway, Ireland); Marco Pasion, Simona Di Meo and Giulia Matrone (University of Pavia, Italy); Bilal Amin (University of Galway, Ireland)

Microwave Tomography (MWT) is an emerging diagnostic tool for assessing bone health. This study introduces a realistic calcaneus-shaped bone phantom with an outer skin layer to investigate its impact on MWT bone reconstruction. Simulated data was collected using 16 antennas, and reconstructed using the Distorted Born Iterative Method (DBIM) and an Iterative Method with Adaptive Thresholding for Compressed Sensing (IMATCS) with L2-regularization. Results demonstrate successful inner bone tissue reconstruction, but challenges arise when the skin layer exceeds 2 mm. This underscores the importance of including the skin layer in numerical investigations for accurate clinical replication.

11:00 On the In-Vivo Electrical Properties of Human Forearm at Microwave Frequency

Martina Teresa Bevaacqua (Università Mediterranea di Reggio Calabria, Italy); Michele Ambrosanio (University of Naples Parthenope, Italy); Joe LoVetri (University of Manitoba, Canada); Vito Pascazio (Università di Napoli Parthenope, Italy); [Tommaso Isernia](#) (University of Reggio Calabria, Italy)

The paper proposes a new microwave procedure to extract the in-vivo electrical properties of biological tissues. The procedure is tested against microwave experimental data collected at the Electromagnetic Imaging Laboratory of the University of Manitoba and allows the estimation of the electrical properties of in-vivo human forearms.

11:20 *Analysis of Return Loss with an Uncooled Coaxial Monopole Antenna During Microwave Ablation*

[Federico Cilia](#), Lourdes Farrugia, Julian Bonello, Charles Sammut and Iman Farhat (University of Malta, Malta); Evan Dimech (University of Malta & University of York, Malta)

Microwave tumour ablation is a percutaneous cancer treatment that irreversibly destroys tumour cells with heat, where high temperatures over 100°C are reached. The process involves the interaction of microwave electric fields with biological tissue. This interaction is dependent on the temperature-dependent dielectric permittivity and effective conductivity. A dual-mode microwave ablation system was developed to measure dielectric properties utilising an uncooled insulated monopole. As a preliminary study, the return loss during ablation was investigated at 2.45 GHz. This was measured using a power meter during powered conditions and a Vector Network Analyser (VNA) with controlled switching. Three different power conditions were employed: 10 W, 30 W and 50 W. Although deviations were obtained during specific instances, a relative agreement was obtained between the return losses measured with the power meter and VNA. Ultimately, this paper briefly discusses the possible causes that led to the measurement deviations experienced with the presented ablation technique.

11:40 *Developments in Open-Source Tools for Microwave Breast Imaging*

Declan O'Loughlin (Trinity College Dublin, Ireland)

Open-source models, datasets and toolboxes are becoming increasingly common in the microwave breast literature, including numerical breast models, simulated and experimental datasets and imaging and analysis tools. These tools lower the barrier to entry for researchers interested in radar-based breast imaging, and also present the opportunity to test algorithms and approaches on multiple datasets with difference advantages and disadvantages. In this work, recent developments in open-source tools for radar-based breast imaging are reviewed. Moreover, uses of the MERIT toolbox and BRIGID dataset are examined and recent developments highlighted. Finally, gaps in the open-source landscape in terms of simulation and antenna design and standardised approaches are identified.

12:00 *Wideband Dielectric Characterization of Biological Tissues and Realistic Phantom Preparation at Microwave Frequencies*

Flavia Liporace (Sapienza University of Rome, Italy); Klementina Vidjak (Sapienza, University of Rome, Italy); Marco Di Cristofano and Marta Cavagnaro (Sapienza University of Rome, Italy)

Oncological hyperthermia is a medical technique whose aim is to heat tumours at 41-43 °C for one hour through the application of an electromagnetic field (EMF). Hyperthermia proved to improve both chemotherapy and radiotherapy. For best hyperthermia performances, the knowledge of the dielectric properties (permittivity and conductivity) of the patient is essential, since these properties represent the response of materials to the applied EMF. This information can be used to optimize the treatment's results but also to validate the hyperthermia device before the application on the patient. The validation procedure is usually done on phantoms, i.e., mixtures of materials which mimic the dielectric properties of biological tissues. This work presents the realization of a muscle equivalent mixture and the measurement of its dielectric properties with the open-ended probe technique. Results were compared with the dielectric properties of ex-vivo animal muscle samples that were measured with the same procedure.

Tuesday, March 19 10:40 - 12:20

CS44b: Near Field mmWave and THz Communication and Sensing Systems (continued)

T07 THz and high frequency technologies / Convened Session / Antennas

Room: [Dochart 1](#)

Chairs: Josep M Jornet (Northeastern University & Institute for the Wireless Internet of Things, USA), Mauricio Rodríguez (Pontificia Universidad Católica de Valparaíso, Chile)

10:40 *Spherical Wavefront Near-Field DoA Estimation in THz Automotive Radar*

Ahmet M Elbir (University of Luxembourg, Luxembourg); Kumar Vijay Mishra (United States DEVCOM Army Research Laboratory, USA); Symeon Chatzinotas (University of Luxembourg, Luxembourg)

Automotive radar at terahertz (THz) band have the potential to provide compact design and achieve high angular and range resolution thanks to the abundant bandwidth and very narrow beamwidth. These features are one of the key enabling factors to achieve milli-degree level direction-of-arrival (DoA) estimation. Due to high frequency operations in THz-band, the signal wavefront becomes spherical in the near-field. Therefore, this paper examines near-field DoA estimation problem for THz automotive radar. To that end, we employ the multiple signal classification (MUSIC) algorithm to estimate target DoAs and ranges. The impact of beam-squint in near-field is also taken into account. Specifically, we propose an array transformation approach, and obtain the corrected noise subspaces to compensate for the impact of near-field beam-squint and construct the beam-squint-free MUSIC spectra. Via numerical experiments, we show the effectiveness of the proposed method to accurately estimate the target parameters.

11:00 *Design and Characterization of an Imaging System Using Photoconductive Connected Arrays*

Martijn D. Huiskes, Nuria LLombart, Juan Bueno and Andrea Neto (Delft University of Technology, The Netherlands)

Photoconductive antennas allow for sub-mm depth resolution in imaging scenarios because of their large bandwidth in the THz range. In this work, for the first time, we present the design and characterization of an imaging system using a leaky wave photoconductive connected array both as transmitter and receiver. The transfer function of the channel between Tx and Rx is evaluated using Fourier Optics together with a field-correlation technique. This methodology is then exploited to include an arbitrary dielectric stratification in the imaging plane of the system, and can be extended to evaluate the received pulse shape and amplitude of an imaging radar illuminating complex targets. The time-evolution of the transmitted pulse is evaluated using a TD Norton circuit in transmission. Using the transmitter pulse together with the channel transfer function, the received pulses are evaluated using a TD Norton model for receivers.

11:20 *Multibeam Metal-Only Groove Gap Waveguide-Based Array in E-Band*

[Sergio Menéndez Feito](#) (University of Oviedo, Spain); Álvaro F. Vaquero and Manuel Arrebola (Universidad de Oviedo, Spain)

Radar technology, particularly at the 76-81 GHz band, plays a central role in ADAS (Advanced Driver Assistance Systems) development, offering precise measurements and robustness in obstacle detection. This study presents a gap waveguide-based, metal-only antenna, combining low transmission losses with scalable design. The proposed 1×8 slotted array antenna, fed through groove gap waveguide technology, provides multi-channel and multibeam operation. Its metal-only construction ensures seamless integration into vehicle chassis while maintaining efficiency in automotive frequency bands. The proposed structure behavior has been simulated and validated through full-wave simulations in CST Microwave Studio. The results present a potential candidate for antennas with multibeam performance in E-band.

11:40 *Curving THz Beams in the near Field: A Framework to Compute Link Budgets*

Hichem Guerboukha (University of Missouri-Kansas City, USA); Bin Zhao (Rice University, USA); Zhaoji Fang (Brown University, USA); Edward W. Knightly (Rice University, USA); Daniel Mittleman (Brown University, USA)

We present a framework to engineer the trajectory of curved THz beams in the near-field region, with a focus on computing link budgets.

12:00 *Graph Neural Network Based 77 GHz MIMO Radar Array Processor for Autonomous Robotics*

Ransara Wijitharathna (University of Moratuwa, Sri Lanka); Pahan Mendis (University of Moratuwa, Sri Lanka); Rahal Perera and Punsara Mahawela (University of Moratuwa, Sri Lanka); Nilan Udayanga (University of Akron, USA); Chamira U. S. Edussooriya (University of Moratuwa, Sri Lanka); Arjuna Madanayake (Florida International University, USA)

Frequency-modulated continuous-wave (FMCW) multiple-input multiple-output (MIMO) long range radars currently employed for autonomous robotics have limited maximum range. By employing transmit beamforming and beam scanning, the range can be increased, however, the beam scanning time reduces the achievable velocity resolution. In this paper, we propose an FMCW MIMO radar, operating at 77 GHz, with transmit (TX) beamforming with subarrays to increase the range. We employ four TX subarrays, each having three antennas, with analog beamforming. Compared to TX beamforming as one TX array, our approach provides sufficiently wide beams alleviating beam scanning, further, without substantially reducing the virtual elements of the MIMO radar. We implement the radar signal processing pipeline on an ZYNQ Ultrascale+ ZCU106 FPGA to achieve real-time processing. Furthermore, we employ a graph neural network to detect objects using the radar point cloud. Preliminary results are presented to confirm the operation of

Tuesday, March 19 10:40 - 12:20

P04b: Propagation theory and modeling (continued)

T08 EM modelling and simulation tools // Propagation

Room: Dochart 2

Chairs: Thomas Kürner (Technische Universität Braunschweig, Germany), Claude Oestges (Université Catholique de Louvain, Belgium)

10:40 Grid-Based Shadowing Gain Modeling for Handling Dynamic Objects in Wireless Channel Emulation

Nopphon Keerativoranan, Siraphop Saisa-ard and Jun-ichi Takada (Tokyo Institute of Technology, Japan)

Adopting deterministic channel modeling to accurately assess wireless system performance with a wireless channel emulator (WCE) presents a challenge due to the substantial computational time required, which contrasts with the real-time computation demand of WCEs. Grid-based channel modeling technique had previously conceptualized to address this issue. This technique enables real-time emulation of the deterministic channel of the mobile station (MS) by interpolating precomputed path parameters at adjacent grid nodes. However, the modeling framework cannot account for the shadowing effect caused by moving objects introduced during emulation. In this paper, grid-based shadowing gain modeling is introduced to incorporate the shadowing effect into the emulated channel. The shadowing contribution at the MS is interpolated from values computed at the grid nodes using the approximated knife-edge diffraction model. The applicability and limitations of the proposed model are investigated analytically, and rigorous simulations are provided to numerically validate the proposed method.

11:00 Ray-Tracing Calibration from Channel Sounding Measurements in a Millimeter-Wave Industrial Scenario

Grégory Gougeon (SIRADEL, France); Frederic Munoz (CEA LETI & University of Grenoble-Alpes, France); Yoann Corre (SIRADEL, France); Raffaele D'Errico (CEA, LETI & Université Grenoble-Alpes, France)

New-generation communication and sensing systems are gaining strong interest in the context of Industry 4.0 e.g., related to mapping techniques, environmental sensing, automation or hyper-vision. The radio propagation in confined, cluttered and heavily metalized factory environments is a critical challenge; thus an evaluation by accurate propagation channel models is necessary. Site-specific channel emulation can be obtained from Ray-tracing (RT), but RT validation for factory environments is still an on-going work. For this purpose, a measurement campaign was performed in a machine room with many metallic objects and machines, using a mmWave channel sounder. Wideband channel responses were collected and compared to RT simulations. The RT prediction tool was calibrated to minimize the error observed on some large scale statistics, thus reaching a very good agreement between the simulation and the measurement. Average error in received power, delay spread and azimuth spread is below 1.5 dB, 5 ns and 2° respectively.

11:20 Ray Tracing and Measurement-Based Characterization of Inter/Intra-Machine THz Wireless Channels

Steffen Pahlke (Technische Universität Braunschweig, Germany); Tommaso Zugno and Mate Boban (Huawei Technologies Duesseldorf GmbH, Germany); Diego Andrés Dupleich (Technische Universität Ilmenau, Germany & Fraunhofer Institute for Integrated Circuits IIS, Germany); Thomas Kürner (Technische Universität Braunschweig, Germany)

We characterize the wireless propagation channels at 300 GHz in an industrial environment through measurements and ray tracing simulations. Two different scenarios are considered representing wireless connections between an access point and an industrial machine (inter-machine scenario), and between two components inside the same machine (intra-machine scenario) are considered. For both scenarios, we compute the channel response in terms of power angle delay profile and compare the results obtained through measurements and simulations, which show a good match.

11:40 Fast Indoor Radio Propagation Prediction Using Deep Learning

Andres J. Florez-Gonzalez (University of Nariño, Colombia); Carlos A. Viteri-Mera and Wilson Achicanoy (Universidad de Nariño, Colombia)

We introduce efficient deep-learning models that estimate maps of two indoor radio propagation parameters: i) received power and ii) cell association. These models, based on U-Net architectures, take floor plans and transmitter positions as inputs, and estimate the two maps. Training data was obtained from simulations using the IEEE 802.11ax path-loss model at 5GHz without co-channel interference. Validation shows errors below 1 dB (received power) and 1% pixel error rate (cell association). Our models reduce simulation times by 30x to 40x compared to traditional methods (e.g., ray-tracing, dominant path), making them valuable for wireless network planning and deployment.

12:00 Conceptual Design and Propagation Characteristics of an Underwater Electromagnetic Communication System for Ocean Environment Sensor Systems

Takashi Kawamura, Takuma Matsushita, Yukio Kaneko, Nobuaki Kawai, Yasuhiro Matsui and Akihiro Horii (Sony Group Corporation, Japan); Hiroshi Yoshida (Japan Agency for Marine-Earth Science and Technology (JAMSTEC), Japan)

As an attempt to protect the ocean environment, a system design for fixed-point observation in a small-scale blue carbon test site is presented. Designed system requires an underwater wireless communication system for data transmission, and electromagnetic (EM) waves are effective for this purpose from the viewpoint of cost and targeted underwater environment. We assume 1-Kbps data rate based on the above use case, select 50-kHz and 100-kHz carrier frequencies, and investigate the propagation of EM waves near seabed at these frequencies by an experiment and numerical calculations. As a result, we show that the closer the distance to the seabed and the lower the frequency, the less attenuation and the wider the coverage area. We also show that low-conductivity layers below the surface layer of seabed affect the propagation, indicating that the layer configuration of seabed is important in the link budget of proposed system.

Tuesday, March 19 10:40 - 11:25

IW4: Ansys workshop

Room: M2

Design Flow Methodology Including Thermal and Active Circuit Impact in Antenna Design and Antenna Integration

Presenter: Dave Prestaux (Ansys HFSS)

Tuesday, March 19 10:40 - 12:20

IW2: Advanced solutions for modern antenna test challenges (Antenna Systems Solutions and Next Phase Measurements)

Room: M3

10:40 IW2 Introduction

Presenter: Sergiy Pivnenko (Antenna Systems Solutions)

10:50 Recent Advances in Robotic Antenna Measurements for Aerospace Applications

Presenter: Dennis Lewis (The Boeing Company)

11:20 Advanced Post Processing for Robotic Applications

Presenter: Stuart Gregson (Next Phase Measurements, Queen Mary University of London)

11:50 Advances in Compact Antenna Test Range Design

Presenter: Marc Dirix (Antenna Systems Solutions)

Tuesday, March 19 10:40 - 12:20

IW9: Dassault Systemes and Simuserv GmbH workshop

Room: M4

10:40 Installed Antenna Performance in Complex Environments

Presenter: Yingjie You (Dassault Systemes)

11:30 Antenna Array Design Workflow - from Single Element to Array Installed Performance

Presenter: Frank Demming Janssen (Simuserv GmbH)

Tuesday, March 19 10:40 - 12:20

AMTA: AMTA Meeting

//

Room: Fyne

Tuesday, March 19 11:25 - 12:20

IW13: CADFEM workshop

Room: M2

Physics Based Workflow for the Design of THz Lens Antennas

Presenter: Alexander Shalaby; Steven Jones (CADFEM)

Tuesday, March 19 13:10 - 14:40

PE2: Poster Session on Electromagnetics I

// Electromagnetics

Chairs: Victoria Gómez-Guillamón Buendía (TNO, The Netherlands), Christos Monochristou (University of Rennes, France)

Geometry Reconstruction from Entries of Impedance Matrices 61

Quanfeng Wang and Alexander H. Paulus (Technical University of Munich, Germany)

The privacy and security of sensitive data are critical concerns when outsourcing computational tasks to external cloud service providers. This paper explores the feasibility of extracting confidential simulated models from method of moments (MoM) matrices. The study focuses on impedance matrices employing Rao-Wilton-Glisson (RWG) functions and the electric field integral equation. Reverse-engineering the simulated geometry can be formulated as an optimization problem. However, the presence of dyadic Green's functions imposes ambiguities when simultaneously reconstructing both the relative angle and distance between RWG source pairs in three-dimensional space. We introduce a local reconstruction method which mitigates these ambiguities. The approach gradually reconstructs the geometric structure locally by employing a reduced set of optimization variables. Numerical examples showcase that the local method can potentially reconstruct the original geometry.

A Two-Component 2-D FDFD Eigenmode Method Incorporated with the Conformal Technique 63

Yong Wang and Scott Langdon (Remcom Inc., USA)

A two-component two-dimensional (2-D) finite difference frequency domain (FDFD) eigenmode method incorporated with the conformal technique is proposed. The new formulations of the coefficients for filling the matrix equation have been derived by combining the conventional two-component eigenmode method with the conformal technique or by eliminating the two magnetic field components from the four-component conformal eigenmode method. The resulting matrix equation size is only a quarter compared with the four-component counterpart. The numerical results are given to show the accuracy and efficacy of the proposed method.

Management of Radiofrequency Compatibility on Aircraft 65

Alexandre Piche (Airbus Operations, France); Richard Perraud and Guillaume Sylvand (Airbus Central Research and Technology); Isabelle Terrasse (Airbus Central Research and Technology, France); Pierre Benjamin and Jerome Robert (Airbus Central Research and Technology); Toufic Abboud and Benoit Chaigne (IMACS, France); Lucia Scialacqua (Italian Ministry of Health, Italy); Lars Foged (Microwave Vision Italy, Italy); Dominique Donval (Microwave Vision, France); Robert Keibel and Stefan

Boerninck (Airbus Operations, Germany)

Radiofrequency Compatibility is becoming a major problematic on aircraft with a main objective of ensuring RF interoperability between Radio Communications, Navigation and Surveillance systems and the growing needs for Global Connectivity. In this framework, electromagnetic modeling based on Near Field Huygens Box approach and High Performance Computing is a powerful way to rigorously assess the behavior of antennas mounted on aircraft platforms as well as RF decoupling. Huygens Box formalism captures antenna broadband behavior for antenna positioning and RF interoperability analyses at aircraft level, with a clearly established industrial boundary between integrators and equipment manufacturers (i.e. no access to antenna internal structure for aircraft integrators). This paper presents in detail this methodology and its experimental validation on representative aircraft configurations.

Applying Neural Networks for Predicting Feed Weights of an Antenna Array 66

Juho Tyrväinen, Anu Lehtovuori and Pasi Ylä-Oijala (Aalto University, Finland); Ville Viikari (Aalto University & School of Electrical Engineering, Finland)

Artificial neural networks (ANN) are applied to find appropriate phasing for beam steering of patch antenna arrays. To obtain this goal, an ANN is trained using simulated far-field data. Two loss functions are tested and their performance is compared with a uniform and a non-uniform antenna array. The results show that in most cases both tested loss functions perform well, but are not able to find the best solution in all cases.

Gain Improvement of a DRA Using Deep Reinforcement Learning with Polygon Mesh Deformation 73

Kirill Kurskiy, Xiantao Yang and Yi Huang (University of Liverpool, United Kingdom (Great Britain))

A new approach for improving the gain of a hemispherical dielectric resonator antenna (DRA) operating at its fundamental mode using Deep Reinforcement Learning (RDL) is introduced. Unlike conventional optimization method, the key idea here is to avoid antenna parametrization during the optimization process so that the surface shape of the DRA can be directly manipulated. The simulated results show that the proposed DRA structure can achieve a high gain over the bandwidth of 2.23-2.7 GHz with its maximum value of 7.4 dBi. This is higher than the typical value dictated by this DRA shape and the data available in the literature.

Machine-Learning-Based Optimization for Wideband Metasurface Mosaic Antenna 69

Peiqin Liu, Xiangrui Yan and Zhi Ning Chen (National University of Singapore, Singapore)

In this paper, a machine-learning-based optimization method is proposed to enhance the bandwidth of metasurface Mosaic antennas. The artificial neural network (ANN) algorithm is utilized to build an effective neural network model to optimize the antenna geometry parameters for desired antenna performance. The input data of the proposed neural network is the target reflection coefficients and gain of the metasurface antenna, and the neural network predicts the geometry parameters that satisfy the target performance. The proposed antenna evolves from a metasurface Mosaic antenna. By dividing the patch cells into fractional pieces and optimizing the dimensions of cutting slots, the proposed antenna realized wideband in terms of both impedance and gain. A prototype antenna was fabricated to verify the design strategy. Measurement results show that the $|S_{11}| < -10$ -dB impedance bandwidth of the proposed antenna is 37.6% or ranging from 4.91 GHz to 7.18 GHz and the measured results of realized gain are

Non-Uniform Metamaterial Mushroom Antennas via a Genuine Multi-Objective Bayesian Optimization Method 67

Yunjia Zeng, Xianming Qing and Michael Chia (Institute for Infocomm Research, Singapore)

Three broadband non-uniform metamaterial mushroom antennas are designed with distinct mushroom configurations. The design trade-offs among the input impedance bandwidth, boresight gain, and the front-to-back ratio are considered with a genuine multi-objective Bayesian optimization method. The three non-uniform antennas attain a notable increase in impedance bandwidth with different degrees of trade-off in terms of the other two design targets when compared to the reference antenna with uniform mushroom configuration. All the four antennas are prototyped and measured, with strong alignment between simulation and measurement. The optimized designs can function in the n77 band of 5G New Radio.

The Role of Arrays in Pulsed Radiation 71

Jakub Liška, Lukas Jelinek and Miloslav Capek (Czech Technical University in Prague, Czech Republic)

The radiation of high-power narrow pulses is addressed with an emphasis on multiport structures, especially antenna arrays, which might significantly improve the pulse quality. The methodology is demonstrated on linear arrays of dipole and bowtie antennas. Significant improvement over single port radiators is reported.

Human- Vs Machine Design of Antennas: Evolution Behavior in Genetic Shape Optimization 75

Leonardo Pollini (Politecnico di Torino & Thales DMS, Italy); Marcello Zucchi and Giuseppe Vecchi (Politecnico di Torino, Italy)

Random-based global optimization algorithms have found extensive application in the domain of antenna shape design, especially when conventional solutions relying on human expertise are lacking. In this research contribution, we investigate the performance of random-based global optimization in scenarios where the design problem could otherwise be tackled through conventional human-guided design methods and parameter adjustments driven by simulations. The present case study involves shape optimization of a 2D pixelated domain, performed via binary coding and a Genetic Algorithm (GA). The reference geometry is a square resonant patch-type antenna with optimized probe feeding position. The initial domain is a pin-centered rectangle larger than the patch itself, so that the optimizer is eventually free to indirectly find the best pin position corresponding to the best design of the patch.

FDTD Modelling of RF Circuits Based on Lumped Components and Transmission Lines Using Modified Telegrapher's Equations 70

Anand Kumar and Debdeep Sarkar (Indian Institute of Science, India); Dimitra Psychogiou (University College Cork and Tyndall National Institute, Ireland)

This paper reports for the first time a finite-difference time-domain (FDTD) method to model discrete lumped L, C components and RF circuits in general by modifying the Telegraph equations of the transmission line (TL) equivalent. The proposed equations enable the modeling of circuits that comprise of lumped-element components and TL and can be exploited for the realization of a variety of RF circuits. Two test case scenarios are shown as examples, a 2nd order bandstop filter and a 3rd order bandpass filter. The results are validated by obtaining S-parameters for the circuits and matched against ADS.

Full Wave Verification of Radome Edge Scattering Treatments Using Open Source Tools 68

Daniel Sjöberg (Lund University, Sweden)

Scattering against radomes is an electrically large problem, typically requiring algorithms making some sort of approximations. In order to check the validity of such algorithms, it is important to define reference cases that can be computed by full wave solvers. In this contribution, we show how such cases can be simulated using open source software. In particular, we demonstrate how a method for reducing edge scattering from a radome-fuselage electrical discontinuity can be studied using open source software for a rotationally symmetric geometry.

A Discontinuous Galerkin Time-Domain Scheme to Model Lasing Dynamics in Four-Level Two-Electron Atomic Systems 64

Ming Dong (King Abdullah University of Science and Technology (KAUST), Saudi Arabia); Liang Chen and Ran Zhao (King Abdullah University of Science and Technology, Saudi Arabia); Hakan Bagci (King Abdullah University of Science and Technology (KAUST), Saudi Arabia)

A discontinuous Galerkin time-domain scheme is formulated and implemented to analyze three-dimensional transient lasing dynamics. The proposed scheme solves a coupled system of the Maxwell and the rate equations. The atomic transitions through different energy levels are quantum-mechanically described by a four-level two-electron model, while the electromagnetic interactions are treated using the Maxwell equations. The resulting solver accounts for the Pauli Exclusion Principle and permits robust simulation of lasing dynamics under optical pumping. Numerical results are presented to demonstrate the applicability and the accuracy of the proposed scheme.

Novel Quantum Computation Based Selection Operator for Genetic Algorithms Applied to Electromagnetic Problems 72

Gabriel Felipe Martinez and Riccardo Enrico Zich (Politecnico di Milano, Italy)

Quantum computing is an extremely promising tool that could dramatically change many engineering fields where computationally heavy tasks have to be dealt with such as electromagnetic optimization. Electromagnetic problems, in fact, are extremely computationally expensive, and an heuristic optimization may need thousands of generations. In this paper, the problems and the potential of the introduction of quantum computing in optimization has been investigated. Numerical results on the preliminary test are provided here while more detailed results will be directly presented at the conference.

Tunable Rectangular Waveguide Bandpass Filter Based on Plasma Technology 74

Atefeh Ashrafiyan (University of Tehran, Iran); Fatemeh Sadeghikia (Wireless Telecommunication Group, ARI, Ministry of Science, Research and Technology, Iran); Jalil A Rashed Mohassel (School of Electrical and Computer Engineering, Iran); Mohammad Himdi (University of Rennes Rennes Cedex France, France); Mirko Magarotto (University of Padova, Italy)

This paper introduces a novel tunable bandpass filter utilizing plasma conductors within a standard hollow waveguide framework. The operational principle of the filter leverages the reconfigurability of plasma and its tunable properties, allowing dynamic control over the lower frequency boundary. By adjusting the plasma frequency, the filter demonstrates remarkable adaptability, transitioning the lower cutoff frequency within a range from 1.72 GHz to 2 GHz, thereby enabling a highly flexible bandpass response. Additionally, a parametric analysis examines the impact of post dimensions on filter performance, emphasizing the role of initial post dimensions in shaping the bandwidth of the filter. The findings underscore the feasibility of this novel filter concept and its potential application in next-generation RF and microwave systems.

Influence of the Incidence Angle on the Focusing of Luneburg Lens Partially Covered with Graphene 62

Iryna O. Mikhailikova (V. N. Karazin Kharkiv National University, Ukraine); Sergii V. Dukhopelnykov (V. N. Karazin Kharkiv National University & Universite de Rennes 1, Ukraine); Mario Lucido (University of Cassino and Southern Lazio, Italy)

We consider the plane wave focusing characteristics of a layered cylindrical Luneburg lens equipped with a conformal strip of graphene, in the H-polarization case. The angular width of the strip is arbitrary and its surface impedance is characterized with the aid of the quantum-physics Kubo formalism. We use mathematically accurate full-wave analytical regularization technique, which is based on the analytic inversion of the problem static part. This guarantees the convergence of the resulting numerical algorithm. We compute the focusing ability of microsize lens as a function of the frequency in wide range up to 30 THz. This analysis shows that a graphene strip, placed into the focal area of the Luneburg lens, enhances its focusing ability at a certain resonance frequency proportionally to the quality factor of the plasmon mode of the strip.

Tuesday, March 19 13:10 - 14:40

PA2: Poster session on Antennas for Aerospace, new space and non-terrestrial networks

T03 Aerospace, new space and non-terrestrial networks // Antennas

Room: Expo/Poster

Chairs: Nelson Fonseca (Anywaves, France), Yannis Iliopoulos (TNO, The Netherlands)

Leading Edge Conformal ARMA Antenna in X Band 11

Pierre-Etienne Portalier (Xlim, France); Hassan Chreim (Dassault Systemes, France); Philippe Leveque (CNRS & XLIM, France); Bernard Jecko (XLIM, France)

This paper presents a conformal multi-source antenna using ARMA (Agile Radiating Matrix Antenna) principle. This antenna has the shape of an airplane wing leading edge. It performs radar or communication application in X band. A technique using a commercial software to compute the phase shift of excitations is proposed. It compensates antenna curve to obtain a radiation pattern with a directivity in the axial direction of 20 dB and side lobe levels below -13 dB. Moreover, the antenna provides beam steering using a phase law.

Compact Wideband Circularly Polarized Antenna Array for Satellite Applications 6

N Nasimuddin and Xianming Qing (Institute for Infocomm Research, Singapore)

A wideband circularly polarized (CP) 2x2 antenna array is proposed for INMARSAT/GNSS applications. The single-feed antenna element consists of an asymmetric-ring-slotted square patch radiator, an asymmetric-slit-slotted square stacked patch, and a coaxial feeding probe. The miniaturized slotted patches with a grounded shorted circular ring are utilized to generate the CP radiation and the stacked configuration to widen the bandwidth. The presented antenna is implemented using an arrangement of RO4003-dielectric substrate and air gap. The measured 10-dB return loss and 3-dB axial ratio (AR) bandwidths of a 2x2 antenna array prototype at the L-band are 16.8% (1.456 GHzx1.724 GHz) and 10.7% (1.51 GHzx1.68 GHz), respectively; the gain is greater than 11.0 dBi across the 3-dB AR bandwidth. The overall antenna volume is 185 mm x 185 mm x 18.0 mm (0.931 λ_{emda0} x 0.931 λ_{emda0} x 0.091 λ_{emda0} , where λ_{emda0} is free space wavelength at 1.51 GHz).

Compact Vivaldi Antenna Application in High-Power Design at X-Band 20

Liangliang Zhao and Yongmao Wang (Northwestern Polytechnical University, China); Dengyang Song (Northwestern Polytechnical University, China); Chenlu Liu (Northwestern Polytechnical University, China); Chuwei Li (China Academy of Space Technology, China); Huiling Zhao and Chufeng Hu (Northwestern Polytechnical University, China)

In this paper, a miniaturized antipodal Vivaldi antenna (AVA) with circularly shaped loads and several elliptic slits embedded around the tapered slot is presented. Firstly, the several elliptic slits embedded in two tapered slots are introduced for wideband design at X-band. Next, two circularly shaped loads are utilized to make the value of max power capacitive grow from 0.47MW to 0.82MW. Meanwhile, the overall size of the prototype is minimized to 0.44 λ_{middle} x 0.42 λ_{middle} (13.2mm x 12.6mm). The measurements of this prototype are presented and are in good agreement with simulations.

Antenna Design for TriHex: A Future Soil Moisture and Ocean Salinity Radiometer Mission 13

Quiterio García, Ana Lopez-Yela, Alberto M Zurita and Ana Olea Garcia (Airbus Defence and Space, Spain); Manuel Martin-Neira (ESA-ESTEC, The Netherlands); Erio Gandini (ESA - European Space Agency, The Netherlands); Martin Suess (ESA/ESTEC, The Netherlands)

ESA's Soil Moisture and Ocean Salinity (SMOS) mission, is providing L-band observations of the Earth surface since November 2009. In preparation of a future L-band mission, ESA is involved in several technological activities intended to develop the components for an advanced L-band radiometer mission. In this context this paper presents the current design status of the antenna element that constitutes the first stage of the advanced L-band receiver unit that populate the aperture synthesis radiometer instrument.

Genetic Algorithm-Based Beamforming in Subarray Architectures for GEO Satellites 9

Juan A. Vázquez Peralvo, Victor Monzon Baeza, Jorge Querol, Eva Lagunas, Jorge L González-Rios, Luis Manuel Garcés-Socarrás, Flor Ortiz and Symeon Chatzinotas (University of Luxembourg, Luxembourg)

The incorporation of subarrays in Direct Radiating Array for satellite missions is fundamental in reducing the number of radio frequency chains, which diminishes cost, power consumption, space, and mass. Despite the advantages, previous beamforming schemes incur significant losses during beam scanning, particularly when hybrid beamforming is not employed. Consequently, this paper introduces an algorithm capable of compensating for these losses by increasing the power, for this, the algorithm will activate radiating elements required to address a specific Effective Isotropic Radiated Power for a beam pattern over Earth, projected from a Geostationary satellite. In addition to the aforementioned compensation, other beam parameters have been addressed in the algorithm, such as beamwidth and Side Lobe Levels. To achieve these, we propose employing array thinning concept through genetic algorithms, which enable beam shaping with the desired characteristics. The array design considers an open-ended waveguide, configured to operate in circular polarization within the Ka-band.

Modular Ka-Band Transmit Phased Array Antenna for SATCOM Applications 3

Bo Shi and N Nasimuddin (Institute for Infocomm Research, Singapore); Francois Chin (Institute for InfoComm Research, Singapore); Xianming Qing (Institute for Infocomm Research, Singapore)

An active electronically scanned dual circularly polarized wideband transmit (Tx) phased array antenna at Ka-band is proposed for satellite communications. The modular phased array is designed with 256 dual-polarized antenna elements fed by 64 eight-channel Tx beamforming chips on a multi-layered PCB. The antenna element has a stacked square-ring slotted patch structure with two orthogonally positioned proximity-feed ports. The dual-feed can be excited orthogonally for circular polarization (CP) and offers the flexibility to reconfigure the CP radiation, either left-handed CP or right-handed CP. Furthermore, each 2x2 antenna cell is arranged using sequential rotation manner to enhance the CP performance. The 256-element transmit array has an aperture size of 80mm x 80mm and a measured EIRP of 58 dBm, 6.2° half-power beam width, sub 1 dB AR, and $\pm 60^\circ$ scanning range free of grating lobes. Scalability of the design is validated by implementing a 1024-element array with four 256-element array modules.

Design and Prototyping of a Low-Cost Parasitic Element Antenna for a Telemetry-Telecommand Link on Ariane 6 Space Launcher 14

Charles Couty (University of Limoges, France); Marc Thevenot (XLIM-UMR CNRS 7252, University of Limoges, France); Nathalie Lecerc (Arianegroup, France); Cyrille Menudier (XLIM Université de Limoges, France); Anthony Disserand (CRT Systeme, France)

This work presents a first prototype of a TMTC (telemetry-telecommand) S-band reconfigurable antenna, validating the architecture of ESPAR (Electronically steerable parasitic array radiator) in terms of performances, integration and power handling for use on space launcher environment. The originality of this work is based on the design of high efficiency-high power handling reflective phase shifters reduced in size and their association with a large radiating surface.

Design of Reconfigurable Reflectarray Antennas on Flexible Substrates with Varactor Diodes Mounted on Slot-Coupled Microstrip Lines 21

Takashi Tomura, Yuki Takeda, Haruki Kurokawa and Hiraku Sakamoto (Tokyo Institute of Technology, Japan)

In this paper, we propose reconfigurable reflectarray antennas with varactor diodes on flexible substrate. Diodes are mounted on slot-coupled microstrip lines and reconfigurability is realized by controlling the reverse bias voltages applied to diodes. The voltage characteristics of the reflectarray element are analyzed with the measured S-parameter of the diode. As a result, it is confirmed that a variable reflection phase range of 343 deg. could be obtained with a reflection loss of 0.53 dB or less.

Sub-7 GHz Circularly Polarized Dielectric Resonator Antenna Array for Full-Duplex Applications 17

Shadi Danesh (5GIC & 6GIC, Institute for Communication Systems (ICS), University of Surrey, United Kingdom (Great Britain)); Mohammad Abedian (HID GLOBAL, United Kingdom (Great Britain)); Ali Araghj and Pei Xiao (University of Surrey, United Kingdom (Great Britain)); Mohsen Khalily (University of Surrey & 5G Innovation Centre, Institute for Communication Systems (ICS), United Kingdom (Great Britain))

A novel high-isolation, monostatic, circularly polarized (CP) simultaneous transmit and receive (STAR) array dielectric resonator antenna (DRA) is presented. The proposed in-band full-duplex (IBFD) CP DRA system consists of 32 identical elements for each transmit and receiver part. Each element includes two rectangular dielectric resonators with different permittivity of 5 and 10 excited by a vertical strip connected to the microstrip line at the backplane. A stub connected to the ground plane is added between Rx and Tx to improve the isolation. In addition, an inverted U-shaped parasitic strip is carefully placed between two feeding networks to further enhance the TX/RX isolation. The measured results exhibit high TX/RX isolation of more than 50 dB over the desired operating bandwidth from 4.8 GHz to 4.95 GHz with a high total efficiency greater than 85% and a peak gain of about 18.7 dBi for both Port 1 and Port 2.

Conceptual Design of Antenna Arrays for Satellite Direct-To-Cell Connectivity 19

Mingtao Zhang (Yinhe Hangtian (Xi'an) Technology Co., Ltd. & Xi'an Institute of Space Radio Technology, China); Chao Gu (Queen's University Belfast, United Kingdom (Great Britain)); Zhengxian Zhu and Shiju Wei (Yinhe Hangtian Technology, China); Zhiwei Zhang (Hangzhou Dianzi University, Hangzhou, China)

Direct satellite-to-smartphone communication using standard mobile frequency bands without hardware modifications is a novel and promising application for satellite communications. This paper presents an antenna architecture for low earth orbit (LEO) satellites to establish the link with a given power budget. Using an array layout with random antenna positions, the antenna elements can be arranged in an expanded aperture to reduce the beamwidth and obtain enough power. This random array can be partitioned into two groups for 900 MHz and S-band application, respectively, to scan the beam in a wide angle range without a grating lobe. The array design concept can be applied in both independent satellites and satellite swarm. The proposed antenna array technique is expected to provide the satellite payload with the capability to reconfigure the radio frequency and antenna system, enhancing mission capabilities.

Multi-Bit Wideband Transmitarray Aperture with Independent Phase and Amplitude Control for High Gain with Low Sidelobe Mm-Wave Applications 15

Noureddine Melouki (University of Quebec INRS, Canada); Fahad Ahmed (University of Quebec, Canada & INRS, Canada); Hassan Naseri Gheisanab (University of Quebec, INRS, Canada); Peyman Pourmohammadi (University of Quebec INRS, Canada); Amjad Iqbal and Tayeb Denidni (INRS, Canada)

In this paper, a multi-bit transmitarray (TA) is proposed, as a system for beam-steering. The full structure is composed of 400 meta-atoms independently adjustable in both phase and amplitude. The far-field beam-steering mechanism of the proposed antenna is achieved by calculating the required phase compensations for each meta-atom, to redirect the beam to a predefined angle, in addition to a multi-bit system for amplitude distribution, for side-lobe level reduction. Simulation results show two unique beam scanning techniques, one for a phase only beam steering system with a maximum peak gain and SLL of 20.1 dBi and -12.3 dB, respectively, and the second one for independent phase/amplitude mechanism, at different angles of 0°, and 30°, and the maximum achieved peak gain and SLL were 25 dBi and -20.4 dB, respectively, making the proposed TA a potential candidate for high-gain and low SLL beam steering mm-wave communication system.

Fabrication and RF Characterization of Fully Additive Manufactured Transmission Lines 4

Chao Gu (Queen's University Belfast, United Kingdom (Great Britain)); Dmitry E Zelenchuk (Queen's University of Belfast, United Kingdom (Great Britain)); Gerard O'Connor and Noel Harrison (National University of Ireland Galway, Ireland)

This study introduces a fully additive manufacturing (AM) approach for microwave devices. The AM technology employed here has the capability to inkjet print conductive circuit elements onto 3D-printed dielectric materials. This all-in-one 3D manufacturing method enables the rapid and precise prototyping of RF and antenna components on flat or curved surfaces. Using the proposed method, several test vehicles are printed, and the electrical characteristics of both conductive ink and dielectric material are assessed up to Ka band using planar microstrip line and waveguide transmission lines (TLs). To showcase the advantages of this technology, the dielectric substrate with different infill densities is manufactured. For validation purposes, measurements of the complex permittivity and ink effective conductivity are conducted. These measurements demonstrate a satisfactory RF performance in the L and Ku bands, with acceptable performance in the Ka band, providing substantial proof of concept for this innovative approach.

Closely-Spaced Groove Gap Waveguides with Reduced Coupling 1

Miguel Angel Fuentes-Pascual (Universidad Politécnica de Valencia (UPV) & Antennas and Propagation Laboratory (APL), Spain); Jose I Herranz-Herruzo (Universitat Politècnica de València & APL - iTEAM, Spain); Miguel Ferrando-Rocher (Universitat Politècnica de València & Antennas and Propagation Lab, Spain); Alejandro Valero-Nogueira and Mariano Baquero-Escudero (Universidad Politécnica de Valencia, Spain)

In this communication, novel Gap Waveguide (GW) versions are presented with the objective of minimizing coupling. These innovations stem from minor modifications to conventional GW designs. As a result of this reduced coupling, it becomes possible to achieve channel spacing below half of a wavelength. Simulated results indicate that the Inverted Imbricated Groove Gap Waveguide and the Fingerprinted Groove Gap Waveguide both demonstrate an isolation level between channels exceeding 35 dB within the target bandwidth of 28 to 32 GHz. This design is noteworthy for its straightforward fabrication process, offering the potential for miniaturization and allowing for arrays with a spacing of less than a half of a wavelength.

Synthesis of a Planar 2D Butler Matrix: A Showcase with a 3x3 Array 2

Arman Bordbar, Raffaele De Marco, Luigi Boccia and Emilio Arneri (University of Calabria, Italy); Giandomenico Amendola (Università della Calabria, Italy)

A method for synthesizing a 2D Butler Matrix for a 3x3 array is introduced. This method can be extended for any number of orthogonal beams and antennas. The synthesis method relies on two techniques: Jordan decomposition and QR decomposition. For synthesis, first, Jordan decomposition is utilized to decompose the transmission matrix of the beamformer, then considering computer programming implementation any real matrices are decomposed to several Givens rotation matrices. To verify the accuracy of this method the circuit is simulated through ADS software. This straightforward and efficient synthesis method is valuable for designing Beamforming Networks (BFN) in contemporary applications of multi-beam antenna arrays.

Feasibility Study of 3D Printed Luneburg Lens Using Fused Deposit Material 3D Printing Technology for Ku-Band Application 12

Lionel Tombakdjian (CNRS & Université Côte d'AZUR, France); Fabien Ferrero (Université Cote d'Azur, CNRS, LEAT & CREMANT, France); Noori BniLam (University of Antwerp - imec, IDLab Research Group, Belgium); Fabio Principe (European Space Agency (ESA), The Netherlands & ESTEC, The Netherlands); Paolo Crosta (European Space Agency (ESA), The Netherlands)

In this work, the feasibility of manufacturing a Luneburg lens with standard FDM (Fused Deposit Material) 3D printing technology is studied for Ku-band application. In a first part, the collimating system design and fabrication process is described. In a second part, measurement results of the complete system is presented to assess the 3D printed lens performance.

Study on CFM Method for Beam Compensation of Array-Fed Space-Borne Reflector Antennas 8

YanJin Cui and Yali Zong (Northwestern Polytechnical University, China); Longteng Yi (China Academy of Space Technology, China); Kang Wang (Northwestern Polytechnical University, China); Bo Sun and Kaiqiang Qi (China Academy of Space Technology, China)

Space-borne reflector antennas have gain wide application for their unique advantages, and if they are fed by array antennas, the beam can be controlled freely. However, for the factors of extremely changing space temperature, repeated development, assembly errors and so on, the beams of deployable antennas will be deteriorated. To achieve anticipative performance, beam compensation should be performed. In the study, influences of the reflector's global, local and mixed deformations on the antenna performances are investigated by physical optics (PO) method, and the conjugate field matching (CFM) method, an easy and time-efficient method, is employed to compensate the beam degradation. The effectiveness of beam compensation by CFM for different kinds of reflector surface deformations are researched and compared. The results show that the beam pointing accuracy can be well compensated for all types of deformations, while the compensation effect is good under global deformations, but bad under local deformations.

Dual-Polarized Connected-Slot Array Technological Demonstrator Targeting a 5:1 Bandwidth 22

Stefan Varault (THALES Defence Mission Systems, France); José Zevallos (Thales DMS, France); Nicolas Cheval (Thales DMS, Italy); Valérie Rananjason (Thales DMS, France); Isabelle LeRoy-Naneix (THALES AIRBORNE SYSTEMS, France)

This contribution presents a technological demonstrator of a connected slot array (CSA) aperture developed in the framework of the European PADR CROWN project. This CSA has been developed for dual-polarized, multi-octave radar operation, targeting a bandwidth ratio of 5:1 and scanning angles up to 60° in all planes. The array is manufactured using printed-circuit board (PCB) process. A digital twin is implemented and used to accurately compare measurements to simulations of the manufactured finite-sized array, in order to assess the fabrication process.

Study of Different Feed Layout Configurations for Hybrid Active VHTS Antennas 7

Carolina Tienda (Airbus Defence and Space, United Kingdom (Great Britain)); Peter Webster (Airbus Defense and Space, United Kingdom (Great Britain)); Sonya Amos and Simon J Stirland (Airbus Defence and Space, United Kingdom (Great Britain))

This paper presents some of the layout configurations considered in recent studies on Very High Throughput Satellites (VHTS) antenna configurations. Four different subarray layouts have been considered for the feed array that illuminates a parabolic reflector of 8m.

Improving the Strut Modelling of the European Space Agency Deep Space Antennas to Evaluate Efficiency and Sidelobe Impact 5

Davide Arenare (University of Pavia, Italy); Fabio Pelorossi (ESOC, ESA, Germany); Filippo Concaro (European Space Agency, Germany); Marco Pasian (University of Pavia, Italy)

Large reflector antennas necessitate the presence of struts to support, according to the configuration, feeds or sub-reflectors. This paper presents the results of an investigation, in terms of sidelobe level and efficiency, of the impact on the antenna performance of the struts, considering the upcoming European Deep Space Antenna 4 (DSA4). In particular, for the first time in the framework of the DSA4 project, the strut model includes a tapering of the diameter of the strut itself, and a service platform and ladder (needed to reach the sub-reflector for maintenance), thus modeling with greater accuracy the real situation. The simulations presented here, carried out using Physical Optics, represent a rare opportunity to investigate these aspects, most often discarded due to the large computational time, and show that the impact on the antenna performance, for such high-end antennas, may be not negligible.

Compact Ka Band Orthomode Transducer with Conical Horn Antenna 10

Simon Fojtik, Samuel Travnicek and Pavel Hazdra (Czech Technical University in Prague, Czech Republic); Zdenek Hradecky (RFspin, Czech Republic); Jan Kracek (Czech Technical University in Prague, Czech Republic)

Orthomode transducers (OMTs) are essential microwave devices designed to separate or mix orthogonal modes, often using waveguide technology. This paper presents the design of a compact wideband OMT operating in the Ka band (26 - 40 GHz) with enhancements through a circular 20 dBi horn antenna. The OMT is designed to radiate vertical, horizontal or circular polarizations, due to its coaxial input ports and the use of a square waveguide carrying TE₁₀ and TE₀₁ modes. The design of the OMT incorporates a Bofot junction, optimizing the septum shape, axial port transformers, side port combination, and an innovative output configuration. The final design also includes rounding sharp edges and corners for improved manufacturing precision. The results of the simulation and measurement demonstrate the effectiveness of the design. This compact Ka band OMT with a conical horn antenna holds promise for a wide range of electromagnetic measurement applications.

Wideband Low-Profile Circularly Polarized All-Metal Antenna for Triton Exploration 25

Niyonzima Laetitia, Pauline Vryghem, Modeste Bodehou and Christophe Craeye (Université Catholique de Louvain, Belgium); Sébastien Lemaistre (Université Catholique de Louvain, Belgium)

A broadband low-profile 2x2 planar array constructed only of metal is proposed for space application. The single element of the array is capable of generating circular polarization with a non-symmetrical (with respect to broadside) radiation pattern. Sequential rotation is introduced at the array level to correct the asymmetry of the beam and for improving the polarization purity. The resulting antenna radiates at broadside with a 12.5 dBi gain. It has been shown that the product gain-bandwidth is competitive as compared to available solutions in the literature.

Compact Circularly Polarized Patch Antenna with Enhanced Axial Ratio and Impedance Bandwidth 16

Hanieh Ahmadi (University of Surrey, United Kingdom (Great Britain)); Chunxu Mao (South China University of Technology, China); Pei Xiao (University of Surrey, United Kingdom (Great Britain))

This paper presents a novel design of wideband circularly polarized (CP) patch antenna based on an aperture coupled feeding method. The properties of the CP structure are derived by introducing a novel coupled resonator-based configuration, which incorporates the inherent 90° phase difference between the two coupled resonant channels. The proposed low profile patch antenna aims to enhance the impedance bandwidth, axial ratio (AR) bandwidth. In contrast to prior works, the antenna demonstrates a reduced physical footprint while also showcasing broad impedance and 3 dB axial ratio bandwidths. This antenna can be used in the satellite communication applications to maintain quality of signal in a wide range of frequency simultaneously with the low axial ratio in the wide impedance bandwidth for mobile satellite services.

Ka-Band Phased Antenna Array Concept for High-EIRP Satellite Connections 18

Stefano Moscato, Alessandro Fonte and Steven Caicedo Mejillones (SIAE Microelettronica, Italy); Alessandro Di Carlofelice, Emidio Di Giampaolo and Piero Tognolatti (University of L'Aquila, Italy); Emilio Amieri (University of Calabria, Italy); Giandomenico Amendola (Università della Calabria, Italy); Luigi Boccia (University of Calabria, Italy); Matteo Oldoni (Politecnico di Milano, Italy)

This work deals with an innovative architecture of a phased antenna array operating in the Ka band. It envisages the adoption of custom designed PA together with 64 hollow metallic horns as radiating elements. The proposed architecture is designed to work in the 25.5 to 27 GHz frequency span with a target EIRP higher than 70 dBm, even considering the maximum beam steering configuration of ±20°. The proposed concept highlights the flexibility in targeting different power levels, antenna gain and steering capabilities to finally address a large number of use-cases. The exploitation of non-uniform array is also taken into account to prevent grating lobes and increasing the steering capabilities of the phased array.

The Design of Re-Imaging Optics for Passing Several Beams Through Small Cryostat Windows 23

Takaho Masai (The Graduate University for Advanced Studies, Japan); Hiroaki Imada and Alvaro Gonzalez (National Astronomical Observatory of Japan, Japan)

In this paper, we present a method to design re-imaging optics for receivers under heavy physical and mechanical constraints introduced by an antenna and cryostat window. Multibeam receivers will face many challenges optics to fit inside compact receiver cabins and to pass multiple beams through small windows. The optics can be solved and filtered to obtain solutions that work under the strong mechanical constraints. This method was used to design a two-beam multibeam receiver for the ALMA 12-m antenna and cryostat. The optics were successfully able to pass a beam through the small cryostat window and achieve a frequency-independent illumination on the sub-reflector.

Tuesday, March 19 13:10 - 14:40

PA7: Poster session on Antenna analysis, design and technology

T09 Fundamental research and emerging technologies // Antennas

Room: Expo/Poster

Chairs: Léonin Lassauce (Université de Rennes 1 & IETR, France), Cristina Yepes (TNO, The Netherlands)

Inconsistency in Modes of Circular Microstrip Antennas and Its Rectification 29

Deepankar Shri gyan (Defence Institute of Advanced Technology, India); KP Ray (DIAT, Pune, India)

Inconsistency in the interpretation of modes in Circular Microstrip Antenna (CMA) has been brought out and explained. The prevalent methods for CMA modes have been shown to be inconsistent with standing wave equation. It is emphasized that the current or field maxima along radius, diameter or half-circumference, have been incorrectly used to infer the mode indices in various books and academic papers. This paper aims to bring out the disconnection between mathematical model and physical interpretation of CMA modes. Further, a method to accurately interpret modes of CMA has been presented and has been demonstrated. Additionally, the presented method has been extended to annular ring antennas.

On the Radiation Resistance of Folded Antennas 27

Marcus C Walden (Plextek, United Kingdom (Great Britain))

The antenna literature appears divided regarding the input impedance of a folded antenna. Is the increase in feed-point impedance for a folded antenna simply an impedance transformation of the single element radiation resistance with no change in radiation resistance or does the folding process actually lead to an increase in the radiation resistance? This paper shows through theory and numerical simulations that the radiation resistance of a folded antenna is effectively - but not exactly - the same as that of a single element. This work serves as a point of clarification regarding the theory of folded antennas.

A Compact Horn Antenna with Low Sidelobes 30

Haim Matzner (HIT-Holon Institute of Technology, Israel)

An X-band (8.2- 12.4 GHz) compact horn antenna based on two shaped horns at the output with a single input horn is proposed. The antenna is matched for VSWR of 2 in this frequency range. The antenna is made of lossy aluminum. The sizes of the antenna are 171 x 86 mm with height of 102 mm. The directivity of the antenna varies between 16.6 to 17.3 dBi. The sidelobes are -30.7 dB and -37.1 dB in the E-plane and H-plane respectively. The gain of the proposed antenna is greater by 2 to 4 dB relatively to the gain of a conventional horn having the same height as that of the proposed antenna, and its sidelobes are lower than the sidelobe of the conventional horn. The simulations were carried by the CST Microwave Studio Software.

Passive Beamforming with Liquid Antennas: Techniques and Implementation 26

Viswanadh Raviteja Gudivada (The University of Liverpool, United Kingdom (Great Britain)); Yi Huang (University of Liverpool, United Kingdom (Great Britain)); Hanyang Wang (Huawei Technologies, United Kingdom (Great Britain)); Kexin Liu (Shanghai Huawei Technologies Company Ltd, China); Elliot L. Bennett (The University of Liverpool, United Kingdom (Great Britain))

This paper presents the concept of passive beamforming using liquid antennas for wireless applications. The work focuses on the usage of liquid dielectrics. The theory of achieving passive beamforming is explained with two different techniques. One focuses on the liquid fluidic behavior and the other takes advantage of liquids. Both the liquid dielectric antennas are subjected to different physical orientations and still, the radiation pattern is preserved and retained towards a fixed intended direction. This presented concept is supported by experimental verification and the results are presented.

Design of Optimized Cylindrical Structural Antenna with Quasi Length Insensitivity Using CMA 42

Raphael Notter (Université de Rennes & French-German Research Institute of Saint-Louis, France); Sylvain Collardey (University of Rennes 1, France); Ala Sharaiha (Université de Rennes & IETR, France); Loic Bernard (ISL & IETR, France); Pouliguen Philippe and Paul Karmann (DGA, France)

This paper deals with the design of cylindrical structures, whose dimensions are larger than the wavelength and which is usually difficult to handle due to the excitation of higher order. Using CMA (Characteristic Mode Analysis) give us the current modes of such structure. We then selected the modes that met our specifications in terms of radiation pattern and currents that have been excited through slots. We show that this structural antenna have a 7% of bandwidth with a gain of 5.5dBi at 4.6 GHz.

Dual-Feed Wideband Folded Waveguide Antenna for Handset Devices 33

Yunfeng Dong (vivo Mobile Communication Co., Ltd, China); Shen Wang (vivo Mobile Communication co., Ltd, China)

This paper presents a dual-feed folded waveguide antenna for handset devices. The proposed antenna can be implemented into devices with seamless metallic back cavity and it radiates through an open slot realized on the front by the corner edges of the display module and the main frame of the device. As a novel way of utilizing antenna cluster technique, an extra feed is added while the phase is adjusted for different operating frequencies. In order to prove the concept, a dual-feed folded waveguide antenna is designed for WiFi applications. The radiation efficiency of the proposed antenna remains higher than -6 dB within the frequency ranges of both 2.19-3.09 GHz and 4.73-6.44 GHz. The proposed antenna exhibits a wideband behavior. It achieves fractional bandwidths of 36% and 31% at 2.50 GHz and 5.50 GHz, respectively. Besides, the directivity is less than 5.5 dBi at both 2.50 GHz and 5.50 GHz.

A Brief Analysis of the Latest Research Progress and Future Direction of Low-Frequency Transmitting Antenna 40

Chao Wu, Jinghui Qiu and Shuang Qiu (Harbin Institute of Technology, China); Vasyi Molebny (Hainan Hongke Innovation Research Institute Co. LTD Lingshui China, China)

Low frequency electromagnetic wave is widely used in global communication and underwater vehicle communication because of its long propagation distance. However, due to the long wavelength of the electromagnetic wave in this frequency band, low-frequency transmitting antennas (LTAs) usually have the problems of large size, high profile height and low efficiency. Engineers have struggled for decades to design miniaturized, efficient low-frequency transmitting antennas. In this paper, the form of traditional LTAs is briefly sorted out, and the latest research progress of miniaturized low-frequency antenna is summarized, and its future development direction is simply analyzed.

Shaping the Sub-Reflector of a Ring Focus Antenna for Tailored Beamwidth Applications 28

Giuseppe Dell'Aere (Université de Rennes, France); Christophe Melle and Pascal Cousin (Safran Data Systems, France); Nelson Fonseca (Anywaves, France); Ronan Sauleau (Universite de Rennes, France); David González-Ovejero (Centre National de La Recherche Scientifique - CNRS, France); Mauro Ettore (University of Rennes 1 & UMR CNRS 6164, France)

This paper introduces a comprehensive investigation on the possibility to tailor the ring focus antenna's beamwidth by manipulating the shape of the sub-reflector, and more specifically its eccentricity, determining the location of the focal points of the dual reflector system. Eccentricity variation affects the sub-reflector's reflected field and thus the main reflector's illumination. The examined antenna configuration includes a main reflector with a diameter of 13.5 m, a sub-reflector with a diameter of 1.35 m, and employs a linearly polarized Gaussian beam as feed. Changing the sub-reflector's eccentricity from the original value of 0.6 to 0.66 reduces the directivity from 70 dB to 55 dB, widening the beamwidth from 0.05° to 0.45° at 26 GHz. This feature is of great interest for applications needing adjustable beamwidth, such as satellite location acquisition. The beamwidth switching may be implemented using a reconfigurable transmitarray providing two states equivalent to the two sub-reflector shapes.

Input Impedance of Radiation Efficiency Deterioration State 37

Kyoichi Iigusa, Hirokazu Sawada, Amame Miura and Hiroyuki Tsuji (National Institute of Information and Communications Technology, Japan)

The factors of radiation efficiency and impedance matching were investigated for a variable reactor-loaded antenna. It was found that when the conductivity decreases, there are reactance regions where the input power increases, and the radiation efficiency deteriorates in the regions. These reactance regions overlap with the regions of low input resistance, but in low frequency they overlap with the regions of low input

reactance. This is thought to be because its absolute value becomes large in wide reactance ranges in the low frequency and the input reactance becomes dominant. Since impedance matching is improved when the input reactance is near 0, controlling the reactance value to achieve matching in low frequency leads to reducing radiation efficiency. Therefore, it is difficult to achieve high antenna efficiency for electrically small antennas.

Radiation Pattern Shaping Using Generalized Luneburg Lenses for Automotive RADAR Antennas 36

Coen van de Ven (University of Twente & Gapwaves AB, Sweden); Abolfazi Haddadi (Gapwaves AB, Gothenburg, Sweden); Andrés Alayón Glazunov (Linköping University, Sweden)

This paper introduces an approach using the Generalized Luneburg Lens as a modular design element to shape automotive RADAR antennas at mmWave frequencies. An optimization routine that includes unwanted effects associated with manufacturing constraints is presented by adding mechanical constraints in the lens design and using a full-wave solver with the feeding antenna. Two lenses are designed; the first increases the directivity from 14.1 to 15.7 dBi, while the second increases the HPBW of the antenna from 57.6 to 129.6 degrees, demonstrating the flexibility of the presented approach.

Electromagnetic Assessment of Tolerances of the Square Kilometre Array Log Periodic Antenna Using Uncertainty Quantification 34

Mark Whale and Pasquale Giuseppe Nicolaci (TICRA, Denmark); Pietro Bolli (INAF Arcetri Astrophysical Observatory, Italy); Antonio Sganzerla and Lorenzo Mezzadrelli (Sirio Antenne, Italy)

This work details the results of a so-called uncertainty quantification analysis conducted on the SKALA 4.2 log-periodic antenna, itself the intended production model of the antenna element for the SKA-Low Antenna Array. The antenna is modelled using the high-order Method of Moments software tool ESTEAM while the tolerance analysis is conducted using the Uncertainty Quantification software tool within TICRA Tools. The results of these analyses are presented, and conclusions drawn regarding the antenna model's electromagnetic robustness against geometrical deviations.

A Novel Quad-Band Electrically Small Antenna 32

Hanguang Liao and Atif Shamim (King Abdullah University of Science and Technology, Saudi Arabia)

Multi-band Electrically Small (ES) antennas are promising candidates for wireless sensing nodes and wearable devices. However, designing ES antennas for multi-band operation is challenging. In this paper, a novel method to design a quad-band completely ES antenna is presented. The proposed method is based on the even and odd modes of a split-ring antenna (SRA) and uses RF trap loading to get dual-band operation for each mode. The proposed antenna is ES for all bands, and at each band, the radiating structure uses almost the whole available volume, so a good bandwidth is obtained for all four bands. The proposed antenna is fabricated, and the performance at each band is measured in a proper ES antenna setup. The measured results validate the proposed method, with Qs only roughly 3 to 8 times of Chu's limit among four bands, given that the proposed antenna is cylindrical rather than spherical.

Experimental Investigation of the Nullifier-Based Monopole 43

Bar Ohana (Merchavim Institute of Research and Development Negev, Israel); Daniel Wolfshtein (Ben Gurion University, Israel); Zion Menachem (SCE, Israel); Motti Haridim (Holon Institute of Technology, Israel)

In this paper, the feasibility and the radiation properties of the nullifier-based monopole is studied and analyzed. Simulation and experimental results for two versions of this antenna are presented. The results partially confirm the feasibility of such antennas. The radiation properties of such antennas depend on the orientation of the nullifier circuit. Further studies are needed to explore the full potential of the proposed antenna.

UWB Circular Metal Mesh Transparent Antenna 39

Umair Rafique (University of Oulu, Finland); Syed Muzahir Abbas (Macquarie University, Australia); Shobit Agarwal (Indian Institute of Technology, Roapr, India); Hijab Zahra (Macquarie University, Australia); Moath Alathbah (King Saud University, Saudi Arabia)

In this paper, a novel co-planar waveguide (CPW)-fed circular metal mesh (MM) transparent antenna (TA) is presented for ultra-wideband (UWB) applications. To achieve transparency, the MM technique is utilized on both conductors and dielectric substrate. To achieve broadband impedance matching in the band of interest, the corners of the CPW ground are truncated in a curved pattern. It is observed from the simulation results that the proposed UWB MM TA is resonating from 2.88 to 20 GHz, offering an impedance bandwidth of 17.12 GHz. In addition, acceptable radiation characteristics are observed in the proposed design, which makes it suitable for indoor wireless infrastructure.

A Novel Reconfigurable Planar Switched-Beam Filtenna with 360-Degree Beam Scanning 31

Behrooz Rezaee and Hossein Sarbandi Farahani (Graz University of Technology, Austria); Wolfgang Bosch (Graz University of Technology & Institute of Microwave and Photonic Engineering, Austria)

This paper presents a novel reconfigurable planar switched-beam filter (SBF). The substrate-integrated cavity (SIC) resonators, terminated by antipodal dipoles, deliver the filtering response with a third-degree Chebyshev response. By integrating the PIN diodes, the structure has effectively divided the azimuthal plane into eight sectors, enabling a reconfigurable pattern. The operating frequency of the proposed SBF is 12.7-13.3 GHz with a return loss of 20 dB, a realized gain of about 5 dBi, and a covering beam of 360 degrees. The simulated and synthesized results are compared and show good agreement.

Single Layer Cavity-Backed Filtenna with Ultra-Wide Out-Of-Band Suppression 41

Behrooz Rezaee (Graz University of Technology, Austria); Wolfgang Bosch (Graz University of Technology & Institute of Microwave and Photonic Engineering, Austria)

This paper presents a single layer cavity-backed patch Filtenna with ultra-wide out-of-band rejection. A cavity-backed patch antenna in a single-layer structure is designed and fabricated. It exhibits satisfactory performance of a maximum realized gain of 7 dBi at a frequency of 13 GHz. The parallel-coupled lines with capacitive terminations are employed to design a third-order bandpass filter. The capacitive endings in the parallel coupled lines facilitate filter miniaturization and suppression of higher harmonics. The designed antenna and filter are combined to form a Filtenna, demonstrating both functionalities of the antenna and filter. Measurement results of this Filtenna verify its performance, with a return loss of 15 dB and a maximum realized gain of 5 dBi within the 12.8 to 13.2 GHz. Additionally, the proposed Filtenna achieves a realized gain suppression of -20 dBi and -10 dBi up to 32 GHz and 46 GHz, respectively.

An Investigation into the Effects of Multi-Path and NLOS Propagation on Antenna-Based Soil Moisture Sensors in the RFID Band 35

James Stephenson and Mahmoud Wagih (University of Glasgow, United Kingdom (Great Britain))

Antenna-based soil moisture sensors are a growing technology, there is limited research into the impact of the reader antenna's placement and polarization. Studies assume a clear Line-of-Sight (LoS) link. This paper presents the first investigation into the effects of multi-path propagation on antenna-based sensors using an omnidirectional loop antenna designed for the 868 MHz ISM band. The performance of the sensing antenna is evaluated using two polarizations for the reader in both LoS and Non-Line-of-Sight (NLOS). It is shown that the loop antenna achieves a gain sensitivity of around -7dB to the added water content, multi-path effects can significantly vary this when the orientation of the sensor is changed. It is demonstrated that polarization mismatches between the reader antenna and the sensor are not as significant as the multi-path interference. It is concluded that the placement of the reader is more significant than the polarization alignment in a multi-path environment.

Generation of Dual Band OAM Wave Using Single Patch Antenna for WLAN/WiMAX Applications 38

Umar Fayyaz, Shahab Ahmad Niazi and Abdul Aziz (The Islamia University of Bahawalpur, Pakistan); Rifaqat Hussain and Akram Alomayni (Queen Mary University of London, United Kingdom (Great Britain))

Characteristic mode theory (CMT) provides valuable guidance to realize the current wave modes and distribution features of a single patch antenna. However, there is still a lack of theoretical guidance for the simultaneous generation of multiple orbital angular momentum (OAM) modes using a single patch antenna in multiple frequency ranges. In this paper, CMT is performed to analyze a single patch ring antenna. Then, the corresponding orthogonal degenerate modes of TM₄₁ and TM₆₁ modes are selected and excited through an appropriate feeding mechanism. As a result, the single patch ring antenna is able to radiate third and fourth-order OAM waves in the frequency ranges of 3.96 GHz and 5.18 GHz, respectively. The proposed antenna is recommended for dual-band WiMAX and WLAN applications with more spectral efficiency.

Tuesday, March 19 13:10 - 14:40

PE1: Poster Session on Metasurfaces and Metamaterials

T10 Novel materials, metamaterials, metasurfaces and manufacturing processes // Electromagnetics

Room: Expo/Poster

Chairs: Enrica Martini (University of Siena, Italy), Jérôme Taillieu (Université de Rennes 1, France)

Broadening the Spectrum: Extending the Finite Crystal Method to Characterize Static Multi-Atomic Active Metamaterial Systems 48

Rahul Dutta and Flynn Castles (Queen Mary University of London, United Kingdom (Great Britain)); Yang Hao (Queen Mary University, United Kingdom (Great Britain))

This paper introduces novel applications of the "finite crystal method" to assess the stability of multi-atomic static active metamaterial systems exhibiting negative static polarizability. While this method has conventionally been applied to systems assuming positive static polarizability and more recently to monoatomic systems with negative static polarizability, its application to multi-atomic systems represents a unique contribution. This work demonstrates the method's adaptability to a more general case with systems composed of multiple atoms per primitive cell and multiple types of atoms, illustrated with the help of a diatomic system.

Smart Propagation Environments Empowered by Metasurfaces: A Self-Consistent Study 49

Hamidreza Taghvaei (University of Surrey, United Kingdom (Great Britain)); Mohsen Khalili (University of Surrey & 5G Innovation Centre, Institute for Communication Systems (ICS), United Kingdom (Great Britain)); Gabriele Gradoni (University of Surrey, United Kingdom (Great Britain))

Smart environments are expected to constitute a distributed wireless network that will support the physical and digital layers in a sustainable manner. Metasurfaces can be used to control radio waves in a way that is compliant with the current operation of wireless communications. In order to control wave propagation, we need a mathematical framework that captures the metasurface operation in the presence of the surrounding propagation environment. The scattering properties of such a complex propagation scenario need to be found self-consistently, i.e., requires a general method that captures multiple interactions between metasurface and environment. This translates into solving a Burton-Miller formulation for the associated boundary-value wave problem. Our methodology overcomes the non-uniqueness difficulties generated by inconsistent theories where the propagation problem and metasurface scattering are solved in isolation and then coupled afterward. Importantly, the use of the fast multipole method is adopted to improve the overall computational efficiency.

A Polarization-Insensitive Ultra-Broadband FSS Absorber with Low-Profile Based on the ITO Film 47

Nan Wang, Guobin Wan, Qimin Ding and Xin Ma (Northwestern Polytechnical University, China)

In this paper, an ultra-broadband and low-profile absorber is proposed based on frequency selective surfaces (FSS). The proposed FSS absorber consists of three layers of indium tin oxide (ITO) patterned films with dielectric substrate between the films and a metal ground plate. Operating principle of ultra-broadband is analyzed based on the reflection characteristics of each FSS layer and the electromagnetic loss distribution of the structure. The simulation result of the equivalent circuit model (ECM) agrees well with the full-wave simulation. The designed structure has a reflection coefficient of less than -10dB at 1.01GHz to 18.80GHz, obtaining a remarkable relative bandwidth of 179.6% while the thickness is only (0.084 λ). The absorber is also able to maintain a stable absorption at large incidence angles for both TE and TM polarized wave incidence.

A Multifunctional Reconfigurable Metagrating for Wavefront Manipulations 54

Jiahui Ji (Xi'an Jiaotong University, China); Zhen Tan (Xi'an Jiaotong University, France); Jianjia Yi (Xi'an Jiaotong University, China); Lina Zhu (Xidian University, China); Shixiong Wang (Xi'an Jiaotong University & School of Information and Communication Engineering, China)

Passive metagratings often face the challenges of single function due to the fact that one of their structures can only correspond to one function. To solve this problem, a multifunctional reconfigurable metagrating composed of tunable elements (varactor diodes) is proposed in this paper. With the loading varactor diodes, the load impedance of elements (meta-atoms) on the metagrating can be flexibly manipulated by varying the bias voltage, so that various functions such as beam scanning and beam splitting can be realized in the same device. Consequently, the simulation results are in agreement with the theoretical predictions.

An Innovative Metasurface Polarizer Working in 5G Frequency Bands 59

Abdulkadir Cildir, Farooq A Tahir, Muhammad Ali Imran and Qammer H Abbasi (University of Glasgow, United Kingdom (Great Britain))

The research introduces an innovative metasurface design to provide multi-band capabilities for both cross-polarization and circular polarization. The metasurface consists of unit cells based on a ring-shaped configuration with a star inside. It is designed on a substrate made of Roger 5880. The thickness of this substrate is 1.575 mm, and the loss tangent is 0.009. The design acts like an efficient cross-polarizer, attaining a fractional bandwidth of 66% within the frequency bands spanning 23.24-34.64 GHz and 36.68-41.12 GHz. Additionally, this design functions as a circular polarizer in the frequency bands of 11.76-13 GHz, 19.43-21.6 GHz, 35.94-36.58 GHz, and 41.28-42.28 GHz.

Characterization of a Metamaterial-Enabled Waveguide Diplexer for Ka-Band Satellite Communication Systems 56

Robin F. Bonny (École Polytechnique Fédérale de Lausanne & MinWave Technologies SA, Switzerland); Mehri Ziaee Bideskan (MinWave Technologies SA, Switzerland); Romain Fleury (EPFL, Switzerland); Maliheh Khatibi Moghaddam and Mostafa Khosrownejad (MinWave Technologies SA, Switzerland)

This paper presents a novel miniaturized metamaterial-enabled diplexer designed for Ka-band. We introduce a measurement methodology to characterize noncontiguous channels within a waveguide structure. The diplexer efficiently separates receive (17.3 - 20.2 GHz) and transmit (27 - 31 GHz) satellite communication channels utilizing an innovative design approach that integrates locally resonant metamaterials (LRMs) and an evanescent mode junction. This integration allows for high rejection and low loss in an ultra-small volume, effectively showcasing the diplexer's capabilities. The measurement techniques implemented for the proposed component employ various waveguide transitions to cover the whole frequency band (15 - 40 GHz) and de-embedding procedures for manual calibration of the device under test (DUT). We precisely measure the passband and stopband of both the receive and transmit channels and compare the results with simulations. The results show less than 0.7 dB insertion loss for this ultra-compact diplexer.

Design of a Concentric Circular Holographic Metasurface Using Hexagonal Anisotropic Unit-Cell for Wireless Communications 60

Swarnadipto Ghosh (Indian Institute of Space Science and Technology, Thiruvananthapuram, India); Dipankar Saha (Indian Institute of Space Science and Technology, India); Rishabh Aalayathil (Government Engineering College Barton-Hill, India); Aakash Bansal and William Whittow (Loughborough University, United Kingdom (Great Britain))

In this article, the surface impedance, Z_{surf} of a cross slotted anisotropic hexagonal unit-cell has been characterized by analyzing the effects of rotation factor and effective length of the slot. A closed form empirical relation has been determined to characterize the Z_{surf} on the basis of the two parameters. Finally, a multibeam Impedance modulated surface is presented using the proposed study and the results are verified in simulation.

Modeling of 3D Feeding Structures in the Automated Design of Metasurface Antennas 57

Lucia Teodorani, Marcello Zucchi and Giuseppe Vecchi (Politecnico di Torino, Italy)

We present an automatic procedure to fully design a metasurface antenna, including the feeding structure. This feature is achieved by performing preliminary full-wave simulations of the feeding structure and by properly modelling PEC regions inside a current-based numerical design method. The synthesized metasurface antennas are implemented and simulated with a full-wave commercial solver, showing excellent agreement with the predicted performances.

A Compact Fabry-Perot Cavity Antenna with Circular Polarization 53

Chiara Scarselli, Edoardo Giusti and Danilo Brizi (University of Pisa, Italy); Agostino Monorchio (University of Pisa & CNIT, Italy)

In this paper, a compact, circularly polarized Fabry-Perot Cavity (FPC) antenna is presented. The proposed solution consists of an opportunely designed microstrip resonator inserted within a closed cavity, measuring only $3\lambda \times 3\lambda$ at the working frequency of 412 MHz. The microstrip resonator is a dual circularly polarized slot-patch antenna. On the cavity top layer, a Partially Reflective Surface (PRS), based on an inductive

Frequency Selective Surface (FSS) structure, is positioned. To verify the conceived design, accurate numerical simulations have been carried out. The obtained results show a gain value of about 19 dBi and an Axial Ratio (AR) less than 3 dB inside the 17° Half Power Beamwidth (HPBW). Moreover, the Side Lobe Level (SLL) remains under -13 dB. The compactness and the excellent radiative properties of the proposed cavity antenna are promising for challenging environments, such as satellite and space applications.

Nonreciprocal Metasurfaces Analyzing Temperature Characteristics 55

Kazuhiro Takahagi (University of Sheffield & Acquisition, Technology and Logistics Agency, Ministry of Defence, United Kingdom (Great Britain)); Alan Tennant (University of Sheffield, United Kingdom (Great Britain))

In recent years, there has been an increasing interest in electromagnetic metasurfaces. This paper presents a novel, non-reciprocal, electromagnetic metasurface based on ferrite control elements. Specifically, the metasurface structure combines cylindrical ferrite elements and metal patch arrays and operates at C-band. The ferrite elements are controlled by electromagnets. A theoretical analysis based on a commercial, full-wave, electromagnetic simulator is presented to demonstrate non-reciprocal behavior in terms of S21 and S12 parameters. Experimental results are presented to confirm theoretical predictions. A detailed, investigation in to the thermal dependence of the electromagnetic characteristics of the metasurface are presented and analyzed.

Compact Polarization Converter on a Thin Ferrite-Based Metasurface for Enhanced 5G Wireless Communication 44

AmirMasood Bagheri (5GIC & 6GIC, Institute for Communication Systems (ICS), University of Surrey, United Kingdom (Great Britain)); Zahra Rahimian Omam, Seyed Ehsan Hosseinejad and Pei Xiao (University of Surrey, United Kingdom (Great Britain)); Mohsen Khalily (University of Surrey & 5G Innovation Centre, Institute for Communication Systems (ICS), United Kingdom (Great Britain))

This paper highlights the crucial importance of polarization control within 5G wireless communication. We propose a compact polarization converter on a thin ferrite-based metasurface, which enables flexible manipulation of polarization in the reflected waves. The direction of applied magnetics bias allows the metasurface to polarize reflected waves in either co- or cross-polarization with respect to the incident wave. To optimize ferrite utilization, the adoption of a cubic lattice structure in metasurface design is recommended. This design approach has successfully delivered efficient polarization conversion and showcased impressive frequency reconfigurability. Each unit cell within the proposed metasurface can be independently controlled for spatial modulation. Utilizing the distinct material properties associated with various polarizations, the suggested metasurface exhibits remarkable potential in creating reflective intelligent surfaces. These surfaces have the capacity to substantially enhance coverage and elevate the performance of 5G networks.

Design of an Ultra-Wideband RCS Reduction Metasurface with Pure Metal-Pattern Layer 52

Shuaipeng Li, Yali Zong, Xinyu Ma, Weijie Yu and Zicheng Liu (Northwestern Polytechnical University, China)

To achieve the perfect stealth of targets, the ultra-wideband RCS (Radar Cross Section) reduction technique is in urgent demand nowadays. The introduction of metasurface brings the advantages of design flexibility and low profile. However, metal-pattern-layer metasurface usually has narrow frequency characteristics. To widen the band and avoid shortcomings of the higher manufacturing cost and lower reliability, the present research designs an ultra-wideband RCS reduction metasurface with pure metal-pattern layer. Based on the impedance matching, absorbing bandwidth is gradually widened by improving the design of the metal-pattern layer. Finally, 85% (7.64-19GHz) and 104% (7.2-22.8GHz) relative bandwidths for the periodic unit and array are realized for RCS reduction, respectively. The maximum absorptivity reaches 0.9996 for the metasurface unit. The maximum RCS reduction of 22.28dBsm and the average one of 10.2dBsm are realized for the metasurface array. The design has some application potential for targets with RCS reduction requirement.

Multi-Channel Beam-Splitting Metasurface for Millimeter Wave Communication Systems 50

Jibrán Zahoor Ahmad Pandit (Univ Gustave Eiffel, France); Mohammed Kalaagi (Institut de Recherche Technologique Railenium, Famars, France & Railenium, France); Divitha Seetharamdoo (Univ Gustave Eiffel COSYS LEOST Univ Lille Nord de France & Univ Lille Nord de France, France); Caroline Maye (Univ Gustave Eiffel, France)

In this paper we propose the design of a metasurface based on the methodology of high periodicity super-cell designs (5.76λ) and impedance modulation to achieve a various number of beam splitting angles, while maintaining the same coverage at multiple incident angles for millimeter wave (mmWave) frequency. Our proposed design achieves a reflection efficiency up to 96.65% and 97.36% in TE and TM mode at 28 GHz with 11 beam directions $\theta_i = 0^\circ$, $\theta_a = 0^\circ$, $\pm 10^\circ$, $\pm 20.32^\circ$, $\pm 31.40^\circ$, $\pm 44^\circ$ and $\pm 60.25^\circ$ while maintaining similar performances for various incident angles which makes it a valuable complementary solution to enhance coverage for mmWave communication applications compared to conventional beam splitters. The performance of the metasurface is determined by calculating the bistatic radar cross section (RCS) compared to a flat metallic plate of similar dimensions. A prototype is fabricated and tested to validate the simulation results.

Integral Equation-Based Solver for the Simulation of Metasurface Designs 58

Hans P Schreckenbach (CEMWorks, Canada); Chen Niu (University of Manitoba, Canada); Nima Chamanara (Ecole Polytechnique de Montreal, Canada); Andre Fecteau and David Abraham (Computational Scientist, Canada); Jonatan Aronsson (CEMWorks Inc., Canada)

A full-wave simulation is conducted on metasurface designs using an integral equation-based solver. This approach offers two distinct advantages over conventional and hybrid Finite-Element Method (FEM) based solvers, namely the use of a surface-based mesh instead of a volumetric representation and excellent efficiency for large-scale structures. The solver is tested against measurements, a Hybrid FEM solver, as well as theoretical models for accuracy.

D-Band Absorber Comprising Tantalum Nitride-Based Resistively-Loaded High Impedance Surfaces 51

Rana Muhammad Hasan Bilal (University of Pisa, Italy); Michele Borgese (Siae Microelettronica, Italy); Simone Genovesi, Giuliano Manara and Filippo Costa (University of Pisa, Italy)

This paper proposes a D-band absorber that employs periodic resistive surface made of Tantalum Nitride (Ta2N) deposited on a gold-backed alumina dielectric substrate. The top resistive surface consists of square loop-based unit cells and demonstrates an absorption rate of over 90% across the frequency range from 100 GHz to 166 GHz. The performance of the designed absorber is evaluated through a full-wave simulation method and has been verified using an equivalent circuit model approach. The proposed absorber could be useful in the sub-THz band for various applications, including enhancing MIMO antenna isolation, reducing Electromagnetic Interference (EMI), and integration into other microwave circuits.

Mechatronic Phase-Control Reflector System with In-Plane Axis Control 46

Hrishit M Das (Birla Institute of Technology and Science, Pilani & Carleton University, Canada); Keigan MacDonell and Shulabh Gupta (Carleton University, Canada)

A simple mechatronic reflector system is proposed using an array of motorized resonator panels to dynamically control the reflection phase of an incoming waves. The proposed design features a static meshed metallic layer coupled with a ring-resonator array rotating about an axis parallel to the surface. A full-wave design in the X-band is presented here to illustrate this system, where electromagnetic couplings between the fixed mesh and resonator rings are exploited to achieve a near 2π phase variation with low reflection losses compared to their all-electronic counterparts using varactor diode, for instance. Two numerical examples are further shown to illustrate the beamforming features of the system - a binary phase surface and a linear phase gradient for steering the reflected beam. This proposed system thus features an in-plane mechanical actuation compared to vertical displacements or in-plane rotation of the unit cell resonators.

A Novel Metasurface Inverse Design Based on Back Propagation Neural Network 45

Tao Qin (University of Electronic Science and Technology of China & Lund University, China); Su Wen (Lanzhou Jiaotong University, China); XianQi Lin (University of Electronic Science and Technology of China, China); Yuyan Cao (Lund University, Sweden); Yang Cai and Peng Mei (Aalborg University, Denmark)

This paper proposes a novel reflective meta-surface inverse design by utilizing a back propagation neural network. A reflective meta-surface, measuring 0.92 m in width, 0.92 m in height, and 0.508 cm in thickness, is synthesized. This meta-surface is composed of twelve distinct unit types, each possessing unique phase-shifting characteristics. When illuminated by a multi-mode waveguide horn employing the offset design, the meta-surface demonstrates a gain of 31.65 dB at a frequency of 5.8 GHz. Furthermore, the simulated design achieves a side lobe level of 23 dB in the far-field region, accompanied by a system efficiency of 36% and a relative 3-dB bandwidth of 7%. By incorporating more training data and enhancing the machine learning algorithms, this design methodology could be applied to generate complex meta-surface structures with multi-frequencies and multi-polarization responses, demonstrating significant potential in multi-functional meta-surface integration.

Tuesday, March 19 13:10 - 14:40

PM1: Poster Session on Measurements I

T04 RF sensing for automotive, security, IoT, and other applications // Measurements

Room: Expo/Poster

Chairs: Maria Alonso-delPino (Delft University of Technology, The Netherlands), Shuai Zhang (Aalborg University, Denmark)

Preliminary Investigation of an Innovative RF Sensor for Deformation and Failure Evaluation in Composite Materials 76

Angelica Masi and Danilo Brizi (University of Pisa, Italy); Eliana Canicatti and Guido Nenna (Free Space, Italy); Agostino Monorchio (University of Pisa & CNIT, Italy)

This paper introduces the design of a high-sensitivity, low-cost, easy-integrable radiofrequency sensor for structural health monitoring. The hardware system is composed of an array of three self-resonant spiral-coils, working in the 100-300 MHz frequency range, inductively coupled to a feed-line. The sensing spirals design is the result of the corresponding Q-factor maximization through an optimization process, ensuring a good compromise between penetration depth and sensitivity. The analysis of the resonance frequency shift and the amplitude variation of the system input impedance are both exploited to identify composite irregularities. In order to validate the methodology, we performed full-wave simulations to evaluate the radiating system performance in presence of normal conditions, deformation of the composite, and presence of a delamination and crack within the sample. The obtained results validated the theoretical approach, confirming both the ability to identify the presence of an irregularity within the composite material and also its spatial position.

A Numerical Analysis of Microwave Hyperthermia of Deep-Seated Tumors Using Magneto-Dielectric Implants 77

Matteo Bruno Lodi (University of Cagliari, Italy)

MW energy can be adopted to treat cancers through hyperthermia treatment (HT). HT is a thermal therapy used in oncology to enhance chemotherapy and improve radiotherapy effectiveness. Despite these advantages, neoplasms such as deep-seated tumors cannot be treated effectively with existing HT modalities. Magnetic implant to be used as thermo-seeds excited by an external RF field has been studied as tool for administering a new HT approach. To date, it has been preliminary proposed to use MW energy to perform the local HT of deep-seated tumor using magneto-dielectric biomaterial implants. However, further studies must be performed. This work deals with the 2D electromagnetic simulations of the MW HT of deep-seated tumors using magneto-dielectric implants. The multiphysics model is presented and used to investigate the key treatment parameters. The electric and magnetic fields distributions, SAR patterns and the temperature profiles achieved in the case of RF and MW hyperthermia are compared.

Impact of 6D Mobility on Doppler Characteristics of UAV-To-Vehicle Channels 78

Junwei Bao (Nanjing University of Aeronautics and Astronautics, China); Zhuangzhuang Cui (KU Leuven, Belgium); Yang Miao (University of Twente, The Netherlands);

Qiuming Zhu, Boyu Hua, Kai Mao and Haoran Ni (Nanjing University of Aeronautics and Astronautics, China)

Unmanned aerial vehicle (UAV) empowered vehicular networks are capable of providing flexible radio access, efficient data transmission, and secure driving operation. For this promising application, we focus on channel modeling for UAV-to-vehicle (U2V) communications in this paper. Based on stochastic geometry and six-dimensional (6D) mobility patterns, a geometry-based stochastic model (GBSM) framework for U2V communication is studied. Specifically, we consider the movement of a UAV in both 3D translational and 3D rotational directions, while a ground vehicle is capable of moving in any direction with varying velocities. Then, the expressions of Doppler shift in different components are derived, and eventually, Doppler power spectral density (PSD) is obtained by integrating Doppler shifts in each path. Simulation results demonstrate that the distinct impacts on Doppler characteristics led by linear velocity, rotation velocity, the direction of the rotation axis when the UAV rotates, and the direction of translation.

A Highly Compact Double-Sided Orientation Insensitive Chipless Tag for Radio Frequency Identification Applications 79

Muhammad Noman (University of Glasgow, United Kingdom (Great Britain)); Usman Haider (NUST, Pakistan); Farooq A Tahir, Muhammad Ali Imran and Qammer Abbasi

(University of Glasgow, United Kingdom (Great Britain))

In this paper, a simple highly compact orientation insensitive frequency-domain strip-based chipless RFID tag design is presented. To achieve the compactness of the tag, resonating copper strips are placed on the front side as well as on the back side of the substrate. In this way, the overall 50% reduction in the tag size is achieved. The proposed tag is design using Roger's RT5880LZ, that has an overall size of 12x12 mm². The tag is capable of encoding 16-bits within a frequency band of 5.7 to 19 GHz. The performance of the tag at different oblique incidence angles show that it is angularly stable for up to 75°. The proposed tag achieves a high code density of 11.11 bits/cm² and is readable from the front and back side of the tag.

Minimum Coherence Bandwidth for OFDM Signal Testing in Reverberation Chambers 80

Miguel Á. García-Fernández (EMITE Ingeniería, S. L., Spain); David A Sánchez-Hernández (Universidad Politécnica de Cartagena, Spain)

This contribution provides a mathematical derivation aimed at establishing the minimum coherence bandwidth necessary within a reverberation chamber (RC) to effectively prevent inter-symbol interference (ISI) when testing standards that make use of orthogonal frequency division multiplex (OFDM) signals, such as 4G Long Term Evolution (LTE) or 5G New Radio (NR). The derived minimum coherence bandwidth is found to be no less than 5.5133 times the sub-carrier spacing (SCS).

Intermodulation Mitigation Through Surrounding Impedance Manipulation 81

Amir Dayan (University of Liverpool, United Kingdom (Great Britain)); Farhad Ghorbani (University of Liverpool, UK); Yi Huang and Jiafeng Zhou (University of Liverpool,

United Kingdom (Great Britain)); Mattias Gustafsson (Huawei Technologies Sweden AB, Sweden); Alex Schuchinsky (University of Liverpool, United Kingdom (Great Britain))

Intermodulation products in antennas and connectors are a serious problem for signal integrity and can significantly reduce the performance and capacity of mobile and satellite systems. The elusive nature of intermodulation, especially in metal contacts, leads to complexity in the analysis and understanding of the characteristics of these weak spurious signals. This paper investigates the effects of load and source impedances on third-order intermodulation (IM3). The analysis is conducted using a power series approach, which is validated through ADS simulations. Both the ADS simulation and the analytical results demonstrate that manipulating the impedance seen by the nonlinear element can improve IM3. Simulation results confirm that a 12 dB reduction in IM3 can be achieved when we increase the impedance seen by a nonlinear source (BAR64-02V PIN diode in our example) from 43 Ω to 100 Ω which has been verified by measurements.

Virus Detection in the Microwave Regime Through an Antenna Workbench 82

Anderson Falcón-Gómez (University Carlos III de Madrid, Spain); Daniel Segovia Vargas (Universidad Carlos III de Madrid, Spain); Vicente González Posadas

(Polytechnic University of Madrid, Spain)

This paper addresses a sensing approach for virus detection harnessing the microwave resonant absorption property thereof. To this end, we contemplate two viruses, COVID-19 and the H3N2. Upon interacting with the virus, an incident monochromatic electromagnetic field makes electric charges distributed in their structure to move harmonically in accordance with Lorentz's force law. This, in turn, excites a mechanical vibration with resonant characteristics that dissipates the energy in the system. By modeling it as a damped double mass-spring system, we estimate the electromagnetic absorption cross-section of virus samples under consideration, and thereafter, we compute their microwave absorption spectrum in an antenna-based sensor and estimate the 3 dB sensitivity limit of the device. Overall, this approach provides a method to implement an economical detection system sensitive to multiple pathogens that can leverage both the RF and the communication platforms of the 5G and 6G technologies.

Dielectric Differences in Biological Tissues: A Comparison Between Excised and Non-Excised Tissues Under the Influence of Chemotherapy 83

E Fernandez-Aranzamendi (Universidad Carlos III de Madrid, Peru & Universidad Católica San Pablo, Peru); Sandra Santiago-Mesas (Universidad Carlos III de Madrid,

Spain); Gelber E Eguiluz (Regional Institute of Neoplastic Diseases, Peru); Ebert G San Roman Castillo and Patricia Castillo (Universidad Católica San Pablo, Peru);

Daniel Segovia-Vargas (Universidad Carlos III de Madrid, Spain)

Breast cancer is one of the most common types of cancer worldwide. Currently, electromagnetic technologies can play a crucial role in monitoring systems. However, achieving precise dielectric characterization is essential to ensure result accuracy. The main objective of this article is to contribute to chemotherapy monitoring systems by analyzing tissue permittivity in vivo and ex vivo, both with and without chemotherapy effects. For the experiment design, an open-ended coaxial probe was used within a frequency range of 1 to 8 GHz, following a measurement protocol. The obtained data were classified into four groups based on the type. It was observed that the permittivity increased by 30% under the influence of chemotherapy, presenting significant changes in tumor tissues within a range of 15% to 20%. These findings demonstrate the possibilities of effective monitoring under the influence of chemotherapy.

Investigation of Correlation Between Absorbed Power Density and Incident Power Density for User Equipment Antennas at Sub-THz Frequencies 84

Ming Yao, Wen Fu, Gert Pedersen and Shuai Zhang (Aalborg University, Denmark)

In the international guidelines, absorbed power density and incident power density have been proposed as local exposure limits above 6 GHz to protect humans from electromagnetic field exposure. Incident power density has attracted more interest because of easier assessment compared to absorbed power density. However, the correlation between incident power density and absorbed power density should be examined in the near field before using it for the electromagnetic field compliance assessment. The reason is that incident power density is derived from the absorbed power density in the far field. Currently, there is no relevant study focusing on practical antennas used for user equipment at sub-THz frequencies. In this paper, the correlation between incident power density and absorbed power density is studied using an antenna at sub-THz frequencies. The results show that incident power density has a good correlation when they are averaged over four square centimeters, except for 100 GHz.

Tuesday, March 19 13:10 - 14:40

PP01: Poster session on Propagation I

// Propagation

Room: Expo/Poster

Chairs: Yuan Ding (Heriot-Watt University, United Kingdom (Great Britain)), Sana Salous (Durham University, United Kingdom (Great Britain))

A Deep Learning-Based Approach for Inverse Design of Reconfigurable Metasurfaces 91

Xin You and Panagiotis Kosmas (Kings College London, United Kingdom (Great Britain))

Reconfigurable metasurfaces (RMTs) have attracted increasing attention for various practical applications thanks to their intriguing ability to manipulate electromagnetic (EM) waves dynamically. However, conventional modelling and optimization methodologies of RMTs can be ad-hoc and time-consuming, which restricts their development. This paper proposes a novel inverse design methodology based on deep learning (DL) techniques to train an inverse artificial neural network (ANN) to predict the corresponding physical dimensions of RMTs with a given EM response in real time with high predictive accuracy. This methodology is modified from the conventional forward and inverse design by introducing performance indices including resonant frequency, max amplitude, and 3dB bandwidth of the reflection coefficient S_{11} 's first resonant frequency band as the inverse ANN model's input and the criteria to separate the datasets. Based on the efficient and accurate inverse ANN model, RMTs can be easily optimized to fit various applications in 5G wireless communications.

Analysis of the Capacity and Energy Efficiency of Metalodielectric Surface Wave Links Operating Beyond Y Band 101

Jie Qing (University of Electronic Science and Technology, China); Miguel Navarro-Cía (University of Birmingham, United Kingdom (Great Britain))

The ability to reconfigure surface wave links has the potential to mitigate manufacturing issues unavoidable on microtextured surfaces as well as to introduce some level of signal processing. To this end, this work proposes a surface wave link based on a silicon-aluminium periodic structure supporting surface waves in the THz range. The dispersion and power budget of a link based on such surface wave supporting metalodielectric structure is presented. This work provides an effective guide for the layout of terahertz surface wave links.

The Time Modulated Array for Channel Sounding Measurements - Concept and Initial Field Tests 98

Edward Ball (University of Sheffield, United Kingdom (Great Britain)); Sumin David Joseph (The University of Sheffield, United Kingdom (Great Britain)); Alan Tennant (University of Sheffield, United Kingdom (Great Britain))

We present a technique to use a Time Modulated Array as the transmitter in a 5.8 GHz propagation channel sounder. The 5.8 GHz signal is first modulated with a pseudo random binary sequence, to allow a correlation in the receiver to detect multi-beam relative path delays and powers, so supporting angle of departure measurements for the transmitter. The system can resolve delays down to 250 ns and the receiver measurement floor is -120 dBm. We present the system concepts and initial field test results.

A Study on W-Band Frequency Attenuation in the Presence of Human Blockage 87

Juan E. Galeote-Cazorla, Alejandro Ramírez-Arroyo and Salvador Moreno-Rodríguez (University of Granada, Spain); Jose-Maria Molina-Garcia-Pardo (Universidad Politécnica de Cartagena, Spain); Maria-Teresa Martínez-Ingles (University Centre of Defence at the Spanish Air Force Academy, MDE-UPCT, Spain); Pablo Padilla (University of Granada, Spain); Juan Valenzuela-Valdés (Universidad de Granada, Spain)

The fifth generation (5G) of mobile communications has been established as the current paradigm. Nevertheless, it has some limitations for cutting-edge applications. The sixth generation (6G) is being conceived to approach these new services. It is expected to reach 1 Tbps with ultra-low latency communications, which will be possible by enabling sub-THz and THz frequency bands. These bands are challenging in terms of propagation since the diffraction phenomenon is degraded by blocking due to the size of the objects in terms of wavelength. Therefore, Non Line-of-Sight (NLoS) condition produced by the human blockage is not negligible for communication reliability. In this work, the signal attenuation and the blockage duration produced by human blockage are analyzed in the W-Band (75 - 110 GHz). The study shows significant differences in terms of the frequency within the W-Band, the distance between antennas, the human blockage orientation, or the blockage human sample.

Field Trials for Different 5G NSA Cellular Networks 93

George Tsoulos and Georgia E. Athanasiadou (University of Peloponnese, Greece); George Nikitopoulos and Vassilis Tsoulos (University of Peloponnese, Greece); Nikos Christopoulos and Dimitra Zarbouti (University of Peloponnese, Greece)

With the introduction of 5G networks, network operators are encountering novel challenges regarding network coverage, capacity, and quality of service. Therefore, it has become imperative to measure and monitor the performance of networks to identify anomalies and optimize performance. This is particularly crucial for NSA 5G networks, as they are constructed on top of the existing 4G infrastructure and may not offer the full potential of 5G technology. In this study, we underscore the importance of system measurements in recently deployed 5G networks, specifically NSA 5G networks, in a town that comprises diverse operational environments. To accomplish this, we utilized handheld devices to gauge the system parameters simultaneously for 4G and 5G networks, and reported critical parameters that assess coverage, capacity, and quality performance, for three cellular network operators.

A New Approach for Line of Sight Prediction with Geometry Analysis and Machine Learning in Diverse Environments 94

Mostafa Jassim and Thomas Kürner (Technische Universität Braunschweig, Germany)

This paper discusses a new method to predict the line of sight condition between the transmitter and receiver implementing a hybrid model of geometry extraction and machine learning.

Path Gain Measurements and Models at 60 GHz in Street Canyons from Rooftop Sites for Outdoor Coverage 88

Andreia Lopes and Mauricio Rodríguez (Pontificia Universidad Católica de Valparaíso, Chile)

Good coverage with high-gain antennas unlocks the full potential of wide bandwidth at mm/cm bands. We report an extensive outdoor measurement campaign at 60 GHz, with over 470 links in both LOS and NLOS measured on 4 streets in Chile using a specialized narrowband channel sounder. We use a 10° (24.7 dBi) receiving horn antenna rotating at 300 RPM to capture azimuthal angular power and a 50° (10.7 dBi) transmitting antenna. The street-to-street path gain is well represented by a log-normal model with an RMS error of 4.5 dB, and the Standard 3GPP models produced a 4-18 dB RMS error loss relative to our data. The measured path gain around the corner indicates that after turning a corner, the signal suffered an excess loss about 26 dB 10m into the corner and about 30 dB after 100m.

Dual-Polarized Diffraction Measurements and Modeling at D-Band Frequencies 92

Cihan Barış Fındık (CWC Radio Technologies - University of Oulu, Finland); Peize Zhang, Veikko Hovinen, Marko E Leinonen and Aarno Pärssinen (University of Oulu, Finland); Pekka Kyösti (Keysight Technologies & University of Oulu, Finland)

This paper investigates the diffraction mechanism at D-band and its polarization dependency in a concise way. The results are compared with the conventional knife edge diffraction (KED) model. A thin metal, laminated board, and a slab of absorber are used as blockage for characterization. Logarithmic fit functions are provided to demonstrate the impact of material properties in diffraction. In most of the cases, KED model provided a good agreement with measurements. The findings also suggest that the XPR is preserved in diffraction for both co-polarized and cross-polarized scenarios.

Development of a Site-Specific Building Entry Loss Model for High-Rise Buildings 97

Shoma Tanaka (SoftBank Corp., Japan); Akihiro Sato, Sho Kimura, Ho-Yu Lin and Hideki Omote (Softbank Corp., Japan)

Recently, not only mobile networks using ground base stations but also Non-Terrestrial Networks (NTN) have been attracting attention, and the development of ubiquitous networks combining these networks is expected to expand communication coverage. In order to build such networks efficiently, it is necessary to estimate radio propagation characteristics accurately according to various terrestrial environments. In this paper, the authors focus on the study the radio propagation loss characteristics from outdoor to indoor areas, i.e., Building Entry Loss (BEL). 3rd Generation Partnership Project (3GPP) and International Telecommunication Union Radiocommunication sector (ITU-R) have standardized the BEL models. However, these models are not appropriate detailed studies because of the small number of parameters taken into account. Therefore, the authors carried out field measurements in office buildings with various elevation/azimuth angle between the outdoor station and the building and various location of the indoor station, clarified the BEL characteristics, and developed a site-specific model.

Sub-THz Propagation Measurement and Analysis in Indoor Corridor Environment at 159 GHz 89

Juyul Lee, Jae-Joon Park, Heon Kook Kwon, Byung Su Kang and Myung-Don Kim (ETRI, Korea (South))

Numerous studies on propagation characteristics in corridor environments have been conducted. Furthermore, several standardized models have been developed and released by organizations such as ITU-R, 3GPP, ETSI, etc. However, most of these models are not applicable for frequencies above 100 GHz. Nevertheless, the sub-THz band, which encompasses frequencies between 100 GHz and 300 GHz, is being considered as a potential candidate band for 6G. In this context, this paper presents corridor environment measurements at 159 GHz and analyzes their propagation characteristics. The measurements were conducted using a 5-GHz-bandwidth channel sounder for high-resolution delay domain analysis. Horn antennas were installed at both the Tx and the Rx, and they were rotated for angular domain analysis. Both the best directional characteristics (among all the rotational Tx-Rx combinations), denoted by "Max-Dir", and synthesized omnidirectional characteristics, denoted by "Syn-Omni", were derived for path loss and delay spread. Additionally, angular spread statistics were calculated.

Achievable Rate Approximation of Large Intelligent Surface Based on Deep Learning 100

Yifan Mao and Zhirun Hu (University of Manchester, United Kingdom (Great Britain))

In order to enhance the achievable rate of large intelligent surfaces (LIS) afflicted by hardware impairment (HWI), existing LIS systems have adopted a distributed deployment scheme that takes into consideration the impact of HWI. This study aims to investigate the optimization problem of matrix design for distributed LIS in the presence of HWI, as well as to reduce the required number of channel samples and computational complexity for calculating the HWI equivalent noise density and utility. A deep learning-based approach is proposed in this work, which not only learns environment-related information between LISs aiming for maximizing the achievable rate of LIS systems with HWI, but also uses small training samples so to ease the system complexity.

The Effect of Beam Misalignment in Data Center Environment at 285GHz Band 95

Jinhyung Oh (Electronics and Telecommunications Research Institute, Korea (South)); Jong Ho Kim (ETRI, Korea (South)); Jangsuk Choi (RRA, Korea (South)); Jae Ho Seok (National Radio Research Agency, Korea (South))

In this paper, we investigate changes in received power intensity and R.M.S. delay spread due to antenna beam width misalignment when using a terahertz band directional antenna in an inter-rack communication environment within a data center. Because the terahertz band has a relatively short radio distance due to the frequency characteristics, directional antennas are expected to be mainly utilized. However, when using a directional antenna with a narrow antenna beamwidth, a situation where the beamwidths of the transmitting antenna and the receiving antenna do not overlap may occur, resulting in antenna beamwidth misalignment. In particular, in an inter-rack communication environment within a data center, we assume that the transmitting and receiving antennas are horizontally or vertically misaligned with the antenna beam widths, and we confirm the resulting effect in propagation characteristics.

Half Mode Corrugated Substrate Integrated Waveguide (HM-CSIW) Band-Stop Filter Using Hexagonal Ring Resonators 99

Amit Kumar Patel, Aakash Bansal, Chinthana J Panagamuwa and William Whitlow (Loughborough University, United Kingdom (Great Britain))

This article presents a novel wideband bandstop filter using a half-mode corrugated substrate integrated waveguide (HM-CSIW) coupled with hexagonal ring resonators (HRRs). The HM-CSIW is designed to operate at the TE₁₀ mode with a cut-off frequency of 22 GHz. The device is fed with integrated digitated capacitor (IDC) in microstrip feed to achieve a full DC-bias. A reconfigurable bandstop behavior has been reported with the introduction of HRR defects within the CSIW. A simulated insertion loss < 1 dB is shown for the passband of the HM-CSIW with a rejection > -30 dB for the stop-band at 26.5 to 33.5 GHz.

Analog Self-Interference Cancellation by Means of a Synchronised Signal Injection 102

Sarmad Ozan and Geoffrey Hilton (University of Bristol, United Kingdom (Great Britain)); Tommaso Cappello (Villanova University, USA); Mark Beach (University of Bristol, United Kingdom (Great Britain))

Full-duplex communications have the potential to double the spectral efficiency. Self-interference hinders the realization of full-duplex communications, thus significant suppression needs to be achieved to enable simultaneous transmit and receive. This paper presents a digitally-assisted analog self-interference cancellation by pre-coding a cancellation waveform on an auxiliary transmitter using a modified copy of the transmitted signal. Over 30 dB self-interference cancellation has been achieved over a bandwidth of 20 MHz.

A Modified Channel Model for the MIMO System Deployed RIS Elements with Imperfect Surface 103

Shaoxuan Xue, Jianing Zhao and Weikang Yang (Southeast University, China)

In this paper, we propose a modified millimeter wave band RIS-assisted end-to-end MIMO channel model, in which the transmission line model is adopted to analyze the RIS element with microdamage. Normally, by independently adjusting the phase shift of RIS elements, incident waves can be reflected in the desired direction by RIS elements working collaboratively. However, the working states of RIS elements are not always ideal. The influence of imperfect elements on channel response and channel capacity is discussed, modeled and simulated in this paper. The simulation results show that, compared with the normal RIS, the anomalous reflection performance will be affected and RIS-assisted channel capacity will decrease.

Breaking the Myth of RIS: Investigating the Role of User Equipment for Achieving Robust mmWave Wireless Channel Links Under NLOS Environments 86

Bumhyun Kim and Wonbin Hong (Pohang University of Science and Technology (POSTECH), Korea (South))

Reconfigurable Intelligent Surfaces (RIS) are being explored as a solution to tackle millimeter-wave (mmWave) coverage gaps in wireless communication. However, quantitative analysis to synergize the RIS and the beamforming capacity of user equipment (UE) remains elusive. This paper delves into the challenges of mmWave blind spot resulting from insufficient terminal coverage despite the addition of RIS through empirical quantification. For in-depth investigation, a mobile configuration that employs Antenna-on-Display (AoD) situated on the farside of the UE is compared with a conventional Antenna-in-Package (AiP) on the side and backside of UE. The forward reception decreases less than 3 dB, whereas side and back receptions drop by at least 7 dB. Comprehensive total scan patterns and cumulative distribution function analyses highlight the importance of farside coverage. The AoD integration results in a lowered attenuation of 2.04 dB, whereas the conventional AiP setup shows a 4.47 dB reduction at the 90% CDF level.

Scenario Classification and Channel Modeling for MIMO Communications in Dense Urban Street Scenarios 96

Hancheng Li (Southeast University, China); Chen Huang (Purple Mountain Laboratories & Southeast University, China); Cheng-Xiang Wang (Southeast University, China & Purple Mountain Laboratories, China); Junling Li (Southeast University, China)

As one of the most typical wireless communication scenarios, urban communication scenarios draw significant attention in recent years. The full-coverage vision of sixth generation (6G) wireless communications requires a more accurate scenario classification. However, the classification of urban communication scenarios in the existing standard channel models is still rough, which can not meet the requirements of 6G wireless communications. In this paper, based on the physical environmental factors, e.g., building height and density, we classify urban dense street scenarios into three individual sub-scenarios, i.e., major streets, minor streets, and branch streets. Specifically, by optimizing the model parameters, we transform the pervasive channel model into customized channel models for each sub-scenario. The proposed channel models are validated by using the channel data collected from practical communication networks. Furthermore, we analyse the impact of physical environmental factors on channel characteristics.

Channel Characterization and Modeling for Wireless MIMO Communication Systems in Intersection Scenarios 85

Deyuan Zhao (Southeast University, China); Chen Huang (Purple Mountain Laboratories & Southeast University, China); Cheng-Xiang Wang (Southeast University, China & Purple Mountain Laboratories, China); Junling Li, Zhongyu Qian and Wenqi Zhou (Southeast University, China)

As a typical communication scenario, the intersection scenario is not well defined and studied in 3GPP TR 38.901. Therefore, to provide higher-quality communication services, it is necessary to study more refined intersection scenarios. In this paper, we propose a new categorization of the intersection scenarios based on the physical environmental parameters. According to the classification results, the corresponding channel model parameters can be determined to build adaptive channel models, which can avoid further extensive channel measurements to study the channels. Besides, to verify the model accuracy, the synthetic data generated by the proposed channel models are compared with the channel data collected from the practical cell communication networks in Meishan City. The results show that the synthetic data are well matched with the collected channel data. Then, channel characteristics of all types of intersection scenarios are compared and analyzed to verify the reasonableness of the categorization.

Ray-Tracing Based Channel Modeling and Characteristics Analysis for LEO Satellite-To-Ground Systems 90

Kaiyuan Zhang (Southeast University, China); Songjiang Yang and Yinghua Wang (Purple Mountain Laboratories, China); Jie Huang (Southeast University, China); Cheng-Xiang Wang (Southeast University, China & Purple Mountain Laboratories, China)

With the vision of global coverage for the sixth generation (6G) wireless communication systems, the low earth orbit (LEO) satellite systems have drawn considerable attention. In this paper, a LEO satellite-to-ground channel model for urban scenarios is proposed based on ray-tracing. The channel model is divided into the atmospheric part and near-ground part, and the effects of ionospheric scintillation, rainfall, and multipath are studied. The model analyzes the multipath effect in the near-ground with the image method, assuming that the incident rays come from a circular plane transmitter over the ground. Channel characteristics such as delay power spectral density (PSD) and received power of signals are derived. The simulation results show that the received power increases with the satellite elevation angle increasing in urban scenarios.

Tuesday, March 19 14:40 - 15:20

IN1: Hybrid Hardware and Digital Processing for energy efficient space phased arrays; Dr. Hervé Legay, Thales Alenia Space, France

//

Room: Lomond Auditorium

Chairs: Nelson Fonseca (Anywaves, France), George Goussetis (Heriot-Watt University, United Kingdom (Great Britain))

Tuesday, March 19 14:40 - 15:20

IN3: Measurement Techniques for mmW and THz Propagation Channel Characterization; Dr. Pekka Kyösti, University of Oulu, Finland

//

Room: M1

Chairs: Rafael F. S. Caldeirinha (Polytechnic Institute of Leiria & Instituto de Telecomunicações, Portugal), Sana Salous (Durham University, United Kingdom (Great Britain))

Tuesday, March 19 15:20 - 16:00

IN2: Self-Phasing Antenna Array Technology for Real World Wireless; Prof. Vincent Fusco, Queens University of Belfast, N Ireland, UK

//

Room: Lomond Auditorium

Chairs: Nelson Fonseca (Anywaves, France), George Goussetis (Heriot-Watt University, United Kingdom (Great Britain))

Tuesday, March 19 15:20 - 16:00

IN4: Radiowave Propagation Development in the ITU-R; Carol Wilson, CSIRO Space & Astronomy, Australia

//

Room: M1

Chairs: Rafael F. S. Caldeirinha (Polytechnic Institute of Leiria & Instituto de Telecomunicações, Portugal), Sana Salous (Durham University, United Kingdom (Great Britain))

Tuesday, March 19 16:30 - 18:10

CS32: AMTA Session: Novel Antenna Measurement and Post Processing Techniques

T09 Fundamental research and emerging technologies / Convened Session / Measurements

Room: Lomond Auditorium

Chairs: Dennis Lewis (Boeing, USA), Janet O'Neil (ETS-Lindgren, USA)

16:30 Delving into Time Domain Gating: An Extensive Study on Parameter Selection and Its Implications

Zhong Chen (ETS-Lindgren, USA); Dennis Lewis (Boeing, USA)

Time Domain Gating is a convenient function offered in commercial Vector Network Analyzers. Users can easily apply a gate by configuring gating parameters without needing to delve into the intricacies of gating implementation. The selection of these parameters can impact the outcomes, and differences in manufacturers' implementations can also lead to variations. This study explores the detailed implementations of gating algorithms, providing insights on how gating operates in typical commercial analyzers and how the choice of the parameters influences the gated results. Furthermore, we introduce a gating library which allows offline gating on a PC. The library includes all the functions found in a VNA. In addition to incorporating the conventional "edge renormalization" commonly found in VNAs, this library integrates an alternative edge treatment technique known as Spectrum Extension Edgeless Gating, which reduces edge errors for a wide class of measurement data.

16:50 A Comparison of Near-Field to Far-Field Transformation Algorithms for Use with Industrial Multi-Axis Robotic Antenna Measurement Systems

Stuart F Gregson (Queen Mary, University of London, United Kingdom (Great Britain)); Clive Parini (Queen Mary University of London, United Kingdom (Great Britain))

This paper compares and contrasts a number of different near-field to far-field transformation algorithms that can be used for the purpose of processing near-field data acquired using multi-axis industrial robots. The merits and limitations of these various, commonly encountered algorithms are highlighted with comparison far-field data presented. Furthermore, the paper explores the viability of using mixed mode acquisition geometries when performing antenna gain measurements. Here, we verify that at 8 GHz and above, where truncation effects are minimal, for this circa 30 dBi gain (at 8 GHz) test antenna the far-field peaks were in agreement to better than ± 0.02 dB, at 3 SD irrespective of the acquisition geometry and transform algorithm being utilised

17:10 In-Flight Calibration of the Measurement System for UAV-Based Near-Field Antenna Measurements

Mohammad Mirmohammadsadeghi (Technical University of Munich, Germany); Stefan Punzet (Technical University of Munich & School of Computation, Information and Technology, Chair of High-Frequency Engineering (HFT), Germany); Thomas F. Eibert (Technical University of Munich (TUM) & Chair of High-Frequency Engineering (HFT), Germany); Alexander H. Paulus (Technical University of Munich, Germany)

The measurement systems used for outdoor uninhabited aerial vehicle (UAV)-based near-field measurements are typically sensitive to environmental influences, such as temperature. These factors manifest as a drift in the measured signal over time. To detect and compensate such variations in UAV-based near-field measurements, we propose an in-flight calibration approach. This approach involves a near-field interpolation based on local measurements taken repeatedly around fixed reference points, eliminating the need for precise UAV positioning. The interpolation is achieved by solving an inverse source problem. Based on this interpolation technique, which is verified through several simulations, we give a flight strategy that allows for monitoring possible changes in the received signal. We test the effectiveness of the interpolation method using real measurement data.

17:30 Simplified Techniques to Estimate Uncertainties for Antenna Gain Patterns Determined via Near-Field to Far-Field Transformation

David Ulm (Physikalisch-Technische Bundesanstalt, Germany); Thomas Kleine-Ostmann (Physikalisch-Technische Bundesanstalt (PTB), Germany)

Depending on the frequency range of interest, the influence of chamber reflections can be a dominant contribution to the measurement uncertainty when calibrating antennas. Estimating this measurement uncertainty contribution is relatively cumbersome and, strictly speaking, requires a new analysis for each unknown antenna, since the influence of chamber reflections depends on the probe, the measurement chamber, the frequency being examined and the antenna under test.

This article shows how modern transformation algorithms can be used to determine the influence of chamber reflections through redundant measurements. The focus here is on measurement procedures that are simple to carry out and can be integrated automatically into an existing measurement process without having to dismount the antenna under test.

17:50 Stable Phaseless Spherical Antenna Measurements via Mixed-Norm Regularization

Nicolas Mezieres (Centre National d'Etudes Spatiales, France); Benjamin Fuchs (Federal Office of Communications, Switzerland); Laurent Le Coq (University of Rennes 1 & IETR, France)

The phaseless characterization of radiated field of antennas is a promising alternative to ease the measurements and to reduce the cost of measurement setups. However, phaseless procedures are dragged down by significant constraints such as the number of required field samples and convergence problems. This article improves on a previous work by proposing a simple yet efficient spherical, phaseless, measurement procedure based on an adaptive mixed-norm regularization.

Tuesday, March 19 16:30 - 18:10

EXR: Exhibitors' reception

Room: M1

Tuesday, March 19 16:30 - 18:10

A04: Shared apertures and multiband antennas

T01 Sub-6 GHz for terrestrial networks (5G/6G) // Antennas

Room: Alsh 1

Chairs: Santi Conchetto Pavone (Università degli Studi di Catania, Italy), Daniel Sjöberg (Lund University, Sweden)

16:30 Implementation of a Novel Triband Antenna Array in a FR1/FR2 5G-NR System

Tiago Brandão (Inatel, Brazil); Eduardo Saia (Instituto Nacional de Telecomunicações, Brazil); Hugo R. D. Filgueiras (VS Telecom, Brazil); Arismar Cerqueira S. Jr. (INATEL, Brazil)

This paper reports on the implementation of a novel triband antenna array in a FR1/FR2 5G New Radio (5G-NR) system. The proposed array combines three different dipole-shaped antenna subarrays with the following bandwidths: 650- 880 MHz, 2.76-4.2 GHz and 24.9-27.8 GHz. Its adjacent element mutual coupling is kept lower than -20 and -30 dB for interband and intraband conditions, respectively. Furthermore, all array elements provide a beamwidth of approximately 60°, cross-polarization lower than -20 dB and gain from 7 to 9.7 dBi over the designed 5G bands. The performance experimental results demonstrate the applicability of proposed antenna array under real microwaves and mm-waves indoor propagation conditions in accordance to the 3GPP requirements, as a function of the Root Mean Square Error Vector Magnitude (EVMRMS). The new triband antenna array topology enables to perform high-quality simultaneous intraband and interband transmission/reception over different FR1 and FR2 standardized channels.

16:50 Design of A Dual-Circular Polarized Antenna Array for Dual-Band Aperture-Shared Applications

Lianwei Zhu and Shigang Zhou (Northwestern Polytechnical University, China)

This paper presents a shared aperture antenna for 5G applications in FR1 and FR2 bands. The design concept exploits the relevant difference in size between the radiating elements to embed a high frequency patch array in the same area where a low frequency patch lays. The antenna system is designed on a single substrate, with a coaxial probe feeding for the FR2 array. The performances of the antenna system are evaluated for both the operating frequency bands, achieving a 10-dB bandwidth equal to 0.14 GHz (3.8%) for FR1, and to 2.32 GHz (8.6%) for FR2. In FR2, a $\pm 30^\circ$ steering capability along the H-plane is shown.

17:10 A Shared-Aperture Planar Antenna for 5G

Marco Simone (University of Catania, Italy); Santi Conchetto Pavone (Università degli Studi di Catania, Italy); Matteo Bruno Lodi (University of Cagliari, Italy); Nicola Curreli (Italian Institute of Technology, Italy); Giacomo Muntoni and Alessandro Fanti (University of Cagliari, Italy); Gino Sorbello (University of Catania, Italy); Giuseppe Mazzarella (University of Cagliari, Italy)

This paper presents a shared aperture antenna for 5G applications in FR1 and FR2 bands. The design concept exploits the relevant difference in size between the radiating elements to embed a high frequency patch array in the same area where a low frequency patch lays. The antenna system is designed on a single substrate, with a coaxial probe feeding for the FR2 array. The performances of the antenna system are evaluated for both the operating frequency bands, achieving a 10-dB bandwidth equal to 0.14 GHz (3.8%) for FR1, and to 2.32 GHz (8.6%) for FR2. In FR2, a $\pm 30^\circ$ steering capability along the H-plane is shown.

17:30 Simulated Far-Field Pattern Disruption from a 1 GHz Cloaked Array Above a 10 GHz Array

Alexandros Pallaris and Daniel Sjöberg (Lund University, Sweden)

This paper presents a design enabling two antenna arrays to use the same aperture. Starting from a 1 GHz dipole element designed to be cloaked for a frequency band around 10 GHz, we designed a 1 GHz array

including a feeding network to allow us to place 6 of these elements on top of a co-polarized 10 GHz array without adversely disturbing its function. A balun was designed, transmission lines were decided upon, and an array placement was chosen. The effect of the 1 GHz cloaked array with its feeding network on the 10 GHz array's radiation pattern was then simulated, showing that the 10 GHz pattern was not greatly disturbed.

17:50 A Penta-Band Shared Aperture Antenna with A Very Ratio Frequency for 5G and B5G Smartphone Applications

Amjaad Altakhaineh and Saqer S Alja'afreh (Mutah University, Jordan); Chaoyun Song (King's College London, United Kingdom (Great Britain)); Yi Huang (University of Liverpool, United Kingdom (Great Britain))

A penta-band (3.2/5.7/28/38/130 GHz) substrate-integrated waveguide (SIW) shared-aperture based-antenna is proposed. A 2×2 compact hook-shaped (0.6x5 mm²) is proposed for 5.7 GHz band (Port1 and Port3). For structure reuse at millimeter wave frequencies, each hook-shaped antenna composed of two orthogonal quarter wavelength-mode SIW slotted cavities (QMSIW). A triple-band 4×4 MIMO millimeter-wave (mm-W) antenna is resulted from QMSIW cavities (Port4, Port5, Port6, and Port7). Their radiations are at 28/38/130 GHz bands. Furthermore, a single T-shaped strip monopole antenna at mid-wad between hook-shaped structures to operate as a 3.2GHz antenna (Port2) and to maintain isolation between 5.7 hook-shaped antennas. The simulated results show that the presented antenna achieves excellent penta-band performance with a very high frequency ratio (about 37%), high isolation levels (above 15dB) at mm-W frequency bands, and above 12dB isolation level at low bands.

Tuesday, March 19 16:30 - 18:10

A21: Mm-wave antenna technologies II

T02 Mm-wave for terrestrial networks 5G/6G // Antennas

Room: Alsh 2

Chairs: Lukasz Kulas (Gdansk University of Technology, Poland), Francesco Prudeniano (Politecnico di Bari, Italy)

16:30 A Dual Linear-Polarized Gap Waveguide Antenna Element for Radar and Communications at 77 GHz

Reza Gheybi Zarnagh (University of Twente, The Netherlands); Abolfazl Haddadi (Gapwaves AB, Gothenburg, Sweden); Andrés Alayón Glazunov (Linköping University, Sweden)

A novel two-port antenna employing Gap Waveguide technology introduces $\pm 45^\circ$ slant polarizations for Joint Communication and Sensing (JCAS) systems or polarimetric radars in the 76 – 81 GHz frequency band. The subarray antenna comprises a two-layer radiating structure: the lower part features vertical slots radiating horizontal polarization, while the upper part integrates a septum polarizer and side metallic ridges. The septum polarizer converts horizontal to circular polarization by creating orthogonal electric field components with a 90° phase difference, while side ridges compensate for this phase difference, generating slant-polarized waves. This method achieves slant polarization by exciting the antenna ports without needing cavities to alter electric field orientation. The antenna, with two elements, attains a peak gain of 8.97 dBi within the 76 – 81 GHz frequency band, demonstrating an axial ratio exceeding 30 dB at $\pm 45^\circ$ slant polarization.

16:50 Dual-Linearly Polarized Pillbox Beamformer in Hybrid CNC-PCB Technologies at W-Band

Thi-Kim-Ngan Nguyen (Universite de Rennes, France); Mauro Ettore (University of Rennes 1 & UMR CNRS 6164, France); Ronan Sauleau (University of Rennes 1, France); David González-Ovejero (Centre National de La Recherche Scientifique - CNRS, France); Ahmed Alwakil (Universite de Rennes, France)

This work introduces a novel low-profile dual-linearly polarized pillbox beamformer operating at W-band in hybrid CNC-PCB technologies. The dual-linear polarization is achieved by exciting two orthogonal modes in an overmoded parallel plate waveguide (OPPW) namely: the quasi-TEM mode (qTEM) and the quasi-TE1 mode (qTE1). The pillbox transition is made of two distinct couplers that transfer efficiently the energy of the two operation modes that propagate from the feeding source in the lower PPW to the uppermost PPW layer via separate coupling regions. The qTEM-mode coupler is built in Aluminum, whereas a multilayer PCB stack-up is used for the qTE1-mode coupler. To the best of our knowledge, this is the first time that this topology has been proposed to achieve dual-linear polarization in a single pillbox beamformer at mm-wave frequency.

17:10 Millimeter Wave Retrodirective Van Atta Arrays in LTCC Technology

Kamil Trzebiatowski (Gdansk University of Technology, Poland); Martin Ihle (Fraunhofer Institute for Ceramic Technologies and Systems IKTS, Germany); Benedykt Sikorski, Lukasz Kulas and Krzysztof Nyka (Gdansk University of Technology, Poland)

The millimeter wave Van Atta arrays, intended for chipless RFID applications and fabricated in LTCC technology, are presented in this paper. The arrays are designed for 24 GHz and 60 GHz bands. The method for an easy modification of the RCS characteristic by increasing the number of single-dimensional arrays, intended for increasing the RCS level, is also presented. The LTCC manufacturing process is described in detail. The fabricated arrays are characterized in an anechoic chamber and exhibit RCS levels up to -26 dBsm with a small 51 x 17 mm footprint.

17:30 Assessment of MFE-Based Multiport Waveguide Crossing for Use with Low-Cost, Low-Loss Dielectric Interconnects in Millimeter Wave Arrays

Nona Messhenas and Werner L. Schroeder (RheinMain University of Applied Sciences, Germany); Thomas Kaiser (Universität Duisburg-Essen, Germany)

Practical feasibility of multi-port waveguide crossings for dielectric waveguides in millimeter-wave arrays is addressed by simulation. An idealized model of a 6-port waveguide crossing which is derived from a two-dimensional Maxwell's Fish-eye lens using concepts from transformation optics is considered as example. Results for the 77 GHz automotive radar band are presented. Conclusions with respect to required device size, dielectric material and acceptable loss factor are drawn.

17:50 Feasibility Investigation on a Low-Cost an Air-Filled Substrate Integrated Waveguide Array Antenna in V-Band

Antonella Maria Loconsole (Politecnico di Bari, Italy); Adham Mahmoud (Institut d'Électronique et de Télécommunications de Rennes, France); Francesco Anelli and Vito Vincenzo Francione (Politecnico di Bari, Italy); Mauro Ettore (University of Rennes 1 & UMR CNRS 6164, France); Francesco Prudeniano (Politecnico di Bari, Italy)

In this work, Printed Circuit Board technology is considered for the design and fabrication of a multilayer air-filled Substrate Integrated Waveguide array antenna in V-band. Different alternative stack-ups are investigated for lamination considering prepreg materials or assembling with dielectric screws. Performances are compared via simulation in terms of bandwidth, maximum gain, total losses, and easiness of construction. The prototype for the stack-up assembled with dielectric screws is chosen for fabrication for easiness.

Tuesday, March 19 16:30 - 18:10

A19: Antennas for space systems

T03 Aerospace, new space and non-terrestrial networks // Antennas

Room: Boisdale 1

Chairs: Nelson Fonseca (Anywaves, France), Christophe Granet (Lyrebird Antenna Research Pty Ltd, Australia)

16:30 Compact Dual-Band Dual-Polarization Feed for Broadband Communication Satellites

Nelson Fonseca (Anywaves, France)

This paper describes a novel compact dual-band dual-polarization feed design with reduced cross-section. This is achieved using a developable H-plane coupler wrapped around the orthomode junction. This design approach enables to reduce significantly the cross-section of the feed without compromising its longitudinal length. A prototype of a specific design in the K/Ka-band is described and experimental results are reported,

showing good agreement between simulated and measured data. The functional part of the feed occupies a volume of only 18mm×18mm×30 mm. The mechanical multi-layer assembly design of the prototype has an hexagonal outline compatible with a feed spacing as small as 25 mm. The feed spacing may be reduced further using additive manufacturing techniques for the design of highly integrated clusters. This feed is of interest for the design of innovative multiple-feed-per-beam feed clusters onboard broadband communication satellites.

16:50 Polymer-Based Additive Manufacturing of a Complex RF Front-End for New Space Applications

Carlos Suárez García and Beatriz Bedia (TTI, Spain); Norica Godja and Gregor Palczynski (CEST, Austria); Konstanze Seidler (Cubicure GmbH, Austria); Christian Gorsche (CUBICURE, Austria)

An innovative 3D-printed wideband monolithic passive array breadboard for space applications has been designed, manufactured, and tested with outstanding results in the K/Ka band. Among the main specifications of the antenna, it has double switchable circular polarization and represents a significant forty-seven percent of relative bandwidth in a single aperture, covering both the Tx and Rx bands. This achievement represents a viable strategy to manufacture satellite antennas using high-performance polymers via additive manufacturing (AM) and surface metallization techniques. The proposed approach for satellite on-board antenna arrays displays significant advantages with respect to traditional antennas in terms of low profile, weight, number of pieces, time-consuming assembly, and payload-reducing parts.

17:10 Non-Regular Multibeam Coverage Antenna for Ka-Band High-Throughput Satellite Communications

Enrica Cala (Swisst012, Switzerland); Marco Baldelli (Airbus Italy, Italy); Alfredo Catalani (ESA ESTEC, Italy); Esteban Menargues (SWISSt012, Switzerland); Giovanni Toso (European Space Agency, ESA ESTEC, The Netherlands); Piero Angeletti (European Space Agency, The Netherlands)

The paper describes a novel multibeam antenna configuration for high-throughput satellite communications. The spatial traffic demand is assumed proportional to population distribution and is balanced at payload level using a Voronoi diagram-based approach. This approach optimizes beam coverage and traffic per beam while minimizing co-channel interference. The non-regular multibeam coverage is obtained by means of a focal array fed reflector (FAFR) with a passive multi-feed-per-beam (MFPB) beamforming network. An innovative strategy is described for sharing feeds in subarrays while reducing complexity of the beamforming network (BFN). The FAFR-MFPB antenna configuration is applied to a 70 beams scenario and advanced 3D additive manufacturing techniques are demonstrated to create the complex BFN.

17:30 A Possible Way to Reduce the High Sidelobe Levels Due to Reflector Struts: Curly Struts

Christophe Granet (Lyrebird Antenna Research Pty Ltd, Australia); Thomas A. Milligan (Milligan and Associates, USA); Robert Hoferer (Spacetime Machine Co, unknown); Stig Sørensen (TICRA, Denmark)

The brand new concept of curly-struts is proposed as a way to mitigate the high sidelobes generated by reflector struts. The curly-struts concept is applied to two basic examples: a Cassegrain reflector and a prime-focus parabolic dish.

17:50 Exploring the Potential of Spatially Modulated Full-Metal Dichroic Mirrors for Deep Space Antennas

Andrea Guarriello (Thales Alenia Space, France); Charalampos Stoumpos and María García-Vigueras (IETR-INSA Rennes, France); Renaud Loison (IETR & INSA, France); Jean-Jacques Herren (Thales Alenia Space, France); Hervé Legay (Thalès Alenia Space, France)

This paper introduces a novel approach to designing Frequency Selective Surfaces (FSS) for dichroic mirrors in Deep Space antennas. Unlike conventional periodic FSS designs, the proposed method employs a quasi-periodic structure, with each unit cell tailored to its specific local incidence angle. This approach aims to compensate for losses induced by extreme incidence angles, enhancing the overall performance of the dichroic mirror. The unit cell chosen for this study exhibits a range of design degrees of freedom, making it well-suited for this novel approach. Additionally, this unit cell offers advantages in terms of broad bandwidth behavior and 3D-printing compatibility, addressing key requirements for Deep Space antenna applications. The paper outlines the methodology for constructing the quasi-periodic structure and presents preliminary performance metrics, demonstrating the potential for improved performance in Deep Space antenna systems. Future work will focus on implementing the proposed design methodology and further optimizing the quasi-periodic surface.

Tuesday, March 19 16:30 - 18:10

P03: Detection and estimation

T04 RF sensing for automotive, security, IoT, and other applications // Propagation

Room: Boisdale 2

Chairs: Yi Huang (University of Liverpool, United Kingdom (Great Britain)), Timothy Pelham (University of Bristol, United Kingdom (Great Britain))

16:30 Seasonal Snow Melting Process Investigation in Polar Environment Using a Dual-Receiver Radar Architecture

Martina Lodigiani and Lorenzo Silvestri (University of Pavia, Italy); Pedro Espín-López (CTTC, Spain); Marco Pasian (University of Pavia, Italy)

With the arrival of spring and the rise in temperatures, seasonal snow coverage starts its melting process and undergoes significant metamorphic changes. Daily monitoring can help to improve the knowledge about this process. Field investigations conducted over a 15-day period in the polar station of Sodankylä-Tähtelä, Finland, utilizing the SNOWAVE system, a dual-receiver multiband and portable radar system in direct contact with the snow surface, revealed substantial day-to-day variations during the spring period. Through meticulous analysis of radar traces, researchers can discern trends in snow depth, density, and liquid water content in response to temperature fluctuations throughout this extended period. The paper presents the outcomes of this field campaign, demonstrating the possibility of employing innovative technologies for a monitoring throughout the snow melting process.

16:50 Advanced Microwave Radiometry: Refining Sun-Tracking Technique for Atmospheric Attenuation Retrieval and Sun Brightness Temperature Estimation

Giovanni Stazi and Marianna Biscarini (Sapienza University of Rome, Italy); Luca Milani (European Space Agency, Germany); George Brost (Air Force Research Laboratory, USA)

Sun-Tracking (ST) is a novel ground-based microwave radiometric technique that allows the retrieval of the slant-path atmospheric attenuation in all-weather conditions as well as the estimation of the Sun brightness temperature. This work proposes a refinement procedure of the ST technique based on taking into account the Sun's angular size variability throughout the year. We have obtained a reduction up to more than 50% of the standard deviation of the estimated Sun's brightness temperature. On the other hand, we have demonstrated that the approximation of a constant value for the Sun's angular size, that strongly limits the precision of the Sun brightness temperature estimation, is acceptable for the ST-based attenuation retrieval algorithm. The study is performed exploiting a three-years dataset of ST measurements collected in Rome NY between 2015 and 2018 at 23.8 (K-band), 31.4 (Ka-band), 72.5 (V-band), and 82.5 (W-band) GHz.

17:10 Influence of the Atmospheric Plasma Sheath on the RCS of a Hypersonic Reentry Vehicle

Florian Mitanchey, Pascal Pagani, Vivien Loridan, Pierre Bonnemason and Claire Latappy (CEA - CESTA, France)

During the atmospheric reentry of a hypersonic vehicle, generation of plasma occurs as a result of its velocity (above Mach 5), yielding complex physics phenomena. Consequently, the object's Radar Cross Section (RCS) strongly varies, depending on the plasma parameters. This paper presents an approach to simulate the RCS behavior of a hypersonic reentry object, by seamlessly integrating a fluid dynamics code implementing Navier-Stokes equations with nonequilibrium chemistry, and an electromagnetic code resolving Maxwell equations by combining a Finite Elements Method and a Boundary Elements Method. As a first validation, the method is applied to a PEC sphere. Further results are provided for the NASA space probe RAM C-II.

17:30 Neural Network Based Microwave Tumour Detection Using Breast Pairs

Fatimah Eashour and Stephen Pistorius (University of Manitoba, Canada)

This study investigated the quality of tumour detection using radar microwave signals from paired breasts (simulating bilateral breast pairs) as input to a neural network classifier. The detection quality was compared to that of a classifier that used single breasts as test samples. The samples consisted of sinograms of experimental microwave scans of MRI-derived breast phantoms. The results demonstrate an improvement in

detection quality of 3% in terms of the receiver operating characteristic - area under the curve (ROC AUC) and 5% in sensitivity for a classifier that used paired breasts. Notably, the classifier exhibited higher detection quality for smaller and denser breasts.

17:50 Utilization of Wi-Fi Signal for Validation of Micro-Doppler Model in a Person Falling Scenario

Nopphon Keerativoranan, Yikai Wang and Jun-ichi Takada (Tokyo Institute of Technology, Japan)

With the growing demand for medical care among the elderly, it is increasingly important to have intelligent detection of falling incidents. Understanding the micro-Doppler signature during a fall event with the accurate channel model is important for future development of the effective falling detection algorithm. In this work, the micro-Doppler channel model is presented based on a combination of radar cross-section (RCS) scattering and spheroid human models. A simplified 3D human fall model is created by creating spheroids between skeleton joints to represent different body parts. The scattering wave from each spheroid body component is computed on the basis of the scattering geometry and the RCS. The channel is then synthesized by superposition of these scattering waves. The measurement system that consists of the Wi-Fi-based channel sounder and the Kinect motion capture system is utilized to validate the proposed model with the captured skeleton during the falling incident.

Tuesday, March 19 16:30 - 18:10

CS13: Applications of RFID Antennas and Systems

T05 Positioning, localization, identification & tracking / Convened Session / Antennas

Room: Carron 1

Chairs: Giulio M. Bianco (University of Roma Tor Vergata, Italy), Mahmoud Wagih (University of Glasgow, United Kingdom (Great Britain))

16:30 Antenna System for Simultaneous Wireless Power and Information Transfer to Brain Implants

Ali Khaleghi (NTNU, Norway & OUS, Norway); Aminolah Hasanvand (NTNU - Norwegian University of Science and Technology, Norway); Ilanko Balasingham (Norwegian Institute of Science and Technology, Norway)

Brain-Computer Interfaces (BCIs) have revolutionized neuroscience applications, from motor rehabilitation to neuroergonomics. Traditional implantable BCIs with invasive microelectrode arrays pose challenges, notably the need for wired connections and inherent implantation risks. This paper introduces a battery-free wireless BCI system, consolidating an implant and its external supporting system. Our design centers on a dual-function antenna system: firstly, an inductive coupling mechanism enables wireless power transfer, sufficiently powering the implant's Application-Specific Integrated Circuit (ASIC) for stimulation and readout without an implant battery. Secondly, a backscatter antenna in the implant facilitates battery-free, high-data-rate wireless connectivity (up to 32 Mbps). This system not only enhances the BCI experience by eliminating wires but also retains data fidelity and energy efficiency, promising a safer, more efficient interface for tasks like robotic arm control.

16:50 Understanding UHF RFID Sensor Systems: A Summary

Jasmin Grosinger (Graz University of Technology, Austria)

The paper provides an extensive summary of ultra-high-frequency radio frequency identification (RFID) systems, with a particular emphasis on the use of the antenna as a sensor. The overview begins with a general explanation of RFID systems, including backscatter communication, which involves absorption and reflection at the tag. The reader, especially the reader receiver, is then discussed in detail. The paper further presents a clear relationship between the received backscattered tag signal at the reader receiver and the tag's absorbing and reflecting mode, as well as its respective backscattered electric field. This signal model allows for a systematic design of sensor tags that use the antenna as a sensor.

17:10 Exploiting Near-Field Antenna Detuning in Collision Avoidance Systems for RFID-Equipped Robots

Glauco Cecchi, Andrea Motroni and Paolo Nepa (University of Pisa, Italy)

This paper presents a collision avoidance system for mobile robots equipped with UHF-RFID (Ultra-High Frequency - Radio Frequency Identification) readers. The proposed system requires the presence of RFID tags with self-tuning chips to recognize the tag antenna mismatch caused by the near-field interaction with the robot-installed antenna. The self-tuning tags are provided with a capacitors network used to re-tune the antenna in presence of mismatches. The network configuration is transmitted to the reader through modulated backscattering. The onboard computing intelligence can use this information to recognize a hazardous situation, stop the robot, and calculate a new safe route. The system is implemented and tested in a real environment where a statistical analysis with a large dataset is conducted to provide an optimized and reliable low-cost system.

17:30 Enabling Living Spaces Through Customizable NFC-Enabled Smart Table System

Mustasin Mahmood Sakif and Tiina Ihalainen (Tampere University, Finland); Sari Merilampi (Satakunta University of Applied Sciences, Finland); Sanna-Mari Petäjistö (Junet Ltd., Finland); Pasi Raunonen, Tiina Vuohijoki and Johanna Virkki (Tampere University, Finland)

This paper presents a near field communication based smart table with a cloud-based web user interface for controlling. The user needs for a smart furniture system were gathered and based on the expert stakeholders, the main needs were synthesized into 1) environment supporting the resident's possibilities for communication and participation, 2) simple to use, easy to modify, unnoticeable, 3) supports several actions. Based on these needs, the technical development work presented in this publication was carried out. As proof-of-concept applications, the system allows the user several functionalities: sending text message, sending email, making phone call, playing music, opening coffeemaking tutorial or useful contact information. Preliminary testing for system functionality and practical use were conducted. The testing results indicate that the system is working reliably. Also, the NFC tags integrated performed well in terms of read range and surface reading area. The paper presents an innovative platform for smart home applications.

17:50 UHF RFID Sensor Antenna for Fat Content and Adulteration Detection of Milk

Abubakar Sharif (University of Electronic Science and Technology China, China); Kamran Arshad and Khaled Assaleh (Ajman University, United Arab Emirates); Muhammad Ali Imran and Qammer H Abbasi (University of Glasgow, United Kingdom (Great Britain))

This paper proposes an ultrahigh frequency (UHF) radio frequency identification (RFID) tag based sensor for fat content and spoilage detection of milk. This dual-slot based tag is designed and optimized using characteristic mode analysis (CMA) for whole milk (with 3.6% fat content). The two open triangular slots provide improved impedance matching over milk bottles. The tag antenna achieved a good impedance match and bandwidth (880 MHz - 950 MHz). Fabricated prototypes of tag are pasted on milk bottles with fat contents 1.5% (low fat cow's milk), 3.6% (full cream cow's milk) and 4.5% (full cream buffalo's milk). The RFID reader setup with EIRP 30 dBm (1W). The experiment results show the capabilities of proposed sensor tag for detecting milk's fat contents. Furthermore, this tag paves a non-invasive way for detection of milk adulteration (mainly dilution of milk using water) and spoilage of milk.

Tuesday, March 19 16:30 - 18:10

CS27: Implantable antennas and intra-body wave propagation

T06 Biomedical and health / Convened Session / Antennas

Room: Carron 2

Chairs: Sema Dumanli (Bogazici University, Turkey), Ali Khaleghi (NTNU, Norway & OUS, Norway)

16:30 Link Budget Estimation for Implantable Antennas: From In-Body Coupling to Free-Space Radiation

Mingxiang Gao (EPFL, Switzerland); Sujith Raman (University of Twente, The Netherlands); Zvonimir Sipus (University of Zagreb, Croatia); Anja K. Skrivervik (EPFL, Switzerland)

In wireless communication systems, the Friis transmission equation is commonly used to quickly estimate wireless transmission efficiency between the transmitter and the receiver. In the case of wireless implantable bioelectronic systems, the gain of the implantable antenna is significantly decreased by the high-loss nature of the host body. Additionally, numerical analysis of implantable antennas considering the host bodies is time-consuming and laborious. On this basis, this work proposes a method for quickly estimating the link efficiency between an implant and an external node, which is applicable for implantable miniature antenna located in a large-scale host body. This method uses closed-form expressions that consider various parameters, including implant dimension, implantation depth, and the dielectric characteristics of the host body. A measurement example is provided, validating the effectiveness of the proposed method in the assessment of the link budget for wireless bioelectronic systems.

16:50 An Electromagnetic Metasurface for Impedance Matching in Microwave Biomedical Applications

Alessandro Luigi Dellabate and Danilo Brizi (University of Pisa, Italy); Tarakeswar Shaw (Postdoctoral Researcher, Uppsala University, Sweden); Mauricio D Perez (Uppsala University, Department of Electrical Engineering); Robin Augustine (Uppsala University, Sweden); Agostino Monorchio (University of Pisa & CNIT, Italy)

This paper presents the design of an electromagnetic metasurface to be employed as a matching layer to improve the electric field transmission inside the human body, for microwave imaging and sensing. The approach used to develop the matching layer is based on the transmission line model and it can be useful to tailor the metasurface properties for different applications. In particular, by retrieving the MS impedance and tuning it in order to compensate for the body impedance, the reflection coefficient at the air-tissues interface can be minimized. We demonstrated that the conceived MS is capable of improving the transmitted electric field by 6.6 dB at 1.61 GHz. Moreover, the array reduced dimensions allow to realize systems suitable for different anatomical districts. The results show the possibility to improve the electric field transmission inside human body at microwaves, leading to safer and more effective solutions with respect to the actual state-of-the-art.

17:10 Theoretical Insights and Engineering of Wireless Body-Implanted Bioelectronics

Denys Nikolayev (Institut d'Électronique et des Technologies du Numérique (IETR) - UMR CNRS 6164, France); Erdem Cil (University of Rennes 1, France); Hajar Benaicha and Gabriel Gaugain (University of Rennes, France); Pratik V Vadher (IETR, CNRS & University of Rennes 1, France); Lorette Queguiner (University of Rennes, France); Ronan Sauleau (University of Rennes 1, France); Giulia Sacco (IETR - CNRS, France); Icaro V Soares (IETR & Université de Rennes 1, France)

The development and widespread adoption of body-implanted bioelectronics face significant challenges due to limited wireless performance and reliance on batteries. This contribution provides an overview of recent theoretical advancements and practical applications in antenna design for body-implanted bioelectronics. It explores performance indicators, including bandwidth, robustness, radiation efficiency, and the impact of loss mechanisms. Additionally, it discusses the role of antennas in wireless sensing and strategies to mitigate reflection losses, offering insights into efficient and safe power transfer.

17:30 A Compact Wideband Biocompatible Circularly Polarized Implantable Flexible Antenna for Biomedical Applications

Tarakeswar Shaw (Postdoctoral Researcher, Uppsala University, Sweden); Bappadiya Mandal (Uppsala University, Uppsala, Sweden); Gopinath Samanta (The LNM Institute of Information Technology, India); Mauricio D Perez (Uppsala University, Department of Electrical Engineering); Robin Augustine (Uppsala University, Sweden)

This article presents the design of a compact, biocompatible, implantable circularly polarized (CP) antenna on a flexible substrate for biomedical use within the 920 MHz Industrial, Scientific, and Medical (ISM) frequency band. To ensure compatibility with human tissue and reduce the antenna's profile, a biocompatible alumina (Al₂O₃) coating surrounds the CP antenna. The antenna employs a thin 0.2 mm dielectric substrate to maintain flexibility. The antenna's compact dimensions, including the coating, are $0.03 \lambda_0 \times 0.03 \lambda_0 \times 0.0007 \lambda_0$, with λ_0 being the free-space wavelength at 920 MHz. It achieves an impressive 21.87% high axial ratio bandwidth (ARBW) covering the 902-928 MHz ISM band. Additionally, it provides a peak gain of -23.35 dBi and outstanding co-cross polarization discrimination of 22 dB at 920 MHz when oriented along the bore sight direction. This antenna design offers significant potential for various biomedical applications.

17:50 Biodegradable Implant Antenna Utilized for Real-Time Sensing Through Genetically Modified Bacteria

Ahmet Bilir and [Sema Dumanli](#) (Bogazici University, Turkey)

This work presents a wireless in-vivo sensing system. The sensing system consist a bio-hybrid implant and a wearable reader antenna pair. The bio-hybrid implant has two parts: a biodegradable implant antenna and genetically modified bacteria. The biodegradable implant antenna operates as a passive reflector and genetically modified bacteria controls the degradation speed according to the presence of a specific molecule of interest. As the implant antenna degrades, changes in its geometry shift its resonant frequency. This shift is tracked by the wearable reader antennas. Therefore, the presence of the molecule of interest can be wirelessly tracked in-vivo in real time from outside the body.

Tuesday, March 19 16:30 - 18:10

CS7: Antenna for emerging applications at sub-THz frequencies

T07 THz and high frequency technologies / Convened Session / Antennas

Room: [Dochart 1](#)

Chairs: Antonio Clemente (CEA-Leti, France), Tomas Thuroczy (Univ Rennes, France)

16:30 Low Profile and High Gain Folded Transmitarray in Quartz for Radiometry at 310 GHz

Tomas Thuroczy (Univ Rennes, France); Orestis Koutsos (CEA Leti, France); Olivier De Sagazan (University Rennes 1, France); Ronan Sauleau (Universite de Rennes, France); David González-Ovejero (Centre National de La Recherche Scientifique - CNRS, France)

This manuscript presents the design, analysis, and simulations of a high-gain and compact folded 310 GHz transmitarray, manufactured in quartz for radiometric applications on compact satellite platforms. The antenna performance is analyzed using an in-house method based on geometrical optics that utilizes unit-cell simulations building on a local periodicity approximation. The antenna has an electrical size of $46\lambda \times 46\lambda \times 17\lambda$ and achieves a peak gain and aperture efficiency of 41.4 dBi and 50%, respectively. The -1 dB gain bandwidth of the antenna is 8%.

16:50 Simultaneously Dual-Polarization Convertible Sub-THz Reconfigurable Intelligent Surface Enabled by Through-Quartz VIAs

[Byeongju Moon](#), Jungsuek Oh, Hogyeon Kim and Seungwoo Bang (Seoul National University, Korea (South))

In this paper, simultaneously dual-polarization convertible sub-THz reconfigurable intelligent surface (RIS) enabled by through-quartz VIAs is proposed. The proposed RIS has two functionalities: beam steering and polarization conversion. Liquid crystal (LC) is placed under the metal pattern and works as a tunable substrate, which makes it possible to steer the beam. The metal pattern, placed above the LC layer, converts the TE polarization to the TM polarization and vice versa. To avoid the polarization conversion performance degradation, the through-VIA on quartz substrate, a sanding technique with um-sized particles is used and copper is filled in the holes to form VIAs. Then the conventional display manufacturing process is utilized to fabricate the proposed RIS. The proposed RIS unit cell has 130° of phase tuning range with 45 um cell gap. The experimental results show that the proposed RIS satisfies both intended functions.

17:10 Experimental Characterization of a Core-Shell Lens for Antenna On-Package Integration at D-Band

Nick van Rooijen, Maria Alonso-delPino, Juan Bueno, Marco Spirito and Nuria LLombart (Delft University of Technology, The Netherlands)

Recently, we introduced a core-shell lens antenna architecture for D-band applications. The antenna uses an electrically small, non-diffractive core lens made of dense thermoplastics, and a large shell lens. Leaky-wave double-slot feeding antennas are used to generate a near-Gaussian pattern, and are fabricated on low-loss glass substrates, enabling future on-package antenna solutions. In this contribution, we report the first results of the experimental characterization of the antenna. A prototype with two types of feeding networks has been developed and characterized: coplanar waveguide based (single-layer), and microstrip based (double-layer). The single-layer design has an estimated total loss of less than 2dB, with a high gain of more than 30dB over a bandwidth of 28 percent. Measurements for the microstrip feed are currently on-going.

17:30 Characterization of a D-Band Active Transmitarray System for Efficient Point-To-Point Links

[Francesco Foglia Manzillo](#) (CEA-LETI, France); Jose Luis Gonzalez Jimenez (Université Grenoble-Alpes/CEA-Leti, France); Abdelaziz Hamani (CEA, France); Alexandre Silligaris (Cea, Leti, Minatec, France); Antonio Clemente (CEA-Leti, France)

We present the design and characterization of an innovative D-band transmitting antenna system. It comprises an active focal-plane array with two separate antennas which radiate two different signals, with adjacent bands, generated by an integrated circuit, and a flat discrete lens. The lens is designed to form a high-directivity broadside beam in both bands, i.e. from 139.3 GHz to 156.6 GHz. The use of two narrowband signals enhances the spectral efficiency and power consumption. Measurements show a remarkable improvement of transmitted power with respect to similar transmitters performing channel aggregation with guided components. The effective isotropic radiated power is higher than 25 dBm in a relative bandwidth of 11% and attains a peak value of 30.5 dBm. The measured radiation patterns are stable with frequency in each of the two sub-bands. The estimated antenna gain of the system (about 26 dBi) is in tight agreement with numerical data.

17:50 Reconfigurable Intelligent Surfaces for THz: Signal Processing and Hardware Design Challenges

Luis M. Pessoa (INESC TEC & Faculty of Engineering, University of Porto, Portugal); George C. Alexandropoulos (University of Athens, Greece); Antonio Clemente (CEA-Leti, France); Sergio Matos (ISCTE-IUL / Instituto de Telecomunicações, Portugal); Ryan Husbands (British Telecoms, United Kingdom (Great Britain)); Sean Ahearne (Dell EMC, Ireland); Qi Luo (University of Herfordshire, United Kingdom (Great Britain)); Veronica Lain-Rubio (ACST, Germany); Thomas Kürner (Technische Universität Braunschweig, Germany)

Wireless communications in the THz frequency band is an envisioned revolutionary technology for sixth generation networks. However, such frequencies impose certain coverage and device design challenges that need to be efficiently overcome. To this end, the development of cost- and energy-efficient technologies for scaling these networks to realistic scenarios constitute a necessity. Among the recent research trends contributing to these objectives belongs the technology of reconfigurable intelligent surfaces (RISs). In fact, several high-level descriptions of THz systems based on RISs have been populating the literature. Nevertheless, hardware implementations of those systems are still very scarce, and not at the scale intended for most envisioned THz scenarios. In this paper, we overview some of the most significant signal processing and hardware design challenges with THz RISs, and present a preliminary analysis of their impact on the overall link budget and system performance, conducted in the framework of the ongoing TERRAMETA project.

Tuesday, March 19 16:30 - 18:10

CS11: AI-Driven Antenna Design Contemporary Methodologies and Practical Applications

T08 EM modelling and simulation tools / Convened Session / Antennas

Room: [Dochart 2](#)

Chairs: Bo Liu (University of Glasgow, United Kingdom (Great Britain)), Lei Wang (Heriot-Watt University, United Kingdom (Great Britain))

16:30 AI-Assisted Design and Experimental Testing of a Compact UWB Antenna for the Inspection of Food and Beverage Products

Jorge A. Tobon Vasquez, Marco Ricci and Calin I Maraloiu (Politecnico di Torino, Italy); Mobayode Akinsolu (Wrexham University, United Kingdom (Great Britain));

Mingwei He (Nanyang Technological University, Singapore); Francesca Vipiana (Politecnico di Torino, Italy)

Detecting physical contamination caused by foreign bodies is an ongoing challenge faced by the food and beverage industries. To overcome the limitations of existing devices, a novel detection principle based on microwave imaging (MWI) has been assessed. MWI enables non-invasive analysis of the sample under test through a 3-D reconstruction obtained from the alteration that the electromagnetic scattered waves undergo due to the foreign body. We propose an antenna that can cover a broad set of food types, permitting the adaptability of the system's operating frequency depending on the products' dielectric properties and the containers' type. The proposed antenna is designed with the help of artificial intelligence (AI). Thanks to its low cost and small dimensions, we can increase the acquired information by increasing the number of antennas placed around the product. A functioning system using the designed antenna is presented, assessing the image reconstruction with realistic products and contaminants.

16:50 AI-Driven Design of a Quasi-Digitally-Coded Wideband Microstrip Patch Antenna Array

Mobayode O. Akinsolu (Wrexham University, United Kingdom (Great Britain)); Yasir Ismael Abdulraheem Al-Yasir (University of Bradford, United Kingdom (Great Britain));

Qiang Hua (University of Huddersfield, United Kingdom (Great Britain)); Chan Hwang See (Edinburgh Napier University, United Kingdom (Great Britain)); Bo Liu

(University of Glasgow, United Kingdom (Great Britain))

Artificial intelligence (AI) is enabling the automated design of contemporary antennas for numerous applications. Specifically, the use of machine learning (ML)-assisted global optimization techniques for the efficient design of modern antennas is now fast becoming a popular method. In this work, we demonstrate for the first time, the ML-assisted global optimization of a high-dimensional non-uniform overlapping quasi-digitally coded microstrip patch antenna array using a new AI-driven antenna design technique, called TR-SADEA (the training cost-reduced surrogate model-assisted hybrid differential evolution for complex antenna optimization). The TR-SADEA-generated array showed very promising simulated frequency responses for potential wideband applications with a -10 dB impedance bandwidth of 5.75 GHz to 10 GHz, a minimum in-band realized gain of 5.82 dBi, and a minimum in-band total radiation efficiency of 87.84%.

17:10 Reflecting/Absorbing Dual-Mode Textile Metasurface with AI-Driven Parametric Studies

Qiang Hua (University of Huddersfield, United Kingdom (Great Britain)); Menglin Zhai and Rui Pei (Donghua University, China); Mobayode O. Akinsolu (Wrexham University, United Kingdom (Great Britain))

This paper presents a textile-based reflecting/absorbing dual-mode metasurface, and emphasizes the role of AI-driven parametric studies in the designing process. The proposed textile metasurface can achieve a reflecting mode with the zero-degree reflection phase centre at 2.4 GHz, and an absorbing mode at the same resonance frequency. The absorption and reflection band of the design are centered at the same frequency by applying a state-of-the-art AI-driven antenna design technique, self-adaptive Bayesian neural network surrogate model-assisted differential evolution for antenna optimization (SB-SADEA) method. The proposed design can also achieve polarization insensitivity and a certain level of incident angle insensitivity. The fabricated prototype of the design achieves a maximal absorption rate of 99.8% and maintains an absorption over 90% in the frequency range of 2.39 to 2.43 GHz. Moreover, a textile linear polarized monopole antenna was fabricated and tested along with the reflection metasurface.

17:30 Automated Design of Antennas Using AI Techniques: A Review of Contemporary Methods and Applications

Mobayode O. Akinsolu (Wrexham University, United Kingdom (Great Britain)); Qiang Hua (University of Huddersfield, United Kingdom (Great Britain)); Bo Liu (University of Glasgow, United Kingdom (Great Britain))

The automated design of antennas made possible through the use of artificial intelligence (AI) techniques is attracting much attention. This development can be mainly attributed to the reduced design time and the higher quality of design solutions that AI-driven antenna optimization methods provide in comparison to their more traditional counterparts. Due to the growing need to fulfill more stringent design specifications and functional requirements for both present-day and future wireless communication systems, the design and development of antennas and antenna systems have increased both in scope and complexity such that conventional methodologies are often not fit for an efficient practical implementation. In this paper, a brief overview of some of the latest AI-based techniques for the design and optimization of contemporary antennas is provided with the goal of providing information on recent research to researchers in this growing area of interest.

17:50 Fine Tuning an AI-Based Indoor Radio Propagation Model with Crowd-Sourced Data

Cheick T Cissé (University of Bourgogne Franche-Comté & Orange Lab Compagny, France); Valery Guillet (Orange Labs, France); Oumaya Baala (FEMTO-ST Institute, Université Bourgogne Franche-Comté, CNRS & UTBM, France); François Spies (University of Franche Comte, France); Alexandre Caminada (Université Cote d'Azur & Polytech Nice Sophia - Ecole Polytechnique de l'Université de Nice, France)

Recent years have known the development of radio propagation models (RPM) and specially the AI-based ones. These models are interesting for many applications such as radio planning and design, fingerprinting-based localization, radio resources management etc. However most of the proposed AI-based RPMs have been trained on simulated radio data making them not ready or reliable for real condition applications. In this work we tackle the problem of learning and fine-tuning an AI-based RPM from simulated data to real world radio measurements. We raise the inherent problems and limitations and then propose solutions to overcome them. The study has been focused on 5 GHz Wi-Fi and Home network environment.

Tuesday, March 19 16:30 - 18:10

IW11: Applying AI/ML to 6G PHY Research, Keysight Technologies

Room: M2

16:30 Applying AI/ML to 6G PHY Research

Presenter: Eva Ribes-Vilanova (Keysight)

17:15 New Sub-THz & Test Techniques for 6G Research

Presenter: Sara Parrella (Keysight)

Tuesday, March 19 16:30 - 18:10

IW3: 5G & 6G Communication Testbeds, TMYTEK

Vincent Lee, TMY Technology Inc. (TMYTEK)

Room: M3

Part I: Introduction

Challenges in mmWave Research High cost and limited accessibility of mmWave. Industry Insight Sharing (5G/B5G and 6G, SATCOM and Radar sensing)

Part II - Barrier Breakthrough: TMYTEK Rapid mmWave Prototyping Solution

Collaboration with NI USRP platform. Comprehensive Coverage in Wireless Communication Prototyping Presenter: Vincent Lee (TMY Technology Inc. - TMYTEK)

Part III - Research Enabling Features

Facilitating 5G/B5G and 6G Research. Addressing Key Research Topics MIMO. Communication and Sensing. mmWave Beamforming. Reflective Intelligent Surface (RIS)

Part - IV - Case Study

Part V - Conclusion

Tuesday, March 19 16:30 - 18:10

E07: Optimization Methods in Metasurface Design

T10 Novel materials, metamaterials, metasurfaces and manufacturing processes // Electromagnetics

Room: M4

Chairs: Enrica Martini (University of Siena, Italy), Oskar Zetterstrom (KTH Royal Institute of Technology, Sweden)

16:30 Model-Based Deep Learning for High-Dimensional Periodic Structures

[Lucas Polo-López](#) and Luc Le Magoarou (IETR-INSA Rennes, France); Romain Contreres (CNES, France); María García-Vigueras (IETR-INSA Rennes, France)

This work presents a deep learning surrogate model for the fast simulation of high-dimensional frequency selective surfaces. We consider unit-cells which are built as multiple concatenated stacks of screens and their design requires the control over many geometrical degrees of freedom. Thanks to the introduction of physical insight into the model, it can produce accurate predictions of the S-parameters of a certain structure after training with a reduced dataset. The proposed model is highly versatile and it can be used with any kind of frequency selective surface, based on either perforations or patches of any arbitrary geometry. Numerical examples are presented here for the case of frequency selective surfaces composed of screens with rectangular perforations, showing an excellent agreement between the predicted performance and such obtained with a full-wave simulator.

16:50 Tunable Optimal Anomalous Reflection Using Discrete Impedance Metasurfaces

Mohammadjavad Shabanpourshepoli and Constantin Simovski (Aalto University, Finland)

The cutting-edge RIS technology enables accurate management of electromagnetic waves within wireless environments. In this study, we aim to achieve the maximal efficiency of the targeted anomalous reflection without scattering at unwanted angles even if the needed reflection angle is very large. To address this, we present a robust optimization technique that utilizes a mode-matching approach for a periodically non-uniform metasurface. It uses the apparatus of discretized sheet impedance and ensures the easy implementation and passivity of the metasurface.

17:10 Adaptive Weighting Scheme for Multi-Objective Optimization in Metasurface Antenna Design

[Marcello Zucchi](#), Amedeo Guida and Giuseppe Vecchi (Politecnico di Torino, Italy)

We present a novel adaptive weighting scheme suited to the current-based optimization of metasurface antennas. The problem is formulated in terms of a weighted sum of individual objective functions corresponding to different constraints. A non-linear conjugate gradient optimization algorithm is combined with an hyperplane adaptive weighting scheme to improve the convergence properties. The proposed approach is inspired by a geometrical interpretation of the properties of the Pareto front, and guarantees a balancing of the individual goals. The procedure has been applied to the design of broadside-radiating metasurface antenna working at 23 GHz, and demonstrated its effectiveness in improving both the speed of convergence and quality of the solution with respect to existing algorithms.

17:30 Multilayer Reflectionless Wide-Angle Anomalous Refractors Based on Surface Field Optimization

Federico Giusti, Enrica Martini, Stefano Maci and Matteo Albani (University of Siena, Italy)

In this work, we discuss the application of a numerically efficient tool based on the optimization of surface field harmonics for the design of reflectionless multilayer wide-angle anomalous refractors. In the proposed design approach, a certain number of evanescent Floquet modes are introduced through an optimization procedure aiming at minimizing the real part of the sheets surface impedance. Unlike the standard three-layer design, the one presented here offers the flexibility to choose an arbitrary number of layers as an input parameter during the design phase, providing an additional degree of freedom to explore novel solutions. Here, we compare the performance of three-layer and four-layer designs for achieving a -20° to $+40^\circ$ anomalous refraction. The optimized four-layer design exhibits spatially bounded admittance profiles, resulting in more effective anomalous refraction compared to the three-layer counterpart, which features asymptotes. The results are obtained using an in-house full wave analysis tool.

17:50 *An Accurate Semi-Analytical Model for Periodic Tunable Metasurfaces Electromagnetic Response*

Savvas Raptis (Aristotle University of Thessaloniki, Greece); Alexandros Papadopoulos (University of Ioannina, Greece); Loizos Symeonidis (Aristotle University of Thessaloniki, Greece); Antonios Lalas (Centre for Research and Technology - Hellas (CERTH), Greece); Christos Liaskos (University of Ioannina, Greece & Foundation of Research and Technology Hellas, Greece); Konstantinos Votis (Information Technologies Institute, Centre For Research and Technology Hellas, Greece); Dimitrios Tzouvaras (Centre for Research and Technology Hellas, Greece); Traianos Yioultsis (Aristotle University of Thessaloniki, Greece)

Tunable metasurfaces, that is, 2D metamaterial structures with programmable functionalities have been a significant subject of research. The consideration of non-local effects in metasurfaces has been proven to be highly important in modeling the electromagnetic response of such structures. In this paper a highly accurate semi-analytical model is presented, taking into consideration the non-local effects of a periodic metasurface. The model is validated through comparison with full wave simulations of tunable metasurfaces' supercells, providing accurate and almost zero computational cost calculations of the radiating Floquet modes. The efficiency of the proposed model allows optimization algorithms to run fast, without multiple repeats of full wave simulations, rendering an effortless extraction of the tunable variables' proper values for the desired behavior of the structure. This advantage is used for the design of programmable anomalous reflectors' supercells for V2X communications.

Tuesday, March 19 16:30 - 18:10

DA -: DA - EurAAP DA

//

Room: Fyne

Wednesday, March 20

Wednesday, March 20 8:30 - 10:10

SW11a: Wi-Fi Antenna Innovation for FTTR (Fiber-To-The-Room) Multi-Access Points F5G-A Scenarios

Room: Lomond Auditorium

Chair: Francis Keshmiri (Huawei Technologies, France)

8:30 *Giga Home Broadband FTTR, an Overview of Wi-Fi 8 Techniques, Spectrums, and Standardizations*

Presenter: Francis Keshmiri (Huawei Technologies, France)

8:45 *On Implementation of SEME-Paradigm in Indoor - New Trends for Wi-Fi Connectivity and UE Improvements*

Presenter: Andrea Massa (University of Trento, Italy)

9:15 *Wi-Fi Antenna with Reconfigurable Metasurfaces*

Presenter: Cristian Della Giovampaola (Wave Up, Italy)

9:45 *Multi-Antenna Systems for Future Wi-Fi Technologies*

Presenter: Fabien Ferrero (Université Côte d'Azur, France)

Wednesday, March 20 8:30 - 10:10

CS31: AMTA Session: New Applications for Compressive Sensing in Antenna Measurements

T09 Fundamental research and emerging technologies / Convened Session / Measurements

Room: M1

Chairs: Zhong Chen (ETS-Lindgren, USA), Stuart F Gregson (Queen Mary, University of London, United Kingdom (Great Britain))

8:30 *Compressive Sensing Applied to Production Testing of Array Antennas Using a Robotic Arm and Very Sparsely Sampled Near-Field Measurements*

Clive Parini (Queen Mary University of London, United Kingdom (Great Britain)); [Stuart F Gregson](#) (Queen Mary, University of London, United Kingdom (Great Britain))

Compressive Sensing (CS) has been deployed in a variety of fields. In massive MIMO arrays, CS has been applied to reduce the number of measurements required to verify array excitation in a production environment. The authors have applied CS to planar near-field measurements offering a compact test facility well suited to the production environment for these antennas with a mean square error of -30dB using just 1.5% of the samples needed for a conventional NF measurement. In this paper we address the optimal sampling strategy needed for this NF approach to diagnose arrays with up to a 4% failure rate by employing a statistical performance analysis of the reconstruction accuracy. Previous publications concerning CS based array diagnostics have exclusively studied the reconstructed array element amplitude, in this work we consider both array element amplitude and phase reconstruction performance that is critical in applying the technique to a production environment.

8:50 *High Resolution ISAR Imaging Methods for RCS Data Analysis*

Christer Larsson (Lund University & Saab Dynamics, Sweden); Andreas Gällström (Lund University and Saab Dynamics)

Radar Cross Section measurement data is often analyzed using Inverse Synthetic Aperture Radar images. Backprojection is the conventional method to create these images but is limited in resolution. This paper builds on developments of ℓ_1 -minimization and iterative smooth reweighted ℓ_1 -minimization to get super resolution and adding another processing step with Gaussian smoothing. This step improves the visualization of the produced high resolution images making them smoother and easier to interpret.

9:10 *Application of Compressed Sensing to Antenna Far-Field Calibration in an Extrapolation Range*

Zhong Chen (ETS-Lindgren, USA); Yibo Wang (ETS Lindgren, USA)

Antenna calibration in an extrapolation range is considered the most accurate method for acquiring far-field gain in an indoor chamber. This method requires one antenna to move linearly to collect the responses. The responses exhibit ripples due to multipath reflections. Post processing is needed to remove these ripples before fitting to a generalized equation to extrapolate data to the far field. The ripples are traditionally smoothed out by using a moving average method, and this requires collecting data densely. Recent proposals using k-space filtering can relax the sampling requirement. However, as the interactions between antennas occur at high spectral frequencies, a dense sampling is required to avoid aliasing. Here we propose to use Compressed Sensing (CS) to recover the spectrum coefficients, and then apply filtering. CS scheme can significantly

reduce the number of sampling points required and speed up the measurements while maintaining the accuracy of the extrapolation method.

9:30 Analysis of Time and Direction of Arrival (TADOA) Data Using Basis Pursuit in the AFRL One-RY Antenna Measurement Range

[Brian Fischer](#) (Resonant Sciences)

Time and Direction of Arrival (TADOA) analysis of field probe data has been an accepted method for characterizing stray signals in an antenna measurement range for many years. Recent uncertainty investigations at the OneRY compact antenna range have shown a need for increased resolution to isolate and characterize energy in TADOA images so that resources can be carefully applied to reduce the uncertainty from these stray signals. This is accomplished by modeling the TADOA image as the solution to a Basis Pursuit (BP) ℓ_1 minimization problem. This paper outlines the model development and shows concrete examples from OneRY field probe data where BP allows for the identification of stray energy which was previously difficult to find. We also show how the BP optimization context can be used to remove contamination from the data through the inclusion of additional basis functions and better isolate stray signal sources in three dimensions.

9:50 An Overview of the Potential of Compressed Sensing in Antenna Measurements

Adrien Antoine Guth (Institute of High Frequency Technology, RWTH Aachen University, Germany); Dirk Heberling (RWTH Aachen University, Germany)

Compressed sensing (CS) has found great popularity and application in various fields. In antenna measurements as well, several applications enable or at least show potential for the use of CS. In the spherical near-field to far-field transformation based on the spherical wave expansion, the radiation of an antenna under test is first represented in terms of spherical mode coefficients. These coefficients are sparse or compressible, allowing CS to retrieve them from fewer measurements. Moreover, in antenna array diagnosis, CS can be used to retrieve defective excitations of array elements. A compressible representation is achieved through an array element's excitation comparison between an array under test and a reference array. This paper summarizes implementations and investigations of current research on the above applications.

Wednesday, March 20 8:30 - 10:10

CS35a: Propagation for Smart Mobility Scenarios

T01 Sub-6 GHz for terrestrial networks (5G/6G) / Convened Session / Propagation

Room: Alsh 1

Chairs: Ke Guan (Beijing Jiaotong University, China), Ibrahim Rashdan (German Aerospace Center (DLR), Germany)

8:30 Design and Validation of a Wireless Network for Intra-Train Communications

Jorge Elizalde (Ikerlan & BRTA, Spain); Aitor Arriola (IKERLAN, Spain); Marti Roset (Comsa, Spain); Igor Lopez (Construcciones y Auxiliar de Ferrocarriles (CAF), Spain); Marvin Straub (Alstom, Germany)

In this work the RF propagation at 2.45 GHz has been characterized in the Advanced Train Lab of Deutsche Bahn, both in simulation and measurement, and path loss models have been obtained. The results indicate two different behaviours: a path loss exponent lower than free-space ($n \approx 1$) inside the train car, due to the waveguide effect of the reflective train structure, and a path loss higher than free-space ($n \approx 5$) in the adjacent car, due to the blockage of the Line-Of-Sight in the transition between train cars.

8:50 Beam Coverage Model of Ultra-Massive MIMO Communication Systems for Intelligent Transportation

Peng Chen (Chang'an University, China); Xiaoyu Huang (ChangAn University, China); Zhe Chen (Guilin University of Electronic Technology, China); Wei Wang (Chang'an University, China)

Ultra-massive MIMO (UM-MIMO) hopes to further expand the antenna scale, and use beamforming technology to greatly increase spatial gain. UM-MIMO will reduce the width of the main lobe of the antenna beam and expand the range of the near-field area, thereby reduce the effective coverage of the beam, making it unable to meet the coverage needs of highly mobile users in intelligent transportation. Therefore, it is necessary to select an appropriate beam width based on different position and motion parameters. To this end, this paper first proposes a beam coverage model that considers propagation attenuation, thereby providing a theoretical model of the beamwidth coverage. Then, a main-lobe synthesis method based on Dolph-Chebyshev (DC) weighting is proposed to obtain the weighting vector of the array under the specified main lobe beam width. Simulation results shows that the proposed method can effectively adjust the beamwidth.

9:10 AttentionRNN: Novel Propagation Channel Time-Domain State Predictor

Congcong Wang, Pengqi Zhu, José Rodríguez-Piñeiro and Xuefeng Yin (Tongji University, China)

Real-time communication-based applications are becoming more popular in the fifth generation (5G) and beyond systems, increasing the demand for accurate near to real-time channel estimation. Channel time-domain state prediction poses as a viable alternative to satisfy these demands. Traditional channel prediction methods usually suffer from high complexity or inaccuracies in their underlying mathematical models, severely limiting their performance. In this paper, a novel channel time-domain state predictor, named AttentionRNN, based on a recurrent neural network with a self-attention mechanism, is proposed. The predictor introduces a self-attention mechanism, allowing the network to focus on the parts of the data that provide more useful information for the channel prediction. The superiority of our proposal with respect to other available solutions in both prediction accuracy and training cost is verified based on measured data from actual vehicular radar scenarios. Our work constitutes a practical framework for real-time channel state prediction for time-varying applications.

9:30 Time-Varying Channel Measurement and Analysis at 105 GHz in an Indoor Factory

Yufeng Qin (Beijing University of Posts Telecommunications, China); Pan Tang (Beijing University of Posts and Telecommunications, China); Lei Tian (Beijing University of Posts and Telecommunications & Wireless Technology Innovation Institute, China); Jiaxin Lin, Zhaowei Chang, Peijie Liu and Jianhua Zhang (Beijing University of Posts and Telecommunications, China); Tao Jiang (China Mobile Research Institution Future Research Lab, China)

As one of the sixth-generation (6G) candidate technologies, terahertz (THz) communication is considered a promising way to achieve high-precision capability and large capacity in the Industrial Internet of Things (IIoT) due to its wide bandwidth and short wavelength. This paper presents time-varying THz channel measurements at 105 GHz in an indoor factory (InF). Firstly, the number of the multipath components (MPC) and root-mean-square delay spread (RMS DS) in line-of-sight (LoS) and non-line-of-sight (NLoS) environments are analyzed and compared. Secondly, the correlation between power delay profiles (PDP) is described by the temporal PDP correlation coefficient (TPCC). Finally, the local region of stationarity (LRS) method is employed to characterize the stationary distance. A Burr distribution is used to fit the distribution of stationary distance. The work contributes to modeling the THz channel in the time-varying environment in InF.

9:50 Link-Level Performance of Vehicle-To-Vulnerable Road Users Communication Using Realistic Channel Models

[Ibrahim Rashdan](#) and Stephan Sand (German Aerospace Center (DLR), Germany)

In this work, we present link-level performance analysis of the IEEE 802.11p protocol in terms of packet error rate (PER) and effective communication range using different fading channel models in critical VRU scenarios. The results show that contrary to the AWGN and the tapped-delay line (TDL) channels, regardless of the signal-to-noise ratio (SNR), an error-free link is out of reach for the realistic geometry-based stochastic channel models (GSCMs). Furthermore, the achieved effective communication ranges in different modulation and coding schemes (MCSs) are presented. It has been found that the IEEE 802.11p protocol with an equivalent isotropic radiated power (EIRP) of 23 dBm is able to achieve an effective communication range that exceeds 100 m for all scenarios except for scenario 1 at 16-QAM 3/4.

Wednesday, March 20 8:30 - 10:10

A12a: Advances in modelling and design of phased arrays

T02 Mm-wave for terrestrial networks 5G/6G // Antennas

Room: Alsh 2

Chairs: Daniele Cavallo (Delft University of Technology, The Netherlands), Marc Thevenot (XLIM-University of Limoges, France)

8:30 Analytical Model of a Parallel Plate Waveguide Feeding a Connected Slot Array

Caspar M Coco Martin and Daniele Cavallo (Delft University of Technology, The Netherlands)

We present an analytical model to describe arrays of connected slots fed by parallel plate waveguides (PPWs). Connected slot arrays are planar wideband arrays with wide scanning capability. PPW feeds can be used to reduce the complexity of the unit cell design. However, existing analytical expressions of the active input impedance of the array cannot account for the presence of PPWs. Here, we derive new models that can include PPW structures in the stratification, enabling the optimization of the design together with the feed. Full-wave simulations are used to validate the model.

8:50 Wide-Scan Active Highly Integrated Phased Array Antenna for Tx/Rx Application at K-Band

Ahmad Emadeddin and Lars Jonsson (KTH Royal Institute of Technology, Sweden)

A new wide-scan ($\pm 50^\circ$) active direct-integrated phased array antenna (AIPAA), designed for Tx/Rx mm-Wave applications, is introduced in this paper. This novel AIPAA offers seamless switching performance between transmitting (Tx) and receiving (Rx) modes without the need for lossy intermediate RF components, such as RF switches, circulators, and duplexers. The unitcell of the AIPAA consists of three miniaturized tapered slot elements operating in the K-band frequency range. In the Tx mode, a GaN high electron mobility transistor serves as the power amplifier (PA), while in the Rx mode, a GaAs MMIC low noise amplifier (LNA) is employed. The unitcell's center antenna element is reshaped to match closely to the optimal load impedance of the PA ($Z_{opt} = 6 + j36\Omega$) while the other elements are tuned to maintain a 50 Ω input impedance suitable for the LNA. The AIPAA achieves matching at both PA and LNA ports with 6% and 16% fractional bandwidth.

9:10 Behavioral Models for the Cosimulation and Optimization of Active Electronically Scanned Arrays

Charlotte Deville and Silvia Hernandez Rodriguez (XLIM - University of Limoges, France); Cyrille Menudier (XLIM Université de Limoges, France); Marc Thevenot (XLIM-University of Limoges, France); Benoît Lesur (Safran Data Systems, France); Wissam Saabe, Christophe Maziere and Tony Gasseling (AMCAD Engineering, France)

Active Electronically Scanned Arrays are versatile antenna solutions when high reconfiguration capabilities are required. However, they remain difficult to optimize due to their important degrees of freedom and their non linear components, sensitive to antenna impedance variation. This contribution describes the use of behavioral models for both non linear components and antenna radiating elements, allowing large arrays cosimulation and opening paths to several optimizations.

9:30 X-Band Receiving Phased Array with Digital Beamforming Using RFSoc

Gong Chen and Peizhuo Yang (National University of Singapore, Singapore); Fujiang Lin (USTC, China); Koen Mouthaan (National University of Singapore, Singapore)

The radio frequency system-on-a-chip (RFSoc) has recently become a promising candidate for replacing traditional analog and digital front ends, facilitating the development of phased-array systems. Unfortunately, due to the limitation of the maximum sampling frequency, RFSoc can not be directly used in the X-band phased array system. In this paper, a calibration-free phased array receiver system with RFSoc is presented at X-band. A rigid-flexible antenna array is designed and fabricated for the demonstration and verification. The proposed method achieves good beamforming patterns disregarding the channel imbalance introduced by the RF front-ends. Thus it is a good candidate for the high frequency phased array system beyond its sampling limitation.

9:50 Antenna Array and GaAs Phase Shifter MMIC for Millimeter Wave Beamforming - Co-Simulation and Measurements

Sumin David Joseph (The University of Sheffield, United Kingdom (Great Britain)); Edward Ball (University of Sheffield, United Kingdom (Great Britain))

Novel millimeter wave microstrip line antenna arrays and a GaAs phase shifter MMIC using 0.1 μ m pHEMTs are realized to demonstrate compact, high gain beamforming. The proposed microstrip arrays are small and easy to integrate with MMICs and millimeter wave platforms. The surface current cancellation of an ideal microstrip line is altered to make an effective radiator. High gain, good radiation pattern and low side lobe levels makes the array feasible and attractive for future integrated millimeter wave arrays. A reflective phase shifter using a hybrid coupler and cold FETs are proposed in the MMIC design. A continuous 160 degree phase shift with compensating adjustable gain values is offered by the MMIC. Measured gain of MMIC can vary from a peak gain of 8 to -6.5 dBi. Co-simulation of the fabricated MMIC phase shifter and the 4 \times 1 series-fed microstrip array achieved gain of 15.5dBi, while steered to 18 degree.

Wednesday, March 20 8:30 - 10:10

A16: User terminal antennas for satellite systems

T03 Aerospace, new space and non-terrestrial networks // Antennas

Room: Boisdale 1

Chairs: Christos Bilitos (University of Rennes, France), Hervé Legay (Thalès Alenia Space, France)

8:30 Novel Risley Prism Design Approach with Improved Side Lobe Levels Using Multi-Layer Transmit-Arrays

Sergio Matos (ISCTE-IUL / Instituto de Telecomunicações, Portugal); Nelson Fonseca (Anywaves, France); João Câmara Serra (Universidade de Lisboa - Instituto Superior Técnico & Instituto de Telecomunicações, Portugal); Joao M. Felicio (Escola Naval, Portugal & CINAV - Instituto de Telecomunicações, Portugal); Jorge R. Costa (Instituto de Telecomunicações / ISCTE-IUL, Portugal); Carlos A. Fernandes (Instituto de Telecomunicações, Instituto Superior Técnico, Portugal)

Cost-effective millimeter wave antennas are fundamental for the deployment of the next generation of terrestrial and satellite communication systems. The increase of the operation frequency changes the antenna design paradigm, where high gain and wide-angle beam steering are fundamental requisites. Electronic scanning approaches still face significant technological challenges, increasing the antenna costs. Therefore, low-cost designs based on mechanical steering are still relevant. The Risley prism (beam steering concept adapted from optics) is attracting significant attention in the antenna community as it can provide wide-angle azimuth and zenith beam coverage. However, this scanning mechanism tends to have high side lobe levels with typical prism implementations in the microwave domain. In this work, we use a new framework (recently proposed by the authors) based on a co-design of the phase correction of the two rotating surfaces, instead of considering each surface as a separate prism (the conventional approach). In our previous work, the improvement of SLL mitigation was demonstrated using fully dielectric TA composed of hollow square dielectric prism. However, these unit cells are far from being the optimal solution for the design transmit arrays, due to their thickness (1.4 λ) and high insertion losses (1.7 dB). Herein, we design a set of multi-layer metallized unit cell with thickness 0.3 λ and insertion losses below -1 dB. We show by full-wave simulations that the previous reported SLL mitigation of the generalized Risley Prism approach is indeed a general result also effective for multi-layer TA designs.

8:50 Low-Profile 2D-Mechanical-Beam-Steering Antenna with Large Field-Of-View

Thi Quynh Van Hoang and Erika Vandelle (Thales Research & Technology, France); Matthieu Bertrand (Thales Research and Technology, France); Brigitte Loiseaux (Thales Research & Technology, France)

This contribution presents a compact Risley-based 2D-beam-steering antenna in Ka-band featuring a large Field-of-View (FoV), which is up to 75° steering angle with 360° coverage in azimuth. The antenna presented in this paper is an improved version of our previous work in which the steering capacity was limited to 66° steering angle. The proposed Risley-based antenna is composed of a circularly polarized Radial Line Slot Array (RLSA) and two high-permittivity dielectric deflectors manufactured by 3D-printing. A 28-cm-diameter prototype was assembled with a total height of only 4 cm, corresponding to 3.8 free-space wavelengths at 29 GHz. In this new version, the two deflectors' design are modified to achieve a higher deflection angle, leading to a wider FoV. Simulation and preliminary measurement results show a good agreement, validating the steering capacity of the antenna up to 75° at 29 GHz.

9:10 Wideband Beam-Steering Continuous Transverse Stub Array Enabled by a Reflecting Luneburg Lens at Ka-Band

Christos Bilitos (University of Rennes, France); Adham Mahmoud (Institut d'Électronique et de Télécommunications de Rennes, France); Ronan Sauleau (University of Rennes 1, France); Enrica Martini and Stefano Maci (University of Siena, Italy); David González-Ovejero (Centre National de La Recherche Scientifique - CNRS, France)

This paper presents the design of a beam-steering parallel-fed Continuous Transverse Stub (CTS) array at Ka-band enabled by a Reflecting Luneburg Lens (RLL) beamformer. The latter consists of two stacked

circular parallel plate waveguides (PPW), where a graded index medium in the bottom one ensures ray collimation in the top PPW. Owing to the rotational symmetry of this medium, one can displace the feed along the inner focal region to change the direction of the planar wavefront in the top PPW. This wavefront then excites the CTS array in parallel thanks to a corporate feed network. The antenna system provides continuous beam-steering capabilities within the H-plane by mechanically adjusting the position of the feed, covering a range of 30 degrees. Stable performance is achieved within the band of interest, featuring a -3 dB fractional bandwidth (BW) of approximately 38.9%, along with consistently low side-lobe levels (SLL) below -13 dB.

9:30 **Compact Hybrid Optical/RF User Segment (CHORUS): RF Terminal Design**

Christophe Granet (Lyrebird Antenna Research Pty Ltd, Australia); John Ness and Glen Callaghan (EM Solutions Pty Ltd, Australia); Glenn Mason (EM Solutions, Australia); Peter Kerr (SmartSat Cooperation Research Centre, Australia)

The CHORUS project aims to build on existing world leading Australian technology in compact RF tactical terminals and optical communication to develop "leap-frogging" technology that exploits bearer diversity through a highly integrated hybrid Optical/RF tactical terminal. The development of a hybrid RF-optical SATCOM terminal is seen to be a critical step to the acceptance of optical communications by users that require high availability and the performance advantages offered by free-space optical communications. If successful, this will place Australia in a leading position to create new capabilities for compact, high data rate, high availability satellite earth terminals for commercial and national security markets. In this paper, we will concentrate on the performance of the RF element of CHORUS.

9:50 **Design of a Wideband Dual-Polarized Stacked Antenna Array for SATCOM Applications**

Davide Guarnera (University of Reggio Calabria Mediterranea, Italy); Santi Concetto Pavone (Università degli Studi di Catania, Italy); Ottavio Crisafulli (Università Mediterranea di Reggio Calabria, Italy); Loreto Di Donato (University of Catania, Italy); Andrea Francesco Morabito (University Mediterranea di Reggio Calabria, Italy); Tommaso Isernia (University of Reggio Calabria, Italy); Gino Sorbello (University of Catania, Italy)

In this contribution, we present a dual-polarized stacked-patch antenna for mobile satellite communication (SATCOM) applications in the Ku-band. The proposed antenna has been designed to cover the entire Rx/Tx Ku-band frequency range, namely from 10.7 GHz to 14.5 GHz. Dual polarization has been achieved by exploiting two different feeding lines, one for each polarization. After the design of the single radiating element, a 2x2 array has been also studied and simulated. The array is fed through an impedance matching network realized by exploiting wideband T-junctions composed of a cascade of quarter-wave transformers. The results show high impedance matching over the entire operating bandwidth ($|S_{11}| < -20$ dB for the single element and < -15 dB for the array), high cross-polarization rejection for both vertical and horizontal polarizations (> 38 dB at broadside), and finally high isolation between the two feeding networks (> 30 dB).

Wednesday, March 20 8:30 - 10:10

CS40a: New challenges on small antennas for emerging wireless technologies

T04 RF sensing for automotive, security, IoT, and other applications / Convened Session / Antennas

Room: Boisdale 2

Chairs: Halim Boutayeb (Université du Québec en Outaouais, Canada), Marta Cabedo-Fabrés (Universidad Politécnica de Valencia, Spain)

8:30 **Tunable Segmented Loop Antenna Reader for Miniaturized Chipless Tag Detection**

Adrián Fernández Camicero and Anja K. Skrivervik (EPFL, Switzerland)

This paper presents a 7.5x7.5 mm² tunable segmented square loop reader antenna working in UHF band for magnetic near field RFID applications. The proposed reader is combined with a post-processing method based on frequency sweep envelope (FSE) for detecting miniaturized chipless tags. Using FSE method, the reader can detect octagonal single turn loop resonators of 17.89 mm², 2.92 mm², 1.65 mm² and 0.75 mm² dimensions at 19.5 mm, 10 mm, 6.5 mm and 1 mm distances, respectively. These results improve the ones obtained with others chipless systems based on phase-dip, reflection distortion (PRD), group delay distortion (GDD) and splitting frequency (SF) detection methods. Moreover, the designed chipless system is capable of reaching detection ranges comparable to chipped systems with similar dimensions. In view of the promising results obtained with the proposed system, some possible modifications for improving the detection range are suggested.

8:50 **Optimizing RF Energy Harvesting in IoT: A Machine Learning Estimation Considering Polarization Effects**

Khatereh Nadali (Technological University Dublin, Ireland); Adnan Shahid (Ghent University - imec, Belgium); Nicolas Claus (Ghent University & Imec, Belgium); Sam Lemey (Ghent University-imec, Belgium); Patrick Van Torre (Ghent University, Belgium); Max James Ammann (Technological University Dublin, Ireland)

The rapid evolution of wireless technology has led to the proliferation of small, low-power IoT devices, often constrained by traditional battery limitations, resulting in size, weight, and maintenance challenges. In response, ambient radio frequency (RF) energy harvesting has emerged as a promising solution to power IoT devices using RF energy from the environment. However, optimizing the placement of energy harvesters is crucial for maximizing energy reception. This paper employs machine learning (ML) techniques to predict areas with high power intensity for RF energy harvesting. Five supervised ML algorithms are compared across four scenarios using antennas with circular and linear polarization. The impact of noise filtering on accuracy is also assessed. Results show that random forest outperforms other ML algorithms, demonstrating the effectiveness of ML in estimating optimal energy harvesting locations and providing insights for sustainable energy network development.

9:10 **Mm-Wave Monopulse Radar System for Detecting Space Debris in Satellite Exploration Missions**

Farzad Karami (University of Quebec in Outaouais, Canada); Halim Boutayeb (Université du Québec en Outaouais, Canada); Larbi Talbi (University of Quebec - Outaouais, Canada)

Monopulse radar systems are essential for managing space debris during satellite exploration missions due to its high precision, angular measurement capabilities, and ability to track multiple objects at once, ensuring the safety and integrity of space assets. In this paper, a compact mm-wave, end-fire, high gain monopulse antenna is presented that could be fabricated on a thin PCB laminate. The reported results show good performances, a -10-dB impedance bandwidth of 60.6% (23-43 GHz) for the sum and difference ports, better than 24 dB isolation between the input ports, the difference radiation patterns better than -25 dB null-depth. The proposed monopulse radar system could be used in a wide range of practical applications in detecting and managing space debris in satellite exploration missions.

9:30 **Design of Microstrip UWB Antenna with Full Ground Plane for Wearable Applications**

Ozuem Chukwuka (University Gustave Eiffel & MC2 Technologies, France); Florent Gamand and Christophe Gaquiere (MC2 Technologies, France); Divitha Seetharamdoo (Univ Gustave Eiffel COSYS LEOST Univ Lille Nord de France & Univ Lille Nord de France, France)

This paper presents the design of a microstrip ultra-wide band rigid antenna that has a full ground plane acting as a reflector and operates from 1 GHz to 7.3 GHz. The antenna can be used for wearable applications such as on backpacks and helmets. The antenna structure includes a UWB radiator (microstrip patch) on top of a substrate, an optimized ground plane on the reverse side of the substrate, a vacuum and a full ground plane acting as a reflector. The overall size of the antenna is 100 mm x 75 mm x 25 mm (0.33 x 0.25 x 0.083λ). In comparison to other full ground plane UWB antennas, the proposed design uses a rigid substrate and operates from a lower frequency of 1 GHz. Additionally, the reflector makes the antenna operational in the vicinity of the human body with minimal body coupling and back radiation to ensure safety.

9:50 **A Self Deployable and Reconfigurable Antenna in VHF Band for a New Space Mission**

Ségolène Tubau (Thales Alenia Space, France); Hervé Legay (Thalès Alenia Space, France); Thibaud Calmettes, Gilles Lubrano Di Scampamorte and Julie De Martres (Thales Alenia Space, France)

A disruptive antenna subsystem was developed for Space based AIS Systems. It consists of an array of six monopoles implemented with a 60° rotational symmetry, that takes benefit of the radiation of the nanosatellite on which it is accommodated. Conjugate beamforming permits to form a beam in an arbitrary polarization in any direction. From our best knowledge the first reconfigurable and deployable antenna in VHF band for nanosatellite.

Wednesday, March 20 8:30 - 10:10

CS23a: Recent Advances on Propagation Research and Its Impact on Localizations

T05 Positioning, localization, identification & tracking / Convened Session / Propagation

Room: Carron 1

Chairs: Christian Gentner (German Aerospace Center (DLR), Germany), Wei Wang (Chang'an University, China)

8:30 Gaussian Processes for Received Signal Strength Based Device-Free Localization

[Ossi Kaltiokallio](#) (Tampere University, Finland); Roland Hostettler (Uppsala University, Sweden); Jukka Talvitie and Mikko Valkama (Tampere University, Finland)

Data-driven Gaussian process models for received signal strength-based device-free localization are presented. The models have physically interpretable parameters that can be explained by analytical models. Moreover, the presented models can approximate highly nonlinear signal propagation patterns such as a target's influence on existing multipath components which is generally treated as unwanted noise that degrades the system performance. The models are evaluated with experimental data and the results indicate that the proposed models decrease the modeling error and improve the localization accuracy, especially in multipath rich indoor environments.

8:50 Terahertz Channel Modeling Based on Scattering Characterization

Ran Pan, Danping He and Ke Guan (Beijing Jiaotong University, China); Bile Peng (TU Braunschweig, Germany); Jianwu Dou (ZTE Corporation, China); Lantu Guo (Beijing Institute of Technology, China); Zhangdui Zhong (Beijing Jiaotong University, China); Thomas Kuerner (Braunschweig Technical University, Germany)

Terahertz (THz) communication is one of the key technologies of the sixth-generation mobile communication system (6G) and is receiving more and more attention for its large bandwidth and ultra-high data rate features. To support the performance evaluation of THz wireless communication devices, it is critical to model wireless channels that can characterize the channel properties. In this paper, a THz channel model is proposed based on the scattering characterization. The channel model is then applied to generate channel coefficients and power delay profiles (PDPs) in an indoor scenario. The evaluation results indicate that the proposed channel model can appropriately characterize THz scattering properties and support THz communication system design. Finally, we summarize the advantages of this model and point out the next research content.

9:10 Robust Tensor Positioning Based on Channel Parameter Estimation Under Spatially Colored Noise

[Yuzhe Sun](#) and Wei Wang (Chang'an University, China); Haochuan Yue (Chang'an University, China); Yue Lyu (Chang'an University, China)

In communication systems, the ubiquitous time-frequency interference, such as co-channel interference (CCI) and RF front-end interference (FEI), constitutes spatially correlated colored noise. They can not only result in increased bit error rates and reduced system capacity, but also introduce distortions and errors in phase estimation. Consequently, for the channel impulse response (CIR) testing, the separation of interference components has become a prominent research focus. This paper deduces a complex-domain robust variational Bayesian method for channel parameter estimation, along with the estimation of interference locations. Simultaneously, by using variational mean-field theory and automatic rank reduction, it achieves the automatic determination of the number of multipath and low-rank approximations of the CIR. Finally, the channel harmonic parameters are employed in the angle positioning algorithm. Performance comparisons are made with traditional information-theoretic rank estimation methods and the space alternating generalized expectation maximization (SAGE) parameter estimation algorithm, confirming the feasibility of the proposed approach.

9:30 Analysis of Channel Characteristics for FMCW Millimeter-Wave Radar in Traffic Scenarios

Biaobiao Ji, Bingjie Xue, Peng Chen and Wei Wang (Chang'an University, China)

Millimeter-wave radar technology has gained significant attention due to its promising applications in various fields, including autonomous vehicles, wireless communications, and remote sensing. According to the survey, research on the propagation characteristics of vehicle-mounted radar in the high-frequency range is relatively limited, and there is even less research on channel propagation characteristics in non line-of-sight (NLOS) scenarios. Therefore, this paper focuses on the measurement and characterization of frequency-modulated continuous wave (FMCW) millimeter-wave radar channels at traffic intersections, including channel impulse response (CIR) extraction, Doppler frequency, K-factor and root mean square time delay spread (RMS Time Delay Spread). The findings of this study contribute to a deeper understanding of millimeter-wave radar channels and lay the foundation for the design and optimization of millimeter-wave radar systems in various applications.

9:50 HRPE-Enhanced AI-Based 5G Indoor Localization in Presence of Specular and Dense Multipaths

Yuchen Shi (Tongji University, China); Xiaoxiao Yang and YuYing Sun (Xiamen University, China); José Rodríguez-Piñero (Tongji University, China); Xuemin Hong (Xiamen University, China); Tomás Domínguez-Bolaño (University of A Coruña, Spain); Xuefeng Yin (Tongji University, China)

Fifth generation (5G) communication systems are expected to provide an ubiquitous solution for indoor positioning, and deep neural networks (DNNs) have been recently proposed for this purpose. However, DNN-based positioning solutions are in general very dependent on the training data. In this paper, an architecture for positioning based on wireless signals is proposed, namely the SAGE-Enhanced CEAP (SE-CEAP). The architecture considers firstly an enhancement of the acquired Channel State Information (CSI) data by means of a high-resolution parameter estimation (HRPE) method, namely the space-alternating generalized-expectation maximization (SAGE) algorithm, and secondly a specifically designed DNN for localization, namely the CNN-Enblock AI Positioning (CEAP). The provided results, considering a realistic 5G New Radio (NR) deployment in an indoor scenario, show that the proposed architecture outperforms other classical DNN-based localization approaches, not only in localization accuracy, but also in generalizability of the results, which is a common drawback of DNN-based solutions.

Wednesday, March 20 8:30 - 10:10

CS45: Direct and inverse EM modelling for biomedical microwave imaging systems

T06 Biomedical and health / Convened Session / Electromagnetics

Room: Carron 2

Chairs: Cristina Ponti (Roma Tre University, Italy), Andrea Randazzo (University of Genoa, Italy)

8:30 MR/Microwave Tomography Integrated Breast Cancer Imaging

Paul M Meaney, Zamzam Kordiboroujeni and Grace Player (Dartmouth College, USA); Amir H Golnabi (Fresenius Medical Care, USA); Xiaoyu Yang (Quality Electrodynamics, USA); Thomas Eastlake (Quality ElectroDynamics, USA); Keith D. Paulsen (Dartmouth College, USA)

We are developing a new, compact microwave breast imaging tank that will allow us to acquire data from the patients' breasts while simultaneously being imaged in an MR system. Compatibility issues regarding mutual disruption of the MR and microwave images have been addressed and the microwave tanks has been sufficiently reduced in size to allow a modestly sized woman to fit inside the MR bore with the tank. A custom MR coil has been integrated into the tank to minimize the space it requires while also increasing the MR SNR by a factor of 3. We present images of an initial experiment where the object is a realistic breast phantom with a spherical tumor inclusion. The microwave images are generated while incorporating the spatial information from the MR scans. The initial results are promising as we prepare for initial clinical use.

8:50 Physics-Informed Regularization for Microwave Imaging in Biomedical Applications

[Brendon C. Besler](#) and Elise Fear (University of Calgary, Canada)

Microwave tomography is a promising imaging modality in which the dielectric properties of an unknown object are reconstructed quantitatively. Microwave tomography requires solving the non-linear and ill-posed inverse scattering problem. A priori information is typically required to regularize the problem and generate useful images. In this work, electromagnetic power balance is introduced as a physics-informed regularizer. Electromagnetic power balance is incorporated with the conventional data mismatch cost function to produce a new multiplicative regularizer. The technique is validated with low loss dielectric cylinders and a simplified forearm model in simulation.

9:10 Preliminary Clinical Trial Results of MammoWave in the Context of RadioSpin Project

Navid Ghavami (Umbria Bioengineering Technology (UBT), United Kingdom (Great Britain)); Arianna Fracassini (UBT - Umbria Bioengineering Technologies, Italy); Lorenzo Papini (UBT - Umbria Bioengineering Technologies, Perugia, Italy); Daniel Álvarez Sánchez-Bayuela (University of Castilla - La Mancha & University Hospital of Toledo, Spain); Alessandra Bigotti (UBT - Umbria Bioengineering Technologies, Perugia, Italy); Mario Badia and Giovanni Raspa (UBT - Umbria Bioengineering Technologies, Italy); Gianmarco Palomba (UBT - Umbria Bioengineering Technologies, Perugia, Italy); Cristina Romero Castellano (Hospital Virgen de la Salud, Toledo, Spain); Mohammad Ghavami (London South Bank University, United Kingdom (Great Britain)); Riccardo Loretoni (Breast Unit, Foligno Hospital, Italy); Alberto Tagliafico (University of Genoa, Italy); Massimo Calabrese (IRCCS Ospedale Policlinico San Martino, Genoa, Italy); Gianluigi Tiberi (London South Bank University, United Kingdom (Great Britain) & UBT - Umbria Bioengineering Technologies, Italy)

In this work, we present our preliminary findings from a prospective multicentric microwave breast imaging clinical trial involving 218 women, within the framework of the RadioSpin project. In addition to the prospective performance evaluation of our microwave imaging device, MammoWave, in classifying breasts with and without radiological findings (using features with appropriate thresholds), we conducted further investigations and analyses to assess the impact of individual frequency sub-bands and the classification of breasts into healthy (without any findings or with benign findings) and non-healthy (malignant findings), based on selected features obtained from a prior clinical trial. Our results reveal the potential for achieving a sensitivity of up to 78% in the detection of radiological findings and up to 89% in the detection of non-healthy (with cancer) breasts.

9:30 On Enhancing Efficiency of Transmission in Imaging Systems by Wearable Scatterers

Ludovica Tognolatti, Cristina Ponti and Giuseppe Schettini (Roma Tre University, Italy)

The application of electromagnetic fields within biological tissues proves to be a powerful technology with a wide range of applications, including the monitoring of physiological parameters, microwave imaging, hyperthermia therapy and deep brain stimulation. In those cases, the maximization of the transmitted field is desired. Here, several solutions to enhance the transmitted electromagnetic field inside biological tissues are investigated. An exact solution to the problem of electromagnetic scattering of a planewave from an array of dielectric or conducting cylinders placed above a multilayer medium is presented. An analytical approach is considered to solve the scattered field by the cylinders in each medium through expansions into cylindrical waves, expressed through plane-wave spectra. The multilayer models the dielectric properties of biological tissues. Numerical results obtained at $f = 2.4$ GHz are presented considering different configurations of the multilayer.

9:50 Brain Stroke Microwave Diagnostics in Children Through a Nonlinear Inverse-Scattering Technique

Valentina Schenone and Alessandro Fedeli (University of Genoa, Italy); Costanza Parodi (IRCCS Istituto Giannina Gaslini, Italy); Igor Bisio and Andrea Sciarrone (University of Genoa, Italy); Andrea Rossi (IRCCS Istituto Giannina Gaslini, Italy); Fabio Lavagetto and Andrea Randazzo (University of Genoa, Italy)

This paper proposes the use of microwave techniques for the diagnosis and monitoring of stroke in children. The main objective is to initiate an investigation into paediatric stroke diagnosis through a preliminary assessment using numerical simulations with realistic 3D models representing the heads of stroke-affected children. A Newton-type iterative procedure with variable exponent Lebesgue space regularisation is proposed as a quantitative microwave-based reconstruction approach.

Wednesday, March 20 8:30 - 10:10

A05: Optical, THz and sub-THz antennas

T07 THz and high frequency technologies // Antennas

Room: Dochart 1

Chairs: Ioan E. Lager (Delft University of Technology, The Netherlands), Enrica Martini (University of Siena, Italy)

8:30 Sub-THz Substrate Integrated Waveguide Signal Transitions in Backend-Of-Line of a Silicon Process

Akanksha Bhutani (Karlsruhe Institute of Technology, Germany); Mehmet Kaynak (IHP, Germany & IHP Microelectronics, Turkey); Matthias Wietstruck (IHP, Germany); Elizabeth Bekker, Ibrahim Kagan Aksoyak and Joachim Hebler (Karlsruhe Institute of Technology, Germany); Thomas Zwick (Karlsruhe Institute of Technology (KIT), Germany)

This paper presents a sub-THz substrate integrated waveguide (SIW)-to-microstrip and an SIW-to-grounded coplanar waveguide (GCPW) transition, realized in the backend-of-line (BEOL) of a silicon (Si) process. The transitions are realized in a back-to-back configuration with ground-signal-ground (GSG) pads on both ends to enable probe-based S-parameter measurement. The influence of the GSG probe pads is de-embedded based on the bisection of a Thru structure. The measured and de-embedded S-parameters show good agreement with the simulation results. The measured average insertion loss of the SIW-to-microstrip and SIW-to-GCPW transitions, in the range of 200 GHz to 310 GHz, is 1.2 dB and 0.9 dB, respectively, which represents the lowest insertion loss demonstrated for an on-chip SIW-to-microstrip and SIW-to-GCPW transition to date. In addition, these transitions are implemented with the smallest chip area required for an on-chip SIW-to-microstrip and SIW-to-GCPW transition demonstrated to date.

8:50 High-Gain and Circular Polarization Silicon-Micromachined Lens Antennas at 500-750 GHz

Alireza Madannejad and Mohammad Mehrabi Gohari (KTH Royal Institute of Technology, Sweden); Umer Shah (Royal Institute of Technology (KTH), Sweden); Joachim Oberhammer (KTH Royal Institute of Technology, Sweden)

This paper introduces an innovative silicon-micromachined antenna operating in the 500-750 GHz range, based on an optimized elliptical Fresnel Zone Plate Lens (FZPL) design. The antenna radiates a circularly polarized wavefront without additional phase compensation components. With a gain of 25.7 dBi and a 15 dB return loss over the whole waveguide band, this low-profile, compact antenna presents a promising solution for upcoming wideband THz communication applications. This work highlights the potential of silicon micromachining in achieving high-performance antennas with a compact footprint in the THz bands.

9:10 110 to 170 GHz High-Gain Antenna with Embedded Surface Mount Short Horn and Baseband PCB Horn Antenna

Elizabeth Bekker, Alexander Quint, Georg Gramlich and Luca Valenziano (Karlsruhe Institute of Technology, Germany); Thomas Zwick (Karlsruhe Institute of Technology (KIT), Germany); Akanksha Bhutani (Karlsruhe Institute of Technology, Germany)

This wideband, high-gain Antenna-in-Package (AiP) concept for D-band applications, features a wideband Dielectric Resonator Antenna (DRA) housed within an Embedded Surface Mount Short Horn (ESMSH), to enhance its gain. The AiP is placed on a standard 4-layer baseband printed circuit board (PCB). The gain is further improved by forming a multilayer pyramidal horn antenna in the PCB. Using the simple 4-layer baseband PCB to double as an extension to the ESMSH, is a low-cost solution that improves the gain of the AiP with up to 5 dBi. The resultant measured peak gain is 12.7 dBi and the gain is above 9 dBi from 110-170 GHz. The AiP and PCB assembly is low-profile with a height of $0.9\lambda_c$, and the antenna aperture is only $1.8\lambda_c \times 1.8\lambda_c$. Lastly, the reflection coefficient remains below -10 dB within the range of 112 to 169 GHz, corresponding to a relative bandwidth of 41%.

9:30 Time Domain Analysis of Pulsed Photo-Conductive Antenna Sources: Distributed Excitations

Laurens F.E. Beijnen, Martijn D. Huiskes and Andrea Neto (Delft University of Technology, The Netherlands)

Distributed feeding in photo-conducting antennas (PCAs) leads to simple optical design, less prone to overheating, as well to THz antennas that can operate non-dispersively over wide bandwidths. However, the efficient analysis of pulsed PCAs was so far limited to architectures characterized by feeds small with respect to the THz wavelengths. In this contribution, an efficient procedure for the time domain analysis of an infinitely long slot antenna printed on photo-conductive material and excited by a distributed pulsed laser is presented. The procedure is electromagnetically rigorous, and relies on spectral representations of the fields in both the frequency and spatial domains.

9:50 Sub-THz U-Slot Coupled Stacked-Patch Radiating Elements for Dual-Polarized MIMO Array Antennas

Elena Shepeleva (Samsung Research, Moscow, Russia); Artem Vilenskiy (Chalmers University of Technology, Sweden); Gennadiy Evtushkin and Anton Lukyanov

(Samsung Research, Moscow, Russia)

Several sub-THz (D-band, 136 - 148 GHz) dual-polarized array elements (unit cells, UCs) implemented in a multi-layer PCB technology are investigated in the infinite array environment. The elements are stacked-patch antennas with unbalanced aperture-coupled feeds (U-slots), having a slant 45 deg. polarization. We demonstrate that a baseline half-wavelength cavity-backed UC is capable of achieving ≤ 3.7 dB scan loss in the 60 deg. conical scan range and (132-149) GHz bandwidth. For the increased UC size, however, active polarization channel isolation drastically degrades and the element experiences scan blindness. To address this problem, a UC modification is introduced that suggests using a single-row mushroom-type electromagnetic band-gap structure along the UC sidewalls. Simulated results evidence the realized UC decoupling and elimination of the scan-blindness anomalies in the full visible scan range, with scan loss ≤ 4.2 dB in the 55 deg. conical scan range and (136-148) GHz bandwidth.

Wednesday, March 20 8:30 - 10:10

E10a: Electromagnetic Modelling and Analytical Methods

T08 EM modelling and simulation tools // Electromagnetics

Room: Dochart 2

Chairs: Pilar Castillo-Tapia (KTH Royal Institute of Technology, Sweden), Andrea Neto (Delft University of Technology, The Netherlands)

8:30 *Spectral Domain Green's Function of an Infinite Dipole with Non-Zero Metal Thickness*

Erik Speksnijder, [Riccardo Ozzola](#) and Andrea Neto (Delft University of Technology, The Netherlands)

The calculation of the transmission line Green's function of an infinite metal line of rectangular cross-section embedded in a generalized stratification is presented. The proposed procedure is quasi-analytical and extends prior models to account effectively for the non-zero thickness of the conductors. From the Green's function of an infinite dipole, an equivalent network is derived to represent the current propagating along the dipole and the reactive loading due to the feeding gap dimensions. The method is validated with numerical simulations and available experimental results.

8:50 *Vector Potentials for Uniaxial Media with Sources*

Michael J Havrilla (Air Force Institute of Technology, USA)

A vector potential formulation is developed for uniaxial media and now includes source terms. It is shown that a Debye-like gauge reduces the resulting vector-potential Helmholtz-like equation to a simple form. Applications of the vector potentials include propagation in rectangular or cylindrical waveguides filled with uniaxial media and material characterization of uniaxial media using a clamped parallel-plate waveguide fixture.

9:10 *Analysis of the Dispersion Diagrams of 3D Cubic Periodic Arrangements of Metallic Spheres*

Hairu Wang, Oskar Zetterstrom and Pilar Castillo-Tapia (KTH Royal Institute of Technology, Sweden); Francisco Mesa (University of Seville, Spain); Oscar Quevedo-Teruel (KTH Royal Institute of Technology, Sweden)

This paper investigates the dispersion properties exhibited by three different three-dimensional (3D) periodic arrangements of metallic spheres with the following underlying lattices: simple cubic (sc), body-centered cubic (bcc) and face-centered cubic (fcc) lattice. Their Brillouin zone (BZ) and the corresponding irreducible BZ are introduced. We then examine the dispersion properties along the edges of their respective irreducible BZs. The findings demonstrate that structures with a non-sc arrangement and higher symmetry can improve design versatility while simultaneously reducing the anisotropy of the structure and broadening the operating frequency range. These advantages are beneficial for the development of 3D graded-index (GRIN) lenses.

9:30 *Platform Scattering Analysis of the Copernicus Imaging Microwave Radiometer*

Pasquale Giuseppe Nicolaci and Cecilia Cappellin (TICRA, Denmark); Roberto Mizzoni (Italy); Vincenzo Lubrano (Thales Alenia Space Italy, Italy); Salvatore Contu (Thales Alenia Space, Italy); Benedetta Fiorelli (European Space Agency, The Netherlands)

The CIMR employs a 7.1 m conical scanning mesh reflector antenna rotating at 7.8 r.p.m that operates from L to Ka band. Demanding radiometric accuracies and sensitivities at few tenths of Kelvin at high spatial resolution are targeted for the instrument. These require a high accuracy in the characterization and modelling of the antenna pattern over 4π , considering any nearby scattering structure and/or any potential multipath due to the antenna installation over the S/C. Moreover, the quantification of the fractional power hitting each scatter entering by reciprocity into the feeds is also of primary importance, since it can bias the antenna temperature. A platform scattering analysis of the reflector antenna on the CIMR satellite was thus undertaken for a subset of feeds at L, C, X, K and Ka bands. In this paper we describe the analyses done and summarize the effect of these scatters over the antenna RF performances.

9:50 *Investigation of Near-Field Contribution in Shooting and Bouncing Rays for Installed Antenna Performance on a Simple Platform*

[Harald Hultin](#) (KTH Royal Institute of Technology & Saab AB, Sweden); Lars Jonsson (KTH Royal Institute of Technology, Sweden); Johan Malmström (Saab Surveillance, Sweden); Henrik Frid (Saab, Sweden)

The near-field contribution in the high-frequency method Shooting and Bouncing Rays (SBR) is investigated for installed antenna performance. Three SBR solvers, the in-house solver SIENT and two commercial solvers, are compared to a commercial full-wave solver. SIENT and one commercial solver have an option to disable near-field effects, which allows the strength of these effects to be investigated. The last solver also includes near-field effects. The results indicate an increase in accuracy when including near-field effects. The most notable difference in the far-field phase and the induced surface current are obtained for the in-house solver. Improvements for the surface current density is seen close to the antenna. On the tested platform, the difference in gain is not as notable but it is overestimated for both the in-house solver and the commercial solvers when excluding near-field terms.

Wednesday, March 20 8:30 - 10:10

E08: Efficient Methods for Metasurfaces Design

T10 Novel materials, metamaterials, metasurfaces and manufacturing processes // Electromagnetics

Room: M2

Chairs: Marko Bosiljevac (University of Zagreb, Croatia), Ariel Epstein (Technion - Israel Institute of Technology, Israel)

8:30 *Multibeam Radiation by Multipoint Fed Modulated MTS Apertures*

Marco Faenzi and Stefano Maci (University of Siena, Italy)

In this paper we introduce a very simple design approach to design multibeam devices from an individual aperture based on modulated metasurface apertures, at the Ku-band range. The presented aperture examples are capable of working both in linear and circular polarization and feature a single impedance modulation profile that is illuminated by four sources, constituted by simple monopoles immersed into the dielectric slab. The latter are displaced wrt the modulation phase center, in analogy to offset reflectors design. By individually activating each of the sources the apertures can produce four off-axis beams, while by simultaneous activation of all the sources the apertures radiate a broadside sum beam. Finally, by a simple phasing scheme between the four feeds the apertures can also produce beams typical of a monopulse aperture for radar applications

8:50 *Reflective Intelligent Surfaces: Reducing Complexity by Controlling the Illuminating Field*

[Mirko Barbutto](#) (Niccolò Cusano University, Italy); Zahra Hamzavi-Zarghani (RomaTre University, Italy); Mohsen Karamirad (Roma Tre University, Italy); Michela Longhi

(Niccolò Cusano University, Italy); Alessio Monti (Roma Tre University, Italy); Davide Ramaccia (RomaTre University, Italy); Luca Stefanini (Roma Tre University, Italy); Stefano Vellucci (Niccolò Cusano University, Italy); Andrea Alù (CUNY Advanced Science Research Center, USA); Filiberto Bilotti (ROMA TRE University, Italy); Alessandro Toscano (Roma Tre University, Italy)

Reflective Intelligent Surfaces (RIS) could play a pivotal role in the implementation of a smart electromagnetic environment. However, achieving efficient and simple reconfigurability of RIS and their deployment in real-world environments remain challenging tasks. In this contribution, we discuss a possible solution to reduce the complexity of RISs by exploiting the properties of composite vortices and moving the reconfigurability to the illuminating field. In this way, static RISs could be deployed, whose scattering patterns could be manipulated by controlling the beam-width of the impinging field.

9:10 Tailoring Surface Impedance for Cascaded Cylindrical Metasurfaces

Zvonimir Sipus and Marko Bosiljevac (University of Zagreb, Croatia)

In this paper, we aim to demonstrate a method for designing cascaded azimuthally varying cylindrical metasurfaces, with particular insight into the process of tailoring the surface impedance of unit cells while taking curvature effects into account. We begin with the design requirements specified by S-parameters and present details of a tool for analyzing cascaded cylindrical metasurfaces. This tool also gives us detailed insight into the properties and selection of surface impedance for specific design parameters. Although a common approach is to approximate the surface admittance by its planar counterpart, we analyze this principle and show the limitations of this approximation through a parametric analysis.

9:30 Rigorous Susceptibility-Based Design of Generalized Huygens' Metasurface Radomes

[Amit Shaham](#) and Ariel Epstein (Technion - Israel Institute of Technology, Israel)

In this paper, we utilize the profound generalized Huygens' condition (GHC) to rigorously devise all-angle transparent metasurface (MS) radomes. We extend our recent configuration of double-layered admittance-sheet cascades, which allows only one Huygens' condition to hold (at grazing angle), by incorporating a third middle layer; we thus fully satisfy Huygens' condition both at normal and grazing angles in closed form. Our meticulous analysis introduces a universal nonlocal link between macroscopic MS constituents and their corresponding effective meta-atom susceptibilities. Particularly, it reveals that the trilayered composite inevitably manifests effective normal susceptibilities overlooked by common tangentially-polarized MS design practices. A printed-circuit-board version of the radome is realized and inspected in theory and simulation. Its excellent observed performance validates the GHC in a fundamental practical situation and sets the stage to cutting edge performance in advanced nonlocal wave-moulding functionalities.

9:50 Static and Reconfigurable Phase-Gradient Metasurfaces for Antenna Applications

[Alessio Monti](#) (Roma Tre University, Italy); Stefano Vellucci, Michela Longhi and Mirko Barbuto (Niccolò Cusano University, Italy); Mohsen Karamirad (Roma Tre University, Italy); Zahra Hamzavi-Zarghani and Davide Ramaccia (RomaTre University, Italy); Luca Stefanini, Alessandro Toscano and Filiberto Bilotti (Roma Tre University, Italy)

In this contribution, we report our recent findings in the design of static and reconfigurable transmissive phase-gradient metasurfaces for antenna applications. In particular, we show that transmissive metasurfaces can be efficiently used to manipulate the radiative characteristics of phased-arrays or single antennas, achieving an extension of the scan range or a dynamic transformation of the radiation pattern, respectively. For these purposes, we explore the design of both local- and non-local phase-gradient Huygens metasurfaces. Several realistic antenna configurations are proposed and checked with extensive full-wave simulations that confirm the huge potentialities of this design scheme for conceiving next-generation antenna systems characterized by enriched radiative capabilities, especially useful in beyond-5G and 6G wireless systems.

Wednesday, March 20 8:30 - 10:10

IW6: Advances in TICRA Tools and Future Developments for AI and Array Antennas, TICRA

Erik Jørgensen and Tonny Rubæk, TICRA

Room: M3

8:30 Introduction to TICRA Tools

What it is and what it can do. The software tools available in the TICRA Tools framework can be used to model advanced antenna systems including arrays, reflector antennas, feed systems, reflectarrays and FSS, as well as satellite structures and more general antennas. Presenters: Erik Jørgensen; Tonny Rubæk (TICRA)

9:00 Recent Additions to TICRA Tools

Presenters: Erik Jørgensen; Tonny Rubæk (TICRA)

9:30 Presentation of TICRA's Latest R&D Within AI and Full-Wave Modelling Algorithms for Large Antenna Arrays

Several application examples are shown to illustrate how AI-based design approaches and dedicated array modelling algorithms will benefit future releases of TICRA Tools. Presenters: Erik Jørgensen; Tonny Rubæk (TICRA)

Wednesday, March 20 8:30 - 10:10

A08a: Leaky-wave antennas

T09 Fundamental research and emerging technologies // Antennas

Room: M4

Chairs: Jose-Luis Gómez-Tornero (Polytechnic University of Cartagena, Spain), Edoardo Negri (Sapienza University of Rome, Italy)

8:30 Efficient Ray-Tracing Approach to Analyze Arbitrarily Shaped Leaky-Wave Antennas Embedded in Lenses

Miguel Poveda-García (Technical University of Cartagena, Spain); Francisco Mesa (University of Seville, Spain); Jose-Luis Gómez-Tornero (Polytechnic University of Cartagena, Spain); Astrid Algaba-Brazález (Ericsson AB, Sweden); Oscar Quevedo-Teruel (KTH Royal Institute of Technology, Sweden)

This paper introduces a computationally efficient ray-tracing approach to study the radiation pattern of a leaky-wave antenna embedded in a lens with an arbitrary shape. The ray-tracing technique, based on geometrical optics, is used to calculate the phase and amplitude of the fields at the lens aperture, taking into account reflections due to the transition from the lens to the free space. To validate the results, the radiation patterns obtained in some examples are compared with full-wave simulations, demonstrating a considerable time reduction in the analysis of up to 99.6% in some cases.

8:50 On the Asymptotic Evaluation of the Near-Field in Resonant Leaky-Wave Antennas Using a Non-Uniform Phase Center

[Alexandros Bechrakis Triantafyllos](#) and Nuria LLombart (Delft University of Technology, The Netherlands)

In this work, an approach for the asymptotic evaluation of the near field in resonant leaky-wave antennas is presented. The employed spectral domain formulation is based on the steepest descent path (SDP) method of integration and utilizes a non-uniform phase center choice to improve the estimation of the first order saddle point (SP). In turn, the near field is asymptotically evaluated through accounting for the leaky-wave poles-saddle point interactions. To demonstrate the applicability of the proposed approach, the near field is combined with a set of physical optics (PO) techniques to examine a small spherical lens integrated on

a leaky-wave supporting stratification with low dielectric contrast between the cavity and lens regions. Good agreement is obtained with the same results extracted using the numerically calculated near field. The computationally efficient asymptotic near field evaluation can facilitate the shaping of small lenses by improving the efficiency of the optimization process.

9:10 **Frequency Scanning Leaky-Wave Antenna for On-Body Radar: Design and Conformal Analysis**

Pratik V Vadher (IETR, CNRS & University of Rennes 1, France); Giulia Sacco (IETR CNRS, France); Denys Nikolayev (Institut d'Électronique et des Technologies du Numérique (IETR) - UMR CNRS 6164, France)

Wearable on-body millimeter-wave (mmWave) radars can help visually impaired people navigate their surroundings by creating a live 3D map and offer safety and motion guidance. Antenna, being a critical component of radar system, must be specifically designed to function while bent on user's body. This contribution details the design of a meandering microstrip leaky wave antenna (LWA) and analyzes its performance when placed on different body parts. The frequency scanning LWA, operates in unlicensed V-band (57-71 GHz). Analyzing return loss, beam steering range, and radiation pattern of the designed LWA positioned on human body at different locations (i.e., wrist, knee, chest) shows that bending has low impact on antenna performance. Simulations show that when the LWA is bent to be placed conformally on the wrist (corresponding to 40 mm radius) it remains well-matched throughout the operating band but radiation pattern is deformed and gain reduces by 1.75dB.

9:30 **Ka-Band USS Enterprise (NCC-1701) Antenna**

Miguel Navarro-Cía (University of Birmingham, United Kingdom (Great Britain)); Unai Beaskoetxea (Anteral, Spain); Jorge Teniente-Vallinas (Public University of Navarra & Institute of Smart Cities, Spain); Miguel Beruete (Universidad Publica de Navarra, Spain)

An all-metallic bull's eye antenna resembling the Enterprise (NCC-1701) Star Trek starship is reported with record side lobe levels (SLLs). The reduced SLLs are achieved by exciting the leaky-wave antenna via a resonant slot with effective out-of-plane electric dipole moment that inhibits the broadside space wave responsible for the relative high SLLs in other bull's eye designs

9:50 **Wideband Half-Elliptical Ring Slot Array Loaded Leaky Wave Antenna on a Half-Mode Corrugated Substrate Integrated Waveguide**

Aakash Bansal (Loughborough University, United Kingdom (Great Britain))

This paper presents a leaky-wave antenna with elliptical ring slot array loaded on a half-mode corrugated substrate integrated waveguide (HM-CSIW) operating at 25 to 36.5 GHz. The half-mode CSIW is designed to have a cut-off frequency of 20 GHz and is shown to operate in the TE₁₀ mode. The corrugated SIW is used as a guiding structure to host an array of half-elliptical ring-shaped slots to behave as a leaky-wave antenna. The antenna presents a frequency-controlled beam-scanning of 3 deg/GHz. It has an approximately stable gain of 14 dBi with an efficiency >75% throughout the bandwidth. The antenna is 0.51 mm thick, and flexible, hence, making them suitable for wearable devices and telecommunications for future 5G/6G applications.

Wednesday, March 20 8:30 - 10:10

SW12a: Open Source Electromagnetic Modelling Tools

Room: Fyne

Chairs: Francesco Lisi (Heriot-Watt University, United Kingdom (Great Britain)), Timothy Pelham (University of Bristol, United Kingdom (Great Britain))

8:30 **Introduction**

8:50 **gprMax (www.gprmax.org)**

Presenter: Antonis Giannopoulos (University of Edinburgh, UK)

9:50 **HERAS: Heriot-Watt Reflector Antenna Solver (www.github.com/Microwave-Antenna-Engineering-Group-HWU/HERAS)**

Francesco Lisi (Heriot-Watt University, UK)

Wednesday, March 20 10:40 - 12:20

SW11b: Wi-Fi Antenna Innovation for FTTR (Fiber-To-The-Room) Multi-Access Points F5G-A Scenarios (continued)

Room: Lomond Auditorium

Chair: Francis Keshmiri (Huawei Technologies, France)

10:40 **Technology for Radiation Pattern Manipulation of Wi-Fi Antennas**

Presenter: Zhi Ning Chen (National University of Singapore)

11:10 **Surface-Wave Communication Platform for Indoor Wireless Networks**

Presenter: Enrica Martini (University of Siena, Italy)

11:40 **Passive RIS to Improve Near-Field Coverage in mm-Wave 5G and Wi-Fi Indoor Networks**

Presenter: Manuel Arrebola (University of Oviedo, Spain)

12:10 **SW11 Pannel Discussions**

Wednesday, March 20 10:40 - 12:20

SW13: 20 Years Anniversary ESoA

Room: M1

Chairs: Angelo Freni (Università degli studi Firenze, Italy), Cristina Yepes (TNO, The Netherlands)

10:40 ESoA 2004-2024: 20 Years of Success

Presenter: Stefano Maci

10:50 It Was 20 Years Ago Today ...

Presenter: Olav Breinbjerg

11:00 ESoA, Arrays and Networks

Presenter: Christopher Craeye

11:10 ESoA: A Friendly Access to the European Antenna Academy

Presenter: Lluis Jofre

11:20 20 Years of ESoA: A (Subjective) View on Its Success

Presenter: Anja Skrivervik

11:30 ESoA: My Personal Experience as Student, Teacher and Course Organizer. What a Journey!

Presenter: Mauro Ettore

11:40 How to Successfully Create an ESoA Course from a Student Perspective

Presenter: Oscar Quevedo-Teruel

11:50 From ACE to ESoA Courses: Impact on Our Careers as Early Participants

Presenters: Nuria Llombart; Simona Bruni

12:00 Journey of Learning, Growth and Community - A Peek Inside ESoA

Presenter: Marko Bosiljevac

12:10 Online Antenna Courses

Presenter: Miguel Ferrando Bataller

Wednesday, March 20 10:40 - 12:20

CS35b: Propagation for Smart Mobility Scenarios (continued)

T01 Sub-6 GHz for terrestrial networks (5G/6G) / Convened Session / Propagation

Room: Alsh 1

Chairs: Ke Guan (Beijing Jiaotong University, China), Ibrahim Rashdan (German Aerospace Center (DLR), Germany)

10:40 Fading Distribution Model for the Maritime Radio Channel

Torbjörn Ekman (Norwegian University of Science and Technology, Norway)

The envelope fading distribution is derived for the round earth loss maritime radio channel. The propagation environment considered consists of a line of sight (LOS), and from the sea a specular reflection and a diffuse component. The phase difference between LOS and specular component is given by the relative path lengths and the change of phase in the sea reflection. The relative path length changes locally with the vertical movement of a ship-mounted antenna. The height variations are modeled as Normal distributed, resulting in a Normal distributed phase difference. This is an extension of the two-wave diffuse power (TWDP) model in which the phase difference between LOS and specular reflection is modeled as uniformly distributed.

11:00 Stationarity of Multiband Channels for OTFS-Based Intelligent Transportation Systems

Danilo Radović and Faruk Pasic (TU Wien, Austria); Markus Hofer (AIT Austrian Institute of Technology, Austria); Thomas Zemen (AIT Austrian Institute of Technology GmbH, Austria); Christoph F Mecklenbräuker (TU Wien, Austria)

The development of communication systems for intelligent transportation systems (ITS) relies on their performance in high-mobility scenarios. Such scenarios introduce rapid fluctuations in wireless channel properties. As a promising solution for vehicle-to-everything (V2X) communication, the orthogonal time frequency space (OTFS) approach has emerged. Nevertheless, the performance of OTFS systems is closely tied to time- and frequency diversity of the wireless propagation channel. However, there is a lack of understanding of the stationarity of the wireless channels, especially in the millimeter wave (mmWave) frequency bands. In this paper, we address this research gap by conducting a comprehensive stationarity analysis of measured sub-6 GHz and mmWave high-speed wireless channels. We evaluate the spatial stationarity of a scenario, where the transmitter is moving at high velocity. Furthermore, we investigate the influence of the transmit antenna orientation on the channel spatial stationarity. We could show that the spatial stationarity is proportional to the wavelength.

11:20 mmWave Channel Sounding for Vehicular Communications

Nicholas Atwood, Francois Gallée and Patrice Pajusco (IMT Atlantique, France); Marion Berbineau (COSYS, Université Gustave Eiffel, IFSTTAR, Univ Lille & Railenium, France)

This paper present some preliminary results of a Vehicle-to-Infrastructure channel measurement campaign. The IMT Atlantique SIMO (Single Input Multiple Output) SDR (Software Define Radio) based channel sounder with a working frequency of 60 GHz and a bandwidth of 180 MHz is used. The Tx (Transmitter) is placed on the top of a moving car and the Rx (Receiver) is placed on a top of a ladder. The scenario of measurement represent a street with vehicle parked on each side near the laboratory. From a measure we present for each channel: the CTF (Channel Transfer Function) gain, the PDP (Power Delay Profile) and the doppler spread function.

11:40 Experimental Evaluation of V2X Connectivity Technologies with V2X Channel Models

Dereje Mechal Molla (Gustave Eiffel University & COSYS-LEOST, France); Sassi Maaloul (Université Gustave Eiffel, France); Marion Berbineau (COSYS, Université Gustave Eiffel, IFSTTAR, Univ Lille & Railenium, France); Massamaesso Narouwa and Leo Mendiboure (Université Gustave Eiffel, France); Hakim Badis (University of Gustave Eiffel, France)

A new concept of on-demand automatic electric vehicle able to circulate on road and tracks is under development to revitalize secondary railway lines. The operation of this new system requires dynamic, flexible, and safe supervision system. This supervision system will be based on exchange of information between vehicles, level crossing, infrastructure and hubs. ITS-G5, LoRA, LTE and 5G NR are potential wireless technologies able to be deployed to guarantee connectivity. In these conditions, it is important to evaluate the foreseen key performance indicators to support the different services. This paper presents an in-lab experimental evaluation of V2X connectivity technologies with vehicular channel models

12:00 Indoor Propagation Measurements with a Reconfigurable Intelligent Surface at 3.5 GHz

[Jesper Ø Nielsen](#) (Aalborg University, Denmark); Ondřej Franek (Aalborg University & APMS Section, Denmark); Ying Zhinong (Aalborg University, Denmark)

This paper describes an investigation of the practical impact of a reconfigurable intelligent surface on indoor radio propagation. The evaluation is based on measurements of the instantaneous channel impulse response (CIR) between a static transmitter (Tx) and moving receiver (Rx) antennas in non-line of sight (NLOS), where the reconfigurable intelligent surface (RIS) was placed to potentially improve the channel. Different configurations of the RIS were employed and a mean power gain of up to 22 dB was found when introducing the RIS, but the gain was highly dependent on the distance between the Tx antenna and the RIS as well as the polarization, where gains of only about 1 dB were found for a 5 m distance. Also the correct focus point of the RIS was found to be important for close distances. In addition, statistics of the instantaneous power level were investigated.

Wednesday, March 20 10:40 - 12:20

A12b: Advances in modelling and design of phased arrays (continued)

T02 Mm-wave for terrestrial networks 5G/6G // Antennas

Room: **Alsh 2**

Chairs: Daniele Cavallo (Delft University of Technology, The Netherlands), Marc Thevenot (XLIM-University of Limoges, France)

10:40 Design, Measurements, and Performance Assessment of a Massive MIMO Wideband Phased Array

Riccardo Ozzola, Cesare Tadolini and Roderick Giosevan Tapia Barroso (Delft University of Technology, The Netherlands); Ulrik Imberg (Huawei Technologies, Sweden AB, Sweden); Daniele Cavallo and Andrea Neto (Delft University of Technology, The Netherlands)

In this paper, a wideband and wide-angle scanning array is designed to reduce the volume occupation in wireless base stations. It is realized as a dual-polarized connected array, which uses two interchangeable radomes of artificial dielectric layers to operate between 6 and 8 GHz and between 2 and 8 GHz, while scanning up to 60° on the main planes. An 8x8 array has been manufactured and tested in terms of matching and radiation patterns. Finally, the number of beams that the prototype can generate in a Multiple-Input Multiple-Output (MIMO) configuration is assessed by using the observable field concept.

11:00 An L-Band Receiving Array with Full Digital Simultaneous Quad-Polarization Beamforming

Peizhuo Yang, Gong Chen, Jiahao Wang and Koen Mouthaan (National University of Singapore, Singapore)

Traditionally, beamforming is a technique that deals with signal of one polarization. In this paper, simultaneous quadpolarization digital beamforming is demonstrated on a Radio Frequency System-on-chip (RFSoc) radio platform. An L-band polarization-reconfigurable antenna array is fabricated for the demonstration.

11:20 Synthesis of Circularly Polarized Microstrip Planar Array with Cross-Polarization Suppression

[Gabriel P Paulena](#) (Federal University of Pampa, Brazil); Juner M. Vieira (National Institute for Space Research (INPE), Brazil); Edson R. Schlosser and Marcos V. T. Heckler (Universidade Federal do Pampa, Brazil)

This paper describes the application of the differential evolution (DE) method to synthesize the radiation pattern of a 4x4 microstrip planar antenna array. The excitation coefficients are optimized to achieve beamsteering with sidelobe level control simultaneously. Additionally, the optimization process realizes the minimization of the cross-polarization level to, at least, 25 dB below of right-hand circular polarization (RHCP) in the main beam direction. The applied technique presents fast convergence and good performance in terms of pattern shape and polarization purity.

11:40 6:1 Connected Slot Array in PCB Technology

Mattia Maggi (Université de Rennes 1 & Centre National Etudes Spatiales, France); Rémi Fragner and Romain Contreres (CNES, France); Ronan Sauleau (University of Rennes 1, France); Mauro Ettorre (University of Rennes 1 & UMR CNRS 6164, France)

This work shows the design of connected slot arrays in PCB technology. A capacitive load is introduced over the radiating slots to enlarge the operating band scanning range. The stack-up of the array is presented and discussed for a PCB fabrication. The features of every element are illustrated from the top of the structure to the end of the feeding network. The antenna can operate in the band 2 - 20 GHz with a field of view of 60° in elevation along the E- and D-planes.

12:00 Study of Finite Edge Effects in Compact Ultra-Wide-Band Connected Arrays

Roderick Giosevan Tapia Barroso, Andrea Neto and Daniele Cavallo (Delft University of Technology, The Netherlands)

Connected array antennas have recently emerged as viable solutions to realize phased arrays with very large bandwidth and wide scanning capability. One of the key properties that enables the broadband operation is the high inter-element mutual coupling. However, the high coupling also causes large variations of the active impedance in finite arrays, due to edge effects. This is particularly problematic for applications in which the number of elements is limited by the available space to accommodate the array. A study of the truncation effects on the array performance is presented, and a number of possible improvement strategies are investigated.

Wednesday, March 20 10:40 - 12:20

A13: Emerging antennas for space systems

T03 Aerospace, new space and non-terrestrial networks // Antennas

Room: **Boisdale 1**

Chairs: Hervé Legay (Thalès Alenia Space, France), Ashraf Uz Zaman (Chalmers University of Technology, Sweden)

10:40 Ultra-Miniature Circularly Polarized Antenna with Omni-Directional Pattern for Sat-IoT

Serge Bories (CEA, France); Jean-François Pintos, Marwan Jadid and Christophe Delaveaud (CEA-LETI, France)

This paper presents the design and performance of a $\lambda/15 \times \lambda/15 \times \lambda/25$ antenna that radiates circular polarisation with a dipole-like pattern. The simple structure of the miniaturized monopole loaded with a loop is optimized by adjusting the phasing between the monopole and loop excitations through reactive loading component calculation. While the circular polarization remains good ($AR < 3$ dB) over the 0.75 % fractional bandwidth, the total efficiency reaches 12% for such ultra-miniature antenna.

11:00 Compact Circularly Polarized Antenna Based on Gapwaveguide for SATCOM Applications

Raha Roosefid (Chalmers University of Technology & Satcube AB, Sweden); Jian Yang and Ashraf Uz Zaman (Chalmers University of Technology, Sweden)

In this study, we introduce a novel compact cavity design specifically tailored for generating circular polarization. By optimizing the structure and dimensions, our proposed cavity demonstrates a significant reduction in size compared to conventional cavities. This compactness not only facilitates the design of more simplified individual components but also sets the way for the development of more compact arrays for the purpose of larger scanning angles in scanning array antennas. The dimensions of the cavity are 5.46×5.46mm at a center frequency of 28.5GHz. The impedance bandwidth ranges from 27.75GHz to 29.75GHz and the axial ratio is less than 3dB, aligning with the impedance matching with a bandwidth of 5.08%. The design has low loss and high efficiency due to its fully metal structure. Given its inherent attributes and performance metrics, this compact cavity emerges as a promising choice for Satellite Communication (SATCOM) applications.

11:20 Wide-Angle Quasi-Optical Beamformer for LEO Applications

Léonin Lassaue (Université de Rennes 1 & IETR, France); Jean-Philippe Fraysse and Ségolène Tubau (Thales Alenia Space, France); Romain Contreres (CNES, France); Mauro Ettore (University of Rennes 1 & UMR CNRS 6164, France)

In this article, the design of a low profile double mirror quasi-optical beamformer is presented for low Earth orbit Satcom megaconstellations. The beamformer consists of stacked parallel plate waveguides operating with the principal transverse electromagnetic mode. Vertical mirrors shape in amplitude and phase the guided mode for feeding a linear array located at one edge of the beamformer. A physical optics tool is used to optimize the shape and location of the mirrors for wide scanning. The final design is based on an integrated solution for high beam crossover in PCB technologies. Full-wave simulations validate the system based on a dual-mirror system radiating 23 beams in a field of view of $\pm 55^\circ$ with increased beam crossover in the Ka-band (17.3 GHz - 20.2 GHz).

11:40 Low Profile Wideband Dual-Polarized Antenna Array for Ku/Ka-Band Satcom Applications

Qingchun You, Lu Qian and Yi Wang (University of Birmingham, United Kingdom (Great Britain))

This paper introduces a design method for an ultra-wideband dual-polarized array antenna. It consists of open-boundary quad-ridged horn antenna elements and a novel waveguide parallel coupled differential feeding network. The design of the open-boundary quad-ridged horn antenna enhances the low-frequency radiation performance. The differential feeding network achieves good impedance matching over a bandwidth from 10 to 32GHz within a confined space of 8mm. Based on this approach, an ultra-wideband dual-polarized array antenna is designed for satellite communication in the Ku/Ka frequency bands. Simulation results demonstrate that the antenna exhibits a return loss better than +12 dB over the 10-32 GHz range, with the antenna aperture efficiency exceeding 75% across the band.

12:00 Circularly-Polarized Wideband Conformal Magneto-Electric Antenna Covering the GNSS Bands

Alexandre Causse (Université de Rennes 1, France); Loïc Bernard (ISL & IETR, France); Sylvain Collardey (University of Rennes 1, France); Ala Sharaiha (Université de Rennes & IETR, France)

A circularly-polarized wideband conformal magneto-electric antenna is introduced; the conformation radius is of 77 mm and this antenna aims at covering all the GPS and Galileo bands ([1164;1300] MHz + [1559;1591] MHz). The antenna dimensions are 88 × 75 × 38.4 mm. The simulation results are validated by the measurement results of a prototype.

Wednesday, March 20 10:40 - 12:20

CS40b: New challenges on small antennas for emerging wireless technologies (continued)

T04 RF sensing for automotive, security, IoT, and other applications / Convened Session / Antennas

Room: Boisdale 2

Chairs: Halim Boutayeb (Université du Québec en Outaouais, Canada), Marta Cabedo-Fabrés (Universidad Politécnica de Valencia, Spain)

10:40 Small On-Metal Passive UHF RFID Transponders with Long Read Ranges

Mohamed Räsänen, Jari Holopainen and Jan H. S. Bergman (Aalto University, Finland); Matti Kuosmanen (Aalto University & Saab Finland Oy, Finland); Ville Viikari (Aalto University & School of Electrical Engineering, Finland)

This paper presents two small wide-band passive on-metal ultra-high frequency (UHF) radio frequency identification (RFID) tags for on-metal applications. The first single resonant design is for long-range RFID applications, whereas the second dual-resonant design targeted for wide-band purposes. Both designs are free of external matching components, the second design utilizes dual-stub matching. Both designs are based on the planar inverted L antenna (PILA), in which the planar radiator is placed on top of the ground plane. The tags operate in the passive mode. The first design achieves a measured reading distance of 15.2 m at 872 MHz. For the second design, the achieved maximum read range is 7.2 m, and a minimum read range of 3.0 m within 902 MHz - 958 MHz. Both tags are designed to operate in the passive mode. The used PCB substrate is the commercially available and widely used FR-4.

11:00 A WiFi-Based System for Ice Monitoring in Harsh Environment Using 2.7 GHz Microwave Sensor

Dima Kilani (The University of British Columbia, Canada); Aaryaman Shah and Fatemeh Niknahad (University of British Columbia, Canada); Mohammad H. Zarifi (The University of British Columbia, Canada)

The integration of microwave sensors within wireless sensor nodes (WSN) enables remote real-time monitoring and detection across diverse sectors. However, the conventional use of a bulky vector network analyzer (VNA) to stimulate the microwave sensor poses limitations for practical applications. This paper presents a WSN utilizing a microwave sensor integrated with a readout printed circuit board (PCB) that inherently excites the sensor eliminating the need for a VNA. The microwave sensor is designed to monitor ice accumulation in harsh environment and is composed of three split-ring resonator tags coupled to the transmission line. The data collected from the microwave sensor is processed and sampled using the integrated readout (PCB), and transmitted to the server via a WiFi module. The WSN has been successfully tested within a temperature range of 20-C to -40-C and a frequency range of 1.75 GHz to 2.8 GHz.

11:20 Compact 868 MHz RFID-Based Antenna for Queen Bee Identification and Location Inside Hives

Laura Pérez Beltrán (Universitat Politècnica de València, Spain); José Lorenzo López and Javier Fernández Caballero (Universidad Politécnica de Cartagena, Spain); Marta Cabedo-Fabrés (Universidad Politécnica de Valencia, Spain); Miguel Ferrando-Bataller (Universitat Politècnica de València, Spain); Leandro Juan-Llacer (Universidad Politécnica de Cartagena, Spain); Manuel Delgado-Restituto (Institute of Microelectronics of Seville, Spain)

The traditional method of identifying and locating queen bees within a hive involves laborious and time-consuming processes, such as visual inspections and paint marking on the thorax. In contrast, this work focuses on leveraging RFID (Radio-Frequency Identification) technology to streamline this task. A compact antenna, intended for use in conjunction with a commercial transponder, is designed and manufactured. The dimensions of the antenna are 3.09 × 2.61 mm, making it suitable for placement on the thorax of a queen bee. This antenna provides sufficient range for the identification and location of queen bees from the exterior of hives, even in hives with maximum dimensions of approximately 54 cm. Measurement reveal that the antenna's range increases when located inside the hive compared to open space. Furthermore, the effectiveness of the antenna in locating queen bees is assessed by conducting extensive measurements within the honeycomb where the bee is situated.

11:40 Efficient Wireless Power Transfer to an Ultra-Miniaturized Antenna for Future Cardiac Leadless Pacemaker

Farooq Faisal (National Institute of Scientific Research Montreal, Canada); Ahmed Moulay (INRS (EMT), Canada); Mohamed Chaker (INRS, Canada); Tarek Djerafi (Institut National de la Recherche Scientifique, Canada)

An ultra-wideband antenna with an ultra-miniaturized size of only 10.66 mm³ is proposed for a leadless pacemaker. The antenna was integrated with the dummy electronics of an LP to consider the components' effects. The specific absorption rates were found in the safety limits. The antenna is tested by experiments in minced pork and the measured results are found in close agreement with simulation results. To convert the received radio frequency (RF) energy into direct current (DC), a multi-section rectifier with a wideband functionality was integrated with the proposed antenna. To improve the RF-dc conversion efficiency of the rectifier, spatial power combining techniques have been employed. In these techniques, two signals (1.5 GHz and 1.52 GHz) components have been generated separately and transmitted through an ultra-wideband horn antenna. It is observed that transferring two signals improved the received dc voltage by 28.2 % compared to using a single frequency.

12:00 Challenges and Limits of Designing Wide Band and Efficient Compact Superdirective Antenna

Abdellah Touhami (University RENNES1, France); Sylvain Collardey (University of Rennes 1, France); Ala Sharaiha (Université de Rennes & IETR, France)

The design of efficient and wideband superdirective array is a challenging task. The challenges lie in the inverse proportionality between the maximal directivity in one hand and the efficiency as well as the impedance bandwidth in the other hand. In this paper we present a simple optimization strategy to address these issues. It consists of two key elements: the embedding of passive loads inside the antenna structure to ensure a wideband behaviour and the optimization of the array realized gain instead of its directivity. Such optimization allows establishing a best trade-off between the array performances. The proposed method is used afterwards for designing a two elements array with a separation distance of $d = 0.1\lambda$. The simulations show that the array presents a wide impedance bandwidth of 11.8%, a large -1 dB bandwidth of directivity and gain of 18.2% and 13.6% respectively and a high total efficiency $> 80\%$.

Wednesday, March 20 10:40 - 12:20

CS23b: Recent Advances on Propagation Research and Its Impact on Localizations (continued)

T05 Positioning, localization, identification & tracking / Convened Session / Propagation

Room: Carron 1

Chairs: Christian Gentner (German Aerospace Center (DLR), Germany), Wei Wang (Chang'an University, China)

10:40 SARFID for Fine-Scale Localization of Passive Backscattering Devices at 2.4 GHz ISM Band

Andrea Motroni, Glauco Cecchi, Alice Buffi and Paolo Nepa (University of Pisa, Italy)

Indoor localization systems have gained prominence across various industries for their ability to determine the location of objects, people, vehicles, and assets. This paper delves into the localization of 2.4 GHz passive devices based on modulated backscattering communications with a Synthetic Aperture Radar (SAR) approach, traditionally associated with UHF-RFID (Ultra-High-Frequency Radio Frequency Identification) devices at around 900 MHz. The shift from 900 MHz band to the 2.4 GHz ISM (Industrial-Scientific-Medical) band necessitates considerations on the effects of the higher frequency on localization accuracy, antenna trajectory parameters, and synthetic array aperture. This study aims to understand the advantages and challenges of applying these techniques in an unexplored frequency range and discusses potential applications.

11:00 Path Loss Modeling for Air-To-Ground Channels in a Suburban Environment

Sander Coene (Universiteit Gent, Belgium); Achiel Colpaert (KU Leuven, Belgium); Emmeric Tanghe (Ghent University, Belgium); David Plets (Ghent University - imec, Belgium); Zhuangzhuang Cui and Sofie Pollin (KU Leuven, Belgium); Wout Joseph (Ghent University/IMEC, Belgium)

In the context of intelligent transportation systems and smart cities, vehicle-to-vehicle communications will play a major role in providing localized information services. Unmanned aerial vehicles are an important part of this infrastructure, as they provide flexibility and enable demand-based (re)deployment of network nodes. However, these drone-based scenarios have unique propagation channel characteristics that are not yet fully explored. In this paper, we investigate channels measured between a ground base station and drone-mounted platform, emulating air-to-ground communications at different heights and for different propagation conditions. Using a log-distance path loss model, we obtain line-of-sight path loss exponents of 6.3-8.4, increasing with height (12.1-49.2m). Vegetation obstruction resulted in values 15.0 and 13.2, at 33 m and 49 m heights, respectively. Addition of an angle-dependent loss component improved the fit slightly in only two scenarios. Its new component exponent was statistically significant at a 5% significance level in only half of the cases.

11:20 Mixture Density Networks for Multipath Assisted Positioning-Based Fingerprinting

Markus Ulmschneider, Christian Gentner and Armin Dammann (German Aerospace Center (DLR), Germany)

In multipath assisted positioning schemes, the spatial information contained in multipath propagation of wireless radio systems is exploited for localization of a receiver. However, such schemes suffer from a high computational complexity. We have proposed before a fingerprinting localization system based on multipath assisted positioning, where the fingerprinting database is encoded in a deep neural network (DNN). Within this paper, we propose and evaluate a mixture density network approach in our DNN to analyze ambiguities among fingerprints at different locations. We show that our scheme shows a very good positioning performance with an error of around 2m for the most part, while having a low computational complexity in the online stage and a very low effort compared to traditional fingerprinting schemes.

11:40 Angle of Arrival Measurements with Ultra-Wide Band Transceivers: Design and Evaluation

Josef Kraska (Czech Technical University in Prague, Czech Republic); Christian Gentner (German Aerospace Center (DLR), Germany); Vaclav Navratil (Czech Technical University in Prague, Czech Republic)

Ultra-wide Band (UWB) positioning systems estimate the user's position from several time-based measurements. While usually achieving decimeter-level accuracy, enhancing the measurements by additional measurements, such as Angle of Arrival (AoA), should improve the positioning performance and robustness. In this work, the design of our custom UWB-AoA board capable of time-based and angle-based measurements is presented. The board contained two DW1000 UWB transceiver chips with a common clock source and with independent communication interfaces, enabling parallel control of the chips. The AoA measurements using Time Difference of Arrival (TDoA) and Phase Difference of Arrival (PDoA) methods are discussed. The AoA estimation accuracy using TDoA and PDoA is evaluated experimentally with turntable experiments, done for several antenna configurations. The results show that with PDoA measurements it is possible to achieve AoA errors with 6.1 degrees standard deviation and +0.73 degrees mean for half-wavelength antenna separation and even better for longer antenna separations.

12:00 Characterization of Propagation from Measurements at Sub-THz for ISAC Applications in an Emulated Dynamic Industrial Scenario

Diego Andrés Dupleich (Technische Universität Ilmenau, Germany & Fraunhofer Institute for Integrated Circuits IIS, Germany); Alexander Ebert, Yanneck Völker-Schöneberg and Damir Sitdikov (Technische Universität Ilmenau, Germany); Mate Boban (Huawei Technologies Duesseldorf GmbH, Germany); Giovanni Del Galdo (Fraunhofer Institute for Integrated Circuits IIS & Technische Universität Ilmenau, Germany); Reiner S. Thomä (Ilmenau University of Technology, Germany)

The large blocks of free instantaneous bandwidth at (sub-)THz and the utilization of high gain radio interfaces makes the (sub-)THz suitable for sensing applications. In this paper we present the analysis of novel dual-polarized double directional measurements at 190-GHz in an industrial setting with integrated sensing and communication applications in view. The set-up consists of a bi-static configuration emulating two access points with beam-steering capabilities in a machine room. One access point serves a machine with a wireless link, while the other access point senses the environment to detect moving objects. The objective is to detect possible obstructions that could interrupt the communication link or cause accidents on the production line. The results have shown that the system aspects as narrow beams and large bandwidths allow the early identification of objects in the environment from the measured channel impulse response.

Wednesday, March 20 10:40 - 12:20

E01: Inverse Scattering and Imaging for Biomedical Applications

T06 Biomedical and health // Electromagnetics

Room: Carron 2

Chairs: Tommaso Isernia (University of Reggio Calabria, Italy), Sergio Matos (ISCTE-IUL / Instituto de Telecomunicações, Portugal)

10:40 Optimal Design of Planar Micro-NMR Coils for High Signal-To-Noise Ratio

Natachai Terawatsakul and Alireza Saberkari (Linköping University, Sweden); Morgan Madec (iCube, France)

This paper introduces a design methodology for optimizing a micro nuclear magnetic resonance (NMR) planar coil to ensure maximum signal-to-noise ratio (SNR) in NMR systems. Although the SNR is influenced by

multiple factors, some remain nearly impossible to model using electromagnetic simulators. To address this challenge, we propose the coil performance factor (CPF) concept, which exclusively considers coil-related parameters. Utilizing this methodology, we evaluated multiple planar coils, each with varying turn numbers, trace widths, and shapes but maintaining a diameter consistent with 5 mm, within an identical environment. Notably, unlike coils designed for other applications prioritizing high-quality factor (Q), NMR coils necessitate a balance between high homogeneity and other factors. Comparative analysis revealed that the optimized octagonal coil, comprising 3 turns and a 0.27 mm trace width, exhibited a CPF of 0.0214 millitesla per the square root of Kelvin ohms, while the high-Q coil demonstrated 0.0102.

11:00 *Assessment of the Feasibility of Breast Lesion Detection with Contrast Source Inversion for Microwave Tomography: A Virtual Experiment*

[Alessandra Ronca](#) (Istituto Nazionale di Ricerca Metrologica (INRIM) & Politecnico di Torino, Italy); [Alessandro Arduino](#), [Luca Zilberti](#) and [Oriano Bottauscio](#) (INRIM, Italy); [Gianluigi Tiberi](#) (London South Bank University, United Kingdom (Great Britain) & UBT - Umbria Bioengineering Technologies, Italy)

In this paper, the microwave tomography performed using the contrast source inversion method was investigated. A two-dimensional model problem, composed of a cylindrical phantom positioned at the center of the receiving antennas' circular distribution, provided the setup for virtual experiments. Both a homogeneous phantom, with electrical properties that approximate the ones of a dense breast, and several heterogeneous phantoms, with an inclusion whose high electrical properties simulate those of a breast lesion, were considered. The effect of the initial guess on the reconstruction of the homogeneous phantom was assessed for a first investigation. Then, the detectability of the inclusion in the heterogeneous phantom was tested varying its size, position, and electrical properties. Results suggested that a priori information is useful to build a robust initial guess. The inclusion was detectable in the permittivity maps independently of the considered dimension and position, whereas structured noise was predominant in the conductivity maps.

11:20 *Estimating the Signal Strength for Microwave Breast Cancer Detection with a Magnetic Near-Field Applicator in Air*

[Christoph Jannick Salomon](#), [Nikola Petrovic](#) and [Per Olov Risman](#) (Mälardalen University, Sweden)

In this paper, we present a numerical simulation scenario to estimate the signal strength of a tumor in a microwave detection scenario containing a magnetic near-field applicator and a quarter-wave dipole as transmitter and receiver, respectively. Two different receiver orientations are tested on two different breast phantoms representing high-adipose and low-adipose bulk breast tissue. The tumor signal strength is estimated by subtracting the received signals acquired with and without a tumor being present. The results indicate that in the horizontally aligned receiver case, the presence of a tumor can be estimated from the receiver positions exhibiting the highest difference signals. The strongest difference signals however do not occur at the frequency of operation but below. The other cases are not conclusive, but a stronger tumor signal was received with the horizontally aligned receiver than with the vertically aligned one throughout.

11:40 *Huygens Principle Imaging Method Powered by Deep Learning for Brain Stroke Classification*

[Moein Movafagh](#) (London South Bank University, United Kingdom (Great Britain)); [Navid Ghavami](#) (Umbria Bioengineering Technology (UBT), United Kingdom (Great Britain)); [Gianluigi Tiberi](#) (London South Bank University, United Kingdom (Great Britain) & UBT - Umbria Bioengineering Technologies, Italy); [Mirco Cosottini](#) (University of Pisa, United Kingdom (Great Britain)); [Sandra Dudley-McEvoy](#) and [Mohammad Ghavami](#) (London South Bank University, United Kingdom (Great Britain))

In our study, we investigate the potential of deep learning to elevate the effectiveness of the Huygens principle (HP) imaging method in detecting brain strokes. While HP has proven successful in breast cancer imaging, it faces some challenges when applied to more complex structures such as the brain. To overcome these challenges, we use Finite-Difference Time Domain (FDTD) simulations to build a comprehensive dataset. Subsequently, we employ the U-net model to map HP-generated images to strokes, yielding impressive results. Our findings indicate an accuracy rate of 93.2% for the brain phantom, showcasing the promising prospect of this approach for brain imaging enhancement.

12:00 *A Smart Convenient Rewriting of the Inverse Scattering Equations for the 3D Scalar Problem*

[Martina Teresa Bevacqua](#) (Università Mediterranea di Reggio Calabria, Italy); [Tommaso Isernia](#) (University of Reggio Calabria, Italy)

The contribution addresses the tridimensional inverse scattering scalar problem, by introducing a new smart rewriting of the scattering equations such to reduce the degree of nonlinearity of the inverse problem. The analysis of the norm of the relevant internal radiation operator is performed in comparison with the standard one. This analysis can open the way for exploring new possibilities and opportunities for imaging and detection of unknown targets.

Wednesday, March 20 10:40 - 12:20

E05: Periodic Structures for mmWave and THz Applications

T07 THz and high frequency technologies // Electromagnetics

Room: [Dochart 1](#)

Chairs: [Alexandros Feresidis](#) (University of Birmingham, United Kingdom (Great Britain)), [Agnese Mazzinghi](#) (University of Florence, Italy)

10:40 *From Bulk Toward Micro-Structured TiO₂ Ceramics for All-Dielectric Metamaterials at Terahertz Frequencies*

[Djihad Amina Djemah](#) (C2N, France); [Delphine Gourdonnaud](#) (Université de Limoges, France); [Pierre-Marie Geoffroy](#) (SPCTS - UMR CNRS 7315 - University of Limoges, France); [Jean-Francois Roux](#) (Université Savoie Mont-Blanc, France); [Fayçal Bouamrane](#) (Unité Mixte de Physique CNRS, France); [Eric Akmansoy](#) (Université Paris Sud & Institut d'Electronique Fondamentale, France)

In this study, we aimed to develop high permittivity TiO₂ ceramics ideal for the fabrication of All-Dielectric Meta- materials operational in the terahertz frequency. TiO₂ ceramic pellets are fabricated from a commercial powder. A comparative analysis was conducted between Spark Plasma Sintering (SPS) and conventional sintering process. Characterizations were then carried out in the range of 0.2 to 1.4 THz using THz time-domain spectroscopy. We observed that the samples fabricated by the spark plasma sintering and post-annealing treatment exhibit a high refractive permittivity associated with minimal loss ($\epsilon'' \approx 100$ and $\tan \delta < 0.015$). These characteristics make these samples optimal candidates for achieving a negative refractive index in all-dielectric metamaterials. In addition, two micro-structuring processes were investigated for the realization of metamaterials operating in the terahertz range: micro-molding and direct TiO₂ etching by Inductively Coupled Plasma (ICP).

11:00 *On the Rigorous Design of Graphene-Based Periodic Structures Exploiting the Fundamental Resonances*

[Pablo H. Zapata Cano](#) (Aristotle University of Thessaloniki, Greece); [Stamatis A. Amanatiadis](#) (Aristotle University of Thessaloniki & Ormylia Foundation, Greece); [Zaharias D. Zaharis](#) and [Traianos Yioultsis](#) (Aristotle University of Thessaloniki, Greece); [Pavlos Lazaridis](#) (University of Huddersfield, United Kingdom (Great Britain)); [Nikolaos V. Kantartzis](#) (Aristotle University of Thessaloniki, Greece)

The electromagnetic response of graphene plasmonic scatterers is realized in the present work by exploiting their natural modes. Initially, a formulation to extract the latter is presented, where the planar material is modeled as an equivalent surface current. Then, a simple disk scatterer is considered and the fundamental modes are evaluated to distinguish them between edge and bulk ones, taking into account the field distribution. Moreover, the resonance frequencies for the case of incident plane-wave scattering are connected to the characteristics of the fundamental modes. Finally, a periodic array of graphene scatterers is investigated to highlight the additional plasmonic coupling resonances, corresponding to natural modes of different attributes.

11:20 *SIW Slot Leaky-Wave Antenna Using Low-Index Metamaterial*

[Amir Jafargholi](#) and [Romain Fleury](#) (EPFL, Switzerland)

This paper presents a wideband leaky-wave substrate-integrated wave guide (SIW) slot antenna. The proposed structure comprises slots loaded with a low-index metamaterial (MTM). The MTM is realized using an array of thin wires. Loading the antenna with low-index material not only improves the antenna's impedance bandwidth but also improves radiation, introducing a slight variation in the main lobe direction as the frequency changes. This is a feature that is challenging to attain with conventional leaky-wave antennas. The antenna operating frequency covers the frequency range of 25.2 to 33.5 GHz, with a bandwidth of 28.3%. Based on the proposed SIW slot antenna, a 16-element leaky-wave antenna with a maximum gain of 14.2 dBi is presented. The final prototype is a single-layer, compact, and cost-effective structure.

11:40 *Design of Novel Fully Metallic mm-Wave Reflectarray Antenna*

[Savvas Chalkidis](#) and [Evangelos Vassos](#) (University of Birmingham, United Kingdom (Great Britain)); [Thomas Whittaker](#) and [William Whittow](#) (Loughborough University,

United Kingdom (Great Britain)); Alexandros Feresidis (University of Birmingham, United Kingdom (Great Britain))

The design of a novel fully metallic reflectarray antenna at millimetre-wave frequencies is presented. The reflectarray consists of 3-D metallic unit cells resembling four layers of thick metallic patches connected by metallic vias. Full phase control and low losses are achieved by generating numerous unit cells with different combinations of the patches' size. Simulations have been carried out using CST Microwave Studio and TICRA QUPES to evaluate the response of the unit cells and the proposed reflectarray. The unconventional multi-layer design suggested can be implemented by exploiting recently emerged additive manufacturing techniques. In terms of the reflectarray performance, the operating frequency is centered at 30GHz whilst the directivity is approximately 28dBi.

12:00 A Novel Topologically Protected Hollow Dielectric Waveguide for Robust mmWave Guiding

Menglin Chen (Hong Kong Polytechnic University, Hong Kong); Rui Zhou (Central China Normal University, Hong Kong)

Waveguide devices are fundamental components in microwave systems. While operation frequencies of communication systems are migrating to millimeter wave regime, it makes design requirements for electronic components more demanding. With the rapid development of topological photonics, it has been found that topology of artificial structures can provide prospects for optical circuits to achieve unprecedented features. Inspired by the idea of topology, here, we propose a new protection mechanism for hollow dielectric waveguides to achieve robust millimeter wave propagation against path bends or defects. By decorating the boundaries of the conventional waveguide with valley photonic crystals, topologically protected hybrid modes consisting of transverse electric modes and valley edge states are generated. The proposed waveguide is highly compatible with substrate-integrated waveguide technology. Our work provides a novel method of leveraging topological effects from optics to millimeter wave engineering and significantly expands the application scope of topological devices in millimeter wave regime.

Wednesday, March 20 10:40 - 12:20

E10b: Electromagnetic Modelling and Analytical Methods (continued)

T08 EM modelling and simulation tools // Electromagnetics

Room: [Dochart 2](#)

Chairs: Pilar Castillo-Tapia (KTH Royal Institute of Technology, Sweden), Andrea Neto (Delft University of Technology, The Netherlands)

10:40 Radiation Efficiency Cost of Optimal Current Density Generating Specific Far-Field Pattern

Miloslav Capek and Lukas Jelinek (Czech Technical University in Prague, Czech Republic)

This paper addresses the question of how closely can a prescribed far field be generated by the current density optimal in radiation efficiency. Two types of current optimization problems are introduced and solved with the tools of convex programming. The theory is demonstrated in several examples utilizing in-house software tools. The complexity of the problems is discussed, showing that the complete problem, including an unspecified phase of the desired far field, is an NP-hard problem, requiring one of the iterative approaches known in the literature.

11:00 Analytical Circuit Models: From Purely Spatial to Space-Time Structures

Carlos Moleró and Salvador Moreno-Rodríguez (University of Granada, Spain); Antonio Alex-Amor (Universidad San Pablo-CEU, Spain); Pablo Padilla (University of Granada, Spain); Juan Valenzuela-Valdés (Universidad de Granada, Spain)

This work presents an insight into a theoretical framework for deriving fully-analytical and multi-modal equivalent circuits for periodic structures, FSSs and general metasurfaces. By including time as a new variable, the classical version of the model can be extended from the analysis of purely spatial structures to time- and spacetime-varying metasurfaces. Several kind of periodic structures are considered from the circuit point of view along the document, being periodic in space, time and spacetime. The performance the analytical circuits is validated via external full-wave solvers, leading the models to become an excellent tool to explore novel and advanced spacetime scenarios.

11:20 Proving the Circular Polarization of the Fundamental Modes in Rotationally Symmetric Waveguides

Gines Garcia-Contreras (Universidad Autonoma de Madrid, Spain); Juan Córcoles and Jorge A Ruiz-Cruz (Universidad Politécnica de Madrid, Spain)

Second-order symmetric waveguides are especially suitable for dual polarization applications, since they present clear, mathematically proven, degeneracy schemes in their spectrum. In this work we will prove that, in second order rotationally-symmetric waveguides, the fundamental mode presents circular polarization in the circumcenter of the cross-section for any symmetry factor greater than three, and regardless of its geometry. Moreover we will show that certain mode classes do not carry any power at the circumcenter.

11:40 Efficient Analysis Method for Artificial Dielectric Layers with Vertical Metal Inclusions

Alexander J van Katwijk, Andrea Neto and Daniele Cavallo (Delft University of Technology, The Netherlands)

Artificial dielectric superstrates have recently been studied due to their ability to enhance the bandwidth and scanning range of antenna arrays. One such superstrate consists of artificial dielectric layers (ADLs) and forms an effective medium that is anisotropic, which enables a larger scanning volume without supporting surface waves. When arrays that employ these ADLs scan to large angles on the diagonal plane, this anisotropy increases the cross-polarization of the array. This problem can be reduced by introducing vertical metal pins in the ADL superstrate which enables control over the vertical component of the permittivity tensor. This work shows an ongoing effort to develop an efficient analysis method based on a spectral domain method of moments. Entire-domain basis functions are used in a hybrid cartesian and cylindrical coordinate system to accurately model the currents on the structure under plane wave incidence.

12:00 Numerical Results on the Use of the L-SVD Approach for the Solution of the Inverse Source Problem from Amplitude-Only Data

Amedeo Capozzoli (Università di Napoli Federico II, Italy); Ilaria Catapano (IREA-CNR, Italy); Claudio Curcio (Università di Napoli Federico II, Italy); Giuseppe Esposito and Gianluca Gennarelli (IREA-CNR, Italy); Angelo Liseno (Università di Napoli Federico II, Italy); Giovanni Ludeno (IREA-CNR, Italy); Francesco Soldovieri (CNR, Italy)

We consider a Learned Singular Value Decomposition (L-SVD) approach to face a canonical 2D scalar inverse source problem from amplitude-only, far-field data. We compare the reconstruction performance of L-SVD from amplitude-only data against the Truncated SVD (TSVD) regularized inversion using amplitude and phase (complex) information. The numerical tests show that phaseless L-SVD provides, with a proper training on a well-organized dataset accommodating significant a priori information on the set of relevant unknown current distributions, superior performance as compared to TSVD.

Wednesday, March 20 10:40 - 12:20

IW12: Teleco Renta: An opportunity to conduct research in Spain

Adrián Amor Martín

Room: [M2](#)

Wednesday, March 20 10:40 - 12:20

IW5: From Planar Antennas to Multi-Beam Phased Array Systems, Celestia

Room: [M3](#)

10:40 *Planar Antennas and Electronic Steerable Antennas Applications*

Presenter: Manuel J. González; Alberto Pellón (CELESTIA TTI)

11:25 *Multi-Beam Phased Array Systems for SatCom Gateway Applications*

Presenters: Ed Totten; Daniel White; Colum Tucker (CELESTIA UK)

Wednesday, March 20 10:40 - 12:20

A08b: Leaky-wave antennas (continued)

T09 Fundamental research and emerging technologies // Antennas

Room: M4

Chairs: Jose-Luis Gómez-Tornero (Polytechnic University of Cartagena, Spain), Edoardo Negri (Sapienza University of Rome, Italy)

10:40 *Proactively Conformed Near-Field Focused Modulated Leaky-Wave Antennas*

Jose-Luis Gómez-Tornero (Polytechnic University of Cartagena, Spain)

The simultaneous use of conformation of a leaky-wave antenna (LWA) and local modulation of its leaky mode, is proposed for near-field focusing. Theoretical expressions are derived to obtain the local tapering of the complex propagation constant along the conformal shape, in order to focus the radiation at the desired coordinates. A design example with a curved tapered slitted leaky waveguide is illustrated to validate this theory, showing good agreement between theory and full-wave simulations. Finally, potential applications of curved near-field focused proactively conformed LWAs are discussed.

11:00 *High Efficiency Groove Gap Waveguide Leaky Wave Antenna Array with Flat Top Radiation Pattern*

Nelson Castro and Eva Rajo-Iglesias (University Carlos III of Madrid, Spain)

The combination of two leaky wave antennas implemented in Groove Gap Waveguide (GGWG) technology is proposed in this work as a simple way to obtain a flat-top radiation pattern. The design consists of two stacked GGWG leaky wave antennas with different pointing directions and full control on the amplitude distribution of the field to achieve low side-lobes and high radiation efficiency. GGWG technology allows the simple combination of the two antennas by stacking them and adding a coupler.

11:20 *Hybrid Metal-Graphene Unit Cells for THz Reconfigurable Leaky-Wave Antennas*

Edoardo Negri (Sapienza University of Rome, Italy); Walter Fuscaldo (Consiglio Nazionale delle Ricerche (CNR), Italy); Marco Toni, Paolo Burghignoli and Alessandro Galli (Sapienza University of Rome, Italy)

Graphene terahertz (THz) antennas are a subject of intense research due to the tunable properties of graphene that may allow for realizing dynamically steering planar antennas. Still, most of these studies remain at a theoretical level due to the very high ohmic losses exhibited by graphene at THz frequencies. In this work, we propose an original metasurface based on a hybrid metal-graphene unit cell that can profitably be used to realize a high-directivity reconfigurable Fabry-Perot cavity leaky-wave antenna. It is shown that by controlling the graphene filling factor of the unit cell it is possible to achieve a satisfactory trade-off between the range of reconfigurability and the antenna directivity. Preliminary results are obtained with a rigorous leaky-wave analysis and compared with full-wave simulations.

11:40 *Beam Steerable Half Mode Substrate Integrated Waveguide Based Composite Right/Left Handed Leaky-Wave Antenna Using Field Programmable Microwave Substrate*

Shahinshah Ali (Lakehead University, Canada)

This paper presents the design and experimental validation of a novel leaky wave antenna (LWA) incorporating field-programmable microwave substrate (FPMS) unit cells. Integrating cross-shaped slots on a Half-Mode Substrate Integrated Waveguide (HMSIW) the impedance of the propagating wave has been carefully modulated to achieve the desired antenna performance. The presence of FPMS unit cells on the antenna structure allows the control of the substrate properties that helps in steering the main antenna beam around broadside direction. The simulated results demonstrate 72 degree of steering with stable impedance response. The applicability of the design is also validated with the help of an actual prototype which provides decent radiation performance. The proposed antenna could prove to be a stepping-stone towards other smart antenna systems that rely on FPMS technology.

12:00 *Open Stopband Suppression of Periodic Leaky-Wave Antenna Based on Theory of Small Reflections*

Feiyu Ge and Shunli Li (Southeast University, China); Hongxin Zhao (State Key Laboratory of Millimeter Waves, Southeast University, China); Xiaoxing Yin (State Key Laboratory of Millimeter Waves, China)

A technology based on theory of small reflections for open stopband suppression in the periodic leaky-wave antennas (PLWA) is presented. The open stopband suppression is realized by the superposition and cancellation of multiple reflected waves generated by discontinuities of periodic structures. Through modifying the discontinuities, the phase and amplitude of each reflected wave could be modulated separately within a certain frequency band. Choosing the proper phase and amplitude of reflected waves, the total reflected wave could be reduced to a low level, even to zero, and then, the abnormally large reflection in the open stopband is suppressed. Two spoof surface plasmon polaritons (SSPP) based PLWA are developed to verify the technology. The results show that good VSWRs and radiation performances are achieved when the beam scans through broadside direction. This technology could have applications in the design of various types of PLWA, such as microstrip, waveguide, and SSPP PLWAs.

Wednesday, March 20 10:40 - 12:20

SW12b: Open Source Electromagnetic Modelling Tools (continued)

Room: Fyne

Chairs: Francesco Lisi (Heriot-Watt University, United Kingdom (Great Britain)), Timothy Pelham (University of Bristol, United Kingdom (Great Britain))

10:40 *"HERAS: Heriot-Watt Reflector Antenna Solver (Part 2) (www.github.com/Microwave-Antenna-Engineering-Group-HWU/HERAS)"*

Francesco Lisi (Heriot-Watt University, UK)

11:20 *LyceanEM (Documentation.lyceanem.com)*

Presenter: Timothy Pelham (Bristol University, UK)

Wednesday, March 20 13:10 - 14:40

PA4: Poster session on mm-wave and sub mm-wave Antennas I

T02 Mm-wave for terrestrial networks 5G/6G // Antennas

Room: Expo/Poster

Chairs: Daniel E. Serup (Aalborg University, Denmark), A. B. (Bart) Smolders (Eindhoven University of Technology, The Netherlands)

A Linear Wide-Angle Scanning Phased Array Antenna Using Heterogeneous Beam Element Technology 12

Yinglu Wan, Shaowei Liao, Yuqi Wang, Wenquan Che and Quan Xue (South China University of Technology, China)

Heterogeneous beam element (HBE) technology leverages the pattern shape of each element as a novel design degree of freedom (DoF) to enhance the scanning performance of phased array antennas (PAAs). Through strategic arrangements of HBEs, this technology effectively synthesizes a wide average active element pattern (AAEP), enabling wide-angle scanning. This study presents a novel HBE configuration that facilitates customized tilted element beams by controlling the current distribution on the radiating section. Based on the HBEs, the performance of a 4-element linear PAA is evaluated. Simulation results indicate that the 4-element linear HBE-based PAA (HBE PAA) can enhance the scan range from 60 to 70° within the 5G mmWave band (24.25-29.5 GHz, 19.5%) at the cost of a broadside gain loss of less than 1 dB compared to its standard counterpart using standard dipole elements.

A Fully Additive Manufactured D-Band SIW Antenna 1

Chao Gu (Queen's University Belfast, United Kingdom (Great Britain)); Zhiwei Zhang (China); Fan Qin (Xidian University, China); Fei Cheng (Sichuan University, China); Xiaobang Shang (National Physical Laboratory, United Kingdom (Great Britain)); Simon Cotton (Queen's University, Belfast, United Kingdom (Great Britain)); Jawad Ullah (Ulster University, United Kingdom (Great Britain)); Abraham Contreras (Nano Dimension, Germany)

This paper presents a D-band horn antenna designed using the substrate integrated waveguide (SIW) technique. The horn's flare can be adjusted by controlling the substrate thickness using an additive manufacturing process. To increase the antenna directivity, a dielectric loading and two-element stacking are employed. Additionally, the metal vias for conventional SIW can be replaced with solid metal walls to reduce leakage loss. The antenna has wideband impedance bandwidth over the full D band. Through simulation, we have achieved a gain higher than 7 dBi over the operating band. A SIW-to-waveguide transition is integrated in the single-layer design for ease of measurement. The fabricated antenna shows good dimensional accuracy with the smallest feature size of less than 0.2 mm. This study is the first demonstration that the additive manufacturing process can produce D-band integrated antennas for system-in-package (SiP) applications while providing end-fire radiation capabilities.

A Two-Port Metamaterial Antenna for mm-Wave 5G MIMO Applications with Enhanced Bandwidth and Gain 2

Hlias Tzouras (' University of Patras', Greece); Stavros Koulouridis (University of Patras, Greece)

A two-port wideband Multiple Input Multiple Output antenna with a metamaterial surface for mm-Wave 5G MIMO Applications is proposed. The MIMO antenna has a compact size of 10x 20x 0.78 mm³ and is realized using Rogers Duroid 5880 substrate. Each one of the radiation elements is composed of a square cut at the corners, patch antenna. In addition, three metasurface array structures of 8x2 metacells are used at the same level with the radiation elements and consequently the impedance bandwidth and the isolation are improved. The performance of the antenna is investigated in terms of MIMO parameters such as Envelope Correlation Coefficient and Diversity Gain. The proposed two-port metamaterial antenna achieves impedance bandwidth 3.37 GHz or 12.48%, an overall Peak Realized Gain of 10.02 dB and isolation between antenna elements bigger than 20 dB. Additionally, the calculated MIMO performance parameters confirms satisfactory behavior of the proposed antenna.

Prototype of Multi-Sector Indoor mmW Base Station Based on 5G NR Beam Control 19

Yuki Inoue (NTT DOCOMO, INC., Japan); Yasuko Kimura (NTT DoCoMo, Inc., Japan); Masashi Yamamoto and Keiya Uchida (NTT DOCOMO, INC., Japan); Hiroyuki Arai (Yokohama National University, Japan)

High-frequency radio waves such as millimeter waves and terahertz waves, which are used in the 5G and beyond, have a wide bandwidth enabling high-speed and high-capacity communications. Because of their strong linearity, there is a trend toward large-scale arraying of base stations. However, the increase in the size of the array antenna, calibration circuits, and circuit size, as well as the increase in power consumption, will be affected by the increase in the calculation load due to larger antennas and digitalization. This has become a challenge to widespread use of millimeter-wave band base stations. To address these issues, we developed a 5G multi-sector antenna indoor base station that efficiently delivers radio waves over a wide area with a small number of base station units. This paper introduces a multi-sector antenna indoor base station prototype based on 5G NR beam control and presents experimental results.

A Simple Technique to Maximize Isolation in Compact mmWaves Antenna Arrays 18

Amélia Ramos (Universidade de Aveiro, Instituto de Telecomunicações, Portugal); Tiago Varum and João Matos (Instituto de Telecomunicações, Universidade de Aveiro, Portugal)

The 5G Era is demanding better and more reliable communication systems. Microstrip antenna arrays operating in mmWaves play an important role in achieving the required performance, however they impose a great deal of design challenges. Besides, densely populated communication environments force those who design RF systems to miniaturize. The impact of reducing the distance between elements in microstrip antenna arrays is very noticeable in isolation. This work studies a method to maximize isolation in very compact antenna arrays. It consists of a direct 45° rotation of the radiating elements and the goal is to test whether it is possible to obtain similar isolation levels in very compact antenna arrays using this technique in comparison with the traditional patches' layout and 0.5λ interelement spacing. This strategy presents a good compromise since it did not damage the antenna's performance and it has improved isolation from 11.2 dB to 15.7 dB.

Detailed Design Procedure for Low-Cost High-Efficiency 3D Printed Transmitarray Antennas for mm-Wave Applications 4

Daniel E. Serup, Shuai Zhang and Gert Pedersen (Aalborg University, Denmark)

In this work, a measurement-validated mm-wave 3D-printed transmitarray antenna together with a detailed description of its design procedure will be presented. The purpose is to provide the reader with a comprehensive all-in-one guide for the transmitarray design process to allow for rapid deployment of cheap 3D-printed transmitarray antennas. The description will provide an example of a unit element and detail the mathematics required to calculate and realize a transmitarray transmission surface. Additionally, the paper will present a design example of an mm-wave 3D-printed transmitarray realization of the proposed antenna structure with accompanying measurement validation of its performance. The measurement shows extremely good agreement with the simulation and confirms the proposed design methods' ability to provide cheap and easily manufacturable 3D-printed transmitarray antennas, even for mm-wave frequencies.

3D Printed Horn Antennas for Millimeter Wave and Sub-THz Bands 25

Lauri Vähä-Savo and Iida Luoma (Aalto University, Finland); Clemens Icheln (Aalto University & School of Electrical Engineering, Finland); Katsuyuki Haneda (Aalto University, Finland)

3D printing has grown in popularity in many fields including antenna manufacturing. Fast and low-cost prototyping of lightweight product is desired for many electronic applications. This paper presents Ka- and D-band vertically polarized sectoral horn antennas, which are manufactured using 3D printing technologies. Dimensions of both antennas are based on reference metallic antennas. 3D printed antennas are compared against metallic antennas in terms of reflection coefficient, maximum realized gain and half-power beamwidth to show their efficacy. The 3D printed antennas at both bands reproduce the beam shapes of the respective metallic reference antenna while their maximum realized gain is on average 3 dB lower than the reference due to surface roughness and different feeding structures that affect matching.

A Novel GO Analysis Tool for GRIN Lenses Based on the Fast Sweeping Method 5

Illir Gashi (University of Siena, Italy); Anastasios Paraskevopoulos (NCSR Demokritos, Institute of Informatics & Telecommunications, Greece & University of Siena, Italy); Stefano Maci and Matteo Albani (University of Siena, Italy)

Additive manufacturing has facilitated the straightforward development and prototyping of Graded Index (GRIN) lenses. These lenses are constructed using inhomogeneous dielectric materials and leverage a refractive index gradient to manipulate the path of light within the lens. This technology allows for creating lenses with flat surfaces and a high level of design flexibility. The Fast Sweeping Method (FSM) is a numerical approach designed to efficiently address both wavefront propagation and field amplitude in GRIN lenses. The utility of the FSM is evaluated by establishing its accuracy and effectiveness, making it a viable alternative to traditional ray-tracing methods. Due to its robust performance, FSM emerges as a strong candidate for serving as the analytical engine in an optimization process for the automatic design of GRIN lenses.

5x7 Nolen Matrix in K-Band Implemented in Rectangular Waveguide 10

Miguel Angel Fuentes-Pascual (Universidad Politécnic de Valencia (UPV) & Antennas and Propagation Laboratory (APL), Spain); Mariano Baquero-Escudero (Universidad Politécnic de Valencia, Spain); Miguel Ferrando-Rocher (Universitat Politécnic de València & Antennas and Propagation Lab, Spain); Jose I Herranz-Herruzo (Universitat Politécnic de València & APL - iTEAM, Spain); Alejandro Valero-Nogueira (Universidad Politécnic de Valencia, Spain)

In this work, the design of a 5x7 Nolen Matrix (NM) at 26 GHz with a rectangular waveguide is presented. At first, the array weights are chosen in order to achieve the desired beams. Using these weights, and ordering them optimally, a theoretical calculation of the NM coupling coefficients and phase shifter values is done. The size of the rectangular waveguide is chosen with the goal of reducing loss and dispersion effects. Couplers and phase shifters are designed with such a rectangular waveguide in a plane-E orientation. Matching networks at the input and output waveguides are also designed to permit connecting the standard rectangular waveguide WR34 at inputs and to connect the outputs to the array elements. A full electromagnetic simulation of the designed MN has been carried out, with promising results.

Analysis and Design of Robust Reconfigurable Intelligent Surfaces Using a Statistical Approach 6

Luca Stefanini (Roma Tre University, Italy); Davide Ramaccia (Roma Tre University, Italy); Mirko Barbuto (Niccolò Cusano University, Italy); Mohsen Karamirad (Roma Tre University, Italy); Michela Longhi (Niccolò Cusano University, Italy); Alessio Monti (Roma Tre University, Italy); Stefano Vellucci (Niccolò Cusano University, Italy); Alessandro Toscano and Filiberto Bilotti (Roma Tre University, Italy)

Reconfigurable Intelligent Surfaces (RIS) and Smart Skins are well-established metasurface-based technologies for the wireless electromagnetic environments of the future. Despite the accurate modeling and fabrication techniques of such devices, their performances may be affected by unpredictable mutual coupling, fabrication defects, mechanical and thermal/mechanical stress that change the local response of the metasurface, realizing an electromagnetic roughness of the surface properties. In this contribution, we statistically model such electromagnetic roughness to predict the modifications to the local surface impedance. We derive a profile transformation function for the surface impedance that allows making the RIS more resilient to such unpredictable defects. A proper set of numerical simulations demonstrates the robustness of such design considering an anomalous reflective metasurface operating at 10 GHz.

Pixel Antenna Design for mm-Wave Wireless Communications to Achieve Wide Scanning 9

Gabriele Federico (Eindhoven University of Technology, The Netherlands); Diego Caratelli (The Antenna Company, The Netherlands); Pierre-Etienne Portaler (Xlim, France); A. B. (Bart) Smolders (Eindhoven University of Technology, The Netherlands); Bernard Jecko (XLIM, France)

In this paper, we illustrate the feasibility of achieving extensive scan capabilities through the integration of a pixel antenna into a radiating matrix, designed for millimeter-wave communications. The antenna element is a combination of a capacitively coupled patch antenna and a partially reflective surface, that operates in the frequency range between 27 GHz and 29 GHz. With the integration of a linear matrix, we can achieve a scan range from -74° to $+74^\circ$. In an 8×8 matrix, the scan range extends from -63° to $+63^\circ$ in the $\phi = 0^\circ$ -plane and from -57° to $+57^\circ$ in the $\phi = 90^\circ$ -plane, with only a 3 dB scan loss. The planar matrix is arranged in a triangular grid, which significantly reduces mutual coupling with adjacent elements when compared to the regular grid.

A Dual Linearly Polarized Array for 5G FR2 21

Marco Simone (University of Catania, Italy); Santi Concetto Pavone (Università degli Studi di Catania, Italy); Matteo Bruno Lodi (University of Cagliari, Italy); Nicola Curreli (Italian Institute of Technology, Italy); Giacomo Muntoni and Alessandro Fanti (University of Cagliari, Italy); Gino Sorbello (University of Catania, Italy); Giuseppe Mazzarella (University of Cagliari, Italy)

A dual linear polarized antenna array for the mm-wave 5G. The antenna element is a cross-dipole, suitable to obtain two orthogonal radiated fields, independently steerable in array arrangement. The design is conceived to allow its manufacturing in PCB technology, so that the main focus of the work is to simplify as much as possible the geometry and the constructive critical issues. The antenna conductors and the feeding network (engineered in coplanar waveguide technology) are realized in the same laminate, and a second board is applied onto to implement the balun. This upper dielectric layer acts as superstrate on the dipoles. The overall structure, which consists of two printed circuit board laminates and a low-loss resin layer that holds them together, is less than 2 mm thick. The antenna has a 7% bandwidth around 27.28 GHz, and a steering capability which covers a $\pm 30\%$ angular width for both the linear polarizations.

A Novel Precise Approach for Digital Metasurface Configuration for Sensing Application 14

AmirMasood Bagheri (5GIC & 6GIC, Institute for Communication Systems (ICS), University of Surrey, United Kingdom (Great Britain)); Seyed Ehsan Hosseininejad, Gabriele Gradoni and Pei Xiao (University of Surrey, United Kingdom (Great Britain)); Mohsen Khalily (University of Surrey & 5G Innovation Centre, Institute for Communication Systems (ICS), United Kingdom (Great Britain))

A novel mathematical approach is proposed for the placement of unit-cells at digital metasurfaces with applications in holography, imaging, coverage improvement and antenna array. As a proof of concept, the idea is applied to a simple unit-cell capable of providing 180 degrees of phase difference between two states of it. Used unit-cell is working at 90GHz although the idea can be used in any other frequencies. It has been shown that the proposed method is capable of providing better results compare to conventional techniques in terms of concentration of intensity and quality of produced field pattern.

RFID-Based Reconfigurable Intelligent Surfaces: Towards Wireless and Ultra-Low-Power Reconfigurability 17

Francesco Lestini and Gaetano Marrocco (University of Rome Tor Vergata, Italy); Cecilia Occhiuzzi (University of Roma Tor Vergata, Italy)

Reconfigurable Intelligent Surfaces (RISs) are innovative smart surfaces, composed by several tunable sub-wavelength scatterers, which provide the capability to control the wireless propagation environment. However, RIS widespread adoption faces obstacles such as high-power requirements for the driving hardware and the need for physical wires for reprogramming. In this study, we propose an architecture that leverages Radio Frequency Identification (RFID) antennas as wireless controllers for RIS unit cells. The rationale is that modern RFID Integrated Circuits (ICs) are programmable and can act as DC power sources using a coin battery. The proposed architecture could significantly reduce costs compared to traditional reprogramming hardware, eliminating the need for physical wiring. As a preliminary proof of concept, we developed a Yagi-Uda antenna with pattern reconfiguration capabilities. Our results demonstrated the feasibility of this approach, with a close match between simulations and measurements. Future research will explore the potential of battery-less ICs for this application.

Low-Cost 3-D Printed Lens Antenna for Ka-Band Connectivity Applications 11

Kamil Trzebiatowski and Weronika Kalista (Gdansk University of Technology, Poland); Mateusz Rzymowski (Gdansk University of Technology & WiComm Center of Excellence, Poland); Lukasz Kulas and Krzysztof Nyka (Gdansk University of Technology, Poland)

This paper discusses the use of low-cost 3-D printing technology to fabricate dielectric lenses for Ka-band wireless networks. A low-cost FDM alternative to previously presented 3-D printed lens in SLA technology with high performance resin is presented. The presented approach has been demonstrated for a 39 GHz MU-MIMO antenna array modified to realize multibeam or switched-beam antenna that can support demanding energy-efficient applications in millimeter waves. The impact of different 3-D printing settings on the lens performance is also investigated. The results demonstrate that with proper printing settings, low-cost 3-D printed lenses created using FDM process are a viable alternative for high-frequency applications.

Design of Wide Band Multi-Lens Focal Plane Arrays for the TIFUUN Instrument 3

Shahab Oddin Dabironezare (Delft University of Technology, The Netherlands); Alexandra Mavropoulou (European Space Agency, The Netherlands); Jochem Baselmans (SRON, The Netherlands); Akira Endo (Delft University of Technology, The Netherlands)

Terahertz Integral Field Unit with Universal Nanotechnology (TIFUUN) is a wideband spectral mapper operating at (sub)-millimeter wavelengths. The instrument is under development for ground-based astronomy and will be deployed to the ASTE telescope in Chile. In this work, the building blocks for TIFUUN's wideband (2:1) mappers are discussed. These components are based on multi-lens focal plane arrays of leaky lens antennas coupled to filter banks based on Microwave Kinetic Inductance Detectors. Two types of multi-lens architecture are proposed and designed here: i) an array of leaky antenna feeders below a hyper-hemispherical lens coupled to a plano-convex lens to achieve wide band operation with moderate scanning capabilities, and ii) focal plane arrays of leaky lens antennas coupled to a plano-convex lens to achieve wide scanning and moderate wide band operation. These architectures are optimized to enlarge their field-of-views and operation bandwidths using a rapid kernel based on a field matching technique.

Wideband Dual-Polarized Lens Antenna for Future mm-Wave Applications 23

Valentina Cicchetti (Queen Mary University of London, United Kingdom (Great Britain)); Yang Hao (Queen Mary University, United Kingdom (Great Britain))

A wideband dual-polarized lens antenna, useful for future millimeter wave applications, is presented in this paper. The proposed antenna consists of a rectangular waveguide, a rectangular-to-circular transition, a circular waveguide, a conical reflector, and a dielectric lens with a spherical-axicon section to enhance the performance of the radiating structure. The antenna operates in the frequency range of 190-300 GHz, providing a maximum gain of 9 dBi in the azimuthal plane. CST Studio Suite, employing a locally conformal full-wave finite integration technique (FIT), was utilized to design and characterize the antenna. The structure offers the advantages of robustness, cost-effectiveness, and ease of fabrication in waveguide configurations.

A Wideband 3D Printed Digital Metasurface Transmitarray Antenna for mm-Wave Applications 15

Gazali Bashir (IIT JAMMU & None, India); Amit Kumar Singh (IIT Patna, India); Ankit Dubey (Indian Institute of Technology Jammu, India)

A low cost dual polarized 3D printed digital metasurface transmitarray antenna for mm-wave applications is presented in this paper. The unit cell element is composed of a dielectric prorated elliptical cylinder with a square base. The height of the elliptical cylinder is varied to control the transmission phase of the incoming electromagnetic wave. Four quantized phase state (00, 01, 10 and 11) are obtained by varying the height of the unit cell. A $4.5\lambda_0 \times 4.5\lambda_0$ transmitarray is designed and illuminated by the wide-band 3d printed horn antenna. The measured results show a wide-band performance with a 3 dB gain bandwidth of 33 %. A measured peak gain of 20 dBi is obtained at 30 GHz corresponding to an aperture efficiency of 38%

A Compact High-Gain 28 GHz Antenna Array for Beyond 5G Wireless Networks 24

Ieuan Meates (Aberystwyth University, United Kingdom (Great Britain)); Shaker Alkaraki (University of Nottingham, United Kingdom (Great Britain)); Muhammad Aslam (Aberystwyth University, United Kingdom (Great Britain)); Qammer H Abbasi (University of Glasgow, United Kingdom (Great Britain)); David Andrew Evans and Syeda Fizzah Jilani (Aberystwyth University, United Kingdom (Great Britain))

In this paper a novel, high-gain corporate-fed 16-element circular patch array featuring a coplanar waveguide (CPW) feed and parasitic loop is proposed for beyond 5G and future 6G applications. An ultra-thin Rogers RO4003C substrate of 0.02 mm thickness is used, and the overall size of the antenna is 31.09 × 41.45 mm. The proposed antenna operates at 28 GHz and achieves a bandwidth of 220 MHz between 27.84 GHz and 28.12 GHz, with a maximum realized gain of 16.85 dBi at 28.05 GHz. The antenna prototype was fabricated using an HPC Laser Cutter (LSE110 Fibre Engraver model). The proposed antenna array is well-fitted for high-gain line-of-sight communication links at the 28GHz band.

A Comparative Study of Decoupling Techniques for Waveguide Slot Array Antennas 7

Mu Fang (Chalmers University of Technology & Chalmers, Sweden); Jian Yang and Ashraf Uz Zaman (Chalmers University of Technology, Sweden)

In this paper, we present a comparative study of three decoupling techniques for waveguide slot array antennas, including half wall, corrugation and fence. Their decoupling efficacy and impact on element patterns are investigated under two typical element spacings: 0.5 λ_0 and 1 λ_0 . A summary highlighting the differences among these decoupling techniques is provided to gain insight into which specific application scenarios are best suited for each technique.

Terahertz Microstrip Leaky-Wave Antenna for WR1.0 Band 16

Thomas Haddad and Rihab Hamad (University of Duisburg-Essen, Germany); Hacer Kaya (Löwenstein Medical SE Co. KG, Germany); Mohamed Damerji and Andreas Stöhr (University of Duisburg-Essen, Germany)

This paper presents the first THz periodic microstrip Leaky-wave antenna (LWA) with a suppressed open stopband for WR1.0 band between 0.75 and 1.1 THz for future communication applications. The designed 20-unit cell LWA on 20 μm InP substrate has been simulated in CST. The return loss is better than 17 dB, and the insertion loss is higher than 20 dB for the whole domain. Furthermore, the LWA has a maximum total efficiency of 76.12% at 0.77 THz. In addition, the beam steering capabilities show a scanning range of 92° in the WR1.0 band when sweeping the frequency from 0.75 THz (-35°) to 1.1 THz (57°). On the other hand, the realized gain varies between 12.6 and 14.1 dBi at 0.75 and 1.0 THz, respectively. Finally, the paper discusses a concept to enable the fabrication of very thin InP substrate and a technique to facilitate the characterization on wide InP substrate.

Effect of Phase Errors on Performance of Ka-Band Reflectarray with DRA Unit Cells 13

Irina Munina (Trinity College Dublin, Ireland); Igor Grigoriev (St. Petersburg Electrotechnical University LETI, Russia); Garret O Donnell (Trinity College Dublin, Ireland)

This paper focuses on investigating the impact of phase errors in 1-bit unit cells on the directional properties of a reflectarray antenna. The simulations were conducted for reflectarray antennas using unit cells with varying numbers of phase states, specifically focusing on 1-bit unit cells with two-phase states. Each unit cell comprises an aperture-coupled dielectric resonator antenna with a pin-diode serving as the switching element. The performance of these unit cells was examined under different incident angles of electromagnetic waves. It was observed that when the unit cell operates at incidence angles exceeding 45°, significant phase errors occur, resulting in elevated side lobe levels in the reflectarray antenna. To mitigate this issue, phase error compensation was explored to reduce the side lobe levels of the reflectarray antenna.

A Wideband Aperture-Shared Dual-Polarized End-Fire Antenna with Low Profile and High Isolation 8

Liangying Li, Shaowei Liao, Yinglu Wan, Wenquan Che and Quan Xue (South China University of Technology, China)

This paper proposes a new wideband aperture-shared dual-polarized end-fire antenna for millimeter-wave (mmWave) applications. Firstly, a reshaped quasi-PIFA element with L-probe feeding is adopted to produce end-fire single vertical polarization (VP) radiation. A pair of dual-layer patches are then loaded in front of the quasi-PIFA element, which serve as both resonator and director towards simultaneous impedance bandwidth and gain improvement. U-slot is further introduced to the quasi-PIFA element to broaden the impedance bandwidth. This results in a low profile, wideband and high gain VP end-fire element. Secondly, based on the single VP end-fire antenna element, by using the two VP elements' dual-layer patches as the two arms of a dipole with horizontal polarization (HP), a dual-polarized element can be realized. The dual-layer patches function as both the resonator/director of VP and the radiator of HP, leading to a compact dual-polarized design with good performances.

Design and Investigation of 2x2 Dielectric Resonator Antennas Array for Sub-THz Applications 22

Muhammad Faisal Bashir (IHP - Leibniz-Institut Fuer Innovative Mikroelektronik, Germany); Matthias Wietstruck (IHP, Germany)

A 2x2 dielectric resonator antennas (DRAs) array consisting of four high-resistivity silicon rectangular radiating structures, is designed. The radiating structures are placed upon a low-resistivity silicon block. All four antennas are aperture-coupled fed by four microstrip (MS) feedlines, with a ground reflector between the MS feedlines and the antennas. The antenna elements of the array have S11 <-10 dB from 220 GHz to 260 GHz and the realized gain at 240 GHz is 11.1 dB. Overall, the realized gain of the array is above 10.5 dB from 235GHz to 245 GHz.

Beam-Steerable Microstrip-Line Based Leaky Wave Antenna with Reconfigurable Slits 20

Yujiro Kushiya (National Institute of Information and Communications Technology, Japan)

In this study, we propose a leaky wave antenna capable of forming beams through radiation from slits on a microstrip line, with the beam direction adjustable based on the pattern of the slits. The pattern of the slits can be changed by the opening and closing of switches loaded onto the slits, and the patterns are determined from the desired beam angle. Based on this proposed structure, we designed an antenna with 16 slits operating at 28 GHz. The initial design exhibits large reflection coefficients when forming beams in the 0° direction. In order to reduce the reflection, we added matching slots in the microstrip line and adjusted the slot length to suppress the reflection. The final antenna shows the beam scanning capability from -30° to +30° by setting the radiation phase of the slits.

Amplitude-Tapered Half-Mode Gap Waveguide Distribution Network for Flat Panel Antennas 29

Adrián Castellá-Montoro (INSA Rennes, France); Miguel Ferrando-Rocher (Universitat Politècnica de València & Antennas and Propagation Lab, Spain); Jose I Herranz-Herruzo (Universitat Politècnica de València & APL - ITEAM, Spain); Alejandro Valero-Nogueira (Universitat Politècnica de Valencia, Spain)

This communication centers around the design and evaluation of a feeding network for a slot array antenna utilizing Gap Waveguide (GW) technology. The core innovation lies in the integration of a single-layer amplitude-tapering network within a Half-Mode Groove Gap Waveguide (HM-GGW), resulting in a compact, low-sidelobe feeding network. This design holds great promise for applications requiring high gain and minimal interference. Simulated results reveal a reduction in sidelobe levels compared to uniform arrays. What sets this approach apart is its cost-effective, additive manufacturing potential, which simplifies fabrication and enhances practicality. The work underscores the significance of this technology in modern wireless communication systems, particularly in the millimeter-wave band, and highlights the potential for mass production.

PA6: Poster session on Metamaterials and metasurface antennas and systems

T10 Novel materials, metamaterials, metasurfaces and manufacturing processes // Antennas

Room: Expo/Poster

Chairs: Bo Liu (University of Glasgow, United Kingdom (Great Britain)), Oskar Zetterstrom (KTH Royal Institute of Technology, Sweden)

Orthogonal Coding for Millimeter-Wave Imaging Using MIMO Dynamic Metasurface Apertures 30

[Vasiliki Skourliakou](#), Amir Masoud Molaei, María García Fernández, Guillermo Alvarez Narciandi and Okan Yurduseven (Queen's University Belfast, United Kingdom (Great Britain))

The recent advent of dynamic metasurface antennas (DMAs) as a millimeter-wave computational imaging (CI) platform has mitigated the hardware limitations of traditional imaging systems in terms of acquisition time, flexibility and cost. Considering a multiple-input multiple-output (MIMO) system fully realized by DMA panels, real-time simultaneous data acquisition can occur by adopting an orthogonal coded approach which enables concurrent transmission and reception by all DMA panels. The image is then reconstructed in the frequency domain by utilizing a signal decompression step that enables the use of a range migration algorithm (RMA) for the compressed signal received by the DMA panels. In that way, the time for the signal processing layer is also significantly reduced compared to the traditional image reconstruction methods usually applied to DMA-based systems. Simulation results of resolution targets are presented to demonstrate the efficiency of the suggested technique.

An Eigenvector-Supported Optimization Method for Holographic-Based Leaky Wave Antennas 28

Thomas Frey (University Ulm - Institute of Microwave Engineering, Germany); Maximilian Döring and Christian Waldschmidt (University of Ulm, Germany); Tobias Chaloun (Hensoldt Sensors GmbH, Germany & University of Ulm, Institute of Microwave Engineering, Germany)

A novel eigenvector-supported optimization method for holographic-based leaky wave antennas is presented. To assign the analytical impedance tensor hologram onto a pixel geometry, a 3D-eigenmode tensor database is utilized. The optimization process calculates the pixel orientation angles of the analytical tensor and the assigned eigenmode impedance tensor based on their respective eigenvectors for each unit cell. If a pixel angle deviation is observed, the correction algorithm is applied to minimize the error between the analytical tensor and the eigenmode tensor. This results in an optimized impedance tensor hologram and a more accurate realization of the anisotropy degree through the corresponding pixel geometry parameters. Employing the eigenvector-based optimization approach, a holographic-based leaky wave antenna is fabricated on a fused silica wafer for an operational frequency of 160GHz. The far field measurements show a gain of 33.2dBi, leading to an aperture efficiency of 34.6% and a side-lobe level of -29dB at 160GHz.

Dual-Polarization Multi-Functional Metasurface for Wireless Communications 38

Guangwei Yang (Northwestern Polytechnical University, China); Juan A. Vázquez Peralvo (University of Luxembourg, Luxembourg); Lei Wang (Heriot-Watt University, United Kingdom (Great Britain)); Symeon Chatzinotas (University of Luxembourg, Luxembourg)

In this paper, a reconfigurable multi-functional metasurface with dual-polarization is presented for operating reflective wave independently. In this design, a simple structure is applied to realize multi-function characteristics, where is composed of the cross patch printed on the thin substrate, four pin diodes and the controlling devices. To show the design performance, the metasurface is simulated to verify the application, which can achieve dual-polarization beam steering, linear polarization (LP) converting to right-hand circular polarization (RHCP) and left-hand circular polarization (LHCP), respectively. Therefore, the proposed design can be the candidate of the terminal device for future wireless communication due to its multi-functionality and reconfigurability.

A High Gain Spoof Surface Plasmon Polaritons (SSPPs) Antenna Based on a Metamaterial-Inspired Substrate Integrated Waveguide 37

Yibo Ning and Zhirun Hu (University of Manchester, United Kingdom (Great Britain))

This article presents a high gain broadside radiation antenna based on spoof surface plasmon polaritons (SSPPs). It is designed on the metamaterial-inspired substrate integrated waveguide (SIW) with two rows broadside-coupled complementary split ring resonators (BC-CSRs). The overall dimension of the SSPPs antenna is $1.15\lambda \times 0.61\lambda \times 0.04\lambda$. The gain is more than 9.19 dBi and achieve 11 dBi at 23 GHz. The proposed SSPPs antenna has the merits of high gain, low cost and easy fabrication. Such antennas will be highly desirable in millimetre-wave applications.

A Pattern-Reconfigurable Water Antenna Based on the Fabry-Perot Cavity 33

Fan Qin, Yifei Liu and Xuan Zhang (Xidian University, China); Chao Gu (Queen's University Belfast, United Kingdom (Great Britain))

In this paper, a distilled water antenna with pattern-reconfigurable characteristics based on the Fabry-Perot cavity (FPC) is presented. The proposed antenna consists of a water source antenna, a two-layer water partially reflective surface (WPRS) and a water ground plane (WGP). An FPC is constructed between WPRS and WGP to increase antenna directivity. Periodic air lattices are embedded in the top layer of WPRS to adjust the reflection coefficient of WPRS. By injecting distilled water into different WPRS layers, three working states of wide-beam, pencil-beam and bi-directional pencil-beam are obtained. The simulations verify the design, showing that the pattern reconfiguration is achieved successfully. The peak gain reaches 10.66 dBi. The proposed method has unique features of flexible pattern reconfiguration, high-gain, low-cost and optically transparent.

Experimental Results for Carbon Nanotube-Sheet Based Microstrip Patch Antenna 35

Aakash Bansal and Thomas Whittaker (Loughborough University, United Kingdom (Great Britain)); Peter Hansen (Hive Composites Ltd, United Kingdom (Great Britain)); William Whittow (Loughborough University, United Kingdom (Great Britain))

The paper presents the potential of carbon nanotube-sheet (CNS) for microstrip antennas. A 20 μm CNS was measured for conductivity using a single post dielectric resonator (SIPDR), and then a microstrip patch was fabricated on a Rogers RT5880 substrate. The measured results of the patch antenna showed good agreement with the simulated version using the CNS measured conductivity. Results were also compared to the simulated PEC version for comparison.

Metasurface-Based Bessel-Beam Launcher with 100 λ Non-Diffractive Range 29

[Konstantinos D. Paschaloudis](#) (Université de Rennes, CNRS, IETR, France); Ravel C. M. Pimenta (Aix-Marseille Université, France); David González-Ovejero (Centre National de La Recherche Scientifique - CNRS, France); Gabriel Soriano (Aix-Marseille University, France); Mauro Ettorre (University of Rennes 1 & UMR CNRS 6164, France)

This work presents the design of a metasurface-based Bessel beam launcher in Ka-band. The launcher uses a modulated metasurface to generate the non-diffractive beam in its near-field. The key advantage of the proposed structure is the large non-diffractive range. The radial size of launcher rises up to 8.75 λ , while the axicon angle decreases to $\theta\alpha = 5^\circ$ to achieve the high non-diffractive range. Full-wave numerical results validate the operation of the systems.

Anisotropic Circularly Polarising Graded Index Lenses Enabling High Gain CP Antennas 27

Thomas Whittaker (Loughborough University, United Kingdom (Great Britain)); Evangelos Vassos and Alexandros Feresidis (University of Birmingham, United Kingdom (Great Britain)); William Whittow (Loughborough University, United Kingdom (Great Britain))

This paper presents the theory and design of a circularly polarising lens utilising anisotropic metamaterials. This design combines the functionality of a lens and a polarisation converter into a single device which cuts down on cost, size, weight and material losses. Theory of the design is presented along with a simulated demonstrator. Anisotropic metamaterials are utilised to create a 90° phase shift between orthogonal wave components to generate circular polarisation. The lens can be fed with a wide range on antenna sources angled at a 45° offset. An example lens was designed in the K-band (18 - 30 GHz) and was capable of achieving high directivity values, between 22.8 dBi and 23.3 dBi, with a wide circular polarisation bandwidth of 9.8 GHz.

Study of the Frequency Dispersion of 3D-Printed Dielectric Crystals for Dielectric Resonator Antenna Applications 32

Gaëtan Antoine (ISAE-SUPAERO, France); Romain Pascaud (ISAE-SUPAERO, Université de Toulouse, France); Christophe Morlaas and Alexandre Chabory (ENAC, France); Vincent Laquerbe (CNES, France); Gautier Mazingue (Anywaves, France)

In this paper, the study of simple cubic (SC) and face-centered cubic (FCC) crystals, in addition to the use of the plane wave expansion method allows us to understand the dispersive behavior of electrically-large unit cells. From numerical analyzes, we demonstrate that we can take this dispersive behavior into account for the design of a dielectric resonator antenna (DRA) made up of electrically-large 3D-printed SC unit cells.

Generation of Narrow Divergence Angle OAM Beams for mmWave Communication Links Using Metasurface 26

Mustafa Khalid Taher Al-Nuaimi (Loughborough University, United Kingdom (Great Britain) & Wireless Communications Research Group, United Kingdom (Great Britain)); William Whittow (Loughborough University, United Kingdom (Great Britain)); Guan-Long Huang and Rui-Sen Chen (Foshan University, China)

This paper presents an efficient and fast strategy to generate single and multiple non-diffractive narrow divergence angle orbital angular momentum (OAM) beams for the 80 to 100 GHz millimeter wave band using a single circularly polarized (CP) feed and single layer reflectarray metasurface (RAMS). Then to generate four OAM beams, a 1-bit binary coding sequence with 10101010 based on the chessboard configuration was added to achieve the phase distribution required for generation of four OAM beams each with small divergence angle. To demonstrate the feasibility of the proposed strategy, single and multiple OAM beams RAMS were designed and fabricated. Both simulation and measured results demonstrated that the proposed strategy is efficient and can reduce the divergence angle of conventional OAM beams from 32° to 7°. In addition, the OAM beam gain improved by 4 ~ 8 dB with mode purity greater than 91%.

User and Passive Beam Scheduling Scheme for Liquid Crystal IRS-Assisted mmWave Communications 31

Keiji Yoshikawa, Takuya Ohto and Takahiro Hayashi (KDDI Research, Inc., Japan)

Intelligent reflecting surfaces (IRS) have been considered a strong solution for coverage holes in millimeter wave communication. We focus on liquid crystal (LC) IRS, which has low power consumption. However, it has a longer response time to change the reflection direction than the symbol length in new radio (NR). Generally, user scheduling at an NR BS is performed on a time-division basis, assuming instantaneous beam switching. However, during the response time of the LC IRS, the radio waves are not reflected in the desired direction, resulting in a decrease in throughput. This paper proposes a user selection and reflection direction control method to improve the throughput reduction in an environment with an LC IRS. The proposed method formulates the problem to optimize the reflection pattern and switching timing, considering the loss due to switching. Simulation evaluations demonstrate the improvement in throughput in an environment with an LC IRS.

An Efficient Wireless Power Transfer System Using Transmission and Reflection Characteristics of Metamaterial 34

Tarakeswar Shaw (Postdoctoral Researcher, Uppsala University, Sweden); Pratim Dasmahapatra (University of Minnesota, Twin Cities, India); Bappaditya Mandal (Uppsala University, Uppsala, Sweden); Debasis Mitra (Indian Institute of Engineering Science & Technology, Shibpur, India); Robin Augustine (Uppsala University, Sweden)

In a study to improve Wireless Power Transfer (WPT) system efficiency, metamaterials (MTMs) were used for their transmission and reflection attributes. The design minimizes losses from scattered beams away from the transmitter (Tx), boosting efficiency. A 1x5 MTM grid array directs scattering from the Tx towards the Receiver (Rx). A 4x4 MTM slab boosts coupling between Tx and Rx. Operating in the 2.45 GHz industrial, scientific, and medical (ISM) bands, comparisons were made with and without metamaterials. Results show a 23% efficiency increase at 75 mm when using MTMs, indicating a notable efficiency advancement with this MTM-based approach.

On-Chip mm-Wave Artificial Magnetic Conductor Backed Dipole Antenna on Low-Ohmic Substrate 36

Armen Harutyunyan (Barkhausen Institut, Germany); Padmanava Sen (Research Group Leader, Barkhausen Institut gGmbH, Germany)

The paper presents an on-chip mm-wave dipole antenna working at 61 GHz. It utilizes artificial magnetic conductor (AMC) surface to boost the gain and efficiency. It is designed for the integration on low-ohmic substrate in 22-nm FDSOI process. In order to create a fabrication tolerant AMC surface, an enhanced Jerusalem cross (JC) structure is used as a unit cell. AMC unit cell design procedure is analyzed for the low-ohmic substrate. The procedure is later used to optimize the antenna design. Deploying a 8 by 3 AMC array, 0.5 dBi antenna gain and 42% efficiency have been achieved on high conductivity substrate. Considering the importance of ground plane in on-chip antenna design, its impact on the antenna performance is also discussed. To the best of authors' knowledge, such a structure is proposed for the first time in an on-chip antenna.

Wednesday, March 20 13:10 - 14:40

PA8: Poster session on Antenna systems

T05 Positioning, localization, identification & tracking // Antennas

Room: Expo/Poster

Chairs: Luigi Boccia (University of Calabria, Italy), Simona Bruni (IMST GmbH, Germany)

Design and Measurement of a 2x2 Array of Coaxial Periodic Leaky-Wave Antennas 50

Syed Osama Kamal and Lai Bun Lok (University College London, United Kingdom (Great Britain))

A 2x2 array of coaxial periodic leaky-wave antennas at X-band has been designed, fabricated and measured. It achieved a gain of more than 10 dBi at 9.8 GHz, input return loss better than 10 dB from 8 GHz to 12 GHz (other than the broadside frequency) and a 3 dB beamwidth of 9 degrees. The sidelobe level is better than 10 dB from 8 GHz to 10.5 GHz. The antenna also achieved a reduced open stopband attenuation at 9.8 GHz. A beam scanning range of 35 degrees from backward to forward direction over a 4 GHz span was measured. Good agreement between the simulated and measured results was obtained.

Dual-Polarized Substrate Integrated Waveguide Antenna with High Isolation for Polarimetric Radar 56

Iram Shahzadi (The University of Edinburgh, United Kingdom (Great Britain)); Alexander Thorburn Don, Jr., Maksim Kuznetsov and Symon K. Podilchak (University of Edinburgh, United Kingdom (Great Britain))

Polarimetric radar systems use dual-polarized antennas to send and receive orthogonally polarized signals, and this can enable detection of target characteristics. This not only enhances the reliability of the radar, but improves the ability to differentiate objects, like vehicles, humans, and stationary items, in particular, by analyzing the polarization responses. In the context of a millimeter-wave frequency-modulated continuous wave (FMCW) radar system, a novel dual-polarized antenna concept which is suitable for both single-input single-output (SISO) and single-input multiple-output (SIMO) setups is demonstrated. This designed antenna, which is a single-layer structure using substrate integrated waveguide (SIW) technology, consists of a network of two-dimensional sub-arrays arranged in a crossshaped configuration and the design is extended to an array for angular target tracking. Moreover, the measured FMCW radar system successfully estimated the target parameters, including range and angular position.

Flexible Antenna with Microfluidics for the Quantification of Liquid Micro-Volumes 39

Giulio M. Bianco (University of Roma Tor Vergata, Italy); Gaetano Marrocco (University of Rome Tor Vergata, Italy)

Microfluidics has been a significant technology for over a decade, particularly in medical and wearable devices. It allows for the manipulation of small amounts of fluid in a confined space and can synergize with auto-tuning microchips that are able to modify their internal capacitance to maximize power delivery to the antenna. Hence, the first prototype of an auto-tuning RFID sensor exploiting a microfluidic channel is designed, manufactured, and tested in this contribution. A small liquid volume of 1050 μL is successfully monitored by the auto-tuning sensor in a continuous way when using 155- μm - and 775- μm -thick microfluidic. The investigated technology could be used to monitor sweating in pathological conditions according to the point-of-care paradigm or estimate food degradation through smart packaging.

An IQ Modulator-Based RF Phase Shifter 40

Xu Qin (University of Aerospace Technology, Guilin, China); Zhiwei Zhang (Hangzhou Dianzi University Hangzhou, China); Chao Gu and Adrian D McKernan (Queen's University Belfast, United Kingdom (Great Britain))

This paper presents a design of a radio frequency phase shifter based on an IQ modulator. In contrast to traditional phase shifter architectures, this design employs an off-the-shelf quadrature modulator featuring a wide operating frequency range and attractive power consumption to achieve phase-shifting functionality. The performance of the proposed approach is validated through a case study involving Analog Devices'

AD8349 chip, and the measured results show a full 360° phase tuning range. The findings indicate that despite inherent performance deviations in IQ modulator IC for phase shifter design, these discrepancies can be effectively mitigated through calibration algorithms, facilitating precise phase control. This design offers advantages such as low cost, compact size, and broad operational bandwidth, making it suitable for applications like smart antennas.

Low-Profile Electrically Small Antenna with Pattern and Polarization Diversity 43

Abel Abdul Zandamela and Nicola Marchetti (Trinity College Dublin, Ireland); Adam Narbudowicz (Trinity College Dublin, Ireland & Wroclaw University of Science and Technology, Poland)

A low-profile electrically small antenna capable of pattern and polarization diversity is presented in this paper. The cavity model analysis is used to describe the antenna design concept, where a step-by-step surface current distribution-based approach is applied to discuss the antenna diversity characteristics. Rectangular and V-like shaped slits are used for isolation enhancement and antenna miniaturization, respectively. It is demonstrated that the antenna can generate multiple patterns to enable good coverage across the elevation plane, with linear and circularly polarized patterns. In contrast, an omnidirectional pattern is produced with horizontal polarization. The design is planar and operates at 3.75 GHz, with 0.35λ diameter and 0.016λ profile. The -10 dB impedance bandwidth covers 20MHz, and the peak realized gain is 2.94 dBi

Bandwidth-Enhanced Compact Beamsteering Antenna for IoT Platforms 42

Abel Abdul Zandamela and Nicola Marchetti (Trinity College Dublin, Ireland); Adam Narbudowicz (Trinity College Dublin, Ireland & Wroclaw University of Science and Technology, Poland)

A technique to enhance the bandwidth characteristics of spherical modes-based beamsteering antennas is investigated in this work. The solution comprises a top-loaded monopole, a shorted ring antenna, and a metasurface layer used for bandwidth enhancement. It is demonstrated that the proposed antenna solution can scan continuously across the entire azimuthal plane. The antenna operates at the centre frequency of 4.42 GHz, where the size with respect to wavelength is $0.73\lambda \times 0.73\lambda \times 0.18\lambda$. The overlapping -10 dB impedance bandwidth covers 265 MHz, where the total efficiency stays above 77%. Owing to its compact size, low profile, and enhanced bandwidth performance, the design is proposed as a good candidate to enable advanced modern wireless applications in small-scale Internet of Things (IoT) platforms.

Compact Size Frequency-Agile Antenna Enabling Multi-Mode Functionality for Internet of Things Applications 45

Wahaj Abbas Awan (Chungbuk National University, Korea (South)); Qasid Hussain (Chungbuk National University, South Korea, Korea (South)); Anees Abbas and Md. Abu Sufian (Chungbuk National University, Korea (South)); Niamat Hussain (Sejong University, Korea (South)); Sangmin Lee (Korea National University of Transportation, Korea (South)); Nam Kim (Chungbuk National University, Korea (South))

To meet the multiband operation by Internet of Things (IoT) applications, a compact size antenna is presented in this manuscript. The antenna is capable of reconfiguring its operational frequency by switching the state of diode along with multimode operation among broadband, dual band and tri-band. The compactness is achieved using serpentine shape stubs without compromising the overall performance of antenna in terms of gain and bandwidth. The results show that the proposed work is capable of working for frequencies of 4-7 GHz, 3.5 GHz, 2.6 GHz, 2.45 GHz, 2.1 GHz, and 1.8 GHz that correspond to C-band, 5G-ub-6-GHz, Wi-Max, ISM-band and LTE applications. The analysis of antenna performance involves evaluating its impedance bandwidth, gain, and radiation pattern, and a comparison is carried out with cutting-edge antennas to demonstrate the potential of the proposed research.

Sidelobe Suppression and Bandwidth Enhancement of Series-Fed Patch Antenna Arrays Using Coplanar Ground Conductor 41

Thipamas Phakaew (King Mongkuts University of Technology North Bangkok, Thailand); Suramate Chalermwisutkui (King Mongkut's University of Technology North Bangkok & The Sirindhorn International Thai-German Graduate School of Engineering, Thailand)

Sidelobe suppression and bandwidth enhancement technique for a series-fed 1x4 microstrip patch antenna array is proposed. The array designed with the proposed technique is a modification of a series-fed antenna array comprising four microstrip patch elements connected together via a single straight transmission line fed by a grounded coplanar waveguide port. Sidelobe suppression was achieved with amplitude tapering and by surrounding the radiating elements with a coplanar ground conductor. The proposed antenna offers a wide impedance bandwidth from 9.25 GHz to 9.81GHz, a gain of 13.79 dBi, a sidelobe level of 21.80 dB and a half power beam width of 20.39° at the center frequency of 9.55 GHz. The proposed technique provides a good solution for applications requiring a wideband series-fed antenna array with a low sidelobe level.

Whip Antenna Miniaturization at VHF Band Using Magneto-Dielectric Materials 48

Lotfi Batel (CEA-Leti, France); Jean-François Pintos and Christophe Delaveaud (CEA-LETI, France)

This article presents a strategy of miniaturization for electrically small wire antennas using Magneto Dielectric Material. The loading strategy is studied in order to strengthen the interaction of antenna's radiation fields with the properties of the material. Typically, with this particular technique, the electrical size of a Whip antenna are significantly reduced (factor 5.6) in the VHF frequency band to reach a $\lambda_{0/22}$ height

Octagonal Patch Tag Antenna and 3 × 3 Array Locator for DoA Applications 52

Ottavio Crisafulli (Università Mediterranea di Reggio Calabria, Italy); Davide Guarnera (University of Reggio Calabria Mediterranea, Italy); Giuseppe Giammello (University of Catania, Italy); Andrea Francesco Morabito (University Mediterranea of Reggio Calabria, Italy); Santi Concetto Pavone (Università degli Studi di Catania, Italy); Loreto Di Donato and Gino Sorbello (University of Catania, Italy)

In this paper, a new circular polarized microstrip antenna with an octagonal patch for Bluetooth Low Energy (BLE) application is presented. In the antenna configuration, a two-layer stack-up between the patch and ground plane has been exploited to simplify the routing of the grounded coplanar waveguides (GCW) on the back of the antenna. This configuration ensures minimal crosstalk in the 3 × 3 array arrangement. A circular via fence has been used to emulate the behavior of a coaxial cable, effectively mitigating the inductive effects of the probe. The comparison between measurements and simulations has been performed with good agreement between measured and simulated radiation patterns.

Development of Passive Chipless RFID Temperature Sensor 53

Hafsa Anam, Syed Muzahir Abbas, Iain B. Collings and Subhas Mukhopadhyay (Macquarie University, Australia)

This research presents a low-cost solution towards passive identification and sensing of temperature for multi-applications being vital enablers to sense remote parameters in pervasive artificial intelligent networks. The paper provides a glimpse of temperature sensitive tags with varying parameters, number of bits and layout. Two different techniques are encountered for temperature sensing outcomes, later their behavior towards varying temperature is analyzed. In first technique, a stanyl Polyamide is used as temperature sensitive material; filled in between unique identifier bit slots in CRFID tag. Whereas temperature dependent substrate is used in the second technique for three different bit combination tags. Multi-bit tag yielding 2-bits, 4-bits and 10-bits response are analyzed for tagging and temperature sensing. Sensor tag can be deployed for solo applications as well as multi-parametric analysis. Ultimately, robust, printable, low-cost flexible tags are suitable for irregular surfaces for temperature sensing and tracking of goods for long-term RF sensing applications.

Towards Array and Curve Analysis: Flexible Passive Chipless RFID Tags 54

Hafsa Anam, Syed Muzahir Abbas and Subhas Mukhopadhyay (Macquarie University, Australia)

This research is intended to characterize the performance of chipless RFID tags for curved surface utilizing array-based structures. It covers design of tag, simulation results of proposed array tag, fabrication, and experimental results of bent/curved chipless RFID tags. Semi octagonal shape passive chipless RFID tags have been fabricated using polyethylene terephthalate (PET) substrate with silver nano particle-based ink as top layer both as single unit tag having 10-bit data and 5 × 5 array-based structures. Extensive simulation and experimental results detail out the response of array based chipless RFID tag along with bending effects. Complete analysis and study of folding effects provides an alteration in radar cross section (RCS) of chip-free tag along with variation in bending radius of the tag. A bend radius of (100mm to 3mm) for material under test (MUT) is analyzed. The original single unit tag has dimensions of (13mm x 7mm), whereas 5 × 5....

A Near-Field Focusing Circularly Polarized Radial Line Slot Array Antenna 46

Liyuan Zhong and Shufeng Zheng (Xidian University, China); Qi Luo (University of Herfordshire, United Kingdom (Great Britain)); Chao Gu (Queen's University Belfast, United Kingdom (Great Britain)); Hangqi Yang (Xidian University, China); Yanxiang Yi (Nanjing Electronic Devices Institute, China)

This paper presents the implementation of a near-field focusing (NFF) antenna on basis of radial line slot array (RLSA). The proposed NFF-RLSA antenna is derived from the conventional single-layer spiral-patterned RLSA with circular polarizations, and near-field focused radiation characteristics is realized by adjusting the arrangements of radiating slot pairs and hence the amplitude and phase distribution of RLSA aperture. The

designed NFF-RLSA antenna is 14.4 λ_0 in diameter and 0.17 λ_0 in height, where λ_0 donates the wavelength in free space at the operating frequency, namely 10GHz. Simulation results show that the focus spot is 22.5 λ_0 away from the antenna aperture, while a focusing gain of 31.2dBi is achieved, and the size of focus spot is 2.48 λ_0 in width and 11.3 λ_0 in depth of focus, respectively.

An Annular Ring Shorted Logarithmic Spiral Antenna with Planar Integrated Feed 49

Ayush Seth (Entuple Technologies Private Limited, India); Kush Parikh (Entuple Technologies, India)

A novel concept of overall lateral and normal dimensions reduction of a spiral antenna is described in this work. Specifically we try to use a combination of techniques that complement each other to achieve overall profile reduction. A microstrip line that is integrated into the annular ring shorted logarithmic spiral is used as a feed to achieve size reduction. A prototype of is fabricated and tested. Simulation and measured results are discussed. Impedance and axial ratio bandwidth of 260.9% are achieved. Limitations and their potential causes are elaborated.

Miniaturized and Lightweight ESPAR Antenna for WSN and IoT Applications 51

Luiza Leszkowska and Mateusz Czelen (Gdansk University of Technology, Poland); Mateusz Rzymowski (Gdansk University of Technology & WiComm Center of Excellence, Poland); Krzysztof Nyka and Lukasz Kulas (Gdansk University of Technology, Poland)

A new compact ESPAR antenna is investigated in this paper. The proposed antenna has 12 directional radiation patterns based on 12 passive elements and can be successfully used in Wireless Sensor Network applications. In proposed antenna design, the possibilities of 3D printing were used to implement a dielectric miniaturization overlay that allowed for reducing antenna occupied area by almost 60% and antenna profile by 27% in comparison to the standard ESPAR antenna. The total dimensions of the antenna are 98 mm in diameter and 20.25 mm in height, while the weight of the antenna is only 86 g, which makes it much more suitable for potential use in UAV-based wireless communication applications.

Performance Estimation of In-Vessel Resonant Communications 58

Vitalii Kirillov, Dmitry Kozlov, Holger Claussen and Senad Bulja (Tyndall National Institute, Ireland)

This paper presents simulation and experimental results for the estimation of in-vessel resonant communications performance. The efficiency of the excitation of cavity resonators filled with lossy liquids is analyzed. Further, the influence of antenna sizes and dielectric properties of liquids on the transmission characteristics between two antennas is investigated. Finally, measurements of monopole antennas located inside a tap water-filled barrel were performed. It is demonstrated that the determination of optimal antenna size providing communication links is one of the most important practical tasks for the development of an in-vessel communication system.

A Systematic Design Method of Miniaturizing Microstrip Patch Antenna Using Theory of Characteristic Modes 55

Angel Abreu and Mahrukh Khan (The College of New Jersey, USA)

A systematic design method of miniaturizing microstrip patch antenna using characteristic modes has been presented. The TCM is applied to investigate and control the currents to excite the lowest resonance mode of the rectangular patch. The first current mode, J1, showed horizontal current distribution, and J2 showed current distribution in the vertical direction of the width of the patch. A systematic analysis has been done to procure the desired excitation of the specific modes. The slot etching was used to elongate the current path first in vertical and then in horizontal directions of the width of the patch. The successful excitation of the lowest resonant mode, i.e., J1, was achieved by etching a slot parallel to the direction of J1. After optimization, the final version showed 60 % miniaturization than the original rectangular patch size with no significant deterioration in performance.

Bandwidth Manipulated Leaky-Wave Antenna Using a Sinusoidal Ridge in Folded Substrate Integrated Waveguide 57

Adan Simon El Hadri (Heriot Watt University, United Kingdom (Great Britain)); Samuel Arthur Rotenberg, George Goussetis and Lei Wang (Heriot-Watt University, United Kingdom (Great Britain))

The impedance bandwidth for leaky-wave antennas (LWAs) is usually very broad, leading to wide signal interference from unwanted spectrums. For instance, the uplink signals will cause jamming effect to the downlink for Satellite communication systems. Hence, an integrated LWA with a bandpass filter is proposed in this paper. A folded substrate integrated waveguide (FSIW) LWA is utilized to reduce the SIW width to build a 2D LWA array with low side lobes. Periodic fan-shaped slots are etched on the top of the FSIW for circular polarization in a band centered at 11.5 GHz. A bandpass filter is investigated by elaborating a sinusoidal ridge in the FSIW LWA. It has been successfully validated through full-wave simulation that the bandpass filtering can be manipulated by varying the amplitude of the sine curve, whereas the circular polarization is well maintained. The proposed antenna is a very promising candidate for next-generation satellite communication systems.

Design of a Semitransparent Dual-Mode Filter for Antenna Applications 44

Luis Inclan-Sanchez (University Carlos III of Madrid, Spain)

A new dual-mode filter that allows the passage of most of the visible light is designed in this paper. The proposed filter is based on a square ring resonator that is perturbed by a square patch at its corner. The filter is designed using a metallic mesh that produces the effect of its metallic surfaces but has sufficient spacing to offer optical transparency greater than 75%. The manufacture of the filter through 3D printing allows the substrate to be eliminated, thereby reducing its insertion losses to 1.5 dB. The selective filter offers a flat passband frequency response with a 3 dB fractional bandwidth of more than 8% and rejection levels greater than 20 dB. This work allows the integration of this device together with optically transparent antennas to add filtering functionality to systems that require transparency due to their location.

A Compact Flexible BLE Antenna for a Remote-Control Application 47

Ihsan El Masri (4MOD Technology, France); Jean-Philippe Coupez (IMT Atlantique/ Lab-STICC, France)

This paper presents simulations and measurements of compact flexible antennas printed on environmentally friendly substrates. These antennas have been designed for a green Remote-Control Unit (RCU) application. First, we present the state of the art of flexible antennas. Then, we present the design of a compact meander dipole at the Bluetooth Low Energy (BLE) frequency (2.45 GHz), highlighting the constraints induced by surrounding elements. Simulation and measurement results are presented, showing the antenna's performance respectively in free space and within an RCU casing. The effects of the casing and of a partial ground plane on the antenna's resonance frequency and radiation pattern are analyzed. This study concludes by emphasizing the potential of the proposed antenna solution for integration into remote control units and IoT devices and suggests perspectives for further optimization.

Wednesday, March 20 13:10 - 14:40

PE3: Poster Session on Electromagnetics II

// Electromagnetics

Room: Expo/Poster

Chairs: Davide Comite (Sapienza University of Rome, Italy), Riccardo Ozzola (Delft University of Technology, The Netherlands)

Cost-Efficient Large-Scale Re-Design of Multi-Band Antennas Using Orthogonal Scaling Directions 64

Anna Pietrenko-Dabrowska and Slawomir Koziel (Gdansk University of Technology, Poland)

This paper proposes a novel and cost-efficient technique for multi-band antenna re-design. The keystone of our method is identification of a set of orthogonal scaling directions, which allow for approximately independent relocation of individual center frequencies. Large-scale design adjustment along these vectors is interleaved with local tuning, executed to correct unavoidable scaling errors and to improve the primary performance parameters. The scaling and correction steps are iterated until convergence. The presented procedure has been validated using two microstrip antennas, both re-designed for target frequencies unattainable through traditional tuning techniques. The obtained results corroborate the ability of our algorithm to precisely control the operating conditions, as well as low running cost corresponding to just about 170 EM simulations of the antenna under design.

Polarization Insensitive Broadband Frequency Selective Resorber with Improved Selectivity for Stealth Applications 65

Baisakhi Bandyopadhyay, Arun Kumar Shahi, Alka Dileep, Mondeep Saikia and Kumar Vaibhav Srivastava (Indian Institute of Technology Kanpur, India)

This article describes a broadband polarization insensitive Absorption-Transmission-Absorption (A-T-A) resorber for stealth applications. The proposed structure is a two tiered structure comprised of one lossy layer with lumped resistors for broadband absorption and one lossless layer for transmission. Under normal incidence, the proposed resorber has two absorption bands and one transmission band (A-T-A), with the first absorption band being from 4.12 GHz to 7.85 GHz with 62.32% of bandwidth and the second absorption band being from 9.3 GHz to 13.82 GHz with 39.1% of bandwidth. The transmission band spans from 8.22-8.84 GHz with 7.26% fractional transmission bandwidth with improved selectivity and the lowest IL of 1.64 dB at 8.49 GHz. The measured reflection and transmission coefficients of the structure correspond well with the results of the simulation when fabrication and alignment errors being taken into account.

Metamaterial-Based Ku-Band Flat-Panel High-Gain Antenna for Satcom Applications 72

Muhammad S Rabbani (Plextek, United Kingdom (Great Britain)); James R Henderson (Queen Mary University of London & Plextek, United Kingdom (Great Britain))

This paper presents a circularly polarised (CP) high-gain (+23 dBi) Fabry-Perot resonant cavity (F-PRC) type antenna design at Ku-band (12-18 GHz) for satellite communications (satcom). The antenna operates at 12.4 GHz with 200 MHz bandwidth. The F-PRC comprises a partially reflective surface (PRS) and a metallic ground plane. The F-PRC is excited by a CP microstrip patch antenna placed at the ground centre. The simulated realised gain is over +20 dBi and total efficiency is better than 90% over the band of interest.

RIS-Enabled Near-Field Localization with EMI 61

Saber Hassouna (University of Glasgow, United Kingdom (Great Britain)); Muhammad Ali Jamshed (University of Glasgow, Glasgow G12 8QQ, United Kingdom (Great Britain)); Masood Ur-Rehman, Muhammad Ali Imran and Qammer H Abbasi (University of Glasgow, United Kingdom (Great Britain))

Controlling the characteristics of electromagnetic signals in terms of scattering, reflection, and refraction can be achieved through the utilization of reconfigurable intelligent surfaces (RIS). This research delves into the assessment of both communication and localization performance, using the achievable data rate and the position error bound (PEB) respectively for random and positional RIS configurations. Previous investigations have overlooked the presence of electromagnetic interference (EMI), which encompasses unavoidable incoming waves from external sources. Our study takes EMI into account when modelling the system, focusing on a single-user single-input single-output (SISO) communication system. The presence of EMI significantly affects communication and localization performance, emphasizing the importance of addressing this performance degradation in the existing literature. This underscores the need to develop more realistic algorithms and frameworks for RIS technology.

Analysis of the Interaction of Laser-Induced Solid-State Plasma with Electromagnetic Waves in Silicon Waveguides at 67-220 GHz 59

Mehrdad Rezaei Golghand and Alireza Madannejad (KTH Royal Institute of Technology, Sweden); Umer Shah (Royal Institute of Technology (KTH), Sweden); Joachim Oberhammer (KTH Royal Institute of Technology, Sweden)

This study investigates the influence of laser parameters on electromagnetic wave attenuation within a silicon waveguide over a wide frequency range of 67-220 GHz using 3-D full-wave simulations. A 10-layer cylindrical model mimicking the energy distribution of a Gaussian laser beam shape is utilized for the analysis. The conductivity of each layer is calculated, and the S-parameters are simulated via CST Studio Suite. Significantly different attenuation levels are observed for different laser wavelengths used in this study. A 980 nm laser resulted in a substantially higher attenuation comparison to a 405 nm laser which had a minimal impact. Furthermore, by increasing the laser intensity, an increase in attenuation is observed. Moreover, the low level of simulated return loss indicates that solid-state plasma absorption dominates the reflections.

Development of an Ultrawideband Wire-Grid Polarizer Measurement Standard for Focus Beam System Cross-Polarization Calibration 70

Jeffrey P. Massman (United States Air Force Institute of Technology & United States Air Force Research Laboratory Sensors Directorate, USA); Michael J Havrilla (Air Force Institute of Technology, USA)

This paper introduces an ultrawideband wire-grid polarizer measurement standard for focus beam system cross-polarization calibration. The low-cost design enables polarimetric calibration techniques of precision non-destructive material measurements. Principles from wire-grid polarizers and A-sandwich radomes are combined to develop a highly planar standard. An infinite array simulation is included to predict the insertion loss and cross-polarization isolation from 0.1-100 GHz at incidence angles from 0-60 degrees. The design is physically realizable with a specialized printed circuit board technique allowing for low-cost manufacturing and electrically significant polarizer calibration standards. A prototype 12in x 12in design is fabricated and mechanically assessed to determine tolerances. Finally, a time-domain gated response isolation scheme is used to characterize the prototype RF performance from 3-18 GHz. The design introduced in this paper may be extended to achieve wire-grid polarizer measurement standards more than 48in diameter for calibration from very low frequencies all the way through W-band.

Electromagnetic Modelling in Modern Vehicles: A Pathway to Efficiency and Performance 62

Shiyu Zhang, Emma Kowalczyk, Christopher Davenport, Shaozhen Zhu, Alex Ibbotson, George De Bolla, Aitor Muñoz Lao and Ailian Cai (Jaguar Land Rover, United Kingdom (Great Britain))

The rapid development of modern vehicles has brought significant challenges and opportunities within electromagnetic (EM) design. This paper presents the contributions of simulation tools in assessing vehicle electromagnetic performance. Electromagnetic interference (EMI) due to cable coupling is discussed. The study also examines effect of the low-emission (Low-E) coatings on vehicle glazing on in-cabin antenna performance. Furthermore, the paper presents how simulation methods can be used to evaluate installed antenna propagation performance in real-world traffic environments.

Design of a Conformal and Low-Frequency Metasurface for Magnetic Field Shielding in Wireless Power Transfer Systems 63

Valeria Lazzoni (University of Pisa & Consorzio Nazionale Interuniversitario per Le Telecomunicazioni, Italy); Alessandro Luigi Dellabate and Danilo Brizi (University of Pisa, Italy); Agostino Monorchio (University of Pisa & CNIT, Italy)

This paper investigates the use of an arbitrarily conformal and low-frequency metasurface for magnetic field shielding in WPT systems. Firstly, we carry out the metasurface design by employing an analytical approach, which enables the manipulation of its response, despite the finite nature of the array and the near-field excitation. In particular, we are able to set a 180° phase shift between the current flowing in the WPT active RF driver and those in the metasurface unit-cells. In this way, the metasurface, by interacting with the driver, will produce a magnetic field opposite to the inducing one, accomplishing the desired shielding behavior. The results, obtained through accurate full-wave simulations, show that it is possible to achieve a maximum level of shielding effectiveness of approximately 8 dB. The study demonstrates the potential application of conformal magnetic metasurfaces for enhancing WPT systems safety, thereby addressing certain constraints associated with existing devices

Concentration Detection of Sodium Chloride and Glucose Solutions Using an IDC-Based Microwave Sensor with Eliminating Environmental Effects 68

Haneul Woo (Yonsei University, Korea (South)); Hee-Jo Lee (Daegu University, Korea (South)); Jong-Gwan Yook (Yonsei University, Korea (South))

In this paper, a microwave sensor based on Interdigital Capacitor (IDC) structure using a switching circuit is proposed for the non-invasive detection of sodium chloride (NaCl) and glucose concentrations. Sodium chloride and glucose concentrations were set at 500-900 mg/dL and 0-400 mg/dL, respectively, considering the substances in human blood. The sensor could detect the concentration via a fluidic channel, which in the strongest electric field region of the resonator. A switching circuit was used to eliminate environmental effects, and according to the experimental results, the proposed sensor exhibited an increase in reflection coefficient of 0.41 dB and 1.43 dB for sodium chloride and glucose solutions, respectively. Furthermore, reproducibility was confirmed by conducting measurements ten times for each concentration.

Highly Reflective, Low-Loss, Homogenized Fishnet Metasurfaces at Terahertz: Design and Experiment 74

Walter Fuscaldo (Consiglio Nazionale delle Ricerche (CNR), Italy); Francesco Maita (IMM-CNR, Italy); Luca Maiolo (CNR-IMM, Italy); Romeo Beccherelli (Consiglio Nazionale delle Ricerche, Italy); Dimitrios Zografopoulos (CNR-IMM, Italy)

A metasurface based on a fishnet-like unit cell is designed, realized, and measured at terahertz frequencies through time-domain spectroscopy in reflection mode. While most of fishnet-like metasurfaces are designed in the resonant regime (i.e., with $p \approx \lambda$), (p and λ), being the period and the free-space wavelength), the proposed one is designed in the homogenized regime (i.e., with $p \ll \lambda$). Experimental results show that the proposed metasurface exhibits very high reflectivity, which makes it particularly attractive for the design of high-gain Fabry-Perot cavity leaky-wave antennas.

Flexible and Transparent Metamaterial Absorber Using Metal Mesh Structure 75

Daecheon Lim (Chung-Ang University, Korea (South)); Tae-Yeob Kim (Electronics and Telecommunications Research Institute, Korea (South)); Sungjoon Lim (Chung-Ang University, Korea (South))

In this paper, we introduce a transparent and flexible metamaterial absorber using a screen-printed metal mesh structure. This metamaterial absorber is implemented on PET film through screen printing, providing flexibility and the capability to absorb electromagnetic waves even in a bent state. To ensure consistent performance even when bent, we designed metamaterial pattern based on a circular sector structure that is insensitive to the angle of incidence. We measured reflection and transmission coefficients of the fabricated prototype in a far-field environment, confirming its absorption efficiency as an electromagnetic wave absorber. In the measurement results, this absorber exhibited an absorptivity of approximately 95% at 9.2 GHz in the flat state, with reflected waves decreasing by -15 dB and transmitted waves decreasing by -20 dB. Furthermore, it demonstrated an absorptivity of over 90% in the TE mode and over 85% in the TM mode at 9.22 GHz in the bent state.

High-Order Quasi-Elliptical Bandpass FSS Based on Substrate-Integrated Waveguide Technology for 60 GHz Applications 66

Hao Jiang (South China University of Technology & School of Electronic and Information Engineering, China); Yinghao Zhang, [Yuqi Wang](#), Shaowei Liao and Quan Xue (South China University of Technology, China)

This paper presents a high-order quasi-elliptical bandpass frequency-selective surface (FSS) using substrate-integrated waveguide (SIW) technology for 60 GHz applications. First, a planar double-layer criss-cross slot FSS is employed to achieve second-order bandpass characteristics and introduce a low-frequency transmission zero (TZ). Second, a long-period SIW FSS, composed of four identical criss-cross slot elements within a single period, is utilized to introduce an additional high-frequency TZ, thereby realizing a high roll-off feature. Third, additional planar octagonal slot elements are integrated into the long-period SIW FSS to excite higher-frequency resonant modes, and a semiopen SIW cavity is utilized to improve high-frequency out-of-band rejection. Simulation results are presented to validate the outstanding performance proposed two FSSs, including the wide passband, low insertion loss, and dual passband with quasi-elliptical response.

Design of Intelligent Reflective Surface Unit Cell for 5G mmWave Applications 71

Mirza Shujaat Ali, Jalil ur Rehman Kazim, Farooq A Tahir, Muhammad Ali Imran and Qammer Abbasi (University of Glasgow, United Kingdom (Great Britain))

This paper presents a single bit millimeter wave (mmWave) intelligent reflective surface (IRS) unit cell for use in 5G communication enhancement. A PIN diode switch is used to introduce a 180° phase shift in reflection mode between ON and OFF state. The geometry of the top layer of the unit cell allows for transverse electric (TE) polarized reflection with an angular stability of 30°, both in azimuth and elevation plane. The design is intended for use in the n257 FR-2 band for 5G applications with the center frequency at 28 GHz. The proposed unit cell design covers a bandwidth of 3 GHz while achieving the required phase difference of 180° ± 20°. The magnitude of reflection is greater than 78.5% throughout the band. These performance characteristics allow the proposed unit cell to be useful in digitally programmable metasurface applications with features such as beam focusing, beam steering and beam scattering.

An Angularly Stable Wideband Low Profile Single-Layer Linear to Circular Polarization Converter for Millimeter Wave Satellite Communications 67

Javid Ahmad Ganie and Kushmanda Saurav (Indian Institute of Technology Jammu, India)

This paper presents a wideband linear-to-circular polarization (LP to CP) converter, utilizing a single-layer substrate and offering exceptional angular stability. The proposed converter achieves a generous 3-dB axial ratio bandwidth of 29% within the frequency span of 29.5 - 39.5 GHz. The unit cell dimensions for the LP to CP converter are 0.38λ x 0.38λ x 0.15λ (λ corresponds to the frequency of 30 GHz). Notably, the design demonstrates remarkable angular stability, reaching 50° and 60° for TE and TM polarizations, respectively. To enhance practical utility, we integrate a wideband Vivaldi antenna with the LP to CP converter, resulting in a wideband CP antenna. The wideband Vivaldi CP antenna exhibits an axial ratio and 1-dB gain bandwidth of 16.5% and 12.5%, respectively. This wideband CP antenna holds promise for measuring CP characteristics and serving as a feed source for high-gain transmit arrays.

Frequency-Selective Surface Generating Two-Band Pseudo-Elliptic Frequency Response 60

Dmitry E Zelenchuk (Queen's University of Belfast, United Kingdom (Great Britain)); Lyudmila Mospan (Computational Electromagnetics Lab, Ukraine)

A novel frequency-selective surface (FSS) is introduced in this paper. The structure proposed is a single-sided printed circuit board (PCB) that generates a pseudo-elliptic type response with two closely spaced passbands. Such a multi-band operating regime is realized owing to additional higher modes excited in the meander-like apertures and involved in electromagnetic interaction. Passbands at the response are independently tuned by adjusting the geometrical parameters of the aperture. Numerical and measured data for X-band FSS are presented for different angles of incidence. Due to the high selectivity, a small frequency ratio of 1.27 for central frequencies of passbands of 4.2% and 5.5% bandwidths is achieved.

Ultra Wide Dynamic Range High Power RF Rectifier 73

Xiaochen Yu (National Tsing Hua University, Taiwan & University of Liverpool, United Kingdom (Great Britain)); Jinyao Zhang, Minzhang Liu and Yi Huang (University of Liverpool, United Kingdom (Great Britain)); Ta-Jen Yen (National Tsing Hua University, Taiwan); Jiafeng Zhou (University of Liverpool, United Kingdom (Great Britain))

A new high-power RF-to-DC rectifier applied to wireless power transfer (WPT) with ultra-wide input power dynamic range is proposed in this paper. GaN (gallium nitride) HEMT (high electron mobility transistor) is utilized to realize rectification at 12W high power and a Schottky diode is used for lower-power rectification. Excellent switching between the two circuits' rectification modes is achieved by adding a circulator. The rectifier has a 30 dB dynamic range with an efficiency of over 50% at 2.4 GHz.

Enhancing Signal Transmission in Energy-Saving Glass Through Tri-Bandpass Frequency Selective Surface Design 69

Zifeng Wan (University of Manchester, United Kingdom (Great Britain)); Farhad Ghorbani, Yi Huang and Jiafeng Zhou (University of Liverpool, United Kingdom (Great Britain))

This study introduces a tri-bandpass frequency selective surface applied to ESG. The design incorporates a square loop and two hexagonal loop slots etched into the metallic coating to enable the transmission of sub-bands of 5G signals and common UMTS signals. Simulation results demonstrate that the -3dB range effectively encompasses the frequency bands of 700MHz, 1.9GHz, and 3.5GHz. Furthermore, the study also proposed an optimized approach involving the selective removal of additional lines along the middle of both hexagonal sides from the coating to enhance current distribution. The improved transmission coefficient has a significant improvement at bandwidths of 1.9GHz and 3.5GHz while constraining total coating removal to a mere 13.8%. This achievement ensures favorable signal transmission for 5G and UMTS signals, preserves thermal insulation properties, and holds significant promise for enhancing signal performance in ESG applications.

Wednesday, March 20 13:10 - 14:40

PM2: Poster Session on Measurements II

T09 Fundamental research and emerging technologies // Measurements

Room: Expo/Poster

Chairs: Jayakrishnan Methapettyparambu Purushothama (Heriot-Watt University, United Kingdom (Great Britain)), Okan Yurduseven (Queen's University Belfast, United Kingdom (Great Britain))

Using a Radio-Frequency System on a Chip in the Development of a Phased Radio Array for the Bustling Universe Radio Survey Telescope in Taiwan 76

Homin Jiang (Academia Sinica, Taiwan)

The Bustling Universe Radio Survey Telescope in Taiwan (BURSTT) employs the Xilinx ZCU216 RFSoc FPGA board as its digital backend. In this study, we used a firmware library available on an online community (called Collaboration for Astronomy Signal Processing and Electronics Research) for hardware implementation. The FPGA board used in the BURSTT accommodates 16-channel analog-to-digital inputs, samples data at 1600 MHz, and has a bandwidth of 800 MHz. Phase alignment, which is key to the success of radio telescopes, was verified through cross-correlation tests for the same device and between different devices. Phase closure was successfully achieved for three inputs in two devices, which indicated system readiness. An optimal power input level, which is crucial for achieving optimal system performance, was identified. The successful acquisition of spectra from 16 on-site inputs confirmed the applicability of the RFSoc chip in phased systems with a single device or multiple devices.

Design Effects of the Junction Contour of a Blended Rolled Edge Compact Range Reflector 77

[Marc Dirix](#) (Antenna Systems Solutions, Spain); Stuart F Gregson (Queen Mary, University of London, United Kingdom (Great Britain))

This paper is an extension of the authors prior work examining the design and optimisation of blended rolled edge (BRE) compact antenna test ranges (CATR) using evolutionary algorithms. The authors existing approach was initially improved and extended to provide broadband optimization of blended rolled edge (BRE) CATRs including refining the algorithm to take account of and reducing chamber wall illumination which is a recognized deficiency of the BRE CATR approach. In this paper the design approach is further extended to include the junction contour which in this study is adapted to remove the discontinuity in the reflector surface that is typically present in BRE CATRs, and further increases the available CATR design envelope. Worthwhile improvements in predicted QZ performance are obtained together with a further reduction in chamber wall illumination. These are highlighted together with the important reduction in the BRE reflector volume and mass.

Leveraging Radar Back-Scattered Data for Classification of Imaging Targets 78

Rahul Sharma and Okan Yurduseven (Queen's University Belfast, United Kingdom (Great Britain))

Employing deep learning methodologies for computer vision tasks, particularly in the domain of radar image analysis, necessitates access to a large and diverse dataset. The creation of such a dataset often entails the intricate task of reconstructing images from raw radar back-scattered data. This reconstruction process involves handling substantial data volumes, which can be computationally intensive and time-consuming. In this research, a deep learning framework is proposed for target classification utilizing solely the radar back-scattered data, completely bypassing the need for image reconstruction procedure, thereby significantly reducing the classification time. To make the dataset generation easier, a computational imaging numerical model is employed. Subsequently, the deep learning model is trained using this dataset, and following the training phase, it is tested with novel radar back-scattered data. The results confirm the benefit of training a deep learning model to perform image identification tasks based on radar back-scattered signatures.

Validation of the DTU ETC Scattering Test Facility for Radar Cross Section Measurements 79

Rasmus E. Jacobsen and Samel Arslanagic (Technical University of Denmark, Denmark)

Accurate measurements of electromagnetic wave scattering is essential in many applications including radars, antennas, and metasurfaces, among others. In this work, we use the recently established DTU Electromagnetic Test Centre Scattering Test Facility to measure the monostatic radar cross section (RCS) of well-known objects with the purpose of validating the facility. The achieved results for metallic spheres of various sizes demonstrate measurable RCS levels down to -50 dBsm (-70 dBsm) with an accuracy of ± 0.5 dB (± 2 dB) from 4 GHz to 18 GHz. A rectangular metallic plate with a larger RCS was also characterized in the Ku-band. The initial measurements exhibit a dynamic range of 80 dB with ± 2 dB accuracy for the upper and lower RCS levels. Future works involve lower-frequency RCS measurements and further analysis of the dynamic range and the obtained results will be presented at the conference together with the RCS measurements of complex scatterers.

Dielectric Characterization of Materials at 5G mm-Wave Frequencies 80

Rocio Rodriguez-Cano (Aalborg University, Denmark); Steven Perini and Michael T Lanagan (The Pennsylvania State University, USA)

The development of the next-generation 5G wireless networks depends critically on the engineering of optimized high-frequency devices, employing dielectric materials. This work presents a comprehensive broadband dielectric characterization of polymers, ceramics and glasses from 5 GHz until 115 GHz. Various measurement techniques including split-post, split cavity, open resonator and free-space transmission are utilized to obtain wideband spectra. The frequency-dependent permittivity and loss tangent are analyzed to identify suitable candidate materials exhibiting minimal dispersion and loss in the 5G millimeter-wave bands. The characterization reveals almost constant permittivity and a loss tangent that increases linearly with the frequency.

Detection Capability of a CNN-Based Imageless Millimeter Wave System for Static Concealed Objects 81

Hadi Mahdipour (University of Oviedo, Spain); Jaime Laviada (Universidad de Oviedo, Spain); Fernando Las-Heras (University of Oviedo, Spain)

Regarding the benefits of millimeter-wave (MMW) systems such as cost-effective, easy to use and safety for humans, this paper proposes an imageless concealed object detection system based on MMW radar and convolutional neural network (CNN). The proposed method is an accurate, portable, compact, real-time, without impeding the privacy of the people, and capable to detect different metallic and non-metallic objects system. A static person with different concealed objects in different angle of view is captured by the MMW radar and the captured data is fed to a CNN after some preprocessing (mapping from captured fast-slow time domain to range-doppler domain) to detect the concealed object. Different parts of the proposed system, including new structure of CNN, data augmentation (for the CNN training) and background removing steps, are designed to achieve the aforementioned. Experimental results show efficiency of the different parts of the proposed method resulting in a promising detection capability.

Near-Field Bistatic Microwave Imaging with Dynamic Metasurface Antennas 82

Amir Masoud Molaei (Queen's University Belfast, United Kingdom (Great Britain)); The Viet Hoang (Novocomms Limited, United Kingdom (Great Britain)); Thomas Fromenteze (University of Limoges & Xlim Research Institute CNRS, France); Vasiliki Skourliakou (Queen's University Belfast, United Kingdom (Great Britain)); Rupesh Kumar (WSI, SRM University AP, India); Mengran Zhao (Queen's University Belfast, United Kingdom (Great Britain) & Xi'an Jiaotong University, China); María García Fernández, Guillermo Alvarez Narciandi, Vincent Fusco and Okan Yurduseven (Queen's University Belfast, United Kingdom (Great Britain))

In recent decades, microwave imaging technology has been used in a variety of applications including security, medicine, nondestructive testing and structural health monitoring. Traditional microwave imaging systems often suffer from drawbacks such as long acquisition times and complex array structures. To address these issues, this paper introduces a panel-to-panel microwave computational imaging (CI) technique for near-field operation using dynamic metasurface antennas for both transmission and reception, enhancing system diversity and enabling real-time applications. The paper also outlines mathematical models for three-dimensional image reconstruction algorithms tailored to this scenario. The results of numerical and electromagnetic simulations show the feasibility of this approach for CI-based imaging, with both Fourier and least squares-based image reconstruction techniques.

Uncertainties in the Estimation of the Gain of a Standard Gain Horn in the Frequency Range of 90 GHz to 140 GHz 83

Purnima Yadav, Laurens A. Bronckers, A. B. (Bart) Smolders and Ad Reniers (Eindhoven University of Technology, The Netherlands)

This paper examines the validity of employing the Naval Research Laboratory's (NRL) on-axis gain calibration curves as a standard reference, as specified in the commercial Standard Gain Horn (SGH) antenna datasheets, for the frequency range of 90 GHz to 140 GHz for antenna gain measurements. We present a comprehensive analysis of the on-axis gain calibration curve characteristics and the dimensions of the SGH antenna by employing three different dimensional measurement techniques and quantifying the discrepancies in comparison to the on-axis calibration curve found in datasheets. Additionally, we demonstrate that inaccuracies in the dimensional data provided in the commercial SGH antenna datasheet can lead to a gain deviation of ± 1 dB from the anticipated gain. We validate the on-axis gain curves obtained from simulation by conducting measurements in a spherical anechoic chamber.

Complex Permittivity Extraction of Typical Wooden Furniture Materials Based on Multi-Objective Particle Swarm Optimization over 40-50 GHz 84

Pan Li, Yu Shao and Ran Xu (Chongqing University of Posts and Telecommunications, China)

In order to facilitate the study of indoor propagation characteristics of millimeter waves, it is necessary to extract electromagnetic parameters of indoor materials in the millimeter wave frequency band. It is understood that there is currently limited research on the electromagnetic characteristics of materials with the same material and different internal structures. In the 40-50 GHz frequency band, the free-space method is used to measure three types of materials: plywood, particle wood, and solid wood. To avoid the ripples and ambiguity problems in the common methods, we propose a multi-objective particle swarm optimization scheme to extract the dielectric constant and conductivity of the materials using the measured values and formula calculated values at 30° incidence angle. Comparing with measurements at other incidence angles, the extraction results are validated and analyzed, and the fitting curve shows good results.

Assessing Performance of Transparent Conductive Films for Microwave Industrial Applications 85

Anastasios Paraskevopoulos (NCSR Demokritos, Institute of Informatics & Telecommunications, Athens, Greece); Dimitrios C. Tzarouchis (University of Pennsylvania, USA); Maria Koutsoupidou (King's College London, United Kingdom (Great Britain)); Konstantinos Dovelos (Queen's University Belfast, United Kingdom (Great Britain)); Panagiotis Kosmas (Kings College London, United Kingdom (Great Britain)); Shimul Saha (SEMwaves Ltd., United Kingdom (Great Britain)); Efthymios Kallos (Medical Wireless Sensing Ltd. - Meta Materials Inc., United Kingdom (Great Britain)); Ragip Pala (Meta Materials Inc., USA); George Palikaras (Meta Materials Inc., Canada); Fotis Lazarakis (NCSR Demokritos, Institute of Informatics & Telecommunications, Greece); Antonis A Alexandridis (NCSR Demokritos, Greece)

Transparent conductive films (TCFs) are gaining increasing attention in microwave industrial applications such as indoor signal coverage for 5G, transparent antennas etc. This work discusses methods to predict and assess performance of such TCF-based applications, which can be useful in their design and characterization stage, respectively.

Quiet-Zone Profiling in a mmWave Spherical Anechoic Chamber: An Evaluation Approach 86

Naïla Rubab, Laurens A. Bronckers, A. B. (Bart) Smolders and Ad Reniers (Eindhoven University of Technology, The Netherlands); Antonius Johannes van den Biggelaar

(ANTENNEX, The Netherlands)

To ensure effective plane wave illumination of an antenna under test in an Anechoic Chamber(AC), a specific region known as the Quiet Zone(QZ) is typically specified. conventional ACs often employ the industry-standard free-space voltage standing wave method utilizing a horn antenna for the QZ characterization. However, to define the QZ in distinctive AC designs, it is essential to assess scanning methodologies that align with their unique working characterization mechanisms. In the mmWave spherical AC at Eindhoven University of Technology a planar scanning methodology using open-ended waveguide antenna has been explored to determine its applicability for the QZ assessment. An evaluation approach, incorporating spatial spread factor and probe pattern compensation, is first analyzed on a digital twin simulations and subsequently applied on practical measurements to study the chamber behaviour. The agreement between the simulated and measured results validates the proposed planar scanning methodology and the evaluation approach for the QZ assessment.

Over-The-Air Testing Environments with Spatial-Directional Selectivity for Characterizing Wireless Devices and Systems 87

Andrés Alayón Glazunov (Linköping University, Sweden)

Various over-the-air (OTA) testing environments are presented, focusing on their capability to produce single- or multidirectional channels, i.e., producing a single path or multipath components. The OTA systems are discussed in terms of the chambers used, either anechoic, reverberation, or hybrid, and the capabilities to produce different channels. It is suggested that future developments in OTA testing technology will require the development of smart testing environments that can accommodate the diverse increasing demands of emerging applications.

Study on Antenna-Phantom Model of Aperture Antennas for SAR Analysis 88

Wenfu Fu (KTH Royal Institute of Technology, Sweden); Bo Xu (Ericsson AB, Sweden); Sailing He (Royal Institute of Technology, Sweden)

In the conventional model to explain the antenna-phantom interaction for specific absorption rate (SAR) analysis, antenna structures are treated as perfect electric conductors. However, such a model does not suffice to analyze complementary antenna structures, i.e., aperture antennas. In this paper, an antenna-phantom model for aperture antennas is introduced considering the tangential electric field generated by the equivalent magnetic currents as the primary contributor to the peak SAR level. When the out-of-phase tangential electric field of the second-order modes for a slot antenna is achieved, the peak 10-g SAR levels are lower than that is caused by a conventional slot antenna with the first-order mode in the same condition due to destructive superposition. Therefore, the proposed antenna-phantom model is helpful to guide the aperture antenna design for the SAR compliance purposes.

A Wideband Free Space Material Characterization Method for Extracting Dielectric Permittivity 89

Orestis Christogeorgos (Queen Mary University of London, United Kingdom (Great Britain)); Ernest Okon (University of Bedfordshire, United Kingdom (Great Britain)); Yang Hao (Queen Mary University, United Kingdom (Great Britain))

The extraction of dielectric properties of materials has been central to the antennas and propagation community, especially since the introduction of metamaterials and/or engineered materials with desired electromagnetic response. These materials can help with enhancing the performance of existing designs and provide capabilities that are unobtainable with conventional materials. As such, it becomes very important to characterize these new materials and through measurements, extract their dielectric properties with a high degree of certainty. Here, we propose a non-destructive and easy to implement methodology for characterizing the dielectric properties of different types of materials, including two types of Radiation Absorbent Materials (RAM) and extract the corresponding effective dielectric permittivity for each case in the 10 – 18 GHz range.

Wednesday, March 20 13:10 - 14:40

PP02: Poster session on Propagation II

// Propagation

Room: Expo/Poster

Chairs: Thomas F. Eibert (Technical University of Munich (TUM) & Chair of High-Frequency Engineering (HFT), Germany), Guido Valerio (Sorbonne Université, France)

Improving Air-Writing Accuracy Through Data Regression and Interpolation in a Single Radar System 107

Seunghoon Kwak, Chanul Park and Seongwook Lee (Chung-Ang University, Korea (South))

In the radar-based air-writing, the hand movement may not be completely detected depending on the transmission cycle of the radar waveform, which potentially reduces the legibility of the air-writing results. Therefore, in this paper, we propose a method of interpolating the unmeasured portions of the air-writing using polynomial regression. First, using a radar sensor, we acquire range and angle detection results for hand motion over time. Then, the trajectory of the hand motion is expressed in two-dimensional distance coordinates using the range and angle information. Subsequently, the polynomial regression is used to derive the relationship between the observation time and the change of distance coordinates in each dimension. Next, we interpolate the unmeasured portions using the derived regression model and generate the interpolated air-writing results. Finally, to verify the performance of the proposed method, the recognition accuracy of non-interpolated and interpolated air-writing results is evaluated.

Pathloss-Based Non-Line-Of-Sight Identification in an Indoor Environment: An Experimental Study 102

Muhammad Asim (Information Technology University, Pakistan); Muhammad Ozair Iqbal (Information Technology University Lahore, Pakistan); Waqas Aman (HBKU, Qatar); Muhammad Mahboob Ur Rahman (Information Technology University, Pakistan); Qammer Abbasi (University of Glasgow, United Kingdom (Great Britain))

We report the findings of an experimental study on the problem of line-of-sight (LOS)/non-line-of-sight (NLOS) classification in an indoor environment. Specifically, we deploy a pair of NI 2901 USRP software-defined radios (SDR) in a large hall, which communicate on a center frequency of 2.4 GHz, using three different signal-to-noise ratios (SNR). The receive SDR constructs a dataset of pathloss measurements from the received signal as it moves across 15 equi-spaced positions on a 1D grid (for both LOS and NLOS scenarios). This allows us to estimate the pathloss parameters using the least-squares method to construct a parameterized pathloss model for a binary hypothesis test (BHT) for NLOS identification. Since the pathloss measurements slightly deviate from Gaussian distribution, we also feed our custom dataset to a range of machine learning (ML) algorithms. It turns out that the performance of the ML algorithms is only slightly superior to the Neyman-Pearson-based BHT.

Feasibility Study of Joint Modeling of Environmental and Morphological Effects for WBAN 92

Badre Youssef (Télécom ParisTech-Institut Mines-Télécom & LTCI, France); Christophe Roblin (Telecom Paris - Institut Polytechnique de Paris & LTCI - Institut Mines-Télécom, France)

In this article, we assess the feasibility of the joint modeling of the effects of the environment and morphology in the context of the Wireless Body Area Networks (WBAN) for the scenario based approach in the 1st Ultra Wide Band (UWB) sub-band [3.1, 4.8] GHz. Previous works have enabled to obtain important representative statistical samples for these two variables, to our knowledge not reached to date for WBAN communications, with a dedicated methodology combining simulations results and experimental designs supported by measurements. Our approach is to combine these variables in a disjointed manner in order to extract a more complete model and naturally limit the simulations campaigns to a reference subject for all the environments to be considered. Thus, for a given subject we therefore estimate the propagation channel transfer function from its on-body contribution and that of the environment obtained with the reference subject. This feasibility study is the first step in extracting interesting future models and a huge saving of time. The comparison results obtained between the estimated transfer function and the nominally calculated one highlight fairly small differences in the majority of cases, which is encouraging for the use of this simplifying approach.

Multipath Model Improvement for Automotive Radar Application 105

Antonin Locatelli (ENAC, France); Jose Luis Alvarez-Perez (University of Alcalá, Spain); Alexander Yaroyov (TU Delft, The Netherlands)

Multi-path propagation over asphalt road surfaces at automotive radar frequencies is studied. A new expression for the reflection coefficient from asphalt which takes into account asphalt surface roughness is proposed. The classic twoway method to take into account the multi-path is improved using antenna radiation patterns and the antenna tilt. A new method to estimate elevation of a reflector above road surface based on reflectivity variations is proposed.

Measurement-Based Channel Characteristics for Air-To-Ground Communications Under Rural Areas 100

[Xuchao Ye](#), Hanpeng Li, Kai Mao, [Qiuming Zhu](#), Farman Ali, Xiao-min Chen, Yanheng Qiu and Hangang Li (Nanjing University of Aeronautics and Astronautics, China)

As an important part of the beyond fifth generation (B5G) and sixth generation (6G) network, unmanned aerial vehicle (UAV) communication has been widely used in various application scenarios. The measurement and analysis of UAV air-to-ground (A2G) channel characteristics is vital to the design of future UAV communication systems. In this paper, we introduce a channel sounder that supports real-time measurements but has smaller data storage sizes. The developed channel sounder is used to carry out channel measurement campaigns in two typical rural scenarios, i.e., farmland and river. Based on the measurement data, some key channel characteristics, including multipath components (MPCs) and path loss (PL), are analyzed and compared. The results can provide a valuable reference for UAV channel modeling and UAV communication system design in rural areas.

Antenna Pattern Tracking Algorithm for Low Terahertz Communications 101

Lorenz Helmut Wolfgang Löser, [Tobias Doeker](#) and Thomas Kürner (Technische Universität Braunschweig, Germany)

In this paper, a novel beam tracking algorithm is presented which is based on the change of the path loss. Due to the movement, the antenna gain is different as the angle of departure and angle of arrival changes. The proposed algorithm draws conclusions to the angular change from information about the measured gain difference. However, in order to provide a unique solution and directly get information about the angular direction of the movement, at least one additional antenna has to be added. By means of simulations, it is shown that the proposed algorithm works perfectly for line-of-sight and with some constraints also for non line-of-sight cases.

Electromagnetic Beerline Cleaning Using Radio Frequency Signals 109

[Maksim Kuznetsov](#) (Heriot Watt University, United Kingdom (Great Britain)); Symon K. Podilchak (University of Edinburgh, United Kingdom (Great Britain)); Louis Arnold and David Arnold (Beerline Wizard, United Kingdom (Great Britain))

In this work, a study on radio frequency (RF) beer-cleaning has been reported. Particularly, a device used to generate pulse-wide modulation (PWM) signals and a simple antenna dipole wound around the beer pipe was shown to mitigate yeast generation. This setup not only reduces and simplifies maintenance of the pipes but also can reduce operating costs. A particular study was investigated using a 60 V PWM signal ranging from 1.6 to 6 KHz. This not only reduced the yeast waste by about 75% but also improved the manual cleaning cycles from 1 week to 4 weeks.

Comparison of Propagation Characteristics Between 5G Bands in a Reflective Industrial Environment 99

[Nora Meyne](#) (Physikalisch-Technische Bundesanstalt, Germany); Johannes Dommel (Fraunhofer Heinrich Hertz Institute, Germany); Thomas Kleine-Ostmann (Physikalisch-Technische Bundesanstalt (PTB), Germany); Martin Kasparick (Fraunhofer Heinrich Hertz Institute & Technical University Berlin, Germany)

New frequency bands, such as the upper mid-band from 7 to 24 GHz, are currently heavily discussed for 5G and beyond, not least for industrial use cases. This study examines the propagation characteristics within a reflective industrial environment, with a specific focus on parts of this novel frequency band (10-12 GHz). Through a dedicated measurement campaign, we compare signal attenuation and delay spread in different settings using channel-sounding equipment in the 5G bands FR1, FR2, and upper mid-band. We give particular attention to both, the impact of reflective industrial environments and the effect of different blockage scenarios, for example, from metal plates or human blockage. In addition, we compare the propagation characteristics using functional measurements for FR1, providing insights into the performance using realistic hardware.

Synthesis of Drop Counter Rain Rate from a Tipping Bucket Rain Gauge 97

Armando Rocha (University of Aveiro & Instituto de Telecomunicações, Portugal); José E. Silva (Universidade de Aveiro, Portugal); Susana Mota (University of Aveiro & Institute of Telecommunications, Portugal)

Earth-Satellite propagation models for Ka-band and above require measured rain rate statistics, preferably locally, with an integration time of 1 minute. In this paper we explore the possibility of deriving 1 minute-integrated precipitation rate time series using a rain gauge tipping bucket and evaluate the performance with a co-sited drop counter rain gauge. The method consists of distributing, using several algorithms, a fixed number of drops corresponding to a tip of the tipping bucket in the interval between two tips. The performance of the retrieval is compared with the results obtained with a co-located drop counter on a per-day time series basis, time correlation and in terms of the CCDFs, using more than two hundred days with rain events. The results are promising, offering reasonable confidence in using a tipping bucket device as a backup.

Designing a Data Pre-Processing Tool for MEO Satellites Propagation Measurements 95

Marlene Gomes Brás (University of Aveiro and Institute of Telecommunications, Portugal); Susana Mota (University of Aveiro & Institute of Telecommunications, Portugal); Armando Rocha (University of Aveiro & Instituto de Telecomunicações, Portugal)

Medium Earth Orbit (MEO) satellite constellations have revolutionized global communications, offering reduced latency and extensive coverage compared to traditional geostationary satellites. However, these systems are vulnerable to atmospheric conditions that can deteriorate signal quality and impact the service performance. This article focuses on the planning strategy of a tool to facilitate the pre-processing of data acquired in the framework of an experimental propagation program with the O3b MEO satellites constellation. These measurements capture valuable insights into atmospheric phenomena, particularly the signal attenuation dependency with the azimuth and elevation - a critical aspect of this kind of satellite communication. The designed tool streamlines data processing and facilitates the extraction of attenuation-related information.

AlphaSat Ka-Band and Q-Band Receiving Station in Rome: Measurements and Data Analysis 96

Stefano Barbieri (Sapienza University of Rome, Italy); Fernando Consalvi (FUB, Italy); Gianmarco Fusco (Istituto Superiore delle Comunicazione e delle Tecnologie dell'Informazione, Italy); [Marianna Biscarini](#) (Sapienza University of Rome, Italy); Lorenzo Luini and Carlo Riva (Politecnico di Milano, Italy)

The AlphaSat TDP#5 experiment, dedicated to Prof. Aldo Paraboni, is an Italian Space Agency (ASI) science experiment to investigate radio propagation channel in the Ka and Q bands. Sapienza University of Rome, in collaboration with the Higher Institute of Communications and Information Technology (ISCTI) and the Ugo Bordononi Foundation (FUB), has joined the experiment with two receivers, one for each frequency, installed at the Ministry of Business and Made in Italy (MIMIT) in Rome. In this paper, we present a methodology for the retrieval of the excess attenuation and tropospheric scintillation from the Alphasat received beacon signal at Ka and Q band. Scintillation amplitude results in clear-air condition acquired over three months are compared with the ITU-R model. Experiment characteristics and data processing details are also presented.

Comparison of Indoor Propagation Channels at 28 GHz and 140 GHz Bands 103

Mar Francis De Guzman (Aalto University, Finland & Advanced Science and Technology Institute, Philippines); Katsuyuki Haneda (Aalto University, Finland)

In this paper, a comparison between the measured 28GHz and 140GHz channels in an entrance hall is presented. The path loss, angular spread, delay spread, and composite power angular spectrum (PAS) are evaluated and compared with reference indoor channels in an office, existing model, and shopping mall. The existing model and office path loss curves align with the path loss of line-of-sight (LOS) and non-LOS (NLOS) links, respectively. When using the full dynamic range, the angular spread does not change with frequency, while the delay spread decreases with frequency in the entrance hall. The differences in angular spread and delay spread vary between the entrance hall and other indoor environments due to differences in layout. The composite PAS at both bands are similar for both LOS and NLOS links. The channels have larger angular and delay spread at 140GHz than 28GHz when the same dynamic range is used.

Radiometeorological Forecasts for Satellite Links Operations: Validation with Measurements from BepiColombo Mission 93

Simone Bellofiore and [Marianna Biscarini](#) (Sapienza University of Rome, Italy); Maria Montagna (VisionSpace @ European Space Agency (ESA/ESOC)); Saverio Di Fabio and Livio Bernardini (CETEMPS, Italy); Paolo Antonelli and Paolo Scaccia (AdaptiveMeteo, Italy); Davide Comite (Sapienza University of Rome, Italy)

This work describes the experimental validation of a radio-meteorological operative model-chain: The first weather-forecast-driven tool for the optimization of satellite links for Ka-band deep-space missions. The proposed model-chain has the capability to provide daily forecast statistics of radiopropagation variables customized on the specific transmission day, thus allowing dynamic link optimization. The radio-meteorological operative chain is tested with two different global scale data for the model-chain initialization (European Centre for Medium-Range Weather Forecasts, ECMWF, and National Centers for Environmental Prediction, NCEP). The optimization results are compared with the optimization performed with standard ITU-R annual statistics and with the link data collected during the operations of the BepiColombo ESA mission to Mercury. The results confirm the great advantage (in terms of received data-volume) deriving from the usage of a radiometeorological operative model chain for the optimization of the satellite link, confirming the theoretical estimation provided by feasibility and design studies.

Modeling Atmospheric Effects on over Land UHF Propagation Links 94

Abby R Anderson (US Naval Research Laboratory, USA); Chris Anderson (National Telecommunications and Information Administration & Institute for Telecommunication Sciences, USA); Henry S. Owen (HS Owen LLC, USA)

Propagation modeling for over land paths has historically been performed using semi-empirical models. These models capture median propagation expected over a month or season; however, they cannot model expected propagation for smaller time scales. Variability in atmospheric conditions, which influences radio frequency electromagnetic propagation, occurs on time scales of minutes to hours. Deterministic models, such as parabolic equation (PE) models, are required to accurately capture the effects of atmospheric variability on these small timescales; however, these models are traditionally used only in maritime environments.

In this manuscript we evaluate the performance of a PE model for two over land propagation paths. Propagation measurement data and atmospheric model data were collected in July 2022 for 43.5 and 112 km UHF links. Ducting conditions are found to exist approximately 20% of the time. Evaluation of PE model output demonstrates accurate characterization of the measured ≈ 10 dB magnitude variability in received signal level.

Large-Scale Site Diversity Experiment in Ljubljana and Budapest at Ka-Band with Alphasat Satellite 91

[Arsim Kelmendi](#) (Jozef Stefan Institute, Slovenia); László Csurgai-Horváth (Budapest University of Technology and Economics, Hungary); Mihael Mohorcic (Jozef Stefan Institute & Jozef Stefan International Postgraduate School, Slovenia); Ales Svigelj and Tomaz Javornik (Jozef Stefan Institute, Slovenia); Andrej Hrovat (Jozef Stefan Institute, Slovenia)

High throughput satellite communication systems, need to utilize less congested high frequency bands, such as Ka- and Q-bands and above with a large available radio channel bandwidth. However, the disadvantage of radio wave propagation at these frequencies is the increased attenuation and impairment caused from tropospheric phenomena, in particular by rainfall. Site diversity is an efficient technique to mitigate the attenuation due to rain. In this paper, we present the performance evaluation of the large-scale dual site diversity system based on the long-term beacon signal measurement of geosynchronous Alphasat satellite at 19.701 GHz between the Earth stations in Ljubljana and Budapest. The statistical analysis of one-year measurement of rain attenuation of the site diversity system is presented. The results show that the mitigation of the rain attenuation in site diversity is significant.

Analysis of the Effects of Rainwater Covered Bumper on the Automotive Radar Signals 108

[Nancy Modi](#), Mahesh Kumar Busineni and Jayanta Mukherjee (Indian Institute of Technology Bombay, India)

This paper studies the effect of the rainwater covered bumper on the automotive radar signal. The rainwater on the painted bumper is modeled in two ways: continuous thin layer and droplets. In the continuous thin layer approach, a uniform water layer is considered on the painted bumper's surface. In contrast, for the droplet approach, multiple hemispheres with equal diameter and spacing are considered on the painted bumper's surface. Moreover, to replicate a real scenario, the presented study considers a water covered painted bumper near a radar antenna. Different cases are studied using the transmission coefficient, S-parameter, and gain parameters to analyze the effect of rainwater on the radar performance. Based on this study, it is found that the transmission through the continuous thin film of water is better than that of droplets. Also, this study aids in selecting the appropriate paint layer such that transmission through the bumper is significant.

Machine Learning Approaches for EM Signature Analysis in Chipless RFID Technology 90

[Nadeem Rether](#) and Roy B. V. B. Simorangkir (Tyndall National Institute, Ireland); John Laurence Buckley (Tyndall National Institute & University College Cork, Ireland); Brendan O'Flynn (Tyndall National Institute, Ireland); Salvatore Tedesco (Tyndall National Institute, Ireland)

In this paper, for the first time, we provide a comprehensive review of Machine Learning (ML) approaches in Chipless Radio Frequency Identification (CRFID) technology, which is a fast-developing sector with applications in inventory management, anti-counterfeiting, health monitoring, and environmental monitoring, to name a few. ML techniques are rapidly being integrated to improve CRFID systems' capabilities for robust detection of information. The combination of ML with CRFID technology is presented, examining various ML approaches, applications, challenges, and future perspectives. It is observed that ML has been successfully deployed in CRFID with high accuracy in the detection of information from CRFID tags. Challenges, such as data quality, security, and scalability are identified. The literature currently struggles in the application of ML models on high-capacity tags, and lacks standardized data collection and sharing methodologies. We suggest the development of common data collection protocols, data sharing initiatives, and collaboration to establish a cohesive framework.

Investigating the Interference Induced by NGSO Constellations on GSO System Ground Stations: A Simulation Approach 98

[Enrico Polo](#) (Politecnico di Milano, Italy); Luis D. Emiliani (SES S.A., Luxembourg); Lorenzo Luini (Politecnico di Milano, Italy)

This contribution describes the development and application of a physically-based simulator to investigate the interference caused by NGSO satellite constellations onto GSO fixed-satellite services. The simulator calculates the yearly statistics of the Carrier to Interference Ratio (CI) of the gateway link of a GSO system ground station, considering all the variables at play, including the impact of precipitation. The analysis relies on the principle of protection of GSO systems by means of an exclusion zone, defined via an avoidance angle (α) and limiting the maximum number of NGSO satellites that can concurrently transmit in the area of the GSO ground station, Max_co_freq . Preliminary results, reported as a function of α and Max_co_freq , show the usefulness of the CI results to design future NGSO constellations while limiting their impact on GSO systems.

Annual Statistics from 5 Years of 1-Minute Rainfall Rate Measurements at a Specific Site in Bolivia 104

[Gustavo Siles](#) and Noelia Ayllon (Universidad Privada Boliviana, Bolivia)

1-minute precipitation data is crucial for evaluating the accuracy of rainfall rate prediction methods. In this paper, we present findings after conducting a 5-year rainfall rate measurement campaign at a single site in Bolivia, spanning from September 2018 to August 2023. Additionally, we utilized 6 years of 15-minute rainfall data from a nearby site. The widely-accepted EXCELL RCS model, with slight adjustments to account for the specific geographical characteristics of the study area, was applied to convert rainfall rate cumulative distributions from 15-minutes to 1-minute. The accuracy analysis performed reveals that long-term statistics of rain intensity predicted by the currently adopted version of the ITU-R P.837 model closely match the experimental results. The results indicate that the mean and RMS values of the relative error remain below 10%. This similarity is particularly notable when we incorporate monthly mean local values of surface temperature and rainfall amounts into the ITU-R model.

Comparison Between ERA5 Cloud Parameters and Rainfall Rate in Madrid 106

[Ana Benarroch](#) (Universidad Politécnica de Madrid, Spain); Gustavo Siles and Mishel Cuiza (Universidad Privada Boliviana, Bolivia); Jose M Riera (Universidad Politécnica de Madrid, Spain)

This ongoing study, conducted at UPM, investigates the relationship between rainfall rate and cloud parameters, leveraging data sourced from ERA5 and experimental rainfall rate measurements collected with a disdrometer. The findings presented in this paper have been obtained using a comprehensive dataset spanning 6 years, including total cloud liquid water, cloud base height, total cloud cover, and rainfall rate. The statistical analysis presented comprises cumulative distributions, histograms, as well as scatter plots of the ERA5 cloud parameters against both the hourly average and maximum hourly rainfall rates. It has been found that low values of total cloud liquid water and cloud base height are more probable with simultaneous rain occurrence, whereas total cloud cover yields values equal or close to one, which is its highest value.

Wednesday, March 20 13:10 - 14:40

WG Propagation: WG meeting

Room: M4

Wednesday, March 20 13:10 - 14:40

CM-SI: CM-SIG Characteristic Modes Special Interest Group.

//

Room: Fyne

Wednesday, March 20 14:40 - 15:20

IN5: Terahertz Antennas and Systems for Space Applications; Dr. Goutam Chattopadhyay, NASA-JPL, USA

//

Room: Lomond Auditorium

Chairs: Mauro Ettore (University of Rennes 1 & UMR CNRS 6164, France), Jiro Hirokawa (Tokyo Institute of Technology, Japan)

Wednesday, March 20 14:40 - 15:20

IN7: Spaceborne antenna testing: Status, Perspectives and Challenges; Dr. Luis Rolo, ESTEC, ESA, The Netherlands

//

Room: M1

Chairs: Olav Breinbjerg (EIMaReCo, Denmark), Lars Foged (Microwave Vision Italy, Italy)

Wednesday, March 20 15:20 - 16:00

IN6: Quasi-Optical Antenna Systems for THz Communications and Sensing; Prof. Nuria Llombart, Tu Delft, Netherlands

//

Room: Lomond Auditorium

Chairs: Mauro Ettore (University of Rennes 1 & UMR CNRS 6164, France), Jiro Hirokawa (Tokyo Institute of Technology, Japan)

Wednesday, March 20 15:20 - 16:00

IN8: How Compressive Sensing Approaches Can Enhance RF Hardware Capability; Dr. Brian E. Fischer, Resonant Sciences, USA

//

Room: M1

Chairs: Olav Breinbjerg (EIMaReCo, Denmark), Lars Foged (Microwave Vision Italy, Italy)

Wednesday, March 20 16:30 - 18:10

SWM: In Memory of Ross Stone

//

Room: Lomond Auditorium

Chairs: Stefania Monni (TNO Defence Security and Safety, The Netherlands), Branislav Notaros (Colorado State University at Fort Collins, USA)

Time	Duration	Title	Presenter(s)	Institute
16:30	5 mins	Introductory remarks	Stefania Monni (EurAAP); Branislav Notaros (IEEE AP-S)	
16:35	15 mins	Ross contribution to IEEE AP-S	Branislav Notaros	IEEE AP-S
16:50	15 mins	Ross contribution to EurAAP	Stefania Monni; Cyril Mangelot	EurAAP
17:05	15 min	Ross contribution to URSI	Peter van Daele	URSI
17:20	15 min	Ross contribution to RoE	Oscar Quevedo Teruel	EurAAP
17:35	15 mins	Ross contribution to IEEE AP-S, ESoA	Stefano Maci	IEEE AP-S, EurAAP
17:50	15 mins	Ross family memory	Sue Stone	
18:05	10 mins	Remembering Ross, conversation with the audience	All	

Wednesday, March 20 16:30 - 18:10

M3: Innovative Approaches for Antenna Measurements

T09 Fundamental research and emerging technologies // Measurements

Room: M1

Chairs: Stuart F Gregson (Queen Mary, University of London, United Kingdom (Great Britain)), Shintaro Hisatake (Gifu University, Japan)

16:30 *Enhancing THz Antenna Characterization Precision in WR-1.5 Band Using Vacuum Waveguide Flange*

[Marius Kretschmann](#) (Karlsruhe Institute of Technology, Germany); [Thomas Zwick](#) (Karlsruhe Institute of Technology (KIT), Germany); [Akanksha Bhutani](#) (Karlsruhe Institute of Technology, Germany)

Measurement fixture for free-space characterization of dielectric resonator antennas up to the THz frequency range is presented. By using a modified waveguide flange with vacuum channels, environmental influences in the half-space of the antenna are minimized. The concept is verified by characterizing a dielectric resonator antenna in the WR-1.5 frequency band. S-parameters of the vacuum flange are measured to perform a de-embedding of the RF losses of the holder.

16:50 *A Demonstration of Diffraction-Limited Images Using a CMOS Chessboard Array at THz Frequencies*

[Martijn Hoogelander](#), [Robbin van Dijk](#), [Nuria LLombart](#), [Marco Spirito](#) and [Maria Alonso-delPino](#) (Delft University of Technology, The Netherlands)

This paper presents the diffraction-limited terahertz imaging capabilities of a silicon-integrated focal plane array (FPA) of antenna-coupled direct-detectors. The FPA prototype is a tightly sampled, 12-pixel array that was developed in a 22 nm CMOS technology and covers a relative bandwidth of 3:1, from 200 GHz to 600 GHz. A quasi-optical (QO) system has been developed to realize images with a dynamic range of 25dB, a resolution of 2.1 mm and a beam overlap around 1.4 dB at 400GHz. The images created by this QO system will be the first demonstration of a diffraction-limited FPA imager at THz frequencies, making it very attractive for future commercial THz imaging applications.

17:10 *Dielectric Characterization of Adhesives for THz Packaging in WR6.5, WR3.4 and WR2.2 Bands*

[Georg Gramlich](#) and [Kilian Speder](#) (Karlsruhe Institute of Technology, Germany); [Martin Roemhild](#) (University of Stuttgart, Germany); [Holger Baur](#) (University Stuttgart, Germany); [Norbert Fruehauf](#) (University of Stuttgart, Germany); [Thomas Zwick](#) (Karlsruhe Institute of Technology (KIT), Germany); [Akanksha Bhutani](#) (Karlsruhe Institute of Technology, Germany)

This study presents, for the first time to our knowledge, measurements of permittivity and loss tangent ranging from 110 GHz to 500 GHz for technical adhesives. Measurements were conducted using the material characterization kits by Swissto12. To ensure a high accuracy, the samples were carefully prepared to achieve optimal surface parallelism, since any deviation in thickness measurement directly affects the derived values of permittivity and loss tangent. For validation purposes, we measured reference materials and benchmarked our findings against independent research, proving the precision of our measurements. Our observations showed nearly constant permittivity in the WR 6.5, WR 3.4, and WR 2.2 bands for all adhesives. Specifically, for UV adhesives NEA 121 and NEA 123M, as well as the single-component epoxy EP501, a permittivity of 3.0 was identified, while for the two-component epoxy Duralco 4460, an ϵ_r of 2.8 was determined.

17:30 *Numerical Assessment of a Cognitive Chamber: TMz Case*

[Christophe Craeye](#) (Université Catholique de Louvain, Belgium); [Sidina Wane](#) (eV-Technologies, France); [Khalidoun Alkhalifeh](#) and [Denis Tihon](#) (Université Catholique de Louvain, Belgium)

A numerical analysis based on the Method of Moments is conducted to study the feasibility of absorbing chambers made of arrays of metallic elements, named here as cognitive chambers. The array is covering the inner surface of a perfectly conducting cylindrical shield. The analysis is so far limited to the TM^z case. Very low perturbation of the field from a device under test, represented by a collection of axial dipoles is observed. The non-disturbance of the incident fields correlates well with a criterion based on the active impedance. A significant dependence of the optimal load impedance versus azimuthal and axial modes has been observed.

17:50 *Highly Precised and Efficient Robot-Based ESPAR Antenna Measurements in Realistic Environments*

[Mateusz Groth](#), [Kamil Domanski](#), [Krzysztof Nyka](#) and [Lukasz Kulas](#) (Gdansk University of Technology, Poland)

In this paper, we present a novel approach utilizing a small Unmanned Surface Vehicle (USV) equipped with Global Navigation Satellite System (GNSS) technology to facilitate large-scale outdoor automated measurements. The system employs dedicated software and measurement scripts to autonomously navigate the robot along predefined routes, stopping at multiple points for data collection. This method minimizes observational error and enables the efficient verification and validation of DoA and positioning algorithms. We provide a detailed overview of the robot's architecture, operating modes, and system performance, demonstrating its capability to achieve high accuracy and repeatability in measurements. Additionally, we present results from a DoA estimation experiment using an electronically steerable parasitic array radiator (ESPAR) antenna, showcasing the system's ability to provide precise and consistent measurements across various transmission module heights.

Wednesday, March 20 16:30 - 18:10

CS34: Propagation measurements and modelling for RIS-aided wireless communications

T01 Sub-6 GHz for terrestrial networks (5G/6G) / Convened Session / Propagation

Room: Alsh 1

Chairs: [Placido Mursia](#) (NEC Laboratories Europe GmbH, Germany), [Enrico M. Vitucci](#) (University of Bologna, Italy)

16:30 *RIS with Practical Reflection Coefficients: Modeling and Experimental Measurements*

[Lin Cao](#), [Haifan Yin](#), [Xilong Pei](#) and [Li Tan](#) (Huazhong University of Science and Technology, China)

In this paper, we consider reconfigurable intelligent surfaces (RIS)-aided wireless communication systems, where the reflection coefficients suffer from the realistic limitations of non-uniform amplitudes and insufficient phase shifting capabilities. We introduce a reflection coefficient model for RIS based on measurements, accounting for these practical factors. We then propose a group-based query algorithm that takes the imperfect coefficients into consideration while calculating the reflection coefficients. We analyze the performance of the proposed algorithm and derive a closed-form expression of the received power. The performance gains of our proposed algorithm are confirmed in simulations. Finally, we validate the proposed theoretical results by experiments with our fabricated RIS prototype system. The simulation and measurement results match well with the theoretical analysis.

16:50 *An Automated Over-The-Air Radiated Testing Platform for Reconfigurable Intelligent Surface*

[Yifa Li](#) (Aalborg University, USA); [Fengchun Zhang](#), [Kim Olesen](#), [Ying Zhinong](#) and [Gert Pedersen](#) (Aalborg University, Denmark); [Wei Fan](#) (Southeast University, China)

Inquest to enhance wireless communication capabilities, reconfigurable intelligent surface (RIS) has emerged as a technology of immense promise. Armed with the beamforming capabilities, RIS can intelligently engineer and control wireless propagation environments. Consequently, an in-depth knowledge of RIS radiation characteristics has become important. This paper presents an automated over-the-air (OTA) radiated testing platform designed for characterizing RIS radiation. Operating in an anechoic chamber setup in a fully automated manner, the platform system utilizes multiple probes to expedite testing and employs a vector network analyzer (VNA) for testing signal measurement and recording. Controlled by a programmed controller, the system efficiently manages RIS operation with predefined code-book while the controller directs the system to conduct radiation measurements. To validate the designed testing platform system, RIS beam steering radiation measurements were conducted using a 2-bit 10×10 RIS. The measured results demonstrate the capabilities and reliability of the automated testing system.

17:10 *Validating Properties of RIS Channel Models with Prototypical Measurements*

[Kevin Weinberger](#) (Ruhr-Universität Bochum, Germany); [Simon Tewes](#) (Ruhr-Universität Bochum, Germany); [Aydin Sezgin](#) (RUB, Germany)

The integration of Reconfigurable Intelligent Surfaces (RIS) holds substantial promise for revolutionizing 6G wireless networks, offering unprecedented capabilities for real-time control over communication environments. However, determining optimal RIS configurations remains a pivotal challenge, necessitating the development of accurate analytical models. While theoretically derived models provide valuable insights, their potentially idealistic assumptions do not always translate well to practical measurements. This becomes especially problematic in mobile environments, where signals arrive from various directions. This study deploys an RIS prototype on a turntable, capturing the RIS channels' dependency on the angle of incoming signals. The difference between theory and practice is bridged by refining a model with angle-dependent reflection coefficients. The improved model exhibits a significantly closer alignment with real-world measurements. Analysis of the reflect coefficients reveals that non-perpendicular receiver angles can induce an additional attenuation of up to -14.5dB. Additionally, we note significant phase shift deviations, varying for each reflect element.

17:30 Empirical Validation of the Impedance-Based RIS Channel Model in an Indoor Scattering Environment

Placido Mursia (NEC Laboratories Europe GmbH, Germany); Taghrid Mazloum (CEA- LETI, France); Frederic Munoz (CEA LETI & University of Grenoble-Alpes, France); Vincenzo Sciancalepore (NEC Laboratories Europe GmbH, Germany); Gabriele Gradoni (University of Surrey, United Kingdom (Great Britain)); Raffaele D'Errico (CEA, LETI & Université Grenoble-Alpes, France); Marco Di Renzo (Paris-Saclay University / CNRS, France); Xavier Costa-Perez (ICREA and i2cat & NEC Laboratories Europe, Spain); Antonio Clemente (CEA-Leti, France); Geoffroy Lerosey (Greenewave, France)

Ensuring the precision of channel modeling plays a pivotal role in the development of wireless communication systems, and this requirement remains a persistent challenge within the realm of networks supported by Reconfigurable Intelligent Surfaces (RIS). Achieving a comprehensive and reliable understanding of channel behavior in RIS-aided networks is an ongoing and complex issue that demands further exploration. In this paper, we empirically validate a recently-proposed impedance-based RIS channel model that accounts for the mutual coupling at the antenna array and precisely models the presence of scattering objects within the environment as a discrete array of loaded dipoles. To this end, we exploit real-life channel measurements collected in an office environment to demonstrate the validity of such a model and its applicability in a practical scenario. Finally, we provide numerical results demonstrating that designing the RIS configuration based upon such model leads to superior performance as compared to reference schemes.

17:50 RIS Performance in a Comprehensive Fading Environment

Pedro Marcio Raposo Pereira (National Institute of Telecommunications, Brazil); Rausley Adriano Amaral de Souza (National Institute of Telecommunications (INATEL), Brazil); Michel Daoud Yacoub (State University of Campinas, Brazil); Yonghui Li (University of Sydney, Australia)

Recent years have witnessed the emergence of reconfigurable intelligent surfaces (RISs) as a promising technology that can enhance the wireless communication performance by softening the harshness of the propagation conditions of the environment. However, the impact of mobility on RIS-assisted communication systems remains a critical yet understudied aspect. In this article, we conduct a comprehensive analysis of RIS-enabled systems under various fading conditions, considering the influence of phase noise and the role of the direct channel. We investigate scenarios with both static and mobile receiving terminals, highlighting the interplay between fading, phase noise, and the effects of the direct channel. Our findings reveal the significance of effectively managing phase noise to optimize RIS configurations, whose vulnerability becomes more evident in the presence of higher order modulations.

Wednesday, March 20 16:30 - 18:10

P09: Rain attenuation

T02 Mm-wave for terrestrial networks 5G/6G // Propagation

Room: Alsh 2

Chairs: Ana Benarroch (Universidad Politécnica de Madrid, Spain), Lorenzo Luini (Politecnico di Milano, Italy)

16:30 Variability of Rain Attenuation at Millimeter Waves Due to Fluctuations of the Drop Size Distribution

Leyre Egozcue-Angulo (Universidad Politécnica de Madrid, Spain); Ignacio Mata-Alonso (Universidad Politecnica de Madrid, Spain); Jose M Riera, Domingo Pimenta-del-Valle and Ana Benarroch (Universidad Politécnica de Madrid, Spain)

Rain attenuation at millimeter waves is progressively more influenced by the Drop Size Distributions (DSD) as the frequency gets higher. This paper continues the work carried out on DSD data gathered in Madrid, Spain, over a long period of 15 years. Rain specific attenuation in the frequency range 30-300 GHz has been calculated using the DSD data and extinction cross-sections obtained for horizontal and vertical polarization using electromagnetic simulations. Previous results showed a significant variability around its reference value obtained from the rainfall rate. This variability was attributed to DSD fluctuations. This attribution is analyzed in the present study, that addresses three additional aspects: the relation between the variability parameter V and the rainfall rate; the average DSD obtained for different ranges of V ; and finally the seasonal variations of the two previous ones. The paper includes some examples of application of the Gaussian model proposed for the parameter V .

16:50 Rain Attenuation at Millimeter Waves in Different Climatic Zones Estimated from Drop Size Distributions

Ignacio Mata-Alonso (Universidad Politecnica de Madrid, Spain); Jose M Riera (Universidad Politécnica de Madrid, Spain); Lorenzo Luini (Politecnico di Milano, Italy); Hong Yin Lam (Universiti Tun Hussein Onn Malaysia, Malaysia); Domingo Pimenta-del-Valle (Universidad Politécnica de Madrid, Spain)

Rain attenuation at millimeter waves is progressively more influenced by the Drop Size Distributions (DSD). In this paper, DSD data collected in Madrid, Spain, with continental climate; Milan, Italy, with Mediterranean climate; and Kuala Lumpur, Malaysia, with tropical climate are used to study this effect. The first two sites use the same model of laser disdrometer whereas the equipment available at Kuala Lumpur is an impact disdrometer. Rain specific attenuation at different frequencies (30-300 GHz) as well as rainfall rate have been calculated. The data have then been used to assess the validity of the ITU-R Rec. P.838-3 model. Results show that the ITU-R model tends to underestimate the specific attenuation, and confirm a significant variability around its reference value obtained from the rainfall rate, with a similar extent in Madrid and Milan, and a different trend in Kuala Lumpur, attributed to the different disdrometer and to the tropical climate.

17:10 Ka-Band Rain Attenuation Derived from a MEO Satellite Constellation

Lorenzo Luini, Carlo Riva, Francesco Capelletti and Alef Comisso (Politecnico di Milano, Italy); Armando Rocha (University of Aveiro & Instituto de Telecomunicações, Portugal); Susana Mota (University of Aveiro & Institute of Telecommunications, Portugal); Marlene Gomes Brás (University of Aveiro and Institute of Telecommunications, Portugal); Marianna Biscarini and Stefano Barbieri (Sapienza University of Rome, Italy); Fernando Consalvi (FUB, Italy); Antonio Martellucci (European Space Agency, The Netherlands)

A procedure to extract rain attenuation from MEO satellite signals is presented in the framework of MEKaP (MEO Ka-band Propagation), a European Space Agency (ESA) funded project. This task, far from being a trivial one, involves removing from the received signal the effects induced by the presence of gases along the path, by the change in the distance to the satellite and by the variation of the onboard antenna gain as perceived at the ground station. To this aim, ancillary data are exploited, such as satellite ephemeris, ERA5 products and some basic information on the onboard antenna. Some preliminary examples of the rain attenuation derived in three sites with different climatic conditions (Milan and Rome, Italy; Aveiro, Portugal) are reported, showing the effectiveness of the proposed procedure, which will be applied to all the data collected during the experimental campaign (from 1/1/2022 to 31/12/2023) to produce rain attenuation statistics.

17:30 Rain Attenuation at mmWave and Optical Bands from Visibility and Rainfall Intensity Measurements

Elizabeth Verdugo (Consiglio Nazionale delle Ricerche, Italy & PUC RIO, Brazil); Lorenzo Luini and Carlo Riva (Politecnico di Milano, Italy); Luiz da Silva Mello (CETUC-PUC-Rio & Inmetro, Brazil); Laura Resteghini (Huawei Technologies, European Research Center, Italy); Renato Lombardi (Milan Microwave Competence Center, Italy); Angelo Milani (Huawei Technologies, Italy); Roberto Nebuloni (Ieiiit - Cnr, Italy)

Wireless communications at very high frequencies from mmWave to Free-Space Optics (FSO) dramatically increase link capacity, but their performance falls under adverse weather. Existing global models for rain attenuation, such as the Rec. ITU-R 838-3 are straightforward as they rely on statistics of rainfall intensity only, but they do not capture the complexity of rain microphysics. This study investigates the potential of visibility measurements to enhance the understanding of rain attenuation. Specifically, we show the preliminary results of an experimental study in Milan started in late 2022 involving collocated E-band (83 GHz) and FSO links (1.550 μm) as well as visibility and rainfall sensors on either side of the links. Rainfall intensity and visibility, though correlated, get scattered during heavy rain, probably due to the microphysical effects. Moreover, the accuracy of mmWave and FSO rainfall attenuation from visibility and rainfall is comparable.

17:50 Predicting Rain Attenuation at D Band for 6G Backhaul Link Design: A Frequency Scaling Approach

Francesco Capelletti (Politecnico di Milano, Italy); Giuseppe Roveda (Huawei Microwave Centre, Italy); Roberto Nebuloni (Ieiiit - Cnr, Italy); Lorenzo Luini (Politecnico di Milano, Italy)

A frequency scaling model is presented for predicting rain-induced attenuation affecting a short terrestrial link operating at D band, to be potentially used as backhaul link in future sixth generation (6G) networks. The methodology, which aims at estimating rain attenuation at a target higher frequency from measurements collected at a lower band, requires as input local rain rate time series and defines a scaling ratio dependent on

the specific attenuations at the two frequencies. Data from a long-term propagation study, conducted in collaboration between Politecnico di Milano and Huawei, are employed to assess the accuracy of the proposed model in scaling rain attenuation from E band (83 GHz) to D band (156 GHz). Results indicate high prediction accuracy. This corroborates its use as a tool to fill the current lack of tropospheric impairment data at carrier frequencies not currently licensed but to be potentially employed in the upcoming 6G networks.

Wednesday, March 20 16:30 - 18:10

A07: Lens antennas

T03 Aerospace, new space and non-terrestrial networks // Antennas

Room: Boisdale 1

Chairs: Erio Gandini (ESA - European Space Agency, The Netherlands), Andrea Neto (Delft University of Technology, The Netherlands)

16:30 A Wideband Half-Circle Metasurface Augmented Luneburg Lens for Millimeter-Wave Applications

Bader Alali (Queen's University Belfast, United Kingdom (Great Britain)); Dmitry E Zelenchuk (Queen's University of Belfast, United Kingdom (Great Britain)); Muhammad Ali Babar Abbasi (Queen's University Belfast & The Institute of Electronics, Communications and Information Technology (ECIT), United Kingdom (Great Britain)); Irina Munina (Trinity College Dublin, Ireland)

This paper presents a method for the design of a wideband two-dimensional (2D) metasurface Luneburg lens antenna optimized for millimeter-wave (mm-wave) applications. The metasurface, with overall dimensions of 12 x 200 mm, operates in a reflective mode and consists of an 80-element array of Phoenix unit cells. We demonstrated that the 2D metasurface Luneburg lens antenna can steer the radiated beam with a wideband performance of 24-38 GHz. It is shown that the steering angle can be controlled to a desired direction within an angular range of 75 degrees, contingent on the distribution of phasing elements and the position of the feeding source. In specific cases, we demonstrate beam-steering towards 0, 30, and 45 degrees, achieved when the feeding source is oriented at -15 degrees as well as towards 0, 15, and 45 degrees achieved when the feeding source is oriented at -30 degrees.

16:50 Metal-Only Additive-Manufactured Geodesic Lens Antennas for the mmWave Band

Jose Rico-Fernandez (Northern Waves AB, Sweden); Pilar Castillo-Tapia, Sarah E Clendinning, Qiao Chen and Oscar Quevedo-Teruel (KTH Royal Institute of Technology, Sweden)

This paper evaluates the suitability of additive manufacturing, with AlSi10Mg using the Laser Powder-Bed Fusion (LPBF) technique, for geodesic lens antennas. This evaluation is carried out with three different geodesic lens antennas operating in Ka-, V- and G-band. In the Ka-band, an elliptically-compressed geodesic lens antenna was designed, manufactured and tested; in the V-band, the experimental results of a geodesic lens array antenna composed of four elements are shown. These two designs were manufactured monolithically to avoid leakage and misalignment between the plates. Finally, the challenges of additive manufacturing at G-band are discussed. A dual-polarized geodesic Luneburg lens antenna working at 122.5 GHz has been produced in three parts, so polishing can be carried out to reduce the surface roughness. The overall results corroborate that additive manufacturing with the LPBF technique is a promising method to produce metal-only solutions for geodesic lens antennas in the millimetre-wave regime.

17:10 On the Design of Wide-Scanning Lenses with Integrated Focal Arrays

Dunja Lončarević, Shahab Oddin Dabironezare, Andrea Neto and Nuria LLombart (Delft University of Technology, The Netherlands)

The optimization of an integrated homogeneous lens over a wide angular region (-60,60)° is presented. The optimization is conducted in terms of the aperture efficiency which is obtained by resorting to the antenna in reception methodology. The optimization procedure is sequential. Firstly, the shape of the lens is optimized for 30° scanning, and then the position of the feed and its tilt are optimized for such fixed lens shape. The reported results show that a nearly-flat aperture efficiency is achieved for wide-angle scanning for different values of the permittivity and the diameter of the lens. In order to compare the explored integrated homogeneous lens design with the spherical lenses found in literature, the aperture efficiency with respect to the antenna aperture as a whole is defined. With this metric, it is shown that for a fixed volume the presented design achieves higher aperture efficiency, owing to the integrated focal array.

17:30 Fully Metallic Wideband Lens Design Using a Highly Refractive Glide-Symmetric Unit Cell at W-Band

Sergio Garcia-Martinez (Universidad Politécnica de Madrid, Spain); Adrián Tamayo-Domínguez and Pablo Sanchez-Olivares (Universidad Politécnica de Madrid, Spain)

This paper presents the design of Luneburg lens at W-band using a fully metallic periodic structure. The use of glide symmetry in the unit cell produces a highly isotropic behavior; however, conventional shaped holes such as circular and square holes do not present a sufficient refractive index for the design of this type of lenses. A cross-shaped hole is proposed to significantly increase the obtainable refractive index while maintaining an isotropic behavior. By terminating the holey metasurface with a flare and feeding it with multiple waveguides, a high efficiency multibeam antenna with 45° scanning range is achieved without scanning losses.

17:50 A Cylindrical Mismatched Luneburg Lens Implemented on PCB at V-Band

Vincent Kaschten, Dimitri Lederer and Christophe Craeye (Université Catholique de Louvain, Belgium)

We implement a cylindrical mismatched Luneburg lens at V-band, following the related theory and design rules. The lens has a relative dielectric permittivity of 2.6 at its edge, while the exterior medium is air. The implementation is done on a Printed Circuit Board, and includes the lens itself as well as Substrate-Integrated Waveguides acting as feeds and a transition from Grounded Co-planar Waveguide transmission lines to the feeds. The whole structure is fabricated as a single-piece board with standard processes. Measurements confirm that this design can produce a fan-shaped beam at multiple excitation points covering a 40 degrees angular range.

Wednesday, March 20 16:30 - 18:10

E04: Electromagnetic Imaging

T04 RF sensing for automotive, security, IoT, and other applications // Electromagnetics

Room: Boisdale 2

Chairs: Ilaria Catapano (IREA-CNR, Italy), Francesca Vipiana (Politecnico di Torino, Italy)

16:30 Towards Optimal Binary Patterns for Compressive Terahertz Single-Pixel Imaging

Adolphe Ndagijimana (Public University of Navarre, Spain); Iñigo Ederra (Universidad Pública de Navarra & Institute of Smart Cities, Universidad Pública de Navarra, Spain); Miquel Heredia Conde (Center for Sensorsystems (ZESS), University of Siegen, Germany)

Terahertz (THz) radiation's properties make it ideal for various imaging applications. However, creating simple, cost-effective, and high-resolution THz array detectors is challenging. Mechanical scanning is commonly used but creates a trade-off between frame rate and resolution. Fortunately, Compressive Sensing (CS) offers a solution by reducing the required number of measurements needed compared to Shannon-Nyquist's sampling theory. CS-THz imaging is usually implemented using a single-pixel camera with spatial modulation patterns, mostly binary patterns. However, the non-uniform and diffraction propagation present in the THz range affects the mutual coherence of the resulting sensing matrices resulting in image reconstruction degradation. In this paper, we introduce an optimization procedure for generating binary patterns that consider THz diffraction and non-uniform illumination of the mask. The produced sensing matrices exhibit low coherence compared to other typical binary sensing matrices, resulting in a higher reconstruction performance than all others.

16:50 *Contactless 3D Subsurface Imaging: Considerations to Set the Measurement Spacing*

Gianluca Gennarelli, Giovanni Ludeno and Giuseppe Esposito (IREA-CNR, Italy); Rosa Scapatucci (CNR-National Research Council of Italy, Italy); Francesco Soldovieri (CNR, Italy); Ilaria Catapano (IREA-CNR, Italy)

Nowadays, contactless subsurface imaging deserves huge attention thanks to the availability of autonomous moving platforms, which simplify and speed up the measurement stage. However, some constraints arise on the number of scattered field samples that can be collected and thus on the achievable imaging capabilities. By focusing the attention on the three-dimensional imaging performed using a multi-monostatic ground penetrating radar system, this communication deals with a criterion to properly define the spatial offset among the measurement points. Synthetic data are used to assess the effectiveness of the provided criterion and investigate how the data under-sampling affects the imaging performance.

17:10 *A Case Study of Misalignment Errors for Range-Migration-Based Microwave Imaging with Multistatic Dynamic Metasurface Apertures*

[Vasiliki Skouroliakou](#), Amir Masoud Molaei, María García Fernández, Guillermo Alvarez Narciandi and Okan Yurduseven (Queen's University Belfast, United Kingdom (Great Britain))

In this paper, we study the effect of antenna positioning errors for a multiple-input multiple-output (MIMO) dynamic metasurface aperture (DMA) system. In this case, the term antenna refers to transmitting or receiving DMA panels that comprise the imaging system. The range migration algorithm (RMA) along with a multistatic-to-monostatic (MTM) interpolation step is employed to address the image reconstruction step. Both the RMA and the MTM steps entail knowledge of the precise locations of the panels with respect of the center of the investigation domain. However, in practical applications, this requirement is not always met and displacement errors can be present. In this work, we study the behavior of the proposed DMA-based multiple-input multiple-output (MIMO) computational imaging (CI) system and image reconstruction algorithm under various range displacement or rotational errors.

17:30 *GPR Imaging Relying on Frequency-Diverse Compressive Antennas*

[María García Fernández](#), Guillermo Alvarez Narciandi and Okan Yurduseven (Queen's University Belfast, United Kingdom (Great Britain))

Ground penetrating radar (GPR) systems have demonstrated their ability to successfully detect both metallic and non-metallic targets, making them very attractive for multiple applications. In addition, the use of synthetic aperture radar (SAR) techniques enables GPR systems to retrieve high-resolution images of buried targets. However, the dense sampling required by GPR-SAR systems limits their survey speed or results in high-complexity hardware. Computational imaging (CI) has emerged as a promising alternative to overcome some of the drawbacks of SAR-based systems. CI enables a significantly faster survey relying on compressive antennas that compress the scene information into a single channel (or a reduced number of them). This contribution proposes, for the first time, the idea of resorting to CI for GPR, and presents a frequency-diverse compressive antenna specifically tailored for GPR applications working at S- and C-bands. In addition, the feasibility of imaging buried targets from a single acquisition is successfully demonstrated.

17:50 *Preliminary Description of a 2D Near-Field Electromagnetic Imaging Database*

Seth J Cathers, Ben J Martin, Noah Stieler, Ian Jeffrey and Colin Gilmore (University of Manitoba, Canada)

With the goal of improving machine learning approaches in inverse scattering, we overview an experimental data set collected with a near-field microwave imaging system. Machine learning approaches often train solely on synthetic data, and one of the reasons for this is that no experimentally-derived public data set exists. The imaging system consists of 24 antennas surrounding the imaging region, connected via a switch to a vector network analyzer. The data set contains over 1000 full Scattering parameter scans of three targets from 3-5 GHz. In this work, we show preliminary results of a direct data-to-image inversion algorithm.

Wednesday, March 20 16:30 - 18:10

CS21: mm-Wave Antennas for Radar Applications

T05 Positioning, localization, identification & tracking / Convened Session / Antennas

Room: Carron 1

Chairs: Marta Martínez-Vázquez (Renesas Electronics, Germany), Eva Rajo-Iglesias (University Carlos III of Madrid, Spain)

16:30 *Imaging Radar Frontend with SIW Feeding Networks*

Marta Martínez-Vázquez and Stephan Renner (Renesas Electronics, Germany); Rakesh Kumar, Alok Prakash Joshi and Anamika Verma (Renesas Electronics, India); Akshay Ashok Hublikar (Renesas Electronics, India)

Using radar for imaging implies increasing the number of transmit and receive channels, which complicates the routing of the signals to the antennas. This paper shows a practical implementation of a 12x12 imaging radar with patch antennas using SIW lines to optimize the performance.

16:50 *New Efficient Waveguide Antenna for Future Automotive Radar Applications*

Simona Bruni, Markus Krengel, Oliver Litschke and Aline Friedrich (IMST GmbH, Germany); Marta Martínez-Vázquez (Renesas Electronics, Germany)

This paper presents the design and the realized prototype of a slotted air-waveguide antenna based on a new technology concept. The antenna is designed combining standard Printed Circuit Board technology (PCB) and a metal frame to cover the 76-81 GHz band for automotive radar applications. Although low cost PCBs are used, the performance of the antenna is comparable to that of a slotted air waveguide antenna. It will be shown that this concept can be used on the next generation MMICs with launcher in package.

17:10 *From mmWave Radar Nodes to Multistatic Arrays: Design Considerations and Applications*

[Ignacio Sardinero-Meirás](#), Ignacio E. López-Delgado and Elías Antolinos (Universidad Politécnica de Madrid, Spain); Francisco N. Pérez-Fernández (Universidad Politécnica de Madrid & Georgia Institute of Technology, Spain); Marta Ferreras (Universidad Politécnica de Madrid, Spain); Lorena María Pérez-Eijo (Universidade de Vigo, Spain); Marcos Arias and Borja Gonzalez-Valdes (University of Vigo, Spain); Jesús Grajal (Universidad Politécnica de Madrid, Spain)

The potential of single-node mmWave radar systems can be expanded with more sophisticated configurations: multi-frequency, multistatic, or phased-array radars. Several radar nodes have been designed with emphasis on transitioning to multistatic or phased-array configurations. This approach involves addressing critical factors often overlooked by commercial radar systems, including synchronization and data handling. This paper presents a 120 GHz phased-array radar, comprising 15 individual nodes. Additionally, we highlight the potential advantages of incorporating phased-arrays and multistatic radars in biomedical and structural health monitoring applications.

17:30 *Low-Cost Coaxial Slot Array Antenna for E-Band Automotive Corner Radar Applications Based on Gap Waveguide MLW Technology*

[Juan Luis Albadalejo Lijarcio](#) (Chalmers University of Technology & Gapwaves AB, Sweden); Abbas Vosoogh and Carlo Bencivenni (Gapwaves AB, Sweden); Ashraf Uz Zaman (Chalmers University of Technology, Sweden)

This paper presents an E-band automotive radar antenna based on multilayer waveguide (MLW) technology. The electromagnetic fields propagate through a low-loss air-filled coaxial transmission line created by the stacking of three separate metal sheets. The fundamental antenna element consist of a single side-fed column composed of six in-line slots. An electromagnetic bandgap (EBG) structure is integrated along the transmission lines in order to mitigate the unwanted leakage resulting from small air-gaps between the metal sheets. The fabrication of the prototype was realized by using the quick and cost-effective 3D chemical etching process, which has proven to be highly suitable for large-scale production. The measurement results for both radiation pattern and reflection coefficient exhibit a good agreement with the corresponding simulations within the operating frequency band ranging from 76 to 81 GHz.

17:50 *Effects of Bumper Integration on Low-, Mid-, and High-Resolution Imaging Radars*

[Dominik Schwarz](#), Matthias Linder, Ron Riekenbrauck and Robin Bord (Ulm University, Germany); Christian Waldschmidt (University of Ulm, Germany)

Radar sensors are widely used for driver assistance systems as they enable an accurate perception of the surroundings. Typically, the sensors are hidden behind bumpers or radomes. Since the bumper affects not only the receive power but also the DoA estimation, the bumper is typically taken into account in the calibration. Thus, a re-calibration is required after a bumper change or paint job. In this work, the influence of the bumper on the DoA estimation performance and radar image quality is compared for low-, mid-, and high-resolution sensors. As reference, a setup without bumper is deployed and no re-calibrations are conducted. The degradation due to a muddy bumper that cannot be included in the calibration is analyzed. In all cases, the high-resolution radar shows the greatest robustness, with a DoA estimation error of only 0.2° for the muddy bumper, compared to 0.8° and 22° for the mid- and low-resolution sensor.

Wednesday, March 20 16:30 - 18:10

P06: Body propagation, sensing and communication

T06 Biomedical and health // Propagation

Room: Carron 2

Chairs: Joao M. Felicio (Escola Naval, Portugal & CINAV - Instituto de Telecomunicacoes, Portugal), Pyry Kiviharju (Aalto University, Finland)

16:30 Localization of a Nasogastric Feeding Tube Using High-Frequency Harmonic Radar - a Feasibility Study

Lieke A. M. Geubbels, Ad Reniers and Rob Mestrom (Eindhoven University of Technology, The Netherlands)

Certain patients, for instance, preterm born babies (neonates), are not capable of feeding themselves. These patients can be helped by getting enteral nutrition by means of a nasogastric feeding tube. When inserted, the location of the feeding tube is obtained via so-called bedside methods. However, these localization techniques are not accurate enough which introduces health risks for the patients. Therefore, a new localization technique is desired to minimize or eliminate the misplacement of the feeding tube. For this purpose, we introduce a high-frequency harmonic radar localization system consisting of an out-of-body transceiver and a passive electromagnetic reflector that is located at the distal end of the feeding tube. By means of a link budget, such a system with a transmitted power of 30 dBm is proven to be feasible for an operation frequency in the industrial, scientific, medical band of 5.75 GHz (second harmonic of 11.5 GHz) for neonatal patients.

16:50 Development of Tissue Emulatory Models/Phantoms of Lungs at Microwave Frequency for Acute Respiratory Distress Syndrome

Laya Joseph (FTE, Angstrom Laboratory, Lägerhyddsvägen 1 & Uppsala University, Sweden); Arvind Selvan Chezhan (Uppsala University, Sweden); Thiemo Voigt (RISE Computer Science & Uppsala University, Sweden); Mauricio D Perez (Uppsala University, Department of Electrical Engineering); Robin Augustine (Uppsala University, Sweden)

Acute respiratory distress syndrome is a severe and life-threatening condition when our lungs are injured by infection or trauma. In this paper, we discuss human lung emulators or phantoms with similar dielectric properties of human lungs to study and treat ARDS as testing precursors. We have developed two semi-solid inflated and deflated lung phantoms to analyze the respiratory distress due to the change in the lung permittivity. The size, shape and volume of the phantoms are chosen from the study done on 166 patients' CT image sets. The performance of the phantoms is carried out by measuring the dielectric properties at frequency range 0.5 - 10 GHz using an open-ended coaxial slim probe technique by Agilent Keysight Technologies. The measured data is compared with Istituto di Fisica Applicata "Nello Carrara" (IFAC) database. The measured dielectric properties of emulatory models show good degree of alliance with respect to the IFAC data.

17:10 Potential of Polarized MIMO in In-Body to Out-Body Radio Links

Pyry Kiviharju (Aalto University, Finland); Kenichi Takizawa (National Institute of Information and Communications Technology, Japan); Clemens Icheln (Aalto University & School of Electrical Engineering, Finland); Katsuyuki Haneda (Aalto University, Finland)

Multiple-Input-Multiple-Output (MIMO) technology is considered to be a viable method for spectral efficiency and capacity enhancement in wireless communications. This article presents characterization of a polarized MIMO radio channel for wireless capsule endoscopy (WCE) application. A full-wave simulation method for 3-by-3 MIMO systems is presented. Furthermore, channel eigenvalue ratios and capacity are derived from channel matrices simulated at five different locations inside a realistic human body model. The results show that also the second and third eigenvalue of the channel matrix contribute to the overall channel performance. Furthermore, using polarized MIMO increases the channel capacity compared to SISO.

17:30 Antenna Position Layout and Frequency Impact on Tumor Detection in Microwave Breast Imaging

Raquel A. Martins (Instituto de Telecomunicações/Instituto Superior Técnico, Portugal); Joao M. Felicio (Escola Naval, Portugal & CINAV - Instituto de Telecomunicacoes, Portugal); Jorge R. Costa (Instituto de Telecomunicações / ISCTE-IUL, Portugal); Carlos A. Fernandes (Instituto de Telecomunicacoes, Instituto Superior Tecnico, Portugal)

We present a systematic study in which we assess the antenna position layout and frequency point distribution of a MWI system, that can potentially improve tumor detection and minimize acquisition time. To this end, we performed measurements on a dry MW setup, using a slot-based antenna in the [2-5] GHz frequency range to scan an anthropomorphic breast phantom, with two different tumor positions, for 40 angular positions. Imaging and tumor-to-clutter ratio metric showed that there is a specific number of angular positions and frequency points beyond which the quality of imaging results does not increase substantially. We found the optimal frequency band for this kind of setup and that the use of lower frequencies seems more beneficial than the use of higher ones. Moreover, distributions of antenna position other from the regular circular one, should be explored further since it showed a decrease of imaging artefacts.

17:50 A Time-Efficient Model for Estimating Far-Field Wireless Power Transfer to Biomedical Implants

Brendan Callaghan (TYNDALL NATIONAL INSTITUTE, Ireland); Dinesh R. Gawade (Tyndall National Institute, Ireland); Sanjeev Kumar (Tyndall National Institute & University College Cork, Ireland); Daniel OHare (Tyndall National Institute and University College Cork, Ireland); John Laurence Buckley (Tyndall National Institute & University College Cork, Ireland)

This paper presents a time-efficient, far-field analytical model for wireless power transfer in the human body for biomedical implantable applications. The proposed method presents a means of rapidly computing received RF power levels in an implantable device compared to finite-element methods. For the first time, the Cole-Cole Dispersion Model and Transfer Matrix Method are combined to model frequency dependent dielectric and signal reflection losses in a multi-layered biological tissue structure. This model can be applied to any arbitrary N-layer biological tissue profile. The model was validated using Ansys HFSS at 403.5 MHz, and can estimate the received RF power at the implant with a mean error of 3.27 dB, compared to FEM methods. In addition, the presented model computes in a fraction of the time, 280 ms versus 39 minutes, for the studied simulation test-case. This model is useful for preliminary analysis of potential performance of implantable devices.

Wednesday, March 20 16:30 - 18:10

A23: Antenna modelling techniques

T07 THz and high frequency technologies // Antennas

Room: Dochart 1

Chairs: Marcus C Walden (Plextek, United Kingdom (Great Britain)), Arthur D Yaghjian (Electromagnetics Research Consultant, USA)

16:30 Generalized Far-Field Distance of Antennas and the Concept of Classical Photons

Arthur D Yaghjian (Electromagnetics Research Consultant, USA)

A generalized far-field (Rayleigh) distance is derived for a frequency-domain or time-domain antenna in terms of the radius of the significant reactive power of the antenna, where this radius is given in terms of the

maximum degree number of the significant spherical waves in the far field of the antenna. Although pulses from finite-radiated-energy, finite-extent sources are always dispersive, and the far fields of "electromagnetic missiles" produced by such sources must decay, it is shown that wavelength-size wavepackets with a well-defined center frequency can remain localized in free-space for a limited amount of travel time and distance. These quasi-monochromatic "classical photons" are used, along with Planck's constant, to determine the electromagnetic energy density below which quantum scattering theory, rather than the classical Maxwell equations, may be required to determine electromagnetic scattering.

16:50 Adaptive Polynomial Chaos Expansion for Uncertainty Quantification of SubTHz Horn Antennas with Flat-Top Radiation Patterns

[Aristeides D Papadopoulos](#) (National and Kapodistrian University of Athens (NKUA), Greece); [Yihan Ma](#) (University of Hertfordshire, Greece); [Qi Luo](#) (University of Hertfordshire, United Kingdom (Great Britain)); [George C. Alexandropoulos](#) (University of Athens, Greece)

Sub-terahertz (subTHz) antennas will play an important role in the next generations of wireless communications. Since the physical antenna size is proportional to the wavelength at its targeted central operation frequency, when comes to the subTHz frequency spectrum, the antenna fabrication tolerance needs to be accurately considered during the design stage. The classic approach to studying the average performance of the design considering fabrication tolerances is through the use of the Monte Carlo (MC) Method. In this paper, we propose an adaptive polynomial chaos expansion (PCE) method for the uncertainty quantification of subTHz horn antennas with flat-top radiation patterns. The proposed method builds a surrogate model of the antenna's response to electromagnetic excitation and estimates its statistical moments with accuracy close to the reference MC method, but with a much smaller computational complexity of roughly two orders of magnitude. This complexity gain claim is supported by the presented numerical experiments.

17:10 Analysis of Radiating Transverse Slot Unit Cell and Reflection Cancellation at D-Band

[Usman Shehryar](#), [Jian Yang](#) and [Ashraf Uz Zaman](#) (Chalmers University of Technology, Sweden)

The purpose of this paper is to analyze and propose a design for a transverse slot on a parallel plate waveguide (PPWG) as a unit cell. It aims to study radiation coupling and reflections at the radiating slot. It also aims to propose a design of a unit cell for cancellation of reflections near the coupling slot to relax fabrication constraints at sub-THz frequencies. The study employed simulations in commercial software CST to investigate the design. The analysis revealed that coupling levels vary based on different widths of radiating transverse slot (RTS). Additionally, the proposed design with edge reflection cancellation notch successfully canceled reflections near the coupling slot that is suitable for manufacturing at sub-THz frequencies. The array of these RTS unit cells can provide directive beam with high efficiency. The precise knowledge of the characteristics of RTS unit cell is beneficial in the design of an antenna array.

17:30 The Kootwijk VLF Antenna: A Numerical Model

[Marcus C Walden](#) (Plextek, United Kingdom (Great Britain))

The first documented numerical modelling of the historical Kootwijk VLF antenna is presented. Simulations using NEC-5 show the operation of this electrically short antenna at resonance. Simulation results agree with theoretical expectations but indicate the radiation efficiency - although comparable with other antenna systems of the same historical era - is lower than it potentially could be. Potential causes of the low radiation efficiency are discussed. This modelling also provides further validation of the relatively new NEC-5 simulation software on a complex antenna design having substantially different wire diameters at acute angles.

17:50 Modeling of Quasi-Optical Systems and Measurements with a Cobot in the J-Band

[Gregory Gaudin](#) (IMT Atlantique & Terakalis, France); [Daniel Bourreau](#), [Clément Henry](#) and [Alain Peden](#) (IMT Atlantique, France)

Terahertz waves bring together the assets of microwave and infrared waves and open up new possibilities in structure analysis and material characterization. In order to optimize a J-band material characterization bench (220-330 GHz), this work proposes a novel simulation tool based on a Gaussian beam formalism enabling the modeling and design of large size quasi-optical components. Numerical results showing the applicability of this framework in the modeling of a J-band lens antenna are provided and validated through measurements performed with a robotic bench.

Wednesday, March 20 16:30 - 18:10

A22: Modelling and design techniques for lens antennas

T08 EM modelling and simulation tools // Antennas

Room: [Dochart 2](#)

Chairs: [Pilar Castillo-Tapia](#) (KTH Royal Institute of Technology, Sweden), [Caspar M Coco Martin](#) (Delft University of Technology, The Netherlands)

16:30 Experimental Validation of Ray-Tracing and Physical-Optics Model for Geodesic H-Plane Horn Antennas

[Mingzheng Chen](#) (KTH Royal Institute of Technology, Sweden); [Francisco Mesa](#) (University of Seville, Spain); [Oscar Quevedo-Teruel](#) (KTH Royal Institute of Technology, Sweden)

In this contribution, we provide an experimental validation of a ray-tracing and physical-optics model for geodesic horn antennas. The proposed model employs a ray-tracing technique to obtain electric fields in the horn aperture and applies the field equivalence principle in physical optics to evaluate the three-dimensional radiation characteristics of the geodesic horn antennas. The numerical results agree well with the measurements in terms of radiation patterns in the uv-plane, the principal E- and H-plane patterns, and directivities.

16:50 Analysis and Design of mmWave Wideband Artificial Dielectric Flat Lens Antenna

[Caspar M Coco Martin](#), [Weiya Hu](#) and [Daniele Cavallo](#) (Delft University of Technology, The Netherlands)

We present the design of a wideband flat lens based on artificial dielectric layers (ADLs). To achieve a large bandwidth, true-time-delay phase shift is implemented across the lens aperture, without any phase wrapping. The lens is based on ADLs, which are an arrangement of sub-wavelength metal patches embedded in a host dielectric, designed to locally control the effective permittivity of the lens and to reduce the lens thickness. An efficient modelling procedure is introduced to simulate the lens, which combines ray tracing in anisotropic and inhomogeneous materials, equivalent transmission line models of ADLs, and physical optics. A lens operating from 30 to 60 GHz, with a diameter of 6 wavelengths at the highest frequency and maximum directivity of 25 dB, is designed, manufactured and tested.

17:10 Tailoring the Performance of Geodesic Lens Antennas by Defining Their Footprint

[Sarah E Clendinning](#) and [Oskar Zetterstrom](#) (KTH Royal Institute of Technology, Sweden); [Jose Rico-Fernandez](#) (Northern Waves AB, Sweden); [Francisco Mesa](#) (University of Seville, Spain); [Oscar Quevedo-Teruel](#) (KTH Royal Institute of Technology, Sweden)

This paper discusses non-rotationally symmetric geodesic lens antennas. By defining the shape of the lens footprint, additional degrees of freedom are introduced into the design process, allowing for further tailoring of the electromagnetic performance of the lens while simultaneously reducing the volume occupied by the lens. An in-house ray-tracing model for geodesic lenses has been developed to analyze this class of lenses. Examples showing the effect of modifying the lens profile are presented, with a more detailed discussion on profile presenting improved side-lobe levels at the extreme ports. The examples presented operate at 30GHz.

17:30 Flat Gradient Index Lenses with Planar or Spherical Output Wavefront

[Daniele Cavallo](#), [Weiya Hu](#) and [Caspar M Coco Martin](#) (Delft University of Technology, The Netherlands)

A semi-analytical method is presented for the design of gradient index (GRIN) flat lenses. Closed-form expressions are derived to define the refractive index distribution of the lens, for several cases: collimating lenses with on-axis feed, collimating lenses with off-axis feed, lenses converting spherical wavefronts with different wavenumbers, lenses changing the focal number of a quasi-optical systems, Fresnel zone lenses. The design equations are validated by ray-tracing simulations in inhomogeneous media, implemented by numerical solution of the Eikonal equation.

17:50 Ray-Tracing Model for the Design and Efficiency Calculation of a Monolithic Geodesic Lens Array Antenna

[Pilar Castillo-Tapia](#) (KTH Royal Institute of Technology, Sweden); [Jose Rico-Fernandez](#) (Northern Waves AB, Sweden); [Francisco Mesa](#) (University of Seville, Spain);

Oscar Quevedo-Teruel (KTH Royal Institute of Technology, Sweden)

We propose the use of a generalized ray-tracing model to design geodesic lens array antennas. This model is capable of computing the radiation patterns and taking into account losses due to finite conductivity and surface roughness, which are essential when producing prototypes as single monolithic pieces. The ray-tracing model is used to design a modified Rinehart-Luneburg lens that shows very good agreement with simulations while significantly decreasing computation time. The profile of the lens is designed in such a way that it can be vertically stacked in an array and produced as a single piece. The lens array antenna is manufactured as a single monolithic piece using the laser powder-bed fusion technique. The tests of this prototype validate the use of additive manufacturing for geodesic lens antennas operating in V-band.

Wednesday, March 20 16:30 - 18:10

SW9: Rydberg Atom-Based Sensors: Transforming Measurements and Detection of Radio-Frequency Fields and Communication Signals

Room: M2

Chair: Joshua Gordon (US National Institute of Standards and Technology, USA)

16:30 Rydberg Atom-Based Sensors

Chris Holloway (NIST)

Wednesday, March 20 16:30 - 18:10

E11: Fundamental Research and Emerging Technology

T09 Fundamental research and emerging technologies // Electromagnetics

Room: M3

Chairs: Jordan Budhu (Virginia Tech, USA), Anthony Grbic (University of Michigan, Ann Arbor, USA)

16:30 Isometric Symmetries in Non-Reflecting Structures

Roeve Geva and Raphael Kastner (Tel Aviv University, Israel); Mario Silveirinha (University of Lisbon - Instituto Telecomunicacoes, Portugal)

Non-reflective electromagnetic systems remain unaltered under sequential application of duality and certain geometrical operators. The latter are classified as the two non-overlapping cases: (1) P . T . D symmetric cases of the mirror type and (2) the rotational R . T . D symmetric cases that include self-dual structures. Out of these two building blocks, a host of complex structures can be synthesized, adhering to arbitrary design constraints.

16:50 Exact Maxwell Solution for Arbitrary Transverse Electric Multipole Radiation for Spherical Electric Current Density

David A. Garren (Naval Postgraduate School, USA)

A recent analysis has examined a possible new type of magnetic antenna design wherein the electric current flows on the surface of a sphere in the azimuthal direction such that the magnitude of the electric current density is proportional to the sine of the spherical polar angle. The developed analytical derivations gave an exact solution of Maxwell's equations for the electro-magnetic (EM) fields for all space, and the corresponding theoretical profile for the radiation resistance was shown to give approximately equal amplitude resonances over a multitude of frequency octaves. In the present investigation, the electric currents that flow on the surface of a sphere are permitted to be non-uniform via calculations in terms of vector spherical harmonic (VSH) series. The resulting analysis yields exact transverse electric (TE) solutions of Maxwell's equations for these more general electric current profiles.

17:10 Bound States in the Continuum in Cylindrical Impedance Surface Cavities

Rasmus E. Jacobsen and Samel Arslanagić (Technical University of Denmark, Denmark)

Bound states in the continuum are highly localized modes, which are typically found in periodic photonic structures as well as multilayer structures utilizing exotic materials. However, recent efforts have demonstrated versions of such states in single dielectric and metallic resonators, as well as in cavity slabs formed by surface impedance sheets. Although the latter represents a simple configuration with many interesting properties, it is not suitable for free-space excitations due to large sizes of the underlying impedance surfaces. Presently, we investigate open cavities made of single cylindrical impedance surfaces for extreme field localizations. When the resonances in the cavity and the impedance surface overlap, a bound state in the continuum emerges. The resonant properties are investigated analytically and numerically showing large quality factor and great field localization. The proposed resonator may find applications within filters, antennas, sensing and nonlinear devices.

17:30 Observation of Exceptional Points in Parity-Time Symmetric Coupled Impedance Sheets

Afshin Abbaszadeh and Jordan Budhu (Virginia Tech, USA)

Two identical impedance sheets separated by a subwavelength distance form a coupled waveguide system. If the impedance sheets also employ balanced gain and loss forming a parity-time (PT) symmetric system, an exceptional point can be observed. Exceptional points are points in the parameter space of the coupled mode system (balanced loss/gain factor) where both the eigenmodes and the eigenvalues coalesce forming an overall lossless degenerate mode. The dispersion relation is derived in two ways: (1) by considering the mathematical form of propagating modes and applying the PT-symmetric impedance boundary conditions, and (2) by transmission line modeling and the transverse resonance condition. Identical results are obtained using the two approaches. To validate the obtained results, modal analysis in COMSOL Multiphysics is used. The modal electric field profiles and complex wavenumbers are plotted against the loss/gain factor. It is shown that at the exceptional point, both the eigenmodes and the eigenvalues coalesce.

17:50 Preliminary Study on Gain Maximization via Density-Based Topology Optimization

Jonas Tuček, Miloslav Capek and Lukas Jelínek (Czech Technical University in Prague, Czech Republic)

Density formulation of topology optimization is utilized within method-of-moments formalism to optimize antenna gain. The structure of the problem's solution space is outlined and compared to a solution space formed by Q-factor minimization. Dependence of antenna gain on ohmic losses includes additional complexity to the optimization problem and may negatively influence the progress of the optimization in early stages. The influence of the utilized interpolation scheme is also investigated. Optimized designs from the current state of the formulation are also presented.

Wednesday, March 20 16:30 - 18:10

E12: Novel Materials, Metamaterials, and Metasurfaces II

T10 Novel materials, metamaterials, metasurfaces and manufacturing processes // Electromagnetics

Room: M4

Chairs: Davide Ramaccia (RomaTre University, Italy), Sajjad Taravati (University of Southampton & University of Oxford, United Kingdom (Great Britain))

16:30 *Reducing the Cross-Polarization Levels in Artificial Dielectric Layers for Wideband Arrays*

Alexander J van Katwijk (Delft University of Technology, The Netherlands); Giovanni Toso (European Space Agency, ESA ESTEC, The Netherlands); Daniele Cavallo (Delft University of Technology, The Netherlands)

Wide-scanning arrays often use dielectric superstrates above the radiating aperture as wide-angle impedance matching (WAIM) structures. Artificial dielectric layers (ADLs) are an example of WAIM that can be exploited to improve the scan range and the bandwidth in broadband arrays. However, WAIM structures can also affect the polarization purity of the array. The characteristic cross-polarization (X-pol) of an ideal linearly polarized current sheet in the presence of ADLs is investigated. The primary mechanism that causes increased X-pol is highlighted. We then propose an approach to reduce the X-pol by the inclusion of vertical vias within the WAIM to control the vertical component of the permittivity tensor. The intrinsic X-pol performance of artificial dielectrics with and without vias is also experimentally verified by placing the WAIM above an open-ended waveguide acting as an ideal linearly polarized source.

16:50 *Nonreciprocal Phase-Shifting in Linear Magnet-Free Reconfigurable Temporal Loops*

Sajjad Taravati (University of Southampton & University of Oxford, United Kingdom (Great Britain))

Recently, nonreciprocal (NR) phase shifters have attracted a surge of interest thanks to the advent of NR electromagnetic systems, such as NR metasurfaces, nonreciprocal-beam antennas, and invisibility cloaks. To overcome the limitations associated with conventional technologies for realizing NR phase shifters and gyrators, here we propose a magnet-free NR phase shifter comprising temporal loops. The proposed temporal device is lightweight and offers low-profile and linear responses. Such a unique nonmagnetic NR device operates based on the generation of time-harmonic signals and destructive/constructive interferences for the spurious side-band and targeted time harmonics (THs), respectively, at different locations of the structure. We utilize a time-harmonic signal to temporally modulate varactor diodes and control the phase and frequency of two temporal loops. Our temporal NR phase shifter is equipped with low insertion loss, and high power handling. Furthermore, this controllable NR phase shifter is compatible with integrated circuit technology.

17:10 *Time-Modulated Metasurface-Based System for the Generation of False Radar Targets*

Xinyu Fang (Nanjing University of Science and Technology, China); Mengmeng Li (Nanjing University of Science and Technology & Communication Engineering, China); Shiyuan Li (University of Science and Technology of China, China); Davide Ramaccia (RomaTre University, Italy); Alessandro Toscano and Filiberto Bilotti (Roma Tre University, Italy); Dazhi Ding (Nanjing University of Science and Technology, China)

A novel concept is introduced here for thwarting the linear frequency modulated (LFM) radar's susceptibility to false target jamming. This innovative approach involves the creation of a non-uniform frequency time-modulated metasurface (NF-MTS). The NF-MTS consists of numerous distinct elements, each undergoing individual temporal modulation at varying frequencies. This intricate system empowers the generation of spurious targets strategically positioned within the radar's range profile. The capability to control the modulation patterns of each metasurface element, coupled with the collective non-uniform frequency response across the entire surface, endows the NF-MTS with superior performance in the manipulation of false targets from diverse observation angles. This approach surpasses conventional metasurface-based false target jamming, which relies solely on uniform frequency time modulation, by offering a significantly enhanced and more adaptable capacity for the manipulation of scattered radar signals.

17:30 *Compact Dual-Band Crossover with Enhanced Band Ratio Using Interdigital Capacitor for 5G Applications*

Abdulkadir Bello Shallah (Universiti Teknologi Malaysia & Kebbi State University of Science and Technology, Aliero, Malaysia); Farid Zubir (Universiti Teknologi Malaysia & Faculty of Electrical Engineering, Malaysia); Mohamad Kamal A. Rahim and Osman Bin Ayop (Universiti Teknologi Malaysia, Malaysia)

This research paper introduces a compact dual-band crossover optimized for the lower 5G frequency of 0.7 GHz and 3.5 GHz. The design utilizes T-shaped transmission lines (TLs) with folded arms and stubs to reduce size and integrates metamaterial (MTM) structures with Interdigital capacitor (IDC) unit cells, achieving an impressive 84% size reduction. The crossover operates on a Rogers RT5880 substrate and is simulated using CST-MW Studio.

17:50 *GPS Interference Cancellation Using Magneto-Dielectric Metamaterials*

Amir Jafarholi and Romain Fleury (EPFL, Switzerland)

This paper presents a new method and structure to suppress unwanted interference in conventional Global Positioning System (GPS) applications. In contrast to traditional antennas that usually utilize high-impedance structures with limited enhancement or the arrays that employ null-steering techniques at the expense of increasing complexity and cost, here, a single-element circularly polarized truncated microstrip patch antenna is loaded by a magneto-dielectric metamaterial (MTM). The antenna constitutes a simple microstrip patch radially loaded by a magneto-dielectric MTM cover. The simulations show that thanks to the magnetic behavior of the capacitively-loaded loop (CLL), the CLL is an effective structure to suppress the unwanted incident plane wave up to 30 dB. The proposed antenna has a cylindrical shape with a radius and height of 0.29 of operating wavelength, while the gain and efficiency of 6.8 dBi and 89% are obtained.

Wednesday, March 20 16:30 - 18:10

WG Measurements: WG meeting

//

Room: Fyne

Thursday, March 21

Thursday, March 21 8:30 - 10:10

SW2a: Activities of ITU-R Study Group 3 on radio wave propagation

Room: Lomond Auditorium

Chairs: Clare Allen (Ofcom, United Kingdom (Great Britain)), Carol D Wilson (CSIRO ICT Centre, Australia)

8:30 *Introduction to ITU, SG 3 and Working Methods*

Presenters: David Botha, Clare Allen (ITU, Switzerland; Ofcom, UK)

8:55 *WP 3J - Propagation Fundamentals - Key Recommendations and Topics*

Presenter: Laurent Castanet

9:20 *WP 3K - Point-To-Area Propagation - Key Recommendations and Topics*

Presenter: Paul McKenna

Thursday, March 21 8:30 - 10:10

CS22a: Quantum Electromagnetics - From Photonics to Quantum Computing

T09 Fundamental research and emerging technologies / Convened Session / Electromagnetics

Room: M1

Chairs: Gabriele Gradoni (University of Surrey, United Kingdom (Great Britain)), Paolo Rocca (University of Trento & ELEDIA Research Center, Italy)

8:30 Development of an Analytical Quantum Full-Wave Solution for a Transmon Qubit in a 3D Cavity

Soomin Moon and [Thomas E. Roth](#) (Purdue University, USA)

Circuit quantum electrodynamics is one of the most promising platforms for building quantum information processors. To meet the stringent performance requirements, high-fidelity general-purpose numerical methods are increasingly needed to improve designs. Currently, there exist a limited number of methods for analyzing these systems and they suffer from problematic efficiency limitations. One challenge in developing more efficient methods is the lack of available reference data that can be generated to validate them. Here, we develop an analytical quantum full-wave solution for a transmon qubit in a 3D cavity that can validate numerical methods in the future. We start by reviewing the basics of the field-based quantization method used before showing how classical electromagnetic theories can be used to analytically evaluate all field-based parameters in our formulation. We validate our analytical solution by calculating experimentally-relevant system parameters and comparing against approaches that use numerical EM eigenmodes in their solution.

8:50 The Predictions of Quantum and Classical Models for the Thermal Energy Emitted in the Sub-mm Ranges by Doped Silicon

Andrea Neto, Juan Bueno and Yanwen Chen (Delft University of Technology, The Netherlands)

The thermal energy expected to be radiated by silicon samples according to the classical Planck's model and according to a newly developed classic model are compared. To this goal samples of different doping levels are considered. The expected differences are in measurable ranges. Accordingly a plan is presented for the experimental comparison for frequencies of interest for a large number of the sensing and communication applications: the few hundreds of GHz band. The samples are kept at room temperature, their thermal radiation is captured by open ended waveguides and is then detected via power detectors. Unfortunately the first campaign of measured showed a problem with the minimal resolution of the read out. New measurements should be available at the time of the conference.

9:10 Quantum and Thermal Noise Engineering with Metamaterials

Iñigo Liberal (Public University of Navarre, Spain)

Quantum metamaterials offer multiple possibilities for the generation of non-classical light and the engineering of quantum and thermal noise. In our talk, we will review our latest advanced in the topic, describing how temporal metamaterials enable the generation of squeezed states of light, how antireflection temporal coatings facilitate quantum state frequency shifting and ultra-fast switching without thermal noise amplification, as well as the design of optical amplifiers with an enhanced noise performance based on noise correlations.

9:30 Quantum Optimisation of Reconfigurable Surfaces in Complex Propagation Environments

Emanuel Colella (CNIT, Parma & Università Politecnica Delle Marche, Italy); Luca Bastianelli (Università Politecnica delle Marche, Italy); Mohsen Khalily (University of Surrey & 5G Innovation Centre, Institute for Communication Systems (ICS), United Kingdom (Great Britain)); Franco Moglie (Università Politecnica delle Marche, Italy); Zhen Peng (University of Illinois at Urbana-Champaign, USA); Gabriele Gradoni (University of Surrey, United Kingdom (Great Britain))

The design and analysis of reconfigurable meta-surfaces operating within rich multi-path propagation fading is of crucial importance for the development of real-life programmable electromagnetic environments. Previous work has shown that impedance-based channel models under rich multi-path propagation possess an isomorphism with Sherrington-Kirkpatrick (SK) Hamiltonians. We focus on received power minimisation, which is equivalent to the hard-to-solve task of finding the ground state of the SK Hamiltonian. It has been recently discovered that the Quantum Approximate Optimisation Algorithm (QAOA) predicts the ground state of SK Hamiltonians accurately. However, the landscape parameters of QAOA are dependent on the specific realisation of the random SK Hamiltonian, which hinders the full usage of quantum hardware to optimise reconfigurable surfaces dynamically. We show by Monte Carlo simulations that a concentration property cures this impediment thus making QAOA an excellent candidate for surface optimisation under fast multi-path fading.

9:50 Real-System Variational Quantum Eigensolver for Electromagnetic Waveguides: A Benchmark Study

Emanuel Colella (CNIT, Parma & Università Politecnica Delle Marche, Italy); Spencer Beloin (Naval Surface Warfare Center, Italy); Luca Bastianelli (Università Politecnica delle Marche, Italy); Valter Mariani Primiani (Polytechnic University of Marche, Italy); Franco Moglie (Università Politecnica delle Marche, Italy); Gabriele Gradoni (University of Surrey, United Kingdom (Great Britain))

Current NISQ machines have a relatively small number of qubits and a limited circuit depth. In this regard, a class of quantum variational algorithms (VQAs) have been developed to be able to split the computational cost between classical and quantum hardware. In this study, the VQE algorithm has been used in order to solve the problem of propagation modes in rectangular waveguides described analytically by the Helmholtz partial differential equation. The IBM quantum device called manila was used in these calculations to provide noise present in physical hardware. In order to implement the VQE, IBM's proprietary framework called Qiskit has been used. The results show good agreement between calculations run on simulated quantum hardware and those run on real quantum hardware. This agreement between theory and experiment is evidence that high fidelity modeling of electromagnetic fields utilizing quantum hardware is possible.

Thursday, March 21 8:30 - 10:10

A03a: Antenna analysis and design for sub-6GHz

T01 Sub-6 GHz for terrestrial networks (5G/6G) // Antennas

Room: Alsh 1

Chairs: Christophe Delaveaud (CEA-LETI, France), Federico Puggelli (University of Siena, Italy)

8:30 Low-Profiled Wideband Dual-Polarized Conformal Antenna Array

[Zhan Chen](#), Wei Hu and Yuchen Gao (Xidian University, China); Lehu Wen (Brunel University London, United Kingdom (Great Britain)); Qi Luo (University of Herfordshire, United Kingdom (Great Britain))

A novel wideband dual-polarized conformal antenna array with low profile is presented by using dual characteristic modes (CMs) in this paper. First, by utilizing two sets of orthogonal CMs that operate at the adjacent bands, a wide impedance bandwidth with dual-polarized operation is achieved in the antenna element design. Then, a columnar surface bending study is performed, leading to the development of a 4×5 cylindrical conformal array. The suggested conformal array exhibits a wide impedance bandwidth of 10.4%, a high polarized isolation of 15.1 dB and a low profile of 1.3mm (0.015λ), under 100-mm (1.16λ) radius of curvature. Such a low-profile wideband dual-polarized conformal antenna array provides an attractive option for contemporary and future communications systems.

8:50 **Loaded and Load-Less Supergain Parasitic End-Fire Arrays**

Alessio Tornese (Université Grenoble Alpes & CEA Leti, France); [Antonio Clemente](#) (CEA-Leti, France); Christophe Delaveaud (CEA-LETI, France)

This paper introduces a compact three-bent-dipole end-fire array operating at 916 MHz, exhibiting remarkably high realized gain in relation to its electrical size. The optimization process maximizes directive properties in a chosen direction while upholding high efficiency as a constraint. Complex excitation coefficients are transformed into equivalent impedance loads for implementing a parasitic array. Two antennas are designed, fabricated, and characterized. For the first prototype (loaded), the central element is actively fed, and the external elements are loaded with reactive components. A second prototype (load-less) is designed to incorporate the required complex excitations by adjusting the imaginary parts of the dipoles. Both array versions are matched with a T-match on the active elements. Experimental results reveal outstanding agreement between simulations and measurements. A peak realized gain of 8.9 dBi at 910 MHz is achieved for the parasitic loaded array, and 8.3 dBi at 911 MHz for the load-less array.

9:10 **The Role of Ground Currents in the Co-Simulation of Matching Components and Layout Models in Matching Circuit Optimization**

Sergei Kosulnikov, Mikko Honkala and Jussi Rahola (Optenni Ltd, Finland)

Components exhibiting high ground currents can introduce inaccuracies in the modeling of matching circuits if these ground currents are not accounted for in the simulation. In this paper, we provide a comparative analysis of two different techniques for simulating matching components and a layout model of a printed circuit board. Our discussion incorporates a suggested figure of merit for the estimation of a component's ground current. We illustrate with a practical example how the omission of ground currents can influence the accuracy of the estimated matching performance. We provide an example based on a co-simulation model integrating full-wave electromagnetic model of the layout and circuit models of the matching components. Our findings underscore the importance for modeling ground currents, as this aspect can have a crucial impact on practical implementations for antenna matching circuits.

9:30 **Circular Loop Antennas with Quasi-Two Sources for Broadband Circular Polarization**

[Kazuhide Hirose](#) and Mitsuki Hirose (Shibaura Institute of Technology, Japan); Hisamatsu Nakano (Hosei University, Japan)

Three loop antennas are analyzed using the moment method for an increase in a 3 dB axial ratio bandwidth. Each antenna is excited with a branched feedline vertical to the ground plane. First, circular and square (reference) loop antennas are investigated to compare the radiation characteristics. It is found that the present and reference antennas have axial ratio bandwidths of 17% and 12%, respectively. Subsequently, the present wire loop is replaced with a plate one. It is revealed that the plate-loop antenna shows an axial ratio bandwidth of 28%, wider than the reference antenna by a factor of two.

9:50 **Reducing Mutual Coupling in 2x2 MIMO Circularly Polarized Patch Antenna Array Using Reflecting Polarization Conversion Metasurface**

Muhammad Usman Raza (Xian Jiaotong University, China); Sen Yan (Xi'an Jiaotong University, China)

The 2x2 MIMO circularly polarized (CP) patch antenna is presented with an effective technique for reducing mutual coupling. The Reflecting Polarization Conversion Metasurface (RPCM), featuring symmetrically X-shaped patches, enables this enhancement by generating an additional neutralization wave strategically placed over the CP array. The proposed decoupling structure employs circular-to-circular polarization conversion to counteract this effect. Circular polarization involves the rotation of the electric field, and the decoupling structure utilizes this characteristic to isolate fields from each antenna, mitigating interference and improving the array's overall performance. The 2x2 MIMO CP patches are placed at a narrow separation distance of 4.05mm, leading to a notable reduction in mutual coupling at 3.5 GHz. Sii consistently remains below -25 dB, and overall mutual coupling within the 2.28–4.02 GHz band remains higher than -26 dB. The evaluation of key diversity parameters like ECC and DG underscores the potential of this antenna array for 5G applications.

Thursday, March 21 8:30 - 10:10

CS8: Advanced mm-Wave Substrate Integrated Antennas and Systems for Future Wireless Communication

T02 Mm-wave for terrestrial networks 5G/6G / Convened Session / Antennas

Room: Alsh 2

Chairs: Chun-Mei Liu (École Polytechnique de Montréal, Canada), Ya Fei Wu (UESTC, China)

8:30 **Millimeter-Wave 3D Folded Strip Antennas and Arrays: Diverse Polarizations Realization Under Robust Input Impedance**

Jun Xu, Xiaoyue Xia, Zhi Hao Jiang and Dongze Zheng (Southeast University, China); Yan Huang (Southeast University, Nanjing, China); Kwai-Man Luk (City University of Hong Kong, Hong Kong); Wei Hong (Southeast University, China)

A folded strip radiating element is developed for millimeter-wave applications. Configuration and operating mechanism of the proposed millimeter-wave folded strip radiating element are firstly clarified. Then, three differently polarized Ka-band 3D folded strip antennas, i.e., horizontal linearly polarized (LP) antenna, 45° LP antenna and circularly polarized (CP) antenna, are designed by simply modifying the radiating strips without large impact on the input impedance. Each of the designed antenna element is used to construct a 2x2-element array, and all these three differently polarized array antennas are fabricated and measured. The measured results indicate that, the proposed three array antennas own merits such as wide operating band, low-profile, low-cost, etc., thus, should be promising for many millimeter-wave applications.

8:50 **Optimization of Contiguously Clustered Multibeam Scanning Planar Array for 5G/6G Application**

Yuhan Fan (National University of Singapore, Singapore)

The design of a physically continuous clustered planar array capable of generating multiple scanning beams is addressed. An optimal beam is afforded by predefined excitation coefficients at the element level (EL) while compromised scanning beams are synthesized by aggregating array elements into physically contiguous subarrays and with only additional phase shifters at the subarray level (SL). The beam scanning synthesis problem is formulated as a pattern-matching problem and then relaxed and simplified as a weighted clustering problem, which can be solved by the weighted clustering method to yield an optimal trade-off solution between architecture complexity and matching with respect to the reference pattern. Afterwards, phase coefficients at the SL for compromised scanning beams can be quickly computed according to obtained cluster centroids. Numerical results of a large-scale planar array are presented to validate the effectiveness of the proposed method.

9:10 **A Wideband Filtering Linear-To-Circular Polarization Converter for Ka-Band Satellite Communication**

Xin Ran Li (University of Electronic Science and Technology of China, China); Hong Bin Wang, Ya Fei Wu and Yu Jian Cheng (UESTC, China)

In this paper, a wideband filtering linear-to-circular polarization converter (LCPC) for Ka-band satellite communication is presented. The proposed converter element consists of two-layer PCBs. To achieve the filtering function, the upper board is a frequency selective surface (FSS) and the lower is a LCPC. Both of two structures have wideband characteristics. By co-design of both two boards, the proposed filtering converter performs a wide 3-dB axial ratio (AR) bandwidth and high frequency selectivity at the right side of the passband. The final prototype working at the center frequency of 32.5 GHz is fabricated and measured. The measured results have a good agreement with the simulated ones. The relative 3-dB bandwidths of the passband and AR are 12.3% and 15.4% respectively, where the overlapping bandwidth is 12.3%. Besides, a transmission zero at 36.5 GHz to enhance filtering performance is achieved. This design is suitable for the satellite communication.

9:30 **Generation of Highly-Pure OAM Beams with Simple Slotted SIW Antenna Array**

[Yuvraj Baburao Dhanade](#) (Indian Institute of Technology Roorkee, India); Amalendu Patnaik (IIT Roorkee, India)

In this paper, the design and analysis of a slotted substrate integrated waveguide (SIW) antenna array for the generation of orbital angular momentum (OAM) beams is presented. The antenna comprises four U-shaped slots that act as radiators and are placed in a sequentially rotated manner in the top metal plane of the SIW to radiate vortex waves. The proposed antenna array can generate first-order OAM beams with +1 and -1 modes simultaneously, and most importantly, the mode purity of the generated OAM beams is high. Compared to the traditional circular arrays utilized for OAM generation, the proposed antenna uses a simple feeding scheme that doesn't require any external phase shifter, which paves a new way to design the antennas generating OAM.

9:50 **Dual-Resonance SIW-Based Reflectarray Unit Cell for Broadband Applications**

[Andrés Gómez-Álvarez](#) (Universidad de Oviedo, Spain); Nicolò Delmonte (University of Pavia, Italy); Lorenzo Silvestri (Università di Pavia, Italy); Maurizio Bozzi (University of Pavia, Italy); Manuel Arrebola and Marcos R. Pino (Universidad de Oviedo, Spain)

A novel concept is introduced for a reflectarray unit cell based on substrate integrated waveguide (SIW) technology in Ku band. Two half-mode resonances are excited inside a slot-coupled single-layer SIW cavity. The two are independently tunable through two tuning vias, allowing for simple broadband design optimizations. This structure achieves more than a full cycle of phase shifting from 15.5 GHz to 22 GHz, for a 35% bandwidth. The use of a resonant cavity also introduces excellent angular stability to the cell response across the band.

Thursday, March 21 8:30 - 10:10

A18: Algorithms, modelling and system analysis for aerospace systems

T03 Aerospace, new space and non-terrestrial networks // Antennas

Room: Boisdale 1

Chairs: Carolina Tienda (Airbus Defence and Space, United Kingdom (Great Britain)), Mark Whale (TICRA, Denmark)

8:30 *Uncertainty Quantification for the Reflector Antenna in the Copernicus Imaging Microwave Radiometer*

Tonny Rubæk and Mustafa Murat Bilgic (TICRA, Denmark); Roberto Mizzoni (Italy); Vincenzo Lubrano (Thales Alenia Space Italy, Italy); Benedetta Fiorelli (European Space Agency, The Netherlands)

The European Space Agency is currently working on realizing the Copernicus Imaging Microwave Radiometer (CIMR) which is a satellite-based multi-frequency microwave radiometer and one of the most ambitious missions of the Copernicus space segment. In this paper, results from the uncertainty-quantification analyses that have been carried out for the CIMR reflector antenna are presented. The analyses focus on the effects of random distortions of the facets of the reflector surface and on distortions of the geometry in the reflective mesh which will make up the surface of the reflector. It is shown that distortion of the surface facets has a greater impact on the antenna parameters than changes in the mesh geometry. As expected, the impact is significantly greater at the high frequencies than at the lower frequencies.

8:50 *Self-Interference Suppression for SatCom Active Antenna Arrays Through Joint Transmit and Receive Beamforming*

Teanette van der Spuy (Chalmers University of Technology, Sweden & Satcube AB, Sweden); Rob Maaskant (CHALMERS, Sweden); Marianna Ivashina (Chalmers University of Technology, Sweden); Lukas Nystrom (Satcube AB, Sweden); Thomas Eriksson (Chalmers University of Technology, Sweden)

A novel joint transmit and receive beamformer algorithm to suppress self-interference (SI) in shared aperture full duplex active antennas for LEO user terminals is presented. The algorithm ensures regulatory radiation mask compliance while also maximizing realized gain for a given SI level. Simulation results for a 1024-element Vivaldi array at Ku-band illustrate the trade-off between achievable SI suppression and gain. In the absence of frequency duplexers or isolators, a total isolation in excess of 100 dB over scan angles of $5^\circ - 60^\circ$ is achieved, with an isolation of 5 dB at broadside, while the per-channel coupled power levels at the input of the LNAs are suppressed by 5 dB through transmit beamforming over the entire scan range.

9:10 *Active Antenna Design for Lunar-Based Detection of Global 21cm-Signals from the Dark Ages*

Jordi C.F. Zandboer (Eindhoven University of Technology, The Netherlands); David S Prinsloo & Netherlands Institute for Radio Astronomy, The Netherlands); Ulf Johannsen (Eindhoven University of Technology, The Netherlands); Mark Bentum (Eindhoven University of Technology & ASTRON, The Netherlands)

This paper concerns the parameters, simulations and techniques involved in designing an active antenna system for detection of global 21cm-signals originating from the Dark Ages at the Lunar far side. A 10.5 m diameter equiangular spiral plate antenna is fashioned to operate from 10 to 70 MHz whilst maintaining a virtually frequency-independent impedance characteristic and radiation pattern. Combined with the stable and low noise performance of the measured PHA-13LN+ amplifier evaluation board, the simulations show that the full active antenna system is well suited to the science objective of this paper.

9:30 *Method of Moment Simulation of Full Arctic Weather Satellite Structure*

Roland Albers (University of Bern, Switzerland); Mustafa Murat Bilgic and Mark Whale (TICRA, Denmark); Axel Murk (IAP, Switzerland)

The Arctic Weather Satellite is a single payload prototype for a meteorological constellation of SmallSats called EPS-Sterna. Previous analysis showed that the Arctic Weather Satellite radiometer suffers from significant spillover in the 54 GHz band. To accurately model the scattering of the spillover, new analysis using method of moments was conducted including the structure of the instrument. This paper details the results of these simulations and the resulting mitigation of the spillover.

9:50 *On the Cost-Effectiveness of Using Beamforming at the Ground Station for Aeronautical Communications*

Ayten Guerbuez (German Aerospace Center, Germany); Alexander Steingass (DLR Oberpfaffenhofen, Germany); Dennis Becker (German Aerospace Center (DLR), Germany)

In recent years, beamforming techniques have become increasingly popular, primarily because of their ability to enhance the performance of communication systems. These techniques might also yield improvements in aeronautical communications systems. However, the deployment of beamforming techniques comes with additional cost. In this paper, we assess the cost-effectiveness of employing beamforming techniques for air-ground communications to determine its feasibility. The study compares the antenna gain-cost ratio of using beamforming techniques to using a single-omnidirectional antenna. The cost function is determined by both the number of antenna elements in a single station and the total number of ground stations needed to cover an area. The cost-effectiveness evaluations are conducted for two use cases: The L-band Digital Aeronautical Communications System (LDACS) and the implementation of beamforming at higher frequencies. According to the cost-effectiveness metric defined in this paper, beamforming is not cost-effective at frequencies below 4 GHz, including LDACS.

Thursday, March 21 8:30 - 10:10

SW7a: Stand on the IEEE Antennas & Propagation Standards

Room: Boisdale 2

Chairs: Lars Foged (Microwave Vision Italy, Italy), Vikass Monebhurrin (SUPELEC, France), Vince Rodriguez (NSI-MI Technologies & University of Mississippi, USA)

8:30 *Introduction to IEEE SA & AP-S Standards*

Presenter: Vikass Monebhurrin (CentraleSupélec)

9:10 *IEEE Terminology Standards: IEEE Std 145 & IEEE Std 211*

Presenter: Vikass Monebhurrin (CentraleSupélec)

9:40 *IEEE P2816: Computational Standard*

Presenter: Vikass Monebhurrin (CentraleSupélec)

Thursday, March 21 8:30 - 10:10

A01a: Sensing, communication and identification antennas and systems

T05 Positioning, localization, identification & tracking // Antennas

Room: Carron 1

Chairs: Luis Jofre (Universitat Politècnica de Catalunya, Spain), Yang Miao (University of Twente, The Netherlands)

8:30 Millimeter-Wave Uniform Amplitude SIW Series Power Divider for 2D Leaky-Wave Antenna Arrays

Weiguang Song, George Goussetis and Lei Wang (Heriot-Watt University, United Kingdom (Great Britain))

This paper proposes a millimeter-wave uniform amplitude substrate integrated waveguide (SIW) series power divider for 2D leaky-wave antenna arrays, which is built by connecting 10 elaborately designed unit cells in series. The unit cell consists of an SIW to slot and microstrip line coupling structure, which can be further extended to a low-cost phase shifter by introducing varactors or other active components. Theoretical analysis is made firstly to specify the necessary conditions for uniform amplitude power division. A full wave simulation is conducted to extract the normalized admittance and transmission characteristics of the unit cell. A 1-to-10 SIW series power divider is implemented by connecting unit cells with aimed transmission characteristics. The proposed uniform amplitude SIW series power divider for 2D leaky-wave antennas works between 24 GHz and 29 GHz, which is competitive for millimeter-wave communication and wireless power transfer systems.

8:50 Design of Broadband Stacked Patch Microstrip Antennas Fed by Differential Microstrip Lines with Large Common-Mode Rejection

Ignacio María Delgado-Lozano and Armando Fernández (Universidad de Sevilla, Spain); Rafael R. Boix (University of Seville, Spain); Vicente Losada and Francisco Medina (University of Sevilla, Spain)

This paper proposes the design of broadband microstrip antennas fed by differential microstrip lines with a feeding scheme that ensures a large common-mode rejection provided by its own geometrical construction. The broadband antennas are made of two capacitively coupled rectangular stacked patches excited through a rectangular aperture by a short-circuited differential microstrip line.

A two-port feeding mechanism involving a 180° hybrid is introduced, which makes it possible to analyze and measure the excitation of the differential-mode in the first port, and the rejection of the common-mode in the second port.

2×2 arrays of these antennas are presented in which each antenna is excited by a 180° hybrid only supporting the differential mode excitation. Single antennas and arrays are designed at center frequencies of 2.5, 5.5 and 9GHz. Fractional bandwidths larger than 30% are typically achieved, and gains around 14 dBi are attained in the array cases.

9:10 Generation of Non-Diffractive Bessel Beams for Near-Field Links Applications Using Meta-Axicons

Ravel C. M. Pimenta (Aix-Marseille Université, France); Gabriel Soriano (Aix-Marseille University, France); Matthieu Bertrand (Thales Research and Technology, France); Konstantinos D. Paschaloudis (Université de Rennes, CNRS, IETR, France); Mauro Ettore (University of Rennes 1 & UMR CNRS 6164, France); Myriam Zerrad (Aix-Marseille Université, France); Claude Amra (CNRS & Aix Marseille University, France)

This contribution explores the generation of a linearly-polarized Bessel-Gauss beam generated by a fully dielectric metasurface axicon (meta-axicon) illuminated with a Gaussian beam. It is shown that this Bessel launcher generates a beam with similar characteristics as compared to the one that would be radiated by an ideal aperture. A theoretical model is presented, which allows to estimate the wireless power transfer efficiency (WLTE) of a system composed of two identical such launchers. We investigate the radiated fields, both in the direct and spectral domains obtained with the model and full-wave simulations.

9:30 Dual-Polarized OAM Antenna with Frequency and Mode Agility for Intelligent OAM Communications

Hassan Naseri Gheisani (University of Quebec, INRS, Canada); Peyman Pourmohammadi and Nouredine Melouki (University of Quebec INRS, Canada); Fahad Ahmed (University of Quebec, Canada & INRS, Canada); Amjad Iqbal and Tayeb Denidni (INRS, Canada)

A new dual-polarized Orbital Angular Momentum antenna is proposed with the capability of mode and frequency reconfigurability to pave the way for designing smarter OAM communication systems. At the first step, a dual-polarized Multiple-Input Multiple-Output (MIMO) antenna is introduced. Later, a 2×2 Uniform Circular Array (UCA) is considered using the mentioned MIMO antennas. Since each MIMO antenna owns two input ports, two 2×2 sub-UCA is obtained having orthogonal polarizations. Reconfigurable feeding networks can produce the necessary phase gradients for generating OAM modes +1 and -1 in each sub-UCA. Frequency-tunability of the structure is achieved due to the frequency-adjustability of MIMO antennas as well. According to the simulated results, the frequency tuning range is from 3.8 GHz up to 4.4 GHz, preserving the OAM characteristics. Maximum gains over 6.75 dBi are achieved over the band.

9:50 Low-Profile Multibeam Beam-Scanning Antenna for Vehicular Radar Systems

Siyuan Lei, Gao Wei, Kangkang Han, Tiancheng Qiu and Min Wang (Northwestern Polytechnical University, China)

In this work, a novel low-profile multibeam beam-scanning antenna (BSA) based on a Luneburg lens (LL) beamforming network (BFN) for vehicular radar applications is proposed. The antenna is composed of three parts, concluding seven microstrip line input ports, an LL BFN, and eleven high-scanning rate leaky-wave antennas. The gradient index of the LL beamforming network is achieved by discretizing the LL into a series of concentric rings filled with air. To obtain a larger scanning range of the BSA, the spoof surface plasmon polaritons transmission line is used to achieve higher scanning rate. The proposed antenna is designed in X-band. The simulated results demonstrate that the antenna achieves a beam-scanning range of -54° to 62° in the H-plane and a multibeam coverage range of 88° in the E-plane with the realized antenna gain more than 10 dBi from 8 to 11 GHz.

Thursday, March 21 8:30 - 10:10

M4: Measurements, characterization and apparatus

T09 Fundamental research and emerging technologies // Measurements

Room: Carron 2

Chairs: Alexander H. Paulus (Technical University of Munich, Germany), Alexander Schuchinsky (University of Liverpool, United Kingdom (Great Britain))

8:30 Inverse Source-Based Three-Antenna Methods in the near Field

Alexander H. Paulus (Technical University of Munich, Germany); Thomas F. Eibert (Technical University of Munich (TUM) & Chair of High-Frequency Engineering (HFT), Germany)

The two- and three-antenna methods are well established measurement techniques for determining the gains of unknown antennas under test (AUTs) without the need for a known probe antenna. In its original versions, both approaches require far-field (FF) conditions and can only be approximately applied to near-field (NF) antenna measurements. We present a three-antenna method suitable for any measurement distance, including NF measurements. Based on an inverse-source formulation, nonlinear systems of equations corresponding to an NF FF transformation (NFFFT) with unknown probe behavior are formulated and solved via two iterative approaches. Simulations indicate that accurate results can be obtained despite the inherent nonconvexity of the problem even at close distances where the classical three-antenna method is highly imprecise.

8:50 Exploring Uniformity of Reverberation Chambers: Insights from Antenna Reflection Coefficient

Nazanin Farid (Eindhoven University of Technology, The Netherlands); Jonas Fridén (Ericsson AB, Sweden); Marianna Ivashina (Chalmers University of Technology, Sweden); A. B. (Bart) Smolders and Laurens A. Bronckers (Eindhoven University of Technology, The Netherlands)

Reverberation chambers are widely recognized as a time-efficient testing facility for various applications. The spatial uniformity based on the power transfer function is a critical characteristic of the chamber that affects the measurement uncertainty. To gain more insights into the chamber behavior we introduce a complementary metric: the K-gamma factor. This metric, inspired by the well-established K-factor, quantifies the unstirred contributions of the chamber for each antenna individually and is highly sensitive to the chamber configuration and antenna placement. Analyzing this metric can help identify any undesired effect, such as specular reflections, and, ultimately, improve measurement accuracy. To highlight the usefulness of this metric, two different loading configurations of a reverberation chamber at millimeter-wave frequencies are evaluated as examples.

9:10 Numerical Study of the Dielectric Properties of Lung Tissue Measured with Two Different Open-Ended Coaxial Probes

Fabiana Capitanio and Klementina Vidjak (Sapienza, University of Rome, Italy); Flavia Liporace and Marta Cavagnaro (Sapienza University of Rome, Italy)

The open-ended coaxial probe technique is a widely used technique for microwave characterization of different materials, especially biological tissues. The measurements with this technique can be performed with different types of probes which enable measurements in different frequency ranges. However, the size of the sensing volume of the probe changes with its diameter, and this can become a drawback of the technique when measuring heterogeneous media where different inclusions are present. Therefore, it is necessary to characterize the probes themselves, to understand how the presence of inclusions influences the bulk properties perceived by the probe. To this end, in this work two probes, with different diameters, were numerically modeled and the influence of the proximity of inclusions to the probe's aperture was studied. Finally, an explicit expression for bulk properties depending on the distance and properties of the inclusion is obtained.

9:30 Quad-Junction Self-Biased Circulator with Wide Operational Bandwidth

Lingqi Kong, Yi Huang and Alexander Schuchinsky (University of Liverpool, United Kingdom (Great Britain))

The choice of hexaferrites has always been crucial in the design of self-biased circulators, as it directly affects the device's performance. The available hexaferrite materials are only suitable for operation in high-frequency bands. At low frequencies, they often cause high insertion loss (IL) and limited bandwidth. This paper introduces a novel approach to the design of self-biased circulators. Parallel connection of two hexaferrite junctions with opposite directions of internal magnetic bias achieves a fractional bandwidth (FBW) of 3.67% for self-biased circulators operating in the C-band. This FBW is 2.5 times the traditional single-junction self-biased circulators. The self-biased circulator presented in this paper, operating in the frequency range of 5.35-5.55GHz, exhibits return loss (RL) and isolation both exceeding 20dB, with insertion loss below 1dB over 50% of the operational bandwidth.

9:50 Phase-Variation Microwave Displacement Sensor with High Resolution, Sensitivity, and Dynamic Range

Amirhossein Karami-Horestani (CIMITEC, Departament d'Enginyeria Electrònica & Universitat Autònoma de Barcelona, Spain); Ferran Paredes (Universitat Autònoma de Barcelona, Spain); Ferran Martín (Universidad autónoma de Barcelona, Spain)

A microwave displacement sensor based on the phase of the reflection coefficient of a transmission line is presented in this paper. The proposed sensor consists of a static part, which is a microstrip line terminated with a matched load, and a movable part, consisting of two resonators with two different resonance frequencies. The movable part is placed on top of the reader with a small airgap between them, and it can move along the microstrip line. Two single-frequency signals with frequencies equal to the resonance frequencies of the resonators are injected into the input port of the reader. The phase of the reflection coefficient of the signal at higher frequency is used to improve resolution and sensitivity, whereas the phase of the reflection coefficient of the signal with lower frequency is used to enhance the dynamic range.

Thursday, March 21 8:30 - 10:10

P10a: mmWave and THz propagation modeling and measurements

T02 Mm-wave for terrestrial networks 5G/6G // Propagation

Room: Dochart 1

Chairs: Bo Kum Jung (Technische Universität Braunschweig, Germany), Lorenzo Luini (Politecnico di Milano, Italy)

8:30 Automatic Planning Algorithm of 300 GHz Backhaul Links Using Mesh Topology

Yunming Liu, [Bo Kum Jung](#) and Thomas Kürner (Technische Universität Braunschweig, Germany)

In 5G and beyond, cell sites are expected to be deployed ultra-densely in order to provide users the possibility of high data transmission. Providing fiber backhaul links to all new cell sites is costly and time-consuming. Wireless backhaul links in the terahertz band are expected to be a strong alternative to traditional fiber backhaul links. Planning THz backhaul links in urban scenarios with numerous cell sites is especially a challenging task to complete manually. Therefore, there is a need to design an automatic planning tool for those backhaul links. In this paper, an automatic planning algorithm of 300 GHz backhaul links in a mesh form is introduced. The performance of the algorithm will then be analyzed using an in-house developed simulation tool, known as SIMoNe.

8:50 Cloud Attenuation in the Q Band: Estimation from Experimental Data of Excess Attenuation

Domingo Pimienta-del-Valle (Universidad Politécnica de Madrid, Spain); [Gustavo Siles](#) (Universidad Privada Boliviana, Bolivia); Jose M Riera (Universidad Politécnica de Madrid, Spain); Pedro Garcia-del-Pino (Universidad Politécnica de Madrid, Spain)

Although rain is the main atmospheric impairment to millimeter waves, the adverse impact of clouds becomes more relevant. This contribution presents a study carried out at the Universidad Politécnica de Madrid, in which cloud attenuation has been estimated from 5-year of experimental data of excess attenuation, gathered with a Q-band beacon receiver, using a novel method to separate the contribution of clouds in the absence of rain in site and along the path. In this method, different ancillary data obtained from co-located instruments - a disdrometer and a Ka-band beacon receiver - are used to detect in-site rain, whereas possible rain events along the path are detected from fade slope information, since fade slope is expected to be higher with rain than with cloud attenuation. Results are compared with available cloud attenuation models including the recently published Rec. ITU-R P.840-9.

9:10 Performance Analysis of THz Backhaul Links Assisted by Reconfigurable Intelligent Surfaces

[Bo Kum Jung](#) and Thomas Kürner (Technische Universität Braunschweig, Germany)

Reconfigurable Intelligent Surfaces (RIS) are one attractive key technology for future mobile communications. It is expected to bring numerous benefits to shaping wireless channels favorably by providing anomalous reflection. Apparently, THz backhaul link is conceived as one of the future application scenarios of RIS. Using RIS, more cell sites can be facilitated to have their backhaul links wirelessly via one reflection by RIS. This paper presents an algorithm to find additional THz backhaul links under the given THz backhaul network that can potentially be operated by the use of RIS. The feasibility and performance of those THz backhaul links are assessed by simulations comparing the signal-to-interference plus noise ratio in various simulation set-ups.

9:30 Direct Clustering and Multi-Path Component Identification on THz Channel Measurements in a Factory Environment

Mengfan Wu, Tommaso Zugno and Mate Boban (Huawei Technologies Duesseldorf GmbH, Germany); Falko Dressler (TU Berlin, Germany)

Multi-path components pose both a challenge and an opportunity in high-frequency wireless communication, especially in environments with complex propagation conditions. In this paper, we derive a clustering algorithm to be applied directly to the measurements of indoor THz propagation. We show that such method does not require preprocessing to identify the peaks of multi-path components, but rather extract the time range of clustered multipath components in measurements. Ray-tracing experiments are performed together with classic clustering methods to validate our solution on the corresponding measurements. Our solution facilitates the identification of both clusters and multi-path components directly on measurements without the need to reconstruct scenario in ray-tracing to identify the sources of specular components.

9:50 Dual-Band MmWave Measurements of Human Body Scattering and Blockage Effects Using Distributed Beamforming for ISAC Applications

Yang Miao (University of Twente, The Netherlands); Minseok Kim (Niigata University, Japan); CheChia Kang (Tokyo Institute of Technology, Japan); Naoya Suzuki (Niigata University, Japan); Sofie Pollin (KU Leuven, Belgium); Jun-ichi Takada (Tokyo Institute of Technology, Japan)

The millimeter-wave (mmWave) systems are designed for shorter transmission distances and with directive beams. Their performances are easily impacted by the presence of human. Although the impact of single human body blocking the direct path between mmWave transmitter and receiver has been investigated in literature, the effect of multiple humans as not only blocker but also reflector/scatterer is lacking. It is also

crucial to study human scattering and blockage effects altogether in distributed multi-input multi-output (MIMO) setups exploiting mono-/bi-/multi-static links. We present our distributed multi-static double-directional measurement using a 24/60 GHz dual-band channel sounder with commercial phased arrays. We've performed novel quasi-static measurements with the presence of up to 3 persons standing at diverse locations with various facing directions. The measurement setup also incorporated four distributed depth-cameras to capture groundtruth. The angular-delay domain power spectra of the distributed links at the concurrent dual bands are visualized and insights are given.

Thursday, March 21 8:30 - 10:10

E02a: Computational Electromagnetics

T08 EM modelling and simulation tools // Electromagnetics

Room: Dochart 2

Chairs: Christophe Craeye (Université Catholique de Louvain, Belgium), Giuseppe Pettanice (University of L'Aquila, Italy)

8:30 Efficient NUFFT-Based Spectral Domain Method of Moments Analysis of Multilayered Periodic Structures with Subsectional Basis Functions

[Juan Córcoles](#) (Universidad Politécnica de Madrid, Spain); [Miguel Camacho](#) (Universidad de Sevilla, Spain); [Rafael R. Boix](#) (University of Seville, Spain)

In this communication a novel spectral domain Method of Moments (MoM) implementation is presented which employs asymmetric rooftop basis functions defined by a non-uniform cartesian mesh. Such a mesh can be tailored to any Manhattan-type metalization or aperture in such a way that rooftops basis functions represent either the unknown electric or magnetic current excited by an incoming plane wave. The slowly convergent double infinite summations resulting from the use of the spectral version of the MoM are calculated exploiting Non-Uniform Fast Fourier Transforms (NUFFT). This implementation has been used to analyze several representative examples of frequency selective surfaces (FSS) and reflectarray antennas (RA) showing three orders of magnitude acceleration when compared to the brute-force summation-based approach and two orders of magnitude when compared to commercial software.

8:50 Crank-Nicolson FDTD Method in Media Described by Time-Fractional Constitutive Relations

[Damian Trofimowicz](#) and Tomasz P Stefanski (Gdansk University of Technology, Poland); [Jacek Gulgowski](#) (University of Gdansk, Poland)

In this contribution, we present the Crank-Nicolson finite-difference time-domain (CN-FDTD) method implemented for simulations of the wave propagation in media described by time-fractional (TF) constitutive relations. That is, the considered constitutive relations involve fractional-order (FO) derivatives based on the Grunwald-Letnikov definition allowing to describe hereditary properties and memory effects of media and processes. Therefore, the TF constitutive relations allow for the inclusion of diffusion processes in a dielectric response, which are modelled mathematically by the diffusion-wave equation. We formulate fundamental equations of the proposed CN-FDTD method and, then, we execute simulations which confirm its accuracy and applicability. The proposed method is useful for researchers investigating numerical techniques in media described by FO derivatives.

9:10 Efficient Optimization-Assisted Full-Wave MoM Unit-Cell Design for Dual-Band Transmitarrays

[Juan Córcoles](#) (Universidad Politécnica de Madrid, Spain); [Sergio Matos](#) (ISCTE-IUL / Instituto de Telecomunicações, Portugal); [Miguel Camacho](#) (Universidad de Sevilla, Spain); [Joao M. Felício](#) (Escola Naval, Portugal & CINAV - Instituto de Telecomunicações, Portugal); [Jorge R. Costa](#) (Instituto de Telecomunicações / ISCTE-IUL, Portugal); [Carlos A. Fernandes](#) (Instituto de Telecomunicações, Instituto Superior Técnico, Portugal); [Rafael R. Boix](#) (University of Seville, Spain)

In dual-band transmitarrays, unit-cell design becomes more challenging, since simultaneous and related strict phase specifications at both bands must be met (e.g., to enable beam-steering through mechanical displacement of the feed). In this work, we present an efficient methodology for unit-cell design based on an ad-hoc implementation of the spectral-domain method of moments (SD-MoM), which computes the full-wave unit-cell response at an affordable computational expense (two to four orders of magnitude lower than general-purpose commercial software). An innovative approach consisting of a genetic-algorithm assisted search of unit-cell solutions is carried out. This approach can be applied because of the efficiency and full-wave accuracy provided by SD-MoM in each fitness function evaluation. As an application example, a set of unit cells is designed to operate in the satellite communications Ka-bands 19.7-20.2 GHz and 29.5-30 GHz. The achieved unit cells have a much lower profile than previous designs for the same bands.

9:30 Dispersion Curve Calculation Using the Method of Moments: The Impact of Macro Basis Functions

[Denis Tihon](#), Modeste Bodehou and Christophe Craeye (Université Catholique de Louvain, Belgium)

The Method of Moments is a powerful tool for computing the dispersion curves of open and possibly lossy structures. However, the brute-force computation of the dispersion curves associated to a 2D periodic structure using the Method of Moments can be computationally intensive. One way to accelerate the computation is to reduce the number of unknowns used to model the periodic structure using Macro Basis Functions (MBFs). In this paper, we investigate the error introduced by the use of MBFs when computing the dispersion curves of printed periodic structure on a layered substrate. We study both the impact of the selected set of excitations used to build the MBFs and, for a given set of excitations, the impact of the number of MBFs used to model the printed patches. From the obtained results, practical rules are proposed for metasurface-type periodic array of printed patches.

9:50 Improved PEEC Modeling of Antennas Through Time-Dependent Partial Elements

[Fabrizio Loreto](#) and [Giuseppe Pettanice](#) (University of L'Aquila, Italy); [Martin Štumpf](#) (Brno University of Technology, Czech Republic); [Albert Ruehli](#) (Missouri University of Science and Tech, Jordan); [Jonas Ekman](#) (Lulea University of Technology, Sweden); [Giulio Antonini](#) (Università degli Studi dell'Aquila, Italy)

Over the last twenty years, the evolution of communications has extended the systems' operating frequency range to the tens of GHz. In this framework, time domain integral equation-based (TDIE) methods for antenna modeling have gained increasing interest. Among them, the Partial Elements Equivalent Circuit (PEEC) method turns out to be attractive for its capability to provide compact circuit models. Similarly to other integral equation-based methods, like the method of moments (MoM) in the time domain (TD), the PEEC method can suffer from late-time instabilities. This work shows that a rigorous computation of the time-dependent partial elements leads to an improved TD formulation of the PEEC method that exhibits better behavior at high frequencies. This is the fundamental premise for having more stable results, preventing the late-time instabilities from appearing in the time domain.

Thursday, March 21 8:30 - 10:10

A06a: Advances in reflectarray antennas for wave control, space and 5G applications

T03 Aerospace, new space and non-terrestrial networks // Antennas

Room: M2

Chairs: Manuel Arrebola (Universidad de Oviedo, Spain), Pablo Camacho (Polytechnique Montreal, Canada)

8:30 Large and Deployable Multi-Faceted Antennas Based on Single-Layer Reflectarrays

[Borja Imaz-Lueje](#) (Universidad Rey Juan Carlos, Spain); [Daniel Martínez-de-Rioja](#) (Universidad Politécnica de Madrid, Spain); [Marcos R. Pino](#) and [Manuel Arrebola](#) (Universidad de Oviedo, Spain)

This paper presents two designs of electrically large multi-faceted structures composed by reflectarray panels. The former comprises rectangular panels assembled edge-to-edge following a parabolic profile along the largest dimension of the aperture. The latter is composed of panels with different shapes, arranged to mimic the equivalent reflector in multiple planes. Both antennas operate in the Ka-band using a simple cell based on a single-layer substrate. The multi-faceted designs exhibit a substantial enhancement in the gain bandwidth compared to a conventional deployable reflectarray, maintaining the low-profile storage load and low losses of this type of antenna technology.

8:50 *Direct Optimisation of a Five-State Reconfigurable Reflectarray for 5G Applications*

Mustafa Murat Bilgic and Min Zhou (TICRA, Denmark)

This paper presents the preliminary design of a reconfigurable reflectarray using a direct optimisation approach, which has not been done before. The reflectarray employs a five-state configuration based on an aperture-coupled stacked patch element, offering phase quantisation within a 320° dynamic range. It operates in the 24.5-27.5 GHz band and is tailored for 5G applications. Several reflectarrays have been optimised to achieve beam scanning over $\pm 70^\circ$ with strict side lobe suppression. The study confirms the suitability of this array element for beam-steering reflectarrays and highlights the simplicity of using the direct optimisation approach in antenna design.

9:10 *3-D Reflectarray Unit Cell with Wideband Performance and Integrated Sensing Capability*

Angel Palomares-Caballero (IETR-INSA Rennes, France); Carlos Molero and Pablo Padilla (University of Granada, Spain); María García-Vigueras (IETR-INSA Rennes, France); Raphael Gillard (IETR & INSA, France)

A reflectarray unit cell design with sensing capability at millimeter-wave frequencies is presented in this paper. The proposed unit cell is based on slotlines spatially arranged in 3-D. There are different parts that conform the reflectarray unit cell, these are: an impedance transformer, a main slotline, an EBG filter and a sensing zone. By modifying the length of the main slotline, phase tuning of the reflected wave is achieved while preserving good level of reflection. Moreover, the phase response is linear in the frequency range that goes from 30 GHz to 50 GHz. To implement the sensing function, the EBG filter is placed after the main slotline to allow some level of leakage through the unit cell. The simulated results show that depending on the angular direction of an incident wave, there is a certain phase difference value among the sensors located in the sensing zone of the unit cell.

9:30 *Large, Multi-Faceted Reflectarray with Quasi-Constant Directivity in the V-Band*

Pablo Camacho (Polytechnique Montreal, Canada); Karim Glatre (MDA Corporation, Canada); Elham Baladi (École Polytechnique de Montréal, Canada); Mohammad S. Sharawi (Blue Origin LLC, USA)

This work presents the simulations of an electrically large, multi-faceted reflectarray with a quasi-constant directivity of 44 dBi in the V-band. The paper shows the performance of an equivalent planar reflectarray to contrast the results. The comparison shows that the multi-faceted reflectarray renders a reduction in phase error. Moreover, this configuration increases the bandwidth up to the Q-band. It achieves a directivity of around 40 dB in contrast to the noisy radiation pattern from the equivalent planar reflectarray.

9:50 *Multibeam Compact Dual Reflectarray Antenna for High-Throughput Satellites in Ka-Band*

Daniel Martínez-de-Rioja (Universidad Politécnica de Madrid, Spain); Eduardo Martínez-de-Rioja (Universidad Rey Juan Carlos, Spain); Yolanda Rodríguez-Vaqueiro, Antonio Pino and Carlos Mosquera (University of Vigo, Spain); Jose A. Encinar (Universidad Politécnica de Madrid, Spain); Giovanni Toso (European Space Agency, ESA ESTEC, The Netherlands)

This contribution describes the design of a dual-reflector multibeam antenna based on a parabolic polarizing main reflector with a flat reflectarray subreflector. This antenna concept is proposed to produce multiple beams in orthogonal CP for enabling broadband satellite communications in Ka-band. The antenna generates two orthogonal beams per feed at transmit (19.7 GHz) and receive (29.5 GHz) frequencies in Ka-band, which would make it possible to reduce by half the number of conventional reflector antennas required onboard the satellite to produce the same multipoint coverage. The antenna generates a set of high-gain circularly polarized beams when illuminated by dual-linearly polarized feed-horns, which avoids the use of linear-to-circular polarizers in the feed-chains.

Thursday, March 21 8:30 - 10:10

CS33a: Multiscale, Multiphysics and Unconventional Techniques for Electromagnetic Imaging

T08 EM modelling and simulation tools / Convened Session / Electromagnetics

Room: M3

Chairs: Tommaso Isernia (University of Reggio Calabria, Italy), Rosa Scapatucci (CNR-National Research Council of Italy, Italy)

8:30 *A Mild Data-Driven Approach Based on a Lebesgue-Space Inversion Procedure for Microwave Imaging Applications*

Claudio Estatico, Valentina Schenone, Alessandro Fedeli and Andrea Randazzo (University of Genoa, Italy)

In this paper, a mild data driven inversion technique for microwave imaging applications is proposed. The developed approach relies upon the use of a variable-exponent inversion procedure, in which a-priori information about the class of inspected targets is included through a data-driven regularization term. The developed technique has been preliminarily tested considering the characterization of inclusions in partially known host structures, showing enhanced reconstruction capabilities with respect to the bare inversion scheme.

8:50 *Recent Advances in Multiscale-Multiphysics Inverse Scattering*

Marco Salucci (ELEDIA Research Center, Italy); Lorenzo Poli (ELEDIA Research Center, University of Trento, Italy); Samantha Lusa (ELEDIA Research Center, Italy); Zhichao Lin (Tsinghua University, Italy); Maokun Li (Tsinghua University, China); Andrea Massa (University of Trento, Italy)

An innovative inverse scattering (IS) methodology is presented for imaging targets within inhomogeneous media. It consists of a joint inversion scheme enabling the simultaneous processing of electromagnetic (EM) and acoustic (AC) data while iteratively zooming on the detected region-of-interest (RoI) in which the scatterer has been detected. Robust and reliable guesses are yielded thanks to the combination of multiphysics data, providing complementary information on the imaged domain, with the available a-priori knowledge of the reference inhomogeneous distribution. Furthermore, the integration within a multiscale procedure allows one to keep the ratio between unknowns and data as low as possible, thus counteracting the non-linearity while further regularizing the inversion thanks to the introduction of progressively-acquired information. A preliminary numerical benchmark is shown to assess the capabilities of the proposed multiscale-multiphysics methodology.

9:10 *Advancements in Broadband Electromagnetic Sensing for Food Quality Control*

Sonia Zappia (IREA-CNR, Italy); Sabrina Zumbo (University of Naples Federico II & Università Mediterranea di Reggio Calabria, Italy); Noemi Zeni (Federico II University of Naples, Italy); Alessio Buzzin and Antonio Mastrandrea (Sapienza University of Rome, Italy); Marco Ricci (Politecnico di Torino, Italy); Ilaria Catapano (IREA-CNR, Italy); Rosa Scapatucci (CNR-National Research Council of Italy, Italy); Nicola Pasquino (University of Naples Federico II, Italy); Nicola Lovecchio (Sapienza University of Rome, Italy); Jorge A. Tobon Vasquez (Politecnico di Torino, Italy); Gennaro Bellizzi (University of Naples Federico II, Italy); Marta Cavagnaro (Sapienza University of Rome, Italy); Francesca Vipiana (Politecnico di Torino, Italy); Lorenzo Crocco (CNR - National Research Council of Italy, Italy)

The problem of quality control is of one of the most relevant issues in food industry, because it impacts both consumers safety and manufacturers reliability. While current technologies have reduced this issue, accidents still occur, especially due to the difficulty of detecting low-density contaminants. To cope with this problem, electromagnetic sensing techniques can provide a viable solution, thanks to the non-negligible electric contrast existing when low-density materials are immersed in food items. In this respect, the authors of this contribution have proposed the synergic use of terahertz and microwaves frequencies, in order to both exploit the high spatial resolution of THz images and the capability of inspecting items in-depth using microwaves. In this paper, the ongoing work concerned with THz time continuous monitoring, experimental demonstration of a low complexity microwave imaging algorithm, as well as with the use of machine-learning techniques to process microwave data will be described.

9:30 *An Electric Properties Tomography Approach Inspired by the Boundary Element Method*

Luca Zilberti, Alessandro Arduino, Umberto Zanollo and Oriano Bottauscio (INRIM, Italy)

A novel approach to perform Electric Properties Tomography starting from data collected during a Magnetic Resonance Imaging exam is proposed. The underlying theory, inspired by the Boundary Element Method, is described, and the reliability of the proposed approach is evaluated through a virtual experiment. Promising results are obtained.

9:50 *Generating a Library of Head Phantoms for Microwave Imaging Using Spherical Harmonic Approximation*

[Anja R Kovačević](#) and Darko Ninković (University of Belgrade, Serbia); Lorenzo Crocco (CNR - National Research Council of Italy, Italy); Branko Kolundzija and [Marija Stevanovic](#) (University of Belgrade, Serbia)

A novel method for generating a library of numerical head phantoms is presented. The parent model is created by parametrizing head tissue boundaries defined in the NEVA woman's model using spherical harmonic approximation. The parent model was then modified by stochastically altering the expansion coefficients. Electromagnetic simulations of the parent and modified model showed a notable difference in the scattering parameters. A large dataset essential for implementing microwave imaging algorithms based on artificial intelligence can be created using the proposed technique.

Thursday, March 21 8:30 - 10:10

A10: Metasurfaces and resonant cavity antennas

T10 Novel materials, metamaterials, metasurfaces and manufacturing processes // Antennas

Room: M4

Chairs: Ahmed A Kishk (Concordia University, Canada), Davide Ramaccia (RomaTre University, Italy)

8:30 *Multi-Fed Resonant Cavity Antenna with In-Antenna Power Combination for mm-Wave Communication*

Khushboo Singh (University of Technology Sydney, Australia & Macquarie University, Australia); Manik Attygalle (DST Group Edinburgh, Australia); Dush Thalakatuna and Karu Esselle (University of Technology Sydney, Australia)

In this paper, an on-chip dielectric resonator-fed millimeter-wave high-gain antenna system with in-antenna power combining capability is presented. A low-profile resonant cavity antenna (RCA) is fed by multiple spherical dielectric resonators (DRs), demonstrating its multi-feed capabilities. Each of the DR is fed by two microstrip resonators on a planar circuit board. The design incorporates a printed superstrate as a partially reflecting superstrate (PRS), reducing the antenna's overall size and profile. The antenna exhibits a wide band matching and measured results are in concurrence with the simulations.

8:50 *Analysis and Design of Metasurface Antennas Based on Temporal Metastructures*

Luca Stefanini (Roma Tre University, Italy); Davide Ramaccia (RomaTre University, Italy); Mirko Barbutto (Niccolò Cusano University, Italy); Mohsen Karamirad (Roma Tre University, Italy); Michela Longhi (Niccolò Cusano University, Italy); Alessio Monti ("Roma Tre" University, Italy); Stefano Vellucci (Niccolò Cusano University, Italy); Alessandro Toscano (Roma Tre University, Italy); Andrea Alù (CUNY Advanced Science Research Center, USA); Vincenzo Galdi (University of Sannio, Italy); Filiberto Bilotti (Roma Tre University, Italy)

In this contribution, we present the analysis and design of a novel class of metasurface-based antennas, whose radiative capabilities are enabled by temporal (time-switched) metamaterials. In particular, we consider a thin metasurface supporting the propagation of a surface wave that can switch instantaneously from a finite capacitive value of the surface impedance to an open circuit, resulting in a temporal interface. We demonstrate that after the temporal switch of the metasurface properties, the surface wave is instantaneously coupled to free space realizing a highly directive beam in end-fire direction. Thanks to wavenumber conservation across a temporal interface, we demonstrate that the proposed metasurface-based antenna can radiate at a much higher frequency with respect to the source frequency. Analytical formulations and numerical simulations are provided to predict and verify the frequency upshift and the radiation characteristics of the proposed novel antenna.

9:10 *Curved Electromagnetic Skins for Urban Scenarios*

Michele Beccaria (Politecnico di Torino, Italy); Angelo Freni (Università degli studi Firenze, Italy); Agnese Mazzinghi (University of Florence, Italy); Andrea Massaccesi and Paola Pirinoli (Politecnico di Torino, Italy)

Recently, the possibility of increasing the performance of 5G and beyond wireless networks with the use of "smart electromagnetic skin," able to provide coverage in blind zones for a base station, is becoming an object of several studies. In this framework, the use of a curved configuration, which can be easily integrated into a cylindrical radome enclosing a street light or traffic light pole, is analyzed. The obtained numerical results prove that the proposed solution guarantees performance even better than a planar configuration occupying the same volume, with further advantages. In fact, it is simpler to mount, it has a lower visual impact, and it does not suffer from the influence of the supporting structure.

9:30 *"The Diminished Edge Diffraction Effect Bull's Eye Antenna "*

[Christineh Shahbazian](#) and Ahmed A Kishk (Concordia University, Canada)

This paper describes the Bull's Eye antenna operating at the V-band and featuring three concentric narrow grooves. The design includes two extended grooves close to the antenna rim with a depth of a quarter wavelength depth to reduce edge diffraction, which enhances the radiation pattern. An analytical approach is used to obtain the radiation pattern. The analysis is based on resampling the grooves with magnetic current rings. A comparison is made between circular and rectangular waveguides on the center to excite the antenna. Finally, the proposed antenna is fabricated, and the radiation patterns are measured and will be given during the presentation. The antenna is simulated using CST Microwave Studio, and there is a good match between the simulation and measured results.

9:50 *Fabry-Perot Antenna with High-Permittivity Grounded Walls for Side Lobe Level Reduction*

Edoardo Giusti and Danilo Brizi (University of Pisa, Italy); Agostino Monorchio (University of Pisa & CNIT, Italy)

In this paper, a compact $3\lambda \times 3\lambda$ Fabry-Perot antenna with high permittivity grounded walls is proposed. The use of high permittivity materials as the cavity side walls, when backed by an opportune metallic sheet, allows a significant enhancement in the overall radiating performance. In particular, while both gain and Half Power Bandwidth improvements can be achieved also by sealing the cavity with purely metal walls, nevertheless, with grounded HPMs, a dramatic reduction of the Side Lobe Level can be accomplished. Indeed, the high value of the dielectric constant of the walls material makes them closely approximating the behavior of an ideal perfect magnetic conductor at the selected working frequency, with an extremely reduced thickness and large angular stability. By comparing the purely metallic with the grounded HPM walls configurations, we observed a maximum reduction in the SLL value for both the E and H planes, respectively of 15.9 and 16.2 dB.

Thursday, March 21 8:30 - 10:10

A25: Additive manufactured antennas

T10 Novel materials, metamaterials, metasurfaces and manufacturing processes // Antennas

Room: Fyne

Chairs: Jeff Fordham (USA), Francesco Prudenzano (Politecnico di Bari, Italy)

8:30 *Long Slot Dielectric-Loaded Periodic Leaky-Wave Antenna Based on 3D Printing Technology*

[Ali Araghi](#) (University of Surrey, United Kingdom (Great Britain)); Mohsen Khalily (University of Surrey & 5G Innovation Centre, Institute for Communication Systems (ICS), United Kingdom (Great Britain)); Rahim Tafazolli (University of Surrey, United Kingdom (Great Britain))

Substrate integrated waveguides (SIW) technology is employed to design a uniform long slot leaky-wave antenna (LWA) in millimeter-wave (mmWave) band. The structure is then loaded by a 3D printed sinusoidal periodic pattern of Photopolymer VeroClear dielectric. This makes a periodic LWA which means that it is possible to regulate a desired higher order space harmonic to form the beam and to tilt it to the direction of interest. To showcase the practicality of method, the dielectric pattern is designed in such a way that the beam is tilted to the backward-quadrant at $(\theta_m = -15^\circ)$ at $f = 35$ GHz. The structure is fabricated

and the S-parameters are measured which shows a good agreement with the simulated results.

8:50 3D Printed Cascaded Cavity-Backed Millimeter-Wave Filtering Antenna

Bing Xue (Aalto University, Finland); Fan Jiang (Guangdong University of Technology, China); Katsuyuki Haneda (Aalto University, Finland); Xiantao Yang (University of Liverpool, United Kingdom (Great Britain)); Clemens Icheln (Aalto University & School of Electrical Engineering, Finland)

In this manuscript, a cascaded filtering antenna structure is proposed. To realize this concept, we leverage the cavity-backed slot antenna as a foundation and take advantage of cutoff frequencies of waveguides to achieve it in the millimeter-wave (mmW) bands. The working principle and parameter analyses are introduced. Subsequently, we present the fabrication process and measurement results, which are then compared with simulation results. The obtained results demonstrate acceptable performance in terms of reflection coefficients and radiation patterns. Furthermore, by comparing our proposed antenna with published works, we highlight its advantages in terms of out-of-band rejection and similar beam width in E-plane and H-plane.

9:10 Design and Characterization of a Flexible Fabry-Perot Antenna Fabricated Using Conductive Inkjet Printing

Francesco Anelli, Antonella Maria Loconsole, Andrea Annunziato, Vito Vincenzo Francione and Francesco Prudenzeno (Politecnico di Bari, Italy)

The broadband directivity of a trapezoidal coplanar waveguide fed monopole antenna is enhanced by leveraging Fabry-Perot resonance. The single layer partially reflective surface consists of printed square patches. The fabrication involves the use of inkjet printing with silver-based conductive ink to obtain a low-profile partially Fabry-Perot resonator antenna, suitable for conformal and wearable applications. Our measurements demonstrate that the designed inkjet-printed Fabry-Perot resonator antenna exhibits a wide 3-dB gain bandwidth and a maximum gain of 10.6 dBi.

9:30 3D-Printed Circular Polarized Dielectric Resonator Antenna with Enhanced Axial Ratio Bandwidth Using Anisotropic Material

Sebastian Diaz (Pontificia Universidad Catolica de Valparaiso, Chile); Romain Pascaud (ISAE-SUPAERO, Université de Toulouse, France); Gaëtan Antoine (ISAE-SUPAERO, France); Christophe Morlaas and Alexandre Chabory (ENAC, France); Francisco Pizarro (Pontificia Universidad Catolica de Valparaiso, Chile)

In this article, we propose a wideband circularly polarized (CP) dielectric resonator antenna (DRA). The CP bandwidth is achieved by combining two stacked anisotropic DRAs, which are fed by a simple aperture-coupling feed. Using this straightforward technique, it is possible to increase the axial ratio bandwidth (ARBW). The DRA is designed to be manufactured using low-cost 3D-printing dielectric filaments and a low-cost 3D-printing additive manufacturing process. The final design achieves an ARBW of over twenty percent, which is approximately three times larger than that of the single CP DRA.

9:50 Additively Manufactured Horn Antennas

Jeff Fordham (USA); Jon Swarner, Eric Kim, Griffin Fox and Corey Agan (NSI-MI Technologies, USA)

Additive manufacturing methods have proven to offer many advantages in manufacturing a wide range of products. These methods have advantages of rapid prototyping, rapid production, and the ability to produce mechanical parts that cannot be realized with subtractive methods. Recent work toward the development of horn antennas produced using additive methods has been accomplished. The methods have been shown to produce horn antennas capable of meeting a variety of applications where accuracy and repeatability are key metrics. A comparison of methods is presented along with advantages and disadvantages

Thursday, March 21 10:40 - 12:20

IW14: IMST workshop Efficient Dual Polarised Omnidirectional 5G/6G mmWave Tx/Rx Frontend Module Design using EMPIRE-XPU

Simona Bruni , Thorsten Liebig

Room: [Etive](#)

Thursday, March 21 10:40 - 12:20

SW2b: Activities of ITU-R Study Group 3 on radio wave propagation (continued)

Room: [Lomond Auditorium](#)

Chairs: Clare Allen (Ofcom, United Kingdom (Great Britain)), Carol D Wilson (CSIRO ICT Centre, Australia)

10:40 WP 3M - Point-To-Point and Earth-Space Propagation - Key Recommendations and Topics

Presenter: Richard Rudd

11:05 SG3 Software, Experimental Data and Model Testing - How to Contribute

Presenter: Antonio Martellucci

11:30 SW2 Panel Discussion - Future Requirements

Moderator: Carol Wilson

Thursday, March 21 10:40 - 12:20

CS22b: Quantum Electromagnetics - From Photonics to Quantum Computing (continued)

T09 Fundamental research and emerging technologies / Convened Session / Electromagnetics

Room: [M1](#)

Chairs: Gabriele Gradoni (University of Surrey, United Kingdom (Great Britain)), Paolo Rocca (University of Trento & ELEDIA Research Center, Italy)

10:40 Optimized Design Parameters for a Flux-Driven SNAIL-Based Traveling-Wave Parametric Amplifier

[Michael Haider](#), Yongjie Yuan and Christian Jirawschek (Technical University of Munich, Germany)

We present an analytic approach for finding optimized design parameters for flux-driven traveling-wave parametric amplifiers with superconducting nonlinear asymmetric inductive elements. The parameter to be optimized, i.e., the gain coefficient, is extracted from a Hamiltonian quantum model for three-wave mixing flux-driven amplifiers. Analytic expressions for the nonlinear coefficients up to the third order in the current-phase relation are derived. The minimum potential energy can be solved by finding the roots of a polynomial function. Candidates for optimal operation points are identified by minimizing the residual cross-phase modulation while at the same time maximizing the gain coefficient. Finally, the gain of a TWPA implementation with optimized parameters is evaluated using a quantum model, including substrate losses and chromatic dispersion.

11:00 A Quantum Optimization Method for Antenna Array Thinning

Luca Tosi (ELEDIA Research Center, Italy); Paolo Rocca (University of Trento & ELEDIA Research Center, Italy)

An innovative design methodology based on a hybrid quantum computing technique aimed at optimizing the thinning configuration of the array elements for interference suppression purposes is presented in this work. The optimization approach exploits the Quantum Approximate Optimization Algorithm (QAOA) and a set of selected numerical results, carried out through a quantum computer emulator, is discussed to point out the peculiarities of the proposed method.

11:20 A Modelling Scheme for the Nonclassical Optical Response in the Nanosphere on Mirror Structure

Xuezhi Zheng (Katholieke Universiteit Leuven, Belgium); Xiaotian Yan (KU Leuven, Belgium); Guy Vandenbosch (Katholieke Universiteit Leuven (KU Leuven), Belgium)

Within the framework of the T-matrix method, we present a modeling tool that predicts the optical response from the Nanosphere-on-Mirror (NSoM) construct. The nonclassical effects in metals are accounted for by the nonlocal hydrodynamic Drude model (NLHDM). Two essential elements in the T-matrix method, i.e., the T-matrix of the sphere and the R matrix accounting for the effects of the mirror, have been fully upgraded to include longitudinal waves for the NLHDM. The proposed tool is quantitatively validated both in the near and the far field by an in-house developed Boundary Element solver for the NLHDM where the gap between the sphere and the mirror is as small as 1 nm.

11:40 Non-Reciprocity in a Three-Mode Quantum Magnomechanical System with Magnetostrictive Interaction

Muhib Ullah (Zhejiang University, China); Said Mikki (University of Illinois Urbana Champaign Institute, China)

We demonstrate non-reciprocity through the utilization of the nonlinear magnetostrictive interaction within a ferrimagnetic material enclosed within a magnomechanical cavity system. This system comprises two cavity modes, a magnonic mode, and phononic modes. Externally, it is driven by two classical electromagnetic fields: a strong driving field and a weak probe field. Internally, a Yttrium Iron Garnet (YIG) sphere is subjected to a strong magnetic field, resulting in a significant number of spins generating phonon modes within the YIG sphere. These phonon modes are coupled to magnons through the magnetostrictive nonlinear interaction. Furthermore, magnons interact with cavity microwave photons through a magnetic dipole interaction. The nonlinear magnetostrictive interaction induces a phase shift in the cavity's photons, causing the breaking of time-reversal symmetry and ultimately leading to the observed non-reciprocal phenomenon in our hybrid magnomechanical cavity system.

Thursday, March 21 10:40 - 12:20

A03b: Antenna analysis and design for sub-6GHz (continued)

T01 Sub-6 GHz for terrestrial networks (5G/6G) // Antennas

Room: Alsh 1

Chairs: Christophe Delaveaud (CEA-LETI, France), Federico Puggelli (University of Siena, Italy)

10:40 An Upper Bound for Envelope Correlation Coefficient of Antenna Clusters

Vojtech Neuman, Miloslav Capek and Lukas Jelinek (Czech Technical University in Prague, Czech Republic)

A method for finding the upper bound on the envelope correlation coefficient for an arbitrary number of antenna clusters is introduced. In the described case, the envelope correlation coefficient depends on applied feeding. The theory below shows a matrix description of the problem, which overcomes the need for repeated evaluations of far-field integration for different feeding vectors. This work further presents a formula for finding the highest possible value of the envelope correlation coefficient when the feeding of one antenna cluster is fixed and only the feeding weights of the second one can be manipulated. The proposed theory is shown in a simple example of six parallel dipoles divided into three antenna clusters.

11:00 Radiation Resistance Enhancement Techniques for Ultracompact Half-Wavelength Helical Omnidirectional Circularly Polarized Antennas

Wei Lin and Huacheng Li (The Hong Kong Polytechnic University, Hong Kong); Zhenxin Hu (School of Automation, Guangdong University of Technology, China)

This paper demonstrates the techniques that effectively enhance the radiation resistance of a conventional $\lambda/2$ omnidirectional circularly polarized (OCP) normal mode helical antenna. The original single-arm OCP antenna, although has a very compact size, only exhibits an extremely low radiation resistance that makes it impossible for practical applications. To sufficiently enhance the radiation resistance while maintaining a compact size, innovative techniques as folding the radiator, adding near-field coupled parasitic elements and their hybrid combination have been successfully developed. An OCP antenna based on above techniques has been designed. Results show that the radiation resistance has a substantial enhancement from 3.5 to 80 ohms. Meanwhile, the overall size is still ultracompact, e. g., only 0.0006 λ . It is electrically small with the ka value less than 0.42. These techniques are generally effective approaches that also enable a fundamental understanding of the methodology to enhance radiation resistance of small antennas.

11:20 Low-Profile In-Band Pattern Diversity Antenna with Improved Bandwidth

Chunxu Mao (South China University of Technology, China); Long Zhang (Shenzhen University, China); Xiuyin Zhang (South China University of Technology, China)

In this paper, a low-profile, pattern diversity antenna with improved bandwidth and isolation is proposed for wireless and Internet-of-Thing (IoT) applications. The antenna is composed of a pair of shorted patches with four stubs, a hybrid ring coupler, and a pair of hairpin resonators. The coupler is to provide the shorted patch pair with in-phase and out-of-phase excitations, generating the unidirectional radiation and omni-directional radiations, respectively. In order to enhance the bandwidths, two hairpin resonators are integrated and coupled with the shorted patches through coupling slots, generating 2nd-order filtering responses. As a result, the impedance bandwidths of the two operating modes are significantly improved without increasing antenna's thickness. The antenna is prototyped with the concept verified, exhibiting a good impedance bandwidth (4.9-5.1 GHz) when the antenna is working at different modes (uni-directional or omni-directional). The isolation between the two ports is about 30 dB.

11:40 High Gain and Dual Band SIW-Fed Stacked Conical DRA for 5G NR FR1 Application

Sidhartha Kumar Sahu (IIT Guwahati, India); Rakhesh Singh Kshetrimayum and Ramesh Kumar Sonkar (Indian Institute of Technology Guwahati, India)

This work presents a high gain and dual band slotted Substrate Integrated Waveguide (SIW) fed Dielectric Resonator Antenna (DRA). In this study, integrating both these technologies, an antenna with high gain and dual bandwidth is proposed. A stacked conical DRA structure is placed on SIW to attain high gain. A superstrate is placed above the stacked conical DRA to increase the antenna's directivity. The simulation result shows that the proposed antenna can operate for dual-band with the bandwidth of 210 MHz (5.24 - 5.45 GHz) and 60 MHz (6.10 - 6.16 GHz). This antenna is linearly polarized and shows a peak total gain of 9.62 dBi. The co-polarization and cross-polarization differences are above 50 dB for the E-plane and H-plane. The DRA is fabricated using 3D printing. The measurements are done for antenna prototype. It is suitable for 5G New Radio (NR) Frequency Range 1 (FR1) n46 and n96 bands.

12:00 Wireless Re-Configurable Intelligent Surface for Sub 6 GHz 5G Frequency

Vladimir Lenets, Vladislav Popov, Mikhail Odit, Jean-Baptiste Gros and Geoffroy Lerosey (Greenerwave, France)

The advent of Reconfigurable Intelligent Surfaces (RISs) promises a transformative leap in wireless communication and electromagnetic systems. However, the complexities and costs associated with cable connections and intricate control mechanisms have hindered their practical deployment.

In this paper, we introduce the concept of wireless RIS, revolutionizing the control and power supply through electromagnetic waves, drawing inspiration from legacy telecommunication standards such as GSM. We leverage a patch-based RFID tag integrated into the RIS design to demonstrate the feasibility of this wireless vision.

This research showcases the potential of wireless RIS to reshape the landscape of wireless communication and electromagnetic systems, offering a glimpse of a promising future in the domain.

Thursday, March 21 10:40 - 12:20

A11: Developments in mm-wave antennas

T02 Mm-wave for terrestrial networks 5G/6G // Antennas

Room: Alsh 2

Chairs: Koh Hashimoto (Toshiba Corporation, Japan), Jose Luis Masa-Campos (Universidad Politécnica de Madrid, Spain)

10:40 Millimeter-Wave Corporate-Fed Slot Array Antenna Fed by Partially Dielectric-Filled Transmission Line

Koh Hashimoto (Toshiba Corporation, Japan)

Corporate-fed array antennas can direct the main beam toward the boresight regardless of the frequency. Reduction of the transmission loss in corporate-fed arrays is one of the key issues because corporate-fed arrays have longer feed lines than series-fed arrays. Although the configuration using hollow waveguides can achieve low loss, the manufacturing cost and difficulty of production are problematic. On the other hand, microstrip antennas, which can be manufactured at low cost, are not suitable for the millimeter-wave band, where transmission loss is large. In this paper, cost-effective partially dielectric-filled transmission lines with characteristics intermediate between hollow waveguides and printed transmission lines are applied to a corporate-fed array antenna. A design of a 16×16-element corporate-fed slot array antenna is presented.

11:00 A Low-Profile Wide-Scan Magneto-Electric Dipole Antenna for 5G mm-Wave Communications

[Maximilian Döring](#) and Nico Kästle (University of Ulm, Germany); Thomas Frey (University Ulm - Institute of Microwave Engineering, Germany); Felix Matt (Ulm University, Germany); Christian Waldschmidt (University of Ulm, Germany); Tobias Chaloun (Hensoldt Sensors GmbH, Germany & University of Ulm, Institute of Microwave Engineering, Germany)

A low-profile magneto-electric dipole antenna for 5G communication networks is presented. The novel unit cell design exhibits a low complexity, facilitating a straightforward fabrication process. The antenna design operates from 24.25 GHz to 29.5 GHz, covering multiple frequency bands in the 5G New Radio Frequency Range 2. Across the operating band, a scan volume of up to 60° in the E- and 30° in the H-plane is achieved. The unit cell design was initially subjected to an infinite array analysis for optimization, followed by the fabrication of an 11 × 11 prototype antenna to validate the simulation results. The measured impedance bandwidth and the antenna gain are in good agreement with the simulations. The scan capability of the proposed magneto-electric dipole is validated through embedded element pattern measurements at 24.25 GHz, 27 GHz, and 29.5 GHz.

11:20 Pinwheel-Shaped Polarizer for Generating Dual-Circularly Polarized Conical Radiation Patterns in the Ka-Band

Javier Melendro-Jimenez (Universidad Politécnica de Madrid, Spain); Pablo Sanchez-Olivares and Adrián Tamayo-Domínguez (Universidad Politécnica de Madrid, Spain); [Sergio Garcia-Martínez](#) and Jose Luis Masa-Campos (Universidad Politécnica de Madrid, Spain)

In this contribution, the design of a 3D-printed dual-mode anisotropic dielectric polarizer is presented for millimeter-wave applications within the Ka-band (28-30 GHz). The dielectric polarizer, fed by a conical horn antenna, can convert the linearly polarized conical radiation patterns obtained when exciting TE₀₁ and TM₀₁ modes into right-handed circularly polarized (RHCP) and left-handed circularly polarized (LHCP) conical radiation patterns, respectively. The horn antenna is fed by a mode-converter with two input ports and one output port. When TE₁₀ mode is excited at input port 1, TE₀₁ mode is radiated by the horn, and the polarizer converts the phi-polarized wave into a RHCP wave. Conversely, when TE₁₀ is excited at input port 2, TM₀₁ mode is radiated by the horn, and the polarizer converts the linearly theta-polarized wave into a LHCP wave. Simulated results show an axial ratio (AR) below 2 dB across the entire frequency range for dual-mode operation.

11:40 A Multilayer Dual-Polarized Stacked Patch Antenna with Enhanced Port Isolation for mmWave Highly Integrated Applications

Qingling Yang, Yi Wang and Qingchun You (University of Birmingham, United Kingdom (Great Britain)); Lehu Wen (Brunel University London, United Kingdom (Great Britain)); Sampson Zhenhua Hu (Novocomms Ltd, United Kingdom (Great Britain))

This paper introduces a dual-polarized stacked patch antenna for millimeter-wave (mmWave) antenna-in-package (AiP) applications, utilizing a multilayer stack-up consisting of 14 metallic layers. In order to ensure high port isolation even at large scan angles of ±60 degrees, a metallic isolation wall is introduced into the feed cavity. The prototyping process utilizes high density interconnect (HDI) technology due to its ability to create densely populated microvias. This paper details the working principle, design process, fabrication details, and measurement results of the antenna. The results demonstrate that the designed AiP operates in the frequency range of 24.25-27.5 GHz with an isolation of 28 dB between the ports within the antenna element. Additionally, the antenna exhibits stable radiation patterns and low cross-polarization levels of less than -19 dB over the operation bandwidth.

12:00 Mutual Coupling Reduction in 5G MIMO Antenna Using Dielectric Bridge and Superstrate

[Oludayo Sokunbi](#) and Ahmed A Kishk (Concordia University, Canada)

A dielectric bridge and superstrate are combined to reduce the mutual coupling between 4- and 8-element ME-Dipole antenna at the millimetre-wave (MMW) frequency range of 52-66 GHz (15.2 % bandwidth). The dielectric bridge consists of a carefully inserted metallic plate inside a high dielectric substrate material. This combination is inserted on top of 15-row vias between the 4 and 8 antenna elements. When the superstrate is placed at 2.5 mm (0.5 λ) (λ is the free-space wavelength at the center frequency of 62 GHz) above the 4- and 8-element antenna, a maximum mutual coupling of 70 dB and 55 dB is achieved within the 4-element and 8-antenna ME Dipole antenna, respectively, in the H-plane. The edge-to-edge separation between the elements is 0.62 mm (0.12λ). The radiation pattern, S-parameters, and surface current of the reference and proposed antenna are compared to validate the proposed technique.

Thursday, March 21 10:40 - 12:20

CS4: Antennas for Radio Astronomy

T03 Aerospace, new space and non-terrestrial networks / Convened Session / Antennas

Room: Boisdale 1

Chairs: Quentin Gueuning (University of Cambridge, United Kingdom (Great Britain)), David S Prinsloo (ASTRON & Netherlands Institute for Radio Astronomy, The Netherlands)

10:40 Analysis of a Small LOFAR Low-Band Test Array Using a Sky Map, Simulated Embedded Element Patterns and Measured LNA-Impedances

[Michel Arts](#) (ASTRON, the Netherlands Institute for Radio Astronomy, The Netherlands); Mark Ruiters and Paulus Kruger (ASTRON, The Netherlands); David S Prinsloo (ASTRON & Netherlands Institute for Radio Astronomy, The Netherlands); Mark Bentum (Eindhoven University of Technology & ASTRON, The Netherlands); A. B. (Bart) Smolders (Eindhoven University of Technology, The Netherlands)

This paper describes the analysis of a nine element test array of inverted V-antennas for the frequency range 20-90 MHz. The array is used as a small radio telescope. The purpose of this test array is to verify a system model using simulated embedded element patterns and measured impedances of the low noise amplifiers in a representative system. The output power of the array is measured over a period of 24 hours. This measurement will be compared with a simulation where the output power due to the sky noise as a function of time is calculated. Results for 35, 55 and 70 MHz showed an agreement between measurements and simulations within 1 dB.

11:00 Mitigating Zenith Blindness from Mutual Coupling in a Sunflower Phased Array

Dominic Anstey, John Cumner, Quentin Gueuning, Oscar OHara and Eloy de Lera Acedo (University of Cambridge, United Kingdom (Great Britain)); Anthony Keith Brown (University of Manchester, United Kingdom (Great Britain)); Andrew Faulkner, Fred Dulwich and Paul Scott (University of Cambridge, United Kingdom (Great Britain))

The most recent Aperture Array Verification System for the SKA-Low, AAVS3, has been designed with a regular sunflower head 'Vogel' layout with a 19 m radius. We use a fast Method-of-Moments solver to investigate the effects of mutual coupling of this style of regular layout in comparison to a more randomised layout. We show that this layout produces a blind spot at zenith at 125 MHz, where the embedded element pattern and station beam show a drop of around 5 dB. We then demonstrate that randomising the locations of the elements reduces the scale of this drop in beam, with greater randomisation producing greater reduction. We find that randomising each element position within an area of around 1.5 m radius is sufficient to eliminate this blind spot.

11:20 A Performance Comparison of Sub-Octave Band Corrugated Horns to a Quadruple-Ridged Flared Horn for the ngVLA Radio Telescope

Robert Lehmensiek (National Radio Astronomy Observatory, USA & Stellenbosch University, South Africa); Dirk de Villiers (Stellenbosch University, South Africa)

The radiation performance of quadruple-ridged flared horns (QRFHs) has in recent years improved greatly due to the more detailed geometries, such as the addition of corrugation rings in the aperture plane (enhanced performance at the lower part of the frequency band) and the addition of dielectric material in the throat of the horn (for improved upper-frequency performance). Over a narrower frequency band, the QRFH can achieve performance levels that are similar to those of the sub-octave band corrugated horns. This is shown in this paper for the lowest (3:1) frequency band of the ngVLA radio telescope.

11:40 The Hydrogen Intensity Real-Time Analysis eXperiment: Overview and Status Update

Anthony Walters and Keshav Bechoo (University of KwaZulu-Natal, South Africa); Shruti Bhatporia (University of Cape Town, South Africa); H. Cynthia Chiang (McGill University, Canada); Devin Crichton (ETH Zürich, Switzerland); Jacobus Diener (Botswana International University of Science and Technology, Botswana); Sindhu Gaddam (University of KwaZulu-Natal, South Africa); Kit Gerodias (McGill University, Canada); Austin Gumba (University of KwaZulu-Natal, South Africa); Neeraj Gupta (Inter-University Centre for Astronomy and Astrophysics, India); Surajit Kalita (University of Cape Town, South Africa); Emily Kuhn (NASA Jet Propulsion Laboratory, USA); Martin Kunz (Université de Genève, Switzerland); Kavilan Moodley and Warren Naidoo (University of KwaZulu-Natal, South Africa); Viraj Nistane (Université de Genève, Switzerland); Tasmiya Papiiah (University of KwaZulu-Natal, South Africa); Aditi Pattabhiraman (Stanford University, USA); Aritha Pillay (Durban University of Technology, South Africa); Alice Pisani (Flatiron Institute, USA); Isibabale Qhoboshiyane (University of KwaZulu-Natal, South Africa); Alexandre Refregier (ETH Zürich, Switzerland); Edwin Retana-Montenegro (University of KwaZulu-Natal, South Africa); Benjamin Saliwanchik (Brookhaven National Laboratory, USA); Ajith Sampath and Tsepo Sekhoasha (University of KwaZulu-Natal, South Africa); Mugundhan Vijayaraghavan (Chalmers University of Technology, Sweden); Amanda Weltman (University of Cape Town, South Africa)

The Hydrogen Intensity Real-time Analysis eXperiment (HIRAX) will be a large interferometric array of drift-scan radio telescopes designed to map the large-scale spatial fluctuations of neutral hydrogen in the Universe, in order to better understand the nature of dark energy. It will operate between 400-800 MHz, and is currently under construction in the Karoo desert of South Africa. It will also be a powerful tool for studying astronomical transients and the evolution of galaxies. Here we present an overview of the project, its anticipated deployment timelines, and highlight some of the characterisation and calibration efforts that are currently underway, or planned for the future.

12:00 CSIRO Radio Astronomy Receiver Update - Ultra Wideband and Phased Array Feeds

Alex Dunning and Steve Barker (CSIRO, Australia); Michael Bourne (CSIRO Astronomy and Space Science, Australia); Mark Bowen (CSIRO, Australia); Nick Carter and Santiago Castillo (CSIRO Astronomy and Space Science, Australia); Aaron Chippendale, Yoon Chung, Paul Doherty, Douglas B Hayman and Daniel George (CSIRO, Australia); Kanapathippillai Jegathanan (Commonwealth Scientific and Industrial Research Organisation (CSIRO), Australia); Simon Mackay, Natasha Maimbo, Les Reilly, Paul Roberts, Peter Roush, Sean Severs and Robert Shaw (CSIRO, Australia); Ken Smart (CSIRO Space and Astronomy, Australia); [Stephanie Smith](#) (CSIRO & Astronomy and Space Science, Australia); John Tuthill, Tasso Tzioumis and Jason van Aardt (CSIRO, Australia)

We present details on recent ultra wideband receiver development at CSIRO for the Parkes radio telescope, Effelsberg radio telescope and ngVLA with almost constant beamwidth achieved up to a 6:1 bandwidth. A large field of view cryogenic phased array feed for the Parkes radio telescope is also discussed.

Thursday, March 21 10:40 - 12:20

SW7b: Stand on the IEEE Antennas & Propagation Standards (continued)

Room: [Boisdale 2](#)

Chairs: Lars Foged (Microwave Vision Italy, Italy), Vikass Monebhurrn (SUPELEC, France), Vince Rodriguez (NSI-MI Technologies & University of Mississippi, USA)

10:40 IEEE Std 149: Recommended Practice for Antenna Measurements

Presenter: Vince Rodriguez (NSI-MI/AMETEK)

11:30 IEEE Std 1720: Recommended Practice for Near-Field Antenna Measurements

Presenter: Lars Foged (MVG-Group)

Thursday, March 21 10:40 - 12:20

A01b: Sensing, communication and identification antennas and systems (continued)

T05 Positioning, localization, identification & tracking // Antennas

Room: [Carron 1](#)

Chairs: Luis Jofre (Universitat Politècnica de Catalunya, Spain), Yang Miao (University of Twente, The Netherlands)

10:40 Tiled Subarray Design for Multibeam Joint Communication and Sensing

Hadi Alidoustaghdam, Andre Kokkeler and Yang Miao (University of Twente, The Netherlands)

The multibeam technology is a promising solution for joint communication and sensing (JCAS) in a base station (BS). Tiling of apertures with rectangular, hexagonal, and circular boundaries is studied which improves cost-efficiency, modularity, and scalability of the design. The optimization of tiling configuration considers the matching of the communication channel and the ambiguity function of sensing before and after tiling. The performance metrics are the capacity for communication and the maximum side lobe level (MSLL) of the array radiation pattern for sensing. The numerical results show that the tiling of various apertures with 64 antennas does not influence the capacity of communication largely. Only-communication, only-sensing, and JCAS apertures are compared in regard to the MSLL, where the aperture for only-sensing has the lowest MSLL without deteriorating the capacity of communication. The metrics show the tiled aperture with a hexagonal boundary has the best JCAS performance.

11:00 Magnetolectric Dipole Antenna Extending NLOS Short-Distance Vehicular Communication with Orbital Angular Momentum Modes

Luis Jofre (Universitat Politècnica de Catalunya, Spain)

The ability to utilize resources to meet the need of growing diversity in services and user behavior marks the future of cognitive wireless communication systems. Cognitive wireless technologies for vehicular communications, in combination with Orbital Angular Momentum (OAM) modes aim at extending direct Non-Line-Of-Sight (NLOS) short-distance communications for smart mobility. In this regard, OAM antennas need

to be developed to support these technologies. To this end, here we describe a compact antenna supporting the first OAM modes. Also, the antenna properties are discussed and are numerically and experimentally validated for OAM modes of $l = \pm 1$. Particularly, for the considered OAM modes, the antenna achieves more than 500 MHz operation bandwidth at the frequency of operation of 3.5 GHz. Also, for $l = \pm 1$ OAM modes, the null beamwidth aligns precisely with the anticipated dimensions theoretically computed.

11:20 *Roof-Glass Integrated Antenna for Vehicular GNSS Applications*

Hanieh Aliakbari (Lund University, Sweden); Xiaotian Li and Christian Lötbäck (Volvo Car Corporation, Sweden); Buon Kiong Lau (Lund University, Sweden)

In this paper, a wideband circularly polarized antenna is designed for integration into the glass roof of a modern car for GNSS positioning applications. Characteristic mode analysis is used to obtain more physical insight into the problem and hence satisfy the polarization and bandwidth requirements. The antenna has a low profile and uses a single coplanar waveguide feed to cover all GNSS bands. The measured 10 dB impedance bandwidth of the prototype is 52% and the 3 dB axial-ratio (AR) bandwidth is 39%. Full-car simulation results are presented for different antenna positions on the roof. It is shown that the middle and rear-right positions are preferred in terms of the AR performance.

11:40 *Traveling-Wave Fed Dielectric Rod Antenna for 3D Scanning MIMO Sensor*

[Alexander Khripkov](#) (Huawei Technologies LTD, Finland)

Designed multiple-input and multiple-output (MIMO) millimeter-wave (mmWave) radar antennas, enabling beamshaping and beam tilting for uniform indoor area coverage. Guidelines and design steps for traveling-wave fed dielectric rod antenna are provided. 62 GHz MIMO mmWave radar antenna design and topology described, illustrating achievable performance of the indoor radar, featuring human presence perception, accurate positioning and trajectory tracking; functional area customization, precise subdivision of spaces and scenes and AI super-sensing recognition

12:00 *Array-Fed Transmitarray with Designated Beam Directions and Coverages*

Xin Guo (Ministerial Key Laboratory, JGMT, Nanjing University of Science and Technology, Nanjing, China); Liting Zhu and Wen Wu (Nanjing University of Science and Technology, China)

An array-fed transmitarray is proposed to radiate various beams with designated directions and coverages. It is proposed based on the superposition principle. An array is used as the feed. When the feed sources are excited individually, multiple elemental beams pointing at different angles are generated. Then the expected beam can be obtained by adding up these elemental beams. The detailed and effective control of beam directions and coverages are put forward. Flattop beams and multi-beams with different coverages and directions are finally designed for validation.

Thursday, March 21 10:40 - 12:20

CS41: Electrically Small Antenna Measurement Technique

T09 Fundamental research and emerging technologies / Convened Session / Measurements

Room: Carron 2

Chairs: Fabien Ferrero (Université Cote d'Azur, CNRS, LEAT & CREMANT, France), Adam Narbudowicz (Trinity College Dublin, Ireland & Wroclaw University of Science and Technology, Poland)

10:40 *UnderGround-To-AboveGround IoT Communication Links Insurance at 915 MHz Using LoRa Technology*

Saeed Haydhah (Concordia University, Canada); Xavier Bernard (Lynkz Instruments, Canada)

At 915 MHz, this study proposes sophisticated wire- less insurance approaches for UnderGround-to-AboveGround (UG-to-AG) communications. Antenna solutions were proposed to ensure the availability of the UG-to-AG link in the face of soil fluctuations and uncertain sensor orientations. IoT antennas must be constructed to be as compact as possible while consuming the least amount of power possible. The difficulties in designing IoT antennas were also discussed. It was discovered that the soil properties must be properly examined in order to construct the appropriate antenna. Finally, a measuring approach for IoT antennas at Ultra-High Frequencies is proposed in order to show underground antenna performance and robustness under various soil conditions.

11:00 *VHF/UHF Antenna Measurements Based on Multi Probe Array Technology*

[Francesco Saccardi](#) (Microwave Vision Italy, Italy); Andrea Giacomini (Microwave Vision Italy SRL, Italy); Nicolas Gross and Thierry Blin (MVG Industries, France); Per Iversen (Orbit/FR, USA); Lars Foged (Microwave Vision Italy, Italy)

Accurately measuring the radiation characteristics of electrically small antennas, particularly those with low directivity, presents a challenge due to the inevitable coupling between the antenna, the measurement chamber, and the associated equipment. This challenge becomes even more pronounced when dealing with antennas operating at frequencies in the VHF/UHF range, which introduces complexity to the measurement instrumentation, testing chamber, and the absorbing materials used. Spherical Near Field (SNF) testing techniques are widely recognized as the most precise and suitable methods for such measurements, primarily because they allow for the overall system dimensions to be minimized. The application of a multiprobe acquisition further enhances the compactness and efficiency of these measurement setups. This paper provides an in-depth investigation of measurement accuracy for low-directivity antennas at VHF/UHF frequencies using multiprobe systems. Specifically, the main errors contributions affecting the measurement uncertainty of the radiation pattern and gain are discussed and analyzed.

11:20 *Design of Electrically Small Antennas and Radiation Efficiency Measurement Using MQFM with Radian Wheeler Cap Sizes*

Marwan Jadid and Christophe Delaveaud (CEA-LETI, France)

The Modified Quality Factor Method (MQFM) was revisited in this paper to measure electrically small antennas (ESAs) radiation efficiency. The method is used to measure the radiation efficiency for three ESAs of maximum electrical dimension $N/12$ at frequencies 433 MHz, 868 MHz, and 2400 MHz using three Wheeler caps, each having the exact size of the radian sphere ($N/2\pi$) at the considered antenna operating frequency. The measurement results show agreement with simulations.

11:40 *Contactless Impedance and Far-Field Characterization of Electrically Small Antennas*

Majid Manteghi (Virginia Tech, USA)

Due to their small size and versatility, electrically small antennas (ESAs) must be precisely characterized in modern wireless communication systems. Traditional methods involving direct cable connections are susceptible to induced currents, resulting in imprecise input impedance and far-field radiation pattern measurements. This paper presents a novel contactless measurement technique that employs an oscilloscope to capture the time-domain impulse response of ESAs, mitigating induced current issues and enabling precise impedance measurement. In addition, we present an indirect method for characterizing far-field patterns and polarization, thereby enhancing the ESA's characterization. Our contactless method is adaptable to various ESA designs and frequencies and offers versatility and non-intrusiveness. Experimental results validate the efficacy of our method, which represents a significant advance in ESA characterization for wireless system design optimization.

12:00 *Cost-Effective Dual Circularly Polarized Antennas for Phase Calibration*

Rasmus Luomaniemi, Riku Kormilainen and Mikko K. Leino (Radiantum Oy, Finland)

The relative phase of the measured electric field components needs to be known accurately when measuring certain antenna parameters, for example, radiation patterns of circularly polarized antennas. Typical methods for phase calibration are expensive and do not necessarily suit very well for cases where the measurement setup is changed occasionally for only a small number of measurements. This work presents a cost-effective dual circularly polarized PCB antenna that can be easily designed for different operation frequencies. The design method and measured antenna properties are presented along with the method to determine and apply phase correction to improve phase accuracy of antenna measurements.

Thursday, March 21 10:40 - 12:20

P10b: mmWave and THz propagation modeling and measurements (continued)

T02 Mm-wave for terrestrial networks 5G/6G // Propagation

Room: Dochart 1

Chairs: Bo Kum Jung (Technische Universität Braunschweig, Germany), Lorenzo Luini (Politecnico di Milano, Italy)

10:40 Empirical Path Loss Model and Small-Scale Fading Statistics in an Indoor Office Environment in 6 and 37 GHz Shared Bands

[Ruoyu Sun](#) and Dorin G Viorel (CableLabs, USA); Wilhelm Keusgen (Technische Universität Berlin, Germany); Ruth G Gebremedhin (New York University, USA)

The low-cost 6-GHz unlicensed and 37-GHz shared spectra are of interest for operators to deploy hotspot 5G/6G or Wi-Fi for Fixed Wireless Access (FWA) and mobile services. The wireless propagation channel determines the coverage, capacity, radio link design, and network planning. CableLabs conducted a measurement campaign in an indoor-office environment to study the channel characteristics. The measurement data, path loss models, and small-scale fading statistics are presented. The channel sounding system uses 500 MHz bandwidth centered at 6.175 and 37.3 GHz. The receiver was mounted near the ceiling mimicking BS or AP and the transmitter was 1.1 m above ground mimicking cellphone or laptop. 76 test positions were measured with distances 3-85 m in line-of-sight (LOS), obstructed-LOS (OLOS), non-LOS (NLOS), and deep NLOS conditions. The experimental path loss models, K-factor, root-mean-square delay spread (RMS-DS), and angular spread (RMS-AS) are reported and compared with the 3GPP TR 38.901 models.

11:00 Validation of Ray-Tracing Simulated Channels for Massive MIMO Systems at Millimeter-Wave Bands

Jingyun Di (Aalborg University, Germany); Zhiqiang Yuan (Beijing University of Posts and Telecommunications, Denmark & Aalborg University, Denmark); Yejian Lyu and Fengchun Zhang (Aalborg University, Denmark); Wei Fan (Southeast University, China)

Employing large-scale antenna configuration is seen as a key enabling radio technology for 5G and beyond communication systems. This work presents validation of a home-developed ray tracing (RT) tool for massive multiple-input multiple-output (MIMO) system in the millimeter-wave (mmWave) frequency bands. For this purpose, a channel sounding campaign in an indoor entrance scenario using a massive MIMO systems based on virtual array concept is presented. The channel measurement of 6 GHz bandwidth (26.5-32.5 GHz) is first demonstrated, with a virtual uniform circular array (UCA) consisting of 720 antenna elements located at the transmitter position on the turntable and one antenna at the receiver position. The impact of order of interactions e.g. reflections and diffractions on the channel impulse responses (CIRs) is analyzed in the RT simulation. The comparison between RT simulated and measured results shows a reasonable level of agreement.

11:20 Exploiting Numerical Weather Prediction Data for Radiopropagation Modeling of SatCom Links

Roberto Nebuloni (Ieiti - Cnr, Italy); Marianna Biscarini (Sapienza University of Rome, Italy); Laura Dossi (CNR-IEIT, Italy); Saverio Di Fabio (CETEMPS, Italy); Paolo Scaccia and Paolo Antonelli (AdaptiveMeteo, Italy); Livio Bernardini (CETEMPS, Italy); Carlo Riva and Lorenzo Luini (Politecnico di Milano, Italy)

Propagation data based on numerical weather prediction (NWP) models are not mature for an operational use in applications such as adaptive fade mitigation in SatCom systems. However, these datasets are useful in the design and system simulation stage. In the framework of the RadioSatMet ESA-funded project, we have developed a software tool that includes a parametric radiopropagation model (PRM) for Earth-to-space links based on NWP data for the atmospheric channel assessment. We run the tool and generated 28-days time series of path attenuation components over a large continental area. Here we describe the NWP+PRM modeling chain and compare the synthetic path attenuation data obtained by our tool with beacon measurements collected during the Alphasat experiment

11:40 Wind-Induced Backscatter Clustering from Vegetation at W-Band

Mario Vala (Instituto de Telecomunicações de Portugal, Portugal); João Ricardo Reis (Instituto de Telecomunicações and Polytechnic Institute of Leiria, Portugal); Joao M. Felício (Escola Naval, Portugal & CINAVAL - Instituto de Telecomunicações, Portugal); Nuno R. Leonor (Polytechnic Institute of Leiria (IPL) & Instituto de Telecomunicações (IT), Leiria, Portugal); Carlos A. Fernandes (Instituto de Telecomunicações, Instituto Superior Técnico, Portugal); [Rafael F. S. Caldeirinha](#) (Polytechnic Institute of Leiria & Instituto de Telecomunicações, Portugal)

In this paper, the wind-induced backscattering from vegetation at W-band frequencies is studied and characterised through practical validation in a controlled environment. Wideband analyses of the backscatter clustering from a simple tree show that leaves and trunk play an important role in the generation of diffuse scattering which is the dominant propagation mechanism in random scattering media. Multiple internal reflections may introduce tails in the power delay profile, yielding a radar signature of about twice the dimensions of the tree canopy. Also, wideband signal statistics are affected in the presence of wind.

12:00 E-Band Measured Propagation Characteristics for Urban Backhaul Communications

[Bofan Wu](#), Haifeng Mou, Hang Yang, Zhenyang Guo, Xianbing Zou and Xiang Gao (University of Electronic Science and Technology of China, China)

E-band millimeter-wave (mm-wave), due to its large bandwidth, is considered promising for building high-speed wireless backhuls. However, link availability and transmission rate can be greatly affected by E-band propagation characteristics. In the paper, we study E-band propagation in urban backhaul scenarios and evaluate system performance. We conducted channel measurements in a campus environment, where on-ground pole-mounted backhauling and rooftop outdoor-to-indoor (O2I) scenarios were considered. Based on the measurement data, we find that the measured E-band pathloss is close to free-space propagation loss. Additionally, there is an around 4-dB penetration loss caused by glass window in the O2I propagation. Fading is found to be severe in the on-ground scenario, but insignificant in the rooftop O2I link. Performance evaluation shows that an uncoded rate of 3 Gbps can be easily achieved over a 750-MHz bandwidth. The results help understand E-band propagation characteristics and are useful for backhaul system design.

Thursday, March 21 10:40 - 12:20

E02b: Computational Electromagnetics (continued)

T08 EM modelling and simulation tools // Electromagnetics

Room: Dochart 2

Chairs: Giuseppe Vecchi (Politecnico di Torino, Italy), Jong-Gwan Yook (Yonsei University, Korea (South))

10:40 Frequency-Domain TLM Method with Cartesian Block Meshing

[Abdelrahman Abdallah Ijeh](#) (Université Côte d'Azur, France); Marylène Cueille (University of Nice Sophia Antipolis CNRS, France); Soukaina Mifdal (Université Côte d'Azur, France); Jean-Lou Dubard (UCA, LEAT, France); Michel Ney (IMT Atlantique, France)

A frequency-domain TLM with Cartesian block meshing scheme is presented in this article. This approach allows arbitrary Cartesian non-structured local mesh refinement in critical regions (e.g., discontinuities and important fine details). This versatile meshing technique is very useful in handling multiscale problems without exhausting computational resources. Moreover, this proposed approach permits the computation of the EM-fields at specific frequencies using fast linear-solvers without the need to run many time-domain iterations especially for highly resonating structures. Simulation experiments and comparison to other computational EM schemes are presented to show the validity and the performance of the proposed approach.

11:00 Stabilization of EFIE-IBC by Spatial Filtering

Margaux Bruliard and Giuseppe Vecchi (Politecnico di Torino, Italy)

Impedance Boundary Condition (IBC) is a widely used approximation in the analysis of metasurfaces, and it greatly simplifies the design process. However, for some ranges of impedance values of practical interest in metasurface applications, the Integral Equation formulation has shown instabilities. This contribution proposes a way to improve that shortcoming; the method is based on the property of the involved operators and the nature of the IBC approximation

11:20 *Mixed Spatial-Spectral Domain Integral Equation Solver for Higher-Order Boundary Conditions in Electromagnetics*

Jordan R. Dugan, Tom Smy and Shulabh Gupta (Carleton University, Canada)

Higher-order boundary conditions are a useful tool for simplification of complex electromagnetic problems. Recently, a systematic technique, known as the Extended GSTC method, has been developed for simulating spatially dispersive metasurfaces using higher-order boundary conditions. In general, if we want to perfectly capture the angular scattering response of a metasurface using higher-order boundary conditions, it would require the computation of derivatives of infinite order. Therefore, achieving a good approximation of the metasurface scattering response may require the calculation of numerical derivatives up to a prohibitively high order, leading to an ill-conditioned system of equations. Here we develop a mixed spatial-spectral Integral Equation (IE) solver in 2D that allows for the simulation of electromagnetic problems involving higher-order boundary conditions without the explicit computation of any numerical derivatives.

11:40 *A Higher-Order Spectral Element Method to Model Eccentric Anisotropic Two-Layer Waveguides via Conformal Transformation Optics*

Raul Oliveira Ribeiro (Pontifical Catholic University of Rio de Janeiro, Brazil); Guilherme Simon da Rosa (São Paulo State University, Brazil); Jose R Bergmann (PUC-Rio, Brazil); Fernando Teixeira (The Ohio State University, USA)

We present an improved spectral element method (SEM) to analyze eccentric two-layer waveguides filled with anisotropic non-reciprocal media. The formulation employs conformal transformation optics (TO) theory to map the original eccentric waveguide into an equivalent concentric problem. The TO is extended to include non-symmetric and non-Hermitian media tensors. In the concentric domain, we apply higher-order two-dimensional basis functions associated with the zeros of the completed Lobatto polynomial to model the fields. We validated our approach against finite-element method (FEM) solutions, and the preliminary results show that our technique requires far fewer degrees of freedom than FEM.

12:00 *Generalized Transition Matrix Model Using Characteristic Basis Function Method for Open-Ended Cavities*

Inhwan Kim and Hyeong-Rae Im (Yonsei University, Korea (South)); Ic-Pyo Hong (Kongju National University, Korea (South)); Hyunsoo Lee (Inha University, Korea (South)); Jong-Gwan Yook (Yonsei University, Korea (South))

This paper proposes a novel method for large open-ended cavity problems using generalized transition matrix (GTM) method accelerated by the characteristic basis function method (CBFM). The electric surface currents on both exterior and interior walls of a cavity are represented by the characteristic basis functions (CBFs), resulting in the compression of the number of unknowns. The paper introduces the GTM model formulation with the CBFs. The GTM model is calculated efficiently using the CBFs, which has lower computational complexity. The numerical results are also introduced using an example of open-ended cavity structure, and evaluated computational efficiency compared with the conventional method.

Thursday, March 21 10:40 - 12:20

A06b: Advances in reflectarray antennas for wave control, space and 5G applications (continued)

T03 Aerospace, new space and non-terrestrial networks // Antennas

Room: M2

Chairs: Manuel Arrebola (Universidad de Oviedo, Spain), Pablo Camacho (Polytechnique Montreal, Canada)

10:40 *Folded Dielectric Reflectarray with Spherical Polarizer*

Andrea Massacesi and Michele Beccaria (Politecnico di Torino, Italy); Agnese Mazzinghi (University of Florence, Italy); Angelo Freni (Università degli studi Firenze, Italy); Paola Pirinoli (Politecnico di Torino, Italy)

A novel folded reflectarray, distinguished by the use of dielectric resonator elements and the integration of a spherical polarizer realized with a metalized plastic structure, is presented in this work. The adopted unit cell consists of a rectangular dielectric resonator placed over a thin substrate. It is designed to produce the required phase shift between the incident and the reflected field and to twist the field polarization by 90 degrees. To reduce the thickness of the reflecting surface, a 3D-printable dielectric material with a high value of the dielectric constant is used. Additionally, a spherical polarizer is exploited to enhance the reflectarray bandwidth compared to a flat configuration. Preliminary results on the design of a 408-element circular reflectarray demonstrate very good performance, with a gain of 28.2 dBi and a 1-dB bandwidth of 14.2%.

11:00 *Experimental Validation of Reflectarray-Based Base Station Antenna for Simultaneous Front- and Radio Back-Haul Links in mm-Wave Frequencies*

Álvaro F. Vaquero (Universidad de Oviedo, Spain); Borja Imaz-Lueje (Universidad Rey Juan Carlos, Spain); Marcos R. Pino and Manuel Arrebola (Universidad de Oviedo, Spain)

This work presents a reflectarray designed for indoor base station operation in mm-Wave bands. The reflectarray operates in dual orthogonal polarization (either circular or linear), using one polarization to create a femtocell tailored to the specific scenario, while the orthogonal polarization establishes a high-gain link with an external base station. Thus, a single antenna is utilized to simultaneously establish both the Front- and Back-haul links. The Front-haul design involves shaping the near field, achieved through synthesis techniques, while the Back-haul is addressed analytically. A design operating with two orthogonal linear polarizations is performed. The physical elements are implemented using a two-layer unit cell based on coplanar dipoles. The manufactured demonstrator closely aligns with simulations, showing that such antennas offer potential solutions in mm-Wave communication to enhance indoor coverage where polarization diversity is unnecessary. Furthermore, they enable a dual Front-haul and Back-haul link.

11:20 *A Wideband Reflectarray with Reconfigurable Polarization and Beam-Scanning by Using Liquid Crystal Delay Line for Millimeter-Wave*

Peyman Aghabeyki and Shuai Zhang (Aalborg University, Denmark)

A wideband reflective unit cell based on aperture-coupled delay line is proposed that leverages the Liquid Crystal (LC) technology and controls the vertical and horizontal polarizations separately. By illuminating the unit cell with linear slant polarization and controlling the phase of vertical and horizontal polarization components through separate delay lines, the phase and polarization of the reflective wave can be dynamically controlled. The proposed unit cell can generate Right-hand and Left-Hand circular, +45 Linear, and +135 Linear polarizations with 360° phase shift control. A 20x20 element Reflectarray (RA) is simulated, and beam-steering is demonstrated for different polarizations only by using a single polarized horn feed. For circular polarization mode, the RA achieves ±45° beam-steering range with a maximum 24.7 dBi realized gain, 20% Axial Ratio bandwidth, and 15% gain bandwidth in boresight at 29 GHz.

11:40 *Dual-Band Reflectarray-Based Electromagnetic Skin to Provide Millimeter-Wave Coverage in the 28/60-GHz Bands*

Jorge Vallejo, Eduardo Martínez-de-Rioja and Ana Arbolea (Universidad Rey Juan Carlos, Spain)

In this contribution, a low-profile dual-band smart electromagnetic skin (SES) is proposed to improve wireless communications in millimeter-wave 5G. The SES is based on a single-layer reflectarray panel that can operate simultaneously at the 28 and 60 GHz bands. The reflectarray unit-cell consists of a central lower frequency element which is surrounded by four higher frequency elements. The SES has been designed to provide a different coverage for each frequency (i.e., two separate beams with different pointing directions). A beamforming technique has been applied to broaden the beams in azimuth and achieve a wider coverage. The proposed device can be used to enable wireless communications in millimeter-wave 5G by providing enhanced coverage in non-line-of-sight (NLOS) scenarios.

12:00 *A High-Efficiency Reconfigurable Reflectarray Antenna Using Two Types of Active Unit Cells*

Yong-Hyun Nam (Hongik University, Korea (South)); Sun-Gyu Lee (Electronics and Telecommunications Research Institute, Korea (South)); Jeong-Hae Lee (Hongik University, Korea (South))

A reconfigurable reflectarray antenna (RRA) using two types of active unit cells is presented for high efficiency and simplification of the bias circuit. By combining two types of 1-bit active unit cell, a quasi 2-bit RRA is designed, which achieves four quantized phase states. In particular, this RRA is confirmed to have quantization efficiency equal to the ideal 2-bit for specific angle and similar to 1-bit for the other angles. The quasi 2-bit RRAs for two specific angles of 0° and 20° in the E-plane are simulated at 10.1 GHz, and the aperture efficiencies are calculated to be 35.0% and 37.4%, respectively. Compared to 1-bit RRA, the improvement of aperture efficiency is confirmed to be 73.3% for the 0° beam and 86.1% for the 20° beam, respectively.

Thursday, March 21 10:40 - 12:20

CS33b: Multiscale, Multiphysics and Unconventional Techniques for Electromagnetic Imaging (continued)

T08 EM modelling and simulation tools / Convened Session / Electromagnetics

Room: M3

Chairs: Tommaso Isernia (University of Reggio Calabria, Italy), Rosa Scapatucci (CNR-National Research Council of Italy, Italy)

10:40 *Nonlinear Correction of the Direct Inverse Problem Solution in Real-Time Imaging*

Cristina Origlia, David O. Rodriguez-Duarte and Jorge A. Tobon Vasquez (Politecnico di Torino, Italy); Natalia Nikolova (McMaster University, Canada); Francesca Vipiana (Politecnico di Torino, Italy)

This paper proposes a direct method for quantitative real-time imaging based on a nonlinear correction of the approximate linearized imaging kernel. The correction process relies on a pseudo-Rytov approximation employing the ratio between the total and incident fields in the scattering model, which can be estimated analytically. Unlike traditional iterative algorithms, there is no need for multiple computations of the direct scattering model, gaining computational speed and robustness to numerical inaccuracies. First, a fast direct inversion algorithm based on the Born approximation provides the initial guess for the permittivity distribution; this study employs the Truncated Singular Value Decomposition (TSVD) and an in-house finite element-based solver to compute the imaging operator. Then, the field correction factor is transferred onto the object's permittivity to enhance its quantitative accuracy. The proposal viability is verified in 2D synthetic experiments at microwave frequencies, verifying improvements in the reconstructed unknown permittivity.

11:00 *Supervised Learning Applied to Microwave Imaging System Calibration*

Ben J Martin, Seth J Cathers, Ian Jeffrey and Colin Gilmore (University of Manitoba, Canada)

Near-field microwave imaging systems seek a quantitative reconstruction of the permittivity in a region of interest. These systems measure raw S-parameters which contain the effects of antennas, cables, and other non-ideal aspects of the imaging system. Imaging algorithms use a computational forward model to make images, often assuming that fields are measured at points. In the absence of a sufficiently complex forward model that can model the physical system perfectly, these S-parameters need to be calibrated to facilitate the reconstruction. Herein, using a data set with three known targets over 300 collected S-parameter/electric field pairs, we evaluate a novel calibration method via supervised learning with a U-Net neural network

11:20 *Microwave Inversion of Measured S-Parameters Using a Thin-Wire Antenna Model*

Lucas Banting, Ian Jeffrey and Joe LoVetri (University of Manitoba, Canada)

An imaging procedure based on the minimization of an objective function that incorporates measured S-parameters is presented. Experimentally measured S-parameters are used to link modelled incident and reflected power waves at the antenna ports. The S-parameter objective function is incorporated into the Contrast Source Inversion method. A sub-grid thin-wire model is used to model these incident and reflected power waves. The new procedure is used to image a simple breast phantom, consisting of a tumour within a homogeneous fat region, placed within an air-based quasi-resonant breast imaging chamber. Single frequency S-parameters measurements at the ports of 24 half-loop antennas on the chamber walls constitutes the inversion data. The thin-wire antenna model, which reduces modelling error, together with the new objective function, lessens the burden on calibration procedures that often fail when the objective function is formulated using field components. Experimental results show promising imaging performance over a large frequency band.

11:40 *Deep-Learning Optimized Reconfigurable Metasurface for Magnetic Resonance Imaging*

Johannes Müller (University of Bremen & Fraunhofer MEVIS, Germany); Martina Falchi (University of Pisa, Italy); Endri Stoja (Fraunhofer FHR, Germany); Simon Konstandin (Fraunhofer MEVIS, Germany); Matthias Günther (Fraunhofer Mevis, Bremen, Germany); Danilo Brizi and Pierpaolo Usai (University of Pisa, Italy); Agostino Monorchio (University of Pisa & CNIT, Italy); Dennis Philipp (Fraunhofer MEVIS, Germany)

In this work, a one-dimensional metasurface prototype ($N = 14$) is presented that is digitally controlled in combination with deep learning (DL)-driven optimization. Both, the forward and inverse problem are addressed. The forward problem, involving the mapping of capacitance values to a desired magnetic field distribution, is well-posed and can be effectively solved through a variety of methods. The inverse problem, i.e., deriving capacitance values from observed magnetic fields, is tackled by deep learning, specifically through a Multi-Layer Perceptrons (MLPs) approach. The feasibility of training a neural network with simulation data, achieving sufficient agreement between numerical and experimental results is demonstrated. Deep learning-driven optimization of MTMs in MRI applications holds a huge potential for many applications in the future and it represents a significant step towards bridging the gap between simulated and experimental results.

12:00 *Impact of Antenna Radiation Pattern Linear Phase Shift in SAR Image Quality*

[Alicia Flórez Berdasco](#) (University of Oviedo, Spain); Jaime Laviada (Universidad de Oviedo, Spain); Fernando Las-Heras (University of Oviedo, Spain)

The effect of linear phase changes along the antenna radiation pattern beamwidth on synthetic aperture radar (SAR) imaging is evaluated by means of electromagnetic simulations. Electromagnetic images have been obtained for a set of linear phase offsets to characterize the effect of the non-uniform phase of the antenna radiation pattern on this type of measurements. From the study, a maximum threshold has been established to avoid target displacement and distortion, and thus, prevent the degradation of the electromagnetic image quality.

Thursday, March 21 10:40 - 12:20

IW8: Regulatory and Performance Testing Considerations for Future Wireless Communication Technologies, ETS-Lindgren

Room: M4

10:40 *Wi-Fi 6E/7: Amazing New Frontiers and Challenges*

Presenter: Bill Koerner (Keysight Technologies)

11:15 *Continued Evaluation of the Modern 5G Millimeter Wave Antenna Array Evaluation in Near- and Far-Field Environments*

Presenter: Jari Vikstedt (ETS-Lindgren)

11:50 *Trials and Tribulations of a Wireless and Digital Services Test Lab*

Presenter: Daniel Churchill (Cambridge Consultants)

Thursday, March 21 10:40 - 12:20

WG Active Array Antennas: WG meeting

Room: Fyne

Thursday, March 21 13:10 - 14:40

PA1: Poster session on Antennas for biomedical and health applications

T06 Biomedical and health // Antennas

Room: Expo/Poster

Chairs: Erdem Cil (University of Rennes 1, France), Joseph Costantine (American University of Beirut, Lebanon)

Omnidirectional Cylindrical Dielectric Resonator Antenna for off & on Body Communications 1

Tarek Saleh Abdou (The University of Sheffield, United Kingdom (Great Britain)); Salam Khamas (University of Sheffield, United Kingdom (Great Britain))

An innovative millimetre wave (mmWave) cylindrical dielectric resonator antenna (DRA) for off/on-body communication is presented. The proposed antenna offers broadside and omnidirectional patterns at two different frequency bands and make use of a planar feed network. The omnidirectional radiation has been achieved with a gain of 4.53 dBi and an impedance bandwidth of 2.1% by exciting the HEM₂₁₀ omnidirectional mode at 25.5 GHz. In addition, the HEM₁₁₁ fundamental mode has been excited to provide broadside radiation at 21.5 GHz. This dual-band performance was confirmed by measurements, exhibiting high agreement with simulations. Therefore, the proposed configuration is flexible and suitable for both on-body and off-body communications.

Dual-Band 3-D MIMO Antenna for Deep Tissue Devices 2

Amjad Iqbal (INRS, Canada); Penchala Reddy Sura (Visvodaya Engineering College, India); Muath Al-Hasan (Al Ain University, United Arab Emirates); Ismail Ben Mabrouk (Al Ain University & Princeton University, United Arab Emirates); Tayeb Denidni (INRS, Canada)

In this paper, a multiple-input multiple-output (MIMO) capsule endoscopic antenna is proposed for the 915 and 2450 MHz Industrial, Scientific, and Medical (ISM) bands. The single element of the MIMO antenna system has a small size of 5×4.75×0.1 mm³. It has simulated 10-dB bandwidths of 90 and 730 MHz at the low-frequency (915 MHz) and high-frequency (2.45 GHz) bands, respectively. Then, four elements are arranged in a cubical form to develop a quad-element MIMO antenna. The proposed three-dimensional (3-D) MIMO antenna has an overall size of 5×5×4.75 mm³. It has simulated realized gains of -28.85 and -20.68 dBi at 915 and 2450 MHz, respectively. The proposed antenna is designed and integrated into a capsule device. The other parts of the capsule device include batteries, a camera, light-emitting diodes (LEDs), a printed circuit board (PCB), and surface-mounted devices (SMDs). The endoscope is placed in the human model's stomach.

Eco-Friendly and Conformable PIFA Based on PEDOT: PSS and a Sustainable Chitosan Substrate for 5G Communications 4

Ilaria Marasco (Politecnico di Bari, Italy); Gaia de Marzo (Istituto Italiano di Tecnologia, Italy); Giovanni Niro (Politecnico di Bari, Italy); Francesco Rizzi (Istituto Italiano di Tecnologia, Italy); Antonella D'Orazio and Marco Grande (Politecnico di Bari, Italy); Massimo De Vittorio (Istituto Italiano di Tecnologia, Italy)

According to many institutions, the number of connected devices will be 125 billion in 2030. Hence, the need to minimize the environmental impact of the plastics derived from circuitry is self-evident. In this context, we present the design, fabrication and characterization of an eco-friendly and conformable Planar Inverted-F Antenna made of a conductive polymer blend based on PEDOT: PSS and placed on a sustainable chitosan substrate. The characterization of the fabricated prototypes is fully in line with the numerical simulations. This work shows the potentiality of the combination of the PEDOT: PSS and chitosan substrate for the realization of a new class of eco-friendly antennas for health monitoring sensors.

Phase Variation of Ingestible Dipole, Loop, and Patch Antennas in Gastrointestinal Tract 5

Erdem Cil (University of Rennes 1, France); Denys Nikolayev (Institut d'Électronique et des Technologies du Numérique (IETR) - UMR CNRS 6164, France)

This paper examines the behavior of magnitude and phase of reflection coefficient of ingestible antennas in the gastrointestinal tract for the purpose of sensing and distinguishing the gastrointestinal tissues. In this context, the paper presents the changes in these parameters for three common antenna types (dipole, loop, patch) in the interval of electromagnetic properties of the gastrointestinal tissues. The antennas operate in the 433 MHz ISM Band and conform to the inner surface of polylactic-acid capsules with shell thicknesses of 0.2, 0.5, and 1 mm. They are optimized in a homogeneous spherical phantom having time-averaged electromagnetic properties of gastrointestinal tissues. The changes in the magnitude and phase are presented in the intervals of 57-72 for relative permittivity and 0.5-2.1 S/m for the conductivity. The results show that the phase varies in wider intervals than the magnitude, indicating that it is better to track the phase for distinguishing the gastrointestinal tissues.

Monitoring Eye States Based on Transparent and Flexible Antenna in WBAN 6

Yu Yang and Yu Shao (Chongqing University of Posts and Telecommunications, China); Yu Yao (University of Sussex, United Kingdom (Great Britain)); Yanyang Zhang (Chongqing University of Posts and Telecommunications, China)

With the development of wireless body area network (WBAN), the integration of transparent and flexible antennas into wearable devices has been widely studied. Transparent and flexible antennas can be compatible with devices of different shapes, sizes and materials, achieving device miniaturization. Wearable antennas can achieve lightweight, flexible, low-cost, and portable wireless communication and sensing. This letter aims to design and fabricate a transparent and flexible monopole antenna operating at 5.8 GHz, fed by coplanar waveguide (CPW). We selected 650-nm-thick indium tin oxide (ITO) as conductors and 0.125-mm-thick polyethylene terephthalate (PET) as substrate. The antenna's surface resistance is 2-3 (Ω/sq), the average transparency is 73%, and the gain at 5.8 GHz is 1.074 dBi. We integrate this antenna into the lens for eye states monitoring and use vector network analyzer to measure return loss in three states: closing, opening, and blinking. And after data processing, the blinking frequency can be accurately calculated.

Miniaturised Magnetic Antenna for Wireless Implanted Medical Device 7

Mélusine Pigeon (University of Bath, Bath, UK); John Barton (Tyndall National Institute, Ireland)

This paper presents a miniaturised magnetic antenna that can be used for Wireless Implanted Medical device (WIMD). This antenna is designed for data transmission. The miniaturisation factor achieved is 1/9th of the size of a loop antenna in free space. The antenna was designed to work at Ultra High Frequency (UHF) frequencies range with an UHF Radio Frequency Identification (RFID) chip. This design could be used for other frequency ranges. Due to the high miniaturization factor the performances of the antenna are impacted but a read range of up to 80mm was achieved within a simplified phantom representing blood and fat.

Development of a Wearable IoT-Optimized Textile Antenna with Low Specific Absorption Rate in Three Frequency Bands 8

Niamat Hussain (Sejong University, Korea (South)); Md. Abu Sufian, Anees Abbas and Jaemin Lee (Chungbuk National University, Korea (South)); Seonggyoon Park (Kongju National University, Korea (South)); Nam Kim (Chungbuk National University, Korea (South))

This paper introduces a textile antenna designed for wearable Internet-of-Things (IoT) use, employing a slotted patch configuration. The antenna is constructed on standard textile material and operates within crucial IoT frequency bands, encompassing the 1.9 GHz, 3.5 GHz and 5.8 GHz band of Global System for Mobile Communications (GSM), 5G-sub-6-GHz, and industrial, scientific, and medical radio bands, respectively. Antenna offers -10 dB impedance bandwidths corresponding to 7.34, 3.4, and 5.03% with respect to resonating frequencies while having radiation efficiencies of 64.2, 76.2, and 75.9 %, respectively. This antenna have a high gain of 5.04, 6.35, and 6.9 dBi at first, second and third resonance, respectively. Most notably, it maintains relatively low specific absorption rates (SAR) of 0.7 W/kg, 1.04 W/kg, and 0.532 W/kg when averaged across 1 gram of tissue. These features make the proposed textile antenna well-suited for wearable IoT applications.

Embroidered Antenna-Based Sensor for Real-Time Natriemia Monitoring 10

Mariam El gharbi (Universitat Politècnica de Catalunya, Spain); Raul Fernandez-Garcia (Universitat Politècnica de Catalunya, Spain); Ignacio Gil (Universitat Politècnica de Catalunya, Spain)

This paper presents a feasibility study of a textile antenna-based sensor to monitor natriemia levels in real-time. The proposed device is composed of a square ring implemented on a textile substrate to detect different concentration of sodium chloride (NaCl). The textile substrate can absorb different concentration solutions of sodium through a square ring slot which contains maximum electric field distribution. Consequently, the dielectric properties of the substrate are changed according to the properties of the liquid absorbed in the sensing area. The designed antenna-based sensor is optimized to operate at 2.4GHz. The results demonstrated the capability of the proposed antenna sensor to detect different natriemia levels, including hyponatremia (110-130mmol/L), normonatremia (135-145mmol/L) and hypernatremia (150-170mmol/L), with a sensitivity of 39 kHz/(mg/dL). In addition to its capacity for detecting varying sodium concentrations associated with different natriemia levels, the proposed antenna sensor offers several advantages, including low cost, compact size and simplistic design.

A Compact Implantable Camera Integrated MIMO Antenna with Polarization Diversity for Wireless-Capsule-Endoscopy Applications 11

Muhammad Qamar (Queen Mary University of London, United Kingdom (Great Britain)); Kamil Yavuz Kapusuz (Ghent University & IMEC, Belgium); Mohamed Thaha and Akram Alomainy (Queen Mary University of London, United Kingdom (Great Britain))

In this paper, we present the development and performance evaluation of a MIMO ultra-compact camera-integrated antenna, uniquely equipped with polarization diversity. This antenna is designed for seamless integration into a pill-shaped capsule, custom-tailored for ingestible and implantable applications at 868 MHz. Extensive numerical analysis substantiates the antenna's robust impedance and radiation characteristics across diverse body tissues. Additionally, MIMO analysis affirms the appropriateness of this design for high-data-rate wireless capsule endoscopy (WCE) systems.

Textile Waveguide Antennas for On-Body Sensor and Communication Systems 12

Davorin Mikulic, Davor Bonefačić, Juraj Bartolić and Zvonimir Sipus (University of Zagreb, Croatia)

The integration of on-body sensors and communication networks is increasingly vital in fields such as sports, healthcare, elderly people support and military services. This paper explores the design and evaluation of textile waveguide antennas for on-body communication, focusing on efficient wave launching and performance assessment. The proposed miniaturized textile bidirectional waveguide antenna offers compact dimensions without sacrificing performance, thus advancing on-body communication technology.

Design of an UWB Conformal Antenna for Wireless Capsule Endoscopy 13

Chang Liu, Abdullah Alshammari and Abdulwahab Alghamdi (Durham University, United Kingdom (Great Britain)); Amjad Iqbal (INRS, Canada); Ismail Ben Mabrouk (Ain University & Princeton University, United Arab Emirates)

This paper introduces a novel, compact antenna for Wireless Capsule Endoscopy (WCE), operating at the 915 MHz, Industrial, Scientific, and Medical (ISM) frequency band. The suggested antenna achieves Ultra Wide-Band (UWB) operation. This design allows the antenna to operate across a broad frequency range from 0.59 to 1.36 GHz, with a fractional bandwidth of 96.25% centered at 0.8 GHz. The antenna's large bandwidth is able to provide higher channel capacity and address frequency detuning issues. A compact design, measuring 30.5mm × 9mm × 0.04mm, is achieved by implementing a meander path shape. This design achieves an average peak gain of up to -45.93 dBi. The specific absorption rate (SAR) is evaluated to be 0.0002W/Kg. The findings demonstrate that, under various scenarios, the designed antenna maintains communication at distances exceeding 6 meters, with a 15 dB margin.

Miniaturization of Wireless Power Transfer for Implantable Devices Using Voltage Doubler Rectifier 14

Abdenasser Lamkaddem (Carlos III University of Madrid, Madrid, Spain); Ahmed El Yousfi (Universidad Carlos III De Madrid, Spain); Vicente González Posadas (Polytechnic University of Madrid, Spain); Daniel Segovia-Vargas (Universidad Carlos III de Madrid, Spain)

In this paper, we present a new and high efficient wireless power transfer system for biomedical implants. The system composes of a dual-band implantable antenna, a wearable patch antenna, and a voltage doubler rectifier. The transmitter has an impedance bandwidth below -10 dB from 1.461 up to 1.48 GHz. On the other hand, the dual-band receiver has a 23.4 % and 16.5 % impedance bandwidths at 915 MHz (the industrial, scientific and medical -ISM) and 1.47 GHz, respectively. Good agreement has been observed between the measured results inside minced pork and salmon fish. Finally, a 8.7 x 3.15 mm² ultra-small rectifier has been developed to be integrated with the implantable device for wireless power transfer purposes.

Sensitivity of the Dielectric Spectroscopy with the Microwave Thermal Ablation Antenna to the Immersion Depth and Longitudinal Dimension of the Measured Media 15

Klementina Vidjak (Sapienza, University of Rome, Italy); Marta Cavagnaro (Sapienza University of Rome, Italy)

Microwave thermal ablation is an electromagnetic-based technique for treating malignant tissue. However, the success of such treatment highly depends on the design of the ablation antenna, its positioning in the targeted tissue and the matching of the antenna into the tissue. The common parameter on which all three conditions depend are the dielectric properties of the tissue. Therefore, to improve the ablation technique it would be beneficiary to develop a methodology for in-situ real-time dielectric spectroscopy with the ablation antenna itself. Until now, some studies dealing with this type of measurements have been published, but further analysis of the factors influencing the measurements need to be performed. In this work, the sensitivity of dielectric spectroscopy with asymmetric dipole applicators operating at 2.45 and 5.8 GHz in respect to their immersion depth into the tissue and the longitudinal dimension of the tissue was studied numerically.

Miniaturized Implantable Antenna with Ultra-Wide Bandwidth Characteristics for Leadless Pacemakers 3

Abdulwahab Alghamdi, Abdullah Alshammari and Liu Chang (Durham University, United Kingdom (Great Britain)); Amjad Iqbal (INRS, Canada); Ismail Ben Mabrouk (Ain University & Princeton University, United Arab Emirates)

This article presents a miniaturized antenna with a broad bandwidth tailored for use in cardiac leadless pacemakers. The proposed antenna has a compact size with a footprint of 9.44 mm², and an ultra-wide bandwidth of 3380 MHz, which effectively mitigates detuning effects. This bandwidth covers the frequencies from 0.77 GHz to 4.15 GHz, ensuring optimal performance across medical frequency bands, including ISM, Wireless Medical Telemetry Service (WMTS), and the midfield bands. The achievement of this ultra-wide bandwidth is attributed to the insertion of a meandered line in the ground plane and a large rectangular slot in the patch. Furthermore, to ensure patient safety, Specific Absorption Rate (SAR) examinations were conducted within a homogeneous heart phantom (HHP). In this HHP scenario, the proposed antenna, housed within a dummy leadless pacemaker, demonstrated high gain values of -27.5 dBi, -27.7 dBi, and -30.5 dBi at 0.915 GHz, 1.4 GHz, and 2.45 GHz, respectively.

CVNN Approach for Microwave Imaging Applications in Brain Cancer: Preliminary Results 9

Sandra Costanzo and Alexandra Flores (University of Calabria, Italy)

The application of Complex-Valued Neural Network (CVNN) is proposed in this work to significantly enhance the image quality derived from the solution of Inverse Scattering Problem (ISP) which are faced with Quadratic Born Iterative Method (BIM). The proposed approach takes advantage from the exploitation of the full information contained into complex-valued data inherent to the microwave imaging context, thus leading to directly reconstruct the conductivity parameter.

Thursday, March 21 13:10 - 14:40

PA3: Poster session on mm-wave and sub mm-wave Antennas II

T02 Mm-wave for terrestrial networks 5G/6G // Antennas

Room: Expo/Poster

Chairs: Michael A Dittman (Michigan State University, USA), Charikleia Tzimiragka (Université de Rennes, France)

Dynamic Programming-Based Beam Codebook Design for mmWave Multi-Antenna Module in Mobile Devices 38

Bing-Jia Chen (Academia Sinica, Taiwan); Yun-Ting Tsai and Sheng-Yeh Yang (National Taiwan University, Taiwan); Sung Mao Liao, Chien Ming Hsu and Chuanchien Huang (Taiwan); Kuo-Chu Liao (AsusTek Computer, Inc., Taiwan); Shih-Yuan Chen (National Taiwan University, Taiwan)

Beam codebook design is essential for enhancing the signal spherical coverage of multi-antenna module in mobile mmWave devices. Meanwhile, power consumption of the antenna module poses a significant challenge for 5G/B5G mobile devices. Therefore, the trade-off between power saving and degradation in spherical coverage gain should be simultaneously considered in the beam codebook design. In this paper, a dynamic programming (DP)-based algorithm is proposed to address this issue by hybridizing the full-chain and sub-chain codebooks in two schemes. The first scheme aims to minimize the degradation in the spherical coverage gain under a specific power saving ratio, while the second focuses on improving the power saving ratio given the level of degradation in the spherical coverage gain. The optimal beam codebooks thus obtained that the proposed DP-based algorithm achieves over 10% more power saving and less degradation in coverage gain, respectively, in the two schemes compared to the sub-chain codebook.

Design of Ultra-Wideband Dual-Polarized Corrugated Horn Antenna for 5G Application 22

Nan Hu (A-INFO INC, USA); Shuang Liu, Jianrui Liu and Lixin Zhao (Chengdu A-INFO Inc., China); Wenqing Xie (A-INFO Inc., China)

An ultra-wideband(UWB) dual-polarized corrugated horn antenna is proposed in this paper. The operating frequency band is 24-50GHz, covering the 5G communication frequency band. This antenna makes up for the deficiency of the traditional horn antenna in bandwidth and radiation characteristics. The combination structure of quad-ridge corrugated horn antenna and orthonode transducer(OMT) is used to realize the UWB, dual-polarization and high isolation radiation characteristics. In practical application, the waveguide coaxial transfer structure is required for installation and connection. The measured results meet the design requirements. The measured VSWR results are 2.2 Max., the port isolation results are -30dB Max. The proposed antenna has good far field characteristics. The gain results are 20dB Typ. and the cross polarization isolation are -35dB Max. The proposed horn antenna has been processed and applied in the practical systems.

A Wearable Open-Ring Dielectric Resonator Antenna with Frequency Reconfiguration 37

Xuewen Jiang and Zhijiao Chen (Beijing University of Posts and Telecommunications, China); Benito Sanz-Izquierdo (University of Kent, United Kingdom (Great Britain))

A wearable open-ring dielectric resonator antenna (DRA) with frequency reconfiguration is proposed in this paper. The travelling wave mode inside DRA is utilized to achieve wideband characteristic. By varying the insertion depth of the feeding probe, three different operating frequencies can be realized located at 21.2 GHz, 26.3 GHz and 32.7 GHz, respectively. The three operating bands achieve relative bandwidths of 15.6% (19.5 GHz - 22.8 GHz), 12.9% (24.6 GHz - 28 GHz) and 12.2% (30.7 GHz - 34.7 GHz), covering several frequency ranges from K band to Ka band. The simple structure and compact size of the proposed antenna present great potential in the millimeter-wave (mmWave) body area network (BAN) applications.

A 2x2 Dual-Band Open Loop Array with Circular Polarisation 25

Erendira Merlos-Garza and Rola Saad (The University of Sheffield, United Kingdom (Great Britain)); Salam Khamas (University of Sheffield, United Kingdom (Great Britain))

A novel dual band circularly polarised mmWave open circular loop antenna array is proposed. The antenna has been fabricated on a double sided Rogers RT5880 substrate with a double-sided parallel strip line (DSPSL) and mounted in a three layer Polytetrafluoroethylene (PTFE) case. The microstrip array offers an average gain of 13.85 dBi, impedance bandwidths of 4.60% and 3.55% at 30 GHz and 34 GHz respectively, and a CP bandwidth of 10.16%. Close agreement has been achieved between measured and simulated results

5G Millimeter-Wave Reflectarray Antenna Design with a Good Gain-Filtering Characteristic Based on a High-Efficiency Polarization Converter 31

Wen Fu, Gert Pedersen and Shuai Zhang (Aalborg University, Denmark)

A shuttle-shaped polarization converter with high-efficiency is designed in the paper, which can operate at 5G millimeter wave and can realize polarization conversion rate (PCR) over 90% from 27.7 GHz to 29.2 GHz. Rotating the polarization converter unit clockwise results in another unit with the same reflection coefficient and a phase difference of 180 degrees. Based on these two units, a high gain reflectarray antenna (RA) with a good and stable gain-filtering characteristic is presented. The maximum realized gain is 23.7 dBi at 28.5 GHz. For a beam at any angle, the realized gain versus frequency exhibits a filter-like curve with a zero.

Beam-Tilted All-Metal Radial-Line Slot Array Antenna with Uniform Spacing 20

Jose I Herranz-Herruzo (Universitat Politècnica de València & APL - ITEAM, Spain); Alejandro Valero-Nogueira (Universidad Politècnica de Valencia, Spain); Miguel Ferrando-Rocher (Universitat Politècnica de València & Antennas and Propagation Lab, Spain)

This communication proposes an all-metal radial-line slot array antenna with a tilted beam, intended to mm-wave communications. Instead of modifying the array spacing along the beam tilt plane, an azimuthal variation of the propagation constant within the feeding waveguide is introduced. With this aim, the parallel-plate waveguide is loaded with a non-uniform bed of nails, tailoring each pin height accordingly. The operation principle and the design guidelines of this uniformly-spaced array are explained, and the beam-tilting performance is assessed.

A Single-Layer Quadruple-Band Millimeter-Wave Antenna Using Split-Rings for 5G Application 18

Nan Hu (A-INFO INC, USA); Shuang Liu, Jianrui Liu and Lixin Zhao (Chengdu A-INFO Inc., China); Wenqing Xie (A-INFO Inc., China)

This manuscript presents a single-layer quadruple-band millimeter-wave antenna for 5G application. Its upper layer is made up of a hexagonal patch fed by a 50 Ω microstrip line. By etching two symmetric split-ring slots on the hexagonal patch, it allows to operate at three frequencies which are 27.5 GHz, 44.6 GHz, and 50.7 GHz. Then, a pair of L-shaped branches are coupled on both sides of the microstrip line to realize the resonance point of 36.7 GHz. The gains at these four frequencies respectively are 6.4 dBi, 7.6 dBi, 9.2 dBi, and 7.1 dBi while the -10 dB impedance bandwidth cover 27.2 GHz-27.8 GHz, 37.3 GHz-37.6 GHz, 44.3 GHz-44.9 GHz, and 50.1-51.7 GHz. These results indicate that the proposed antenna is a promising candidate for 5G millimeter-wave applications.

1-Bit RIS Unit Cell with Mechanical Reconfiguration at 28 GHz 21

Marcos Baena-Molina (University of Granada, Spain); Angel Palomares-Caballero (IETR-INSA Rennes, France); Ginés Martínez-García, Rubén Padial-Allué and Pablo Padilla (University of Granada, Spain); Juan Valenzuela-Valdés (Universidad de Granada, Spain)

In this paper, a mechanically tunable unit cell for reconfigurable intelligent surfaces (RIS) is presented. The RIS unit cell design is based on a metallic cylinder with a metallic cone-shaped element placed at one end. Thanks to the two positions provided by the mechanically reconfigurable cylinder, the cone-shaped element produces a phase shift in reflection of 180° at 28 GHz and therefore, giving the 1-bit reconfiguration. A comparison of the cone-shaped element with other types of geometries such as a cube and a cylinder has been performed. Besides, in view of the unit cell design, a cost-effective fabrication using 3-D printing and spray metallization is considered. A study of dimensional tolerances and conductivity values for the proposed RIS unit cell is done. The simulated results show the robustness of the RIS unit cell for both main dimensions and conductivity values for a frequency range between 25 GHz and 30 GHz.

Impact of the Antenna Topology on the Combination of Full-Duplex Spatial Modulation and RF Energy Harvesting 34

Andriamanohisoa Hery Zo Jean Baptiste (Univ Lyon, INSA Lyon, INRIA, CITI, France); Florin Hutu (Univ Lyon, INSA Lyon, Inria, CITI, France); Guillaume Villemaud (Université de Lyon, INSA-Lyon, INRIA, CITI, France)

In the context of full-duplex spatial modulation (FDSM) systems, this paper proposes a strategy that exploits the subset of antenna that is not used by the transmitter nor by the receiver to perform RF energy harvesting (RFEH). Through the mutual coupling effect, the transmitting antenna transfers a part of its power to the other antennas. Our idea is to recycle this power in complement to the ambient RF sources. Our study shows that the level of the available power may be greater than the RF ambient sources. The impact of the spacing d between the elements of an array of four antennas on the performance of the FDSM-RFEH was studied. By analysing the transfer coefficients extracted from S-parameters simulations, the role of each antenna (emission, reception, RF energy harvesting) may be established.

A Millimeter-Wave Binary Reconfigurable Intelligent Surface on a Low-Cost FR4 Substrate 19

Chen-Yi Chang (Graduate Institute of Communication Engineering, National Taiwan University, Taiwan); Hsi-Tseng Chou (National Taiwan University, Taiwan)

In this work, a reconfigurable intelligent surface (RIS) is designed and implemented on a FR4 dielectric substrate for cost-effective fabrication to improve the electromagnetic (EM) wave propagation degradation in an indoor environment at the millimeter-wave (mmWave) frequency band from 27.9 GHz to 28.5 GHz. The proposed reflecting element is an impedance tunable slot-based structure that can provide low reflection loss and binary phase modulation. A modified analytic model of RIS based on the discrete summation of elemental complex radio cross sections (RCSs) is developed for easy RIS pattern estimation and optimization. Numerical results of RIS multi-beam patterns are presented to demonstrate its feasibility.

Broadband Waveguide Magneto-Electric Dipole Antenna for F-Band Applications 26

Felix Matt and David Zimmermann (Ulm University, Germany); Maximilian Döring and Christian Waldschmidt (University of Ulm, Germany)

This paper describes a waveguide-fed magneto-electric dipole with a relative bandwidth of 46%. The antenna has been milled from an aluminum block, constructed as two half-shells, and is fed by a standard WR8 rectangular waveguide. The antenna element is coupled to the waveguide through an aperture, allowing for a low profile configuration. This, combined with the choice of aluminum material as a good thermal conductor, makes the antenna an attractive option for industrial and high power radar or future 6G applications. The full-wave simulation results were validated through far-field antenna measurements. The antenna exhibits a gain of 10 dBi with unidirectional radiation pattern and its impedance bandwidth and 3 dB gain bandwidth cover the entire F-band from 90 GHz to 140 GHz.

Shorted Stacked Patch Array for Photonic Beam Steering at mm-Waves 28

Charikleia Tzimoragka (Université de Rennes, France); Ronan Sauleau (University of Rennes 1, France); Mehdi Alouini (Institut de Physique de Rennes - Université Rennes 1 - CNRS, France); Cyril Paranthoen (FOTON-INSA lab, France); David González-Ovejero (Centre National de La Recherche Scientifique - CNRS, France)

We present the design of a mm-wave phased array antenna enabled by photonic beam steering. The mm-wave signal is generated by InP uni-traveling-carrier (UTC) photodiodes within the photonic integrated chip (PIC). The antenna array consists of four sub-arrays, each comprising two stacked patch elements. The bottom patch is shorted to create a compact element, enabling a half-wavelength spacing in the scanning plane. This configuration results in a relatively wide scanning range of $\pm 1-30^\circ$ without significant sidelobe levels. The complexity of this structure lies in the heterogeneous integration of the InP chip with the antenna array and biasing network, all printed on a low-loss substrate with low relative permittivity. The proposed array exhibits a simulated peak directivity of 16 dBi and an impedance and -3 dB gain bandwidth ranging from 43.8 GHz to 58.8 GHz.

MIMO Array Decoupling with SSR Structure in Joint Communication and Sensing System 30

Zizhen Zhang and Zhirun Hu (University of Manchester, United Kingdom (Great Britain))

The weight-beamforming algorithm utilized in the joint communication and sensing (JCAS) system has shown promise in mitigating system coupling. However, the algorithm's tendency to set excessive frequency nulls can lead to signal loss. Consequently, this work examines the decoupling process from the perspective of antenna array design and proposes a MIMO antenna array design scheme that operates in the 28 GHz frequency band. This design scheme effectively addresses the coupling issue between the transmitting and receiving antennas by integrating it with beamforming algorithms. By employing SSR metasurface decoupling structures, this approach significantly reduces coupling by approximately 33 dB, resulting in improved system performance and the preservation of transmission information.

Study of Environmentally-Friendly Radomes Using Cork-Rubber Composites for 5G Backhaul Links at E-Band 32

Joao M. Felício (Escola Naval, Portugal & CINAV - Instituto de Telecomunicações, Portugal); Eduardo Motta Cruz (Radio Frequency Systems, France); Jorge R. Costa (Instituto de Telecomunicações / ISCTE-IUL, Portugal); Sergio Matos (ISCTE-IUL / Instituto de Telecomunicações, Portugal); Carlos A. Fernandes (Instituto de Telecomunicações, Instituto Superior Tecnico, Portugal)

Polymer-based materials face increasing limitations imposed by European legislation due to their environmental impact, namely carbon footprint and recycling capabilities. Radome antennas often use these materials due to their electrical and mechanical properties and, therefore, there is a search for alternative dielectrics. Here, we evaluate the performance of cork + nitrile rubber and cork + chloroprene rubber composites to be used in radomes at E-band for 5G backhaul communications. Both materials present a dielectric constant of around 1.6 and a loss tangent of 5×10^{-2} at 50 GHz. We fabricate a 1ft reflector antenna which we covered with a cork-rubber radome. We measure the radiation pattern and isotropic gain across the 71-86 GHz frequency band. Results indicate that the cross-polarization slightly deteriorates with the use of cork+rubber and the gain drops by around 1 dB, when compared to an ABS radome used by Radio Frequency Systems.

Self-Isolated MIMO Antenna Using SIW Cavity Antenna for Dual-Band (28, 38 GHz) Applications 33

Mahesh Kumar Busineni, Nancy Modi and Jayanta Mukherjee (Indian Institute of Technology Bombay, India)

This paper introduces a substrate integrated waveguide (SIW) antenna for dual-band applications. The antenna comprises a SIW cavity and a rectangular ring slot on the top metal layer for the radiation. Two different modes, i.e., TM₁₀₀ patch mode and half-TE₃₁₀ cavity mode, are excited in the cavity so that the antenna operates in 28/38 GHz band. Also, the radiation mechanism of the proposed SIW antenna with its electric and magnetic field distributions is provided. The single antenna element achieves a fractional bandwidth of 6.65% (26.91-28.76 GHz) and 1.45% (37.71-38.25 GHz) at the two resonant frequencies. Also, the peak gain of 6.57 dBi and 4.56 dBi is achieved in their respective bands. Further, utilizing the SIW cavity property of self-isolation, a four-element MIMO antenna is presented. The MIMO antenna exhibits the fractional bandwidth of 6.69% and 1.23% with minimum port-to-port isolation of 28.48 dB and 22.45 dB within the operating bands.

Frequency Reconfigurable Flexible Printed Antenna Based on Non-Volatile RF Switches for Wearable Applications 24

Yize Li (The University of Manchester, United Kingdom (Great Britain)); Xiaoyu Xiao, Zirui Zhang and Zhirun Hu (University of Manchester, United Kingdom (Great Britain))

This paper presents an innovative frequency-reconfigurable, flexible printed inverted F-shaped monopole antenna, explicitly engineered for wearable applications, and designed to operate across multiple bands without necessitating complex structures or exhaustive optimizations. Constructed on a pliable Kapton substrate and utilizing non-volatile RF switches, the antenna can function assertively across four distinct operating modes, rendering dynamic frequency responses in the L-band, S-band, and C-band. This versatile approach is apt for a range of applications, from weather radar systems to global navigation satellite systems, whilst potentially integrating with wearable technologies. Notably, the employment of non-volatile switches obviates the need for static power during mode switches, markedly minimizing DC power consumption.

Beam Steering Range Enhancement of Bifocal Reflectarray Using Irregular Distribution of Meta-Atoms 16

Mustafa Khalid Taher Al-Nuaimi (Loughborough University, United Kingdom (Great Britain) & Wireless Communications Research Group, United Kingdom (Great Britain)); William Whittow (Loughborough University, United Kingdom (Great Britain)); Guan-Long Huang and Rui-Sen Chen (Foshan University, China)

The beam steering range improvement in this work is realized via breaking the symmetry (periodicity) along x- and y-axes and using an irregular (aperiodic) distribution of meta-atoms on the BiRA aperture. This is accomplished without the need to optimize the reflection phase using complicated and time-consuming algorithms. The geometric phased meta-atoms of the proposed irregular BiRA are distributed without any transitional periodicity in the xy-plane in a way similar to the distribution of seeds of a sunflower. Bifocal parabolic phase distribution is imposed on all the aperiodic geometric phased meta-atoms across the irregular BiRA aperture. It is shown that the proposed BiRA with irregular distribution of geometric phased meta-atoms can realize 140° ($\pm 70^\circ$) beam steering range (with less than 3 dB gain loss) from 14 GHz to 24 GHz. The maximum measured gain is 26.8 dBi at 19 GHz, and a maximum aperture efficiency of 50.9%.

Embedded Graded Index Lens for Mitigating the Phase Error of an SIW Horn Lens Antenna 23

Hossein Eskandari and William Whittow (Loughborough University, United Kingdom (Great Britain))

A graded index lens embedded in the body of a substrate-integrated waveguide horn antenna is designed using transformation optics to mitigate the phase error at the antenna aperture. A conformal transformation is established in the design procedure, which leads to an all-dielectric inhomogeneous medium that can be realized by perforating a Rogers RO4350B substrate. Compared to the conventional horn antenna with the optimum length, the proposed lens antenna is 30% shorter and enhances the directivity by a value of 2.5 dB at 40 GHz.

Sub-THz Spatially Modulated Beam Splitting Reflectors for Potential RIS Implementations 35

Tung Duy Phan and Jaakko Palosaari (University of Oulu, Finland); Di Kong (University of Oulu, China); Tuomo Siponkoski, Sami Myllymaki, Marko E Leinonen, Aarno Pärssinen and Jari Juuti (University of Oulu, Finland); Ping Jack Soh (University of Oulu & Katholieke Universiteit Leuven, Finland)

Reconfigurable intelligent surfaces (RISs) promise to revolutionize wireless communications by creating a smart electromagnetic environment. They facilitate beamsplitting and beamsteering of EM waves in sub-THz communications. In this work, we design and demonstrate concept of a spatially modulated RIS that can potentially operate as a reconfigurable beam splitter. Unlike traditional reflectors based on resonating structures, this design uses non-resonating elements, offering broader operational frequency range with potential variable-frequency beamsplitting. The proposed structures are first theoretically designed using theoretical calculations, followed by simulations and experimental validations. By adjusting only the element spacing, it can split a 150 GHz normal incident wave into multiple beams at varying reflection angles. Such multi-beam control capability in reflectors promises a potential pathway towards enabling reconfigurable intelligent surfaces in future joint communications and sensing systems.

Sub-THz On-Chip CPW Monopole on InP with Cross-Shaped Slot for Bandwidth Enhancement 27

Andrzej Dudek (AGH University Krakow, Poland); Abdullah Al-Khalidi (University of Glasgow, United Kingdom (Great Britain)); Krzysztof Wincza (AGH University of Science and Technology, Poland); Mahmoud Wagih (University of Glasgow, United Kingdom (Great Britain))

THz communications call for highly integrated wireless chips. This paper presents the first, on-chip sub-THz coplanar waveguide (CPW)-fed monopole antenna covering the full J-band (220-330 GHz), on an Indium Phosphide (InP) substrate. The antenna is designed on a high-permittivity Indium Phosphide (InP) dielectric substrate with a single layer of metallization. Targeting multi-GBPS communication applications, the antenna is designed to have an S₁₁ bandwidth covering 230-330 GHz. Through the addition of a cross-shaped slot to the monopole's radiator, the fractional bandwidth is improved by nearly three-fold, from 11.1% to 29.6%. The designed antenna features stable radiation patterns throughout the entire operational frequency range, with a single element gain over 3.8 dBi, while maintaining a small footprint of 330 $\mu\text{m} \times 225 \mu\text{m}$ (0.25 $\lambda \times 0.17\lambda$ at 230 GHz).

MIMO Signals Processing Utilizing Optical Crossbar Linear Operator 36

Ronis Maximidis, Stefanos Kovaivos and Ioannis Roumpos (Aristotle University of Thessaloniki, Greece); Apostolos Tsakyridis (Aristotle University of Thessaloniki, CIRI, Greece); George Giamougiannis, Miltiadis Moralis-Pegios, Dimitra Ketzaki and Nikos Pleros (Aristotle University of Thessaloniki, Greece)

This paper introduces an innovative photonic MIMO processing architecture through the adaptation of a crossbar linear operator. The merits of this approach, such as restorable fidelity and reduced programming complexity, are highlighted. Experimental validation is conducted using a 4x4 integrated crossbar photonic chip, resulting in the reporting of an 8.4 dB power tunability and a complete pi-phase shift for every node, validating in this way the tunable weight matrix implementation. Furthermore, the paper outlines the potential directions for further enhanced performance.

Wideband Array Antenna with Single-Layer Feeding Network at Ka-Band 17

Ying Sun and Peiye Liu (Aalborg University, Denmark); Ondřej Franek (Aalborg University & APMS Section, Denmark); Gert Pedersen and Shuai Zhang (Aalborg University, Denmark)

This work presents a wideband slot array antenna with a single-layer feeding network at Ka-band for the fixed wireless communication system. To improve the bandwidth, the circular arm dipole slot is used as the radiating element, fed by open-ended rectangular waveguides. Then, a combination of the ridged waveguide and the hollow waveguide is implemented to realize the corresponding one-to-one excitation between the output ports of the feeding network and the radiation slots. The 4 by 4 slot array antenna achieves a wide bandwidth of 34.3% with a reflection coefficient remaining below -14dB, reasonably good radiation patterns, and a total efficiency of over 90%.

Wideband Aperture-Coupled Array Design for Automotive Radar Applications 39

Lazaros Alexios Iliadis and Achilles D. Boursianis (Aristotle University of Thessaloniki, Greece); Panagiotis Sarianniadis (University of Western Macedonia, Greece); Zaharias D. Zaharis and Sotirios Sotiroudis (Aristotle University of Thessaloniki, Greece); Maria S. Papadopoulou (International Hellenic University & Aristotle University of Thessaloniki, Greece); Christos Christodoulou (The University of New Mexico, USA); Sotirios Goudos (Aristotle University of Thessaloniki, Greece)

Advanced driver assistance systems (ADAS) technology has been developed to improve driver safety and is a major part of today's autonomous vehicle functionalities. Automotive radars operate as core sensors in modern ADAS systems since they can detect the speed and range of objects near the vehicle. This work uses a recent variant of the Runge-Kutta algorithm, namely RUN, to design an aperture-coupled antenna array for automotive radars. The proposed array consists of five U-shaped patch elements and achieves low return loss, high gain, and high efficiency at 77 GHz - 81 GHz.

Thursday, March 21 13:10 - 14:40

PA5: Poster session on Sub-6GHz antennas for terrestrial networks

T01 Sub-6 GHz for terrestrial networks (5G/6G) // Antennas

Room: Expo/Poster

Chairs: Daniele Cavallo (Delft University of Technology, The Netherlands), Sarah E Clendinning (KTH Royal Institute of Technology, Sweden)

High-Gain Shared-Aperture Patch Phased Array and Reflectarray Antenna 61

Senlin Lu and Shi-Wei Qu (University of Electronic Science and Technology of China, China)

A dual-band shared-aperture antenna, integrating a patch phased array and a reflectarray antenna (RA), is presented in this paper. The X-band phased array uses stacked patches as radiators, while the Ka-band RA also employs patches but with various sizes to achieve desired phase compensation, placing above the X-band array. In addition, the upper ones of stacked patches serve as the ground plane for Ka-band RA operation. Due to this configuration, the X-/Ka-band shared-aperture operation is realized with high-gain property. The proposed shared-aperture antenna achieves an active VSWR below 3 in 10.2 ~ 12 GHz during $\pm 45^\circ$ beam scanning in E/H planes. Moreover, the 3-dB gain bandwidth is 16.6% (27.1 ~ 32.0 GHz), with a peak gain of 26.2 dBi at 29 GHz, corresponding to an aperture efficiency of 53%.

DC Bias Routing Design for Wideband Reconfigurable Transmitarray Based on 1-Bit Phase-Switching Elements 51

Bo-Ting Lin, Sheng-Wei Wu and Shih-Yuan Chen (National Taiwan University, Taiwan)

DC bias routing design is critical but challenging for a wideband reconfigurable transmitarray (RTA) to control unit cells without compromising performance. To analyze the impact of routing and to eliminate the need for discrete RF choke components, three common routing rules are first summarized, followed by a proposed advanced rule: to disperse the modal deterioration areas of each mode. Based on these rules, four DC bias routing cases are designed for an RTA composed of 8-by-8 wideband 1-bit phasing elements (based on our previous work) and analyzed using modal deterioration analysis. The simulated radiation patterns of the 8-by-8 RTA under the four routing cases are compared to assess the impact of different routing strategies. The results are coherent with the modal deterioration analysis and verify that the proposed routing rule is beneficial for wideband RTA design in keeping the radiation performance unaffected without using discrete components for RF choking.

Characterization of All-Metal Multi-Feed Antenna for High Power Applications 54

Alessandro Garufo (TNO Defense Safety and Security, The Netherlands); Erwin M. Suijker (TNO, The Netherlands); Diogo C. Ribeiro and Christian Trampuz (TNO Defense Safety and Security, The Netherlands); Stefania Monni (TNO Defence Security and Safety, The Netherlands)

An all-metal antenna with multiple feeding points for high power applications is presented in this paper. The radiating element is a stacked patch fed by coupled slots, and it is composed only by stacked metal layers realized by milling machining, ensuring a reliable thermal behaviour of the antenna for high input power level applications. The multi-feed strategy of the antenna is realized on a multi-layer substrate, enclosed in a metal cavity within the antenna structure, supporting four striplines feeding the slots. such transmission lines are meant to be connected to four HPAs. The demonstrator is a stand-alone radiating element, which has been returned from the radiating element designed in array environment in order to support an EIRP of 30dBW over a wide scanning range, max $s = 50$ for all θ -planes, over 15% bandwidth.

A Dual-Port Antenna for Colinearly Polarized Full Duplex and Pattern Reconfigurable Applications 42

Yuqi Wang, Quan Xue, Zhipeng Hu and Shaowei Liao (South China University of Technology, China)

This article introduces a symmetrical dual-port antenna designed to operate under distinct excitation strategies for two specific purposes. First, it enables co-polarized in-band monostatic full-duplex communication by independently operating the transmitter (TX) and receiver (RX) channels. Second, it exhibits radiation pattern reconfigurability when the two ports collaborate with different phase differences. Regarding the decoupling mechanism, the mutual coupling is suppressed based on the odd and even modes, by incorporating an LC resonator. It not only achieves antenna decoupling but also enables pattern reconfigurability. The antenna can realize main beam scanning between the broadside (odd mode) and end-fire (even mode) directions, maintaining stable active reflection coefficients and cross-polarization levels. The proposed versatile antenna serves as a good candidate for multi-scenario applications and array setups.

Pulse Preserving Capability of an Ultrawideband Dispersive Dielectric Resonator Antenna 48

Xiantao Yang and Yi Huang (University of Liverpool, United Kingdom (Great Britain)); Elliot L. Bennett (The University of Liverpool, United Kingdom (Great Britain)); Ilkan Calisir and Jianliang Xiao (University of Liverpool, United Kingdom (Great Britain))

The pulse preserving capability in terms of system fidelity factor (SFF) of a new ultrawideband dielectric resonator antenna (DRA) made of a dispersive material is evaluated in this paper. The proposed antenna is developed based on a special frequency-dependent dispersive material whose relative permittivity is inversely proportional to the frequency square. Due to the small variation of gain and stable radiation pattern of the proposed antenna, the calculated SFF is very close to unity, showing the high quality of pulse transmission through the proposed antenna system. Overall, the proposed antenna shows ultrawide bandwidth, stable radiation pattern and gain, and excellent pulse-preserving capability, which is promising for future wideband high-speed wireless communication systems.

Bifunctional Stubs Enabled MIMO System for Wideband Mobile 5G and Wi-Fi 6E Applications 40

Zhipeng Hu, Quan Xue and Yuqi Wang (South China University of Technology, China); Xuekang Liu (University of kent, United Kingdom (Great Britain)); Zhiheng Zhou

(South China University of Technology, China)

A dual-function grounded stubs (DFGSs) structure is presented to demonstrate the design philosophy of wideband radiation enhancement and coupling suppression simultaneously. It improves the impedance matching and bandwidth under multi-resonant modes enabled by DFGSs while maintaining a good isolation level across the operating band. To verify the feasibility and effectiveness of the operating mechanisms, a 4 × 4 MIMO antenna system is prototyped. Measured results show good agreement with simulations. A straightforward working mechanism, with the merits of enhanced radiation properties and compatibility with MIMO, exhibits a promising solution for future Wi-Fi 6/6E and 5G NR MIMO modularized integration design.

Analysis and Measurement of Key Performance Indicators for MIMO Antennas 57

Ossian Kynman (Umeå University & Abracon LLC, Sweden); Jonatan Lindahl and Jonas Starck (Abracon LLC, Sweden); Claes Beckman (KTH Royal Institute of Technology, Sweden)

Predicting the performance of antenna arrays designed for MIMO communications is difficult. To determine the benefits that additional antenna elements may provide to a wireless system, the statistical correlation between the signals received from the antennas needs to be evaluated. In 2003 Blanch, proposed a simple method to estimate the correlation coefficient from S-parameters and in 2005 Hallbjörner proposed a modified version including the effect of antenna efficiency. We investigate the validity of these methods. Three different antenna arrays, with four elements each, and with varying efficiency and mutual coupling were designed, manufactured and measured. The method proposed by Blanch was found to be inaccurate whereas the Hallbjörner method produced better results but required determination of antenna efficiencies. S-parameter measurements alone do not provide valid estimates of the MIMO performance of antenna arrays. In order to evaluate MIMO performance, the antenna efficiency is paramount and needs to be measured accurately.

A Linearly Polarized Wideband Antenna with A Stable Omnidirectional Radiation Pattern 59

Hong-Tien Vu (Research Institute of Embedded Electronic Systems (IRSEEM), ESIGELEC & University of Rouen Normandy, France); Constant M. A. Niamien (Normandie Univ, UNIROUEN, ESIGELEC/IRSEEM, Rouen, France)

This paper presents a wideband linearly polarized antenna with a stable omnidirectional radiation pattern. The proposed technique combines linear parasitic radiators with a main dipole to create and control additional resonant modes. This enlarges the impedance bandwidth while maintaining linear polarization and stable radiation characteristics over a broad-covered band. Simulations and experiments confirm these results on a fabricated prototype showing a wide impedance bandwidth of 41% (0.65 - 0.99 GHz), a stable omnidirectional radiation pattern, and a high efficiency of 80%.

A Cascaded Resonator Decoupling Network for Two Filtering Antennas with Adjacent Operating Bands 43

Qian Jianfeng and Benito Sanz-Izquierdo (University of Kent, United Kingdom (Great Britain)); Steven Shichang Gao (Chinese University of Hong Kong, China); Hanyang Wang (Huawei Technologies, United Kingdom (Great Britain))

In this paper, the mutual coupling problem between two adjacent-band filtering antennas is addressed. A coupled-resonator DN is co-designed with the coupled filtering antennas with little effect on the original filtering responses. By connecting this network to the coupled antennas in parallel, the mutual coupling between two 2nd order filtering antennas can be suppressed dramatically, even when they are operating over the closely arranged frequency bands. A step-by-step realization of the DN is provided. To verify the concept, a prototype of decoupled antennas using the DN is presented. Full-wave simulations and measurements indicate that this coupled-resonator DN can enhance the isolation between two filtering antennas up to 30 dB with little effect on the filtering performance of each antenna for both in-band and adjacent-band operations.

A High Efficiency and Ultra-Wideband Rectenna for RF Energy Harvesting Application 49

Meghdad Khodaei (University of Quebec in Outaouais, Canada); Halim Boutayeb (Université du Québec en Outaouais, Canada); Larbi Talbi (University of Quebec - Outaouais, Canada)

In this letter, an ultra wideband rectenna using a novel wideband matching circuit for energy harvesting systems is proposed. A new simple and wide band matching circuit configuration that operates from 0.9 to 2.5 GHz is connected to an ultra wideband (UWB) antenna to make a rectenna system. Simulation results of proposed rectenna exhibits good matching performance ($S_{11} < -10$ dB) and a high RF-dc conversion efficiency (>55%) throughout a broad frequency range from 0.9 to 2.5 GHz, covering GSM, Wi-Fi, and WLAN bands. The maximum efficiency of the rectenna is around 61% an output voltage is over 1.9 Volt, for an input power of 10dBm and load resistance of 750Ω. Based on the proposed structure for matching scheme, a highly efficient UWB rectenna over a wide frequency band is achievable with stable high efficiency.

Circularly Polarized Wide-Angle Scanning Phased Array Based on Heterogeneous Beam Element 41

Jia Wei, Shaowei Liao, Yinglu Wan, Quan Xue and Wenquan Che (South China University of Technology, China)

A circularly polarized (CP) phased array antennas (PAA) based on wide heterogeneous beam elements (HBEs) is presented to realize wide-angle scanning for the first time. The proposed HBEs PAA is formed by two elements at two sides with inclined beams and two elements between two sides elements with broadside beams. A 5-GHz CP HBE antenna with wide beamwidth is designed, whose beam can be inclined up to 50° by loading a parasitic director. Then, based on it, a 1×4-element HBE PAA is designed, fabricated, and measured, whose 3-dB gain fluctuation and 3-dB axial ratio scanning range reaches ±80° (±14° wider than its standard counterpart) with 8.3 dBi broadsides scanning gain (1.2dB lower than its standard counterpart). To the authors' best knowledge, compared with the former linear CP PAA with similar amount of elements, the proposed design shows the widest scanning range.

Highly Transparent and Efficient Flexible Antenna for Vehicle-To-Everything (V2X) Applications 56

Mehmet Emre Eralt (Middle East Technical University & Accelerate Simulation Technologies, Turkey); Ozlem Aydin Civi (Middle East Technical University, Turkey); Reyhan Baktur (Utah State University, USA)

This paper presents a single-sided planar transparent monopole antenna for vehicle-to-everything application. The fundamental limiting factor for the antenna's efficiency is studied, and a simple yet effective antenna topology as well as methods to improve antenna's efficiency are presented. Low-cost fabrication methods are proposed and the antenna prototypes are projected to have optical transparency as high as 90% and efficiency higher than reported prior art.

A Reactively Coupled Bi-Directional Dual CP Antenna 45

Ratul De (Indian Institute of Technology Delhi, India); Mahesh P Abegaonkar (IIT Delhi, India); Ananjan Basu (Indian Institute of Technology, Delhi, India)

This paper presents the design of a bi-directional, dual CP antenna at S band. It is a two layer structure and reactive coupling is used to excite the antenna. This antenna provides a bandwidth of 100 MHz, a maximum gain of 6.2 dBi in the positive z direction and 4.84 dBi in the negative z direction at 2.27 GHz. It produces RHCP in the +z direction and LHCP in the -z direction. This antenna can find applications in situations where two orthogonal polarizations are required in two different directions. It can also be used for communication in tunnels and in corridors.

Super-Realized Gain Huygens Antennas 44

Donal P Lynch (Queen's University, United Kingdom (Great Britain)); Vincent Fusco (Queen's University Belfast, United Kingdom (Great Britain)); Manos M. Tentzeris (Georgia Institute of Technology, USA); Stylianos D. Asimonis (Queen's University Belfast, United Kingdom (Great Britain))

This study presents a superdirective antenna array specifically designed for the sub-6 5G frequency range, incorporating pioneering Huygens antenna elements. The optimized structure achieves a realized gain that surpasses Harrington's well-known maximum theoretical limit for antenna directivity, effectively addressing practical concerns related to ohmic and return losses. Additionally, the compact size of the proposed antenna array, as opposed to a uniform linear array, offers the potential to fabricate highly radiation-efficient, high-directivity antennas in a compact form.

A Decoupling Scheme for Closely Spaced Microstrip Patch Antenna 47

Rupa Laller and Mahesh P Abegaonkar (IIT Delhi, India); Ananjan Basu (Indian Institute of Technology, Delhi, India)

This article introduces a simple decoupling method aimed at achieving high isolation among closely spaced antennas. The study focuses on evaluating the impact of the gap between antenna elements on coupling for an H-plane array antenna. The decoupling structure comprises transmission line resonators and vias, which effectively mitigate coupling when two antennas are positioned with a minimal 2 mm edge-to-edge separation. The inclusion of resonators effectively diminishes the coupling between these antennas. To affirm the practical utility of this configuration, the design is implemented and rigorously validated through measurements. The proposed structure demonstrates an impressive 40 dB isolation with a gain of 2.3 dBi. Furthermore, a three-element array is examined to confirm the effectiveness of this proposed approach for linear element arrays.

Design of the 3D-Printed Rectangular Dielectric Resonator Antenna for WLAN Applications 62

Zhenyi Shou and Zhipeng Wu (University of Manchester, United Kingdom (Great Britain)); Hanyang Wang (Huawei Technologies, United Kingdom (Great Britain)); Hai Zhou (Huawei Technology (UK), United Kingdom (Great Britain)); Meng Hou (Huawei Technologies CO., LTD, China)

A probe-fed 3D-printed rectangular dielectric resonator antenna (RDRA) for 2.4/5.2-GHz wireless local area network (WLAN) applications is demonstrated in this study. It validates the first successful utilization of Barium Titanate (BaTiO₃) powder and UV-curing resin in conjunction with Stereolithography Apparatus (SLA) 3D printing technology to create a ceramic DRA with a dielectric constant of 8. Through using notched slots and a metal strip on the antenna structure, three distinct modes within the designed RDRA are excited, achieving complete coverage of the 2.4/5.2-GHz frequency bands. A strong agreement between the simulated and measured results is achieved, highlighting the potential of the SLA technique for future DRA designs and applications.

Low-Profile Super-Realised Gain Antennas 60

James Moore and [Aron M Graham](#) (Queens University Belfast, United Kingdom (Great Britain)); Manos M. Tentzeris (Georgia Institute of Technology, USA); Vincent Fusco and Stylianos D. Asimonis (Queen's University Belfast, United Kingdom (Great Britain))

This study introduces a novel approach to the design of low-profile superdirective antenna arrays, employing parasitic elements. The proposed design concept was verified through the analysis of a two-element antenna array consisting of strip dipoles, operating at a frequency of 3.5 GHz within the sub-6 5G frequency band. The antenna array was optimized for realized gain, a key antenna parameter considering both ohmic and return losses. The design parameters included the lengths and widths of the strip dipoles, along with a reactance load connected to the parasitic element. The driven element was excited by a sinusoidal voltage signal with a magnitude of 1 V, eliminating the need for amplifiers, attenuators, phase shifters, or impedance matching networks. Results demonstrated that this design concept enables the achievement of superdirectivity, with inter-element distances as small as 0.1λ, resulting in low-profile, compact, high directional antenna systems.

Realizing Flat-Top Radiation Pattern with Sharp Cutoff for Reducing Lobing Fades 50

Mohammad Hossein Amini and Amirhossein Ghasemi (TeleMonTech Inc., Canada); Maryam Khodadadi and Alireza Mallahzadeh (University of Surrey, United Kingdom (Great Britain)); [Mohsen Khalily](#) (University of Surrey & 5G Innovation Centre, Institute for Communication Systems (ICS), United Kingdom (Great Britain))

In this paper, synthesis of the flat-top radiation pattern with sharp cutoff for reducing the lobing fades due to the presence of the earth is investigated. To this end, first the propagation factor is investigated. Then based on the propagation factor, the antenna pattern is examined at different levels of the cutoff to achieve a flat-top radiation with low level of lobing fades. Finally, synthesizing the desired radiation pattern is investigated through Woodward-Lawson method. Our studies reveal that that antenna with large length (>12λ) provides the desired flat-top pattern with the appropriate cutoff. The aperture distribution of the desired pattern is provided and discussed.

Beam Steering Performance Improvements Using a Layered Permittivity Dielectric 46

Stefan Andersson and Jari Holopainen (Aalto University, Finland); Matti Kuosmanen (Aalto University & Saab Finland Oy, Finland)

This paper presents simulated performance improvements utilizing a layered dielectric for a truncated tapered slotline array targeted in the 2 – 7-GHz frequency range. It will be shown that a dielectric loading may significantly improve the bandwidth and beam-steering characteristics of the antenna array. Furthermore, it will be demonstrated that a layered dielectric structure with different permittivities can further improve the performance compared to a homogeneous dielectric. Namely, the antenna with layered dielectrics display a further increase in bandwidth and wider beam steering angles in the H-plane.

A Wideband Circularly Polarized Filtering Array Antenna Using Dual-Layer Circular Cross Slotted Patch 55

Min Wang and Hao Zhang (Chongqing University of Posts and Telecommunications, China); Nan Hu (A-INFO INC, China); Wenqing Xie (A-INFO Inc., China); Shu-Lin Chen (University of Technology, Sydney, Australia); Zhengchuan Chen (Chongqing University, China)

The array element consists of a feeding structure designed as a 2-way power division with a 90° phase difference and a dual-layer patch structure. An aperture-couple driven patch spatially placed between the parasitic patch and feeding structure is used to introduce magnetic coupling with parasitic patch for a resonant mode at high frequency and a radiation null. Meanwhile, four arc-shaped patches fitted with four shorting via surround the driven patch to generate electric coupling with it. It allows to achieve a resonant mode at low frequencies and a radiation null to improve the bandwidth. Then, a four-way sequential rotation feed network is designed with the same amplitude and a 90° clockwise incremental phase, which is fed a 2×2-element circularly polarized filtering array antenna. The results demonstrate that the array achieves a 3 dB gain bandwidth of 22.9% and the axial ratio bandwidth of 22.0%.

Design of a Dual-Polarization Ultra-Wideband Horn Antenna 58

Nan Hu (A-INFO INC, USA); Shuang Liu, Jianrui Liu and Lixin Zhao (Chengdu A-INFO Inc., China); Wenqing Xie (A-INFO Inc., China)

A dual-polarization ultra-wideband(UWB) horn antenna is proposed in this paper. This antenna uses quad-ridge structure to achieve broadband and dual-polarization characteristics. In order to reduce the overall weight, there is no metal wall structure and part of the ridge structure which has little effect on the electric field is removed. The operating frequency band is 1-20GHz. The measured VSWR results are 2 Typ., the port isolation results are less than -25dB, the gain results are 10dB Typ. and the cross polarization isolation are less than -20dB. The weight is around 0.56 Kg around. The proposed antenna has been processed and applied in measured systems.

DRL-Based Sidelobe Suppression for Multi-Focus Reconfigurable Intelligent Surface 53

[Wei Wang](#) (University of Bristol, United Kingdom (Great Britain)); Peizheng Li (Toshiba Europe Ltd., United Kingdom (Great Britain)); Angela Doufexi and Mark Beach (University of Bristol, United Kingdom (Great Britain))

Reconfigurable intelligent surface (RIS) technology is receiving significant attention as a key enabling technology for 6G communications, with much attention given to coverage infill and wireless power transfer. However, relatively little attention has been paid to the radiation pattern fidelity, for example, sidelobe suppression. When considering multi-user coverage infill, direct beam pattern synthesis using superposition can result in undesirable sidelobe levels. To address this issue, this paper introduces and applies deep reinforcement learning (DRL) as a means to optimize the far-field pattern, offering a 4dB reduction in the unwanted sidelobe levels, thereby improving energy efficiency and decreasing the co-channel interference levels.

Wideband Decoupling Smartphone Antenna with Integrated Metal Rim 52

Yi-Min Gan and [Qing-Xin Chu](#) (South China University of Technology, China)

A wideband decoupling four-element multipleinput-multiple-output (MIMO) antenna based on Common and Differential Mode (CDM) impedances Analysis for 5G smartphones is proposed. For the antenna pairs, in high frequency band, self-decoupling is realized. In low frequency band, a shorting stripe is added to adjust CM and DM impedances so that they can be close to each other and high isolation is obtained. Finally, the isolation is better than 13 dB in the whole operating band (3.3-5.0 GHz). The model is also fabricated and measured, and both simulated and measured results are discussed.

Thursday, March 21 13:10 - 14:40

PP03: Poster session on Propagation III

// Propagation

Room: Expo/Poster

Chairs: Edoardo Negri (Sapienza University of Rome, Italy), Enrico Polo (Politecnico di Milano, Italy)

Wideband Characterization of Wireless Power Transfer in Ventilation (HVAC) Ducts for the Internet of Things and Smart Buildings 69

Guillaume Villemaud (Université de Lyon, INSA-Lyon, INRIA, CITI, France); Regis Rousseau and Jules-Henri Paques (Univ Lyon, France)

This study aims at demonstrating the potential efficiency of a wideband wireless power transfer system used to remotely feed communicating objects through radiowave propagation in ventilation ducts. After justifying and describing such a system, an OFDM-based channel sounding experimentation is detailed and some results are analyzed to deeply characterize the channel both in frequency and time. Finally, the impact of the waveform and of the load of the rectifier is also studied in order to show clearly the key parameters influencing the global efficiency of this system.

A Deep Split-Step Wavelet Model for the Long-Range Propagation 67

[Thomas Bonnafant](#) (Lab-STICC & ENSTA Bretagne, France); Benjamin Chauvel and Abdelmalek Toumi (ENSTA Bretagne, France)

This article presents a new approach based on a deep-learning method using a U-Net architecture to generate electromagnetic propagation over a specific terrain. For this purpose, the learning dataset is constructed artificially using a fast split-step wavelet (SSW) method. For this phase, the synthetic 1D profiles are randomly generated from rectangle and triangle shapes. This latter allows for conveying the "staircase" model used in SSW. To ensure a precise sampling of the underlying manifold, the study employs Latin Hypercube Sampling. To achieve robust and precise predictions, a specific loss function is proposed. To evaluate this approach, numerical tests are realized. These tests demonstrate the effectiveness of the proposed method in realistic terrain.

Propagation Path Analysis with Propagation QUBO Model in Urban Area 78

Keita Fujita, Keisuke Hayashi and Tetsuro Imai (Tokyo Denki University, Japan); Wataru Yamada and Minoru Inomata (NTT, Japan)

At present, model for radio propagation path finding that can be applied to quantum annealing (QA) has been proposed (Propagation QUBO model). The model is that finds for a propagation path with the minimum propagation loss between transmitter (Tx) to receiver (Rx) at a given number of scattering times, ϕ . Here, the maximum number of scatterings that should be considered in propagation path finding when applying the proposed model to a real environment is unknown. The probability of the existence of a propagation path with a low scattering frequency is expected to decrease as the distance between Tx and Rx increases. In this paper, "desired propagation path" is defined as the propagation path that radio wave can reach Rx with a set number of scattering, and spatial distribution characteristics of Rx where desired propagation path exists are evaluated in urban Macro-cell environment.

Effect of Wave Polarization in On-Body Propagation for the 2.4, 24 and 60 GHz ISM Bands 81

Wasi Ur Rehman Khan and Max James Ammann (Technological University Dublin, Ireland); William G. Scanlon (Tyndall National Institute, Ireland)

A skin-based phantom is used to numerically model on-body propagation at three different frequencies, 2.4, 24 and 60 GHz. Linearly-polarized open-ended waveguides are used as antennas. The influence of polarization on path gain and antenna radiation efficiency are analyzed. The results show that path gain is highly sensitive to the antenna/body separation at 24 and 60 GHz

Modeling Received Power from 4G and 5G Networks in Greece Using Machine Learning 65

Vasileios P. Rekkas and Sotirios Sotiroudis (Aristotle University of Thessaloniki, Greece); George Tsoulos and Georgia E. Athanasiadou (University of Peloponnese, Greece); Achilles D. Boursianis and Zaharias D. Zaharis (Aristotle University of Thessaloniki, Greece); Panagiotis Sarigiannidis (University of Western Macedonia, Greece); Christos Christodoulou (The University of New Mexico, USA); Sotirios Goudos (Aristotle University of Thessaloniki, Greece)

Wireless propagation modeling is crucial for designing 5G networks and deploying base stations. Traditional models are constrained by different propagation environments, and deterministic models using ray tracing demand extensive computational resources. In recent years, advances in data-driven artificial intelligence (AI) have significantly improved the fitting of intelligent propagation models for 5G systems. Using artificial intelligence (AI) and substantial measured data, we conduct a comparative study of various machine learning (ML) models to perform accurate regression predictions for Reference Signal Receiving Power (RSRP). The results of the proposed ML models are compared and analyzed, exhibiting great accuracy in the prediction of RSRP values in a diverse range of urban, suburban, and rural environments.

Target Classification Through ISAR for Autonomous Vehicles Based on Federated Learning 68

Vincenzo Violi (University of Pisa & universitmediterranea di Reggio Calabria, Italy); Pierpaolo Usai and Danilo Brizi (University of Pisa, Italy); Gurtaj Singh (University Mediterranea of Reggio Calabria, Italy); Marco Fisichella (L3S Research Center, Germany); Tommaso Isernia (University of Reggio Calabria, Italy); Agostino Monorchio (University of Pisa & CNIT, Italy)

This study explores the use of Federated Learning (FL) in classifying ISAR images for autonomous driving. Automotive radar systems, operating at millimeter-wave frequencies, offer critical safety features. ISAR images are powerful for target recognition but pose challenges in real-world scenarios. FL, a decentralized training approach, is employed for data privacy while maintaining competitive accuracy. Our findings reveal that FL achieves commendable performance compared to centralized models, ensuring data confidentiality by keeping the information on local devices and centrally sharing only the model weights. In conclusion, this research demonstrates FL's potential in improving ISAR-based target classification for autonomous driving, making it suitable for privacy-sensitive applications.

SINTEC Comparative Body-Centric Communication Study: Bluetooth Vs Fat-Intrabody Communication 73

Mauricio D Perez (Uppsala University, Department of Electrical Engineering); Bappaditya Mandal, Pramod K B Rangaiah, Laya Joseph and [Robin Augustine](#) (Uppsala University, Sweden)

Here we present a comparative study between Bluetooth Low Energy (BLE) and fat-intrabody communication (Fat-IBC) done with two advanced torso phantom models and two human volunteers, representing low-fat and high-fat content, in the context of the H2020-funded project SINTEC. The phantom tests were done in a small made-for-the-job semi-shielded chamber with the possibility of suppressing the surface wave in the air-skin surface. Two Fat-IBC antennas were designed and they were found to perform better than the BLE one both on phantom and volunteers in most cases, particularly in the front-to-back (10 - 20 dB times better). Fat-IBC propagation mechanism and surface wave suppression need to be further studied, but the current results are positive on the significance of the Fat-IBC mechanism to reduce surface leakage and associated security/safety concerns in body-centric communication scenarios.

Empirical Characterization of Doppler in Industrial Wireless Channels 74

Dreyelian Morejon Betancourt, Jon Montalban and Eneko Iradier (University of the Basque Country, Spain); Mohamed Kashef (National Institute of Standards and Technology (NIST), USA); Richard Candell (National Institute of Standards and Technology, USA); Pablo Angueira (University of the Basque Country, Spain)

This paper analyzes the temporal variation of the radio propagation channel in industrial environments. The results have been obtained by processing empirical data from the National Institute of Standards and Technology (NIST) in a field measurement campaign, at different industrial premises, with various dimensions and clutter densities. The paper analyzes the shape of the Doppler spectra and related parameters such as Doppler bandwidth and coherence time. The results are supplemented with maximum Delay Times and RMS Delay Spread data. The influence of factors such as the operational frequency band, environment, and polarization is also analyzed.

Indoor Localization of Smartphones Thanks to Zero-Energy-Devices Beacons 71

[Shanglin Yang](#) (INSA Lyon, Inria & Orange Labs, France); Yohann Benedic (Orange Innovation, France); Dinh-Thuy Phan-Huy (Orange, France); Jean-Marie Gorce (INSA-Lyon & CITI, Inria, France); Guillaume Villemaud (Université de Lyon, INSA-Lyon, INRIA, CITI, France)

In this paper, we present a novel ultra-low power method of indoor localization of smartphones (SM) based on zero-energy-devices (ZEDs) beacons instead of active wireless beacons. The ZED backscatters ambient waves from base stations (BSs) of the cellular network. The smartphone detects the ZED message in the variations of received ambient signal from the BS. Thanks to a ray-tracing based propagation simulation tool, we accurately simulate the ambient waves from a BS of Orange 4G commercial network, inside an existing large building covered with ZED beacons. Our first performance evaluation study, in a realistic and challenging propagation scenario, shows that the proposed localization system enables to locate in which room is the smartphone.

Electromagnetic Detection and Identification of Perturbed Wire Resonators 79

[Qingyan Zhu](#), Oleksiy Sydoruk and Richard R. A. Syms (Imperial College London, United Kingdom (Great Britain))

The resonances of metal wire resonators may change due to a localized variation of the surrounding dielectric, coupling to nearby resonators, or the introduction of bends. We used shifts in the resonant frequencies to detect and identify perturbed wire resonators. In this paper, we present measurements, a perturbation model based on a lumped-element circuit, and full-wave simulations of perturbed resonators. Resonances of four resonators with different structures and perturbations were excited with near-field probes, and the variations of normalized resonant frequency with perturbation position were shown to agree with the results obtained from full-wave simulations. The experimental and simulated data match the perturbation theory, which suggests the feasibility of identifying perturbed metal resonators by exciting and detecting their resonances.

Brain Hemorrhage Detection Using Antenna System Integrated with Imaging Algorithm 75

Bishakha Biswas (Indian Institute of Engineering Science and Technology Shibpur, India); Adarsh Singh (IEST, India); Debasis Mitra (Indian Institute of Engineering Science & Technology, Shibpur, India); Bappaditya Mandal (Uppsala University, Uppsala, Sweden); [Robin Augustine](#) (Uppsala University, Sweden)

Brain bleeding, also known as hemorrhage, is a potentially fatal condition. A four-antenna system for brain hemorrhage imaging has been introduced, which offers a more accessible and faster diagnosis. Microwave imaging has been utilized for over a decade to diagnose health-related issues, providing a more convenient alternative to traditional imaging procedures. Hemorrhage poses a significant risk to life, and this streamlined system, consisting of just four antennas and a highly efficient imaging algorithm, can effectively detect the presence of blood clots or blood pools within the skull.

Supervised Machine Learning for Breast Cancer Detection Using Microwave Imaging in the Frequency Domain 64

Marwa Dridi (SogetiLabs Research and Innovation, Issy-les-Moulineaux, France); Leila Gharsalli (Polytechnic Institute of Advanced Sciences (IPSA), France)

Due to its non-invasive and non-ionizing properties, microwave imaging has emerged as an efficient alternative to conventional screening techniques. This paper presents a Supervised Machine Learning (ML) framework for Breast Microwave classification where chosen features rely on measured scattering (S-parameters) in the frequency domain. An open source dataset from the university of Manitoba based on a preclinical Breast Microwave Imaging (BMI) system using breast phantoms (UM-BMD) is considered to illustrate that problem of detecting whether a tumor exists or not. The obtained results with maximum achieved accuracy of 98% highlight the relevance of the frequency domain features by comparing them to previously published results where features were chosen in the time domain and show the potential advantages of applying ML classification methods in that BMI system.

Filter Integrated Microstrip 3-Port Power Combiner 66

[Nisamol Thevaruparambu Abdul Nazer](#) (Deutsches Elektronen-Synchrotron DESY, Germany); Bernhard E. J. Scheible (Mittelhessen University of Applied Sciences, Germany); Rahul Yadav (Technische Universität Darmstadt & Technische Hochschule Mittelhessen, Giessen-Friedberg, Germany); Marie Kristin Czwalinna (Deutsches Elektronen-Synchrotron, Germany); Holger Schlarb (Deutsches Elektronen Synchrotron, Germany); Andreas Penirschke (Mittelhessen University of Applied Sciences, Germany)

Modern wireless communication systems demand the integration of filter-to-signal combiner circuits owing to a significant rise in enthusiasm for the integration of frequency-dependent circuits in a single network. The proposed circuits are important since it has the capacity to incorporate signal frequency filtering of thirty-five harmonics with high-end suppression and power combining capabilities below 2 GHz. The radial microstrip transmission line has been designed to ensure compactness when the filter resonator units are integrated into the circuit. The design, analysis, and practical verification of the circuit have also been presented. The scaled version of the proposed circuit would be the most suitable solution for the high-frequency noise rejection

Generation of Electromagnetic Exposure Maps for 5G Communications 77

[Esteban Egea-Lopez](#) (Universidad Politécnic de Cartagena (UPCT), Spain); Mohammed Mallik (Institute Mines Telecom, IMT Nord Europe & IRCICA, IEMN, France); Laurent Clavier (Institut Mines-Telecom, IMT Nord Europe, France); Davy P Gaillot (University of Lille, France)

Monitoring human exposure to electro magnetic field sources is a growing concern. An approach for the evaluation of exposure is the generation of radio-frequency electro-magnetic fields (RF EMF) exposure maps via simulation, which is complex due to the need to simulate the multiple sources involved. As an alternative, it has been explored the automatic generation of EMF exposure maps by machine learning (ML) methods using as input the measurements from sensors located in the area of interest. These methods, due to the scarcity of measurements, still require simulation for generating the dataset for training the algorithms. In this paper we describe how to generate exposure maps for 5G networks with our ray-tracing tool Opal, to generate a large number of EMF maps that can be used to train ML algorithms. We describe how we generate them without the need to execute demanding higher level simulations whose details are not necessary.

Analytical Fitting of Dielectric Response of Basal Cell Carcinoma 70

Enrico Mattana, Matteo Bruno Lodi, Giuseppe Mazzarella and Alessandro Fanti (University of Cagliari, Italy)

Terahertz spectroscopy and imaging are non-ionizing and non-invasive tools to investigate skin. It is therefore necessary to accurately describe the dielectric response of both skin and basal cell carcinoma in the THz range. Due to the high sensitivity of THz radiation to polar substances and the significant water content in the skin, the traditional model to describe its dielectric permittivity has been the double Debye one. This paper shows that a third order Cole-Cole model has the potential to accurately approximate the dielectric permittivity of both skin and basal cell carcinoma. We fitted experimental data taken from the literature using a genetic algorithm routine and we found a minimum root-mean-square error of 0.0466, which is approximately two order of magnitude less than the dielectric permittivity. The proposed third order Cole-Cole model could be used to advance THz-based technologies for skin cancers diagnosis.

Advances in Core-Shell Nanocrystals: A Multiphysics Approach to Multispectral Electromagnetic Shielding 63

Nicola Curreli (Italian Institute of Technology, Italy); Matteo Bruno Lodi and Alessandro Fanti (University of Cagliari, Italy)

The proliferation of electronic devices operating across a wide spectrum of frequencies has given rise to a multitude of new applications. However, it has also led to a significant increase in electromagnetic interference, resulting in unwanted effects, such as device malfunctions and human exposure to electromagnetic radiation. To mitigate these effects, there is a growing demand for multispectral shielding materials in various domains, including electronics, healthcare, defense, and aerospace. Existing shielding materials are typically tailored for specific frequency bands, and the need for materials that can effectively attenuate radiation across multiple bands is pressing. In this paper, we explore the design and simulation of novel multispectral shielding nanomaterials for a wide range of frequencies, from microwave to ultraviolet. We specifically investigate the optical properties and electromagnetic responses of core-shell nanoparticles. Our study provides insights into the development of advanced shielding materials capable of addressing multispectral challenges in contemporary applications.

Propagation Modeling in an Indoor Environment at Sub-THz Frequencies Based on Ray Tracing 72

[Nektarios Moraitis](#) (National Technical University of Athens & Institute of Communications and Computers Systems, Greece); Konstantina Nikita (National Technical University of Athens, Greece)

This paper presents extensive deterministic simulations in an indoor environment at sub-THz frequencies. All the relative wideband parameters of the channel are determined and assessed, including the time delay and spatial characteristics. It is demonstrated that simulations with an accurate description of the materials and representation of the propagation environment produce reliable results, given the fact that the parameters, obtained from the simulation study, are found to be consistent with measurement results that exist in the literature for similar indoor locations. The root-mean-square delay spread exhibits values in the range of 0.6-5.4 ns and 1.7-23.0 ns, for line-of-sight (LOS) and non-line-of-sight (NLOS) conditions, respectively. A multi-cluster model characterizes very well the power delay profiles of the indoor channel, which are found to be formed by 3 up to 4, and 5 up to 7 cluster groups for LOS and NLOS conditions, respectively. All the relative clusters and ray's decay patterns, as well as their inter-arrival times are also evaluated.

Best Practices for Accurate Results Using Numerical Solvers for Microwave Body Screening 76

Raquel A. Martins (Instituto de Telecomunicações/Instituto Superior Técnico, Portugal); [Daniela M. Godinho](#) (Instituto de Biofísica e Engenharia Biomédica - Faculdade de Ciências - Universidade de Lisboa, Portugal); Joao M. Felicio (Escola Naval, Portugal & CINAV - Instituto de Telecomunicações, Portugal); Matteo Savazzi (Universidade de Lisboa, Portugal); Jorge R. Costa (Instituto de Telecomunicações / ISCTE-IUL, Portugal); Raquel C. Conceição (Instituto de Biofísica e Engenharia Biomédica, Faculdade de Ciências, Universidade de Lisboa, Portugal); Carlos A. Fernandes (Instituto de Telecomunicações, Instituto Superior Técnico, Portugal)

In this paper, we indicate best practices that should be observed when using numerical solvers for microwave body sensing. We show the impact of not minding these aspects in the case of microwave breast scanning using the Computer Simulation Technology tool. To this end we simulate a homogeneous breast with a 5-mm radius spherical tumor placed inside. The breast is illuminated by a broadband antenna that operates in the 2-6 GHz band. The scattering parameters are then processed to reconstruct the reflectivity map of the breast. The results highlight that the conclusions drawn from simulations may be misleading or meaningless when the solver type or positioning of model elements (body and antennas) are not carefully applied. This is particularly critical when considering more complex scenarios, such as inhomogeneous or multilayer body models.

Microwave Sensor for Detection of Optical Transparent Foreign Body in Soft Tissue: Eye 80

Soroush Rasti Boroujeni (Pigeon Comm Inc., Canada); Javad Ebrahimzadeh (Kuleuven University, Belgium)

This paper introduces a novel sensor for detecting toxic metals in the human eye. The sensor is a microwave open-ended circular waveguide that excites the dominant modes TE₁₁, TM₀₁ within a probe. By covering

the eye with the opening aperture, the sensor can detect changes in the reflection parameters caused by the presence of foreign metal objects in the eye. The proposed sensor is capable of detecting cylindricalshaped foreign bodies as small as 2 mm in length and located 1 cm deep within the eye. The sensor was validated through ex-vivo measurements on a cadaveric pig eye using a WR90 rectangular waveguide at the x-band. A small piece of glass with dimensions less than 5 mm was inserted at a depth of 1 cm, and the sensor was able to detect it successfully.

Thursday, March 21 13:10 - 14:40

PS1: Best Paper Awards

//

Room: Expo/Poster

Analysis and Design of mmWave Wideband Artificial Dielectric Flat Lens Antenna

Caspar M Coco Martin (Delft University of Technology, The Netherlands); Weiya Hu (Delft University of Technology, The Netherlands); Daniele Cavallo (Delft University of Technology, The Netherlands)

Generation of Narrow Divergence Angle OAM Beams for mmWave Communication Links Using Metasurface

Mustafa Khalid Taher Al-Nuaimi (Loughborough University, United Kingdom); William Whittow (Loughborough University, United Kingdom); Guan-Long Huang and Rui-Sen Chen (Foshan University, China)

Low-Profiled Wideband Dual-Polarized Conformal Antenna Array

Zhan Chen (Xidian University, China); Wei Hu (Xidian University, China); Yuchen Gao (Xidian University, China); Lehu Wen (Brunel University London, United Kingdom); Qi Luo (University of Herfordshire, United Kingdom)

Beam Steering Range Enhancement of Bifocal Reflectarray Using Irregular Distribution of Meta-Atoms

Mustafa Khalid Taher Al-Nuaimi (Loughborough University, United Kingdom); William Whittow (Loughborough University, United Kingdom); Guan-Long Huang (Foshan University, China); Rui-Sen Chen (Foshan University, China)

Compact Dual-Band Dual-Polarization Feed for Broadband Communication Satellites

Nelson Fonseca (Anywaves, France)

Flexible Antenna with Microfluidics for the Quantification of Liquid Micro-Volumes

Giulio M. Bianco (University of Rome Tor Vergata, Italy); Gaetano Marrocco (University of Rome Tor Vergata, Italy)

Feed Assembly Development for INCUS

Gaurangi Gupta (NASA Jet Propulsory Laboratory & Caltech, USA); Paolo Focardi (NASA Jet Propulsory Laboratory & Caltech, USA)

High Data-Rate Sub-THz Coherent Near-Field Wireless Links Enabled by Spline-Profile Bessel Launchers

Jérôme Taillieu (University of Rennes 1, France); David González-Ovejero (Centre National de la Recherche Scientifique, CNRS, France); Walter Fuscaldo (Consiglio Nazionale Ricerche, CNR, Italy); Laurent Bramerie (Foton CNRS UMR & ENSSAT / Université de Rennes 1, France); Paul Desombre (IETR/CentraleSupélec, France); Mathilde Gay(ENSSAT /Université de Rennes 1, France); Mehdi Alouini (Institut de Physique de Rennes - Université Rennes 1 - CNRS, France); Haifa Farès (Centrale Supélec, France); Yves Louet (CentraleSupélec, France);Mauro Ettorre (Michigan State University, USA)

A Completely Overlapped Ku- and Ka-Band Dual-Polarized Phased Array for Simultaneous Terrestrial and Satellite Communications

Bumhyun Kim (Pohang University of Science and Technology POSTECH, Korea (South)); Wonbin Hong (Pohang University of Science and Technology POSTECH, Korea (South))

Characterization of a D-Band Active Transmitarray System for Efficient Point-To-Point Links

Francesco Foglia Manzillo (CEA-LETI, France); Jose Luis Gonzalez Jimenez (Université Grenoble-Alpes/CEA-LETI, France); Abdelaziz Hamani (CEA, France); Alexandre Siligaris(CEA-LETI, Minatec, France); Antonio Clemente (CEA-LETI, France)

Optimizing RF Energy Harvesting in IoT: A Machine Learning Estimation Considering Polarization Effects

Khatereh Nadali (Technological University Dublin, Ireland); Adnan Shahid (Gent University - IMEC, Belgium); Nicolas Claus (Ghent University & IMEC, Belgium); Sam Lemey (Ghent University & IMEC, Belgium); Patrick Van Torre (Ghent University, Belgium); Max James Ammann (Technological University Dublin, Ireland)

Quantification and Correction of Signal Averaging with On-The-Fly Sampling in Near-Field Antenna Measurements

Olav Breinbjerg (EIMaReCo, Denmark)

Application of Compressed Sensing to Antenna Far-Field Calibration in an Extrapolation Range

Zhong Chen (ETS-Lindgren, USA); Yibo Wang (ETS Lindgren, USA)

Characterization of Typical Instantaneous Exposure and Usage Scenarios in the Vicinity of 5G Massive-MIMO Base Stations

Anna-Malin Schiffrath (RWTH Aachen University, Germany); Thanh Tam Julian Ta (RWTH Aachen University, Germany); Lisa-Marie Schilling (Technische Universität Ilmenau, Germany); Christian Bornkessel (Technische Universität Ilmenau, Germany); Matthias Hein (Technische Universität Ilmenau, Germany); Dirk Heberling (RWTH Aachen University, Germany)

A Demonstration of Diffraction-Limited Images Using a CMOS Chessboard Array at THz Frequencies

Martijn Hoogelander (Delft University of Technology, The Netherlands); Robbin van Dijk (Delft University of Technology, The Netherlands); Nuria LLombart (Delft University of Technology, The Netherlands); Marco Spirito (Delft University of Technology, The Netherlands); Maria Alonso-del Pino (Delft University of Technology, The Netherlands)

Grid-Free Harmonic Retrieval and Model Order Selection Using Convolutional Neural Networks

Steffen Schieler (Technische Universität Ilmenau, Germany); Sebastian Semper (Ilmenau University of Technology, Germany); Reza Faramarzanagari (Technische Universität Ilmenau, Germany); Michael Döbereiner (Fraunhofer Institute for Integrated Circuits IIS & Technische Universität Ilmenau, Germany); Christian Schneider (Technische Universität Ilmenau, Germany); Reiner S. Thomä (Ilmenau University of Technology, Germany)

Channel Characterization and Modeling for Wireless MIMO Communication Systems in Intersection Scenarios

Dayuan Zhao (Southeast University, China); Chen Huang (Purple Mountain Laboratories & Southeast University, China); Cheng-Xiang Wang (Southeast University, China & Purple Mountain Laboratories, China); Junling Li, Zhongyu Qian and Wenqi Zhou (Southeast University, China)

Cloud Attenuation in the Q Band: Estimation from Experimental Data of Excess Attenuation

Domingo Pimienta-del-Valle (Universidad Politécnica de Madrid, Spain); Gustavo Siles (Universidad Privada Boliviana, Bolivia); Jose M Riera (Universidad Politécnica de Madrid, Spain); Pedro Garcia-del-Pino (Universidad Politécnica de Madrid, Spain)

RIS-Based Over-The-Air Channel Equalization in Resource-Constrained Wireless Networks

Hugo Prodhomme (CNRS, France); Mohammadreza F. Imani (Arizona State University, USA); Sergi Abadal (Universitat Politècnica de Catalunya (UPC) & NaNoNetworking Center in Catalunya (N3Cat), Spain); Philipp del Hougne (CNRS, Univ Rennes, France)

Advanced Microwave Radiometry: Refining Sun-Tracking Technique for Atmospheric Attenuation Retrieval and Sun Brightness Temperature Estimation

Giovanni Stazi and Marianna Biscarini (Sapienza University of Rome, Italy); Luca Milani (European Space Agency, Germany); George Brost (Air Force Research Laboratory, USA)

Rigorous Susceptibility-Based Design of Generalized Huygens' Metasurface Radomes

Amit Shaham (Technion, Israel), Ariel Epstein, (Technion, Israel)

A Multi-Region Hierarchical Preconditioning Scheme for the MoM Simulation of Complex Composite Structures

Victor Martín (Universidad de Extremadura, Spain), Jose M. Taboada (University of Extremadura, Spain), Francesca Vipiana (Politecnico di Torino, Italy)

Radiation Control by Space-Time-Modulated Anisotropic Impedance Surfaces

Oscar Senlis, (University Rennes, CNRS, IETR, France), David González-Ovejero (Centre National de La Recherche Scientifique - CNRS, France), Mauro Ettore (Michigan State University, USA), Vincent Laquerre (CNES, France), Pouliguen Philippe (DGA, France)

Spectral Domain Green's Function of an Infinite Dipole with Non-Zero Metal Thickness

Erik Speksnijder (Delft University of Technology, The Netherlands), Riccardo Ozzola (Delft University of Technology, The Netherlands), Andrea Neto (Delft University of Technology, The Netherlands)

Emulating Spatial Dispersion Using Non-Spatially Dispersive Periodic Metasurfaces

Jordan R. Dugan (Carleton University, Canada), Tom Smy (Carleton University, Canada), Shulabh Gupta (Carleton University, Canada)

Experimental Analysis of Physical Interacting Objects of a Building at mmWave Frequencies

Hedieh Khosravi (Lund University, Sweden); Xuesong Cai (Lund University, Sweden); Fredrik Tufvesson (Lund University, Sweden)

Reduced-Order Maximum Determinant Sampling Grids by Acquisition of Additional Arbitrary Sampling Points on an Optimized Path

Henrik Jansen (RWTH Aachen University, Germany); Roland Moch (RWTH Aachen University, Germany); Dirk Heberling (RWTH Aachen University, Germany)

Thursday, March 21 14:40 - 15:20

IN9: Versatile metagratings for diverse field manipulation; Prof. Ariel Epstein, Technion – Israel Institute of Technology, Israel

//

Room: Lomond Auditorium

Chairs: Zvonimir Sipus (University of Zagreb, Croatia), Richard W Ziolkowski (University of Arizona, USA & University of Arizona, USA)

Thursday, March 21 14:40 - 15:20

IN12: Filtering Antenna Techniques for 5G/B5G Wireless Communication Applications; Prof. Wenquan Che, South China University of Technology, China

Room: M1

Chairs: Astrid Algaba-Brazález (Ericsson AB, Sweden), Luigi Boccia (University of Calabria, Italy)

Thursday, March 21 15:20 - 16:00

IN10: Perfectly-Matched Metamaterials; Prof. Anthony Grbic, University of Michigan, USA

Room: Lomond Auditorium

Chairs: Zvonimir Sipus (University of Zagreb, Croatia), Richard W Ziolkowski (University of Arizona, USA & University of Arizona, USA)

Thursday, March 21 15:20 - 16:00

IN11: Crafting the Future of Smart EM Environments Through the System-by-Design - The SEME@Trentino Initiative; Prof. Paolo Rocca, University of Trento, Italy

Room: M1

Chairs: Astrid Algaba-Brazález (Ericsson AB, Sweden), Luigi Boccia (University of Calabria, Italy)

Thursday, March 21 16:30 - 18:10

SW4: EurAAP Early Careers and Women in Antennas and Propagation

Room: Lomond Auditorium

Chairs: Davide Comite (Sapienza University of Rome, Italy), Francesca Vipiana (Politecnico di Torino, Italy)

16:30 *Brief Presentation of the ECAP and WiAP WGs*

Presenters: Davide Comite; Francesca Vipiana (Sapienza, University of Rome and Politecnico di Torino, Italy)

16:40 (Nearly) *Four Decades in the Antennas and Propagation Community*

Presenter: Anja Skrivervik (Ecole Polytechnique Fédérale de Lausanne, Switzerland)

17:10 *Preparing the Workforce of Tomorrow*

Presenter: Lucy van der Tas (European Space Agency, The Netherlands)

17:40 *Beyond Antennas: Challenges and Rewards of an Engineer's Life*

Presenter: Marta Martínez-Vázquez (Renesas Electronics, Düsseldorf, Germany)

Thursday, March 21 16:30 - 18:10

CS18: Characteristic Modes Analysis for Next-Generation Wireless Technologies

T09 Fundamental research and emerging technologies / Convened Session / Electromagnetics

Room: M1

Chairs: Mats Gustafsson (Lund University, Sweden), Kurt Schab (Santa Clara University, USA)

16:30 *Metasurfaces Meet Characteristic Modes*

[Feng Han Lin](#), YiHui Zhu, Yi An Mao, Jia Fan Gao and Si Yu Miao (ShanghaiTech University, China); Yi Zheng (ShanghaiTech University, China); Tong Wu (ShanghaiTech University, China)

This paper briefly reviews the recent development of metasurface (MTS) antennas with the aid of characteristic mode analysis (CMA), focusing on the unique advantages and new explanations offered by CMA for modeling an MTS, simplifying the analysis, mode excitation, mode manipulation and mode synthesis. Examples of multi-mode MTS antennas are given in three different levels, including MTS antenna element, MTS antenna array and multi-port MTS antenna for bandwidth enhancement, pattern mitigation, isolation improvement, accelerated analysis and clearer physical understanding. Future directions are also briefly introduced.

16:50 *Circularly Polarized Transmitarray Design Using Characteristic Modes Theory*

Francesco Alessio Dicandia (National Research Council (CNR), Italy); Simone Genovesi (University of Pisa, Italy)

A novel strategy for the design of a circularly polarized (CP) transmitarray (TA) is proposed by resorting to the characteristic modes theory (CMT). The described TA working principle relies on the use of two transmitting unit cells that support a pair of characteristic modes characterized by either right-handed CP (RHCP) or left-handed CP (LHCP) scattered field. The measured results emphasized a notable 3 dB gain bandwidth of 15.22 % (7.77 GHz - 9.05 GHz) and a maximum TA gain of around 22 dBi at 8 GHz.

17:10 *Generation of a Square Multi-Mode Multi-Port Aperture Antenna by Selective Modal Excitation*

[Tim Hahn](#) (Leibniz University Hannover, Germany); Dirk Manteuffel (University of Hannover, Germany)

A methodology for the generation of a multi-mode multi-port aperture antenna is proposed based on the selective excitation of magnetic current modes. The magnetic current modes are determined based on the analytical solution of waveguide modes with the same aperture dimensions. An excitation technique for the modal magnetic aperture currents is shown by placing multiple ports within the aperture. Guidelines for the port placement within the aperture are given based on the magnetic current distribution. Further, a feeding network topology is proposed to selectively excite the magnetic current modes of the aperture. The theory is evaluated and validated by an analysis of the radiation patterns of the individual antenna ports as well as an investigation of the envelope correlation coefficient of the radiation patterns. It is shown that the excited far-fields are orthogonal, which confirms the claimed selective excitation of the magnetic current modes.

17:30 *Circularly Polarized Sub-THz Antenna Design for Distributed Deployment*

Yuyan Cao (Lund University, Sweden); Maciej Wojnowski (Infineon Technologies, Germany); Buon Kiong Lau (Lund University, Sweden)

Sub-THz deployment is challenging due to high propagation losses, necessitating dense deployment. To reduce cost, RF signal can be distributed via plastic fiber to remote radio units to increase coverage area. In this paper, we propose an antenna-in-package concept for the single-layer substrate on low-cost embedded wafer level ball grid array (eWLB) packages. To suppress the distortion in the broadside pattern from the coplanar waveguide feed line, the circularly polarized patch antenna is surrounded by an integrated loop structure. The loop also enhances the antenna bandwidth by adding a second resonance. Simulation results show that the proposed antenna offers broadside coverage with the 10 dB impedance and 3 dB axial ratio bandwidths of 14.2% and 11.2% at 145 GHz, as well as realized gain of 7.8 dBi. The antenna shows good promise for array implementation on eWLB packages.

17:50 *Material-Independent Scattering Formulations of Characteristic Modes*

Kurt Schab (Santa Clara University, USA); Miloslav Capek and Lukas Jelinek (Czech Technical University in Prague, Czech Republic); Johan Lundgren and Mats Gustafsson (Lund University, Sweden)

Various approaches to extending characteristic mode analysis to the study of arbitrary material bodies are reviewed. Recent work on a scattering-based formulation's general features, extensibility to cases involving

complex background media, application to periodic systems, and acceleration via iterative methods are summarized. Emphasis is placed on unifying these features and extensions of characteristic mode analysis under a single, general framework. Implementation details are briefly discussed, highlighting the computational strengths and weaknesses of the scattering formulation as compared to the well-known impedance formulation.

Thursday, March 21 16:30 - 18:10

A02: Emerging antenna technologies for sub-6GHz

T01 Sub-6 GHz for terrestrial networks (5G/6G) // Antennas

Room: Alsh 1

Chairs: Sumin David Joseph (The University of Sheffield, United Kingdom (Great Britain)), Haim Matzner (HIT-Holon Institute of Technology, Israel)

16:30 A Low Profile Dual-Band Dual-Polarized Filtering Antenna with No Extra Circuit

[Xuekang Liu](#) (University of Kent, United Kingdom (Great Britain)); Benito Sanz-Izquierdo (University of Kent, United Kingdom (Great Britain)); Steven Shichang Gao (Chinese University of Hong Kong, China)

This research introduces an innovative, compact dual-band dual-polarized antenna equipped with filtering capabilities for 5G sub-6GHz base stations. Using the concept of multipath coupling, two controllable radiation nulls are achieved independently. The antenna's impedance bandwidth is widened by skillfully exciting the anti-phase TM₂₂ mode and shifting it to a lower frequency band while preserving other resonant modes. Additionally, incorporating four shorted strips around the radiator effectively increases the average half power beamwidth in the higher frequency band from 51° to 61°. Finally, the integration of two wide-band planar baluns, linked to the input terminals of the differentially fed antenna, results in the creation of this dual-polarized filtering antenna with dual operating frequency bands. Experimental prototypes of the antenna element and 1×4 array were fabricated and tested. The reflection coefficients demonstrate the antenna's functionality across the 3.24-3.90 GHz (18.5%) and 4.74-5.06 GHz (6.5%) frequency bands, maintaining $|S_{11}| < -14$ dB. Additionally, a high isolation level of 31 dB was measured from the input ports.

16:50 Subsampling Time-Modulated Array for Reduced Hardware down Conversion and Beamforming

[Sumin David Joseph](#) (The University of Sheffield, United Kingdom (Great Britain)); Edward Ball and Alan Tennant (University of Sheffield, United Kingdom (Great Britain))

A Subsampling Time Modulated Array (STMA) with eight elements at 2.4 GHz is introduced to reduce the hardware complexity in a conventional analog beamformer. By applying the concept of TMA in a SDR based downconverter, the proposed RF hardware can perform beamforming and down conversion with a minimal circuitry. Experimental tests confirm the ability of the hardware to steer the desired incoming RF receive beam at the carrier frequency and resolve it at the subsampled intermediate frequency IF output. The analysis extends to the correlation between the hardware of the STMA and the performance of sidelobe levels within the array. The beam steering capability of each harmonic beams and the corresponding side lobe levels is also analyzed. The proposed STMA system with beamforming and down conversion is suitable for future receiver systems to reduce the complexity and power consumption.

17:10 Spherical Active Frequency-Selective Surface for 3-D Beam-Scanning Antenna

[Ali Hassan](#) (Higher Institute of Applied Sciences and Technology, Syria)

This paper presents a novel design of active frequency-selective surface (AFSS) in a spherical form where an omnidirectional planar monopole antenna is placed at the sphere's center. The proposed design can achieve beam steering in both the azimuth and elevation planes. Hexagonal cells are used with incorporated high frequency PIN-Diodes to form the spherical (AFSS) surface. Every cell can reflect incident EM waves in the operating frequency band when diodes are in ON state and be transparent when diodes are in OFF state. The antenna beam is formed by activating the appropriate cells and making a dish reflector which is focusing the EM waves in the desired direction. The reflecting dish can be formed freely from any part of the spherical (AFSS) surface for realizing the switched beam antenna.

17:30 Two-Dimensional, Un-Equal, Series Power Dividers for Feeding Antenna Arrays

[Haim Matzner](#) (HIT-Holon Institute of Technology, Israel)

Two-dimensional, un-equal, series power dividers based on microstrip line sections and quadrature couplers are proposed. The dividers can easily be designed to feed two-dimensional antenna arrays with specified amplitudes excitations and equal phases for each element at the center frequency. The design method is presented, together with a simple example of a 4 x 4 microstrip antenna array fed by the proposed divider with binomial distribution. The performance of the couplers is first analyzed by the MATHEMATICA (Wolfram) software, and then checked by the Keysight Advanced Design System software (ADS). The simulation of the microstrip array antenna is performed by the CST Microwave Studio software. The bandwidth of the antenna is approximately 10% at 1.9 GHz.

17:50 A Four-Channel In-Band Full-Duplex (IBFD) Antenna System with Shared Radiation Aperture

[Yuenian Chen](#) (University of Technology Sydney, Australia); [Can Ding](#) (University of Technology Sydney (UTS), Australia); [He Zhu](#) (CSIRO, Australia); [Ying Liu](#) (Xidian University, China); [Y. Jay Guo](#) (University of Technology Sydney, Australia)

A four-channel in-band full-duplex (IBFD) antenna array system with shared radiation aperture based on common-mode (CM) and differential-mode (DM) combination is developed in this paper. The IBFD antenna system B is created by two subarrays. Exciting any of the four input ports simultaneously excites one subarray in CM and the other subarray in DM. The inclusion of both CM and DM in both the xoz and yoz planes leads to identical radiation patterns when any of the four ports are excited. The IBFD antenna system designed, fabricated, and measured to verify the effectiveness of the method. The isolation between any two ports is >38 dB within the bandwidth of 3.3 - 3.8 GHz (14.4%). The gains of all four ports are > 8 dBi with large cross-polarization discrimination (XPD) > 20 dB.

Thursday, March 21 16:30 - 18:10

A28: Antennas for 5G and beyond

T02 Mm-wave for terrestrial networks 5G/6G // Antennas

Room: Alsh 2

Chairs: Yannis Iliopoulos (TNO, The Netherlands), Lucas Nogueira Ribeiro (Ericsson Antenna Technology GmbH, Germany)

16:30 Antenna and Mechanical Co-Design for Auto-Beam-Tracking in Backhaul Systems

[Enlin Wang](#) (Chalmers University of Technology, Sweden); [Anders Wennergren](#), [Henrik Stalrud](#), [Carlo Bencivenni](#) and [Esperanza Alfonso](#) (Gapwaves AB, Sweden); [Ashraf Uz Zaman](#) and [Jian Yang](#) (Chalmers University of Technology, Sweden)

This paper addresses the electrical-mechanical co-design challenges of beam alignment in ultra-high-gain antennas due to mast sway by adopting a defocusing strategy for the reflector antenna feed in order to meet the requirements of 5G mmWave backhaul communication systems. Three automatic beam tracking methods have been investigated and evaluated: a sensor-motor-based control method, a gear-driven compensation method by using a secondary mast as a reference, and a gravity-driven pendulum method that leverages gravitational force as the reference. Detailed description of the integrated design approach combining both antenna design and mechanical structure is given in the paper, providing potential platform for further improved system developments.

16:50 A High-Isolation Dual-Band Base Station Antenna Design for Full Duplex Technologies

[Lucas Nogueira Ribeiro](#) (Ericsson Antenna Technology GmbH, Germany); [Duy Hai Nguyen](#) (Ericsson Antenna System Germany GmbH, Germany); [Philipp Gentner](#) (Ericsson Antenna Technology Germany GmbH, Germany); [Maximilian Göttl](#) (Ericsson, Germany)

Full duplex schemes technologies have considerable potential to improve the performance of future generations of mobile communication systems. While promising, these technologies face several challenges, particularly self- and cross-link- interference. This paper addresses the self-interference issue, which can severely impact the performance of full duplex systems. A novel dual-band antenna architecture tailored for full duplex systems is presented alongside the design of two shielding structures and their performance are evaluated in electromagnetic simulation software. The simulation results indicate that the isolation between a transmit beam and a receive radio branch can reach more than 80 dB over a support of 500 MHz for different beam steering directions.

17:10 *Base Station Radome Design for 5G and Beyond*

Lauri Vähä-Savo (Aalto University, Finland); Nasrin Shoghi Badr (Aalto University); Clemens Icheln (Aalto University & School of Electrical Engineering, Finland); Katsuyuki Haneda (Aalto University, Finland)

Increasing data use forces mobile communication to move higher carrier frequencies. The 71-76 GHz band has been newly assigned for communication use. The base station needs radome for protection against the environment. At millimeter waves, the thickness of the radome may become significant compared to the wavelength, making the radome design more challenging. In this manuscript, we design and manufacture two planar radomes, i.e., a single-layer radome and an A-sandwich radome with dielectric lenses. These two radomes are evaluated using maximum realized gain and a new metric (it gain envelope variation). The A-sandwich lens radome achieves higher realized gains with smaller gain envelope variation than traditional single-layer radome.

17:30 *Ground Base Station Antenna Design for Air-To-Ground Communications*

Lucas Nogueira Ribeiro (Ericsson Antenna Technology GmbH, Germany); Sertan Hastürkoglu and Jan Gräwendieck (Ericsson Antenna Systems, Germany)

The sixth generation (6G) of mobile communication networks aims to bring innovations in mobile broadband solutions and airborne communications. This paper proposes an antenna solution for direct air-to-ground (ATG) communications, particularly focusing on the challenges and potential of the digital airspace vision. The intra- and inter-cell interference caused by sidelobes of ground base station (BS) antennas and the bandwidth constraints at sub-6 GHz bands are important limitations. The paper introduces a ground BS antenna design for the 5.9-8.5 GHz band. The main contributions include wide-band, high-isolation antenna array concept for the ground BS antenna, along with an analysis of how the antenna array dimension affects the signal-to-noise-and-interference ratio and throughput in ATG systems.

17:50 *Indoor Wireless Signal Modeling with Smooth Surface Diffraction Effects*

Ruichen Wang, Samuel J Audia and Dinesh Manocha (University of Maryland, USA)

We introduce a novel algorithm that enhances the accuracy of electromagnetic field simulations in indoor environments by incorporating the Uniform Geometrical Theory of Diffraction (UTD) for surface diffraction. The additional phenomenology is important for the design of modern wireless systems and allows us to capture the effects of more complex scene geometries. Central to our methodology is the Dynamic Coherence-Based EM Ray Tracing Simulator, which we have augmented with smooth surface UTD. We validate our additions by comparing them to analytical solutions of a sphere, method of moments solutions from FEKO, and ray-traced indoor scenes from WinProp. Our algorithm improves shadow region predicted powers by about 5dB compared to our previous work, and captures nuanced field effects beyond shadow boundaries. This paper underscores the performance benefits of our method (60% faster computation time compared to WinProp under default settings), emphasizing its potential to revolutionize indoor wireless system design and testing.

Thursday, March 21 16:30 - 18:10

A17: Deployable antenna solutions for space applications

T03 Aerospace, new space and non-terrestrial networks // Antennas

Room: Boisdale 1

Chairs: Paolo Focardi (Jet Propulsion Laboratory & California Institute of Technology, USA), German Augusto Ramirez Arroyave (EPFL - École Polytechnique Fédérale de Lausanne & Universidad Nacional de Colombia, Switzerland)

16:30 *Feed Assembly Development for INCUS*

Gaurangi Gupta (NASA Jet Propulsion Laboratory, Caltech, USA); Paolo Focardi (Jet Propulsion Laboratory & California Institute of Technology, USA)

INCUS (INvestigation of Convective Updrafts) is an Earth Science project approved by NASA in 2022. The goal of the mission is to study in detail how water vapor and droplets move inside tropical storms and thunderstorms and understand their effects on weather and climate models. To carry out this study, the mission will use three almost identical SmallSats, each one equipped with a Ka-band radar heritage of Raincube. The deployable mesh reflector antenna is a new 1.6 m design provided by Tendeg. This paper presents the general architecture of the three observatories with particular emphasis on the radar antenna subsystem design. In particular, the approach used to design and fabricate the feed assembly will be presented along with measured and calculated RF performance parameters.

16:50 *Series-Fed Loop Antenna Array Deployable by a Scissors Mechanism*

German Augusto Ramirez Arroyave (EPFL - École Polytechnique Fédérale de Lausanne & Universidad Nacional de Colombia, Switzerland); Anja K. Skrivervik (EPFL, Switzerland); Javier Leonardo Araque Quijano (Universidad Nacional de Colombia, Colombia)

A series-fed loop antenna array, deployable by means of a scissors-type stretchable mechanism is presented. The antenna topology uses a continuous conductor with proper size to produce in-phase vertical currents that creates a highly directive pattern. The design methodology and simple guidelines for obtaining desired input impedance, gain and front-to-backlobe-ratio (FBR) are presented. A wire prototype was realized as proof of concept, demonstrating input impedance and radiation characteristics according to expectations.

17:10 *Design and Test of a UHF Deployable Conical Log Spiral Antenna for Small Satellites*

Lewis Raymond Williams (University of Oslo, Norway); Karina Hoel (FFI & University of Oslo, Norway); Lars Erling Bråten (Norwegian Defence Research Establishment (FFI), Norway); Bendik Sagsveen (FFI, Norway)

The design and experimental test results for a deployable broadband conical log spiral antenna intended for small satellites are presented. A performance trade-off was conducted, resulting in a feasible mechanical design whilst retaining good radiation characteristics. A deployment mechanism is proposed, and electrical and mechanical prototypes manufactured. The antenna has a measured directivity of approximately 6 dBi from 600 to 1500 MHz and is well matched at 100 Ω input impedance.

17:30 *RF Modelling and Validation of the Breadboard Antenna of the Copernicus Imaging Microwave Radiometer*

Cecilia Cappellin and Pasquale Giuseppe Nicolaci (TICRA, Denmark); Roberto Mizzi (Italy); Cyril Mangenot (Api-Space, France); Vincenzo Lubrano and Eva Trippanera (Thales Alenia Space Italy, Italy); Leri Datashvili (Large Space Structures (LSS) GmbH, Germany); Benedetta Fiorelli (European Space Agency, The Netherlands)

A 1.4 m representative breadboard of the Copernicus Imaging Microwave Radiometer (CIMR) mesh reflector antenna was manufactured and its radiated field was measured using the planar near-field scanner of TASI in Rome. In this paper we describe the RF modelling of the CIMR breadboard in its measurement conditions and correlate the measured fields with the predicted fields in Ka bands.

17:50 *The Novel Method for Deployable Parabolic Reflector Based on Uchiwa Origami*

Amit Kumar Baghel (AVENIDA DE ARTUR RAVARA 4 1ESQ & IT AVEIRO, Portugal); Vinicius Magno Uchoa Lima Oliveira (University of Aveiro & Instituto de Telecomunicações, Portugal); Pedro Pinho (UA - Universidade de Aveiro & IT - Instituto de Telecomunicações, Portugal); Nuno Borges Carvalho (Universidade de Aveiro, Portugal & Instituto de Telecomunicações, Portugal)

In this paper the authors proposed a novel method for the deploying parabolic reflector antenna (PRA). The idea of the same comes from the Japanese silk fan called Uchiwa. The PRA is designed for 2.45 GHz frequency of operation with $F/D = 0.5$ having diameter (D) = 1.3 m. The PRA surface is broken down in 18 segments. While deployment, the first segment is fixed and the other segments are moved in the steps of 200 with the help of stepper motor. For the fully deployability, the segments are attached at the back with the closing and opening V-shaped hinge. The proposed method uses mechanical robust items rather than

the spring mechanism, thus making it more reliable solution for the deployment. For lower D of 0.5 m and same F/D ratio, the volume occupied by the structure is less than 1.5 U (10 × 10 × 15 cm³).

Thursday, March 21 16:30 - 18:10

P02: Imaging, detection and estimation

T04 RF sensing for automotive, security, IoT, and other applications / / Propagation

Room: Boisdale 2

Chairs: Joao M. Felicio (Escola Naval, Portugal & CINAV - Instituto de Telecomunicacoes, Portugal), Sergio Matos (ISCTE-IUL / Instituto de Telecomunicações, Portugal)

16:30 Multistatic OFDM Radar Fusion of MUSIC-Based Angle Estimation

Martin Willame (Université Catholique de Louvain (UCLouvain) & Université Libre de Bruxelles (ULB), Belgium); Hasan Can Yildirim (Université Libre de Bruxelles (ULB), Belgium); Laurent Storrer (Université Libre de Bruxelles (ULB), Belgium); François Horlin (Université Libre de Bruxelles, Belgium); Jerome Louveaux (Université catholique de Louvain, Belgium)

This study investigates the problem of angle-based localization of multiple targets using a multistatic OFDM radar. Although the maximum likelihood (ML) approach can be employed to merge data from different radar pairs, this method requires a high complexity multi-dimensional search process. The multiple signal classification (MUSIC) algorithm simplifies the complexity to a two-dimensional search, but no framework is derived for combining MUSIC pseudo-spectrums in a multistatic configuration. This paper exploits the relationship between MUSIC and ML estimators to approximate the multidimensional ML parameter estimation with a weighted combination of MUSIC pseudo-spectrum. This enables the computation of a likelihood map on which a peak selection is applied for target detection. In addition to reducing the computational complexity, the proposed method relies only on transmitting the estimated channel covariance matrices of each radar pair to the central processor. A numerical analysis is conducted to assess the benefits of the proposed fusion.

16:50 Learning-Based Procedures for Inverse Design of Electromagnetic Devices: A Preliminary Investigation

Roberta Palmeri (IREA-CNR, Napoli, Italy); Álvaro Yago Ruiz (CNR, National Research Council, Italy); Rosa Scapatucci (CNR-National Research Council of Italy, Italy); Tommaso Isernia (University of Reggio Calabria, Italy); Lorenzo Crocco (CNR - National Research Council of Italy, Italy)

The concept of Inverse Design (ID) has grown in the last years in many branches of engineering. In this contribution, the possibility of performing optimal ID within the inverse scattering (IS) framework is presented. In particular, the possibility of exploiting deep learning (DL) based approaches is discussed by focusing on the joint exploitation of the most suitable DL architecture and IS techniques.

17:10 Feature Selection for Identifying Optimal Microwave Frequencies to Detect Floating Macroplastic Litter in C and X Bands

Tomás Soares da Costa (ULisboa - Instituto Superior Técnico & Instituto Telecomunicações, Portugal); Joao M. Felicio (Escola Naval, Portugal & CINAV - Instituto de Telecomunicacoes, Portugal); Mario Vala (Instituto de Telecomunicações de Portugal, Portugal); Nuno R. Leonor (Polytechnic Institute of Leiria (IPL) & Instituto de Telecomunicações (IT), Leiria, Portugal); Jorge R. Costa (Instituto de Telecomunicações / ISCTE-IUL, Portugal); Paulo Marques (ISEL-IT Lisboa, Portugal); Antonio A Moreira (IST - University of Lisbon & Instituto de Telecomunicações/ Lisbon, Portugal); Rafael F. S. Caldeirinha (Polytechnic Institute of Leiria & Instituto de Telecomunicações, Portugal); Sergio Matos (ISCTE-IUL / Instituto de Telecomunicações, Portugal); Carlos A. Fernandes (Instituto de Telecomunicacoes, Instituto Superior Tecnico, Portugal); Nelson Fonseca (Anywaves, France); Peter de Maagt (European Space Agency, The Netherlands)

Recently, the utilisation of microwave (MW) frequencies in remote sensing has emerged as a promising and complementary technology to optical methods for effectively detecting and monitoring floating plastic litter. Still, there is a scarce number of existing studies evaluating the optimal MW band for detection, in particular making use of machine learning (ML) techniques. To contribute to this topic, we propose and adapt the use of a simple and reliable feature selection (FS) algorithm based on the weighted principal component analysis (WPCA) to study the backscattering response in C and X-bands of floating macroplastic clusters (made of plastic bottles, straws, lids, and cylinder foams). Specific backscattering radio measurements were carried out in a controllable indoor scenario that mimics deep sea conditions. The results attained show that, under the tested conditions, that X-band is preferable and that the floating macroplastics shows a consistent behaviour through the MW frequencies.

17:30 Measuring and Modelling the Scattering Parameters of the Wet Radome of the Swiss Weather Radars

Philipp Joachim Schmid (University of Bern, Switzerland); Maurizio Sartori (Meteoswiss, Switzerland); Marco Gabella (Meteoswiss, Germany); Matthias Renker (Armasuisse, Switzerland); Mikko Kotiranta and Axel Murk (University of Bern, Switzerland)

The radome of weather radars can be covered with a layer of water, degrading the quality of the radar products. Considering a simplified setup with a planar sample of the Swiss weather radar's radome, we measure and model analytically the scattering parameters of the multilayered structure, with and without water. The measured reflectance of the dry radome sample is consistent with the one modelled according to the manufacturer specifications. As regards the wet radome sample, for thick layers the distribution of the water complies with the model's hypothesis of a homogeneous film of uniform thickness. Qualitative agreement is also found for the meteorologically relevant thin layers, but because the water forms droplets the quantitative comparison is limited. GRASP antenna simulations of the wet radome complement the study for a more realistic setup with a spherical radome.

17:50 Mechanical Vibrations on a Deployable Nanosatellite Antenna: SAR Performance Analysis

Andrew C M Austin and Timothy Pelham (University of Bristol, United Kingdom (Great Britain)); Simone Mencarelli (The University of Auckland, New Zealand); Annalisa Tresoldi (University of Auckland, New Zealand); Mohammed Daboor (Environment and Climate Change Canada, Government of Canada, Canada); Guglielmo Aglietti (University of Auckland, New Zealand); Michael J Neve (The University of Auckland, New Zealand)

The mechanical vibrations of a high-strain glass-fibre composite deployable X-band antenna structure are investigated using a finite element method. The antenna is approximately 2 m x 0.3 m, and exhibits natural frequencies at 2.8 Hz and 7.6 Hz. The radiation patterns for a reflectarray formed from the structure are calculated using a ray-tracing approach for the nominal and mechanically deformed cases. The mechanically deformed antenna pattern is defocused, and a synthetic aperture radar system model shows this reduces the signal-to-noise ratio of a point scattering target by approximately 6 dB.

Thursday, March 21 16:30 - 18:10

CS29: Propagation for Integrated Sensing and Communication

T05 Positioning, localization, identification & tracking / Convened Session / Propagation

Room: Carron 1

Chairs: Yang Miao (University of Twente, The Netherlands), Carsten Jan Smeenk (Fraunhofer Institute for Integrated Circuits & TU Ilmenau, Germany)

16:30 AI-Based Environment Segmentation Using a Context-Aware Channel Sounder

Anuraag Bodi and Samuel Berweger (NIST, USA); Raied Caromi (National Institute of Standard and Technology, USA); Jihoon Bang, Jelena Senic and Camillo Gentile (NIST, USA)

We describe how the data acquired from the camera and Lidar systems of our context-aware radio-frequency (RF) channel sounder is used to reconstruct a 3D mesh of the surrounding environment, segmented and classified into discrete objects. First, the images captured by the camera are segmented into objects through an AI-based algorithm. Then the segmented images are projected onto the point cloud captured by the Lidar. Since the receiver end of the channel sounder is mounted on a mobile robot, the data is acquired in the local coordinate system and so must be transformed to a global coordinate system to synthesize a

single, holistic point cloud of the environment. Finally, the synthesized point cloud is tessellated into a 3D mesh. The segmented mesh can be used for the automated - i.e., without human analysis - reduction of the data acquired by the RF system of the sounder into an object-specific channel model.

16:50 Physics-Informed Generative Neural Networks for RF Propagation Prediction with Application to Indoor Body Perception

Federica Fieramosca (Politecnico di Milano, Italy); Vittorio Rampa (National Research Council of Italy (CNR), Italy); Michele D'Amico (Politecnico di Milano, Italy); Stefano Savazzi (Consiglio Nazionale delle Ricerche CNR, Italy)

Electromagnetic (EM) body models designed to predict the Radio-Frequency (RF) propagation are time-consuming methods which prevent their adoption in strict real-time computational imaging problems, such as localization and human body sensing. Physics-informed Generative Neural Network (GNN) models have been recently proposed to reproduce a EM effects, namely to simulate or reconstruct missing data or samples by incorporating relevant EM principles and constraints. The paper discusses a variational auto-encoder (VAE) model which is trained to reproduce the effects of human motions on the EM field, namely the channel state information (CSI), as well as incorporate EM body diffraction concepts. Proposed EM-informed generative models are verified against both classical diffraction-based EM tools and full-wave EM body simulations.

17:10 Computer Vision Enabled Sub-THz Radio Channel Characterization of Dynamic Objects

[Ankit Regmi](#), Praneeth Susarla, Peize Zhang and Nuutti Tervo (University of Oulu, Finland); Miguel Bordallo Lopez (University of Oulu, Finland & VTT Technical Research Centre of Finland Ltd., Finland); Olli Silvén (University of Oulu, Finland); Pekka Kyösti (Keysight Technologies & University of Oulu, Finland); Marko E Leinonen and Aarno Pärssinen (University of Oulu, Finland)

To enable a wide range of joint communications and sensing applications, future channel models must support dynamic variations of the propagation environment. Moreover, when discovering sensing applications, it is essential to connect physical objects and actions to the radio channel characteristics. In this paper, we perform computer vision (CV) aided automatic mapping and showcase that channel measurements can be linked to the dynamic actions and objects in the environment, thus supporting sensing applications. The proposed method employs a vector network analyzer-based channel measurement system operating at 300 GHz and a camera to enable CV for tracking the object in the radio link. Using human hand as the blockage object, the CV-extracted coordinates and the measured channel responses are combined to generate radio channel footprints for different hand movements.

17:30 Accurate Time Synchronization Exploiting Integrated Sensing and Communication

Davide Scazzoli, Francesco Linsalata, Dario Tagliaferrì, Maurizio Magarini and Umberto Spagnolini (Politecnico di Milano, Italy)

The design of waveforms catering to both communication and sensing functionalities emerges as a pivotal aspect in Integrated Sensing and Communication (ISAC) systems. The Orthogonal Frequency Division Multiplexing (OFDM), currently used for communication purposes, requires accurate time synchronization. This paper presents an experimental exploration of a novel ISAC waveform, which superimposes the legacy OFDM onto a low power and wide bandwidth signal, with the specific focus being synchronizing transmitters and receivers. Our proposed method requires a simple yet effective correlation technique with the transmitted low power signal to identify OFDM symbols timing at the communication receiver. The experimental results shows the superiority of our approach compared to the state of the art, showcasing enhanced accuracy, also in harsh channel conditions, compared to the existing synchronization methods. Our approach leverages the processing typically done to sense the environment for the goal of synchronisation, reusing computationally expensive results for multiple purposes.

17:50 Multi-Scattering Centers Extraction and Modeling for ISAC Channel Modeling

Yi Chen (Huawei Technologies CO. LTD., China); Ziming Yu (Huawei Technologies CO., LTD, China); Jia He, Wenfei Yang, Jian Li and Guangjian Wang (Huawei Technologies Co., Ltd., China)

Integrated sensing and communication (ISAC), has many potential applications, like localization, environment reconstruction, identification, and communication assistance purposes. Also, it has been adopted as one of the key 6 usage scenarios specified in IMT-2030 (6G) framework by ITU. ISAC performance evaluation depends critically on channel modeling, but because traditional models are oriented only to communication, such models cannot meet the requirements imposed by ISAC. Consequently, we need to explore a new channel model for ISAC. In this paper, we first present a hybrid channel modeling method that incorporates statistical and deterministic modeling. This modeling method independently considers sensing targets and background channels, and adopts the multi-scattering center theory to model the target's electromagnetic features. Second, we present multi-scattering center model and parameter extraction algorithm, which are then verified through electromagnetic (EM) simulation.

Thursday, March 21 16:30 - 18:10

A20: Biomedical and health

T06 Biomedical and health // Antennas

Room: Carron 2

Chairs: Giovanni Buonanno (University of Calabria, Italy), Giuseppe Vecchi (Politecnico di Torino, Italy)

16:30 Errors Correlation in Near-Field Focused Arrays for Biosafe Microwave Applications

Sandra Costanzo and Giovanni Buonanno (University of Calabria, Italy)

The most common errors in antenna arrays are those affecting the magnitudes and phases of the excitation coefficients, as well as those related to faults occurring in the radiating elements. Such errors can affect the performance of near-field focused arrays by causing relatively high levels of the electric field even into unwanted regions. Obviously, this aspect is also harmful in receiving mode. This can be a severe problem if applied to a biomedical context, where field levels must be properly controlled to ensure biological integrity. Correlations between magnitude errors as well as between phase errors are analysed in the present work, to take into account simultaneous effects produced by the same components and/or phenomena.

16:50 Stretchable Multi-Band Radio Frequency Sensor for Strain Measurement

Zaynab Attoun, Youssef Tawk, Joseph Costantine and Elie Shammam (American University of Beirut, Lebanon)

A stretchable Radio Frequency (RF) tension sensor is presented in this paper. The sensor is based on a filter that, in the absence of strain, operates as a dual band-pass filter at 1.2 GHz and 1.95 GHz and a dual band-stop filter at 1.67 GHz and 2.27 GHz. Two logarithmically scaled spiral-shaped Defected Ground Structures (DGS) are etched from the ground planes of a Coplanar Waveguide Transmission Line (CPW) to produce the dual band-stop operation. In addition, two U-shaped slot capacitors are etched from the feeding line of the CPW to ensure the appropriate operation of the filter when stretched. The magnitudes of the reflection and transmission coefficients undergo a gradual shift in their operational frequencies, which corresponds to the degree of stretching. The filter is fabricated and tested in different stretching states where its ability to accurately sense the applied strain level is validated.

17:10 Compact Antenna Solutions for Data Transmission Using Fat-Intrabody Communication (Fat-IBC)

[Rossella Gaffoglio](#) (Fondazione LINKS, Italy); Giorgio Giordanengo (LINKS Foundation, Italy); Giuseppe Musacchio Adorisio (Fondazione LINKS, Italy); Bappaditya Mandal, Johan Engstrand and Robin Augustine (Uppsala University, Sweden); Giuseppe Vecchi (Politecnico di Torino, Italy)

Fat intra-body communication (Fat-IBC) is a novel communication technique aiming at exploiting the very low electrical conductivity of subcutaneous fat tissue to convey electromagnetic signals among implantable and wearable biomedical devices. This paper describes the design of two on-body antenna solutions, optimized to transmit signals along the body exploiting the subcutaneous fat tissue as a communication channel. The designed antennas have been fabricated and tested on a three-layer phantom model emulating the dielectric properties of skin, fat and muscle, inserted in a portable chamber to reduce external interference and minimize alternative propagation paths, i.e., outside the fat channel. Preliminary data rate transmission measurements computed using two Raspberry Pi units allowed link speeds in the range of 90 Mbps for one of the two considered antenna pairs, demonstrating the ability of the designed solution to efficiently couple the radiation into the tissue-mimicking phantoms and transmit signals through the fat layer.

17:30 *The Impact of a Phantom's Size on the Performance of an Implanted Antenna*

Mohammed Aldosari (University of Sheffield, United Kingdom (Great Britain) & Prince Sattam Bin Abdulaziz University, Saudi Arabia); Salam Khamas (University of Sheffield, United Kingdom (Great Britain))

This study investigates the impact of the size of a tissue-equivalent phantom on the implanted antenna performance at 2.45 GHz. A planar inverted-F antenna (PIFA), which is implanted in a single layer of skin at a depth of 4 mm, has been selected to investigate the impact of the phantom's size on the antenna's impedance matching, radiation efficiency, realized gain, and radiation pattern. Furthermore, a minimum phantom size that can provide an accurate model of the body, or semi-infinite phantom, has been suggested. In addition, the reliability of the suggested phantom model has been examined using different implanted antennas and compared with a semi-infinite model, as well as recommended models in the literature.

17:50 *Quad-Band Meandered Implantable Planar Inverted-F Antenna for Wireless Brain Health Monitoring*

Uzman Ali (Tampere University, Finland); Muhammad Waqas Ahmad Khan (Tampere University, Sweden); Nikta Pourmoori, Leena Ukkonen, Lauri Sydänheimo and Toni Björminen (Tampere University, Finland)

We've developed and optimized a quad-band meandered implantable Planar Inverted-F Antenna (PIFA) for brain health monitoring. By utilizing numerical optimization and full-wave EM simulations, we successfully enabled operation across four vital healthcare communication bands: Medical Device Radiocommunication Service (MedRadio) band (401-406 MHz), Wireless Medical Telemetry Service (WMTS) band (1427-1432 MHz), and Industrial, Scientific, and Medical (ISM) bands (902.8-928 MHz, 2400-2483.5 MHz) with reflection coefficients below -10 dB. Employing meandered miniaturization techniques reduced antenna size. A biocompatible silicone coating safeguards against direct body contact, and Rogers RO3210 high-permittivity substrate was employed. We utilized a 7-layer human head model, implanting the antenna at a depth of 13.25 mm within the cranial cavity's cerebrospinal fluid (CSF) layer, resulting in an antenna volume of $11 \times 19.8 \times 1.8 \text{ mm}^3$.

Thursday, March 21 16:30 - 18:10

P01: Channel modeling and measurements

T02 Mm-wave for terrestrial networks 5G/6G // Propagation

Room: Dochart 1

Chairs: Raffaele D'Errico (CEA, LETI & Université Grenoble-Alpes, France), Ruth G Gebremedhin (New York University, USA)

16:30 *5G Radio Channel Characterization in an Underground Mining Environment*

Marko E Leinonen and Veikko Hovinen (University of Oulu, Finland); Risto Vuohoniemi (Centre for Wireless Communications, Finland); Aarno Pärssinen (University of Oulu, Finland)

The development and usage of wireless communication systems in underground mines are essential for the digitalization of the mining industry. The 5G systems have been widely deployed at frequency range 1 (FR1) below 6 GHz as terrestrial networks. The first 5G network installations have been done for underground mines but the optimized 5G network planning in the mine requires a specific understanding of the radio propagation characteristics of the mine tunnels.

This paper provides radio channel measurement results for 5G FR1 and FR2 bands from the underground mine tunnels of Sandvik's test mine. In a cross-section scenario, the 5G signal travels up to 18 meters from the main tunnel to the side tunnel at FR1, but only 6 meters at FR2. The signal blocking in different scoop positions of the loader at FR1 was measured, and the topmost position attenuates the signal by 10 to 15 dB.

16:50 *Grid-Free Harmonic Retrieval and Model Order Selection Using Convolutional Neural Networks*

Steffen Schieler (Technische Universität Ilmenau, Germany); Sebastian Semper (Ilmenau University of Technology, Germany); Reza Faramarzanagari (Technische Universität Ilmenau, Germany); Michael Döbereiner (Fraunhofer Institute for Integrated Circuits IIS & Technische Universität Ilmenau, Germany); Christian Schneider (Technische Universität Ilmenau, Germany); Reiner S. Thomä (Ilmenau University of Technology, Germany)

Harmonic retrieval techniques are the foundation of radio channel sounding, estimation and modeling. This paper introduces a Deep Learning approach for joint delay- and Doppler estimation from frequency and time samples of a radio channel transfer function.

Our work estimates the two-dimensional parameters from a signal containing an unknown number of paths. Compared to existing deep learning-based methods, the signal parameters are not estimated via classification but in a quasi-grid-free manner. This alleviates the bias, spectral leakage, and ghost targets that grid-based approaches produce. The proposed architecture also reliably estimates the number of paths in the measurement. Hence, it jointly solves the model order selection and parameter estimation task. Additionally, we propose a multi-channel windowing of the data to increase the estimator's robustness.

We compare the performance to other harmonic retrieval methods and integrate it into an existing maximum likelihood estimator for efficient initialization of a gradient-based iteration.

17:10 *Scenario Classification and Channel Modeling for MIMO Communications in Suburban Road Scenarios*

Dayuan Zhao (Southeast University, China); Chen Huang (Purple Mountain Laboratories & Southeast University, China); Cheng-Xiang Wang (Southeast University, China & Purple Mountain Laboratories, China); Junling Li (Southeast University, China)

Suburban road scenario is one of the most typical communication scenarios for the sixth generation (6G) wireless communications. Therefore, it is essential to conduct a more thorough investigation and modeling of suburban road wireless channels. Physical environmental factors, including building height and width, usually have a significant influence on channel characteristics. In this paper, through an analysis of physical environmental factors and channel characteristics, we classify the suburban road scenarios into two sub-scenarios, i.e., main roads and branch roads. Subsequently, we propose specific channel models for each sub-scenario. To validate the accuracy of our proposed channel models, we compare synthetic data generated by these models with channel data collected from practical communication networks in Meishan City. Furthermore, we conduct a comparative analysis of channel characteristics for all types of suburban road scenarios to verify the effectiveness of the classification.

17:30 *Frequency Domain Channel Characteristics in an Outdoor-To-Indoor Environment at 6 and 37 GHz*

Ruth G Gebremedhin (New York University, USA); Ruoyu Sun and Dorin G Viorel (CableLabs, USA); Wilhelm Keusgen (Technische Universität Berlin, Germany)

Fixed Wireless Access (FWA) aims to provide users with high data rates. The unlicensed 6-GHz band (5.925 - 7.125 GHz) and the shared lower-37-GHz band (37.0 - 37.6 GHz) are considered for FWA due to their low cost and high bandwidth availability. We studied the frequency domain characteristics of multiple outdoor-to-indoor channel realizations at 6.175 and 37.3 GHz, emulating FWA scenarios. Channel transfer functions from a measurement campaign were analyzed to study the impact of frequency-selective fading on OFDM. Power flatness within each subcarrier and power variation across multiple subcarriers were studied. Subcarrier channels were generally flat-fading with a 95% probability of less than 1 dB variation. Channel power gain across subcarriers followed a Log-Normal distribution with an average standard deviation of 3.2 and 5.2 for outdoor and indoor receivers, respectively. The channel was more dispersive at 37 GHz compared to 6 GHz with respect to both intra-subcarrier power flatness and power gain variation across subcarriers.

17:50 *Analysis of 5G Channel Characteristics Based on Ray Tracing for the Straight Tunnel of High Speed Railway*

Lei Liu, Bo Ai and Yuanyuan Qiao (Beijing Jiaotong University, China)

The tunnel is one of the most important scenarios for high-speed railway (HSR). However, it exists many gaps about the coverage, the path loss and the number of signal paths in the HSR tunnel. In this paper, we first simulate the coverage of base station (BS) at the 2.6, 3.5 and 4.9 GHz by the ray tracing (RT) simulator, when the BS is arranged outside the tunnel. Simulation results show that the BS outside the tunnel can cover more than 200 meters of the tunnel. And decreasing the elevation angle between the BS and the tunnel can increase the covered tunnel distance of the BS. Moreover, we propose the three-slope path loss model to predict signal attenuation at different areas for the tunnel scenario. Finally, we analyze the number of signal paths and find that the multipath effect is more severe at the tunnel entrance, rather than inside the tunnel.

Thursday, March 21 16:30 - 18:10

A24: Superdirectivity and synthesis techniques

T08 EM modelling and simulation tools // Antennas

Room: Dochart 2

Chairs: Okan Yurduseven (Queen's University Belfast, United Kingdom (Great Britain)), Richard W Ziolkowski (University of Arizona, USA & University of Arizona, USA)

16:30 Self-Resonant Broadside-Radiating Superdirective Unidirectional Mixed-Multipole Antennas

Richard W Ziolkowski (University of Arizona, USA)

Two 28 GHz broadside-radiating unidirectional mixed-multipole antenna (UMMA) designs are presented. These UMMAs are self-resonant metamorphoses of previously reported systems. Both versions are matched to a 50 ohm source. Details of their directivity, front-to-back ratio, realized gain, and radiation efficiency performance characteristics are reported. It is demonstrated that both of them are superdirective, highly efficient and have interesting bandwidths. Their intrinsic attributes surpass several recognized bounds. These results add further credence to the fact that superdirective systems with useful properties are indeed practical in contradistinction to the general perception that they are not.

16:50 Synthesis of Flat-Top Beams Based on Modified Chebyshev Polynomials

Goran Molnar and Marko Matijašić (Ericsson Nikola Tesla d. d. & Research and Development Centre, Croatia)

Real-time beamforming applications require computationally efficient methods for the beam pattern synthesis. This feature is usually met by analytical techniques or simple iterative procedures. On the other hand, many of these applications utilize flat-top beam patterns with adjustable parameters. In this paper, we present an analytical method for the design of symmetrical linear arrays which form flat-top beam patterns. The method is based on matching the array factor with a given polynomial, thus ensuring a closed form expression for array's weights. To obtain flat-top beam patterns with adjustable sidelobe level and beamwidth, we use a modification of Chebyshev polynomials. To adjust the beam patterns, we provide two straightforward procedures, one for a given sidelobe level and the other for a given beamwidth.

17:10 Optimization of Super-Directive Linear Arrays with Differential Evolution for High Realized Gain

Ihsan Kanbaz (Gazi University, Turkey); Okan Yurduseven and Michail Matthaiou (Queen's University Belfast, United Kingdom (Great Britain))

Due to the low impedance and high feeding currents, it is naturally challenging to design super-directive antenna arrays that perfectly match the feed line, and this becomes almost impossible as the number of elements increases. In this paper, we assert that it is crucial to consider the trade-off between directivity and overall efficiency (to achieve high realized gain) before employing super-directive arrays in real-world applications. Given this trade-off (high directivity and low mismatch for high realized gain), a 4-element dipole array (unit array) is optimized using the differential evolution (DE) algorithm. Then, the performance of the unit array in subarray configuration scenarios is analyzed. Finally, the obtained parameters are verified using the CST full-wave simulation software. The results clearly indicate that the proposed unit array is a strong candidate for dense array applications, particularly in the context of massive multiple-input multiple-output (MIMO), thanks to its notable high gain and efficiency.

17:30 Superdirective Broadside-Radiating Unidirectional Mixed-Multipole Antenna Arrays

Richard W Ziolkowski (University of Arizona, USA)

A realistic superdirective broadside-radiating unidirectional mixed-multipole antenna (UMMA) design is presented and then used as the radiators of two two-element arrays. The single and two element systems are self-resonant in the 5G 28 GHz band being matched to 75 ohm sources without any intervening matching networks. Details of the designs along with their key performance attributes: directivity, realized gain, front-to-back ratio, radiation efficiency, and bandwidth, are given. It is demonstrated that these systems are not only highly efficient and have usable bandwidths, but they are all superdirective with their directivities surpassing several recognized bounds. They also further the recognition that traditional perceptions of superdirective systems being impractical are no longer tenable.

17:50 Design Recommendations for Minimal Antenna Mutual Coupling Using Current Optimization

Hannes Bartle (Ecole Polytechnique Federale de Lausanne & ClearSpace SA, Switzerland); Jakub Liška and Miloslav Capek (Czech Technical University in Prague, Czech Republic); Anja K. Skrivervik (EPFL, Switzerland); Lukas Jelinek (Czech Technical University in Prague, Czech Republic)

This work addresses a first attempt at using current density optimization algorithms to gain insight into the relation between maximum achievable gain in a given direction and the mutual coupling to another antenna nearby. The methodology is presented on the example of the coupling between two patch antennas placed above an infinite ground plane. The optimized antenna gain is shown to have a strong relation to the geometry of the problem. The obtained insight is then formulated into design recommendations that can help in an actual design.

Thursday, March 21 16:30 - 18:10

M2: MIMO, OTA and 6G Antenna Testing

T09 Fundamental research and emerging technologies // Measurements

Room: M2

Chairs: Andrés Alayón Glazunov (Linköping University, Sweden), Thorsten Hertel (Keysight Technologies, USA)

16:30 A Novel MIMO OTA Methodology for UE Performance Testing

Thorsten Hertel (Keysight Technologies, USA); Lassi Hentila (Keysight Technologies, Finland); Jukka Kyröläinen (Keysight Technologies Finland oy, Finland); Pekka Kyösti (Keysight Technologies & University of Oulu, Finland); Huaizhi Yang (Keysight Technologies China co. Ltd, China)

This paper provides an overview of a novel MIMO OTA methodology using dynamic channel models and link adaptation being developed for CTIA's NR FR1 MIMO OTA performance test plan using dynamic channel models with link adaptation. The test setup comprises a base station emulator, fading/channel emulator, anechoic chamber, and probe antennas. Purpose of the testing is to evaluate UE antenna system and its overall adaptation to transitions and time variant radio environments. Initial end-to-end measurement results are provided that clearly demonstrate the efficacy of this test methodology.

16:50 Real-Time Near-Field Measurements of mmWave Devices Using a Metasurface and IR Camera

Johan Lundgren (Lund University, Sweden); Torleif Martin (Qamcom Research and Technology, Sweden); Hamza Khalid and Deyu Tu (Linköping University, Sweden); Daniel Sjöberg and Mats Gustafsson (Lund University, Sweden); Isak Engquist (Linköping University, Sweden)

With a metasurface consisting of elements absorbing incident mmWaves and an infrared camera tracking temperature evolution, this paper introduces an alternative approach to rapidly image incident power density. This offers an effective non-contact assessment of power levels without direct antenna connections for validating and characterizing radiating devices operating in the mmWave regime. We display how the technique of the metasurface along with modulating the transmit signal enables the detection of typical mmWave power levels rapidly by demonstrating it in the Ka-band for fault detection on a 16 x 16 element phased array antenna and incident power density imaging in the near-field of a mobile phone mock-up. Both time and frequency domain analyses can be employed for processing and comprehension of the results.

17:10 Data-Driven Optimization of an Array of Steered Sub-Arrays for Enhanced Fairness in MU-MIMO

Noud Kanters (University of Twente, The Netherlands); Andrés Alayón Glazunov (Linköping University, Sweden)

This paper investigates arrays of steered sub-arrays (SAs) in multi-user scenarios. We optimize the SA steering angles based on rate-based and gain-based objective functions which naturally balance aggregate system performance and user fairness. Numerical simulations show that, compared to a full-digital array with the same number of RF-chains, rate-optimized arrays increase the array gain in small sector scenarios and compensate for low element gains in large sector scenarios. An array with 4-element SAs achieves the highest rate at all sectors at both low and high signal-to-noise ratios (SNRs). Improvements vary from

2% (120-degree sector, high SNR) to 113% (30-degree sector, low SNR). Hence, adjusting the steering angles to the long-term channel statistics yields significant rate improvements if users are confined to a small sector, without sacrificing performance if this is not the case. Similar results are obtained for gain-based optimized arrays, which is important and convenient for array design.

17:30 *K-Factor Evaluation in a Hybrid Reverberation Chamber plus CATR OTA Testing Setup*

[Alejandro Antón Ruiz](#) (University of Twente, The Netherlands); Samar Hosseinzadegan (Bluetest, Sweden); John Kvarnstrand and Klas Arvidsson (Bluetest AB, Sweden); Andrés Alayón Glazunov (Linköping University, Sweden)

This paper investigates achieving diverse K-factors using a Reverberation Chamber (RC) with a Compact Antenna Test Range (CATR) system. It explores six hybrid "RC plus CATR" configurations, involving different excitations of the Rich Isotropic Multipath (RIMP) field and CATR-generated plane waves, with some setups including absorbers. A fixed horn antenna points towards the CATR in all configurations. The study found that the null hypothesis of Rayleigh or Rician probability distributions for received signal envelope could not be rejected, with RIMP setups primarily conforming to Rayleigh distribution and all setups showing Rician distribution. Various K-factors were obtained, but no generalizable method for achieving the desired K-factor was identified. The paper also estimates K-factor as a function of frequency in the 24.25-29.5 GHz band. Smaller K-factors exhibit larger fluctuations, while larger K-factors remain relatively stable, with consistent fluctuations across the frequency range.

17:50 *Optimization of the TRP Evaluation in Anechoic-Reverberation Hybrid Chamber*

[Pavlo Krasov](#) and Oleg Iupikov (Chalmers University of Technology, Sweden); Rob Maaskant (CHALMERS, Sweden); Jonas Fridén (Ericsson AB, Sweden); Marianna Ivashina (Chalmers University of Technology, Sweden)

A hybrid, reconfigurable anechoic-reverberation antenna measurement chamber has recently been introduced. The chamber is developed for fast characterization of the active antenna radiated power and directive characteristics in a single measurement environment. In the present work, we propose optimizations of the hybrid chamber design in the configuration that uses E-field scanner. Introducing the wedge reflector in the chamber allows for a reduction in the total number of acquisition samples four times compared to $\lambda/2$ spaced scan during the total radiated power (TRP) measurements.

Thursday, March 21 16:30 - 18:10

ESoA: ESoA Board

//

Room: M3

Thursday, March 21 16:30 - 18:10

E09: Frequency Selective Surfaces

T10 Novel materials, metamaterials, metasurfaces and manufacturing processes // Electromagnetics

Room: M4

Chairs: Agostino Monorchio (Pisa University, Sweden), Jesús Sánchez-Pastor (Technische Universität Darmstadt, Germany)

16:30 *Design of an L-S-Band Frequency Selective Resorber for Dual-Band Absorption and In-Band Transmission*

Francesca Pascarella and Danilo Brizi (University of Pisa, Italy); Agostino Monorchio (University of Pisa & CNIT, Italy)

In this paper, a passive Frequency Selective Resorber (FSR) for dual-band absorption and in-band transmission operating in the L and S bands is presented. The proposed FSR consists of two lossy Frequency Selective Surface (FSS) layers and a lossless FSS layer, with opportune substrates between them for a total thickness of 32 mm. The design procedure of each layer is investigated, and full-wave simulations are performed. The lossy FSSs comprise a modified square loop element loaded with lumped elements. On the other hand, the lossless FSS layer includes a band-pass filter made of a square patch inserted in a connected grid. The simulated results show that the proposed FSR achieves a transmission band from 2.4 to 2.9 GHz with a minimum insertion loss of 1.4 dB. The dual-band absorption covers the range from 0.8-1 GHz and from 3.4-3.9 GHz. Furthermore, the presented structure exhibits stable performance against oblique incidences.

16:50 *Double-Layer Frequency Selective Surface-Based Corner Reflector for Indoor Self-Localization Systems in the W-Band*

[Jesús Sánchez-Pastor](#) (Technische Universität Darmstadt, Germany); Martin Schüßler (TU Darmstadt, Germany); Rolf Jakoby (Institute for Microwave Engineering and Photonics, Technische Universität Darmstadt, Germany); Alejandro Jiménez-Sáez (Technische Universität Darmstadt, Germany)

One possibility to enable low complexity and robust indoor self-localization systems operating at the W-band (75 GHz to 110 GHz) is the deployment of chipless infrastructure. To do so, frequency-coded radar targets are placed in designated coordinates, where a stopband structure is placed into the aperture of a metallic corner reflector (CR). In this work, an alternative is presented by designing a passband double-layer frequency selective surface (FSS) and assembling it in the shape of a CR. The FSS is formed by a Jerusalem cross on one side and a square ring on the other side. The measured resonance frequency, f_{res} , differs for both transverse electric (92 GHz) and transverse magnetic (79 GHz) plane waves, which is attributed to manufacturing tolerances. Regardless, the f_{res} shifts less than 3.5% up to 45° for both polarizations. The resulting CR assembly presents a notch as frequency-coded response between 80 GHz to 90 GHz.

17:10 *Analysis and Design of a Wideband Jaumann-Like Radar Absorber Offering High Angular Stability and Polarization Insensitivity*

Aqsa Ahmad (The University of Edinburgh, United Kingdom (Great Britain)); Callum J Hodgkinson (University of Edinburgh & Heriot Watt University, United Kingdom (Great Britain)); Dimitris E. Anagnostou (Heriot Watt University, United Kingdom (Great Britain)); Symon K. Podilchak (University of Edinburgh, United Kingdom (Great Britain))

A circuit model of a frequency selective absorber exhibiting absorption properties in a wide frequency band (1 to 11 GHz) and a transmission window around 5.5 GHz is developed. The structure offers wideband absorption, low insertion losses, and polarization insensitivity to incident TM and TE fields. In addition, the three-layer structure is symmetric and defined by a compact Jaumann-like stack-up of PCBs and is composed of two resistive layers placed on top of a lossless layer. The resistive layers are defined by a Jerusalem cross surrounded by a square-ring structure and tapered dipole arms in both the horizontal and vertical planes. This symmetry supports the noted polarization insensitivity. The unit cell of the bottom metamaterial layer (also referred to as the lossless layer) is composed of a small square-ring slot bridged with the same capacitors as the upper resistive layers.

17:30 *Progressive Ultra-Wideband Circularly Periodic High Impedance Surface Integrated with a Spiral Antenna*

Kshiti Lele and Chris Bartone (Ohio University, USA)

A progressive ultra-wideband (UWB) circularly periodic High Impedance Surface (HIS) is designed and integrated with a UWB spiral antenna while maintaining a low height profile. The HIS is designed to perform across the full frequency range between 1.1-8.0GHz. The proposed design methodology divides the HIS into two zones - heterogenous and homogenous zones. In the heterogenous zone, multiple HIS rings are designed at specific frequencies across the band with the zero-degree reflection-phase of each ring coinciding with a frequency represented by the ring's circumference. The homogenous zone consists of multiple rings designed for a single frequency to provide additional frequency and spatial coverage. The UWB HIS is integrated with a spiral antenna placed at a height of $1/10$ th wavelength above the HIS and is enclosed in an aluminum cavity to further suppress back-lobe radiation. S11, gain and radiation patterns are presented to demonstrate UWB performance of the full antenna structure.

17:50 *Multifunctional Linear Dichroism and Polarization Transforming Metasurface for mm-Wave Application*

Ahsaan Gul Hassan (National University of Science and Technology, Pakistan); Anum Zulqarnain and Muhammad Danial Shafi (National University of Sciences and Technology NUST, Pakistan); Adnan Nadeem (School of Electrical Engineering and Computer Science (SEECs), NUST, Islamabad, Pakistan.); Sultan Shoaib (Wrexham Glyndwr University & HITEC University Taxila, United Kingdom (Great Britain)); [Imran Shoaib](#) (Queen Mary University of London, London, UK); Mohaira Ahmad (National

University of Sciences & Technology, Pakistan); Noshawan Shoaib (School of Electrical Engineering and Computer Science (SEECs), NUST, Islamabad, Pakistan.)

In this paper, a multifunctional metasurface is designed and developed to achieve linear-to-linear (LP-LP) and linear-to-circular (LP-CP) polarization conversion along with linear dichroism functionality. The proposed metasurface consists of split ring resonator structures printed on the top layer which perform the LP-LP, LP-CP, and absorption at two distinct frequency bands. Overall, the polarization conversion ratio (PCR) for cross-polarization conversion is greater than 90 %. The absorption ratio for linear dichroism in TM mode is higher than 85%, while the axial ratio for circular polarization conversion is less than 3 dB. The proposed metasurface can be utilized in wireless communication and satellite communication applications.

Friday, March 22

Friday, March 22 8:30 - 10:10

SW10a: Sub-Terahertz Antenna and Packaging Solutions for Future Radar and Wireless Communication

Room: Lomond Auditorium

Chairs: Akanksha Bhutani (Karlsruhe Institute of Technology, Germany), Matthias Wietstruck (IHP, Germany)

8:30 *Advancements in Sub-THz Antenna and Package Integration for Miniaturized Surface Mount Device Modules Up to 420 GHz - Part II*

Presenter: Akanksha Bhutani (Karlsruhe Institute of Technology - KIT)

9:00 *SiGe BiCMOS and Wafer-Level Packaging Technologies for Sub-THz Applications*

Presenter: Matthias Wietstruck (IHP - Leibniz Institut für innovative Mikroelektronik)

9:30 *Towards Achieving Reliable On-Wafer Measurement of Millimetre-Wave and Terahertz Planar Circuits*

Presenter: Xiaobang Shang (National Physical Laboratory, UK)

Friday, March 22 8:30 - 10:10

CS30a: Approaching optimal performance through automated design techniques

T08 EM modelling and simulation tools / Convened Session / Antennas

Room: M1

Chairs: Miloslav Capek (Czech Technical University in Prague, Czech Republic), Johan Lundgren (Lund University, Sweden)

8:30 *Unconventional Surrogate-Assisted Approaches to EM-Driven Antenna Design. Modeling and Optimization: Global, Multi-Objective, Statistical*

Slawomir Koziel and Anna Pietrenko-Dabrowska (Gdansk University of Technology, Poland)

Design of contemporary antenna systems relies heavily on full-wave electromagnetic (EM) simulation tools. EM analysis ensures reliability but tends to be computationally expensive, which becomes a serious issue in the context of design automation. In recent years, utilization of surrogate modeling methods has been fostered to alleviate the cost-related difficulties. Yet, the existing procedures typically follow a few major approaches, e.g., different architectural variations of deep neural networks, hyper-parameter/model adjustments in Bayesian optimization, or more or less standard machine learning frameworks. This paper reviews several unconventional surrogate-assisted techniques that employ less common algorithmic tools such as the response feature technology, domain confinement, dimensionality reduction, or supplementary inverse predictors. We demonstrate how these tools can be incorporated into practical procedures for global and multi-criterial optimization, statistical analysis, and design-oriented behavioral modeling. A discussion of the algorithm operating principles is supplemented by antenna design cases.

8:50 *Additively Manufactured Waveguide Hybrid Septum Coupler Optimized Using Machine Learning*

Nelson Fonseca (Anywaves, France); Mobayode Akinsolu (Wrexham University, United Kingdom (Great Britain)); Jose Rico-Fernandez (Northern Waves AB, Sweden); Bo Liu (University of Glasgow, United Kingdom (Great Britain)); Jean-Christophe Angevain (ESA, The Netherlands)

This paper describes a waveguide septum coupler design having a smooth profile well suited for additive manufacturing. The large aperture of this hybrid coupler is shaped with even-degree Legendre polynomials. Machine learning-assisted global optimization is employed to extend the operating bandwidth of the component. A design in K-band is detailed and a prototype is manufactured and tested. The experimental results confirm an improvement of 19% in operating bandwidth compared to the previously reported design in the same band while keeping all other key properties mostly unchanged, specifically the physical dimensions. The use of additive manufacturing leads to a mechanically simple and lightweight component of interest for the design of integrated microwave devices, such as beamforming networks and compact feed systems.

9:10 *On Efficient Representations of Frequency Dependent Far-Field Information for Array Antennas*

Lars Jonsson (KTH Royal Institute of Technology, Sweden); Harald Hultin (KTH Royal Institute of Technology & Saab AB, Sweden)

This paper investigates the number of required data points to accurately represent the vector far-field information over the radiation sphere and its frequency variation for array antennas. The method needs to be explicit in terms of the excitation of the elements.

We compare representations of far-field data on the sphere with two different approaches to spherical wave expansion representations and apply a data-driven model-order reduction to find a small-size representation. As is well known, a spherical wave expansion strongly reduces the number of required data points. Here, we show that accounting for the phase center of the elements further strongly reduces the number of required coefficients in the tested cases. The Loewner framework data-driven model-order reduction shrinks the required far-field data by an additional factor of 8-14 per mode coefficients, depending on the acceptable level of error. This reduction works well for the two investigated cases.

9:30 *Validating Convex Optimization of Reconfigurable Intelligent Surfaces via Measurements*

Hans-Dieter Lang (OST Eastern Switzerland University of Applied Sciences Rapperswil & ICOM Institute for Communication Systems, Switzerland); Michel A Nyffenegger, Sven Keller, Patrik Stöckli and Nathan Hoffman (OST Eastern Switzerland University of Applied Sciences Rapperswil, Switzerland); Heinz Mathis (OST-Eastern Switzerland University of Applied Sciences, Switzerland); Xingqi Zhang (University of Alberta, Canada)

Reconfigurable Intelligent Surfaces (RISs) can be designed in various ways. A previously proposed semidefinite relaxation-based optimization method for maximizing power transfer efficiency showed promise, but earlier results were only theoretical. This paper evaluates a small RIS at 3.55GHz, the center of the 5G band "n78", for practical verification of this method. The presented results not only empirically confirm the desired performance of the optimized RIS, but also affirm the optimality of the resulting reactance values. Additionally, this paper discusses several practical aspects of RIS design and measurement, such as the operation of varactor diodes and time gating to omit the direct line-of-sight (LOS) path.

9:50 Alternate Optimization with Deep Learning to Design Beam Deflector Under Aperiodic Near-Field Coupling Conditions

Qimin Ding, Guobin Wan, Nan Wang and Xin Ma (Northwestern Polytechnical University, China)

When designing metasurface beam deflectors, the near-field coupling under aperiodic conditions is significantly different from that under periodic conditions, and the electromagnetic (EM) responses are distorted which finally leads to an inaccurate design result. A deep learning (DL) model is proposed to estimate the EM responses of each metasurface element in the deflector under aperiodic conditions, and an alternate optimization (AO) process is used to determine the arrangement for elements so that the real responses of these elements can be aligned with the design target. The proposed method is validated by both transmissive and reflective deflectors in microwave bands. Simulation results show that the DL model can estimate the responses of elements accurately in aperiodic conditions. Also, compared with conventional optimization with time-consuming full-wave simulation, the AO based on the DL model can design the deflector in just several iterations with 3% error of phase responses.

Friday, March 22 8:30 - 10:10

CS43a: COST-INTERACT, Propagation Measurement and Modelling for 6G and Beyond

T01 Sub-6 GHz for terrestrial networks (5G/6G) / Convened Session / Propagation

Room: Alsh 1

Chairs: Xuesong Cai (Lund University, Sweden), Golsa Ghiaasi (Silicon Austria Lab, Austria), Richard Rudd (Plum Consulting Ltd, United Kingdom (Great Britain))

8:30 On the Importance of Scattering from Poles in Ray Tracing Simulations

Remco Heijs (Eindhoven University of Technology, The Netherlands); Gerhard Steinbock (Ericsson AB, Sweden); Martin Johansson (Ericsson Research, Sweden); Bengt-Erik Olsson (Ericsson AB, Sweden); A. B. (Bart) Smolders (Eindhoven University of Technology, The Netherlands)

For enhancing the latest mobile networks, a more precise approximation of ray propagation in complex environments is necessary to position base stations and optimize network performance. The scattering from a cylindrical metallic object, which could represent lampposts, poles of traffic signs or flag poles, is implemented in ray tracing simulations. In this paper, the addition of cylindrical metallic objects in ray tracing simulations is done via analytically derivable radar cross-sections. Furthermore, objects are decomposed to utilize plane wave excitation in the near field of the object. Implementing this approach results in an augmentation of the channel richness and increases the best available path gain. The comparison of simulation results to measurements clearly indicates that poles contribute significantly and should not be ignored in ray tracing simulations.

8:50 Millimeter-Wave and Sub-THz Channel Measurements and Characterization Analysis in a Street Canyon Scenario

Amar Al-Jzari, Jiahao Hu and Sana Salous (Durham University, United Kingdom (Great Britain))

Wireless communication systems that operate at frequencies higher than 100 GHz are becoming increasingly important in the future due to the availability of wide unused bandwidth (BW) that supports high data rates. In this paper, propagation characteristics of the E-band and D-band are compared based on wideband channel measurements conducted in an outdoor environment for both line-of-sight (LoS) and non-LoS (NLoS) scenarios. The channel statistics including the power delay profile (PDP), path loss (PL), Root Mean Square (RMS) Delay Spread (DS), and Ricean K factor (KF) are presented and analyzed. In addition, the path loss exponents in both frequency bands estimated using the close-in (CI) and floating-intercept (FI) models are presented.

9:10 A Deep Learning Based Surface Current Generation Method for Scattering Modeling at Terahertz Band

Zhao Zhang, Danping He, Ke Guan and Ben Chen (Beijing Jiaotong University, China); Jianwu Dou (ZTE Corporation, China); Wei E. I. Sha (Zhejiang University, China); Zhangdui Zhong (Beijing Jiaotong University, China)

The terahertz band is an important candidate frequency band for next-generation communications. Due to comparable wavelength to surface undulation, scattering modeling becomes the core part of the propagation mechanism characterization. In this paper, a deep learning model is proposed to learn the generation paradigm of surface currents (SC) under multiple input factors. Then, based on the generated SC, we use the dyadic Green's function to reconstruct the scattered electric field in the incidence plane and scattering hemisphere space. Experiments, among which the root mean square error of SC and electric field amplitude draws to 1.33~4.41 dB and 1.55~6.10 dB respectively, demonstrate the excellent generation ability of the proposed model and the feasibility of scattering reconstruction based on induced currents. This deterministic modeling approach can be used to generate SC distribution and scattering beams of a specific surface more efficiently compared with full-wave simulation, providing a novel direction for scattering modeling.

9:30 Propagation Study of Vision-Based RIS Beam Tracking for mmWave Communications

Juan D Sanchez, Xuesong Cai and Fredrik Tufvesson (Lund University, Sweden)

Reconfigurable intelligent surfaces have emerged as a technology with the potential to enhance wireless communication performance for 5G and beyond. This paper focuses on analyzing the multipath components that arise from the insertion of such a device into the wireless channel. A computer vision-based beam tracking algorithm was used for continuously steering the reconfigurable intelligent surface towards the target. The results show that a reconfigurable intelligent surface can provide additional multipath components whose corresponding power contribution could be crucial to overcome blockage situations. A received power boost of up to 3 dB can be perceived in both line-of-sight and non line-of-sight regions.

9:50 Feasibility of High Throughput Wireless Communication Above 100 GHz in Indoor Scenarios

Christina Larsson (Ericsson Research & Ericsson AB, Sweden); Bengt-Erik Olsson (Ericsson AB, Sweden); Henrik Asplund (Ericsson Research, Ericsson AB, Sweden)

In this paper, we compare measured pathloss results from two indoor scenarios at 143 GHz with a simplified link budget to visualize the feasibility of high throughput wireless communication at these high frequencies. The paper concludes that the high-throughput communication can be achieved in indoor open areas, even if the Tx and Rx is not in LOS, but the increased penetration loss at these high frequencies together with a limited link budget make coverage through even thin indoor walls difficult and hence coverage predictions without floorplans difficult. The high penetration losses must also be considered if indoor stochastic propagation models above 100 GHz should be developed.

Friday, March 22 8:30 - 10:10

CS48: MIMO Beamforming Design and Optimization in future 6G Wireless Systems

T02 Mm-wave for terrestrial networks 5G/6G / Convened Session / Antennas

Room: Alsh 2

Chairs: Paul Zheng (RWTH Aachen University, Germany), Yao Zhu (RWTH Aachen, Germany)

8:30 Beamforming Orthogonality in Coupled Directional Modulation Arrays

Jiayu Hou, Haijun Fan and Yuan Ding (Heriot-Watt University, United Kingdom (Great Britain)); Yue Xiao (University of Electronic Science and Technology of China, China); Symon K. Podilchak (University of Edinburgh, United Kingdom (Great Britain))

This paper studies the orthogonality in a directional modulation (DM) transmitter equipped with an antenna array whose mutual coupling is considered. The antenna coupling will generate backward waves at the power amplifier (PA) outputs. This dynamic interaction will drive the PA load away from the system characteristic impedance thus introducing the load-pulling effect to the system which would result in the distortion to the DM system orthogonality. When the antenna coupling is considered, for a certain target user, the leakage radiation from the information beams designed for other users and from the generated artificial noise would become the interference to this user, and in one example given in this paper, the signal to interference ratios (SIR) of around 20 dB are observed. This compromise of the DM orthogonality would put a performance upper limit to a DM system with coupled antenna array.

8:50 Cooperative Power Control and Beamforming Design for Multi-Source Enabled Wireless Power Transfer Networks

Xiaopeng Yuan, HuanYu Zhang, Paul Zheng and Anke Schmeink (RWTH Aachen University, Germany)

In this paper, we study wireless power transfer (WPT) network with multiple WPT stations and multiple low-power devices. With installed uniform linear antenna array, WPT stations emit independent radio-frequency (RF) signals for cooperatively harvesting all devices. Analog beamforming has been applied for efficiently concentrating the emitted energy. Combining beamforming with multi-source WPT, we characterize out the harvested power for each device based on a practically nonlinear energy harvesting (EH) model. Allowing different beamforming schemes in multiple time slots, we formulate a joint power control and beamforming design problem fairly maximizing the total harvested energy at all devices. To tackle the problem non-convexity, we apply proved convexity in both antenna gain model and nonlinear EH model, and build convex problem approximation, which enables an iterative algorithm efficiently converging to a suboptimal solution. At last, we verify our proposed algorithm and highlight the WPT profits of our proposed solution via numerical results.

9:10 Joint Resource Allocation and Beamforming Design for Secure Short Packet Communication in RIS-Aided MISO Systems

Wei Gao (Wuhan University, China); Cunxiang Wang (Ministry of Industry and Information Technology, China); Jie Wang (School of Electronic Information, Wuhan University, China); Yulin Hu (RWTH Aachen University, Germany)

In this work, we consider the physical-layer security problem in multi-user secure RIS-aided MISO short packet communication systems. To enhance the secrecy transmission rate, a novel Riemannian conjugate gradient (RCG) based joint optimization algorithm is proposed for blocklength, beamforming, and RIS phase shift optimization, while subject to resource limitation, unit norm, and unit modulus constraints. More specifically, we first derive the closed-form expression of blocklength and convert the original problem to a more manageable form, which only involves beamforming and RIS phase design. To address the unit norm and unit modulus constraints, the RCG algorithm is utilized for beamforming and RIS phase shift joint optimization. Numerical results demonstrate that our proposed algorithm outperforms the baseline scheme.

9:30 Joint Wide Illumination and Null Insertion Design in RIS-Assisted System

Xinyi Lin, Ziyi Zhou and Lei Zhang (University of Glasgow, United Kingdom (Great Britain)); Anvar Tukmanov (BT, United Kingdom (Great Britain)); Qammer H Abbasi and Muhammad Ali Imran (University of Glasgow, United Kingdom (Great Britain))

In this paper, we focus on reconfigurable intelligent surface (RIS)-aided wide illumination and null insertion design. This design can be applied in cellular networks, broadcasting, and radar systems, enabling multiple wide null and illumination at arbitrary directions. Our objective is to minimize the deviation between the target and practical pattern by designing the passive beamforming at RIS, while the RIS unit modulus weights constraint is illustrated. To tackle the non-convex problem, the low-complexity alternating direction method of multipliers (ADMM) algorithm is proposed. The augmented objective function is first formulated with introduced auxiliary variables, which is then rephrased as a Lagrangian function. By alternatively updating the variables, the objective function converges with the optimized RIS phase shifts. The convergence of simulation results proves the validity of our proposed algorithm, and the proposed algorithm matches the desired and actual power patterns well under different numbers and sizes of illumination and null areas.

9:50 A Varactor-Based Reconfigurable Intelligent Surface Concept for 5G/6G mm-Wave Applications

Yuqing Zhu, Artem Vilenskiy, Oleg Lupikov and Pavlo Krasov (Chalmers University of Technology, Sweden); Thomas Emanuelsson (Ericsson AB, Sweden); Gregor Lasser and Marianna Ivashina (Chalmers University of Technology, Sweden)

A varactor-based reconfigurable intelligent surface (RIS) concept is presented for low-cost, high-precision beamforming of 5G/6G mm-waves. To enable this, we maximize the RIS unit cell (UC) phase coverage by (i) employing a varactor diode-tuned slotted-patch UC, and (ii) adding a metallic loop and via fence across the UC boundary, which also improves the bandwidth and angular insensitivity. In an infinite RIS environment, the UC exhibits a phase coverage of 330.7 degrees while maintaining the insensitivity of reflection coefficients up to 50-degree elevation angle. This UC design demonstrates a phase coverage that exceeds 315 degrees with under 0.7-dB reflection loss across a 11.6% bandwidth, where the capacitance tuning ratio of the considered commercial off-the-shelf varactor diode is only 1.8. A 15x15 RIS model with a 3-bit phase quantization is used for beam steering performance validation; it predicts the realized gain of 19.5 dBi for the 30-degree beam-steering direction at 28 GHz.

Friday, March 22 8:30 - 10:10

CS15: GigaScale Antenna Arrays for Space based Solar Power

T03 Aerospace, new space and non-terrestrial networks / Convened Session / Antennas

Room: Boisdale 1

Chairs: Xiaodong Chen (Queen Mary University of London, United Kingdom (Great Britain)), Timothy Pelham (University of Bristol, United Kingdom (Great Britain))

8:30 Time-Modulated Arrays for Simultaneous Wireless Information and Power Transfer in Near-Field

Álvaro Pendás-Recondo (University of Oviedo, Spain); Rafael González Ayeararán and Jesús López-Fernández (Universidad de Oviedo, Spain)

A novel approach for enabling Simultaneous Wireless Information and Power Transfer (SWIPT) through Time Modulated Arrays (TMAs) is proposed. The presented system employs a transmitting TMA based on periodic Sum-of-Weighted-Cosine (SWC) pulses with a Single-Sideband (SSB) modulation for maximum power efficiency. Wireless Power Transfer (WPT) is achieved through Near-Field Focus (NFF) of the transmitted array, while Information Transfer (IT) is performed based on Frequency Domain Index Modulation (FDIM). An application example is studied for two users.

8:50 Validation of a Large Retrodirective CASSIOPeIA Solar Power Satellite Antenna Array

Neil Buchanan (Queens University Belfast, United Kingdom (Great Britain)); Yat Hin Chan (Queens University Belfast & ECIT, United Kingdom (Great Britain)); Hossein Mardani and Dmitry E Zelenchuk (Queen's University of Belfast, United Kingdom (Great Britain))

The CASSIOPeIA Solar power satellite (SPS) helix antenna array has been shown to provide a viable concept for the SPS. The important feature of the CASSIOPeIA antenna is that it can provide 360 degrees azimuth electronic beam steering, pointing a highly directional beam, to a rectenna farm on earth. Modelling of the CASSIOPeIA antenna to date has only included setting up pre-defined phase/amplitude distributions across the array. These results are promising but to model the array for retrodirective operation, the phase distributions across the array need to be determined from phase conjugation of a received pilot tone. This mode of operation, to our knowledge, has never been theoretically validated within the triple dipole beam steering configuration of the CASSIOPeIA. In this paper we present the first simulated validation of a 10,000 unit cell (100x100) CASSIOPeIA array as a retrodirective antenna, providing a well-defined steerable main beam and good sidelobe suppression.

9:10 Large and Simple Phased Array System at 28 GHz for Beam Wireless Power Transfer

Naoki Shinohara, Bo Yang and Wenyi Shao (Kyoto University, Japan)

Space-based solar power (SBSP) is envisioned as a future CO₂-free power station in space. One of the critical technologies for SBSP is beam wireless power transfer (WPT). In this paper, we present the development of a new large and straightforward phased array system operating at 28GHz, designed for simultaneous wireless information and power transfer (SWIPT). We believe that SWIPT is a crucial step toward realizing SBSP. This paper introduces the developed phased array, focusing on its applications in SWIPT as a business system and its potential as the primary technology for SBSP, the largest anticipated application of WPT.

9:30 An Overview of Gigascale Antenna Arrays and Electromagnetics for Space Based Solar Power

Timothy Pelham (University of Bristol, United Kingdom (Great Britain)); Xiaodong Chen (Queen Mary University of London, United Kingdom (Great Britain)); Brian S Collins (BSC Associates Ltd & Queen Mary, University of London, United Kingdom (Great Britain)); Clive Parini (Queen Mary University of London, United Kingdom (Great Britain)); Anthony Keith Brown (University of Manchester, United Kingdom (Great Britain))

Gigascale antenna arrays (3 to 4 orders of magnitude more elements than the largest ever built) are a critical component of proposed space-based solar power (SBSP) systems. The transmitting antenna arrays in orbit are expected to be up to 3 km², while the receiving arrays on Earth have been proposed at up to 77 km². There are many challenges and risks in the design, modelling, operation and deployment of the gigascale antenna arrays in the SBSP system. This paper highlights these challenges and risks, reviews existing solution and proposes novel approaches.

9:50 A Digital Beamforming Antenna for Space Based Solar Power Transmitting Array

Long Qian, Jin Zhang, Chao Shu, [Noaman Nasser](#), Brian Collins and Xiaodong Chen (Queen Mary University of London, United Kingdom (Great Britain))

This paper presents a beam-steerable quadrifilar helix antenna (QHA) on an artificial magnetic conductor (AMC) surface for space based solar power application. The AMC surface is composed of 8×8 square unit cells to suppress the surface current. By controlling the input phases to the QHA ports through a digital beamforming circuit, the circular polarized (CP) patterns can be steered within upper half space. To verify the working mechanism, two passive phase feeding networks are employed in the measurement of the proposed QHA at 5.8GHz. The measured results show the proposed antenna can steer the beam from boresight to 26 degree in elevation without dropping the gain, while keeping the sidelobe level to -8.1dB.

Friday, March 22 8:30 - 10:10

CS1a: Advances in Microwave and mmWave Wireless Power Transfer

T04 RF sensing for automotive, security, IoT, and other applications / Convened Session / Antennas

Room: [Boisdale 2](#)

Chairs: Chaoyun Song (King's College London, United Kingdom (Great Britain)), Mahmoud Wagih (University of Glasgow, United Kingdom (Great Britain))

8:30 Microwave to mmWave Wireless Power Transfer: An Overview of the Design Challenges with a Focus on UK-Based R&D

[Mahmoud Wagih](#) (University of Glasgow, United Kingdom (Great Britain)); Chaoyun Song (King's College London, United Kingdom (Great Britain))

Microwave and mmWave wireless power transfer (WPT) continues to attract significant interest. This paper presents an overview of selected UK-based activities in WPT and energy harvesting, and highlights the emerging research trends and future directions, with focus on mmWave power transfer. The justification for mmWave power transfer, fueled by beyond-5G hardware, is first introduced. Rectenna and WPT-specific innovations such as beam-forming, bandwidth enhancement, and frequency scanning are then highlighted. The developments are then reviewed from an application perspective, highlighting the novel material and implementations of rectennas, along with the outstanding research challenges. Quantitative performance comparisons are presented summarizing state-of-the-art rectifiers, rectennas, and antennas.

8:50 Single-Branch Hybrid Resistance Compression Technique for Enhanced Rectifier Performance

Furong Yang (King's College London, United Kingdom (Great Britain)); Apostolos Georgiadis (United Kingdom (Great Britain)); Spyridon Nektarios Daskalakis (Heriot-Watt University, United Kingdom (Great Britain)); Kyriaki Niotaki (Telecom Paris & Institut Polytechnique de Paris, France); Yichao Hu (Imperial College London, United Kingdom (Great Britain)); Jichao Yang (Cornell University, USA); Chaoyun Song (King's College London, United Kingdom (Great Britain))

In this paper, we introduce a novel resistance compression technique which is termed as the Single-branch Hybrid Resistance Compression Technique (SHRCT) aimed at enhancing the performance of rectifiers. While the conventional Resistance Compression Network (RCN) mitigates non-linear impedance variation effects in rectifier circuits, ensuring stable operation under varying input power and load resistance conditions, it typically necessitates at least two branches and consequently multiple surface-mount devices (SMD), resulting in substantial power losses. The introduction of SHRCT revolutionizes resistance compression by eliminating the need for multiple branches, thus reducing the requirement for SMDs, and improving overall efficiency.

9:10 Far-Field Beam Wireless Power Transfer with Combination of Beam Forming and Optical Target Detection

Naoki Shinohara, Bo Yang and Katsumi Kawai (Kyoto University, Japan)

Far-field wireless power transfer (WPT) is an efficient unconscious wireless power system with high efficiency. The present study used optical target-detecting and beam-forming technology to build an unconscious WPT tracking system. The coordinate position of the target is obtained from the image recognition module and transformed into the phase information of the phased array, which transmits microwave waves beyond the target position by controlling the microwave beam. The camera and microcomputer unit are adopted to control the beam in the proposed system. Here, the transmitting array receives the voltage data from the rectenna array via Bluetooth low energy. Then, the transmitting array readjusts the amplitude and the phase. The transmitting system can also adjust the phase with a resolution of 0.09 degree. We showed that a smartphone can be charged at a transmission distance of 40 cm.

9:30 Substrate-Integrated Mode Composite Waveguide

[Chun-Mei Liu](#) (École Polytechnique de Montréal, Canada); Ke Wu (Polytechnique Montréal, Canada)

This work introduces a metallo-dielectric mode-composite waveguide (MCW) architecture, which consists of an inner substrate-integrated non-radiative dielectric (SINRD) waveguide operating in LSM01 mode in a terahertz (THz) band and an outer partially perforated substrate-integrated waveguide (PPSIW) operating in TE10 mode in a millimeter-wave (mmW) band. This arrangement is set to create and optimize two integrated guided-wave structures in both frequency bands, which is believed to exhibit the highest density waveguide integration of this type. SINRD waveguide shows a promising potential in making THz integrated circuits and systems because of its low conductor loss performance. SIW still maintains its advantages in the development of mm-W band circuits and systems. The operating frequency bands of such an aperture-shared SINRD waveguide and PPSIW are independently adjustable. The proposed MCW architecture presents an attractive option for the design of future highly integrated circuits and systems.

9:50 Design of Dual-Band CPW Rectenna for Wireless Power Transmission

Zeyu Liu, [Jingchen Wang](#), Eng Gee Lim and Mark Leach (Xi'an Jiaotong-Liverpool University, China); Zhao Wang (Xi'an Jiaotong Liverpool University & University of Liverpool, China); Yi Huang (University of Liverpool, United Kingdom (Great Britain))

This article features a compact four-port dual-band Co-Planar Waveguide (CPW) rectenna. The two bands (2.3 GHz) and (5.65 GHz) of the proposed antenna are cover the standard Wi-Fi bands (2.412-2.484 GHz) and WLAN bands (5.745-5.825 GHz). The gain of the proposed antenna is 3.72 dBi at 2.4 GHz and 3.73 dBi at 5.8 GHz. A double voltage rectifying circuit with a load of 6.2 kΩ is designed to achieve relatively high power conversion efficiency. When the input power is 0 dBm, the proposed rectifier can achieve RF-to-DC efficiencies of 66% at 2.4 GHz and 58% at 5.8 GHz. The combined output voltage can reach to 10 V, which is suitable for wireless charging in Internet of Things (IoT) applications.

Friday, March 22 8:30 - 10:10

CS12a: AMTA Session: Robotic Antenna Measurements

T05 Positioning, localization, identification & tracking / Convened Session / Measurements

Room: [Carron 1](#)

Chairs: Joshua Gordon (US National Institute of Standards and Technology, USA), Roland Moch (RWTH Aachen University, Germany)

8:30 A High-Precision Approach to Eliminate Positioning Errors in Radar Calibrations

[Matthias Linder](#), Dominik Schwarz, Robin Bord and Nico Riese (Ulm University, Germany); Christian Waldschmidt (University of Ulm, Germany)

To improve the angular separation capability of radar sensors, large apertures with respect to the wavelength are increasingly used. With the help of MIMO operation, even larger virtual apertures than the physical ones are realized. This improvement in performance requires an extremely accurate calibration setup in order to avoid systematic errors and to achieve the best possible performance of the sensor. Thus, robotic arms are increasingly used for accurate characterizations of antennas due to their high position accuracy. In this work, an efficient method for the alignment of radar sensor and radar target is outlined which is within the repeatability range of the robot arm deployed for calibration measurements amounting to only 50 micro meters.

8:50 *Rapid Automated Antenna Alignment on Robotic Antenna Ranges*

[Benjamin L Moser](#) (National Institute of Standards and Technology, USA); [Joshua Gordon](#) (US National Institute of Standards and Technology, USA)

We present methods to automate antenna-probe alignment on a robotic antenna range using iterative fitting methods. Pose measurements are used to characterize offsets to the robot motion frame and the end effector measurement frame with minimal additional information. The fitted offsets are then used to solve the inverse kinematics problem to align the antennas. We detail variations of the approach that use external or controller-integrated kinematic models. Experimental alignments for a 3-pair antenna measurement were performed on the Large Antenna Positioning System (LAPS) robot antenna range with this technique, resulting in 7.59 μm RMS position error and 40.7 μrad RMS rotation error.

9:10 *Characterisation of a D-Band Horn Antenna: Comparison of Near-Field and OTA Measurements*

Asad Husein, Kimmo Rasilainen and Klaus Nevala (University of Oulu, Finland); Jani Kallankari, Sami Laukkanen and Veli-Matti Niemitalo (Verkotan Ltd., Finland); Aarno Pärssinen and Marko E Leinonen (University of Oulu, Finland)

The small wavelength, typically in the range of millimeters to micrometers, makes characterisation of antennas at sub-THz band of frequencies particularly challenging as it requires measurement systems to accurately capture the details of the antenna radiation patterns. Additionally, sub-THz signals experience significant free-space path loss, making it harder to measure radiation patterns accurately over reasonable distances. This paper presents the characterisation of a D-band (110- 170 GHz) horn antenna having nominal gain of 25 dBi using both planar near-field and over-the-air far-field measurement techniques. The E-plane co-polar patterns are determined from both measurement techniques and compared to electromagnetic simulations. Analysis of measured results is carried out to illustrate the validation of the planar near-field and OTA measurement systems at sub-THz frequencies.

9:30 *Use of Model Based Systems Engineering and Development in the Design of a Commercial Nose-Radome Test System Employing a Multi-Axis Cobot*

Stuart F Gregson (Queen Mary, University of London, United Kingdom (Great Britain)); [Dennis Lewis](#) (Boeing, USA); Patrick Schluper and Greg Hindman (Next Phase Measurements, USA)

The move towards antenna measurement ranges employing multi-axis industrial robotic positioners that provide a near limitless degree of flexibility in terms of measurement types and scan geometries complicates design and development tasks. The available flexibility and ability to continuously adapt and refine the acquisitions results in an ongoing need to evaluate each unique setup and application. Model based Systems Engineering and Development (MBSE/MBD) techniques can be employed to dramatically reduce the time, cost, and effort of developing and validating new measurement scenarios. This paper illustrates the use of MBSE in the implementation of a new nose-mounted radome test system employing industrial multi-axis robots. In this novel application, a collaborative robot (Cobot) is used to emulate a classical antenna gimbal, requiring extensive use of MBSE to develop and verify the measurement and control sub-systems.

9:50 *Reduced-Order Maximum Determinant Sampling Grids by Acquisition of Additional Arbitrary Sampling Points on an Optimized Path*

[Henrik Jansen](#), Roland Moch and Dirk Heberling (RWTH Aachen University, Germany)

A maximum determinant sampling grid (MDSG) presents a fully determinant non-redundant sampling grid for spherical near-field antenna measurements which can be efficiently measured using robot-based antenna measurement systems. Although the position of the sampling points is determined by the sampling grid, the sequence of data acquisition can still be optimized to reduce measurement time. A new trajectory optimization approach is proposed which reduces sharp curves in the path at the cost of a longer total path length. It is shown that this approach significantly increases the average path speed and reduces the measurement time for sparse grids compared to an optimization for the shortest path. Furthermore, the acquisition of additional sampling points on the resulting path is investigated, allowing for lower-order MDSGs without sacrificing accuracy of the transformation results. As a result, this combination allows to reduce the measurement time by more than 60 % compared to conventional equiangular measurements.

Friday, March 22 8:30 - 10:10

CS19a: Fundamental challenges and novel methodologies in the next-generation computational electromagnetics

T08 EM modelling and simulation tools / Convened Session / Electromagnetics

Room: Carron 2

Chairs: Zhen Peng (University of Illinois at Urbana-Champaign, USA), Francesca Vipiana (Politecnico di Torino, Italy)

8:30 *The d'Alembertian Representation of Green's Functions and Evaluation of Surface Integrals over Non-Parallel Planes*

Elizabeth Bleszynski (Monopole Researach, USA); Marek Bleszynski (Monopole Researach, USA); Thomas Jaroszewicz (Monopole Research, USA)

We present progress in analytic evaluation, in the static limit, of matrix elements of electromagnetic operators for the RWG basis functions located on non-coplanar planes. Our method employs the previously reported d'Alembertian representation of Green's function g , such that a certain d'Alembert-type operator, when acting on an auxiliary function Φ , reproduces g . Integration by parts allows then converting four-fold surface integrals to double integrals of Π (which turns out to be a fairly simple expression involving only elementary functions) over perimeters of the triangles. Here we describe our ongoing work on two approaches reducing the latter double integral to a single numerical integral.

8:50 *Surface Partial Differential Equations and Its Applications to Scattering Problems*

Felipe Vico (Universidad Politécnica de Valencia, Spain); Miguel Ferrando-Bataller and Eva Antonino-Daviu (Universitat Politècnica de València, Spain); Marta Cabedo-Fabrés (Universidad Politécnica de Valencia, Spain)

Curved spaces, such as surfaces, provide a rich setting for the study of partial differential equations (PDEs). Building upon the extensive research conducted on PDEs in flat spaces, the extension of these equations to curved spaces has garnered considerable attention in the field of mathematics. One prominent example is the Laplace Beltrami equation. In this work, we employ efficient direct solvers to obtain solutions for PDEs on surfaces and demonstrate their applicability in solving conventional electromagnetic scattering problems.

9:10 *Modal Analysis of Thermal Noise from Lossy Dielectric Medium*

Jean Cavillot (Université Catholique de Louvain (UCL), Belgium); Denis Tihon (Université Catholique de Louvain, Belgium); Eloy de Lera Acedo (University of Cambridge, United Kingdom (Great Britain)); Christophe Craeye (Université Catholique de Louvain, Belgium)

The modal characterization of the thermal noise generated by lossy dielectric media can be used to improve the design of antenna arrays and improve the overall system performance. In this paper we study the thermal noise generated above a circular ground plane by a lossy semi-infinite medium. To do so, we consider an array of infinitesimal dipoles above the ground plane. The fields generated by the dipoles in presence of the finite ground plane are computed using the Method of Moments and used to compute the power dissipated by the dielectric medium. Combining the fluctuation-dissipation theorem to Lorentz reciprocity, the noise correlation matrix at the location of the dipoles is obtained. Using this matrix, we apply the eigenmode decomposition to obtain a modal representation of the noise. We show that increasing the size of the ground plane decreases the noise power and increases its coherence, potentially facilitating its filtering.

9:30 *Combined Ray-Tracing and Physical-Optics Model for Flat-Aperture PPW Lens Antennas*

Mingzheng Chen (KTH Royal Institute of Technology, Sweden); Francisco Mesa (University of Seville, Spain); Oscar Quevedo-Teruel (KTH Royal Institute of Technology, Sweden)

This paper proposes a combined ray-tracing and physical-optics model to analyze parallel-plate-waveguide lens antennas with a flat aperture. A family of rays is traced from the source to a set of target points on the lens radiating aperture, giving a description of the aperture electric field. On the basis of the physical-optics approximation, an equivalent magnetic current is then assumed and used to evaluate the far-field radiation characteristics in every direction. This numerical approach is validated by applying it to a particular planar Mikaelian lens antenna and comparing the results with those obtained using a commercial full-wave simulator.

9:50 Platform-Aware Optimization of Conformal Antenna Array via Simulated Bifurcation

Qi Jian Lim (University of Illinois Urbana-Champaign, USA); Incheol Jung (University of Illinois at Urbana-Champaign, USA); Hong-Wei Gao (Beijing Institute of Technology, China); Zhen Peng (University of Illinois at Urbana-Champaign, USA)

In this paper, we introduce a platform-aware, quantum-inspired optimization framework for large conformal antenna arrays. The proposed work starts with the calculation of element-wise radiation vectors by leveraging recent advances in the domain decomposition method and reduced order model. Subsequently, we introduce a modified Simulated Bifurcation algorithm, which is capable of finding the optimal excitation vector of a large-scale array within 10 to 50 milliseconds. To illustrate the effectiveness of our methodology, we demonstrate its performance across various array synthesis and optimization scenarios, including array thinning for planar antenna arrays, maximum gain optimization with conformal arrays, and enabling multiple beamforming capabilities on large platforms.

Friday, March 22 8:30 - 10:10

SW6a: Recent advances in antenna measurement traceability and uncertainty at reduced distances

Room: Dochart 1

Chairs: Dennis Lewis (Boeing, USA), Janet O'Neil (ETS-Lindgren, USA)

8:30 Real World Challenges with Antenna Calibration in Industry

Presenter: Dennis Lewis (Boeing, USA)

9:15 Evaluation/Comparison of Post Processing Techniques for Antenna Gain Extrapolation Measurements

Presenter: Zhong Chen (ETS-Lindgren, USA)

Friday, March 22 8:30 - 10:10

CS26a: COST Session CA18223 (SyMat) Modeling and Applications of Higher Symmetries

T08 EM modelling and simulation tools / Convened Session / Antennas

Room: Dochart 2

Chairs: Sara Mugnaini (OneWeb Communication Ltd, United Kingdom (Great Britain)), Eva Rajo-Iglesias (University Carlos III of Madrid, Spain)

8:30 Glide-Symmetric SIH Unit Cells Implemented in Parallel-Plate Waveguides at mmWaves

[Andrés Biedma-Pérez](#) and Cleofás Segura-Gómez (University of Granada, Spain); Angel Palomares-Caballero (IETR-INSA Rennes, France); Juan Valenzuela-Valdés (Universidad de Granada, Spain); Pablo Padilla (University of Granada, Spain)

This work studies the behaviours of unit cells based on substrate integrated holes (SIH) in parallel-plate waveguides (PPW). The basic SIH unit cell has been improved through the incorporation of a metallic patch. A comparison between the perfect dielectric hollow with patch unit cell and a SIH with patch unit cell has been carried out. The unit cell dimensions are used to study the different effective refractive indices. High order symmetries as a means to control dispersion and effective refractive indices are also introduced. By applying glide symmetry on different planes, we aim to enhance the effective refractive index and reduce dispersion across different frequency ranges. It is demonstrated that 1D glide-symmetric configurations reduce dispersion at higher frequencies, while 2D glide-symmetric configurations are able to reduce dispersion at high frequencies and also, to increase the effective refractive index simultaneously.

8:50 On the Use of Resonant Cavities for Experimental Validation of the Dispersion Diagram of Periodic Glide Symmetric Waveguides

Nelson Castro (University Carlos III of Madrid, Spain); Miguel Saavedra-Melo and Filippo Capolino (University of California, Irvine, USA); Eva Rajo-Iglesias (University Carlos III of Madrid, Spain)

This article presents a discussion on the synthetic technique to experimentally determine the wavenumber dispersion diagram of modes in periodic waveguides with glide symmetry. The method involves reconstructing the dispersion diagram using resonance frequencies obtained from a cavity created from the waveguide. The variation in the number of resonances required for periodic structures with glide symmetry, in contrast to the non-glide scenario, is the main topic of exploration. We also verify the proposed modification of the method through simulations involving an ideal cavity.

9:10 Higher Symmetries in Hexagonal Periodic Structures

[Oskar Zetterstrom](#) (KTH Royal Institute of Technology, Sweden); Francisco Mesa (University of Seville, Spain); Oscar Quevedo-Teruel (KTH Royal Institute of Technology, Sweden)

We study higher-symmetric periodic structures with hexagonal lattice arrangement. We define three ways to synthesize a glide symmetry in a hexagonal lattice. If the periodic motifs have sufficient symmetry, the three resulting structures are related through a rotation. Furthermore, we define two ways of synthesizing a mirrored half-turn symmetry in a hexagonal lattice. Again, if the periodic motifs have sufficient symmetry, the two resulting structures are related through a rotation. We analyze a structure with mirrored half-turn symmetry and compare its response to that of a periodic structure with conventional hexagonal symmetry. The mirrored half-turn-symmetric structure provides a higher effective refractive index for the same geometrical dimensional. As a result, the higher-symmetric structure is useful for devices in future wireless applications.

9:30 Wiener-Hopf Type Analysis of PTD Symmetric Waveguides: A Novel Methodology Procedure

[Xenofon Mitsalas](#), Enrica Martini and Stefano Maci (University of Siena, Italy)

The current paper analyses the wave propagation and excitation mechanisms on parity time-reversal duality (PTD) symmetric waveguide structures on the basis of the Wiener-Hopf technique. It aims to propose an efficient procedure for investigating complex PTD symmetric structures in the spectral domain, covering both planar and cylindrical configurations. The adopted formulation enables the physical interpretation of solution regarding field components and potential functions.

9:50 Efficient Numerical Computation of Dispersion Diagrams for Glide-Symmetric Periodic Structures with a Hexagonal Lattice

Martin Petek (Politecnico di Torino, Italy & KTH Royal Institute of Technology, Sweden); Jorge A. Tobon Vasquez (Politecnico di Torino, Italy); Guido Valerio (Sorbonne Université, France); Francisco Mesa (University of Seville, Spain); Oscar Quevedo-Teruel (KTH Royal Institute of Technology, Sweden); Francesca Vipiana (Politecnico di Torino, Italy)

In this work, we present a modeling methodology to solve the eigenvalue problem for periodic structures with a hexagonal lattice. The method is based on the previously proposed multi-modal transfer matrix method, which is a hybrid method that takes into account the coupling between the multiple modes of the ports surrounding the single unit cell. Commercial software can be used to obtain the generalized scattering parameters which are used to solve the eigenvalue problem of the periodic structure. This approach has the ability to obtain complex solutions. Here, we extend the multimodal transfer matrix method to the efficient solution of the resulting eigenvalue problem for the case of a hexagonal lattice, detailing the selection of the appropriate supercells and the appropriate irreducible Brillouin zones. Two types of structures are analyzed: a mirror-symmetric structure and a glide-symmetric structure. Very good agreement is obtained for real solutions with commercial software.

Friday, March 22 8:30 - 10:10

A15a: Developments in antenna arrays

T08 EM modelling and simulation tools // Antennas

Room: M2

Chairs: Yanki Aslan (Delft University of Technology, The Netherlands), Christopher G Hynes (Simon Fraser University, Canada)

8:30 *Multiple-User Full-Duplex Hybrid Beamforming Design for mmWave Systems with A Joint Interference Cancellation Design*

Xinping Xia, Jianing Zhao, Xuenan Ni, Yunfei Wang and Jianyi Zhou (Southeast University, China)

With the continuous growth of capacity demand, millimeter-wave (mmWave) massive multiple-input multiple-output (MIMO) systems have been considered as one of the primary research focuses of the next sixth generation (6G) wireless communication networks. Full-duplex (FD) technology can further enhance the capacity of mmWave massive MIMO systems. However, the strong self-interference (SI) and inter-user interference (IUI) severely limit the performance of multiple-user (MU) FD mmWave massive MIMO systems. In this paper, a hybrid beamforming (HBF) scheme with joint optimization is proposed for MU FD mmWave massive MIMO systems. The Lagrange multiplier method is adopted to minimize the interference energy. Then, considering the power consumption problem of massive MIMO systems at the base station (BS), the beamforming matrixes are decomposed into analog and digital parts based on the manifold optimization-alternating minimization (MO-AltMin) algorithm. Simulation results show that the proposed system has made good achievements in interference cancellation.

8:50 *Extending Spectral Factorization to the 2-D Mask-Constrained Power Synthesis of Shaped Beams with Arbitrary Footprints*

Giada Maria Battaglia (Università Mediterranea di Reggio Calabria, Italy); Andrea Francesco Morabito (University Mediterranea di Reggio Calabria, Italy); Roberta Palmeri (IREA-CNR, Napoli, Italy); Tommaso Isernia (University of Reggio Calabria, Italy)

A new method is proposed for the mask-constrained power synthesis of planar sources and exemplified for antenna arrays. In particular, by resorting to recent results achieved in the Phase Retrieval of radiated power patterns exploiting only one measurement surface, we extend the Spectral Factorization method to the case of 2-D shaped beams having arbitrary footprints. The presented method is fast and effective as it avoids exploiting global optimization algorithms, and it also allows identifying the minimum number of array elements (i.e., the minimum source size) required in order to fulfill the 2-D power-pattern mask.

9:10 *Impact of Deformations on Beamforming Performance of Uniform Rectangular Arrays*

Jiahao Wang and Koen Mouthaan (National University of Singapore, Singapore)

Phased arrays often use a uniform rectangular array (URA) with phasing of the elements. In large phased arrays, deformations may occur due to fabrication tolerances and other influences, which will cause errors in the position of the antenna elements. The impact of such errors on the antenna pattern can be analyzed by sampling the distribution of the deformations and computing the mean radiation pattern (MRP). However, this will be time-consuming when the number of elements is large and it will not give much insight into the impact of the deformations. Here, an analytical expression is presented for the MRP of a deformed URA considering different distributions of the deformation in x , y , and z including uniform distribution, normal distribution, and triangular distribution. The analytical expression is further used to investigate the impact of the deformation on the pattern and the gain of the array under different distributions.

9:30 *Beamforming Optimization for Full-Duplex Relay in SIC-Enhanced Cooperative NOMA System*

Xuenan Ni, Jianing Zhao, Xiaoying Zhang, Xinping Xia and Jianyi Zhou (Southeast University, China)

In this paper, a beamforming optimization method for a full-duplex relay in a SIC-enhanced cooperative non-orthogonal multiple access (NOMA) system is proposed, in which the information contained in the signal transferred by the relay is utilized to enhance the successive interference cancellation (SIC) performance at the local "target user". The beamforming optimization problem is considered in a specific scenario that involves maximizing the rate of the target user while only ensuring the business requirements of the remote "conditional user". This paper demonstrates that this optimization problem can be formulated as a semidefinite relaxation (SDR) problem. The results indicate that the proposed beamforming optimization method can enhance the rate of the target user and the system sum capacity.

9:50 *Tapering Impact on the Spatial and Frequency Responses of Broadband Asymmetrically Routed Phased Arrays*

Duccio Delfino, Nuutti Tervo, Muhammad Yasir Javed, Marko E Leinonen and Aarno Pärssinen (University of Oulu, Finland)

Asymmetrical feeding networks can be used to amplify the beam squint phenomena of the phased arrays and to make their frequency domain behavior very angle-dependent. The aim of this paper is to demonstrate the analogy between the far field of a side-fed uniform linear array (ULA) and its frequency response in the beam steering direction. Indeed, by using simplified array equations, we show that the beam pattern of an asymmetrical series-fed ULA is similar to the frequency response observed at the steering angle. Furthermore, we show that amplitude tapering which is used to reduce the sidelobe level (SLL) of the array also reduces the corresponding sidebands of the frequency response in the given steering angle, to facilitate frequency domain filtering. Moreover, a modified tapering method is introduced to showcase the generality of the analysis.

Friday, March 22 8:30 - 10:10

SW8a: Waveguide Antenna Array Technologies for Space and Beyond

Room: M3

Chairs: Nelson Fonseca (Anywaves, France), Yi Wang (University of Birmingham, United Kingdom (Great Britain))

8:30 *Welcome Introduction*

Presenter: Yi Wang (The University of Birmingham, UK)

8:35 *Waveguide Slot Array Antennas by Diffusion Bonding of Laminated Thin Plates*

Presenter: Jiro Hirokawa (Tokyo Institute of Technology, Japan)

9:05 *Gap Waveguide Technology for mm-Wave Antennas*

Presenter: Ashraf Uz Zaman (Chalmers University of Technology, Sweden)

9:35 *Design and Development of Full-Metal Planar Array Antennas*

Presenter: Jifu Huang (Ningbo University, China)

Friday, March 22 8:30 - 10:10

CS14a: Shape-morphing metamaterials, antennas and electromagnetic components

T10 Novel materials, metamaterials, metasurfaces and manufacturing processes / Convened Session / Electromagnetics

Room: M4

Chairs: Alex W Powell (University of Exeter, United Kingdom (Great Britain)), Christopher Stevens (University of Oxford, United Kingdom (Great Britain))

8:30 Enabling Shape Morphing Communications at mmWave with Spray on Antenna Arrays

Rola Saad (The University of Sheffield, United Kingdom (Great Britain)); Benedict EG Davies and Stephen Henthorn (University of Sheffield, United Kingdom (Great Britain))

Flexible and shape-morphing antennas have increasing applications in soft robotics and future factories, but fabricating them at mmWave frequencies for high throughput is a challenge, especially as higher gain is often required to overcome pathloss. Aerosol Jet Printing (AJP) has been used to produce two different designs of mmWave antennas on different flexible substrates. The designs are simulated, fabricated and measured, demonstrating simulated gains of 8.4dBi and 5.3dBi on Rogers and Kapton, respectively. When flexed, the design on polyimide showed 20% change in operating frequency.

8:50 Ambient Pressure Responsive Shape-Morphing Electromagnetic Components

Alex W Powell (University of Exeter, United Kingdom (Great Britain))

This work presents the concept of active electromagnetic components whose response is driven by a new class of shape-morphing materials, which dramatically reconfigure their geometry in response to changes in the ambient pressure of their environment. We discuss, and experimentally demonstrate examples of these components including deployable antennas and wireless, battery free ambient pressure sensors. This principle can be used to design soft, deployable components for applications that will experience large pressure gradients, such as satellites, underwater vehicles and pressurized tanks and pipes.

9:10 Hybrid Reconfigurable Reflective Metasurface with Both Phase and Space Modulation

Kyoungwan Kim and Ratanak Phon (Chung-Ang University, Korea (South)); Park Eiyong (University of Chung-Ang, Korea (South)); Sungjoon Lim (Chung-Ang University, Korea (South))

Reconfigurable reflective metasurfaces offer diverse functionalities to manipulate the incident electromagnetic waves. They generally employ phase modulation using positive-intrinsic-negative diodes to achieve beam steering functions. With only phase modulation, however, the metasurfaces can only reflect the beams to discrete angles that are determined by the size of the unit cell. In this work, we propose a hybrid reconfigurable reflective metasurface using both phase and space modulation for a reflection enhancement. We theoretically and numerically demonstrated the function, and experimentally verified it using a 4D printed structure for space modulation. The metasurface is expected to be used in 5G/6G indoor wireless communications as an intelligent reflecting surface.

9:30 Optimal Morphing Metasurface Lens for Next Generation RF Sensing and Communications

Aakash Bansal (Loughborough University, United Kingdom (Great Britain)); Robert Hewson and Matthew Santer (Imperial College London, United Kingdom (Great Britain)); William Whittow (Loughborough University, United Kingdom (Great Britain))

This paper introduces a new intelligent 3D metasurface with mechanical morphing abilities to act as an RF beam-steering lens and manipulate electromagnetic (EM) waves for applications in RF sensing and communications. The mechanical metasurface can be controlled using low-power actuators on the sides to deform the surface and mechanically move the lens structure. The metasurface is fed with a horn antenna and the mechanical movement of the lens with respect to the horn feed provides a beam-steering function. In this paper, a beam-steering of $\pm 30^\circ$ is achieved within simulations with a mechanical movement of ± 40 mm. Furthermore, the 1D lens created using the shape morphing metasurface offers a gain enhancement of approximately 8 dBi throughout the frequency band.

9:50 Time-Modulated Metasurface for Harmonic Signals Frequency Conversion

Tanguy Lopez (ONERA & LEME, France); Thomas Lepetit (ONERA, France); Badreddine Ratni (Univ Paris Nanterre, France); Shah Nawaz Burokur (LEME, France)

Radar stealth relies on various deception and camouflage strategies. However, at the lower frequencies used by long-range surveillance systems, there are still very few functional strategies. The emergence of metasurfaces fortunately brought hopeful new horizons to this issue. In parallel, thanks to the integration of time-based elements, metasurface research has reached new heights in the last few years. One subsequent feature of particular interest in this work is the frequency shifting of waves granted by time modulation. In radar stealth context, such mechanism can be harnessed to serve Doppler cloaking strategies. By compensating the Doppler shift induced by the target's movement, one can tamper with velocity readings. This work therefore focuses on the development of a frequency-converting metasurface, evaluating its frequency shifting abilities along with some undesired effects, notably induced by incomplete phase variations and the use of varactor diodes and their parasitic resistive elements.

Friday, March 22 8:30 - 10:10

RoE: RoE meeting

//

Room: Fyne

Friday, March 22 10:40 - 12:20

SW10b: Sub-Terahertz Antenna and Packaging Solutions for Future Radar and Wireless Communication (continued)

Room: Lomond Auditorium

Chairs: Akanksha Bhutani (Karlsruhe Institute of Technology, Germany), Matthias Wietstruck (IHP, Germany)

10:40 Antennas and Systems at Sub-THz Frequencies for Space Applications

Presenter: Goutam Chattopadhyay (NASA's Jet Propulsion Laboratory)

11:30 Silicon-Micromachined THz Antennas and Systems

Joachim Oberhammer (KTH Royal Institute of Technology)

Friday, March 22 10:40 - 12:20

CS30b: Approaching optimal performance through automated design techniques (continued)

T08 EM modelling and simulation tools / Convened Session / Antennas

Room: M1

Chairs: Miloslav Capek (Czech Technical University in Prague, Czech Republic), Johan Lundgren (Lund University, Sweden)

10:40 Overview of State-Of-The-Art Methods for Determining Performance Bounds on Electromagnetic Systems

Kurt Schab (Santa Clara University, USA); Miloslav Capek and Lukas Jelinek (Czech Technical University in Prague, Czech Republic); Johan Lundgren and Mats Gustafsson (Lund University, Sweden)

Motivations for studying physical bounds in electromagnetics are reviewed, with emphasis on applications involving the assessment of automated (inverse) design algorithms. Details are given for two broad classes of commonly used bounds: those based on sum-rules and those based on single-frequency source-based optimization. Applications in inverse design and open problems are discussed.

11:00 Fundamental Limits on Characteristic Modes

Mats Gustafsson (Lund University, Sweden); Miloslav Capek and Lukas Jelinek (Czech Technical University in Prague, Czech Republic); Johan Lundgren (Lund University, Sweden); Kurt Schab (Santa Clara University, USA)

Characteristic modes (CM) is a powerful technique to analyze and design antennas and scatterers. In this paper, we show how the slope of characteristic eigenvalue traces is constrained for all possible designs that fit within a given design region. The results are based on reformulating the frequency derivative of the CM eigenvalues as an optimization problem over the current density in the design region. The results show that the slope of the eigenvalues are constrained similar to antenna Q-factors. They also show that resonances must be approached from the capacitive side for electrically small to medium-sized objects.

11:20 Automated Design and Characterization of a Scalar Metasurface Antenna Radiating a Linearly-Polarized Broadside Beam

Marcello Zucchi (Politecnico di Torino, Italy); Andrea Scarabosio (LINKS Foundation, Italy); Francesco Verni (Huawei Technologies, Italy); Lucia Teodorani (Politecnico di Torino, Italy); Giorgio Giordanengo (LINKS Foundation, Italy); Giuseppe Vecchi (Politecnico di Torino, Italy)

We present the automated design of a broadside-radiating, linearly-polarized metasurface antenna. The design is carried out with a numerical optimization procedure based on the equivalent surface current only. A non-linear conjugate gradient algorithm is applied to minimize an objective function that includes both realizability and far field requirements. A suitable configuration of circular unit cells, chosen from a database of precomputed shapes, is then used to implement the antenna. The proposed antenna has a diameter $\approx 12\lambda$, working at a frequency of 23 GHz. The obtained design has been validated with commercial software simulations, then prototyped and tested.

11:40 Port Generation for Multi-Mode Multi-Port Antennas Based on Group Theory

Lukas Warkentin (Leibniz University Hannover, Germany); Dirk Manteuffel (University of Hannover, Germany)

A port generation method for Multi-Mode Multi-Port Antennas is explained with focus on easy feasibility. This port generation method uses the symmetry of a given antenna structure. With this method it is possible to create the maximum number of uncorrelated antenna ports. As an example, port configurations for a cuboidal antenna are calculated.

12:00 Optimization of Loads for Antenna-Based Scattering Systems Using Feedforward Neural Networks

Aleksandr D. Kuznetsov and Jari Holopainen (Aalto University, Finland); Ville Viikari (Aalto University & School of Electrical Engineering, Finland)

In this paper, we optimize the passive loads of a scattering system consisting of multiple coupled antennas using multi-layer feedforward neural networks. The developed in this study architectures, trained to solve a classification task, predict the load impedance values connected to unit antenna scatterers based on the bistatic radar cross-section of a structure. Trained networks exhibit potential in optimizing load values for scattering redirection among predefined directions. To demonstrate the applicability of the proposed method, two multi-layer feedforward neural networks are trained and used to predict proper load impedances for different scattering objectives. Additionally, existing limitations of the method usage are discussed with the potential ways to mitigate them.

Friday, March 22 10:40 - 12:20

CS43b: COST-INTERACT, Propagation Measurement and Modelling for 6G and Beyond (continued)

T01 Sub-6 GHz for terrestrial networks (5G/6G) / Convened Session / Propagation

Room: Alsh 1

Chairs: Xuesong Cai (Lund University, Sweden), Golsa Ghiaasi (Silicon Austria Lab, Austria), Richard Rudd (Plum Consulting Ltd, United Kingdom (Great Britain))

10:40 Channel Measurements and Characterization in Industrial Environment at 60 GHz

Jiri Blumenstein (Brno University of Technology, Czech Republic); Josef Vychodil (Brno University of Technology & BUT Brno, Czech Republic); Radek Zavorka, Jan Bolcek and Malek Abdulmalek Ali (Brno University of Technology, Czech Republic); Golsa Ghiaasi (Silicon Austria Lab, Austria); Roman Marsalek (Brno University of Technology, Czech Republic)

This paper presents novel channel sounding and parametrization campaign outcomes in terms of both Doppler and delay statistics. The utilized frequency band is centered at 60 GHz with a 500 MHz of bandwidth. The experimentation is conducted within an industrial setting featuring a substantial presence of highly reflective metallic surfaces. We utilize our developed Orthogonal time-frequency space (OTFS)-based channel sounder/communication device. The presented sounding campaign encompasses a range of diverse human activities conducted during the measurement procedures

11:00 Comparison of Sub-THz Radio Channel Characteristics at 158 GHz and 300 GHz in a Shopping Mall Scenario

Alper Schultze, Mathis Schmieder, Ramez Askar and Michael Peter (Fraunhofer Institute for Telecommunications, Heinrich Hertz Institute, Germany); Wilhelm Keusgen (Technische Universität Berlin, Germany); Taro Eichler (Rohde & Schwarz, Germany)

This paper compares the sub-THz radio channel characteristics at 158 GHz and 300 GHz in a shopping mall scenario by extracting three different path loss models and various channel parameters. The path loss models extracted are two single frequency models, that include the close-in (CI) and floating-intercept (FI) model, and the alpha-beta-gamma (ABG) model being a multi frequency model. The extracted channel parameters include K-factor, delay spread and angular spread. The extraction of mentioned models and parameters is based on two measurement campaigns executed at the mentioned center frequencies in the same shopping mall like environment with a time-domain correlative channel sounder. The subsequent comparison gives an assessment on the extracted path loss models and the multipath behaviour of the sub-THz radio channel. The paper presents for the first time a comparison between a D-band and H/J-band channel measurements taken both in the same shopping mall environment.

11:20 Machine Learning Approach to Delay Spread Estimation in Industrial Environments

Mohammad Hossein zadeh, Simone Del Prete, Franco Fuschini, Marina Barbiroli, Enrico M. Vitucci and Vittorio Degli-Esposti (University of Bologna, Italy)

Delay spread is a measure of the multipath characteristics of the wireless channel and predicting it is very important as the time dispersion of the wireless channel leads to intersymbol interference and thus signal distortion. Existing models dealing with delay spread estimation are basically lacking in flexibility, as they tackle specific deterministic cases. In this work, a flexible approach machine learning tool for the assessment of delay spread values in an industrial environment is presented. The model is tailored to the industrial environment characterized by few macro-parameters, where wireless technologies have been gaining increasing importance in the development of next-generation smart factories. Machine learning is leveraged to get flexibility and fast predictions, i.e. to evaluate the delay spread value based on the geometry of the environment. Results show good performance and confirm the overall physical soundness of the tool.

11:40 A Study on Satellite-To-Ground Propagation in Urban Environment

Nicolò Cenni, Vittorio Degli-Esposti, Enrico M. Vitucci, Franco Fuschini and Marina Barbiroli (University of Bologna, Italy)

Non-Terrestrial Networks are going to play an important role in future 6G wireless networks as they can enhance global connectivity in cooperation with terrestrial networks. In order to properly design and deploy non-terrestrial networks, the satellite-to-ground channel must be properly characterized, with particular focus on the urban environment. This paper uses a Ray-Tracing simulation tool to analyze the primary propagation mechanisms and the behaviour of the Rician K-factor as a function of satellite position in a reference urban environment. Non-specular reflection due to surface irregularities emerges as a primary propagation

mechanism in non-line-of-sight cases. Additionally, the Rician K-factor shows a slight increase with the elevation angle, in contrast with previous studies.

12:00 *Experimental Analysis of Physical Interacting Objects of a Building at mmWave Frequencies*

Hedieh Khosravi, Xuesong Cai and Fredrik Tufvesson (Lund University, Sweden)

The evolution of multipath components (MPCs) in real radio channels is crucial for channel characterization, modeling, and multipath-assisted positioning. This paper provides an experimental analysis at millimeter wave (mmWave) frequencies of the behavior of MPCs originating from a standard building facade. Using a high resolution channel parameter estimation method, clustering, and tracking, we identify physical interacting points and analyze the lifetime and number of trackable MPCs. Our findings shed light on reflection patterns from standard building elements, highlighting the significant impact of these elements on mmWave propagation modeling and positioning accuracy. The building wall under study is shown to have many distributed distinct backscattering points due to the windows highlighting the importance of including those in channel models and ray tracing simulations.

Friday, March 22 10:40 - 12:20

A26: Reconfigurable Intelligent Surface (RIS) technologies

T10 Novel materials, metamaterials, metasurfaces and manufacturing processes // Antennas

Room: Alsh 2

Chairs: Julien de Rosny (CNRS, ESPCI Paris, PSL Research University, France), Raafat R. Mansour (University of Waterloo, Canada)

10:40 *An Electromagnetic-Compliant Scattering Model for Reconfigurable Intelligent Surfaces*

Hussein Ezzeddine (ESPCI Paris & Institut Langevin, France); Abdelwaheb Ourir (Institut Langevin ESPCI Paris CNRS, France); Julien de Rosny (CNRS, ESPCI Paris, PSL Research University, France)

This paper presents the development of a novel communication model for reconfigurable intelligent surface (RIS)-assisted wireless systems, utilizing a 2D formulation of electromagnetic (EM) fields based on Green's theorem. The proposed 2D model is both simple and accurate, adhering to the laws of electromagnetism for the generation, propagation, and scattering of EM fields. Specifically, we establish a direct relationship between the scattered field and the current and impedance of the scattering antenna, resulting in a tractable expression for the total field scattered by the RIS. Moreover, our model successfully explains and analyzes the various diffraction orders present in the scattered field. Through this analysis, we derive an analytical model that predicts and elucidates the different diffraction order components, including the central and replica components. The presented communication model offers valuable insights and predictions for RIS-assisted wireless systems, paving the way for improved system design and performance optimization.

11:00 *A Wideband Dual-Polarized 1-Bit Unit Cell for Reconfigurable Intelligent Surface Applications*

Jalaledin Tayebpour and Raafat R. Mansour (University of Waterloo, Canada)

In this paper, a wideband 1-bit dual-polarized unit cell has been presented at Ku-band. It comprises three substrates and four metallic layers. The proposed structure uses polarization conversion technique, and out of phase characteristic of electric field in patch dominant mode to get two phase states. Using this characteristic provides the proposed structure with considerable bandwidth and accurate phase difference between two states. Two PIN diodes are used as switches for two phase states. Activating one diode for each state results in the conversion of x-polarized to y-polarized (and vice versa) incident wave with a 180° phase difference between the two states. Notably, only one control voltage suffices for both diodes, simplifying the design of the control system. The proposed structure has been simulated using CST software. Numerical results show good matching and 180°±2° phase difference between two states from 11.2 GHz -14.2 GHz with 25 % relative bandwidth.

11:20 *Non-Volatile Memristor-Based 1-Bit Reconfigurable Intelligent Surface Towards a Greener 6G*

Mohamed Elsaid Ghatas (INESCTEC and Faculty of Engineering, University of Porto, Portugal); Luis M. Pessoa (INESC TEC & Faculty of Engineering, University of Porto, Portugal)

Reconfigurable Intelligent Surfaces (RISs) are in significant focus within 6G research. However, RISs face a power consumption challenge in the reconfigurable elements which may restrict its future scale-up to large areas. We address this issue by proposing a unit cell based on a non-volatile memristor-based switching mechanism. A 1-bit memristor-based reconfigurable RIS unit cell was designed in the Ka-band, and validated using CST and HFSS simulation platforms. The required control circuit to enable the digital control of the memristor has also been proposed. The proposed unit cell achieves losses of less than 1 dB over a frequency band of 25 - 28.3 GHz and a phase difference of 180° ± 20° at a central frequency of 26.7 GHz, with an operational bandwidth of approximately 1 GHz. Furthermore, an exemplary 8x8 RIS was designed and simulated based on the proposed unit cell to demonstrate its capability to achieve beam steering.

11:40 *1-Bit Graphene-Based Reconfigurable Intelligent Surface Design in Ka-Band*

Sofia Inacio (INESC TEC, Portugal); Luis M. Pessoa (INESC TEC & Faculty of Engineering, University of Porto, Portugal)

This paper presents a 1-bit graphene-based reflective reconfigurable intelligent surface (RIS), namely a reflectarray antenna, that operates in the Ka-band (27-31GHz). The reflectarray unit-cell features a simple structure with one metal layer, a Rogers RT5880 substrate and a Graphene Sandwich Structure (GSS) on top. The GSS comprises two layers of graphene separated by a diaphragm paper and a PVC layer to enhance its durability. The reflectarray can ensure a 1-bit phase shift resolution, by alternating the bias voltage applied to the graphene. The unit-cell simulation shows that the losses are around 3dB over the studied band for both unit-cell states. An equivalent lumped circuit model is also presented to facilitate the analysis and design of GSS-based unit-cells. The full-wave simulation results of a 32x32 reflectarray indicate a gain of 25dBi for a steering angle of 10deg., displaying a 1dB gain bandwidth of 15%, confirming the promise of the graphene-based elements.

12:00 *Improved Performance of a 1-Bit RIS by Using Two Switches per Bit Implementation*

Fábio Martinho Cardoso (Iscte - Instituto Universitário de Lisboa & Instituto de Telecomunicações, Portugal); Sergio Matos (ISCTE-IUL / Instituto de Telecomunicações, Portugal); Luis M. Pessoa (INESC TEC & Faculty of Engineering, University of Porto, Portugal); Antonio Clemente (CEA-Leti, France); Jorge R. Costa (Instituto de Telecomunicações / ISCTE-IUL, Portugal); Carlos A. Fernandes (Instituto de Telecomunicações, Instituto Superior Técnico, Portugal); Joao M. Felício (Escola Naval, Portugal & CINAV - Instituto de Telecomunicações, Portugal)

Reconfigurable Intelligent Surfaces (RIS) are an enabling technology widely investigated towards 6G. The viability of large active metasurfaces is constrained by the RF performance, cost, and power consumption. The number of switches per unit cell is a key design parameter that designers aim to minimize following cost and power consumption drivers. However, an efficient use of the aperture is ultimately required and although a one-to-one correspondence between number of switches and phase-quantization bits seems intuitive, one may question its impact. Here we present a full-wave evaluation of a 30x30 1-bit reflective RIS, implemented considering two pin diodes per unit cell. The RIS allows scanning up to 60 degrees from 28 to 29 GHz with a maximum aperture efficiency of 22%. This superior performance provides tantalizing evidence that the multiple switches per bit approach should not be discarded a priori due to its apparent higher complexity.

Friday, March 22 10:40 - 12:20

CS46: GNSS Reflectometry Antenna Topics

T03 Aerospace, new space and non-terrestrial networks / Convened Session / Antennas

Room: Boisdale 1

Chairs: Philip Jales (Spire Global, United Kingdom (Great Britain)), Manuel Martin-Neira (ESA-ESTEC, The Netherlands)

10:40 *Dual All Metal Patch Antenna for the HydroGNSS Mission*

Martin J Unwin, Kevin Maynard, Patrick Hope, Reynolt de Vos van Steenwijk and David Sanderson (SSTL, United Kingdom (Great Britain)); Manuel Martin-Neira (ESA-ESTEC, The Netherlands)

HydroGNSS is a small satellite mission under the ESA Scout Programme tapping into NewSpace, as part of ESA's FutureEO Programme, within a budget of €30m and a schedule of three years from mission kick-off to launch. The mission comprises of two satellites using an innovative GNSS-Reflectometry instrument to collect parameters related to the Essential Climate Variables (ECVs): soil moisture, inundation, freeze/thaw, biomass, ocean wind speed and sea ice extent. Previous GNSS Reflectometry antennas on UK-DMC on CYGNSS missions employed fixed arrays of single frequency, single polarisation patch elements. TDS-1 used wide-band flared spiral array to give a wider bandwidth suitable for multiple frequencies. The HydroGNSS mission, however, requires dual polarisation and dual frequency reception. An array of four Dual All-Metal Patch antennas was designed to cover GPS L1 and L5 bands and collect signals from both polarisations, with a feed network to phase and combine signals for the receiver.

11:00 *Digital Beamformer for GNSS Reflectometry and Radio Occultation Applications*

Neil Boasman (European Space Agency, The Netherlands); Manuel Martin-Neira (ESA-ESTEC, The Netherlands); Salvatore D' Addio (European Space Agency, The Netherlands)

This paper presents the specifications for the design and prototyping of a digital-beamforming processor demonstrator breadboard, suitable for new-space payloads, in LEO, for small/nano platforms, capable of generating multiple simultaneous beams for GNSS Reflectometry and Radio-Occultation applications.

This constitutes the objective of an ESA technology activity which includes the development of on-board autonomous, dynamic digital beamforming with multiple beams for small/compact/low-power new-space payloads, where a medium/large number of channels are supported. The main output of the activity consists of a representative digital beamforming breadboard demonstrator

11:20 *CubeSat Formation Antenna Array Synchronization for GNSS-R*

Laurent Paucot, Eliott Hubin and Maxime Drouguet (Université catholique de Louvain, Belgium); Volodymyr Kudriashov (ESA, Netherlands); Jan Thoemel (University of Luxembourg, Luxembourg); Christophe Craeye (Université Catholique de Louvain, Belgium)

This paper presents an approach to improving GNSS-R Earth observation resolution. The proposed method involves using a large antenna array comprising CubeSats flying in formation to synthetically increase the aperture. The paper discusses how the orbital constraints necessitate changes to the formation over time and require the formation plane to be inclined relative to the Earth's surface. The study examines a 1 km resolution target, side lobe level restrictions, and the isotropy of the ground spot. Synchronization challenges are explored by characterizing an antenna array involving CubeSat prototypes.

11:40 *Antenna Digital Beamforming on Spire's GNSS-Reflectometry CubeSat Constellation*

Philip Jales (Spire Global, United Kingdom (Great Britain)); Takayuki Yuasa (Spire Global Singapore, Singapore); Surabhi Guruprasad and Oleguer Nogués-Correig (Spire Global UK, United Kingdom (Great Britain)); Jessica Cartwright (Spire Global Luxembourg, Luxembourg)

Spire operates a constellation of satellites that perform remote sensing of the Earth using the Global Navigation Satellite System (GNSS) signals. Spire's STRATOS payload has been modified for sensing using GNSS-Reflectometry (GNSS-R). This has found successful application in sensing ocean wind / wave state and for retrieving volumetric soil moisture amongst others physical properties. In this paper the motivation for using antenna digital beamforming is described. The design elements that have been added, include the internal calibration, the digital signal processing and phase control. The calibration method uses the injection of a spread-spectrum signal into each of the radio inputs. This allows for absolute and relative calibration of signal amplitude and phase. A novel RF coupling device is devised to make a realisable RF coupler multitude of input channels. The scheme is tested on a two antenna system and the expected 3 dB improvement in receiver sensitivity is demonstrated.

12:00 *Low-Cost Hybrid Additive Manufacturing of a Miniaturized Dual Band Stacked Patch Antenna for GNSS Applications*

Simon P Hehenberger (DLR- German Aerospace Center & TU Delft, Germany); Stefano Caizzone (German Aerospace Center (DLR), Germany); Alexander Yarovoy (TU Delft, The Netherlands)

The utilization of low-cost hybrid additive manufacturing equipment for creating a fully integrated patch antenna system is demonstrated. A miniaturized stacked dual-band patch antenna for GNSS applications with integrated feed, amplifier, matching, and bias network is considered. Design and manufacturing challenges due to the peculiarities of hybrid additive manufacturing like anisotropic substrates, thermal curing steps, and low layer adhesion between different materials are discussed and solutions proposed. In this paper, the passive part of the antenna is manufactured and its measured performance is compared to results obtained via numerical simulations. An excellent agreement between simulation and measurement of the passive antenna is observed. The results of the fully integrated and active antenna will be demonstrated at the conference.

Friday, March 22 10:40 - 12:20

CS1b: Advances in Microwave and mmWave Wireless Power Transfer (continued)

T04 RF sensing for automotive, security, IoT, and other applications / Convened Session / Antennas

Room: Boisdale 2

Chairs: Chaoyun Song (King's College London, United Kingdom (Great Britain)), Mahmoud Wagih (University of Glasgow, United Kingdom (Great Britain))

10:40 *A Compact Microwave Rectifier for Wireless Power Transfer and Energy Harvesting Applications*

Gholamhosein Moloudian (Tyndall National Institute, Ireland); Sanjeev Kumar (Tyndall National Institute & University College Cork, Ireland); Brendan O'Flynn (Tyndall National Institute, Ireland); John Laurence Buckley (Tyndall National Institute & University College Cork, Ireland)

This paper presents a microwave rectifier with compact size and high efficiency for radio frequency (RF) energy harvesting and low-power internet of things (IoT) applications. The proposed rectifier consists of a matching network, a doubler rectifier, a lowpass (LPF) structure and a low-power electronic circuit. An LPF structure is employed to pass a direct current (DC) rectified signal and to control harmonics which increases the output voltage (V_{OUT}-DC) as well as power conversion efficiency (PCE). The proposed rectifier is designed to operate at $f = 1.8$ GHz which shows a maximum PCE of 62% for an RF input power (PIN) level of 8 dBm and optimum load (RL) of 820 Ω . A DC-DC boost converter and a super capacitor (COUT = 370 μ F) is employed to deliver sufficient DC voltage to power a low-power electronic circuit. The proposed rectifier is demonstrated to be capable of powering a low-power circuit at varying PIN levels. The developed rectifier can be used in RF energy harvesting and wireless power transmission systems to power sensor nodes and IoT devices.

11:00 *Matching Network Elimination in Multiband Metasurface-Structured Rectennas for Wireless Power Transfer and Energy Harvesting*

Wenzhang Zhang (Xi'an Jiaotong-Liverpool University & University of Liverpool, United Kingdom (Great Britain)); Rui Pei (Donghua University, China); Jinyao Zhang (University of Liverpool, United Kingdom (Great Britain)); Bintao Hu (Xi'an Jiaotong-Liverpool University, China); Jiafeng Zhou (University of Liverpool, United Kingdom (Great Britain))

This paper presents a multiband metasurface-structured rectenna without using an impedance matching network for wireless power transfer and energy harvesting applications. The impedance matching network for nonlinear devices like rectifiers in multi- or broadband frequency bands is difficult to design, so matching network elimination can improve the conversion efficiency of the rectenna. Due to the special properties of a metasurface-structured antenna (which can potentially excite multiple frequency bands and tune the ratio between different frequencies), it becomes an appropriate candidate to achieve the high impedance values at different frequency bands to realize the matching network elimination in WPT and EH operating frequency bands. The simulated and measured results verify that this proposed rectenna can operate at 0.9, 1.4 and 2.45 GHz without the need for a matching network. In addition, the conversion efficiency of this rectenna is around 50%, 60%, and 40% at 0.9, 1.4, and 2.45 GHz.

11:20 *A mmWave Leaky-Wave Antenna for Efficiency Enhanced Near-Field Wireless Power Transfer and Communication*

Shan Han (Heriot Watt University, United Kingdom (Great Britain)); Miguel Poveda-García (Technical University of Cartagena, Spain); Yuan Ding, George Goussetis and

Lei Wang (Heriot-Watt University, United Kingdom (Great Britain))

A mmWave near-field-focused and beam steerable circularly polarized (CP) leaky-wave antenna (LWA) for wireless power transfer (WPT) with multiple users and communication is presented. The proposed design is achieved by etching uniform fan-shaped slots in a rectangular substrate integrated waveguide (SIW). The slots are elaborately designed and positioned for beam focusing at a desired focal distance of 0.5 m. Compared to the conventional LWA, the power density of the proposed design is enhanced by 1.4 dB. It allows a dual beam scanning propriety with a wide angular coverage of 43.18° and 33° in near field and far field, respectively. The proposed design benefits WPT systems by eliminating the beam forming network and offering wide power coverage. Moreover, it offers high realized no less than 12.62 dBi in the bandwidth of 22.5 GHz to 26 GHz. Hence, the LWA proposed is a promising transmitter candidate for integrated WPT and communication.

11:40 Power Handling Test of a L-Band Antenna Using Infrared Thermography

Adrien Laffont and Stéphane Fauré (Anyfields, France); Gautier Mazingue (Anywaves, France)

This paper presents power handling tests performed on an antenna using infrared thermography. Infrared thermography measurement allows to quickly verify that the antenna radiation is not affected by the power increase. The tests are carried out on an L-band antenna for a maximum input power of 6.3 W at its frequency of interest of 1.7 GHz.

12:00 Plug-In Plug-Out Multibeam Dielectric Rod Antenna for Target Dedicated mm-Wave RF-WPT Applications

Amir Mohsen Ahmadi Najafabadi (EPFL, Switzerland & CSEM SA, Switzerland); German Augusto Ramirez Arroyave (EPFL - École Polytechnique Fédérale de Lausanne & Universidad Nacional de Colombia, Switzerland); Mohsen Ghorbanpoor (ETHZ, Switzerland); Alexander Vorobyov (CSEM & Center Suisse d'Electronique et de Microtechnique SA, Switzerland); Pascal Nussbaum (CSEM, Switzerland); Anja K. Skrivervik (EPFL, Switzerland)

This paper introduces a beam-adjustable multibeam dielectric rod antenna for mm-wave RF-WPT applications. The unique multibeam setup allows the generation of several adjustable beams simultaneously. This is conceptualized by utilizing three and five rods to create a beam coverage between -30° to 30° in the azimuth plane. In the proposed configuration, the peak gain value of each generated beam is 13 dBi at 23.8 GHz. A gain value above 12 dBi is maintained between 20 GHz and 24 GHz. The Rexolite rod is fed through an annular slot fabricated on a Rogers RO4003 substrate. The adjustable nature of this configuration makes the solution agile, with the possibility of adaptation to different scenarios either by altering the number of unit elements employed or their orientation. This capability, together with the low cost of the proposed solution, makes it a promising power delivery solution for Internet of Things (IoT).

Friday, March 22 10:40 - 12:20

CS12b: AMTA Session: Robotic Antenna Measurements (continued)

T05 Positioning, localization, identification & tracking / Convened Session / Measurements

Room: Carron 1

Chairs: Joshua Gordon (US National Institute of Standards and Technology, USA), Roland Moch (RWTH Aachen University, Germany)

10:40 KRISS Robot-Based Antenna Measurement System

Jae-Yong Kwon (Korea Research Institute of Standards and Science, Korea (South)); Woohyun Chung and Chihyun Cho (Korea Research Institute of Standard and Science, Korea (South))

A Robot-based antenna measurement system is proposed. The system configuration and initial operating procedure are briefly introduced. Three models of robots were tested their positional accuracy using a laser tracker. The vertical and horizontal accuracies of robots are within ± 0.15 mm in the working distance of 400 mm. We performed three-antenna method and present the preliminary antenna gain data of one KRISS W-band standard gain horn antenna to compare the measurement accuracy of KR-MANMS with a conventional full anechoic chamber.

11:00 Robotic Antenna Characterization System Based on Wideband FMCW Transceiver Modules

Kristof Dausien (Ruhr University Bochum, Germany); Michael Tomasz Kleinschmidt (Ruhr Universität Bochum, Germany); Ilona Rolfes (Ruhr-Universität Bochum, Germany); Nils Pohl (Ruhr-University Bochum & Fraunhofer FHR, Germany); Jan Barowski (Ruhr-Universität Bochum, Germany)

This paper evaluates an automated antenna characterization system with two robotic arms, performing measurements through the use of two wideband radar transceivers based on the frequency-modulated continuous wave (FMCW) principle. For this purpose, a radar system is used that covers large parts of the D-band and can perform measurements in the frequency range from 126 GHz to 182 GHz. In contrast to vector network analyzer (VNA) extension modules, the FMCW transceivers are lightweight, compact, and do not have sensitive RF cables to connect to the large host device. This allows for faster scanning, and better positioning accuracies and is much more cost efficient, providing an interesting solution in fabrication facilities. To demonstrate the capabilities, the paper presents antenna pattern measurements from 4 different (lens) antennas: an open waveguide, a 25 dBi horn antenna, a spherical (low gain), and an elliptic lens (high gain).

11:20 Safety Considerations for Robotic Antenna Measurement Systems

Chris Smith (NSI-MI Technologies, USA)

This paper discusses safety considerations when using industrial robots as positioning devices in near field antenna measurement systems. Robotic systems allow for exceptional flexibility and speed but can also pose hazards to both range personnel and test articles. Special consideration needs to be given to ensuring the motion profile of the robotic system stays within proscribed motion and velocity limits. Layered safety systems including physical barriers, light curtains, LIDARs, software, and independent control safety features will be explored and will be presented to the reader with a holistic approach to safety.

11:40 Robotic near Field Scanning for High Throughput Phased Array Production Test

Ernestus J Vermeulen (NSI-MI Technologies Ametek & NSI-MI Technologies, USA); John Demas (NSI-MI Technologies, USA)

During the past 5 years robot based near field measurement systems have evolved and become increasingly used in the testing of phased array antennas. Robotic positioning systems offer greater positioning range and flexibility than traditional scanning systems by allowing the use of different test tools and geometries. These benefits allow for faster and more efficient testing. For all the benefits they bring, robot based systems have different facility interface and safety requirements that must be considered as part of specifying them for a particular test application. This paper provides a high-level comparison between traditional, and robot based near field scanner systems and provides a high-level summary of the key benefits, limitations and unique attributes of robotic systems specifically focused on phased array production testing applications. It also provides an example of how a robotic system was implemented to test phased array tiles for one application.

12:00 Robotic Arm-Based Antenna Metrology System for Aerospace Applications

Marie Piasecki (NASA, USA); Bryan Schoenholz and James Downey (NASA Glenn Research Center, USA); Christine Chevalier and Kevin Lambert (HX5 LLC, USA)

Robotic antenna metrology presents interesting opportunities to investigate novel approaches to traditional antenna and communication system evaluation. In 2018 the National Aeronautics and Space Administration (NASA) Glenn Research Center (GRC) began exploring the use of robotic measurement for antenna and communication system metrology to address unique needs for traceability and in situ testing of a novel antenna for use in unmanned aerial systems (UAS). Since that initial development of the Portable Laser Guided Robotic Metrology (PLGRM) system many additional capabilities have been added to support a wide variety of aerospace applications. This paper provides an overview of the system itself, existing capabilities, benefits over other measurement approaches, and future work.

Friday, March 22 10:40 - 12:20

CS19b: Fundamental challenges and novel methodologies in the next-generation computational electromagnetics (continued)

T08 EM modelling and simulation tools / Convened Session / Electromagnetics

Room: Carron 2

Chairs: Zhen Peng (University of Illinois at Urbana-Champaign, USA), Francesca Vipiana (Politecnico di Torino, Italy)

10:40 A Loop-Star Decomposition for the B-Spline Based Discretization of the Electric Field Integral Equation

Mohammad Mirmohammadsadeghi and Bernd Hofmann (Technical University of Munich, Germany); Thomas F. Eibert (Technical University of Munich (TUM) & Chair of High-Frequency Engineering (HFT), Germany); Francesco P. Andriulli (Politecnico di Torino, Italy); Simon B Adrian (Universität Rostock, Germany)

The electric field integral equation (EFIE) is widely employed to determine the field that is scattered from perfectly electrically conducting (PEC) structures. However, it is known to suffer from a low-frequency breakdown. In order to overcome this breakdown for a B-spline based (isogeometric) discretization of arbitrary polynomial order of the EFIE employing the method of moments, we propose a loop-star decomposition of the discretized surface current density resulting in a preconditioner involving solely sparse matrices. The proposed decomposition is applicable to open and closed simply-connected surfaces described by a single or by multiple patches. To verify the correctness of the proposed method, numerical examples are provided.

11:00 A Multi-Region Hierarchical Preconditioning Scheme for the MoM Simulation of Complex Composite Structures

Victor Martín (Universidad de Extremadura, Spain); Jose M. Taboada (University of Extremadura, Spain); Francesca Vipiana (Politecnico di Torino, Italy)

The hierarchical quasi-Helmholtz decomposition multiresolution preconditioner has been widely studied and proven effective in addressing surface integral equation breakdowns and improving convergence in multiscale problems, but, until now, it has been applied to perfect electrical conductors only. In this paper, we present a new methodology that utilizes this efficient preconditioner to solve complex geometries built of piecewise homogeneous composite objects that meet boundary conditions automatically. The proposed approach represents the first known use of a multi-level quasi-Helmholtz decomposition to solve objects with dielectric junctions without resorting to weak enforcement of continuity or reducing the number of unknowns. Numerical examples show that this method can efficiently solve geometrically complex problems involving multiple materials, including dielectrics and conductors.

11:20 Automatic MoM Source Integral Quadrature Selection via a Machine Learning Approach

Victor Martín (Universidad de Extremadura, Spain); Marco Ricci (Politecnico di Torino, Italy); Donald Wilton (University of Houston, USA); William Johnson (Private Consultant, USA); Francesca Vipiana (Politecnico di Torino, Italy)

In this paper, a new technique, based on machine learning (ML) and dimensionality reduction, is proposed for drastically improving the performance in the evaluation of the singular and near singular potential integrals in the method of moments (MoM). The MoM source surface integral is first reduced to a line integral via a dimensionality reduction method, and, then, an ML algorithm is trained on a set of line integrals evaluated with Gauss-Legendre (GL) quadrature schemes of different orders. Finally, the trained ML algorithm is used to determine the minimum number of GL sample points and weights required for each potential line integral to get the requested accuracy.

11:40 Supervised Learning Based Real-Time Adaptive Beamforming On-Board Multibeam Satellites

Flor Ortiz, Juan A. Vázquez Peralvo, Jorge Querol, Eva Lagunas and Jorge L González-Rios (University of Luxembourg, Luxembourg); Marcelo O K Mendonça (University of Luxembourg & SNT, Luxembourg); Luis Manuel Garcés-Socarrás, Victor Monzon Baeza and Symeon Chatzinotas (University of Luxembourg, Luxembourg)

Satellite communications (SatCom) are crucial for global connectivity, especially in the era of emerging technologies like 6G and narrowing the digital divide. Traditional SatCom systems struggle with efficient resource management due to static multibeam configurations, hindering quality of service (QoS) amidst dynamic traffic demands. This paper introduces an innovative solution - real-time adaptive beamforming on multibeam satellites with software-defined payloads in geostationary orbit (GEO). Utilizing a Direct Radiating Array (DRA) with circular polarization in the 17.7 - 20.2 GHz band, the paper outlines DRA design and a supervised learning-based algorithm for on-board beamforming. This adaptive approach not only meets precise beam projection needs but also dynamically adjusts beamwidth, minimizes sidelobe levels (SLL), and optimizes effective isotropic radiated power (EIRP).

12:00 Impact of the Unit Cell Distribution of 1-D Dynamic Metasurface Antennas on the Performance of a Computational Imaging System

Guillermo Alvarez Narciandi, María García Fernández and Okan Yurduseven (Queen's University Belfast, United Kingdom (Great Britain))

Computational imaging (CI) enables to bypass the significantly demanding sampling requirements imposed by synthetic aperture radar (SAR) techniques. For that purpose, CI systems rely on compressive antennas to achieve a physical-layer compression of the scene information. In this context, among the different compressive antenna implementations, dynamic metasurface antennas (DMAs) are of significant interest due to their compactness, ease of fabrication, and their ability to reconstruct the scene information without the need of large bandwidths. This contribution analyzes the impact of using different unit cell distributions for a 1-D DMA on the performance of a single-pixel CI system. Results show that the use of a sparse unit cell distribution does not jeopardize the imaging performance of the system, and, in addition, it enables to reduce the hardware complexity of the antenna.

Friday, March 22 10:40 - 12:20

SW6b: Recent advances in antenna measurement traceability and uncertainty at reduced distances (continued)

Room: Dochart 1

Chairs: Dennis Lewis (Boeing, USA), Janet O'Neil (ETS-Lindgren, USA)

10:40 High-Accuracy Near-Field Calibration Techniques for Gain Reference Antennas

Presenter: Olav Breinbjerg (EIMaReCo, Denmark)

11:25 Near-Field Antenna Gain Calibrations Employing Spherical Near-Field Techniques

Presenter: David Ulm (Physikalisch-Technische Bundesanstalt, Germany)

Friday, March 22 10:40 - 12:20

CS26b: COST Session CA18223 (SyMat) Modeling and Applications of Higher Symmetries (continued)

T08 EM modelling and simulation tools / Convened Session / Antennas

Room: Dochart 2

Chairs: Sara Mugnaini (OneWeb Communication Ltd, United Kingdom (Great Britain)), Eva Rajo-Iglesias (University Carlos III of Madrid, Spain)

10:40 Ridge Gap Waveguide Implementation with a 3D Glide Symmetric Hole Metasurface for Slotted Antenna Array Feeding

Panagiotis Petroustos and Stavros Koulouridis (University of Patras, Greece)

This work focuses on integrating Electromagnetic Band Gap (EBG) multi-layer glide symmetric holes (GSH) in a Ridge Gap Waveguide (RGW) feeding. The presented RGW structure consists of four stacked metal layers. A formed path is generated between the bottom and top layer while each layer integrates a periodic pattern of holes. The integrated holes are arranged to configure a GSH metasurface. Glide symmetric metasurface is used to form boundary conditions for RGW feeding, effectively dealing with energy leakage. Also, EBG conditions allow the assembly of distinct layers without any galvanic connection to be required. In addition, the hole metasurface utilization takes advantage of larger periodicity and reduced milling depth, providing a related lower manufacturing cost. To highlight potential applications, a slot array antenna fed by the RGW with a 3D GSH configuration is presented. It covers an impedance bandwidth from 37.02GHz to 42.36GHz and provides a gain of over 11dB.

11:00 Glide-Symmetric Reconfigurable Substrate-Integrated Holey Waveguide

Boris Fischer, Julien Sarrazin and Guido Valerio (Sorbonne Université, France)

Glide-symmetric metasurfaces have been recently employed to realize integrated microwave devices exhibiting a reduced frequency dispersion and thus capable to operate in a wide band: planar lenses, gap waveguides, filters. They have been successfully realized with fully metallic holey metasurfaces. However, substrate-integrated technology can be adopted to ease the fabrication of this class of devices by mimicking drilled holes with tightly spaced metallized via holes. Here we investigate the possibility to reconfigure the unit cells of glide-symmetric substrate-integrated holey surfaces by modifying the effective height of its holes. Since the height of the holes cannot be reconfigured after the realization of a device, we place a high-impedance surface close to the bottom of each hole and move it to achieve a variation of the effective reactive load of each hole.

11:20 Thinned Connected Slot Array Design Using Higher Symmetries

[Christos Monochristou](#) (University of Rennes, France); Ronan Sauleau (University of Rennes 1, France); Mauro Ettore (University of Rennes 1 & UMR CNRS 6164, France)

Arrays with a reduced number of active elements have garnered considerable attention due to their potential to simplify phased arrays while preserving their operational versatility. Nevertheless, most research has concentrated on numerical synthesis methods, with limited emphasis on the practical implementations of these arrays. In this work, we introduce realizable thinned arrays based on the connected slot architecture. The unit-cell performance is enhanced with glide-symmetric artificial dielectric superstrates which enable the unidirectional radiation of the antenna and significantly increase its bandwidth. The thinned lattices are synthesized using a compressive sensing algorithm which is integrated with a semi-analytical Method of Moments (MoM) for connected slot topologies. Consequently, the array's layout and the inter-element coupling are accounted for during the optimization procedure. The resulting arrays are near-optimal, they demonstrate high efficiency and their realization is feasible.

11:40 All-Metal Glide-Symmetric Slotted Planar Antennas: Modal Analysis

Yuhuan Tong and Guido Valerio (Sorbonne Université, France); Beatrice Ambrogio (Sapienza University, Italy); Davide Comite (Sapienza University of Rome, Italy)

Glide-symmetric periodic structures have attracted increasing interest in the last decade thanks to their unconventional dispersion features. They have been proposed to design electromagnetic bandgap materials, planar lenses, and, more generally, microwave and millimeter waves devices. A glide-symmetric load within a metallic waveguide produces linear dispersion within the first pass band, then an open stop-band with maximized spectral width. The modes propagating within the structures become a slow wave and, therefore, an all-metal glide-symmetric load defines an artificial dielectric. This contribution proposes, for the first time, a preliminary dispersive analysis of the complex mode supported by an open glide-symmetric all-metal waveguide loaded with glide-symmetric corrugations. To this aim, an ad-hoc method-of-moments approach is introduced, whose results are compared with full-wave simulations achieved by implementing a Bloch analysis.

12:00 Design of Glide-Symmetric Dielectric Mikaelian Lens Antenna for K/Ka-Band

Jose-Manuel Poyanco (University Carlos III of Madrid, Spain); Dubravko Tomić, Marko Bosiljevac and Zvonimir Sipus (University of Zagreb, Croatia); Eva Rajo-Iglesias (University Carlos III of Madrid, Spain)

This paper outlines the optimization procedure for designing a planar dielectric Mikaelian lens with the emphasis on achieving one-dimensional beam steering. The lens unique flat shape is a key feature that enables a straightforward and cost-effective planar feed. To verify the design procedure, a lens prototype made out of a dielectric glide-symmetric periodic structure embedded in a parallel plate waveguide is constructed. The propagation constant and dielectric losses of the glide-symmetric periodic structure are analyzed using the rigorous coupled wave analysis method. The antenna design has a focused fan-shaped beam that can be steered over a 100 degrees range through 11 ports, with scan loss below 3 dB. The Mikaelian lens has a flat feeding interface, minimizing the mutual coupling between ports. These characteristics have great potential for realizing affordable multi-beam antennas for 5G/6G.

Friday, March 22 10:40 - 12:20

A15b: Developments in antenna arrays (continued)

T08 EM modelling and simulation tools // Antennas

Room: M2

Chairs: Yanki Aslan (Delft University of Technology, The Netherlands), Christopher G Hynes (Simon Fraser University, Canada)

10:40 Maximum Gain Estimates for Corporate-Fed Arrays

[Christopher G Hynes](#) and Rodney Vaughan (Simon Fraser University, Canada)

Unlike adaptive or reconfigurable systems such as phased arrays, the feed network can limit the maximum realized gain of fixed-beam corporate-fed arrays. For any corporate-fed array, the total transmission loss increases with the array size, so for a fixed element gain, there is a maximum array gain for a given transmission loss. This paper derives accurate estimates for the maximum gain of a corporate-fed planar rectangular antenna array in terms of the performance of the feed network components and the array element. The theoretical results are validated using simulation.

11:00 Ultra-Wideband Wide-Scanning Dual-Polarized Vivaldi Antenna Unit with Novel Pendulum-Shaped Slots

Shigang Fang and Shi-Wei Qu (University of Electronic Science and Technology of China, China)

An ultra-wideband (UWB) wide-scanning dual-polarized Vivaldi antenna unit is proposed in this paper. Vivaldi antennas always suffer from the high-profile problem. As a solution, the novel pendulum-shaped slots are designed, which notably reduces the profile and enhances the wide-scanning ability. Thus, the proposed dual-polarized Vivaldi antenna unit achieves $\pm 60^\circ$ beam scanning in E/H/D planes with an active VSWR below 2.5 in 6~18GHz. The orthogonal port coupling during beam scanning is lower than -30dB in E/H planes, -10dB in D plane. Computed performances prove that the proposed dual-polarized antenna unit is of great potential to be employed for large-scale Vivaldi arrays.

11:20 Array Scattering Synthesis for Anomalous Deflection Using Passive Aperiodic Loadings

[Sravan Kumar Reddy Vuyyuru](#) (Aalto University & Nokia Bell Labs, Finland); Risto Valkonen (Nokia Bell Labs, Finland); Do-Hoon Kwon (University of Massachusetts Amherst, USA); Sergei Tretyakov (Aalto University, Finland)

Large-scale anomalous reflectors in reconfigurable intelligent surface applications require a scanning capability to deflect the beam to an arbitrary angle without incurring parasitic scattering. In this study, we propose a design methodology for linear loaded antenna arrays by synthesizing the scattering characteristics with respect to impedance loads to attain perfect anomalous reflection. It relies on accurate prediction of the induced element port currents and their associated scattering behavior for any given set of load impedances. We develop a linear array with a fixed half wavelength spacing for scanning into extreme deflection angles. Using continuous and discretized load reactances, the tunability prospect of high-efficiency anomalous reflection is demonstrated.

11:40 Sunflower Array of Infinitesimal Dipoles for Constrained Antenna Modeling

[Nehir Berk Onat](#) (Delft University of Technology, The Netherlands); Alexander Yarovoy (TU Delft, The Netherlands); Yanki Aslan (Delft University of Technology, The Netherlands)

Netherlands)

The sunflower array topology concept is introduced, for the first time, to the constrained infinitesimal dipole modeling (IDM) technique to increase the computational efficiency and reduce the modeling errors. The concept is applied to embedded element pattern predictions via matrix inversion. A novel study on the impact of the type and orientation of the dipoles on the IDM performance in pattern mean square error (MSE) and stability against noise (linked to the matrix condition number) is conducted. A 5 by 5 patch antenna array modeled with 81 dipoles is used for demonstration. It is shown that using magnetic dipoles (oriented in the direction of a radiating edge of the patch) in IDM yields the optimal performance. Besides, the sunflower topology significantly lowers the MSE (by 5 dB, on average), while reducing the condition number by a factor of 10.

12:00 *Dual UWB Antennas on AoA Anchor Node*

Hossein Raghbi Hokmabadi, Khatereh Nadali and Patrick McEvoy (Technological University Dublin, Ireland); Sam Lemey (Ghent University, Belgium); Max James Ammann (Technological University Dublin, Ireland)

This paper investigates the performance impact of mounting UWB antennas on small anchor nodes for angle-of-arrival indoor positioning systems. A slot antenna and a monopole are designed to support UWB channels 5 to 10 (6.2-8.6 GHz). The antennas are evaluated when connected to a 76.6 × 51.6 mm anchor node PCB. The study assesses the performance of compact slot and monopole antennas, complying with IEEE 802.15.4z-2020 standards. The results provide valuable insights into optimizing UWB antenna performance for AoA applications

Friday, March 22 10:40 - 12:20

SW8b: Waveguide Antenna Array Technologies for Space and Beyond (continued)

Room: M3

Chairs: Nelson Fonseca (Anywaves, France), Yi Wang (University of Birmingham, United Kingdom (Great Britain))

10:40 *Array Antennas for Space Applications*

Presenter: Nelson Fonseca (Anywaves, Toulouse, France)

11:10 *Long Slot Arrays for Space Applications*

Presenter: Mauro Ettore (Michigan State University, USA)

11:40 *Multi-Band and Wideband Waveguide Arrays for Satcom and 5G Backhaul*

Presenter: Yi Wang (The University of Birmingham, UK)

12:05 *SW8 Discussions*

Friday, March 22 10:40 - 12:20

CS14b: Shape-morphing metamaterials, antennas and electromagnetic components (continued)

T10 Novel materials, metamaterials, metasurfaces and manufacturing processes / Convened Session / Electromagnetics

Room: M4

Chairs: Alex W Powell (University of Exeter, United Kingdom (Great Britain)), Christopher Stevens (University of Oxford, United Kingdom (Great Britain))

10:40 *Reconfiguration of Electromagnetic Metasurfaces Using Tunable Shape Morphing Structures*

David L West and William D Pavlick (Georgia Institute of Technology, USA); Jay S Sim, Jize Dai and Shuai Wu (Stanford University, USA); Jack Eichenberger (The Ohio State University, USA); Ruike Renee Zhao (Stanford University, USA); Nima Ghalichechian (Georgia Institute of Technology, USA)

Reconfigurable metamaterials and metasurfaces are of interest for a variety of functionalities for next-generation communications and sensing. However, electronically controlling large arrays is difficult, and traditional PCB technology has limited capabilities for conforming to curved surfaces. We demonstrate the use of novel magnetically reconfigurable shape morphing structures for metasurface applications. The reconfiguration is performed using a quasi-DC magnetic field, which decouples the electrical control problem from the electromagnetic design. In addition, the magnetic composite is flexible and can conform to various shapes. We have previously demonstrated the use of these structures for reconfigurable on-off filters. We also demonstrate fully wrapped conformability to cylindrical shapes.

11:00 *Multistable Structures for Deployable and Reconfigurable Antennas*

Maria Sakovsky (Stanford University, USA); Joseph Costantine and Youssef Tawk (American University of Beirut, Lebanon)

This paper presents the integration of multi-stable structures in deployable antennas to reconfigure their performance characteristics. The integration of the multi-stability of structures into electromagnetic antenna designs from the outset results in minimizing the need for actuation mechanisms and renders the reconfiguration passive. Furthermore, the paper delves into the mechanical aspects of multi-stability, describing how materials with strain energy storage can exhibit multiple stable states due to pre-stress. It discusses various multi-stability mechanisms, including fiber-reinforced polymer composites and tape springs, which enable antennas to achieve stable geometric configurations. The paper also provides examples of bi-stable reconfigurable deployable antennas and explores the broader potential of multi-stable structures in shape-morphing surfaces for future communication applications.

11:20 *Analyzing the Performance of Phased Array Geometries with Aperture Projection Analysis*

David Elliott Williamstyer (Hofstra University, USA); Ali Hajimiri (California Institute of Technology, USA)

Geometry plays an important role in phased array performance. There is thus an opportunity to improve array performance by including geometry as a design variable. This is the core idea in the emerging field of shape-changing phased arrays. Therefore, formal analytic tools are needed for assessing the performance of different geometries. This work establishes a solid theoretical foundation for a commonly used analysis technique, aperture projection analysis. Using this tool, the fundamental trade-offs between gain and steering range for common array geometries are explored. Analytic formulas of the maximum gain are established and numeric calculations directly compare the relationship between maximum gain and steering range. It is demonstrated that planar arrays have the highest gain, that spherical and cylindrical arrays have the highest steering range, and conic arrays offer the best compromise.

11:40 *Wideband Dual-Polarized 1-Bit Unit-Cell Design for mmWave Reconfigurable Intelligent Surface*

Gabriel G. Machado (Ulster University, United Kingdom (Great Britain)); Muhammad Ali Babar Abbasi (Queen's University Belfast & The Institute of Electronics, Communications and Information Technology (ECIT), United Kingdom (Great Britain)); Adrian D McKernan and Chao Gu (Queen's University Belfast, United Kingdom (Great Britain)); Dmitry E Zelenchuk (Queen's University of Belfast, United Kingdom (Great Britain))

This study presents a novel reflective unit-cell with wideband characteristics at millimeter-wave (mmWave) bands for application in Reconfigurable Intelligent Surfaces (RIS). The proposed unit-cell design

demonstrates through full-wave simulations a superior bandwidth performance over the 26.50-29.45 GHz, targeting the n257 band of mmWave 5G. The design was created for dual-polarization operation, each controlled by a p-n diode to realise a 1-bit RIS. The design achieves impressive performance, maintaining a phase difference error within ± 20 degrees across most of the 3 GHz bandwidth while reflecting over 80% of the energy. The increased reflectivity minimizes losses, while precise phase control improves beam pointing accuracy, crucial in low-complexity 1-bit systems. Numerical simulations also indicate that this unit-cell performs effectively in a 6-layer PCB stack-up. A comparison with state-of-the-art unit-cells for RIS design is also presented, demonstrating the advantages of the proposed design in terms of bandwidth, dual-polarization operation, and phase accuracy.

12:00 Multi-Band Anisotropic Metasurface: Simultaneous Linear and Circular Polarization for Robust Satellite Communication

Humayun Zubair Khan, Farooq A Tahir, Abdul Jabbar, Qammer H Abbasi and Muhammad Ali Imran (University of Glasgow, United Kingdom (Great Britain))

This paper presents a novel metasurface design for efficient polarization conversion in electromagnetic wave applications. To achieve linear-to-linear polarization (LLP) and linear-to-circular polarization (LCP) conversions, the metasurface was meticulously engineered. The co-reflection and cross-reflection coefficients were carefully controlled to meet specific criteria for successful LCP conversion. The results demonstrated that within the frequency bands of 11.02-11.88 GHz, 12.92-15.20 GHz, and 15.14-16.42 GHz, the metasurface effectively achieved LCP conversion with high efficiency, meeting the handedness requirements for both left-circularly polarized (LHCP) and right-circularly polarized (RHCP) waves. The proposed design exhibited excellent performance not only for normal incidence but also at oblique incidence angles of up to 45 degrees, ensuring its robustness in practical scenarios. This versatile metasurface design holds promise for a wide range of applications in satellite communications, offering efficient and stable polarization conversion capabilities within multiple frequency bands.

Friday, March 22 12:40 - 13:10

CC: Closing ceremony

Room: Lomond Auditorium

Friday, March 22 14:00 - 17:00

SC07: Fundamental equations of electromagnetics from classical to quantum

Room: Alsh 1

Friday, March 22 14:00 - 17:00

SC08: Microwave Imaging and Sensing and their Innovative Applications

Room: Alsh 2

Friday, March 22 14:00 - 17:00

SC02: Optimal Antennas: Operators, Limits, and Design

Room: Boisdale 1

Friday, March 22 14:00 - 17:00

SC01: Modelling and Design of Space-Time Modulated Electromagnetic Structures

Room: Boisdale 2

Friday, March 22 14:00 - 17:00

SC05: AI Techniques for Microwave Antenna Design

Room: Carron 1

Friday, March 22 14:00 - 17:00

SC06: Machine Learning-Enabled Optimization and Synthesis of Metasurface Antennas

Room: Carron 2

Friday, March 22 14:00 - 17:00

SC04: Multibeam Antennas and Beamforming Networks

Room: Dochart 1

Friday, March 22 14:00 - 17:00

SC03: Advanced impedance matching and impedance analysis for antenna applications

Room: Dochart 2

Friday, March 22 14:00 - 17:00

SC09: Planar near-field measurements of phased array antennas in millimetre-wave bands

Room: M2

Friday, March 22 14:00 - 17:00

SC10: Spherical Near-Field Antenna Measurements – Theory and Practical Implementation

Room: M3

Author	Session	Start page	Title
A			
A. Rahim, Mohamad Kamal	E12.4	2832	<i>Compact Dual-Band Crossover with Enhanced Band Ratio Using Interdigital Capacitor for 5G Applications</i>
Aalayathil, Rishabh	PE1.7	1265	<i>Design of a Concentric Circular Holographic Metasurface Using Hexagonal Anisotropic Unit-Cell for Wireless Communications</i>
Abadal, Sergi	CS17b.5	335	<i>RIS-Based Over-The-Air Channel Equalization in Resource-Constrained Wireless Networks</i>
Abbas, Anees	PA8.7	2298	<i>Compact Size Frequency-Agile Antenna Enabling Multi-Mode Functionality for Internet of Things Applications</i>
	PA1.7	3359	<i>Development of a Wearable IoT-Optimized Textile Antenna with Low Specific Absorption Rate in Three Frequency Bands</i>
Abbas, Hasan	P05.6	266	<i>Contactless Respiration Variability Detection and Accuracy Test Using UWB Radar</i>
	E13.1	270	<i>Ultrahigh Sensitive Terahertz Metasurface with 2D MoS₂ for Refractive Index Biosensing</i>
Abbas, Syed Muzahir	PA7.14	1222	<i>UWB Circular Metal Mesh Transparent Antenna</i>
	PA8.11	2315	<i>Development of Passive Chipless RFID Temperature Sensor</i>
	PA8.12	2320	<i>Towards Array and Curve Analysis: Flexible Passive Chipless RFID Tags</i>
Abbasi, Muhammad Ali Babar	P05.5	261	<i>Sequential Phase Optimization for Coherent Long-Range Distributed Wireless Power Transfer to a Non-Communicative Receiver</i>
	CS36b.3	906	<i>Towards a Reconfigurable Metacavity Antenna for Computational Imaging and DoA Estimation</i>
	A07.1	2659	<i>A Wideband Half-Circle Metasurface Augmented Luneburg Lens for Millimeter-Wave Applications</i>
	CS14b.4	4362	<i>Wideband Dual-Polarized 1-Bit Unit-Cell Design for mmWave Reconfigurable Intelligent Surface</i>
Abbasi, Qammer	E13.1	270	<i>Ultrahigh Sensitive Terahertz Metasurface with 2D MoS₂ for Refractive Index Biosensing</i>
	PM1.4	1323	<i>A Highly Compact Double-Sided Orientation Insensitive Chipless Tag for Radio Frequency Identification Applications</i>
	PE3.13	2408	<i>Design of Intelligent Reflective Surface Unit Cell for 5G mmWave Applications</i>
	PP02.2	2495	<i>Pathloss-Based Non-Line-Of-Sight Identification in an Indoor Environment: An Experimental Study</i>
Abbasi, Qammer H	CS17a.6	24	<i>RIS-Enhanced MIMO Channels in Urban Environments: Experimental Insights</i>
	P05.6	266	<i>Contactless Respiration Variability Detection and Accuracy Test Using UWB Radar</i>
	A27a.2	636	<i>Impact of Dielectric Substrate, Feed Connector, and Fabrication Tolerances on the Performance of Planar Millimeter-Wave Antenna Arrays</i>
	PE1.5	1256	<i>An Innovative Metasurface Polarizer Working in 5G Frequency Bands</i>

	CS13.5	1568	<i>UHF RFID Sensor Antenna for Fat Content and Adulteration Detection of Milk</i>
	PA4.19	2186	<i>A Compact High-Gain 28 GHz Antenna Array for Beyond 5G Wireless Networks</i>
	PE3.4	2374	<i>RIS-Enabled Near-Field Localization with EMI</i>
	CS48.4	3992	<i>Joint Wide Illumination and Null Insertion Design in RIS-Assisted System</i>
	CS14b.5	4366	<i>Multi-Band Anisotropic Metasurface: Simultaneous Linear and Circular Polarization for Robust Satellite Communication</i>
Abbaszadeh, Afshin	E11.4	2810	<i>Observation of Exceptional Points in Parity-Time Symmetric Coupled Impedance Sheets</i>
Abboud, Toufic	PE2.3	999	<i>Management of Radiofrequency Compatibility on Aircraft</i>
Abdou, Tarek	PA1.1	3331	<i>Omnidirectional Cylindrical Dielectric Resonator Antenna for off & on Body Communications</i>
Abedian, Mohammad	PA2.9	1091	<i>Sub-7 GHz Circularly Polarized Dielectric Resonator Antenna Array for Full-Duplex Applications</i>
Abegaonkar, Mahesh	PA5.13	3546	<i>A Reactively Coupled Bi-Directional Dual CP Antenna</i>
	PA5.15	3552	<i>A Decoupling Scheme for Closely Spaced Microstrip Patch Antenna</i>
Abohmra, Abdoalbasat	E13.1	270	<i>Ultrahigh Sensitive Terahertz Metasurface with 2D MoS2 for Refractive Index Biosensing</i>
Abolhasan, Mehran	E13.6	289	<i>Highly Efficient Polarization-Insensitive EM Energy Harvester</i>
Abou Nasa, Mohamad	P05.4	256	<i>A Small-Sized Antenna System for Direction Finding Applications on a Single Plane (1D) Using BT 5.1</i>
Abraham, David	PE1.14	1292	<i>Integral Equation-Based Solver for the Simulation of Metasurface Designs</i>
Abrardo., Andrea.	CS20a.2	91	<i>Analysis and Optimization of Reconfigurable Intelligent Surfaces Based on S-Parameters Multiport Network Theory</i>
Abreu, Angel	PA8.17	2340	<i>A Systematic Design Method of Miniaturizing Microstrip Patch Antenna Using Theory of Characteristic Modes</i>
Achicanoy, Wilson	P04b.4	980	<i>Fast Indoor Radio Propagation Prediction Using Deep Learning</i>
Addamo, Giuseppe	CS6b.5	505	<i>Multi-Beam Arrays for Future LEO SatCom Payloads</i>
Addo, Ernest	CS25.2	659	<i>A Modular, Low-Cost Ka-Band Antenna Subarray as Building Block for Phased Arrays of Arbitrary Size and Shape</i>
Adrian, Simon	CS19b.1	4282	<i>A Loop-Star Decomposition for the B-Spline Based Discretization of the Electric Field Integral Equation</i>
Afzal, Muhammad Usman	CS9a.5	233	<i>Beam Steering 2D Leaky Wave Resonant Cavity Antenna for Ka-Band Satellite Communication</i>
Agan, Corey	A25.5	3105	<i>Additively Manufactured Horn Antennas</i>
Agarwal, Shobit	PA7.14	1222	<i>UWB Circular Metal Mesh Transparent Antenna</i>
Aghabeyki, Peyman	A06b.3	3296	<i>A Wideband Reflectarray with Reconfigurable Polarization and Beam-Scanning by Using Liquid Crystal Delay Line for Millimeter-Wave</i>
Aglietti, Guglielmo	P05.3	251	<i>Characterisation of Thin Glass-Fibre Substrates for Deployable SAR Antennas</i>
	P02.5	3782	<i>Mechanical Vibrations on a Deployable Nanosatellite Antenna: SAR Performance Analysis</i>

Ahearne, Sean	CS7.5	1611	<i>Reconfigurable Intelligent Surfaces for THz: Signal Processing and Hardware Design Challenges</i>
Ahmad, Aqsa	E09.3	3914	<i>Analysis and Design of a Wideband Jaumann-Like Radar Absorber Offering High Angular Stability and Polarization Insensitivity</i>
Ahmad, Mohaira	E09.5	3924	<i>Multifunctional Linear Dichroism and Polarization Transforming Metasurface for mm-Wave Application</i>
Ahmadi, Hanieh	PA2.22	1150	<i>Compact Circularly Polarized Patch Antenna with Enhanced Axial Ratio and Impedance Bandwidth</i>
Ahmadi Najafabadi, Amir Mohsen	CS1b.5	4254	<i>Plug-In Plug-Out Multibeam Dielectric Rod Antenna for Target Dedicated mm-Wave RF-WPT Applications</i>
Ahmed, Fahad	PA2.11	1101	<i>Multi-Bit Wideband Transmitarray Aperture with Independent Phase and Amplitude Control for High Gain with Low Sidelobe Mm-Wave Applications</i>
	A01a.4	2941	<i>Dual-Polarized OAM Antenna with Frequency and Mode Agility for Intelligent OAM Communications</i>
Ahmed, Fayyadh	A27b.5	845	<i>Flexible Phase-Reconfigurable Branch Line Coupler for Millimeter-Wave Phased Array Antenna</i>
Ai, Bo	P01.5	3852	<i>Analysis of 5G Channel Characteristics Based on Ray Tracing for the Straight Tunnel of High Speed Railway</i>
Akinsolu, Mobayode	CS11.1	1616	<i>AI-Assisted Design and Experimental Testing of a Compact UWB Antenna for the Inspection of Food and Beverage Products</i>
Akinsolu, Mobayode	CS11.2	1620	<i>AI-Driven Design of a Quasi-Digitally-Coded Wideband Microstrip Patch Antenna Array</i>
	CS11.3	1624	<i>Reflecting/Absorbing Dual-Mode Textile Metasurface with AI-Driven Parametric Studies</i>
	CS11.4	1627	<i>Automated Design of Antennas Using AI Techniques: A Review of Contemporary Methods and Applications</i>
Akinsolu, Mobayode	CS30a.2	3933	<i>Additively Manufactured Waveguide Hybrid Septum Coupler Optimized Using Machine Learning</i>
Akmansoy, Eric	E05.1	2036	<i>From Bulk Toward Micro-Structured TiO₂ Ceramics for All-Dielectric Metamaterials at Terahertz Frequencies</i>
Aksoyak, Ibrahim	A05.1	1820	<i>Sub-THz Substrate Integrated Waveguide Signal Transitions in Backend-Of-Line of a Silicon Process</i>
Al-Dabbagh, Mohanad	CS5a.3	66	<i>Horn Antenna Phase Center Position Influence on Sub-THz Measurements Uncertainties</i>
Al-Hasan, Muath	PA1.2	3336	<i>Dual-Band 3-D MIMO Antenna for Deep Tissue Devices</i>
Al-Jzari, Amar	CS5a.4	71	<i>Indoor Channel Characterization Based on Directional Measurements at 140 GHz</i>
	CS43a.2	3957	<i>Millimeter-Wave and Sub-THz Channel Measurements and Characterization Analysis in a Street Canyon Scenario</i>
Al-Khalidi, Abdullah	PA3.20	3479	<i>Sub-THz On-Chip CPW Monopole on InP with Cross-Shaped Slot for Bandwidth Enhancement</i>
Al-Nuaimi, Mustafa Khalid Taher	PA6.10	2250	<i>Generation of Narrow Divergence Angle OAM Beams for mmWave Communication Links Using Metasurface</i>
	PA3.17	3467	<i>Beam Steering Range Enhancement of Bifocal Reflectarray Using</i>

			<i>Irregular Distribution of Meta-Atoms</i>
Al-Yasir, Yasir	CS11.2	1620	<i>AI-Driven Design of a Quasi-Digitally-Coded Wideband Microstrip Patch Antenna Array</i>
Ala-Laurinaho, Juha	CS38.1	112	<i>Improving Scan Gain of Sparse Vivaldi Array with Parasitic Scatterers</i>
	CS37b.2	348	<i>Crack Stop as a Coupling Element Between an IC Chip and Antenna</i>
Alali, Bader	A07.1	2659	<i>A Wideband Half-Circle Metasurface Augmented Luneburg Lens for Millimeter-Wave Applications</i>
Alathbah, Moath	PA7.14	1222	<i>UWB Circular Metal Mesh Transparent Antenna</i>
Alayón Glazunov, Andrés	PA7.10	1205	<i>Radiation Pattern Shaping Using Generalized Luneburg Lenses for Automotive RADAR Antennas</i>
	A21.1	1480	<i>A Dual Linear-Polarized Gap Waveguide Antenna Element for Radar and Communications at 77 GHz</i>
	PM2.12	2477	<i>Over-The-Air Testing Environments with Spatial-Directional Selectivity for Characterizing Wireless Devices and Systems</i>
	M2.3	3890	<i>Data-Driven Optimization of an Array of Steered Sub-Arrays for Enhanced Fairness in MU-MIMO</i>
Albadalejo Lijarcio, Juan Luis	M2.4	3895	<i>K-Factor Evaluation in a Hybrid Reverberation Chamber plus CATR OTA Testing Setup</i>
	CS21.4	2717	<i>Low-Cost Coaxial Slot Array Antenna for E-Band Automotive Corner Radar Applications Based on Gap Waveguide MLW Technology</i>
Albani, Matteo	CS20b.2	398	<i>A Macroscopic Bilateral Modeling Approach for Reflective and Transmissive Metasurfaces</i>
	E07.4	1649	<i>Multilayer Reflectionless Wide-Angle Anomalous Refractors Based on Surface Field Optimization</i>
	PA4.8	2139	<i>A Novel GO Analysis Tool for GRIN Lenses Based on the Fast Sweeping Method</i>
Albers, Roland	A18.4	2919	<i>Method of Moment Simulation of Full Arctic Weather Satellite Structure</i>
Aldosari, Mohammed	A20.4	3822	<i>The Impact of a Phantom's Size on the Performance of an Implanted Antenna</i>
Alex-Amor, Antonio	E10b.2	2064	<i>Analytical Circuit Models: From Purely Spatial to Space-Time Structures</i>
Alexandridis, Antonis	PM2.10	2469	<i>Assessing Performance of Transparent Conductive Films for Microwave Industrial Applications</i>
Alexandropoulos, George	CS20b.1	393	<i>1-Bit SubTHz RIS with Planar Tightly Coupled Dipoles: Beam Shaping and Prototypes</i>
	CS7.5	1611	<i>Reconfigurable Intelligent Surfaces for THz: Signal Processing and Hardware Design Challenges</i>
	A23.2	2752	<i>Adaptive Polynomial Chaos Expansion for Uncertainty Quantification of SubTHz Horn Antennas with Flat-Top Radiation Patterns</i>
Alfonso, Esperanza	A28.1	3714	<i>Antenna and Mechanical Co-Design for Auto-Beam-Tracking in Backhaul Systems</i>
Algaba-Brazález, Astrid	CS36a.2	705	<i>GHz Prism: Frequency-Scanned Antennas to Improve Localization with Separate-Channel Fingerprinting</i>
	CS36a.3	710	<i>Compact Amplitude-Monopulse Microstrip Antenna Design for Wide Field-Of-View Direction Finding</i>

	CS10.1	850	<i>Efficient Ray-Tracing Model for Generalized 2D Dielectric Lenses Combined with Arrays</i>
	A08a.1	1883	<i>Efficient Ray-Tracing Approach to Analyze Arbitrarily Shaped Leaky-Wave Antennas Embedded in Lenses</i>
Alghamdi, Abdulwahab	PA1.11	3376	<i>Design of an UWB Conformal Antenna for Wireless Capsule Endoscopy</i>
	PA1.14	3390	<i>Miniaturized Implantable Antenna with Ultra-Wide Bandwidth Characteristics for Leadless Pacemakers</i>
Ali, Farman	PP02.5	2510	<i>Measurement-Based Channel Characteristics for Air-To-Ground Communications Under Rural Areas</i>
Ali, Malek Abdulmalek	CS43b.1	4168	<i>Channel Measurements and Characterization in Industrial Environment at 60 GHz</i>
Ali, Mirza Shujaat	PE3.13	2408	<i>Design of Intelligent Reflective Surface Unit Cell for 5G mmWave Applications</i>
Ali, Shahinshah	A08b.4	2096	<i>Beam Steerable Half Mode Substrate Integrated Waveguide Based Composite Right/Left Handed Leaky-Wave Antenna Using Field Programmable Microwave Substrate</i>
Ali, Uzman	A20.5	3827	<i>Quad-Band Meandered Implantable Planar Inverted-F Antenna for Wireless Brain Health Monitoring</i>
Aliakbari, Hanieh	A01b.3	3206	<i>Roof-Glass Integrated Antenna for Vehicular GNSS Applications</i>
Alidoustaghdam, Hadi	A01b.1	3197	<i>Tiled Subarray Design for Multibeam Joint Communication and Sensing</i>
Alja'afreh, Saqer	A04.5	1475	<i>A Penta-Band Shared Aperture Antenna with A Very Ratio Frequency for 5G and B5G Smartphone Applications</i>
Alkaraki, Shaker	A09b.1	872	<i>X-Band Reconfigurable Phase Shifters Based on SIW and Liquid Metal Technologies</i>
	A09b.5	891	<i>Liquid Metal Reconfigurable Phased Array Antenna</i>
	PA4.19	2186	<i>A Compact High-Gain 28 GHz Antenna Array for Beyond 5G Wireless Networks</i>
Alkhalifeh, Khaldoun	M3.4	2600	<i>Numerical Assessment of a Cognitive Chamber: TMz Case</i>
Allasia, Andrea	CS20b.3	402	<i>Measurements of Reconfigurable Intelligent Surface in 5G System Within a Reverberation Chamber at mmWave</i>
Almutawa, Ahmad	CS9a.6	534	<i>Strategies for Enhancing the Gain Bandwidth of Fabry-Pérot Cavity Antennas: A Review of Recent Advances</i>
Alomainy, Akram	PA7.18	1238	<i>Generation of Dual Band OAM Wave Using Single Patch Antenna for WLAN/WiMAX Applications</i>
	PA1.9	3366	<i>A Compact Implantable Camera Integrated MIMO Antenna with Polarization Diversity for Wireless-Capsule-Endoscopy Applications</i>
Alonso-delPino, Maria	CS37b.3	352	<i>Chessboard Focal Plane Array in Silicon Technologies for Terahertz Imaging</i>
	CS7.3	1601	<i>Experimental Characterization of a Core-Shell Lens for Antenna On-Package Integration at D-Band</i>
	M3.2	2590	<i>A Demonstration of Diffraction-Limited Images Using a CMOS Chessboard Array at THz Frequencies</i>
Alouini, Mehdi	CS44a.4	757	<i>High Data-Rate Sub-THz Coherent Near-Field Wireless Links Enabled by Spline-Profile Bessel Launchers</i>

	PA3.12	3442	<i>Shorted Stacked Patch Array for Photonic Beam Steering at mm-Waves</i>
Alshammari, Abdullah	PA1.11	3376	<i>Design of an UWB Conformal Antenna for Wireless Capsule Endoscopy</i>
	PA1.14	3390	<i>Miniaturized Implantable Antenna with Ultra-Wide Bandwidth Characteristics for Leadless Pacemakers</i>
Altakhaineh, Amjaad	A04.5	1475	<i>A Penta-Band Shared Aperture Antenna with A Very Ratio Frequency for 5G and B5G Smartphone Applications</i>
Alù, Andrea	E08.2	1868	<i>Reflective Intelligent Surfaces: Reducing Complexity by Controlling the Illuminating Field</i>
	A10.2	3071	<i>Analysis and Design of Metasurface Antennas Based on Temporal Metastructures</i>
Alvarez Narciandi, Guillermo	PA6.1	2213	<i>Orthogonal Coding for Millimeter-Wave Imaging Using MIMO Dynamic Metasurface Apertures</i>
	PM2.7	2454	<i>Near-Field Bistatic Microwave Imaging with Dynamic Metasurface Antennas</i>
	E04.3	2693	<i>A Case Study of Misalignment Errors for Range-Migration-Based Microwave Imaging with Multistatic Dynamic Metasurface Apertures</i>
	E04.4	2698	<i>GPR Imaging Relying on Frequency-Diverse Compressive Antennas</i>
	CS19b.5	4300	<i>Impact of the Unit Cell Distribution of 1-D Dynamic Metasurface Antennas on the Performance of a Computational Imaging System</i>
Álvarez Sánchez-Bayuela, Daniel	CS45.3	1808	<i>Preliminary Clinical Trial Results of MammoWave in the Context of RadioSpin Project</i>
Alvarez-Perez, Jose Luis	PP02.4	2505	<i>Multipath Model Improvement for Automotive Radar Application</i>
Alwakil, Ahmed	A21.2	1484	<i>Dual-Linearly Polarized Pillbox Beamformer in Hybrid CNC-PCB Technologies at W-Band</i>
Aman, Waqas	PP02.2	2495	<i>Pathloss-Based Non-Line-Of-Sight Identification in an Indoor Environment: An Experimental Study</i>
Amanatiadis, Stamatis	E05.2	2041	<i>On the Rigorous Design of Graphene-Based Periodic Structures Exploiting the Fundamental Resonances</i>
Ambroggi, Beatrice	CS26b.4	4318	<i>All-Metal Glide-Symmetric Slotted Planar Antennas: Modal Analysis</i>
Ambrosanio, Michele	CS24b.2	925	<i>On the In-Vivo Electrical Properties of Human Forearm at Microwave Frequency</i>
Amendola, Giandomenico	A27a.3	641	<i>K-Band Microstrip ESPAR Antenna Integrated into Large Array</i>
	PA2.14	1114	<i>Synthesis of a Planar 2D Butler Matrix: A Showcase with a 3x3 Array</i>
	PA2.23	1154	<i>Ka-Band Phased Antenna Array Concept for High-EIRP Satellite Connections</i>
Ameya, Michitaka	CS39b.4	823	<i>Millimeter Wave Vector Measurement System Using Low Frequency Band Oscilloscope</i>
Amin, Bilal	CS28.1	465	<i>Dielectric Characterisation of Human Parathyroid Glands at Microwave Frequencies</i>
	CS24b.1	920	<i>Microwave Tomography Bone Imaging: Analysing the Impact of Skin Thickness on the Reconstruction of Numerical Bone Phantoms</i>
Amini, Mohammad	PA5.18	3564	<i>Realizing Flat-Top Radiation Pattern with Sharp Cutoff for Reducing</i>

Hossein			<i>Lobing Fades</i>
Amiri, Majid	E13.6	289	<i>Highly Efficient Polarization-Insensitive EM Energy Harvester</i>
Ammann, Max	CS40a.2	1758	<i>Optimizing RF Energy Harvesting in IoT: A Machine Learning Estimation Considering Polarization Effects</i>
	PP03.4	3601	<i>Effect of Wave Polarization in On-Body Propagation for the 2.4, 24 and 60 GHz ISM Bands</i>
	A15b.5	4345	<i>Dual UWB Antennas on AoA Anchor Node</i>
Amos, Sonya	PA2.18	1132	<i>Study of Different Feed Layout Configurations for Hybrid Active VHTS Antennas</i>
Amra, Claude	A01a.3	2938	<i>Generation of Non-Diffractive Bessel Beams for Near-Field Links Applications Using Meta-Axicons</i>
An, Hao	CS39a.4	622	<i>Addressing PIM Challenges in Radio Base Stations: Field Issues and Testing Methods for Large-Scale Deployments</i>
Anagnostou, Dimitris	CS3.3	303	<i>Reconfigurable Polarisation Conversion Metasurface for mm-Wave Applications Using Vanadium Dioxide (VO₂)</i>
	E06b.4	804	<i>A Reconfigurable Phase Gradient Metasurface Resorber Offering Enhanced Beam Steering Capability and a Tuneable Transmission Band</i>
	E09.3	3914	<i>Analysis and Design of a Wideband Jaumann-Like Radar Absorber Offering High Angular Stability and Polarization Insensitivity</i>
Anam, Hafsa	PA8.11	2315	<i>Development of Passive Chipless RFID Temperature Sensor</i>
	PA8.12	2320	<i>Towards Array and Curve Analysis: Flexible Passive Chipless RFID Tags</i>
Anderson, Abby	PP02.14	2552	<i>Modeling Atmospheric Effects on over Land UHF Propagation Links</i>
Anderson, Chris	PP02.14	2552	<i>Modeling Atmospheric Effects on over Land UHF Propagation Links</i>
Andersson, Stefan	PA5.19	3569	<i>Beam Steering Performance Improvements Using a Layered Permittivity Dielectric</i>
Andriamiharivolamena, Tsitoha	CS39b.5	827	<i>Antennas and Power Measurement Techniques for Wireless Applications</i>
Andriulli, Francesco P.	CS19b.1	4282	<i>A Loop-Star Decomposition for the B-Spline Based Discretization of the Electric Field Integral Equation</i>
Andújar, Aurora	CS38.3	120	<i>Reconfigurable Architecture in a 130 x 80 mm² PCB with Antenna Booster Element for Multiband Operation in IoT Devices</i>
	CS38.4	124	<i>Ground Plane Width Analysis for IoT Devices Embedding Antenna Boosters</i>
Anelli, Francesco	A21.5	1498	<i>Feasibility Investigation on a Low-Cost an Air-Filled Substrate Integrated Waveguide Array Antenna in V-Band</i>
	A25.3	3095	<i>Design and Characterization of a Flexible Fabry-Perot Antenna Fabricated Using Conductive Inkjet Printing</i>
Angeletti, Piero	CS6a.6	216	<i>Development of a Circuit-Type Multiple-Agile Beamforming and Interference Mitigation Network</i>
	CS25.3	663	<i>Multibeam Phased Arrays Exploiting Frequency Dispersion for Massive MIMO Satellite Communications</i>
	CS25.4	668	<i>Aperture Distribution Method for Array-Fed Reflectors: A System Level Performance Case Study</i>

	CS10.5	868	<i>On the Scanning Properties of Bidimensional Discrete Lens Antennas with 1, 3, Infinite Focal Points</i>
	A19.3	1513	<i>Non-Regular Multibeam Coverage Antenna for Ka-Band High-Throughput Satellite Communications</i>
Angevain, Jean-Christophe	CS30a.2	3933	<i>Additively Manufactured Waveguide Hybrid Septum Coupler Optimized Using Machine Learning</i>
Angueira, Pablo	PP03.8	3620	<i>Empirical Characterization of Doppler in Industrial Wireless Channels</i>
Anguera, Jaume	CS38.3	120	<i>Reconfigurable Architecture in a 130 x 80 mm² PCB with Antenna Booster Element for Multiband Operation in IoT Devices</i>
	CS38.4	124	<i>Ground Plane Width Analysis for IoT Devices Embedding Antenna Boosters</i>
Anlage, Steven	CS20b.5	409	<i>Scattering Singularities of Complex Systems Probed with Continuously Variable Metasurfaces</i>
Annunziato, Andrea	A25.3	3095	<i>Design and Characterization of a Flexible Fabry-Perot Antenna Fabricated Using Conductive Inkjet Printing</i>
Ansari, Maral	CS6b.6	509	<i>3D-Printed Multi-Beam Flat Lens Antenna System</i>
Anstey, Dominic	CS4.2	3181	<i>Mitigating Zenith Blindness from Mutual Coupling in a Sunflower Phased Array</i>
Antar, Yahia	P05.2	246	<i>Multifunction Over-The-Horizon Radar for Space Domain Awareness</i>
Antoine, Gaëtan	PA6.9	2245	<i>Study of the Frequency Dispersion of 3D-Printed Dielectric Crystals for Dielectric Resonator Antenna Applications</i>
	A25.4	3100	<i>3D-Printed Circular Polarized Dielectric Resonator Antenna with Enhanced Axial Ratio Bandwidth Using Anisotropic Material</i>
Antolinos, Elías	CS21.3	2712	<i>From mmWave Radar Nodes to Multistatic Arrays: Design Considerations and Applications</i>
Antón Ruiz, Alejandro	M2.4	3895	<i>K-Factor Evaluation in a Hybrid Reverberation Chamber plus CATR OTA Testing Setup</i>
Antonelli, Paolo	PP02.13	2547	<i>Radiometeorological Forecasts for Satellite Links Operations: Validation with Measurements from BepiColombo Mission</i>
	P10b.3	3254	<i>Exploiting Numerical Weather Prediction Data for Radiopropagation Modeling of SatCom Links</i>
Antonini, Giulio	E02a.5	3016	<i>Improved PEEC Modeling of Antennas Through Time-Dependent Partial Elements</i>
Antonino-Daviu, Eva	CS19a.2	4072	<i>Surface Partial Differential Equations and Its Applications to Scattering Problems</i>
Antonsen, Thomas	CS20b.5	409	<i>Scattering Singularities of Complex Systems Probed with Continuously Variable Metasurfaces</i>
Antony, Linta	CS36a.1	700	<i>Angle of Arrival Estimation Methods Using Spherical-Modes-Driven Multiport Antennas</i>
Anwar, Shoaib	CS2.4	180	<i>Advanced Post-Processing Technique to Evaluate Specific Absorption Rate (SAR) for a Standard Dipole Antenna</i>
	CS5b.3	374	<i>Industrial Design Validation for a Plane Wave Generator at 28GHz</i>
Araghi, Ali	PA2.9	1091	<i>Sub-7 GHz Circularly Polarized Dielectric Resonator Antenna Array for Full-Duplex Applications</i>
	A25.1	3087	<i>Long Slot Dielectric-Loaded Periodic Leaky-Wave Antenna Based on</i>

3D Printing Technology

Arai, Hiroyuki	CS36a.5	719	<i>A Parasitic Element Technique for Deep Null Synthesis and the Application to Received Signal Strength (RSS)-Based Localization</i>
	PA4.4	2119	<i>Prototype of Multi-Sector Indoor mmW Base Station Based on 5G NR Beam Control</i>
Araque Quijano, Javier Leonardo	A17.2	3744	<i>Series-Fed Loop Antenna Array Deployable by a Scissors Mechanism</i>
Araújo, Nuno	CS28.2	470	<i>The Effect of Pressure of the Open-Ended Coaxial Probe on the Measurement of Ex Vivo Biological Tissues Dielectric Properties</i>
Arboleya, Ana	A06b.4	3301	<i>Dual-Band Reflectarray-Based Electromagnetic Skin to Provide Millimeter-Wave Coverage in the 28/60-GHz Bands</i>
Arduino, Alessandro	E01.2	2019	<i>Assessment of the Feasibility of Breast Lesion Detection with Contrast Source Inversion for Microwave Tomography: A Virtual Experiment</i>
	CS33a.4	3057	<i>An Electric Properties Tomography Approach Inspired by the Boundary Element Method</i>
Arenare, Davide	PA2.19	1136	<i>Improving the Strut Modelling of the European Space Agency Deep Space Antennas to Evaluate Efficiency and Sidelobe Impact</i>
Arias, Marcos	CS21.3	2712	<i>From mmWave Radar Nodes to Multistatic Arrays: Design Considerations and Applications</i>
Arias Campo, Marta	CS10.3	860	<i>D-Band Active Antenna Array with Lens Enabling Quasi-Optical and Analogue Beam Reconfiguration for 6G Applications</i>
Arnieri, Emilio	A27a.3	641	<i>K-Band Microstrip ESPAR Antenna Integrated into Large Array</i>
	PA2.14	1114	<i>Synthesis of a Planar 2D Butler Matrix: A Showcase with a 3x3 Array</i>
	PA2.23	1154	<i>Ka-Band Phased Antenna Array Concept for High-EIRP Satellite Connections</i>
Arnold, David	PP02.7	2520	<i>Electromagnetic Beerline Cleaning Using Radio Frequency Signals</i>
Arnold, Louis	PP02.7	2520	<i>Electromagnetic Beerline Cleaning Using Radio Frequency Signals</i>
Aronsson, Jonatan	PE1.14	1292	<i>Integral Equation-Based Solver for the Simulation of Metasurface Designs</i>
Arrebola, Manuel	CS44b.3	950	<i>Multibeam Metal-Only Groove Gap Waveguide-Based Array in E-Band</i>
	CS8.5	2899	<i>Dual-Resonance SIW-Based Reflectarray Unit Cell for Broadband Applications</i>
	A06a.1	3021	<i>Large and Deployable Multi-Faceted Antennas Based on Single-Layer Reflectarrays</i>
	A06b.2	3291	<i>Experimental Validation of Reflectarray-Based Base Station Antenna for Simultaneous Front- and Radio Back-Haul Links in mm-Wave Frequencies</i>
Arriola, Aitor	CS35a.1	1683	<i>Design and Validation of a Wireless Network for Intra-Train Communications</i>
Arshad, Kamran	CS13.5	1568	<i>UHF RFID Sensor Antenna for Fat Content and Adulteration Detection of Milk</i>
Arshed, Talha	CS20a.4	99	<i>Accurate Design of Surface-Wave Enabled Reflective Intelligent Surfaces Through the Generalized Oliner Method</i>
Arslanagić, Samel	PM2.4	2443	<i>Validation of the DTU ETC Scattering Test Facility for Radar Cross Section Measurements</i>

	E11.3	2806	<i>Bound States in the Continuum in Cylindrical Impedance Surface Cavities</i>
Arts, Michel	CS4.1	3176	<i>Analysis of a Small LOFAR Low-Band Test Array Using a Sky Map, Simulated Embedded Element Patterns and Measured LNA-Impedances</i>
Arvidsson, Klas	M2.4	3895	<i>K-Factor Evaluation in a Hybrid Reverberation Chamber plus CATR OTA Testing Setup</i>
Ashrafian, Atefeh	PE2.14	1044	<i>Tunable Rectangular Waveguide Bandpass Filter Based on Plasma Technology</i>
Asim, Muhammad	PP02.2	2495	<i>Pathloss-Based Non-Line-Of-Sight Identification in an Indoor Environment: An Experimental Study</i>
Asimonis, Stylianos	PA5.14	3549	<i>Super-Realized Gain Huygens Antennas</i>
	PA5.17	3560	<i>Low-Profile Super-Realised Gain Antennas</i>
Askar, Ramez	CS43b.2	4173	<i>Comparison of Sub-THz Radio Channel Characteristics at 158 GHz and 300 GHz in a Shopping Mall Scenario</i>
Aslam, Muhammad	PA4.19	2186	<i>A Compact High-Gain 28 GHz Antenna Array for Beyond 5G Wireless Networks</i>
Aslan, Yanki	CS6a.6	216	<i>Development of a Circuit-Type Multiple-Agile Beamforming and Interference Mitigation Network</i>
	A15b.4	4340	<i>Sunflower Array of Infinitesimal Dipoles for Constrained Antenna Modeling</i>
Asplund, Henrik	CS43a.5	3972	<i>Feasibility of High Throughput Wireless Communication Above 100 GHz in Indoor Scenarios</i>
Asrih, Nawfal	CS39b.5	827	<i>Antennas and Power Measurement Techniques for Wireless Applications</i>
Assaleh, Khaled	CS13.5	1568	<i>UHF RFID Sensor Antenna for Fat Content and Adulteration Detection of Milk</i>
Ataloglou, Vasileios	CS17a.2	6	<i>3D Method-Of-Moment Design of Huygens' Metasurfaces</i>
Athanasiadou, Georgia	PP01.5	1365	<i>Field Trials for Different 5G NSA Cellular Networks</i>
	PP03.5	3605	<i>Modeling Received Power from 4G and 5G Networks in Greece Using Machine Learning</i>
Attila, Géczy	CS3.5	311	<i>Exploring PLA/Flax Substrates for Antenna Applications: Assessing Moisture, Temperature and Dielectric Constant Homogeneity</i>
Attoun, Zaynab	A20.2	3816	<i>Stretchable Multi-Band Radio Frequency Sensor for Strain Measurement</i>
Attwood, Nicholas	CS35b.3	1913	<i>mmWave Channel Sounding for Vehicular Communications</i>
Attygalle, Manik	A10.1	3066	<i>Multi-Feed Resonant Cavity Antenna with In-Antenna Power Combination for mm-Wave Communication</i>
Audia, Samuel	A28.5	3734	<i>Indoor Wireless Signal Modeling with Smooth Surface Diffraction Effects</i>
Augustine, Robin	CS27.2	1575	<i>An Electromagnetic Metasurface for Impedance Matching in Microwave Biomedical Applications</i>
	CS27.4	1584	<i>A Compact Wideband Biocompatible Circularly Polarized Implantable Flexible Antenna for Biomedical Applications</i>
	PA6.12	2260	<i>An Efficient Wireless Power Transfer System Using Transmission and</i>

			<i>Reflection Characteristics of Metamaterial</i>
	P06.2	2732	<i>Development of Tissue Emulatory Models/Phantoms of Lungs at Microwave Frequency for Acute Respiratory Distress Syndrome</i>
	PP03.7	3615	<i>SINTEC Comparative Body-Centric Communication Study: Bluetooth Vs Fat-Intrabody Communication</i>
	PP03.11	3635	<i>Brain Hemorrhage Detection Using Antenna System Integrated with Imaging Algorithm</i>
	A20.3	3818	<i>Compact Antenna Solutions for Data Transmission Using Fat-Intrabody Communication (Fat-IBC)</i>
Austin, Andrew	P05.3	251	<i>Characterisation of Thin Glass-Fibre Substrates for Deployable SAR Antennas</i>
	P02.5	3782	<i>Mechanical Vibrations on a Deployable Nanosatellite Antenna: SAR Performance Analysis</i>
awada Mislmani, Narimane	E06b.5		<i>Metasurface Solution for Generating 3D-Curved Beams in Road Environments: A Numerical Study</i>
Awan, Wahaj	PA8.7	2298	<i>Compact Size Frequency-Agile Antenna Enabling Multi-Mode Functionality for Internet of Things Applications</i>
Aydin Civi, Ozlem	PA5.12	3542	<i>Highly Transparent and Efficient Flexible Antenna for Vehicle-To-Everything (V2X) Applications</i>
Ayestarán, Rafael	CS15.1	4001	<i>Time-Modulated Arrays for Simultaneous Wireless Information and Power Transfer in Near-Field</i>
Ayllon, Noelia	PP02.19	2577	<i>Annual Statistics from 5 Years of 1-Minute Rainfall Rate Measurements at a Specific Site in Bolivia</i>
Ayop, Osman	E12.4	2832	<i>Compact Dual-Band Crossover with Enhanced Band Ratio Using Interdigital Capacitor for 5G Applications</i>
Aziz, Abdul	PA7.18	1238	<i>Generation of Dual Band OAM Wave Using Single Patch Antenna for WLAN/WiMAX Applications</i>

B

Baala, Oumaya	CS11.5	1631	<i>Fine Tuning an AI-Based Indoor Radio Propagation Model with Crowd-Sourced Data</i>
Babae, Amirhossein	CS37b.4	357	<i>Increasing the Efficiency-Bandwidth Product and Impedance Bandwidth of Electrically-Small Antennas Through Parametric Space-Time Variation</i>
Baccarelli, Paolo	CS9b.5	531	<i>Modal Analysis in Woodpile Dielectric Structures</i>
Baccin-Smith, Francis	CS36b.5	916	<i>Multi-Directional Leaky-Wave Antenna with Independent Beam-Scanning Laws</i>
Badia, Mario	CS45.3	1808	<i>Preliminary Clinical Trial Results of MammoWave in the Context of RadioSpin Project</i>
Badis, Hakim	CS35b.4	1917	<i>Experimental Evaluation of V2X Connectivity Technologies with V2X Channel Models</i>
Baena-Molina, Marcos	PA3.8	3424	<i>1-Bit RIS Unit Cell with Mechanical Reconfiguration at 28 GHz</i>
Bagci, Hakan	PE2.12	1036	<i>A Discontinuous Galerkin Time-Domain Scheme to Model Lasing Dynamics in Four-Level Two-Electron Atomic Systems</i>
Baghel, Amit	A17.5	3759	<i>The Novel Method for Deployable Parabolic Reflector Based on Uchiwa Origami</i>

Baghel, Naman	A27a.5	650	<i>A Novel Substrate Integrated Broadband Dielectric Resonator Antenna (DRA) in SICL for Millimeter Wave Application</i>
Bagheri, AmirMasood	PE1.11	1279	<i>Compact Polarization Converter on a Thin Ferrite-Based Metasurface for Enhanced 5G Wireless Communication</i>
	PA4.13	2160	<i>A Novel Precise Approach for Digital Metasurface Configuration for Sensing Application</i>
Bakr, Mustafa	E13.3	275	<i>Superconducting Space-Time Modulation: Theoretical Implications and Mixing-Beamsplitting Functionality</i>
Baktur, Reyhan	PA5.12	3542	<i>Highly Transparent and Efficient Flexible Antenna for Vehicle-To-Everything (V2X) Applications</i>
Baladi, Elham	A06a.4	3036	<i>Large, Multi-Faceted Reflectarray with Quasi-Constant Directivity in the V-Band</i>
Balasingham, Ilangko	CS13.1	1553	<i>Antenna System for Simultaneous Wireless Power and Information Transfer to Brain Implants</i>
Baldelli, Marco	A19.3	1513	<i>Non-Regular Multibeam Coverage Antenna for Ka-Band High-Throughput Satellite Communications</i>
Ball, Edward	PP01.3	1355	<i>The Time Modulated Array for Channel Sounding Measurements - Concept and Initial Field Tests</i>
	A12a.5	1724	<i>Antenna Array and GaAs Phase Shifter MMIC for Millimeter Wave Beamforming - Co-Simulation and Measurements</i>
	A02.2	3696	<i>Subsampling Time-Modulated Array for Reduced Hardware down Conversion and Beamforming</i>
Bandyopadhyay, Baisakhi	PE3.2	2364	<i>Polarization Insensitive Broadband Frequency Selective Resorber with Improved Selectivity for Stealth Applications</i>
Bang, Jihoon	CS29.1	3787	<i>AI-Based Environment Segmentation Using a Context-Aware Channel Sounder</i>
Bang, Seungwoo	CS17b.4	330	<i>Indoor Coverage Enhancement Employing Liquid Crystal-Based Massive Reconfigurable Intelligent Surface Linked to 5G FR2 Base Station</i>
	CS7.2	1596	<i>Simultaneously Dual-Polarization Convertible Sub-THz Reconfigurable Intelligent Surface Enabled by Through-Quartz VIAs</i>
Bansal, Aakash	PE1.7	1265	<i>Design of a Concentric Circular Holographic Metasurface Using Hexagonal Anisotropic Unit-Cell for Wireless Communications</i>
	PP01.13	1404	<i>Half Mode Corrugated Substrate Integrated Waveguide (HM-CSIW) Band-Stop Filter Using Hexagonal Ring Resonators</i>
	A08a.5	1900	<i>Wideband Half-Elliptical Ring Slot Array Loaded Leaky Wave Antenna on a Half-Mode Corrugated Substrate Integrated Waveguide</i>
	PA6.6	2235	<i>Experimental Results for Carbon Nanotube-Sheet Based Microstrip Patch Antenna</i>
	CS14a.4	4142	<i>Optimal Morphing Metasurface Lens for Next Generation RF Sensing and Communications</i>
Banting, Lucas	CS33b.3	3317	<i>Microwave Inversion of Measured S-Parameters Using a Thin-Wire Antenna Model</i>
Bao, Junwei	PM1.3	1318	<i>Impact of 6D Mobility on Doppler Characteristics of UAV-To-Vehicle Channels</i>

Baquero-Escudero, Mariano	PA2.13 PA4.9	1110 2142	<i>Closely-Spaced Groove Gap Waveguides with Reduced Coupling</i> <i>5x7 Nolen Matrix in K-Band Implemented in Rectangular Waveguide</i>
Barbary, Ines	CS42b.1	439	<i>An Antenna Measuring System Based on a Cable Suspended Dolly and Inverse Source</i>
Barbieri, Stefano	PP02.11	2538	<i>AlphaSat Ka-Band and Q-Band Receiving Station in Rome: Measurements and Data Analysis</i>
Barbiroli, Marina	P09.3	2644	<i>Ka-Band Rain Attenuation Derived from a MEO Satellite Constellation</i>
	CS20b.2	398	<i>A Macroscopic Bilateral Modeling Approach for Reflective and Transmissive Metasurfaces</i>
	CS43b.3	4178	<i>Machine Learning Approach to Delay Spread Estimation in Industrial Environments</i>
Barbuto, Mirko	CS43b.4	4183	<i>A Study on Satellite-To-Ground Propagation in Urban Environment</i>
	E08.2	1868	<i>Reflective Intelligent Surfaces: Reducing Complexity by Controlling the Illuminating Field</i>
	E08.5	1880	<i>Static and Reconfigurable Phase-Gradient Metasurfaces for Antenna Applications</i>
	PA4.10	2147	<i>Analysis and Design of Robust Reconfigurable Intelligent Surfaces Using a Statistical Approach</i>
Barendsz, Laura	A10.2	3071	<i>Analysis and Design of Metasurface Antennas Based on Temporal Metastructures</i>
	CS28.4	480	<i>Phantom Material with Biological Composition for Muscle Equivalent Radiofrequency, Thermal and Magnetic Resonance Properties</i>
	CS4.5	3194	<i>CSIRO Radio Astronomy Receiver Update - Ultra Wideband and Phased Array Feeds</i>
Barowski, Jan	CS12b.2	4263	<i>Robotic Antenna Characterization System Based on Wideband FMCW Transceiver Modules</i>
Bartle, Hannes	A24.5	3876	<i>Design Recommendations for Minimal Antenna Mutual Coupling Using Current Optimization</i>
Bartolić, Juraj	PA1.10	3371	<i>Textile Waveguide Antennas for On-Body Sensor and Communication Systems</i>
Bartolomei, Nicola	CS25.5	673	<i>TX/RX Terminal Based on Metascreen Technology for Ka-Band Satcom with Dual Switchable Polarization</i>
Barton, John	PA1.6	3354	<i>Miniaturised Magnetic Antenna for Wireless Implanted Medical Device</i>
Bartone, Chris	E06a.1	586	<i>Contiguous Broadband Circularly Periodic High Impedance Surface Integrated with a Spiral Antenna</i>
	E09.4	3919	<i>Progressive Ultra-Wideband Circularly Periodic High Impedance Surface Integrated with a Spiral Antenna</i>
Baselmans, Jochem	PA4.16	2174	<i>Design of Wide Band Multi-Lens Focal Plane Arrays for the TIFUUN Instrument</i>
Bashir, Gazali	PA4.18	2181	<i>A Wideband 3D Printed Digital Metasurface Transmitarray Antenna for mm-Wave Applications</i>
Bashir, Muhammad Faisal	PA4.24	2206	<i>Design and Investigation of 2x2 Dielectric Resonator Antennas Array for Sub-THz Applications</i>
Bastia, Lorenzo	CS36b.4	911	<i>Simplified Frequency-Diverse Array Architecture for Surveillance Purposes</i>

Bastianelli, Luca	CS20b.3	402	<i>Measurements of Reconfigurable Intelligent Surface in 5G System Within a Reverberation Chamber at mmWave</i>
	CS22a.4	2853	<i>Quantum Optimisation of Reconfigurable Surfaces in Complex Propagation Environments</i>
	CS22a.5	2858	<i>Real-System Variational Quantum Eigensolver for Electromagnetic Waveguides: A Benchmark Study</i>
Basu, Ananjan	PA5.13	3546	<i>A Reactively Coupled Bi-Directional Dual CP Antenna</i>
	PA5.15	3552	<i>A Decoupling Scheme for Closely Spaced Microstrip Patch Antenna</i>
Batel, Lotfi	PA8.9	2306	<i>Whip Antenna Miniaturization at VHF Band Using Magneto-Dielectric Materials</i>
Battaglia, Giada	M5.5	557	<i>Near Field Phase Recovery Exploiting Only One Measurement Surface and A Smart Warping Sampling Strategy</i>
	A15a.2	4115	<i>Extending Spectral Factorization to the 2-D Mask-Constrained Power Synthesis of Shaped Beams with Arbitrary Footprints</i>
Baur, Holger	M3.3	2595	<i>Dielectric Characterization of Adhesives for THz Packaging in WR6.5, WR3.4 and WR2.2 Bands</i>
Beach, Mark	PP01.14	1407	<i>Analog Self-Interference Cancellation by Means of a Synchronised Signal Injection</i>
	PA5.22	3581	<i>DRL-Based Sidelobe Suppression for Multi-Focus Reconfigurable Intelligent Surface</i>
Beaskoetxea, Unai	A08a.4	1897	<i>Ka-Band USS Enterprise (NCC-1701) Antenna</i>
Beccaria, Michele	A10.3	3074	<i>Curved Electromagnetic Skins for Urban Scenarios</i>
	A06b.1	3287	<i>Folded Dielectric Reflectarray with Spherical Polarizer</i>
Beccherelli, Romeo	PE3.10	2398	<i>Highly Reflective, Low-Loss, Homogenized Fishnet Metasurfaces at Terahertz: Design and Experiment</i>
Bechoo, Keshav	CS4.4	3189	<i>The Hydrogen Intensity Real-Time Analysis eXperiment: Overview and Status Update</i>
Bechrakis Triantafyllos, Alexandros	A08a.2	1888	<i>On the Asymptotic Evaluation of the Near-Field in Resonant Leaky-Wave Antennas Using a Non-Uniform Phase Center</i>
Becker, Dennis	A18.5	2923	<i>On the Cost-Effectiveness of Using Beamforming at the Ground Station for Aeronautical Communications</i>
Beckman, Claes	PA5.7	3519	<i>Analysis and Measurement of Key Performance Indicators for MIMO Antennas</i>
Bedia, Beatriz	A19.2	1508	<i>Polymer-Based Additive Manufacturing of a Complex RF Front-End for New Space Applications</i>
Behdad, Nader	CS37a.3	37	<i>A Class-E, Switched-Mode, Non-LTI Electrically-Small Transmit Antenna Design for Overcoming the Fundamental Bandwidth-Efficiency Product Limits</i>
Beijnen, Laurens	A05.4	1833	<i>Time Domain Analysis of Pulsed Photo-Conductive Antenna Sources: Distributed Excitations</i>
Bekker, Elizabeth	A05.1	1820	<i>Sub-THz Substrate Integrated Waveguide Signal Transitions in Backend-Of-Line of a Silicon Process</i>
	A05.3	1828	<i>110 to 170 GHz High-Gain Antenna with Embedded Surface Mount Short Horn and Baseband PCB Horn Antenna</i>
Bellizzi, Gennaro	CS33a.3	3054	<i>Advancements in Broadband Electromagnetic Sensing for Food Quality</i>

			<i>Control</i>
Bellofiore, Simone	PP02.13	2547	<i>Radiometeorological Forecasts for Satellite Links Operations: Validation with Measurements from BepiColombo Mission</i>
Beloin, Spencer	CS22a.5	2858	<i>Real-System Variational Quantum Eigensolver for Electromagnetic Waveguides: A Benchmark Study</i>
Ben Mabrouk, Ismail	PA1.2	3336	<i>Dual-Band 3-D MIMO Antenna for Deep Tissue Devices</i>
	PA1.11	3376	<i>Design of an UWB Conformal Antenna for Wireless Capsule Endoscopy</i>
	PA1.14	3390	<i>Miniaturized Implantable Antenna with Ultra-Wide Bandwidth Characteristics for Leadless Pacemakers</i>
Benaicha, Hajar	CS27.3	1579	<i>Theoretical Insights and Engineering of Wireless Body-Implanted Bioelectronics</i>
Benarroch, Ana	PP02.20	2582	<i>Comparison Between ERA5 Cloud Parameters and Rainfall Rate in Madrid</i>
	P09.1	2634	<i>Variability of Rain Attenuation at Millimeter Waves Due to Fluctuations of the Drop Size Distribution</i>
Bencivenni, Carlo	CS21.4	2717	<i>Low-Cost Coaxial Slot Array Antenna for E-Band Automotive Corner Radar Applications Based on Gap Waveguide MLW Technology</i>
	A28.1	3714	<i>Antenna and Mechanical Co-Design for Auto-Beam-Tracking in Backhaul Systems</i>
Benedic, Yohann	PP03.9	3625	<i>Indoor Localization of Smartphones Thanks to Zero-Energy-Devices Beacons</i>
Benjamin, Pierre	PE2.3	999	<i>Management of Radiofrequency Compatibility on Aircraft</i>
Benjelloun, Nabil	M5.4	552	<i>Thermoelectric Cooling Solution for Active Antennas</i>
Bennett, Elliot L.	PA7.4	1176	<i>Passive Beamforming with Liquid Antennas: Techniques and Implementation</i>
	PA5.5	3511	<i>Pulse Preserving Capability of an Ultrawideband Dispersive Dielectric Resonator Antenna</i>
Bentum, Mark	A18.3	2914	<i>Active Antenna Design for Lunar-Based Detection of Global 21cm-Signals from the Dark Ages</i>
	CS4.1	3176	<i>Analysis of a Small LOFAR Low-Band Test Array Using a Sky Map, Simulated Embedded Element Patterns and Measured LNA-Impedances</i>
Berbineau, Marion	CS35b.3	1913	<i>mmWave Channel Sounding for Vehicular Communications</i>
	CS35b.4	1917	<i>Experimental Evaluation of V2X Connectivity Technologies with V2X Channel Models</i>
Bergman, Jan	CS38.1	112	<i>Improving Scan Gain of Sparse Vivaldi Array with Parasitic Scatterers</i>
	CS37b.2	348	<i>Crack Stop as a Coupling Element Between an IC Chip and Antenna</i>
	CS40b.1	1969	<i>Small On-Metal Passive UHF RFID Transponders with Long Read Ranges</i>
Bergmann, Jose	E02b.4	3279	<i>A Higher-Order Spectral Element Method to Model Eccentric Anisotropic Two-Layer Waveguides via Conformal Transformation Optics</i>
Bermudez Arboleda, Maria	CS37b.1	344	<i>3D Spatially Reconfigurable Circularly Polarized Antenna in Package with Embedded Electronics</i>

Bernard, Loic	PA7.5	1180	<i>Design of Optimized Cylindrical Structural Antenna with Quasi Length Insensitivity Using CMA</i>
	A13.5	1965	<i>Circularly-Polarized Wideband Conformal Magneto-Electric Antenna Covering the GNSS Bands</i>
Bernard, Xavier	CS41.1	3220	<i>UnderGround-To-AboveGround IoT Communication Links Insurance at 915 MHz Using LoRa Technology</i>
Bernardini, Livio	PP02.13	2547	<i>Radiometeorological Forecasts for Satellite Links Operations: Validation with Measurements from BepiColombo Mission</i>
	P10b.3	3254	<i>Exploiting Numerical Weather Prediction Data for Radiopropagation Modeling of SatCom Links</i>
Bertrand, Matthieu	A16.2	1734	<i>Low-Profile 2D-Mechanical-Beam-Steering Antenna with Large Field-Of-View</i>
	A01a.3	2938	<i>Generation of Non-Diffractive Bessel Beams for Near-Field Links Applications Using Meta-Axicons</i>
Beruete, Miguel	A08a.4	1897	<i>Ka-Band USS Enterprise (NCC-1701) Antenna</i>
Berweger, Samuel	CS5a.1	56	<i>Context-Aware Channel Sounder for AI-Assisted Radio-Frequency Channel Modeling</i>
	CS29.1	3787	<i>AI-Based Environment Segmentation Using a Context-Aware Channel Sounder</i>
Besler, Brendon	CS45.2	1803	<i>Physics-Informed Regularization for Microwave Imaging in Biomedical Applications</i>
Beumer, Steven	CS28.4	480	<i>Phantom Material with Biological Composition for Muscle Equivalent Radiofrequency, Thermal and Magnetic Resonance Properties</i>
Bevacqua, Martina Teresa	CS24b.2	925	<i>On the In-Vivo Electrical Properties of Human Forearm at Microwave Frequency</i>
	E01.5	2033	<i>A Smart Convenient Rewriting of the Inverse Scattering Equations for the 3D Scalar Problem</i>
Bevilacqua, Florindo	CS42b.3	446	<i>Phaseless Characterization of Flat Sources with a Planar Wide-Mesh Scanning Strategy</i>
Bhatia, Gurjot Singh	CS17a.3	10	<i>Exploring RIS Coverage Enhancement in Factories: From Ray-Based Modeling to Use-Case Analysis</i>
Bhatporia, Shruti	CS4.4	3189	<i>The Hydrogen Intensity Real-Time Analysis eXperiment: Overview and Status Update</i>
Bhutani, Akanksha	A05.1	1820	<i>Sub-THz Substrate Integrated Waveguide Signal Transitions in Backend-Of-Line of a Silicon Process</i>
	A05.3	1828	<i>110 to 170 GHz High-Gain Antenna with Embedded Surface Mount Short Horn and Baseband PCB Horn Antenna</i>
	M3.1	2586	<i>Enhancing THz Antenna Characterization Precision in WR-1.5 Band Using Vacuum Waveguide Flange</i>
	M3.3	2595	<i>Dielectric Characterization of Adhesives for THz Packaging in WR6.5, WR3.4 and WR2.2 Bands</i>
Bianco, Giulio	PA8.3	2278	<i>Flexible Antenna with Microfluidics for the Quantification of Liquid Micro-Volumes</i>
Biedma-Pérez, Andrés	CS26a.1	4090	<i>Glide-Symmetric SIH Unit Cells Implemented in Parallel-Plate Waveguides at mmWaves</i>

Bigotti, Alessandra	CS45.3	1808	<i>Preliminary Clinical Trial Results of MammoWave in the Context of RadioSpin Project</i>
Bilal, Rana Muhammad Hasan	PE1.15	1295	<i>D-Band Absorber Comprising Tantalum Nitride-Based Resistively-Loaded High Impedance Surfaces</i>
Bilgic, Mustafa Murat	CS39a.3	618	<i>Full Wave Modelling and Design of a Baffle for the HERTZ 2.0 Compact Antenna Test Range</i>
	A18.1	2904	<i>Uncertainty Quantification for the Reflector Antenna in the Copernicus Imaging Microwave Radiometer</i>
	A18.4	2919	<i>Method of Moment Simulation of Full Arctic Weather Satellite Structure</i>
	A06a.2	3026	<i>Direct Optimisation of a Five-State Reconfigurable Reflectarray for 5G Applications</i>
Bilir, Ahmet	CS28.5	485	<i>Temperature-Dependent Electrical Characterization of a Thermally Sensitive Hepatic Tumor Phantom</i>
	CS27.5	1588	<i>Biodegradable Implant Antenna Utilized for Real-Time Sensing Through Genetically Modified Bacteria</i>
Bilitos, Christos	A16.3	1739	<i>Wideband Beam-Steering Continuous Transverse Stub Array Enabled by a Reflecting Luneburg Lens at Ka-Band</i>
Bilotti, Filiberto	E08.2	1868	<i>Reflective Intelligent Surfaces: Reducing Complexity by Controlling the Illuminating Field</i>
Bilotti, Filiberto	E08.5	1880	<i>Static and Reconfigurable Phase-Gradient Metasurfaces for Antenna Applications</i>
	PA4.10	2147	<i>Analysis and Design of Robust Reconfigurable Intelligent Surfaces Using a Statistical Approach</i>
	E12.3	2829	<i>Time-Modulated Metasurface-Based System for the Generation of False Radar Targets</i>
	A10.2	3071	<i>Analysis and Design of Metasurface Antennas Based on Temporal Metastructures</i>
Biscarini, Marianna	P03.2	1533	<i>Advanced Microwave Radiometry: Refining Sun-Tracking Technique for Atmospheric Attenuation Retrieval and Sun Brightness Temperature Estimation</i>
	PP02.11	2538	<i>AlphaSat Ka-Band and Q-Band Receiving Station in Rome: Measurements and Data Analysis</i>
	PP02.13	2547	<i>Radiometeorological Forecasts for Satellite Links Operations: Validation with Measurements from BepiColombo Mission</i>
	P09.3	2644	<i>Ka-Band Rain Attenuation Derived from a MEO Satellite Constellation</i>
	P10b.3	3254	<i>Exploiting Numerical Weather Prediction Data for Radiopropagation Modeling of SatCom Links</i>
Bischoff, Jens	CS2.3	175	<i>Long-Term Network-Based Assessment of the Actual Output Power of Base Stations in a 5G Network</i>
Bisio, Igor	CS45.5	1815	<i>Brain Stroke Microwave Diagnostics in Children Through a Nonlinear Inverse-Scattering Technique</i>
Biswas, Bishakha	PP03.11	3635	<i>Brain Hemorrhage Detection Using Antenna System Integrated with Imaging Algorithm</i>
Björninen, Toni	A20.5	3827	<i>Quad-Band Meandered Implantable Planar Inverted-F Antenna for Wireless Brain Health Monitoring</i>

Björnson, Emil	CS17a.5	19	<i>Nonlinear Distortion Issues Created by Active Reconfigurable Intelligent Surfaces</i>
Blanco, Darwin	CS16.6	582	<i>A Multiband Leaky-Wave Phased Array Antenna for 5G Fixed Link Communications</i>
Bland, Xavier	M5.2	542	<i>Uncertainty Analysis of Linear Multi-Probe Array Systems for Fast Antenna Measurements</i>
Bleszynski, Elizabeth	CS19a.1	4068	<i>The d'Alembertian Representation of Green's Functions and Evaluation of Surface Integrals over Non-Parallel Planes</i>
Bleszynski, Marek	CS19a.1	4068	<i>The d'Alembertian Representation of Green's Functions and Evaluation of Surface Integrals over Non-Parallel Planes</i>
Blin, Thierry	M5.2	542	<i>Uncertainty Analysis of Linear Multi-Probe Array Systems for Fast Antenna Measurements</i>
	CS41.2	3225	<i>VHF/UHF Antenna Measurements Based on Multi Probe Array Technology</i>
Blumenstein, Jiri	CS43b.1	4168	<i>Channel Measurements and Characterization in Industrial Environment at 60 GHz</i>
BniLam, Noori	PA2.15	1119	<i>Feasibility Study of 3D Printed Luneburg Lens Using Fused Deposit Material 3D Printing Technology for Ku-Band Application</i>
Boasman, Neil	CS46.2	4219	<i>Digital Beamformer for GNSS Reflectometry and Radio Occultation Applications</i>
Boban, Mate	P04b.3	975	<i>Ray Tracing and Measurement-Based Characterization of Inter/Intra-Machine THz Wireless Channels</i>
	CS23b.5	2009	<i>Characterization of Propagation from Measurements at Sub-THz for ISAC Applications in an Emulated Dynamic Industrial Scenario</i>
	P10a.4	2987	<i>Direct Clustering and Multi-Path Component Identification on THz Channel Measurements in a Factory Environment</i>
Boccia, Luigi	A27a.3	641	<i>K-Band Microstrip ESPAR Antenna Integrated into Large Array</i>
	PA2.14	1114	<i>Synthesis of a Planar 2D Butler Matrix: A Showcase with a 3x3 Array</i>
	PA2.23	1154	<i>Ka-Band Phased Antenna Array Concept for High-EIRP Satellite Connections</i>
Bodehou, Modeste	PA2.21	1145	<i>Wideband Low-Profile Circularly Polarized All-Metal Antenna for Triton Exploration</i>
	E02a.4	3012	<i>Dispersion Curve Calculation Using the Method of Moments: The Impact of Macro Basis Functions</i>
Bodi, Anuraag	CS5a.1	56	<i>Context-Aware Channel Sounder for AI-Assisted Radio-Frequency Channel Modeling</i>
	CS29.1	3787	<i>AI-Based Environment Segmentation Using a Context-Aware Channel Sounder</i>
Boerninck, Stefan	PE2.3	999	<i>Management of Radiofrequency Compatibility on Aircraft</i>
Boix, Rafael	A01a.2	2933	<i>Design of Broadband Stacked Patch Microstrip Antennas Fed by Differential Microstrip Lines with Large Common-Mode Rejection</i>
	E02a.1	2997	<i>Efficient NUFFT-Based Spectral Domain Method of Moments Analysis of Multilayered Periodic Structures with Subsectional Basis Functions</i>
	E02a.3	3007	<i>Efficient Optimization-Assisted Full-Wave MoM Unit-Cell Design for Dual-Band Transmitarrays</i>

Bolcek, Jan	CS43b.1	4168	<i>Channel Measurements and Characterization in Industrial Environment at 60 GHz</i>
Boldi, Mauro	CS20b.3	402	<i>Measurements of Reconfigurable Intelligent Surface in 5G System Within a Reverberation Chamber at mmWave</i>
Bolli, Pietro	PA7.11	1210	<i>Electromagnetic Assessment of Tolerances of the Square Kilometre Array Log Periodic Antenna Using Uncertainty Quantification</i>
Bonefačić, Davor	PA1.10	3371	<i>Textile Waveguide Antennas for On-Body Sensor and Communication Systems</i>
Bonello, Julian	CS24b.3	928	<i>Analysis of Return Loss with an Uncooled Coaxial Monopole Antenna During Microwave Ablation</i>
Bonnafont, Thomas	PP03.2	3592	<i>A Deep Split-Step Wavelet Model for the Long-Range Propagation</i>
Bonnemason, Pierre	P03.3	1538	<i>Influence of the Atmospheric Plasma Sheath on the RCS of a Hypersonic Reentry Vehicle</i>
Bonny, Robin	PE1.6	1261	<i>Characterization of a Metamaterial-Enabled Waveguide Diplexer for Ka-Band Satellite Communication Systems</i>
Bord, Robin	CS21.5	2722	<i>Effects of Bumper Integration on Low-, Mid-, and High-Resolution Imaging Radars</i>
	CS12a.1	4043	<i>A High-Precision Approach to Eliminate Positioning Errors in Radar Calibrations</i>
Bordallo Lopez, Miguel	CS29.3	3797	<i>Computer Vision Enabled Sub-THz Radio Channel Characterization of Dynamic Objects</i>
Bordbar, Arman	A27a.3	641	<i>K-Band Microstrip ESPAR Antenna Integrated into Large Array</i>
	PA2.14	1114	<i>Synthesis of a Planar 2D Butler Matrix: A Showcase with a 3x3 Array</i>
Borgese, Michele	PE1.15	1295	<i>D-Band Absorber Comprising Tantalum Nitride-Based Resistively-Loaded High Impedance Surfaces</i>
Bories, Serge	A13.1	1949	<i>Ultra-Miniature Circularly Polarized Antenna with Omni-Directional Pattern for Sat-IoT</i>
Borja, Alejandro	A09b.1	872	<i>X-Band Reconfigurable Phase Shifters Based on SIW and Liquid Metal Technologies</i>
Bornkessel, Christian	CS42a.6	160	<i>Hybrid Antenna Measurement and Post-Processing for 5G Small Cell Exposure Assessment with Site-Specific Mounting Conditions</i>
	CS2.2	170	<i>Characterization of Typical Instantaneous Exposure and Usage Scenarios in the Vicinity of 5G Massive-MIMO Base Stations</i>
	CS2.6	189	<i>Reproducibility Studies of Instantaneous and 6-Minute Average Exposure Measurements Around 5G Massive-MIMO Base Stations</i>
Bosch, Wolfgang	PA7.15	1226	<i>A Novel Reconfigurable Planar Switched-Beam Filtenna with 360-Degree Beam Scanning</i>
	PA7.16	1229	<i>Single Layer Cavity-Backed Filtenna with Ultra-Wide Out-Of-Band Suppression</i>
Bosiljevac, Marko	E08.3	1870	<i>Tailoring Surface Impedance for Cascaded Cylindrical Metasurfaces</i>
	CS26b.5	4321	<i>Design of Glide-Symmetric Dielectric Mikaelian Lens Antenna for K/Ka-Band</i>
Botham, Christopher	CS3.2	298	<i>From Reconfigurable Intelligent Surfaces to Holographic MIMO Surfaces and Back</i>
Bottauscio, Oriano	E01.2	2019	<i>Assessment of the Feasibility of Breast Lesion Detection with Contrast</i>

			<i>Source Inversion for Microwave Tomography: A Virtual Experiment</i>
	CS33a.4	3057	<i>An Electric Properties Tomography Approach Inspired by the Boundary Element Method</i>
Bouamrane, Fayçal	E05.1	2036	<i>From Bulk Toward Micro-Structured TiO₂ Ceramics for All-Dielectric Metamaterials at Terahertz Frequencies</i>
Boulos, Federico	CS25.2	659	<i>A Modular, Low-Cost Ka-Band Antenna Subarray as Building Block for Phased Arrays of Arbitrary Size and Shape</i>
Boulzazen, Habib	M5.4	552	<i>Thermoelectric Cooling Solution for Active Antennas</i>
Bourne, Michael	CS4.5	3194	<i>CSIRO Radio Astronomy Receiver Update - Ultra Wideband and Phased Array Feeds</i>
Bourreau, Daniel	A23.5	2767	<i>Modeling of Quasi-Optical Systems and Measurements with a Cobot in the J-Band</i>
Boursianis, Achilles	PA3.23	3490	<i>Wideband Aperture-Coupled Array Design for Automotive Radar Applications</i>
	PP03.5	3605	<i>Modeling Received Power from 4G and 5G Networks in Greece Using Machine Learning</i>
Boutayeb, Halim	CS40a.3	1763	<i>Mm-Wave Monopulse Radar System for Detecting Space Debris in Satellite Exploration Missions</i>
	PA5.10	3533	<i>A High Efficiency and Ultra-Wideband Rectenna for RF Energy Harvesting Application</i>
Bowen, Mark	CS4.5	3194	<i>CSIRO Radio Astronomy Receiver Update - Ultra Wideband and Phased Array Feeds</i>
Bozzi, Maurizio	CS8.5	2899	<i>Dual-Resonance SIW-Based Reflectarray Unit Cell for Broadband Applications</i>
Bradshaw, Benjamin	CS17b.6	340	<i>Wave-Controlled Biasing of RIS for Multi-Beam Scattering Pattern Generation</i>
Bramerie, Laurent	CS44a.4	757	<i>High Data-Rate Sub-THz Coherent Near-Field Wireless Links Enabled by Spline-Profile Bessel Launchers</i>
Brandão, Tiago	A04.1	1458	<i>Implementation of a Novel Triband Antenna Array in a FR1/FR2 5G-NR System</i>
Brás, Marlene	PP02.10	2533	<i>Designing a Data Pre-Processing Tool for MEO Satellites Propagation Measurements</i>
	P09.3	2644	<i>Ka-Band Rain Attenuation Derived from a MEO Satellite Constellation</i>
Bråten, Lars	A17.3	3749	<i>Design and Test of a UHF Deployable Conical Log Spiral Antenna for Small Satellites</i>
Braun, Roni	M5.2	542	<i>Uncertainty Analysis of Linear Multi-Probe Array Systems for Fast Antenna Measurements</i>
Breinbjerg, Olav	CS42a.2	141	<i>Quantification and Correction of Signal Averaging with On-The-Fly Sampling in Near-Field Antenna Measurements</i>
Brizi, Danilo	E06a.4	601	<i>Design of a Low-Frequency Magnetic Metasurface for Extremely Focused and Long Range Wireless Power Transfer Applications</i>
	PE1.9	1272	<i>A Compact Fabry-Perot Cavity Antenna with Circular Polarization</i>
	PM1.1	1308	<i>Preliminary Investigation of an Innovative RF Sensor for Deformation and Failure Evaluation in Composite Materials</i>
	CS27.2	1575	<i>An Electromagnetic Metasurface for Impedance Matching in Microwave</i>

Biomedical Applications

	PE3.8	2392	<i>Design of a Conformal and Low-Frequency Metasurface for Magnetic Field Shielding in Wireless Power Transfer Systems</i>
	A10.5	3083	<i>Fabry-Perot Antenna with High-Permittivity Grounded Walls for Side Lobe Level Reduction</i>
	CS33b.4	3321	<i>Deep-Learning Optimized Reconfigurable Metasurface for Magnetic Resonance Imaging</i>
	PP03.6	3610	<i>Target Classification Through ISAR for Autonomous Vehicles Based on Federated Learning</i>
	E09.1	3905	<i>Design of an L-S-Band Frequency Selective Resorber for Dual-Band Absorption and In-Band Transmission</i>
Bronckers, Laurens	PM2.8	2459	<i>Uncertainties in the Estimation of the Gain of a Standard Gain Horn in the Frequency Range of 90 GHz to 140 GHz</i>
	PM2.11	2472	<i>Quiet-Zone Profiling in a mmWave Spherical Anechoic Chamber: An Evaluation Approach</i>
	M4.2	2955	<i>Exploring Uniformity of Reverberation Chambers: Insights from Antenna Reflection Coefficient</i>
Brost, George	P03.2	1533	<i>Advanced Microwave Radiometry: Refining Sun-Tracking Technique for Atmospheric Attenuation Retrieval and Sun Brightness Temperature Estimation</i>
Brown, Anthony	CS4.2	3181	<i>Mitigating Zenith Blindness from Mutual Coupling in a Sunflower Phased Array</i>
	CS15.4	4015	<i>An Overview of Gigascale Antenna Arrays and Electromagnetics for Space Based Solar Power</i>
Bruliard, Margaux	E02b.2	3273	<i>Stabilization of EFIE-IBC by Spatial Filtering</i>
Bruni, Simona	CS10.3	860	<i>D-Band Active Antenna Array with Lens Enabling Quasi-Optical and Analogue Beam Reconfiguration for 6G Applications</i>
	CS21.2	2709	<i>New Efficient Waveguide Antenna for Future Automotive Radar Applications</i>
Buchanan, Neil	P05.5	261	<i>Sequential Phase Optimization for Coherent Long-Range Distributed Wireless Power Transfer to a Non-Communicative Receiver</i>
	CS15.2	4006	<i>Validation of a Large Retrodirective CASSIOPeiA Solar Power Satellite Antenna Array</i>
Buckley, John	PP02.17	2567	<i>Machine Learning Approaches for EM Signature Analysis in Chipless RFID Technology</i>
	P06.5	2747	<i>A Time-Efficient Model for Estimating Far-Field Wireless Power Transfer to Biomedical Implants</i>
	CS1b.1	4238	<i>A Compact Microwave Rectifier for Wireless Power Transfer and Energy Harvesting Applications</i>
Budé, Roel	CS47.4	426	<i>Over-The-Air Noise-Figure Measurements of Active Integrated Antennas at W-Band</i>
Budhu, Jordan	E11.4	2810	<i>Observation of Exceptional Points in Parity-Time Symmetric Coupled Impedance Sheets</i>
Bueno, Juan	CS44b.2	945	<i>Design and Characterization of an Imaging System Using Photoconductive Connected Arrays</i>

	CS7.3	1601	<i>Experimental Characterization of a Core-Shell Lens for Antenna On-Package Integration at D-Band</i>
	CS22a.2	2846	<i>The Predictions of Quantum and Classical Models for the Thermal Energy Emitted in the Sub-mm Ranges by Doped Silicon</i>
Buffi, Alice	CS23b.1	1989	<i>SARFID for Fine-Scale Localization of Passive Backscattering Devices at 2.4 GHz ISM Band</i>
Bui, Cong Danh	CS3.1	294	<i>Chipless RFID Sensor on Paper Substrate</i>
Buisman, Koen	CS39b.2	813	<i>Estimation of Obtainable Data-Rates in an Over-The-Air mm-Wave MIMO Testbed</i>
Bulja, Senad	PA8.16	2336	<i>Performance Estimation of In-Vessel Resonant Communications</i>
Buonanno, Giovanni	A20.1	3812	<i>Errors Correlation in Near-Field Focused Arrays for Biosafe Microwave Applications</i>
Burghignoli, Paolo	CS9a.2	225	<i>2D-Scanning of Circularly Polarized Beams via Array-Fed Fabry--Perot Cavity Antennas</i>
	CS16.4	573	<i>Leaky-Wave Design of Hybrid-, TE-, and TM-Polarized Resonant Bessel-Beam Launchers for Millimeter- and Submillimeter-Wave Applications</i>
	A08b.3	2091	<i>Hybrid Metal-Graphene Unit Cells for THz Reconfigurable Leaky-Wave Antennas</i>
Burokur, Shah Nawaz	E13.5	284	<i>Transmissive-Type Metagratings with Few Meta-Atoms for Beam Splitting</i>
	E06b.2	797	<i>Direction-Of-Arrival Estimation by a Programmable Metasurface</i>
	CS14a.5	4145	<i>Time-Modulated Metasurface for Harmonic Signals Frequency Conversion</i>
Burton, Fraser	CS3.2	298	<i>From Reconfigurable Intelligent Surfaces to Holographic MIMO Surfaces and Back</i>
Busineni, Mahesh Kumar	PP02.16	2562	<i>Analysis of the Effects of Rainwater Covered Bumper on the Automotive Radar Signals</i>
	PA3.15	3454	<i>Self-Isolated MIMO Antenna Using SIW Cavity Antenna for Dual-Band (28, 38 GHz) Applications</i>
Buxton, Bob	CS39b.5	827	<i>Antennas and Power Measurement Techniques for Wireless Applications</i>
Buzzin, Alessio	CS33a.3	3054	<i>Advancements in Broadband Electromagnetic Sensing for Food Quality Control</i>
Byrne, Benedikt	CS25.5	673	<i>TX/RX Terminal Based on Metascreen Technology for Ka-Band Satcom with Dual Switchable Polarization</i>
Byun, Gangil	CS37a.5	47	<i>Display-Integrated MIMO Antennas for Gesture-Sensing Radars</i>
	CS6b.3	499	<i>Anisotropic Metagrating for Beamforming with Polarization Conversion</i>
C			
Cabedo-Fabrés, Marta	CS40b.3	1976	<i>Compact 868 MHz RFID-Based Antenna for Queen Bee Identification and Location Inside Hives</i>
	CS19a.2	4072	<i>Surface Partial Differential Equations and Its Applications to Scattering Problems</i>
Cai, Ailian	PE3.7	2388	<i>Electromagnetic Modelling in Modern Vehicles: A Pathway to Efficiency and Performance</i>

Cai, Xuesong	CS47.3	421	<i>Millimeter-Wave Scattering from Building Facade: A Simulation and Verification Study</i>
	CS43a.4	3967	<i>Propagation Study of Vision-Based RIS Beam Tracking for mmWave Communications</i>
	CS43b.5	4187	<i>Experimental Analysis of Physical Interacting Objects of a Building at mmWave Frequencies</i>
Cai, Yang	CS6b.4	502	<i>Millimeter-Wave Beam-Steerable Lens with Reduced Profile and Enhanced Gain</i>
	PE1.17	1303	<i>A Novel Metasurface Inverse Design Based on Back Propagation Neural Network</i>
Caicedo Mejillones, Steven	PA2.23	1154	<i>Ka-Band Phased Antenna Array Concept for High-EIRP Satellite Connections</i>
Caizzone, Stefano	CS25.2	659	<i>A Modular, Low-Cost Ka-Band Antenna Subarray as Building Block for Phased Arrays of Arbitrary Size and Shape</i>
	CS46.5	4233	<i>Low-Cost Hybrid Additive Manufacturing of a Miniaturized Dual Band Stacked Patch Antenna for GNSS Applications</i>
Cala, Enrica	A19.3	1513	<i>Non-Regular Multibeam Coverage Antenna for Ka-Band High-Throughput Satellite Communications</i>
Calabrese, Massimo	CS45.3	1808	<i>Preliminary Clinical Trial Results of MammoWave in the Context of RadioSpin Project</i>
Caldeirinha, Rafael	P05.1	241	<i>Small-Scale Passive Millimetre-Wave Imaging Measurements for Marine Litter Detection at W-Band</i>
	P10b.4	3259	<i>Wind-Induced Backscatter Clustering from Vegetation at W-Band</i>
	P02.3	3772	<i>Feature Selection for Identifying Optimal Microwave Frequencies to Detect Floating Macroplastic Litter in C and X Bands</i>
Calisir, Ilkan	PA5.5	3511	<i>Pulse Preserving Capability of an Ultrawideband Dispersive Dielectric Resonator Antenna</i>
Callaghan, Brendan	P06.5	2747	<i>A Time-Efficient Model for Estimating Far-Field Wireless Power Transfer to Biomedical Implants</i>
Callaghan, Glen	A16.4	1744	<i>Compact Hybrid Optical/RF User Segment (CHORUS): RF Terminal Design</i>
Calmettes, Thibaud	CS40a.5	1770	<i>A Self Deployable and Reconfigurable Antenna in VHF Band for a New Space Mission</i>
Camacho, Miguel	E02a.1	2997	<i>Efficient NUFFT-Based Spectral Domain Method of Moments Analysis of Multilayered Periodic Structures with Subsectional Basis Functions</i>
	E02a.3	3007	<i>Efficient Optimization-Assisted Full-Wave MoM Unit-Cell Design for Dual-Band Transmitarrays</i>
Camacho, Pablo	A06a.4	3036	<i>Large, Multi-Faceted Reflectarray with Quasi-Constant Directivity in the V-Band</i>
Caminada, Alexandre	CS11.5	1631	<i>Fine Tuning an AI-Based Indoor Radio Propagation Model with Crowd-Sourced Data</i>
Caminita, Francesco	CS25.5	673	<i>TX/RX Terminal Based on Metascreen Technology for Ka-Band Satcom with Dual Switchable Polarization</i>
Candell, Richard	PP03.8	3620	<i>Empirical Characterization of Doppler in Industrial Wireless Channels</i>
Cañete Rebenaque,	CS36a.3	710	<i>Compact Amplitude-Monopulse Microstrip Antenna Design for Wide</i>

David			<i>Field-Of-View Direction Finding</i>
Canicatti, Eliana	PM1.1	1308	<i>Preliminary Investigation of an Innovative RF Sensor for Deformation and Failure Evaluation in Composite Materials</i>
Cannatà, Alessia	CS24b.1	920	<i>Microwave Tomography Bone Imaging: Analysing the Impact of Skin Thickness on the Reconstruction of Numerical Bone Phantoms</i>
Caño-García, Manuel	CS17a.4	15	<i>Reflective Surfaces Based on Semi-Passive Reconfigurable Polymer Network Liquid Crystal</i>
Cao, Lin	CS34.1	2610	<i>RIS with Practical Reflection Coefficients: Modeling and Experimental Measurements</i>
Cao, Yuyan	PE1.17	1303	<i>A Novel Metasurface Inverse Design Based on Back Propagation Neural Network</i>
	CS18.4	3683	<i>Circularly Polarized Sub-THz Antenna Design for Distributed Deployment</i>
Capek, Miloslav	CS38.5	128	<i>Substructure Modes and Bounds</i>
	PE2.8	1020	<i>The Role of Arrays in Pulsed Radiation</i>
	E10b.1	2059	<i>Radiation Efficiency Cost of Optimal Current Density Generating Specific Far-Field Pattern</i>
	E11.5	2815	<i>Preliminary Study on Gain Maximization via Density-Based Topology Optimization</i>
	A03b.1	3128	<i>An Upper Bound for Envelope Correlation Coefficient of Antenna Clusters</i>
	CS18.5	3687	<i>Material-Independent Scattering Formulations of Characteristic Modes</i>
	A24.5	3876	<i>Design Recommendations for Minimal Antenna Mutual Coupling Using Current Optimization</i>
	CS30b.1	4149	<i>Overview of State-Of-The-Art Methods for Determining Performance Bounds on Electromagnetic Systems</i>
	CS30b.2	4153	<i>Fundamental Limits on Characteristic Modes</i>
Capelletti, Francesco	P09.3	2644	<i>Ka-Band Rain Attenuation Derived from a MEO Satellite Constellation</i>
	P09.5	2654	<i>Predicting Rain Attenuation at D Band for 6G Backhaul Link Design: A Frequency Scaling Approach</i>
Capitanio, Fabiana	M4.3	2959	<i>Numerical Study of the Dielectric Properties of Lung Tissue Measured with Two Different Open-Ended Coaxial Probes</i>
Capobianco, Antonio-D.	A09b.2	877	<i>Recent Advances in Plasma Surfaces</i>
Capolino, Filippo	CS17b.6	340	<i>Wave-Controlled Biasing of RIS for Multi-Beam Scattering Pattern Generation</i>
	CS9a.6	534	<i>Strategies for Enhancing the Gain Bandwidth of Fabry-Pérot Cavity Antennas: A Review of Recent Advances</i>
	CS26a.2	4094	<i>On the Use of Resonant Cavities for Experimental Validation of the Dispersion Diagram of Periodic Glide Symmetric Waveguides</i>
Capozzoli, Amedeo	CS42b.3	446	<i>Phaseless Characterization of Flat Sources with a Planar Wide-Mesh Scanning Strategy</i>
	CS42b.4	451	<i>Discretizing 2D Equivalent Radiating Panels by Legendre Quadrature</i>
	E10b.5	2077	<i>Numerical Results on the Use of the L-SVD Approach for the Solution of the Inverse Source Problem from Amplitude-Only Data</i>

Cappellin, Cecilia	CS39a.3	618	<i>Full Wave Modelling and Design of a Baffle for the HERTZ 2.0 Compact Antenna Test Range</i>
	E10a.4	1854	<i>Platform Scattering Analysis of the Copernicus Imaging Microwave Radiometer</i>
	A17.4	3754	<i>RF Modelling and Validation of the Breadboard Antenna of the Copernicus Imaging Microwave Radiometer</i>
Cappello, Tommaso	PP01.14	1407	<i>Analog Self-Interference Cancellation by Means of a Synchronised Signal Injection</i>
Caratelli, Diego	PA4.11	2150	<i>Pixel Antenna Design for mm-Wave Wireless Communications to Achieve Wide Scanning</i>
Cardoso, Fábio	A26.5	4212	<i>Improved Performance of a 1-Bit RIS by Using Two Switches per Bit Implementation</i>
Caromi, Raied	CS5a.1	56	<i>Context-Aware Channel Sounder for AI-Assisted Radio-Frequency Channel Modeling</i>
	CS29.1	3787	<i>AI-Based Environment Segmentation Using a Context-Aware Channel Sounder</i>
Carrasco, Eduardo	CS17a.4	15	<i>Reflective Surfaces Based on Semi-Passive Reconfigurable Polymer Network Liquid Crystal</i>
Carslake, Lawrence	CS5b.5	383	<i>Design and Preliminary Indoor Assessment of a Long-Range Sub-THz VNA-Based Channel Sounder Between 500 GHz and 750 GHz</i>
Carter, Nick	CS4.5	3194	<i>CSIRO Radio Astronomy Receiver Update - Ultra Wideband and Phased Array Feeds</i>
Cartwright, Jessica	CS46.4	4228	<i>Antenna Digital Beamforming on Spire's GNSS-Reflectometry CubeSat Constellation</i>
Carvalho, Nuno	A17.5	3759	<i>The Novel Method for Deployable Parabolic Reflector Based on Uchiwa Origami</i>
Castellá-Montoro, Adrián	PA4.26	3459	<i>Amplitude-Tapered Half-Mode Gap Waveguide Distribution Network for Flat Panel Antennas</i>
Castellano, Cristina Romero	CS45.3	1808	<i>Preliminary Clinical Trial Results of MammoWave in the Context of RadioSpin Project</i>
Castillo, Patricia	PM1.8	1339	<i>Dielectric Differences in Biological Tissues: A Comparison Between Excised and Non-Excised Tissues Under the Influence of Chemotherapy</i>
Castillo, Santiago	CS4.5	3194	<i>CSIRO Radio Astronomy Receiver Update - Ultra Wideband and Phased Array Feeds</i>
Castillo-Tapia, Pilar	CS10.1	850	<i>Efficient Ray-Tracing Model for Generalized 2D Dielectric Lenses Combined with Arrays</i>
	CS10.2	855	<i>Design of a Dielectric Lens Using a Ray-Tracing Model for Satellite Communications</i>
	E10a.3	1850	<i>Analysis of the Dispersion Diagrams of 3D Cubic Periodic Arrangements of Metallic Spheres</i>
	A07.2	2664	<i>Metal-Only Additive-Manufactured Geodesic Lens Antennas for the mmWave Band</i>
	A22.5	2791	<i>Ray-Tracing Model for the Design and Efficiency Calculation of a Monolithic Geodesic Lens Array Antenna</i>

Castles, Flynn	PE1.1	1241	<i>Broadening the Spectrum: Extending the Finite Crystal Method to Characterize Static Multi-Atomic Active Metamaterial Systems</i>
Castro, Nelson	A08b.2	2086	<i>High Efficiency Groove Gap Waveguide Leaky Wave Antenna Array with Flat Top Radiation Pattern</i>
	CS26a.2	4094	<i>On the Use of Resonant Cavities for Experimental Validation of the Dispersion Diagram of Periodic Glide Symmetric Waveguides</i>
Catalani, Alfredo	A19.3	1513	<i>Non-Regular Multibeam Coverage Antenna for Ka-Band High-Throughput Satellite Communications</i>
Catapano, Ilaria	CS24a.2	727	<i>Microwave Imaging for Monitoring Bone Healing Using Magnetic Scaffolds: An Initial Analysis</i>
	E10b.5	2077	<i>Numerical Results on the Use of the L-SVD Approach for the Solution of the Inverse Source Problem from Amplitude-Only Data</i>
	E04.2	2689	<i>Contactless 3D Subsurface Imaging: Considerations to Set the Measurement Spacing</i>
	CS33a.3	3054	<i>Advancements in Broadband Electromagnetic Sensing for Food Quality Control</i>
Cathers, Seth	E04.5	2703	<i>Preliminary Description of a 2D Near-Field Electromagnetic Imaging Database</i>
	CS33b.2	3313	<i>Supervised Learning Applied to Microwave Imaging System Calibration</i>
Causse, Alexandre	A13.5	1965	<i>Circularly-Polarized Wideband Conformal Magneto-Electric Antenna Covering the GNSS Bands</i>
Cavagnaro, Marta	CS28.3	475	<i>Dielectric Characterization of Biological Tissues at Microwave Frequencies Based on Water Content</i>
	CS24a.4	736	<i>Analytical and Numerical Solution of the One Dimensional Steady State Bioheat Transfer Equation</i>
	CS24b.5	936	<i>Wideband Dielectric Characterization of Biological Tissues and Realistic Phantom Preparation at Microwave Frequencies</i>
	M4.3	2959	<i>Numerical Study of the Dielectric Properties of Lung Tissue Measured with Two Different Open-Ended Coaxial Probes</i>
	CS33a.3	3054	<i>Advancements in Broadband Electromagnetic Sensing for Food Quality Control</i>
	PA1.13	3385	<i>Sensitivity of the Dielectric Spectroscopy with the Microwave Thermal Ablation Antenna to the Immersion Depth and Longitudinal Dimension of the Measured Media</i>
Cavallo, Daniele	CS37b.3	352	<i>Chessboard Focal Plane Array in Silicon Technologies for Terahertz Imaging</i>
	A12a.1	1707	<i>Analytical Model of a Parallel Plate Waveguide Feeding a Connected Slot Array</i>
	A12b.1	1927	<i>Design, Measurements, and Performance Assessment of a Massive MIMO Wideband Phased Array</i>
	A12b.5	1944	<i>Study of Finite Edge Effects in Compact Ultra-Wide-Band Connected Arrays</i>
	E10b.4	2073	<i>Efficient Analysis Method for Artificial Dielectric Layers with Vertical Metal Inclusions</i>
	A22.2	2776	<i>Analysis and Design of mmWave Wideband Artificial Dielectric Flat</i>

			<i>Lens Antenna</i>
	A22.4	2786	<i>Flat Gradient Index Lenses with Planar or Spherical Output Wavefront</i>
	E12.1	2820	<i>Reducing the Cross-Polarization Levels in Artificial Dielectric Layers for Wideband Arrays</i>
Cavillot, Jean	CS19a.3	4077	<i>Modal Analysis of Thermal Noise from Lossy Dielectric Medium</i>
Caytan, Olivier	CS2.5	184	<i>New Hybrid Ray-Tracing/FDTD for EMF Exposure in 6G Networks Using Semantically Classified Google Earth Photogrammetry with Measurement Validation</i>
Cecchi, Glauco	CS13.3	1558	<i>Exploiting Near-Field Antenna Detuning in Collision Avoidance Systems for RFID-Equipped Robots</i>
	CS23b.1	1989	<i>SARFID for Fine-Scale Localization of Passive Backscattering Devices at 2.4 GHz ISM Band</i>
Cenni, Nicolò	CS43b.4	4183	<i>A Study on Satellite-To-Ground Propagation in Urban Environment</i>
Chabory, Alexandre	PA6.9	2245	<i>Study of the Frequency Dispersion of 3D-Printed Dielectric Crystals for Dielectric Resonator Antenna Applications</i>
	A25.4	3100	<i>3D-Printed Circular Polarized Dielectric Resonator Antenna with Enhanced Axial Ratio Bandwidth Using Anisotropic Material</i>
Chahat, Nacer	CS9a.1	221	<i>Dual-Frequency Metasurface Antenna for Earth Science Remote Sensing</i>
Chaigne, Benoit	PE2.3	999	<i>Management of Radiofrequency Compatibility on Aircraft</i>
Chaker, Mohamed	CS40b.4	1981	<i>Efficient Wireless Power Transfer to an Ultra-Miniaturized Antenna for Future Cardiac Leadless Pacemaker</i>
Chalermwisutkul, Suramate	PA8.8	2301	<i>Sidelobe Suppression and Bandwidth Enhancement of Series-Fed Patch Antenna Arrays Using Coplanar Ground Conductor</i>
Chalkidis, Savvas	E05.4	2050	<i>Design of Novel Fully Metallic mm-Wave Reflectarray Antenna</i>
Chaloun, Tobias	PA6.2	2218	<i>An Eigenvector-Supported Optimization Method for Holographic-Based Leaky Wave Antennas</i>
	A11.2	3157	<i>A Low-Profile Wide-Scan Magneto-Electric Dipole Antenna for 5G mm-Wave Communications</i>
Chamanara, Nima	PE1.14	1292	<i>Integral Equation-Based Solver for the Simulation of Metasurface Designs</i>
Chan, Yat Hin	CS15.2	4006	<i>Validation of a Large Retrodirective CASSIOPeiA Solar Power Satellite Antenna Array</i>
Chang, Chen-Yi	PA3.10	3434	<i>A Millimeter-Wave Binary Reconfigurable Intelligent Surface on a Low-Cost FR4 Substrate</i>
Chang, Liu	PA1.14	3390	<i>Miniaturized Implantable Antenna with Ultra-Wide Bandwidth Characteristics for Leadless Pacemakers</i>
Chang, Zhaowei	CS35a.4	1697	<i>Time-Varying Channel Measurement and Analysis at 105 GHz in an Indoor Factory</i>
Chattopadhyay, Goutam	CS9a.1	221	<i>Dual-Frequency Metasurface Antenna for Earth Science Remote Sensing</i>
Chatzinotas, Symeon	CS44b.1	940	<i>Spherical Wavefront Near-Field DoA Estimation in THz Automotive Radar</i>
	PA2.5	1074	<i>Genetic Algorithm-Based Beamforming in Subarray Architectures for GEO Satellites</i>

	PA6.3	2223	<i>Dual-Polarization Multi-Functional Metasurface for Wireless Communications</i>
	CS19b.4	4295	<i>Supervised Learning Based Real-Time Adaptive Beamforming On-Board Multibeam Satellites</i>
Chauvel, Benjamin	PP03.2	3592	<i>A Deep Split-Step Wavelet Model for the Long-Range Propagation</i>
Che, Wenquan	PA4.1	2105	<i>A Linear Wide-Angle Scanning Phased Array Antenna Using Heterogeneous Beam Element Technology</i>
	PA4.23	2201	<i>A Wideband Aperture-Shared Dual-Polarized End-Fire Antenna with Low Profile and High Isolation</i>
	PA5.11	3537	<i>Circularly Polarized Wide-Angle Scanning Phased Array Based on Heterogeneous Beam Element</i>
Chen, Ben	CS43a.3	3962	<i>A Deep Learning Based Surface Current Generation Method for Scattering Modeling at Terahertz Band</i>
Chen, Bing-Jia	PA3.1	3398	<i>Dynamic Programming-Based Beam Codebook Design for mmWave Multi-Antenna Module in Mobile Devices</i>
Chen, Chen	M5.2	542	<i>Uncertainty Analysis of Linear Multi-Probe Array Systems for Fast Antenna Measurements</i>
Chen, Gong	A12a.4	1719	<i>X-Band Receiving Phased Array with Digital Beamforming Using RFSoc</i>
	A12b.2	1932	<i>An L-Band Receiving Array with Full Digital Simultaneous Quad-Polarization Beamforming</i>
Chen, Jiahong	A27b.1	830	<i>A Wideband High-Gain Circularly-Polarized Metasurface Antenna with a Large Element Spacing SIW Array at Ka Band</i>
Chen, Ke	CS6a.2	199	<i>Designing Transmissive Metasurface for Multibeam Transmitarray at 5G Millimeter-Wave Band</i>
Chen, Liang	PE2.12	1036	<i>A Discontinuous Galerkin Time-Domain Scheme to Model Lasing Dynamics in Four-Level Two-Electron Atomic Systems</i>
Chen, Menglin	E05.5	2055	<i>A Novel Topologically Protected Hollow Dielectric Waveguide for Robust mmWave Guiding</i>
Chen, Mingzheng	A22.1	2772	<i>Experimental Validation of Ray-Tracing and Physical-Optics Model for Geodesic H-Plane Horn Antennas</i>
	CS19a.4	4081	<i>Combined Ray-Tracing and Physical-Optics Model for Flat-Aperture PPW Lens Antennas</i>
Chen, Na	E06b.1	792	<i>Variable Multi-Band Metasurface Reflector with Controllable Direction Using Varactor Diodes Mounted Large-Via Mushroom-Type Structure</i>
Chen, Peng	CS35a.2	1688	<i>Beam Coverage Model of Ultra-Massive MIMO Communication Systems for Intelligent Transportation</i>
	CS23a.4	1790	<i>Analysis of Channel Characteristics for FMCW Millimeter-Wave Radar in Traffic Scenarios</i>
Chen, Qiang	CS5a.2	61	<i>Validation of Pseudo-Scale Model for the Air-Sea Two-Layer Near-Field Problem by Using FDTD Simulations and Measurements in a Tank</i>
Chen, Qiao	CS17b.3	326	<i>Information Metasurface for Simultaneous Wave Manipulations and Signal Modulations</i>
	A07.2	2664	<i>Metal-Only Additive-Manufactured Geodesic Lens Antennas for the mmWave Band</i>

Chen, Rui-Sen	PA6.10	2250	<i>Generation of Narrow Divergence Angle OAM Beams for mmWave Communication Links Using Metasurface</i>
	PA3.17	3467	<i>Beam Steering Range Enhancement of Bifocal Reflectarray Using Irregular Distribution of Meta-Atoms</i>
Chen, Shengjian	CS37a.1	29	<i>3D-Printed Wearable Antenna Integrated with Rectifier for Wireless Power Transfer</i>
Chen, Shih-Yuan	PA3.1	3398	<i>Dynamic Programming-Based Beam Codebook Design for mmWave Multi-Antenna Module in Mobile Devices</i>
	PA5.2	3498	<i>DC Bias Routing Design for Wideband Reconfigurable Transmitarray Based on 1-Bit Phase-Switching Elements</i>
Chen, Shu-Lin	PA5.20	3574	<i>A Wideband Circularly Polarized Filtering Array Antenna Using Dual-Layer Circular Cross Slotted Patch</i>
Chen, Xiao-min	PP02.5	2510	<i>Measurement-Based Channel Characteristics for Air-To-Ground Communications Under Rural Areas</i>
Chen, Xiaodong	CS15.4	4015	<i>An Overview of Gigascale Antenna Arrays and Electromagnetics for Space Based Solar Power</i>
	CS15.5	4019	<i>A Digital Beamforming Antenna for Space Based Solar Power Transmitting Array</i>
Chen, Xiaoming	CS39a.2	614	<i>Measurement of Total Radiated Power Using a TEM Cell</i>
Chen, Yanwen	CS22a.2	2846	<i>The Predictions of Quantum and Classical Models for the Thermal Energy Emitted in the Sub-mm Ranges by Doped Silicon</i>
Chen, Yi	CS29.5	3807	<i>Multi-Scattering Centers Extraction and Modeling for ISAC Channel Modeling</i>
Chen, Yuenian	A02.5	3710	<i>A Four-Channel In-Band Full-Duplex (IBFD) Antenna System with Shared Radiation Aperture</i>
Chen, Zhan	A03a.1	2862	<i>Low-Profiled Wideband Dual-Polarized Conformal Antenna Array</i>
Chen, Zhe	CS35a.2	1688	<i>Beam Coverage Model of Ultra-Massive MIMO Communication Systems for Intelligent Transportation</i>
Chen, Zhengchuan	PA5.20	3574	<i>A Wideband Circularly Polarized Filtering Array Antenna Using Dual-Layer Circular Cross Slotted Patch</i>
Chen, Zhi Ning	PE2.6	1012	<i>Machine-Learning-Based Optimization for Wideband Metasurface Mosaic Antenna</i>
Chen, Zhijiao	PA3.3	3407	<i>A Wearable Open-Ring Dielectric Resonator Antenna with Frequency Reconfiguration</i>
Chen, Zhizhang (David)	A27b.1	830	<i>A Wideband High-Gain Circularly-Polarized Metasurface Antenna with a Large Element Spacing SIW Array at Ka Band</i>
Chen, Zhong	CS32.1	1433	<i>Delving into Time Domain Gating: An Extensive Study on Parameter Selection and Its Implications</i>
	CS31.3	1668	<i>Application of Compressed Sensing to Antenna Far-Field Calibration in an Extrapolation Range</i>
Cheng, Fei	PA4.2	2109	<i>A Fully Additive Manufactured D-Band SIW Antenna</i>
Cheng, Qiang	CS17b.3	326	<i>Information Metasurface for Simultaneous Wave Manipulations and Signal Modulations</i>
Cheng, Yin-Han	E13.4	280	<i>Thin-Film Terahertz Metamaterials Manufactured by Laser Direct Writing</i>

Cheng, Yu Jian	CS8.3	2892	<i>A Wideband Filtering Linear-To-Circular Polarization Converter for Ka-Band Satellite Communication</i>
Cheng, Yu-Hsiang	E13.4	280	<i>Thin-Film Terahertz Metamaterials Manufactured by Laser Direct Writing</i>
Cheval, Nicolas	PA2.17	1128	<i>Dual-Polarized Connected-Slot Array Technological Demonstrator Targeting a 5:1 Bandwidth</i>
Chevalier, Christine	CS12b.5	4278	<i>Robotic Arm-Based Antenna Metrology System for Aerospace Applications</i>
Chevalier, Nicolas	CS3.5	311	<i>Exploring PLA/Flax Substrates for Antenna Applications: Assessing Moisture, Temperature and Dielectric Constant Homogeneity</i>
Chezian, Arvind Selvan	P06.2	2732	<i>Development of Tissue Emulatory Models/Phantoms of Lungs at Microwave Frequency for Acute Respiratory Distress Syndrome</i>
Chia, Michael	PE2.7	1015	<i>Non-Uniform Metamaterial Mushroom Antennas via a Genuine Multi-Objective Bayesian Optimization Method</i>
Chiang, H. Cynthia	CS4.4	3189	<i>The Hydrogen Intensity Real-Time Analysis eXperiment: Overview and Status Update</i>
Chin, Francois	PA2.6	1079	<i>Modular Ka-Band Transmit Phased Array Antenna for SATCOM Applications</i>
Chippendale, Aaron	CS4.5	3194	<i>CSIRO Radio Astronomy Receiver Update - Ultra Wideband and Phased Array Feeds</i>
Cho, Chihyun	CS12b.1	4259	<i>KRISS Robot-Based Antenna Measurement System</i>
Choi, Domin	A27b.2	834	<i>A Radial Waveguide Power Divider Inspired Antenna for mmWave IoT Sensing Applications</i>
Choi, Jae Ryung	E13.2		<i>Magnetic Composites with M-Type Hexaferrites for Q/V-Band Electromagnetic Wave Absorption</i>
Choi, Jaeuk	CS37a.5	47	<i>Display-Integrated MIMO Antennas for Gesture-Sensing Radars</i>
Choi, Jangsuk	PP01.12	1399	<i>The Effect of Beam Misalignment in Data Center Environment at 285GHz Band</i>
Chou, Hsi-Tseng	PA3.10	3434	<i>A Millimeter-Wave Binary Reconfigurable Intelligent Surface on a Low-Cost FR4 Substrate</i>
Choudhury, Noor	CS39a.4	622	<i>Addressing PIM Challenges in Radio Base Stations: Field Issues and Testing Methods for Large-Scale Deployments</i>
Chreim, Hassan	PA2.1	1052	<i>Leading Edge Conformal ARMA Antenna in X Band</i>
Christodoulou, Christos	PA3.23	3490	<i>Wideband Aperture-Coupled Array Design for Automotive Radar Applications</i>
	PP03.5	3605	<i>Modeling Received Power from 4G and 5G Networks in Greece Using Machine Learning</i>
Christogeorgos, Orestis	PM2.14	2486	<i>A Wideband Free Space Material Characterization Method for Extracting Dielectric Permittivity</i>
Christopoulos, Nikos	PP01.5	1365	<i>Field Trials for Different 5G NSA Cellular Networks</i>
Chu, Qing-Xin	PA5.23	3586	<i>Wideband Decoupling Smartphone Antenna with Integrated Metal Rim</i>
Chukwuka, Ozuem	CS40a.4	1766	<i>Design of Microstrip UWB Antenna with Full Ground Plane for Wearable Applications</i>
Chun, Yangbae	A27b.2	834	<i>A Radial Waveguide Power Divider Inspired Antenna for mmWave IoT Sensing Applications</i>

Chung, Woohyun	CS12b.1	4259	<i>KRISS Robot-Based Antenna Measurement System</i>
Chung, Yoon	CS4.5	3194	<i>CSIRO Radio Astronomy Receiver Update - Ultra Wideband and Phased Array Feeds</i>
Churm, James	A09b.3	882	<i>Ultra-Low-Loss Millimeter Wave Beam Scanning Antenna Using Piezoelectric Actuation</i>
Ciarleglio, Gianluca	CS28.3	475	<i>Dielectric Characterization of Biological Tissues at Microwave Frequencies Based on Water Content</i>
Cicchetti, Valentina	PA4.17	2178	<i>Wideband Dual-Polarized Lens Antenna for Future mm-Wave Applications</i>
Cil, Erdem	CS27.3	1579	<i>Theoretical Insights and Engineering of Wireless Body-Implanted Bioelectronics</i>
	PA1.4	3345	<i>Phase Variation of Ingestible Dipole, Loop, and Patch Antennas in Gastrointestinal Tract</i>
Cildir, Abdulkadir	PE1.5	1256	<i>An Innovative Metasurface Polarizer Working in 5G Frequency Bands</i>
Cilia, Federico	CS24b.3	928	<i>Analysis of Return Loss with an Uncooled Coaxial Monopole Antenna During Microwave Ablation</i>
Ciociola, Antonio	CS42b.5	456	<i>A Greedy Approach for Reducing Data in Near-Field Measurements</i>
Cissé, Cheick	CS11.5	1631	<i>Fine Tuning an AI-Based Indoor Radio Propagation Model with Crowd-Sourced Data</i>
Claus, Nicolas	CS40a.2	1758	<i>Optimizing RF Energy Harvesting in IoT: A Machine Learning Estimation Considering Polarization Effects</i>
Claussen, Holger	PA8.16	2336	<i>Performance Estimation of In-Vessel Resonant Communications</i>
Clavier, Laurent	PP03.14	3647	<i>Generation of Electromagnetic Exposure Maps for 5G Communications</i>
Clemente, Antonio	CS6b.2	494	<i>Hybrid Analog-Digital Beamforming System with Quad-Steerable Beams Based on Programmable Transmitarray</i>
	A09a.2	683	<i>Sub-Wavelength Anisotropic Unit-Cells for Low-Profile Transmitarray Antennas</i>
	CS7.4	1606	<i>Characterization of a D-Band Active Transmitarray System for Efficient Point-To-Point Links</i>
	CS7.5	1611	<i>Reconfigurable Intelligent Surfaces for THz: Signal Processing and Hardware Design Challenges</i>
	CS34.4	2625	<i>Empirical Validation of the Impedance-Based RIS Channel Model in an Indoor Scattering Environment</i>
	A03a.2	2867	<i>Loaded and Load-Less Supergain Parasitic End-Fire Arrays</i>
	A26.5	4212	<i>Improved Performance of a 1-Bit RIS by Using Two Switches per Bit Implementation</i>
Clendinning, Sarah	CS10.1	850	<i>Efficient Ray-Tracing Model for Generalized 2D Dielectric Lenses Combined with Arrays</i>
	A07.2	2664	<i>Metal-Only Additive-Manufactured Geodesic Lens Antennas for the mmWave Band</i>
	A22.3	2781	<i>Tailoring the Performance of Geodesic Lens Antennas by Defining Their Footprint</i>
Coco Martin, Caspar	A12a.1	1707	<i>Analytical Model of a Parallel Plate Waveguide Feeding a Connected Slot Array</i>
	A22.2	2776	<i>Analysis and Design of mmWave Wideband Artificial Dielectric Flat</i>

			<i>Lens Antenna</i>
	A22.4	2786	<i>Flat Gradient Index Lenses with Planar or Spherical Output Wavefront</i>
Coene, Sander	CS23b.2	1994	<i>Path Loss Modeling for Air-To-Ground Channels in a Suburban Environment</i>
Coesoij, Richard	CS47.6	435	<i>The Antenna Dome High-Speed Characterization System for OTA Characterization of FR2 5G Active Antenna Panels</i>
Colella, Emanuel	CS20b.3	402	<i>Measurements of Reconfigurable Intelligent Surface in 5G System Within a Reverberation Chamber at mmWave</i>
	CS22a.4	2853	<i>Quantum Optimisation of Reconfigurable Surfaces in Complex Propagation Environments</i>
	CS22a.5	2858	<i>Real-System Variational Quantum Eigensolver for Electromagnetic Waveguides: A Benchmark Study</i>
Collardey, Sylvain	PA7.5	1180	<i>Design of Optimized Cylindrical Structural Antenna with Quasi Length Insensitivity Using CMA</i>
	A13.5	1965	<i>Circularly-Polarized Wideband Conformal Magneto-Electric Antenna Covering the GNSS Bands</i>
	CS40b.5	1985	<i>Challenges and Limits of Designing Wide Band and Efficient Compact Superdirective Antenna</i>
Collings, Iain	PA8.11	2315	<i>Development of Passive Chipless RFID Temperature Sensor</i>
Collins, Brian	CS15.4	4015	<i>An Overview of Gigascale Antenna Arrays and Electromagnetics for Space Based Solar Power</i>
Collins, Brian	CS15.5	4019	<i>A Digital Beamforming Antenna for Space Based Solar Power Transmitting Array</i>
Colombi, Davide	CS2.3	175	<i>Long-Term Network-Based Assessment of the Actual Output Power of Base Stations in a 5G Network</i>
Colombo, Michele	CS20b.3	402	<i>Measurements of Reconfigurable Intelligent Surface in 5G System Within a Reverberation Chamber at mmWave</i>
Colpaert, Achiel	CS23b.2	1994	<i>Path Loss Modeling for Air-To-Ground Channels in a Suburban Environment</i>
Comisso, Alef	P09.3	2644	<i>Ka-Band Rain Attenuation Derived from a MEO Satellite Constellation</i>
Comite, Davide	CS9a.2	225	<i>2D-Scanning of Circularly Polarized Beams via Array-Fed Fabry--Perot Cavity Antennas</i>
	PP02.13	2547	<i>Radiometeorological Forecasts for Satellite Links Operations: Validation with Measurements from BepiColombo Mission</i>
	CS26b.4	4318	<i>All-Metal Glide-Symmetric Slotted Planar Antennas: Modal Analysis</i>
Concaro, Filippo	PA2.19	1136	<i>Improving the Strut Modelling of the European Space Agency Deep Space Antennas to Evaluate Efficiency and Sidelobe Impact</i>
Conceição, Raquel	CS28.2	470	<i>The Effect of Pressure of the Open-Ended Coaxial Probe on the Measurement of Ex Vivo Biological Tissues Dielectric Properties</i>
	PP03.18	3660	<i>Best Practices for Accurate Results Using Numerical Solvers for Microwave Body Screening</i>
Consalvi, Fernando	PP02.11	2538	<i>AlphaSat Ka-Band and Q-Band Receiving Station in Rome: Measurements and Data Analysis</i>
	P09.3	2644	<i>Ka-Band Rain Attenuation Derived from a MEO Satellite Constellation</i>
Contreras, Abraham	PA4.2	2109	<i>A Fully Additive Manufactured D-Band SIW Antenna</i>

Contreres, Romain	E07.1	1636	<i>Model-Based Deep Learning for High-Dimensional Periodic Structures</i>
	A12b.4	1941	<i>6:1 Connected Slot Array in PCB Technology</i>
	A13.3	1958	<i>Wide-Angle Quasi-Optical Beamformer for LEO Applications</i>
Contu, Salvatore	E10a.4	1854	<i>Platform Scattering Analysis of the Copernicus Imaging Microwave Radiometer</i>
Córcoles, Juan	E10b.3	2069	<i>Proving the Circular Polarization of the Fundamental Modes in Rotationally Symmetric Waveguides</i>
	E02a.1	2997	<i>Efficient NUFFT-Based Spectral Domain Method of Moments Analysis of Multilayered Periodic Structures with Subsectional Basis Functions</i>
	E02a.3	3007	<i>Efficient Optimization-Assisted Full-Wave MoM Unit-Cell Design for Dual-Band Transmitarrays</i>
Corrao, Nicolas	CS3.5	311	<i>Exploring PLA/Flax Substrates for Antenna Applications: Assessing Moisture, Temperature and Dielectric Constant Homogeneity</i>
Corre, Samuel	CS42b.2	442	<i>Multiple Reduced Order Models for Antenna Measurements</i>
Corre, Yoann	CS17a.3	10	<i>Exploring RIS Coverage Enhancement in Factories: From Ray-Based Modeling to Use-Case Analysis</i>
	P04b.2	970	<i>Ray-Tracing Calibration from Channel Sounding Measurements in a Millimeter-Wave Industrial Scenario</i>
Cosottini, Mirco	E01.4	2028	<i>Huygens Principle Imaging Method Powered by Deep Learning for Brain Stroke Classification</i>
Costa, Filippo	PE1.15	1295	<i>D-Band Absorber Comprising Tantalum Nitride-Based Resistively-Loaded High Impedance Surfaces</i>
Costa, Jorge	P05.1	241	<i>Small-Scale Passive Millimetre-Wave Imaging Measurements for Marine Litter Detection at W-Band</i>
	CS6b.1	490	<i>Multibeam Antenna for Wide-Angle 95-Beam Coverage at Ka-Band Using a Multifocal Transmit-Array</i>
	A16.1	1729	<i>Novel Risley Prism Design Approach with Improved Side Lobe Levels Using Multi-Layer Transmit-Arrays</i>
	P06.4	2742	<i>Antenna Position Layout and Frequency Impact on Tumor Detection in Microwave Breast Imaging</i>
	E02a.3	3007	<i>Efficient Optimization-Assisted Full-Wave MoM Unit-Cell Design for Dual-Band Transmitarrays</i>
	PA3.14	3450	<i>Study of Environmentally-Friendly Radomes Using Cork-Rubber Composites for 5G Backhaul Links at E-Band</i>
	PP03.18	3660	<i>Best Practices for Accurate Results Using Numerical Solvers for Microwave Body Screening</i>
	P02.3	3772	<i>Feature Selection for Identifying Optimal Microwave Frequencies to Detect Floating Macroplastic Litter in C and X Bands</i>
	A26.5	4212	<i>Improved Performance of a 1-Bit RIS by Using Two Switches per Bit Implementation</i>
Costa-Perez, Xavier	CS20b.4	406	<i>Impedance-Based RIS Channel Model and Optimization in Fast-Fading Environments</i>
	CS34.4	2625	<i>Empirical Validation of the Impedance-Based RIS Channel Model in an Indoor Scattering Environment</i>
Costantine, Joseph	A20.2	3816	<i>Stretchable Multi-Band Radio Frequency Sensor for Strain</i>

			<i>Measurement</i>
Costanzo, Alessandra	CS14b.2	4353	<i>Multistable Structures for Deployable and Reconfigurable Antennas</i>
	CS36b.4	911	<i>Simplified Frequency-Diverse Array Architecture for Surveillance Purposes</i>
Costanzo, Sandra	PA1.15	3395	<i>CVNN Approach for Microwave Imaging Applications in Brain Cancer: Preliminary Results</i>
	A20.1	3812	<i>Errors Correlation in Near-Field Focused Arrays for Biosafe Microwave Applications</i>
Cotton, Simon	PA4.2	2109	<i>A Fully Additive Manufactured D-Band SIW Antenna</i>
Coupez, Jean-Philippe	PA8.20	2354	<i>A Compact Flexible BLE Antenna for a Remote-Control Application</i>
Cousin, Pascal	PA7.8	1195	<i>Shaping the Sub-Reflector of a Ring Focus Antenna for Tailored Beamwidth Applications</i>
Couty, Charles	PA2.7	1084	<i>Design and Prototyping of a Low-Cost Parasitic Element Antenna for a Telemetry-Telecommand Link on Ariane 6 Space Launcher</i>
Craeye, Christophe	PA2.21	1145	<i>Wideband Low-Profile Circularly Polarized All-Metal Antenna for Triton Exploration</i>
	M3.4	2600	<i>Numerical Assessment of a Cognitive Chamber: TMz Case</i>
	A07.5	2679	<i>A Cylindrical Mismatched Luneburg Lens Implemented on PCB at V-Band</i>
	E02a.4	3012	<i>Dispersion Curve Calculation Using the Method of Moments: The Impact of Macro Basis Functions</i>
	CS19a.3	4077	<i>Modal Analysis of Thermal Noise from Lossy Dielectric Medium</i>
Crichton, Devin	CS46.3	4223	<i>CubeSat Formation Antenna Array Synchronization for GNSS-R</i>
	CS4.4	3189	<i>The Hydrogen Intensity Real-Time Analysis eXperiment: Overview and Status Update</i>
Crisafulli, Ottavio	A16.5	1749	<i>Design of a Wideband Dual-Polarized Stacked Antenna Array for SATCOM Applications</i>
	PA8.10	2311	<i>Octagonal Patch Tag Antenna and 3 × 3 Array Locator for DoA Applications</i>
Crocco, Lorenzo	CS24a.1	724	<i>Advancements in the Experimental Validation of a Wearable Microwave Imaging System for Brain Stroke Monitoring</i>
	CS24a.2	727	<i>Microwave Imaging for Monitoring Bone Healing Using Magnetic Scaffolds: An Initial Analysis</i>
	CS24a.5	740	<i>Polynomial Basis Functions for Qualitative Head Tissue Segmentation via Linearized Microwave Imaging</i>
	CS33a.3	3054	<i>Advancements in Broadband Electromagnetic Sensing for Food Quality Control</i>
	CS33a.5	3062	<i>Generating a Library of Head Phantoms for Microwave Imaging Using Spherical Harmonic Approximation</i>
Crosta, Paolo	P02.2	3768	<i>Learning-Based Procedures for Inverse Design of Electromagnetic Devices: A Preliminary Investigation</i>
	PA2.15	1119	<i>Feasibility Study of 3D Printed Luneburg Lens Using Fused Deposit Material 3D Printing Technology for Ku-Band Application</i>
Crozzoli, Maurizio	CS20b.3	402	<i>Measurements of Reconfigurable Intelligent Surface in 5G System Within a Reverberation Chamber at mmWave</i>

Csurgai-Horváth, László	PP02.15	2557	<i>Large-Scale Site Diversity Experiment in Ljubljana and Budapest at Ka-Band with Alphasat Satellite</i>
Cueille, Marylène	E02b.1	3268	<i>Frequency-Domain TLM Method with Cartesian Block Meshing</i>
Cuesta, Francisco	CS20a.1	86	<i>Comparison of Simplistic System-Level RIS Models and Diffraction-Theory Solutions</i>
Cui, Tie Jun	CS17b.2	322	<i>Challenges and Opportunities of Amplified Information Metasurfaces for Simultaneous Wireless Communications and Power Transfers</i>
	CS17b.3	326	<i>Information Metasurface for Simultaneous Wave Manipulations and Signal Modulations</i>
Cui, YanJin	PA2.16	1123	<i>Study on CFM Method for Beam Compensation of Array-Fed Space-Borne Reflector Antennas</i>
Cui, Zhuangzhuang	PM1.3	1318	<i>Impact of 6D Mobility on Doppler Characteristics of UAV-To-Vehicle Channels</i>
	CS23b.2	1994	<i>Path Loss Modeling for Air-To-Ground Channels in a Suburban Environment</i>
Cuiza, Mishel	PP02.20	2582	<i>Comparison Between ERA5 Cloud Parameters and Rainfall Rate in Madrid</i>
Cumner, John	CS4.2	3181	<i>Mitigating Zenith Blindness from Mutual Coupling in a Sunflower Phased Array</i>
Curcio, Claudio	CS42b.3	446	<i>Phaseless Characterization of Flat Sources with a Planar Wide-Mesh Scanning Strategy</i>
	CS42b.4	451	<i>Discretizing 2D Equivalent Radiating Panels by Legendre Quadrature</i>
	E10b.5	2077	<i>Numerical Results on the Use of the L-SVD Approach for the Solution of the Inverse Source Problem from Amplitude-Only Data</i>
Curreli, Nicola	CS24a.2	727	<i>Microwave Imaging for Monitoring Bone Healing Using Magnetic Scaffolds: An Initial Analysis</i>
	A04.3	1467	<i>A Shared-Aperture Planar Antenna for 5G</i>
	PA4.12	2155	<i>A Dual Linearly Polarized Array for 5G FR2</i>
	PP03.16		<i>Advances in Core-Shell Nanocrystals: A Multiphysics Approach to Multispectral Electromagnetic Shielding</i>
Curto, Sergio	CS28.4	480	<i>Phantom Material with Biological Composition for Muscle Equivalent Radiofrequency, Thermal and Magnetic Resonance Properties</i>
Czarnowske, Kyra	P05.2	246	<i>Multifunction Over-The-Horizon Radar for Space Domain Awareness</i>
Czelen, Mateusz	PA8.15	2332	<i>Miniaturized and Lightweight ESPAR Antenna for WSN and IoT Applications</i>
Czwalinna, Marie	PP03.13	3643	<i>Filter Integrated Microstrip 3-Port Power Combiner</i>

D

D' Addio, Salvatore	CS46.2	4219	<i>Digital Beamformer for GNSS Reflectometry and Radio Occultation Applications</i>
D'Agostino, Francesco	CS42a.3	146	<i>Reconstruction of the Far-Field Pattern Radiated by an Elongated Antenna Measured over a Perfectly Electric Conducting Ground Plane in a Spherical Spiral Near-Field Facility</i>
	CS42b.3	446	<i>Phaseless Characterization of Flat Sources with a Planar Wide-Mesh Scanning Strategy</i>
	CS42b.4	451	<i>Discretizing 2D Equivalent Radiating Panels by Legendre Quadrature</i>

D'Amico, Michele	CS29.2	3792	<i>Physics-Informed Generative Neural Networks for RF Propagation Prediction with Application to Indoor Body Perception</i>
D'Errico, Raffaele	CS6b.2	494	<i>Hybrid Analog-Digital Beamforming System with Quad-Steerable Beams Based on Programmable Transmitarray</i>
	P04b.2	970	<i>Ray-Tracing Calibration from Channel Sounding Measurements in a Millimeter-Wave Industrial Scenario</i>
	CS34.4	2625	<i>Empirical Validation of the Impedance-Based RIS Channel Model in an Indoor Scattering Environment</i>
D'Orazio, Antonella	PA1.3	3340	<i>Eco-Friendly and Conformable PIFA Based on PEDOT: PSS and a Sustainable Chitosan Substrate for 5G Communications</i>
da Costa, Tomás	P05.1	241	<i>Small-Scale Passive Millimetre-Wave Imaging Measurements for Marine Litter Detection at W-Band</i>
	P02.3	3772	<i>Feature Selection for Identifying Optimal Microwave Frequencies to Detect Floating Macroplastic Litter in C and X Bands</i>
da Silva Mello, Luiz	P09.4	2649	<i>Rain Attenuation at mmWave and Optical Bands from Visibility and Rainfall Intensity Measurements</i>
Dabboor, Mohammed	P02.5	3782	<i>Mechanical Vibrations on a Deployable Nanosatellite Antenna: SAR Performance Analysis</i>
Dabironezare, Shahab Oddin	CS44a.1	745	<i>Development of a Shaped Quartz Lens Antenna for Wide Scanning Sub-Millimeter Imagers</i>
	PA4.16	2174	<i>Design of Wide Band Multi-Lens Focal Plane Arrays for the TIFUUN Instrument</i>
	A07.3	2669	<i>On the Design of Wide-Scanning Lenses with Integrated Focal Arrays</i>
Dai, Jize	CS14b.1	4349	<i>Reconfiguration of Electromagnetic Metasurfaces Using Tunable Shape Morphing Structures</i>
Dai, Jun Yan	CS17b.3	326	<i>Information Metasurface for Simultaneous Wave Manipulations and Signal Modulations</i>
Damerji, Mohamed	PA4.21	2193	<i>Terahertz Microstrip Leaky-Wave Antenna for WR1.0 Band</i>
Damm, Frieso	CS39a.4	622	<i>Addressing PIM Challenges in Radio Base Stations: Field Issues and Testing Methods for Large-Scale Deployments</i>
Dammann, Armin	CS23b.3	1999	<i>Mixture Density Networks for Multipath Assisted Positioning-Based Fingerprinting</i>
Danesh, Shadi	PA2.9	1091	<i>Sub-7 GHz Circularly Polarized Dielectric Resonator Antenna Array for Full-Duplex Applications</i>
Das, Hrishit	PE1.16	1300	<i>Mechatronic Phase-Control Reflector System with In-Plane Axis Control</i>
Dasari, Sree Adinarayana	CS37a.4	42	<i>Integrated Low-Loss mmWave On-Chip Arrays</i>
Daskalakis, Spyridon Nektarios	CS1a.2	4027	<i>Single-Branch Hybrid Resistance Compression Technique for Enhanced Rectifier Performance</i>
Dasmahapatra, Pratim	PA6.12	2260	<i>An Efficient Wireless Power Transfer System Using Transmission and Reflection Characteristics of Metamaterial</i>
Datashvili, Leri	A17.4	3754	<i>RF Modelling and Validation of the Breadboard Antenna of the Copernicus Imaging Microwave Radiometer</i>
Dausien, Kristof	CS12b.2	4263	<i>Robotic Antenna Characterization System Based on Wideband FMCW Transceiver Modules</i>

Davenport, Christopher	PE3.7	2388	<i>Electromagnetic Modelling in Modern Vehicles: A Pathway to Efficiency and Performance</i>
Davies, Benedict	CS14a.1	4132	<i>Enabling Shape Morphing Communications at mmWave with Spray on Antenna Arrays</i>
Dayan, Amir	PM1.6	1331	<i>Intermodulation Mitigation Through Surrounding Impedance Manipulation</i>
De, Ratul	PA5.13	3546	<i>A Reactively Coupled Bi-Directional Dual CP Antenna</i>
De Bolla, George	PE3.7	2388	<i>Electromagnetic Modelling in Modern Vehicles: A Pathway to Efficiency and Performance</i>
de Cos Gómez, María Elena	CS3.4	306	<i>Eco-Friendly Meta-Radomized Antenna for Millimeter Wave Radar</i>
De Guzman, Mar Francis	PP02.12	2542	<i>Comparison of Indoor Propagation Channels at 28 GHz and 140 GHz Bands</i>
de la Rosa del Val, Pablo	CS17a.4	15	<i>Reflective Surfaces Based on Semi-Passive Reconfigurable Polymer Network Liquid Crystal</i>
de Lera Acedo, Eloy	CS4.2	3181	<i>Mitigating Zenith Blindness from Mutual Coupling in a Sunflower Phased Array</i>
de Lustrac, André	CS19a.3	4077	<i>Modal Analysis of Thermal Noise from Lossy Dielectric Medium</i>
	E13.5	284	<i>Transmissive-Type Metagratings with Few Meta-Atoms for Beam Splitting</i>
De Marco, Raffaele	A27a.3	641	<i>K-Band Microstrip ESPAR Antenna Integrated into Large Array</i>
	PA2.14	1114	<i>Synthesis of a Planar 2D Butler Matrix: A Showcase with a 3x3 Array</i>
De Martres, Julie	CS40a.5	1770	<i>A Self Deployable and Reconfigurable Antenna in VHF Band for a New Space Mission</i>
de Marzo, Gaia	PA1.3	3340	<i>Eco-Friendly and Conformable PIFA Based on PEDOT: PSS and a Sustainable Chitosan Substrate for 5G Communications</i>
de Rosny, Julien	CS36a.4	715	<i>Compact Metamaterial Antenna for Three-Dimensional Angular Localization of Multiple Radio-Frequency Sources</i>
	A26.1	4192	<i>An Electromagnetic-Compliant Scattering Model for Reconfigurable Intelligent Surfaces</i>
De Sagazan, Olivier	CS7.1	1592	<i>Low Profile and High Gain Folded Transmitarray in Quartz for Radiometry at 310 GHz</i>
de Souza, Rausley	CS34.5	2629	<i>RIS Performance in a Comprehensive Fading Environment</i>
de Villiers, Dirk	CS4.3	3186	<i>A Performance Comparison of Sub-Octave Band Corrugated Horns to a Quadruple-Ridged Flared Horn for the ngVLA Radio Telescope</i>
De Vittorio, Massimo	PA1.3	3340	<i>Eco-Friendly and Conformable PIFA Based on PEDOT: PSS and a Sustainable Chitosan Substrate for 5G Communications</i>
de Vos van Steenwijk, Reynolt	CS46.1	4215	<i>Dual All Metal Patch Antenna for the HydroGNSS Mission</i>
Degli-Esposti, Vittorio	CS20b.2	398	<i>A Macroscopic Bilateral Modeling Approach for Reflective and Transmissive Metasurfaces</i>
	CS43b.3	4178	<i>Machine Learning Approach to Delay Spread Estimation in Industrial Environments</i>
	CS43b.4	4183	<i>A Study on Satellite-To-Ground Propagation in Urban Environment</i>
Del Galdo, Giovanni	CS23b.5	2009	<i>Characterization of Propagation from Measurements at Sub-THz for</i>

			<i>ISAC Applications in an Emulated Dynamic Industrial Scenario</i>
del Hougne, Philipp	CS20a.3	95	<i>Load Impedances Vs Polarizabilities: On the Compactness of Physics-Compliant Models of RIS-Parametrized Wireless Channels</i>
	CS17b.5	335	<i>RIS-Based Over-The-Air Channel Equalization in Resource-Constrained Wireless Networks</i>
Del Prete, Simone	CS43b.3	4178	<i>Machine Learning Approach to Delay Spread Estimation in Industrial Environments</i>
Del Real, Juan Antonio	CS39b.5	827	<i>Antennas and Power Measurement Techniques for Wireless Applications</i>
Delamotte, Thomas	CS25.1	654	<i>Beamforming Schemes for 6G Direct-To-Cell Connectivity Using Satellite Swarms</i>
Delaveaud, Christophe	A13.1	1949	<i>Ultra-Miniature Circularly Polarized Antenna with Omni-Directional Pattern for Sat-IoT</i>
	PA8.9	2306	<i>Whip Antenna Miniaturization at VHF Band Using Magneto-Dielectric Materials</i>
	A03a.2	2867	<i>Loaded and Load-Less Supergain Parasitic End-Fire Arrays</i>
	CS41.3	3230	<i>Design of Electrically Small Antennas and Radiation Efficiency Measurement Using MQFM with Radian Wheeler Cap Sizes</i>
Delfini, Duccio	A15a.5	4127	<i>Tapering Impact on the Spatial and Frequency Responses of Broadband Asymmetrically Routed Phased Arrays</i>
Delgado-Lozano, Ignacio Maria	A01a.2	2933	<i>Design of Broadband Stacked Patch Microstrip Antennas Fed by Differential Microstrip Lines with Large Common-Mode Rejection</i>
Delgado-Restituto, Manuel	CS40b.3	1976	<i>Compact 868 MHz RFID-Based Antenna for Queen Bee Identification and Location Inside Hives</i>
Dell'Aere, Giuseppe	PA7.8	1195	<i>Shaping the Sub-Reflector of a Ring Focus Antenna for Tailored Beamwidth Applications</i>
Della Giovampaola, Cristian	CS25.5	673	<i>TX/RX Terminal Based on Metascreen Technology for Ka-Band Satcom with Dual Switchable Polarization</i>
Dellabate, Alessandro	CS27.2	1575	<i>An Electromagnetic Metasurface for Impedance Matching in Microwave Biomedical Applications</i>
	PE3.8	2392	<i>Design of a Conformal and Low-Frequency Metasurface for Magnetic Field Shielding in Wireless Power Transfer Systems</i>
Delmonte, Nicolò	CS8.5	2899	<i>Dual-Resonance SIW-Based Reflectarray Unit Cell for Broadband Applications</i>
Demas, John	CS12b.4	4273	<i>Robotic near Field Scanning for High Throughput Phased Array Production Test</i>
Demeester, Piet	CS2.5	184	<i>New Hybrid Ray-Tracing/FDTD for EMF Exposure in 6G Networks Using Semantically Classified Google Earth Photogrammetry with Measurement Validation</i>
Demmer, David	CS6b.2	494	<i>Hybrid Analog-Digital Beamforming System with Quad-Steerable Beams Based on Programmable Transmitarray</i>
Deng, Lei	CS39a.4	622	<i>Addressing PIM Challenges in Radio Base Stations: Field Issues and Testing Methods for Large-Scale Deployments</i>
Denidni, Tayeb	PA2.11	1101	<i>Multi-Bit Wideband Transmitarray Aperture with Independent Phase and Amplitude Control for High Gain with Low Sidelobe Mm-Wave</i>

Applications

	A01a.4	2941	<i>Dual-Polarized OAM Antenna with Frequency and Mode Agility for Intelligent OAM Communications</i>
	PA1.2	3336	<i>Dual-Band 3-D MIMO Antenna for Deep Tissue Devices</i>
Desombre, Paul	CS44a.4	757	<i>High Data-Rate Sub-THz Coherent Near-Field Wireless Links Enabled by Spline-Profile Bessel Launchers</i>
Deville, Charlotte	A12a.3	1715	<i>Behavioral Models for the Cosimulation and Optimization of Active Electronically Scanned Arrays</i>
Dhanade, Yuvraj	CS8.4	2896	<i>Generation of Highly-Pure OAM Beams with Simple Slotted SIW Antenna Array</i>
Di, Jingyun	P10b.2	3249	<i>Validation of Ray-Tracing Simulated Channels for Massive MIMO Systems at Millimeter-Wave Bands</i>
Di Carlofelice, Alessandro	PA2.23	1154	<i>Ka-Band Phased Antenna Array Concept for High-EIRP Satellite Connections</i>
Di Cristofano, Marco	CS24a.4	736	<i>Analytical and Numerical Solution of the One Dimensional Steady State Bioheat Transfer Equation</i>
	CS24b.5	936	<i>Wideband Dielectric Characterization of Biological Tissues and Realistic Phantom Preparation at Microwave Frequencies</i>
Di Donato, Loreto	A16.5	1749	<i>Design of a Wideband Dual-Polarized Stacked Antenna Array for SATCOM Applications</i>
	PA8.10	2311	<i>Octagonal Patch Tag Antenna and 3 × 3 Array Locator for DoA Applications</i>
Di Fabio, Saverio	PP02.13	2547	<i>Radiometeorological Forecasts for Satellite Links Operations: Validation with Measurements from BepiColombo Mission</i>
	P10b.3	3254	<i>Exploiting Numerical Weather Prediction Data for Radiopropagation Modeling of SatCom Links</i>
Di Giampaolo, Emidio	PA2.23	1154	<i>Ka-Band Phased Antenna Array Concept for High-EIRP Satellite Connections</i>
Di Meo, Simona	CS24b.1	920	<i>Microwave Tomography Bone Imaging: Analysing the Impact of Skin Thickness on the Reconstruction of Numerical Bone Phantoms</i>
Di Paola, Carla	CS2.3	175	<i>Long-Term Network-Based Assessment of the Actual Output Power of Base Stations in a 5G Network</i>
Di Renzo, Marco	CS17a.3	10	<i>Exploring RIS Coverage Enhancement in Factories: From Ray-Based Modeling to Use-Case Analysis</i>
	CS20a.2	91	<i>Analysis and Optimization of Reconfigurable Intelligent Surfaces Based on S-Parameters Multiport Network Theory</i>
Di Renzo, Marco	CS20b.4	406	<i>Impedance-Based RIS Channel Model and Optimization in Fast-Fading Environments</i>
	CS34.4	2625	<i>Empirical Validation of the Impedance-Based RIS Channel Model in an Indoor Scattering Environment</i>
Diamanti, Riccardo	CS20b.3	402	<i>Measurements of Reconfigurable Intelligent Surface in 5G System Within a Reverberation Chamber at mmWave</i>
Diaz, Sebastian	A25.4	3100	<i>3D-Printed Circular Polarized Dielectric Resonator Antenna with Enhanced Axial Ratio Bandwidth Using Anisotropic Material</i>
Dicandia, Francesco	CS6a.5	212	<i>Multibeam Phased Array with Reduced Transmit and Receive Modules</i>

	CS18.2	3674	<i>Circularly Polarized Transmitarray Design Using Characteristic Modes Theory</i>
Diener, Jacobus	CS4.4	3189	<i>The Hydrogen Intensity Real-Time Analysis eXperiment: Overview and Status Update</i>
Dileep, Alka	PE3.2	2364	<i>Polarization Insensitive Broadband Frequency Selective Resorber with Improved Selectivity for Stealth Applications</i>
Dimech, Evan	CS24b.3	928	<i>Analysis of Return Loss with an Uncooled Coaxial Monopole Antenna During Microwave Ablation</i>
Ding, Can	CS10.1	850	<i>Efficient Ray-Tracing Model for Generalized 2D Dielectric Lenses Combined with Arrays</i>
	A02.5	3710	<i>A Four-Channel In-Band Full-Duplex (IBFD) Antenna System with Shared Radiation Aperture</i>
Ding, Dazhi	E12.3	2829	<i>Time-Modulated Metasurface-Based System for the Generation of False Radar Targets</i>
Ding, Qimin	PE1.3	1249	<i>A Polarization-Insensitive Ultra-Broadband FSS Absorber with Low-Profile Based on the ITO Film</i>
	CS30a.5	3947	<i>Alternate Optimization with Deep Learning to Design Beam Deflector Under Aperiodic Near-Field Coupling Conditions</i>
Ding, Yuan	CS48.1	3977	<i>Beamforming Orthogonality in Coupled Directional Modulation Arrays</i>
	CS1b.3	4246	<i>A mmWave Leaky-Wave Antenna for Efficiency Enhanced Near-Field Wireless Power Transfer and Communication</i>
Dirix, Marc	PM2.2	2433	<i>Design Effects of the Junction Contour of a Blended Rolled Edge Compact Range Reflector</i>
Disharoon, Walter	CS37a.4	42	<i>Integrated Low-Loss mmWave On-Chip Arrays</i>
Disserand, Anthony	PA2.7	1084	<i>Design and Prototyping of a Low-Cost Parasitic Element Antenna for a Telemetry-Telecommand Link on Ariane 6 Space Launcher</i>
Dittman, Michael	CS9a.3	227	<i>Beam Focusing with a Conformal Leaky-Wave Antenna Described by a Spline Curve</i>
Djemmah, Djihad Amina	E05.1	2036	<i>From Bulk Toward Micro-Structured TiO₂ Ceramics for All-Dielectric Metamaterials at Terahertz Frequencies</i>
Djerafi, Tarek	CS40b.4	1981	<i>Efficient Wireless Power Transfer to an Ultra-Miniaturized Antenna for Future Cardiac Leadless Pacemaker</i>
Döbereiner, Michael	CS5a.6	81	<i>Excitation Signal Design for THz Channel Sounding and Propagation Parameter Estimation</i>
	P01.2	3837	<i>Grid-Free Harmonic Retrieval and Model Order Selection Using Convolutional Neural Networks</i>
Doeker, Tobias	PP02.6	2515	<i>Antenna Pattern Tracking Algorithm for Low Terahertz Communications</i>
Doherty, Paul	CS4.5	3194	<i>CSIRO Radio Astronomy Receiver Update - Ultra Wideband and Phased Array Feeds</i>
Domanski, Kamil	M3.5	2605	<i>Highly Precised and Efficient Robot-Based ESPAR Antenna Measurements in Realistic Environments</i>
Domínguez-Bolaño, Tomás	CS23a.5	1794	<i>HRPE-Enhanced AI-Based 5G Indoor Localization in Presence of Specular and Dense Multipaths</i>
Dommel, Johannes	PP02.8	2523	<i>Comparison of Propagation Characteristics Between 5G Bands in a Reflective Industrial Environment</i>

Don, Alexander	PA8.2	2274	<i>Dual-Polarized Substrate Integrated Waveguide Antenna with High Isolation for Polarimetric Radar</i>
Dong, Ming	PE2.12	1036	<i>A Discontinuous Galerkin Time-Domain Scheme to Model Lasing Dynamics in Four-Level Two-Electron Atomic Systems</i>
Dong, Yunfeng	PA7.6	1185	<i>Dual-Feed Wideband Folded Waveguide Antenna for Handset Devices</i>
Donval, Dominique	PE2.3	999	<i>Management of Radiofrequency Compatibility on Aircraft</i>
Doré, Jean-Baptiste	CS6b.2	494	<i>Hybrid Analog-Digital Beamforming System with Quad-Steerable Beams Based on Programmable Transmitarray</i>
Döring, Maximilian	PA6.2	2218	<i>An Eigenvector-Supported Optimization Method for Holographic-Based Leaky Wave Antennas</i>
	A11.2	3157	<i>A Low-Profile Wide-Scan Magneto-Electric Dipole Antenna for 5G mm-Wave Communications</i>
	PA3.11	3438	<i>Broadband Waveguide Magneto-Electric Dipole Antenna for F-Band Applications</i>
Dossi, Laura	P10b.3	3254	<i>Exploiting Numerical Weather Prediction Data for Radiopropagation Modeling of SatCom Links</i>
Dou, Jianwu	CS23a.2	1780	<i>Terahertz Channel Modeling Based on Scattering Characterization</i>
	CS43a.3	3962	<i>A Deep Learning Based Surface Current Generation Method for Scattering Modeling at Terahertz Band</i>
Doufexi, Angela	PA5.22	3581	<i>DRL-Based Sidelobe Suppression for Multi-Focus Reconfigurable Intelligent Surface</i>
Dovelos, Konstantinos	PM2.10	2469	<i>Assessing Performance of Transparent Conductive Films for Microwave Industrial Applications</i>
Downey, James	CS12b.5	4278	<i>Robotic Arm-Based Antenna Metrology System for Aerospace Applications</i>
Dressler, Falko	P10a.4	2987	<i>Direct Clustering and Multi-Path Component Identification on THz Channel Measurements in a Factory Environment</i>
Dridi, Marwa	PP03.12	3639	<i>Supervised Machine Learning for Breast Cancer Detection Using Microwave Imaging in the Frequency Domain</i>
Drouguet, Maxime	CS46.3	4223	<i>CubeSat Formation Antenna Array Synchronization for GNSS-R</i>
Du, Jia	CS6a.3	204	<i>Wideband Transmissive Metasurfaces for Sub-THz Frequency-Dependent Beam Scanning</i>
Dubard, Jean-Lou	E02b.1	3268	<i>Frequency-Domain TLM Method with Cartesian Block Meshing</i>
Dubey, Ankit	PA4.18	2181	<i>A Wideband 3D Printed Digital Metasurface Transmitarray Antenna for mm-Wave Applications</i>
Dudek, Andrzej	PA3.20	3479	<i>Sub-THz On-Chip CPW Monopole on InP with Cross-Shaped Slot for Bandwidth Enhancement</i>
Dudley-McEvoy, Sandra	E01.4	2028	<i>Huygens Principle Imaging Method Powered by Deep Learning for Brain Stroke Classification</i>
Dugan, Jordan	CS9b.1	512	<i>Emulating Spatial Dispersion Using Non-Spatially Dispersive Periodic Metasurfaces</i>
	E02b.3	3276	<i>Mixed Spatial-Spectral Domain Integral Equation Solver for Higher-Order Boundary Conditions in Electromagnetics</i>
Dukhopelnykov, Sergii	PE2.15	1048	<i>Influence of the Incidence Angle on the Focusing of Luneburg Lens Partially Covered with Graphene</i>

Dulwich, Fred	CS4.2	3181	<i>Mitigating Zenith Blindness from Mutual Coupling in a Sunflower Phased Array</i>
Dumanli, Sema	CS28.5	485	<i>Temperature-Dependent Electrical Characterization of a Thermally Sensitive Hepatic Tumor Phantom</i>
	CS27.5	1588	<i>Biodegradable Implant Antenna Utilized for Real-Time Sensing Through Genetically Modified Bacteria</i>
Dun, Gwenael	M5.1	537	<i>On the RF Absorber Coverage of Antenna Under Test Positioners</i>
Dunne, Eoghan	CS28.1	465	<i>Dielectric Characterisation of Human Parathyroid Glands at Microwave Frequencies</i>
Dunning, Alex	CS4.5	3194	<i>CSIRO Radio Astronomy Receiver Update - Ultra Wideband and Phased Array Feeds</i>
Dupleich, Diego	P04b.3	975	<i>Ray Tracing and Measurement-Based Characterization of Inter/Intra-Machine THz Wireless Channels</i>
	CS23b.5	2009	<i>Characterization of Propagation from Measurements at Sub-THz for ISAC Applications in an Emulated Dynamic Industrial Scenario</i>
Dutta, Rahul	PE1.1	1241	<i>Broadening the Spectrum: Extending the Finite Crystal Method to Characterize Static Multi-Atomic Active Metamaterial Systems</i>

E

E. J. Scheible, Bernhard	PP03.13	3643	<i>Filter Integrated Microstrip 3-Port Power Combiner</i>
Eashour, Fatimah	CS24a.3	731	<i>Evaluating System Design in Breast Microwave Sensing: Data and Image Quality in Multiple Systems</i>
	P03.4	1543	<i>Neural Network Based Microwave Tumour Detection Using Breast Pairs</i>
Eastlake, Thomas	CS45.1	1799	<i>MR/Microwave Tomography Integrated Breast Cancer Imaging</i>
Ebert, Alexander	CS23b.5	2009	<i>Characterization of Propagation from Measurements at Sub-THz for ISAC Applications in an Emulated Dynamic Industrial Scenario</i>
Ebrahimizadeh, Javad	CS47.3	421	<i>Millimeter-Wave Scattering from Building Facade: A Simulation and Verification Study</i>
	PP03.19	3665	<i>Microwave Sensor for Detection of Optical Transparent Foreign Body in Soft Tissue: Eye</i>
Ederra, Iñigo	E04.1	2684	<i>Towards Optimal Binary Patterns for Compressive Terahertz Single-Pixel Imaging</i>
Edussooriya, Chamira	CS44b.5	960	<i>Graph Neural Network Based 77 GHz MIMO Radar Array Processor for Autonomous Robotics</i>
Eertmans, Jérôme	P04a.4	782	<i>Fully Differentiable Ray Tracing via Discontinuity Smoothing for Radio Network Optimization</i>
Egea-Lopez, Esteban	PP03.14	3647	<i>Generation of Electromagnetic Exposure Maps for 5G Communications</i>
Egozcue-Angulo, Leyre	P09.1	2634	<i>Variability of Rain Attenuation at Millimeter Waves Due to Fluctuations of the Drop Size Distribution</i>
Eguiluz, Gelber	PM1.8	1339	<i>Dielectric Differences in Biological Tissues: A Comparison Between Excised and Non-Excised Tissues Under the Influence of Chemotherapy</i>
Eibert, Thomas F.	CS42a.1	136	<i>Inverse Source Solutions with Spectral Filtering</i>
	CS32.3	1443	<i>In-Flight Calibration of the Measurement System for UAV-Based Near-Field Antenna Measurements</i>

	M4.1	2950	<i>Inverse Source-Based Three-Antenna Methods in the near Field</i>
	CS19b.1	4282	<i>A Loop-Star Decomposition for the B-Spline Based Discretization of the Electric Field Integral Equation</i>
Eichenberger, Jack	CS14b.1	4349	<i>Reconfiguration of Electromagnetic Metasurfaces Using Tunable Shape Morphing Structures</i>
Eichler, Taro	CS43b.2	4173	<i>Comparison of Sub-THz Radio Channel Characteristics at 158 GHz and 300 GHz in a Shopping Mall Scenario</i>
Eiyong, Park	CS14a.3	4139	<i>Hybrid Reconfigurable Reflective Metasurface with Both Phase and Space Modulation</i>
Ekman, Jonas	E02a.5	3016	<i>Improved PEEC Modeling of Antennas Through Time-Dependent Partial Elements</i>
Ekman, Torbjörn	CS35b.1	1903	<i>Fading Distribution Model for the Maritime Radio Channel</i>
El gharbi, Mariam	PA1.8	3362	<i>Embroidered Antenna-Based Sensor for Real-Time Natremia Monitoring</i>
El Hajj, Walid	CS39b.5	827	<i>Antennas and Power Measurement Techniques for Wireless Applications</i>
El Korso, Mohammed	E06b.2	797	<i>Direction-Of-Arrival Estimation by a Programmable Metasurface</i>
El Masri, Ihsan	PA8.20	2354	<i>A Compact Flexible BLE Antenna for a Remote-Control Application</i>
El Yousfi, Ahmed	PA1.12	3381	<i>Miniaturization of Wireless Power Transfer for Implantable Devices Using Voltage Doubler Rectifier</i>
Elahi, Adnan	CS28.1	465	<i>Dielectric Characterisation of Human Parathyroid Glands at Microwave Frequencies</i>
	CS24b.1	920	<i>Microwave Tomography Bone Imaging: Analysing the Impact of Skin Thickness on the Reconstruction of Numerical Bone Phantoms</i>
Elbir, Ahmet	CS44b.1	940	<i>Spherical Wavefront Near-Field DoA Estimation in THz Automotive Radar</i>
Eleftheriades, George V.	CS17a.2	6	<i>3D Method-Of-Moment Design of Huygens' Metasurfaces</i>
Elesina, Varvara	CS5b.4	378	<i>Channel Measurements in Workspace with Robotic Manipulators at 300 GHz and Recent Results</i>
Elizalde, Jorge	CS35a.1	1683	<i>Design and Validation of a Wireless Network for Intra-Train Communications</i>
Elzanaty, Ahmed	CS44a.2	750	<i>Dual Functional mmWave RIS for Radar and Communication Coexistence in near Field</i>
Emadeddin, Ahmad	A12a.2	1711	<i>Wide-Scan Active Highly Integrated Phased Array Antenna for Tx/Rx Application at K-Band</i>
Emanuelsson, Thomas	CS48.5	3996	<i>A Varactor-Based Reconfigurable Intelligent Surface Concept for 5G/6G mm-Wave Applications</i>
Emiliani, Luis	PP02.18	2572	<i>Investigating the Interference Induced by NGSO Constellations on GSO System Ground Stations: A Simulation Approach</i>
Encinar, Jose	A06a.5	3041	<i>Multibeam Compact Dual Reflectarray Antenna for High-Throughput Satellites in Ka-Band</i>
Endo, Akira	PA4.16	2174	<i>Design of Wide Band Multi-Lens Focal Plane Arrays for the TIFUUN Instrument</i>
Engquist, Isak	M2.2	3886	<i>Real-Time Near-Field Measurements of mmWave Devices Using a</i>

			<i>Metasurface and IR Camera</i>
Engstrand, Johan	A20.3	3818	<i>Compact Antenna Solutions for Data Transmission Using Fat-Intrabody Communication (Fat-IBC)</i>
Epstein, Ariel	E08.4	1875	<i>Rigorous Susceptibility-Based Design of Generalized Huygens' Metasurface Radomes</i>
Eralp, Mehmet	PA5.12	3542	<i>Highly Transparent and Efficient Flexible Antenna for Vehicle-To-Everything (V2X) Applications</i>
Erb, Jared	CS20b.5	409	<i>Scattering Singularities of Complex Systems Probed with Continuously Variable Metasurfaces</i>
Eriksson, Thomas	CS39b.2	813	<i>Estimation of Obtainable Data-Rates in an Over-The-Air mm-Wave MIMO Testbed</i>
	A18.2	2909	<i>Self-Interference Suppression for SatCom Active Antenna Arrays Through Joint Transmit and Receive Beamforming</i>
Erman, Fuad	A09b.5	891	<i>Liquid Metal Reconfigurable Phased Array Antenna</i>
Ermolov, Vladimir	A27b.3	837	<i>Single Material Multilayer Radome for D Band Applications</i>
Eskandari, Hossein	PA3.18	3472	<i>Embedded Graded Index Lens for Mitigating the Phase Error of an SIW Horn Lens Antenna</i>
Espín-López, Pedro	P03.1	1528	<i>Seasonal Snow Melting Process Investigation in Polar Environment Using a Dual-Receiver Radar Architecture</i>
Esposito, Giuseppe	E10b.5	2077	<i>Numerical Results on the Use of the L-SVD Approach for the Solution of the Inverse Source Problem from Amplitude-Only Data</i>
	E04.2	2689	<i>Contactless 3D Subsurface Imaging: Considerations to Set the Measurement Spacing</i>
Esselle, Karu	CS9a.5	233	<i>Beam Steering 2D Leaky Wave Resonant Cavity Antenna for Ka-Band Satellite Communication</i>
	A10.1	3066	<i>Multi-Feed Resonant Cavity Antenna with In-Antenna Power Combination for mm-Wave Communication</i>
Estatico, Claudio	CS33a.1	3045	<i>A Mild Data-Driven Approach Based on a Lebesgue-Space Inversion Procedure for Microwave Imaging Applications</i>
Ettorre, Mauro	CS9a.3	227	<i>Beam Focusing with a Conformal Leaky-Wave Antenna Described by a Spline Curve</i>
	CS16.2	567	<i>On the Data Rate Capability of Near-Field Communications Links Based on Bessel Beams</i>
	CS16.5	578	<i>Radiation Control by Space-Time-Modulated Anisotropic Impedance Surfaces</i>
	CS44a.4	757	<i>High Data-Rate Sub-THz Coherent Near-Field Wireless Links Enabled by Spline-Profile Bessel Launchers</i>
	PA7.8	1195	<i>Shaping the Sub-Reflector of a Ring Focus Antenna for Tailored Beamwidth Applications</i>
	A21.2	1484	<i>Dual-Linearly Polarized Pillbox Beamformer in Hybrid CNC-PCB Technologies at W-Band</i>
	A21.5	1498	<i>Feasibility Investigation on a Low-Cost an Air-Filled Substrate Integrated Waveguide Array Antenna in V-Band</i>
	A12b.4	1941	<i>6:1 Connected Slot Array in PCB Technology</i>
	A13.3	1958	<i>Wide-Angle Quasi-Optical Beamformer for LEO Applications</i>

	PA6.7	2238	<i>Metasurface-Based Bessel-Beam Launcher with 100λ Non-Diffractive Range</i>
	A01a.3	2938	<i>Generation of Non-Diffractive Bessel Beams for Near-Field Links Applications Using Meta-Axicons</i>
	CS26b.3	4314	<i>Thinned Connected Slot Array Design Using Higher Symmetries</i>
Eun, Hae Soo	CS37a.5	47	<i>Display-Integrated MIMO Antennas for Gesture-Sensing Radars</i>
Evans, David Andrew	PA4.19	2186	<i>A Compact High-Gain 28 GHz Antenna Array for Beyond 5G Wireless Networks</i>
Evtushkin, Gennadiy	A05.5	1836	<i>Sub-THz U-Slot Coupled Stacked-Patch Radiating Elements for Dual-Polarized MIMO Array Antennas</i>
Ezzeddine, Hussein	A26.1	4192	<i>An Electromagnetic-Compliant Scattering Model for Reconfigurable Intelligent Surfaces</i>

F

F. Vaquero, Álvaro	CS44b.3	950	<i>Multibeam Metal-Only Groove Gap Waveguide-Based Array in E-Band</i>
	A06b.2	3291	<i>Experimental Validation of Reflectarray-Based Base Station Antenna for Simultaneous Front- and Radio Back-Haul Links in mm-Wave Frequencies</i>
Faenzi, Marco	E06b.3	800	<i>Multi-Beam Dual Polarised Metasurface Antenna in Ka-Band</i>
	E08.1	1864	<i>Multibeam Radiation by Multipoint Fed Modulated MTS Apertures</i>
Faisal, Farooq	CS40b.4	1981	<i>Efficient Wireless Power Transfer to an Ultra-Miniaturized Antenna for Future Cardiac Leadless Pacemaker</i>
Falchi, Martina	E06a.4	601	<i>Design of a Low-Frequency Magnetic Metasurface for Extremely Focused and Long Range Wireless Power Transfer Applications</i>
	CS33b.4	3321	<i>Deep-Learning Optimized Reconfigurable Metasurface for Magnetic Resonance Imaging</i>
Falcón-Gómez, Anderson	PM1.7	1335	<i>Virus Detection in the Microwave Regime Through an Antenna Workbench</i>
Fan, Haijun	CS48.1	3977	<i>Beamforming Orthogonality in Coupled Directional Modulation Arrays</i>
Fan, Wei	CS5b.1	364	<i>Enabling VNA Based Channel Sounder for 6G Research: Challenges and Solutions</i>
	CS34.2	2615	<i>An Automated Over-The-Air Radiated Testing Platform for Reconfigurable Intelligent Surface</i>
	P10b.2	3249	<i>Validation of Ray-Tracing Simulated Channels for Massive MIMO Systems at Millimeter-Wave Bands</i>
Fan, Yuhan	CS8.2	2889	<i>Optimization of Contiguously Clustered Multibeam Scanning Planar Array for 5G/6G Application</i>
Fang, Mu	PA4.20	2189	<i>A Comparative Study of Decoupling Techniques for Waveguide Slot Array Antennas</i>
Fang, Shigang	A15b.2	4331	<i>Ultra-Wideband Wide-Scanning Dual-Polarized Vivaldi Antenna Unit with Novel Pendulum-Shaped Slots</i>
Fang, Xinyu	E12.3	2829	<i>Time-Modulated Metasurface-Based System for the Generation of False Radar Targets</i>
Fang, Zhaoji	CS44b.4	955	<i>Curving THz Beams in the near Field: A Framework to Compute Link Budgets</i>
Fanti, Alessandro	CS24a.2	727	<i>Microwave Imaging for Monitoring Bone Healing Using Magnetic</i>

Scaffolds: An Initial Analysis

	A04.3	1467	<i>A Shared-Aperture Planar Antenna for 5G</i>
	PA4.12	2155	<i>A Dual Linearly Polarized Array for 5G FR2</i>
	PP03.15	3651	<i>Analytical Fitting of Dielectric Response of Basal Cell Carcinoma</i>
	PP03.16		<i>Advances in Core-Shell Nanocrystals: A Multiphysics Approach to Multispectral Electromagnetic Shielding</i>
Famarzahanagri, Reza	P01.2	3837	<i>Grid-Free Harmonic Retrieval and Model Order Selection Using Convolutional Neural Networks</i>
Farès, Haifa	CS44a.4	757	<i>High Data-Rate Sub-THz Coherent Near-Field Wireless Links Enabled by Spline-Profile Bessel Launchers</i>
Farhat, Iman	CS24b.3	928	<i>Analysis of Return Loss with an Uncooled Coaxial Monopole Antenna During Microwave Ablation</i>
Farid, Nazanin	M4.2	2955	<i>Exploring Uniformity of Reverberation Chambers: Insights from Antenna Reflection Coefficient</i>
Farooq, Muhammad	P05.6	266	<i>Contactless Respiration Variability Detection and Accuracy Test Using UWB Radar</i>
Farrugia, Lourdes	CS24b.3	928	<i>Analysis of Return Loss with an Uncooled Coaxial Monopole Antenna During Microwave Ablation</i>
Faulkner, Andrew	CS4.2	3181	<i>Mitigating Zenith Blindness from Mutual Coupling in a Sunflower Phased Array</i>
Fauré, Stéphane	CS1b.4	4251	<i>Power Handling Test of a L-Band Antenna Using Infrared Thermography</i>
Fayyaz, Umar	PA7.18	1238	<i>Generation of Dual Band OAM Wave Using Single Patch Antenna for WLAN/WiMAX Applications</i>
Fazzini, Enrico	CS36b.4	911	<i>Simplified Frequency-Diverse Array Architecture for Surveillance Purposes</i>
Fear, Elise	CS45.2	1803	<i>Physics-Informed Regularization for Microwave Imaging in Biomedical Applications</i>
Fecteau, Andre	PE1.14	1292	<i>Integral Equation-Based Solver for the Simulation of Metasurface Designs</i>
Fedeli, Alessandro	CS45.5	1815	<i>Brain Stroke Microwave Diagnostics in Children Through a Nonlinear Inverse-Scattering Technique</i>
	CS33a.1	3045	<i>A Mild Data-Driven Approach Based on a Lebesgue-Space Inversion Procedure for Microwave Imaging Applications</i>
Federico, Gabriele	PA4.11	2150	<i>Pixel Antenna Design for mm-Wave Wireless Communications to Achieve Wide Scanning</i>
Feito, Sergio	CS44b.3	950	<i>Multibeam Metal-Only Groove Gap Waveguide-Based Array in E-Band</i>
Feix, Noel	CS3.6	316	<i>Use of Ecofriendly Geopolymer Ceramics in Antenna Design and Microwave Applications</i>
Felicio, Joao	P05.1	241	<i>Small-Scale Passive Millimetre-Wave Imaging Measurements for Marine Litter Detection at W-Band</i>
	CS6b.1	490	<i>Multibeam Antenna for Wide-Angle 95-Beam Coverage at Ka-Band Using a Multifocal Transmit-Array</i>
	A16.1	1729	<i>Novel Risley Prism Design Approach with Improved Side Lobe Levels Using Multi-Layer Transmit-Arrays</i>

	P06.4	2742	<i>Antenna Position Layout and Frequency Impact on Tumor Detection in Microwave Breast Imaging</i>
	E02a.3	3007	<i>Efficient Optimization-Assisted Full-Wave MoM Unit-Cell Design for Dual-Band Transmitarrays</i>
	P10b.4	3259	<i>Wind-Induced Backscatter Clustering from Vegetation at W-Band</i>
	PA3.14	3450	<i>Study of Environmentally-Friendly Radomes Using Cork-Rubber Composites for 5G Backhaul Links at E-Band</i>
	PP03.18	3660	<i>Best Practices for Accurate Results Using Numerical Solvers for Microwave Body Screening</i>
	P02.3	3772	<i>Feature Selection for Identifying Optimal Microwave Frequencies to Detect Floating Macroplastic Litter in C and X Bands</i>
	A26.5	4212	<i>Improved Performance of a 1-Bit RIS by Using Two Switches per Bit Implementation</i>
Feng, Yijun	CS6a.2	199	<i>Designing Transmissive Metasurface for Multibeam Transmitarray at 5G Millimeter-Wave Band</i>
Feresidis, Alexandros	CS9b.3	521	<i>Dual-Polarized Reconfigurable Metasurface for Leaky-Wave Antenna Design Using Air-Bridged Schottky Diode Technology</i>
	A09b.3	882	<i>Ultra-Low-Loss Millimeter Wave Beam Scanning Antenna Using Piezoelectric Actuation</i>
	E05.4	2050	<i>Design of Novel Fully Metallic mm-Wave Reflectarray Antenna</i>
	PA6.8	2241	<i>Anisotropic Circularly Polarising Graded Index Lenses Enabling High Gain CP Antennas</i>
Fernandes, Carlos	P05.1	241	<i>Small-Scale Passive Millimetre-Wave Imaging Measurements for Marine Litter Detection at W-Band</i>
	CS6b.1	490	<i>Multibeam Antenna for Wide-Angle 95-Beam Coverage at Ka-Band Using a Multifocal Transmit-Array</i>
	A16.1	1729	<i>Novel Risley Prism Design Approach with Improved Side Lobe Levels Using Multi-Layer Transmit-Arrays</i>
	P06.4	2742	<i>Antenna Position Layout and Frequency Impact on Tumor Detection in Microwave Breast Imaging</i>
	E02a.3	3007	<i>Efficient Optimization-Assisted Full-Wave MoM Unit-Cell Design for Dual-Band Transmitarrays</i>
	P10b.4	3259	<i>Wind-Induced Backscatter Clustering from Vegetation at W-Band</i>
	PA3.14	3450	<i>Study of Environmentally-Friendly Radomes Using Cork-Rubber Composites for 5G Backhaul Links at E-Band</i>
	PP03.18	3660	<i>Best Practices for Accurate Results Using Numerical Solvers for Microwave Body Screening</i>
	P02.3	3772	<i>Feature Selection for Identifying Optimal Microwave Frequencies to Detect Floating Macroplastic Litter in C and X Bands</i>
	A26.5	4212	<i>Improved Performance of a 1-Bit RIS by Using Two Switches per Bit Implementation</i>
Fernández, Alejandro	CS38.4	124	<i>Ground Plane Width Analysis for IoT Devices Embedding Antenna Boosters</i>
Fernández, Armando	A01a.2	2933	<i>Design of Broadband Stacked Patch Microstrip Antennas Fed by Differential Microstrip Lines with Large Common-Mode Rejection</i>

Fernández Caballero, Javier	CS40b.3	1976	<i>Compact 868 MHz RFID-Based Antenna for Queen Bee Identification and Location Inside Hives</i>
Fernández Carnicero, Adrián	CS40a.1	1753	<i>Tunable Segmented Loop Antenna Reader for Miniaturized Chipless Tag Detection</i>
Fernandez-Aranzamendi, E	PM1.8	1339	<i>Dielectric Differences in Biological Tissues: A Comparison Between Excised and Non-Excised Tissues Under the Influence of Chemotherapy</i>
Fernandez-Garcia, Raul	PA1.8	3362	<i>Embroidered Antenna-Based Sensor for Real-Time Natremia Monitoring</i>
Ferrando-Bataller, Miguel	CS40b.3	1976	<i>Compact 868 MHz RFID-Based Antenna for Queen Bee Identification and Location Inside Hives</i>
	CS19a.2	4072	<i>Surface Partial Differential Equations and Its Applications to Scattering Problems</i>
Ferrando-Rocher, Miguel	PA2.13	1110	<i>Closely-Spaced Groove Gap Waveguides with Reduced Coupling</i>
	PA4.9	2142	<i>5x7 Nolen Matrix in K-Band Implemented in Rectangular Waveguide</i>
	PA3.6	3417	<i>Beam-Tilted All-Metal Radial-Line Slot Array Antenna with Uniform Spacing</i>
	PA4.26	3459	<i>Amplitude-Tapered Half-Mode Gap Waveguide Distribution Network for Flat Panel Antennas</i>
Ferrara, Flaminio	CS42a.3	146	<i>Reconstruction of the Far-Field Pattern Radiated by an Elongated Antenna Measured over a Perfectly Electric Conducting Ground Plane in a Spherical Spiral Near-Field Facility</i>
	CS42b.3	446	<i>Phaseless Characterization of Flat Sources with a Planar Wide-Mesh Scanning Strategy</i>
Ferreras, Marta	CS21.3	2712	<i>From mmWave Radar Nodes to Multistatic Arrays: Design Considerations and Applications</i>
Ferrero, Fabien	PA2.15	1119	<i>Feasibility Study of 3D Printed Luneburg Lens Using Fused Deposit Material 3D Printing Technology for Ku-Band Application</i>
Fieramosca, Federica	CS29.2	3792	<i>Physics-Informed Generative Neural Networks for RF Propagation Prediction with Application to Indoor Body Perception</i>
Filgueiras, Hugo	A04.1	1458	<i>Implementation of a Novel Triband Antenna Array in a FR1/FR2 5G-NR System</i>
Fiorelli, Benedetta	E10a.4	1854	<i>Platform Scattering Analysis of the Copernicus Imaging Microwave Radiometer</i>
	A18.1	2904	<i>Uncertainty Quantification for the Reflector Antenna in the Copernicus Imaging Microwave Radiometer</i>
	A17.4	3754	<i>RF Modelling and Validation of the Breadboard Antenna of the Copernicus Imaging Microwave Radiometer</i>
Fischer, Boris	CS26b.2	4310	<i>Glide-Symmetric Reconfigurable Substrate-Integrated Holey Waveguide</i>
Fischer, Brian	CS31.4	1673	<i>Analysis of Time and Direction of Arrival (TADOA) Data Using Basis Pursuit in the AFRL One-RY Antenna Measurement Range</i>
Fisichella, Marco	PP03.6	3610	<i>Target Classification Through ISAR for Autonomous Vehicles Based on Federated Learning</i>
Findik, Cihan Barış	CS5a.5	76	<i>A Modular COTS-Based High-Efficient Sub-THz Channel Sounder and</i>

			<i>Experimental Validations</i>
	PP01.8	1380	<i>Dual-Polarized Diffraction Measurements and Modeling at D-Band Frequencies</i>
Fleury, Romain	PE1.6	1261	<i>Characterization of a Metamaterial-Enabled Waveguide Diplexer for Ka-Band Satellite Communication Systems</i>
	E05.3	2045	<i>SIW Slot Leaky-Wave Antenna Using Low-Index Metamaterial</i>
	E12.5	2836	<i>GPS Interference Cancellation Using Magneto-Dielectric Metamaterials</i>
Flores, Alexandra	PA1.15	3395	<i>CVNN Approach for Microwave Imaging Applications in Brain Cancer: Preliminary Results</i>
Flores-Espinosa, N�ria	CS10.2	855	<i>Design of a Dielectric Lens Using a Ray-Tracing Model for Satellite Communications</i>
Fl�rez Berdasco, Alicia	CS3.4	306	<i>Eco-Friendly Meta-Randomized Antenna for Millimeter Wave Radar</i>
	CS33b.5	3326	<i>Impact of Antenna Radiation Pattern Linear Phase Shift in SAR Image Quality</i>
Florez-Gonzalez, Andres	P04b.4	980	<i>Fast Indoor Radio Propagation Prediction Using Deep Learning</i>
Focardi, Paolo	CS42b.6	460	<i>Uncertainty Quantification of the Gain Budget for INCUS</i>
	A17.1	3739	<i>Feed Assembly Development for INCUS</i>
Foged, Lars	CS42a.4	151	<i>Planar Near-Field Phaseless Measurements Using Multi-Probe Arrays</i>
	CS42a.5	156	<i>Antenna Coupling Evaluation in Arrays and Complex Structures Using Measured Sources and Simulations</i>
	CS2.4	180	<i>Advanced Post-Processing Technique to Evaluate Specific Absorption Rate (SAR) for a Standard Dipole Antenna</i>
	CS5b.3	374	<i>Industrial Design Validation for a Plane Wave Generator at 28GHz</i>
	M5.2	542	<i>Uncertainty Analysis of Linear Multi-Probe Array Systems for Fast Antenna Measurements</i>
	PE2.3	999	<i>Management of Radiofrequency Compatibility on Aircraft</i>
	CS41.2	3225	<i>VHF/UHF Antenna Measurements Based on Multi Probe Array Technology</i>
Foglia Manzillo, Francesco	A09a.2	683	<i>Sub-Wavelength Anisotropic Unit-Cells for Low-Profile Transmitarray Antennas</i>
	CS7.4	1606	<i>Characterization of a D-Band Active Transmitarray System for Efficient Point-To-Point Links</i>
Fojtik, Simon	PA2.20	1140	<i>Compact Ka Band Orthomode Transducer with Conical Horn Antenna</i>
Fonseca, Nelson	CS6a.6	216	<i>Development of a Circuit-Type Multiple-Agile Beamforming and Interference Mitigation Network</i>
	P05.1	241	<i>Small-Scale Passive Millimetre-Wave Imaging Measurements for Marine Litter Detection at W-Band</i>
	CS6b.1	490	<i>Multibeam Antenna for Wide-Angle 95-Beam Coverage at Ka-Band Using a Multifocal Transmit-Array</i>
	PA7.8	1195	<i>Shaping the Sub-Reflector of a Ring Focus Antenna for Tailored Beamwidth Applications</i>
	A19.1	1503	<i>Compact Dual-Band Dual-Polarization Feed for Broadband Communication Satellites</i>
	A16.1	1729	<i>Novel Risley Prism Design Approach with Improved Side Lobe Levels</i>

			<i>Using Multi-Layer Transmit-Arrays</i>
	P02.3	3772	<i>Feature Selection for Identifying Optimal Microwave Frequencies to Detect Floating Macroplastic Litter in C and X Bands</i>
	CS30a.2	3933	<i>Additively Manufactured Waveguide Hybrid Septum Coupler Optimized Using Machine Learning</i>
Fontaine, Gabrielle	CS24a.3	731	<i>Evaluating System Design in Breast Microwave Sensing: Data and Image Quality in Multiple Systems</i>
Fonte, Alessandro	PA2.23	1154	<i>Ka-Band Phased Antenna Array Concept for High-EIRP Satellite Connections</i>
Fordham, Jeff	A25.5	3105	<i>Additively Manufactured Horn Antennas</i>
Fox, Griffin	A25.5	3105	<i>Additively Manufactured Horn Antennas</i>
Fracassini, Arianna	CS45.3	1808	<i>Preliminary Clinical Trial Results of MammoWave in the Context of RadioSpin Project</i>
Fragnier, Rémi	A12b.4	1941	<i>6:1 Connected Slot Array in PCB Technology</i>
Francione, Vito Vincenzo	A21.5	1498	<i>Feasibility Investigation on a Low-Cost an Air-Filled Substrate Integrated Waveguide Array Antenna in V-Band</i>
	A25.3	3095	<i>Design and Characterization of a Flexible Fabry-Perot Antenna Fabricated Using Conductive Inkjet Printing</i>
Franek, Ondřej	CS20a.6	107	<i>Electromagnetics-Based RIS Channel Model with Near-Field Accuracy Improvement</i>
	CS35b.5	1922	<i>Indoor Propagation Measurements with a Reconfigurable Intelligent Surface at 3.5 GHz</i>
	PA3.22	3486	<i>Wideband Array Antenna with Single-Layer Feeding Network at Ka-Band</i>
Fransson, Anders	CS39b.1	808	<i>Exploring the Properties of Reverberation Chambers in the THz Range: A Pilot Study</i>
Fraysse, Jean-Philippe	A13.3	1958	<i>Wide-Angle Quasi-Optical Beamformer for LEO Applications</i>
Freni, Angelo	A09a.2	683	<i>Sub-Wavelength Anisotropic Unit-Cells for Low-Profile Transmitarray Antennas</i>
	A10.3	3074	<i>Curved Electromagnetic Skins for Urban Scenarios</i>
	A06b.1	3287	<i>Folded Dielectric Reflectarray with Spherical Polarizer</i>
Frey, Thomas	PA6.2	2218	<i>An Eigenvector-Supported Optimization Method for Holographic-Based Leaky Wave Antennas</i>
	A11.2	3157	<i>A Low-Profile Wide-Scan Magneto-Electric Dipole Antenna for 5G mm-Wave Communications</i>
Frid, Henrik	E10a.5	1859	<i>Investigation of Near-Field Contribution in Shooting and Bouncing Rays for Installed Antenna Performance on a Simple Platform</i>
Fridén, Jonas	CS47.5	430	<i>In-Field Measurement of Total Radiated Power from Active Antenna Arrays</i>
	M4.2	2955	<i>Exploring Uniformity of Reverberation Chambers: Insights from Antenna Reflection Coefficient</i>
	M2.5	3900	<i>Optimization of the TRP Evaluation in Anechoic-Reverberation Hybrid Chamber</i>
Friedrich, Aline	CS10.3	860	<i>D-Band Active Antenna Array with Lens Enabling Quasi-Optical and Analogue Beam Reconfiguration for 6G Applications</i>

	CS21.2	2709	<i>New Efficient Waveguide Antenna for Future Automotive Radar Applications</i>
Fritts, Zachary	CS37b.4	357	<i>Increasing the Efficiency-Bandwidth Product and Impedance Bandwidth of Electrically-Small Antennas Through Parametric Space-Time Variation</i>
Fromenteze, Thomas	CS36b.3	906	<i>Towards a Reconfigurable Metacavity Antenna for Computational Imaging and DoA Estimation</i>
	PM2.7	2454	<i>Near-Field Bistatic Microwave Imaging with Dynamic Metasurface Antennas</i>
Fruehauf, Norbert	M3.3	2595	<i>Dielectric Characterization of Adhesives for THz Packaging in WR6.5, WR3.4 and WR2.2 Bands</i>
Fu, Wen	PM1.9	1343	<i>Investigation of Correlation Between Absorbed Power Density and Incident Power Density for User Equipment Antennas at Sub-THz Frequencies</i>
	PA3.5	3414	<i>5G Millimeter-Wave Reflectarray Antenna Design with a Good Gain-Filtering Characteristic Based on a High-Efficiency Polarization Converter</i>
Fu, Wenfu	PM2.13	2482	<i>Study on Antenna-Phantom Model of Aperture Antennas for SAR Analysis</i>
Fuchs, Benjamin	CS42b.2	442	<i>Multiple Reduced Order Models for Antenna Measurements</i>
	CS32.5	1453	<i>Stable Phaseless Spherical Antenna Measurements via Mixed-Norm Regularization</i>
Fuentes-Pascual, Miguel	PA2.13	1110	<i>Closely-Spaced Groove Gap Waveguides with Reduced Coupling</i>
	PA4.9	2142	<i>5x7 Nolen Matrix in K-Band Implemented in Rectangular Waveguide</i>
Fujita, Keita	P04a.5	787	<i>Proposal on Application of Quantum Annealers for Analysis of Multiple Scattered Waves</i>
	PP03.3	3597	<i>Propagation Path Analysis with Propagation QUBO Model in Urban Area</i>
Fumeaux, Christophe	CS37a.1	29	<i>3D-Printed Wearable Antenna Integrated with Rectifier for Wireless Power Transfer</i>
Fuscaldo, Walter	CS9a.2	225	<i>2D-Scanning of Circularly Polarized Beams via Array-Fed Fabry--Perot Cavity Antennas</i>
	CS9a.4	230	<i>Characterization and Comparison of Formulas for Optimizing Broadside Radiation in a 2-D Leaky-Wave Antenna</i>
	CS16.4	573	<i>Leaky-Wave Design of Hybrid-, TE-, and TM-Polarized Resonant Bessel-Beam Launchers for Millimeter- and Submillimeter-Wave Applications</i>
	CS44a.4	757	<i>High Data-Rate Sub-THz Coherent Near-Field Wireless Links Enabled by Spline-Profile Bessel Launchers</i>
	A08b.3	2091	<i>Hybrid Metal-Graphene Unit Cells for THz Reconfigurable Leaky-Wave Antennas</i>
	PE3.10	2398	<i>Highly Reflective, Low-Loss, Homogenized Fishnet Metasurfaces at Terahertz: Design and Experiment</i>
Fuschini, Franco	CS43b.3	4178	<i>Machine Learning Approach to Delay Spread Estimation in Industrial Environments</i>

	CS43b.4	4183	<i>A Study on Satellite-To-Ground Propagation in Urban Environment</i>
Fusco, Gianmarco	PP02.11	2538	<i>AlphaSat Ka-Band and Q-Band Receiving Station in Rome: Measurements and Data Analysis</i>
Fusco, Vincent	P05.5	261	<i>Sequential Phase Optimization for Coherent Long-Range Distributed Wireless Power Transfer to a Non-Communicative Receiver</i>
	PM2.7	2454	<i>Near-Field Bistatic Microwave Imaging with Dynamic Metasurface Antennas</i>
	PA5.14	3549	<i>Super-Realized Gain Huygens Antennas</i>
	PA5.17	3560	<i>Low-Profile Super-Realised Gain Antennas</i>
G			
G. Machado, Gabriel	CS14b.4	4362	<i>Wideband Dual-Polarized 1-Bit Unit-Cell Design for mmWave Reconfigurable Intelligent Surface</i>
Gabella, Marco	P02.4	3777	<i>Measuring and Modelling the Scattering Parameters of the Wet Radome of the Swiss Weather Radars</i>
Gaddam, Sindhu	CS4.4	3189	<i>The Hydrogen Intensity Real-Time Analysis eXperiment: Overview and Status Update</i>
Gaffoglio, Rossella	A20.3	3818	<i>Compact Antenna Solutions for Data Transmission Using Fat-Intrabody Communication (Fat-IBC)</i>
Gaillot, Davy	PP03.14	3647	<i>Generation of Electromagnetic Exposure Maps for 5G Communications</i>
Galdi, Vincenzo	A10.2	3071	<i>Analysis and Design of Metasurface Antennas Based on Temporal Metastructures</i>
Galeote-Cazorla, Juan	PP01.4	1360	<i>A Study on W-Band Frequency Attenuation in the Presence of Human Blockage</i>
Gallée, Francois	CS35b.3	1913	<i>mmWave Channel Sounding for Vehicular Communications</i>
Galli, Alessandro	CS9a.2	225	<i>2D-Scanning of Circularly Polarized Beams via Array-Fed Fabry--Perot Cavity Antennas</i>
	CS9a.4	230	<i>Characterization and Comparison of Formulas for Optimizing Broadside Radiation in a 2-D Leaky-Wave Antenna</i>
	CS16.4	573	<i>Leaky-Wave Design of Hybrid-, TE-, and TM-Polarized Resonant Bessel-Beam Launchers for Millimeter- and Submillimeter-Wave Applications</i>
	A08b.3	2091	<i>Hybrid Metal-Graphene Unit Cells for THz Reconfigurable Leaky-Wave Antennas</i>
Gällström, Andreas	CS31.2	1663	<i>High Resolution ISAR Imaging Methods for RCS Data Analysis</i>
Galtarossa, Andrea	A09b.2	877	<i>Recent Advances in Plasma Surfaces</i>
Gamand, Florent	CS40a.4	1766	<i>Design of Microstrip UWB Antenna with Full Ground Plane for Wearable Applications</i>
Gan, Yi-Min	PA5.23	3586	<i>Wideband Decoupling Smartphone Antenna with Integrated Metal Rim</i>
Gandini, Erio	PA2.4	1069	<i>Antenna Design for TriHex: A Future Soil Moisture and Ocean Salinity Radiometer Mission</i>
Ganie, Javid	PE3.14	2412	<i>An Angularly Stable Wideband Low Profile Single-Layer Linear to Circular Polarization Converter for Millimeter Wave Satellite Communications</i>
Gao, Hong-Wei	CS19a.5	4085	<i>Platform-Aware Optimization of Conformal Antenna Array via Simulated Bifurcation</i>

Gao, Jia	CS18.1	3669	<i>Metasurfaces Meet Characteristic Modes</i>
Gao, Mingxiang	CS27.1	1571	<i>Link Budget Estimation for Implantable Antennas: From In-Body Coupling to Free-Space Radiation</i>
Gao, Steven	CS6a.1	194	<i>Irregular Subarray with Gathered Elements for Sidelobe Suppression</i>
	PA5.9	3529	<i>A Cascaded Resonator Decoupling Network for Two Filtering Antennas with Adjacent Operating Bands</i>
	A02.1	3691	<i>A Low Profile Dual-Band Dual-Polarized Filtering Antenna with No Extra Circuit</i>
Gao, Wei	CS48.3	3987	<i>Joint Resource Allocation and Beamforming Design for Secure Short Packet Communication in RIS-Aided MISO Systems</i>
Gao, Xiang	P10b.5	3263	<i>E-Band Measured Propagation Characteristics for Urban Backhaul Communications</i>
Gao, Yuchen	A03a.1	2862	<i>Low-Profiled Wideband Dual-Polarized Conformal Antenna Array</i>
Gaquierie, Christophe	CS40a.4	1766	<i>Design of Microstrip UWB Antenna with Full Ground Plane for Wearable Applications</i>
Garcés-Socarrás, Luis	PA2.5	1074	<i>Genetic Algorithm-Based Beamforming in Subarray Architectures for GEO Satellites</i>
	CS19b.4	4295	<i>Supervised Learning Based Real-Time Adaptive Beamforming On-Board Multibeam Satellites</i>
García, Elena	CS38.3	120	<i>Reconfigurable Architecture in a 130 x 80 mm² PCB with Antenna Booster Element for Multiband Operation in IoT Devices</i>
García, Quiterio	PA2.4	1069	<i>Antenna Design for TriHex: A Future Soil Moisture and Ocean Salinity Radiometer Mission</i>
García Fernández, Joaquín	CS10.4	864	<i>Metasurface Dome Enhancing Beam Scanning of AESA Panels</i>
García Fernández, María	PA6.1	2213	<i>Orthogonal Coding for Millimeter-Wave Imaging Using MIMO Dynamic Metasurface Apertures</i>
	PM2.7	2454	<i>Near-Field Bistatic Microwave Imaging with Dynamic Metasurface Antennas</i>
	E04.3	2693	<i>A Case Study of Misalignment Errors for Range-Migration-Based Microwave Imaging with Multistatic Dynamic Metasurface Apertures</i>
	E04.4	2698	<i>GPR Imaging Relying on Frequency-Diverse Compressive Antennas</i>
	CS19b.5	4300	<i>Impact of the Unit Cell Distribution of 1-D Dynamic Metasurface Antennas on the Performance of a Computational Imaging System</i>
Garcia-Contreras, Gines	E10b.3	2069	<i>Proving the Circular Polarization of the Fundamental Modes in Rotationally Symmetric Waveguides</i>
Garcia-del-Pino, Pedro	P10a.2	2977	<i>Cloud Attenuation in the Q Band: Estimation from Experimental Data of Excess Attenuation</i>
García-Fernández, Miguel	PM1.5	1327	<i>Minimum Coherence Bandwidth for OFDM Signal Testing in Reverberation Chambers</i>
Garcia-Marin, Eduardo	A27a.1	632	<i>Full-Metal Single-Block Antenna Arrays with Waveguide Corporative Feeding Networks at Ka and V Bands</i>
Garcia-Martinez, Sergio	A07.4	2674	<i>Fully Metallic Wideband Lens Design Using a Highly Refractive Glide-Symmetric Unit Cell at W-Band</i>
	A11.3	3162	<i>Pinwheel-Shaped Polarizer for Generating Dual-Circularly Polarized</i>

			<i>Conical Radiation Patterns in the Ka-Band</i>
Garcia-Pardo, Concepcion	CS2.1	165	<i>Instantaneous Vs Theoretical Maximum Exposure Under Real Traffic Conditions: Example in the City of Valencia</i>
García-Vigueras, María	A19.5	1523	<i>Exploring the Potential of Spatially Modulated Full-Metal Dichroic Mirrors for Deep Space Antennas</i>
	E07.1	1636	<i>Model-Based Deep Learning for High-Dimensional Periodic Structures</i>
	A06a.3	3031	<i>3-D Reflectarray Unit Cell with Wideband Performance and Integrated Sensing Capability</i>
Garren, David	E11.2	2801	<i>Exact Maxwell Solution for Arbitrary Transverse Electric Multipole Radiation for Spherical Electric Current Density</i>
Garufo, Alessandro	PA5.3	3503	<i>Characterization of All-Metal Multi-Feed Antenna for High Power Applications</i>
Gashi, Ilir	PA4.8	2139	<i>A Novel GO Analysis Tool for GRIN Lenses Based on the Fast Sweeping Method</i>
Gasseling, Tony	A12a.3	1715	<i>Behavioral Models for the Cosimulation and Optimization of Active Electronically Scanned Arrays</i>
Gaudin, Gregory	A23.5	2767	<i>Modeling of Quasi-Optical Systems and Measurements with a Cobot in the J-Band</i>
Gaugain, Gabriel	CS27.3	1579	<i>Theoretical Insights and Engineering of Wireless Body-Implanted Bioelectronics</i>
Gawade, Dinesh	P06.5	2747	<i>A Time-Efficient Model for Estimating Far-Field Wireless Power Transfer to Biomedical Implants</i>
Gay, Mathilde	CS44a.4	757	<i>High Data-Rate Sub-THz Coherent Near-Field Wireless Links Enabled by Spline-Profile Bessel Launchers</i>
Ge, Feiyu	A08b.5	2100	<i>Open Stopband Suppression of Periodic Leaky-Wave Antenna Based on Theory of Small Reflections</i>
Ge, Yuehe	A27b.1	830	<i>A Wideband High-Gain Circularly-Polarized Metasurface Antenna with a Large Element Spacing SIW Array at Ka Band</i>
Gebremedhin, Ruth	P10b.1	3244	<i>Empirical Path Loss Model and Small-Scale Fading Statistics in an Indoor Office Environment in 6 and 37 GHz Shared Bands</i>
	P01.4	3847	<i>Frequency Domain Channel Characteristics in an Outdoor-To-Indoor Environment at 6 and 37 GHz</i>
Gedschold, Jonas	CS5a.6	81	<i>Excitation Signal Design for THz Channel Sounding and Propagation Parameter Estimation</i>
Geffroy, Pierre-Marie	E05.1	2036	<i>From Bulk Toward Micro-Structured TiO₂ Ceramics for All-Dielectric Metamaterials at Terahertz Frequencies</i>
Gennarelli, Claudio	CS42a.3	146	<i>Reconstruction of the Far-Field Pattern Radiated by an Elongated Antenna Measured over a Perfectly Electric Conducting Ground Plane in a Spherical Spiral Near-Field Facility</i>
	CS42b.3	446	<i>Phaseless Characterization of Flat Sources with a Planar Wide-Mesh Scanning Strategy</i>
Gennarelli, Gianluca	E10b.5	2077	<i>Numerical Results on the Use of the L-SVD Approach for the Solution of the Inverse Source Problem from Amplitude-Only Data</i>
	E04.2	2689	<i>Contactless 3D Subsurface Imaging: Considerations to Set the Measurement Spacing</i>

Genovesi, Simone	CS6a.5	212	<i>Multibeam Phased Array with Reduced Transmit and Receive Modules</i>
	PE1.15	1295	<i>D-Band Absorber Comprising Tantalum Nitride-Based Resistively-Loaded High Impedance Surfaces</i>
	CS18.2	3674	<i>Circularly Polarized Transmitarray Design Using Characteristic Modes Theory</i>
Gentile, Camillo	CS5a.1	56	<i>Context-Aware Channel Sounder for AI-Assisted Radio-Frequency Channel Modeling</i>
	CS29.1	3787	<i>AI-Based Environment Segmentation Using a Context-Aware Channel Sounder</i>
Gentner, Christian	CS23b.3	1999	<i>Mixture Density Networks for Multipath Assisted Positioning-Based Fingerprinting</i>
	CS23b.4	2004	<i>Angle of Arrival Measurements with Ultra-Wide Band Transceivers: Design and Evaluation</i>
Gentner, Philipp	A28.2	3719	<i>A High-Isolation Dual-Band Base Station Antenna Design for Full Duplex Technologies</i>
George, Daniel	CS4.5	3194	<i>CSIRO Radio Astronomy Receiver Update - Ultra Wideband and Phased Array Feeds</i>
Georgiadis, Apostolos	CS1a.2	4027	<i>Single-Branch Hybrid Resistance Compression Technique for Enhanced Rectifier Performance</i>
Gerafentis, Ioannis	CS9b.3	521	<i>Dual-Polarized Reconfigurable Metasurface for Leaky-Wave Antenna Design Using Air-Bridged Schottky Diode Technology</i>
	A09b.3	882	<i>Ultra-Low-Loss Millimeter Wave Beam Scanning Antenna Using Piezoelectric Actuation</i>
Geraghty, Michael	CS44a.3	754	<i>A Wideband Reflector-Based Mm-Wave/THz Nearfield Line Scanner for Rapidly Sensing Materials in Envelopes</i>
Gerodias, Kit	CS4.4	3189	<i>The Hydrogen Intensity Real-Time Analysis eXperiment: Overview and Status Update</i>
Geubbels, Lieke	P06.1	2727	<i>Localization of a Nasogastric Feeding Tube Using High-Frequency Harmonic Radar - a Feasibility Study</i>
Geva, Roe	E11.1	2796	<i>Isometric Symmetries in Non-Reflecting Structures</i>
Ghalichechian, Nima	CS37a.4	42	<i>Integrated Low-Loss mmWave On-Chip Arrays</i>
	CS14b.1	4349	<i>Reconfiguration of Electromagnetic Metasurfaces Using Tunable Shape Morphing Structures</i>
Gharbieh, Samara	CS6b.2	494	<i>Hybrid Analog-Digital Beamforming System with Quad-Steerable Beams Based on Programmable Transmitarray</i>
Gharsalli, Leila	PP03.12	3639	<i>Supervised Machine Learning for Breast Cancer Detection Using Microwave Imaging in the Frequency Domain</i>
Gharzouni, Ameni	CS3.6	316	<i>Use of Ecofriendly Geopolymer Ceramics in Antenna Design and Microwave Applications</i>
Ghasemi, Amirhossein	PA5.18	3564	<i>Realizing Flat-Top Radiation Pattern with Sharp Cutoff for Reducing Lobing Fades</i>
Ghatas, Mohamed	A26.3	4202	<i>Non-Volatile Memristor-Based 1-Bit Reconfigurable Intelligent Surface Towards a Greener 6G</i>
Ghavami, Mohammad	CS45.3	1808	<i>Preliminary Clinical Trial Results of MammoWave in the Context of RadioSpin Project</i>

	E01.4	2028	<i>Huygens Principle Imaging Method Powered by Deep Learning for Brain Stroke Classification</i>
Ghavami, Navid	CS45.3	1808	<i>Preliminary Clinical Trial Results of MammoWave in the Context of RadioSpin Project</i>
	E01.4	2028	<i>Huygens Principle Imaging Method Powered by Deep Learning for Brain Stroke Classification</i>
Gheybi Zarnagh, Reza	A21.1	1480	<i>A Dual Linear-Polarized Gap Waveguide Antenna Element for Radar and Communications at 77 GHz</i>
Ghiaasi, Golsa	CS43b.1	4168	<i>Channel Measurements and Characterization in Industrial Environment at 60 GHz</i>
Ghorbani, Farhad	PM1.6	1331	<i>Intermodulation Mitigation Through Surrounding Impedance Manipulation</i>
	PE3.17	2423	<i>Enhancing Signal Transmission in Energy-Saving Glass Through Tri-Bandpass Frequency Selective Surface Design</i>
Ghorbanpoor, Mohsen	CS1b.5	4254	<i>Plug-In Plug-Out Multibeam Dielectric Rod Antenna for Target Dedicated mm-Wave RF-WPT Applications</i>
Ghosh, Anirban	CS5b.2	369	<i>Double-Directional Angle-Resolved Wideband Channel Measurements and Path Loss Characterization in Corridor at 300 GHz</i>
Ghosh, Swarnadipto	PE1.7	1265	<i>Design of a Concentric Circular Holographic Metasurface Using Hexagonal Anisotropic Unit-Cell for Wireless Communications</i>
Giacomini, Andrea	CS42a.4	151	<i>Planar Near-Field Phaseless Measurements Using Multi-Probe Arrays</i>
Giacomini, Andrea	CS5b.3	374	<i>Industrial Design Validation for a Plane Wave Generator at 28GHz</i>
Giacomini, Andrea	M5.2	542	<i>Uncertainty Analysis of Linear Multi-Probe Array Systems for Fast Antenna Measurements</i>
Giacomini, Andrea	CS41.2	3225	<i>VHF/UHF Antenna Measurements Based on Multi Probe Array Technology</i>
Giammello, Giuseppe	PA8.10	2311	<i>Octagonal Patch Tag Antenna and 3 × 3 Array Locator for DoA Applications</i>
Giamougiannis, George	PA3.21	3483	<i>MIMO Signals Processing Utilizing Optical Crossbar Linear Operator</i>
Gil, Ignacio	PA1.8	3362	<i>Embroidered Antenna-Based Sensor for Real-Time Natremia Monitoring</i>
Gil Martinez, Alejandro	CS36a.2	705	<i>GHz Prism: Frequency-Scanned Antennas to Improve Localization with Separate-Channel Fingerprinting</i>
	CS36a.3	710	<i>Compact Amplitude-Monopulse Microstrip Antenna Design for Wide Field-Of-View Direction Finding</i>
Gillard, Raphael	A06a.3	3031	<i>3-D Reflectarray Unit Cell with Wideband Performance and Integrated Sensing Capability</i>
Gilmore, Colin	E04.5	2703	<i>Preliminary Description of a 2D Near-Field Electromagnetic Imaging Database</i>
	CS33b.2	3313	<i>Supervised Learning Applied to Microwave Imaging System Calibration</i>
Giordanengo, Giorgio	CS42b.1	439	<i>An Antenna Measuring System Based on a Cable Suspended Dolly and Inverse Source</i>
	A20.3	3818	<i>Compact Antenna Solutions for Data Transmission Using Fat-Intrabody Communication (Fat-IBC)</i>

	CS30b.3	4156	<i>Automated Design and Characterization of a Scalar Metasurface Antenna Radiating a Linearly-Polarized Broadside Beam</i>
Giorgia Venturini, Giorgia	CS42a.5	156	<i>Antenna Coupling Evaluation in Arrays and Complex Structures Using Measured Sources and Simulations</i>
Giusti, Edoardo	PE1.9	1272	<i>A Compact Fabry-Perot Cavity Antenna with Circular Polarization</i>
	A10.5	3083	<i>Fabry-Perot Antenna with High-Permittivity Grounded Walls for Side Lobe Level Reduction</i>
Giusti, Federico	E07.4	1649	<i>Multilayer Reflectionless Wide-Angle Anomalous Refractors Based on Surface Field Optimization</i>
Glatre, Karim	A06a.4	3036	<i>Large, Multi-Faceted Reflectarray with Quasi-Constant Directivity in the V-Band</i>
Godinho, Daniela	CS28.2	470	<i>The Effect of Pressure of the Open-Ended Coaxial Probe on the Measurement of Ex Vivo Biological Tissues Dielectric Properties</i>
	PP03.18	3660	<i>Best Practices for Accurate Results Using Numerical Solvers for Microwave Body Screening</i>
Godja, Norica	A19.2	1508	<i>Polymer-Based Additive Manufacturing of a Complex RF Front-End for New Space Applications</i>
Golmie, Nada	CS5a.1	56	<i>Context-Aware Channel Sounder for AI-Assisted Radio-Frequency Channel Modeling</i>
Golnabi, Amir	CS45.1	1799	<i>MR/Microwave Tomography Integrated Breast Cancer Imaging</i>
Gómez-Álvarez, Andrés	CS8.5	2899	<i>Dual-Resonance SIW-Based Reflectarray Unit Cell for Broadband Applications</i>
Gómez-Tornero, Jose- Luis	CS9b.2	516	<i>Mechanically Re-Configurable Leaky-Wave Antenna for Fix-Frequency Beam Scanning</i>
	CS9b.4	526	<i>Design of Modulated Dielectric Leaky-Wave Antennas for Efficient Bessel-Beam Synthesis</i>
	CS36a.2	705	<i>GHz Prism: Frequency-Scanned Antennas to Improve Localization with Separate-Channel Fingerprinting</i>
	CS36a.3	710	<i>Compact Amplitude-Monopulse Microstrip Antenna Design for Wide Field-Of-View Direction Finding</i>
	A08a.1	1883	<i>Efficient Ray-Tracing Approach to Analyze Arbitrarily Shaped Leaky-Wave Antennas Embedded in Lenses</i>
	A08b.1	2081	<i>Proactively Conformed Near-Field Focused Modulated Leaky-Wave Antennas</i>
Gonzalez, Alvaro	PA2.24	1159	<i>The Design of Re-Imaging Optics for Passing Several Beams Through Small Cryostat Windows</i>
Gonzalez Jimenez, Jose Luis	CS7.4	1606	<i>Characterization of a D-Band Active Transmitarray System for Efficient Point-To-Point Links</i>
González Posadas, Vicente	PM1.7	1335	<i>Virus Detection in the Microwave Regime Through an Antenna Workbench</i>
	PA1.12	3381	<i>Miniaturization of Wireless Power Transfer for Implantable Devices Using Voltage Doubler Rectifier</i>
González-Ovejero, David	CS16.5	578	<i>Radiation Control by Space-Time-Modulated Anisotropic Impedance Surfaces</i>
	CS44a.4	757	<i>High Data-Rate Sub-THz Coherent Near-Field Wireless Links Enabled</i>

			<i>by Spline-Profile Bessel Launchers</i>
	E06b.3	800	<i>Multi-Beam Dual Polarised Metasurface Antenna in Ka-Band</i>
	PA7.8	1195	<i>Shaping the Sub-Reflector of a Ring Focus Antenna for Tailored Beamwidth Applications</i>
	A21.2	1484	<i>Dual-Linearly Polarized Pillbox Beamformer in Hybrid CNC-PCB Technologies at W-Band</i>
	CS7.1	1592	<i>Low Profile and High Gain Folded Transmitarray in Quartz for Radiometry at 310 GHz</i>
	A16.3	1739	<i>Wideband Beam-Steering Continuous Transverse Stub Array Enabled by a Reflecting Luneburg Lens at Ka-Band</i>
	PA6.7	2238	<i>Metasurface-Based Bessel-Beam Launcher with 100λ Non-Diffractive Range</i>
	PA3.12	3442	<i>Shorted Stacked Patch Array for Photonic Beam Steering at mm-Waves</i>
González-Rios, Jorge	PA2.5	1074	<i>Genetic Algorithm-Based Beamforming in Subarray Architectures for GEO Satellites</i>
	CS19b.4	4295	<i>Supervised Learning Based Real-Time Adaptive Beamforming On-Board Multibeam Satellites</i>
Gonzalez-Rubio, Jesus	CS2.1	165	<i>Instantaneous Vs Theoretical Maximum Exposure Under Real Traffic Conditions: Example in the City of Valencia</i>
González-Suárez, Ana	CS28.1	465	<i>Dielectric Characterisation of Human Parathyroid Glands at Microwave Frequencies</i>
Gonzalez-Valdes, Borja	CS21.3	2712	<i>From mmWave Radar Nodes to Multistatic Arrays: Design Considerations and Applications</i>
Gorce, Jean-Marie	PP03.9	3625	<i>Indoor Localization of Smartphones Thanks to Zero-Energy-Devices Beacons</i>
Gordon, Joshua	CS12a.2	4048	<i>Rapid Automated Antenna Alignment on Robotic Antenna Ranges</i>
Gorsche, Christian	A19.2	1508	<i>Polymer-Based Additive Manufacturing of a Complex RF Front-End for New Space Applications</i>
Goto, Makoto	CS5a.2	61	<i>Validation of Pseudo-Scale Model for the Air-Sea Two-Layer Near-Field Problem by Using FDTD Simulations and Measurements in a Tank</i>
Göttl, Maximilian	A28.2	3719	<i>A High-Isolation Dual-Band Base Station Antenna Design for Full Duplex Technologies</i>
Goudos, Sotirios	PA3.23	3490	<i>Wideband Aperture-Coupled Array Design for Automotive Radar Applications</i>
	PP03.5	3605	<i>Modeling Received Power from 4G and 5G Networks in Greece Using Machine Learning</i>
Gougeon, Grégory	P04b.2	970	<i>Ray-Tracing Calibration from Channel Sounding Measurements in a Millimeter-Wave Industrial Scenario</i>
Gourdonnaud, Delphine	E05.1	2036	<i>From Bulk Toward Micro-Structured TiO₂ Ceramics for All-Dielectric Metamaterials at Terahertz Frequencies</i>
Gourley, Grant	CS3.3	303	<i>Reconfigurable Polarisation Conversion Metasurface for mm-Wave Applications Using Vanadium Dioxide (VO₂)</i>
Goussetis, George	CS9b.2	516	<i>Mechanically Re-Configurable Leaky-Wave Antenna for Fix-Frequency Beam Scanning</i>

	CS25.3	663	<i>Multibeam Phased Arrays Exploiting Frequency Dispersion for Massive MIMO Satellite Communications</i>
	CS25.4	668	<i>Aperture Distribution Method for Array-Fed Reflectors: A System Level Performance Case Study</i>
	PA8.18	2344	<i>Bandwidth Manipulated Leaky-Wave Antenna Using a Sinusoidal Ridge in Folded Substrate Integrated Waveguide</i>
	A01a.1	2928	<i>Millimeter-Wave Uniform Amplitude SIW Series Power Divider for 2D Leaky-Wave Antenna Arrays</i>
	CS1b.3	4246	<i>A mmWave Leaky-Wave Antenna for Efficiency Enhanced Near-Field Wireless Power Transfer and Communication</i>
Gouzouasis, Ioannis	P05.4	256	<i>A Small-Sized Antenna System for Direction Finding Applications on a Single Plane (1D) Using BT 5.1</i>
Gradoni, Gabriele	CS20b.4	406	<i>Impedance-Based RIS Channel Model and Optimization in Fast-Fading Environments</i>
	E06a.3	596	<i>Fully Autonomous Reconfigurable Metasurfaces with Integrated Sensing and Communication</i>
	PE1.2	1245	<i>Smart Propagation Environments Empowered by Metasurfaces: A Self-Consistent Study</i>
	PA4.13	2160	<i>A Novel Precise Approach for Digital Metasurface Configuration for Sensing Application</i>
	CS34.4	2625	<i>Empirical Validation of the Impedance-Based RIS Channel Model in an Indoor Scattering Environment</i>
	CS22a.4	2853	<i>Quantum Optimisation of Reconfigurable Surfaces in Complex Propagation Environments</i>
	CS22a.5	2858	<i>Real-System Variational Quantum Eigensolver for Electromagnetic Waveguides: A Benchmark Study</i>
Graham, Aaron	PA5.17	3560	<i>Low-Profile Super-Realised Gain Antennas</i>
Grajal, Jesús	CS21.3	2712	<i>From mmWave Radar Nodes to Multistatic Arrays: Design Considerations and Applications</i>
Gramlich, Georg	A05.3	1828	<i>110 to 170 GHz High-Gain Antenna with Embedded Surface Mount Short Horn and Baseband PCB Horn Antenna</i>
	M3.3	2595	<i>Dielectric Characterization of Adhesives for THz Packaging in WR6.5, WR3.4 and WR2.2 Bands</i>
Grande, Marco	PA1.3	3340	<i>Eco-Friendly and Conformable PIFA Based on PEDOT: PSS and a Sustainable Chitosan Substrate for 5G Communications</i>
Granet, Christophe	A19.4	1518	<i>A Possible Way to Reduce the High Sidelobe Levels Due to Reflector Struts: Curly Struts</i>
	A16.4	1744	<i>Compact Hybrid Optical/RF User Segment (CHORUS): RF Terminal Design</i>
Granich, Anna	M5.3	547	<i>Simulation Based Uncertainty Analysis for Active Two-Way-Radiation Pattern Measurements of Circularly Polarized Antennas</i>
Grävendieck, Jan	A28.4	3729	<i>Ground Base Station Antenna Design for Air-To-Ground Communications</i>
Gray, Douglas	CS47.2		<i>Advanced Thermal-Imaging for OTA Industrial-Testing of Active-In-Package, Antenna-On-Chip and Antenna on PCB</i>

Grbic, Anthony	CS37b.4	357	<i>Increasing the Efficiency-Bandwidth Product and Impedance Bandwidth of Electrically-Small Antennas Through Parametric Space-Time Variation</i>
	CS16.3	570	<i>All-Metal Perfectly-Matched Metamaterials</i>
Greco, Francesco	A27a.3	641	<i>K-Band Microstrip ESPAR Antenna Integrated into Large Array</i>
Gregson, Stuart	CS32.2	1438	<i>A Comparison of Near-Field to Far-Field Transformation Algorithms for Use with Industrial Multi-Axis Robotic Antenna Measurement Systems</i>
	CS31.1	1658	<i>Compressive Sensing Applied to Production Testing of Array Antennas Using a Robotic Arm and Very Sparsely Sampled Near-Field Measurements</i>
	PM2.2	2433	<i>Design Effects of the Junction Contour of a Blended Rolled Edge Compact Range Reflector</i>
	CS12a.4	4058	<i>Use of Model Based Systems Engineering and Development in the Design of a Commercial Nose-Radome Test System Employing a Multi-Axis Cobot</i>
Grennerat, Vincent	CS3.5	311	<i>Exploring PLA/Flax Substrates for Antenna Applications: Assessing Moisture, Temperature and Dielectric Constant Homogeneity</i>
Grigoriev, Igor	PA4.22	2197	<i>Effect of Phase Errors on Performance of Ka-Band Reflectarray with DRA Unit Cells</i>
Gros, Jean-Baptiste	CS20b.3	402	<i>Measurements of Reconfigurable Intelligent Surface in 5G System Within a Reverberation Chamber at mmWave</i>
	A03b.5	3147	<i>Wireless Re-Configurable Intelligent Surface for Sub 6 GHz 5G Frequency</i>
Grosinger, Jasmin	CS13.2		<i>Understanding UHF RFID Sensor Systems: A Summary</i>
Gross, Nicolas	CS2.4	180	<i>Advanced Post-Processing Technique to Evaluate Specific Absorption Rate (SAR) for a Standard Dipole Antenna</i>
	CS5b.3	374	<i>Industrial Design Validation for a Plane Wave Generator at 28GHz</i>
	M5.2	542	<i>Uncertainty Analysis of Linear Multi-Probe Array Systems for Fast Antenna Measurements</i>
	CS41.2	3225	<i>VHF/UHF Antenna Measurements Based on Multi Probe Array Technology</i>
Groth, Mateusz	M3.5	2605	<i>Highly Precised and Efficient Robot-Based ESPAR Antenna Measurements in Realistic Environments</i>
Gu, Chao	PA2.10	1096	<i>Conceptual Design of Antenna Arrays for Satellite Direct-To-Cell Connectivity</i>
	PA2.12	1105	<i>Fabrication and RF Characterization of Fully Additive Manufactured Transmission Lines</i>
	PA4.2	2109	<i>A Fully Additive Manufactured D-Band SIW Antenna</i>
	PA6.5	2231	<i>A Pattern-Reconfigurable Water Antenna Based on the Fabry-Perot Cavity</i>
	PA8.4	2283	<i>An IQ Modulator-Based RF Phase Shifter</i>
	PA8.13	2324	<i>A Near-Field Focusing Circularly Polarized Radial Line Slot Array Antenna</i>
	CS14b.4	4362	<i>Wideband Dual-Polarized 1-Bit Unit-Cell Design for mmWave Reconfigurable Intelligent Surface</i>

Guan, Ke	CS23a.2	1780	<i>Terahertz Channel Modeling Based on Scattering Characterization</i>
	CS43a.3	3962	<i>A Deep Learning Based Surface Current Generation Method for Scattering Modeling at Terahertz Band</i>
Guarnera, Davide	A16.5	1749	<i>Design of a Wideband Dual-Polarized Stacked Antenna Array for SATCOM Applications</i>
	PA8.10	2311	<i>Octagonal Patch Tag Antenna and 3 × 3 Array Locator for DoA Applications</i>
Guarriello, Andrea	A19.5	1523	<i>Exploring the Potential of Spatially Modulated Full-Metal Dichroic Mirrors for Deep Space Antennas</i>
Gudivada, Viswanadh Raviteja	PA7.4	1176	<i>Passive Beamforming with Liquid Antennas: Techniques and Implementation</i>
Guerboukha, Hichem	CS44b.4	955	<i>Curving THz Beams in the near Field: A Framework to Compute Link Budgets</i>
Guerbuez, Ayten	A18.5	2923	<i>On the Cost-Effectiveness of Using Beamforming at the Ground Station for Aeronautical Communications</i>
Guerra, Anna	CS44a.2	750	<i>Dual Functional mmWave RIS for Radar and Communication Coexistence in near Field</i>
Guerrero, Rocco	CS42a.3	146	<i>Reconstruction of the Far-Field Pattern Radiated by an Elongated Antenna Measured over a Perfectly Electric Conducting Ground Plane in a Spherical Spiral Near-Field Facility</i>
	CS42b.3	446	<i>Phaseless Characterization of Flat Sources with a Planar Wide-Mesh Scanning Strategy</i>
Gueuning, Quentin	CS4.2	3181	<i>Mitigating Zenith Blindness from Mutual Coupling in a Sunflower Phased Array</i>
Gugliermi, Martina	CS24a.1	724	<i>Advancements in the Experimental Validation of a Wearable Microwave Imaging System for Brain Stroke Monitoring</i>
Guida, Amedeo	E07.3	1645	<i>Adaptive Weighting Scheme for Multi-Objective Optimization in Metasurface Antenna Design</i>
Guidi, Francesco	CS44a.2	750	<i>Dual Functional mmWave RIS for Radar and Communication Coexistence in near Field</i>
Guillet, Valery	CS11.5	1631	<i>Fine Tuning an AI-Based Indoor Radio Propagation Model with Crowd-Sourced Data</i>
Guirado, Robert	CS17a.4	15	<i>Reflective Surfaces Based on Semi-Passive Reconfigurable Polymer Network Liquid Crystal</i>
Gul Hassan, Ahsaan	E09.5	3924	<i>Multifunctional Linear Dichroism and Polarization Transforming Metasurface for mm-Wave Application</i>
Gulgowski, Jacek	E02a.2	3002	<i>Crank-Nicolson FDTD Method in Media Described by Time-Fractional Constitutive Relations</i>
Gülten, Engin	CS39b.3	818	<i>Broadband Performance Assessment of Compensated Compact Antenna Test Range CCR 75/60 of Airbus at L-Band for Navigation Applications</i>
Gumba, Austin	CS4.4	3189	<i>The Hydrogen Intensity Real-Time Analysis eXperiment: Overview and Status Update</i>
Gunenc Tuncel, Nezahat	CS39a.4	622	<i>Addressing PIM Challenges in Radio Base Stations: Field Issues and Testing Methods for Large-Scale Deployments</i>

Günther, Matthias	CS33b.4	3321	<i>Deep-Learning Optimized Reconfigurable Metasurface for Magnetic Resonance Imaging</i>
Guo, Lantu	CS23a.2	1780	<i>Terahertz Channel Modeling Based on Scattering Characterization</i>
Guo, Lu	CS6a.4	208	<i>A Beam-Scanning Metal-Only Folded Reflectarray Antenna</i>
Guo, Xin	A01b.5	3216	<i>Array-Fed Transmitarray with Designated Beam Directions and Coverages</i>
Guo, Y Jay	CS6a.3	204	<i>Wideband Transmissive Metasurfaces for Sub-THz Frequency-Dependent Beam Scanning</i>
Guo, Y. Jay	CS6b.6	509	<i>3D-Printed Multi-Beam Flat Lens Antenna System</i>
	CS10.1	850	<i>Efficient Ray-Tracing Model for Generalized 2D Dielectric Lenses Combined with Arrays</i>
	A02.5	3710	<i>A Four-Channel In-Band Full-Duplex (IBFD) Antenna System with Shared Radiation Aperture</i>
Guo, Zhenyang	P10b.5	3263	<i>E-Band Measured Propagation Characteristics for Urban Backhaul Communications</i>
Gupta, Gaurangi	CS42b.6	460	<i>Uncertainty Quantification of the Gain Budget for INCUS</i>
	A17.1	3739	<i>Feed Assembly Development for INCUS</i>
Gupta, Neeraj	CS4.4	3189	<i>The Hydrogen Intensity Real-Time Analysis eXperiment: Overview and Status Update</i>
Gupta, Shulabh	CS9b.1	512	<i>Emulating Spatial Dispersion Using Non-Spatially Dispersive Periodic Metasurfaces</i>
	CS36b.5	916	<i>Multi-Directional Leaky-Wave Antenna with Independent Beam-Scanning Laws</i>
	PE1.16	1300	<i>Mechatronic Phase-Control Reflector System with In-Plane Axis Control</i>
	E02b.3	3276	<i>Mixed Spatial-Spectral Domain Integral Equation Solver for Higher-Order Boundary Conditions in Electromagnetics</i>
Guruprasad, Surabhi	CS46.4	4228	<i>Antenna Digital Beamforming on Spire's GNSS-Reflectometry CubeSat Constellation</i>
Gustafsson, Mats	CS38.5	128	<i>Substructure Modes and Bounds</i>
	CS18.5	3687	<i>Material-Independent Scattering Formulations of Characteristic Modes</i>
	M2.2	3886	<i>Real-Time Near-Field Measurements of mmWave Devices Using a Metasurface and IR Camera</i>
	CS30b.1	4149	<i>Overview of State-Of-The-Art Methods for Determining Performance Bounds on Electromagnetic Systems</i>
Gustafsson, Mattias	CS30b.2	4153	<i>Fundamental Limits on Characteristic Modes</i>
	PM1.6	1331	<i>Intermodulation Mitigation Through Surrounding Impedance Manipulation</i>
Guth, Adrien	CS31.5	1678	<i>An Overview of the Potential of Compressed Sensing in Antenna Measurements</i>
Gutruf, Philipp	CS37a.1	29	<i>3D-Printed Wearable Antenna Integrated with Rectifier for Wireless Power Transfer</i>

H

Haddad, Thomas	PA4.21	2193	<i>Terahertz Microstrip Leaky-Wave Antenna for WR1.0 Band</i>
Haddadi, Abolfazl	PA7.10	1205	<i>Radiation Pattern Shaping Using Generalized Luneburg Lenses for</i>

			<i>Automotive RADAR Antennas</i>
	A21.1	1480	<i>A Dual Linear-Polarized Gap Waveguide Antenna Element for Radar and Communications at 77 GHz</i>
Hahn, Tim	CS18.3	3679	<i>Generation of a Square Multi-Mode Multi-Port Aperture Antenna by Selective Modal Excitation</i>
Haider, Michael	CS22b.1	3109	<i>Optimized Design Parameters for a Flux-Driven SNAIL-Based Traveling-Wave Parametric Amplifier</i>
Haider, Usman	PM1.4	1323	<i>A Highly Compact Double-Sided Orientation Insensitive Chipless Tag for Radio Frequency Identification Applications</i>
Hajimiri, Ali	CS14b.3	4357	<i>Analyzing the Performance of Phased Array Geometries with Aperture Projection Analysis</i>
Hamad, Rihab	PA4.21	2193	<i>Terahertz Microstrip Leaky-Wave Antenna for WR1.0 Band</i>
Hamada, Ahmad	P04a.3	777	<i>Analysis of Propagation Models for Frequency Coordination Between 5G Base Stations and Satellite Earth Stations at FR1</i>
Hamani, Abdelaziz	CS7.4	1606	<i>Characterization of a D-Band Active Transmitarray System for Efficient Point-To-Point Links</i>
Hameed, Hira	P05.6	266	<i>Contactless Respiration Variability Detection and Accuracy Test Using UWB Radar</i>
Hamzavi-Zarghani, Zahra	E08.2	1868	<i>Reflective Intelligent Surfaces: Reducing Complexity by Controlling the Illuminating Field</i>
	E08.5	1880	<i>Static and Reconfigurable Phase-Gradient Metasurfaces for Antenna Applications</i>
Han, Jiaqi	CS17b.2	322	<i>Challenges and Opportunities of Amplified Information Metasurfaces for Simultaneous Wireless Communications and Power Transfers</i>
Han, Kangkang	A01a.5	2945	<i>Low-Profile Multibeam Beam-Scanning Antenna for Vehicular Radar Systems</i>
Han, Ruobin	E13.1	270	<i>Ultrahigh Sensitive Terahertz Metasurface with 2D MoS₂ for Refractive Index Biosensing</i>
Han, Shan	CS1b.3	4246	<i>A mmWave Leaky-Wave Antenna for Efficiency Enhanced Near-Field Wireless Power Transfer and Communication</i>
Han, Yu	CS44a.5	762	<i>Interference-Free Transmission for Near-Field Communication with Unlimited Antennas</i>
Haneda, Katsuyuki	P04a.1	767	<i>On the Use of Adaptive-Density Point Cloud for Site-Specific Ray-Optics Simulations</i>
	PA4.7	2134	<i>3D Printed Horn Antennas for Millimeter Wave and Sub-THz Bands</i>
	PP02.12	2542	<i>Comparison of Indoor Propagation Channels at 28 GHz and 140 GHz Bands</i>
	P06.3	2737	<i>Potential of Polarized MIMO in In-Body to Out-Body Radio Links</i>
	A25.2	3090	<i>3D Printed Cascaded Cavity-Backed Millimeter-Wave Filtering Antenna</i>
	A28.3	3724	<i>Base Station Radome Design for 5G and Beyond</i>
Hansen, Peter	PA6.6	2235	<i>Experimental Results for Carbon Nanotube-Sheet Based Microstrip Patch Antenna</i>
Hao, Le	CS20a.1	86	<i>Comparison of Simplistic System-Level RIS Models and Diffraction-Theory Solutions</i>
Hao, Yang	PE1.1	1241	<i>Broadening the Spectrum: Extending the Finite Crystal Method to</i>

			<i>Characterize Static Multi-Atomic Active Metamaterial Systems</i>
	PA4.17	2178	<i>Wideband Dual-Polarized Lens Antenna for Future mm-Wave Applications</i>
	PM2.14	2486	<i>A Wideband Free Space Material Characterization Method for Extracting Dielectric Permittivity</i>
Haridim, Motti	PA7.13	1219	<i>Experimental Investigation of the Nullifier-Based Monopole</i>
Harrison, Noel	PA2.12	1105	<i>Fabrication and RF Characterization of Fully Additive Manufactured Transmission Lines</i>
Harutyunyan, Armen	PA6.13	2264	<i>On-Chip mm-Wave Artificial Magnetic Conductor Backed Dipole Antenna on Low-Ohmic Substrate</i>
Hasanvand, Aminolah	CS13.1	1553	<i>Antenna System for Simultaneous Wireless Power and Information Transfer to Brain Implants</i>
Hashimoto, Koh	A11.1	3152	<i>Millimeter-Wave Corporate-Fed Slot Array Antenna Fed by Partially Dielectric-Filled Transmission Line</i>
Hassan, Ali	A02.3	3701	<i>Spherical Active Frequency-Selective Surface for 3-D Beam-Scanning Antenna</i>
Hassouna, Saber	PE3.4	2374	<i>RIS-Enabled Near-Field Localization with EMI</i>
Hastürkoglu, Sertan	A28.4	3729	<i>Ground Base Station Antenna Design for Air-To-Ground Communications</i>
Haun, Martin	CS39a.4	622	<i>Addressing PIM Challenges in Radio Base Stations: Field Issues and Testing Methods for Large-Scale Deployments</i>
Havrilla, Michael	E10a.2	1846	<i>Vector Potentials for Uniaxial Media with Sources</i>
	PE3.6	2383	<i>Development of an Ultrawideband Wire-Grid Polarizer Measurement Standard for Focus Beam System Cross-Polarization Calibration</i>
Hayashi, Keisuke	PP03.3	3597	<i>Propagation Path Analysis with Propagation QUBO Model in Urban Area</i>
Hayashi, Takahiro	PA6.11	2255	<i>User and Passive Beam Scheduling Scheme for Liquid Crystal IRS-Assisted mmWave Communications</i>
Haydhah, Saeed	CS41.1	3220	<i>UnderGround-To-AboveGround IoT Communication Links Insurance at 915 MHz Using LoRa Technology</i>
Hayman, Douglas	CS4.5	3194	<i>CSIRO Radio Astronomy Receiver Update - Ultra Wideband and Phased Array Feeds</i>
Hazdra, Pavel	PA2.20	1140	<i>Compact Ka Band Orthomode Transducer with Conical Horn Antenna</i>
He, Danping	CS23a.2	1780	<i>Terahertz Channel Modeling Based on Scattering Characterization</i>
	CS43a.3	3962	<i>A Deep Learning Based Surface Current Generation Method for Scattering Modeling at Terahertz Band</i>
He, Jia	CS29.5	3807	<i>Multi-Scattering Centers Extraction and Modeling for ISAC Channel Modeling</i>
He, Meng	M5.2	542	<i>Uncertainty Analysis of Linear Multi-Probe Array Systems for Fast Antenna Measurements</i>
He, Mingwei	CS11.1	1616	<i>AI-Assisted Design and Experimental Testing of a Compact UWB Antenna for the Inspection of Food and Beverage Products</i>
He, Sailing	PM2.13	2482	<i>Study on Antenna-Phantom Model of Aperture Antennas for SAR Analysis</i>
Hebeler, Joachim	A05.1	1820	<i>Sub-THz Substrate Integrated Waveguide Signal Transitions in</i>

			<i>Backend-Of-Line of a Silicon Process</i>
Heberling, Dirk	CS2.2	170	<i>Characterization of Typical Instantaneous Exposure and Usage Scenarios in the Vicinity of 5G Massive-MIMO Base Stations</i>
	M5.3	547	<i>Simulation Based Uncertainty Analysis for Active Two-Way-Radiation Pattern Measurements of Circularly Polarized Antennas</i>
	CS31.5	1678	<i>An Overview of the Potential of Compressed Sensing in Antenna Measurements</i>
	CS12a.5	4063	<i>Reduced-Order Maximum Determinant Sampling Grids by Acquisition of Additional Arbitrary Sampling Points on an Optimized Path</i>
Hecht, Kristy	CS9a.1	221	<i>Dual-Frequency Metasurface Antenna for Earth Science Remote Sensing</i>
Heckler, Marcos	A12b.3	1936	<i>Synthesis of Circularly Polarized Microstrip Planar Array with Cross-Polarization Suppression</i>
Hehenberger, Simon	CS46.5	4233	<i>Low-Cost Hybrid Additive Manufacturing of a Miniaturized Dual Band Stacked Patch Antenna for GNSS Applications</i>
Heijs, Remco	CS47.4	426	<i>Over-The-Air Noise-Figure Measurements of Active Integrated Antennas at W-Band</i>
	CS43a.1	3952	<i>On the Importance of Scattering from Poles in Ray Tracing Simulations</i>
Hein, Matthias	CS42a.6	160	<i>Hybrid Antenna Measurement and Post-Processing for 5G Small Cell Exposure Assessment with Site-Specific Mounting Conditions</i>
	CS2.2	170	<i>Characterization of Typical Instantaneous Exposure and Usage Scenarios in the Vicinity of 5G Massive-MIMO Base Stations</i>
	CS2.6	189	<i>Reproducibility Studies of Instantaneous and 6-Minute Average Exposure Measurements Around 5G Massive-MIMO Base Stations</i>
Henault, Simon	P05.2	246	<i>Multifunction Over-The-Horizon Radar for Space Domain Awareness</i>
Henderson, James	PE3.3	2369	<i>Metamaterial-Based Ku-Band Flat-Panel High-Gain Antenna for Satcom Applications</i>
Henry, Clément	A23.5	2767	<i>Modeling of Quasi-Optical Systems and Measurements with a Cobot in the J-Band</i>
Henthorn, Stephen	CS14a.1	4132	<i>Enabling Shape Morphing Communications at mmWave with Spray on Antenna Arrays</i>
Hentila, Lassi	M2.1	3881	<i>A Novel MIMO OTA Methodology for UE Performance Testing</i>
Heo, Jin Myeong	CS37a.5	47	<i>Display-Integrated MIMO Antennas for Gesture-Sensing Radars</i>
Heredia Conde, Miguel	E04.1	2684	<i>Towards Optimal Binary Patterns for Compressive Terahertz Single-Pixel Imaging</i>
Hernandez Rodriguez, Silvia	A12a.3	1715	<i>Behavioral Models for the Cosimulation and Optimization of Active Electronically Scanned Arrays</i>
Herold, Christoph	CS10.3	860	<i>D-Band Active Antenna Array with Lens Enabling Quasi-Optical and Analogue Beam Reconfiguration for 6G Applications</i>
Herranz-Herruzo, Jose	PA2.13	1110	<i>Closely-Spaced Groove Gap Waveguides with Reduced Coupling</i>
	PA4.9	2142	<i>5x7 Nolen Matrix in K-Band Implemented in Rectangular Waveguide</i>
	PA3.6	3417	<i>Beam-Tilted All-Metal Radial-Line Slot Array Antenna with Uniform Spacing</i>
	PA4.26	3459	<i>Amplitude-Tapered Half-Mode Gap Waveguide Distribution Network for Flat Panel Antennas</i>

Herren, Jean-Jacques	A19.5	1523	<i>Exploring the Potential of Spatially Modulated Full-Metal Dichroic Mirrors for Deep Space Antennas</i>
Hertel, Thorsten	M2.1	3881	<i>A Novel MIMO OTA Methodology for UE Performance Testing</i>
Hery Zo Jean Baptiste, Andriamanohisoa	PA3.9	3429	<i>Impact of the Antenna Topology on the Combination of Full-Duplex Spatial Modulation and RF Energy Harvesting</i>
Hewson, Robert	CS14a.4	4142	<i>Optimal Morphing Metasurface Lens for Next Generation RF Sensing and Communications</i>
Hilton, Geoffrey	PP01.14	1407	<i>Analog Self-Interference Cancellation by Means of a Synchronised Signal Injection</i>
Himdi, Mohammad	PE2.14	1044	<i>Tunable Rectangular Waveguide Bandpass Filter Based on Plasma Technology</i>
Hindman, Greg	CS12a.4	4058	<i>Use of Model Based Systems Engineering and Development in the Design of a Commercial Nose-Radome Test System Employing a Multi-Axis Cobot</i>
Hirokawa, Jiro	A27b.4	842	<i>Design of a Hollow-Waveguide Slot Array Antenna for a Channel Sounder in the 150 GHz Band</i>
Hirose, Kazuhide	A03a.4	2877	<i>Circular Loop Antennas with Quasi-Two Sources for Broadband Circular Polarization</i>
Hirose, Masanobu	CS39b.4	823	<i>Millimeter Wave Vector Measurement System Using Low Frequency Band Oscilloscope</i>
Hirose, Mitsuki	A03a.4	2877	<i>Circular Loop Antennas with Quasi-Two Sources for Broadband Circular Polarization</i>
Hisatake, Shintaro	M5.6	560	<i>Spherical Near-Field Measurement and Far-Field Characterization of a 300 GHz Band Antenna Based on an Electrooptic Probe with Compact Tabletop Robotic Arm</i>
Hoad, Richard	P05.5	261	<i>Sequential Phase Optimization for Coherent Long-Range Distributed Wireless Power Transfer to a Non-Communicative Receiver</i>
Hoang, Phuong Linh	CS37a.5	47	<i>Display-Integrated MIMO Antennas for Gesture-Sensing Radars</i>
Hoang, The Viet	PM2.7	2454	<i>Near-Field Bistatic Microwave Imaging with Dynamic Metasurface Antennas</i>
Hoang, Thi Quynh Van	A16.2	1734	<i>Low-Profile 2D-Mechanical-Beam-Steering Antenna with Large Field-Of-View</i>
Hodgkinson, Callum	E06b.4	804	<i>A Reconfigurable Phase Gradient Metasurface Rasorber Offering Enhanced Beam Steering Capability and a Tuneable Transmission Band</i>
	E09.3	3914	<i>Analysis and Design of a Wideband Jaumann-Like Radar Absorber Offering High Angular Stability and Polarization Insensitivity</i>
Hoel, Karina	A17.3	3749	<i>Design and Test of a UHF Deployable Conical Log Spiral Antenna for Small Satellites</i>
Hofer, Markus	CS35b.2	1908	<i>Stationarity of Multiband Channels for OTFS-Based Intelligent Transportation Systems</i>
Hoferer, Robert	A19.4	1518	<i>A Possible Way to Reduce the High Sidelobe Levels Due to Reflector Struts: Curly Struts</i>
Hoffman, Nathan	CS30a.4	3942	<i>Validating Convex Optimization of Reconfigurable Intelligent Surfaces via Measurements</i>

Hofmann, Bernd	CS19b.1	4282	<i>A Loop-Star Decomposition for the B-Spline Based Discretization of the Electric Field Integral Equation</i>
Hofmann, Willi	CS42a.6	160	<i>Hybrid Antenna Measurement and Post-Processing for 5G Small Cell Exposure Assessment with Site-Specific Mounting Conditions</i>
Hole, Sam	P05.5	261	<i>Sequential Phase Optimization for Coherent Long-Range Distributed Wireless Power Transfer to a Non-Communicative Receiver</i>
Holm, Mark	A09a.3	688	<i>1-Bit Reconfigurable Transmitted/Reflected Array (TRA) for 5G/6G Wireless Communication</i>
Holopainen, Jari	CS40b.1	1969	<i>Small On-Metal Passive UHF RFID Transponders with Long Read Ranges</i>
	PA5.19	3569	<i>Beam Steering Performance Improvements Using a Layered Permittivity Dielectric</i>
	CS30b.5	4163	<i>Optimization of Loads for Antenna-Based Scattering Systems Using Feedforward Neural Networks</i>
Hong, Ic-Pyo	E02b.5	3284	<i>Generalized Transition Matrix Model Using Characteristic Basis Function Method for Open-Ended Cavities</i>
Hong, Wei	CS8.1	2885	<i>Milimeter-Wave 3D Folded Strip Antennas and Arrays: Diverse Polarizations Realization Under Robust Input Impedance</i>
Hong, Wonbin	CS37a.6	51	<i>A Completely Overlapped Ku- and Ka-Band Dual-Polarized Phased Array for Simultaneous Terrestrial and Satellite Communications</i>
	CS37b.6		<i>Differentially-Fed Antenna-On-Display Module for SATCOM and Mobile Applications at Ka-Band</i>
	PP01.16	1413	<i>Breaking the Myth of RIS: Investigating the Role of User Equipment for Achieving Robust mmWave Wireless Channel Links Under NLOS Environments</i>
Hong, Xuemin	CS23a.5	1794	<i>HRPE-Enhanced AI-Based 5G Indoor Localization in Presence of Specular and Dense Multipaths</i>
Honkala, Mikko	A03a.3	2872	<i>The Role of Ground Currents in the Co-Simulation of Matching Components and Layout Models in Matching Circuit Optimization</i>
Honma, Naoki	CS36b.1	896	<i>Safe Beamforming Based on Human Area Estimation for Microwave Wireless Power Transfer</i>
Hoogelander, Martijn	CS37b.3	352	<i>Chessboard Focal Plane Array in Silicon Technologies for Terahertz Imaging</i>
	M3.2	2590	<i>A Demonstration of Diffraction-Limited Images Using a CMOS Chessboard Array at THz Frequencies</i>
Hope, Patrick	CS46.1	4215	<i>Dual All Metal Patch Antenna for the HydroGNSS Mission</i>
Horii, Akihiro	P04b.5	985	<i>Conceptual Design and Propagation Characteristics of an Underwater Electromagnetic Communication System for Ocean Environment Sensor Systems</i>
Horlin, François	P02.1	3763	<i>Multistatic OFDM Radar Fusion of MUSIC-Based Angle Estimation</i>
Hossein zadeh, Mohammad	CS43b.3	4178	<i>Machine Learning Approach to Delay Spread Estimation in Industrial Environments</i>
Hosseininejad, Seyed Ehsan	PE1.11	1279	<i>Compact Polarization Converter on a Thin Ferrite-Based Metasurface for Enhanced 5G Wireless Communication</i>
	PA4.13	2160	<i>A Novel Precise Approach for Digital Metasurface Configuration for</i>

			<i>Sensing Application</i>
Hosseinzadegan, Samar	CS39b.1	808	<i>Exploring the Properties of Reverberation Chambers in the THz Range: A Pilot Study</i>
	M2.4	3895	<i>K-Factor Evaluation in a Hybrid Reverberation Chamber plus CATR OTA Testing Setup</i>
Hostettler, Roland	CS23a.1	1775	<i>Gaussian Processes for Received Signal Strength Based Device-Free Localization</i>
Hou, Jiayu	CS48.1	3977	<i>Beamforming Orthogonality in Coupled Directional Modulation Arrays</i>
Hou, Meng	PA5.16	3556	<i>Design of the 3D-Printed Rectangular Dielectric Resonator Antenna for WLAN Applications</i>
Hovinen, Veikko	CS5a.5	76	<i>A Modular COTS-Based High-Efficient Sub-THz Channel Sounder and Experimental Validations</i>
	PP01.8	1380	<i>Dual-Polarized Diffraction Measurements and Modeling at D-Band Frequencies</i>
	P01.1	3832	<i>5G Radio Channel Characterization in an Underground Mining Environment</i>
Hradecky, Zdenek	PA2.20	1140	<i>Compact Ka Band Orthomode Transducer with Conical Horn Antenna</i>
Hrovat, Andrej	PP02.15	2557	<i>Large-Scale Site Diversity Experiment in Ljubljana and Budapest at Ka-Band with Alphasat Satellite</i>
Hsu, Chien Ming	PA3.1	3398	<i>Dynamic Programming-Based Beam Codebook Design for mmWave Multi-Antenna Module in Mobile Devices</i>
Hu, Bintao	CS1b.2	4242	<i>Matching Network Elimination in Multiband Metasurface-Structured Rectennas for Wireless Power Transfer and Energy Harvesting</i>
Hu, Chufeng	PA2.3	1066	<i>Compact Vivaldi Antenna Application in High-Power Design at X-Band</i>
Hu, Jiahao	CS5a.4	71	<i>Indoor Channel Characterization Based on Directional Measurements at 140 GHz</i>
	CS43a.2	3957	<i>Millimeter-Wave and Sub-THz Channel Measurements and Characterization Analysis in a Street Canyon Scenario</i>
Hu, Kai-Chun	E13.4	280	<i>Thin-Film Terahertz Metamaterials Manufactured by Laser Direct Writing</i>
Hu, Nan	PA3.2	3403	<i>Design of Ultra-Wideband Dual-Polarized Corrugated Horn Antenna for 5G Application</i>
	PA3.7	3421	<i>A Single-Layer Quadruple-Band Millimeter-Wave Antenna Using Split-Rings for 5G Application</i>
	PA5.20	3574	<i>A Wideband Circularly Polarized Filtering Array Antenna Using Dual-Layer Circular Cross Slotted Patch</i>
	PA5.21	3577	<i>Design of a Dual-Polarization Ultra-Wideband Horn Antenna</i>
Hu, Sampson	A11.4	3166	<i>A Multilayer Dual-Polarized Stacked Patch Antenna with Enhanced Port Isolation for mmWave Highly Integrated Applications</i>
Hu, Wei	A03a.1	2862	<i>Low-Profiled Wideband Dual-Polarized Conformal Antenna Array</i>
Hu, Weiya	A22.2	2776	<i>Analysis and Design of mmWave Wideband Artificial Dielectric Flat Lens Antenna</i>
	A22.4	2786	<i>Flat Gradient Index Lenses with Planar or Spherical Output Wavefront</i>
	CS1a.2	4027	<i>Single-Branch Hybrid Resistance Compression Technique for Enhanced Rectifier Performance</i>

Hu, Yulin	CS48.3	3987	<i>Joint Resource Allocation and Beamforming Design for Secure Short Packet Communication in RIS-Aided MISO Systems</i>
Hu, Zhenxin	A03b.2	3133	<i>Radiation Resistance Enhancement Techniques for Ultracompact Half-Wavelength Helical Omnidirectional Circularly Polarized Antennas</i>
Hu, Zhipeng	PA5.4	3506	<i>A Dual-Port Antenna for Colinearly Polarized Full Duplex and Pattern Reconfigurable Applications</i>
	PA5.6	3515	<i>Bifunctional Stubs Enabled MIMO System for Wideband Mobile 5G and Wi-Fi 6E Applications</i>
Hu, Zhirun	A09a.5	696	<i>Non-Volatile RF Frequency Reconfigurable Antenna for Wireless Communication</i>
	PP01.11	1395	<i>Achievable Rate Approximation of Large Intelligent Surface Based on Deep Learning</i>
	PA6.4	2227	<i>A High Gain Spoof Surface Plasmon Polaritons (SSPPs) Antenna Based on a Metamaterial-Inspired Substrate Integrated Waveguide</i>
	PA3.13	3446	<i>MIMO Array Decoupling with SSR Structure in Joint Communication and Sensing System</i>
	PA3.16	3463	<i>Frequency Reconfigurable Flexible Printed Antenna Based on Non-Volatile RF Switches for Wearable Applications</i>
Hua, Boyu	PM1.3	1318	<i>Impact of 6D Mobility on Doppler Characteristics of UAV-To-Vehicle Channels</i>
Hua, Qiang	CS11.2	1620	<i>AI-Driven Design of a Quasi-Digitally-Coded Wideband Microstrip Patch Antenna Array</i>
	CS11.3	1624	<i>Reflecting/Absorbing Dual-Mode Textile Metasurface with AI-Driven Parametric Studies</i>
	CS11.4	1627	<i>Automated Design of Antennas Using AI Techniques: A Review of Contemporary Methods and Applications</i>
Huang, Chen	PP01.17	1418	<i>Scenario Classification and Channel Modeling for MIMO Communications in Dense Urban Street Scenarios</i>
	PP01.18	1423	<i>Channel Characterization and Modeling for Wireless MIMO Communication Systems in Intersection Scenarios</i>
	P01.3	3842	<i>Scenario Classification and Channel Modeling for MIMO Communications in Suburban Road Scenarios</i>
Huang, Chuanchien	PA3.1	3398	<i>Dynamic Programming-Based Beam Codebook Design for mmWave Multi-Antenna Module in Mobile Devices</i>
Huang, Guan-Long	PA6.10	2250	<i>Generation of Narrow Divergence Angle OAM Beams for mmWave Communication Links Using Metasurface</i>
	PA3.17	3467	<i>Beam Steering Range Enhancement of Bifocal Reflectarray Using Irregular Distribution of Meta-Atoms</i>
Huang, Jie	PP01.19	1428	<i>Ray-Tracing Based Channel Modeling and Characteristics Analysis for LEO Satellite-To-Ground Systems</i>
Huang, Xiaoyu	CS35a.2	1688	<i>Beam Coverage Model of Ultra-Massive MIMO Communication Systems for Intelligent Transportation</i>
Huang, Yan	CS8.1	2885	<i>Milimeter-Wave 3D Folded Strip Antennas and Arrays: Diverse Polarizations Realization Under Robust Input Impedance</i>
Huang, Yi	CS39a.2	614	<i>Measurement of Total Radiated Power Using a TEM Cell</i>

	PE2.5	1009	<i>Gain Improvement of a DRA Using Deep Reinforcement Learning with Polygon Mesh Deformation</i>
	PA7.4	1176	<i>Passive Beamforming with Liquid Antennas: Techniques and Implementation</i>
	PM1.6	1331	<i>Intermodulation Mitigation Through Surrounding Impedance Manipulation</i>
	A04.5	1475	<i>A Penta-Band Shared Aperture Antenna with A Very Ratio Frequency for 5G and B5G Smartphone Applications</i>
	PE3.16	2419	<i>Ultra Wide Dynamic Range High Power RF Rectifier</i>
	PE3.17	2423	<i>Enhancing Signal Transmission in Energy-Saving Glass Through Tri-Bandpass Frequency Selective Surface Design</i>
	M4.4	2964	<i>Quad-Junction Self-Biased Circulator with Wide Operational Bandwidth</i>
	PA5.5	3511	<i>Pulse Preserving Capability of an Ultrawideband Dispersive Dielectric Resonator Antenna</i>
	CS1a.5	4039	<i>Design of Dual-Band CPW Rectenna for Wireless Power Transmission</i>
Hubin, Elliott	CS46.3	4223	<i>CubeSat Formation Antenna Array Synchronization for GNSS-R</i>
Hublikar, Akshay	CS21.1	2706	<i>Imaging Radar Frontend with SIW Feeding Networks</i>
Hubrechtsen, Anouk	CS47.4	426	<i>Over-The-Air Noise-Figure Measurements of Active Integrated Antennas at W-Band</i>
Huiskes, Martijn	CS44b.2	945	<i>Design and Characterization of an Imaging System Using Photoconductive Connected Arrays</i>
	A05.4	1833	<i>Time Domain Analysis of Pulsed Photo-Conductive Antenna Sources: Distributed Excitations</i>
Hujanen, Arto	A27b.3	837	<i>Single Material Multilayer Radome for D Band Applications</i>
Hultin, Harald	E10a.5	1859	<i>Investigation of Near-Field Contribution in Shooting and Bouncing Rays for Installed Antenna Performance on a Simple Platform</i>
	CS30a.3	3937	<i>On Efficient Representations of Frequency Dependent Far-Field Information for Array Antennas</i>
Humphreys, David	CS5a.3	66	<i>Horn Antenna Phase Center Position Influence on Sub-THz Measurements Uncertainties</i>
Husbands, Ryan	CS7.5	1611	<i>Reconfigurable Intelligent Surfaces for THz: Signal Processing and Hardware Design Challenges</i>
Husein, Asad	CS12a.3	4053	<i>Characterisation of a D-Band Horn Antenna: Comparison of Near-Field and OTA Measurements</i>
Hussain, Niamat	A27b.2	834	<i>A Radial Waveguide Power Divider Inspired Antenna for mmWave IoT Sensing Applications</i>
	PA8.7	2298	<i>Compact Size Frequency-Agile Antenna Enabling Multi-Mode Functionality for Internet of Things Applications</i>
	PA1.7	3359	<i>Development of a Wearable IoT-Optimized Textile Antenna with Low Specific Absorption Rate in Three Frequency Bands</i>
Hussain, Qasid	A27b.2	834	<i>A Radial Waveguide Power Divider Inspired Antenna for mmWave IoT Sensing Applications</i>
	PA8.7	2298	<i>Compact Size Frequency-Agile Antenna Enabling Multi-Mode Functionality for Internet of Things Applications</i>
Hussain, Rifaqat	PA7.18	1238	<i>Generation of Dual Band OAM Wave Using Single Patch Antenna for</i>

WLAN/WiMAX Applications

Hutu, Florin	PA3.9	3429	<i>Impact of the Antenna Topology on the Combination of Full-Duplex Spatial Modulation and RF Energy Harvesting</i>
Hynes, Christopher	A15b.1	4326	<i>Maximum Gain Estimates for Corporate-Fed Arrays</i>

I

Ibbotson, Alex	PE3.7	2388	<i>Electromagnetic Modelling in Modern Vehicles: A Pathway to Efficiency and Performance</i>
Icheln, Clemens	PA4.7	2134	<i>3D Printed Horn Antennas for Millimeter Wave and Sub-THz Bands</i>
	P06.3	2737	<i>Potential of Polarized MIMO in In-Body to Out-Body Radio Links</i>
	A25.2	3090	<i>3D Printed Cascaded Cavity-Backed Millimeter-Wave Filtering Antenna</i>
	A28.3	3724	<i>Base Station Radome Design for 5G and Beyond</i>
Ihalainen, Tiina	CS13.4	1563	<i>Enabling Living Spaces Through Customizable NFC-Enabled Smart Table System</i>
Ihle, Martin	A21.3	1488	<i>Millimeter Wave Retrodirective Van Atta Arrays in LTCC Technology</i>
Iigusa, Kyoichi	PA7.9	1200	<i>Input Impedance of Radiation Efficiency Deterioration State</i>
Ijjeh, Abdelrahman	E02b.1	3268	<i>Frequency-Domain TLM Method with Cartesian Block Meshing</i>
Iliadis, Lazaros Alexios	PA3.23	3490	<i>Wideband Aperture-Coupled Array Design for Automotive Radar Applications</i>
Im, Hyeong-Rae	E02b.5	3284	<i>Generalized Transition Matrix Model Using Characteristic Basis Function Method for Open-Ended Cavities</i>
Imada, Hiroaki	PA2.24	1159	<i>The Design of Re-Imaging Optics for Passing Several Beams Through Small Cryostat Windows</i>
Imai, Tetsuro	P04a.5	787	<i>Proposal on Application of Quantum Annealers for Analysis of Multiple Scattered Waves</i>
	PP03.3	3597	<i>Propagation Path Analysis with Propagation QUBO Model in Urban Area</i>
Imani, Mohammadreza F.	CS17b.5	335	<i>RIS-Based Over-The-Air Channel Equalization in Resource-Constrained Wireless Networks</i>
Imaz-Lueje, Borja	A06a.1	3021	<i>Large and Deployable Multi-Faceted Antennas Based on Single-Layer Reflectarrays</i>
	A06b.2	3291	<i>Experimental Validation of Reflectarray-Based Base Station Antenna for Simultaneous Front- and Radio Back-Haul Links in mm-Wave Frequencies</i>
Imberg, Ulrik	A12b.1	1927	<i>Design, Measurements, and Performance Assessment of a Massive MIMO Wideband Phased Array</i>
Imran, Muhammad Ali	CS17a.6	24	<i>RIS-Enhanced MIMO Channels in Urban Environments: Experimental Insights</i>
	P05.6	266	<i>Contactless Respiration Variability Detection and Accuracy Test Using UWB Radar</i>
	E13.1	270	<i>Ultrahigh Sensitive Terahertz Metasurface with 2D MoS₂ for Refractive Index Biosensing</i>
	A27a.2	636	<i>Impact of Dielectric Substrate, Feed Connector, and Fabrication Tolerances on the Performance of Planar Millimeter-Wave Antenna Arrays</i>
	PE1.5	1256	<i>An Innovative Metasurface Polarizer Working in 5G Frequency Bands</i>

	PM1.4	1323	<i>A Highly Compact Double-Sided Orientation Insensitive Chipless Tag for Radio Frequency Identification Applications</i>
	CS13.5	1568	<i>UHF RFID Sensor Antenna for Fat Content and Adulteration Detection of Milk</i>
	PE3.4	2374	<i>RIS-Enabled Near-Field Localization with EMI</i>
	PE3.13	2408	<i>Design of Intelligent Reflective Surface Unit Cell for 5G mmWave Applications</i>
	CS48.4	3992	<i>Joint Wide Illumination and Null Insertion Design in RIS-Assisted System</i>
	CS14b.5	4366	<i>Multi-Band Anisotropic Metasurface: Simultaneous Linear and Circular Polarization for Robust Satellite Communication</i>
Inacio, Sofia	A26.4	4207	<i>1-Bit Graphene-Based Reconfigurable Intelligent Surface Design in Ka-Band</i>
Inclan-Sanchez, Luis	PA8.19	2349	<i>Design of a Semitransparent Dual-Mode Filter for Antenna Applications</i>
Ingerson, Mark	M5.1	537	<i>On the RF Absorber Coverage of Antenna Under Test Positioners</i>
Inomata, Minoru	CS5b.6	388	<i>Sub-Terahertz MassiveMIMO Channel Sounder for 6G Mobile Communication Systems</i>
	P04a.5	787	<i>Proposal on Application of Quantum Annealers for Analysis of Multiple Scattered Waves</i>
	A27b.4	842	<i>Design of a Hollow-Waveguide Slot Array Antenna for a Channel Sounder in the 150 GHz Band</i>
	PP03.3	3597	<i>Propagation Path Analysis with Propagation QUBO Model in Urban Area</i>
Inoue, Yuki	PA4.4	2119	<i>Prototype of Multi-Sector Indoor mmW Base Station Based on 5G NR Beam Control</i>
Iqbal, Amjad	PA2.11	1101	<i>Multi-Bit Wideband Transmitarray Aperture with Independent Phase and Amplitude Control for High Gain with Low Sidelobe Mm-Wave Applications</i>
	A01a.4	2941	<i>Dual-Polarized OAM Antenna with Frequency and Mode Agility for Intelligent OAM Communications</i>
	PA1.2	3336	<i>Dual-Band 3-D MIMO Antenna for Deep Tissue Devices</i>
	PA1.11	3376	<i>Design of an UWB Conformal Antenna for Wireless Capsule Endoscopy</i>
	PA1.14	3390	<i>Miniaturized Implantable Antenna with Ultra-Wide Bandwidth Characteristics for Leadless Pacemakers</i>
Iqbal, Muhammad Ozair	PP02.2	2495	<i>Pathloss-Based Non-Line-Of-Sight Identification in an Indoor Environment: An Experimental Study</i>
Iradier, Eneko	PP03.8	3620	<i>Empirical Characterization of Doppler in Industrial Wireless Channels</i>
Isernia, Tommaso	M5.5	557	<i>Near Field Phase Recovery Exploiting Only One Measurement Surface and A Smart Warping Sampling Strategy</i>
	CS24b.2	925	<i>On the In-Vivo Electrical Properties of Human Forearm at Microwave Frequency</i>
	A16.5	1749	<i>Design of a Wideband Dual-Polarized Stacked Antenna Array for SATCOM Applications</i>
	E01.5	2033	<i>A Smart Convenient Rewriting of the Inverse Scattering Equations for</i>

			<i>the 3D Scalar Problem</i>
	PP03.6	3610	<i>Target Classification Through ISAR for Autonomous Vehicles Based on Federated Learning</i>
	P02.2	3768	<i>Learning-Based Procedures for Inverse Design of Electromagnetic Devices: A Preliminary Investigation</i>
	A15a.2	4115	<i>Extending Spectral Factorization to the 2-D Mask-Constrained Power Synthesis of Shaped Beams with Arbitrary Footprints</i>
Ishihara, Kento	M5.6	560	<i>Spherical Near-Field Measurement and Far-Field Characterization of a 300 GHz Band Antenna Based on an Electrooptic Probe with Compact Tabletop Robotic Arm</i>
Ishii, Nozomu	CS5a.2	61	<i>Validation of Pseudo-Scale Model for the Air-Sea Two-Layer Near-Field Problem by Using FDTD Simulations and Measurements in a Tank</i>
Iupikov, Oleg	M2.5	3900	<i>Optimization of the TRP Evaluation in Anechoic-Reverberation Hybrid Chamber</i>
	CS48.5	3996	<i>A Varactor-Based Reconfigurable Intelligent Surface Concept for 5G/6G mm-Wave Applications</i>
Ivashina, Marianna	A18.2	2909	<i>Self-Interference Suppression for SatCom Active Antenna Arrays Through Joint Transmit and Receive Beamforming</i>
	M4.2	2955	<i>Exploring Uniformity of Reverberation Chambers: Insights from Antenna Reflection Coefficient</i>
	M2.5	3900	<i>Optimization of the TRP Evaluation in Anechoic-Reverberation Hybrid Chamber</i>
	CS48.5	3996	<i>A Varactor-Based Reconfigurable Intelligent Surface Concept for 5G/6G mm-Wave Applications</i>
Iversen, Per	CS5b.3	374	<i>Industrial Design Validation for a Plane Wave Generator at 28GHz</i>
Iversen, Per	M5.2	542	<i>Uncertainty Analysis of Linear Multi-Probe Array Systems for Fast Antenna Measurements</i>
	CS41.2	3225	<i>VHF/UHF Antenna Measurements Based on Multi Probe Array Technology</i>

J

Jabbar, Abdul	A27a.2	636	<i>Impact of Dielectric Substrate, Feed Connector, and Fabrication Tolerances on the Performance of Planar Millimeter-Wave Antenna Arrays</i>
	CS14b.5	4366	<i>Multi-Band Anisotropic Metasurface: Simultaneous Linear and Circular Polarization for Robust Satellite Communication</i>
Jackson, David	CS9a.4	230	<i>Characterization and Comparison of Formulas for Optimizing Broadside Radiation in a 2-D Leaky-Wave Antenna</i>
Jacobsen, Rasmus	PM2.4	2443	<i>Validation of the DTU ETC Scattering Test Facility for Radar Cross Section Measurements</i>
	E11.3	2806	<i>Bound States in the Continuum in Cylindrical Impedance Surface Cavities</i>
Jacques, Laurent	P04a.4	782	<i>Fully Differentiable Ray Tracing via Discontinuity Smoothing for Radio Network Optimization</i>
Jadid, Marwan	A13.1	1949	<i>Ultra-Miniature Circularly Polarized Antenna with Omni-Directional Pattern for Sat-IoT</i>

	CS41.3	3230	<i>Design of Electrically Small Antennas and Radiation Efficiency Measurement Using MQFM with Radian Wheeler Cap Sizes</i>
Jafargholi, Amir	E05.3	2045	<i>SIW Slot Leaky-Wave Antenna Using Low-Index Metamaterial</i>
	E12.5	2836	<i>GPS Interference Cancellation Using Magneto-Dielectric Metamaterials</i>
Jakoby, Rolf	E09.2	3909	<i>Double-Layer Frequency Selective Surface-Based Corner Reflector for Indoor Self-Localization Systems in the W-Band</i>
Jales, Philip	CS46.4	4228	<i>Antenna Digital Beamforming on Spire's GNSS-Reflectometry CubeSat Constellation</i>
Jamshed, Muhammad Ali	PE3.4	2374	<i>RIS-Enabled Near-Field Localization with EMI</i>
Jandieri, Vakhtang	CS9b.5	531	<i>Modal Analysis in Woodpile Dielectric Structures</i>
Jang, Inseok	CS37b.6		<i>Differentially-Fed Antenna-On-Display Module for SATCOM and Mobile Applications at Ka-Band</i>
Jansen, Henrik	CS12a.5	4063	<i>Reduced-Order Maximum Determinant Sampling Grids by Acquisition of Additional Arbitrary Sampling Points on an Optimized Path</i>
Jaroszewicz, Thomas	CS19a.1	4068	<i>The d'Alembertian Representation of Green's Functions and Evaluation of Surface Integrals over Non-Parallel Planes</i>
Jassim, Mostafa	PP01.6	1370	<i>A New Approach for Line of Sight Prediction with Geometry Analysis and Machine Learning in Diverse Environments</i>
Javed, Muhammad Yasir	A15a.5	4127	<i>Tapering Impact on the Spatial and Frequency Responses of Broadband Asymmetrically Routed Phased Arrays</i>
Javornik, Tomaz	PP02.15	2557	<i>Large-Scale Site Diversity Experiment in Ljubljana and Budapest at Ka-Band with Alphasat Satellite</i>
Jecko, Bernard	PA2.1	1052	<i>Leading Edge Conformal ARMA Antenna in X Band</i>
	PA4.11	2150	<i>Pixel Antenna Design for mm-Wave Wireless Communications to Achieve Wide Scanning</i>
Jeffrey, Ian	E04.5	2703	<i>Preliminary Description of a 2D Near-Field Electromagnetic Imaging Database</i>
	CS33b.2	3313	<i>Supervised Learning Applied to Microwave Imaging System Calibration</i>
	CS33b.3	3317	<i>Microwave Inversion of Measured S-Parameters Using a Thin-Wire Antenna Model</i>
Jeganathan, Kanapathippillai	CS4.5	3194	<i>CSIRO Radio Astronomy Receiver Update - Ultra Wideband and Phased Array Feeds</i>
Jelinek, Lukas	CS38.5	128	<i>Substructure Modes and Bounds</i>
	PE2.8	1020	<i>The Role of Arrays in Pulsed Radiation</i>
	E10b.1	2059	<i>Radiation Efficiency Cost of Optimal Current Density Generating Specific Far-Field Pattern</i>
	E11.5	2815	<i>Preliminary Study on Gain Maximization via Density-Based Topology Optimization</i>
	A03b.1	3128	<i>An Upper Bound for Envelope Correlation Coefficient of Antenna Clusters</i>
	CS18.5	3687	<i>Material-Independent Scattering Formulations of Characteristic Modes</i>
	A24.5	3876	<i>Design Recommendations for Minimal Antenna Mutual Coupling Using Current Optimization</i>
	CS30b.1	4149	<i>Overview of State-Of-The-Art Methods for Determining Performance</i>

			<i>Bounds on Electromagnetic Systems</i>
	CS30b.2	4153	<i>Fundamental Limits on Characteristic Modes</i>
Ji, Biaobiao	CS23a.4	1790	<i>Analysis of Channel Characteristics for FMCW Millimeter-Wave Radar in Traffic Scenarios</i>
Ji, Jiahui	PE1.4	1253	<i>A Multifunctional Reconfigurable Metagrating for Wavefront Manipulations</i>
Jianfeng, Qian	PA5.9	3529	<i>A Cascaded Resonator Decoupling Network for Two Filtering Antennas with Adjacent Operating Bands</i>
Jiang, Fan	A25.2	3090	<i>3D Printed Cascaded Cavity-Backed Millimeter-Wave Filtering Antenna</i>
Jiang, Hao	PE3.12	2404	<i>High-Order Quasi-Elliptical Bandpass FSS Based on Substrate-Integrated Waveguide Technology for 60 GHz Applications</i>
Jiang, Haoran	CS6a.4	208	<i>A Beam-Scanning Metal-Only Folded Reflectarray Antenna</i>
Jiang, Homin	PM2.1	2428	<i>Using a Radio-Frequency System on a Chip in the Development of a Phased Radio Array for the Bustling Universe Radio Survey Telescope in Taiwan</i>
Jiang, Kai	CS39a.2	614	<i>Measurement of Total Radiated Power Using a TEM Cell</i>
Jiang, Tao	CS35a.4	1697	<i>Time-Varying Channel Measurement and Analysis at 105 GHz in an Indoor Factory</i>
Jiang, Xiaoying	CS39a.4	622	<i>Addressing PIM Challenges in Radio Base Stations: Field Issues and Testing Methods for Large-Scale Deployments</i>
Jiang, Xuewen	PA3.3	3407	<i>A Wearable Open-Ring Dielectric Resonator Antenna with Frequency Reconfiguration</i>
Jiang, Zhenzhen	CS1a.5	4039	<i>Design of Dual-Band CPW Rectenna for Wireless Power Transmission</i>
Jiang, Zhi Hao	CS8.1	2885	<i>Millimeter-Wave 3D Folded Strip Antennas and Arrays: Diverse Polarizations Realization Under Robust Input Impedance</i>
Jilani, Syeda Fizzah	A09b.1	872	<i>X-Band Reconfigurable Phase Shifters Based on SIW and Liquid Metal Technologies</i>
	A09b.5	891	<i>Liquid Metal Reconfigurable Phased Array Antenna</i>
	PA4.19	2186	<i>A Compact High-Gain 28 GHz Antenna Array for Beyond 5G Wireless Networks</i>
Jiménez-Sáez, Alejandro	A09b.4	886	<i>Loss Analysis for Compact Liquid Crystal Delay Lines Based on Defective Ground Structures</i>
	E09.2	3909	<i>Double-Layer Frequency Selective Surface-Based Corner Reflector for Indoor Self-Localization Systems in the W-Band</i>
Jin, Shi	CS44a.5	762	<i>Interference-Free Transmission for Near-Field Communication with Unlimited Antennas</i>
Jirauschek, Christian	CS22b.1	3109	<i>Optimized Design Parameters for a Flux-Driven SNAIL-Based Traveling-Wave Parametric Amplifier</i>
Jofre, Luis	A01b.2	3202	<i>Magnetolectric Dipole Antenna Extending NLOS Short-Distance Vehicular Communication with Orbital Angular Momentum Modes</i>
Johannsen, Ulf	CS25.2	659	<i>A Modular, Low-Cost Ka-Band Antenna Subarray as Building Block for Phased Arrays of Arbitrary Size and Shape</i>
	A18.3	2914	<i>Active Antenna Design for Lunar-Based Detection of Global 21cm-Signals from the Dark Ages</i>
Johansson, Martin	CS10.1	850	<i>Efficient Ray-Tracing Model for Generalized 2D Dielectric Lenses</i>

			<i>Combined with Arrays</i>
Johnson, William	CS43a.1	3952	<i>On the Importance of Scattering from Poles in Ray Tracing Simulations</i>
	CS19b.3	4292	<i>Automatic MoM Source Integral Quadrature Selection via a Machine Learning Approach</i>
Jonsson, Lars	CS38.2	116	<i>Model Order Reduction for Parametric Dependence of Q-Factor Bounds in IoT Applications</i>
	A12a.2	1711	<i>Wide-Scan Active Highly Integrated Phased Array Antenna for Tx/Rx Application at K-Band</i>
	E10a.5	1859	<i>Investigation of Near-Field Contribution in Shooting and Bouncing Rays for Installed Antenna Performance on a Simple Platform</i>
Joseph, Laya	CS30a.3	3937	<i>On Efficient Representations of Frequency Dependent Far-Field Information for Array Antennas</i>
	P06.2	2732	<i>Development of Tissue Emulatory Models/Phantoms of Lungs at Microwave Frequency for Acute Respiratory Distress Syndrome</i>
Joseph, Laya	PP03.7	3615	<i>SINTEC Comparative Body-Centric Communication Study: Bluetooth Vs Fat-Intrabody Communication</i>
Joseph, Sumin	PP01.3	1355	<i>The Time Modulated Array for Channel Sounding Measurements - Concept and Initial Field Tests</i>
	A12a.5	1724	<i>Antenna Array and GaAs Phase Shifter MMIC for Millimeter Wave Beamforming - Co-Simulation and Measurements</i>
	A02.2	3696	<i>Subsampling Time-Modulated Array for Reduced Hardware down Conversion and Beamforming</i>
Joseph, Wout	CS2.5	184	<i>New Hybrid Ray-Tracing/FDTD for EMF Exposure in 6G Networks Using Semantically Classified Google Earth Photogrammetry with Measurement Validation</i>
	CS23b.2	1994	<i>Path Loss Modeling for Air-To-Ground Channels in a Suburban Environment</i>
Joshi, Alok	CS21.1	2706	<i>Imaging Radar Frontend with SIW Feeding Networks</i>
Joshi, Paramananda	CS2.3	175	<i>Long-Term Network-Based Assessment of the Actual Output Power of Base Stations in a 5G Network</i>
Juan-Llacer, Leandro	CS40b.3	1976	<i>Compact 868 MHz RFID-Based Antenna for Queen Bee Identification and Location Inside Hives</i>
Jung, Bo Kum	P10a.1	2972	<i>Automatic Planning Algorithm of 300 GHz Backhaul Links Using Mesh Topology</i>
	P10a.3	2982	<i>Performance Analysis of THz Backhaul Links Assisted by Reconfigurable Intelligent Surfaces</i>
Jung, Incheol	CS19a.5	4085	<i>Platform-Aware Optimization of Conformal Antenna Array via Simulated Bifurcation</i>
Juuti, Jari	PA3.19	3475	<i>Sub-THz Spatially Modulated Beam Splitting Reflectors for Potential RIS Implementations</i>

K

Kadi, Moncef	M5.4	552	<i>Thermoelectric Cooling Solution for Active Antennas</i>
Kaiser, Thomas	A21.4	1493	<i>Assessment of MFE-Based Multiport Waveguide Crossing for Use with Low-Cost, Low-Loss Dielectric Interconnects in Millimeter Wave Arrays</i>
Kalaagi, Mohammed	PE1.13	1288	<i>Multi-Channel Beam-Splitting Metasurface for Millimeter Wave</i>

Communication Systems

Kalista, Weronika	PA4.15	2169	<i>Low-Cost 3-D Printed Lens Antenna for Ka-Band Connectivity Applications</i>
Kalita, Surajit	CS4.4	3189	<i>The Hydrogen Intensity Real-Time Analysis eXperiment: Overview and Status Update</i>
Kallankari, Jani	CS12a.3	4053	<i>Characterisation of a D-Band Horn Antenna: Comparison of Near-Field and OTA Measurements</i>
Kallos, Efthymios	PM2.10	2469	<i>Assessing Performance of Transparent Conductive Films for Microwave Industrial Applications</i>
Kaltiokallio, Ossi	CS23a.1	1775	<i>Gaussian Processes for Received Signal Strength Based Device-Free Localization</i>
Kamal, Syed	PA8.1	2269	<i>Design and Measurement of a 2x2 Array of Coaxial Periodic Leaky-Wave Antennas</i>
Kanbaz, Ihsan	A24.3	3866	<i>Optimization of Super-Directive Linear Arrays with Differential Evolution for High Realized Gain</i>
Kaneko, Yukio	P04b.5	985	<i>Conceptual Design and Propagation Characteristics of an Underwater Electromagnetic Communication System for Ocean Environment Sensor Systems</i>
Kang, Byung Su	PP01.10	1390	<i>Sub-THz Propagation Measurement and Analysis in Indoor Corridor Environment at 159 GHz</i>
Kang, CheChia	P10a.5	2992	<i>Dual-Band MmWave Measurements of Human Body Scattering and Blockage Effects Using Distributed Beamforming for ISAC Applications</i>
Kanno, Issei	A09a.4	691	<i>Beam Training of LoS-MIMO Systems Using Subarray-Based Beamforming in the Presence of Ground Reflection</i>
Kantartzis, Nikolaos	E05.2	2041	<i>On the Rigorous Design of Graphene-Based Periodic Structures Exploiting the Fundamental Resonances</i>
Kanters, Noud	M2.3	3890	<i>Data-Driven Optimization of an Array of Steered Sub-Arrays for Enhanced Fairness in MU-MIMO</i>
Kapusuz, Kamil	PA1.9	3366	<i>A Compact Implantable Camera Integrated MIMO Antenna with Polarization Diversity for Wireless-Capsule-Endoscopy Applications</i>
Karami, Farzad	CS40a.3	1763	<i>Mm-Wave Monopulse Radar System for Detecting Space Debris in Satellite Exploration Missions</i>
Karami-Horestani, Amirhossein	M4.5	2968	<i>Phase-Variation Microwave Displacement Sensor with High Resolution, Sensitivity, and Dynamic Range</i>
Karamirad, Mohsen	E08.2	1868	<i>Reflective Intelligent Surfaces: Reducing Complexity by Controlling the Illuminating Field</i>
	E08.5	1880	<i>Static and Reconfigurable Phase-Gradient Metasurfaces for Antenna Applications</i>
	PA4.10	2147	<i>Analysis and Design of Robust Reconfigurable Intelligent Surfaces Using a Statistical Approach</i>
	A10.2	3071	<i>Analysis and Design of Metasurface Antennas Based on Temporal Metastructures</i>
Karlsson, Peter	P05.4	256	<i>A Small-Sized Antenna System for Direction Finding Applications on a Single Plane (1D) Using BT 5.1</i>
Karmann, Paul	PA7.5	1180	<i>Design of Optimized Cylindrical Structural Antenna with Quasi Length</i>

			<i>Insensitivity Using CMA</i>
Karthikeyan, Vaithinathan	E13.1	270	<i>Ultrahigh Sensitive Terahertz Metasurface with 2D MoS2 for Refractive Index Biosensing</i>
Kaschten, Vincent	A07.5	2679	<i>A Cylindrical Mismatched Luneburg Lens Implemented on PCB at V-Band</i>
Kashef, Mohamed	PP03.8	3620	<i>Empirical Characterization of Doppler in Industrial Wireless Channels</i>
Kasparick, Martin	PP02.8	2523	<i>Comparison of Propagation Characteristics Between 5G Bands in a Reflective Industrial Environment</i>
Kästle, Nico	A11.2	3157	<i>A Low-Profile Wide-Scan Magneto-Electric Dipole Antenna for 5G mm-Wave Communications</i>
Kastner, Raphael	E11.1	2796	<i>Isometric Symmetries in Non-Reflecting Structures</i>
Kataoka, Ryochi	A09a.4	691	<i>Beam Training of LoS-MIMO Systems Using Subarray-Based Beamforming in the Presence of Ground Reflection</i>
Kaverine, Evgueni	CS5b.3	374	<i>Industrial Design Validation for a Plane Wave Generator at 28GHz</i>
Kawai, Katsumi	CS1a.3	4031	<i>Far-Field Beam Wireless Power Transfer with Combination of Beam Forming and Optical Target Detection</i>
Kawai, Nobuaki	P04b.5	985	<i>Conceptual Design and Propagation Characteristics of an Underwater Electromagnetic Communication System for Ocean Environment Sensor Systems</i>
Kawamura, Takashi	P04b.5	985	<i>Conceptual Design and Propagation Characteristics of an Underwater Electromagnetic Communication System for Ocean Environment Sensor Systems</i>
Kaya, Hacer	PA4.21	2193	<i>Terahertz Microstrip Leaky-Wave Antenna for WR1.0 Band</i>
Kaynak, Mehmet	A05.1	1820	<i>Sub-THz Substrate Integrated Waveguide Signal Transitions in Backend-Of-Line of a Silicon Process</i>
Kazim, Jalil ur Rehman	PE3.13	2408	<i>Design of Intelligent Reflective Surface Unit Cell for 5G mmWave Applications</i>
Kebel, Robert	PE2.3	999	<i>Management of Radiofrequency Compatibility on Aircraft</i>
Keerativoranan, Nophon	P04b.1	965	<i>Grid-Based Shadowing Gain Modeling for Handling Dynamic Objects in Wireless Channel Emulation</i>
	P03.5	1548	<i>Utilization of Wi-Fi Signal for Validation of Micro-Doppler Model in a Person Falling Scenario</i>
Keller, Sven	CS30a.4	3942	<i>Validating Convex Optimization of Reconfigurable Intelligent Surfaces via Measurements</i>
Kelly, James	A09a.3	688	<i>1-Bit Reconfigurable Transmitted/Reflected Array (TRA) for 5G/6G Wireless Communication</i>
	A09b.1	872	<i>X-Band Reconfigurable Phase Shifters Based on SIW and Liquid Metal Technologies</i>
	A09b.5	891	<i>Liquid Metal Reconfigurable Phased Array Antenna</i>
Kelmendi, Arsim	PP02.15	2557	<i>Large-Scale Site Diversity Experiment in Ljubljana and Budapest at Ka-Band with Alphasat Satellite</i>
Kerr, Peter	A16.4	1744	<i>Compact Hybrid Optical/RF User Segment (CHORUS): RF Terminal Design</i>
Ketzaki, Dimitra	PA3.21	3483	<i>MIMO Signals Processing Utilizing Optical Crossbar Linear Operator</i>
Keusgen, Wilhelm	CS10.3	860	<i>D-Band Active Antenna Array with Lens Enabling Quasi-Optical and</i>

			<i>Analogue Beam Reconfiguration for 6G Applications</i>
	P10b.1	3244	<i>Empirical Path Loss Model and Small-Scale Fading Statistics in an Indoor Office Environment in 6 and 37 GHz Shared Bands</i>
	P01.4	3847	<i>Frequency Domain Channel Characteristics in an Outdoor-To-Indoor Environment at 6 and 37 GHz</i>
	CS43b.2	4173	<i>Comparison of Sub-THz Radio Channel Characteristics at 158 GHz and 300 GHz in a Shopping Mall Scenario</i>
Khaleghi, Ali	CS13.1	1553	<i>Antenna System for Simultaneous Wireless Power and Information Transfer to Brain Implants</i>
Khalid, Hamza	M2.2	3886	<i>Real-Time Near-Field Measurements of mmWave Devices Using a Metasurface and IR Camera</i>
Khalifeh, Rania	M5.4	552	<i>Thermoelectric Cooling Solution for Active Antennas</i>
Khalily, Mohsen	CS17a.1	1	<i>Dual-Polarized Reconfigurable Metacavity Transceiver for Computational Polarimetric Imaging</i>
	CS3.2	298	<i>From Reconfigurable Intelligent Surfaces to Holographic MIMO Surfaces and Back</i>
	E06a.3	596	<i>Fully Autonomous Reconfigurable Metasurfaces with Integrated Sensing and Communication</i>
	CS44a.2	750	<i>Dual Functional mmWave RIS for Radar and Communication Coexistence in near Field</i>
	PA2.9	1091	<i>Sub-7 GHz Circularly Polarized Dielectric Resonator Antenna Array for Full-Duplex Applications</i>
	PE1.2	1245	<i>Smart Propagation Environments Empowered by Metasurfaces: A Self-Consistent Study</i>
	PE1.11	1279	<i>Compact Polarization Converter on a Thin Ferrite-Based Metasurface for Enhanced 5G Wireless Communication</i>
	PA4.13	2160	<i>A Novel Precise Approach for Digital Metasurface Configuration for Sensing Application</i>
	CS22a.4	2853	<i>Quantum Optimisation of Reconfigurable Surfaces in Complex Propagation Environments</i>
	A25.1	3087	<i>Long Slot Dielectric-Loaded Periodic Leaky-Wave Antenna Based on 3D Printing Technology</i>
	PA5.18	3564	<i>Realizing Flat-Top Radiation Pattern with Sharp Cutoff for Reducing Lobing Fades</i>
Khamas, Salam	A27b.5	845	<i>Flexible Phase-Reconfigurable Branch Line Coupler for Millimeter-Wave Phased Array Antenna</i>
	PA1.1	3331	<i>Omnidirectional Cylindrical Dielectric Resonator Antenna for off & on Body Communications</i>
	PA3.4	3410	<i>A 2x2 Dual-Band Open Loop Array with Circular Polarisation</i>
	A20.4	3822	<i>The Impact of a Phantom's Size on the Performance of an Implanted Antenna</i>
Khan, Humayun Zubair	CS14b.5	4366	<i>Multi-Band Anisotropic Metasurface: Simultaneous Linear and Circular Polarization for Robust Satellite Communication</i>
Khan, Mahrukh	PA8.17	2340	<i>A Systematic Design Method of Miniaturizing Microstrip Patch Antenna Using Theory of Characteristic Modes</i>

Khan, Muhammad Waqas Ahmad	A20.5	3827	<i>Quad-Band Meandered Implantable Planar Inverted-F Antenna for Wireless Brain Health Monitoring</i>
Khan, Wasi Ur Rehman	PP03.4	3601	<i>Effect of Wave Polarization in On-Body Propagation for the 2.4, 24 and 60 GHz ISM Bands</i>
Khatibi Moghaddam, Maliheh	PE1.6	1261	<i>Characterization of a Metamaterial-Enabled Waveguide Diplexer for Ka-Band Satellite Communication Systems</i>
Khodadadi, Maryam	E06a.3	596	<i>Fully Autonomous Reconfigurable Metasurfaces with Integrated Sensing and Communication</i>
	PA5.18	3564	<i>Realizing Flat-Top Radiation Pattern with Sharp Cutoff for Reducing Lobing Fades</i>
Khodaei, Meghdad	PA5.10	3533	<i>A High Efficiency and Ultra-Wideband Rectenna for RF Energy Harvesting Application</i>
Khorashadizadeh, Vahid	CS47.3	421	<i>Millimeter-Wave Scattering from Building Facade: A Simulation and Verification Study</i>
Khosravi, Hedieh	CS43b.5	4187	<i>Experimental Analysis of Physical Interacting Objects of a Building at mmWave Frequencies</i>
Khosrownejad, Mostafa	PE1.6	1261	<i>Characterization of a Metamaterial-Enabled Waveguide Diplexer for Ka-Band Satellite Communication Systems</i>
Khripkov, Alexander	A01b.4	3211	<i>Traveling-Wave Fed Dielectric Rod Antenna for 3D Scanning MIMO Sensor</i>
Kikuma, Nobuyoshi	A27a.4	646	<i>Mechanical/Electrical Hybrid 2-Dimensional Beam Scanning Cylindrical Dielectric Lens Antenna</i>
Kilani, Dima	CS40b.2	1973	<i>A WiFi-Based System for Ice Monitoring in Harsh Environment Using 2.7 GHz Microwave Sensor</i>
Kim, Bumhyun	CS37a.6	51	<i>A Completely Overlapped Ku- and Ka-Band Dual-Polarized Phased Array for Simultaneous Terrestrial and Satellite Communications</i>
	PP01.16	1413	<i>Breaking the Myth of RIS: Investigating the Role of User Equipment for Achieving Robust mmWave Wireless Channel Links Under NLOS Environments</i>
Kim, Eric	A25.5	3105	<i>Additively Manufactured Horn Antennas</i>
Kim, Hogyeon	CS17b.4	330	<i>Indoor Coverage Enhancement Employing Liquid Crystal-Based Massive Reconfigurable Intelligent Surface Linked to 5G FR2 Base Station</i>
	CS7.2	1596	<i>Simultaneously Dual-Polarization Convertible Sub-THz Reconfigurable Intelligent Surface Enabled by Through-Quartz VIAs</i>
Kim, Inhwan	E02b.5	3284	<i>Generalized Transition Matrix Model Using Characteristic Basis Function Method for Open-Ended Cavities</i>
Kim, Jong Ho	PP01.12	1399	<i>The Effect of Beam Misalignment in Data Center Environment at 285GHz Band</i>
Kim, Kiseo	CS37a.5	47	<i>Display-Integrated MIMO Antennas for Gesture-Sensing Radars</i>
Kim, Kyoungwhan	CS14a.3	4139	<i>Hybrid Reconfigurable Reflective Metasurface with Both Phase and Space Modulation</i>
Kim, Minseok	CS5b.2	369	<i>Double-Directional Angle-Resolved Wideband Channel Measurements and Path Loss Characterization in Corridor at 300 GHz</i>
	P10a.5	2992	<i>Dual-Band MmWave Measurements of Human Body Scattering and</i>

Kim, Myung-Don	PP01.10	1390	<i>Blockage Effects Using Distributed Beamforming for ISAC Applications Sub-THz Propagation Measurement and Analysis in Indoor Corridor Environment at 159 GHz</i>
Kim, Nam	A27b.2	834	<i>A Radial Waveguide Power Divider Inspired Antenna for mmWave IoT Sensing Applications</i>
	PA8.7	2298	<i>Compact Size Frequency-Agile Antenna Enabling Multi-Mode Functionality for Internet of Things Applications</i>
	PA1.7	3359	<i>Development of a Wearable IoT-Optimized Textile Antenna with Low Specific Absorption Rate in Three Frequency Bands</i>
Kim, Sehun	CS37b.6		<i>Differentially-Fed Antenna-On-Display Module for SATCOM and Mobile Applications at Ka-Band</i>
Kim, Sunghyun	CS17b.4	330	<i>Indoor Coverage Enhancement Employing Liquid Crystal-Based Massive Reconfigurable Intelligent Surface Linked to 5G FR2 Base Station</i>
Kim, Tae-Yeob	PE3.11	2401	<i>Flexible and Transparent Metamaterial Absorber Using Metal Mesh Structure</i>
Kim, Yongwan	CS17b.4	330	<i>Indoor Coverage Enhancement Employing Liquid Crystal-Based Massive Reconfigurable Intelligent Surface Linked to 5G FR2 Base Station</i>
Kimura, Sho	PP01.9	1385	<i>Development of a Site-Specific Building Entry Loss Model for High-Rise Buildings</i>
Kimura, Yasuko	PA4.4	2119	<i>Prototype of Multi-Sector Indoor mmW Base Station Based on 5G NR Beam Control</i>
Kirillov, Vitalii	PA8.16	2336	<i>Performance Estimation of In-Vessel Resonant Communications</i>
Kishi, Yoji	A09a.4	691	<i>Beam Training of LoS-MIMO Systems Using Subarray-Based Beamforming in the Presence of Ground Reflection</i>
Kishk, Ahmed	A10.4	3079	<i>"The Diminished Edge Diffraction Effect Bull's Eye Antenna "</i>
	A11.5	3171	<i>Mutual Coupling Reduction in 5G MIMO Antenna Using Dielectric Bridge and Superstrate</i>
Kitao, Koshiro	CS5b.6	388	<i>Sub-Terahertz MassiveMIMO Channel Sounder for 6G Mobile Communication Systems</i>
Kiviharju, Pyry	P06.3	2737	<i>Potential of Polarized MIMO in In-Body to Out-Body Radio Links</i>
Kleine-Ostmann, Thomas	CS5a.3	66	<i>Horn Antenna Phase Center Position Influence on Sub-THz Measurements Uncertainties</i>
	CS32.4	1448	<i>Simplified Techniques to Estimate Uncertainties for Antenna Gain Patterns Determined via Near-Field to Far-Field Transformation</i>
	PP02.8	2523	<i>Comparison of Propagation Characteristics Between 5G Bands in a Reflective Industrial Environment</i>
Kleinschmidt, Michael	CS12b.2	4263	<i>Robotic Antenna Characterization System Based on Wideband FMCW Transceiver Modules</i>
Knapp, Josef	CS42a.1	136	<i>Inverse Source Solutions with Spectral Filtering</i>
Knightly, Edward	CS44b.4	955	<i>Curving THz Beams in the near Field: A Framework to Compute Link Budgets</i>
Knopp, Andreas	CS25.1	654	<i>Beamforming Schemes for 6G Direct-To-Cell Connectivity Using Satellite Swarms</i>

Kodra, Silvi	CS20b.2	398	<i>A Macroscopic Bilateral Modeling Approach for Reflective and Transmissive Metasurfaces</i>
Koivumäki, Pasi	P04a.1	767	<i>On the Use of Adaptive-Density Point Cloud for Site-Specific Ray-Optics Simulations</i>
Kokkeler, Andre	A01b.1	3197	<i>Tiled Subarray Design for Multibeam Joint Communication and Sensing</i>
Kolomvakis, Nikolaos	CS17a.5	19	<i>Nonlinear Distortion Issues Created by Active Reconfigurable Intelligent Surfaces</i>
Kolundzija, Branko	CS24a.5	740	<i>Polynomial Basis Functions for Qualitative Head Tissue Segmentation via Linearized Microwave Imaging</i>
	CS33a.5	3062	<i>Generating a Library of Head Phantoms for Microwave Imaging Using Spherical Harmonic Approximation</i>
Kong, Di	PA3.19	3475	<i>Sub-THz Spatially Modulated Beam Splitting Reflectors for Potential RIS Implementations</i>
Kong, Lingqi	M4.4	2964	<i>Quad-Junction Self-Biased Circulator with Wide Operational Bandwidth</i>
Konstandin, Simon	CS33b.4	3321	<i>Deep-Learning Optimized Reconfigurable Metasurface for Magnetic Resonance Imaging</i>
Kordiboroujeni, Zamzam	CS45.1	1799	<i>MR/Microwave Tomography Integrated Breast Cancer Imaging</i>
Kormilainen, Riku	CS41.5	3239	<i>Cost-Effective Dual Circularly Polarized Antennas for Phase Calibration</i>
Kosmas, Panagiotis	PP01.1	1347	<i>A Deep Learning-Based Approach for Inverse Design of Reconfigurable Metasurfaces</i>
	PM2.10	2469	<i>Assessing Performance of Transparent Conductive Films for Microwave Industrial Applications</i>
Kosulnikov, Sergei	A03a.3	2872	<i>The Role of Ground Currents in the Co-Simulation of Matching Components and Layout Models in Matching Circuit Optimization</i>
Kotiranta, Mikko	P02.4	3777	<i>Measuring and Modelling the Scattering Parameters of the Wet Radome of the Swiss Weather Radars</i>
Koulouridis, Stavros	PA4.3	2114	<i>A Two-Port Metamaterial Antenna for mm-Wave 5G MIMO Applications with Enhanced Bandwidth and Gain</i>
	CS26b.1	4305	<i>Ridge Gap Waveguide Implementation with a 3D Glide Symmetric Holey Metasurface for Slotted Antenna Array Feeding</i>
Koutsos, Orestis	A09a.2	683	<i>Sub-Wavelength Anisotropic Unit-Cells for Low-Profile Transmitarray Antennas</i>
	CS7.1	1592	<i>Low Profile and High Gain Folded Transmitarray in Quartz for Radiometry at 310 GHz</i>
Koutsoupidou, Maria	PM2.10	2469	<i>Assessing Performance of Transparent Conductive Films for Microwave Industrial Applications</i>
Kovačević, Anja	CS33a.5	3062	<i>Generating a Library of Head Phantoms for Microwave Imaging Using Spherical Harmonic Approximation</i>
Kovaios, Stefanos	PA3.21	3483	<i>MIMO Signals Processing Utilizing Optical Crossbar Linear Operator</i>
Kowalczuk, Emma	PE3.7	2388	<i>Electromagnetic Modelling in Modern Vehicles: A Pathway to Efficiency and Performance</i>
Koziel, Slawomir	PE3.1	2359	<i>Cost-Efficient Large-Scale Re-Design of Multi-Band Antennas Using Orthogonal Scaling Directions</i>
	CS30a.1	3928	<i>Unconventional Surrogate-Assisted Approaches to EM-Driven Antenna</i>

			<i>Design. Modeling and Optimization: Global, Multi-Objective, Statistical</i>
Kozlov, Dmitry	PA8.16	2336	<i>Performance Estimation of In-Vessel Resonant Communications</i>
Kracek, Jan	PA2.20	1140	<i>Compact Ka Band Orthomode Transducer with Conical Horn Antenna</i>
Krasov, Pavlo	M2.5	3900	<i>Optimization of the TRP Evaluation in Anechoic-Reverberation Hybrid Chamber</i>
	CS48.5	3996	<i>A Varactor-Based Reconfigurable Intelligent Surface Concept for 5G/6G mm-Wave Applications</i>
Krengel, Markus	CS21.2	2709	<i>New Efficient Waveguide Antenna for Future Automotive Radar Applications</i>
Krenkevich, Jordan	CS24a.3	731	<i>Evaluating System Design in Breast Microwave Sensing: Data and Image Quality in Multiple Systems</i>
Kretschmann, Marius	M3.1	2586	<i>Enhancing THz Antenna Characterization Precision in WR-1.5 Band Using Vacuum Waveguide Flange</i>
Krishnegowda, Karthik	CS10.3	860	<i>D-Band Active Antenna Array with Lens Enabling Quasi-Optical and Analogue Beam Reconfiguration for 6G Applications</i>
Krska, Josef	CS23b.4	2004	<i>Angle of Arrival Measurements with Ultra-Wide Band Transceivers: Design and Evaluation</i>
Kruger, Paulus	CS4.1	3176	<i>Analysis of a Small LOFAR Low-Band Test Array Using a Sky Map, Simulated Embedded Element Patterns and Measured LNA-Impedances</i>
Kshetrimayum, Rakesh	A03b.4	3142	<i>High Gain and Dual Band SIW-Fed Stacked Conical DRA for 5G NR FR1 Application</i>
Kudriashov, Volodymyr	CS46.3	4223	<i>CubeSat Formation Antenna Array Synchronization for GNSS-R</i>
Kuerner, Thomas	CS23a.2	1780	<i>Terahertz Channel Modeling Based on Scattering Characterization</i>
Kuhn, Emily	CS4.4	3189	<i>The Hydrogen Intensity Real-Time Analysis eXperiment: Overview and Status Update</i>
Kulas, Lukasz	A21.3	1488	<i>Millimeter Wave Retrodirective Van Atta Arrays in LTCC Technology</i>
	PA4.15	2169	<i>Low-Cost 3-D Printed Lens Antenna for Ka-Band Connectivity Applications</i>
	PA8.15	2332	<i>Miniaturized and Lightweight ESPAR Antenna for WSN and IoT Applications</i>
	M3.5	2605	<i>Highly Precised and Efficient Robot-Based ESPAR Antenna Measurements in Realistic Environments</i>
Kumar, Anand	PE2.10	1027	<i>FDTD Modelling of RF Circuits Based on Lumped Components and Transmission Lines Using Modified Telegrapher's Equations</i>
Kumar, Rakesh	CS21.1	2706	<i>Imaging Radar Frontend with SIW Feeding Networks</i>
Kumar, Rupesh	PM2.7	2454	<i>Near-Field Bistatic Microwave Imaging with Dynamic Metasurface Antennas</i>
Kumar, Sanjeev	P06.5	2747	<i>A Time-Efficient Model for Estimating Far-Field Wireless Power Transfer to Biomedical Implants</i>
	CS1b.1	4238	<i>A Compact Microwave Rectifier for Wireless Power Transfer and Energy Harvesting Applications</i>
Kuno, Nobuaki	CS5b.6	388	<i>Sub-Terahertz MassiveMIMO Channel Sounder for 6G Mobile Communication Systems</i>
Kunz, Martin	CS4.4	3189	<i>The Hydrogen Intensity Real-Time Analysis eXperiment: Overview and</i>

			<i>Status Update</i>
Kuosmanen, Matti	CS40b.1	1969	<i>Small On-Metal Passive UHF RFID Transponders with Long Read Ranges</i>
	PA5.19	3569	<i>Beam Steering Performance Improvements Using a Layered Permittivity Dielectric</i>
Kürner, Thomas	CS5b.4	378	<i>Channel Measurements in Workspace with Robotic Manipulators at 300 GHz and Recent Results</i>
	P04a.3	777	<i>Analysis of Propagation Models for Frequency Coordination Between 5G Base Stations and Satellite Earth Stations at FR1</i>
	P04b.3	975	<i>Ray Tracing and Measurement-Based Characterization of Inter/Intra-Machine THz Wireless Channels</i>
	PP01.6	1370	<i>A New Approach for Line of Sight Prediction with Geometry Analysis and Machine Learning in Diverse Environments</i>
	CS7.5	1611	<i>Reconfigurable Intelligent Surfaces for THz: Signal Processing and Hardware Design Challenges</i>
	PP02.6	2515	<i>Antenna Pattern Tracking Algorithm for Low Terahertz Communications</i>
	P10a.1	2972	<i>Automatic Planning Algorithm of 300 GHz Backhaul Links Using Mesh Topology</i>
	P10a.3	2982	<i>Performance Analysis of THz Backhaul Links Assisted by Reconfigurable Intelligent Surfaces</i>
	Kurokawa, Haruki	PA2.8	1088
Kurokawa, Satoru	CS39b.4	823	<i>Millimeter Wave Vector Measurement System Using Low Frequency Band Oscilloscope</i>
Kurskiy, Kirill	PE2.5	1009	<i>Gain Improvement of a DRA Using Deep Reinforcement Learning with Polygon Mesh Deformation</i>
Kushiyama, Yujiro	PA4.25	2210	<i>Beam-Steerable Microstrip-Line Based Leaky Wave Antenna with Reconfigurable Slits</i>
Kuznetcov, Maksim	PA8.2	2274	<i>Dual-Polarized Substrate Integrated Waveguide Antenna with High Isolation for Polarimetric Radar</i>
Kuznetcov, Maksim	PP02.7	2520	<i>Electromagnetic Beerline Cleaning Using Radio Frequency Signals</i>
Kuznetsov, Aleksandr	CS30b.5	4163	<i>Optimization of Loads for Antenna-Based Scattering Systems Using Feedforward Neural Networks</i>
Kvarnstrand, John	CS39b.1	808	<i>Exploring the Properties of Reverberation Chambers in the THz Range: A Pilot Study</i>
	M2.4	3895	<i>K-Factor Evaluation in a Hybrid Reverberation Chamber plus CATR OTA Testing Setup</i>
Kwak, Seungheon	PP02.1	2490	<i>Improving Air-Writing Accuracy Through Data Regression and Interpolation in a Single Radar System</i>
Kwon, Do-Hoon	A15b.3	4335	<i>Array Scattering Synthesis for Anomalous Deflection Using Passive Aperiodic Loadings</i>
Kwon, Heon Kook	PP01.10	1390	<i>Sub-THz Propagation Measurement and Analysis in Indoor Corridor Environment at 159 GHz</i>
Kwon, Jae-Yong	CS12b.1	4259	<i>KRISS Robot-Based Antenna Measurement System</i>
Kwon, Suk Jin	E13.2		<i>Magnetic Composites with M-Type Hexaferrites for Q/V-Band</i>

			<i>Electromagnetic Wave Absorption</i>
Kynman, Ossian	PA5.7	3519	<i>Analysis and Measurement of Key Performance Indicators for MIMO Antennas</i>
Kyösti, Pekka	CS5a.5	76	<i>A Modular COTS-Based High-Efficient Sub-THz Channel Sounder and Experimental Validations</i>
	PP01.8	1380	<i>Dual-Polarized Diffraction Measurements and Modeling at D-Band Frequencies</i>
	CS29.3	3797	<i>Computer Vision Enabled Sub-THz Radio Channel Characterization of Dynamic Objects</i>
	M2.1	3881	<i>A Novel MIMO OTA Methodology for UE Performance Testing</i>
Kyröläinen, Jukka	M2.1	3881	<i>A Novel MIMO OTA Methodology for UE Performance Testing</i>

L

Lacrevaz, Thierry	CS3.5	311	<i>Exploring PLA/Flax Substrates for Antenna Applications: Assessing Moisture, Temperature and Dielectric Constant Homogeneity</i>
Laetitia, Niyonzima	PA2.21	1145	<i>Wideband Low-Profile Circularly Polarized All-Metal Antenna for Triton Exploration</i>
Laffont, Adrien	CS1b.4	4251	<i>Power Handling Test of a L-Band Antenna Using Infrared Thermography</i>
Lagunas, Eva	PA2.5	1074	<i>Genetic Algorithm-Based Beamforming in Subarray Architectures for GEO Satellites</i>
	CS19b.4	4295	<i>Supervised Learning Based Real-Time Adaptive Beamforming On-Board Multibeam Satellites</i>
Lain-Rubio, Veronica	CS7.5	1611	<i>Reconfigurable Intelligent Surfaces for THz: Signal Processing and Hardware Design Challenges</i>
Lalas, Antonios	E07.5	1653	<i>An Accurate Semi-Analytical Model for Periodic Tunable Metasurfaces Electromagnetic Response</i>
Laller, Rupa	PA5.15	3552	<i>A Decoupling Scheme for Closely Spaced Microstrip Patch Antenna</i>
Lam, Hong Yin	P09.2	2639	<i>Rain Attenuation at Millimeter Waves in Different Climatic Zones Estimated from Drop Size Distributions</i>
Lambert, Kevin	CS12b.5	4278	<i>Robotic Arm-Based Antenna Metrology System for Aerospace Applications</i>
Lamkaddem, Abdenasser	PA1.12	3381	<i>Miniaturization of Wireless Power Transfer for Implantable Devices Using Voltage Doubler Rectifier</i>
Lanagan, Michael	PM2.5	2446	<i>Dielectric Characterization of Materials at 5G mm-Wave Frequencies</i>
Lang, Hans-Dieter	CS30a.4	3942	<i>Validating Convex Optimization of Reconfigurable Intelligent Surfaces via Measurements</i>
Langdon, Scott	PE2.2	995	<i>A Two-Component 2-D FDFD Eigenmode Method Incorporated with the Conformal Technique</i>
Laquerbe, Vincent	CS16.5	578	<i>Radiation Control by Space-Time-Modulated Anisotropic Impedance Surfaces</i>
	PA6.9	2245	<i>Study of the Frequency Dispersion of 3D-Printed Dielectric Crystals for Dielectric Resonator Antenna Applications</i>
Larsson, Christer	CS31.2	1663	<i>High Resolution ISAR Imaging Methods for RCS Data Analysis</i>
Larsson, Christina	CS43a.5	3972	<i>Feasibility of High Throughput Wireless Communication Above 100 GHz in Indoor Scenarios</i>

Las-Heras, Fernando	CS3.4	306	<i>Eco-Friendly Meta-Randomized Antenna for Millimeter Wave Radar</i>
	PM2.6	2449	<i>Detection Capability of a CNN-Based Imageless Millimeter Wave System for Static Concealed Objects</i>
	CS33b.5	3326	<i>Impact of Antenna Radiation Pattern Linear Phase Shift in SAR Image Quality</i>
Lassauce, Léonin	A13.3	1958	<i>Wide-Angle Quasi-Optical Beamformer for LEO Applications</i>
Lasser, Gregor	CS48.5	3996	<i>A Varactor-Based Reconfigurable Intelligent Surface Concept for 5G/6G mm-Wave Applications</i>
Latappy, Claire	P03.3	1538	<i>Influence of the Atmospheric Plasma Sheath on the RCS of a Hypersonic Reentry Vehicle</i>
Lau, Buon Kiong	A01b.3	3206	<i>Roof-Glass Integrated Antenna for Vehicular GNSS Applications</i>
	CS18.4	3683	<i>Circularly Polarized Sub-THz Antenna Design for Distributed Deployment</i>
Lauer, Andreas	CS10.3	860	<i>D-Band Active Antenna Array with Lens Enabling Quasi-Optical and Analogue Beam Reconfiguration for 6G Applications</i>
Laukkanen, Sami	CS12a.3	4053	<i>Characterisation of a D-Band Horn Antenna: Comparison of Near-Field and OTA Measurements</i>
Lavagetto, Fabio	CS45.5	1815	<i>Brain Stroke Microwave Diagnostics in Children Through a Nonlinear Inverse-Scattering Technique</i>
Laviada, Jaime	PM2.6	2449	<i>Detection Capability of a CNN-Based Imageless Millimeter Wave System for Static Concealed Objects</i>
	CS33b.5	3326	<i>Impact of Antenna Radiation Pattern Linear Phase Shift in SAR Image Quality</i>
Lazarakis, Fotis	PM2.10	2469	<i>Assessing Performance of Transparent Conductive Films for Microwave Industrial Applications</i>
Lazaridis, Pavlos	E05.2	2041	<i>On the Rigorous Design of Graphene-Based Periodic Structures Exploiting the Fundamental Resonances</i>
Lazzoni, Valeria	PE3.8	2392	<i>Design of a Conformal and Low-Frequency Metasurface for Magnetic Field Shielding in Wireless Power Transfer Systems</i>
Le Coq, Laurent	CS42b.2	442	<i>Multiple Reduced Order Models for Antenna Measurements</i>
	CS32.5	1453	<i>Stable Phaseless Spherical Antenna Measurements via Mixed-Norm Regularization</i>
Le Magoarou, Luc	E07.1	1636	<i>Model-Based Deep Learning for High-Dimensional Periodic Structures</i>
Leach, Mark	CS1a.5	4039	<i>Design of Dual-Band CPW Rectenna for Wireless Power Transmission</i>
Lecerf, Nathalie	PA2.7	1084	<i>Design and Prototyping of a Low-Cost Parasitic Element Antenna for a Telemetry-Telecommand Link on Ariane 6 Space Launcher</i>
Lederer, Dimitri	A07.5	2679	<i>A Cylindrical Mismatched Luneburg Lens Implemented on PCB at V-Band</i>
Lee, Hee-Jo	PE3.9	2395	<i>Concentration Detection of Sodium Chloride and Glucose Solutions Using an IDC-Based Microwave Sensor with Eliminating Environmental Effects</i>
Lee, Horim	E13.2		<i>Magnetic Composites with M-Type Hexaferrites for Q/V-Band Electromagnetic Wave Absorption</i>
Lee, Hyunsoo	E02b.5	3284	<i>Generalized Transition Matrix Model Using Characteristic Basis Function Method for Open-Ended Cavities</i>

Lee, Jaemin	PA1.7	3359	<i>Development of a Wearable IoT-Optimized Textile Antenna with Low Specific Absorption Rate in Three Frequency Bands</i>
Lee, Jeong-Hae	A06b.5	3306	<i>A High-Efficiency Reconfigurable Reflectarray Antenna Using Two Types of Active Unit Cells</i>
Lee, Juyul	PP01.10	1390	<i>Sub-THz Propagation Measurement and Analysis in Indoor Corridor Environment at 159 GHz</i>
Lee, Kyuho	CS37a.5	47	<i>Display-Integrated MIMO Antennas for Gesture-Sensing Radars</i>
Lee, Sang Bok	E13.2		<i>Magnetic Composites with M-Type Hexaferrites for Q/V-Band Electromagnetic Wave Absorption</i>
Lee, Sangmin	PA8.7	2298	<i>Compact Size Frequency-Agile Antenna Enabling Multi-Mode Functionality for Internet of Things Applications</i>
Lee, Seongwook	PP02.1	2490	<i>Improving Air-Writing Accuracy Through Data Regression and Interpolation in a Single Radar System</i>
Lee, Seung Yoon	CS37a.4	42	<i>Integrated Low-Loss mmWave On-Chip Arrays</i>
Lee, Sun-Gyu	A06b.5	3306	<i>A High-Efficiency Reconfigurable Reflectarray Antenna Using Two Types of Active Unit Cells</i>
Legay, Hervé	CS25.3	663	<i>Multibeam Phased Arrays Exploiting Frequency Dispersion for Massive MIMO Satellite Communications</i>
	CS25.4	668	<i>Aperture Distribution Method for Array-Fed Reflectors: A System Level Performance Case Study</i>
	A19.5	1523	<i>Exploring the Potential of Spatially Modulated Full-Metal Dichroic Mirrors for Deep Space Antennas</i>
	CS40a.5	1770	<i>A Self Deployable and Reconfigurable Antenna in VHF Band for a New Space Mission</i>
Lehmensiek, Robert	CS4.3	3186	<i>A Performance Comparison of Sub-Octave Band Corrugated Horns to a Quadruple-Ridged Flared Horn for the ngVLA Radio Telescope</i>
Lehtovuori, Anu	CS38.1	112	<i>Improving Scan Gain of Sparse Vivaldi Array with Parasitic Scatterers</i>
	PE2.4	1004	<i>Applying Neural Networks for Predicting Feed Weights of an Antenna Array</i>
Lei, Siyuan	A01a.5	2945	<i>Low-Profile Multibeam Beam-Scanning Antenna for Vehicular Radar Systems</i>
Leino, Mikko	CS41.5	3239	<i>Cost-Effective Dual Circularly Polarized Antennas for Phase Calibration</i>
Leinonen, Marko	CS5a.5	76	<i>A Modular COTS-Based High-Efficient Sub-THz Channel Sounder and Experimental Validations</i>
	PP01.8	1380	<i>Dual-Polarized Diffraction Measurements and Modeling at D-Band Frequencies</i>
	PA3.19	3475	<i>Sub-THz Spatially Modulated Beam Splitting Reflectors for Potential RIS Implementations</i>
	CS29.3	3797	<i>Computer Vision Enabled Sub-THz Radio Channel Characterization of Dynamic Objects</i>
	P01.1	3832	<i>5G Radio Channel Characterization in an Underground Mining Environment</i>
	CS12a.3	4053	<i>Characterisation of a D-Band Horn Antenna: Comparison of Near-Field and OTA Measurements</i>
	A15a.5	4127	<i>Tapering Impact on the Spatial and Frequency Responses of</i>

			<i>Broadband Asymmetrically Routed Phased Arrays</i>
Lele, Kshitij	E06a.1	586	<i>Contiguous Broadband Circularly Periodic High Impedance Surface Integrated with a Spiral Antenna</i>
	E09.4	3919	<i>Progressive Ultra-Wideband Circularly Periodic High Impedance Surface Integrated with a Spiral Antenna</i>
Lelievre, Aurelien	CS2.4	180	<i>Advanced Post-Processing Technique to Evaluate Specific Absorption Rate (SAR) for a Standard Dipole Antenna</i>
Lemaistre, Sébastien	PA2.21	1145	<i>Wideband Low-Profile Circularly Polarized All-Metal Antenna for Triton Exploration</i>
Lemey, Sam	CS2.5	184	<i>New Hybrid Ray-Tracing/FDTD for EMF Exposure in 6G Networks Using Semantically Classified Google Earth Photogrammetry with Measurement Validation</i>
	CS40a.2	1758	<i>Optimizing RF Energy Harvesting in IoT: A Machine Learning Estimation Considering Polarization Effects</i>
Lemey, Sam	A15b.5	4345	<i>Dual UWB Antennas on AoA Anchor Node</i>
Lenets, Vladimir	A03b.5	3147	<i>Wireless Re-Configurable Intelligent Surface for Sub 6 GHz 5G Frequency</i>
Leonor, Nuno R.	P05.1	241	<i>Small-Scale Passive Millimetre-Wave Imaging Measurements for Marine Litter Detection at W-Band</i>
	P10b.4	3259	<i>Wind-Induced Backscatter Clustering from Vegetation at W-Band</i>
	P02.3	3772	<i>Feature Selection for Identifying Optimal Microwave Frequencies to Detect Floating Macroplastic Litter in C and X Bands</i>
Lepetit, Thomas	CS14a.5	4145	<i>Time-Modulated Metasurface for Harmonic Signals Frequency Conversion</i>
Lerosey, Geoffroy	CS20b.3	402	<i>Measurements of Reconfigurable Intelligent Surface in 5G System Within a Reverberation Chamber at mmWave</i>
	CS34.4	2625	<i>Empirical Validation of the Impedance-Based RIS Channel Model in an Indoor Scattering Environment</i>
	A03b.5	3147	<i>Wireless Re-Configurable Intelligent Surface for Sub 6 GHz 5G Frequency</i>
LeRoux, Daniel	CS42a.5	156	<i>Antenna Coupling Evaluation in Arrays and Complex Structures Using Measured Sources and Simulations</i>
LeRoy-Naneix, Isabelle	PA2.17	1128	<i>Dual-Polarized Connected-Slot Array Technological Demonstrator Targeting a 5:1 Bandwidth</i>
Lestini, Francesco	PA4.14	2165	<i>RFID-Based Reconfigurable Intelligent Surfaces: Towards Wireless and Ultra-Low-Power Reconfigurability</i>
Lesur, Benoît	A12a.3	1715	<i>Behavioral Models for the Cosimulation and Optimization of Active Electronically Scanned Arrays</i>
Leszkowska, Luiza	PA8.15	2332	<i>Miniaturized and Lightweight ESPAR Antenna for WSN and IoT Applications</i>
Leveque, Philippe	PA2.1	1052	<i>Leading Edge Conformal ARMA Antenna in X Band</i>
Lewis, Dennis	CS32.1	1433	<i>Delving into Time Domain Gating: An Extensive Study on Parameter Selection and Its Implications</i>
	CS12a.4	4058	<i>Use of Model Based Systems Engineering and Development in the Design of a Commercial Nose-Radome Test System Employing a Multi-</i>

			<i>Axis Cobot</i>
Li, Chuwei	PA2.3	1066	<i>Compact Vivaldi Antenna Application in High-Power Design at X-Band</i>
Li, Hancheng	PP01.17	1418	<i>Scenario Classification and Channel Modeling for MIMO Communications in Dense Urban Street Scenarios</i>
Li, Hangang	PP02.5	2510	<i>Measurement-Based Channel Characteristics for Air-To-Ground Communications Under Rural Areas</i>
Li, Hanpeng	PP02.5	2510	<i>Measurement-Based Channel Characteristics for Air-To-Ground Communications Under Rural Areas</i>
Li, Huacheng	A03b.2	3133	<i>Radiation Resistance Enhancement Techniques for Ultracompact Half-Wavelength Helical Omnidirectional Circularly Polarized Antennas</i>
Li, Jian	CS29.5	3807	<i>Multi-Scattering Centers Extraction and Modeling for ISAC Channel Modeling</i>
Li, Junling	PP01.17	1418	<i>Scenario Classification and Channel Modeling for MIMO Communications in Dense Urban Street Scenarios</i>
	PP01.18	1423	<i>Channel Characterization and Modeling for Wireless MIMO Communication Systems in Intersection Scenarios</i>
	P01.3	3842	<i>Scenario Classification and Channel Modeling for MIMO Communications in Suburban Road Scenarios</i>
Li, Liangying	PA4.23	2201	<i>A Wideband Aperture-Shared Dual-Polarized End-Fire Antenna with Low Profile and High Isolation</i>
Li, Long	CS17b.2	322	<i>Challenges and Opportunities of Amplified Information Metasurfaces for Simultaneous Wireless Communications and Power Transfers</i>
Li, Maokun	CS33a.2	3050	<i>Recent Advances in Multiscale-Multiphysics Inverse Scattering</i>
Li, Mengmeng	E12.3	2829	<i>Time-Modulated Metasurface-Based System for the Generation of False Radar Targets</i>
Li, Pan	PM2.9	2464	<i>Complex Permittivity Extraction of Typical Wooden Furniture Materials Based on Multi-Objective Particle Swarm Optimization over 40-50 GHz</i>
Li, Peizheng	PA5.22	3581	<i>DRL-Based Sidelobe Suppression for Multi-Focus Reconfigurable Intelligent Surface</i>
Li, Shiyuan	E12.3	2829	<i>Time-Modulated Metasurface-Based System for the Generation of False Radar Targets</i>
Li, Shuaipeng	PE1.12	1283	<i>Design of an Ultra-Wideband RCS Reduction Metasurface with Pure Metal-Pattern Layer</i>
Li, Shunli	A08b.5	2100	<i>Open Stopband Suppression of Periodic Leaky-Wave Antenna Based on Theory of Small Reflections</i>
Li, Xiaotian	A01b.3	3206	<i>Roof-Glass Integrated Antenna for Vehicular GNSS Applications</i>
Li, Xin Ran	CS8.3	2892	<i>A Wideband Filtering Linear-To-Circular Polarization Converter for Ka-Band Satellite Communication</i>
Li, Yifa	CS34.2	2615	<i>An Automated Over-The-Air Radiated Testing Platform for Reconfigurable Intelligent Surface</i>
Li, Yize	A09a.5	696	<i>Non-Volatile RF Frequency Reconfigurable Antenna for Wireless Communication</i>
	PA3.16	3463	<i>Frequency Reconfigurable Flexible Printed Antenna Based on Non-Volatile RF Switches for Wearable Applications</i>
Li, Yonghui	CS34.5	2629	<i>RIS Performance in a Comprehensive Fading Environment</i>

Liang, Haokai	CS3.5	311	<i>Exploring PLA/Flax Substrates for Antenna Applications: Assessing Moisture, Temperature and Dielectric Constant Homogeneity</i>
Liao, Hanguang	PA7.12	1215	<i>A Novel Quad-Band Electrically Small Antenna</i>
Liao, Kuo-Chu	PA3.1	3398	<i>Dynamic Programming-Based Beam Codebook Design for mmWave Multi-Antenna Module in Mobile Devices</i>
Liao, Shaowei	PA4.1	2105	<i>A Linear Wide-Angle Scanning Phased Array Antenna Using Heterogeneous Beam Element Technology</i>
	PA4.23	2201	<i>A Wideband Aperture-Shared Dual-Polarized End-Fire Antenna with Low Profile and High Isolation</i>
	PE3.12	2404	<i>High-Order Quasi-Elliptical Bandpass FSS Based on Substrate-Integrated Waveguide Technology for 60 GHz Applications</i>
	PA5.4	3506	<i>A Dual-Port Antenna for Colinearly Polarized Full Duplex and Pattern Reconfigurable Applications</i>
	PA5.11	3537	<i>Circularly Polarized Wide-Angle Scanning Phased Array Based on Heterogeneous Beam Element</i>
Liao, Sung Mao	PA3.1	3398	<i>Dynamic Programming-Based Beam Codebook Design for mmWave Multi-Antenna Module in Mobile Devices</i>
Liaskos, Christos	E07.5	1653	<i>An Accurate Semi-Analytical Model for Periodic Tunable Metasurfaces Electromagnetic Response</i>
Liben, Marisa	CS37a.3	37	<i>A Class-E, Switched-Mode, Non-LTI Electrically-Small Transmit Antenna Design for Overcoming the Fundamental Bandwidth-Efficiency Product Limits</i>
Liberal, Iñigo	CS22a.3	2850	<i>Quantum and Thermal Noise Engineering with Metamaterials</i>
Lietti, Valerio	CS20b.3	402	<i>Measurements of Reconfigurable Intelligent Surface in 5G System Within a Reverberation Chamber at mmWave</i>
Lim, Daecheon	PE3.11	2401	<i>Flexible and Transparent Metamaterial Absorber Using Metal Mesh Structure</i>
Lim, Eng	CS1a.5	4039	<i>Design of Dual-Band CPW Rectenna for Wireless Power Transmission</i>
Lim, Qi Jian	CS19a.5	4085	<i>Platform-Aware Optimization of Conformal Antenna Array via Simulated Bifurcation</i>
Lim, Sungjoon	PE3.11	2401	<i>Flexible and Transparent Metamaterial Absorber Using Metal Mesh Structure</i>
	CS14a.3	4139	<i>Hybrid Reconfigurable Reflective Metasurface with Both Phase and Space Modulation</i>
Lin, Bo-Ting	PA5.2	3498	<i>DC Bias Routing Design for Wideband Reconfigurable Transmitarray Based on 1-Bit Phase-Switching Elements</i>
Lin, Chih-Han	E13.4	280	<i>Thin-Film Terahertz Metamaterials Manufactured by Laser Direct Writing</i>
Lin, Feng Han	A09a.1	678	<i>Optical Microwave Metasurface Phased Arrays</i>
	CS18.1	3669	<i>Metasurfaces Meet Characteristic Modes</i>
Lin, Fujiang	A12a.4	1719	<i>X-Band Receiving Phased Array with Digital Beamforming Using RFSoc</i>
Lin, Ho-Yu	PP01.9	1385	<i>Development of a Site-Specific Building Entry Loss Model for High-Rise Buildings</i>
Lin, Jiaxin	CS35a.4	1697	<i>Time-Varying Channel Measurement and Analysis at 105 GHz in an</i>

			<i>Indoor Factory</i>
Lin, Quan Wei	A09b.1	872	<i>X-Band Reconfigurable Phase Shifters Based on SIW and Liquid Metal Technologies</i>
	A09b.5	891	<i>Liquid Metal Reconfigurable Phased Array Antenna</i>
Lin, Wei	A03b.2	3133	<i>Radiation Resistance Enhancement Techniques for Ultracompact Half-Wavelength Helical Omnidirectional Circularly Polarized Antennas</i>
Lin, XianQi	CS6b.4	502	<i>Millimeter-Wave Beam-Steerable Lens with Reduced Profile and Enhanced Gain</i>
	PE1.17	1303	<i>A Novel Metasurface Inverse Design Based on Back Propagation Neural Network</i>
Lin, Xinyi	CS48.4	3992	<i>Joint Wide Illumination and Null Insertion Design in RIS-Assisted System</i>
Lin, Zhichao	CS33a.2	3050	<i>Recent Advances in Multiscale-Multiphysics Inverse Scattering</i>
Lindahl, Jonatan	PA5.7	3519	<i>Analysis and Measurement of Key Performance Indicators for MIMO Antennas</i>
Linder, Matthias	CS21.5	2722	<i>Effects of Bumper Integration on Low-, Mid-, and High-Resolution Imaging Radars</i>
	CS12a.1	4043	<i>A High-Precision Approach to Eliminate Positioning Errors in Radar Calibrations</i>
Linsalata, Francesco	CS29.4	3802	<i>Accurate Time Synchronization Exploiting Integrated Sensing and Communication</i>
Lipman, Justin	E13.6	289	<i>Highly Efficient Polarization-Insensitive EM Energy Harvester</i>
Liporace, Flavia	CS28.3	475	<i>Dielectric Characterization of Biological Tissues at Microwave Frequencies Based on Water Content</i>
	CS24b.5	936	<i>Wideband Dielectric Characterization of Biological Tissues and Realistic Phantom Preparation at Microwave Frequencies</i>
	M4.3	2959	<i>Numerical Study of the Dielectric Properties of Lung Tissue Measured with Two Different Open-Ended Coaxial Probes</i>
Lira, Tomas	CS9b.4	526	<i>Design of Modulated Dielectric Leaky-Wave Antennas for Efficient Bessel-Beam Synthesis</i>
Liseno, Angelo	CS42b.3	446	<i>Phaseless Characterization of Flat Sources with a Planar Wide-Mesh Scanning Strategy</i>
	CS42b.4	451	<i>Discretizing 2D Equivalent Radiating Panels by Legendre Quadrature</i>
	E10b.5	2077	<i>Numerical Results on the Use of the L-SVD Approach for the Solution of the Inverse Source Problem from Amplitude-Only Data</i>
Lisi, Francesco	CS25.4	668	<i>Aperture Distribution Method for Array-Fed Reflectors: A System Level Performance Case Study</i>
Liška, Jakub	PE2.8	1020	<i>The Role of Arrays in Pulsed Radiation</i>
	A24.5	3876	<i>Design Recommendations for Minimal Antenna Mutual Coupling Using Current Optimization</i>
Litschke, Oliver	CS10.3	860	<i>D-Band Active Antenna Array with Lens Enabling Quasi-Optical and Analogue Beam Reconfiguration for 6G Applications</i>
	CS21.2	2709	<i>New Efficient Waveguide Antenna for Future Automotive Radar Applications</i>
Liu, Bo	CS11.2	1620	<i>AI-Driven Design of a Quasi-Digitally-Coded Wideband Microstrip Patch</i>

			<i>Antenna Array</i>
	CS11.4	1627	<i>Automated Design of Antennas Using AI Techniques: A Review of Contemporary Methods and Applications</i>
	CS30a.2	3933	<i>Additively Manufactured Waveguide Hybrid Septum Coupler Optimized Using Machine Learning</i>
Liu, Chang	PA1.11	3376	<i>Design of an UWB Conformal Antenna for Wireless Capsule Endoscopy</i>
Liu, Chenlu	PA2.3	1066	<i>Compact Vivaldi Antenna Application in High-Power Design at X-Band</i>
Liu, Chuanting	CS39a.4	622	<i>Addressing PIM Challenges in Radio Base Stations: Field Issues and Testing Methods for Large-Scale Deployments</i>
Liu, Chun-Mei	CS1a.4	4035	<i>Substrate-Integrated Mode Composite Waveguide</i>
Liu, Guanghui	CS39a.5	627	<i>Standardization Progress and Challenges for 5G OTA Testing</i>
Liu, Jianrui	PA3.2	3403	<i>Design of Ultra-Wideband Dual-Polarized Corrugated Horn Antenna for 5G Application</i>
	PA3.7	3421	<i>A Single-Layer Quadruple-Band Millimeter-Wave Antenna Using Split-Rings for 5G Application</i>
	PA5.21	3577	<i>Design of a Dual-Polarization Ultra-Wideband Horn Antenna</i>
Liu, Kexin	PA7.4	1176	<i>Passive Beamforming with Liquid Antennas: Techniques and Implementation</i>
Liu, Lei	P01.5	3852	<i>Analysis of 5G Channel Characteristics Based on Ray Tracing for the Straight Tunnel of High Speed Railway</i>
Liu, Minzhang	PE3.16	2419	<i>Ultra Wide Dynamic Range High Power RF Rectifier</i>
Liu, Peijie	CS35a.4	1697	<i>Time-Varying Channel Measurement and Analysis at 105 GHz in an Indoor Factory</i>
Liu, Peiqin	PE2.6	1012	<i>Machine-Learning-Based Optimization for Wideband Metasurface Mosaic Antenna</i>
Liu, Peiye	PA3.22	3486	<i>Wideband Array Antenna with Single-Layer Feeding Network at Ka-Band</i>
Liu, Shuang	PA3.2	3403	<i>Design of Ultra-Wideband Dual-Polarized Corrugated Horn Antenna for 5G Application</i>
	PA3.7	3421	<i>A Single-Layer Quadruple-Band Millimeter-Wave Antenna Using Split-Rings for 5G Application</i>
	PA5.21	3577	<i>Design of a Dual-Polarization Ultra-Wideband Horn Antenna</i>
Liu, Wei	CS6a.1	194	<i>Irregular Subarray with Gathered Elements for Sidelobe Suppression</i>
Liu, Xuekang	PA5.6	3515	<i>Bifunctional Stubs Enabled MIMO System for Wideband Mobile 5G and Wi-Fi 6E Applications</i>
	A02.1	3691	<i>A Low Profile Dual-Band Dual-Polarized Filtering Antenna with No Extra Circuit</i>
Liu, Yifei	PA6.5	2231	<i>A Pattern-Reconfigurable Water Antenna Based on the Fabry-Perot Cavity</i>
Liu, Ying	A02.5	3710	<i>A Four-Channel In-Band Full-Duplex (IBFD) Antenna System with Shared Radiation Aperture</i>
Liu, Yuanwei	A09a.3	688	<i>1-Bit Reconfigurable Transmitted/Reflected Array (TRA) for 5G/6G Wireless Communication</i>
Liu, Yujie	A09a.3	688	<i>1-Bit Reconfigurable Transmitted/Reflected Array (TRA) for 5G/6G</i>

Wireless Communication

Liu, Yunming	P10a.1	2972	<i>Automatic Planning Algorithm of 300 GHz Backhaul Links Using Mesh Topology</i>
Liu, Zeyu	CS1a.5	4039	<i>Design of Dual-Band CPW Rectenna for Wireless Power Transmission</i>
Liu, Zicheng	PE1.12	1283	<i>Design of an Ultra-Wideband RCS Reduction Metasurface with Pure Metal-Pattern Layer</i>
Lizzi, Leonardo	CS38.6	132	<i>Estimating the Achievable Efficiency and Bandwidth of Small Terminal-Integrated Inverted-F Antennas Using Machine Learning</i>
LLombart, Nuria	CS37b.3	352	<i>Chessboard Focal Plane Array in Silicon Technologies for Terahertz Imaging</i>
	CS44a.1	745	<i>Development of a Shaped Quartz Lens Antenna for Wide Scanning Sub-Millimeter Imagers</i>
	CS44b.2	945	<i>Design and Characterization of an Imaging System Using Photoconductive Connected Arrays</i>
	CS7.3	1601	<i>Experimental Characterization of a Core-Shell Lens for Antenna On-Package Integration at D-Band</i>
	A08a.2	1888	<i>On the Asymptotic Evaluation of the Near-Field in Resonant Leaky-Wave Antennas Using a Non-Uniform Phase Center</i>
	M3.2	2590	<i>A Demonstration of Diffraction-Limited Images Using a CMOS Chessboard Array at THz Frequencies</i>
	A07.3	2669	<i>On the Design of Wide-Scanning Lenses with Integrated Focal Arrays</i>
Locatelli, Antonin	PP02.4	2505	<i>Multipath Model Improvement for Automotive Radar Application</i>
Loconsole, Antonella Maria	A21.5	1498	<i>Feasibility Investigation on a Low-Cost an Air-Filled Substrate Integrated Waveguide Array Antenna in V-Band</i>
	A25.3	3095	<i>Design and Characterization of a Flexible Fabry-Perot Antenna Fabricated Using Conductive Inkjet Printing</i>
Lodi, Matteo Bruno	CS24a.2	727	<i>Microwave Imaging for Monitoring Bone Healing Using Magnetic Scaffolds: An Initial Analysis</i>
	PM1.2	1313	<i>A Numerical Analysis of Microwave Hyperthermia of Deep-Seated Tumors Using Magneto-Dielectric Implants</i>
	A04.3	1467	<i>A Shared-Aperture Planar Antenna for 5G</i>
	PA4.12	2155	<i>A Dual Linearly Polarized Array for 5G FR2</i>
	PP03.15	3651	<i>Analytical Fitting of Dielectric Response of Basal Cell Carcinoma</i>
	PP03.16		<i>Advances in Core-Shell Nanocrystals: A Multiphysics Approach to Multispectral Electromagnetic Shielding</i>
Lodigiani, Martina	P03.1	1528	<i>Seasonal Snow Melting Process Investigation in Polar Environment Using a Dual-Receiver Radar Architecture</i>
Loh, Tian Hong	CS5b.5	383	<i>Design and Preliminary Indoor Assessment of a Long-Range Sub-THz VNA-Based Channel Sounder Between 500 GHz and 750 GHz</i>
Loiseaux, Brigitte	A16.2	1734	<i>Low-Profile 2D-Mechanical-Beam-Steering Antenna with Large Field-Of-View</i>
Loison, Renaud	A19.5	1523	<i>Exploring the Potential of Spatially Modulated Full-Metal Dichroic Mirrors for Deep Space Antennas</i>
Lok, Lai Bun	PA8.1	2269	<i>Design and Measurement of a 2x2 Array of Coaxial Periodic Leaky-Wave Antennas</i>

Lombardi, Renato	P09.4	2649	<i>Rain Attenuation at mmWave and Optical Bands from Visibility and Rainfall Intensity Measurements</i>
Lončarević, Dunja	A07.3	2669	<i>On the Design of Wide-Scanning Lenses with Integrated Focal Arrays</i>
Longhi, Michela	E08.2	1868	<i>Reflective Intelligent Surfaces: Reducing Complexity by Controlling the Illuminating Field</i>
	E08.5	1880	<i>Static and Reconfigurable Phase-Gradient Metasurfaces for Antenna Applications</i>
	PA4.10	2147	<i>Analysis and Design of Robust Reconfigurable Intelligent Surfaces Using a Statistical Approach</i>
	A10.2	3071	<i>Analysis and Design of Metasurface Antennas Based on Temporal Metastructures</i>
Lopes, Andreia	PP01.7	1375	<i>Path Gain Measurements and Models at 60 GHz in Street Canyons from Rooftop Sites for Outdoor Coverage</i>
Lopez, Igor	CS35a.1	1683	<i>Design and Validation of a Wireless Network for Intra-Train Communications</i>
Lopez, Tanguy	CS14a.5	4145	<i>Time-Modulated Metasurface for Harmonic Signals Frequency Conversion</i>
López Pastor, Jose A	CS36a.2	705	<i>GHz Prism: Frequency-Scanned Antennas to Improve Localization with Separate-Channel Fingerprinting</i>
López-Delgado, Ignacio	CS21.3	2712	<i>From mmWave Radar Nodes to Multistatic Arrays: Design Considerations and Applications</i>
López-Fernández, Jesús	CS15.1	4001	<i>Time-Modulated Arrays for Simultaneous Wireless Information and Power Transfer in Near-Field</i>
Lopez-Yela, Ana	PA2.4	1069	<i>Antenna Design for TriHex: A Future Soil Moisture and Ocean Salinity Radiometer Mission</i>
Lorenzo López, José	CS40b.3	1976	<i>Compact 868 MHz RFID-Based Antenna for Queen Bee Identification and Location Inside Hives</i>
Loreto, Fabrizio	E02a.5	3016	<i>Improved PEEC Modeling of Antennas Through Time-Dependent Partial Elements</i>
Loretoni, Riccardo	CS45.3	1808	<i>Preliminary Clinical Trial Results of MammoWave in the Context of RadioSpin Project</i>
Loridan, Vivien	P03.3	1538	<i>Influence of the Atmospheric Plasma Sheath on the RCS of a Hypersonic Reentry Vehicle</i>
Losada, Vicente	A01a.2	2933	<i>Design of Broadband Stacked Patch Microstrip Antennas Fed by Differential Microstrip Lines with Large Common-Mode Rejection</i>
Löser, Lorenz	PP02.6	2515	<i>Antenna Pattern Tracking Algorithm for Low Terahertz Communications</i>
Lötbäck, Christian	A01b.3	3206	<i>Roof-Glass Integrated Antenna for Vehicular GNSS Applications</i>
Louet, Yves	CS44a.4	757	<i>High Data-Rate Sub-THz Coherent Near-Field Wireless Links Enabled by Spline-Profile Bessel Launchers</i>
Louveaux, Jerome	P02.1	3763	<i>Multistatic OFDM Radar Fusion of MUSIC-Based Angle Estimation</i>
Lovecchio, Nicola	CS33a.3	3054	<i>Advancements in Broadband Electromagnetic Sensing for Food Quality Control</i>
LoVetri, Joe	CS24b.2	925	<i>On the In-Vivo Electrical Properties of Human Forearm at Microwave Frequency</i>
	CS33b.3	3317	<i>Microwave Inversion of Measured S-Parameters Using a Thin-Wire</i>

			<i>Antenna Model</i>
Lowery, Aoife	CS28.1	465	<i>Dielectric Characterisation of Human Parathyroid Glands at Microwave Frequencies</i>
Lu, Senlin	PA5.1	3495	<i>High-Gain Shared-Aperture Patch Phased Array and Reflectarray Antenna</i>
Lubrano, Vincenzo	E10a.4	1854	<i>Platform Scattering Analysis of the Copernicus Imaging Microwave Radiometer</i>
	A18.1	2904	<i>Uncertainty Quantification for the Reflector Antenna in the Copernicus Imaging Microwave Radiometer</i>
	A17.4	3754	<i>RF Modelling and Validation of the Breadboard Antenna of the Copernicus Imaging Microwave Radiometer</i>
Lubrano Di Scampamorte, Gilles	CS40a.5	1770	<i>A Self Deployable and Reconfigurable Antenna in VHF Band for a New Space Mission</i>
Luc, Jerome	CS2.4	180	<i>Advanced Post-Processing Technique to Evaluate Specific Absorption Rate (SAR) for a Standard Dipole Antenna</i>
Lucido, Mario	PE2.15	1048	<i>Influence of the Incidence Angle on the Focusing of Luneburg Lens Partially Covered with Graphene</i>
Ludeno, Giovanni	E10b.5	2077	<i>Numerical Results on the Use of the L-SVD Approach for the Solution of the Inverse Source Problem from Amplitude-Only Data</i>
	E04.2	2689	<i>Contactless 3D Subsurface Imaging: Considerations to Set the Measurement Spacing</i>
Ludois, Dan C.	CS37a.3	37	<i>A Class-E, Switched-Mode, Non-LTI Electrically-Small Transmit Antenna Design for Overcoming the Fundamental Bandwidth-Efficiency Product Limits</i>
Luini, Lorenzo	PP02.11	2538	<i>AlphaSat Ka-Band and Q-Band Receiving Station in Rome: Measurements and Data Analysis</i>
	PP02.18	2572	<i>Investigating the Interference Induced by NGSO Constellations on GSO System Ground Stations: A Simulation Approach</i>
	P09.2	2639	<i>Rain Attenuation at Millimeter Waves in Different Climatic Zones Estimated from Drop Size Distributions</i>
	P09.3	2644	<i>Ka-Band Rain Attenuation Derived from a MEO Satellite Constellation</i>
	P09.4	2649	<i>Rain Attenuation at mmWave and Optical Bands from Visibility and Rainfall Intensity Measurements</i>
	P09.5	2654	<i>Predicting Rain Attenuation at D Band for 6G Backhaul Link Design: A Frequency Scaling Approach</i>
	P10b.3	3254	<i>Exploiting Numerical Weather Prediction Data for Radiopropagation Modeling of SatCom Links</i>
Luk, Kwai-Man	CS8.1	2885	<i>Millimeter-Wave 3D Folded Strip Antennas and Arrays: Diverse Polarizations Realization Under Robust Input Impedance</i>
Lukyanov, Anton	A05.5	1836	<i>Sub-THz U-Slot Coupled Stacked-Patch Radiating Elements for Dual-Polarized MIMO Array Antennas</i>
Lundgren, Johan	CS38.5	128	<i>Substructure Modes and Bounds</i>
	CS18.5	3687	<i>Material-Independent Scattering Formulations of Characteristic Modes</i>
	M2.2	3886	<i>Real-Time Near-Field Measurements of mmWave Devices Using a Metasurface and IR Camera</i>

	CS30b.1	4149	<i>Overview of State-Of-The-Art Methods for Determining Performance Bounds on Electromagnetic Systems</i>
	CS30b.2	4153	<i>Fundamental Limits on Characteristic Modes</i>
Luo, Qi	CS6a.1	194	<i>Irregular Subarray with Gathered Elements for Sidelobe Suppression</i>
	CS20b.1	393	<i>1-Bit SubTHz RIS with Planar Tightly Coupled Dipoles: Beam Shaping and Prototypes</i>
	CS7.5	1611	<i>Reconfigurable Intelligent Surfaces for THz: Signal Processing and Hardware Design Challenges</i>
	PA8.13	2324	<i>A Near-Field Focusing Circularly Polarized Radial Line Slot Array Antenna</i>
	A23.2	2752	<i>Adaptive Polynomial Chaos Expansion for Uncertainty Quantification of SubTHz Horn Antennas with Flat-Top Radiation Patterns</i>
	A03a.1	2862	<i>Low-Profiled Wideband Dual-Polarized Conformal Antenna Array</i>
Luoma, Iida	PA4.7	2134	<i>3D Printed Horn Antennas for Millimeter Wave and Sub-THz Bands</i>
Luomaniemi, Rasmus	CS41.5	3239	<i>Cost-Effective Dual Circularly Polarized Antennas for Phase Calibration</i>
Lusa, Samantha	CS33a.2	3050	<i>Recent Advances in Multiscale-Multiphysics Inverse Scattering</i>
Lynch, Donal	PA5.14	3549	<i>Super-Realized Gain Huygens Antennas</i>
Lyu, Yejian	CS5b.1	364	<i>Enabling VNA Based Channel Sounder for 6G Research: Challenges and Solutions</i>
	P10b.2	3249	<i>Validation of Ray-Tracing Simulated Channels for Massive MIMO Systems at Millimeter-Wave Bands</i>
Lyu, Yue	CS23a.3	1785	<i>Robust Tensor Positioning Based on Channel Parameter Estimation Under Spatially Colored Noise</i>

M

Ma, Xianjun	CS20b.1	393	<i>1-Bit SubTHz RIS with Planar Tightly Coupled Dipoles: Beam Shaping and Prototypes</i>
Ma, Xin	PE1.3	1249	<i>A Polarization-Insensitive Ultra-Broadband FSS Absorber with Low-Profile Based on the ITO Film</i>
	CS30a.5	3947	<i>Alternate Optimization with Deep Learning to Design Beam Deflector Under Aperiodic Near-Field Coupling Conditions</i>
Ma, Xinyu	PE1.12	1283	<i>Design of an Ultra-Wideband RCS Reduction Metasurface with Pure Metal-Pattern Layer</i>
Ma, Yihan	CS6a.1	194	<i>Irregular Subarray with Gathered Elements for Sidelobe Suppression</i>
	CS20b.1	393	<i>1-Bit SubTHz RIS with Planar Tightly Coupled Dipoles: Beam Shaping and Prototypes</i>
Ma, Yihan	A23.2	2752	<i>Adaptive Polynomial Chaos Expansion for Uncertainty Quantification of SubTHz Horn Antennas with Flat-Top Radiation Patterns</i>
Maagt, Peter de	P05.1	241	<i>Small-Scale Passive Millimetre-Wave Imaging Measurements for Marine Litter Detection at W-Band</i>
	P02.3	3772	<i>Feature Selection for Identifying Optimal Microwave Frequencies to Detect Floating Macroplastic Litter in C and X Bands</i>
Maaloul, Sassi	CS35b.4	1917	<i>Experimental Evaluation of V2X Connectivity Technologies with V2X Channel Models</i>
Maaskant, Rob	A18.2	2909	<i>Self-Interference Suppression for SatCom Active Antenna Arrays Through Joint Transmit and Receive Beamforming</i>

	M2.5	3900	<i>Optimization of the TRP Evaluation in Anechoic-Reverberation Hybrid Chamber</i>
MacDonell, Keigan	PE1.16	1300	<i>Mechatronic Phase-Control Reflector System with In-Plane Axis Control</i>
Maci, Stefano	CS20a.4	99	<i>Accurate Design of Surface-Wave Enabled Reflective Intelligent Surfaces Through the Generalized Oliner Method</i>
	CS25.5	673	<i>TX/RX Terminal Based on Metascreen Technology for Ka-Band Satcom with Dual Switchable Polarization</i>
	E06b.3	800	<i>Multi-Beam Dual Polarised Metasurface Antenna in Ka-Band</i>
	CS10.4	864	<i>Metasurface Dome Enhancing Beam Scanning of AESA Panels</i>
	E07.4	1649	<i>Multilayer Reflectionless Wide-Angle Anomalous Refractors Based on Surface Field Optimization</i>
	A16.3	1739	<i>Wideband Beam-Steering Continuous Transverse Stub Array Enabled by a Reflecting Luneburg Lens at Ka-Band</i>
	E08.1	1864	<i>Multibeam Radiation by Multipoint Fed Modulated MTS Apertures</i>
	PA4.8	2139	<i>A Novel GO Analysis Tool for GRIN Lenses Based on the Fast Sweeping Method</i>
	CS26a.4	4102	<i>Wiener-Hopf Type Analysis of PTD Symmetric Waveguides: A Novel Methodology Procedure</i>
Mackay, Simon	CS4.5	3194	<i>CSIRO Radio Astronomy Receiver Update - Ultra Wideband and Phased Array Feeds</i>
Madanayake, Arjuna	CS44b.5	960	<i>Graph Neural Network Based 77 GHz MIMO Radar Array Processor for Autonomous Robotics</i>
Madannejad, Alireza	A05.2	1825	<i>High-Gain and Circular Polarization Silicon-Micromachined Lens Antennas at 500-750 GHz</i>
	PE3.5	2379	<i>Analysis of the Interaction of Laser-Induced Solid-State Plasma with Electromagnetic Waves in Silicon Waveguides at 67-220 GHz</i>
Madec, Morgan	E01.1	2014	<i>Optimal Design of Planar Micro-NMR Coils for High Signal-To-Noise Ratio</i>
Madji, Mikhail	CS9a.2	225	<i>2D-Scanning of Circularly Polarized Beams via Array-Fed Fabry--Perot Cavity Antennas</i>
Magarini, Maurizio	CS29.4	3802	<i>Accurate Time Synchronization Exploiting Integrated Sensing and Communication</i>
Magarotto, Mirko	A09b.2	877	<i>Recent Advances in Plasma Surfaces</i>
	PE2.14	1044	<i>Tunable Rectangular Waveguide Bandpass Filter Based on Plasma Technology</i>
Maggi, Mattia	A12b.4	1941	<i>6:1 Connected Slot Array in PCB Technology</i>
Mahawela, Punsara	CS44b.5	960	<i>Graph Neural Network Based 77 GHz MIMO Radar Array Processor for Autonomous Robotics</i>
Mahdipour, Hadi	PM2.6	2449	<i>Detection Capability of a CNN-Based Imageless Millimeter Wave System for Static Concealed Objects</i>
Mahmoud, Adham	A21.5	1498	<i>Feasibility Investigation on a Low-Cost an Air-Filled Substrate Integrated Waveguide Array Antenna in V-Band</i>
	A16.3	1739	<i>Wideband Beam-Steering Continuous Transverse Stub Array Enabled by a Reflecting Luneburg Lens at Ka-Band</i>
Maimbo, Natasha	CS4.5	3194	<i>CSIRO Radio Astronomy Receiver Update - Ultra Wideband and</i>

Phased Array Feeds

Maiolo, Luca	PE3.10	2398	<i>Highly Reflective, Low-Loss, Homogenized Fishnet Metasurfaces at Terahertz: Design and Experiment</i>
Maisto, Maria Antonia	CS42b.5	456	<i>A Greedy Approach for Reducing Data in Near-Field Measurements</i>
	M5.5	557	<i>Near Field Phase Recovery Exploiting Only One Measurement Surface and A Smart Warping Sampling Strategy</i>
Maita, Francesco	PE3.10	2398	<i>Highly Reflective, Low-Loss, Homogenized Fishnet Metasurfaces at Terahertz: Design and Experiment</i>
Mallahzadeh, Alireza	PA5.18	3564	<i>Realizing Flat-Top Radiation Pattern with Sharp Cutoff for Reducing Lobing Fades</i>
Mallik, Mohammed	PP03.14	3647	<i>Generation of Electromagnetic Exposure Maps for 5G Communications</i>
Malmström, Johan	E10a.5	1859	<i>Investigation of Near-Field Contribution in Shooting and Bouncing Rays for Installed Antenna Performance on a Simple Platform</i>
Malotaux, Satoshi	CS37b.3	352	<i>Chessboard Focal Plane Array in Silicon Technologies for Terahertz Imaging</i>
Manara, Giuliano	PE1.15	1295	<i>D-Band Absorber Comprising Tantalum Nitride-Based Resistively-Loaded High Impedance Surfaces</i>
Mancini, Alessio	CS42b.6	460	<i>Uncertainty Quantification of the Gain Budget for INCUS</i>
Mandal, Bappaditya	CS27.4	1584	<i>A Compact Wideband Biocompatible Circularly Polarized Implantable Flexible Antenna for Biomedical Applications</i>
	PA6.12	2260	<i>An Efficient Wireless Power Transfer System Using Transmission and Reflection Characteristics of Metamaterial</i>
Mandal, Bappaditya	PP03.7	3615	<i>SINTEC Comparative Body-Centric Communication Study: Bluetooth Vs Fat-Intrabody Communication</i>
Mandal, Bappaditya	PP03.11	3635	<i>Brain Hemorrhage Detection Using Antenna System Integrated with Imaging Algorithm</i>
Mandal, Bappaditya	A20.3	3818	<i>Compact Antenna Solutions for Data Transmission Using Fat-Intrabody Communication (Fat-IBC)</i>
Mangenot, Cyril	A17.4	3754	<i>RF Modelling and Validation of the Breadboard Antenna of the Copernicus Imaging Microwave Radiometer</i>
Manholm, Lars	CS10.1	850	<i>Efficient Ray-Tracing Model for Generalized 2D Dielectric Lenses Combined with Arrays</i>
Manocha, Dinesh	A28.5	3734	<i>Indoor Wireless Signal Modeling with Smooth Surface Diffraction Effects</i>
Mansour, Raafat	A26.2	4197	<i>A Wideband Dual-Polarized 1-Bit Unit Cell for Reconfigurable Intelligent Surface Applications</i>
Mantash, Mohamad	CS2.4	180	<i>Advanced Post-Processing Technique to Evaluate Specific Absorption Rate (SAR) for a Standard Dipole Antenna</i>
Manteghi, Majid	CS37b.5	361	<i>Front-End Mismatching, Mutual Coupling, Bandwidth, Transmission Line Noise, and SNR</i>
	CS41.4	3235	<i>Contactless Impedance and Far-Field Characterization of Electrically Small Antennas</i>
Manteuffel, Dirk	CS18.3	3679	<i>Generation of a Square Multi-Mode Multi-Port Aperture Antenna by Selective Modal Excitation</i>
	CS30b.4	4159	<i>Port Generation for Multi-Mode Multi-Port Antennas Based on Group</i>

			<i>Theory</i>
Mao, Chunxu	PA2.22	1150	<i>Compact Circularly Polarized Patch Antenna with Enhanced Axial Ratio and Impedance Bandwidth</i>
	A03b.3	3137	<i>Low-Profile In-Band Pattern Diversity Antenna with Improved Bandwidth</i>
Mao, Kai	PM1.3	1318	<i>Impact of 6D Mobility on Doppler Characteristics of UAV-To-Vehicle Channels</i>
	PP02.5	2510	<i>Measurement-Based Channel Characteristics for Air-To-Ground Communications Under Rural Areas</i>
Mao, Yi An	CS18.1	3669	<i>Metasurfaces Meet Characteristic Modes</i>
Mao, Yifan	PP01.11	1395	<i>Achievable Rate Approximation of Large Intelligent Surface Based on Deep Learning</i>
Maraloiu, Calin	CS11.1	1616	<i>AI-Assisted Design and Experimental Testing of a Compact UWB Antenna for the Inspection of Food and Beverage Products</i>
Marasco, Ilaria	PA1.3	3340	<i>Eco-Friendly and Conformable PIFA Based on PEDOT: PSS and a Sustainable Chitosan Substrate for 5G Communications</i>
Marchetti, Nicola	CS36a.1	700	<i>Angle of Arrival Estimation Methods Using Spherical-Modes-Driven Multiport Antennas</i>
	PA8.5	2288	<i>Low-Profile Electrically Small Antenna with Pattern and Polarization Diversity</i>
	PA8.6	2293	<i>Bandwidth-Enhanced Compact Beamsteering Antenna for IoT Platforms</i>
Mardani, Hossein	CS15.2	4006	<i>Validation of a Large Retrodirective CASSIOPeIA Solar Power Satellite Antenna Array</i>
Mariani Primiani, Valter	CS20b.3	402	<i>Measurements of Reconfigurable Intelligent Surface in 5G System Within a Reverberation Chamber at mmWave</i>
	CS22a.5	2858	<i>Real-System Variational Quantum Eigensolver for Electromagnetic Waveguides: A Benchmark Study</i>
Marques, Paulo	P05.1	241	<i>Small-Scale Passive Millimetre-Wave Imaging Measurements for Marine Litter Detection at W-Band</i>
	P02.3	3772	<i>Feature Selection for Identifying Optimal Microwave Frequencies to Detect Floating Macroplastic Litter in C and X Bands</i>
Marrocco, Gaetano	PA4.14	2165	<i>RFID-Based Reconfigurable Intelligent Surfaces: Towards Wireless and Ultra-Low-Power Reconfigurability</i>
	PA8.3	2278	<i>Flexible Antenna with Microfluidics for the Quantification of Liquid Micro-Volumes</i>
Marsalek, Roman	CS43b.1	4168	<i>Channel Measurements and Characterization in Industrial Environment at 60 GHz</i>
Martellucci, Antonio	P09.3	2644	<i>Ka-Band Rain Attenuation Derived from a MEO Satellite Constellation</i>
Martin, Ben	E04.5	2703	<i>Preliminary Description of a 2D Near-Field Electromagnetic Imaging Database</i>
	CS33b.2	3313	<i>Supervised Learning Applied to Microwave Imaging System Calibration</i>
Martín, Ferran	M4.5	2968	<i>Phase-Variation Microwave Displacement Sensor with High Resolution, Sensitivity, and Dynamic Range</i>
Martin, Torleif	M2.2	3886	<i>Real-Time Near-Field Measurements of mmWave Devices Using a</i>

			<i>Metasurface and IR Camera</i>
Martín, Víctor	CS19b.2	4287	<i>A Multi-Region Hierarchical Preconditioning Scheme for the MoM Simulation of Complex Composite Structures</i>
	CS19b.3	4292	<i>Automatic MoM Source Integral Quadrature Selection via a Machine Learning Approach</i>
Martin-Neira, Manuel	PA2.4	1069	<i>Antenna Design for TriHex: A Future Soil Moisture and Ocean Salinity Radiometer Mission</i>
	CS46.1	4215	<i>Dual All Metal Patch Antenna for the HydroGNSS Mission</i>
	CS46.2	4219	<i>Digital Beamformer for GNSS Reflectometry and Radio Occultation Applications</i>
Martinez, Gabriel	PE2.13	1040	<i>Novel Quantum Computation Based Selection Operator for Genetic Algorithms Applied to Electromagnetic Problems</i>
Martinez-de-Rioja, Daniel	A06a.1	3021	<i>Large and Deployable Multi-Faceted Antennas Based on Single-Layer Reflectarrays</i>
	A06a.5	3041	<i>Multibeam Compact Dual Reflectarray Antenna for High-Throughput Satellites in Ka-Band</i>
Martinez-de-Rioja, Eduardo	A06a.5	3041	<i>Multibeam Compact Dual Reflectarray Antenna for High-Throughput Satellites in Ka-Band</i>
	A06b.4	3301	<i>Dual-Band Reflectarray-Based Electromagnetic Skin to Provide Millimeter-Wave Coverage in the 28/60-GHz Bands</i>
Martínez-García, Ginés	PA3.8	3424	<i>1-Bit RIS Unit Cell with Mechanical Reconfiguration at 28 GHz</i>
Martinez-Ingles, Maria-Teresa	PP01.4	1360	<i>A Study on W-Band Frequency Attenuation in the Presence of Human Blockage</i>
Martínez-Vázquez, Marta	CS21.1	2706	<i>Imaging Radar Frontend with SIW Feeding Networks</i>
	CS21.2	2709	<i>New Efficient Waveguide Antenna for Future Automotive Radar Applications</i>
Martini, Enrica	CS20a.4	99	<i>Accurate Design of Surface-Wave Enabled Reflective Intelligent Surfaces Through the Generalized Oliner Method</i>
	CS9a.1	221	<i>Dual-Frequency Metasurface Antenna for Earth Science Remote Sensing</i>
	CS25.5	673	<i>TX/RX Terminal Based on Metascreen Technology for Ka-Band Satcom with Dual Switchable Polarization</i>
	E06b.3	800	<i>Multi-Beam Dual Polarised Metasurface Antenna in Ka-Band</i>
	CS10.4	864	<i>Metasurface Dome Enhancing Beam Scanning of AESA Panels</i>
	E07.4	1649	<i>Multilayer Reflectionless Wide-Angle Anomalous Refractors Based on Surface Field Optimization</i>
	A16.3	1739	<i>Wideband Beam-Steering Continuous Transverse Stub Array Enabled by a Reflecting Luneburg Lens at Ka-Band</i>
Martinod, Edson	CS26a.4	4102	<i>Wiener-Hopf Type Analysis of PTD Symmetric Waveguides: A Novel Methodology Procedure</i>
	CS3.6	316	<i>Use of Ecofriendly Geopolymer Ceramics in Antenna Design and Microwave Applications</i>
Martins, Raquel	P06.4	2742	<i>Antenna Position Layout and Frequency Impact on Tumor Detection in Microwave Breast Imaging</i>
	PP03.18	3660	<i>Best Practices for Accurate Results Using Numerical Solvers for</i>

			<i>Microwave Body Screening</i>
Maruyama, Tamami	E06b.1	792	<i>Variable Multi-Band Metasurface Reflector with Controllable Direction Using Varactor Diodes Mounted Large-Via Mushroom-Type Structure</i>
Masa-Campos, Jose Luis	A27a.1	632	<i>Full-Metal Single-Block Antenna Arrays with Waveguide Corporative Feeding Networks at Ka and V Bands</i>
	A11.3	3162	<i>Pinwheel-Shaped Polarizer for Generating Dual-Circularly Polarized Conical Radiation Patterns in the Ka-Band</i>
Masai, Takaho	PA2.24	1159	<i>The Design of Re-Imaging Optics for Passing Several Beams Through Small Cryostat Windows</i>
Masi, Angelica	PM1.1	1308	<i>Preliminary Investigation of an Innovative RF Sensor for Deformation and Failure Evaluation in Composite Materials</i>
Mason, Glenn	A16.4	1744	<i>Compact Hybrid Optical/RF User Segment (CHORUS): RF Terminal Design</i>
Masotti, Diego	CS36b.4	911	<i>Simplified Frequency-Diverse Array Architecture for Surveillance Purposes</i>
Massa, Andrea	CS20a.5	104	<i>Recent Advances on Multi-Scale Wave Manipulation Through Reconfigurable Intelligent Surfaces</i>
	CS17b.1	320	<i>On the Design of Static Passive Skins for Next Generation Fixed Wireless Access Applications</i>
	CS33a.2	3050	<i>Recent Advances in Multiscale-Multiphysics Inverse Scattering</i>
Massaccesi, Andrea	A10.3	3074	<i>Curved Electromagnetic Skins for Urban Scenarios</i>
	A06b.1	3287	<i>Folded Dielectric Reflectarray with Spherical Polarizer</i>
Massman, Jeffrey	PE3.6	2383	<i>Development of an Ultrawideband Wire-Grid Polarizer Measurement Standard for Focus Beam System Cross-Polarization Calibration</i>
Mastrandrea, Antonio	CS33a.3	3054	<i>Advancements in Broadband Electromagnetic Sensing for Food Quality Control</i>
Mata-Alonso, Ignacio	P09.1	2634	<i>Variability of Rain Attenuation at Millimeter Waves Due to Fluctuations of the Drop Size Distribution</i>
	P09.2	2639	<i>Rain Attenuation at Millimeter Waves in Different Climatic Zones Estimated from Drop Size Distributions</i>
Mathis, Heinz	CS30a.4	3942	<i>Validating Convex Optimization of Reconfigurable Intelligent Surfaces via Measurements</i>
Matijašćić, Marko	A24.2	3861	<i>Synthesis of Flat-Top Beams Based on Modified Chebyshev Polynomials</i>
Matos, João	PA4.5	2124	<i>A Simple Technique to Maximize Isolation in Compact mmWaves Antenna Arrays</i>
Matos, Sergio	P05.1	241	<i>Small-Scale Passive Millimetre-Wave Imaging Measurements for Marine Litter Detection at W-Band</i>
	CS6b.1	490	<i>Multibeam Antenna for Wide-Angle 95-Beam Coverage at Ka-Band Using a Multifocal Transmit-Array</i>
	CS7.5	1611	<i>Reconfigurable Intelligent Surfaces for THz: Signal Processing and Hardware Design Challenges</i>
	A16.1	1729	<i>Novel Risley Prism Design Approach with Improved Side Lobe Levels Using Multi-Layer Transmit-Arrays</i>
	E02a.3	3007	<i>Efficient Optimization-Assisted Full-Wave MoM Unit-Cell Design for</i>

			<i>Dual-Band Transmitarrays</i>
	PA3.14	3450	<i>Study of Environmentally-Friendly Radomes Using Cork-Rubber Composites for 5G Backhaul Links at E-Band</i>
	P02.3	3772	<i>Feature Selection for Identifying Optimal Microwave Frequencies to Detect Floating Macroplastic Litter in C and X Bands</i>
	A26.5	4212	<i>Improved Performance of a 1-Bit RIS by Using Two Switches per Bit Implementation</i>
Matrone, Giulia	CS24b.1	920	<i>Microwave Tomography Bone Imaging: Analysing the Impact of Skin Thickness on the Reconstruction of Numerical Bone Phantoms</i>
Matsui, Yasuhiro	P04b.5	985	<i>Conceptual Design and Propagation Characteristics of an Underwater Electromagnetic Communication System for Ocean Environment Sensor Systems</i>
Matsushita, Takuma	P04b.5	985	<i>Conceptual Design and Propagation Characteristics of an Underwater Electromagnetic Communication System for Ocean Environment Sensor Systems</i>
Matt, Felix	A11.2	3157	<i>A Low-Profile Wide-Scan Magneto-Electric Dipole Antenna for 5G mm-Wave Communications</i>
	PA3.11	3438	<i>Broadband Waveguide Magneto-Electric Dipole Antenna for F-Band Applications</i>
Mattana, Enrico	PP03.15	3651	<i>Analytical Fitting of Dielectric Response of Basal Cell Carcinoma</i>
Mattes, Michael	CS42b.2	442	<i>Multiple Reduced Order Models for Antenna Measurements</i>
Matthaiou, Michail	CS44a.5	762	<i>Interference-Free Transmission for Near-Field Communication with Unlimited Antennas</i>
	A24.3	3866	<i>Optimization of Super-Directive Linear Arrays with Differential Evolution for High Realized Gain</i>
Matzner, Haim	PA7.3	1172	<i>A Compact Horn Antenna with Low Sidelobes</i>
	A02.4	3705	<i>Two-Dimensional, Un-Equal, Series Power Dividers for Feeding Antenna Arrays</i>
Maurer, Michael	CS42b.1	439	<i>An Antenna Measuring System Based on a Cable Suspended Dolly and Inverse Source</i>
Maurin, Julien	CS25.4	668	<i>Aperture Distribution Method for Array-Fed Reflectors: A System Level Performance Case Study</i>
Mavropoulou, Alexandra	PA4.16	2174	<i>Design of Wide Band Multi-Lens Focal Plane Arrays for the TIFUUN Instrument</i>
Maximidis, Ronis	PA3.21	3483	<i>MIMO Signals Processing Utilizing Optical Crossbar Linear Operator</i>
Maye, Caroline	PE1.13	1288	<i>Multi-Channel Beam-Splitting Metasurface for Millimeter Wave Communication Systems</i>
Mayer, Frederick	CS42b.1	439	<i>An Antenna Measuring System Based on a Cable Suspended Dolly and Inverse Source</i>
Maynard, Kevin	CS46.1	4215	<i>Dual All Metal Patch Antenna for the HydroGNSS Mission</i>
Maziere, Christophe	A12a.3	1715	<i>Behavioral Models for the Cosimulation and Optimization of Active Electronically Scanned Arrays</i>
Mazingue, Gautier	PA6.9	2245	<i>Study of the Frequency Dispersion of 3D-Printed Dielectric Crystals for Dielectric Resonator Antenna Applications</i>
	CS1b.4	4251	<i>Power Handling Test of a L-Band Antenna Using Infrared</i>

			<i>Thermography</i>
Mazloun, Taghrid	CS34.4	2625	<i>Empirical Validation of the Impedance-Based RIS Channel Model in an Indoor Scattering Environment</i>
Mazzarella, Giuseppe	A04.3	1467	<i>A Shared-Aperture Planar Antenna for 5G</i>
	PA4.12	2155	<i>A Dual Linearly Polarized Array for 5G FR2</i>
	PP03.15	3651	<i>Analytical Fitting of Dielectric Response of Basal Cell Carcinoma</i>
Mazzinghi, Agnese	A09a.2	683	<i>Sub-Wavelength Anisotropic Unit-Cells for Low-Profile Transmitarray Antennas</i>
	A10.3	3074	<i>Curved Electromagnetic Skins for Urban Scenarios</i>
	A06b.1	3287	<i>Folded Dielectric Reflectarray with Spherical Polarizer</i>
McEvoy, Patrick	A15b.5	4345	<i>Dual UWB Antennas on AoA Anchor Node</i>
McKernan, Adrian	PA8.4	2283	<i>An IQ Modulator-Based RF Phase Shifter</i>
	CS14b.4	4362	<i>Wideband Dual-Polarized 1-Bit Unit-Cell Design for mmWave Reconfigurable Intelligent Surface</i>
Meaney, Paul	CS45.1	1799	<i>MR/Microwave Tomography Integrated Breast Cancer Imaging</i>
Meates, Ieuan	PA4.19	2186	<i>A Compact High-Gain 28 GHz Antenna Array for Beyond 5G Wireless Networks</i>
Mecklenbräuker, Christoph	CS35b.2	1908	<i>Stationarity of Multiband Channels for OTFS-Based Intelligent Transportation Systems</i>
Medina, Francisco	A01a.2	2933	<i>Design of Broadband Stacked Patch Microstrip Antennas Fed by Differential Microstrip Lines with Large Common-Mode Rejection</i>
Meftah, Nawel	E06b.2	797	<i>Direction-Of-Arrival Estimation by a Programmable Metasurface</i>
Mehrabi Gohari, Mohammad	A05.2	1825	<i>High-Gain and Circular Polarization Silicon-Micromachined Lens Antennas at 500-750 GHz</i>
Mei, Peng	CS6b.4	502	<i>Millimeter-Wave Beam-Steerable Lens with Reduced Profile and Enhanced Gain</i>
	PE1.17	1303	<i>A Novel Metasurface Inverse Design Based on Back Propagation Neural Network</i>
Meier, Ingolf	CS39a.4	622	<i>Addressing PIM Challenges in Radio Base Stations: Field Issues and Testing Methods for Large-Scale Deployments</i>
Melendro-Jimenez, Javier	A11.3	3162	<i>Pinwheel-Shaped Polarizer for Generating Dual-Circularly Polarized Conical Radiation Patterns in the Ka-Band</i>
Melle, Christophe	PA7.8	1195	<i>Shaping the Sub-Reflector of a Ring Focus Antenna for Tailored Beamwidth Applications</i>
Melouki, Noureddine	PA2.11	1101	<i>Multi-Bit Wideband Transmitarray Aperture with Independent Phase and Amplitude Control for High Gain with Low Sidelobe Mm-Wave Applications</i>
	A01a.4	2941	<i>Dual-Polarized OAM Antenna with Frequency and Mode Agility for Intelligent OAM Communications</i>
Menachem, Zion	PA7.13	1219	<i>Experimental Investigation of the Nullifier-Based Monopole</i>
Menargues, Esteban	A19.3	1513	<i>Non-Regular Multibeam Coverage Antenna for Ka-Band High-Throughput Satellite Communications</i>
Mencagli, Mario Junior	CS9a.1	221	<i>Dual-Frequency Metasurface Antenna for Earth Science Remote Sensing</i>
Mencarelli, Simone	P05.3	251	<i>Characterisation of Thin Glass-Fibre Substrates for Deployable SAR</i>

Antennas

	P02.5	3782	<i>Mechanical Vibrations on a Deployable Nanosatellite Antenna: SAR Performance Analysis</i>
Mendiboure, Leo	CS35b.4	1917	<i>Experimental Evaluation of V2X Connectivity Technologies with V2X Channel Models</i>
Mendis, Pahan	CS44b.5	960	<i>Graph Neural Network Based 77 GHz MIMO Radar Array Processor for Autonomous Robotics</i>
Mendonça, Marcele	CS19b.4	4295	<i>Supervised Learning Based Real-Time Adaptive Beamforming On-Board Multibeam Satellites</i>
Meng, Shengguo	CS17b.3	326	<i>Information Metasurface for Simultaneous Wave Manipulations and Signal Modulations</i>
Menudier, Cyrille	PA2.7	1084	<i>Design and Prototyping of a Low-Cost Parasitic Element Antenna for a Telemetry-Telecommand Link on Ariane 6 Space Launcher</i>
	A12a.3	1715	<i>Behavioral Models for the Cosimulation and Optimization of Active Electronically Scanned Arrays</i>
Merilampi, Sari	CS13.4	1563	<i>Enabling Living Spaces Through Customizable NFC-Enabled Smart Table System</i>
Merlos-Garza, Erendira	PA3.4	3410	<i>A 2x2 Dual-Band Open Loop Array with Circular Polarisation</i>
Mesa, Francisco	CS10.1	850	<i>Efficient Ray-Tracing Model for Generalized 2D Dielectric Lenses Combined with Arrays</i>
	CS10.2	855	<i>Design of a Dielectric Lens Using a Ray-Tracing Model for Satellite Communications</i>
	E10a.3	1850	<i>Analysis of the Dispersion Diagrams of 3D Cubic Periodic Arrangements of Metallic Spheres</i>
	A08a.1	1883	<i>Efficient Ray-Tracing Approach to Analyze Arbitrarily Shaped Leaky-Wave Antennas Embedded in Lenses</i>
	A22.1	2772	<i>Experimental Validation of Ray-Tracing and Physical-Optics Model for Geodesic H-Plane Horn Antennas</i>
	A22.3	2781	<i>Tailoring the Performance of Geodesic Lens Antennas by Defining Their Footprint</i>
	A22.5	2791	<i>Ray-Tracing Model for the Design and Efficiency Calculation of a Monolithic Geodesic Lens Array Antenna</i>
	CS19a.4	4081	<i>Combined Ray-Tracing and Physical-Optics Model for Flat-Aperture PPW Lens Antennas</i>
	CS26a.3	4098	<i>Higher Symmetries in Hexagonal Periodic Structures</i>
	CS26a.5	4105	<i>Efficient Numerical Computation of Dispersion Diagrams for Glide-Symmetric Periodic Structures with a Hexagonal Lattice</i>
Messhenas, Nona	A21.4	1493	<i>Assessment of MFE-Based Multiport Waveguide Crossing for Use with Low-Cost, Low-Loss Dielectric Interconnects in Millimeter Wave Arrays</i>
Mestrom, Rob	CS28.4	480	<i>Phantom Material with Biological Composition for Muscle Equivalent Radiofrequency, Thermal and Magnetic Resonance Properties</i>
	P06.1	2727	<i>Localization of a Nasogastric Feeding Tube Using High-Frequency Harmonic Radar - a Feasibility Study</i>
Meyne, Nora	PP02.8	2523	<i>Comparison of Propagation Characteristics Between 5G Bands in a Reflective Industrial Environment</i>

Mezieres, Nicolas	CS42b.2	442	<i>Multiple Reduced Order Models for Antenna Measurements</i>
	CS32.5	1453	<i>Stable Phaseless Spherical Antenna Measurements via Mixed-Norm Regularization</i>
Mezzadrelli, Lorenzo	PA7.11	1210	<i>Electromagnetic Assessment of Tolerances of the Square Kilometre Array Log Periodic Antenna Using Uncertainty Quantification</i>
Miao, Si	A09a.1	678	<i>Optical Microwave Metasurface Phased Arrays</i>
	CS18.1	3669	<i>Metasurfaces Meet Characteristic Modes</i>
Miao, Yang	PM1.3	1318	<i>Impact of 6D Mobility on Doppler Characteristics of UAV-To-Vehicle Channels</i>
	P10a.5	2992	<i>Dual-Band MmWave Measurements of Human Body Scattering and Blockage Effects Using Distributed Beamforming for ISAC Applications</i>
	A01b.1	3197	<i>Tiled Subarray Design for Multibeam Joint Communication and Sensing</i>
Micheli, Davide	CS20b.3	402	<i>Measurements of Reconfigurable Intelligent Surface in 5G System Within a Reverberation Chamber at mmWave</i>
Mifdal, Soukaina	E02b.1	3268	<i>Frequency-Domain TLM Method with Cartesian Block Meshing</i>
Migl, Josef	CS39b.3	818	<i>Broadband Performance Assessment of Compensated Compact Antenna Test Range CCR 75/60 of Airbus at L-Band for Navigation Applications</i>
Migliozzi, Massimo	CS42b.3	446	<i>Phaseless Characterization of Flat Sources with a Planar Wide-Mesh Scanning Strategy</i>
Mikhailikova, Iryna	PE2.15	1048	<i>Influence of the Incidence Angle on the Focusing of Luneburg Lens Partially Covered with Graphene</i>
Mikki, Said	CS22b.4	3123	<i>Non-Reciprocity in a Three-Mode Quantum Magnomechanical System with Magnetostrictive Interaction</i>
Mikulic, Davorin	PA1.10	3371	<i>Textile Waveguide Antennas for On-Body Sensor and Communication Systems</i>
Milani, Angelo	P09.4	2649	<i>Rain Attenuation at mmWave and Optical Bands from Visibility and Rainfall Intensity Measurements</i>
Milani, Luca	P03.2	1533	<i>Advanced Microwave Radiometry: Refining Sun-Tracking Technique for Atmospheric Attenuation Retrieval and Sun Brightness Temperature Estimation</i>
Millhaem, Michael	CS5b.6	388	<i>Sub-Terahertz MassiveMIMO Channel Sounder for 6G Mobile Communication Systems</i>
Milligan, Thomas	A19.4	1518	<i>A Possible Way to Reduce the High Sidelobe Levels Due to Reflector Struts: Curly Struts</i>
Minatti, Gabriele	CS25.5	673	<i>TX/RX Terminal Based on Metascreen Technology for Ka-Band Satcom with Dual Switchable Polarization</i>
Mirmohammadsadeghi, Mohammad	CS32.3	1443	<i>In-Flight Calibration of the Measurement System for UAV-Based Near-Field Antenna Measurements</i>
	CS19b.1	4282	<i>A Loop-Star Decomposition for the B-Spline Based Discretization of the Electric Field Integral Equation</i>
Mirmozafari, Mirhamed	CS37a.3	37	<i>A Class-E, Switched-Mode, Non-LTI Electrically-Small Transmit Antenna Design for Overcoming the Fundamental Bandwidth-Efficiency Product Limits</i>
Mishra, Kumar Vijay	CS44b.1	940	<i>Spherical Wavefront Near-Field DoA Estimation in THz Automotive</i>

			<i>Radar</i>
Mitanchey, Florian	P03.3	1538	<i>Influence of the Atmospheric Plasma Sheath on the RCS of a Hypersonic Reentry Vehicle</i>
Mitra, Debasis	PA6.12	2260	<i>An Efficient Wireless Power Transfer System Using Transmission and Reflection Characteristics of Metamaterial</i>
	PP03.11	3635	<i>Brain Hemorrhage Detection Using Antenna System Integrated with Imaging Algorithm</i>
Mitsalass, Xenofon	CS26a.4	4102	<i>Wiener-Hopf Type Analysis of PTD Symmetric Waveguides: A Novel Methodology Procedure</i>
Mittleman, Daniel	CS44b.4	955	<i>Curving THz Beams in the near Field: A Framework to Compute Link Budgets</i>
Miura, Amane	PA7.9	1200	<i>Input Impedance of Radiation Efficiency Deterioration State</i>
Miyake, Takao	CS5b.6	388	<i>Sub-Terahertz MassiveMIMO Channel Sounder for 6G Mobile Communication Systems</i>
Mizzoni, Roberto	E10a.4	1854	<i>Platform Scattering Analysis of the Copernicus Imaging Microwave Radiometer</i>
	A18.1	2904	<i>Uncertainty Quantification for the Reflector Antenna in the Copernicus Imaging Microwave Radiometer</i>
	A17.4	3754	<i>RF Modelling and Validation of the Breadboard Antenna of the Copernicus Imaging Microwave Radiometer</i>
Moch, Roland	CS12a.5	4063	<i>Reduced-Order Maximum Determinant Sampling Grids by Acquisition of Additional Arbitrary Sampling Points on an Optimized Path</i>
Modi, Nancy	PP02.16	2562	<i>Analysis of the Effects of Rainwater Covered Bumper on the Automotive Radar Signals</i>
	PA3.15	3454	<i>Self-Isolated MIMO Antenna Using SIW Cavity Antenna for Dual-Band (28, 38 GHz) Applications</i>
Moerman, Arno	CS2.5	184	<i>New Hybrid Ray-Tracing/FDTD for EMF Exposure in 6G Networks Using Semantically Classified Google Earth Photogrammetry with Measurement Validation</i>
Moglie, Franco	CS20b.3	402	<i>Measurements of Reconfigurable Intelligent Surface in 5G System Within a Reverberation Chamber at mmWave</i>
	CS22a.4	2853	<i>Quantum Optimisation of Reconfigurable Surfaces in Complex Propagation Environments</i>
	CS22a.5	2858	<i>Real-System Variational Quantum Eigensolver for Electromagnetic Waveguides: A Benchmark Study</i>
Mohorcic, Mihael	PP02.15	2557	<i>Large-Scale Site Diversity Experiment in Ljubljana and Budapest at Ka-Band with Alphasat Satellite</i>
Möhring, Björn	CS39b.3	818	<i>Broadband Performance Assessment of Compensated Compact Antenna Test Range CCR 75/60 of Airbus at L-Band for Navigation Applications</i>
Mojabi, Puyan	E06a.2	591	<i>On Solving Inverse Source Problems with Metasurfaces Performing Analog Computations</i>
Molaei, Amir Masoud	PA6.1	2213	<i>Orthogonal Coding for Millimeter-Wave Imaging Using MIMO Dynamic Metasurface Apertures</i>
	PM2.7	2454	<i>Near-Field Bistatic Microwave Imaging with Dynamic Metasurface</i>

Antennas

	E04.3	2693	<i>A Case Study of Misalignment Errors for Range-Migration-Based Microwave Imaging with Multistatic Dynamic Metasurface Apertures</i>
Molebny, Vasyl	PA7.7	1190	<i>A Brief Analysis of the Latest Research Progress and Future Direction of Low-Frequency Transmitting Antenna</i>
Molero, Carlos	E10b.2	2064	<i>Analytical Circuit Models: From Purely Spatial to Space-Time Structures</i>
	A06a.3	3031	<i>3-D Reflectarray Unit Cell with Wideband Performance and Integrated Sensing Capability</i>
Molina-Garcia-Pardo, Jose-Maria	PP01.4	1360	<i>A Study on W-Band Frequency Attenuation in the Presence of Human Blockage</i>
Molisch, Andreas	P04a.1	767	<i>On the Use of Adaptive-Density Point Cloud for Site-Specific Ray-Optics Simulations</i>
Molla, Dereje Mechal	CS35b.4	1917	<i>Experimental Evaluation of V2X Connectivity Technologies with V2X Channel Models</i>
Molnar, Goran	A24.2	3861	<i>Synthesis of Flat-Top Beams Based on Modified Chebyshev Polynomials</i>
Moloudian, Gholamhosein	CS1b.1	4238	<i>A Compact Microwave Rectifier for Wireless Power Transfer and Energy Harvesting Applications</i>
Monni, Stefania	PA5.3	3503	<i>Characterization of All-Metal Multi-Feed Antenna for High Power Applications</i>
Monochristou, Christos	CS26b.3	4314	<i>Thinned Connected Slot Array Design Using Higher Symmetries</i>
Monorchio, Agostino	E06a.4	601	<i>Design of a Low-Frequency Magnetic Metasurface for Extremely Focused and Long Range Wireless Power Transfer Applications</i>
	PE1.9	1272	<i>A Compact Fabry-Perot Cavity Antenna with Circular Polarization</i>
	PM1.1	1308	<i>Preliminary Investigation of an Innovative RF Sensor for Deformation and Failure Evaluation in Composite Materials</i>
	CS27.2	1575	<i>An Electromagnetic Metasurface for Impedance Matching in Microwave Biomedical Applications</i>
	PE3.8	2392	<i>Design of a Conformal and Low-Frequency Metasurface for Magnetic Field Shielding in Wireless Power Transfer Systems</i>
	A10.5	3083	<i>Fabry-Perot Antenna with High-Permittivity Grounded Walls for Side Lobe Level Reduction</i>
	CS33b.4	3321	<i>Deep-Learning Optimized Reconfigurable Metasurface for Magnetic Resonance Imaging</i>
	PP03.6	3610	<i>Target Classification Through ISAR for Autonomous Vehicles Based on Federated Learning</i>
	E09.1	3905	<i>Design of an L-S-Band Frequency Selective Resorber for Dual-Band Absorption and In-Band Transmission</i>
Montagna, Maria	PP02.13	2547	<i>Radiometeorological Forecasts for Satellite Links Operations: Validation with Measurements from BepiColombo Mission</i>
Montalban, Jon	PP03.8	3620	<i>Empirical Characterization of Doppler in Industrial Wireless Channels</i>
Monti, Alessio	E08.2	1868	<i>Reflective Intelligent Surfaces: Reducing Complexity by Controlling the Illuminating Field</i>
	E08.5	1880	<i>Static and Reconfigurable Phase-Gradient Metasurfaces for Antenna</i>

			<i>Applications</i>
	PA4.10	2147	<i>Analysis and Design of Robust Reconfigurable Intelligent Surfaces Using a Statistical Approach</i>
Monti, Alessio	A10.2	3071	<i>Analysis and Design of Metasurface Antennas Based on Temporal Metastructures</i>
Montoya-Roca, Roger	CS6b.5	505	<i>Multi-Beam Arrays for Future LEO SatCom Payloads</i>
Monzon Baeza, Victor	PA2.5	1074	<i>Genetic Algorithm-Based Beamforming in Subarray Architectures for GEO Satellites</i>
	CS19b.4	4295	<i>Supervised Learning Based Real-Time Adaptive Beamforming On-Board Multibeam Satellites</i>
Moodley, Kavilan	CS4.4	3189	<i>The Hydrogen Intensity Real-Time Analysis eXperiment: Overview and Status Update</i>
Moon, Byeongju	CS7.2	1596	<i>Simultaneously Dual-Polarization Convertible Sub-THz Reconfigurable Intelligent Surface Enabled by Through-Quartz VIAs</i>
Moon, Soomin	CS22a.1	2841	<i>Development of an Analytical Quantum Full-Wave Solution for a Transmon Qubit in a 3D Cavity</i>
Moore, James	PA5.17	3560	<i>Low-Profile Super-Realised Gain Antennas</i>
Moore, Lawrence	CS39b.1	808	<i>Exploring the Properties of Reverberation Chambers in the THz Range: A Pilot Study</i>
Morabito, Andrea	M5.5	557	<i>Near Field Phase Recovery Exploiting Only One Measurement Surface and A Smart Warping Sampling Strategy</i>
	A16.5	1749	<i>Design of a Wideband Dual-Polarized Stacked Antenna Array for SATCOM Applications</i>
	PA8.10	2311	<i>Octagonal Patch Tag Antenna and 3 × 3 Array Locator for DoA Applications</i>
	A15a.2	4115	<i>Extending Spectral Factorization to the 2-D Mask-Constrained Power Synthesis of Shaped Beams with Arbitrary Footprints</i>
Moradi, Sina	CS37b.5	361	<i>Front-End Mismatching, Mutual Coupling, Bandwidth, Transmission Line Noise, and SNR</i>
Moraitis, Nektarios	PP03.17	3655	<i>Propagation Modeling in an Indoor Environment at Sub-THz Frequencies Based on Ray Tracing</i>
Moralis-Pegios, Miltiadis	PA3.21	3483	<i>MIMO Signals Processing Utilizing Optical Crossbar Linear Operator</i>
Moreira, Antonio	P05.1	241	<i>Small-Scale Passive Millimetre-Wave Imaging Measurements for Marine Litter Detection at W-Band</i>
	P02.3	3772	<i>Feature Selection for Identifying Optimal Microwave Frequencies to Detect Floating Macroplastic Litter in C and X Bands</i>
Morejon Betancourt, Dreyelian	PP03.8	3620	<i>Empirical Characterization of Doppler in Industrial Wireless Channels</i>
Moreno-Rodríguez, Salvador	PP01.4	1360	<i>A Study on W-Band Frequency Attenuation in the Presence of Human Blockage</i>
	E10b.2	2064	<i>Analytical Circuit Models: From Purely Spatial to Space-Time Structures</i>
Morlaas, Christophe	PA6.9	2245	<i>Study of the Frequency Dispersion of 3D-Printed Dielectric Crystals for Dielectric Resonator Antenna Applications</i>

	A25.4	3100	<i>3D-Printed Circular Polarized Dielectric Resonator Antenna with Enhanced Axial Ratio Bandwidth Using Anisotropic Material</i>
Moroni, Nicolò	CS10.3	860	<i>D-Band Active Antenna Array with Lens Enabling Quasi-Optical and Analogue Beam Reconfiguration for 6G Applications</i>
Moscato, Stefano	PA2.23	1154	<i>Ka-Band Phased Antenna Array Concept for High-EIRP Satellite Connections</i>
Moser, Benjamin	CS12a.2	4048	<i>Rapid Automated Antenna Alignment on Robotic Antenna Ranges</i>
Mospan, Lyudmila	PE3.15	2416	<i>Frequency-Selective Surface Generating Two-Band Pseudo-Elliptic Frequency Response</i>
Mosquera, Carlos	A06a.5	3041	<i>Multibeam Compact Dual Reflectarray Antenna for High-Throughput Satellites in Ka-Band</i>
Mota, Joao	CS25.3	663	<i>Multibeam Phased Arrays Exploiting Frequency Dispersion for Massive MIMO Satellite Communications</i>
Mota, Susana	PP02.9	2528	<i>Synthesis of Drop Counter Rain Rate from a Tipping Bucket Rain Gauge</i>
	PP02.10	2533	<i>Designing a Data Pre-Processing Tool for MEO Satellites Propagation Measurements</i>
	P09.3	2644	<i>Ka-Band Rain Attenuation Derived from a MEO Satellite Constellation</i>
Motroni, Andrea	CS13.3	1558	<i>Exploiting Near-Field Antenna Detuning in Collision Avoidance Systems for RFID-Equipped Robots</i>
	CS23b.1	1989	<i>SARFID for Fine-Scale Localization of Passive Backscattering Devices at 2.4 GHz ISM Band</i>
Motta Cruz, Eduardo	PA3.14	3450	<i>Study of Environmentally-Friendly Radomes Using Cork-Rubber Composites for 5G Backhaul Links at E-Band</i>
Mou, Haifeng	P10b.5	3263	<i>E-Band Measured Propagation Characteristics for Urban Backhaul Communications</i>
Moulay, Ahmed	CS40b.4	1981	<i>Efficient Wireless Power Transfer to an Ultra-Miniaturized Antenna for Future Cardiac Leadless Pacemaker</i>
Mouthaan, Koen	A12a.4	1719	<i>X-Band Receiving Phased Array with Digital Beamforming Using RFSoc</i>
	A12b.2	1932	<i>An L-Band Receiving Array with Full Digital Simultaneous Quad-Polarization Beamforming</i>
	A15a.3	4118	<i>Impact of Deformations on Beamforming Performance of Uniform Rectangular Arrays</i>
Movafagh, Moein	E01.4	2028	<i>Huygens Principle Imaging Method Powered by Deep Learning for Brain Stroke Classification</i>
Mukherjee, Jayanta	PP02.16	2562	<i>Analysis of the Effects of Rainwater Covered Bumper on the Automotive Radar Signals</i>
	PA3.15	3454	<i>Self-Isolated MIMO Antenna Using SIW Cavity Antenna for Dual-Band (28, 38 GHz) Applications</i>
Mukherjee, Soumava	A27a.5	650	<i>A Novel Substrate Integrated Broadband Dielectric Resonator Antenna (DRA) in SICL for Millimeter Wave Application</i>
Mukhopadhyay, Subhas	PA8.11	2315	<i>Development of Passive Chipless RFID Temperature Sensor</i>
	PA8.12	2320	<i>Towards Array and Curve Analysis: Flexible Passive Chipless RFID Tags</i>

Müller, Johannes	CS33b.4	3321	<i>Deep-Learning Optimized Reconfigurable Metasurface for Magnetic Resonance Imaging</i>
Munina, Irina	PA4.22	2197	<i>Effect of Phase Errors on Performance of Ka-Band Reflectarray with DRA Unit Cells</i>
	A07.1	2659	<i>A Wideband Half-Circle Metasurface Augmented Luneburg Lens for Millimeter-Wave Applications</i>
Munoz, Frederic	P04b.2	970	<i>Ray-Tracing Calibration from Channel Sounding Measurements in a Millimeter-Wave Industrial Scenario</i>
	CS34.4	2625	<i>Empirical Validation of the Impedance-Based RIS Channel Model in an Indoor Scattering Environment</i>
Muñoz Lao, Aitor	PE3.7	2388	<i>Electromagnetic Modelling in Modern Vehicles: A Pathway to Efficiency and Performance</i>
Muntoni, Giacomo	A04.3	1467	<i>A Shared-Aperture Planar Antenna for 5G</i>
	PA4.12	2155	<i>A Dual Linearly Polarized Array for 5G FR2</i>
Muramatsu, Kyoshiro	CS36b.1	896	<i>Safe Beamforming Based on Human Area Estimation for Microwave Wireless Power Transfer</i>
Murata, Kentaro	CS36b.1	896	<i>Safe Beamforming Based on Human Area Estimation for Microwave Wireless Power Transfer</i>
Murk, Axel	A18.4	2919	<i>Method of Moment Simulation of Full Arctic Weather Satellite Structure</i>
Murk, Axel	P02.4	3777	<i>Measuring and Modelling the Scattering Parameters of the Wet Radome of the Swiss Weather Radars</i>
Mursia, Placido	CS20b.4	406	<i>Impedance-Based RIS Channel Model and Optimization in Fast-Fading Environments</i>
	CS34.4	2625	<i>Empirical Validation of the Impedance-Based RIS Channel Model in an Indoor Scattering Environment</i>
Musacchio Adoriso, Giuseppe	CS42b.1	439	<i>An Antenna Measuring System Based on a Cable Suspended Dolly and Inverse Source</i>
	A20.3	3818	<i>Compact Antenna Solutions for Data Transmission Using Fat-Intrabody Communication (Fat-IBC)</i>
Mustacchio, Carmine	A27a.3	641	<i>K-Band Microstrip ESPAR Antenna Integrated into Large Array</i>
Musters, Ferry	CS47.6	435	<i>The Antenna Dome High-Speed Characterization System for OTA Characterization of FR2 5G Active Antenna Panels</i>
Myllymaki, Sami	PA3.19	3475	<i>Sub-THz Spatially Modulated Beam Splitting Reflectors for Potential RIS Implementations</i>

N

Nabeel, Maira	CS9a.5	233	<i>Beam Steering 2D Leaky Wave Resonant Cavity Antenna for Ka-Band Satellite Communication</i>
Nadali, Khatereh	CS40a.2	1758	<i>Optimizing RF Energy Harvesting in IoT: A Machine Learning Estimation Considering Polarization Effects</i>
	A15b.5	4345	<i>Dual UWB Antennas on AoA Anchor Node</i>
Nadeem, Adnan	E09.5	3924	<i>Multifunctional Linear Dichroism and Polarization Transforming Metasurface for mm-Wave Application</i>
Naidoo, Warren	CS4.4	3189	<i>The Hydrogen Intensity Real-Time Analysis eXperiment: Overview and Status Update</i>
Najera, Alberto	CS2.1	165	<i>Instantaneous Vs Theoretical Maximum Exposure Under Real Traffic</i>

			<i>Conditions: Example in the City of Valencia</i>
Nakano, Hisamatsu	A03a.4	2877	<i>Circular Loop Antennas with Quasi-Two Sources for Broadband Circular Polarization</i>
Nam, Yong-Hyun	A06b.5	3306	<i>A High-Efficiency Reconfigurable Reflectarray Antenna Using Two Types of Active Unit Cells</i>
Nannetti, Massimo	CS25.5	673	<i>TX/RX Terminal Based on Metascreen Technology for Ka-Band Satcom with Dual Switchable Polarization</i>
Narbudowicz, Adam	CS3.1	294	<i>Chipless RFID Sensor on Paper Substrate</i>
	CS16.2	567	<i>On the Data Rate Capability of Near-Field Communications Links Based on Bessel Beams</i>
	CS36a.1	700	<i>Angle of Arrival Estimation Methods Using Spherical-Modes-Driven Multiport Antennas</i>
	PA8.5	2288	<i>Low-Profile Electrically Small Antenna with Pattern and Polarization Diversity</i>
	PA8.6	2293	<i>Bandwidth-Enhanced Compact Beamsteering Antenna for IoT Platforms</i>
Narita, Takanori	A27a.4	646	<i>Mechanical/Electrical Hybrid 2-Dimensional Beam Scanning Cylindrical Dielectric Lens Antenna</i>
Narouwa, Massamaesso	CS35b.4	1917	<i>Experimental Evaluation of V2X Connectivity Technologies with V2X Channel Models</i>
Naseri Gheisanab, Hassan	PA2.11	1101	<i>Multi-Bit Wideband Transmitarray Aperture with Independent Phase and Amplitude Control for High Gain with Low Sidelobe Mm-Wave Applications</i>
	A01a.4	2941	<i>Dual-Polarized OAM Antenna with Frequency and Mode Agility for Intelligent OAM Communications</i>
Nasimuddin, N	PA2.2	1056	<i>Compact Wideband Circularly Polarized Antenna Array for Satellite Applications</i>
	PA2.6	1079	<i>Modular Ka-Band Transmit Phased Array Antenna for SATCOM Applications</i>
Nasser, Noaman	CS15.5	4019	<i>A Digital Beamforming Antenna for Space Based Solar Power Transmitting Array</i>
Nasser, Youssef	CS20b.3	402	<i>Measurements of Reconfigurable Intelligent Surface in 5G System Within a Reverberation Chamber at mmWave</i>
Navarro-Cía, Miguel	PP01.2	1352	<i>Analysis of the Capacity and Energy Efficiency of Metallodielectric Surface Wave Links Operating Beyond Y Band</i>
	A08a.4	1897	<i>Ka-Band USS Enterprise (NCC-1701) Antenna</i>
Navratil, Vaclav	CS23b.4	2004	<i>Angle of Arrival Measurements with Ultra-Wide Band Transceivers: Design and Evaluation</i>
Ndagijimana, Adolphe	E04.1	2684	<i>Towards Optimal Binary Patterns for Compressive Terahertz Single-Pixel Imaging</i>
Nebuloni, Roberto	P09.4	2649	<i>Rain Attenuation at mmWave and Optical Bands from Visibility and Rainfall Intensity Measurements</i>
	P09.5	2654	<i>Predicting Rain Attenuation at D Band for 6G Backhaul Link Design: A Frequency Scaling Approach</i>
	P10b.3	3254	<i>Exploiting Numerical Weather Prediction Data for Radiopropagation</i>

			<i>Modeling of SatCom Links</i>
Negri, Edoardo	CS9a.2	225	<i>2D-Scanning of Circularly Polarized Beams via Array-Fed Fabry--Perot Cavity Antennas</i>
	CS16.4	573	<i>Leaky-Wave Design of Hybrid-, TE-, and TM-Polarized Resonant Bessel-Beam Launchers for Millimeter- and Submillimeter-Wave Applications</i>
	A08b.3	2091	<i>Hybrid Metal-Graphene Unit Cells for THz Reconfigurable Leaky-Wave Antennas</i>
Nekovee, Maziar	E06a.5	605	<i>An Efficient Wheel-Integrated Wireless Power Transfer System Based on High-Permittivity Metasurface</i>
Nenna, Guido	PM1.1	1308	<i>Preliminary Investigation of an Innovative RF Sensor for Deformation and Failure Evaluation in Composite Materials</i>
Nepa, Paolo	CS13.3	1558	<i>Exploiting Near-Field Antenna Detuning in Collision Avoidance Systems for RFID-Equipped Robots</i>
	CS23b.1	1989	<i>SARFID for Fine-Scale Localization of Passive Backscattering Devices at 2.4 GHz ISM Band</i>
Ness, John	A16.4	1744	<i>Compact Hybrid Optical/RF User Segment (CHORUS): RF Terminal Design</i>
Neto, Andrea	CS44b.2	945	<i>Design and Characterization of an Imaging System Using Photoconductive Connected Arrays</i>
	A05.4	1833	<i>Time Domain Analysis of Pulsed Photo-Conductive Antenna Sources: Distributed Excitations</i>
	E10a.1	1841	<i>Spectral Domain Green's Function of an Infinite Dipole with Non-Zero Metal Thickness</i>
	A12b.1	1927	<i>Design, Measurements, and Performance Assessment of a Massive MIMO Wideband Phased Array</i>
	A12b.5	1944	<i>Study of Finite Edge Effects in Compact Ultra-Wide-Band Connected Arrays</i>
	E10b.4	2073	<i>Efficient Analysis Method for Artificial Dielectric Layers with Vertical Metal Inclusions</i>
	A07.3	2669	<i>On the Design of Wide-Scanning Lenses with Integrated Focal Arrays</i>
	CS22a.2	2846	<i>The Predictions of Quantum and Classical Models for the Thermal Energy Emitted in the Sub-mm Ranges by Doped Silicon</i>
Neuder, Robin	A09b.4	886	<i>Loss Analysis for Compact Liquid Crystal Delay Lines Based on Defective Ground Structures</i>
Neuman, Vojtech	A03b.1	3128	<i>An Upper Bound for Envelope Correlation Coefficient of Antenna Clusters</i>
Nevala, Klaus	CS5a.5	76	<i>A Modular COTS-Based High-Efficient Sub-THz Channel Sounder and Experimental Validations</i>
	CS12a.3	4053	<i>Characterisation of a D-Band Horn Antenna: Comparison of Near-Field and OTA Measurements</i>
Neve, Michael	P05.3	251	<i>Characterisation of Thin Glass-Fibre Substrates for Deployable SAR Antennas</i>
	P02.5	3782	<i>Mechanical Vibrations on a Deployable Nanosatellite Antenna: SAR Performance Analysis</i>

Ney, Michel	E02b.1	3268	<i>Frequency-Domain TLM Method with Cartesian Block Meshing</i>
Nguyen, Anh	CS6b.3	499	<i>Anisotropic Metagrating for Beamforming with Polarization Conversion</i>
Nguyen, Duy Hai	A28.2	3719	<i>A High-Isolation Dual-Band Base Station Antenna Design for Full Duplex Technologies</i>
Nguyen, Thi-Kim-Ngan	A21.2	1484	<i>Dual-Linearly Polarized Pillbox Beamformer in Hybrid CNC-PCB Technologies at W-Band</i>
Nguyen, Tuan Hung	A27a.4	646	<i>Mechanical/Electrical Hybrid 2-Dimensional Beam Scanning Cylindrical Dielectric Lens Antenna</i>
Ni, Haoran	PM1.3	1318	<i>Impact of 6D Mobility on Doppler Characteristics of UAV-To-Vehicle Channels</i>
Ni, Xuenan	A15a.1	4110	<i>Multiple-User Full-Duplex Hybrid Beamforming Design for mmWave Systems with A Joint Interference Cancellation Design</i>
	A15a.4	4122	<i>Beamforming Optimization for Full-Duplex Relay in SIC-Enhanced Cooperative NOMA System</i>
Niamien, Constant	PA5.8	3524	<i>A Linearly Polarized Wideband Antenna with A Stable Omnidirectional Radiation Pattern</i>
Niazi, Shahab	PA7.18	1238	<i>Generation of Dual Band OAM Wave Using Single Patch Antenna for WLAN/WIMAX Applications</i>
Nichols, Roger	CS5b.6	388	<i>Sub-Terahertz MassiveMIMO Channel Sounder for 6G Mobile Communication Systems</i>
Nicolaci, Pasquale Giuseppe	CS39a.3	618	<i>Full Wave Modelling and Design of a Baffle for the HERTZ 2.0 Compact Antenna Test Range</i>
	PA7.11	1210	<i>Electromagnetic Assessment of Tolerances of the Square Kilometre Array Log Periodic Antenna Using Uncertainty Quantification</i>
	E10a.4	1854	<i>Platform Scattering Analysis of the Copernicus Imaging Microwave Radiometer</i>
	A17.4	3754	<i>RF Modelling and Validation of the Breadboard Antenna of the Copernicus Imaging Microwave Radiometer</i>
Nielsen, Jesper	CS35b.5	1922	<i>Indoor Propagation Measurements with a Reconfigurable Intelligent Surface at 3.5 GHz</i>
Nielsen, Jonas	CS47.1	416	<i>Over-The-Air Measurements for mm-Wave Body-Centric Wireless Communication</i>
Niemitalo, Veli-Matti	CS12a.3	4053	<i>Characterisation of a D-Band Horn Antenna: Comparison of Near-Field and OTA Measurements</i>
Nikita, Konstantina	PP03.17	3655	<i>Propagation Modeling in an Indoor Environment at Sub-THz Frequencies Based on Ray Tracing</i>
Nikitopoulos, George	PP01.5	1365	<i>Field Trials for Different 5G NSA Cellular Networks</i>
Niknahad, Fatemeh	CS40b.2	1973	<i>A WiFi-Based System for Ice Monitoring in Harsh Environment Using 2.7 GHz Microwave Sensor</i>
Nikolaou, Symeon	CS24a.5	740	<i>Polynomial Basis Functions for Qualitative Head Tissue Segmentation via Linearized Microwave Imaging</i>
Nikolayev, Denys	CS27.3	1579	<i>Theoretical Insights and Engineering of Wireless Body-Implanted Bioelectronics</i>
	A08a.3	1893	<i>Frequency Scanning Leaky-Wave Antenna for On-Body Radar: Design and Conformal Analysis</i>

	PA1.4	3345	<i>Phase Variation of Ingestible Dipole, Loop, and Patch Antennas in Gastrointestinal Tract</i>
Nikolova, Natalia	CS33b.1	3309	<i>Nonlinear Correction of the Direct Inverse Problem Solution in Real-Time Imaging</i>
Ning, Yibo	PA6.4	2227	<i>A High Gain Spoof Surface Plasmon Polaritons (SSPPs) Antenna Based on a Metamaterial-Inspired Substrate Integrated Waveguide</i>
Ninković, Darko	CS24a.5	740	<i>Polynomial Basis Functions for Qualitative Head Tissue Segmentation via Linearized Microwave Imaging</i>
	CS33a.5	3062	<i>Generating a Library of Head Phantoms for Microwave Imaging Using Spherical Harmonic Approximation</i>
Niotaki, Kyriaki	CS1a.2	4027	<i>Single-Branch Hybrid Resistance Compression Technique for Enhanced Rectifier Performance</i>
Niro, Giovanni	PA1.3	3340	<i>Eco-Friendly and Conformable PIFA Based on PEDOT: PSS and a Sustainable Chitosan Substrate for 5G Communications</i>
Nistane, Viraj	CS4.4	3189	<i>The Hydrogen Intensity Real-Time Analysis eXperiment: Overview and Status Update</i>
Niu, Chen	PE1.14	1292	<i>Integral Equation-Based Solver for the Simulation of Metasurface Designs</i>
Nogués-Correig, Oleguer	CS46.4	4228	<i>Antenna Digital Beamforming on Spire's GNSS-Reflectometry CubeSat Constellation</i>
Noman, Muhammad	PM1.4	1323	<i>A Highly Compact Double-Sided Orientation Insensitive Chipless Tag for Radio Frequency Identification Applications</i>
Notter, Raphael	PA7.5	1180	<i>Design of Optimized Cylindrical Structural Antenna with Quasi Length Insensitivity Using CMA</i>
Nussbaum, Pascal	CS1b.5	4254	<i>Plug-In Plug-Out Multibeam Dielectric Rod Antenna for Target Dedicated mm-Wave RF-WPT Applications</i>
Nyffenegger, Michel	CS30a.4	3942	<i>Validating Convex Optimization of Reconfigurable Intelligent Surfaces via Measurements</i>
Nyka, Krzysztof	A21.3	1488	<i>Millimeter Wave Retrodirective Van Atta Arrays in LTCC Technology</i>
	PA4.15	2169	<i>Low-Cost 3-D Printed Lens Antenna for Ka-Band Connectivity Applications</i>
	PA8.15	2332	<i>Miniaturized and Lightweight ESPAR Antenna for WSN and IoT Applications</i>
	M3.5	2605	<i>Highly Precised and Efficient Robot-Based ESPAR Antenna Measurements in Realistic Environments</i>
Nystrom, Lukas	A18.2	2909	<i>Self-Interference Suppression for SatCom Active Antenna Arrays Through Joint Transmit and Receive Beamforming</i>

O

O Donnell, Garret	PA4.22	2197	<i>Effect of Phase Errors on Performance of Ka-Band Reflectarray with DRA Unit Cells</i>
O Halloran, Martin	CS24b.1	920	<i>Microwave Tomography Bone Imaging: Analysing the Impact of Skin Thickness on the Reconstruction of Numerical Bone Phantoms</i>
O'Flynn, Brendan	PP02.17	2567	<i>Machine Learning Approaches for EM Signature Analysis in Chipless RFID Technology</i>
	CS1b.1	4238	<i>A Compact Microwave Rectifier for Wireless Power Transfer and</i>

Energy Harvesting Applications

O'Halloran, Martin	CS28.1	465	<i>Dielectric Characterisation of Human Parathyroid Glands at Microwave Frequencies</i>
O'Loughlin, Declan	CS24b.4	933	<i>Developments in Open-Source Tools for Microwave Breast Imaging</i>
Oberhammer, Joachim	A05.2	1825	<i>High-Gain and Circular Polarization Silicon-Micromachined Lens Antennas at 500-750 GHz</i>
	PE3.5	2379	<i>Analysis of the Interaction of Laser-Induced Solid-State Plasma with Electromagnetic Waves in Silicon Waveguides at 67-220 GHz</i>
Occhiuzzi, Cecilia	PA4.14	2165	<i>RFID-Based Reconfigurable Intelligent Surfaces: Towards Wireless and Ultra-Low-Power Reconfigurability</i>
OConnor, Gerard	PA2.12	1105	<i>Fabrication and RF Characterization of Fully Additive Manufactured Transmission Lines</i>
Odit, Mikhail	CS20b.3	402	<i>Measurements of Reconfigurable Intelligent Surface in 5G System Within a Reverberation Chamber at mmWave</i>
	A03b.5	3147	<i>Wireless Re-Configurable Intelligent Surface for Sub 6 GHz 5G Frequency</i>
Oestges, Claude	P04a.2	772	<i>Improvements of Scintillation Modelling from Radiosonde Observations in the Arctic Region</i>
	P04a.4	782	<i>Fully Differentiable Ray Tracing via Discontinuity Smoothing for Radio Network Optimization</i>
Oh, Jinhyung	PP01.12	1399	<i>The Effect of Beam Misalignment in Data Center Environment at 285GHz Band</i>
Oh, Jungsuek	CS17b.4	330	<i>Indoor Coverage Enhancement Employing Liquid Crystal-Based Massive Reconfigurable Intelligent Surface Linked to 5G FR2 Base Station</i>
	CS7.2	1596	<i>Simultaneously Dual-Polarization Convertible Sub-THz Reconfigurable Intelligent Surface Enabled by Through-Quartz VIAs</i>
Ohana, Bar	PA7.13	1219	<i>Experimental Investigation of the Nullifier-Based Monopole</i>
OHara, Oscar	CS4.2	3181	<i>Mitigating Zenith Blindness from Mutual Coupling in a Sunflower Phased Array</i>
OHare, Daniel	P06.5	2747	<i>A Time-Efficient Model for Estimating Far-Field Wireless Power Transfer to Biomedical Implants</i>
Ohto, Takuya	PA6.11	2255	<i>User and Passive Beam Scheduling Scheme for Liquid Crystal IRS-Assisted mmWave Communications</i>
Oikonomopoulos-Zachos, Christos	CS10.3	860	<i>D-Band Active Antenna Array with Lens Enabling Quasi-Optical and Analogue Beam Reconfiguration for 6G Applications</i>
Okada, Minoru	E06b.1	792	<i>Variable Multi-Band Metasurface Reflector with Controllable Direction Using Varactor Diodes Mounted Large-Via Mushroom-Type Structure</i>
Okon, Ernest	PM2.14	2486	<i>A Wideband Free Space Material Characterization Method for Extracting Dielectric Permittivity</i>
Oldoni, Matteo	PA2.23	1154	<i>Ka-Band Phased Antenna Array Concept for High-EIRP Satellite Connections</i>
Olea Garcia, Ana	PA2.4	1069	<i>Antenna Design for TriHex: A Future Soil Moisture and Ocean Salinity Radiometer Mission</i>
Olesen, Kim	CS34.2	2615	<i>An Automated Over-The-Air Radiated Testing Platform for</i>

			<i>Reconfigurable Intelligent Surface</i>
Oliveira, Vinicius Magno	A17.5	3759	<i>The Novel Method for Deployable Parabolic Reflector Based on Uchiwa Origami</i>
Oliveri, Giacomo	CS20a.5	104	<i>Recent Advances on Multi-Scale Wave Manipulation Through Reconfigurable Intelligent Surfaces</i>
	CS17b.1	320	<i>On the Design of Static Passive Skins for Next Generation Fixed Wireless Access Applications</i>
Olsson, Bengt-Erik	CS47.5	430	<i>In-Field Measurement of Total Radiated Power from Active Antenna Arrays</i>
	CS43a.1	3952	<i>On the Importance of Scattering from Poles in Ray Tracing Simulations</i>
	CS43a.5	3972	<i>Feasibility of High Throughput Wireless Communication Above 100 GHz in Indoor Scenarios</i>
Omote, Hideki	PP01.9	1385	<i>Development of a Site-Specific Building Entry Loss Model for High-Rise Buildings</i>
Onat, Nehir Berk	A15b.4	4340	<i>Sunflower Array of Infinitesimal Dipoles for Constrained Antenna Modeling</i>
Ono, Akira	E06b.1	792	<i>Variable Multi-Band Metasurface Reflector with Controllable Direction Using Varactor Diodes Mounted Large-Via Mushroom-Type Structure</i>
Origlia, Cristina	CS24a.1	724	<i>Advancements in the Experimental Validation of a Wearable Microwave Imaging System for Brain Stroke Monitoring</i>
	CS33b.1	3309	<i>Nonlinear Correction of the Direct Inverse Problem Solution in Real-Time Imaging</i>
Ortiz, Flor	PA2.5	1074	<i>Genetic Algorithm-Based Beamforming in Subarray Architectures for GEO Satellites</i>
	CS19b.4	4295	<i>Supervised Learning Based Real-Time Adaptive Beamforming On-Board Multibeam Satellites</i>
Ourir, Abdelwaheb	CS36a.4	715	<i>Compact Metamaterial Antenna for Three-Dimensional Angular Localization of Multiple Radio-Frequency Sources</i>
	A26.1	4192	<i>An Electromagnetic-Compliant Scattering Model for Reconfigurable Intelligent Surfaces</i>
Owen, Henry	PP02.14	2552	<i>Modeling Atmospheric Effects on over Land UHF Propagation Links</i>
Ozan, Sarmad	PP01.14	1407	<i>Analog Self-Interference Cancellation by Means of a Synchronised Signal Injection</i>
Ozzola, Riccardo	E10a.1	1841	<i>Spectral Domain Green's Function of an Infinite Dipole with Non-Zero Metal Thickness</i>
	A12b.1	1927	<i>Design, Measurements, and Performance Assessment of a Massive MIMO Wideband Phased Array</i>

P

Padial-Allué, Rubén	PA3.8	3424	<i>1-Bit RIS Unit Cell with Mechanical Reconfiguration at 28 GHz</i>
Padilla, Pablo	PP01.4	1360	<i>A Study on W-Band Frequency Attenuation in the Presence of Human Blockage</i>
	E10b.2	2064	<i>Analytical Circuit Models: From Purely Spatial to Space-Time Structures</i>
	A06a.3	3031	<i>3-D Reflectarray Unit Cell with Wideband Performance and Integrated Sensing Capability</i>

	PA3.8	3424	<i>1-Bit RIS Unit Cell with Mechanical Reconfiguration at 28 GHz</i>
	CS26a.1	4090	<i>Glide-Symmetric SIH Unit Cells Implemented in Parallel-Plate Waveguides at mmWaves</i>
Pagani, Pascal	P03.3	1538	<i>Influence of the Atmospheric Plasma Sheath on the RCS of a Hypersonic Reentry Vehicle</i>
Pahlke, Steffen	P04b.3	975	<i>Ray Tracing and Measurement-Based Characterization of Inter/Intra-Machine THz Wireless Channels</i>
Pajusco, Patrice	CS35b.3	1913	<i>mmWave Channel Sounding for Vehicular Communications</i>
Pala, Ragip	PM2.10	2469	<i>Assessing Performance of Transparent Conductive Films for Microwave Industrial Applications</i>
Palczynski, Gregor	A19.2	1508	<i>Polymer-Based Additive Manufacturing of a Complex RF Front-End for New Space Applications</i>
Palikaras, George	PM2.10	2469	<i>Assessing Performance of Transparent Conductive Films for Microwave Industrial Applications</i>
Pallaris, Alexandros	A04.4	1471	<i>Simulated Far-Field Pattern Disruption from a 1 GHz Cloaked Array Above a 10 GHz Array</i>
Palmeri, Roberta	M5.5	557	<i>Near Field Phase Recovery Exploiting Only One Measurement Surface and A Smart Warping Sampling Strategy</i>
	CS24a.2	727	<i>Microwave Imaging for Monitoring Bone Healing Using Magnetic Scaffolds: An Initial Analysis</i>
	P02.2	3768	<i>Learning-Based Procedures for Inverse Design of Electromagnetic Devices: A Preliminary Investigation</i>
	A15a.2	4115	<i>Extending Spectral Factorization to the 2-D Mask-Constrained Power Synthesis of Shaped Beams with Arbitrary Footprints</i>
Palomares-Caballero, Angel	A06a.3	3031	<i>3-D Reflectarray Unit Cell with Wideband Performance and Integrated Sensing Capability</i>
	PA3.8	3424	<i>1-Bit RIS Unit Cell with Mechanical Reconfiguration at 28 GHz</i>
	CS26a.1	4090	<i>Glide-Symmetric SIH Unit Cells Implemented in Parallel-Plate Waveguides at mmWaves</i>
Palomba, Gianmarco	CS45.3	1808	<i>Preliminary Clinical Trial Results of MammoWave in the Context of RadioSpin Project</i>
Palosaari, Jaakko	PA3.19	3475	<i>Sub-THz Spatially Modulated Beam Splitting Reflectors for Potential RIS Implementations</i>
Pan, Ran	CS23a.2	1780	<i>Terahertz Channel Modeling Based on Scattering Characterization</i>
Panagamuwa, Chinthana	PP01.13	1404	<i>Half Mode Corrugated Substrate Integrated Waveguide (HM-CSIW) Band-Stop Filter Using Hexagonal Ring Resonators</i>
Pandit, Jibran	PE1.13	1288	<i>Multi-Channel Beam-Splitting Metasurface for Millimeter Wave Communication Systems</i>
Papadopoulos, Alexandros	E07.5	1653	<i>An Accurate Semi-Analytical Model for Periodic Tunable Metasurfaces Electromagnetic Response</i>
Papadopoulos, Aristeides	A23.2	2752	<i>Adaptive Polynomial Chaos Expansion for Uncertainty Quantification of SubTHz Horn Antennas with Flat-Top Radiation Patterns</i>
Papadopolou, Maria S.	PA3.23	3490	<i>Wideband Aperture-Coupled Array Design for Automotive Radar Applications</i>
Papapolymerou, John	CS9a.3	227	<i>Beam Focusing with a Conformal Leaky-Wave Antenna Described by a</i>

			<i>Spline Curve</i>
Papiah, Tasmiya	CS4.4	3189	<i>The Hydrogen Intensity Real-Time Analysis eXperiment: Overview and Status Update</i>
Papini, Lorenzo	CS45.3	1808	<i>Preliminary Clinical Trial Results of MammoWave in the Context of RadioSpin Project</i>
Paques, Jules-Henri	PP03.1	3589	<i>Wideband Characterization of Wireless Power Transfer in Ventilation (HVAC) Ducts for the Internet of Things and Smart Buildings</i>
Paranthoen, Cyril	PA3.12	3442	<i>Shorted Stacked Patch Array for Photonic Beam Steering at mm-Waves</i>
Paraskevopoulos, Anastasios	PA4.8	2139	<i>A Novel GO Analysis Tool for GRIN Lenses Based on the Fast Sweeping Method</i>
	PM2.10	2469	<i>Assessing Performance of Transparent Conductive Films for Microwave Industrial Applications</i>
Paredes, Ferran	M4.5	2968	<i>Phase-Variation Microwave Displacement Sensor with High Resolution, Sensitivity, and Dynamic Range</i>
Parikh, Kush	PA8.14	2327	<i>An Annular Ring Shorted Logarithmic Spiral Antenna with Planar Integrated Feed</i>
Parini, Clive	CS32.2	1438	<i>A Comparison of Near-Field to Far-Field Transformation Algorithms for Use with Industrial Multi-Axis Robotic Antenna Measurement Systems</i>
	CS31.1	1658	<i>Compressive Sensing Applied to Production Testing of Array Antennas Using a Robotic Arm and Very Sparsely Sampled Near-Field Measurements</i>
	CS15.4	4015	<i>An Overview of Gigascale Antenna Arrays and Electromagnetics for Space Based Solar Power</i>
Park, Byeongjin	E13.2		<i>Magnetic Composites with M-Type Hexaferrites for Q/V-Band Electromagnetic Wave Absorption</i>
Park, Chanul	PP02.1	2490	<i>Improving Air-Writing Accuracy Through Data Regression and Interpolation in a Single Radar System</i>
Park, Ikmo	CS6b.3	499	<i>Anisotropic Metagrating for Beamforming with Polarization Conversion</i>
Park, Jae-Joon	PP01.10	1390	<i>Sub-THz Propagation Measurement and Analysis in Indoor Corridor Environment at 159 GHz</i>
Park, Junho	CS37b.6		<i>Differentially-Fed Antenna-On-Display Module for SATCOM and Mobile Applications at Ka-Band</i>
Park, Seonggyoon	PA1.7	3359	<i>Development of a Wearable IoT-Optimized Textile Antenna with Low Specific Absorption Rate in Three Frequency Bands</i>
Parodi, Costanza	CS45.5	1815	<i>Brain Stroke Microwave Diagnostics in Children Through a Nonlinear Inverse-Scattering Technique</i>
Pärssinen, Aarno	CS5a.5	76	<i>A Modular COTS-Based High-Efficient Sub-THz Channel Sounder and Experimental Validations</i>
	PP01.8	1380	<i>Dual-Polarized Diffraction Measurements and Modeling at D-Band Frequencies</i>
	PA3.19	3475	<i>Sub-THz Spatially Modulated Beam Splitting Reflectors for Potential RIS Implementations</i>
	CS29.3	3797	<i>Computer Vision Enabled Sub-THz Radio Channel Characterization of Dynamic Objects</i>

	P01.1	3832	<i>5G Radio Channel Characterization in an Underground Mining Environment</i>
	CS12a.3	4053	<i>Characterisation of a D-Band Horn Antenna: Comparison of Near-Field and OTA Measurements</i>
	A15a.5	4127	<i>Tapering Impact on the Spatial and Frequency Responses of Broadband Asymmetrically Routed Phased Arrays</i>
Pascarella, Francesca	E09.1	3905	<i>Design of an L-S-Band Frequency Selective Resorber for Dual-Band Absorption and In-Band Transmission</i>
Pascarella, Luigi	CS42b.4	451	<i>Discretizing 2D Equivalent Radiating Panels by Legendre Quadrature</i>
Pascaud, Romain	PA6.9	2245	<i>Study of the Frequency Dispersion of 3D-Printed Dielectric Crystals for Dielectric Resonator Antenna Applications</i>
	A25.4	3100	<i>3D-Printed Circular Polarized Dielectric Resonator Antenna with Enhanced Axial Ratio Bandwidth Using Anisotropic Material</i>
Pascazio, Vito	CS24b.2	925	<i>On the In-Vivo Electrical Properties of Human Forearm at Microwave Frequency</i>
Paschaloudis, Konstantinos	PA6.7	2238	<i>Metasurface-Based Bessel-Beam Launcher with 100λ Non-Diffractive Range</i>
	A01a.3	2938	<i>Generation of Non-Diffractive Bessel Beams for Near-Field Links Applications Using Meta-Axicons</i>
Pasian, Marco	CS24b.1	920	<i>Microwave Tomography Bone Imaging: Analysing the Impact of Skin Thickness on the Reconstruction of Numerical Bone Phantoms</i>
	PA2.19	1136	<i>Improving the Strut Modelling of the European Space Agency Deep Space Antennas to Evaluate Efficiency and Sidelobe Impact</i>
	P03.1	1528	<i>Seasonal Snow Melting Process Investigation in Polar Environment Using a Dual-Receiver Radar Architecture</i>
Pasic, Faruk	CS35b.2	1908	<i>Stationarity of Multiband Channels for OTFS-Based Intelligent Transportation Systems</i>
Pasquino, Nicola	CS33a.3	3054	<i>Advancements in Broadband Electromagnetic Sensing for Food Quality Control</i>
Patel, Amit	PP01.13	1404	<i>Half Mode Corrugated Substrate Integrated Waveguide (HM-CSIW) Band-Stop Filter Using Hexagonal Ring Resonators</i>
Patnaik, Amalendu	CS8.4	2896	<i>Generation of Highly-Pure OAM Beams with Simple Slotted SIW Antenna Array</i>
Pattabhiraman, Aditi	CS4.4	3189	<i>The Hydrogen Intensity Real-Time Analysis eXperiment: Overview and Status Update</i>
Paucot, Laurent	CS46.3	4223	<i>CubeSat Formation Antenna Array Synchronization for GNSS-R</i>
Paulena, Gabriel	A12b.3	1936	<i>Synthesis of Circularly Polarized Microstrip Planar Array with Cross-Polarization Suppression</i>
Paulides, Margarethus	CS28.4	480	<i>Phantom Material with Biological Composition for Muscle Equivalent Radiofrequency, Thermal and Magnetic Resonance Properties</i>
Paulsen, Keith D.	CS45.1	1799	<i>MR/Microwave Tomography Integrated Breast Cancer Imaging</i>
Paulus, Alexander	CS42a.1	136	<i>Inverse Source Solutions with Spectral Filtering</i>
	PE2.1	990	<i>Geometry Reconstruction from Entries of Impedance Matrices</i>
	CS32.3	1443	<i>In-Flight Calibration of the Measurement System for UAV-Based Near-Field Antenna Measurements</i>

	M4.1	2950	<i>Inverse Source-Based Three-Antenna Methods in the near Field</i>
Pavlick, William	CS14b.1	4349	<i>Reconfiguration of Electromagnetic Metasurfaces Using Tunable Shape Morphing Structures</i>
Pavone, Santi	CS16.1	564	<i>Analytical and Numerical Evaluation of Efficient Power Transfer of Bessel-Shaped Beams in Near-Field Through a Planar Layered Medium</i>
	A04.3	1467	<i>A Shared-Aperture Planar Antenna for 5G</i>
	A16.5	1749	<i>Design of a Wideband Dual-Polarized Stacked Antenna Array for SATCOM Applications</i>
	PA4.12	2155	<i>A Dual Linearly Polarized Array for 5G FR2</i>
	PA8.10	2311	<i>Octagonal Patch Tag Antenna and 3 × 3 Array Locator for DoA Applications</i>
Peden, Alain	A23.5	2767	<i>Modeling of Quasi-Optical Systems and Measurements with a Cobot in the J-Band</i>
Pedersen, Gert	CS5b.1	364	<i>Enabling VNA Based Channel Sounder for 6G Research: Challenges and Solutions</i>
	PM1.9	1343	<i>Investigation of Correlation Between Absorbed Power Density and Incident Power Density for User Equipment Antennas at Sub-THz Frequencies</i>
	PA4.6	2129	<i>Detailed Design Procedure for Low-Cost High-Efficiency 3D Printed Transmitarray Antennas for mm-Wave Applications</i>
	CS34.2	2615	<i>An Automated Over-The-Air Radiated Testing Platform for Reconfigurable Intelligent Surface</i>
	PA3.5	3414	<i>5G Millimeter-Wave Reflectarray Antenna Design with a Good Gain-Filtering Characteristic Based on a High-Efficiency Polarization Converter</i>
	PA3.22	3486	<i>Wideband Array Antenna with Single-Layer Feeding Network at Ka-Band</i>
Pegatoquet, Alain	CS38.6	132	<i>Estimating the Achievable Efficiency and Bandwidth of Small Terminal-Integrated Inverted-F Antennas Using Machine Learning</i>
Pei, Long	CS39a.5	627	<i>Standardization Progress and Challenges for 5G OTA Testing</i>
Pei, Rui	CS11.3	1624	<i>Reflecting/Absorbing Dual-Mode Textile Metasurface with AI-Driven Parametric Studies</i>
Pei, Rui	CS1b.2	4242	<i>Matching Network Elimination in Multiband Metasurface-Structured Rectennas for Wireless Power Transfer and Energy Harvesting</i>
Pei, Xilong	CS34.1	2610	<i>RIS with Practical Reflection Coefficients: Modeling and Experimental Measurements</i>
Pelham, Timothy	P02.5	3782	<i>Mechanical Vibrations on a Deployable Nanosatellite Antenna: SAR Performance Analysis</i>
	CS15.4	4015	<i>An Overview of Gigascale Antenna Arrays and Electromagnetics for Space Based Solar Power</i>
Pelicano, Ana Catarina	CS28.2	470	<i>The Effect of Pressure of the Open-Ended Coaxial Probe on the Measurement of Ex Vivo Biological Tissues Dielectric Properties</i>
Pellet, Margaux	CS25.3	663	<i>Multibeam Phased Arrays Exploiting Frequency Dispersion for Massive MIMO Satellite Communications</i>

Pelorossi, Fabio	PA2.19	1136	<i>Improving the Strut Modelling of the European Space Agency Deep Space Antennas to Evaluate Efficiency and Sidelobe Impact</i>
Pendás-Recondo, Álvaro	CS15.1	4001	<i>Time-Modulated Arrays for Simultaneous Wireless Information and Power Transfer in Near-Field</i>
Peng, Bile	CS23a.2	1780	<i>Terahertz Channel Modeling Based on Scattering Characterization</i>
Peng, Zhen	CS22a.4	2853	<i>Quantum Optimisation of Reconfigurable Surfaces in Complex Propagation Environments</i>
	CS19a.5	4085	<i>Platform-Aware Optimization of Conformal Antenna Array via Simulated Bifurcation</i>
Penirschke, Andreas	PP03.13	3643	<i>Filter Integrated Microstrip 3-Port Power Combiner</i>
Pereira, Pedro Marcio	CS34.5	2629	<i>RIS Performance in a Comprehensive Fading Environment</i>
Perera, Rahal	CS44b.5	960	<i>Graph Neural Network Based 77 GHz MIMO Radar Array Processor for Autonomous Robotics</i>
Perez, Mauricio	CS27.2	1575	<i>An Electromagnetic Metasurface for Impedance Matching in Microwave Biomedical Applications</i>
	CS27.4	1584	<i>A Compact Wideband Biocompatible Circularly Polarized Implantable Flexible Antenna for Biomedical Applications</i>
	P06.2	2732	<i>Development of Tissue Emulatory Models/Phantoms of Lungs at Microwave Frequency for Acute Respiratory Distress Syndrome</i>
	PP03.7	3615	<i>SINTEC Comparative Body-Centric Communication Study: Bluetooth Vs Fat-Intrabody Communication</i>
Pérez Beltrán, Laura	CS40b.3	1976	<i>Compact 868 MHz RFID-Based Antenna for Queen Bee Identification and Location Inside Hives</i>
Pérez-Eijo, Lorena María	CS21.3	2712	<i>From mmWave Radar Nodes to Multistatic Arrays: Design Considerations and Applications</i>
Pérez-Fernández, Francisco N.	CS21.3	2712	<i>From mmWave Radar Nodes to Multistatic Arrays: Design Considerations and Applications</i>
Perez-Palomino, Gerardo	CS17a.4	15	<i>Reflective Surfaces Based on Semi-Passive Reconfigurable Polymer Network Liquid Crystal</i>
Perini, Steven	PM2.5	2446	<i>Dielectric Characterization of Materials at 5G mm-Wave Frequencies</i>
Perraud, Richard	PE2.3	999	<i>Management of Radiofrequency Compatibility on Aircraft</i>
Pessoa, Luis	CS7.5	1611	<i>Reconfigurable Intelligent Surfaces for THz: Signal Processing and Hardware Design Challenges</i>
	A26.3	4202	<i>Non-Volatile Memristor-Based 1-Bit Reconfigurable Intelligent Surface Towards a Greener 6G</i>
	A26.4	4207	<i>1-Bit Graphene-Based Reconfigurable Intelligent Surface Design in Ka-Band</i>
	A26.5	4212	<i>Improved Performance of a 1-Bit RIS by Using Two Switches per Bit Implementation</i>
Petäjistö, Sanna-Mari	CS13.4	1563	<i>Enabling Living Spaces Through Customizable NFC-Enabled Smart Table System</i>
Petek, Martin	CS26a.5	4105	<i>Efficient Numerical Computation of Dispersion Diagrams for Glide-Symmetric Periodic Structures with a Hexagonal Lattice</i>
Peter, Michael	CS43b.2	4173	<i>Comparison of Sub-THz Radio Channel Characteristics at 158 GHz and 300 GHz in a Shopping Mall Scenario</i>

Peters, Georg	CS42b.1	439	<i>An Antenna Measuring System Based on a Cable Suspended Dolly and Inverse Source</i>
Petit, Barnabas	P05.5	261	<i>Sequential Phase Optimization for Coherent Long-Range Distributed Wireless Power Transfer to a Non-Communicative Receiver</i>
Petroutsos, Panagiotis	CS26b.1	4305	<i>Ridge Gap Waveguide Implementation with a 3D Glide Symmetric Holey Metasurface for Slotted Antenna Array Feeding</i>
Petrovic, Nikola	E01.3	2024	<i>Estimating the Signal Strength for Microwave Breast Cancer Detection with a Magnetic Near-Field Applicator in Air</i>
Pettanice, Giuseppe	E02a.5	3016	<i>Improved PEEC Modeling of Antennas Through Time-Dependent Partial Elements</i>
Peverini, Oscar	CS6b.5	505	<i>Multi-Beam Arrays for Future LEO SatCom Payloads</i>
Phakaew, Thipamas	PA8.8	2301	<i>Sidelobe Suppression and Bandwidth Enhancement of Series-Fed Patch Antenna Arrays Using Coplanar Ground Conductor</i>
Phan, Tung Duy	PA3.19	3475	<i>Sub-THz Spatially Modulated Beam Splitting Reflectors for Potential RIS Implementations</i>
Phan-Huy, Dinh-Thuy	PP03.9	3625	<i>Indoor Localization of Smartphones Thanks to Zero-Energy-Devices Beacons</i>
Phaneuf, Mario	E06a.2	591	<i>On Solving Inverse Source Problems with Metasurfaces Performing Analog Computations</i>
Philipp, Dennis	CS33b.4	3321	<i>Deep-Learning Optimized Reconfigurable Metasurface for Magnetic Resonance Imaging</i>
Philippe, Pouliguen	CS16.5	578	<i>Radiation Control by Space-Time-Modulated Anisotropic Impedance Surfaces</i>
	PA7.5	1180	<i>Design of Optimized Cylindrical Structural Antenna with Quasi Length Insensitivity Using CMA</i>
Phon, Ratanak	CS14a.3	4139	<i>Hybrid Reconfigurable Reflective Metasurface with Both Phase and Space Modulation</i>
Piasecki, Marie	CS12b.5	4278	<i>Robotic Arm-Based Antenna Metrology System for Aerospace Applications</i>
Piche, Alexandre	PE2.3	999	<i>Management of Radiofrequency Compatibility on Aircraft</i>
Pietrenko-Dabrowska, Anna	PE3.1	2359	<i>Cost-Efficient Large-Scale Re-Design of Multi-Band Antennas Using Orthogonal Scaling Directions</i>
	CS30a.1	3928	<i>Unconventional Surrogate-Assisted Approaches to EM-Driven Antenna Design. Modeling and Optimization: Global, Multi-Objective, Statistical</i>
Pigeon, Mélusine	PA1.6	3354	<i>Miniaturised Magnetic Antenna for Wireless Implanted Medical Device</i>
Pijoan, Joan	CS38.3	120	<i>Reconfigurable Architecture in a 130 x 80 mm² PCB with Antenna Booster Element for Multiband Operation in IoT Devices</i>
Pikushina, Alena	CS2.6	189	<i>Reproducibility Studies of Instantaneous and 6-Minute Average Exposure Measurements Around 5G Massive-MIMO Base Stations</i>
Pillay, Aritha	CS4.4	3189	<i>The Hydrogen Intensity Real-Time Analysis eXperiment: Overview and Status Update</i>
Pimenta, Ravel	PA6.7	2238	<i>Metasurface-Based Bessel-Beam Launcher with 100λ Non-Diffractive Range</i>
	A01a.3	2938	<i>Generation of Non-Diffractive Bessel Beams for Near-Field Links Applications Using Meta-Axicons</i>

Pimienta-del-Valle, Domingo	P09.1	2634	<i>Variability of Rain Attenuation at Millimeter Waves Due to Fluctuations of the Drop Size Distribution</i>
	P09.2	2639	<i>Rain Attenuation at Millimeter Waves in Different Climatic Zones Estimated from Drop Size Distributions</i>
	P10a.2	2977	<i>Cloud Attenuation in the Q Band: Estimation from Experimental Data of Excess Attenuation</i>
Pinho, Pedro	A17.5	3759	<i>The Novel Method for Deployable Parabolic Reflector Based on Uchiwa Origami</i>
Pino, Antonio	A06a.5	3041	<i>Multibeam Compact Dual Reflectarray Antenna for High-Throughput Satellites in Ka-Band</i>
Pino, Marcos	CS8.5	2899	<i>Dual-Resonance SIW-Based Reflectarray Unit Cell for Broadband Applications</i>
	A06a.1	3021	<i>Large and Deployable Multi-Faceted Antennas Based on Single-Layer Reflectarrays</i>
	A06b.2	3291	<i>Experimental Validation of Reflectarray-Based Base Station Antenna for Simultaneous Front- and Radio Back-Haul Links in mm-Wave Frequencies</i>
Pintos, Jean-François	A13.1	1949	<i>Ultra-Miniature Circularly Polarized Antenna with Omni-Directional Pattern for Sat-IoT</i>
	PA8.9	2306	<i>Whip Antenna Miniaturization at VHF Band Using Magneto-Dielectric Materials</i>
Pires, Tomas	E13.1	270	<i>Ultrahigh Sensitive Terahertz Metasurface with 2D MoS₂ for Refractive Index Biosensing</i>
Pirinoli, Paola	A10.3	3074	<i>Curved Electromagnetic Skins for Urban Scenarios</i>
	A06b.1	3287	<i>Folded Dielectric Reflectarray with Spherical Polarizer</i>
Pisani, Alice	CS4.4	3189	<i>The Hydrogen Intensity Real-Time Analysis eXperiment: Overview and Status Update</i>
Pistorius, Stephen	CS24a.3	731	<i>Evaluating System Design in Breast Microwave Sensing: Data and Image Quality in Multiple Systems</i>
	P03.4	1543	<i>Neural Network Based Microwave Tumour Detection Using Breast Pairs</i>
Pizarro, Francisco	CS9b.4	526	<i>Design of Modulated Dielectric Leaky-Wave Antennas for Efficient Bessel-Beam Synthesis</i>
	A25.4	3100	<i>3D-Printed Circular Polarized Dielectric Resonator Antenna with Enhanced Axial Ratio Bandwidth Using Anisotropic Material</i>
Player, Grace	CS45.1	1799	<i>MR/Microwave Tomography Integrated Breast Cancer Imaging</i>
Pleros, Nikos	PA3.21	3483	<i>MIMO Signals Processing Utilizing Optical Crossbar Linear Operator</i>
Plets, David	CS23b.2	1994	<i>Path Loss Modeling for Air-To-Ground Channels in a Suburban Environment</i>
Podilchak, Symon	CS9b.2	516	<i>Mechanically Re-Configurable Leaky-Wave Antenna for Fix-Frequency Beam Scanning</i>
	E06b.4	804	<i>A Reconfigurable Phase Gradient Metasurface Rasorber Offering Enhanced Beam Steering Capability and a Tuneable Transmission Band</i>
	PA8.2	2274	<i>Dual-Polarized Substrate Integrated Waveguide Antenna with High Isolation for Polarimetric Radar</i>

	PP02.7	2520	<i>Electromagnetic Beerline Cleaning Using Radio Frequency Signals</i>
	E09.3	3914	<i>Analysis and Design of a Wideband Jaumann-Like Radar Absorber Offering High Angular Stability and Polarization Insensitivity</i>
	CS48.1	3977	<i>Beamforming Orthogonality in Coupled Directional Modulation Arrays</i>
Pohl, Nils	CS12b.2	4263	<i>Robotic Antenna Characterization System Based on Wideband FMCW Transceiver Modules</i>
Poli, Lorenzo	CS33a.2	3050	<i>Recent Advances in Multiscale-Multiphysics Inverse Scattering</i>
Pollin, Sofie	CS23b.2	1994	<i>Path Loss Modeling for Air-To-Ground Channels in a Suburban Environment</i>
	P10a.5	2992	<i>Dual-Band MmWave Measurements of Human Body Scattering and Blockage Effects Using Distributed Beamforming for ISAC Applications</i>
Pollini, Leonardo	PE2.9	1024	<i>Human- Vs Machine Design of Antennas: Evolution Behavior in Genetic Shape Optimization</i>
Polo, Enrico	PP02.18	2572	<i>Investigating the Interference Induced by NGSO Constellations on GSO System Ground Stations: A Simulation Approach</i>
Polo-López, Lucas	E07.1	1636	<i>Model-Based Deep Learning for High-Dimensional Periodic Structures</i>
Ponti, Cristina	CS45.4	1812	<i>On Enhancing Efficiency of Transmission in Imaging Systems by Wearable Scatterers</i>
Popov, Vladislav	A03b.5	3147	<i>Wireless Re-Configurable Intelligent Surface for Sub 6 GHz 5G Frequency</i>
Portalier, Pierre- Etienne	PA2.1	1052	<i>Leading Edge Conformal ARMA Antenna in X Band</i>
	PA4.11	2150	<i>Pixel Antenna Design for mm-Wave Wireless Communications to Achieve Wide Scanning</i>
Pourmohammadi, Peyman	PA2.11	1101	<i>Multi-Bit Wideband Transmitarray Aperture with Independent Phase and Amplitude Control for High Gain with Low Sidelobe Mm-Wave Applications</i>
	A01a.4	2941	<i>Dual-Polarized OAM Antenna with Frequency and Mode Agility for Intelligent OAM Communications</i>
Pournoori, Nikta	A20.5	3827	<i>Quad-Band Meandered Implantable Planar Inverted-F Antenna for Wireless Brain Health Monitoring</i>
Poveda-García, Miguel	CS9b.2	516	<i>Mechanically Re-Configurable Leaky-Wave Antenna for Fix-Frequency Beam Scanning</i>
	CS36a.2	705	<i>GHz Prism: Frequency-Scanned Antennas to Improve Localization with Separate-Channel Fingerprinting</i>
	CS36a.3	710	<i>Compact Amplitude-Monopulse Microstrip Antenna Design for Wide Field-Of-View Direction Finding</i>
	A08a.1	1883	<i>Efficient Ray-Tracing Approach to Analyze Arbitrarily Shaped Leaky-Wave Antennas Embedded in Lenses</i>
	CS1b.3	4246	<i>A mmWave Leaky-Wave Antenna for Efficiency Enhanced Near-Field Wireless Power Transfer and Communication</i>
Powell, Alex	CS14a.2	4135	<i>Ambient Pressure Responsive Shape-Morphing Electromagnetic Components</i>
Poyanco, Jose-Manuel	CS26b.5	4321	<i>Design of Glide-Symmetric Dielectric Mikaelian Lens Antenna for K/Ka-Band</i>
Principe, Fabio	PA2.15	1119	<i>Feasibility Study of 3D Printed Luneburg Lens Using Fused Deposit</i>

			<i>Material 3D Printing Technology for Ku-Band Application</i>
Prinsloo, David	A18.3	2914	<i>Active Antenna Design for Lunar-Based Detection of Global 21cm-Signals from the Dark Ages</i>
	CS4.1	3176	<i>Analysis of a Small LOFAR Low-Band Test Array Using a Sky Map, Simulated Embedded Element Patterns and Measured LNA-Impedances</i>
Prodhomme, Hugo	CS17b.5	335	<i>RIS-Based Over-The-Air Channel Equalization in Resource-Constrained Wireless Networks</i>
Prudenzano, Francesco	A21.5	1498	<i>Feasibility Investigation on a Low-Cost an Air-Filled Substrate Integrated Waveguide Array Antenna in V-Band</i>
	A25.3	3095	<i>Design and Characterization of a Flexible Fabry-Perot Antenna Fabricated Using Conductive Inkjet Printing</i>
Psychogiou, Dimitra	PE2.10	1027	<i>FDTD Modelling of RF Circuits Based on Lumped Components and Transmission Lines Using Modified Telegrapher's Equations</i>
Pubill-Font, Maria	CS10.1	850	<i>Efficient Ray-Tracing Model for Generalized 2D Dielectric Lenses Combined with Arrays</i>
Punzet, Stefan	CS32.3	1443	<i>In-Flight Calibration of the Measurement System for UAV-Based Near-Field Antenna Measurements</i>

Q

Qamar, Muhammad	PA1.9	3366	<i>A Compact Implantable Camera Integrated MIMO Antenna with Polarization Diversity for Wireless-Capsule-Endoscopy Applications</i>
Qhoboshiyane, Isibabale	CS4.4	3189	<i>The Hydrogen Intensity Real-Time Analysis eXperiment: Overview and Status Update</i>
Qi, Kaiqiang	PA2.16	1123	<i>Study on CFM Method for Beam Compensation of Array-Fed Space-Borne Reflector Antennas</i>
Qian, Long	CS15.5	4019	<i>A Digital Beamforming Antenna for Space Based Solar Power Transmitting Array</i>
Qian, Lu	A13.4	1961	<i>Low Profile Wideband Dual-Polarized Antenna Array for Ku/K/Ka-Band Satcom Applications</i>
Qian, Zhongyu	PP01.18	1423	<i>Channel Characterization and Modeling for Wireless MIMO Communication Systems in Intersection Scenarios</i>
Qiao, Yuanyuan	P01.5	3852	<i>Analysis of 5G Channel Characteristics Based on Ray Tracing for the Straight Tunnel of High Speed Railway</i>
Qin, Fan	PA4.2	2109	<i>A Fully Additive Manufactured D-Band SIW Antenna</i>
	PA6.5	2231	<i>A Pattern-Reconfigurable Water Antenna Based on the Fabry-Perot Cavity</i>
Qin, Peiyuan	CS6a.3	204	<i>Wideband Transmissive Metasurfaces for Sub-THz Frequency-Dependent Beam Scanning</i>
	CS6b.6	509	<i>3D-Printed Multi-Beam Flat Lens Antenna System</i>
Qin, Tao	PE1.17	1303	<i>A Novel Metasurface Inverse Design Based on Back Propagation Neural Network</i>
Qin, Xu	PA8.4	2283	<i>An IQ Modulator-Based RF Phase Shifter</i>
Qin, Yufeng	CS35a.4	1697	<i>Time-Varying Channel Measurement and Analysis at 105 GHz in an Indoor Factory</i>
Qing, Jie	PP01.2	1352	<i>Analysis of the Capacity and Energy Efficiency of Metallodielectric</i>

			<i>Surface Wave Links Operating Beyond Y Band</i>
Qing, Xianming	PE2.7	1015	<i>Non-Uniform Metamaterial Mushroom Antennas via a Genuine Multi-Objective Bayesian Optimization Method</i>
	PA2.2	1056	<i>Compact Wideband Circularly Polarized Antenna Array for Satellite Applications</i>
	PA2.6	1079	<i>Modular Ka-Band Transmit Phased Array Antenna for SATCOM Applications</i>
Qiu, Jinghui	PA7.7	1190	<i>A Brief Analysis of the Latest Research Progress and Future Direction of Low-Frequency Transmitting Antenna</i>
Qiu, Shuang	PA7.7	1190	<i>A Brief Analysis of the Latest Research Progress and Future Direction of Low-Frequency Transmitting Antenna</i>
Qiu, Tiancheng	A01a.5	2945	<i>Low-Profile Multibeam Beam-Scanning Antenna for Vehicular Radar Systems</i>
Qiu, Tianke	CS17a.2	6	<i>3D Method-Of-Moment Design of Huygens' Metasurfaces</i>
Qiu, Yanheng	PP02.5	2510	<i>Measurement-Based Channel Characteristics for Air-To-Ground Communications Under Rural Areas</i>
Qu, Shi-Wei	PA5.1	3495	<i>High-Gain Shared-Aperture Patch Phased Array and Reflectarray Antenna</i>
	A15b.2	4331	<i>Ultra-Wideband Wide-Scanning Dual-Polarized Vivaldi Antenna Unit with Novel Pendulum-Shaped Slots</i>
Quatresooz, Florian	P04a.2	772	<i>Improvements of Scintillation Modelling from Radiosonde Observations in the Arctic Region</i>
Queguiner, Lorette	CS27.3	1579	<i>Theoretical Insights and Engineering of Wireless Body-Implanted Bioelectronics</i>
Querol, Jorge	PA2.5	1074	<i>Genetic Algorithm-Based Beamforming in Subarray Architectures for GEO Satellites</i>
	CS19b.4	4295	<i>Supervised Learning Based Real-Time Adaptive Beamforming On-Board Multibeam Satellites</i>
Quevedo-Teruel, Oscar	CS10.1	850	<i>Efficient Ray-Tracing Model for Generalized 2D Dielectric Lenses Combined with Arrays</i>
	CS10.2	855	<i>Design of a Dielectric Lens Using a Ray-Tracing Model for Satellite Communications</i>
	E10a.3	1850	<i>Analysis of the Dispersion Diagrams of 3D Cubic Periodic Arrangements of Metallic Spheres</i>
	A08a.1	1883	<i>Efficient Ray-Tracing Approach to Analyze Arbitrarily Shaped Leaky-Wave Antennas Embedded in Lenses</i>
	A07.2	2664	<i>Metal-Only Additive-Manufactured Geodesic Lens Antennas for the mmWave Band</i>
	A22.1	2772	<i>Experimental Validation of Ray-Tracing and Physical-Optics Model for Geodesic H-Plane Horn Antennas</i>
	A22.3	2781	<i>Tailoring the Performance of Geodesic Lens Antennas by Defining Their Footprint</i>
	A22.5	2791	<i>Ray-Tracing Model for the Design and Efficiency Calculation of a Monolithic Geodesic Lens Array Antenna</i>
	CS19a.4	4081	<i>Combined Ray-Tracing and Physical-Optics Model for Flat-Aperture</i>

PPW Lens Antennas

	CS26a.3	4098	<i>Higher Symmetries in Hexagonal Periodic Structures</i>
	CS26a.5	4105	<i>Efficient Numerical Computation of Dispersion Diagrams for Glide-Symmetric Periodic Structures with a Hexagonal Lattice</i>
Quint, Alexander	A05.3	1828	<i>110 to 170 GHz High-Gain Antenna with Embedded Surface Mount Short Horn and Baseband PCB Horn Antenna</i>

R

Rabbani, Muhammad	A09b.3	882	<i>Ultra-Low-Loss Millimeter Wave Beam Scanning Antenna Using Piezoelectric Actuation</i>
	PE3.3	2369	<i>Metamaterial-Based Ku-Band Flat-Panel High-Gain Antenna for Satcom Applications</i>
Radovic, Danilo	CS35b.2	1908	<i>Stationarity of Multiband Channels for OTFS-Based Intelligent Transportation Systems</i>
Rafique, Umair	PA7.14	1222	<i>UWB Circular Metal Mesh Transparent Antenna</i>
Raghib Hokmabadi, Hossein	A15b.5	4345	<i>Dual UWB Antennas on AoA Anchor Node</i>
Rahimian Omam, Zahra	PE1.11	1279	<i>Compact Polarization Converter on a Thin Ferrite-Based Metasurface for Enhanced 5G Wireless Communication</i>
Rahman, Muhammad Mahboob Ur	PP02.2	2495	<i>Pathloss-Based Non-Line-Of-Sight Identification in an Indoor Environment: An Experimental Study</i>
Rahola, Jussi	A03a.3	2872	<i>The Role of Ground Currents in the Co-Simulation of Matching Components and Layout Models in Matching Circuit Optimization</i>
Rains, James	CS17a.6	24	<i>RIS-Enhanced MIMO Channels in Urban Environments: Experimental Insights</i>
Rajo-Iglesias, Eva	CS9b.4	526	<i>Design of Modulated Dielectric Leaky-Wave Antennas for Efficient Bessel-Beam Synthesis</i>
	A08b.2	2086	<i>High Efficiency Groove Gap Waveguide Leaky Wave Antenna Array with Flat Top Radiation Pattern</i>
	CS26a.2	4094	<i>On the Use of Resonant Cavities for Experimental Validation of the Dispersion Diagram of Periodic Glide Symmetric Waveguides</i>
	CS26b.5	4321	<i>Design of Glide-Symmetric Dielectric Mikaelian Lens Antenna for K/Ka-Band</i>
Ramaccia, Davide	E08.2	1868	<i>Reflective Intelligent Surfaces: Reducing Complexity by Controlling the Illuminating Field</i>
	E08.5	1880	<i>Static and Reconfigurable Phase-Gradient Metasurfaces for Antenna Applications</i>
	PA4.10	2147	<i>Analysis and Design of Robust Reconfigurable Intelligent Surfaces Using a Statistical Approach</i>
	E12.3	2829	<i>Time-Modulated Metasurface-Based System for the Generation of False Radar Targets</i>
	A10.2	3071	<i>Analysis and Design of Metasurface Antennas Based on Temporal Metastructures</i>
Raman, Sujith	CS27.1	1571	<i>Link Budget Estimation for Implantable Antennas: From In-Body Coupling to Free-Space Radiation</i>
Ramirez Arroyave,	A17.2	3744	<i>Series-Fed Loop Antenna Array Deployable by a Scissors Mechanism</i>

German	CS1b.5	4254	<i>Plug-In Plug-Out Multibeam Dielectric Rod Antenna for Target Dedicated mm-Wave RF-WPT Applications</i>
Ramírez-Arroyo, Alejandro	PP01.4	1360	<i>A Study on W-Band Frequency Attenuation in the Presence of Human Blockage</i>
Ramos, Amélia	PA4.5	2124	<i>A Simple Technique to Maximize Isolation in Compact mmWaves Antenna Arrays</i>
Rampa, Vittorio	CS29.2	3792	<i>Physics-Informed Generative Neural Networks for RF Propagation Prediction with Application to Indoor Body Perception</i>
Rananjason, Valérie	PA2.17	1128	<i>Dual-Polarized Connected-Slot Array Technological Demonstrator Targeting a 5:1 Bandwidth</i>
Randazzo, Andrea	CS45.5	1815	<i>Brain Stroke Microwave Diagnostics in Children Through a Nonlinear Inverse-Scattering Technique</i>
	CS33a.1	3045	<i>A Mild Data-Driven Approach Based on a Lebesgue-Space Inversion Procedure for Microwave Imaging Applications</i>
Rangaiah, Pramod	PP03.7	3615	<i>SINTEC Comparative Body-Centric Communication Study: Bluetooth Vs Fat-Intrabody Communication</i>
Rappaport, Carey	CS44a.3	754	<i>A Wideband Reflector-Based Mm-Wave/THz Nearfield Line Scanner for Rapidly Sensing Materials in Envelopes</i>
Raptis, Savvas	E07.5	1653	<i>An Accurate Semi-Analytical Model for Periodic Tunable Metasurfaces Electromagnetic Response</i>
Räsänen, Mohamed	CS40b.1	1969	<i>Small On-Metal Passive UHF RFID Transponders with Long Read Ranges</i>
Rashdan, Ibrahim	CS35a.5	1702	<i>Link-Level Performance of Vehicle-To-Vulnerable Road Users Communication Using Realistic Channel Models</i>
Rashed Mohassel, Jalil A	PE2.14	1044	<i>Tunable Rectangular Waveguide Bandpass Filter Based on Plasma Technology</i>
Rasilainen, Kimmo	CS12a.3	4053	<i>Characterisation of a D-Band Horn Antenna: Comparison of Near-Field and OTA Measurements</i>
Raspa, Giovanni	CS45.3	1808	<i>Preliminary Clinical Trial Results of MammoWave in the Context of RadioSpin Project</i>
Rasti Boroujeni, Soroush	PP03.19	3665	<i>Microwave Sensor for Detection of Optical Transparent Foreign Body in Soft Tissue: Eye</i>
Rather, Nadeem	PP02.17	2567	<i>Machine Learning Approaches for EM Signature Analysis in Chipless RFID Technology</i>
Ratni, Badreddine	E13.5	284	<i>Transmissive-Type Metagratings with Few Meta-Atoms for Beam Splitting</i>
	E06b.2	797	<i>Direction-Of-Arrival Estimation by a Programmable Metasurface</i>
	CS14a.5	4145	<i>Time-Modulated Metasurface for Harmonic Signals Frequency Conversion</i>
Raumonen, Pasi	CS13.4	1563	<i>Enabling Living Spaces Through Customizable NFC-Enabled Smart Table System</i>
Ray, KP	PA7.1	1164	<i>Inconsistency in Modes of Circular Microstrip Antennas and Its Rectification</i>
Raza, Muhammad Usman	A03a.5	2881	<i>Reducing Mutual Coupling in 2x2 MIMO Circularly Polarized Patch Antenna Array Using Reflecting Polarization Conversion Metasurface</i>

Razavi, Aidin	CS47.5	430	<i>In-Field Measurement of Total Radiated Power from Active Antenna Arrays</i>
Reddy, CJ	CS42a.5	156	<i>Antenna Coupling Evaluation in Arrays and Complex Structures Using Measured Sources and Simulations</i>
Reddy Sura, Penchala	PA1.2	3336	<i>Dual-Band 3-D MIMO Antenna for Deep Tissue Devices</i>
Refregier, Alexandre	CS4.4	3189	<i>The Hydrogen Intensity Real-Time Analysis eXperiment: Overview and Status Update</i>
Regmi, Ankit	CS29.3	3797	<i>Computer Vision Enabled Sub-THz Radio Channel Characterization of Dynamic Objects</i>
Reilly, Les	CS4.5	3194	<i>CSIRO Radio Astronomy Receiver Update - Ultra Wideband and Phased Array Feeds</i>
Reimer, Tyson	CS24a.3	731	<i>Evaluating System Design in Breast Microwave Sensing: Data and Image Quality in Multiple Systems</i>
Reinhardt, Carla	CS5b.4	378	<i>Channel Measurements in Workspace with Robotic Manipulators at 300 GHz and Recent Results</i>
Reis, João	P10b.4	3259	<i>Wind-Induced Backscatter Clustering from Vegetation at W-Band</i>
Rekkas, Vasileios	PP03.5	3605	<i>Modeling Received Power from 4G and 5G Networks in Greece Using Machine Learning</i>
Reniers, Ad	CS47.1	416	<i>Over-The-Air Measurements for mm-Wave Body-Centric Wireless Communication</i>
	PM2.8	2459	<i>Uncertainties in the Estimation of the Gain of a Standard Gain Horn in the Frequency Range of 90 GHz to 140 GHz</i>
	PM2.11	2472	<i>Quiet-Zone Profiling in a mmWave Spherical Anechoic Chamber: An Evaluation Approach</i>
	P06.1	2727	<i>Localization of a Nasogastric Feeding Tube Using High-Frequency Harmonic Radar - a Feasibility Study</i>
Renker, Matthias	P02.4	3777	<i>Measuring and Modelling the Scattering Parameters of the Wet Radome of the Swiss Weather Radars</i>
Renner, Stephan	CS21.1	2706	<i>Imaging Radar Frontend with SIW Feeding Networks</i>
Resteghini, Laura	P09.4	2649	<i>Rain Attenuation at mmWave and Optical Bands from Visibility and Rainfall Intensity Measurements</i>
Retana-Montenegro, Edwin	CS4.4	3189	<i>The Hydrogen Intensity Real-Time Analysis eXperiment: Overview and Status Update</i>
Rezaee, Behrooz	PA7.15	1226	<i>A Novel Reconfigurable Planar Switched-Beam Filtenna with 360-Degree Beam Scanning</i>
	PA7.16	1229	<i>Single Layer Cavity-Backed Filtenna with Ultra-Wide Out-Of-Band Suppression</i>
Rezaei Golghand, Mehrdad	PE3.5	2379	<i>Analysis of the Interaction of Laser-Induced Solid-State Plasma with Electromagnetic Waves in Silicon Waveguides at 67-220 GHz</i>
Ribeiro, Diogo	PA5.3	3503	<i>Characterization of All-Metal Multi-Feed Antenna for High Power Applications</i>
Ribeiro, Lucas	A28.2	3719	<i>A High-Isolation Dual-Band Base Station Antenna Design for Full Duplex Technologies</i>
	A28.4	3729	<i>Ground Base Station Antenna Design for Air-To-Ground Communications</i>

Ribeiro, Raul	E02b.4	3279	<i>A Higher-Order Spectral Element Method to Model Eccentric Anisotropic Two-Layer Waveguides via Conformal Transformation Optics</i>
Ricci, Marco	CS11.1	1616	<i>AI-Assisted Design and Experimental Testing of a Compact UWB Antenna for the Inspection of Food and Beverage Products</i>
	CS33a.3	3054	<i>Advancements in Broadband Electromagnetic Sensing for Food Quality Control</i>
	CS19b.3	4292	<i>Automatic MoM Source Integral Quadrature Selection via a Machine Learning Approach</i>
Rico-Fernandez, Jose	A07.2	2664	<i>Metal-Only Additive-Manufactured Geodesic Lens Antennas for the mmWave Band</i>
	A22.3	2781	<i>Tailoring the Performance of Geodesic Lens Antennas by Defining Their Footprint</i>
	A22.5	2791	<i>Ray-Tracing Model for the Design and Efficiency Calculation of a Monolithic Geodesic Lens Array Antenna</i>
	CS30a.2	3933	<i>Additively Manufactured Waveguide Hybrid Septum Coupler Optimized Using Machine Learning</i>
Riekenbrauck, Ron	CS21.5	2722	<i>Effects of Bumper Integration on Low-, Mid-, and High-Resolution Imaging Radars</i>
Riera, Jose	PP02.20	2582	<i>Comparison Between ERA5 Cloud Parameters and Rainfall Rate in Madrid</i>
	P09.1	2634	<i>Variability of Rain Attenuation at Millimeter Waves Due to Fluctuations of the Drop Size Distribution</i>
	P09.2	2639	<i>Rain Attenuation at Millimeter Waves in Different Climatic Zones Estimated from Drop Size Distributions</i>
	P10a.2	2977	<i>Cloud Attenuation in the Q Band: Estimation from Experimental Data of Excess Attenuation</i>
Riese, Nico	CS12a.1	4043	<i>A High-Precision Approach to Eliminate Positioning Errors in Radar Calibrations</i>
Righero, Marco	CS42b.1	439	<i>An Antenna Measuring System Based on a Cable Suspended Dolly and Inverse Source</i>
Risman, Per Olov	E01.3	2024	<i>Estimating the Signal Strength for Microwave Breast Cancer Detection with a Magnetic Near-Field Applicator in Air</i>
Riva, Carlo	PP02.11	2538	<i>AlphaSat Ka-Band and Q-Band Receiving Station in Rome: Measurements and Data Analysis</i>
	P09.3	2644	<i>Ka-Band Rain Attenuation Derived from a MEO Satellite Constellation</i>
	P09.4	2649	<i>Rain Attenuation at mmWave and Optical Bands from Visibility and Rainfall Intensity Measurements</i>
	P10b.3	3254	<i>Exploiting Numerical Weather Prediction Data for Radiopropagation Modeling of SatCom Links</i>
Rizzi, Francesco	PA1.3	3340	<i>Eco-Friendly and Conformable PIFA Based on PEDOT: PSS and a Sustainable Chitosan Substrate for 5G Communications</i>
Robert, Jerome	PE2.3	999	<i>Management of Radiofrequency Compatibility on Aircraft</i>
Roberts, Paul	CS4.5	3194	<i>CSIRO Radio Astronomy Receiver Update - Ultra Wideband and Phased Array Feeds</i>

Roblin, Christophe	PP02.3	2500	<i>Feasibility Study of Joint Modeling of Environmental and Morphological Effects for WBAN</i>
Rocca, Paolo	CS22b.2	3114	<i>A Quantum Optimization Method for Antenna Array Thinning</i>
Rocha, Armando	PP02.9	2528	<i>Synthesis of Drop Counter Rain Rate from a Tipping Bucket Rain Gauge</i>
	PP02.10	2533	<i>Designing a Data Pre-Processing Tool for MEO Satellites Propagation Measurements</i>
	P09.3	2644	<i>Ka-Band Rain Attenuation Derived from a MEO Satellite Constellation</i>
Rodríguez, Mauricio	PP01.7	1375	<i>Path Gain Measurements and Models at 60 GHz in Street Canyons from Rooftop Sites for Outdoor Coverage</i>
Rodríguez, Vince	M5.1	537	<i>On the RF Absorber Coverage of Antenna Under Test Positioners</i>
Rodríguez Varela, Fernando	CS42a.4	151	<i>Planar Near-Field Phaseless Measurements Using Multi-Probe Arrays</i>
Rodríguez-Cano, Rocio	PM2.5	2446	<i>Dielectric Characterization of Materials at 5G mm-Wave Frequencies</i>
Rodríguez-Duarte, David	CS24a.1	724	<i>Advancements in the Experimental Validation of a Wearable Microwave Imaging System for Brain Stroke Monitoring</i>
	CS33b.1	3309	<i>Nonlinear Correction of the Direct Inverse Problem Solution in Real-Time Imaging</i>
Rodríguez-Piñeiro, José	CS35a.3	1692	<i>AttentionRNN: Novel Propagation Channel Time-Domain State Predictor</i>
	CS23a.5	1794	<i>HRPE-Enhanced AI-Based 5G Indoor Localization in Presence of Specular and Dense Multipaths</i>
Rodríguez-Vaqueiro, Yolanda	A06a.5	3041	<i>Multibeam Compact Dual Reflectarray Antenna for High-Throughput Satellites in Ka-Band</i>
Roederer, Antoine	CS6a.6	216	<i>Development of a Circuit-Type Multiple-Agile Beamforming and Interference Mitigation Network</i>
Roemhild, Martin	M3.3	2595	<i>Dielectric Characterization of Adhesives for THz Packaging in WR6.5, WR3.4 and WR2.2 Bands</i>
Rogier, Hendrik	CS2.5	184	<i>New Hybrid Ray-Tracing/FDTD for EMF Exposure in 6G Networks Using Semantically Classified Google Earth Photogrammetry with Measurement Validation</i>
Rolfes, Ilona	CS12b.2	4263	<i>Robotic Antenna Characterization System Based on Wideband FMCW Transceiver Modules</i>
Rolo, Luis	CS42b.1	439	<i>An Antenna Measuring System Based on a Cable Suspended Dolly and Inverse Source</i>
	CS39a.3	618	<i>Full Wave Modelling and Design of a Baffle for the HERTZ 2.0 Compact Antenna Test Range</i>
Ronca, Alessandra	E01.2	2019	<i>Assessment of the Feasibility of Breast Lesion Detection with Contrast Source Inversion for Microwave Tomography: A Virtual Experiment</i>
Roosefid, Raha	A13.2	1954	<i>Compact Circularly Polarized Antenna Based on Gapwaveguide for SATCOM Applications</i>
Roqui, Julian	CS38.6	132	<i>Estimating the Achievable Efficiency and Bandwidth of Small Terminal-Integrated Inverted-F Antennas Using Machine Learning</i>
Roset, Marti	CS35a.1	1683	<i>Design and Validation of a Wireless Network for Intra-Train Communications</i>

Rossi, Andrea	CS45.5	1815	<i>Brain Stroke Microwave Diagnostics in Children Through a Nonlinear Inverse-Scattering Technique</i>
Rossignol, Sylvie	CS3.6	316	<i>Use of Ecofriendly Geopolymer Ceramics in Antenna Design and Microwave Applications</i>
Rotenberg, Samuel	CS9b.2	516	<i>Mechanically Re-Configurable Leaky-Wave Antenna for Fix-Frequency Beam Scanning</i>
	PA8.18	2344	<i>Bandwidth Manipulated Leaky-Wave Antenna Using a Sinusoidal Ridge in Folded Substrate Integrated Waveguide</i>
Roth, Thomas	CS22a.1	2841	<i>Development of an Analytical Quantum Full-Wave Solution for a Transmon Qubit in a 3D Cavity</i>
Rouhi, Kasra	CS17b.6	340	<i>Wave-Controlled Biasing of RIS for Multi-Beam Scattering Pattern Generation</i>
Roumpos, Ioannis	PA3.21	3483	<i>MIMO Signals Processing Utilizing Optical Crossbar Linear Operator</i>
Roush, Peter	CS4.5	3194	<i>CSIRO Radio Astronomy Receiver Update - Ultra Wideband and Phased Array Feeds</i>
Rousseau, Regis	PP03.1	3589	<i>Wideband Characterization of Wireless Power Transfer in Ventilation (HVAC) Ducts for the Internet of Things and Smart Buildings</i>
Roux, Jean-Francois	E05.1	2036	<i>From Bulk Toward Micro-Structured TiO₂ Ceramics for All-Dielectric Metamaterials at Terahertz Frequencies</i>
Roveda, Giuseppe	P09.5	2654	<i>Predicting Rain Attenuation at D Band for 6G Backhaul Link Design: A Frequency Scaling Approach</i>
Rubab, Naila	PM2.11	2472	<i>Quiet-Zone Profiling in a mmWave Spherical Anechoic Chamber: An Evaluation Approach</i>
Rubæk, Tonny	A18.1	2904	<i>Uncertainty Quantification for the Reflector Antenna in the Copernicus Imaging Microwave Radiometer</i>
Ruehli, Albert	E02a.5	3016	<i>Improved PEEC Modeling of Antennas Through Time-Dependent Partial Elements</i>
Ruiter, Mark	CS4.1	3176	<i>Analysis of a Small LOFAR Low-Band Test Array Using a Sky Map, Simulated Embedded Element Patterns and Measured LNA-Impedances</i>
Ruiz-Cruz, Jorge	A27a.1	632	<i>Full-Metal Single-Block Antenna Arrays with Waveguide Corporative Feeding Networks at Ka and V Bands</i>
	E10b.3	2069	<i>Proving the Circular Polarization of the Fundamental Modes in Rotationally Symmetric Waveguides</i>
Ruiz-García, Jorge	CS16.3	570	<i>All-Metal Perfectly-Matched Metamaterials</i>
Rytir, Martin	P04a.2	772	<i>Improvements of Scintillation Modelling from Radiosonde Observations in the Arctic Region</i>
Ryynänen, Jussi	CS37b.2	348	<i>Crack Stop as a Coupling Element Between an IC Chip and Antenna</i>
Ryynänen, Kaisa	CS37b.2	348	<i>Crack Stop as a Coupling Element Between an IC Chip and Antenna</i>
Rzymowski, Mateusz	PA4.15	2169	<i>Low-Cost 3-D Printed Lens Antenna for Ka-Band Connectivity Applications</i>
	PA8.15	2332	<i>Miniaturized and Lightweight ESPAR Antenna for WSN and IoT Applications</i>

S

S. Jr., Arismar	A04.1	1458	<i>Implementation of a Novel Triband Antenna Array in a FR1/FR2 5G-NR</i>
-----------------	-------	------	---

			System
Saabe, Wissam	A12a.3	1715	<i>Behavioral Models for the Cosimulation and Optimization of Active Electronically Scanned Arrays</i>
Saad, Rola	A27b.5	845	<i>Flexible Phase-Reconfigurable Branch Line Coupler for Millimeter-Wave Phased Array Antenna</i>
	PA3.4	3410	<i>A 2x2 Dual-Band Open Loop Array with Circular Polarisation</i>
	CS14a.1	4132	<i>Enabling Shape Morphing Communications at mmWave with Spray on Antenna Arrays</i>
Saavedra-Melo, Miguel	CS17b.6	340	<i>Wave-Controlled Biasing of RIS for Multi-Beam Scattering Pattern Generation</i>
	CS26a.2	4094	<i>On the Use of Resonant Cavities for Experimental Validation of the Dispersion Diagram of Periodic Glide Symmetric Waveguides</i>
Saberkari, Alireza	E01.1	2014	<i>Optimal Design of Planar Micro-NMR Coils for High Signal-To-Noise Ratio</i>
Sabra, Ahmad	CS3.5	311	<i>Exploring PLA/Flax Substrates for Antenna Applications: Assessing Moisture, Temperature and Dielectric Constant Homogeneity</i>
Saccardi, Francesco	CS42a.4	151	<i>Planar Near-Field Phaseless Measurements Using Multi-Probe Arrays</i>
	CS2.4	180	<i>Advanced Post-Processing Technique to Evaluate Specific Absorption Rate (SAR) for a Standard Dipole Antenna</i>
	CS5b.3	374	<i>Industrial Design Validation for a Plane Wave Generator at 28GHz</i>
	M5.2	542	<i>Uncertainty Analysis of Linear Multi-Probe Array Systems for Fast Antenna Measurements</i>
	CS41.2	3225	<i>VHF/UHF Antenna Measurements Based on Multi Probe Array Technology</i>
Sacco, Giulia	CS27.3	1579	<i>Theoretical Insights and Engineering of Wireless Body-Implanted Bioelectronics</i>
Sacco, Giulia	A08a.3	1893	<i>Frequency Scanning Leaky-Wave Antenna for On-Body Radar: Design and Conformal Analysis</i>
Sadeghikia, Fatemeh	PE2.14	1044	<i>Tunable Rectangular Waveguide Bandpass Filter Based on Plasma Technology</i>
Sagsveen, Bendik	A17.3	3749	<i>Design and Test of a UHF Deployable Conical Log Spiral Antenna for Small Satellites</i>
Saha, Dipankar	PE1.7	1265	<i>Design of a Concentric Circular Holographic Metasurface Using Hexagonal Anisotropic Unit-Cell for Wireless Communications</i>
Saha, Shimul	PM2.10	2469	<i>Assessing Performance of Transparent Conductive Films for Microwave Industrial Applications</i>
Sahu, Sidhartha	A03b.4	3142	<i>High Gain and Dual Band SIW-Fed Stacked Conical DRA for 5G NR FR1 Application</i>
Saia, Eduardo	A04.1	1458	<i>Implementation of a Novel Triband Antenna Array in a FR1/FR2 5G-NR System</i>
Saikia, Mondeep	PE3.2	2364	<i>Polarization Insensitive Broadband Frequency Selective Resorber with Improved Selectivity for Stealth Applications</i>
Saisa-ard, Siraphop	P04b.1	965	<i>Grid-Based Shadowing Gain Modeling for Handling Dynamic Objects in Wireless Channel Emulation</i>
Sakakibara, Kunio	A27a.4	646	<i>Mechanical/Electrical Hybrid 2-Dimensional Beam Scanning Cylindrical</i>

			<i>Dielectric Lens Antenna</i>
Sakamoto, Hiraku	PA2.8	1088	<i>Design of Reconfigurable Reflectarray Antennas on Flexible Substrates with Varactor Diodes Mounted on Slot-Coupled Microstrip Lines</i>
Sakif, Mustasin	CS13.4	1563	<i>Enabling Living Spaces Through Customizable NFC-Enabled Smart Table System</i>
Sakovsky, Maria	CS14b.2	4353	<i>Multistable Structures for Deployable and Reconfigurable Antennas</i>
Saliwanchik, Benjamin	CS4.4	3189	<i>The Hydrogen Intensity Real-Time Analysis eXperiment: Overview and Status Update</i>
Salmi, Albert	CS38.1	112	<i>Improving Scan Gain of Sparse Vivaldi Array with Parasitic Scatterers</i>
Salomon, Christoph	E01.3	2024	<i>Estimating the Signal Strength for Microwave Breast Cancer Detection with a Magnetic Near-Field Applicator in Air</i>
Salous, Sana	CS5a.4	71	<i>Indoor Channel Characterization Based on Directional Measurements at 140 GHz</i>
	CS43a.2	3957	<i>Millimeter-Wave and Sub-THz Channel Measurements and Characterization Analysis in a Street Canyon Scenario</i>
Salucci, Marco	CS20a.5	104	<i>Recent Advances on Multi-Scale Wave Manipulation Through Reconfigurable Intelligent Surfaces</i>
	CS17b.1	320	<i>On the Design of Static Passive Skins for Next Generation Fixed Wireless Access Applications</i>
	CS33a.2	3050	<i>Recent Advances in Multiscale-Multiphysics Inverse Scattering</i>
Samanta, Gopinath	CS27.4	1584	<i>A Compact Wideband Biocompatible Circularly Polarized Implantable Flexible Antenna for Biomedical Applications</i>
Sammut, Charles	CS24b.3	928	<i>Analysis of Return Loss with an Uncooled Coaxial Monopole Antenna During Microwave Ablation</i>
Sampath, Ajith	CS4.4	3189	<i>The Hydrogen Intensity Real-Time Analysis eXperiment: Overview and Status Update</i>
San Roman Castillo, Ebert	PM1.8	1339	<i>Dielectric Differences in Biological Tissues: A Comparison Between Excised and Non-Excised Tissues Under the Influence of Chemotherapy</i>
Sanchez, Juan	CS43a.4	3967	<i>Propagation Study of Vision-Based RIS Beam Tracking for mmWave Communications</i>
Sánchez Castillo, Jorge	A27a.1	632	<i>Full-Metal Single-Block Antenna Arrays with Waveguide Corporative Feeding Networks at Ka and V Bands</i>
Sánchez-Hernández, David	PM1.5	1327	<i>Minimum Coherence Bandwidth for OFDM Signal Testing in Reverberation Chambers</i>
Sanchez-Olivares, Pablo	A27a.1	632	<i>Full-Metal Single-Block Antenna Arrays with Waveguide Corporative Feeding Networks at Ka and V Bands</i>
	A07.4	2674	<i>Fully Metallic Wideband Lens Design Using a Highly Refractive Glide-Symmetric Unit Cell at W-Band</i>
	A11.3	3162	<i>Pinwheel-Shaped Polarizer for Generating Dual-Circularly Polarized Conical Radiation Patterns in the Ka-Band</i>
Sánchez-Pastor, Jesús	E09.2	3909	<i>Double-Layer Frequency Selective Surface-Based Corner Reflector for Indoor Self-Localization Systems in the W-Band</i>
Sand, Stephan	CS35a.5	1702	<i>Link-Level Performance of Vehicle-To-Vulnerable Road Users Communication Using Realistic Channel Models</i>

Sanderson, David	CS46.1	4215	<i>Dual All Metal Patch Antenna for the HydroGNSS Mission</i>
Santagiustina, Marco	A09b.2	877	<i>Recent Advances in Plasma Surfaces</i>
Santamaria, Luca	CS20b.3	402	<i>Measurements of Reconfigurable Intelligent Surface in 5G System Within a Reverberation Chamber at mmWave</i>
Santer, Matthew	CS14a.4	4142	<i>Optimal Morphing Metasurface Lens for Next Generation RF Sensing and Communications</i>
Santiago-Mesas, Sandra	PM1.8	1339	<i>Dielectric Differences in Biological Tissues: A Comparison Between Excised and Non-Excised Tissues Under the Influence of Chemotherapy</i>
Santonicola, Maria Gabriella	CS28.3	475	<i>Dielectric Characterization of Biological Tissues at Microwave Frequencies Based on Water Content</i>
Sanz-Izquierdo, Benito	PA3.3	3407	<i>A Wearable Open-Ring Dielectric Resonator Antenna with Frequency Reconfiguration</i>
	PA5.9	3529	<i>A Cascaded Resonator Decoupling Network for Two Filtering Antennas with Adjacent Operating Bands</i>
	A02.1	3691	<i>A Low Profile Dual-Band Dual-Polarized Filtering Antenna with No Extra Circuit</i>
Sarbandi Farahani, Hossein	PA7.15	1226	<i>A Novel Reconfigurable Planar Switched-Beam Filtenna with 360-Degree Beam Scanning</i>
Sardinero-Meirás, Ignacio	CS21.3	2712	<i>From mmWave Radar Nodes to Multistatic Arrays: Design Considerations and Applications</i>
Sarigiannidis, Panagiotis	PA3.23	3490	<i>Wideband Aperture-Coupled Array Design for Automotive Radar Applications</i>
	PP03.5	3605	<i>Modeling Received Power from 4G and 5G Networks in Greece Using Machine Learning</i>
Sarkar, Debdeep	PE2.10	1027	<i>FDTD Modelling of RF Circuits Based on Lumped Components and Transmission Lines Using Modified Telegrapher's Equations</i>
Sarrazin, Julien	CS36b.2	901	<i>Direction-Of-Arrival Ambiguities Mitigation in Multibeam Leaky-Wave Antennas</i>
	CS26b.2	4310	<i>Glide-Symmetric Reconfigurable Substrate-Integrated Holey Waveguide</i>
Sartori, Maurizio	P02.4	3777	<i>Measuring and Modelling the Scattering Parameters of the Wet Radome of the Swiss Weather Radars</i>
Sato, Akihiro	PP01.9	1385	<i>Development of a Site-Specific Building Entry Loss Model for High-Rise Buildings</i>
Sauleau, Ronan	A09a.2	683	<i>Sub-Wavelength Anisotropic Unit-Cells for Low-Profile Transmitarray Antennas</i>
Sauleau, Ronan	PA7.8	1195	<i>Shaping the Sub-Reflector of a Ring Focus Antenna for Tailored Beamwidth Applications</i>
Sauleau, Ronan	A21.2	1484	<i>Dual-Linearly Polarized Pillbox Beamformer in Hybrid CNC-PCB Technologies at W-Band</i>
	CS27.3	1579	<i>Theoretical Insights and Engineering of Wireless Body-Implanted Bioelectronics</i>
Sauleau, Ronan	CS7.1	1592	<i>Low Profile and High Gain Folded Transmitarray in Quartz for Radiometry at 310 GHz</i>

Sauleau, Ronan	A16.3	1739	<i>Wideband Beam-Steering Continuous Transverse Stub Array Enabled by a Reflecting Luneburg Lens at Ka-Band</i>
	A12b.4	1941	<i>6:1 Connected Slot Array in PCB Technology</i>
	PA3.12	3442	<i>Shorted Stacked Patch Array for Photonic Beam Steering at mm-Waves</i>
Saurav, Kushmanda	CS26b.3	4314	<i>Thinned Connected Slot Array Design Using Higher Symmetries</i>
	PE3.14	2412	<i>An Angularly Stable Wideband Low Profile Single-Layer Linear to Circular Polarization Converter for Millimeter Wave Satellite Communications</i>
Saurer, Matthias	CS42a.1	136	<i>Inverse Source Solutions with Spectral Filtering</i>
Savazzi, Matteo	PP03.18	3660	<i>Best Practices for Accurate Results Using Numerical Solvers for Microwave Body Screening</i>
Savazzi, Stefano	CS29.2	3792	<i>Physics-Informed Generative Neural Networks for RF Propagation Prediction with Application to Indoor Body Perception</i>
Sawada, Hirokazu	PA7.9	1200	<i>Input Impedance of Radiation Efficiency Deterioration State</i>
Scaccia, Paolo	PP02.13	2547	<i>Radiometeorological Forecasts for Satellite Links Operations: Validation with Measurements from BepiColombo Mission</i>
	P10b.3	3254	<i>Exploiting Numerical Weather Prediction Data for Radiopropagation Modeling of SatCom Links</i>
Scanlon, William	PP03.4	3601	<i>Effect of Wave Polarization in On-Body Propagation for the 2.4, 24 and 60 GHz ISM Bands</i>
Scapatucci, Rosa	CS24a.1	724	<i>Advancements in the Experimental Validation of a Wearable Microwave Imaging System for Brain Stroke Monitoring</i>
	CS24a.2	727	<i>Microwave Imaging for Monitoring Bone Healing Using Magnetic Scaffolds: An Initial Analysis</i>
	E04.2	2689	<i>Contactless 3D Subsurface Imaging: Considerations to Set the Measurement Spacing</i>
	CS33a.3	3054	<i>Advancements in Broadband Electromagnetic Sensing for Food Quality Control</i>
	P02.2	3768	<i>Learning-Based Procedures for Inverse Design of Electromagnetic Devices: A Preliminary Investigation</i>
Scarabosio, Andrea	CS30b.3	4156	<i>Automated Design and Characterization of a Scalar Metasurface Antenna Radiating a Linearly-Polarized Broadside Beam</i>
Scarselli, Chiara	PE1.9	1272	<i>A Compact Fabry-Perot Cavity Antenna with Circular Polarization</i>
Scattone, Francesco	CS5b.3	374	<i>Industrial Design Validation for a Plane Wave Generator at 28GHz</i>
Scazzoli, Davide	CS29.4	3802	<i>Accurate Time Synchronization Exploiting Integrated Sensing and Communication</i>
Schab, Kurt	CS38.5	128	<i>Substructure Modes and Bounds</i>
	CS18.5	3687	<i>Material-Independent Scattering Formulations of Characteristic Modes</i>
	CS30b.1	4149	<i>Overview of State-Of-The-Art Methods for Determining Performance Bounds on Electromagnetic Systems</i>
	CS30b.2	4153	<i>Fundamental Limits on Characteristic Modes</i>
Schenato, Luca	A09b.2	877	<i>Recent Advances in Plasma Surfaces</i>
Schenone, Valentina	CS45.5	1815	<i>Brain Stroke Microwave Diagnostics in Children Through a Nonlinear Inverse-Scattering Technique</i>

	CS33a.1	3045	<i>A Mild Data-Driven Approach Based on a Lebesgue-Space Inversion Procedure for Microwave Imaging Applications</i>
Schettini, Giuseppe	CS45.4	1812	<i>On Enhancing Efficiency of Transmission in Imaging Systems by Wearable Scatterers</i>
Schieler, Steffen	P01.2	3837	<i>Grid-Free Harmonic Retrieval and Model Order Selection Using Convolutional Neural Networks</i>
Schiffarth, Anna-Malin	CS2.2	170	<i>Characterization of Typical Instantaneous Exposure and Usage Scenarios in the Vicinity of 5G Massive-MIMO Base Stations</i>
Schilling, Lisa-Marie	CS42a.6	160	<i>Hybrid Antenna Measurement and Post-Processing for 5G Small Cell Exposure Assessment with Site-Specific Mounting Conditions</i>
	CS2.2	170	<i>Characterization of Typical Instantaneous Exposure and Usage Scenarios in the Vicinity of 5G Massive-MIMO Base Stations</i>
	CS2.6	189	<i>Reproducibility Studies of Instantaneous and 6-Minute Average Exposure Measurements Around 5G Massive-MIMO Base Stations</i>
Schlarb, Holger	PP03.13	3643	<i>Filter Integrated Microstrip 3-Port Power Combiner</i>
Schlosser, Edson	A12b.3	1936	<i>Synthesis of Circularly Polarized Microstrip Planar Array with Cross-Polarization Suppression</i>
Schluper, Patrick	CS12a.4	4058	<i>Use of Model Based Systems Engineering and Development in the Design of a Commercial Nose-Radome Test System Employing a Multi-Axis Cobot</i>
Schmeink, Anke	CS48.2	3982	<i>Cooperative Power Control and Beamforming Design for Multi-Source Enabled Wireless Power Transfer Networks</i>
Schmid, Philipp	P02.4	3777	<i>Measuring and Modelling the Scattering Parameters of the Wet Radome of the Swiss Weather Radars</i>
Schmieder, Mathis	CS43b.2	4173	<i>Comparison of Sub-THz Radio Channel Characteristics at 158 GHz and 300 GHz in a Shopping Mall Scenario</i>
Schneider, Christian	P01.2	3837	<i>Grid-Free Harmonic Retrieval and Model Order Selection Using Convolutional Neural Networks</i>
Schoeman, Marlize	CS42a.5	156	<i>Antenna Coupling Evaluation in Arrays and Complex Structures Using Measured Sources and Simulations</i>
Schoenholz, Bryan	CS12b.5	4278	<i>Robotic Arm-Based Antenna Metrology System for Aerospace Applications</i>
Schreckenbach, Hans	PE1.14	1292	<i>Integral Equation-Based Solver for the Simulation of Metasurface Designs</i>
Schroeder, Werner	A21.4	1493	<i>Assessment of MFE-Based Multiport Waveguide Crossing for Use with Low-Cost, Low-Loss Dielectric Interconnects in Millimeter Wave Arrays</i>
Schuchinsky, Alex	PM1.6	1331	<i>Intermodulation Mitigation Through Surrounding Impedance Manipulation</i>
Schuchinsky, Alexander	M4.4	2964	<i>Quad-Junction Self-Biased Circulator with Wide Operational Bandwidth</i>
Schultze, Alper	CS43b.2	4173	<i>Comparison of Sub-THz Radio Channel Characteristics at 158 GHz and 300 GHz in a Shopping Mall Scenario</i>
Schüßler, Martin	A09b.4	886	<i>Loss Analysis for Compact Liquid Crystal Delay Lines Based on Defective Ground Structures</i>
	E09.2	3909	<i>Double-Layer Frequency Selective Surface-Based Corner Reflector for</i>

			<i>Indoor Self-Localization Systems in the W-Band</i>
Schwarz, Dominik	CS21.5	2722	<i>Effects of Bumper Integration on Low-, Mid-, and High-Resolution Imaging Radars</i>
	CS12a.1	4043	<i>A High-Precision Approach to Eliminate Positioning Errors in Radar Calibrations</i>
Scialacqua, Lucia	CS42a.5	156	<i>Antenna Coupling Evaluation in Arrays and Complex Structures Using Measured Sources and Simulations</i>
	CS2.4	180	<i>Advanced Post-Processing Technique to Evaluate Specific Absorption Rate (SAR) for a Standard Dipole Antenna</i>
	PE2.3	999	<i>Management of Radiofrequency Compatibility on Aircraft</i>
Sciancalepore, Vincenzo	CS20b.4	406	<i>Impedance-Based RIS Channel Model and Optimization in Fast-Fading Environments</i>
	CS34.4	2625	<i>Empirical Validation of the Impedance-Based RIS Channel Model in an Indoor Scattering Environment</i>
Sciarrone, Andrea	CS45.5	1815	<i>Brain Stroke Microwave Diagnostics in Children Through a Nonlinear Inverse-Scattering Technique</i>
Scott, Paul	CS4.2	3181	<i>Mitigating Zenith Blindness from Mutual Coupling in a Sunflower Phased Array</i>
See, Chan	CS11.2	1620	<i>AI-Driven Design of a Quasi-Digitally-Coded Wideband Microstrip Patch Antenna Array</i>
Seetharamdoo, Divitha	E06b.5		<i>Metasurface Solution for Generating 3D-Curved Beams in Road Environments: A Numerical Study</i>
	PE1.13	1288	<i>Multi-Channel Beam-Splitting Metasurface for Millimeter Wave Communication Systems</i>
	CS40a.4	1766	<i>Design of Microstrip UWB Antenna with Full Ground Plane for Wearable Applications</i>
Segovia Vargas, Daniel	PM1.7	1335	<i>Virus Detection in the Microwave Regime Through an Antenna Workbench</i>
Segovia-Vargas, Daniel	PM1.8	1339	<i>Dielectric Differences in Biological Tissues: A Comparison Between Excised and Non-Excised Tissues Under the Influence of Chemotherapy</i>
	PA1.12	3381	<i>Miniaturization of Wireless Power Transfer for Implantable Devices Using Voltage Doubler Rectifier</i>
Segura-Gómez, Cleofás	CS26a.1	4090	<i>Glide-Symmetric SIH Unit Cells Implemented in Parallel-Plate Waveguides at mmWaves</i>
Seidler, Konstanze	A19.2	1508	<i>Polymer-Based Additive Manufacturing of a Complex RF Front-End for New Space Applications</i>
Sekhoasha, Tsepo	CS4.4	3189	<i>The Hydrogen Intensity Real-Time Analysis eXperiment: Overview and Status Update</i>
Semper, Sebastian	CS5a.6	81	<i>Excitation Signal Design for THz Channel Sounding and Propagation Parameter Estimation</i>
	P01.2	3837	<i>Grid-Free Harmonic Retrieval and Model Order Selection Using Convolutional Neural Networks</i>
Sen, Padmanava	PA6.13	2264	<i>On-Chip mm-Wave Artificial Magnetic Conductor Backed Dipole Antenna on Low-Ohmic Substrate</i>

Senic, Jelena	CS5a.1	56	<i>Context-Aware Channel Sounder for AI-Assisted Radio-Frequency Channel Modeling</i>
	CS29.1	3787	<i>AI-Based Environment Segmentation Using a Context-Aware Channel Sounder</i>
Senlis, Oscar	CS16.5	578	<i>Radiation Control by Space-Time-Modulated Anisotropic Impedance Surfaces</i>
Seok, Jae Ho	PP01.12	1399	<i>The Effect of Beam Misalignment in Data Center Environment at 285GHz Band</i>
Seong, Baekjun	CS37b.6		<i>Differentially-Fed Antenna-On-Display Module for SATCOM and Mobile Applications at Ka-Band</i>
Sepúlveda Alancastro, Nelson	CS3.3	303	<i>Reconfigurable Polarisation Conversion Metasurface for mm-Wave Applications Using Vanadium Dioxide (VO₂)</i>
Serra, João	A16.1	1729	<i>Novel Risley Prism Design Approach with Improved Side Lobe Levels Using Multi-Layer Transmit-Arrays</i>
Serup, Daniel	PA4.6	2129	<i>Detailed Design Procedure for Low-Cost High-Efficiency 3D Printed Transmitarray Antennas for mm-Wave Applications</i>
Seth, Ayush	PA8.14	2327	<i>An Annular Ring Shorted Logarithmic Spiral Antenna with Planar Integrated Feed</i>
Severs, Sean	CS4.5	3194	<i>CSIRO Radio Astronomy Receiver Update - Ultra Wideband and Phased Array Feeds</i>
Sezgin, Aydin	CS34.3	2620	<i>Validating Properties of RIS Channel Models with Prototypical Measurements</i>
Sganzerla, Antonio	PA7.11	1210	<i>Electromagnetic Assessment of Tolerances of the Square Kilometre Array Log Periodic Antenna Using Uncertainty Quantification</i>
Sha, Wei	CS43a.3	3962	<i>A Deep Learning Based Surface Current Generation Method for Scattering Modeling at Terahertz Band</i>
Shabanpoursheshpoli, Mohammadjavad	E07.2	1641	<i>Tunable Optimal Anomalous Reflection Using Discrete Impedance Metasurfaces</i>
Shafi, Muhammad Danial	E09.5	3924	<i>Multifunctional Linear Dichroism and Polarization Transforming Metasurface for mm-Wave Application</i>
Shah, Aaryaman	CS40b.2	1973	<i>A WiFi-Based System for Ice Monitoring in Harsh Environment Using 2.7 GHz Microwave Sensor</i>
Shah, Umer	A05.2	1825	<i>High-Gain and Circular Polarization Silicon-Micromachined Lens Antennas at 500-750 GHz</i>
	PE3.5	2379	<i>Analysis of the Interaction of Laser-Induced Solid-State Plasma with Electromagnetic Waves in Silicon Waveguides at 67-220 GHz</i>
Shaham, Amit	E08.4	1875	<i>Rigorous Susceptibility-Based Design of Generalized Huygens' Metasurface Radomes</i>
Shahbazian, Christineh	A10.4	3079	<i>"The Diminished Edge Diffraction Effect Bull's Eye Antenna "</i>
Shahi, Arun	PE3.2	2364	<i>Polarization Insensitive Broadband Frequency Selective Resorber with Improved Selectivity for Stealth Applications</i>
Shahid, Adnan	CS40a.2	1758	<i>Optimizing RF Energy Harvesting in IoT: A Machine Learning Estimation Considering Polarization Effects</i>
Shahzad, Atif	CS28.1	465	<i>Dielectric Characterisation of Human Parathyroid Glands at Microwave Frequencies</i>

Shahzadi, Iram	PA8.2	2274	<i>Dual-Polarized Substrate Integrated Waveguide Antenna with High Isolation for Polarimetric Radar</i>
Shakouri, Ali	CS47.2		<i>Advanced Thermal-Imaging for OTA Industrial-Testing of Active-In-Package, Antenna-On-Chip and Antenna on PCB</i>
Shakouri, Mo	CS47.2		<i>Advanced Thermal-Imaging for OTA Industrial-Testing of Active-In-Package, Antenna-On-Chip and Antenna on PCB</i>
Shallah, Abdulkadir	E12.4	2832	<i>Compact Dual-Band Crossover with Enhanced Band Ratio Using Interdigital Capacitor for 5G Applications</i>
Shamim, Atif	CS37b.1	344	<i>3D Spatially Reconfigurable Circularly Polarized Antenna in Package with Embedded Electronics</i>
	PA7.12	1215	<i>A Novel Quad-Band Electrically Small Antenna</i>
Shammas, Elie	A20.2	3816	<i>Stretchable Multi-Band Radio Frequency Sensor for Strain Measurement</i>
Shang, Xiaobang	PA4.2	2109	<i>A Fully Additive Manufactured D-Band SIW Antenna</i>
Shao, Wenyi	CS37a.2	34	<i>Optimum Structured Phased Array with Novel Beam Forming Circuits for Beam Wireless Power Transfer</i>
	CS15.3	4011	<i>Large and Simple Phased Array System at 28 GHz for Beam Wireless Power Transfer</i>
Shao, Yu	PM2.9	2464	<i>Complex Permittivity Extraction of Typical Wooden Furniture Materials Based on Multi-Objective Particle Swarm Optimization over 40-50 GHz</i>
	PA1.5	3349	<i>Monitoring Eye States Based on Transparent and Flexible Antenna in WBAN</i>
Sharaiha, Ala	PA7.5	1180	<i>Design of Optimized Cylindrical Structural Antenna with Quasi Length Insensitivity Using CMA</i>
	A13.5	1965	<i>Circularly-Polarized Wideband Conformal Magneto-Electric Antenna Covering the GNSS Bands</i>
	CS40b.5	1985	<i>Challenges and Limits of Designing Wide Band and Efficient Compact Superdirective Antenna</i>
Sharawi, Mohammad S.	A06a.4	3036	<i>Large, Multi-Faceted Reflectarray with Quasi-Constant Directivity in the V-Band</i>
Shariati, Negin	E13.6	289	<i>Highly Efficient Polarization-Insensitive EM Energy Harvester</i>
Sharif, Abubakar	CS13.5	1568	<i>UHF RFID Sensor Antenna for Fat Content and Adulteration Detection of Milk</i>
Sharma, Rahul	PM2.3	2438	<i>Leveraging Radar Back-Scattered Data for Classification of Imaging Targets</i>
Shaw, Robert	CS4.5	3194	<i>CSIRO Radio Astronomy Receiver Update - Ultra Wideband and Phased Array Feeds</i>
Shaw, Tarakeswar	CS27.2	1575	<i>An Electromagnetic Metasurface for Impedance Matching in Microwave Biomedical Applications</i>
	CS27.4	1584	<i>A Compact Wideband Biocompatible Circularly Polarized Implantable Flexible Antenna for Biomedical Applications</i>
	PA6.12	2260	<i>An Efficient Wireless Power Transfer System Using Transmission and Reflection Characteristics of Metamaterial</i>
Shehryar, Usman	A23.3	2757	<i>Analysis of Radiating Transverse Slot Unit Cell and Reflection Cancellation at D-Band</i>

Shepeleva, Elena	A05.5	1836	<i>Sub-THz U-Slot Coupled Stacked-Patch Radiating Elements for Dual-Polarized MIMO Array Antennas</i>
Shi, Bo	PA2.6	1079	<i>Modular Ka-Band Transmit Phased Array Antenna for SATCOM Applications</i>
Shi, Yuchen	CS23a.5	1794	<i>HRPE-Enhanced AI-Based 5G Indoor Localization in Presence of Specular and Dense Multipaths</i>
Shikhantsov, Sergei	CS2.5	184	<i>New Hybrid Ray-Tracing/FDTD for EMF Exposure in 6G Networks Using Semantically Classified Google Earth Photogrammetry with Measurement Validation</i>
Shinohara, Naoki	CS37a.2	34	<i>Optimum Structured Phased Array with Novel Beam Forming Circuits for Beam Wireless Power Transfer</i>
	CS15.3	4011	<i>Large and Simple Phased Array System at 28 GHz for Beam Wireless Power Transfer</i>
	CS1a.3	4031	<i>Far-Field Beam Wireless Power Transfer with Combination of Beam Forming and Optical Target Detection</i>
Shmidov, Lior	M5.2	542	<i>Uncertainty Analysis of Linear Multi-Probe Array Systems for Fast Antenna Measurements</i>
Shoaib, Imran	E09.5	3924	<i>Multifunctional Linear Dichroism and Polarization Transforming Metasurface for mm-Wave Application</i>
Shoaib, Noshawan	E09.5	3924	<i>Multifunctional Linear Dichroism and Polarization Transforming Metasurface for mm-Wave Application</i>
Shoaib, Sultan	E09.5	3924	<i>Multifunctional Linear Dichroism and Polarization Transforming Metasurface for mm-Wave Application</i>
Shoghi Badr, Nasrin	A28.3	3724	<i>Base Station Radome Design for 5G and Beyond</i>
Shou, Zhenyi	PA5.16	3556	<i>Design of the 3D-Printed Rectangular Dielectric Resonator Antenna for WLAN Applications</i>
Shri gyan, Deepankar	PA7.1	1164	<i>Inconsistency in Modes of Circular Microstrip Antennas and Its Rectification</i>
Shu, Chao	CS15.5	4019	<i>A Digital Beamforming Antenna for Space Based Solar Power Transmitting Array</i>
Sierra-Castañer, Manuel	CS42a.4	151	<i>Planar Near-Field Phaseless Measurements Using Multi-Probe Arrays</i>
Sikorski, Benedykt	A21.3	1488	<i>Millimeter Wave Retrodirective Van Atta Arrays in LTCC Technology</i>
Siles, Gustavo	PP02.19	2577	<i>Annual Statistics from 5 Years of 1-Minute Rainfall Rate Measurements at a Specific Site in Bolivia</i>
	PP02.20	2582	<i>Comparison Between ERA5 Cloud Parameters and Rainfall Rate in Madrid</i>
	P10a.2	2977	<i>Cloud Attenuation in the Q Band: Estimation from Experimental Data of Excess Attenuation</i>
Siligaris, Alexandre	CS7.4	1606	<i>Characterization of a D-Band Active Transmitarray System for Efficient Point-To-Point Links</i>
Silva, Guto	CS3.6	316	<i>Use of Ecofriendly Geopolymer Ceramics in Antenna Design and Microwave Applications</i>
Silva, José	PP02.9	2528	<i>Synthesis of Drop Counter Rain Rate from a Tipping Bucket Rain Gauge</i>

Silveirinha, Mario	E11.1	2796	<i>Isometric Symmetries in Non-Reflecting Structures</i>
Silvén, Olli	CS29.3	3797	<i>Computer Vision Enabled Sub-THz Radio Channel Characterization of Dynamic Objects</i>
Silvestri, Lorenzo	P03.1	1528	<i>Seasonal Snow Melting Process Investigation in Polar Environment Using a Dual-Receiver Radar Architecture</i>
Silvestri, Lorenzo	CS8.5	2899	<i>Dual-Resonance SIW-Based Reflectarray Unit Cell for Broadband Applications</i>
Sim, Jay	CS14b.1	4349	<i>Reconfiguration of Electromagnetic Metasurfaces Using Tunable Shape Morphing Structures</i>
Simon da Rosa, Guilherme	E02b.4	3279	<i>A Higher-Order Spectral Element Method to Model Eccentric Anisotropic Two-Layer Waveguides via Conformal Transformation Optics</i>
Simon El Hadri, Adan	PA8.18	2344	<i>Bandwidth Manipulated Leaky-Wave Antenna Using a Sinusoidal Ridge in Folded Substrate Integrated Waveguide</i>
Simone, Marco	A04.3	1467	<i>A Shared-Aperture Planar Antenna for 5G</i>
	PA4.12	2155	<i>A Dual Linearly Polarized Array for 5G FR2</i>
Simorangkir, Roy B. V. B.	PP02.17	2567	<i>Machine Learning Approaches for EM Signature Analysis in Chipless RFID Technology</i>
Simovski, Constantin	E07.2	1641	<i>Tunable Optimal Anomalous Reflection Using Discrete Impedance Metasurfaces</i>
Singh, Adarsh	PP03.11	3635	<i>Brain Hemorrhage Detection Using Antenna System Integrated with Imaging Algorithm</i>
Singh, Amit	PA4.18	2181	<i>A Wideband 3D Printed Digital Metasurface Transmitarray Antenna for mm-Wave Applications</i>
Singh, Gurtaj	PP03.6	3610	<i>Target Classification Through ISAR for Autonomous Vehicles Based on Federated Learning</i>
Singh, Khushboo	A10.1	3066	<i>Multi-Feed Resonant Cavity Antenna with In-Antenna Power Combination for mm-Wave Communication</i>
Siponkosk, Tuomo	PA3.19	3475	<i>Sub-THz Spatially Modulated Beam Splitting Reflectors for Potential RIS Implementations</i>
Sipus, Zvonimir	CS27.1	1571	<i>Link Budget Estimation for Implantable Antennas: From In-Body Coupling to Free-Space Radiation</i>
	E08.3	1870	<i>Tailoring Surface Impedance for Cascaded Cylindrical Metasurfaces</i>
	PA1.10	3371	<i>Textile Waveguide Antennas for On-Body Sensor and Communication Systems</i>
	CS26b.5	4321	<i>Design of Glide-Symmetric Dielectric Mikaelian Lens Antenna for K/Ka-Band</i>
Sitdikov, Damir	CS23b.5	2009	<i>Characterization of Propagation from Measurements at Sub-THz for ISAC Applications in an Emulated Dynamic Industrial Scenario</i>
Sjöberg, Daniel	PE2.11	1032	<i>Full Wave Verification of Radome Edge Scattering Treatments Using Open Source Tools</i>
	A04.4	1471	<i>Simulated Far-Field Pattern Disruption from a 1 GHz Cloaked Array Above a 10 GHz Array</i>
	M2.2	3886	<i>Real-Time Near-Field Measurements of mmWave Devices Using a Metasurface and IR Camera</i>

Skinner, James	CS5b.5	383	<i>Design and Preliminary Indoor Assessment of a Long-Range Sub-THz VNA-Based Channel Sounder Between 500 GHz and 750 GHz</i>
Skouroliakou, Vasiliki	PA6.1	2213	<i>Orthogonal Coding for Millimeter-Wave Imaging Using MIMO Dynamic Metasurface Apertures</i>
	PM2.7	2454	<i>Near-Field Bistatic Microwave Imaging with Dynamic Metasurface Antennas</i>
	E04.3	2693	<i>A Case Study of Misalignment Errors for Range-Migration-Based Microwave Imaging with Multistatic Dynamic Metasurface Apertures</i>
Skrivervik, Anja	CS27.1	1571	<i>Link Budget Estimation for Implantable Antennas: From In-Body Coupling to Free-Space Radiation</i>
	CS40a.1	1753	<i>Tunable Segmented Loop Antenna Reader for Miniaturized Chipless Tag Detection</i>
	A17.2	3744	<i>Series-Fed Loop Antenna Array Deployable by a Scissors Mechanism</i>
	A24.5	3876	<i>Design Recommendations for Minimal Antenna Mutual Coupling Using Current Optimization</i>
	CS1b.5	4254	<i>Plug-In Plug-Out Multibeam Dielectric Rod Antenna for Target Dedicated mm-Wave RF-WPT Applications</i>
Smart, Ken	CS4.5	3194	<i>CSIRO Radio Astronomy Receiver Update - Ultra Wideband and Phased Array Feeds</i>
Smith, Chris	CS12b.3	4268	<i>Safety Considerations for Robotic Antenna Measurement Systems</i>
Smith, Stephanie	CS6b.6	509	<i>3D-Printed Multi-Beam Flat Lens Antenna System</i>
	CS4.5	3194	<i>CSIRO Radio Astronomy Receiver Update - Ultra Wideband and Phased Array Feeds</i>
Smolders, A. B. (Bart)	CS47.1	416	<i>Over-The-Air Measurements for mm-Wave Body-Centric Wireless Communication</i>
	PA4.11	2150	<i>Pixel Antenna Design for mm-Wave Wireless Communications to Achieve Wide Scanning</i>
	PM2.8	2459	<i>Uncertainties in the Estimation of the Gain of a Standard Gain Horn in the Frequency Range of 90 GHz to 140 GHz</i>
	PM2.11	2472	<i>Quiet-Zone Profiling in a mmWave Spherical Anechoic Chamber: An Evaluation Approach</i>
	M4.2	2955	<i>Exploring Uniformity of Reverberation Chambers: Insights from Antenna Reflection Coefficient</i>
	CS4.1	3176	<i>Analysis of a Small LOFAR Low-Band Test Array Using a Sky Map, Simulated Embedded Element Patterns and Measured LNA-Impedances</i>
Smy, Tom	CS43a.1	3952	<i>On the Importance of Scattering from Poles in Ray Tracing Simulations</i>
	CS9b.1	512	<i>Emulating Spatial Dispersion Using Non-Spatially Dispersive Periodic Metasurfaces</i>
	E02b.3	3276	<i>Mixed Spatial-Spectral Domain Integral Equation Solver for Higher-Order Boundary Conditions in Electromagnetics</i>
Soares, Icaro	CS27.3	1579	<i>Theoretical Insights and Engineering of Wireless Body-Implanted Bioelectronics</i>
Soh, Ping Jack	PA3.19	3475	<i>Sub-THz Spatially Modulated Beam Splitting Reflectors for Potential RIS Implementations</i>

Sokunbi, Oludayo	A11.5	3171	<i>Mutual Coupling Reduction in 5G MIMO Antenna Using Dielectric Bridge and Superstrate</i>
Soldovieri, Francesco	E10b.5	2077	<i>Numerical Results on the Use of the L-SVD Approach for the Solution of the Inverse Source Problem from Amplitude-Only Data</i>
	E04.2	2689	<i>Contactless 3D Subsurface Imaging: Considerations to Set the Measurement Spacing</i>
Solimene, Raffaele	CS42b.5	456	<i>A Greedy Approach for Reducing Data in Near-Field Measurements</i>
	M5.5	557	<i>Near Field Phase Recovery Exploiting Only One Measurement Surface and A Smart Warping Sampling Strategy</i>
Song, Chaoyun	A04.5	1475	<i>A Penta-Band Shared Aperture Antenna with A Very Ratio Frequency for 5G and B5G Smartphone Applications</i>
Song, Chaoyun	CS1a.1	4023	<i>Microwave to mmWave Wireless Power Transfer: An Overview of the Design Challenges with a Focus on UK-Based R&D</i>
	CS1a.2	4027	<i>Single-Branch Hybrid Resistance Compression Technique for Enhanced Rectifier Performance</i>
Song, Dengyang	PA2.3	1066	<i>Compact Vivaldi Antenna Application in High-Power Design at X-Band</i>
Song, Lizhao	CS6a.3	204	<i>Wideband Transmissive Metasurfaces for Sub-THz Frequency-Dependent Beam Scanning</i>
	CS6b.6	509	<i>3D-Printed Multi-Beam Flat Lens Antenna System</i>
Song, Weiguang	A01a.1	2928	<i>Millimeter-Wave Uniform Amplitude SIW Series Power Divider for 2D Leaky-Wave Antenna Arrays</i>
Sonkar, Ramesh	A03b.4	3142	<i>High Gain and Dual Band SIW-Fed Stacked Conical DRA for 5G NR FR1 Application</i>
Sorbello, Gino	CS16.1	564	<i>Analytical and Numerical Evaluation of Efficient Power Transfer of Bessel-Shaped Beams in Near-Field Through a Planar Layered Medium</i>
	A04.3	1467	<i>A Shared-Aperture Planar Antenna for 5G</i>
	A16.5	1749	<i>Design of a Wideband Dual-Polarized Stacked Antenna Array for SATCOM Applications</i>
	PA4.12	2155	<i>A Dual Linearly Polarized Array for 5G FR2</i>
	PA8.10	2311	<i>Octagonal Patch Tag Antenna and 3 × 3 Array Locator for DoA Applications</i>
Soriano, Gabriel	PA6.7	2238	<i>Metasurface-Based Bessel-Beam Launcher with 100λ Non-Diffractive Range</i>
	A01a.3	2938	<i>Generation of Non-Diffractive Bessel Beams for Near-Field Links Applications Using Meta-Axicons</i>
Sotiroudis, Sotirios	PA3.23	3490	<i>Wideband Aperture-Coupled Array Design for Automotive Radar Applications</i>
	PP03.5	3605	<i>Modeling Received Power from 4G and 5G Networks in Greece Using Machine Learning</i>
Sørensen, Stig	CS39a.3	618	<i>Full Wave Modelling and Design of a Baffle for the HERTZ 2.0 Compact Antenna Test Range</i>
	A19.4	1518	<i>A Possible Way to Reduce the High Sidelobe Levels Due to Reflector Struts: Curly Struts</i>
Spagnolini, Umberto	CS29.4	3802	<i>Accurate Time Synchronization Exploiting Integrated Sensing and</i>

			<i>Communication</i>
Späth, Marc	A09b.4	886	<i>Loss Analysis for Compact Liquid Crystal Delay Lines Based on Defective Ground Structures</i>
Speder, Kilian	M3.3	2595	<i>Dielectric Characterization of Adhesives for THz Packaging in WR6.5, WR3.4 and WR2.2 Bands</i>
Speksnijder, Erik	E10a.1	1841	<i>Spectral Domain Green's Function of an Infinite Dipole with Non-Zero Metal Thickness</i>
Spies, François	CS11.5	1631	<i>Fine Tuning an AI-Based Indoor Radio Propagation Model with Crowd-Sourced Data</i>
Spirito, Marco	CS37b.3	352	<i>Chessboard Focal Plane Array in Silicon Technologies for Terahertz Imaging</i>
	CS47.6	435	<i>The Antenna Dome High-Speed Characterization System for OTA Characterization of FR2 5G Active Antenna Panels</i>
	CS7.3	1601	<i>Experimental Characterization of a Core-Shell Lens for Antenna On-Package Integration at D-Band</i>
	M3.2	2590	<i>A Demonstration of Diffraction-Limited Images Using a CMOS Chessboard Array at THz Frequencies</i>
Srivastava, Kumar Vaibhav	PE3.2	2364	<i>Polarization Insensitive Broadband Frequency Selective Resorber with Improved Selectivity for Stealth Applications</i>
Stadius, Kari	CS37b.2	348	<i>Crack Stop as a Coupling Element Between an IC Chip and Antenna</i>
Stalrud, Henrik	A28.1	3714	<i>Antenna and Mechanical Co-Design for Auto-Beam-Tracking in Backhaul Systems</i>
Starck, Jonas	PA5.7	3519	<i>Analysis and Measurement of Key Performance Indicators for MIMO Antennas</i>
Stazi, Giovanni	P03.2	1533	<i>Advanced Microwave Radiometry: Refining Sun-Tracking Technique for Atmospheric Attenuation Retrieval and Sun Brightness Temperature Estimation</i>
Stefanini, Luca	E08.2	1868	<i>Reflective Intelligent Surfaces: Reducing Complexity by Controlling the Illuminating Field</i>
	E08.5	1880	<i>Static and Reconfigurable Phase-Gradient Metasurfaces for Antenna Applications</i>
	PA4.10	2147	<i>Analysis and Design of Robust Reconfigurable Intelligent Surfaces Using a Statistical Approach</i>
	A10.2	3071	<i>Analysis and Design of Metasurface Antennas Based on Temporal Metastructures</i>
Stefanski, Tomasz	E02a.2	3002	<i>Crank-Nicolson FDTD Method in Media Described by Time-Fractional Constitutive Relations</i>
Steinbock, Gerhard	CS43a.1	3952	<i>On the Importance of Scattering from Poles in Ray Tracing Simulations</i>
Steingass, Alexander	A18.5	2923	<i>On the Cost-Effectiveness of Using Beamforming at the Ground Station for Aeronautical Communications</i>
Stek, Tim	CS47.4	426	<i>Over-The-Air Noise-Figure Measurements of Active Integrated Antennas at W-Band</i>
Stephenson, James	PA7.17	1233	<i>An Investigation into the Effects of Multi-Path and NLOS Propagation on Antenna-Based Soil Moisture Sensors in the RFID Band</i>
Stevanovic, Marija	CS24a.5	740	<i>Polynomial Basis Functions for Qualitative Head Tissue Segmentation</i>

			<i>via Linearized Microwave Imaging</i>
	CS33a.5	3062	<i>Generating a Library of Head Phantoms for Microwave Imaging Using Spherical Harmonic Approximation</i>
Stieler, Noah	E04.5	2703	<i>Preliminary Description of a 2D Near-Field Electromagnetic Imaging Database</i>
Stirland, Simon	PA2.18	1132	<i>Study of Different Feed Layout Configurations for Hybrid Active VHTS Antennas</i>
Stöckli, Patrik	CS30a.4	3942	<i>Validating Convex Optimization of Reconfigurable Intelligent Surfaces via Measurements</i>
Stöhr, Andreas	PA4.21	2193	<i>Terahertz Microstrip Leaky-Wave Antenna for WR1.0 Band</i>
Stoja, Endri	CS33b.4	3321	<i>Deep-Learning Optimized Reconfigurable Metasurface for Magnetic Resonance Imaging</i>
Storrer, Laurent	P02.1	3763	<i>Multistatic OFDM Radar Fusion of MUSIC-Based Angle Estimation</i>
Stoumpos, Charalampos	A19.5	1523	<i>Exploring the Potential of Spatially Modulated Full-Metal Dichroic Mirrors for Deep Space Antennas</i>
Straub, Marvin	CS35a.1	1683	<i>Design and Validation of a Wireless Network for Intra-Train Communications</i>
Struck, Tobias	CS42a.6	160	<i>Hybrid Antenna Measurement and Post-Processing for 5G Small Cell Exposure Assessment with Site-Specific Mounting Conditions</i>
	CS2.6	189	<i>Reproducibility Studies of Instantaneous and 6-Minute Average Exposure Measurements Around 5G Massive-MIMO Base Stations</i>
Stuart, Tucker	CS37a.1	29	<i>3D-Printed Wearable Antenna Integrated with Rectifier for Wireless Power Transfer</i>
Štumpf, Martin	E02a.5	3016	<i>Improved PEEC Modeling of Antennas Through Time-Dependent Partial Elements</i>
Stylianopoulos, Kyriakos	CS20b.1	393	<i>1-Bit SubTHz RIS with Planar Tightly Coupled Dipoles: Beam Shaping and Prototypes</i>
Suárez García, Carlos	A19.2	1508	<i>Polymer-Based Additive Manufacturing of a Complex RF Front-End for New Space Applications</i>
Suess, Martin	PA2.4	1069	<i>Antenna Design for TriHex: A Future Soil Moisture and Ocean Salinity Radiometer Mission</i>
Sufian, Md. Abu	A27b.2	834	<i>A Radial Waveguide Power Divider Inspired Antenna for mmWave IoT Sensing Applications</i>
	PA8.7	2298	<i>Compact Size Frequency-Agile Antenna Enabling Multi-Mode Functionality for Internet of Things Applications</i>
	PA1.7	3359	<i>Development of a Wearable IoT-Optimized Textile Antenna with Low Specific Absorption Rate in Three Frequency Bands</i>
Sugimoto, Yoshiki	A27a.4	646	<i>Mechanical/Electrical Hybrid 2-Dimensional Beam Scanning Cylindrical Dielectric Lens Antenna</i>
Suijker, Erwin	PA5.3	3503	<i>Characterization of All-Metal Multi-Feed Antenna for High Power Applications</i>
Sumser, Kemal	CS28.4	480	<i>Phantom Material with Biological Composition for Muscle Equivalent Radiofrequency, Thermal and Magnetic Resonance Properties</i>
Sun, Bo	PA2.16	1123	<i>Study on CFM Method for Beam Compensation of Array-Fed Space-Borne Reflector Antennas</i>

Sun, Ruoyu	P10b.1	3244	<i>Empirical Path Loss Model and Small-Scale Fading Statistics in an Indoor Office Environment in 6 and 37 GHz Shared Bands</i>
	P01.4	3847	<i>Frequency Domain Channel Characteristics in an Outdoor-To-Indoor Environment at 6 and 37 GHz</i>
Sun, Ying	PA3.22	3486	<i>Wideband Array Antenna with Single-Layer Feeding Network at Ka-Band</i>
Sun, YuYing	CS23a.5	1794	<i>HRPE-Enhanced AI-Based 5G Indoor Localization in Presence of Specular and Dense Multipaths</i>
Sun, Yuzhe	CS23a.3	1785	<i>Robust Tensor Positioning Based on Channel Parameter Estimation Under Spatially Colored Noise</i>
Susarla, Praneeth	CS29.3	3797	<i>Computer Vision Enabled Sub-THz Radio Channel Characterization of Dynamic Objects</i>
Suyama, Satoshi	CS5b.6	388	<i>Sub-Terahertz MassiveMIMO Channel Sounder for 6G Mobile Communication Systems</i>
Suzuki, Naoya	P10a.5	2992	<i>Dual-Band MmWave Measurements of Human Body Scattering and Blockage Effects Using Distributed Beamforming for ISAC Applications</i>
Svigelj, Ales	PP02.15	2557	<i>Large-Scale Site Diversity Experiment in Ljubljana and Budapest at Ka-Band with Alphasat Satellite</i>
Swarner, Jon	A25.5	3105	<i>Additively Manufactured Horn Antennas</i>
Sydänheimo, Lauri	A20.5	3827	<i>Quad-Band Meandered Implantable Planar Inverted-F Antenna for Wireless Brain Health Monitoring</i>
Sydoruk, Oleksiy	PP03.10	3630	<i>Electromagnetic Detection and Identification of Perturbed Wire Resonators</i>
Sylvand, Guillaume	PE2.3	999	<i>Management of Radiofrequency Compatibility on Aircraft</i>
Symeonidis, Loizos	E07.5	1653	<i>An Accurate Semi-Analytical Model for Periodic Tunable Metasurfaces Electromagnetic Response</i>
Syms, Richard	PP03.10	3630	<i>Electromagnetic Detection and Identification of Perturbed Wire Resonators</i>

T

Ta, Thanh Tam Julian	CS2.2	170	<i>Characterization of Typical Instantaneous Exposure and Usage Scenarios in the Vicinity of 5G Massive-MIMO Base Stations</i>
Taboada, Jose	CS19b.2	4287	<i>A Multi-Region Hierarchical Preconditioning Scheme for the MoM Simulation of Complex Composite Structures</i>
Tadolini, Cesare	A12b.1	1927	<i>Design, Measurements, and Performance Assessment of a Massive MIMO Wideband Phased Array</i>
Tafazolli, Rahim	CS3.2	298	<i>From Reconfigurable Intelligent Surfaces to Holographic MIMO Surfaces and Back</i>
	A25.1	3087	<i>Long Slot Dielectric-Loaded Periodic Leaky-Wave Antenna Based on 3D Printing Technology</i>
Taghvaei, Hamidreza	CS3.2	298	<i>From Reconfigurable Intelligent Surfaces to Holographic MIMO Surfaces and Back</i>
	E06a.3	596	<i>Fully Autonomous Reconfigurable Metasurfaces with Integrated Sensing and Communication</i>
	PE1.2	1245	<i>Smart Propagation Environments Empowered by Metasurfaces: A Self-Consistent Study</i>

Tagliaferri, Dario	CS29.4	3802	<i>Accurate Time Synchronization Exploiting Integrated Sensing and Communication</i>
Tagliafico, Alberto	CS45.3	1808	<i>Preliminary Clinical Trial Results of MammoWave in the Context of RadioSpin Project</i>
Taha, Ahmad	P05.6	266	<i>Contactless Respiration Variability Detection and Accuracy Test Using UWB Radar</i>
Tahir, Farooq	E13.1	270	<i>Ultrahigh Sensitive Terahertz Metasurface with 2D MoS2 for Refractive Index Biosensing</i>
	PE1.5	1256	<i>An Innovative Metasurface Polarizer Working in 5G Frequency Bands</i>
	PM1.4	1323	<i>A Highly Compact Double-Sided Orientation Insensitive Chipless Tag for Radio Frequency Identification Applications</i>
	PE3.13	2408	<i>Design of Intelligent Reflective Surface Unit Cell for 5G mmWave Applications</i>
	CS14b.5	4366	<i>Multi-Band Anisotropic Metasurface: Simultaneous Linear and Circular Polarization for Robust Satellite Communication</i>
Taillieu, Jérôme	CS44a.4	757	<i>High Data-Rate Sub-THz Coherent Near-Field Wireless Links Enabled by Spline-Profile Bessel Launchers</i>
Takada, Jun-ichi	P04b.1	965	<i>Grid-Based Shadowing Gain Modeling for Handling Dynamic Objects in Wireless Channel Emulation</i>
	P03.5	1548	<i>Utilization of Wi-Fi Signal for Validation of Micro-Doppler Model in a Person Falling Scenario</i>
	P10a.5	2992	<i>Dual-Band MmWave Measurements of Human Body Scattering and Blockage Effects Using Distributed Beamforming for ISAC Applications</i>
Takahagi, Kazuhiro	PE1.10	1275	<i>Nonreciprocal Metasurfaces Analyzing Temperature Characteristics</i>
Takahashi, Masaharu	CS5a.2	61	<i>Validation of Pseudo-Scale Model for the Air-Sea Two-Layer Near-Field Problem by Using FDTD Simulations and Measurements in a Tank</i>
Takahashi, Riku	CS5b.2	369	<i>Double-Directional Angle-Resolved Wideband Channel Measurements and Path Loss Characterization in Corridor at 300 GHz</i>
Takeda, Yuki	PA2.8	1088	<i>Design of Reconfigurable Reflectarray Antennas on Flexible Substrates with Varactor Diodes Mounted on Slot-Coupled Microstrip Lines</i>
Takigawa, Masahiro	A09a.4	691	<i>Beam Training of LoS-MIMO Systems Using Subarray-Based Beamforming in the Presence of Ground Reflection</i>
Takizawa, Kenichi	P06.3	2737	<i>Potential of Polarized MIMO in In-Body to Out-Body Radio Links</i>
Talbi, Larbi	CS40a.3	1763	<i>Mm-Wave Monopulse Radar System for Detecting Space Debris in Satellite Exploration Missions</i>
	PA5.10	3533	<i>A High Efficiency and Ultra-Wideband Rectenna for RF Energy Harvesting Application</i>
Talvitie, Jukka	CS23a.1	1775	<i>Gaussian Processes for Received Signal Strength Based Device-Free Localization</i>
Tamayo-Domínguez, Adrián	A07.4	2674	<i>Fully Metallic Wideband Lens Design Using a Highly Refractive Glide-Symmetric Unit Cell at W-Band</i>
	A11.3	3162	<i>Pinwheel-Shaped Polarizer for Generating Dual-Circularly Polarized Conical Radiation Patterns in the Ka-Band</i>
Tamura, Jo	CS36a.5	719	<i>A Parasitic Element Technique for Deep Null Synthesis and the Application to Received Signal Strength (RSS)-Based Localization</i>

Tan, Li	CS34.1	2610	<i>RIS with Practical Reflection Coefficients: Modeling and Experimental Measurements</i>
Tan, Zhen	E13.5	284	<i>Transmissive-Type Metagratings with Few Meta-Atoms for Beam Splitting</i>
	PE1.4	1253	<i>A Multifunctional Reconfigurable Metagrating for Wavefront Manipulations</i>
Tanaka, Shoma	PP01.9	1385	<i>Development of a Site-Specific Building Entry Loss Model for High-Rise Buildings</i>
Tanaka, Yusuke	M5.6	560	<i>Spherical Near-Field Measurement and Far-Field Characterization of a 300 GHz Band Antenna Based on an Electrooptic Probe with Compact Tabletop Robotic Arm</i>
Tang, Chengkai	CS20b.6	412	<i>A Vector Differential Coding for Hybrid RIS Aided Zero-Padded OTFS Systems</i>
Tang, Pan	CS35a.4	1697	<i>Time-Varying Channel Measurement and Analysis at 105 GHz in an Indoor Factory</i>
Tang, Shiyang	A09b.1	872	<i>X-Band Reconfigurable Phase Shifters Based on SIW and Liquid Metal Technologies</i>
Tanghe, Emmeric	CS2.5	184	<i>New Hybrid Ray-Tracing/FDTD for EMF Exposure in 6G Networks Using Semantically Classified Google Earth Photogrammetry with Measurement Validation</i>
	CS23b.2	1994	<i>Path Loss Modeling for Air-To-Ground Channels in a Suburban Environment</i>
Taniguchi, Ryotaro	CS5b.6	388	<i>Sub-Terahertz MassiveMIMO Channel Sounder for 6G Mobile Communication Systems</i>
Tantot, Olivier	CS3.6	316	<i>Use of Ecofriendly Geopolymer Ceramics in Antenna Design and Microwave Applications</i>
Tapia Barroso, Roderick	A12b.1	1927	<i>Design, Measurements, and Performance Assessment of a Massive MIMO Wideband Phased Array</i>
	A12b.5	1944	<i>Study of Finite Edge Effects in Compact Ultra-Wide-Band Connected Arrays</i>
Taravati, Sajjad	E13.3	275	<i>Superconducting Space-Time Modulation: Theoretical Implications and Mixing-Beamsplitting Functionality</i>
	E12.2	2824	<i>Nonreciprocal Phase-Shifting in Linear Magnet-Free Reconfigurable Temporal Loops</i>
Tawk, Youssef	A20.2	3816	<i>Stretchable Multi-Band Radio Frequency Sensor for Strain Measurement</i>
	CS14b.2	4353	<i>Multistable Structures for Deployable and Reconfigurable Antennas</i>
Tayebpour, Jalaledin	A26.2	4197	<i>A Wideband Dual-Polarized 1-Bit Unit Cell for Reconfigurable Intelligent Surface Applications</i>
Tedesco, Salvatore	PP02.17	2567	<i>Machine Learning Approaches for EM Signature Analysis in Chipless RFID Technology</i>
Teixeira, Fernando	E02b.4	3279	<i>A Higher-Order Spectral Element Method to Model Eccentric Anisotropic Two-Layer Waveguides via Conformal Transformation Optics</i>
Teniente-Vallinas,	A08a.4	1897	<i>Ka-Band USS Enterprise (NCC-1701) Antenna</i>

Jorge			
Tennant, Alan	PE1.10	1275	<i>Nonreciprocal Metasurfaces Analyzing Temperature Characteristics</i>
	PP01.3	1355	<i>The Time Modulated Array for Channel Sounding Measurements - Concept and Initial Field Tests</i>
	A02.2	3696	<i>Subsampling Time-Modulated Array for Reduced Hardware down Conversion and Beamforming</i>
Tenoux, Thierry	CS17a.3	10	<i>Exploring RIS Coverage Enhancement in Factories: From Ray-Based Modeling to Use-Case Analysis</i>
Tentzeris, Manos M.	PA5.14	3549	<i>Super-Realized Gain Huygens Antennas</i>
	PA5.17	3560	<i>Low-Profile Super-Realised Gain Antennas</i>
Teodorani, Lucia	PE1.8	1269	<i>Modeling of 3D Feeding Structures in the Automated Design of Metasurface Antennas</i>
	CS30b.3	4156	<i>Automated Design and Characterization of a Scalar Metasurface Antenna Radiating a Linearly-Polarized Broadside Beam</i>
Terawatsakul, Natachai	E01.1	2014	<i>Optimal Design of Planar Micro-NMR Coils for High Signal-To-Noise Ratio</i>
Terrasse, Isabelle	PE2.3	999	<i>Management of Radiofrequency Compatibility on Aircraft</i>
Tervo, Nuutti	CS5a.5	76	<i>A Modular COTS-Based High-Efficient Sub-THz Channel Sounder and Experimental Validations</i>
	CS29.3	3797	<i>Computer Vision Enabled Sub-THz Radio Channel Characterization of Dynamic Objects</i>
	A15a.5	4127	<i>Tapering Impact on the Spatial and Frequency Responses of Broadband Asymmetrically Routed Phased Arrays</i>
Tewes, Simon	CS34.3	2620	<i>Validating Properties of RIS Channel Models with Prototypical Measurements</i>
Thaha, Mohamed	PA1.9	3366	<i>A Compact Implantable Camera Integrated MIMO Antenna with Polarization Diversity for Wireless-Capsule-Endoscopy Applications</i>
Thalakotuna, Dush	CS9a.5	233	<i>Beam Steering 2D Leaky Wave Resonant Cavity Antenna for Ka-Band Satellite Communication</i>
	A10.1	3066	<i>Multi-Feed Resonant Cavity Antenna with In-Antenna Power Combination for mm-Wave Communication</i>
Thanikonda, Ravikanth	E06b.3	800	<i>Multi-Beam Dual Polarised Metasurface Antenna in Ka-Band</i>
Thelappilly Joy, Ashwin	CS3.2	298	<i>From Reconfigurable Intelligent Surfaces to Holographic MIMO Surfaces and Back</i>
Thevaruparambu Abdul Nazer, Nisamol	PP03.13	3643	<i>Filter Integrated Microstrip 3-Port Power Combiner</i>
Thevenot, Marc	PA2.7	1084	<i>Design and Prototyping of a Low-Cost Parasitic Element Antenna for a Telemetry-Telecommand Link on Ariane 6 Space Launcher</i>
Thevenot, Marc	A12a.3	1715	<i>Behavioral Models for the Cosimulation and Optimization of Active Electronically Scanned Arrays</i>
Thoemel, Jan	CS46.3	4223	<i>CubeSat Formation Antenna Array Synchronization for GNSS-R</i>
Thomä, Reiner	CS5a.6	81	<i>Excitation Signal Design for THz Channel Sounding and Propagation Parameter Estimation</i>
	CS23b.5	2009	<i>Characterization of Propagation from Measurements at Sub-THz for ISAC Applications in an Emulated Dynamic Industrial Scenario</i>

	P01.2	3837	<i>Grid-Free Harmonic Retrieval and Model Order Selection Using Convolutional Neural Networks</i>
Thuroczy, Tomas	CS7.1	1592	<i>Low Profile and High Gain Folded Transmitarray in Quartz for Radiometry at 310 GHz</i>
Tian, Lei	CS35a.4	1697	<i>Time-Varying Channel Measurement and Analysis at 105 GHz in an Indoor Factory</i>
Tiberi, Gianluigi	CS45.3	1808	<i>Preliminary Clinical Trial Results of MammoWave in the Context of RadioSpin Project</i>
	E01.2	2019	<i>Assessment of the Feasibility of Breast Lesion Detection with Contrast Source Inversion for Microwave Tomography: A Virtual Experiment</i>
	E01.4	2028	<i>Huygens Principle Imaging Method Powered by Deep Learning for Brain Stroke Classification</i>
Tiberi, Tommaso	CS36b.4	911	<i>Simplified Frequency-Diverse Array Architecture for Surveillance Purposes</i>
Tienda, Carolina	PA2.18	1132	<i>Study of Different Feed Layout Configurations for Hybrid Active VHTS Antennas</i>
Tihon, Denis	M3.4	2600	<i>Numerical Assessment of a Cognitive Chamber: TMz Case</i>
	E02a.4	3012	<i>Dispersion Curve Calculation Using the Method of Moments: The Impact of Macro Basis Functions</i>
	CS19a.3	4077	<i>Modal Analysis of Thermal Noise from Lossy Dielectric Medium</i>
Tishchenko, Anton	CS3.2	298	<i>From Reconfigurable Intelligent Surfaces to Holographic MIMO Surfaces and Back</i>
	CS44a.2	750	<i>Dual Functional mmWave RIS for Radar and Communication Coexistence in near Field</i>
Tobon Vasquez, Jorge	CS24a.1	724	<i>Advancements in the Experimental Validation of a Wearable Microwave Imaging System for Brain Stroke Monitoring</i>
	CS11.1	1616	<i>AI-Assisted Design and Experimental Testing of a Compact UWB Antenna for the Inspection of Food and Beverage Products</i>
	CS33a.3	3054	<i>Advancements in Broadband Electromagnetic Sensing for Food Quality Control</i>
	CS33b.1	3309	<i>Nonlinear Correction of the Direct Inverse Problem Solution in Real-Time Imaging</i>
	CS26a.5	4105	<i>Efficient Numerical Computation of Dispersion Diagrams for Glide-Symmetric Periodic Structures with a Hexagonal Lattice</i>
Toccafondi., Alberto.	CS20a.2	91	<i>Analysis and Optimization of Reconfigurable Intelligent Surfaces Based on S-Parameters Multiport Network Theory</i>
Tognolatti, Ludovica	CS45.4	1812	<i>On Enhancing Efficiency of Transmission in Imaging Systems by Wearable Scatterers</i>
Tognolatti, Piero	PA2.23	1154	<i>Ka-Band Phased Antenna Array Concept for High-EIRP Satellite Connections</i>
Tombakdjian, Lionel	PA2.15	1119	<i>Feasibility Study of 3D Printed Luneburg Lens Using Fused Deposit Material 3D Printing Technology for Ku-Band Application</i>
Tomić, Dubravko	CS26b.5	4321	<i>Design of Glide-Symmetric Dielectric Mikaelian Lens Antenna for K/Ka-Band</i>
Tomie, Takahiro	CS5b.6	388	<i>Sub-Terahertz MassiveMIMO Channel Sounder for 6G Mobile</i>

Communication Systems

Tomura, Takashi	A27b.4	842	<i>Design of a Hollow-Waveguide Slot Array Antenna for a Channel Sounder in the 150 GHz Band</i>
	PA2.8	1088	<i>Design of Reconfigurable Reflectarray Antennas on Flexible Substrates with Varactor Diodes Mounted on Slot-Coupled Microstrip Lines</i>
Tong, Yuhuan	CS26b.4	4318	<i>All-Metal Glide-Symmetric Slotted Planar Antennas: Modal Analysis</i>
Toni, Marco	A08b.3	2091	<i>Hybrid Metal-Graphene Unit Cells for THz Reconfigurable Leaky-Wave Antennas</i>
Tornese, Alessio	A03a.2	2867	<i>Loaded and Load-Less Supergain Parasitic End-Fire Arrays</i>
Törnevik, Christer	CS2.3	175	<i>Long-Term Network-Based Assessment of the Actual Output Power of Base Stations in a 5G Network</i>
Toscano, Alessandro	E08.2	1868	<i>Reflective Intelligent Surfaces: Reducing Complexity by Controlling the Illuminating Field</i>
	E08.5	1880	<i>Static and Reconfigurable Phase-Gradient Metasurfaces for Antenna Applications</i>
	PA4.10	2147	<i>Analysis and Design of Robust Reconfigurable Intelligent Surfaces Using a Statistical Approach</i>
	E12.3	2829	<i>Time-Modulated Metasurface-Based System for the Generation of False Radar Targets</i>
	A10.2	3071	<i>Analysis and Design of Metasurface Antennas Based on Temporal Metastructures</i>
Tosi, Luca	CS22b.2	3114	<i>A Quantum Optimization Method for Antenna Array Thinning</i>
Toso, Giovanni	CS25.3	663	<i>Multibeam Phased Arrays Exploiting Frequency Dispersion for Massive MIMO Satellite Communications</i>
	CS25.5	673	<i>TX/RX Terminal Based on Metascreen Technology for Ka-Band Satcom with Dual Switchable Polarization</i>
	CS10.5	868	<i>On the Scanning Properties of Bidimensional Discrete Lens Antennas with 1, 3, Infinite Focal Points</i>
	A19.3	1513	<i>Non-Regular Multibeam Coverage Antenna for Ka-Band High-Throughput Satellite Communications</i>
	E12.1	2820	<i>Reducing the Cross-Polarization Levels in Artificial Dielectric Layers for Wideband Arrays</i>
	A06a.5	3041	<i>Multibeam Compact Dual Reflectarray Antenna for High-Throughput Satellites in Ka-Band</i>
Toubal, Ayoub	CS20b.3	402	<i>Measurements of Reconfigurable Intelligent Surface in 5G System Within a Reverberation Chamber at mmWave</i>
Touhami, Abdellah	CS40b.5	1985	<i>Challenges and Limits of Designing Wide Band and Efficient Compact Superdirective Antenna</i>
Toumi, Abdelmalek	PP03.2	3592	<i>A Deep Split-Step Wavelet Model for the Long-Range Propagation</i>
Trampuz, Christian	PA5.3	3503	<i>Characterization of All-Metal Multi-Feed Antenna for High Power Applications</i>
Travnicek, Samuel	PA2.20	1140	<i>Compact Ka Band Orthomode Transducer with Conical Horn Antenna</i>
Trenta, Damiano	CS39a.3	618	<i>Full Wave Modelling and Design of a Baffle for the HERTZ 2.0 Compact Antenna Test Range</i>
Tresoldi, Annalisa	P05.3	251	<i>Characterisation of Thin Glass-Fibre Substrates for Deployable SAR</i>

			<i>Antennas</i>
	P02.5	3782	<i>Mechanical Vibrations on a Deployable Nanosatellite Antenna: SAR Performance Analysis</i>
Tretyakov, Sergei	CS20a.1	86	<i>Comparison of Simplistic System-Level RIS Models and Diffraction-Theory Solutions</i>
	A15b.3	4335	<i>Array Scattering Synthesis for Anomalous Deflection Using Passive Aperiodic Loadings</i>
Trippanera, Eva	A17.4	3754	<i>RF Modelling and Validation of the Breadboard Antenna of the Copernicus Imaging Microwave Radiometer</i>
Trofimowicz, Damian	E02a.2	3002	<i>Crank-Nicolson FDTD Method in Media Described by Time-Fractional Constitutive Relations</i>
Trzebiatowski, Kamil	A21.3	1488	<i>Millimeter Wave Retrodirective Van Atta Arrays in LTCC Technology</i>
	PA4.15	2169	<i>Low-Cost 3-D Printed Lens Antenna for Ka-Band Connectivity Applications</i>
Tsai, Yun-Ting	PA3.1	3398	<i>Dynamic Programming-Based Beam Codebook Design for mmWave Multi-Antenna Module in Mobile Devices</i>
Tsakyridis, Apostolos	PA3.21	3483	<i>MIMO Signals Processing Utilizing Optical Crossbar Linear Operator</i>
Tsoulos, George	PP01.5	1365	<i>Field Trials for Different 5G NSA Cellular Networks</i>
	PP03.5	3605	<i>Modeling Received Power from 4G and 5G Networks in Greece Using Machine Learning</i>
Tsoulos, Vassilis	PP01.5	1365	<i>Field Trials for Different 5G NSA Cellular Networks</i>
Tsuji, Hiroyuki	PA7.9	1200	<i>Input Impedance of Radiation Efficiency Deterioration State</i>
Tu, Deyu	M2.2	3886	<i>Real-Time Near-Field Measurements of mmWave Devices Using a Metasurface and IR Camera</i>
Tubau, Ségolène	CS40a.5	1770	<i>A Self Deployable and Reconfigurable Antenna in VHF Band for a New Space Mission</i>
	A13.3	1958	<i>Wide-Angle Quasi-Optical Beamformer for LEO Applications</i>
Tucek, Jonas	E11.5	2815	<i>Preliminary Study on Gain Maximization via Density-Based Topology Optimization</i>
Tufvesson, Fredrik	CS47.3	421	<i>Millimeter-Wave Scattering from Building Facade: A Simulation and Verification Study</i>
	CS43a.4	3967	<i>Propagation Study of Vision-Based RIS Beam Tracking for mmWave Communications</i>
	CS43b.5	4187	<i>Experimental Analysis of Physical Interacting Objects of a Building at mmWave Frequencies</i>
Tukmanov, Anvar	CS17a.6	24	<i>RIS-Enhanced MIMO Channels in Urban Environments: Experimental Insights</i>
	CS48.4	3992	<i>Joint Wide Illumination and Null Insertion Design in RIS-Assisted System</i>
Tummolo, Andrea	A09a.2	683	<i>Sub-Wavelength Anisotropic Unit-Cells for Low-Profile Transmitarray Antennas</i>
Tuthill, John	CS4.5	3194	<i>CSIRO Radio Astronomy Receiver Update - Ultra Wideband and Phased Array Feeds</i>
Tuzi, Diego	CS25.1	654	<i>Beamforming Schemes for 6G Direct-To-Cell Connectivity Using Satellite Swarms</i>

Tyrväinen, Juho	PE2.4	1004	<i>Applying Neural Networks for Predicting Feed Weights of an Antenna Array</i>
Tzarouchis, Dimitrios	PM2.10	2469	<i>Assessing Performance of Transparent Conductive Films for Microwave Industrial Applications</i>
Tzimiragka, Charikleia	PA3.12	3442	<i>Shorted Stacked Patch Array for Photonic Beam Steering at mm-Waves</i>
Tzioumis, Tasso	CS4.5	3194	<i>CSIRO Radio Astronomy Receiver Update - Ultra Wideband and Phased Array Feeds</i>
Tzouras, Hlias	PA4.3	2114	<i>A Two-Port Metamaterial Antenna for mm-Wave 5G MIMO Applications with Enhanced Bandwidth and Gain</i>
Tzouvaras, Dimitrios	E07.5	1653	<i>An Accurate Semi-Analytical Model for Periodic Tunable Metasurfaces Electromagnetic Response</i>

U

Uchida, Keiya	PA4.4	2119	<i>Prototype of Multi-Sector Indoor mmW Base Station Based on 5G NR Beam Control</i>
Udayanga, Nilan	CS44b.5	960	<i>Graph Neural Network Based 77 GHz MIMO Radar Array Processor for Autonomous Robotics</i>
Ukkonen, Leena	A20.5	3827	<i>Quad-Band Meandered Implantable Planar Inverted-F Antenna for Wireless Brain Health Monitoring</i>
Ullah, Jawad	PA4.2	2109	<i>A Fully Additive Manufactured D-Band SIW Antenna</i>
Ullah, Muhib	CS22b.4	3123	<i>Non-Reciprocity in a Three-Mode Quantum Magnomechanical System with Magnetostrictive Interaction</i>
Ulm, David	CS5a.3	66	<i>Horn Antenna Phase Center Position Influence on Sub-THz Measurements Uncertainties</i>
	CS32.4	1448	<i>Simplified Techniques to Estimate Uncertainties for Antenna Gain Patterns Determined via Near-Field to Far-Field Transformation</i>
Ulmschneider, Markus	CS23b.3	1999	<i>Mixture Density Networks for Multipath Assisted Positioning-Based Fingerprinting</i>
Unwin, Martin	CS46.1	4215	<i>Dual All Metal Patch Antenna for the HydroGNSS Mission</i>
Ur-Rehman, Masood	A27a.2	636	<i>Impact of Dielectric Substrate, Feed Connector, and Fabrication Tolerances on the Performance of Planar Millimeter-Wave Antenna Arrays</i>
	PE3.4	2374	<i>RIS-Enabled Near-Field Localization with EMI</i>
Urakami, Taisei	E06b.1	792	<i>Variable Multi-Band Metasurface Reflector with Controllable Direction Using Varactor Diodes Mounted Large-Via Mushroom-Type Structure</i>
Usai, Pierpaolo	E06a.4	601	<i>Design of a Low-Frequency Magnetic Metasurface for Extremely Focused and Long Range Wireless Power Transfer Applications</i>
	CS33b.4	3321	<i>Deep-Learning Optimized Reconfigurable Metasurface for Magnetic Resonance Imaging</i>
	PP03.6	3610	<i>Target Classification Through ISAR for Autonomous Vehicles Based on Federated Learning</i>

V

Vadher, Pratik	CS27.3	1579	<i>Theoretical Insights and Engineering of Wireless Body-Implanted Bioelectronics</i>
	A08a.3	1893	<i>Frequency Scanning Leaky-Wave Antenna for On-Body Radar: Design</i>

			<i>and Conformal Analysis</i>
Vähä-Savo, Lauri	PA4.7	2134	<i>3D Printed Horn Antennas for Millimeter Wave and Sub-THz Bands</i>
	A28.3	3724	<i>Base Station Radome Design for 5G and Beyond</i>
Vala, Mario	P05.1	241	<i>Small-Scale Passive Millimetre-Wave Imaging Measurements for Marine Litter Detection at W-Band</i>
	P10b.4	3259	<i>Wind-Induced Backscatter Clustering from Vegetation at W-Band</i>
	P02.3	3772	<i>Feature Selection for Identifying Optimal Microwave Frequencies to Detect Floating Macroplastic Litter in C and X Bands</i>
Valenziano, Luca	A05.3	1828	<i>110 to 170 GHz High-Gain Antenna with Embedded Surface Mount Short Horn and Baseband PCB Horn Antenna</i>
Valenzuela-Valdés, Juan	PP01.4	1360	<i>A Study on W-Band Frequency Attenuation in the Presence of Human Blockage</i>
	E10b.2	2064	<i>Analytical Circuit Models: From Purely Spatial to Space-Time Structures</i>
	PA3.8	3424	<i>1-Bit RIS Unit Cell with Mechanical Reconfiguration at 28 GHz</i>
	CS26a.1	4090	<i>Glide-Symmetric SIH Unit Cells Implemented in Parallel-Plate Waveguides at mmWaves</i>
Valerio, Guido	CS9b.5	531	<i>Modal Analysis in Woodpile Dielectric Structures</i>
	CS36b.2	901	<i>Direction-Of-Arrival Ambiguities Mitigation in Multibeam Leaky-Wave Antennas</i>
	CS26a.5	4105	<i>Efficient Numerical Computation of Dispersion Diagrams for Glide-Symmetric Periodic Structures with a Hexagonal Lattice</i>
	CS26b.2	4310	<i>Glide-Symmetric Reconfigurable Substrate-Integrated Holey Waveguide</i>
	CS26b.4	4318	<i>All-Metal Glide-Symmetric Slotted Planar Antennas: Modal Analysis</i>
Valero-Nogueira, Alejandro	PA2.13	1110	<i>Closely-Spaced Groove Gap Waveguides with Reduced Coupling</i>
	PA4.9	2142	<i>5x7 Nolen Matrix in K-Band Implemented in Rectangular Waveguide</i>
	PA3.6	3417	<i>Beam-Tilted All-Metal Radial-Line Slot Array Antenna with Uniform Spacing</i>
	PA4.26	3459	<i>Amplitude-Tapered Half-Mode Gap Waveguide Distribution Network for Flat Panel Antennas</i>
Valkama, Mikko	CS23a.1	1775	<i>Gaussian Processes for Received Signal Strength Based Device-Free Localization</i>
Valkonen, Risto	A15b.3	4335	<i>Array Scattering Synthesis for Anomalous Deflection Using Passive Aperiodic Loadings</i>
Vallejo, Jorge	A06b.4	3301	<i>Dual-Band Reflectarray-Based Electromagnetic Skin to Provide Millimeter-Wave Coverage in the 28/60-GHz Bands</i>
van Aardt, Jason	CS4.5	3194	<i>CSIRO Radio Astronomy Receiver Update - Ultra Wideband and Phased Array Feeds</i>
van Berkel, Sven	CS37b.3	352	<i>Chessboard Focal Plane Array in Silicon Technologies for Terahertz Imaging</i>
van Boeijen, Rutger	CS39b.1	808	<i>Exploring the Properties of Reverberation Chambers in the THz Range: A Pilot Study</i>
van de Ven, Coen	PA7.10	1205	<i>Radiation Pattern Shaping Using Generalized Luneburg Lenses for Automotive RADAR Antennas</i>

van den Biggelaar, Antonius	CS47.4	426	<i>Over-The-Air Noise-Figure Measurements of Active Integrated Antennas at W-Band</i>
	PM2.11	2472	<i>Quiet-Zone Profiling in a mmWave Spherical Anechoic Chamber: An Evaluation Approach</i>
van der Houwen, Eric	CS42b.1	439	<i>An Antenna Measuring System Based on a Cable Suspended Dolly and Inverse Source</i>
van der Spuy, Teanette	A18.2	2909	<i>Self-Interference Suppression for SatCom Active Antenna Arrays Through Joint Transmit and Receive Beamforming</i>
van Dijk, Robbin	M3.2	2590	<i>A Demonstration of Diffraction-Limited Images Using a CMOS Chessboard Array at THz Frequencies</i>
van Katwijk, Alexander	E10b.4	2073	<i>Efficient Analysis Method for Artificial Dielectric Layers with Vertical Metal Inclusions</i>
	E12.1	2820	<i>Reducing the Cross-Polarization Levels in Artificial Dielectric Layers for Wideband Arrays</i>
van Rooijen, Nick	CS7.3	1601	<i>Experimental Characterization of a Core-Shell Lens for Antenna On-Package Integration at D-Band</i>
Van Torre, Patrick	CS40a.2	1758	<i>Optimizing RF Energy Harvesting in IoT: A Machine Learning Estimation Considering Polarization Effects</i>
Vandelle, Erika	A16.2	1734	<i>Low-Profile 2D-Mechanical-Beam-Steering Antenna with Large Field-Of-View</i>
Vandenbosch, Guy	CS47.3	421	<i>Millimeter-Wave Scattering from Building Facade: A Simulation and Verification Study</i>
	CS22b.3	3118	<i>A Modelling Scheme for the Nonclassical Optical Response in the Nanosphere on Mirror Structure</i>
Vanhoenacker-Janvier, Danielle	P04a.2	772	<i>Improvements of Scintillation Modelling from Radiosonde Observations in the Arctic Region</i>
Varault, Stefan	PA2.17	1128	<i>Dual-Polarized Connected-Slot Array Technological Demonstrator Targeting a 5:1 Bandwidth</i>
Vardaxoglou, Yiannis	CS42b.3	446	<i>Phaseless Characterization of Flat Sources with a Planar Wide-Mesh Scanning Strategy</i>
Varum, Tiago	PA4.5	2124	<i>A Simple Technique to Maximize Isolation in Compact mmWaves Antenna Arrays</i>
Vásquez Peralvo, Juan A.	PA2.5	1074	<i>Genetic Algorithm-Based Beamforming in Subarray Architectures for GEO Satellites</i>
	PA6.3	2223	<i>Dual-Polarization Multi-Functional Metasurface for Wireless Communications</i>
	CS19b.4	4295	<i>Supervised Learning Based Real-Time Adaptive Beamforming On-Board Multibeam Satellites</i>
Vassos, Evangelos	CS9b.3	521	<i>Dual-Polarized Reconfigurable Metasurface for Leaky-Wave Antenna Design Using Air-Bridged Schottky Diode Technology</i>
	E05.4	2050	<i>Design of Novel Fully Metallic mm-Wave Reflectarray Antenna</i>
	PA6.8	2241	<i>Anisotropic Circularly Polarising Graded Index Lenses Enabling High Gain CP Antennas</i>
Vaughan, Rodney	A15b.1	4326	<i>Maximum Gain Estimates for Corporate-Fed Arrays</i>
Vazquez-Sogorb,	CS6b.5	505	<i>Multi-Beam Arrays for Future LEO SatCom Payloads</i>

Carlos			
Vecchi, Giuseppe	CS42b.1	439	<i>An Antenna Measuring System Based on a Cable Suspended Dolly and Inverse Source</i>
	PE2.9	1024	<i>Human- Vs Machine Design of Antennas: Evolution Behavior in Genetic Shape Optimization</i>
	PE1.8	1269	<i>Modeling of 3D Feeding Structures in the Automated Design of Metasurface Antennas</i>
	E07.3	1645	<i>Adaptive Weighting Scheme for Multi-Objective Optimization in Metasurface Antenna Design</i>
	E02b.2	3273	<i>Stabilization of EFIE-IBC by Spatial Filtering</i>
	A20.3	3818	<i>Compact Antenna Solutions for Data Transmission Using Fat-Intrabody Communication (Fat-IBC)</i>
	CS30b.3	4156	<i>Automated Design and Characterization of a Scalar Metasurface Antenna Radiating a Linearly-Polarized Broadside Beam</i>
Vellucci, Stefano	E08.2	1868	<i>Reflective Intelligent Surfaces: Reducing Complexity by Controlling the Illuminating Field</i>
	E08.5	1880	<i>Static and Reconfigurable Phase-Gradient Metasurfaces for Antenna Applications</i>
	PA4.10	2147	<i>Analysis and Design of Robust Reconfigurable Intelligent Surfaces Using a Statistical Approach</i>
	A10.2	3071	<i>Analysis and Design of Metasurface Antennas Based on Temporal Metastructures</i>
Verdugo, Elizabeth	P09.4	2649	<i>Rain Attenuation at mmWave and Optical Bands from Visibility and Rainfall Intensity Measurements</i>
Verma, Anamika	CS21.1	2706	<i>Imaging Radar Frontend with SIW Feeding Networks</i>
Vermeeren, Gunter	CS2.5	184	<i>New Hybrid Ray-Tracing/FDTD for EMF Exposure in 6G Networks Using Semantically Classified Google Earth Photogrammetry with Measurement Validation</i>
Vermeulen, Ernestus	CS12b.4	4273	<i>Robotic near Field Scanning for High Throughput Phased Array Production Test</i>
Verni, Francesco	CS30b.3	4156	<i>Automated Design and Characterization of a Scalar Metasurface Antenna Radiating a Linearly-Polarized Broadside Beam</i>
Vico, Felipe	CS19a.2	4072	<i>Surface Partial Differential Equations and Its Applications to Scattering Problems</i>
Vidjak, Klementina	CS24b.5	936	<i>Wideband Dielectric Characterization of Biological Tissues and Realistic Phantom Preparation at Microwave Frequencies</i>
	M4.3	2959	<i>Numerical Study of the Dielectric Properties of Lung Tissue Measured with Two Different Open-Ended Coaxial Probes</i>
	PA1.13	3385	<i>Sensitivity of the Dielectric Spectroscopy with the Microwave Thermal Ablation Antenna to the Immersion Depth and Longitudinal Dimension of the Measured Media</i>
Vieira, Juner	A12b.3	1936	<i>Synthesis of Circularly Polarized Microstrip Planar Array with Cross-Polarization Suppression</i>
Vigano, Maria Carolina	CS10.2	855	<i>Design of a Dielectric Lens Using a Ray-Tracing Model for Satellite Communications</i>

Viikari, Ville	CS38.1	112	<i>Improving Scan Gain of Sparse Vivaldi Array with Parasitic Scatterers</i>
	CS37b.2	348	<i>Crack Stop as a Coupling Element Between an IC Chip and Antenna</i>
	PE2.4	1004	<i>Applying Neural Networks for Predicting Feed Weights of an Antenna Array</i>
	CS40b.1	1969	<i>Small On-Metal Passive UHF RFID Transponders with Long Read Ranges</i>
	CS30b.5	4163	<i>Optimization of Loads for Antenna-Based Scattering Systems Using Feedforward Neural Networks</i>
Vijayaraghavan, Mugundhan	CS4.4	3189	<i>The Hydrogen Intensity Real-Time Analysis eXperiment: Overview and Status Update</i>
Vilenskiy, Artem	A05.5	1836	<i>Sub-THz U-Slot Coupled Stacked-Patch Radiating Elements for Dual-Polarized MIMO Array Antennas</i>
	CS48.5	3996	<i>A Varactor-Based Reconfigurable Intelligent Surface Concept for 5G/6G mm-Wave Applications</i>
Villaescusa-Tebar, Alvaro	CS2.1	165	<i>Instantaneous Vs Theoretical Maximum Exposure Under Real Traffic Conditions: Example in the City of Valencia</i>
Villemaud, Guillaume	PA3.9	3429	<i>Impact of the Antenna Topology on the Combination of Full-Duplex Spatial Modulation and RF Energy Harvesting</i>
	PP03.1	3589	<i>Wideband Characterization of Wireless Power Transfer in Ventilation (HVAC) Ducts for the Internet of Things and Smart Buildings</i>
	PP03.9	3625	<i>Indoor Localization of Smartphones Thanks to Zero-Energy-Devices Beacons</i>
Violi, Vincenzo	PP03.6	3610	<i>Target Classification Through ISAR for Autonomous Vehicles Based on Federated Learning</i>
Viorel, Dorin	P10b.1	3244	<i>Empirical Path Loss Model and Small-Scale Fading Statistics in an Indoor Office Environment in 6 and 37 GHz Shared Bands</i>
	P01.4	3847	<i>Frequency Domain Channel Characteristics in an Outdoor-To-Indoor Environment at 6 and 37 GHz</i>
Vipiana, Francesca	CS24a.1	724	<i>Advancements in the Experimental Validation of a Wearable Microwave Imaging System for Brain Stroke Monitoring</i>
	CS11.1	1616	<i>AI-Assisted Design and Experimental Testing of a Compact UWB Antenna for the Inspection of Food and Beverage Products</i>
	CS33a.3	3054	<i>Advancements in Broadband Electromagnetic Sensing for Food Quality Control</i>
	CS33b.1	3309	<i>Nonlinear Correction of the Direct Inverse Problem Solution in Real-Time Imaging</i>
	CS26a.5	4105	<i>Efficient Numerical Computation of Dispersion Diagrams for Glide-Symmetric Periodic Structures with a Hexagonal Lattice</i>
	CS19b.2	4287	<i>A Multi-Region Hierarchical Preconditioning Scheme for the MoM Simulation of Complex Composite Structures</i>
	CS19b.3	4292	<i>Automatic MoM Source Integral Quadrature Selection via a Machine Learning Approach</i>
Virkki, Johanna	CS13.4	1563	<i>Enabling Living Spaces Through Customizable NFC-Enabled Smart Table System</i>
Virone, Giuseppe	CS6b.5	505	<i>Multi-Beam Arrays for Future LEO SatCom Payloads</i>

Viteri-Mera, Carlos	P04b.4	980	<i>Fast Indoor Radio Propagation Prediction Using Deep Learning</i>
Vitucci, Enrico M.	CS20b.2	398	<i>A Macroscopic Bilateral Modeling Approach for Reflective and Transmissive Metasurfaces</i>
	CS43b.3	4178	<i>Machine Learning Approach to Delay Spread Estimation in Industrial Environments</i>
	CS43b.4	4183	<i>A Study on Satellite-To-Ground Propagation in Urban Environment</i>
Voigt, Thiemo	P06.2	2732	<i>Development of Tissue Emulatory Models/Phantoms of Lungs at Microwave Frequency for Acute Respiratory Distress Syndrome</i>
Völker-Schöneberg, Yanneck	CS23b.5	2009	<i>Characterization of Propagation from Measurements at Sub-THz for ISAC Applications in an Emulated Dynamic Industrial Scenario</i>
Vorobyov, Alexander	CS1b.5	4254	<i>Plug-In Plug-Out Multibeam Dielectric Rod Antenna for Target Dedicated mm-Wave RF-WPT Applications</i>
Vosoogh, Abbas	CS21.4	2717	<i>Low-Cost Coaxial Slot Array Antenna for E-Band Automotive Corner Radar Applications Based on Gap Waveguide MLW Technology</i>
Votis, Konstantinos	E07.5	1653	<i>An Accurate Semi-Analytical Model for Periodic Tunable Metasurfaces Electromagnetic Response</i>
Vryghem, Pauline	PA2.21	1145	<i>Wideband Low-Profile Circularly Polarized All-Metal Antenna for Triton Exploration</i>
Vu, Hong-Tien	PA5.8	3524	<i>A Linearly Polarized Wideband Antenna with A Stable Omnidirectional Radiation Pattern</i>
Vuohijoki, Tiina	CS13.4	1563	<i>Enabling Living Spaces Through Customizable NFC-Enabled Smart Table System</i>
Vuohtoniemi, Risto	P01.1	3832	<i>5G Radio Channel Characterization in an Underground Mining Environment</i>
Vuyyuru, Sravan Kumar Reddy	A15b.3	4335	<i>Array Scattering Synthesis for Anomalous Deflection Using Passive Aperiodic Loadings</i>
Vychodil, Josef	CS43b.1	4168	<i>Channel Measurements and Characterization in Industrial Environment at 60 GHz</i>

W

Wagih, Mahmoud	PA7.17	1233	<i>An Investigation into the Effects of Multi-Path and NLOS Propagation on Antenna-Based Soil Moisture Sensors in the RFID Band</i>
	PA3.20	3479	<i>Sub-THz On-Chip CPW Monopole on InP with Cross-Shaped Slot for Bandwidth Enhancement</i>
	CS1a.1	4023	<i>Microwave to mmWave Wireless Power Transfer: An Overview of the Design Challenges with a Focus on UK-Based R&D</i>
Walden, Marcus	PA7.2	1168	<i>On the Radiation Resistance of Folded Antennas</i>
	A23.4	2762	<i>The Kootwijk VLF Antenna: A Numerical Model</i>
Waldschmidt, Christian	PA6.2	2218	<i>An Eigenvector-Supported Optimization Method for Holographic-Based Leaky Wave Antennas</i>
	CS21.5	2722	<i>Effects of Bumper Integration on Low-, Mid-, and High-Resolution Imaging Radars</i>
	A11.2	3157	<i>A Low-Profile Wide-Scan Magneto-Electric Dipole Antenna for 5G mm-Wave Communications</i>
	PA3.11	3438	<i>Broadband Waveguide Magneto-Electric Dipole Antenna for F-Band Applications</i>

	CS12a.1	4043	<i>A High-Precision Approach to Eliminate Positioning Errors in Radar Calibrations</i>
Walters, Anthony	CS4.4	3189	<i>The Hydrogen Intensity Real-Time Analysis eXperiment: Overview and Status Update</i>
Wan, Guobin	PE1.3	1249	<i>A Polarization-Insensitive Ultra-Broadband FSS Absorber with Low-Profile Based on the ITO Film</i>
	CS30a.5	3947	<i>Alternate Optimization with Deep Learning to Design Beam Deflector Under Aperiodic Near-Field Coupling Conditions</i>
Wan, Yinglu	PA4.1	2105	<i>A Linear Wide-Angle Scanning Phased Array Antenna Using Heterogeneous Beam Element Technology</i>
	PA4.23	2201	<i>A Wideband Aperture-Shared Dual-Polarized End-Fire Antenna with Low Profile and High Isolation</i>
	PA5.11	3537	<i>Circularly Polarized Wide-Angle Scanning Phased Array Based on Heterogeneous Beam Element</i>
Wan, Zifeng	PE3.17	2423	<i>Enhancing Signal Transmission in Energy-Saving Glass Through Tri-Bandpass Frequency Selective Surface Design</i>
Wane, Sidina	CS47.2		<i>Advanced Thermal-Imaging for OTA Industrial-Testing of Active-In-Package, Antenna-On-Chip and Antenna on PCB</i>
	M3.4	2600	<i>Numerical Assessment of a Cognitive Chamber: TMz Case</i>
Wang, Cheng-Xiang	PP01.17	1418	<i>Scenario Classification and Channel Modeling for MIMO Communications in Dense Urban Street Scenarios</i>
	PP01.18	1423	<i>Channel Characterization and Modeling for Wireless MIMO Communication Systems in Intersection Scenarios</i>
	PP01.19	1428	<i>Ray-Tracing Based Channel Modeling and Characteristics Analysis for LEO Satellite-To-Ground Systems</i>
	P01.3	3842	<i>Scenario Classification and Channel Modeling for MIMO Communications in Suburban Road Scenarios</i>
Wang, Congcong	CS35a.3	1692	<i>AttentionRNN: Novel Propagation Channel Time-Domain State Predictor</i>
Wang, Cunxiang	CS48.3	3987	<i>Joint Resource Allocation and Beamforming Design for Secure Short Packet Communication in RIS-Aided MISO Systems</i>
Wang, Enlin	A28.1	3714	<i>Antenna and Mechanical Co-Design for Auto-Beam-Tracking in Backhaul Systems</i>
Wang, Guangjian	CS29.5	3807	<i>Multi-Scattering Centers Extraction and Modeling for ISAC Channel Modeling</i>
Wang, Hairu	E10a.3	1850	<i>Analysis of the Dispersion Diagrams of 3D Cubic Periodic Arrangements of Metallic Spheres</i>
Wang, Hanyang	PA7.4	1176	<i>Passive Beamforming with Liquid Antennas: Techniques and Implementation</i>
	PA5.9	3529	<i>A Cascaded Resonator Decoupling Network for Two Filtering Antennas with Adjacent Operating Bands</i>
	PA5.16	3556	<i>Design of the 3D-Printed Rectangular Dielectric Resonator Antenna for WLAN Applications</i>
Wang, Hong Bin	CS8.3	2892	<i>A Wideband Filtering Linear-To-Circular Polarization Converter for Ka-Band Satellite Communication</i>

Wang, Jiahao	A12b.2	1932	<i>An L-Band Receiving Array with Full Digital Simultaneous Quad-Polarization Beamforming</i>
	A15a.3	4118	<i>Impact of Deformations on Beamforming Performance of Uniform Rectangular Arrays</i>
Wang, Jie	CS48.3	3987	<i>Joint Resource Allocation and Beamforming Design for Secure Short Packet Communication in RIS-Aided MISO Systems</i>
Wang, Jingchen	CS1a.5	4039	<i>Design of Dual-Band CPW Rectenna for Wireless Power Transmission</i>
Wang, Jingru	A27b.1	830	<i>A Wideband High-Gain Circularly-Polarized Metasurface Antenna with a Large Element Spacing SIW Array at Ka Band</i>
Wang, Kang	PA2.16	1123	<i>Study on CFM Method for Beam Compensation of Array-Fed Space-Borne Reflector Antennas</i>
Wang, Lei	PA6.3	2223	<i>Dual-Polarization Multi-Functional Metasurface for Wireless Communications</i>
	PA8.18	2344	<i>Bandwidth Manipulated Leaky-Wave Antenna Using a Sinusoidal Ridge in Folded Substrate Integrated Waveguide</i>
	A01a.1	2928	<i>Millimeter-Wave Uniform Amplitude SIW Series Power Divider for 2D Leaky-Wave Antenna Arrays</i>
	CS1b.3	4246	<i>A mmWave Leaky-Wave Antenna for Efficiency Enhanced Near-Field Wireless Power Transfer and Communication</i>
Wang, Luyi	CS36b.3	906	<i>Towards a Reconfigurable Metacavity Antenna for Computational Imaging and DoA Estimation</i>
Wang, Min	A01a.5	2945	<i>Low-Profile Multibeam Beam-Scanning Antenna for Vehicular Radar Systems</i>
Wang, Min	PA5.20	3574	<i>A Wideband Circularly Polarized Filtering Array Antenna Using Dual-Layer Circular Cross Slotted Patch</i>
Wang, Nan	PE1.3	1249	<i>A Polarization-Insensitive Ultra-Broadband FSS Absorber with Low-Profile Based on the ITO Film</i>
	CS30a.5	3947	<i>Alternate Optimization with Deep Learning to Design Beam Deflector Under Aperiodic Near-Field Coupling Conditions</i>
Wang, Peng	CS39a.5	627	<i>Standardization Progress and Challenges for 5G OTA Testing</i>
Wang, Quanfeng	PE2.1	990	<i>Geometry Reconstruction from Entries of Impedance Matrices</i>
Wang, Ruichen	A28.5	3734	<i>Indoor Wireless Signal Modeling with Smooth Surface Diffraction Effects</i>
Wang, Shen	PA7.6	1185	<i>Dual-Feed Wideband Folded Waveguide Antenna for Handset Devices</i>
Wang, Shixiong	PE1.4	1253	<i>A Multifunctional Reconfigurable Metagrating for Wavefront Manipulations</i>
Wang, Wei	CS35a.2	1688	<i>Beam Coverage Model of Ultra-Massive MIMO Communication Systems for Intelligent Transportation</i>
	CS23a.3	1785	<i>Robust Tensor Positioning Based on Channel Parameter Estimation Under Spatially Colored Noise</i>
	CS23a.4	1790	<i>Analysis of Channel Characteristics for FMCW Millimeter-Wave Radar in Traffic Scenarios</i>
Wang, Wei	PA5.22	3581	<i>DRL-Based Sidelobe Suppression for Multi-Focus Reconfigurable Intelligent Surface</i>
Wang, Xin	CS17b.2	322	<i>Challenges and Opportunities of Amplified Information Metasurfaces for</i>

			<i>Simultaneous Wireless Communications and Power Transfers</i>
Wang, Yi	A09b.1	872	<i>X-Band Reconfigurable Phase Shifters Based on SIW and Liquid Metal Technologies</i>
	A13.4	1961	<i>Low Profile Wideband Dual-Polarized Antenna Array for Ku/K/Ka-Band Satcom Applications</i>
	A11.4	3166	<i>A Multilayer Dual-Polarized Stacked Patch Antenna with Enhanced Port Isolation for mmWave Highly Integrated Applications</i>
Wang, Yibo	CS31.3	1668	<i>Application of Compressed Sensing to Antenna Far-Field Calibration in an Extrapolation Range</i>
Wang, Yikai	P03.5	1548	<i>Utilization of Wi-Fi Signal for Validation of Micro-Doppler Model in a Person Falling Scenario</i>
Wang, Yinghua	PP01.19	1428	<i>Ray-Tracing Based Channel Modeling and Characteristics Analysis for LEO Satellite-To-Ground Systems</i>
Wang, Yong	PE2.2	995	<i>A Two-Component 2-D FDFD Eigenmode Method Incorporated with the Conformal Technique</i>
Wang, Yongmao	PA2.3	1066	<i>Compact Vivaldi Antenna Application in High-Power Design at X-Band</i>
Wang, Yunfei	A15a.1	4110	<i>Multiple-User Full-Duplex Hybrid Beamforming Design for mmWave Systems with A Joint Interference Cancellation Design</i>
Wang, Yuqi	PA4.1	2105	<i>A Linear Wide-Angle Scanning Phased Array Antenna Using Heterogeneous Beam Element Technology</i>
	PE3.12	2404	<i>High-Order Quasi-Elliptical Bandpass FSS Based on Substrate-Integrated Waveguide Technology for 60 GHz Applications</i>
	PA5.4	3506	<i>A Dual-Port Antenna for Colinearly Polarized Full Duplex and Pattern Reconfigurable Applications</i>
	PA5.6	3515	<i>Bifunctional Stubs Enabled MIMO System for Wideband Mobile 5G and Wi-Fi 6E Applications</i>
Wang, Zhao	CS1a.5	4039	<i>Design of Dual-Band CPW Rectenna for Wireless Power Transmission</i>
Wang, Zhengpeng	A09b.5	891	<i>Liquid Metal Reconfigurable Phased Array Antenna</i>
Warkentin, Lukas	CS30b.4	4159	<i>Port Generation for Multi-Mode Multi-Port Antennas Based on Group Theory</i>
Webster, Peter	PA2.18	1132	<i>Study of Different Feed Layout Configurations for Hybrid Active VHTS Antennas</i>
Wei, Gao	A01a.5	2945	<i>Low-Profile Multibeam Beam-Scanning Antenna for Vehicular Radar Systems</i>
Wei, Jia	PA5.11	3537	<i>Circularly Polarized Wide-Angle Scanning Phased Array Based on Heterogeneous Beam Element</i>
Wei, Shiju	PA2.10	1096	<i>Conceptual Design of Antenna Arrays for Satellite Direct-To-Cell Connectivity</i>
Weinberger, Kevin	CS34.3	2620	<i>Validating Properties of RIS Channel Models with Prototypical Measurements</i>
Weltman, Amanda	CS4.4	3189	<i>The Hydrogen Intensity Real-Time Analysis eXperiment: Overview and Status Update</i>
Wen, Lehu	A03a.1	2862	<i>Low-Profiled Wideband Dual-Polarized Conformal Antenna Array</i>
	A11.4	3166	<i>A Multilayer Dual-Polarized Stacked Patch Antenna with Enhanced Port Isolation for mmWave Highly Integrated Applications</i>

Wen, Su	PE1.17	1303	<i>A Novel Metasurface Inverse Design Based on Back Propagation Neural Network</i>
Wennergren, Anders	A28.1	3714	<i>Antenna and Mechanical Co-Design for Auto-Beam-Tracking in Backhaul Systems</i>
West, David	CS37a.4	42	<i>Integrated Low-Loss mmWave On-Chip Arrays</i>
	CS14b.1	4349	<i>Reconfiguration of Electromagnetic Metasurfaces Using Tunable Shape Morphing Structures</i>
Whale, Mark	PA7.11	1210	<i>Electromagnetic Assessment of Tolerances of the Square Kilometre Array Log Periodic Antenna Using Uncertainty Quantification</i>
	A18.4	2919	<i>Method of Moment Simulation of Full Arctic Weather Satellite Structure</i>
Whittaker, Thomas	E05.4	2050	<i>Design of Novel Fully Metallic mm-Wave Reflectarray Antenna</i>
	PA6.6	2235	<i>Experimental Results for Carbon Nanotube-Sheet Based Microstrip Patch Antenna</i>
	PA6.8	2241	<i>Anisotropic Circularly Polarising Graded Index Lenses Enabling High Gain CP Antennas</i>
Whittow, William	PE1.7	1265	<i>Design of a Concentric Circular Holographic Metasurface Using Hexagonal Anisotropic Unit-Cell for Wireless Communications</i>
	PP01.13	1404	<i>Half Mode Corrugated Substrate Integrated Waveguide (HM-CSIW) Band-Stop Filter Using Hexagonal Ring Resonators</i>
	E05.4	2050	<i>Design of Novel Fully Metallic mm-Wave Reflectarray Antenna</i>
	PA6.6	2235	<i>Experimental Results for Carbon Nanotube-Sheet Based Microstrip Patch Antenna</i>
	PA6.8	2241	<i>Anisotropic Circularly Polarising Graded Index Lenses Enabling High Gain CP Antennas</i>
	PA6.10	2250	<i>Generation of Narrow Divergence Angle OAM Beams for mmWave Communication Links Using Metasurface</i>
	PA3.17	3467	<i>Beam Steering Range Enhancement of Bifocal Reflectarray Using Irregular Distribution of Meta-Atoms</i>
	PA3.18	3472	<i>Embedded Graded Index Lens for Mitigating the Phase Error of an SIW Horn Lens Antenna</i>
	CS14a.4	4142	<i>Optimal Morphing Metasurface Lens for Next Generation RF Sensing and Communications</i>
	Wietstruck, Matthias	A05.1	1820
PA4.24		2206	<i>Design and Investigation of 2x2 Dielectric Resonator Antennas Array for Sub-THz Applications</i>
Wijtharathna, Ransara	CS44b.5	960	<i>Graph Neural Network Based 77 GHz MIMO Radar Array Processor for Autonomous Robotics</i>
Willame, Martin	P02.1	3763	<i>Multistatic OFDM Radar Fusion of MUSIC-Based Angle Estimation</i>
Williams, Lewis	A17.3	3749	<i>Design and Test of a UHF Deployable Conical Log Spiral Antenna for Small Satellites</i>
Williamson, Thomas	CS37a.4	42	<i>Integrated Low-Loss mmWave On-Chip Arrays</i>
Williamstyer, David	CS14b.3	4357	<i>Analyzing the Performance of Phased Array Geometries with Aperture Projection Analysis</i>
Wilton, Donald	CS19b.3	4292	<i>Automatic MoM Source Integral Quadrature Selection via a Machine</i>

Learning Approach

Wincza, Krzysztof	PA3.20	3479	<i>Sub-THz On-Chip CPW Monopole on InP with Cross-Shaped Slot for Bandwidth Enhancement</i>
Wischmann, Wolfgang	CS10.3	860	<i>D-Band Active Antenna Array with Lens Enabling Quasi-Optical and Analogue Beam Reconfiguration for 6G Applications</i>
Wleklinski, Michael	CS10.3	860	<i>D-Band Active Antenna Array with Lens Enabling Quasi-Optical and Analogue Beam Reconfiguration for 6G Applications</i>
Wojnowski, Maciej	CS18.4	3683	<i>Circularly Polarized Sub-THz Antenna Design for Distributed Deployment</i>
Wolfshtein, Daniel	PA7.13	1219	<i>Experimental Investigation of the Nullifier-Based Monopole</i>
Wong, Hang	A09b.1	872	<i>X-Band Reconfigurable Phase Shifters Based on SIW and Liquid Metal Technologies</i>
	A09b.5	891	<i>Liquid Metal Reconfigurable Phased Array Antenna</i>
Woo, Haneul	PE3.9	2395	<i>Concentration Detection of Sodium Chloride and Glucose Solutions Using an IDC-Based Microwave Sensor with Eliminating Environmental Effects</i>
Wu, Bofan	P10b.5	3263	<i>E-Band Measured Propagation Characteristics for Urban Backhaul Communications</i>
Wu, Chao	PA7.7	1190	<i>A Brief Analysis of the Latest Research Progress and Future Direction of Low-Frequency Transmitting Antenna</i>
Wu, Ke	CS1a.4	4035	<i>Substrate-Integrated Mode Composite Waveguide</i>
Wu, Mengfan	P10a.4	2987	<i>Direct Clustering and Multi-Path Component Identification on THz Channel Measurements in a Factory Environment</i>
Wu, Sheng-Wei	PA5.2	3498	<i>DC Bias Routing Design for Wideband Reconfigurable Transmitarray Based on 1-Bit Phase-Switching Elements</i>
Wu, Shuai	CS14b.1	4349	<i>Reconfiguration of Electromagnetic Metasurfaces Using Tunable Shape Morphing Structures</i>
Wu, Tong	CS18.1	3669	<i>Metasurfaces Meet Characteristic Modes</i>
Wu, Wen	A01b.5	3216	<i>Array-Fed Transmitarray with Designated Beam Directions and Coverages</i>
Wu, Ya Fei	CS8.3	2892	<i>A Wideband Filtering Linear-To-Circular Polarization Converter for Ka-Band Satellite Communication</i>
Wu, Zhipeng	PA5.16	3556	<i>Design of the 3D-Printed Rectangular Dielectric Resonator Antenna for WLAN Applications</i>
Wydaeghe, Robin	CS2.5	184	<i>New Hybrid Ray-Tracing/FDTD for EMF Exposure in 6G Networks Using Semantically Classified Google Earth Photogrammetry with Measurement Validation</i>

X

Xavier, Pascal	CS3.5	311	<i>Exploring PLA/Flax Substrates for Antenna Applications: Assessing Moisture, Temperature and Dielectric Constant Homogeneity</i>
Xia, Xiaoyue	CS8.1	2885	<i>Milimeter-Wave 3D Folded Strip Antennas and Arrays: Diverse Polarizations Realization Under Robust Input Impedance</i>
Xia, Xinping	A15a.1	4110	<i>Multiple-User Full-Duplex Hybrid Beamforming Design for mmWave Systems with A Joint Interference Cancellation Design</i>
	A15a.4	4122	<i>Beamforming Optimization for Full-Duplex Relay in SIC-Enhanced</i>

			<i>Cooperative NOMA System</i>
Xiao, Jianliang	PA5.5	3511	<i>Pulse Preserving Capability of an Ultrawideband Dispersive Dielectric Resonator Antenna</i>
Xiao, Pei	PA2.9	1091	<i>Sub-7 GHz Circularly Polarized Dielectric Resonator Antenna Array for Full-Duplex Applications</i>
	PA2.22	1150	<i>Compact Circularly Polarized Patch Antenna with Enhanced Axial Ratio and Impedance Bandwidth</i>
	PE1.11	1279	<i>Compact Polarization Converter on a Thin Ferrite-Based Metasurface for Enhanced 5G Wireless Communication</i>
	PA4.13	2160	<i>A Novel Precise Approach for Digital Metasurface Configuration for Sensing Application</i>
Xiao, Xiaoyu	A09a.5	696	<i>Non-Volatile RF Frequency Reconfigurable Antenna for Wireless Communication</i>
	PA3.16	3463	<i>Frequency Reconfigurable Flexible Printed Antenna Based on Non-Volatile RF Switches for Wearable Applications</i>
Xiao, Yue	CS48.1	3977	<i>Beamforming Orthogonality in Coupled Directional Modulation Arrays</i>
Xie, Wenqing	PA3.2	3403	<i>Design of Ultra-Wideband Dual-Polarized Corrugated Horn Antenna for 5G Application</i>
	PA3.7	3421	<i>A Single-Layer Quadruple-Band Millimeter-Wave Antenna Using Split-Rings for 5G Application</i>
	PA5.20	3574	<i>A Wideband Circularly Polarized Filtering Array Antenna Using Dual-Layer Circular Cross Slotted Patch</i>
	PA5.21	3577	<i>Design of a Dual-Polarization Ultra-Wideband Horn Antenna</i>
Xie, Yanzhao	CS39a.2	614	<i>Measurement of Total Radiated Power Using a TEM Cell</i>
Xu, Bo	CS2.3	175	<i>Long-Term Network-Based Assessment of the Actual Output Power of Base Stations in a 5G Network</i>
	CS39a.4	622	<i>Addressing PIM Challenges in Radio Base Stations: Field Issues and Testing Methods for Large-Scale Deployments</i>
	PM2.13	2482	<i>Study on Antenna-Phantom Model of Aperture Antennas for SAR Analysis</i>
	CS8.1	2885	<i>Millimeter-Wave 3D Folded Strip Antennas and Arrays: Diverse Polarizations Realization Under Robust Input Impedance</i>
Xu, Ran	PM2.9	2464	<i>Complex Permittivity Extraction of Typical Wooden Furniture Materials Based on Multi-Objective Particle Swarm Optimization over 40-50 GHz</i>
Xue, Bing	A25.2	3090	<i>3D Printed Cascaded Cavity-Backed Millimeter-Wave Filtering Antenna</i>
Xue, Bingjie	CS23a.4	1790	<i>Analysis of Channel Characteristics for FMCW Millimeter-Wave Radar in Traffic Scenarios</i>
Xue, Quan	PA4.1	2105	<i>A Linear Wide-Angle Scanning Phased Array Antenna Using Heterogeneous Beam Element Technology</i>
	PA4.23	2201	<i>A Wideband Aperture-Shared Dual-Polarized End-Fire Antenna with Low Profile and High Isolation</i>
	PE3.12	2404	<i>High-Order Quasi-Elliptical Bandpass FSS Based on Substrate-Integrated Waveguide Technology for 60 GHz Applications</i>
	PA5.4	3506	<i>A Dual-Port Antenna for Colinearly Polarized Full Duplex and Pattern Reconfigurable Applications</i>

	PA5.6	3515	<i>Bifunctional Stubs Enabled MIMO System for Wideband Mobile 5G and Wi-Fi 6E Applications</i>
	PA5.11	3537	<i>Circularly Polarized Wide-Angle Scanning Phased Array Based on Heterogeneous Beam Element</i>
Xue, Shaoxuan	PP01.15	1410	<i>A Modified Channel Model for the MIMO System Deployed RIS Elements with Imperfect Surface</i>

Y

Yacoub, Michel Daoud	CS34.5	2629	<i>RIS Performance in a Comprehensive Fading Environment</i>
Yadav, Purnima	PM2.8	2459	<i>Uncertainties in the Estimation of the Gain of a Standard Gain Horn in the Frequency Range of 90 GHz to 140 GHz</i>
Yadav, Rahul	PP03.13	3643	<i>Filter Integrated Microstrip 3-Port Power Combiner</i>
Yaghjian, Arthur	A23.1		<i>Generalized Far-Field Distance of Antennas and the Concept of Classical Photons</i>
Yago Ruiz, Álvaro	CS24a.5	740	<i>Polynomial Basis Functions for Qualitative Head Tissue Segmentation via Linearized Microwave Imaging</i>
	P02.2	3768	<i>Learning-Based Procedures for Inverse Design of Electromagnetic Devices: A Preliminary Investigation</i>
Yamada, Wataru	CS5b.6	388	<i>Sub-Terahertz MassiveMIMO Channel Sounder for 6G Mobile Communication Systems</i>
	P04a.5	787	<i>Proposal on Application of Quantum Annealers for Analysis of Multiple Scattered Waves</i>
	A27b.4	842	<i>Design of a Hollow-Waveguide Slot Array Antenna for a Channel Sounder in the 150 GHz Band</i>
	PP03.3	3597	<i>Propagation Path Analysis with Propagation QUBO Model in Urban Area</i>
Yamaguchi, Rikako	A27b.4	842	<i>Design of a Hollow-Waveguide Slot Array Antenna for a Channel Sounder in the 150 GHz Band</i>
Yamamoto, Haruki	CS36b.1	896	<i>Safe Beamforming Based on Human Area Estimation for Microwave Wireless Power Transfer</i>
Yamamoto, Masashi	PA4.4	2119	<i>Prototype of Multi-Sector Indoor mmW Base Station Based on 5G NR Beam Control</i>
Yan, Sen	A03a.5	2881	<i>Reducing Mutual Coupling in 2x2 MIMO Circularly Polarized Patch Antenna Array Using Reflecting Polarization Conversion Metasurface</i>
Yan, Xiangrui	PE2.6	1012	<i>Machine-Learning-Based Optimization for Wideband Metasurface Mosaic Antenna</i>
Yan, Xiaotian	CS22b.3	3118	<i>A Modelling Scheme for the Nonclassical Optical Response in the Nanosphere on Mirror Structure</i>
Yang, Bo	CS37a.2	34	<i>Optimum Structured Phased Array with Novel Beam Forming Circuits for Beam Wireless Power Transfer</i>
	CS15.3	4011	<i>Large and Simple Phased Array System at 28 GHz for Beam Wireless Power Transfer</i>
	CS1a.3	4031	<i>Far-Field Beam Wireless Power Transfer with Combination of Beam Forming and Optical Target Detection</i>
Yang, Furong	CS1a.2	4027	<i>Single-Branch Hybrid Resistance Compression Technique for Enhanced Rectifier Performance</i>

Yang, Guangwei	PA6.3	2223	<i>Dual-Polarization Multi-Functional Metasurface for Wireless Communications</i>
Yang, Hang	P10b.5	3263	<i>E-Band Measured Propagation Characteristics for Urban Backhaul Communications</i>
Yang, Hangqi	PA8.13	2324	<i>A Near-Field Focusing Circularly Polarized Radial Line Slot Array Antenna</i>
Yang, Huaizhi	M2.1	3881	<i>A Novel MIMO OTA Methodology for UE Performance Testing</i>
Yang, Hyunjun	CS17b.4	330	<i>Indoor Coverage Enhancement Employing Liquid Crystal-Based Massive Reconfigurable Intelligent Surface Linked to 5G FR2 Base Station</i>
Yang, Jian	A13.2	1954	<i>Compact Circularly Polarized Antenna Based on Gapwaveguide for SATCOM Applications</i>
	PA4.20	2189	<i>A Comparative Study of Decoupling Techniques for Waveguide Slot Array Antennas</i>
	A23.3	2757	<i>Analysis of Radiating Transverse Slot Unit Cell and Reflection Cancellation at D-Band</i>
	A28.1	3714	<i>Antenna and Mechanical Co-Design for Auto-Beam-Tracking in Backhaul Systems</i>
Yang, Jichao	CS1a.2	4027	<i>Single-Branch Hybrid Resistance Compression Technique for Enhanced Rectifier Performance</i>
Yang, Peizhuo	A12a.4	1719	<i>X-Band Receiving Phased Array with Digital Beamforming Using RFSoc</i>
	A12b.2	1932	<i>An L-Band Receiving Array with Full Digital Simultaneous Quad-Polarization Beamforming</i>
Yang, Qingling	A11.4	3166	<i>A Multilayer Dual-Polarized Stacked Patch Antenna with Enhanced Port Isolation for mmWave Highly Integrated Applications</i>
Yang, Shanglin	PP03.9	3625	<i>Indoor Localization of Smartphones Thanks to Zero-Energy-Devices Beacons</i>
Yang, Sheng-Yeh	PA3.1	3398	<i>Dynamic Programming-Based Beam Codebook Design for mmWave Multi-Antenna Module in Mobile Devices</i>
Yang, Songjiang	PP01.19	1428	<i>Ray-Tracing Based Channel Modeling and Characteristics Analysis for LEO Satellite-To-Ground Systems</i>
Yang, Weikang	PP01.15	1410	<i>A Modified Channel Model for the MIMO System Deployed RIS Elements with Imperfect Surface</i>
Yang, Weixu	CS6a.2	199	<i>Designing Transmissive Metasurface for Multibeam Transmitarray at 5G Millimeter-Wave Band</i>
Yang, Wenfei	CS29.5	3807	<i>Multi-Scattering Centers Extraction and Modeling for ISAC Channel Modeling</i>
Yang, Xiantao	PE2.5	1009	<i>Gain Improvement of a DRA Using Deep Reinforcement Learning with Polygon Mesh Deformation</i>
	A25.2	3090	<i>3D Printed Cascaded Cavity-Backed Millimeter-Wave Filtering Antenna</i>
	PA5.5	3511	<i>Pulse Preserving Capability of an Ultrawideband Dispersive Dielectric Resonator Antenna</i>
Yang, Xiaoxiao	CS23a.5	1794	<i>HRPE-Enhanced AI-Based 5G Indoor Localization in Presence of Specular and Dense Multipaths</i>

Yang, Xiaoyu	CS45.1	1799	<i>MR/Microwave Tomography Integrated Breast Cancer Imaging</i>
Yang, Yu	CS39a.4	622	<i>Addressing PIM Challenges in Radio Base Stations: Field Issues and Testing Methods for Large-Scale Deployments</i>
Yang, Yu	PA1.5	3349	<i>Monitoring Eye States Based on Transparent and Flexible Antenna in WBAN</i>
Yao, Ming	PM1.9	1343	<i>Investigation of Correlation Between Absorbed Power Density and Incident Power Density for User Equipment Antennas at Sub-THz Frequencies</i>
Yao, Yu	E06a.5	605	<i>An Efficient Wheel-Integrated Wireless Power Transfer System Based on High-Permittivity Metasurface</i>
	PA1.5	3349	<i>Monitoring Eye States Based on Transparent and Flexible Antenna in WBAN</i>
Yarovoy, Alexander	CS6a.6	216	<i>Development of a Circuit-Type Multiple-Agile Beamforming and Interference Mitigation Network</i>
	PP02.4	2505	<i>Multipath Model Improvement for Automotive Radar Application</i>
	CS46.5	4233	<i>Low-Cost Hybrid Additive Manufacturing of a Miniaturized Dual Band Stacked Patch Antenna for GNSS Applications</i>
	A15b.4	4340	<i>Sunflower Array of Infinitesimal Dipoles for Constrained Antenna Modeling</i>
Yatman, William	CS39a.3	618	<i>Full Wave Modelling and Design of a Baffle for the HERTZ 2.0 Compact Antenna Test Range</i>
Ye, Xuchao	PP02.5	2510	<i>Measurement-Based Channel Characteristics for Air-To-Ground Communications Under Rural Areas</i>
Yen, Ta-Jen	PE3.16	2419	<i>Ultra Wide Dynamic Range High Power RF Rectifier</i>
Yi, Jianjia	E13.5	284	<i>Transmissive-Type Metagratings with Few Meta-Atoms for Beam Splitting</i>
	PE1.4	1253	<i>A Multifunctional Reconfigurable Metagrating for Wavefront Manipulations</i>
Yi, Longteng	PA2.16	1123	<i>Study on CFM Method for Beam Compensation of Array-Fed Space-Borne Reflector Antennas</i>
Yi, Xuan	CS39a.5	627	<i>Standardization Progress and Challenges for 5G OTA Testing</i>
Yi, Yanxiang	PA8.13	2324	<i>A Near-Field Focusing Circularly Polarized Radial Line Slot Array Antenna</i>
Yildirim, Hasan Can	P02.1	3763	<i>Multistatic OFDM Radar Fusion of MUSIC-Based Angle Estimation</i>
Yin, Haifan	CS34.1	2610	<i>RIS with Practical Reflection Coefficients: Modeling and Experimental Measurements</i>
Yin, Xiaoxing	A08b.5	2100	<i>Open Stopband Suppression of Periodic Leaky-Wave Antenna Based on Theory of Small Reflections</i>
Yin, Xiaoyang	CS37a.1	29	<i>3D-Printed Wearable Antenna Integrated with Rectifier for Wireless Power Transfer</i>
Yin, Xuefeng	CS35a.3	1692	<i>AttentionRNN: Novel Propagation Channel Time-Domain State Predictor</i>
	CS23a.5	1794	<i>HRPE-Enhanced AI-Based 5G Indoor Localization in Presence of Specular and Dense Multipaths</i>
Yioultsis, Traianos	E07.5	1653	<i>An Accurate Semi-Analytical Model for Periodic Tunable Metasurfaces</i>

			<i>Electromagnetic Response</i>
	E05.2	2041	<i>On the Rigorous Design of Graphene-Based Periodic Structures Exploiting the Fundamental Resonances</i>
Ylä-Oijala, Pasi	PE2.4	1004	<i>Applying Neural Networks for Predicting Feed Weights of an Antenna Array</i>
Yook, Jong-Gwan	PE3.9	2395	<i>Concentration Detection of Sodium Chloride and Glucose Solutions Using an IDC-Based Microwave Sensor with Eliminating Environmental Effects</i>
	E02b.5	3284	<i>Generalized Transition Matrix Model Using Characteristic Basis Function Method for Open-Ended Cavities</i>
Yoshida, Hiroshi	P04b.5	985	<i>Conceptual Design and Propagation Characteristics of an Underwater Electromagnetic Communication System for Ocean Environment Sensor Systems</i>
Yoshikawa, Keiji	PA6.11	2255	<i>User and Passive Beam Scheduling Scheme for Liquid Crystal IRS-Assisted mmWave Communications</i>
You, Qingchun	A13.4	1961	<i>Low Profile Wideband Dual-Polarized Antenna Array for Ku/K/Ka-Band Satcom Applications</i>
	A11.4	3166	<i>A Multilayer Dual-Polarized Stacked Patch Antenna with Enhanced Port Isolation for mmWave Highly Integrated Applications</i>
You, Xin	PP01.1	1347	<i>A Deep Learning-Based Approach for Inverse Design of Reconfigurable Metasurfaces</i>
Young, Steve	CS37b.4	357	<i>Increasing the Efficiency-Bandwidth Product and Impedance Bandwidth of Electrically-Small Antennas Through Parametric Space-Time Variation</i>
Youssef, Badre	PP02.3	2500	<i>Feasibility Study of Joint Modeling of Environmental and Morphological Effects for WBAN</i>
Yu, Weijie	PE1.12	1283	<i>Design of an Ultra-Wideband RCS Reduction Metasurface with Pure Metal-Pattern Layer</i>
Yu, Xiaochen	PE3.16	2419	<i>Ultra Wide Dynamic Range High Power RF Rectifier</i>
Yu, Zhexuan	CS44a.5	762	<i>Interference-Free Transmission for Near-Field Communication with Unlimited Antennas</i>
Yu, Ziming	CS29.5	3807	<i>Multi-Scattering Centers Extraction and Modeling for ISAC Channel Modeling</i>
Yuan, Xiaopeng	CS48.2	3982	<i>Cooperative Power Control and Beamforming Design for Multi-Source Enabled Wireless Power Transfer Networks</i>
Yuan, Yongjie	CS22b.1	3109	<i>Optimized Design Parameters for a Flux-Driven SNAIL-Based Traveling-Wave Parametric Amplifier</i>
Yuan, Zhiqiang	CS5b.1	364	<i>Enabling VNA Based Channel Sounder for 6G Research: Challenges and Solutions</i>
	P10b.2	3249	<i>Validation of Ray-Tracing Simulated Channels for Massive MIMO Systems at Millimeter-Wave Bands</i>
Yuasa, Takayuki	CS46.4	4228	<i>Antenna Digital Beamforming on Spire's GNSS-Reflectometry CubeSat Constellation</i>
Yue, Haochuan	CS23a.3	1785	<i>Robust Tensor Positioning Based on Channel Parameter Estimation Under Spatially Colored Noise</i>

Yue, Xiang	CS39a.4	622	<i>Addressing PIM Challenges in Radio Base Stations: Field Issues and Testing Methods for Large-Scale Deployments</i>
Yurduseven, Okan	CS17a.1	1	<i>Dual-Polarized Reconfigurable Metacavity Transceiver for Computational Polarimetric Imaging</i>
	CS36b.3	906	<i>Towards a Reconfigurable Metacavity Antenna for Computational Imaging and DoA Estimation</i>
	PA6.1	2213	<i>Orthogonal Coding for Millimeter-Wave Imaging Using MIMO Dynamic Metasurface Apertures</i>
	PM2.3	2438	<i>Leveraging Radar Back-Scattered Data for Classification of Imaging Targets</i>
	PM2.7	2454	<i>Near-Field Bistatic Microwave Imaging with Dynamic Metasurface Antennas</i>
	E04.3	2693	<i>A Case Study of Misalignment Errors for Range-Migration-Based Microwave Imaging with Multistatic Dynamic Metasurface Apertures</i>
	E04.4	2698	<i>GPR Imaging Relying on Frequency-Diverse Compressive Antennas</i>
	A24.3	3866	<i>Optimization of Super-Directive Linear Arrays with Differential Evolution for High Realized Gain</i>
	CS19b.5	4300	<i>Impact of the Unit Cell Distribution of 1-D Dynamic Metasurface Antennas on the Performance of a Computational Imaging System</i>

Z

Zaharis, Zaharias	E05.2	2041	<i>On the Rigorous Design of Graphene-Based Periodic Structures Exploiting the Fundamental Resonances</i>
	PA3.23	3490	<i>Wideband Aperture-Coupled Array Design for Automotive Radar Applications</i>
	PP03.5	3605	<i>Modeling Received Power from 4G and 5G Networks in Greece Using Machine Learning</i>
Zahra, Hijab	PA7.14	1222	<i>UWB Circular Metal Mesh Transparent Antenna</i>
Zahran, Sherif	A27a.3	641	<i>K-Band Microstrip ESPAR Antenna Integrated into Large Array</i>
Zakka El Nashef, Georges	CS3.5	311	<i>Exploring PLA/Flax Substrates for Antenna Applications: Assessing Moisture, Temperature and Dielectric Constant Homogeneity</i>
Zaman, Ashraf	A13.2	1954	<i>Compact Circularly Polarized Antenna Based on Gapwaveguide for SATCOM Applications</i>
	PA4.20	2189	<i>A Comparative Study of Decoupling Techniques for Waveguide Slot Array Antennas</i>
	CS21.4	2717	<i>Low-Cost Coaxial Slot Array Antenna for E-Band Automotive Corner Radar Applications Based on Gap Waveguide MLW Technology</i>
	A23.3	2757	<i>Analysis of Radiating Transverse Slot Unit Cell and Reflection Cancellation at D-Band</i>
	A28.1	3714	<i>Antenna and Mechanical Co-Design for Auto-Beam-Tracking in Backhaul Systems</i>
Zandamela, Abel Abdul	CS36a.1	700	<i>Angle of Arrival Estimation Methods Using Spherical-Modes-Driven Multipoint Antennas</i>
	PA8.5	2288	<i>Low-Profile Electrically Small Antenna with Pattern and Polarization Diversity</i>
	PA8.6	2293	<i>Bandwidth-Enhanced Compact Beamsteering Antenna for IoT</i>

Platforms

Zandboer, Jordi	A18.3	2914	<i>Active Antenna Design for Lunar-Based Detection of Global 21cm-Signals from the Dark Ages</i>
Zanella, Alberto	CS44a.2	750	<i>Dual Functional mmWave RIS for Radar and Communication Coexistence in near Field</i>
Zanovello, Umberto	CS33a.4	3057	<i>An Electric Properties Tomography Approach Inspired by the Boundary Element Method</i>
Zapata Cano, Pablo H.	E05.2	2041	<i>On the Rigorous Design of Graphene-Based Periodic Structures Exploiting the Fundamental Resonances</i>
Zappia, Sonia	CS24a.2	727	<i>Microwave Imaging for Monitoring Bone Healing Using Magnetic Scaffolds: An Initial Analysis</i>
	CS33a.3	3054	<i>Advancements in Broadband Electromagnetic Sensing for Food Quality Control</i>
Zarbouti, Dimitra	PP01.5	1365	<i>Field Trials for Different 5G NSA Cellular Networks</i>
Zarifi, Mohammad	CS40b.2	1973	<i>A WiFi-Based System for Ice Monitoring in Harsh Environment Using 2.7 GHz Microwave Sensor</i>
Zavorka, Radek	CS43b.1	4168	<i>Channel Measurements and Characterization in Industrial Environment at 60 GHz</i>
Zelenchuk, Dmitry	PA2.12	1105	<i>Fabrication and RF Characterization of Fully Additive Manufactured Transmission Lines</i>
	PE3.15	2416	<i>Frequency-Selective Surface Generating Two-Band Pseudo-Elliptic Frequency Response</i>
	A07.1	2659	<i>A Wideband Half-Circle Metasurface Augmented Luneburg Lens for Millimeter-Wave Applications</i>
	CS15.2	4006	<i>Validation of a Large Retrodirective CASSIOPeiA Solar Power Satellite Antenna Array</i>
	CS14b.4	4362	<i>Wideband Dual-Polarized 1-Bit Unit-Cell Design for mmWave Reconfigurable Intelligent Surface</i>
Zemen, Thomas	CS35b.2	1908	<i>Stationarity of Multiband Channels for OTFS-Based Intelligent Transportation Systems</i>
Zeng, Yunjia	PE2.7	1015	<i>Non-Uniform Metamaterial Mushroom Antennas via a Genuine Multi-Objective Bayesian Optimization Method</i>
Zeni, Noemi	CS33a.3	3054	<i>Advancements in Broadband Electromagnetic Sensing for Food Quality Control</i>
Zerrad, Myriam	A01a.3	2938	<i>Generation of Non-Diffractive Bessel Beams for Near-Field Links Applications Using Meta-Axicons</i>
Zetterstrom, Oskar	E10a.3	1850	<i>Analysis of the Dispersion Diagrams of 3D Cubic Periodic Arrangements of Metallic Spheres</i>
	A22.3	2781	<i>Tailoring the Performance of Geodesic Lens Antennas by Defining Their Footprint</i>
	CS26a.3	4098	<i>Higher Symmetries in Hexagonal Periodic Structures</i>
Zevallos, José	PA2.17	1128	<i>Dual-Polarized Connected-Slot Array Technological Demonstrator Targeting a 5:1 Bandwidth</i>
Zhai, Menglin	CS11.3	1624	<i>Reflecting/Absorbing Dual-Mode Textile Metasurface with AI-Driven Parametric Studies</i>

Zhang, Fengchun	CS34.2	2615	<i>An Automated Over-The-Air Radiated Testing Platform for Reconfigurable Intelligent Surface</i>
	P10b.2	3249	<i>Validation of Ray-Tracing Simulated Channels for Massive MIMO Systems at Millimeter-Wave Bands</i>
Zhang, Hao	PA5.20	3574	<i>A Wideband Circularly Polarized Filtering Array Antenna Using Dual-Layer Circular Cross Slotted Patch</i>
Zhang, Huanyu	CS48.2	3982	<i>Cooperative Power Control and Beamforming Design for Multi-Source Enabled Wireless Power Transfer Networks</i>
Zhang, Huasheng	CS44a.1	745	<i>Development of a Shaped Quartz Lens Antenna for Wide Scanning Sub-Millimeter Imagers</i>
Zhang, Jianan	CS20b.6	412	<i>A Vector Differential Coding for Hybrid RIS Aided Zero-Padded OTFS Systems</i>
Zhang, Jianhua	CS35a.4	1697	<i>Time-Varying Channel Measurement and Analysis at 105 GHz in an Indoor Factory</i>
Zhang, Jin	CS15.5	4019	<i>A Digital Beamforming Antenna for Space Based Solar Power Transmitting Array</i>
Zhang, Jinyao	PE3.16	2419	<i>Ultra Wide Dynamic Range High Power RF Rectifier</i>
	CS1b.2	4242	<i>Matching Network Elimination in Multiband Metasurface-Structured Rectennas for Wireless Power Transfer and Energy Harvesting</i>
Zhang, Jun	CS44a.5	762	<i>Interference-Free Transmission for Near-Field Communication with Unlimited Antennas</i>
Zhang, Kaiyuan	PP01.19	1428	<i>Ray-Tracing Based Channel Modeling and Characteristics Analysis for LEO Satellite-To-Ground Systems</i>
Zhang, Lei	CS48.4	3992	<i>Joint Wide Illumination and Null Insertion Design in RIS-Assisted System</i>
Zhang, Lingling	CS20b.6	412	<i>A Vector Differential Coding for Hybrid RIS Aided Zero-Padded OTFS Systems</i>
Zhang, Long	A03b.3	3137	<i>Low-Profile In-Band Pattern Diversity Antenna with Improved Bandwidth</i>
Zhang, Mingtao	PA2.10	1096	<i>Conceptual Design of Antenna Arrays for Satellite Direct-To-Cell Connectivity</i>
Zhang, Peize	CS5a.5	76	<i>A Modular COTS-Based High-Efficient Sub-THz Channel Sounder and Experimental Validations</i>
	PP01.8	1380	<i>Dual-Polarized Diffraction Measurements and Modeling at D-Band Frequencies</i>
	CS29.3	3797	<i>Computer Vision Enabled Sub-THz Radio Channel Characterization of Dynamic Objects</i>
Zhang, Queenie	CS39a.4	622	<i>Addressing PIM Challenges in Radio Base Stations: Field Issues and Testing Methods for Large-Scale Deployments</i>
Zhang, Shiyu	PE3.7	2388	<i>Electromagnetic Modelling in Modern Vehicles: A Pathway to Efficiency and Performance</i>
Zhang, Shuai	CS6b.4	502	<i>Millimeter-Wave Beam-Steerable Lens with Reduced Profile and Enhanced Gain</i>
	PM1.9	1343	<i>Investigation of Correlation Between Absorbed Power Density and Incident Power Density for User Equipment Antennas at Sub-THz</i>

Frequencies

	PA4.6	2129	<i>Detailed Design Procedure for Low-Cost High-Efficiency 3D Printed Transmitarray Antennas for mm-Wave Applications</i>
	A06b.3	3296	<i>A Wideband Reflectarray with Reconfigurable Polarization and Beam-Scanning by Using Liquid Crystal Delay Line for Millimeter-Wave</i>
	PA3.5	3414	<i>5G Millimeter-Wave Reflectarray Antenna Design with a Good Gain-Filtering Characteristic Based on a High-Efficiency Polarization Converter</i>
	PA3.22	3486	<i>Wideband Array Antenna with Single-Layer Feeding Network at Ka-Band</i>
Zhang, Ting	CS6a.3	204	<i>Wideband Transmissive Metasurfaces for Sub-THz Frequency-Dependent Beam Scanning</i>
Zhang, Wenzhang	CS1b.2	4242	<i>Matching Network Elimination in Multiband Metasurface-Structured Rectennas for Wireless Power Transfer and Energy Harvesting</i>
Zhang, Xiaoying	A15a.4	4122	<i>Beamforming Optimization for Full-Duplex Relay in SIC-Enhanced Cooperative NOMA System</i>
Zhang, Xingqi	CS30a.4	3942	<i>Validating Convex Optimization of Reconfigurable Intelligent Surfaces via Measurements</i>
Zhang, Xiuyin	A03b.3	3137	<i>Low-Profile In-Band Pattern Diversity Antenna with Improved Bandwidth</i>
Zhang, Xuan	PA6.5	2231	<i>A Pattern-Reconfigurable Water Antenna Based on the Fabry-Perot Cavity</i>
Zhang, Yanyang	PA1.5	3349	<i>Monitoring Eye States Based on Transparent and Flexible Antenna in WBAN</i>
Zhang, Yinghao	PE3.12	2404	<i>High-Order Quasi-Elliptical Bandpass FSS Based on Substrate-Integrated Waveguide Technology for 60 GHz Applications</i>
Zhang, Zhao	CS43a.3	3962	<i>A Deep Learning Based Surface Current Generation Method for Scattering Modeling at Terahertz Band</i>
Zhang, Zhiwei	PA2.10	1096	<i>Conceptual Design of Antenna Arrays for Satellite Direct-To-Cell Connectivity</i>
	PA4.2	2109	<i>A Fully Additive Manufactured D-Band SIW Antenna</i>
	PA8.4	2283	<i>An IQ Modulator-Based RF Phase Shifter</i>
Zhang, Zirui	A09a.5	696	<i>Non-Volatile RF Frequency Reconfigurable Antenna for Wireless Communication</i>
	PA3.16	3463	<i>Frequency Reconfigurable Flexible Printed Antenna Based on Non-Volatile RF Switches for Wearable Applications</i>
Zhang, Zizhen	PA3.13	3446	<i>MIMO Array Decoupling with SSR Structure in Joint Communication and Sensing System</i>
Zhao, Bin	CS44b.4	955	<i>Curving THz Beams in the near Field: A Framework to Compute Link Budgets</i>
Zhao, Deyuan	PP01.18	1423	<i>Channel Characterization and Modeling for Wireless MIMO Communication Systems in Intersection Scenarios</i>
	P01.3	3842	<i>Scenario Classification and Channel Modeling for MIMO Communications in Suburban Road Scenarios</i>
Zhao, Hongxin	A08b.5	2100	<i>Open Stopband Suppression of Periodic Leaky-Wave Antenna Based</i>

			<i>on Theory of Small Reflections</i>
Zhao, Hui	CS39a.1	610	<i>A Comprehensive Mobile Phone Antenna Performance Evaluation Model Based on Deep Learning</i>
Zhao, Hailing	PA2.3	1066	<i>Compact Vivaldi Antenna Application in High-Power Design at X-Band</i>
Zhao, Jianing	PP01.15	1410	<i>A Modified Channel Model for the MIMO System Deployed RIS Elements with Imperfect Surface</i>
	A15a.1	4110	<i>Multiple-User Full-Duplex Hybrid Beamforming Design for mmWave Systems with A Joint Interference Cancellation Design</i>
	A15a.4	4122	<i>Beamforming Optimization for Full-Duplex Relay in SIC-Enhanced Cooperative NOMA System</i>
Zhao, Liangliang	PA2.3	1066	<i>Compact Vivaldi Antenna Application in High-Power Design at X-Band</i>
Zhao, Lixin	PA3.2	3403	<i>Design of Ultra-Wideband Dual-Polarized Corrugated Horn Antenna for 5G Application</i>
	PA3.7	3421	<i>A Single-Layer Quadruple-Band Millimeter-Wave Antenna Using Split-Rings for 5G Application</i>
	PA5.21	3577	<i>Design of a Dual-Polarization Ultra-Wideband Horn Antenna</i>
Zhao, Mengran	CS17a.1	1	<i>Dual-Polarized Reconfigurable Metacavity Transceiver for Computational Polarimetric Imaging</i>
	CS36b.3	906	<i>Towards a Reconfigurable Metacavity Antenna for Computational Imaging and DoA Estimation</i>
	PM2.7	2454	<i>Near-Field Bistatic Microwave Imaging with Dynamic Metasurface Antennas</i>
Zhao, Ran	PE2.12	1036	<i>A Discontinuous Galerkin Time-Domain Scheme to Model Lasing Dynamics in Four-Level Two-Electron Atomic Systems</i>
Zhao, Ruike Renee	CS14b.1	4349	<i>Reconfiguration of Electromagnetic Metasurfaces Using Tunable Shape Morphing Structures</i>
Zhekov, Stanislav	CS2.3	175	<i>Long-Term Network-Based Assessment of the Actual Output Power of Base Stations in a 5G Network</i>
Zheng, Dongze	CS8.1	2885	<i>Milimeter-Wave 3D Folded Strip Antennas and Arrays: Diverse Polarizations Realization Under Robust Input Impedance</i>
Zheng, Paul	CS48.2	3982	<i>Cooperative Power Control and Beamforming Design for Multi-Source Enabled Wireless Power Transfer Networks</i>
Zheng, Shufeng	PA8.13	2324	<i>A Near-Field Focusing Circularly Polarized Radial Line Slot Array Antenna</i>
Zheng, Xuezhi	CS22b.3	3118	<i>A Modelling Scheme for the Nonclassical Optical Response in the Nanosphere on Mirror Structure</i>
Zheng, Yi	CS18.1	3669	<i>Metasurfaces Meet Characteristic Modes</i>
Zhinong, Ying	CS35b.5	1922	<i>Indoor Propagation Measurements with a Reconfigurable Intelligent Surface at 3.5 GHz</i>
	CS34.2	2615	<i>An Automated Over-The-Air Radiated Testing Platform for Reconfigurable Intelligent Surface</i>
Zhong, Liyuan	PA8.13	2324	<i>A Near-Field Focusing Circularly Polarized Radial Line Slot Array Antenna</i>
Zhong, Zhangdui	CS23a.2	1780	<i>Terahertz Channel Modeling Based on Scattering Characterization</i>
	CS43a.3	3962	<i>A Deep Learning Based Surface Current Generation Method for</i>

Scattering Modeling at Terahertz Band

Zhou, Hai	PA5.16	3556	<i>Design of the 3D-Printed Rectangular Dielectric Resonator Antenna for WLAN Applications</i>
Zhou, Jiafeng	PM1.6	1331	<i>Intermodulation Mitigation Through Surrounding Impedance Manipulation</i>
	PE3.16	2419	<i>Ultra Wide Dynamic Range High Power RF Rectifier</i>
	PE3.17	2423	<i>Enhancing Signal Transmission in Energy-Saving Glass Through Tri-Bandpass Frequency Selective Surface Design</i>
	CS1b.2	4242	<i>Matching Network Elimination in Multiband Metasurface-Structured Rectennas for Wireless Power Transfer and Energy Harvesting</i>
Zhou, Jianyi	A15a.1	4110	<i>Multiple-User Full-Duplex Hybrid Beamforming Design for mmWave Systems with A Joint Interference Cancellation Design</i>
	A15a.4	4122	<i>Beamforming Optimization for Full-Duplex Relay in SIC-Enhanced Cooperative NOMA System</i>
Zhou, Kai	CS17b.2	322	<i>Challenges and Opportunities of Amplified Information Metasurfaces for Simultaneous Wireless Communications and Power Transfers</i>
Zhou, Min	A06a.2	3026	<i>Direct Optimisation of a Five-State Reconfigurable Reflectarray for 5G Applications</i>
Zhou, Qun Yan	CS17b.3	326	<i>Information Metasurface for Simultaneous Wave Manipulations and Signal Modulations</i>
Zhou, Rui	E05.5	2055	<i>A Novel Topologically Protected Hollow Dielectric Waveguide for Robust mmWave Guiding</i>
Zhou, Shigang	A04.2	1462	<i>Design of A Dual-Circular Polarized Antenna Array for Dual-Band Aperture-Shared Applications</i>
Zhou, Wenqi	PP01.18	1423	<i>Channel Characterization and Modeling for Wireless MIMO Communication Systems in Intersection Scenarios</i>
Zhou, Yonggang	CS20b.1	393	<i>1-Bit SubTHz RIS with Planar Tightly Coupled Dipoles: Beam Shaping and Prototypes</i>
Zhou, Zhiheng	PA5.6	3515	<i>Bifunctional Stubs Enabled MIMO System for Wideband Mobile 5G and Wi-Fi 6E Applications</i>
Zhou, Ziyi	CS48.4	3992	<i>Joint Wide Illumination and Null Insertion Design in RIS-Assisted System</i>
Zhu, He	A02.5	3710	<i>A Four-Channel In-Band Full-Duplex (IBFD) Antenna System with Shared Radiation Aperture</i>
Zhu, Lianwei	A04.2	1462	<i>Design of A Dual-Circular Polarized Antenna Array for Dual-Band Aperture-Shared Applications</i>
Zhu, Lina	PE1.4	1253	<i>A Multifunctional Reconfigurable Metagrating for Wavefront Manipulations</i>
Zhu, Liting	A01b.5	3216	<i>Array-Fed Transmitarray with Designated Beam Directions and Coverages</i>
Zhu, Pengqi	CS35a.3	1692	<i>AttentionRNN: Novel Propagation Channel Time-Domain State Predictor</i>
Zhu, Qingyan	PP03.10	3630	<i>Electromagnetic Detection and Identification of Perturbed Wire Resonators</i>
Zhu, Qiuming	PM1.3	1318	<i>Impact of 6D Mobility on Doppler Characteristics of UAV-To-Vehicle</i>

Channels

	PP02.5	2510	<i>Measurement-Based Channel Characteristics for Air-To-Ground Communications Under Rural Areas</i>
Zhu, Shaozhen	PE3.7	2388	<i>Electromagnetic Modelling in Modern Vehicles: A Pathway to Efficiency and Performance</i>
Zhu, Shitao	CS36b.3	906	<i>Towards a Reconfigurable Metacavity Antenna for Computational Imaging and DoA Estimation</i>
Zhu, Siting	CS39a.5	627	<i>Standardization Progress and Challenges for 5G OTA Testing</i>
Zhu, YiHui	CS18.1	3669	<i>Metasurfaces Meet Characteristic Modes</i>
Zhu, Yuqing	CS48.5	3996	<i>A Varactor-Based Reconfigurable Intelligent Surface Concept for 5G/6G mm-Wave Applications</i>
Zhu, Zhengxian	PA2.10	1096	<i>Conceptual Design of Antenna Arrays for Satellite Direct-To-Cell Connectivity</i>
Ziaee Bideskan, Mehri	PE1.6	1261	<i>Characterization of a Metamaterial-Enabled Waveguide Diplexer for Ka-Band Satellite Communication Systems</i>
Zich, Riccardo	PE2.13	1040	<i>Novel Quantum Computation Based Selection Operator for Genetic Algorithms Applied to Electromagnetic Problems</i>
Zilberti, Luca	E01.2	2019	<i>Assessment of the Feasibility of Breast Lesion Detection with Contrast Source Inversion for Microwave Tomography: A Virtual Experiment</i>
	CS33a.4	3057	<i>An Electric Properties Tomography Approach Inspired by the Boundary Element Method</i>
Zimaglia, Elisa	CS20b.3	402	<i>Measurements of Reconfigurable Intelligent Surface in 5G System Within a Reverberation Chamber at mmWave</i>
Zimmermann, David	PA3.11	3438	<i>Broadband Waveguide Magneto-Electric Dipole Antenna for F-Band Applications</i>
Ziolkowski, Richard	A24.1	3856	<i>Self-Resonant Broadside-Radiating Superdirective Unidirectional Mixed-Multipole Antennas</i>
	A24.4	3871	<i>Superdirective Broadside-Radiating Unidirectional Mixed-Multipole Antenna Arrays</i>
Zografopoulos, Dimitrios	PE3.10	2398	<i>Highly Reflective, Low-Loss, Homogenized Fishnet Metasurfaces at Terahertz: Design and Experiment</i>
Zong, Yali	PA2.16	1123	<i>Study on CFM Method for Beam Compensation of Array-Fed Space-Borne Reflector Antennas</i>
	PE1.12	1283	<i>Design of an Ultra-Wideband RCS Reduction Metasurface with Pure Metal-Pattern Layer</i>
Zou, Xianbing	P10b.5	3263	<i>E-Band Measured Propagation Characteristics for Urban Backhaul Communications</i>
Zubir, Farid	E12.4	2832	<i>Compact Dual-Band Crossover with Enhanced Band Ratio Using Interdigital Capacitor for 5G Applications</i>
Zucchi, Marcello	PE2.9	1024	<i>Human- Vs Machine Design of Antennas: Evolution Behavior in Genetic Shape Optimization</i>
	PE1.8	1269	<i>Modeling of 3D Feeding Structures in the Automated Design of Metasurface Antennas</i>
	E07.3	1645	<i>Adaptive Weighting Scheme for Multi-Objective Optimization in Metasurface Antenna Design</i>

	CS30b.3	4156	<i>Automated Design and Characterization of a Scalar Metasurface Antenna Radiating a Linearly-Polarized Broadside Beam</i>
Zugno, Tommaso	P04b.3	975	<i>Ray Tracing and Measurement-Based Characterization of Inter/Intra-Machine THz Wireless Channels</i>
	P10a.4	2987	<i>Direct Clustering and Multi-Path Component Identification on THz Channel Measurements in a Factory Environment</i>
Zulqarnain, Anum	E09.5	3924	<i>Multifunctional Linear Dichroism and Polarization Transforming Metasurface for mm-Wave Application</i>
Zumbo, Sabrina	CS33a.3	3054	<i>Advancements in Broadband Electromagnetic Sensing for Food Quality Control</i>
Zurita, Alberto	PA2.4	1069	<i>Antenna Design for TriHex: A Future Soil Moisture and Ocean Salinity Radiometer Mission</i>
Zwick, Thomas	A05.1	1820	<i>Sub-THz Substrate Integrated Waveguide Signal Transitions in Backend-Of-Line of a Silicon Process</i>
	A05.3	1828	<i>110 to 170 GHz High-Gain Antenna with Embedded Surface Mount Short Horn and Baseband PCB Horn Antenna</i>
	M3.1	2586	<i>Enhancing THz Antenna Characterization Precision in WR-1.5 Band Using Vacuum Waveguide Flange</i>
	M3.3	2595	<i>Dielectric Characterization of Adhesives for THz Packaging in WR6.5, WR3.4 and WR2.2 Bands</i>

1 2 3 5 6 A B C D E F G H I J K L M N O P Q R S T U V W X

1

1 2 3 5 6 A B C D E F G H I J K L M N O P Q R S T U V W X

1-Bit Graphene-Based Reconfigurable Intelligent Surface Design in Ka-Band

1-Bit Reconfigurable Transmitted/Reflected Array (TRA) for 5G/6G Wireless Communication

1-Bit RIS Unit Cell with Mechanical Reconfiguration at 28 GHz

1-Bit SubTHz RIS with Planar Tightly Coupled Dipoles: Beam Shaping and Prototypes

110 to 170 GHz High-Gain Antenna with Embedded Surface Mount Short Horn and Baseband PCB Horn Antenna

2

1 2 3 5 6 A B C D E F G H I J K L M N O P Q R S T U V W X

20 Years of ESoA: A (Subjective) View on Its Success

2D-Scanning of Circularly Polarized Beams via Array-Fed Fabry--Perot Cavity Antennas

3

1 2 3 5 6 A B C D E F G H I J K L M N O P Q R S T U V W X

3-D Reflectarray Unit Cell with Wideband Performance and Integrated Sensing Capability

3D Method-Of-Moment Design of Huygens' Metasurfaces

3D Printed Cascaded Cavity-Backed Millimeter-Wave Filtering Antenna

3D Printed Horn Antennas for Millimeter Wave and Sub-THz Bands

3D Spatially Reconfigurable Circularly Polarized Antenna in Package with Embedded Electronics

3D-Printed Circular Polarized Dielectric Resonator Antenna with Enhanced Axial Ratio Bandwidth Using Anisotropic Material

3D-Printed Multi-Beam Flat Lens Antenna System

3D-Printed Wearable Antenna Integrated with Rectifier for Wireless Power Transfer

5

1 2 3 5 6 A B C D E F G H I J K L M N O P Q R S T U V W X

5G Millimeter-Wave Reflectarray Antenna Design with a Good Gain-Filtering Characteristic Based on a High-Efficiency Polarization Converter

5G OTA Testbed of Full-Sized Vehicles in Reverberation Chamber

5G Radio Channel Characterization in an Underground Mining Environment

5x7 Nolen Matrix in K-Band Implemented in Rectangular Waveguide

6

1 2 3 5 6 A B C D E F G H I J K L M N O P Q R S T U V W X

6:1 Connected Slot Array in PCB Technology

- A 2x2 Dual-Band Open Loop Array with Circular Polarisation*
- A Beam-Scanning Metal-Only Folded Reflectarray Antenna*
- A Brief Analysis of the Latest Research Progress and Future Direction of Low-Frequency Transmitting Antenna*
- A Cascaded Resonator Decoupling Network for Two Filtering Antennas with Adjacent Operating Bands*
- A Case Study of Misalignment Errors for Range-Migration-Based Microwave Imaging with Multistatic Dynamic Metasurface Apertures*
- A Class-E, Switched-Mode, Non-LTI Electrically-Small Transmit Antenna Design for Overcoming the Fundamental Bandwidth-Efficiency Product Limits*
- A Compact Fabry-Perot Cavity Antenna with Circular Polarization*
- A Compact Flexible BLE Antenna for a Remote-Control Application*
- A Compact High-Gain 28 GHz Antenna Array for Beyond 5G Wireless Networks*
- A Compact Horn Antenna with Low Sidelobes*
- A Compact Implantable Camera Integrated MIMO Antenna with Polarization Diversity for Wireless-Capsule-Endoscopy Applications*
- A Compact Microwave Rectifier for Wireless Power Transfer and Energy Harvesting Applications*
- A Compact Wideband Biocompatible Circularly Polarized Implantable Flexible Antenna for Biomedical Applications*
- A Comparative Study of Decoupling Techniques for Waveguide Slot Array Antennas*
- A Comparison of Near-Field to Far-Field Transformation Algorithms for Use with Industrial Multi-Axis Robotic Antenna Measurement Systems*
- A Completely Overlapped Ku- and Ka-Band Dual-Polarized Phased Array for Simultaneous Terrestrial and Satellite Communications*
- A Completely Overlapped Ku- and Ka-Band Dual-Polarized Phased Array for Simultaneous Terrestrial and Satellite Communications*
- A Comprehensive Mobile Phone Antenna Performance Evaluation Model Based on Deep Learning*
- A Cylindrical Mismatched Luneburg Lens Implemented on PCB at V-Band*
- A Decoupling Scheme for Closely Spaced Microstrip Patch Antenna*
- A Deep Learning Based Surface Current Generation Method for Scattering Modeling at Terahertz Band*
- A Deep Learning-Based Approach for Inverse Design of Reconfigurable Metasurfaces*

A Deep Split-Step Wavelet Model for the Long-Range Propagation

A Demonstration of Diffraction-Limited Images Using a CMOS Chessboard Array at THz Frequencies

A Demonstration of Diffraction-Limited Images Using a CMOS Chessboard Array at THz Frequencies

A Digital Beamforming Antenna for Space Based Solar Power Transmitting Array

A Discontinuous Galerkin Time-Domain Scheme to Model Lasing Dynamics in Four-Level Two-Electron Atomic Systems

A Dual Linear-Polarized Gap Waveguide Antenna Element for Radar and Communications at 77 GHz

A Dual Linearly Polarized Array for 5G FR2

A Dual-Port Antenna for Colinearly Polarized Full Duplex and Pattern Reconfigurable Applications

A Four-Channel In-Band Full-Duplex (IBFD) Antenna System with Shared Radiation Aperture

A Fully Additive Manufactured D-Band SIW Antenna

A Greedy Approach for Reducing Data in Near-Field Measurements

A High Efficiency and Ultra-Wideband Rectenna for RF Energy Harvesting Application

A High Gain Spoof Surface Plasmon Polaritons (SSPPs) Antenna Based on a Metamaterial-Inspired Substrate Integrated Waveguide

A High-Efficiency Reconfigurable Reflectarray Antenna Using Two Types of Active Unit Cells

A High-Isolation Dual-Band Base Station Antenna Design for Full Duplex Technologies

A High-Precision Approach to Eliminate Positioning Errors in Radar Calibrations

A Higher-Order Spectral Element Method to Model Eccentric Anisotropic Two-Layer Waveguides via Conformal Transformation Optics

A Highly Compact Double-Sided Orientation Insensitive Chipless Tag for Radio Frequency Identification Applications

A Linear Wide-Angle Scanning Phased Array Antenna Using Heterogeneous Beam Element Technology

A Linearly Polarized Wideband Antenna with A Stable Omnidirectional Radiation Pattern

A Loop-Star Decomposition for the B-Spline Based Discretization of the Electric Field Integral Equation

A Low Profile Dual-Band Dual-Polarized Filtering Antenna with No Extra Circuit

A Low-Profile Wide-Scan Magneto-Electric Dipole Antenna for 5G mm-Wave Communications

A Macroscopic Bilateral Modeling Approach for Reflective and Transmissive Metasurfaces

A Metrological Full-Connected Hybrid Beamformer Testbed with a Large Antenna Array for Millimetre-Wave RF-EMF Testing

A Mild Data-Driven Approach Based on a Lebesgue-Space Inversion Procedure for Microwave Imaging Applications

A Millimeter-Wave Binary Reconfigurable Intelligent Surface on a Low-Cost FR4 Substrate

A mmWave Leaky-Wave Antenna for Efficiency Enhanced Near-Field Wireless Power Transfer and Communication

A Modelling Scheme for the Nonclassical Optical Response in the Nanosphere on Mirror Structure

A Modified Channel Model for the MIMO System Deployed RIS Elements with Imperfect Surface

A Modular COTS-Based High-Efficient Sub-THz Channel Sounder and Experimental Validations

A Modular, Low-Cost Ka-Band Antenna Subarray as Building Block for Phased Arrays of Arbitrary Size and Shape

A Multi-Region Hierarchical Preconditioning Scheme for the MoM Simulation of Complex Composite Structures

A Multi-Region Hierarchical Preconditioning Scheme for the MoM Simulation of Complex Composite Structures

A Multiband Leaky-Wave Phased Array Antenna for 5G Fixed Link Communications

A Multifunctional Reconfigurable Metagrating for Wavefront Manipulations

A Multilayer Dual-Polarized Stacked Patch Antenna with Enhanced Port Isolation for mmWave Highly Integrated Applications

A Near-Field Focusing Circularly Polarized Radial Line Slot Array Antenna

A New Approach for Line of Sight Prediction with Geometry Analysis and Machine Learning in Diverse Environments

A Novel GO Analysis Tool for GRIN Lenses Based on the Fast Sweeping Method

A Novel Metasurface Inverse Design Based on Back Propagation Neural Network

A Novel MIMO OTA Methodology for UE Performance Testing

A Novel Precise Approach for Digital Metasurface Configuration for Sensing Application

A Novel Quad-Band Electrically Small Antenna

A Novel Reconfigurable Planar Switched-Beam Filtenna with 360-Degree Beam Scanning

A Novel Substrate Integrated Broadband Dielectric Resonator Antenna (DRA) in SICL for Millimeter Wave Application

A Novel Topologically Protected Hollow Dielectric Waveguide for Robust mmWave Guiding

A Numerical Analysis of Microwave Hyperthermia of Deep-Seated Tumors Using Magneto-Dielectric Implants

A Parasitic Element Technique for Deep Null Synthesis and the Application to Received Signal Strength (RSS)-Based Localization

A Pattern-Reconfigurable Water Antenna Based on the Fabry-Perot Cavity

A Penta-Band Shared Aperture Antenna with A Very Ratio Frequency for 5G and B5G Smartphone Applications

A Performance Comparison of Sub-Octave Band Corrugated Horns to a Quadruple-Ridged Flared Horn for the ngVLA Radio Telescope

A Polarization-Insensitive Ultra-Broadband FSS Absorber with Low-Profile Based on the ITO Film

A Possible Way to Reduce the High Sidelobe Levels Due to Reflector Struts: Curly Struts

A Quantum Optimization Method for Antenna Array Thinning

A Radial Waveguide Power Divider Inspired Antenna for mmWave IoT Sensing Applications

A Reactively Coupled Bi-Directional Dual CP Antenna

A Reconfigurable Phase Gradient Metasurface Resorber Offering Enhanced Beam Steering Capability and a Tuneable Transmission Band

A Self Deployable and Reconfigurable Antenna in VHF Band for a New Space Mission

A Shared-Aperture Planar Antenna for 5G

A Simple Technique to Maximize Isolation in Compact mmWaves Antenna Arrays

A Single-Layer Quadruple-Band Millimeter-Wave Antenna Using Split-Rings for 5G Application

A Small-Sized Antenna System for Direction Finding Applications on a Single Plane (1D) Using BT 5.1

A Smart Convenient Rewriting of the Inverse Scattering Equations for the 3D Scalar Problem

A Study on Satellite-To-Ground Propagation in Urban Environment

A Study on W-Band Frequency Attenuation in the Presence of Human Blockage

A Systematic Design Method of Miniaturizing Microstrip Patch Antenna Using Theory of Characteristic Modes

A Time-Efficient Model for Estimating Far-Field Wireless Power Transfer to Biomedical Implants

A Two-Component 2-D FDFD Eigenmode Method Incorporated with the Conformal Technique

A Two-Port Metamaterial Antenna for mm-Wave 5G MIMO Applications with Enhanced Bandwidth and Gain

A Varactor-Based Reconfigurable Intelligent Surface Concept for 5G/6G mm-Wave Applications

A Vector Differential Coding for Hybrid RIS Aided Zero-Padded OTFS Systems

A Wearable Open-Ring Dielectric Resonator Antenna with Frequency Reconfiguration

A Wideband 3D Printed Digital Metasurface Transmitarray Antenna for mm-Wave Applications

A Wideband Aperture-Shared Dual-Polarized End-Fire Antenna with Low Profile and High Isolation

A Wideband Circularly Polarized Filtering Array Antenna Using Dual-Layer Circular Cross Slotted Patch

A Wideband Dual-Polarized 1-Bit Unit Cell for Reconfigurable Intelligent Surface Applications

A Wideband Filtering Linear-To-Circular Polarization Converter for Ka-Band Satellite Communication

A Wideband Free Space Material Characterization Method for Extracting Dielectric Permittivity

A Wideband Half-Circle Metasurface Augmented Luneburg Lens for Millimeter-Wave Applications

A Wideband High-Gain Circularly-Polarized Metasurface Antenna with a Large Element Spacing SIW Array at Ka Band

A Wideband Reflectarray with Reconfigurable Polarization and Beam-Scanning by Using Liquid Crystal Delay Line for Millimeter-Wave

A Wideband Reflector-Based Mm-Wave/THz Nearfield Line Scanner for Rapidly Sensing Materials in Envelopes

A WiFi-Based System for Ice Monitoring in Harsh Environment Using 2.7 GHz Microwave Sensor

Accurate Design of Surface-Wave Enabled Reflective Intelligent Surfaces Through the Generalized Oliner Method

Accurate Time Synchronization Exploiting Integrated Sensing and Communication

Achievable Rate Approximation of Large Intelligent Surface Based on Deep Learning

Active Antenna Design for Lunar-Based Detection of Global 21cm-Signals from the Dark Ages

Active Array Antennas for Non-Terrestrial Communications

Adaptive Polynomial Chaos Expansion for Uncertainty Quantification of SubTHz Horn Antennas with Flat-Top Radiation Patterns

Adaptive Weighting Scheme for Multi-Objective Optimization in Metasurface Antenna Design

Additively Manufactured Horn Antennas

Additively Manufactured Waveguide Hybrid Septum Coupler Optimized Using Machine Learning

Addressing PIM Challenges in Radio Base Stations: Field Issues and Testing Methods for Large-Scale Deployments

Advanced Materials and Manufacturing Methods Enable New Antenna Solutions - Application Use-Cases with 3D Printable RF Lenses

Advanced Microwave Radiometry: Refining Sun-Tracking Technique for Atmospheric Attenuation Retrieval and Sun Brightness Temperature Estimation

Advanced Microwave Radiometry: Refining Sun-Tracking Technique for Atmospheric Attenuation Retrieval and Sun Brightness Temperature Estimation

Advanced Post Processing for Robotic Applications

Advanced Post-Processing Technique to Evaluate Specific Absorption Rate (SAR) for a Standard Dipole Antenna

Advanced Thermal-Imaging for OTA Industrial-Testing of Active-In-Package, Antenna-On-Chip and Antenna on PCB

Advancements in Broadband Electromagnetic Sensing for Food Quality Control

Advancements in Sub-THz Antenna and Package Integration for Miniaturized Surface Mount Device Modules Up to 420 GHz - Part II

Advancements in the Experimental Validation of a Wearable Microwave Imaging System for Brain Stroke Monitoring

Advances in Compact Antenna Test Range Design

Advances in Core-Shell Nanocrystals: A Multiphysics Approach to Multispectral Electromagnetic Shielding

AI-Assisted Design and Experimental Testing of a Compact UWB Antenna for the Inspection of Food and Beverage Products

AI-Based Environment Segmentation Using a Context-Aware Channel Sounder

AI-Driven Design of a Quasi-Digitally-Coded Wideband Microstrip Patch Antenna Array

All-Metal Glide-Symmetric Slotted Planar Antennas: Modal Analysis

All-Metal Perfectly-Matched Metamaterials

AlphaSat Ka-Band and Q-Band Receiving Station in Rome: Measurements and Data Analysis

Alternate Optimization with Deep Learning to Design Beam Deflector Under Aperiodic Near-Field Coupling Conditions

Ambient Pressure Responsive Shape-Morphing Electromagnetic Components

Amplitude-Tapered Half-Mode Gap Waveguide Distribution Network for Flat Panel Antennas

An Accurate Semi-Analytical Model for Periodic Tunable Metasurfaces Electromagnetic Response

An Angularly Stable Wideband Low Profile Single-Layer Linear to Circular Polarization Converter for Millimeter Wave Satellite Communications

An Annular Ring Shorted Logarithmic Spiral Antenna with Planar Integrated Feed

An Antenna Measuring System Based on a Cable Suspended Dolly and Inverse Source

An Automated Over-The-Air Radiated Testing Platform for Reconfigurable Intelligent Surface

An Efficient Wheel-Integrated Wireless Power Transfer System Based on High-Permittivity Metasurface

An Efficient Wireless Power Transfer System Using Transmission and Reflection Characteristics of Metamaterial

An Eigenvector-Supported Optimization Method for Holographic-Based Leaky Wave Antennas

An Electric Properties Tomography Approach Inspired by the Boundary Element Method

An Electromagnetic Metasurface for Impedance Matching in Microwave Biomedical Applications

An Electromagnetic-Compliant Scattering Model for Reconfigurable Intelligent Surfaces

An Innovative Metasurface Polarizer Working in 5G Frequency Bands

An Investigation into the Effects of Multi-Path and NLOS Propagation on Antenna-Based Soil Moisture Sensors in the RFID Band

An IQ Modulator-Based RF Phase Shifter

An L-Band Receiving Array with Full Digital Simultaneous Quad-Polarization Beamforming

An Overview of Gigascale Antenna Arrays and Electromagnetics for Space Based Solar Power

An Overview of the Potential of Compressed Sensing in Antenna Measurements

An Upper Bound for Envelope Correlation Coefficient of Antenna Clusters

Analog Self-Interference Cancellation by Means of a Synchronised Signal Injection

Analysis and Design of a Wideband Jaumann-Like Radar Absorber Offering High Angular Stability and Polarization Insensitivity

Analysis and Design of Metasurface Antennas Based on Temporal Metastructures

Analysis and Design of mmWave Wideband Artificial Dielectric Flat Lens Antenna

Analysis and Design of mmWave Wideband Artificial Dielectric Flat Lens Antenna

Analysis and Design of Robust Reconfigurable Intelligent Surfaces Using a Statistical Approach

Analysis and Measurement of Key Performance Indicators for MIMO Antennas

Analysis and Optimization of Reconfigurable Intelligent Surfaces Based on S-Parameters Multiport Network Theory

Analysis of 5G Channel Characteristics Based on Ray Tracing for the Straight Tunnel of High Speed Railway

Analysis of a Small LOFAR Low-Band Test Array Using a Sky Map, Simulated Embedded Element Patterns and Measured LNA-Impedances

Analysis of Channel Characteristics for FMCW Millimeter-Wave Radar in Traffic Scenarios

Analysis of Propagation Models for Frequency Coordination Between 5G Base Stations and Satellite Earth Stations at FR1

Analysis of Radiating Transverse Slot Unit Cell and Reflection Cancellation at D-Band

Analysis of Return Loss with an Uncooled Coaxial Monopole Antenna During Microwave Ablation

Analysis of the Capacity and Energy Efficiency of Metallodielectric Surface Wave Links Operating Beyond Y Band

Analysis of the Dispersion Diagrams of 3D Cubic Periodic Arrangements of Metallic Spheres

Analysis of the Effects of Rainwater Covered Bumper on the Automotive Radar Signals

Analysis of the Interaction of Laser-Induced Solid-State Plasma with Electromagnetic Waves in Silicon Waveguides at 67-220 GHz

Analysis of Time and Direction of Arrival (TADOA) Data Using Basis Pursuit in the AFRL One-RY Antenna Measurement Range

Analytical and Numerical Evaluation of Efficient Power Transfer of Bessel-Shaped Beams in Near-Field Through a Planar Layered Medium

Analytical and Numerical Solution of the One Dimensional Steady State Bioheat Transfer Equation

Analytical Circuit Models: From Purely Spatial to Space-Time Structures

Analytical Fitting of Dielectric Response of Basal Cell Carcinoma

Analytical Model of a Parallel Plate Waveguide Feeding a Connected Slot Array

Analyzing the Performance of Phased Array Geometries with Aperture Projection Analysis

Angle of Arrival Estimation Methods Using Spherical-Modes-Driven Multiport Antennas

Angle of Arrival Measurements with Ultra-Wide Band Transceivers: Design and Evaluation

Anisotropic Circularly Polarising Graded Index Lenses Enabling High Gain CP Antennas

Anisotropic Metagrating for Beamforming with Polarization Conversion

Annual Statistics from 5 Years of 1-Minute Rainfall Rate Measurements at a Specific Site in Bolivia

Antenna and Mechanical Co-Design for Auto-Beam-Tracking in Backhaul Systems

Antenna Array and GaAs Phase Shifter MMIC for Millimeter Wave Beamforming - Co-Simulation and Measurements

Antenna Array Design Workflow - from Single Element to Array Installed Performance

Antenna Coupling Evaluation in Arrays and Complex Structures Using Measured Sources and Simulations

Antenna Design for TriHex: A Future Soil Moisture and Ocean Salinity Radiometer Mission

Antenna Digital Beamforming on Spire's GNSS-Reflectometry CubeSat Constellation

Antenna Pattern Tracking Algorithm for Low Terahertz Communications

Antenna Position Layout and Frequency Impact on Tumor Detection in Microwave Breast Imaging

Antenna System for Simultaneous Wireless Power and Information Transfer to Brain Implants

Antennas and Power Measurement Techniques for Wireless Applications

Antennas and Systems at Sub-THz Frequencies for Space Applications

Aperture Distribution Method for Array-Fed Reflectors: A System Level Performance Case Study

Application of Compressed Sensing to Antenna Far-Field Calibration in an Extrapolation Range

Application of Compressed Sensing to Antenna Far-Field Calibration in an Extrapolation Range

Applying AI/ML to 6G PHY Research

Applying Neural Networks for Predicting Feed Weights of an Antenna Array

Array Antennas for Space Applications

Array Calibration for Massive MIMO Antenna System: Challenges and Solutions

Array Scattering Synthesis for Anomalous Deflection Using Passive Aperiodic Loadings

Array-Fed Transmitarray with Designated Beam Directions and Coverages

Assessing Performance of Transparent Conductive Films for Microwave Industrial Applications

Assessment of MFE-Based Multiport Waveguide Crossing for Use with Low-Cost, Low-Loss Dielectric Interconnects in Millimeter Wave Arrays

Assessment of the Feasibility of Breast Lesion Detection with Contrast Source Inversion for Microwave Tomography: A Virtual Experiment

AttentionRNN: Novel Propagation Channel Time-Domain State Predictor

Automated Design and Characterization of a Scalar Metasurface Antenna Radiating a Linearly-Polarized Broadside Beam

Automated Design of Antennas Using AI Techniques: A Review of Contemporary Methods and Applications

Automatic MoM Source Integral Quadrature Selection via a Machine Learning Approach

Automatic Planning Algorithm of 300 GHz Backhaul Links Using Mesh Topology

B

1 2 3 5 6 A B C D E F G H I J K L M N O P Q R S T U V W X

Bandwidth Manipulated Leaky-Wave Antenna Using a Sinusoidal Ridge in Folded Substrate Integrated Waveguide

Bandwidth-Enhanced Compact Beamsteering Antenna for IoT Platforms

Base Station Radome Design for 5G and Beyond

Beam Coverage Model of Ultra-Massive MIMO Communication Systems for Intelligent Transportation

Beam Focusing with a Conformal Leaky-Wave Antenna Described by a Spline Curve

Beam Steerable Half Mode Substrate Integrated Waveguide Based Composite Right/Left Handed Leaky-Wave Antenna Using Field Programmable Microwave Substrate

Beam Steering 2D Leaky Wave Resonant Cavity Antenna for Ka-Band Satellite Communication

Beam Steering Performance Improvements Using a Layered Permittivity Dielectric

Beam Steering Range Enhancement of Bifocal Reflectarray Using Irregular Distribution of Meta-Atoms

Beam Steering Range Enhancement of Bifocal Reflectarray Using Irregular Distribution of Meta-Atoms

Beam Training of LoS-MIMO Systems Using Subarray-Based Beamforming in the Presence of Ground Reflection

Beam-Steerable Microstrip-Line Based Leaky Wave Antenna with Reconfigurable Slits

Beam-Tilted All-Metal Radial-Line Slot Array Antenna with Uniform Spacing

Beamforming Optimization for Full-Duplex Relay in SIC-Enhanced Cooperative NOMA System

Beamforming Orthogonality in Coupled Directional Modulation Arrays

Beamforming Schemes for 6G Direct-To-Cell Connectivity Using Satellite Swarms

Behavioral Models for the Cosimulation and Optimization of Active Electronically Scanned Arrays

Best Practices for Accurate Results Using Numerical Solvers for Microwave Body Screening

Beyond Antennas: Challenges and Rewards of an Engineer's Life

Bifunctional Stubs Enabled MIMO System for Wideband Mobile 5G and Wi-Fi 6E Applications

Biodegradable Implant Antenna Utilized for Real-Time Sensing Through Genetically Modified Bacteria

Bound States in the Continuum in Cylindrical Impedance Surface Cavities

Brain Hemorrhage Detection Using Antenna System Integrated with Imaging Algorithm

Brain Stroke Microwave Diagnostics in Children Through a Nonlinear Inverse-Scattering Technique

Breaking the Myth of RIS: Investigating the Role of User Equipment for Achieving Robust mmWave Wireless Channel Links Under NLOS Environments

Brief Presentation of the ECAP and WiAP WGs

Broadband Performance Assessment of Compensated Compact Antenna Test Range CCR 75/60 of Airbus at L-Band for Navigation Applications

Broadband Waveguide Magneto-Electric Dipole Antenna for F-Band Applications

Broadening the Spectrum: Extending the Finite Crystal Method to Characterize Static Multi-Atomic Active Metamaterial Systems

C

1 2 3 5 6 A B C D E F G H I J K L M N O P Q R S T U V W X

Challenges and Limits of Designing Wide Band and Efficient Compact Superdirective Antenna

Challenges and Opportunities of Amplified Information Metasurfaces for Simultaneous Wireless Communications and Power Transfers

Channel Characterization and Modeling for Wireless MIMO Communication Systems in Intersection Scenarios

Channel Characterization and Modeling for Wireless MIMO Communication Systems in Intersection Scenarios

Channel Measurements and Characterization in Industrial Environment at 60 GHz

Channel Measurements in Workspace with Robotic Manipulators at 300 GHz and Recent Results

Characterisation of a D-Band Horn Antenna: Comparison of Near-Field and OTA Measurements

Characterisation of Frequency Selective Reflections off Indoor Surfaces for Sub-THz Band

Characterisation of Thin Glass-Fibre Substrates for Deployable SAR Antennas

Characterization and Comparison of Formulas for Optimizing Broadside Radiation in a 2-D Leaky-Wave Antenna

Characterization of a D-Band Active Transmitarray System for Efficient Point-To-Point Links

Characterization of a D-Band Active Transmitarray System for Efficient Point-To-Point Links

Characterization of a Metamaterial-Enabled Waveguide Diplexer for Ka-Band Satellite Communication Systems

Characterization of All-Metal Multi-Feed Antenna for High Power Applications

Characterization of Propagation from Measurements at Sub-THz for ISAC Applications in an Emulated Dynamic Industrial Scenario

Characterization of Typical Instantaneous Exposure and Usage Scenarios in the Vicinity of 5G Massive-MIMO Base Stations

Characterization of Typical Instantaneous Exposure and Usage Scenarios in the Vicinity of 5G Massive-MIMO Base Stations

Chessboard Focal Plane Array in Silicon Technologies for Terahertz Imaging

Chipless RFID Sensor on Paper Substrate

Circular Loop Antennas with Quasi-Two Sources for Broadband Circular Polarization

Circularly Polarized Sub-THz Antenna Design for Distributed Deployment

Circularly Polarized Transmitarray Design Using Characteristic Modes Theory

Circularly Polarized Wide-Angle Scanning Phased Array Based on Heterogeneous Beam Element

Circularly-Polarized Wideband Conformal Magneto-Electric Antenna Covering the GNSS Bands

Closely-Spaced Groove Gap Waveguides with Reduced Coupling

Cloud Attenuation in the Q Band: Estimation from Experimental Data of Excess Attenuation

Cloud Attenuation in the Q Band: Estimation from Experimental Data of Excess Attenuation

Combined Ray-Tracing and Physical-Optics Model for Flat-Aperture PPW Lens Antennas

Compact 868 MHz RFID-Based Antenna for Queen Bee Identification and Location Inside Hives

Compact Amplitude-Monopulse Microstrip Antenna Design for Wide Field-Of-View Direction Finding

Compact Antenna Solutions for Data Transmission Using Fat-Intrabody Communication (Fat-IBC)

Compact Circularly Polarized Antenna Based on Gapwaveguide for SATCOM Applications

Compact Circularly Polarized Patch Antenna with Enhanced Axial Ratio and Impedance Bandwidth

Compact Dual-Band Crossover with Enhanced Band Ratio Using Interdigital Capacitor for 5G Applications

Compact Dual-Band Dual-Polarization Feed for Broadband Communication Satellites

Compact Dual-Band Dual-Polarization Feed for Broadband Communication Satellites

Compact Hybrid Optical/RF User Segment (CHORUS): RF Terminal Design

Compact Ka Band Orthomode Transducer with Conical Horn Antenna

Compact Metamaterial Antenna for Three-Dimensional Angular Localization of Multiple Radio-Frequency Sources

Compact Polarization Converter on a Thin Ferrite-Based Metasurface for Enhanced 5G Wireless Communication

Compact Size Frequency-Agile Antenna Enabling Multi-Mode Functionality for Internet of Things Applications

Compact Vivaldi Antenna Application in High-Power Design at X-Band

Compact Wideband Circularly Polarized Antenna Array for Satellite Applications

Comparison Between ERA5 Cloud Parameters and Rainfall Rate in Madrid

Comparison of Indoor Propagation Channels at 28 GHz and 140 GHz Bands

Comparison of Propagation Characteristics Between 5G Bands in a Reflective Industrial Environment

Comparison of Simplistic System-Level RIS Models and Diffraction-Theory Solutions

Comparison of Sub-THz Radio Channel Characteristics at 158 GHz and 300 GHz in a Shopping Mall Scenario

Complex Permittivity Extraction of Typical Wooden Furniture Materials Based on Multi-Objective Particle Swarm Optimization over 40-50 GHz

Compressive Sensing Applied to Production Testing of Array Antennas Using a Robotic Arm and Very Sparsely Sampled Near-Field Measurements

Computer Vision Enabled Sub-THz Radio Channel Characterization of Dynamic Objects

Concentration Detection of Sodium Chloride and Glucose Solutions Using an IDC-Based Microwave Sensor with Eliminating Environmental Effects

Conceptual Design and Propagation Characteristics of an Underwater Electromagnetic Communication System for Ocean Environment Sensor Systems

Conceptual Design of Antenna Arrays for Satellite Direct-To-Cell Connectivity

Contactless 3D Subsurface Imaging: Considerations to Set the Measurement Spacing

Contactless Impedance and Far-Field Characterization of Electrically Small Antennas

Contactless Respiration Variability Detection and Accuracy Test Using UWB Radar

Context-Aware Channel Sounder for AI-Assisted Radio-Frequency Channel Modeling

Contiguous Broadband Circularly Periodic High Impedance Surface Integrated with a Spiral Antenna

Continued Evaluation of the Modern 5G Millimeter Wave Antenna Array Evaluation in Near- and Far-Field Environments

Cooperative Power Control and Beamforming Design for Multi-Source Enabled Wireless Power Transfer Networks

Cost-Effective Dual Circularly Polarized Antennas for Phase Calibration

Cost-Efficient Large-Scale Re-Design of Multi-Band Antennas Using Orthogonal Scaling Directions

Crack Stop as a Coupling Element Between an IC Chip and Antenna

Crank-Nicolson FDTD Method in Media Described by Time-Fractional Constitutive Relations

CSIRO Radio Astronomy Receiver Update - Ultra Wideband and Phased Array Feeds

CubeSat Formation Antenna Array Synchronization for GNSS-R

Curved Electromagnetic Skins for Urban Scenarios

Curving THz Beams in the near Field: A Framework to Compute Link Budgets

CVNN Approach for Microwave Imaging Applications in Brain Cancer: Preliminary Results

D

1 2 3 5 6 A B C D E F G H I J K L M N O P Q R S T U V W X

D-Band Absorber Comprising Tantalum Nitride-Based Resistively-Loaded High Impedance Surfaces

D-Band Active Antenna Array with Lens Enabling Quasi-Optical and Analogue Beam Reconfiguration for 6G Applications

Data-Driven Optimization of an Array of Steered Sub-Arrays for Enhanced Fairness in MU-MIMO

DC Bias Routing Design for Wideband Reconfigurable Transmitarray Based on 1-Bit Phase-Switching Elements

Deep-Learning Optimized Reconfigurable Metasurface for Magnetic Resonance Imaging

Delving into Time Domain Gating: An Extensive Study on Parameter Selection and Its Implications

Design and Characterization of a Flexible Fabry-Perot Antenna Fabricated Using Conductive Inkjet Printing

Design and Characterization of an Imaging System Using Photoconductive Connected Arrays

Design and Development of Full-Metal Planar Array Antennas

Design and Investigation of 2x2 Dielectric Resonator Antennas Array for Sub-THz Applications

Design and Measurement of a 2x2 Array of Coaxial Periodic Leaky-Wave Antennas

Design and Preliminary Indoor Assessment of a Long-Range Sub-THz VNA-Based Channel Sounder Between 500 GHz and 750 GHz

Design and Prototyping of a Low-Cost Parasitic Element Antenna for a Telemetry-Telecommand Link on Ariane 6 Space Launcher

Design and Test of a UHF Deployable Conical Log Spiral Antenna for Small Satellites

Design and Validation of a Wireless Network for Intra-Train Communications

Design Effects of the Junction Contour of a Blended Rolled Edge Compact Range Reflector

Design Flow Methodology Including Thermal and Active Circuit Impact in Antenna Design and Antenna Integration

Design of a Concentric Circular Holographic Metasurface Using Hexagonal Anisotropic Unit-Cell for Wireless Communications

Design of a Conformal and Low-Frequency Metasurface for Magnetic Field Shielding in Wireless Power Transfer Systems

Design of a Dielectric Lens Using a Ray-Tracing Model for Satellite Communications

Design of A Dual-Circular Polarized Antenna Array for Dual-Band Aperture-Shared Applications

Design of a Dual-Polarization Ultra-Wideband Horn Antenna

Design of a Hollow-Waveguide Slot Array Antenna for a Channel Sounder in the 150 GHz Band

Design of a Low-Frequency Magnetic Metasurface for Extremely Focused and Long Range Wireless Power Transfer Applications

Design of a Semitransparent Dual-Mode Filter for Antenna Applications

Design of a Wideband Dual-Polarized Stacked Antenna Array for SATCOM Applications

Design of an L-S-Band Frequency Selective Resorber for Dual-Band Absorption and In-Band Transmission

Design of an Ultra-Wideband RCS Reduction Metasurface with Pure Metal-Pattern Layer

Design of an UWB Conformal Antenna for Wireless Capsule Endoscopy

Design of Broadband Stacked Patch Microstrip Antennas Fed by Differential Microstrip Lines with Large Common-Mode Rejection

Design of Dual-Band CPW Rectenna for Wireless Power Transmission

Design of Electrically Small Antennas and Radiation Efficiency Measurement Using MQFM with Radian Wheeler Cap Sizes

Design of Glide-Symmetric Dielectric Mikaelian Lens Antenna for K/Ka-Band

Design of Intelligent Reflective Surface Unit Cell for 5G mmWave Applications

Design of Microstrip UWB Antenna with Full Ground Plane for Wearable Applications

Design of Modulated Dielectric Leaky-Wave Antennas for Efficient Bessel-Beam Synthesis

Design of Novel Fully Metallic mm-Wave Reflectarray Antenna

Design of Optimized Cylindrical Structural Antenna with Quasi Length Insensitivity Using CMA

Design of Reconfigurable Reflectarray Antennas on Flexible Substrates with Varactor Diodes Mounted on Slot-Coupled Microstrip Lines

Design of the 3D-Printed Rectangular Dielectric Resonator Antenna for WLAN Applications

Design of Ultra-Wideband Dual-Polarized Corrugated Horn Antenna for 5G Application

Design of Wide Band Multi-Lens Focal Plane Arrays for the TIFUUN Instrument

Design Recommendations for Minimal Antenna Mutual Coupling Using Current Optimization

Design, Measurements, and Performance Assessment of a Massive MIMO Wideband Phased Array

Designing a Data Pre-Processing Tool for MEO Satellites Propagation Measurements

Designing Transmissive Metasurface for Multibeam Transmitarray at 5G Millimeter-Wave Band

Detailed Design Procedure for Low-Cost High-Efficiency 3D Printed Transmitarray Antennas for mm-Wave Applications

Detection Capability of a CNN-Based Imageless Millimeter Wave System for Static Concealed Objects

Development of a Circuit-Type Multiple-Agile Beamforming and Interference Mitigation Network

Development of a Shaped Quartz Lens Antenna for Wide Scanning Sub-Millimeter Imagers

Development of a Site-Specific Building Entry Loss Model for High-Rise Buildings

Development of a Wearable IoT-Optimized Textile Antenna with Low Specific Absorption Rate in Three Frequency Bands

Development of an Analytical Quantum Full-Wave Solution for a Transmon Qubit in a 3D Cavity

Development of an Ultrawideband Wire-Grid Polarizer Measurement Standard for Focus Beam System Cross-Polarization Calibration

Development of Passive Chipless RFID Temperature Sensor

Development of Phased Array and Multi-Phase Centre Systems

Development of Tissue Emulatory Models/Phantoms of Lungs at Microwave Frequency for Acute Respiratory Distress Syndrome

Developments in Open-Source Tools for Microwave Breast Imaging

Dielectric Characterisation of Human Parathyroid Glands at Microwave Frequencies

Dielectric Characterization of Adhesives for THz Packaging in WR6.5, WR3.4 and WR2.2 Bands

Dielectric Characterization of Biological Tissues at Microwave Frequencies Based on Water Content

Dielectric Characterization of Materials at 5G mm-Wave Frequencies

Dielectric Differences in Biological Tissues: A Comparison Between Excised and Non-Excised Tissues Under the Influence of Chemotherapy

Differentially-Fed Antenna-On-Display Module for SATCOM and Mobile Applications at Ka-Band

Digital Beamformer for GNSS Reflectometry and Radio Occultation Applications

Direct Clustering and Multi-Path Component Identification on THz Channel Measurements in a Factory Environment

Direct Optimisation of a Five-State Reconfigurable Reflectarray for 5G Applications

Direction-Of-Arrival Ambiguities Mitigation in Multibeam Leaky-Wave Antennas

Direction-Of-Arrival Estimation by a Programmable Metasurface

Discretizing 2D Equivalent Radiating Panels by Legendre Quadrature

Discussion on the Optimization Goals and Methods for Tunable Antenna Design

Dispersion Curve Calculation Using the Method of Moments: The Impact of Macro Basis Functions

Display-Integrated MIMO Antennas for Gesture-Sensing Radars

Double-Directional Angle-Resolved Wideband Channel Measurements and Path Loss Characterization in Corridor at 300 GHz

Double-Layer Frequency Selective Surface-Based Corner Reflector for Indoor Self-Localization Systems in the W-Band

DRL-Based Sidelobe Suppression for Multi-Focus Reconfigurable Intelligent Surface

Dual All Metal Patch Antenna for the HydroGNSS Mission

Dual Functional mmWave RIS for Radar and Communication Coexistence in near Field

Dual UWB Antennas on AoA Anchor Node

Dual-Band 3-D MIMO Antenna for Deep Tissue Devices

Dual-Band MmWave Measurements of Human Body Scattering and Blockage Effects Using Distributed Beamforming for ISAC Applications

Dual-Band Reflectarray-Based Electromagnetic Skin to Provide Millimeter-Wave Coverage in the 28/60-GHz Bands

Dual-Feed Wideband Folded Waveguide Antenna for Handset Devices

Dual-Frequency Metasurface Antenna for Earth Science Remote Sensing

Dual-Linearly Polarized Pillbox Beamformer in Hybrid CNC-PCB Technologies at W-Band

Dual-Polarization Multi-Functional Metasurface for Wireless Communications

Dual-Polarized Connected-Slot Array Technological Demonstrator Targeting a 5:1 Bandwidth

Dual-Polarized Diffraction Measurements and Modeling at D-Band Frequencies

Dual-Polarized OAM Antenna with Frequency and Mode Agility for Intelligent OAM Communications

Dual-Polarized Reconfigurable Metacavity Transceiver for Computational Polarimetric Imaging

Dual-Polarized Reconfigurable Metasurface for Leaky-Wave Antenna Design Using Air-Bridged Schottky Diode Technology

Dual-Polarized Substrate Integrated Waveguide Antenna with High Isolation for Polarimetric Radar

Dual-Resonance SIW-Based Reflectarray Unit Cell for Broadband Applications

Dynamic Programming-Based Beam Codebook Design for mmWave Multi-Antenna Module in Mobile Devices

E

1 2 3 5 6 A B C D E F G H I J K L M N O P Q R S T U V W X

E-Band Measured Propagation Characteristics for Urban Backhaul Communications

Eco-Friendly and Conformable PIFA Based on PEDOT: PSS and a Sustainable Chitosan Substrate for 5G Communications

Eco-Friendly Meta-Randomized Antenna for Millimeter Wave Radar

Effect of Phase Errors on Performance of Ka-Band Reflectarray with DRA Unit Cells

Effect of Wave Polarization in On-Body Propagation for the 2.4, 24 and 60 GHz ISM Bands

Effects of Bumper Integration on Low-, Mid-, and High-Resolution Imaging Radars

Efficiency Use of Electromagnetic and Circuit Simulation Tools for Tunable Antennas

Efficient Analysis Method for Artificial Dielectric Layers with Vertical Metal Inclusions

Efficient NUFFT-Based Spectral Domain Method of Moments Analysis of Multilayered Periodic Structures with Subsectional Basis Functions

Efficient Numerical Computation of Dispersion Diagrams for Glide-Symmetric Periodic Structures with a Hexagonal Lattice

Efficient Optimization-Assisted Full-Wave MoM Unit-Cell Design for Dual-Band Transmitarrays

Efficient Ray-Tracing Approach to Analyze Arbitrarily Shaped Leaky-Wave Antennas Embedded in Lenses

Efficient Ray-Tracing Model for Generalized 2D Dielectric Lenses Combined with Arrays

Efficient Wireless Power Transfer to an Ultra-Miniaturized Antenna for Future Cardiac Leadless Pacemaker

Electromagnetic Assessment of Tolerances of the Square Kilometre Array Log Periodic Antenna Using Uncertainty Quantification

Electromagnetic Beerline Cleaning Using Radio Frequency Signals

Electromagnetic Compatibility for Automotive Applications

Electromagnetic Detection and Identification of Perturbed Wire Resonators

Electromagnetic Modelling in Modern Vehicles: A Pathway to Efficiency and Performance

Electromagnetics-Based RIS Channel Model with Near-Field Accuracy Improvement

Embedded Graded Index Lens for Mitigating the Phase Error of an SIW Horn Lens Antenna

Embroidered Antenna-Based Sensor for Real-Time Natremia Monitoring

Empirical Characterization of Doppler in Industrial Wireless Channels

Empirical Path Loss Model and Small-Scale Fading Statistics in an Indoor Office Environment in 6 and 37 GHz Shared Bands

Empirical Validation of the Impedance-Based RIS Channel Model in an Indoor Scattering Environment

Emulating Spatial Dispersion Using Non-Spatially Dispersive Periodic Metasurfaces

Emulating Spatial Dispersion Using Non-Spatially Dispersive Periodic Metasurfaces

Enabling Living Spaces Through Customizable NFC-Enabled Smart Table System

Enabling Shape Morphing Communications at mmWave with Spray on Antenna Arrays

Enabling VNA Based Channel Sounder for 6G Research: Challenges and Solutions

Enhancing Signal Transmission in Energy-Saving Glass Through Tri-Bandpass Frequency Selective Surface Design

Enhancing THz Antenna Characterization Precision in WR-1.5 Band Using Vacuum Waveguide Flange

Errors Correlation in Near-Field Focused Arrays for Biosafe Microwave Applications

ESoA 2004-2024: 20 Years of Success

ESoA, Arrays and Networks

ESoA: A Friendly Access to the European Antenna Academy

ESoA: My Personal Experience as Student, Teacher and Course Organizer. What a Journey!

Estimating the Achievable Efficiency and Bandwidth of Small Terminal-Integrated Inverted-F Antennas Using Machine

Learning

Estimating the Signal Strength for Microwave Breast Cancer Detection with a Magnetic Near-Field Applicator in Air

Estimation of Obtainable Data-Rates in an Over-The-Air mm-Wave MIMO Testbed

Evaluating System Design in Breast Microwave Sensing: Data and Image Quality in Multiple Systems

Evaluation/Comparison of Post Processing Techniques for Antenna Gain Extrapolation Measurements

Exact Maxwell Solution for Arbitrary Transverse Electric Multipole Radiation for Spherical Electric Current Density

Excitation Signal Design for THz Channel Sounding and Propagation Parameter Estimation

Experimental Analysis of Physical Interacting Objects of a Building at mmWave Frequencies

Experimental Analysis of Physical Interacting Objects of a Building at mmWave Frequencies

Experimental Characterization of a Core-Shell Lens for Antenna On-Package Integration at D-Band

Experimental Evaluation of V2X Connectivity Technologies with V2X Channel Models

Experimental Investigation of the Nullifier-Based Monopole

Experimental Results for Carbon Nanotube-Sheet Based Microstrip Patch Antenna

Experimental Validation of Ray-Tracing and Physical-Optics Model for Geodesic H-Plane Horn Antennas

Experimental Validation of Reflectarray-Based Base Station Antenna for Simultaneous Front- and Radio Back-Haul Links in mm-Wave Frequencies

Exploiting Near-Field Antenna Detuning in Collision Avoidance Systems for RFID-Equipped Robots

Exploiting Numerical Weather Prediction Data for Radiopropagation Modeling of SatCom Links

Exploring PLA/Flax Substrates for Antenna Applications: Assessing Moisture, Temperature and Dielectric Constant Homogeneity

Exploring RIS Coverage Enhancement in Factories: From Ray-Based Modeling to Use-Case Analysis

Exploring the Potential of Spatially Modulated Full-Metal Dichroic Mirrors for Deep Space Antennas

Exploring the Properties of Reverberation Chambers in the THz Range: A Pilot Study

Exploring Uniformity of Reverberation Chambers: Insights from Antenna Reflection Coefficient

Extending Spectral Factorization to the 2-D Mask-Constrained Power Synthesis of Shaped Beams with Arbitrary Footprints

Fabry-Perot Antenna with High-Permittivity Grounded Walls for Side Lobe Level Reduction

Fading Distribution Model for the Maritime Radio Channel

Far-Field Beam Wireless Power Transfer with Combination of Beam Forming and Optical Target Detection

Fast Indoor Radio Propagation Prediction Using Deep Learning

FDTD Modelling of RF Circuits Based on Lumped Components and Transmission Lines Using Modified Telegrapher's Equations

Feasibility Investigation on a Low-Cost an Air-Filled Substrate Integrated Waveguide Array Antenna in V-Band

Feasibility of High Throughput Wireless Communication Above 100 GHz in Indoor Scenarios

Feasibility Study of 3D Printed Luneburg Lens Using Fused Deposit Material 3D Printing Technology for Ku-Band Application

Feasibility Study of Joint Modeling of Environmental and Morphological Effects for WBAN

Feature Selection for Identifying Optimal Microwave Frequencies to Detect Floating Macroplastic Litter in C and X Bands

Feed Assembly Development for INCUS

Feed Assembly Development for INCUS

Field Trials for Different 5G NSA Cellular Networks

Filter Integrated Microstrip 3-Port Power Combiner

Fine Tuning an AI-Based Indoor Radio Propagation Model with Crowd-Sourced Data

Flat Gradient Index Lenses with Planar or Spherical Output Wavefront

Flexible and Transparent Metamaterial Absorber Using Metal Mesh Structure

Flexible Antenna with Microfluidics for the Quantification of Liquid Micro-Volumes

Flexible Antenna with Microfluidics for the Quantification of Liquid Micro-Volumes

Flexible Phase-Reconfigurable Branch Line Coupler for Millimeter-Wave Phased Array Antenna

Folded Dielectric Reflectarray with Spherical Polarizer

Frequency Domain Channel Characteristics in an Outdoor-To-Indoor Environment at 6 and 37 GHz

Frequency Reconfigurable Flexible Printed Antenna Based on Non-Volatile RF Switches for Wearable Applications

Frequency Scanning Leaky-Wave Antenna for On-Body Radar: Design and Conformal Analysis

Frequency-Domain TLM Method with Cartesian Block Meshing

Frequency-Selective Surface Generating Two-Band Pseudo-Elliptic Frequency Response

From ACE to ESoA Courses: Impact on Our Careers as Early Participants

From Bulk Toward Micro-Structured TiO₂ Ceramics for All-Dielectric Metamaterials at Terahertz Frequencies

From mmWave Radar Nodes to Multistatic Arrays: Design Considerations and Applications

From Reconfigurable Intelligent Surfaces to Holographic MIMO Surfaces and Back

Front-End Mismatching, Mutual Coupling, Bandwidth, Transmission Line Noise, and SNR

Front-End Topologies and Calibration Strategies of Active Phased Arrays

Full Wave Modelling and Design of a Baffle for the HERTZ 2.0 Compact Antenna Test Range

Full Wave Verification of Radome Edge Scattering Treatments Using Open Source Tools

Full-Metal Single-Block Antenna Arrays with Waveguide Copractive Feeding Networks at Ka and V Bands

Fully Autonomous Reconfigurable Metasurfaces with Integrated Sensing and Communication

Fully Differentiable Ray Tracing via Discontinuity Smoothing for Radio Network Optimization

Fully Metallic Wideband Lens Design Using a Highly Refractive Glide-Symmetric Unit Cell at W-Band

Fundamental Limits on Characteristic Modes

G

1 2 3 5 6 A B C D E F G H I J K L M N O P Q R S T U V W X

Gain Improvement of a DRA Using Deep Reinforcement Learning with Polygon Mesh Deformation

Gap Waveguide Technology for mm-Wave Antennas

Gaussian Processes for Received Signal Strength Based Device-Free Localization

Generalized Far-Field Distance of Antennas and the Concept of Classical Photons

Generalized Transition Matrix Model Using Characteristic Basis Function Method for Open-Ended Cavities

Generating a Library of Head Phantoms for Microwave Imaging Using Spherical Harmonic Approximation

Generation of a Square Multi-Mode Multi-Port Aperture Antenna by Selective Modal Excitation

Generation of Dual Band OAM Wave Using Single Patch Antenna for WLAN/WiMAX Applications

Generation of Electromagnetic Exposure Maps for 5G Communications

Generation of Highly-Pure OAM Beams with Simple Slotted SIW Antenna Array

Generation of Narrow Divergence Angle OAM Beams for mmWave Communication Links Using Metasurface

Generation of Narrow Divergence Angle OAM Beams for mmWave Communication Links Using Metasurface

Generation of Non-Diffractive Bessel Beams for Near-Field Links Applications Using Meta-Axicons

Genetic Algorithm-Based Beamforming in Subarray Architectures for GEO Satellites

Geometry Reconstruction from Entries of Impedance Matrices

GHz Prism: Frequency-Scanned Antennas to Improve Localization with Separate-Channel Fingerprinting

Giga Home Broadband FTTR, an Overview of Wi-Fi 8 Techniques, Spectrums, and Standardizations

Glide-Symmetric Reconfigurable Substrate-Integrated Holey Waveguide

Glide-Symmetric SIH Unit Cells Implemented in Parallel-Plate Waveguides at mmWaves

GPR Imaging Relying on Frequency-Diverse Compressive Antennas

gprMax (Www.gprmax.org)

GPS Interference Cancellation Using Magneto-Dielectric Metamaterials

Graph Neural Network Based 77 GHz MIMO Radar Array Processor for Autonomous Robotics

Grid-Based Shadowing Gain Modeling for Handling Dynamic Objects in Wireless Channel Emulation

Grid-Free Harmonic Retrieval and Model Order Selection Using Convolutional Neural Networks

Grid-Free Harmonic Retrieval and Model Order Selection Using Convolutional Neural Networks

Ground Base Station Antenna Design for Air-To-Ground Communications

Ground Plane Width Analysis for IoT Devices Embedding Antenna Boosters

H

1 2 3 5 6 A B C D E F G H I J K L M N O P Q R S T U V W X

Half Mode Corrugated Substrate Integrated Waveguide (HM-CSIW) Band-Stop Filter Using Hexagonal Ring Resonators

"HERAS: Heriot-Watt Reflector Antenna Solver (Part 2) (Www.github.com/Microwave-Antenna-Engineering-Group-HWU/HERAS)"

HERAS: Heriot-Watt Reflector Antenna Solver (www.github.com/Microwave-Antenna-Engineering-Group-HWU/HERAS)

High Data-Rate Sub-THz Coherent Near-Field Wireless Links Enabled by Spline-Profile Bessel Launchers

High Data-Rate Sub-THz Coherent Near-Field Wireless Links Enabled by Spline-Profile Bessel Launchers

High Efficiency Groove Gap Waveguide Leaky Wave Antenna Array with Flat Top Radiation Pattern

High Gain and Dual Band SIW-Fed Stacked Conical DRA for 5G NR FR1 Application

High Resolution ISAR Imaging Methods for RCS Data Analysis

High-Accuracy Near-Field Calibration Techniques for Gain Reference Antennas

High-Gain and Circular Polarization Silicon-Micromachined Lens Antennas at 500-750 GHz

High-Gain Shared-Aperture Patch Phased Array and Reflectarray Antenna

High-Order Quasi-Elliptical Bandpass FSS Based on Substrate-Integrated Waveguide Technology for 60 GHz Applications

Higher Symmetries in Hexagonal Periodic Structures

Highly Efficient Polarization-Insensitive EM Energy Harvester

Highly Precised and Efficient Robot-Based ESPAR Antenna Measurements in Realistic Environments

Highly Reflective, Low-Loss, Homogenized Fishnet Metasurfaces at Terahertz: Design and Experiment

Highly Transparent and Efficient Flexible Antenna for Vehicle-To-Everything (V2X) Applications

Historical Perspective of World War II Radar Development

History and Future Directions of Airborne Radars

Horn Antenna Phase Center Position Influence on Sub-THz Measurements Uncertainties

How to Successfully Create an ESoA Course from a Student Perspective

How to Take Layout Effects into Account in Circuit Optimization

HRPE-Enhanced AI-Based 5G Indoor Localization in Presence of Specular and Dense Multipaths

Human- Vs Machine Design of Antennas: Evolution Behavior in Genetic Shape Optimization

Huygens Principle Imaging Method Powered by Deep Learning for Brain Stroke Classification

Hybrid Analog-Digital Beamforming System with Quad-Steerable Beams Based on Programmable Transmitarray

Hybrid Antenna Measurement and Post-Processing for 5G Small Cell Exposure Assessment with Site-Specific Mounting Conditions

Hybrid Metal-Graphene Unit Cells for THz Reconfigurable Leaky-Wave Antennas

Hybrid Reconfigurable Reflective Metasurface with Both Phase and Space Modulation

|

1 2 3 5 6 A B C D E F G H I J K L M N O P Q R S T U V W X

IEEE P2816: Computational Standard

IEEE Std 149: Recommended Practice for Antenna Measurements

IEEE Std 1720: Recommended Practice for Near-Field Antenna Measurements

IEEE Terminology Standards: IEEE Std 145 & IEEE Std 211

Imaging Radar Frontend with SIW Feeding Networks

Impact of 6D Mobility on Doppler Characteristics of UAV-To-Vehicle Channels

Impact of Antenna Radiation Pattern Linear Phase Shift in SAR Image Quality

Impact of Deformations on Beamforming Performance of Uniform Rectangular Arrays

Impact of Dielectric Substrate, Feed Connector, and Fabrication Tolerances on the Performance of Planar Millimeter-Wave Antenna Arrays

Impact of the Antenna Topology on the Combination of Full-Duplex Spatial Modulation and RF Energy Harvesting

Impact of the Unit Cell Distribution of 1-D Dynamic Metasurface Antennas on the Performance of a Computational Imaging System

Impedance-Based RIS Channel Model and Optimization in Fast-Fading Environments

Implementation of a Novel Triband Antenna Array in a FR1/FR2 5G-NR System

Improved PEEC Modeling of Antennas Through Time-Dependent Partial Elements

Improved Performance of a 1-Bit RIS by Using Two Switches per Bit Implementation

Improvements of Scintillation Modelling from Radiosonde Observations in the Arctic Region

Improving Air-Writing Accuracy Through Data Regression and Interpolation in a Single Radar System

Improving Scan Gain of Sparse Vivaldi Array with Parasitic Scatterers

Improving the Strut Modelling of the European Space Agency Deep Space Antennas to Evaluate Efficiency and Sidelobe Impact

In-Field Measurement of Total Radiated Power from Active Antenna Arrays

In-Flight Calibration of the Measurement System for UAV-Based Near-Field Antenna Measurements

Inconsistency in Modes of Circular Microstrip Antennas and Its Rectification

Increasing the Efficiency-Bandwidth Product and Impedance Bandwidth of Electrically-Small Antennas Through Parametric Space-Time Variation

Indoor Channel Characterization Based on Directional Measurements at 140 GHz

Indoor Coverage Enhancement Employing Liquid Crystal-Based Massive Reconfigurable Intelligent Surface Linked to 5G FR2 Base Station

Indoor Localization of Smartphones Thanks to Zero-Energy-Devices Beacons

Indoor Propagation Measurements with a Reconfigurable Intelligent Surface at 3.5 GHz

Indoor Wireless Signal Modeling with Smooth Surface Diffraction Effects

Industrial Design Validation for a Plane Wave Generator at 28GHz

Influence of the Atmospheric Plasma Sheath on the RCS of a Hypersonic Reentry Vehicle

Influence of the Incidence Angle on the Focusing of Luneburg Lens Partially Covered with Graphene

Information Metasurface for Simultaneous Wave Manipulations and Signal Modulations

Input Impedance of Radiation Efficiency Deterioration State

Installed Antenna Performance in Complex Environments

Instantaneous Vs Theoretical Maximum Exposure Under Real Traffic Conditions: Example in the City of Valencia

Integral Equation-Based Solver for the Simulation of Metasurface Designs

Integrated Low-Loss mmWave On-Chip Arrays

Integration of Doherty Power Amplifiers with Antennas: Direct Impedance Matching, Active Load Modulation

Interference-Free Transmission for Near-Field Communication with Unlimited Antennas

Intermodulation Mitigation Through Surrounding Impedance Manipulation

Introduction

Introduction to IEEE SA & AP-S Standards

Introduction to ITU, SG 3 and Working Methods

Introduction to TICRA Tools

Introductory Remarks

Inverse Source Solutions with Spectral Filtering

Inverse Source-Based Three-Antenna Methods in the near Field

Investigating the Interference Induced by NGSO Constellations on GSO System Ground Stations: A Simulation Approach

Investigation of Correlation Between Absorbed Power Density and Incident Power Density for User Equipment Antennas at Sub-THz Frequencies

Investigation of Near-Field Contribution in Shooting and Bouncing Rays for Installed Antenna Performance on a Simple Platform

Irregular Subarray with Gathered Elements for Sidelobe Suppression

Isometric Symmetries in Non-Reflecting Structures

It Was 20 Years Ago Today ...

IW2 Introduction

Joint Wide Illumination and Null Insertion Design in RIS-Assisted System

Journey of Learning, Growth and Community - A Peek Inside ESoA

K

1 2 3 5 6 A B C D E F G H I J K L M N O P Q R S T U V W X

K-Band Microstrip ESPAR Antenna Integrated into Large Array

K-Factor Evaluation in a Hybrid Reverberation Chamber plus CATR OTA Testing Setup

Ka-Band Phased Antenna Array Concept for High-EIRP Satellite Connections

Ka-Band Rain Attenuation Derived from a MEO Satellite Constellation

Ka-Band USS Enterprise (NCC-1701) Antenna

KRISS Robot-Based Antenna Measurement System

L

1 2 3 5 6 A B C D E F G H I J K L M N O P Q R S T U V W X

Large and Deployable Multi-Faceted Antennas Based on Single-Layer Reflectarrays

Large and Simple Phased Array System at 28 GHz for Beam Wireless Power Transfer

Large-Scale Site Diversity Experiment in Ljubljana and Budapest at Ka-Band with Alphasat Satellite

Large, Multi-Faceted Reflectarray with Quasi-Constant Directivity in the V-Band

Leading Edge Conformal ARMA Antenna in X Band

Leaky-Wave Design of Hybrid-, TE-, and TM-Polarized Resonant Bessel-Beam Launchers for Millimeter- and Submillimeter-Wave Applications

Learning-Based Procedures for Inverse Design of Electromagnetic Devices: A Preliminary Investigation

Leveraging Radar Back-Scattered Data for Classification of Imaging Targets

Link Budget Estimation for Implantable Antennas: From In-Body Coupling to Free-Space Radiation

Link-Level Performance of Vehicle-To-Vulnerable Road Users Communication Using Realistic Channel Models

Liquid Metal Reconfigurable Phased Array Antenna

Load Impedances Vs Polarizabilities: On the Compactness of Physics-Compliant Models of RIS-Parametrized Wireless Channels

Loaded and Load-Less Supergain Parasitic End-Fire Arrays

Localization of a Nasogastric Feeding Tube Using High-Frequency Harmonic Radar - a Feasibility Study

Long Slot Arrays for Space Applications

Long Slot Dielectric-Loaded Periodic Leaky-Wave Antenna Based on 3D Printing Technology

Long-Term Network-Based Assessment of the Actual Output Power of Base Stations in a 5G Network

Loss Analysis for Compact Liquid Crystal Delay Lines Based on Defective Ground Structures

Low Profile and High Gain Folded Transmitarray in Quartz for Radiometry at 310 GHz

Low Profile Wideband Dual-Polarized Antenna Array for Ku/K/Ka-Band Satcom Applications

Low-Cost 3-D Printed Lens Antenna for Ka-Band Connectivity Applications

Low-Cost Coaxial Slot Array Antenna for E-Band Automotive Corner Radar Applications Based on Gap Waveguide MLW Technology

Low-Cost Hybrid Additive Manufacturing of a Miniaturized Dual Band Stacked Patch Antenna for GNSS Applications

Low-Profile 2D-Mechanical-Beam-Steering Antenna with Large Field-Of-View

Low-Profile Electrically Small Antenna with Pattern and Polarization Diversity

Low-Profile In-Band Pattern Diversity Antenna with Improved Bandwidth

Low-Profile Multibeam Beam-Scanning Antenna for Vehicular Radar Systems

Low-Profile Super-Realised Gain Antennas

Low-Profiled Wideband Dual-Polarized Conformal Antenna Array

Low-Profiled Wideband Dual-Polarized Conformal Antenna Array

LyceanEM (Documentation.lyceanem.com)

M

1 2 3 5 6 A B C D E F G H I J K L M N O P Q R S T U V W X

Machine Learning Approach to Delay Spread Estimation in Industrial Environments

Machine Learning Approaches for EM Signature Analysis in Chipless RFID Technology

Machine-Learning-Based Optimization for Wideband Metasurface Mosaic Antenna

Magnetic Composites with M-Type Hexaferrites for Q/V-Band Electromagnetic Wave Absorption

Magnetolectric Dipole Antenna Extending NLOS Short-Distance Vehicular Communication with Orbital Angular Momentum Modes

Management of Radiofrequency Compatibility on Aircraft

Matching Network Elimination in Multiband Metasurface-Structured Rectennas for Wireless Power Transfer and Energy Harvesting

Material-Independent Scattering Formulations of Characteristic Modes

Maximum Gain Estimates for Corporate-Fed Arrays

Measurement of Total Radiated Power Using a TEM Cell

Measurement-Based Channel Characteristics for Air-To-Ground Communications Under Rural Areas

Measurements of Reconfigurable Intelligent Surface in 5G System Within a Reverberation Chamber at mmWave

Measuring and Modelling the Scattering Parameters of the Wet Radome of the Swiss Weather Radars

Mechanical Vibrations on a Deployable Nanosatellite Antenna: SAR Performance Analysis

Mechanical/Electrical Hybrid 2-Dimensional Beam Scanning Cylindrical Dielectric Lens Antenna

Mechanically Re-Configurable Leaky-Wave Antenna for Fix-Frequency Beam Scanning

Mechatronic Phase-Control Reflector System with In-Plane Axis Control

Metal-Only Additive-Manufactured Geodesic Lens Antennas for the mmWave Band

Metamaterial-Based Ku-Band Flat-Panel High-Gain Antenna for Satcom Applications

Metasurface Dome Enhancing Beam Scanning of AESA Panels

Metasurface Solution for Generating 3D-Curved Beams in Road Environments: A Numerical Study

Metasurface-Based Bessel-Beam Launcher with 100λ Non-Diffractive Range

Metasurfaces Meet Characteristic Modes

Method of Moment Simulation of Full Arctic Weather Satellite Structure

Microwave Imaging for Monitoring Bone Healing Using Magnetic Scaffolds: An Initial Analysis

Microwave Inversion of Measured S-Parameters Using a Thin-Wire Antenna Model

Microwave Sensor for Detection of Optical Transparent Foreign Body in Soft Tissue: Eye

Microwave to mmWave Wireless Power Transfer: An Overview of the Design Challenges with a Focus on UK-Based R&D

Microwave Tomography Bone Imaging: Analysing the Impact of Skin Thickness on the Reconstruction of Numerical Bone Phantoms

Millimeter-Wave 3D Folded Strip Antennas and Arrays: Diverse Polarizations Realization Under Robust Input Impedance

Millimeter Wave Retrodirective Van Atta Arrays in LTCC Technology

Millimeter Wave Vector Measurement System Using Low Frequency Band Oscilloscope

Millimeter-Wave and Sub-THz Channel Measurements and Characterization Analysis in a Street Canyon Scenario

Millimeter-Wave Beam-Steerable Lens with Reduced Profile and Enhanced Gain

Millimeter-Wave Corporate-Fed Slot Array Antenna Fed by Partially Dielectric-Filled Transmission Line

Millimeter-Wave Scattering from Building Facade: A Simulation and Verification Study

Millimeter-Wave Uniform Amplitude SIW Series Power Divider for 2D Leaky-Wave Antenna Arrays

MIMO Array Decoupling with SSR Structure in Joint Communication and Sensing System

MIMO Signals Processing Utilizing Optical Crossbar Linear Operator

Miniaturised Magnetic Antenna for Wireless Implanted Medical Device

Miniaturization of Wireless Power Transfer for Implantable Devices Using Voltage Doubler Rectifier

Miniaturized and Lightweight ESPAR Antenna for WSN and IoT Applications

Miniaturized Implantable Antenna with Ultra-Wide Bandwidth Characteristics for Leadless Pacemakers

Minimum Coherence Bandwidth for OFDM Signal Testing in Reverberation Chambers

Mitigating Zenith Blindness from Mutual Coupling in a Sunflower Phased Array

Mixed Spatial-Spectral Domain Integral Equation Solver for Higher-Order Boundary Conditions in Electromagnetics

Mixture Density Networks for Multipath Assisted Positioning-Based Fingerprinting

Mm-Wave Monopulse Radar System for Detecting Space Debris in Satellite Exploration Missions

mmWave Channel Sounding for Vehicular Communications

Modal Analysis in Woodpile Dielectric Structures

Modal Analysis of Thermal Noise from Lossy Dielectric Medium

Model Order Reduction for Parametric Dependence of Q-Factor Bounds in IoT Applications

Model-Based Deep Learning for High-Dimensional Periodic Structures

Modeling Atmospheric Effects on over Land UHF Propagation Links

Modeling of 3D Feeding Structures in the Automated Design of Metasurface Antennas

Modeling of Quasi-Optical Systems and Measurements with a Cobot in the J-Band

Modeling Received Power from 4G and 5G Networks in Greece Using Machine Learning

Modular Ka-Band Transmit Phased Array Antenna for SATCOM Applications

Monitoring Eye States Based on Transparent and Flexible Antenna in WBAN

MR/Microwave Tomography Integrated Breast Cancer Imaging

Multi-Antenna Systems for Future Wi-Fi Technologies

Multi-Band and Wideband Waveguide Arrays for Satcom and 5G Backhaul

Multi-Band Anisotropic Metasurface: Simultaneous Linear and Circular Polarization for Robust Satellite Communication

Multi-Beam Arrays for Future LEO SatCom Payloads

Multi-Beam Dual Polarised Metasurface Antenna in Ka-Band

Multi-Beam Phased Array Systems for SatCom Gateway Applications

Multi-Bit Wideband Transmitarray Aperture with Independent Phase and Amplitude Control for High Gain with Low Sidelobe Mm-Wave Applications

Multi-Channel Beam-Splitting Metasurface for Millimeter Wave Communication Systems

Multi-Directional Leaky-Wave Antenna with Independent Beam-Scanning Laws

Multi-Feed Resonant Cavity Antenna with In-Antenna Power Combination for mm-Wave Communication

Multi-Scattering Centers Extraction and Modeling for ISAC Channel Modeling

Multibeam Antenna for Wide-Angle 95-Beam Coverage at Ka-Band Using a Multifocal Transmit-Array

Multibeam Compact Dual Reflectarray Antenna for High-Throughput Satellites in Ka-Band

Multibeam Metal-Only Groove Gap Waveguide-Based Array in E-Band

Multibeam Phased Array with Reduced Transmit and Receive Modules

Multibeam Phased Arrays Exploiting Frequency Dispersion for Massive MIMO Satellite Communications

Multibeam Radiation by Multipoint Fed Modulated MTS Apertures

Multifunction Over-The-Horizon Radar for Space Domain Awareness

Multifunctional Linear Dichroism and Polarization Transforming Metasurface for mm-Wave Application

Multilayer Reflectionless Wide-Angle Anomalous Refractors Based on Surface Field Optimization

Multipath Model Improvement for Automotive Radar Application

Multiple Reduced Order Models for Antenna Measurements

Multiple-User Full-Duplex Hybrid Beamforming Design for mmWave Systems with A Joint Interference Cancellation Design

Multistable Structures for Deployable and Reconfigurable Antennas

Multistatic OFDM Radar Fusion of MUSIC-Based Angle Estimation

Mutual Coupling Reduction in 5G MIMO Antenna Using Dielectric Bridge and Superstrate

N

1 2 3 5 6 A B C D E F G H I J K L M N O P Q R S T U V W X

Near Field Phase Recovery Exploiting Only One Measurement Surface and A Smart Warping Sampling Strategy

Near-Field Antenna Gain Calibrations Employing Spherical Near-Field Techniques

Near-Field Bistatic Microwave Imaging with Dynamic Metasurface Antennas

(Nearly) Four Decades in the Antennas and Propagation Community

Needs and Measurements Challenges over Integrating Adaptive Antenna with Emerging Wireless Systems

Neural Network Based Microwave Tumour Detection Using Breast Pairs

New Efficient Waveguide Antenna for Future Automotive Radar Applications

New Hybrid Ray-Tracing/FDTD for EMF Exposure in 6G Networks Using Semantically Classified Google Earth Photogrammetry with Measurement Validation

New Sub-THz & Test Techniques for 6G Research

Non-Reciprocity in a Three-Mode Quantum Magnomechanical System with Magnetostrictive Interaction

Non-Regular Multibeam Coverage Antenna for Ka-Band High-Throughput Satellite Communications

Non-Uniform Metamaterial Mushroom Antennas via a Genuine Multi-Objective Bayesian Optimization Method

Non-Volatile Memristor-Based 1-Bit Reconfigurable Intelligent Surface Towards a Greener 6G

Non-Volatile RF Frequency Reconfigurable Antenna for Wireless Communication

Nonlinear Correction of the Direct Inverse Problem Solution in Real-Time Imaging

Nonlinear Distortion Issues Created by Active Reconfigurable Intelligent Surfaces

Nonreciprocal Metasurfaces Analyzing Temperature Characteristics

Nonreciprocal Phase-Shifting in Linear Magnet-Free Reconfigurable Temporal Loops

Novel Quantum Computation Based Selection Operator for Genetic Algorithms Applied to Electromagnetic Problems

Novel Risle Prism Design Approach with Improved Side Lobe Levels Using Multi-Layer Transmit-Arrays

Numerical Assessment of a Cognitive Chamber: TMz Case

Numerical Results on the Use of the L-SVD Approach for the Solution of the Inverse Source Problem from Amplitude-Only Data

Numerical Study of the Dielectric Properties of Lung Tissue Measured with Two Different Open-Ended Coaxial Probes



1 2 3 5 6 A B C D E F G H I J K L M N O P Q R S T U V W X

Observation of Exceptional Points in Parity-Time Symmetric Coupled Impedance Sheets

Octagonal Patch Tag Antenna and 3×3 Array Locator for DoA Applications

Omnidirectional Cylindrical Dielectric Resonator Antenna for off & on Body Communications

On Efficient Representations of Frequency Dependent Far-Field Information for Array Antennas

On Enhancing Efficiency of Transmission in Imaging Systems by Wearable Scatterers

On Implementation of SEME-Paradigm in Indoor - New Trends for Wi-Fi Connectivity and UE Improvements

On Solving Inverse Source Problems with Metasurfaces Performing Analog Computations

On the Asymptotic Evaluation of the Near-Field in Resonant Leaky-Wave Antennas Using a Non-Uniform Phase Center

On the Cost-Effectiveness of Using Beamforming at the Ground Station for Aeronautical Communications

On the Data Rate Capability of Near-Field Communications Links Based on Bessel Beams

On the Design of Static Passive Skins for Next Generation Fixed Wireless Access Applications

On the Design of Wide-Scanning Lenses with Integrated Focal Arrays

On the Importance of Scattering from Poles in Ray Tracing Simulations

On the In-Vivo Electrical Properties of Human Forearm at Microwave Frequency

On the Radiation Resistance of Folded Antennas

On the RF Absorber Coverage of Antenna Under Test Positioners

On the Rigorous Design of Graphene-Based Periodic Structures Exploiting the Fundamental Resonances

On the Scanning Properties of Bidimensional Discrete Lens Antennas with 1, 3, Infinite Focal Points

On the Use of Adaptive-Density Point Cloud for Site-Specific Ray-Optics Simulations

On the Use of Resonant Cavities for Experimental Validation of the Dispersion Diagram of Periodic Glide Symmetric Waveguides

On-Chip mm-Wave Artificial Magnetic Conductor Backed Dipole Antenna on Low-Ohmic Substrate

Online Antenna Courses

Open Stopband Suppression of Periodic Leaky-Wave Antenna Based on Theory of Small Reflections

Opening Presentation by Organizers

Optical Microwave Metasurface Phased Arrays

Optimal Design of Planar Micro-NMR Coils for High Signal-To-Noise Ratio

Optimal Morphing Metasurface Lens for Next Generation RF Sensing and Communications

Optimization of Contiguously Clustered Multibeam Scanning Planar Array for 5G/6G Application

Optimization of Loads for Antenna-Based Scattering Systems Using Feedforward Neural Networks

Optimization of Super-Directive Linear Arrays with Differential Evolution for High Realized Gain

Optimization of the TRP Evaluation in Anechoic-Reverberation Hybrid Chamber

Optimized Design Parameters for a Flux-Driven SNAIL-Based Traveling-Wave Parametric Amplifier

Optimizing RF Energy Harvesting in IoT: A Machine Learning Estimation Considering Polarization Effects

Optimizing RF Energy Harvesting in IoT: A Machine Learning Estimation Considering Polarization Effects

Optimum Structured Phased Array with Novel Beam Forming Circuits for Beam Wireless Power Transfer

Orthogonal Coding for Millimeter-Wave Imaging Using MIMO Dynamic Metasurface Apertures

Over-The-Air Measurements for mm-Wave Body-Centric Wireless Communication

Over-The-Air Measurements of Integrated Antennas Using a Reverberation Chamber

Over-The-Air Noise-Figure Measurements of Active Integrated Antennas at W-Band

Over-The-Air Testing Environments with Spatial-Directional Selectivity for Characterizing Wireless Devices and Systems

Overview of Closed-Loop Tuning to Adapt to Varying Impedance Environments

Overview of Frequency Tunable Antenna Concepts, Especially Aperture Tuning

Overview of State-Of-The-Art Methods for Determining Performance Bounds on Electromagnetic Systems

Overview of Tunable Components: Capacitor Banks, Switches and Tuner Chips

P 1 2 3 5 6 A B C D E F G H I J K L M N O P Q R S T U V W X

Packaging of mm-Wave Active Array Antennas for Car Radar: Concepts and Technologies

Panel Discussion

Part - IV - Case Study

Part I: Introduction

Part II - Barrier Breakthrough: TMYTEK Rapid mmWave Prototyping Solution

Part III - Research Enabling Features

Part V - Conclusion

Passive Beamforming with Liquid Antennas: Techniques and Implementation

Passive RIS to Improve Near-Field Coverage in mm-Wave 5G and Wi-Fi Indoor Networks

Path Gain Measurements and Models at 60 GHz in Street Canyons from Rooftop Sites for Outdoor Coverage

Path Loss Modeling for Air-To-Ground Channels in a Suburban Environment

Pathloss-Based Non-Line-Of-Sight Identification in an Indoor Environment: An Experimental Study

Performance Analysis of THz Backhaul Links Assisted by Reconfigurable Intelligent Surfaces

Performance Estimation of In-Vessel Resonant Communications

Phantom Material with Biological Composition for Muscle Equivalent Radiofrequency, Thermal and Magnetic Resonance Properties

Phase Variation of Ingestible Dipole, Loop, and Patch Antennas in Gastrointestinal Tract

Phase-Variation Microwave Displacement Sensor with High Resolution, Sensitivity, and Dynamic Range

Phased Array Antennas for Radar: Research Directions at TNO

Phased Array Technology at FHR - from Early Beginnings to High-End Solutions

Phaseless Characterization of Flat Sources with a Planar Wide-Mesh Scanning Strategy

Physics Based Workflow for the Design of THz Lens Antennas

Physics-Informed Generative Neural Networks for RF Propagation Prediction with Application to Indoor Body Perception

Physics-Informed Regularization for Microwave Imaging in Biomedical Applications

Pinwheel-Shaped Polarizer for Generating Dual-Circularly Polarized Conical Radiation Patterns in the Ka-Band

Pixel Antenna Design for mm-Wave Wireless Communications to Achieve Wide Scanning

Planar Antennas and Electronic Steerable Antennas Applications

Planar Near-Field Phaseless Measurements Using Multi-Probe Arrays

Plane Wave Generator for OTA Testing

Platform Scattering Analysis of the Copernicus Imaging Microwave Radiometer

Platform-Aware Optimization of Conformal Antenna Array via Simulated Bifurcation

Plug-In Plug-Out Multibeam Dielectric Rod Antenna for Target Dedicated mm-Wave RF-WPT Applications

Polarization Insensitive Broadband Frequency Selective Resorber with Improved Selectivity for Stealth Applications

Polymer-Based Additive Manufacturing of a Complex RF Front-End for New Space Applications

Polynomial Basis Functions for Qualitative Head Tissue Segmentation via Linearized Microwave Imaging

Port Generation for Multi-Mode Multi-Port Antennas Based on Group Theory

Potential of Polarized MIMO in In-Body to Out-Body Radio Links

Power Handling Test of a L-Band Antenna Using Infrared Thermography

Predicting Rain Attenuation at D Band for 6G Backhaul Link Design: A Frequency Scaling Approach

Preliminary Clinical Trial Results of MammoWave in the Context of RadioSpin Project

Preliminary Description of a 2D Near-Field Electromagnetic Imaging Database

Preliminary Investigation of an Innovative RF Sensor for Deformation and Failure Evaluation in Composite Materials

Preliminary Study on Gain Maximization via Density-Based Topology Optimization

Preparing the Workforce of Tomorrow

Presentation of TICRA's Latest R&D Within AI and Full-Wave Modelling Algorithms for Large Antenna Arrays

Proactively Conformed Near-Field Focused Modulated Leaky-Wave Antennas

Progressive Ultra-Wideband Circularly Periodic High Impedance Surface Integrated with a Spiral Antenna

Propagation Modeling in an Indoor Environment at Sub-THz Frequencies Based on Ray Tracing

Propagation Path Analysis with Propagation QUBO Model in Urban Area

Propagation Study of Vision-Based RIS Beam Tracking for mmWave Communications

Proposal on Application of Quantum Annealers for Analysis of Multiple Scattered Waves

Prototype of Multi-Sector Indoor mmW Base Station Based on 5G NR Beam Control

Proving the Circular Polarization of the Fundamental Modes in Rotationally Symmetric Waveguides

Pulse Preserving Capability of an Ultrawideband Dispersive Dielectric Resonator Antenna

Q

1 2 3 5 6 A B C D E F G H I J K L M N O P Q R S T U V W X

Quad-Band Meandered Implantable Planar Inverted-F Antenna for Wireless Brain Health Monitoring

Quad-Junction Self-Biased Circulator with Wide Operational Bandwidth

Quantification and Correction of Signal Averaging with On-The-Fly Sampling in Near-Field Antenna Measurements

Quantification and Correction of Signal Averaging with On-The-Fly Sampling in Near-Field Antenna Measurements

Quantum and Thermal Noise Engineering with Metamaterials

Quantum Optimisation of Reconfigurable Surfaces in Complex Propagation Environments

Quiet-Zone Profiling in a mmWave Spherical Anechoic Chamber: An Evaluation Approach

R

1 2 3 5 6 A B C D E F G H I J K L M N O P Q R S T U V W X

Radiation Control by Space-Time-Modulated Anisotropic Impedance Surfaces

Radiation Control by Space-Time-Modulated Anisotropic Impedance Surfaces

Radiation Efficiency Cost of Optimal Current Density Generating Specific Far-Field Pattern

Radiation Pattern Shaping Using Generalized Luneburg Lenses for Automotive RADAR Antennas

Radiation Resistance Enhancement Techniques for Ultracompact Half-Wavelength Helical Omnidirectional Circularly Polarized Antennas

Radiofrequency Compatibility for Aerospace Applications

Radiometeorological Forecasts for Satellite Links Operations: Validation with Measurements from BepiColombo Mission

Rain Attenuation at Millimeter Waves in Different Climatic Zones Estimated from Drop Size Distributions

Rain Attenuation at mmWave and Optical Bands from Visibility and Rainfall Intensity Measurements

Rapid Automated Antenna Alignment on Robotic Antenna Ranges

Ray Tracing and Measurement-Based Characterization of Inter/Intra-Machine THz Wireless Channels

Ray-Tracing Based Channel Modeling and Characteristics Analysis for LEO Satellite-To-Ground Systems

Ray-Tracing Calibration from Channel Sounding Measurements in a Millimeter-Wave Industrial Scenario

Ray-Tracing Model for the Design and Efficiency Calculation of a Monolithic Geodesic Lens Array Antenna

Real World Challenges with Antenna Calibration in Industry

Real-System Variational Quantum Eigensolver for Electromagnetic Waveguides: A Benchmark Study

Real-Time Near-Field Measurements of mmWave Devices Using a Metasurface and IR Camera

Realizing Flat-Top Radiation Pattern with Sharp Cutoff for Reducing Lobing Fades

Recent Additions to TICRA Tools

Recent Advances in Multiscale-Multiphysics Inverse Scattering

Recent Advances in Plasma Surfaces

Recent Advances in Robotic Antenna Measurements for Aerospace Applications

Recent Advances on Multi-Scale Wave Manipulation Through Reconfigurable Intelligent Surfaces

Recent Past, Current, and Future AESA Radar Development at Lincoln Lab

Reconfigurable Architecture in a 130 x 80 mm² PCB with Antenna Booster Element for Multiband Operation in IoT Devices

Reconfigurable Intelligent Surfaces for THz: Signal Processing and Hardware Design Challenges

Reconfigurable Polarisation Conversion Metasurface for mm-Wave Applications Using Vanadium Dioxide (VO₂)

Reconfiguration of Electromagnetic Metasurfaces Using Tunable Shape Morphing Structures

Reconstruction of the Far-Field Pattern Radiated by an Elongated Antenna Measured over a Perfectly Electric Conducting Ground Plane in a Spherical Spiral Near-Field Facility

Reduced-Order Maximum Determinant Sampling Grids by Acquisition of Additional Arbitrary Sampling Points on an Optimized Path

Reduced-Order Maximum Determinant Sampling Grids by Acquisition of Additional Arbitrary Sampling Points on an Optimized Path

Reducing Mutual Coupling in 2x2 MIMO Circularly Polarized Patch Antenna Array Using Reflecting Polarization Conversion Metasurface

Reducing the Cross-Polarization Levels in Artificial Dielectric Layers for Wideband Arrays

Reflecting/Absorbing Dual-Mode Textile Metasurface with AI-Driven Parametric Studies

Reflective Intelligent Surfaces: Reducing Complexity by Controlling the Illuminating Field

Reflective Surfaces Based on Semi-Passive Reconfigurable Polymer Network Liquid Crystal

Reproducibility Studies of Instantaneous and 6-Minute Average Exposure Measurements Around 5G Massive-MIMO Base Stations

RF Modelling and Validation of the Breadboard Antenna of the Copernicus Imaging Microwave Radiometer

RF-Heterointegration for mm-Wave Radar and Communication Antenna-Arrays

RFID-Based Reconfigurable Intelligent Surfaces: Towards Wireless and Ultra-Low-Power Reconfigurability

Ridge Gap Waveguide Implementation with a 3D Glide Symmetric Holey Metasurface for Slotted Antenna Array Feeding

Rigorous Susceptibility-Based Design of Generalized Huygens' Metasurface Radomes

Rigorous Susceptibility-Based Design of Generalized Huygens' Metasurface Radomes

RIS Performance in a Comprehensive Fading Environment

RIS with Practical Reflection Coefficients: Modeling and Experimental Measurements

RIS-Based Over-The-Air Channel Equalization in Resource-Constrained Wireless Networks

RIS-Based Over-The-Air Channel Equalization in Resource-Constrained Wireless Networks

RIS-Enabled Near-Field Localization with EMI

RIS-Enhanced MIMO Channels in Urban Environments: Experimental Insights

Robotic Antenna Characterization System Based on Wideband FMCW Transceiver Modules

Robotic Arm-Based Antenna Metrology System for Aerospace Applications

Robotic near Field Scanning for High Throughput Phased Array Production Test

Robust Tensor Positioning Based on Channel Parameter Estimation Under Spatially Colored Noise

Roof-Glass Integrated Antenna for Vehicular GNSS Applications

Rydberg Atom-Based Sensors

S

1 2 3 5 6 A B C D E F G H I J K L M N O P Q R S T U V W X

Safe Beamforming Based on Human Area Estimation for Microwave Wireless Power Transfer

Safety Considerations for Robotic Antenna Measurement Systems

SARFID for Fine-Scale Localization of Passive Backscattering Devices at 2.4 GHz ISM Band

Scattering Model on Rough Surfaces in the THz Band

Scattering Singularities of Complex Systems Probed with Continuously Variable Metasurfaces

Scenario Classification and Channel Modeling for MIMO Communications in Dense Urban Street Scenarios

Scenario Classification and Channel Modeling for MIMO Communications in Suburban Road Scenarios

Seasonal Snow Melting Process Investigation in Polar Environment Using a Dual-Receiver Radar Architecture

Self-Interference Suppression for SatCom Active Antenna Arrays Through Joint Transmit and Receive Beamforming

Self-Isolated MIMO Antenna Using SIW Cavity Antenna for Dual-Band (28, 38 GHz) Applications

Self-Resonant Broadside-Radiating Superdirective Unidirectional Mixed-Multipole Antennas

Sensitivity of the Dielectric Spectroscopy with the Microwave Thermal Ablation Antenna to the Immersion Depth and Longitudinal Dimension of the Measured Media

Sequential Phase Optimization for Coherent Long-Range Distributed Wireless Power Transfer to a Non-Communicative Receiver

Series-Fed Loop Antenna Array Deployable by a Scissors Mechanism

SG3 Software, Experimental Data and Model Testing - How to Contribute

Shaping the Sub-Reflector of a Ring Focus Antenna for Tailored Beamwidth Applications

Shorted Stacked Patch Array for Photonic Beam Steering at mm-Waves

Sidelobe Suppression and Bandwidth Enhancement of Series-Fed Patch Antenna Arrays Using Coplanar Ground Conductor

SiGe BiCMOS and Wafer-Level Packaging Technologies for Sub-THz Applications

Silicon-Micromachined THz Antennas and Systems

Simplified Frequency-Diverse Array Architecture for Surveillance Purposes

Simplified Techniques to Estimate Uncertainties for Antenna Gain Patterns Determined via Near-Field to Far-Field Transformation

Simulated Far-Field Pattern Disruption from a 1 GHz Cloaked Array Above a 10 GHz Array

Simulation Based Uncertainty Analysis for Active Two-Way-Radiation Pattern Measurements of Circularly Polarized Antennas

Simultaneously Dual-Polarization Convertible Sub-THz Reconfigurable Intelligent Surface Enabled by Through-Quartz VIAs

Single Layer Cavity-Backed Filtenna with Ultra-Wide Out-Of-Band Suppression

Single Material Multilayer Radome for D Band Applications

Single-Branch Hybrid Resistance Compression Technique for Enhanced Rectifier Performance

SINTEC Comparative Body-Centric Communication Study: Bluetooth Vs Fat-Intrabody Communication

SIW Slot Leaky-Wave Antenna Using Low-Index Metamaterial

Small On-Metal Passive UHF RFID Transponders with Long Read Ranges

Small-Scale Passive Millimetre-Wave Imaging Measurements for Marine Litter Detection at W-Band

Smart Propagation Environments Empowered by Metasurfaces: A Self-Consistent Study

Spectral Domain Green's Function of an Infinite Dipole with Non-Zero Metal Thickness

Spectral Domain Green's Function of an Infinite Dipole with Non-Zero Metal Thickness

Spherical Active Frequency-Selective Surface for 3-D Beam-Scanning Antenna

Spherical Near-Field Measurement and Far-Field Characterization of a 300 GHz Band Antenna Based on an Electrooptic Probe with Compact Tabletop Robotic Arm

Spherical Wavefront Near-Field DoA Estimation in THz Automotive Radar

Stabilization of EFIE-IBC by Spatial Filtering

Stable Phaseless Spherical Antenna Measurements via Mixed-Norm Regularization

Standardization Progress and Challenges for 5G OTA Testing

Static and Reconfigurable Phase-Gradient Metasurfaces for Antenna Applications

Stationarity of Multiband Channels for OTFS-Based Intelligent Transportation Systems

Strategies for Enhancing the Gain Bandwidth of Fabry-Pérot Cavity Antennas: A Review of Recent Advances

Stretchable Multi-Band Radio Frequency Sensor for Strain Measurement

Study of Different Feed Layout Configurations for Hybrid Active VHTS Antennas

Study of Environmentally-Friendly Radomes Using Cork-Rubber Composites for 5G Backhaul Links at E-Band

Study of Finite Edge Effects in Compact Ultra-Wide-Band Connected Arrays

Study of the Frequency Dispersion of 3D-Printed Dielectric Crystals for Dielectric Resonator Antenna Applications

Study on Antenna-Phantom Model of Aperture Antennas for SAR Analysis

Study on CFM Method for Beam Compensation of Array-Fed Space-Borne Reflector Antennas

Sub-7 GHz Circularly Polarized Dielectric Resonator Antenna Array for Full-Duplex Applications

Sub-Terahertz MassiveMIMO Channel Sounder for 6G Mobile Communication Systems

Sub-THz On-Chip CPW Monopole on InP with Cross-Shaped Slot for Bandwidth Enhancement

Sub-THz Propagation Measurement and Analysis in Indoor Corridor Environment at 159 GHz

Sub-THz Spatially Modulated Beam Splitting Reflectors for Potential RIS Implementations

Sub-THz Substrate Integrated Waveguide Signal Transitions in Backend-Of-Line of a Silicon Process

Sub-THz U-Slot Coupled Stacked-Patch Radiating Elements for Dual-Polarized MIMO Array Antennas

Sub-Wavelength Anisotropic Unit-Cells for Low-Profile Transmitarray Antennas

Subsampling Time-Modulated Array for Reduced Hardware down Conversion and Beamforming

Substrate-Integrated Mode Composite Waveguide

Substructure Modes and Bounds

Sunflower Array of Infinitesimal Dipoles for Constrained Antenna Modeling

Super-Realized Gain Huygens Antennas

Superconducting Space-Time Modulation: Theoretical Implications and Mixing-Beamsplitting Functionality

Superdirective Broadside-Radiating Unidirectional Mixed-Multipole Antenna Arrays

Supervised Learning Applied to Microwave Imaging System Calibration

Supervised Learning Based Real-Time Adaptive Beamforming On-Board Multibeam Satellites

Supervised Machine Learning for Breast Cancer Detection Using Microwave Imaging in the Frequency Domain

Surface Partial Differential Equations and Its Applications to Scattering Problems

Surface-Wave Communication Platform for Indoor Wireless Networks

SW1 Panel Discussion: Discuss on Future Research Challenges

SW11 Pannel Discussions

SW2 Panel Discussion - Future Requirements

SW5 Panel Discussion

SW8 Discussions

Synthesis of a Planar 2D Butler Matrix: A Showcase with a 3x3 Array

Synthesis of Circularly Polarized Microstrip Planar Array with Cross-Polarization Suppression

Synthesis of Drop Counter Rain Rate from a Tipping Bucket Rain Gauge

Synthesis of Flat-Top Beams Based on Modified Chebyshev Polynomials

T

1 2 3 5 6 A B C D E F G H I J K L M N O P Q R S T U V W X

Tailoring Surface Impedance for Cascaded Cylindrical Metasurfaces

Tailoring the Performance of Geodesic Lens Antennas by Defining Their Footprint

Tapering Impact on the Spatial and Frequency Responses of Broadband Asymmetrically Routed Phased Arrays

Target Classification Through ISAR for Autonomous Vehicles Based on Federated Learning

Technology for Radiation Pattern Manipulation of Wi-Fi Antennas

Temperature-Dependent Electrical Characterization of a Thermally Sensitive Hepatic Tumor Phantom

Terahertz Channel Modeling Based on Scattering Characterization

Terahertz Microstrip Leaky-Wave Antenna for WR1.0 Band

Textile Waveguide Antennas for On-Body Sensor and Communication Systems

The Antenna Dome High-Speed Characterization System for OTA Characterization of FR2 5G Active Antenna Panels

The d'Alembertian Representation of Green's Functions and Evaluation of Surface Integrals over Non-Parallel Planes

The Design of Re-Imaging Optics for Passing Several Beams Through Small Cryostat Windows

"The Diminished Edge Diffraction Effect Bull's Eye Antenna "

The Effect of Beam Misalignment in Data Center Environment at 285GHz Band

The Effect of Pressure of the Open-Ended Coaxial Probe on the Measurement of Ex Vivo Biological Tissues Dielectric Properties

The Hydrogen Intensity Real-Time Analysis eXperiment: Overview and Status Update

The Impact of a Phantom's Size on the Performance of an Implanted Antenna

The Kootwijk VLF Antenna: A Numerical Model

The Novel Method for Deployable Parabolic Reflector Based on Uchiwa Origami

The Predictions of Quantum and Classical Models for the Thermal Energy Emitted in the Sub-mm Ranges by Doped Silicon

The Role of Arrays in Pulsed Radiation

The Role of Ground Currents in the Co-Simulation of Matching Components and Layout Models in Matching Circuit Optimization

The Time Modulated Array for Channel Sounding Measurements - Concept and Initial Field Tests

Theoretical Insights and Engineering of Wireless Body-Implanted Bioelectronics

Thermoelectric Cooling Solution for Active Antennas

Thin-Film Terahertz Metamaterials Manufactured by Laser Direct Writing

Thinned Connected Slot Array Design Using Higher Symmetries

Tiled Subarray Design for Multibeam Joint Communication and Sensing

Time Domain Analysis of Pulsed Photo-Conductive Antenna Sources: Distributed Excitations

Time-Modulated Arrays for Simultaneous Wireless Information and Power Transfer in Near-Field

Time-Modulated Metasurface for Harmonic Signals Frequency Conversion

Time-Modulated Metasurface-Based System for the Generation of False Radar Targets

Time-Varying Channel Measurement and Analysis at 105 GHz in an Indoor Factory

Towards a Reconfigurable Metacavity Antenna for Computational Imaging and DoA Estimation

Towards Achieving Reliable On-Wafer Measurement of Millimetre-Wave and Terahertz Planar Circuits

Towards Array and Curve Analysis: Flexible Passive Chipless RFID Tags

Towards Optimal Binary Patterns for Compressive Terahertz Single-Pixel Imaging

Traceability of 5G Measurements

Transmissive-Type Metagratings with Few Meta-Atoms for Beam Splitting

Traveling-Wave Fed Dielectric Rod Antenna for 3D Scanning MIMO Sensor

Trials and Tribulations of a Wireless and Digital Services Test Lab

Tunable Optimal Anomalous Reflection Using Discrete Impedance Metasurfaces

Tunable Rectangular Waveguide Bandpass Filter Based on Plasma Technology

Tunable Segmented Loop Antenna Reader for Miniaturized Chipless Tag Detection

Two-Dimensional, Un-Equal, Series Power Dividers for Feeding Antenna Arrays

TX/RX Terminal Based on Metascreen Technology for Ka-Band Satcom with Dual Switchable Polarization

U

1 2 3 5 6 A B C D E F G H I J K L M N O P Q R S T U V W X

UHF RFID Sensor Antenna for Fat Content and Adulteration Detection of Milk

Ultra Wide Dynamic Range High Power RF Rectifier

Ultra-Low-Loss Millimeter Wave Beam Scanning Antenna Using Piezoelectric Actuation

Ultra-Miniature Circularly Polarized Antenna with Omni-Directional Pattern for Sat-IoT

Ultra-Wideband Wide-Scanning Dual-Polarized Vivaldi Antenna Unit with Novel Pendulum-Shaped Slots

Ultrahigh Sensitive Terahertz Metasurface with 2D MoS₂ for Refractive Index Biosensing

Uncertainties in the Estimation of the Gain of a Standard Gain Horn in the Frequency Range of 90 GHz to 140 GHz

Uncertainty Analysis of Linear Multi-Probe Array Systems for Fast Antenna Measurements

Uncertainty Quantification for the Reflector Antenna in the Copernicus Imaging Microwave Radiometer

Uncertainty Quantification of the Gain Budget for INCUS

Unconventional Surrogate-Assisted Approaches to EM-Driven Antenna Design. Modeling and Optimization: Global, Multi-Objective, Statistical

UnderGround-To-AboveGround IoT Communication Links Insurance at 915 MHz Using LoRa Technology

Understanding UHF RFID Sensor Systems: A Summary

Use of Ecofriendly Geopolymer Ceramics in Antenna Design and Microwave Applications

Use of Model Based Systems Engineering and Development in the Design of a Commercial Nose-Radome Test System Employing a Multi-Axis Cobot

User and Passive Beam Scheduling Scheme for Liquid Crystal IRS-Assisted mmWave Communications

Using a Radio-Frequency System on a Chip in the Development of a Phased Radio Array for the Bustling Universe Radio Survey Telescope in Taiwan

Utilization of Wi-Fi Signal for Validation of Micro-Doppler Model in a Person Falling Scenario

UWB Circular Metal Mesh Transparent Antenna

V

1 2 3 5 6 A B C D E F G H I J K L M N O P Q R S T U V W X

Validating Convex Optimization of Reconfigurable Intelligent Surfaces via Measurements

Validating Properties of RIS Channel Models with Prototypical Measurements

Validation of a Large Retrodirective CASSIOPeiA Solar Power Satellite Antenna Array

Validation of Pseudo-Scale Model for the Air-Sea Two-Layer Near-Field Problem by Using FDTD Simulations and Measurements in a Tank

Validation of Ray-Tracing Simulated Channels for Massive MIMO Systems at Millimeter-Wave Bands

Validation of the DTU ETC Scattering Test Facility for Radar Cross Section Measurements

Variability of Rain Attenuation at Millimeter Waves Due to Fluctuations of the Drop Size Distribution

Variable Multi-Band Metasurface Reflector with Controllable Direction Using Varactor Diodes Mounted Large-Via Mushroom-Type Structure

Vector Potentials for Uniaxial Media with Sources

VHF/UHF Antenna Measurements Based on Multi Probe Array Technology

Virus Detection in the Microwave Regime Through an Antenna Workbench

W

1 2 3 5 6 A B C D E F G H I J K L M N O P Q R S T U V W X

Wave-Controlled Biasing of RIS for Multi-Beam Scattering Pattern Generation

Waveguide Slot Array Antennas by Diffusion Bonding of Laminated Thin Plates

Welcome and Introduction

Welcome Introduction

Whip Antenna Miniaturization at VHF Band Using Magneto-Dielectric Materials

Wi-Fi 6E/7: Amazing New Frontiers and Challenges

Wi-Fi Antenna with Reconfigurable Metasurfaces

Wide-Angle Quasi-Optical Beamformer for LEO Applications

Wide-Scan Active Highly Integrated Phased Array Antenna for Tx/Rx Application at K-Band

Wideband Aperture-Coupled Array Design for Automotive Radar Applications

Wideband Array Antenna with Single-Layer Feeding Network at Ka-Band

Wideband Beam-Steering Continuous Transverse Stub Array Enabled by a Reflecting Luneburg Lens at Ka-Band

Wideband Characterization of Wireless Power Transfer in Ventilation (HVAC) Ducts for the Internet of Things and Smart Buildings

Wideband Decoupling Smartphone Antenna with Integrated Metal Rim

Wideband Dielectric Characterization of Biological Tissues and Realistic Phantom Preparation at Microwave Frequencies

Wideband Dual-Polarized 1-Bit Unit-Cell Design for mmWave Reconfigurable Intelligent Surface

Wideband Dual-Polarized Lens Antenna for Future mm-Wave Applications

Wideband Half-Elliptical Ring Slot Array Loaded Leaky Wave Antenna on a Half-Mode Corrugated Substrate Integrated Waveguide

Wideband Low-Profile Circularly Polarized All-Metal Antenna for Triton Exploration

Wideband Transmissive Metasurfaces for Sub-THz Frequency-Dependent Beam Scanning

Wiener-Hopf Type Analysis of PTD Symmetric Waveguides: A Novel Methodology Procedure

Wind-Induced Backscatter Clustering from Vegetation at W-Band

Wireless Re-Configurable Intelligent Surface for Sub 6 GHz 5G Frequency

WP 3J - Propagation Fundamentals - Key Recommendations and Topics

WP 3K - Point-To-Area Propagation - Key Recommendations and Topics

WP 3L - Ionospheric Propagation and Radio Noise - Key Recommendations and Topics

WP 3M - Point-To-Point and Earth-Space Propagation - Key Recommendations and Topics

X

1 2 3 5 6 A B C D E F G H I J K L M N O P Q R S T U V W X

X-Band Receiving Phased Array with Digital Beamforming Using RFSoc

X-Band Reconfigurable Phase Shifters Based on SIW and Liquid Metal Technologies